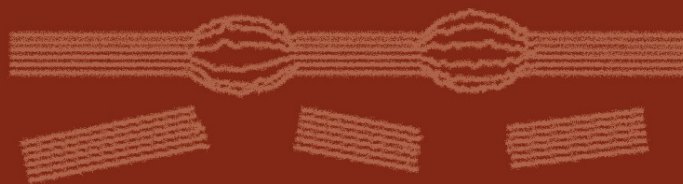


S. Kalia
B. S. Kaith
I. Kaur (Eds.)



Cellulose Fibers: Bio- and Nano- Polymer Composites

Green Chemistry and Technology



Springer

Cellulose Fibers:
Bio- and Nano-Polymer Composites

Susheel Kalia • B. S. Kaith • Inderjeet Kaur
Editors

Cellulose Fibers: Bio- and Nano-Polymer Composites

Green Chemistry and Technology

 Springer

Editors

Dr. Susheel Kalia
Department of Chemistry
Bahra University
Waknaghat (Shimla Hills)-173 234
Dist. Solan
Himachal Pradesh, India
susheel_kalia@yahoo.com
susheel.kalia@gmail.com

Dr. B. S. Kaith
Department of Chemistry
Dr. B.R. Ambedkar National Institute
of Technology
Jalandhar -144 011
Punjab, India
bskaith@yahoo.co.in

Dr. Inderjeet Kaur
Department of Chemistry
Himachal Pradesh University
Shimla – 171 005
Himachal Pradesh, India
ij_kaur@hotmail.com

ISBN 978-3-642-17369-1 e-ISBN 978-3-642-17370-7
DOI 10.1007/978-3-642-17370-7
Springer Heidelberg Dordrecht London New York

Library of Congress Control Number: 2011924897

© Springer-Verlag Berlin Heidelberg 2011

This work is subject to copyright. All rights are reserved, whether the whole or part of the material is concerned, specifically the rights of translation, reprinting, reuse of illustrations, recitation, broadcasting, reproduction on microfilm or in any other way, and storage in data banks. Duplication of this publication or parts thereof is permitted only under the provisions of the German Copyright Law of September 9, 1965, in its current version, and permission for use must always be obtained from Springer. Violations are liable to prosecution under the German Copyright Law.

The use of general descriptive names, registered names, trademarks, etc. in this publication does not imply, even in the absence of a specific statement, that such names are exempt from the relevant protective laws and regulations and therefore free for general use.

Cover design: eStudio Calamar S.L.

Printed on acid-free paper

Springer is part of Springer Science+Business Media (www.springer.com)

Preface

Present is an era of advance materials including polymer composites, nanocomposites, and biocompatible materials. With advancements in science and technology and increase in Industrial growth, there is a continuous deterioration in our environmental conditions. Emission of toxic gases such as dioxin on open burning of plastics in the air and the poisoning of soil-fertility due to nonbiodegradability of plastics disposed in the soil are continuously adding pollution load to our surrounding environment. Therefore, keeping in view the deteriorating conditions of the living planet earth, researchers all over the world have focused their research on eco-friendly materials, and the steps taken in this direction will lead toward Green-Science and Green-Technology.

Cellulosics account for about half of the dry weight of plant biomass and approximately half of the dry weight of secondary sources of waste biomass. At this crucial moment, cellulose fibers are pushed due to their “green” image, mainly because they are renewable and can be incinerated at the end of the material’s lifetime without adding any pollution load in the atmosphere. Moreover, the amount of CO₂ released during incineration process is negligible as compared to the amount of CO₂ taken up by the plant throughout its lifetime. Polysaccharides can be utilized in many applications such as biomedical, textiles, automobiles, etc. One of the promising applications is using them as a reinforcing material for the preparation of biocomposites. The most important factor in obtaining mechanically viable composite material is the reinforcement–matrix interfacial interaction. The extent of adhesion depends upon the chemical structure and polarity of these materials. Owing to the presence of hydroxyl groups in cellulose fibers, the moisture regain is high, leading to poor organic wettability with the matrix material and hence a weak interfacial bonding between the reinforcing agent and hydrophobic matrices. In order to develop composites with better mechanical properties and environmental performance, it becomes necessary to increase the hydrophobicity of the reinforcing agent and to improve the compatibility between the matrix and cellulose fibers. There exist several pretreatments that are conducted on cellulose fibers for modifying not only the interphase but also the morphological changes in fibers. Nowadays, to improve the compatibility between

natural fibers and hydrophobic polymer matrices, various greener methods such as plasma treatment and treatments using fungi, enzymes, and bacteria have been explored.

Reinforcement of thermoplastic and thermosetting composites with cellulose fibers is increasingly regarded as an alternative to glass fiber reinforcement. The environmental issues in combination with their low cost have recently generated considerable interest in cellulose fibers such as isora, jute, flax, hemp, kenaf, pineapple leaf, and man-made cellulose fibers as fillers for polymer matrices-based composites.

Criteria for cleaner and safer environment have directed enormous parts of the scientific research toward bioplastic materials that can easily be degraded or bio-assimilated toward the end of their life cycle. Degradation of the biocomposites could be either a photodegradation or microbial degradation. Photodegradation of biofilms plays an important role as mulching sheets for plants in agricultural practices that ultimately gets degraded in the soil as an organic fertilizer. Microbial degradation plays a significant role in the depolymerization of the biopolymers, and final degradation products are carbon dioxide and water, thereby adding no pollution load to the environment.

Development of polymer nanocomposite is a fast-growing area of research. Significant efforts are focused on the ability to obtain control of the nanoscale structures via innovative synthetic approaches. The properties of nanocomposite materials depend not only on the properties of their individual constituents but also on their morphology and interfacial characteristics. This rapidly expanding field is generating many exciting new materials with novel properties. All types and classes of nanocomposite materials lead to new and improved properties when compared to their macrocomposite counterparts. Therefore, nanocomposites promise new applications in diversified fields such as high-strength and light-weight components for aerospace industry, corrosion-resistant materials for naval purpose, etc.

Researchers all over the world are working in this field, and only a few books are available on cellulose fiber polymer composites and nanocomposites. Therefore, this book is in the benefit of society, covering all the essential components of green chemistry. The book is divided into four parts. It starts off with Part-I: structure and properties of cellulose fibers and nanofibers and their importance in composites, medical applications, and paper making. Part-II of the book covers the polymer composites and nanocomposites reinforced with cellulose fibers, nanofibers, cellulose whiskers, rice husk, etc. Greener surface modifications of cellulose fibers, morphology, and mechanical properties of composites are also covered in this part. Part-III of the book covers the biodegradable plastics and their importance in composite manufacturing, reinforced with natural and man-made cellulose fibers. Present section also discusses the biodegradation of polymer composites. Part-IV of the book includes the use of cellulose fiber-reinforced polymer composites in automotives, building materials, and medical applications.

Book covering such vital issues and topics definitely should be attractive to the scientific community. This book is a very useful tool for scientists, academicians,

research scholars, polymer engineers, and industries. This book is also supportive for undergraduate and postgraduate students in Institutes of Plastic Engineering and Technology and other Technical Institutes. The book is unique with valuable contributions from renowned experts from all over the world.

The Editors would like to express their gratitude to all contributors of this book, who made excellent contributions. We would also like to thank our students, who helped us in the editorial work.

Solan (Shimla Hills), India
Jalandhar, India
Shimla, India
February 2011

Susheel Kalia
Balbir Singh Kaith
Inderjeet Kaur

Contents

Part I Cellulose Fibers and Nanofibers

- 1 Natural Fibres: Structure, Properties and Applications** 3
S. Thomas, S.A. Paul, L.A. Pothan, and B. Deepa
- 2 Chemical Functionalization of Cellulose Derived from Nonconventional Sources** 43
V.K. Varshney and Sanjay Naithani
- 3 Production of Flax Fibers for Biocomposites** 61
Jonn Foulk, Danny Akin, Roy Dodd, and Chad Ulven
- 4 Cellulosic Bast Fibers, Their Structure and Properties Suitable for Composite Applications** 97
Malgorzata Zimniewska, Maria Wladyka-Przybylak, and Jerzy Mankowski
- 5 Potential Use of Micro- and Nanofibrillated Cellulose Composites Exemplified by Paper** 121
Ramjee Subramanian, Eero Hiltunen, and Patrick A.C. Gané

Part II Cellulosic Fiber-Reinforced Polymer Composites and Nanocomposites

- 6 Greener Surface Treatments of Natural Fibres for the Production of Renewable Composite Materials** 155
Koon-Yang Lee, Anne Delille, and Alexander Bismarck
- 7 Nanocellulose-Based Composites** 179
Kelley Spence, Youssef Habibi, and Alain Dufresne

8	Dimensional Analysis and Surface Morphology as Selective Criteria of Lignocellulosic Fibers as Reinforcement in Polymeric Matrices	215
	Kestur Gundappa Satyanarayana, Sergio Neves Monteiro, Felipe Perisse Duarte Lopes, Frederico Muylaert Margem, Helvio Pessanha Guimaraes Santafe Jr., and Lucas L. da Costa	
9	Interfacial Shear Strength in Lignocellulosic Fibers Incorporated Polymeric Composites	241
	Sergio Neves Monteiro, Kestur Gundappa Satyanarayana, Frederico Muylaert Margem, Ailton da Silva Ferreira, Denise Cristina Oliveira Nascimento, Helvio Pessanha Guimarães Santafé Jr., and Felipe Perissé Duarte Lopes	
10	The Structure, Morphology, and Mechanical Properties of Thermoplastic Composites with Lignocellulosic Fiber	263
	Slawomir Borysiak, Dominik Pauksza, Paulina Batkowska, and Jerzy Mańkowski	
11	Isora Fibre: A Natural Reinforcement for the Development of High Performance Engineering Materials	291
	Lovely Mathew, M.K. Joshy, and Rani Joseph	
12	Pineapple Leaf Fibers and PALF-Reinforced Polymer Composites	325
	S.M. Sapuan, A.R. Mohamed, J.P. Siregar, and M.R. Ishak	
13	Utilization of Rice Husks and the Products of Its Thermal Degradation as Fillers in Polymer Composites	345
	S.D. Genieva, S.Ch. Turmanova, and L.T. Vlaev	
14	Polyolefin-Based Natural Fiber Composites	377
	Santosh D. Wanjale and Jyoti P. Jog	
15	All-Cellulosic Based Composites	399
	J.P. Borges, M.H. Godinho, J.L. Figueirinhas, M.N. de Pinho, and M.N. Belgacem	
Part III Biodegradable Plastics and Composites from Renewable Resources		
16	Environment Benevolent Biodegradable Polymers: Synthesis, Biodegradability, and Applications	425
	B.S. Kaith, Hemant Mittal, Rajeev Jindal, Mithu Maiti, and Susheel Kalia	

17 Biocomposites Based on Biodegradable Thermoplastic Polyester and Lignocellulose Fibers 453
 Luc Avérous

18 Man-Made Cellulose Short Fiber Reinforced Oil and Bio-Based Thermoplastics 479
 Johannes Ganster and Hans-Peter Fink

19 Degradation of Cellulose-Based Polymer Composites 507
 J.K. Pandey, D.R. Saini, and S.H. Ahn

20 Biopolymeric Nanocomposites as Environment Benign Materials 519
 Pratheep Kumar Annamalai and Raj Pal Singh

Part IV Applications of Cellulose Fiber-Reinforced Polymer Composites

21 Cellulose Nanocomposites for High-Performance Applications 539
 Bibin Mathew Cherian, Alcides Lopes Leao, Sivoney Ferreira de Souza, Sabu Thomas, Laly A. Pothan, and M. Kottaisamy

22 Sisal Fiber Based Polymer Composites and Their Applications 589
 Mohini Saxena, Asokan Pappu, Ruhi Haque, and Anusha Sharma

23 Natural Fibre-Reinforced Polymer Composites and Nanocomposites for Automotive Applications 661
 James Njuguna, Paul Wambua, Krzysztof Pielichowski, and Kambiz Kayvantash

24 Natural Fiber-Based Composite Building Materials 701
 B. Singh, M. Gupta, Hina Tarannum, and Anamika Randhawa

About the Editors 721

Index 723

Contributors

S.H. Ahn School of Mechanical and Aerospace Engineering Seoul National University, Kwanak-Ro 599, Seoul 151-742, South Korea

Danny Akin Light Light Solutions LLC, PO Box 81486, Athens, GA 30608, USA

Pratheep Kumar Annamalai Division of Polymer Science and Engineering, National Chemical Laboratory, Dr. Homi Bhaba Road, Pune 411 008, India; Laboratoire Génie des Procédés d'élaboration des Bioproduits (GPEB), Université Montpellier II, Place Eugène Bataillon, F-34095, Montpellier, France

Luc Avérous LIPHT-ECPM, EAC (CNRS) 4375, University of Strasbourg, 25 rue Becquerel, 67087 Strasbourg Cedex 2, France

Paulina Batkowska Poznan University of Technology, Institute of Chemical Technology and Engineering, 60-965 Poznan, Poland

M.N. Belgacem Laboratoire de Génie des Procédés Papetiers UMR CNRS 5518, Grenoble INP-Pagora, B.P. 65, 38402 Saint Martin d'Hères Cedex, France

Alexander Bismarck Department of Chemical Engineering, Imperial College London, Polymer and Composite Engineering (PaCE) Group, South Kensington Campus, London SW7 2AZ, UK

J.P. Borges Departamento de Ciência dos Materiais and CENIMAT/I3N, Faculdade de Ciências e Tecnologia, FCT, Universidade Nova de Lisboa, 2829-516 Caparica, Portugal

Slawomir Borysiak Poznan University of Technology, Institute of Chemical Technology and Engineering, Skłodowskiej-Curie 60-965 Poznan, Poland

Lucas L. da Costa Laboratory for Advanced Materials, LAMAV; State University of the Northern Rio de Janeiro, UENF; Av. Alberto Lamego, 2000, 28013-602, Campos dos Goytacazes, RJ, Brazil

B. Deepa Department of Chemistry, Bishop Moore College, Mavelikkara, Kerala, India

Anne Delille Polymer and Composite Engineering (PaCE) Group, Department of Chemical Engineering, Imperial College London, South Kensington Campus, London SW7 2AZ, UK

Roy Dodd Department of Agriculture and Biological Engineering, Clemson University, McAdams Hall, Clemson, SC 29634, USA

Alain Dufresne Grenoble Institute of Technology, The International School of Paper, Print Media and Biomaterials (Pagora), BP 65, 38402 Saint Martin d'Hères cedex, France; Universidade Federal do Rio de Janeiro (UFRJ), Departamento de Engenharia Metalurgica e de Materiais, Coppe, Rio de Janeiro, Brazil

J.L. Figueirinhas Departamento de Física, IST-TU, Av. Rovisco Pais, 1049-001, Lisbon, Portugal

Hans-Peter Fink Fraunhofer Institute for Applied Polymer Research IAP, Geiselbergstr. 69, 14476 Potsdam, Germany

Jonn Foulk Cotton Quality Research Station, USDA-ARS, Ravenel Center room 10, Clemson, SC 29634, USA

Patrick A.C. Gane Omya Development AG, Baslerstrasse 42, 4665 Oftringen, Switzerland; Department of Forest Products Technology, School of Science and Technology, Aalto University, 02150 Espoo, Finland

Johannes Ganster Fraunhofer Institute for Applied Polymer Research IAP, Geiselbergstr. 69, 14476 Potsdam, Germany

S.D. Genieva Department of Inorganic Chemistry, Assen Zlatarov University, 8010, Burgas, Bulgaria

M.H. Godinho Departamento de Ciência dos Materiais and CENIMAT/I3N, Faculdade de Ciências e Tecnologia, FCT, Universidade Nova de Lisboa, 2829-516, Caparica, Portugal

M. Gupta CSIR-Central Building Research Institute, Roorkee 247 667, India

Youssef Habibi Department of Forest Biomaterials, North Carolina State University Campus, PO Box 8005, Raleigh, NC 27695-8005, USA

Ruhi Haque Advanced Materials and Processes Research Institute (AMPRI), CSIR, HabibGanj Naka, Bhopal 462064, India

Eero Hiltunen Department of Forest Products Technology, School of Science and Technology, Aalto University, 02150 Espoo, Finland

Rajeev Jindal Department of Chemistry, Dr. B.R. Ambedkar National Institute of Technology, Jalandhar 144 011, Punjab, India

Jyoti P. Jog Polymer Science and Engineering Division, National Chemical Laboratory, Dr. Homi Bhabha Road, Pashan, Pune 411008, India

Rani Joseph Department of Polymer Science and Rubber Technology, Cochin University of Science and Technology, Kochi, Kerala, India

M.K. Joshy Department of Chemistry, S.N.M. College, Malienkara, Kerala, India

B.S. Kaith Department of Chemistry, Dr. B.R. Ambedkar National Institute of Technology, Jalandhar 144 011, Punjab, India

Susheel Kalia Department of Chemistry, Bahra University, Wagnaghat (Shimla Hills), 173 234, Solan, Himachal Pradesh, India

Kambiz Kayvantash Société CADLM, 9 rue Raoul Dautry, 91190 GIF-SUR-YVETTE, Paris, France

M. Kottaisamy Centre for Nanotechnology, Kalasalingam University, Anand Nagar, Krishnankoil, 626 190 Virudhunagar, Tamil Nadu, India

Koon-Yang Lee Polymer and Composite Engineering (PaCE) Group, Department of Chemical Engineering, Imperial College London, South Kensington Campus, London SW7 2AZ, UK

Felipe Perisse Duarte Lopes Laboratory for Advanced Materials, LAMAV; State University of the Northern Rio de Janeiro, UENF; Av. Alberto Lamego, 2000, 28013-602, Campos dos Goytacazes, RJ, Brazil

Alcides Lopes Leao Department of Natural Science, College of Agricultural Sciences, UNESP – São Paulo State University, Botucatu 18610-307, Brazil

Mithu Maiti Department of Chemistry, Dr. B.R. Ambedkar National Institute of Technology, Jalandhar 144 011, Punjab, India

Jerzy Mankowski Institute of Natural Fibres and Medicinal Plants, Wojska Polskiego 71b, 60-630, Poznan, Poland

Frederico Muylaert Margem Laboratory for Advanced Materials, LAMAV; State University of the Northern Rio de Janeiro, UENF; Av. Alberto Lamego, 2000, 28013-602, Campos dos Goytacazes, RJ, Brazil

Lovely Mathew Department of Chemistry, Newman College, Thodupuzha, Kerala, India

Bibin Mathew Cherian Department of Natural Science, College of Agricultural Sciences, São Paulo State University (UNESP), Botucatu 18610-307, São Paulo, Brazil

Hemant Mittal Department of Chemistry, Dr. B.R. Ambedkar National Institute of Technology, Jalandhar 144 011, Punjab, India

A.R. Mohamed Department of Mechanical and Manufacturing Engineering, Faculty of Engineering, University of Putra Malaysia, 43400 UPM Serdang, Selangor, Malaysia

Sergio Neves Monteiro Laboratory for Advanced Materials, LAMAV; State University of the Northern Rio de Janeiro, UENF; Av. Alberto Lamego, 2000, 28013-602 Campos dos Goytacazes, RJ, Brazil

Sanjay Naithani Chemistry Division, Forest Research Institute, Dehra Dun 248 006, India

Denise Cristina Oliveira Nascimento Laboratory for Advanced Materials, LAMAV; State University of the Northern Rio de Janeiro, UENF; Av. Alberto Lamego, 2000, 28013-602, Campos dos Goytacazes, RJ, Brazil

James Njuguna Department of Sustainable Systems, Cranfield University, Bedfordshire MK43 0AL, UK

J.K. Pandey School of Mechanical and Aerospace Engineering Seoul National University, Kwanak-Ro 599, Seoul 151-742, South Korea

Asokan Pappu Advanced Materials and Processes Research Institute (AMPRI), CSIR, HabibGanj Naka, Bhopal 462064, India

Januar Parlaungan Siregar Department of Mechanical and Manufacturing Engineering, Faculty of Engineering, University of Putra Malaysia, 43400 UPM Serdang, Selangor, Malaysia

Dominik Pauksza Poznan University of Technology, Institute of Chemical Technology and Engineering, 60-965 Poznan, Poland

S.A. Paul Department of Chemistry, Bishop Moore College, Mavelikkara, Kerala, India

Krzysztof Pielichowski Department of Chemistry and Technology of Polymers, Cracow University of Technology, ul. Warszawska 24, 31-155 Kraków, Poland

M.N. de Pinho Departamento de Química and ICEMS, IST-TU, Av. Rovisco Pais, 1049-001 Lisbon, Portugal

L.A. Pothan Department of Chemistry, Bishop Moore College, Mavelikkara, Kerala, India

Maria Wladyka Przybylak Institute of Natural Fibres and Medicinal Plants, Wojska Polskiego 71b, 60-630 Poznan, Poland

Anamika Randhawa CSIR-Central Building Research Institute, Roorkee 247 667, India

Mohamad Ridzwan Ishak Department of Mechanical and Manufacturing Engineering, Faculty of Engineering, University of Putra Malaysia, 43400 UPM Serdang, Selangor, Malaysia

D.R. Saini Department of Polymer Science and Engineering, National Chemical Laboratory, Dr. Homi Bhabha Road, Pune 411008, India

Helvio Pessanha Guimaraes Santafe Jr. Laboratory for Advanced Materials, LAMAV; State University of the Northern Rio de Janeiro, UENF; Av. Alberto Lamego, 2000, 28013-602, Campos dos Goytacazes, RJ, Brazil

Salit Mohd Sapuan Department of Mechanical and Manufacturing Engineering, University of Putra Malaysia, 43400 UPM Serdang, Selangor, Malaysia

Kestur Gundappa Satyanarayana Laboratory for Advanced Materials, LAMAV, State University of the Northern Rio de Janeiro, UENF, Av. Alberto Lamego 2000, Horto, Campos dos Goytacazes, Rio de Janeiro, Brazil; UFPR, Curitiba, Paraná, Brazil; Acharya Institutes, BMS College of Engineering and Poornaprajna Institute of Scientific Research, Bangalore, India

Mohini Saxena Building Materials Development Group, Advanced Materials and Processes Research Institute (AMPRI), CSIR, HabibGanj Naka, Bhopal 462064, India

Anusha Sharma Advanced Materials and Processes Research Institute (AMPRI), CSIR, HabibGanj Naka, Bhopal 462064, India

Ailton da Silva Ferreira Laboratory for Advanced Materials, LAMAV; State University of the Northern Rio de Janeiro, UENF; Av. Alberto Lamego, 2000, 28013-602, Campos dos Goytacazes, RJ, Brazil

B. Singh CSIR-Central Building Research Institute, Roorkee 247 667, India

Raj Pal Singh Division of Polymer Science and Engineering, National Chemical Laboratory, Dr. Homi Bhaba Road, 411 008, Pune, India

Sivoney Ferreira de Souza Department of Natural Science, College of Agricultural Sciences, UNESP – São Paulo State University, Botucatu 18610-307, Brazil

Kelley Spence Department of Forest Biomaterials, North Carolina State University Campus, PO Box 8005, Raleigh, NC 27695-8005, USA

Ramjee Subramanian Omya Development AG, Baslerstrasse 42, 4665, Oftringen, Switzerland

Hina Tarannum CSIR-Central Building Research Institute, Roorkee 247 667, India

Sabu Thomas School of Chemical Sciences, Mahatma Gandhi University, Kottayam, Kerala, India

S. Ch. Turmanova Department of Material Science, Assen Zlatarov University, 8010, Burgas, Bulgaria

Chad Ulven Department of Mechanical Engineering and Applied Mechanics, North Dakota State University, 103 Dolve Hall, Fargo, ND 58105, USA

V.K. Varshney Chemistry Division, Forest Research Institute, Dehra Dun 248 006, India

L.T. Vlaev Department of Physical Chemistry, Assen Zlatarov University, 8010 Burgas, Bulgaria

Paul Wambua Department of Manufacturing, Industrial and Textile Engineering, Moi University, PO Box 3900, Eldoret 30100, Kenya

Santosh D. Wanjale Polymer Science and Engineering Division, National Chemical Laboratory, Dr. Homi Bhabha Road, Pashan, Pune 411008, India

Malgorzata Zimniewska Institute of Natural Fibres and Medicinal Plants, Wojska Polskiego 71b, 60-630, Poznan, Poland

Part I
Cellulose Fibers and Nanofibers

Chapter 1

Natural Fibres: Structure, Properties and Applications

S. Thomas, S.A. Paul, L.A. Pothan, and B. Deepa

Abstract This chapter deals with the structure, properties and applications of natural fibres. Extraction methods of Natural Fibres from different sources have been discussed in detail. Natural fibres have the special advantage of high specific strength and sustainability, which make them ideal candidates for reinforcement in various polymeric matrices. Natural fibres find application in various fields like construction, automobile industry and also in soil conservation. It is the main source of cellulose, an eminent representative of nanomaterial. Extractions of cellulose from plant-based fibres are discussed in detail. Various methods used for characterization of cellulose nanofibres and advantages of these nanofibres have also been dealt with.

Keywords Animal fibre · Cellulose · Nanofibre · Plant fibre

Contents

1.1	Introduction	4
1.2	Natural Fibres	5
1.2.1	Animal Fibres and Their General Structure	5
1.2.2	Plant Fibres and Their General Structure	6
1.2.3	Processing Techniques for Obtaining Natural Fibres	9
1.2.4	Chemical Composition of Plant Fibres	11
1.2.5	Cellulose from Plant Fibres	13
1.2.6	Surface Characteristics of Various Plant Fibres	15
1.2.7	Applications of Natural Fibres	24
1.3	Nanofibres from Natural Fibres	26
1.3.1	Cellulose as a Nanostructured Polymer	27
1.3.2	Extraction Methods for Obtaining Nanocellulose from Natural Fibres	27
1.3.3	Characterisation Techniques for Nanofibres	28

S. Thomas (✉)

School of Chemical Sciences, Mahatma Gandhi University, Kottayam, Kerala, India
e-mail: sabupolymer@yahoo.com; sabuchathukulam@yahoo.co.uk

1.4 Conclusion	36
References	37

1.1 Introduction

The growing ecological, social and economic awareness, high rate of depletion of petroleum resources, concepts of sustainability and new environmental regulations have stimulated the search for green materials compatible with the environment. The waste disposal problems, as well as strong European regulations and criteria for cleaner and safer environment, have directed a great part of the scientific research to eco-composite materials that can be easily degraded or bio-assimilated. The world-wide availability of natural fibres and other abundantly accessible agrowaste is responsible for the new interest in research in sustainable technology [1, 2]. Bio-resources obtained from agricultural-related industries have received much attention, because they can potentially serve as key components of biocomposites. The possibilities of using all the components of the fibre crop provide wide ranging opportunities both in up and down stream processing for developing new applications in packaging, building, automotive, aerospace, marine, electronics, leisure and household [3]. Agricultural crop residues such as cereal straw, corn stalk, cotton, bagasse and grass, which are produced in billions of tonnes around the world, represent an abundant, inexpensive and readily available source of lignocellulosic biomass. Among these enormous amounts of agricultural residues, only a minor quantity of residues is reserved as animal feed or household fuel and a major portion of the straw is burned in the field, creating environmental pollution. The exploration of these inexpensive agricultural residues as bio resource for making industrial products will open new avenues for the utilisation of agricultural residues by reducing the need for disposal and environmental deterioration through pollution, fire and pests and at the same time add value to the creation of rural agricultural-based economy [4].

Most of the natural fibres are lighter due to their favourable density in comparison with other synthetic fibres and metallic materials. This attribute in combination with their excellent mechanical properties are beneficial, where stronger and lighter materials are required especially in transportation application where energy efficiency is influenced by the weight of the fast moving mass. The physical and chemical morphology of natural fibres, their cell wall growth, patterns and thickness, dimensions and shape of the cells, cross-sectional shapes, distinctiveness of lumens, etc., besides their chemical compositions, influence the properties of the fibres [5]. These fibres will also provide important opportunities to improve people's standard of living by helping generate additional employment, particularly in the rural sector. Accordingly, many countries that have these natural sources has started to conduct R&D efforts with lignocellulosic fibres, seeking to take advantage of their potential social advantages.

1.2 Natural Fibres

1.2.1 *Animal Fibres and Their General Structure*

1.2.1.1 Silk Fibre

Silks are protein materials produced by a wide range of insect and spider species. They are used for applications requiring high-performance fibres. Silk is produced by insects and arachnids to make structures such as webs, cocoons and nests. Silk from silkworm cocoons (of the moth *Bombyx mori*) has been used by mankind to make fabrics, because it has excellent mechanical properties, particularly its high tensile modulus [6]. The silk of the domesticated silkworm, *B. mori*, has been used as a suture biomaterial for centuries, and in recent years farmed silkworm silk has also been reprocessed into forms such as films, gels and sponges for medical applications. Spider silks also have outstanding strength, stiffness and toughness that, weight for weight, are unrivalled by synthetic fibres.

Structural proteins are commonly fibrous proteins such as keratin, collagen and elastin. Skin, bone, hair and silk all depend on such proteins for their structural properties. The structures (several types have been recorded) all consist of silk based on anti-parallel sheets of the fibrous protein fibroin. Long stretches of the polypeptide chain consist of sequences (Glycine- Sericin- Glycine-Alanine-Glycine-Alanine), where the symbols indicate different amino acids. The Gly chains extend from one surface of the-sheets and the Ser and Ala from the other, forming an alternating layered structure. The orientation of the chains along the sheet underpins the tensile strength of silk, while the weak forces between sheets ensure that silk fibres are flexible. Silk fibres have a complex hierarchical structure, in which a fibroin core is surrounded by a skin of the protein sericin. Within the core, termed bave, there are crystalline regions containing layered sheets and amorphous regions that may contain isolated sheets [7–9]. Vintage X-ray fibre diffraction work demonstrated that honeybee silk contains α -helical proteins assembled into a higher order coiled coil conformation [10]. A more detailed study indicated a tetrameric coiled coil. As the four silk proteins of honeybees are expressed at approximately equal levels, they likely correspond to the four strands of the coiled coil structure [11].

1.2.1.2 Agriculturally Derived Proteins

Other than animals, agricultural materials can also be considered as an ideal source of protein and are prospective materials for the preparation of fibres. Fibres of regenerated protein were produced commercially in between 1930 and 1950, and by today's standards, they would be considered natural, sustainable, renewable, and biodegradable. Casein from milk was used by M/s Courtaulds Ltd. to make Fibrolane and by M/s Snia to make Lanital; groundnut (peanut) protein was used by

M/s ICI to make Ardil; Vicara was made by the M/s Virginia–Carolina Chemical Corporation from zein (corn protein); and soybean protein fibre was developed by the Ford Motor Company [12]. The regenerated fibres had several qualities typical of the main protein fibres, wool and silk; they were soft, with excellent drape and high moisture absorbency. They could be processed on conventional textile machinery and coloured with conventional dyes. Superior to wool in some regards, they did not prickle, pill or shrink. They could be produced as staple or filament, crimped or straight, with control over diameter, and dope-dyed if required. Regenerated protein fibres are potentially environmentally sustainable, renewable and biodegradable. Two protein sources, feather keratin and wheat gluten, have been considered for their suitability to make an eco-friendly regenerated fibre. Both appear to be viable, although low wet strength may make it problematic. The inclusion of nanoparticles and use of cross-linking technologies offer the potential to improve mechanical strength to make them fit for use in apparel or technical textile applications. Wool is similar to feather in some regards, both keratins being highly cross-linked, although wool proteins are heterogeneous with a generally higher molecular weight (10–55 kDa) and higher cysteine content.

1.2.2 Plant Fibres and Their General Structure

1.2.2.1 Different Types of Plant Fibres

Fibres obtained from the various parts of the plants are known as plant fibres. Plant fibres include bast, leaf and seed/fruit fibres. Bast consists of a wood core surrounded by a stem. Within the stem, there are a number of fibre bundles, each containing individual fibre cells or filaments. Examples include flax, hemp, jute, kenaf and ramie. Leaf fibres such as sisal, abaca, banana and henequen are coarser than bast fibres. Cotton is the most common seed fibre. Other examples include coir and oil palm. Other source of lignocellulosics can be from agricultural residues such as rice hulls from a rice processing plant, sun flower seed hulls from an oil processing unit and bagasse from a sugar mill. The properties of natural fibres vary considerably depending on the fibre diameter, structure, degree of polymerization, crystal structure and source, whether the fibres are taken from the plant stem, leaf or seed, and on the growing conditions [13–15]. List of important plant fibres are given in Table 1.1.

1.2.2.2 General Structure of Plant Fibres

A single or elementary plant fibre is a single cell typically of a length from 1 to 50 mm and a diameter of around 10–50 μm . Plant fibres are like microscopic tubes, i.e., cell walls surrounding the central lumen. The lumen contributes to the water

Table 1.1 List of important plant fibres

Fibre source	Origin
Abaca	Leaf
Bagasse	Grass
Bamboo	Grass
Banana	Stem
Coir	Fruit
Cotton	Seed
Curaua	Leaf
Date palm	Leaf
Flax	Stem
Hemp	Stem
Henequen	Leaf
Isora	Stem
Jute	Stem
Kapok	Fruit
Kenaf	Stem
Oil palm	Fruit
Piassava	Leaf
Pineapple	Leaf
Ramie	Stem
Sisal	Leaf
Sponge gourd	Fruit
Straw (Cereal)	Stalk
Sun hemp	Stem
Wood	Stem

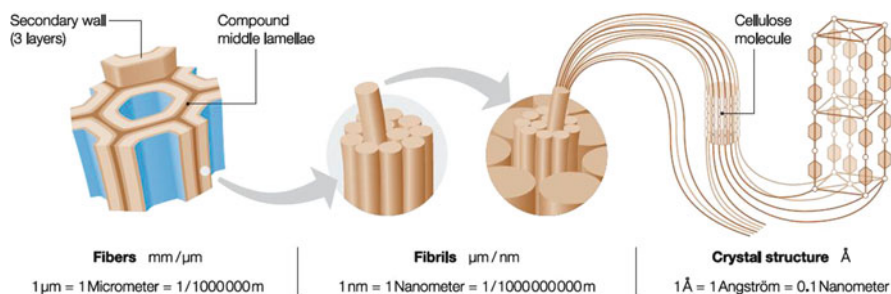


Fig. 1.1 Arrangement of microfibrils and cellulose in the plant cell wall [Zimmermann et al. [17]]

uptake behaviour of plant fibres [16]. The fibre consists of several cell walls. These cell walls are formed from oriented reinforcing semi-crystalline cellulose microfibrils embedded in a hemicellulose–lignin matrix of varying composition. Such microfibrils have typically a diameter of about 10–30 nm and are made up of 30–100 cellulose molecules in extended chain conformation and provide mechanical strength to the fibre. Figure 1.1 shows the arrangement of fibrils, microfibrils and cellulose in the cell walls of a plant fibre.

The hemicellulose molecules of the matrix phase in a cell wall are hydrogen bonded to cellulose and act as a cementing matrix between the cellulose microfibrils, forming the cellulose/hemicellulose network, which is thought to be the main structural component of the fibre cell. The hydrophobic lignins on the other hand act as a cementing agent and increase the stiffness of the cellulose/hemicellulose composite.

The cell walls are divided into two sections, the primary cell wall containing a loose irregular net work of cellulose microfibrils, which are closely packed, and the secondary wall. The secondary wall is composed of three separate and distant layers – S_1 (outer layer), S_2 (middle layer) and S_3 (inner layer). S_2 layer is the thickest and the most important in determining mechanical properties [16]. Schematic representation of the fine structure of a lignocellulosic fibre is presented in Fig. 1.2. These fibre cell walls differ in their composition, i.e., the ratio between cellulose and lignin/hemicellulose and in the orientation or spiral angle of the cellulose microfibrils [18]. The spiral angle is the angle that the helical spirals of cellulose microfibrils form with the fibre axis. The spiral angle or the microfibrillar angle varies from one plant fibre to another. The mechanical properties of the fibre are dependent on the cellulose content, microfibrillar angle and the degree of polymerization. Degree of polymerization also depends on the part of the plant from which fibres are obtained. Fibres with higher cellulose content, higher degree of polymerization and a lower microfibrillar angle exhibit higher tensile strength and modulus.

Cellulosic fibres have amorphous and crystalline domains with a high degree of organisation. The crystallinity rate depends on the origin of the material. Cotton, flax, ramie, sisal and banana have high degrees of crystallinity (65–70%), but the crystallinity of regenerated cellulose is only 35–40%. Progressive elimination of the less organised parts leads to fibrils with ever-increasing crystallinity, until almost 100%, leading to whiskers. Crystallinity of cellulose results partially from hydrogen bonding between the cellulosic chains, but some hydrogen bonding also

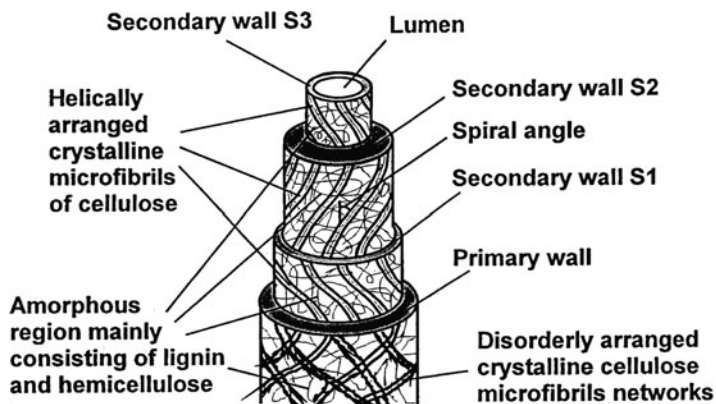


Fig. 1.2 Structural constitution of natural vegetable fibre cell [18]

occurs in the amorphous phase, although its organisation is low [18]. In cellulose, there are many hydroxyl groups available for interaction with water by hydrogen bonding. They interact with water not only at the surface but also in the bulk. The quantity of water absorbed depends on the relative humidity of the confined atmosphere with which the fibre is in equilibrium. The sorption isotherm of cellulosic material depends on the purity of cellulose and the degree of crystallinity. All –OH groups in the amorphous phase are accessible to water, whereas only a small amount of water interacts with the surface –OH groups of the crystalline phase. The main components of natural fibres are cellulose (α -cellulose), hemicellulose, lignin, pectins and waxes.

1.2.3 Processing Techniques for Obtaining Natural Fibres

Extraction of fibres from the plant stems is achieved by various methods. Retting is a process of controlled degradation of the plant stem to allow the fibre to be separated from the woody core and thereby improving the ease of extraction of the fibres from the plant stems [19]. The retting of the straw is caused with time by exposure to moisture and, sometimes, by the help of a mechanical decorticator. Most available methods of retting rely on the biological activity of microorganism, bacteria and fungi from the environment to degrade the pectic polysaccharides from the non-fibre tissue and, thereby, separate the fibre bundles. Microbial/enzymatic retting is one of the widely used techniques to extract good quality cellulosic fibres from the agricultural plants such as hemp, flax and jute [5, 20, 21]. Sain and Panthapulakkal [4] used fungal retting of wheat straw before extracting the fibres. They explored the use of a fungus, which was isolated from the bark of an elm tree, for retting of wheat straw. They mechanically defibrillated wheat straw using a laboratory-scale mechanical refiner before and after fungal retting. The enzymes produced by the fungus or bacteria weaken or remove the pectinic glue that bonds the fibre bundles together and release the cellulosic fibres from the fibre bundle. The fibre separation and extraction process has a major impact on fibre yield and final fibre quality. It influences the structure, chemical composition and properties of the fibres. Retting procedures can be divided into biological, mechanical, chemical and physical fibre separation process.

1.2.3.1 Biological Retting

Biological retting includes natural and artificial retting. Natural retting comprises dew or field retting and cold water retting. Dew or field retting [22] is the most commonly applied retting process in regions that have appropriate moisture and temperature ranges. After being mown, the crops should remain on the fields until the microorganisms have separated the fibres from the cortex and xylem.

After retting, the stalk is dried and baled. The retting process has to be stopped at the right time to prevent over-retting. Under-retting results in fibres that are difficult to separate and to further process. Therefore, it is necessary to monitor the retting process to ensure the quality of the fibres. A modified field-retting process is the thermally induced stand-retting process [23].

Cold water retting [24] utilises anaerobic bacteria that breakdown the pectin of plant straw bundles submerged in huge water tanks, ponds, hamlets or rivers and vats. The process takes between 7 and 14 days and depends on the water type, temperature of the retting water and any bacterial inoculum. Even though the process produces high quality fibres, environmental pollution is high due to unacceptable organic fermentation waste waters.

Artificial retting [25] involves warm-water or canal retting and produces homogeneous and clean fibres of high quality in 3–5 days. Plant bundles are soaked in warm water tanks. After sufficient retting, the bast fibres are separated from the woody parts. The sheaves or hurds are loosened and extracted from the raw fibres in a breaking or scotching process.

1.2.3.2 Mechanical or Green Retting

It is a much simpler and more cost-effective alternative to separate the bast fibre from the plant straw [26]. The raw material for this procedure is either field dried or slightly retted plant straw. The bast fibres are separated from the woody part by mechanical means. Weather-dependent variations of fibre quality are eliminated. However, the produced green fibres are much coarser and less fine as compared to dew or water retted fibres.

1.2.3.3 Physical Retting

Physical retting [27, 28] includes ultrasound and steam explosion method. In ultrasound retting, the stems obtained after the harvest are broken and washed. Slightly crushed stems are immersed in hot water bath that contains small amounts of alkali and surfactants and then exposed to high-intense ultrasound. This continuous process separates the hurds from the fibre. The steam explosion method represents another suitable alternative to the traditional field-retting procedure. Under pressure and increased temperature, steam and additives penetrates the fibre interspaces of the bast fibre bundles. The subsequent sudden relaxation of the steam leads to an effective breaking up of the bast fibre composite, which results in an extensive decomposition into fine fibres. Another alternative for producing high and consistent quality fibres is enzyme retting. This retting procedure uses pectin-degrading enzymes to separate the fibres from the woody tissue. The use of enzymes promotes the controlled retting of the fibre crops through the selective biodegradation of the pectinaceous substances. The enzyme activity increases with

increasing temperature up to an optimum temperature above which the enzyme starts to denature.

1.2.3.4 Chemical and Surfactant Retting

Chemical and surfactant retting [29] refers to all retting process in which the fibre crop's straw is submerged in heated tanks containing water solutions of sulphuric acid, chlorinated lime, sodium or potassium hydroxide and soda ash to dissolve the pectin component. The use of surface active agents in retting allows the simple removal of unwanted non-cellulosic components adhering to the fibres by dispersion and emulsion-forming process. Chemical retting produces high quality fibres but adds costs to the final product. An investigation of the extraction procedures of vakka (*Roystonea regia*), date and bamboo fibres was reported by Murali and Mohana [19]. In their studies, the manually decorticated bamboo fibrous strips were extracted by means of a chemical process of decomposition called degumming, in which the gummy materials and the pectin are removed. The chemical extraction process yields about 33% of fibre on weight basis.

1.2.4 Chemical Composition of Plant Fibres

The chemical composition as well as the morphological microstructure of vegetable fibres is extremely complex due to the hierarchical organisation of the different compounds present at various compositions. Depending on the type of fibre, the chemical composition of natural fibres varies. Primarily, fibres contain cellulose, hemicellulose and lignin. The property of each constituent contributes to the overall properties of the fibre.

1.2.4.1 Cellulose

Cellulose forms the basic material of all plant fibres. It is generally accepted that cellulose is a linear condensation polymer consisting of D-anhydroglucopyranose units joined together by β -1,4-glycosidic linkages. Cellulose is thus a 1,4- β -D-glucan [15]. The molecular structure of cellulose, which is responsible for its supramolecular structure determines many of its chemical and physical properties. In the fully extended molecule, the adjacent chain units are oriented by their mean planes at the angle of 180° to each other. Thus, the repeating unit in cellulose is the anhydrocellobiose unit, and the number of repeating units per molecule is half the DP. This may be as high as 14,000 in native cellulose.

The mechanical properties of natural fibres depend on the cellulose type. Each type of cellulose has its own cell geometry, and the geometrical conditions determine the mechanical properties. Solid cellulose forms a microcrystalline structure

with regions of high order, i.e., crystalline regions, and regions of low order, i.e., amorphous regions. Cellulose is also formed of slender rod like crystalline microfibrils. The crystal nature (monoclinic sphenodic) of naturally occurring cellulose is known as cellulose I. Cellulose is resistant to strong alkali (17.5 wt%) but is easily hydrolyzed by acid to water-soluble sugars. Cellulose is relatively resistant to oxidising agents.

1.2.4.2 Hemicelluloses

Hemicellulose is not a form of cellulose at all. It comprises a group of polysaccharides (excluding pectin) that remains associated with the cellulose after lignin has been removed. The hemicellulose differs from cellulose in three important aspects [15]. In the first place, they contain several different sugar units, whereas cellulose contains only 1,4- β -D-glucopyranose units. Secondly, they exhibit a considerable degree of chain branching, whereas cellulose is strictly a linear polymer. Thirdly, the degree of polymerization of native cellulose is 10–100 times higher than that of hemicellulose. Unlike cellulose, the constituents of hemicellulose differ from plant to plant [15, 30].

1.2.4.3 Lignins

Lignins are complex hydrocarbon polymers with both aliphatic and aromatic constituents [31, 32]. Their chief monomer units are various ring-substituted phenyl propanes linked together in ways that are still not fully understood. Their mechanical properties are lower than those of cellulose. Lignin is totally amorphous and hydrophobic in nature. It is the compound that gives rigidity to the plants. Lignin is considered to be a thermoplastic polymer, exhibiting a glass transition temperature of around 90°C and melting temperature of around 170°C. It is not hydrolyzed by acids, but soluble in hot alkali, readily oxidised and easily condensable with phenol [33].

1.2.4.4 Pectins and Waxes

Pectin is a collective name for heteropolysaccharides, which consist essentially of polygalacturon acid. Pectin is soluble in water only after a partial neutralisation with alkali or ammonium hydroxide. It provides flexibility to plants. Waxes make up the last part of fibres and they consist of different types of alcohols, which are insoluble in water as well as in several acids.

1.2.5 Cellulose from Plant Fibres

A single fibre of all plant-based natural fibres consists of several cells. These cells are formed out of cellulose-based crystalline microfibrils, which are connected to a complete layer by amorphous lignin and hemicellulose. Multiples of such cellulose–lignin–hemicellulose layers in one primary and three secondary cell walls stick together to form a multiple layer composite. The fibre strength increases with increasing cellulose content and decreasing spiral angle with respect to fibre axis.

Cellulose is found not to be uniformly crystalline. However, the ordered regions are extensively distributed throughout the material, and these regions are called crystallites. The threadlike entity, which arises from the linear association of these components, is called the microfibril. It forms the basic structural unit of the plant cell wall. These microfibrils are found to be 10–30 nm wide, less than this in width, indefinitely long containing 2–30,000 cellulose molecules in cross section. Their structure consists of predominantly crystalline cellulose core. Individual cellulose nanocrystals (Fig. 1.3) are produced by breaking down the cellulose fibres and isolating the crystalline regions [34]. These are covered with a sheath of para-crystalline polyglucosan material surrounded by hemicelluloses [35].

In most natural fibres, these microfibrils orient themselves at an angle to the fibre axis called the microfibril angle. The ultimate mechanical properties of natural fibres are found to be dependent on the microfibrillar angle. Gassan et al. [36] have done calculations on the elastic properties of natural fibres. Cellulose exists in the plant cell wall in the form of thin threads with an indefinite length. Such threads are cellulose microfibrils, playing an important role in the chemical, physical and mechanical properties of plant fibres and wood. Microscopists' and crystallographers' studies have shown the green algae *Valonia* to be excellent material for the ultrastructural study of the cellulose microfibril [37]. A discrepancy in the size of the crystalline regions of cellulose, obtained by X-ray diffractometry and electron microscopy, led to differing concepts on the molecular organisation of microfibrils. David et al. [38] regarded the microfibril itself as being made up of a number of crystallites, each of which was separated by a para-crystalline region and later termed "elementary fibril". The term "elementary fibril" is therefore applied to the smallest cellulosic strand. Electron micrograph studies of the disintegrated microfibrils,

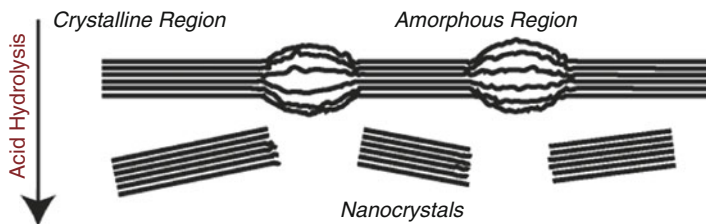


Fig. 1.3 Acid hydrolysis breaks down disordered (amorphous) regions and isolates nanocrystals [34]

showing the crystalline nature of cellulose microfibrils (Magnfn 100 nm) taken by diffraction contrast in the bright field mode, are given in Fig. 1.4. Reports on the characterisation and the make-up of the elementary fibrils and on their association while establishing the fibre structure – usually called fibrillar or fringed fibril structure are there in the literature [39]. According to this concept, the elementary fibril is formed by the association of many cellulose molecules, which are linked together in repeating lengths along their chains. In this way, a strand of elementary crystallites is held together by parts of the long molecules reaching from one crystallite to the next, through less ordered inter-linking regions. Molecular transition from one crystallite strand to an adjacent one is possible, in principle. Apparently, in natural fibres, this occurs only to a minor extent, whereas in man-made cellulosic fibres, such molecular transitions occur more frequently.

The internal cohesion within the elementary fibrils is established by the transition of the long cellulose chain molecules from crystallite to crystallite. The coherence of the fibrils in their secondary aggregation is given either by hydrogen bonds at close contact points or by diverging molecules. Access into this structure is given by large voids formed by the imperfect axial orientation of the fibrillar aggregates, interspaces of nanometre dimensions between the fibrils in the fibrillar aggregations and by the less ordered inter-linking regions between the crystallites within the elementary fibrils. Dufresne has reported on whiskers obtained from a variety of natural and living sources [40]. Cellulose microfibrils and cellulose whisker suspension were obtained from sugar beet root and from tunicin. Typical electron micrographs obtained from dilute suspensions of sugar beet are shown in Fig. 1.5. Individual microfibrils are almost 5 nm in width while their length is of a much higher value, leading to a practically infinite aspect ratio of this filler. They can be used as a reinforcing phase in a polymer matrix.



Fig. 1.4 Electron micrograph of the disintegrated microfibrils [37]

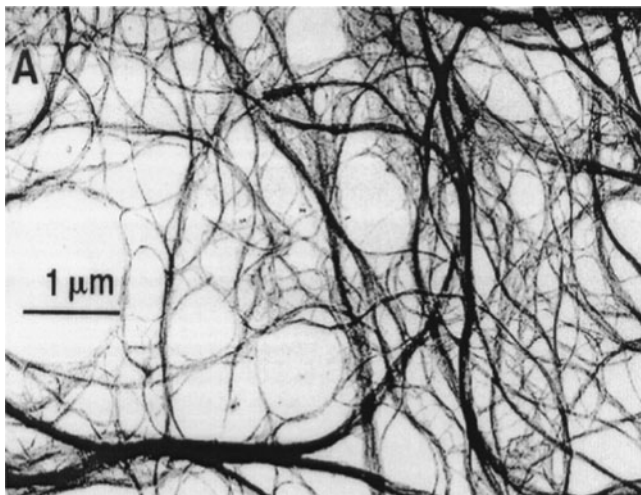


Fig. 1.5 Transmission electron micrograph of a dilute suspension of sugar beet cellulose [40]

1.2.6 Surface Characteristics of Various Plant Fibres

Many natural fibres have a hollow space (the lumen) as well as nodes at irregular distances that divide the fibre into individual cells. The surface of natural fibres is rough and uneven and provides good adhesion to the matrix in a composite structure. The compatibility of fibre surface with the interacting chemicals, such as resin, depends on the smoothness or roughness of the fibre. Rough surfaces increase the number of anchorage points, thus offering a good fibre-resin mechanical interlocking. The presence of waxy substances on the fibre surface contributes immensely to ineffective fibre to resin bonding and poor surface wetting. Also, the presence of free water and hydroxyl groups, especially in the amorphous regions, worsens the ability of plant fibres to develop adhesive characteristics with most binder materials.

Microscopic studies such as optical microscopy, scanning electron microscopy (SEM), transmission electron microscopy (TEM) and atomic force microscopy (AFM) can be used to study the morphology of fibre surface and can predict the extent of mechanical bonding at the interface. AFM is a useful technique to determine the surface roughness of fibres [41].

Morphology of Brazilian coconut fibres was studied by Tomczak et al. [42]. The morphological characterization of the fibres was conducted through an optical microscope and scanning electron microscope. The degree of crystallinity of the fibres was calculated from X-ray diffractograms. It was found that fibre consists of different types of regularly arranged cells, with a large lacuna at the centre of the fibre. Figure 1.6 shows the photomicrograph of transverse section of coir fibre. The cells are almost circular, similar to those reported for coir fibres of other countries. The X-ray diffraction spectrum of the coir fibres (Fig. 1.7) showed peak associated

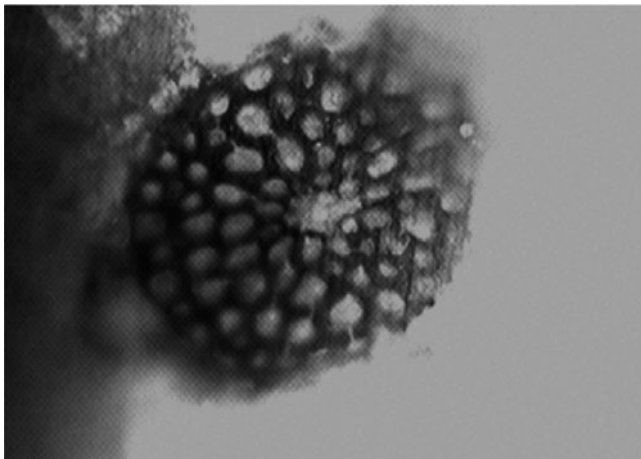


Fig. 1.6 Photomicrograph of transverse section of coir fibre [42]

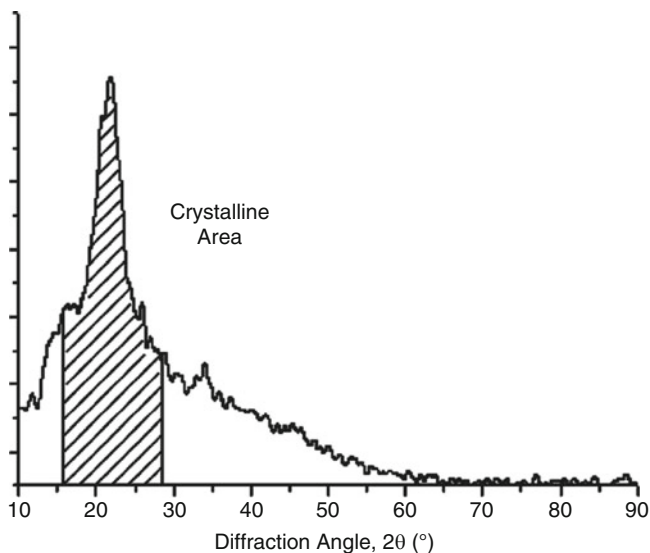


Fig. 1.7 X-ray spectrum of Brazilian coir fibres [42]

with the crystalline part at $2\theta = 22^\circ$. The crystallinity index of coir fibres calculated was 57%, and the microfibrillar angle was found to be 51° .

AFM characterization of the surface wettability of hemp fibre was reported by [41]. These images detailed the rough primary cell wall, which is characteristic of the hemp fibre. The fibres showed lower adhesion force and were presumably hydrophobic. Surface roughness averages of the fibre samples were measured to be between 10 and 20 nm on 1 mm^2 areas, which were significantly rougher than the

model surfaces used for the calibration, with surface roughness averages of 0.5–2 nm measured on 1 mm² areas. The AFM results were complimented by examination of the contact angle of the fibres. Morphology of hemp fibre surface detailing the rough primary cell wall is shown in (Fig. 1.8). Panels (a) and (b) shown in the above figure are deflection images taken at low and high magnifications, while (c) is a friction map taken from an area similar to that shown in (b), resolving fibres (f) embedded in an amorphous matrix (m). High contact angle was evident for hemp fibres, which showed its hydrophobicity (Fig. 1.9).

Bessadok et al. [43] studied the surface characteristics of agave fibres by means of microscopic analysis, infrared spectroscopy and surface energy. Cross-section of an Agave leaf fibre is shown in Fig. 1.10. Infrared spectroscopy revealed the presence of the major absorbance peaks reflecting the carbohydrate backbone of cellulose. The surface energy analysis showed that surface energy of the fibre was high due to the roughness of the fibre.

Fluorescent microscopic images of the fibre (Fig. 1.11) showed how the fibre was able to fix calcofluor, a fluorescent probe well-known to have high affinity with polysaccharides such as cellulose, hemicellulose and pectins. From the figure, it

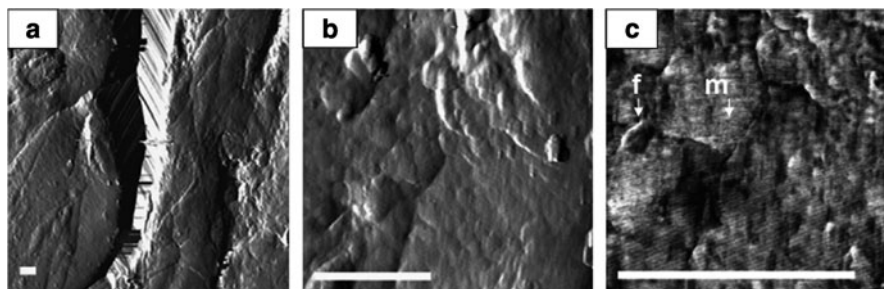


Fig. 1.8 Morphology of hemp fibre surface detailing the rough primary cell wall [41]

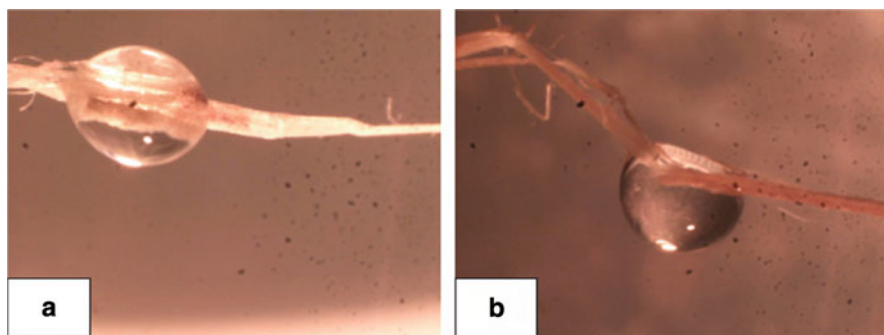


Fig. 1.9 Interaction of water with hemp fibre demonstrating the hydrophobic nature of hemp fibre [42]

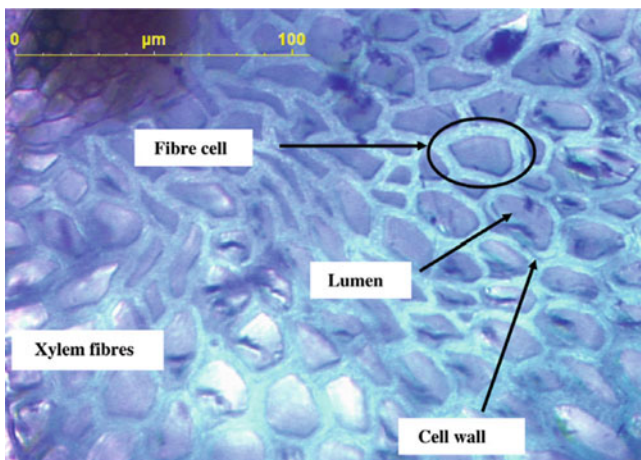


Fig. 1.10 Cross-section of an Agave leaf coloured with Carmin-green [43]

Agave (Untreated)

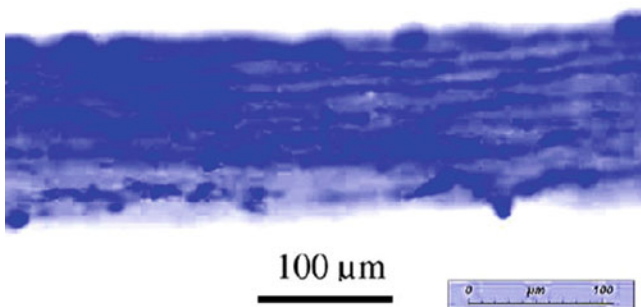


Fig. 1.11 Fluorescent microscopy images of agave fibre [43]

is clear that the fibre is sensitive to calcofluor due to the presence of cellulose, hemicellulose and pectic substances. The study was further supported by SEM studies. SEM studies revealed that agave fibres gathered in a bundle form and constituted spiral tracheids, well-known as water transport materials.

In an innovative study, nanoscale characterization of natural fibres using contact-resonance force microscopy (CR-FM) was reported by Sandeep et al. [44]. This method was used to evaluate the cell wall layers of natural fibres for studying the elastic properties of cell walls. The cell wall layer experiments involved samples collected from a 45-year-old red oak. The studies revealed that there is a thin region between the S1 and S2 layers with apparently lower modulus than that of other secondary layers. Figure 1.12 shows schematic representation of cell wall layers of wood fibre. Figure 1.13 shows images for the topography and indentation modulus. Contrasts in modulus between the compound middle lamellae (CML) and S1 and S2 layers are clearly visible. Mean values of the indentation

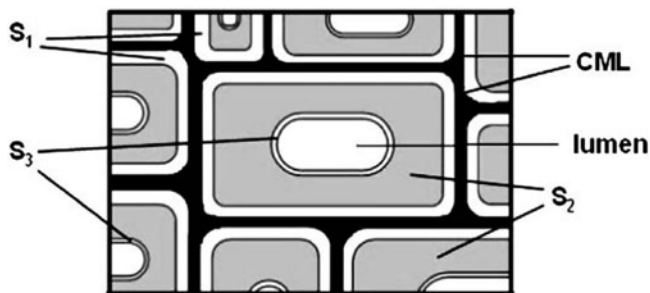


Fig. 1.12 Schematic representation of cell wall layers of wood fibre [44]

modulus for the CML and S1 and S2 layers were obtained from the area enclosed within the box plots, as shown in Fig. 1.13. The average values of indentation modulus obtained for different cell wall layers within a fibre were found to be 22.5–28.0 GPa, 17.9–20.2 GPa, and 15.0–15.5 GPa for the S2 and S1 layers and the CML, respectively. Characterization of natural fibre surfaces of kenaf, hemp and henequen were reported by Sgriccia et al. [45]. The ESEM images of hemp fibre showed the presence of interfibrillar material, hemicellulose and lignin. XPS studies revealed that hemp is more hydrophobic than kenaf as indicated by lower O/C ratio. XPS spectra also revealed that all fibres contained carbon and oxygen, while nitrogen, calcium, silicon and aluminium were detected in some samples. Cellulose, hemicellulose and pectin have an O/C ratio of 0.83 while lignin has a ratio of 0.35. Since the O/C of fibres is found to be less than 0.83, it was concluded that the fibre surface must have a greater proportion of lignin and waxes.

Morphological characterization of okra fibre was studied by Maria et al. [46]. Microscopic examinations of the cross section and longitudinal surface of okra fibres are depicted in Fig. 1.14a and b, respectively. Typically, the structure of an okra fibre consists of several elementary fibres (referred also to as ultimate fibres or cells) overlapped along the length of the fibres and bonded firmly together, by pectin and other non-cellulosic compounds that give strength to the bundle as a whole. However, the strength of the bundle structure is significantly lower than that of elementary cell. The region at the interface of two cells is termed middle lamella (Fig. 1.14a). In common terminology, the bundles of elementary fibres are referred to as technical fibres or single fibres. In longitudinal view, the fibres appear as in Fig. 1.14b, which shows the overlapping of the cells.

Furthermore, the presence of some impurities on the surface of the okra fibre can also be seen, and the fibres are cemented in non-cellulosic compounds. In particular, the cross-sectional shape of okra fibre shows a polygonal shape that varies notably from irregular shape to reasonably circular, as depicted in Fig. 1.15. Their diameter considerably vary in the range of about 40–180 μm . Furthermore, each ultimate cell is roughly polygonal in shape, with a central hole, or lumen like other natural plant fibres, as shown in Fig. 1.15. The cell wall thickness and lumen diameter vary typically between 1–10 μm and 0.1–20 μm , respectively. As a consequence of it,

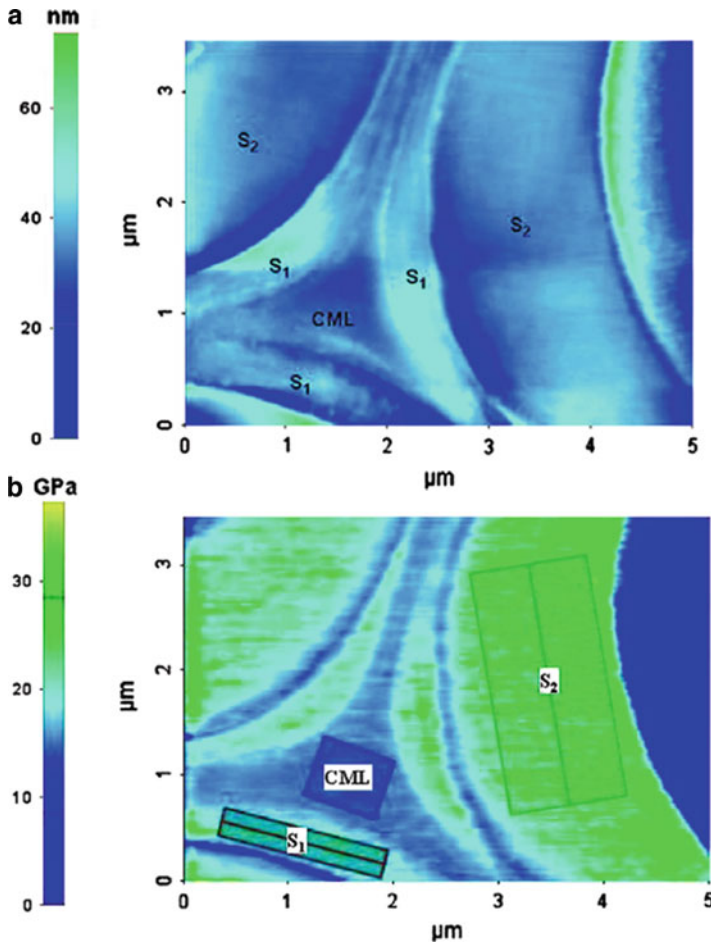


Fig. 1.13 Images of: (a) topography and (b) box plot analysis of indentation modulus image of various cell wall layers [44]

the considerable difference of the diameter values of the single fibre and lumen and their rough shape strongly affect mechanical and dimensional properties of okra fibres.

In another study, surface morphology of curaua fibres was reported by Spinacé et al. [47]. SEM studies revealed that curaua fibre has a smooth and compact surface, with no fibrillation. The X-ray diffractograms of curaua fibres show three peaks at $2\theta = 16; 22.6$ and 34.7° . These are characteristic of the crystal polymorph I of cellulose. For fibres with higher cellulose content, such as cotton or flax, two peaks around 16° are observed, but for curaua fibres, only one broad peak was observed due to the presence of amorphous materials like lignin, hemicelluloses and amorphous cellulose, which cover the two peaks. In an interesting study, the investigation of surface characterization of banana, sugarcane bagasse and sponge gourd fibres of Brazil was reported by Guimarães et al. [48]. It can be seen that the

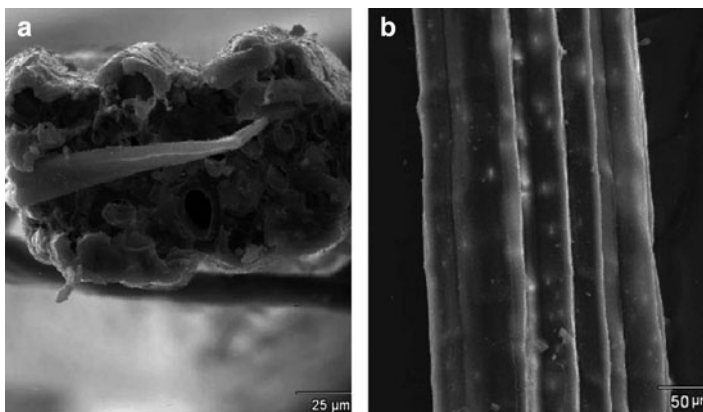


Fig. 1.14 SEM micrographs of (a) cross section and (b) longitudinal view of okra fibre [46]

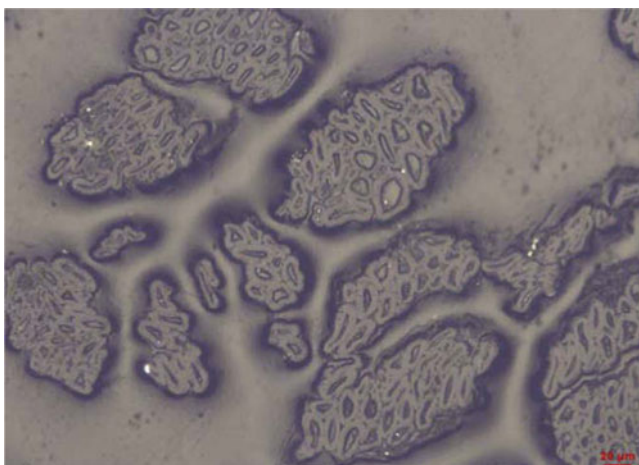


Fig. 1.15 Optical micrograph showing cross section of several okra fibres [46]

three fibres studied (Fig. 1.16) show variations in their structure, namely, different sizes, shape and arrangement of their cells as well as nature of lumen. Cells are non-spherical rather irregular in shape, and cell walls are thick in banana and sponge gourd fibres, while they are almost spherical, compactly arranged and thin walled in the case of bagasse fibre. The central lumen is elliptical (or nearly spherical) and of higher diameter in the case of bagasse fibre compared to other two fibres, which show very narrow and elongated lumen. At higher magnifications, all the fibres show helical winding of microfibrils attached to each other by a binding material (lignin). The interior of these microfibrils show longitudinal array in some cases. The lacuna is present in bagasse fibres, while it seems to be absent in other two fibres. X-ray diffraction patterns of the three fibres exhibited mainly cellulose type I

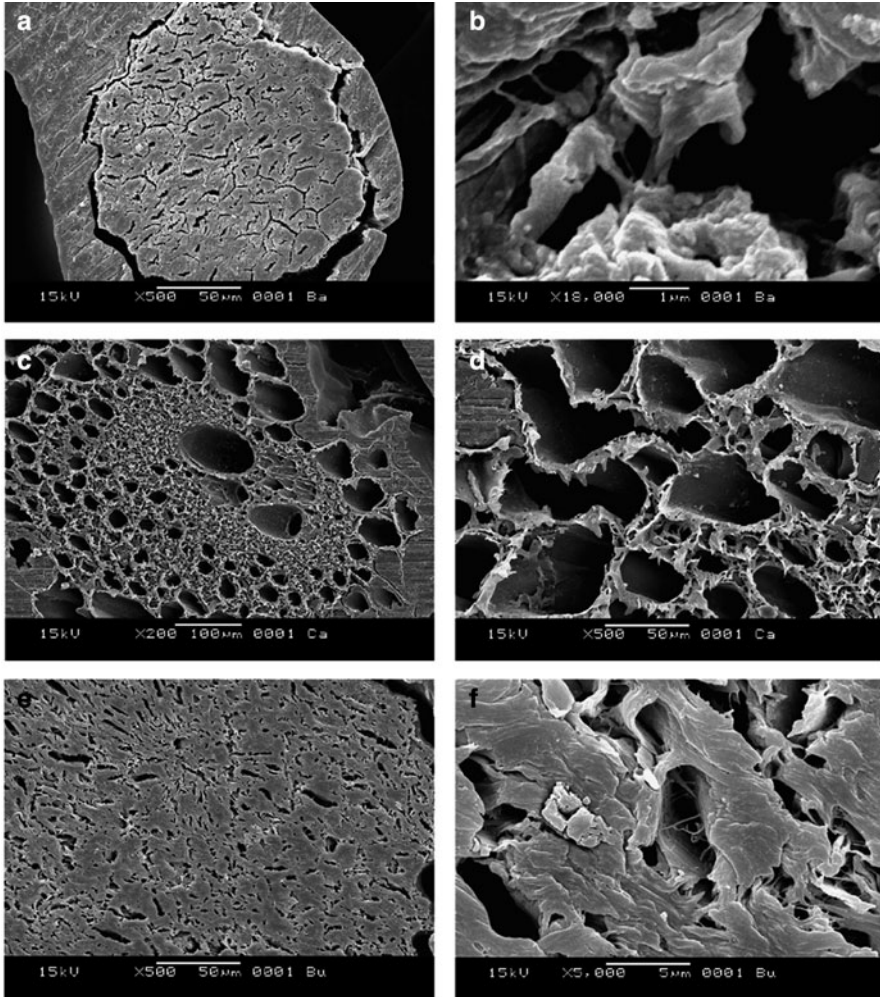


Fig. 1.16 Scanning electron micrographs of cross-sections of fibres (a and b) banana [a: 500 \times ; b: 18,000 \times]; (c and d) bagasse [c: 200 \times ; d: 500 \times]; and (e and f) sponge gourd [e: 500 \times ; b: 5000 \times] [48]

structure with the crystallinity indices of 39%, 48% and 50% for banana, bagasse and sponge gourd fibres, respectively.

In a novel study, Zou et al. [49] reported nanoscale structural and mechanical characterization of the cell wall of bamboo fibres. They reported the discovery of cobble-like polygonal cellulose nanograins with a diameter of 21–198 nm in the cell wall of bamboo fibres. These nanograins are basic building blocks that are used to construct individual bamboo fibres. Nanoscale mechanical tests were carried out on individual fibre cell walls by nanoindentation. It was found that the nanograin structured bamboo fibres are not brittle in nature but somewhat ductile. Figure 1.17a

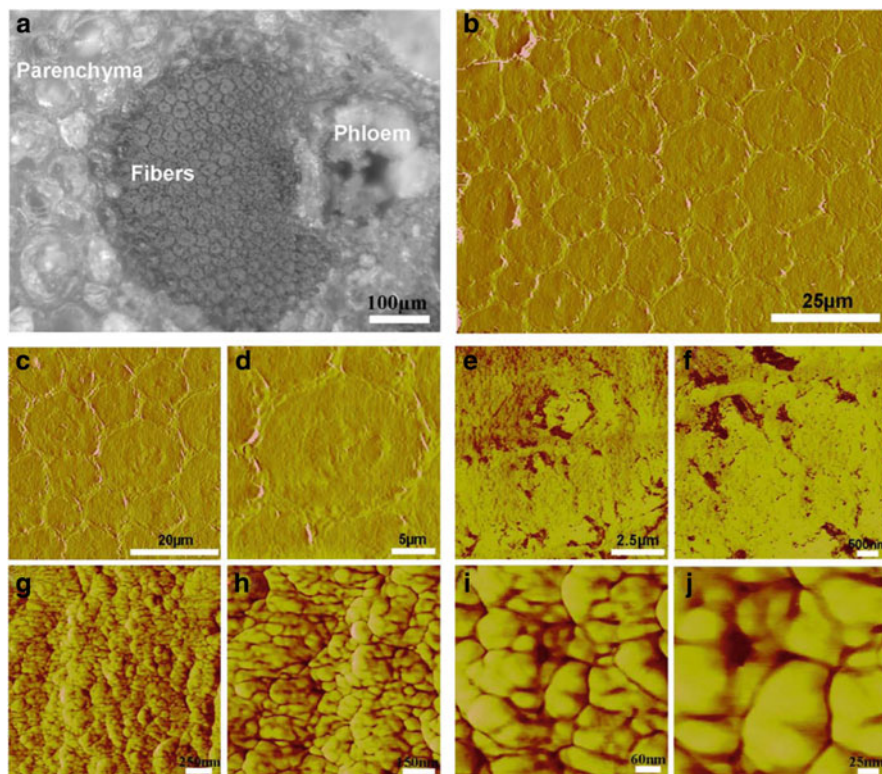


Fig. 1.17 Cross-sectional micrographs of a phloem fibre cap in a vascular bundle of a bamboo culm. (a) Optical micrograph of a fibre cap. (b)–(d) AFM phase images of bamboo fibres. (e)–(j) AFM phase images of the nanoscale structure in the fibre cell wall [49]

shows a representative optical image of the cross-section of bamboo fibres. It can be seen that a fibre cap with bundles of fibres is embedded among ground parenchyma (Pa) cells with connection to a phloem (Ph). AFM observations (Fig. 1.17b–d) show that these fibres are approximately 5–20 μm in diameter and densely packed within the cap.

Surface characterization of wheat straw fibres using X-ray photoelectron spectroscopy (XPS) was reported by Sain and Panthapulakkal [4]. Elemental surface composition and oxygen to carbon ratio (O/C) of the fibres illustrated that there is more lignin-type surface structure for the fibres. However, slightly higher ratio of oxygen to carbon in the retted fibre indicated a more carbohydrate-rich fibre than the un-retted fibre. The surface chemistry and morphology of spruce (*Picea abies*) mechanical pulps were investigated by Electron spectroscopy for chemical analysis (ESCA) and AFM [50]. As determined by ESCA, the content of lignin was slightly higher on the pulp surface than in the whole pulp. The AFM studies showed that the surfaces of mechanical pulp fibres are very heterogeneous, i.e., different cell wall layers are exposed along the fibre surface.

1.2.7 Applications of Natural Fibres

1.2.7.1 Natural Fibre-Based Composites

Natural fibres possess sufficient strength and stiffness but are difficult to use in load bearing applications by themselves because of their fibrous structure. Most plastics themselves are not suitable for load bearing applications due to their lack of sufficient strength, stiffness and dimensional stability [51]. In natural fibre reinforced composites, the fibres serve as reinforcement by giving strength and stiffness to the structure while the plastic matrix serve as the adhesive to hold the fibres in place so that suitable structural components can be made. The matrix for the natural fibres includes thermosets, thermoplastics and rubber. Different plant fibres and wood fibres are found to be interesting reinforcements for rubber, thermoplastics and thermosets [52–58].

In recent years, a new class of fully biodegradable “green” composites [59–63] have been made by combining natural fibres with biodegradable resins. The major attraction of green composites is that they are fully degradable and sustainable, that is, they are truly “green”. Green composites may be used effectively in many applications with short lifecycles or products intended for one-time or short-term use before disposal. A number of natural biodegradable matrices are also available for use in such green composites. Some of them are polysaccharides (starch, cellulose, chitin), proteins (casein, albumin, fibrogen, silks), polyesters (polyhydroxy alkanates) and other polymers, which include lignin, lipids, natural rubber and shellac [64–66]. These natural biodegradable polymers show a range of properties and can compete with non-biodegradable polymers in different industrial field.

To fabricate advanced green composites having high strength, Netravali et al. [67] used cellulose fibres spun using liquid crystalline (LC) solutions prepared by dissolving cellulose in phosphoric acid. The dry-jet wet spinning technique similar to what is used to spin aramid fibres such as Kevlar was used in spinning these fibres. The strengths of these LC cellulose fibres were in the range of 1,700 MPa, which is by far the highest strength achieved for cellulose-based fibres. In another study, to make advanced composites, Huang and Netravali [68] developed soy protein concentrate-based resins that were modified using a cross-linking polycarboxylic acid to form interpenetrating network-like resin systems with excellent mechanical properties.

1.2.7.2 Natural Fibres in Automobiles

The automotive industry is the prime driver of “green composites” because the industry is faced with issues for which green materials offer a solution [69]. Many components for the automotive sector are now made from natural fibre composite materials [70]. Natural fibres have intrinsic properties like mechanical strength, low weight and low cost, ecological sustainability, low energy requirements for

production, end of life disposal and carbon dioxide neutrality – that have made them particularly attractive to the automobile industry. In Europe, car makers are using mats made from abaca, flax and hemp in press-moulded thermoplastic panels for door liners, parcel shelves, seat backs, engine shields and headrests. Daimler Chrysler, already a major user of natural fibre composites in the interior trim components such as dash boards and door panels using polypropylene and natural fibres, has increased its research and development investment in flax/polyester composite for exterior or semi-exterior applications [70, 71].

For consumers, natural fibre composites in automobiles provide better thermal and acoustic insulation than fibre glass and reduce irritation of the skin and respiratory system. The low density of plant fibres also reduces vehicle weight, which cuts fuel consumption [72]. Alves et al. [73] studied the life cycle assessment (LCA) analysis of the replacement of glass fibres by jute fibres as reinforcement of composite materials to produce automotive structural components in the structural frontal bonnet of an off-road vehicle (Buggy).

1.2.7.3 Natural Fibres in Construction

Natural fibre composites offer vast opportunities for an increasing role as alternate materials, especially wood substitutes in the construction market [74]. Various natural fibre-based composites products such as laminates, panels, partitions, door frames, shutters, and roofing have been produced as an alternative to existing wood materials. Production of jute pultruded door frames, coir/cement roofing sheets, sisal/glass fibre-epoxy shutting plate and sisal/polyester roofing sheets were reported by Singh and Gupta [74]. Composite doors can be made by bonding the jute/sisal laminate face sheets with rigid foam cores [75]. Prospects for natural fibre-reinforced concretes in construction application were studied by Aziz et al. [76]. The studies revealed that natural fibre-reinforced concrete products like sheets (both plain and corrugated) and boards are light in weight and are ideal for use in roofing, ceiling and walling for the construction of low cost houses. Performance of “Agave lecheguilla” natural fibre in Portland cement composites exposed to severe environment conditions was reported by Juárez et al. [77]. In another study, fracture and fatigue of natural fibre-reinforced cementitious composites was reported by Savastano et al. [78]. They enumerated the results of an experimental study of resistance-curve behaviour and fatigue crack growth in cementitious matrices reinforced with eco-friendly natural fibres. Study of window frame fabrication by injection moulding process was carried out by Rahman et al. [79]. Rice husk filled high-density polyethylene was used as the raw material. Solid and hollow designs were created to compare the pros and cons of each design. The investigations were carried out on flowing, packing, cooling and costing of injection-moulded window frame. From the analysis, they concluded that window frame with hollow design is preferable, since hollow design has the advantage of filling, packing, and cooling properties. The hollow design also costs less than solid design of window frame. However, high injection pressure and clamping tonnage are unfavourable for hollow design.

Durability of compression-moulded sisal fibre reinforced mortar laminates were reported by Toledo et al. [80].

1.2.7.4 Natural Fibres in Soil Conservation

Natural fibres possess a distinctive characteristic, which makes them excellent materials for soil conservation. Coir fibre has very good application in erosion control markets for landscaping. The mesh of woven coir matting acts as miniature dams and prevents the seeds from washing away by rain and wind and facilitates the growth [81]. Geotextiles are promising new outlet for natural fibre producers. Originally developed in the Netherlands for the construction of dykes, geotextile nets made from hard natural fibres strengthen earthworks and encourage the growth of plants and trees, which provide further reinforcement. Unlike plastic textiles used for the same purpose, natural fibre nets – particularly those made from coir – decay over time as the earthworks stabilise. Mwasha [82] reported the use of environmentally friendly geotextiles for soil reinforcement. The studies demonstrated the potential for the use of sustainable biodegradable vegetable fibres over man-made polymeric materials in ground improvement. Utilisation of palm-leaf geotextile mats to conserve loamy sand soil in the United Kingdom was reported by Bhattacharyya et al. [83]. The studies recommended to cover palm-mat geotextiles as buffer strips for soil and water conservation on erodible moderate slopes.

Subaida et al. [84] reported the beneficial use of woven coir geotextiles as reinforcing material in a two-layer pavement section. The test results indicated that the inclusion of coir geotextiles enhanced the bearing capacity of thin sections. Placement of geotextile at the interface of the subgrade and base course increased the load carrying capacity significantly at large deformations. Datye and Gore [85] presented a review of the development of natural geotextiles and related materials such as wood and bamboo for a wide range of applications. The geotextile is used in conjunction with reinforced soil constructions, where small-dimensioned timber and bamboo were used as reinforcement in the form of cribs.

1.3 Nanofibres from Natural Fibres

Nanofibres are fibres that have diameter equal to or less than 100 nm. One of most significant characteristic of nanofibres is the enormous availability of surface area per unit mass. The high surface area of nanofibres provides a remarkable capacity for the attachment or release of functional groups, absorbed molecules, ions, catalytic moieties and nanometre scale particles of many kinds.

In recent years, considerable research has been done on the isolation of nanofibres from plants to use them as fillers in biocomposites [86–90]. Agricultural crop residues are one of the most valuable sources of natural cellulose nanofibres. It should be noted that in agricultural fibres, the cellulose microfibrils are less tightly wound in the primary cell wall than in the secondary wall in wood, thus fibrillation

to produce nanocellulose should be less energy demanding [91]. Cellulose nanofibres can be extracted from agricultural by-products of different plants such as flax, hemp, sisal, corn, wheat, rice, sorghum, barley, sugar cane, pineapple, banana and coconut crops.

The nanostructure of cellulose can play a significant part in papermaking and manufacture of high quality nanocomposites, as well as in technology of promising health care nano products [92]. The small dimensions of cellulose fibrils enable direct contact between cellulose and matrix polymers, allowing for a large contact surface and thus excellent adhesion. Cellulose nanofibres can be used as a rheology modifier in foods, paints, cosmetics and pharmaceuticals [91]. It seems that among various applications, use of nanocellulose and its derivatives in health care areas will be especially promising due to their high strength and stiffness combined with low weight, biocompatibility and renewability.

1.3.1 Cellulose as a Nanostructured Polymer

Cellulose is the most eminent representative of nanostructures occurring in wood, cotton, hemp, flax and other plant-based materials and serving as the dominant reinforcing phase in plant structures. Cellulose is also synthesised by algae, tunicates, and some bacteria [93–95]. Cellulose fibres are bundles of microfibrils where the cellulose molecules are always biosynthesized in the form of nanosized fibrils. Up to 100 glucan chains are grouped together to form elementary fibrils, which aggregate together to form cellulose nanosized microfibrils or nanofibres [96]. Fibrils have diameters in the nanometre and lengths in the micrometre scale. The production of nanoscale cellulose fibres and the application of cellulose nanofibres in polymer reinforcement is a relatively new research field. Plant-based cellulose nanofibres have great reinforcing potential because of their sustainability, easy availability, and the related characteristics such as a very large surface to volume ratio, high tensile strength, high stiffness, high flexibility and good dynamic mechanical, electrical and thermal properties as compared to other commercial fibres [97, 98]. These nanofibre-reinforced polymer composites give improved properties compared to the neat polymer and micro composites based on the same fibres. The use of cellulose nanofibres as reinforcing elements in the polymer matrix has been predicted to create the next generation of value-added novel eco-friendly nanocomposites.

1.3.2 Extraction Methods for Obtaining Nanocellulose from Natural Fibres

Many studies have been done on extracting cellulose nanofibrils from various sources and on using them as reinforcement in composite manufacturing. The

nano architecture of the cellulose promotes isolation of nanofibrils from initial fibres by various methods that facilitate breaking up of the glycosidic bonds in the disordered nanodomains of nanofibrils and cleaving of interfibrillar contacts [92].

Several sources of cellulose have been used to obtain cellulose nanofibres including banana residues [87, 90], soybean source [99], cotton [100], wheat straw [86], bacterial cellulose [101–104], sisal [88, 105], hemp [89, 106], sugar beet pulp [107, 108], potato pulp [109], bagasse [110], stems of cacti [111] and algae [112].

Cellulose nanofibres can be extracted from the cell walls by different types of isolation processes: simple mechanical methods [113], a combination of chemical and mechanical methods [109, 114] or an enzymatic approach [115] etc. Depending upon the raw materials and fibrillation techniques, the cellulose degree of polymerization, morphology and nanofibre aspect ratio may vary [116]. A purely mechanical process can produce refined fine fibrils having a web-like structure. The chemical treatment mainly involves the hydrolysis of cellulose, followed by mechanical disintegration or ultrasound sonification. The combination of acid hydrolysis and high pressure disintegration permits isolation of nano crystalline particles having lengths of 100–200 nm and widths of 20–40 nm. The enzymatic pre-treatment of cellulose fibres, followed by mechanical splitting in water by means of special high-shear mills or refiners, lead to the formation of nanofibrillated cellulose with average diameters of the nano-bundles about 100 nm and length greater than 1 μm . Repeated milling of the pulp in water over a long period of time permits complete fibrillation of the cellulose nanofibrils and turn these into nanofibrils. Dissolving methods and cryocrushing process of hydrolysed cellulose have also been used for the extraction of nanocellulose [92].

Cryocrushing is an alternative method for producing nanofibres in which fibres are frozen using liquid nitrogen and high shear forces are then applied [117]. When high impact forces are applied to the frozen fibres, ice crystals exert pressure on the cell walls, causing them to rupture and thereby liberating microfibrils. The cryocrushed fibres may then be dispersed uniformly into water suspension using a disintegrator before high pressure fibrillation [91]. Several researchers adopted cryocrushing method to extract cellulose nanofibres from soybean stock [99], chemically treated flax and hemp fibres [106] and wheat straw fibres [86]. Various methods used for the preparation of cellulose nanofibres are shown in Table 1.2.

1.3.3 Characterisation Techniques for Nanofibres

Detailed structural examination is essential to investigate the potential of cellulose nanofibre as reinforcement in polymer composites. Several characterization techniques were used to study the ultrastructure of cellulose obtained from various sources. Various techniques such as TEM, field emission scanning electron microscopy (FESEM), SEM, AFM and wide-angle X-ray scattering (WAXS) have been used to characterise the morphology of cellulose nanofibres. TEM and AFM aid

Table 1.2 Examples of cellulose nanofibre preparation procedures

Method	Raw material	Procedure	Nanofibre dimension
Mechanical treatment	Bleached potato pulp	Disintegration in a Waring blender;	~5 nm in width
	Cladodes of <i>Opuntia ficus indica</i>	Homogenisation by 15 passes through a laboratory homogeniser, operated at 500 bars and 90–95°C	
	Kraft pulp	Passing 2–30 times through a refiner with a gap of 0.1 mm, subsequently passing through a high pressure homogeniser 2–30 times	ND
		Passing through a refiner with a gap of 0.1 mm 30 times, subsequently passing through a high pressure homogeniser up to 30 times and finally grinder treatments up to 10 times	
		Cryocrushing followed by 20 passes through a defibrillator at 500–1,000 bar	50–100 nm in width and several nm in length
	Soybean stock	Beating and refining in a PFI mill; 20 passes through a defibrillator at 500–1,000 Pa	
		Cryocrushing followed by fibrillation using a Cramer disintegrator at 2,000 rpm; homogenization by 20 passes through a laboratory defibrillator at pressure above 300 bar	50–100 nm in width and several nm in length
	Wheat straw	Microfibrillation by super-grinder	20–120 nm in width, the majority around 30–40 nm
		Cryocrushing followed by high shear homogenisation	
	Wood pulps, Tunicin cellulose, chitosan, collagen	Disintegration by means of an Ultra-Turrax mixer at 24,000 rpm followed by homogenisation by a high-pressure laboratory homogeniser at 300 bar for 10–15 passes	20–90 nm in width
	Hemp fibre, spring flax, bleached kraft pulp, Rutabaga		5–80 nm in width, the majority around 10–60 nm
	Dried sugar beet pulp chips		30–100 nm and a length of several nm
	Never-dried bleached sulfite/kraft pulp		Few nanometre in width

(continued)

Table 1.2 (continued)

Method	Raw material	Procedure	Nanofibre dimension
Chemical treatment	Sugar beet pulp	TEMPO-mediated oxidation, followed by disintegration in a Waring blender Disintegration in a Waring blender; homogenisation by 15 passes through a laboratory homogeniser, operated at 500 bars and 90–95°C; TEMPO mediated oxidation Acid treatment coupled with high pressure defibrillation	ND Banana fibre having 4–5 nm in diameter and 200–250 nm in length PALF having 5–60 nm in diameter and 200–300 nm in length around 25–75 nm
Enzymatic pretreatment	Bleached kraft pulp	Enzymatic pre-treatment by fungus OSI (isolated from infected Elm trees), followed by high shear refining, cryocrushing and dispersion in water by a disintegrator	10–250 nm in width, the majority is around 25–75 nm
	Bleached sulfite softwood cellulose pulp	Refining to increase the accessibility of the cell wall to the subsequent monocomponent endoglucanase treatment; enzymatic treatment; second refining stage; high-pressure homogenising	5–30 nm in diameter
	Softwood sulfite pulp	Beating in a PFI-mill; enzymatic treatment with endoglucanase (Novozyme 476); second beating;	5–30 nm in diameter
	Softwood dissolving pulp	High-pressure homogenisation	

Siró and David [91]

the interpretation of structures from the nanometre to the micrometre size scale. Typical information obtained from conventional TEM is length, aspect ratio, shape and the aggregated or isolated state of fibres. AFM has also been used to examine plant cell walls at a similar resolution to that of the TEM. This type of microscopy has the important advantage of reducing the risks of introducing artefacts resulting from the preparative techniques. These techniques were applied to study the cellulose nanofibres obtained from various sources such as banana, cotton, hemp, sisal ramie, wheat straw, soybean stock, bacterial cellulose, sugar beet, etc. In the literature, there are reports of cellulose nanofibre characterisations using various techniques such as AFM, TEM, SEM, etc.

Teixeira et al. [100] extracted cellulose nanofibres from white and naturally coloured cotton (brown, green and ruby) by acid hydrolysis method. The yields of the various cotton nanocelluloses were around 65 wt% for white nanofibres and 52 wt% for others. Morphological study of several cotton nanofibres by scanning transmission electron microscopy (STEM) and AFM analyses revealed that the nanofibres had a length of the 85–225 nm and diameter of 6–18 nm. The micrographs also indicated that there were no significant morphological differences among the nanostructures from different cotton fibres. The thermal studies showed that the coloured nanofibres were thermally more stable in isothermal oxidising conditions at 180°C than white nanofibres. Figures 1.18 and 1.19 show the TEM and AFM images of white cotton fibres.

Menezes et al. [118] also extracted cellulose nanocrystals or whiskers of ramie fibres by acid hydrolysis. Acid hydrolysis of native ramie cellulose fibres leads to aqueous suspensions of elongated nanocrystals with high aspect ratio. The geometric average length and diameter were around 134 ± 59 nm and 10.8 ± 4.5 nm, respectively, giving rise to an aspect ratio around 12. A minimum of 228 and 70 measurements were used to determine the length and the diameter, respectively, of ramie whiskers. They noticed that more than 50% of the

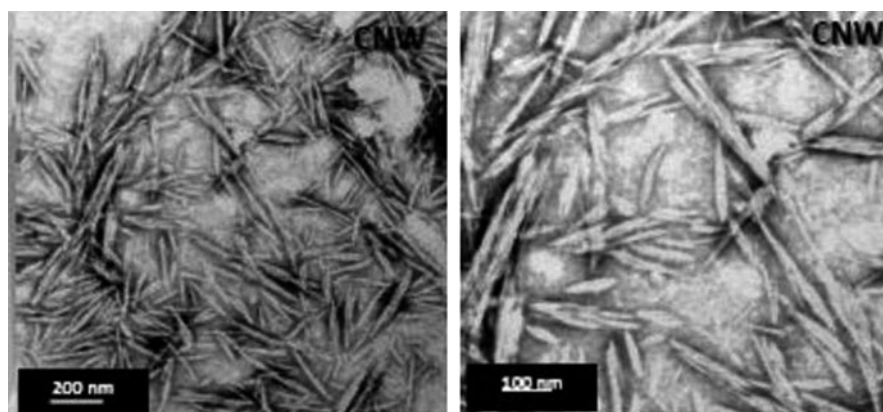


Fig. 1.18 Transmission electron micrographs of nanofibres of white cotton fibres at two magnifications [100]

Fig. 1.19 AFM images of nanofibres of white cotton fibres [100]

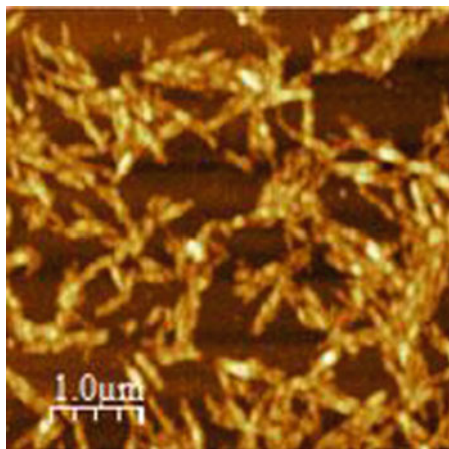
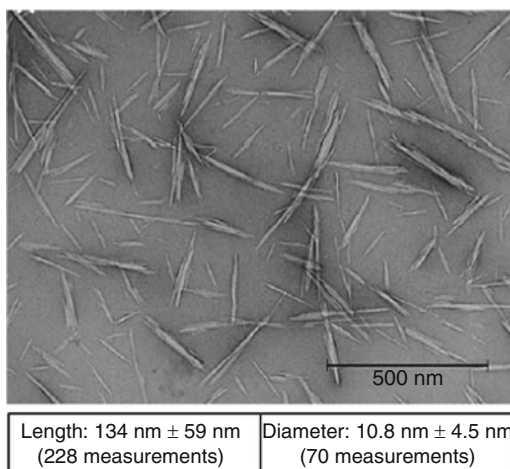


Fig. 1.20 Transmission electron micrograph of ramie cellulose whiskers [118]



nanoparticles have a length lower than 100 nm. Figure 1.20 shows the transmission electron micrograph of ramie cellulose whiskers

Alemdar and Sain [86] extracted Cellulose nanofibres of wheat straw and soy hulls, by a chemi-mechanical technique. They analysed the morphology and physical properties of the nanofibres by scanning and transmission electron microscopy. The wheat straw nanofibres have diameters in the range of 10–80 nm and lengths of a few thousand nanometres, and the soy hull nanofibres have diameters in the range of 20–120 nm and shorter lengths than the wheat straw nanofibres. Fig. 1.21a and b shows the TEM pictures of the wheat straw and soy hull nanofibres. The image shows the separation of the nanofibres from the micro-sized fibres. The thermal properties of the nanofibres were studied by the TGA technique and found that the

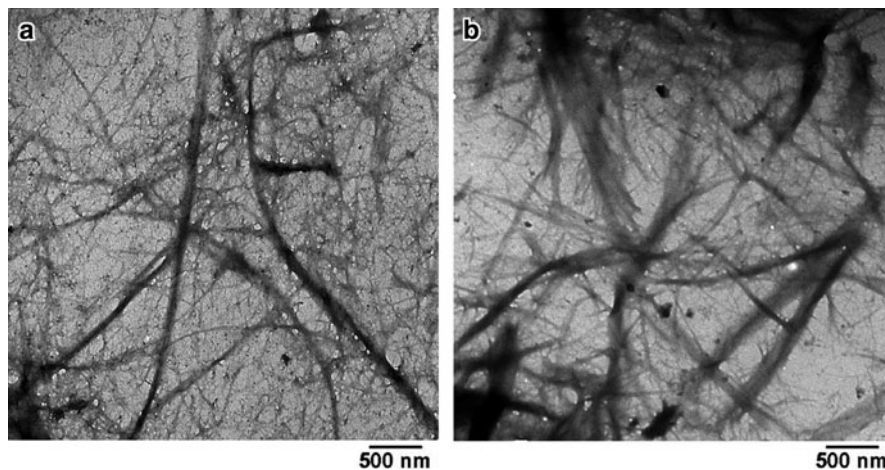


Fig. 1.21 Transmission electron micrographs of the (a) wheat straw and (b) soy hulls nanofibres [86]

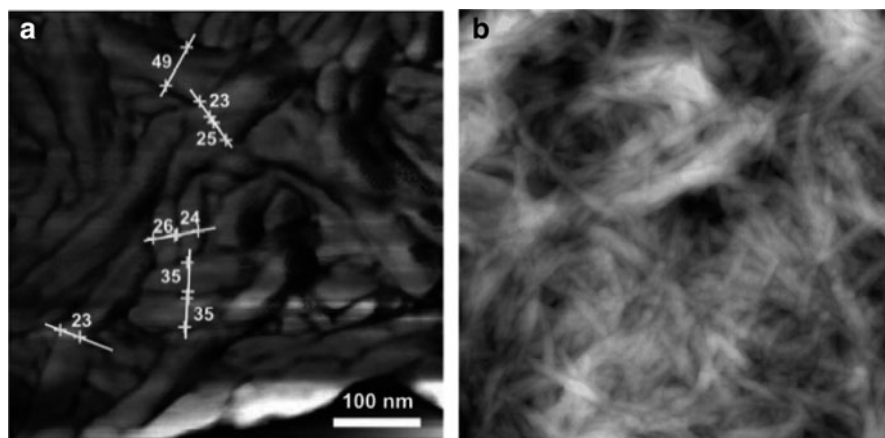


Fig. 1.22 SFM pictures of banana nanofibres [87]

processed fibres shows higher thermal stability. The degradation temperature of both nanofibre types reached beyond 290°C.

Cherian et al. [87] extracted cellulose nanofibres from the pseudo stem of the banana plant by using acid treatment coupled with high pressure defibrillation. Characterization of the fibres by (Scanning Force Microscopy) SFM and TEM showed that there is reduction in the size of banana fibres to the nanometre range (below 40 nm). The average length and diameter of the developed nanofibrils were found to be between 200–250 nm and 4–5 nm, respectively. Figures 1.22a, b and 1.23 show the SFM and TEM pictures of banana nanofibres, respectively.

Fig. 1.23 Transmission electron micrographs of the banana nano fibres [87]

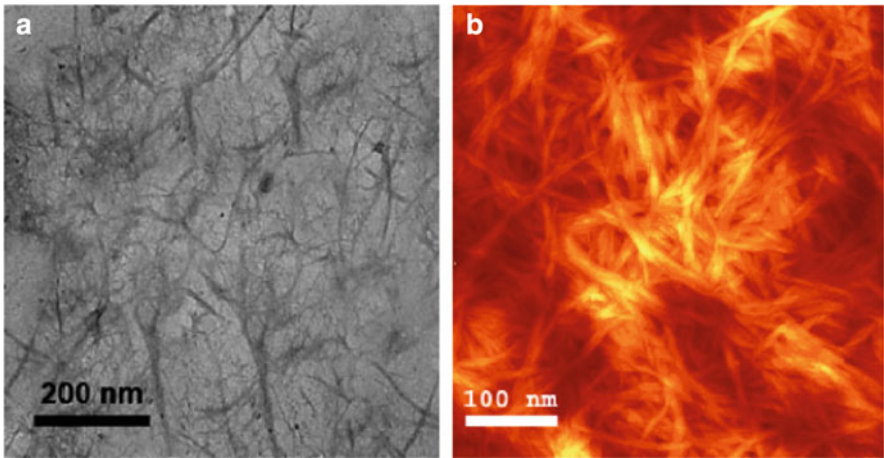
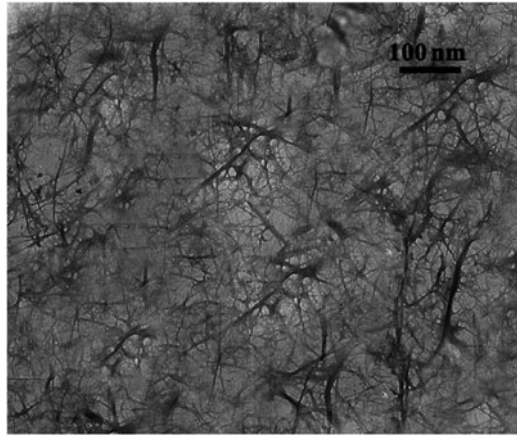


Fig. 1.24 (a) Atomic force micrographs of cellulose nanofibres of PALF (b) TEM of cellulose nanofibres of PALF [119]

Cherian et al. [119] also extracted cellulose nanofibres from pineapple leaf fibres using acid-coupled steam treatment. The structural and physicochemical properties of the pineapple leaf fibres were studied by environmental scanning electron microscopy (ESEM), AFM and TEM and X-ray diffraction (XRD) techniques. The acid-coupled steam explosion process resulted in the isolation of PALF nanofibres having a diameter range of 5–60 nm. Figure 1.24a and b shows the AFM and TEM images of nano fibres obtained from pineapple leaf fibres. AFM and TEM support the evidence for the isolation of individual nanofibres from PALF.

Wang et al. [89] extracted the cellulose nanofibres of hemp fibre by a chemi-mechanical process, and the structural details were studied with SEM, TEM and

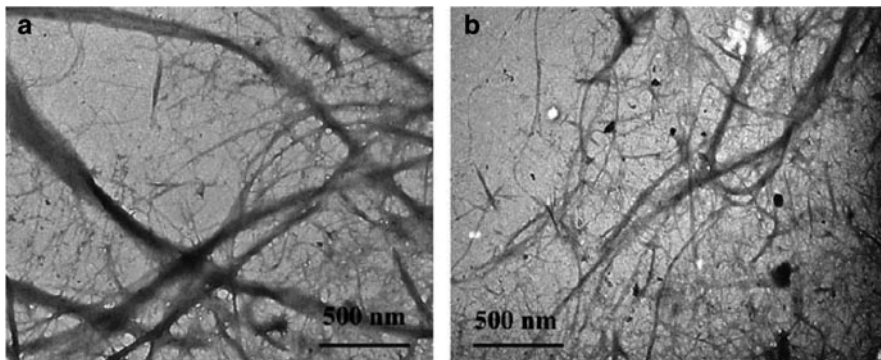
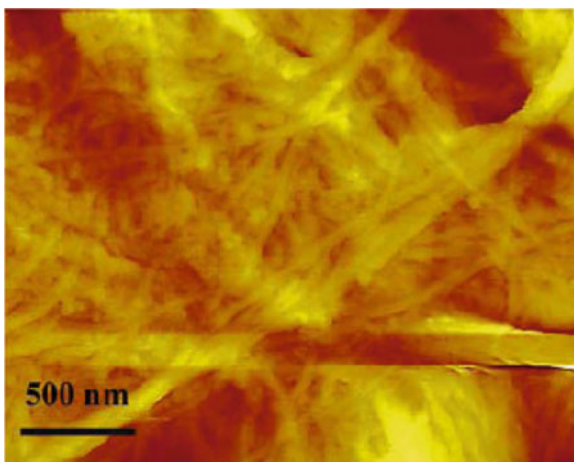


Fig. 1.25 Transmission electron micrographs of (a) unbleached, (b) bleached hemp nanofibres [89]

Fig. 1.26 Atomic force micrographs of unbleached hemp nanofibres [89]



AFM. The widths of unbleached nanofibres of hemp were estimated between 50 and 100 nm, and most of them had a diameter range of 70–100 nm. Bleached nanofibres of hemp produced smaller widths (30–100 nm) compared with that of unbleached nanofibres, and most of the bleached nanofibres had a diameter range of 30–50 nm. Aspect ratios of the extracted cellulose nanofibres were estimated from transmission electron micrographs. The aspect ratio of the bleached and unbleached nanofibres were found to be 82 and 88, respectively. TEM and AFM images of hemp nanofibres are shown in the Figs. 1.25 and 1.26, respectively. TEM and AFM images showed that the high-pressure defibrillation leads to individualization of the cellulose nanofibres from the cell wall.

Wang and Sain [99] extracted cellulose nanofibres from a soybean source by combining chemical and mechanical treatments. Isolated nanofibres were shown to have diameter between 50 and 100 nm and the length in micrometre scale, which

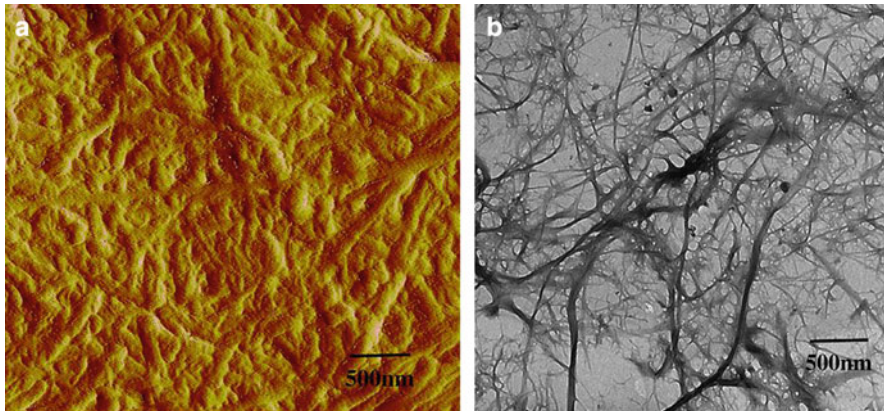


Fig. 1.27 (a) Atomic force micrographs of SBN (b) TEM of diluted suspension of SBN in water (Wang and Sain 2007)

results in very high aspect ratio. The nanofibres were characterised by using SEM, AFM and TEM analysis. AFM was used to investigate the size of the dispersed nanofibres. The atomic force micrograph (Fig. 1.27a) shows the size of the nanofibres within the range of 50–100 nm in width and several nm in length. Figure 1.27b shows the TEM picture of soybean nanofibres in water suspension.

Besides microscopic techniques, the extent of fibrillation can be assessed indirectly by other measurements. Degree of cellulose polymerization (DP) is reported to correlate strongly with the aspect ratio of the nanofibres; longer fibrils are associated with higher cellulose DP [91]. The DP for the raw material (sulfite pulp) is often reported to be around 1,200–1,400, while mechanical isolation of nanofibres may result in about 30–50% decrease in DP [93]. Depending on the nature of the starting material, the DP of microfibrillated cellulose may be even lower. For example, Iwamoto et al. [94] reported that the DP of microfibrillated cellulose decreased from about 770 to 525 after 9 passes through a grinder. High cellulose DP is desirable for microfibrillated cellulose nanofibres since this is correlated with increased nanofibre tensile strength [93].

1.4 Conclusion

“Back to Nature” is the present day mantra of the modern world. The current trend is to find out new materials based on natural substances. Increased environmental awareness and the current economic situations tempt the modern man to make use of Natural fibres in developing new composite materials. Natural fibres are extracted from various parts of plants, and several extraction procedures are in vogue. The fibre properties depend on the part of the plant from which the fibres are obtained and the extraction methods used.

Nowadays, researchers are increasingly acknowledging the importance of Nanomaterials because of their exciting properties due to their high surface area. Natural fibres serve as a very good source for cellulose, which is the most abundant bio polymer and nanomaterial. As a result of its sustainability, biocompatibility and biodegradability, cellulose is gaining more and more importance nowadays. Nanofibre-reinforced polymer composites give improved properties compared to the neat polymer and micro composites based on the same fibres. Nanofibre-reinforced polymer composites are likely to become the next generation of value-added novel eco-friendly composites.

References

1. Bismarck A, Mishra S, Lampke T et al (2005) Plant fibres as reinforcement for green composites. In: Mohanty AK, Misra M, Drzal LT (eds) *Natural fibres biopolymers and biocomposites*. CRC, Boca Raton, p 37
2. Bogoeva-Gaceva G, Avella M, Malinconico M, Buzarovska A, Grozdano A, Gentile G, Errico ME et al (2007) Natural fibre eco-composites. *Polym Compos* 28:98–107
3. Anandjiwala RD (2006) The role of research and development in the global competitiveness of natural fibre products. *Proceedings, Natural fibres vision 2020*, New Delhi 8–9th December
4. Sain M, Panthapulakkal S (2006) Bioprocess preparation of wheat straw fibres and their characterization. *Ind Crops Prod* 23:1–8
5. Morton WE, Hearle JWS (1993) *Physical properties of textile fibres*. The Textile Institute, Manchester, UK
6. Weisman S, Haritos VS, Church JS et al (2010) Honeybee silk: recombinant protein production, assembly and fiber spinning. *Biomaterials* 1–6 DOI:10.1016/j.biomaterials.2009.12.021
7. Kelsall RW, Hamley IW, Geoghegan M (2005) *Handbook of textile fibres II. Man-made fibres*. Wiley, UK
8. Matthew's MH (1954) *Textile fibres: their physical, microscopic, and chemical properties*. John Wiley and Sons Inc., New York
9. Press J (1959) *Man-made textile encyclopedia*. Textbook Publishers Inc., London
10. Shi J, Lua S, Du N, Liu X, Song J et al (2008) Identification, recombinant production and structural characterization of four silk proteins from the Asiatic honeybee *Apis cerana*. *Biomaterials* 29:2820–2828
11. Sutherland TD, Weisman S, Trueman HE, Sriskantha A, Trueman JWH, Haritos VS et al (2007) Conservation of essential design features in coiled coil silks. *Mol Biol Evol* 24:2424–2432
12. Poole AJ, Church JS, Huson MG et al (2009) Environmentally sustainable fibers from regenerated protein. *Biomacromolecules* 10:1–7
13. Bledski AK, Gassan J (1999) Composites reinforced with cellulose-based fibres. *Prog Polym Sci* 24:221–274
14. Franco PHJ, Valadez-Gonzalez M (2005) Fibre-matrix adhesion in natural fibre composites. In: Mohanty AK, Misra M, Drzal LT (eds) *Natural fibres, biopolymers and biocomposites*. CRC, Boca Raton, p 37
15. Nevell TP, Zeronian SH (1985) *Cellulose chemistry and its applications*. Wiley, New York
16. Toumris GT (1991) *Structure, properties and utilization*. Science and technology of wood. Van Nostrand Reinhold, New York, p 494
17. Zimmermann T, Pohlerand E, Geiger T (2004) Cellulose fibrils for polymer reinforcement. *Adv Eng Mater* 6, No. 9

18. Rong MZ, Zhang MQ, Liu Y, Yang GC, Zeng HM et al (2001) Effect of fibre treatment on the mechanical properties of unidirectional sisal-reinforced epoxy composites. *Compos Sci Technol* 61:1437–1447
19. Murali MRK, Mohana RK (2007) Extraction and tensile properties of natural fibres: Vakka, date and bamboo. *Compos Struct* 77:288–295
20. Foulk JA, Akin DE, Dodd RB et al (2001) Processing techniques for improving enzyme-retting of flax. *Ind Crops Prod* 13:239
21. Yu H, Yu C (2007) Study on microbe retting of kenaf fibre. *Enzyme Microb Technol* 40:1806–1809
22. Goodman AM, Ennos AR, Booth I et al (2002) A mechanical study of retting in glyphosate treated flax stems. *Ind Crops Prod* 15:169
23. Heinemann O (1997) Standroste von Flachs-Innovation in der Flachserntetechnik in VDI/MEG Kolloquium Agrartechnik: Erzeugung, Aufbereitung und Verarbeitung von Naturfasern für nichttextile Zwecke. 22 Bonn:101
24. Terentie P, Neacsu H (1995) Die Gewinnung von Textilfasern aus Hanfstengeln. *Proceedings Biorhstoff Hanf-Resource Hemp, Reader zum Technologisch-wissenschaftlichen Symposium*. Nova-Institut (Hrsg.), Frankfurt, March 2–5:278
25. Katalyse-Institut für angewandte Umweltforschung (Hrsg.) Hanf & Co. (1995) Die Renaissance der heimischen Faserpflanzen, Verlag Die Werkstatt, Göttingen
26. Folster Th, Michaeli W (1993) Flachs-eine nachwachsende Verstärkungsfasern für Kunststoffe? *Kunststoffe* 83:687
27. Kessler RW, Kohler BU, Rgoth B et al (1998) Steam explosion of flax- a superior technique for upgrading fibre value. *Biomass Bioenergy* 14:237–249
28. Kohler R, Kessler RW (1999) Designing Natural fibres for advanced materials. *Proceedings of the 5th International Conference on wood fibre plastic composites*, Madison, May 26–28: 29–36
29. Wurster J, Daul D (1988) Flachs, eine durch Forschung modernere alte Kulturpflanze. *Melliland Textilber* 12:551
30. Rowell RM, Han JS, Rowell JS et al (2000) Characterization and factors effecting fibre properties in natural polymers and agro fibres based composites. In: Frollini E, Leao AL, Mattoso LH (eds) *Natural polymers and biobased composites*, USP, Unesp, Embrapa, Brazil p 115–135
31. Gassan J, Bledzki AK (1995) *Internationales Textextil Symposium*, Frankfurt, 20–22 June
32. Kritschewsky GE (1985) *Chemische technology von textil materialien*. Moskau, Legprombitisdat
33. Sadov F, Korchagin M, Matetsky A et al (1978) *Chemical technology of fibrous materials*. Mir Publishers, Moscow
34. Oke IW (2010) Nanoscience in nature: Cellulose nanocrystals. *Studies by undergraduate researchers at Guelph*, Winter 3:77–80
35. Whistler RL, Richards EL (1970) *Carbohydrates*, vol 2A. Academic, New York
36. Gassan J, Chate A, Bledzki AK et al (2001) *J Mater Sci* 36:3715
37. David N, Hon S, Shiraiishi N et al (1991) *Wood and cellulose chemistry*. Marcel Dekker, New York
38. Frey-Wyssling A (1954) The fine structure of cell micro-fibrils. *Science* 119:80
39. Krassig HA (1992) *Cellulose*. Gordon and Breach Science Publishers, New York
40. Dufresne A (1998) In recent research developments in macromolecules. Pandalai SG (eds) *Research Signpost* 3:455–474
41. Pietak A, Korte S, Tan E, Downard A, Staiger MP et al (2007) Atomic force microscopy characterization of the surface wettability of natural fibres. *Appl Surf Sci* 253:3627–3635
42. Tomczak F, Deme'trio Sydenstricker TH, Satyanarayana KG et al (2007) Studies on lignocellulosic fibres of Brazil Part II: morphology and properties of Brazilian coconut fibres. *Compos Part A* 38:1710–1721

43. Bessadok A, Marais S, Roudesli S, Lixon C, Me'tayer M et al (2008) Influence of chemical modifications on water-sorption and mechanical properties of agave fibres. *Compos Part A* 39:29–45
44. Sandeep SN, Wanga S, Hurley DC et al (2010) Nanoscale characterization of natural fibres and their composites using contact-resonance force microscopy. *Compos: Part A* 41:624–631
45. Sgriccia N, Hawley MC, Misra M et al (2008) Characterization of natural fibre surfaces and natural fibre composites. *Compos Part A* 39:1632–1637
46. Maria DRI, Kenny JM, Puglia D, Santulli C, Sarasini F et al (2010) Morphological, thermal and mechanical characterization of okra (*Abelmoschus esculentus*) fibres as potential reinforcement in polymer composites. *Compos Sci Technol* 70:116–122
47. Spinacé MAS, Lambert CS, Femoselli KKG, De Paoli MA et al (2009) Characterization of lignocellulosic curaua fibres. *Carbohydr Polym* 77:47–53
48. Guimarães JL, Frollini E, da Silva CG, Wypych F, Satyanarayanac KG et al (2009) Characterization of banana, sugarcane bagasse and sponge gourd fibres of Brazil. *Ind Crop Prod* 30:407–415
49. Zou L, Jin H, Lu WY, Li X et al (2009) Nanoscale structural and mechanical characterization of the cell wall of bamboo fibres. *Mater Sci Eng* 29:1375–1379
50. Koljonen K, Österberg M, Johansson LS, Stenius P et al (2003) Surface chemistry and morphology of different mechanical pulps determined by ESCA and AFM. *Colloids Surf A: Physicochem Eng Asp* 228:143–148
51. Mohanty AK, Misra M, Drzal LT, Selke SE, Harte BR, Hinrichsen G et al (2005) Natural fibres, biopolymers, and bio composites an introduction. In: Mohanty AK, Misra M, Drzal LT (eds) *Natural fibres, biopolymers and biocomposites*. CRC, Boca Raton, p 37
52. Bax B, Mussig J (2008) Impact and tensile properties of PLA/Cordenka and PLA/flax composites. *Compos Sci Technol* 68:1601–1607
53. Beckermann GW, Pickering KL (2008) Engineering and evaluation of hemp fibre reinforced polypropylene composites: fibre treatment and matrix modification. *Compos Part A* 39: 979–988
54. Bledzki AK, Mamun AA, Jaszkwicz A, Erdmann K et al (2010) Polypropylene composites with enzyme modified abaca fibre. *Compos Sci Technol* 70:854–860
55. Sangthong S, Pongprayoon T, Yanumet N et al (2009) Mechanical property improvement of unsaturated polyester composite reinforced with admicellar-treated sisal fibres. *Compos Part A* 40:687–694
56. Towo AN, Ansell MP (2008) Fatigue of sisal fibre reinforced composites: constant-life diagrams and hysteresis loop capture. *Compos Sci Technol* 68:915–1924
57. Wang ZF, Peng Z, Li SD, Lin H, Zhang KX, She XD, Fu X et al (2009) The impact of esterification on the properties of starch/natural rubber composite. *Compos Sci Technol* 69:1797–1803
58. Yao F, Wu Q, Lei Y, Xu Y et al (2008) Rice straw fibre-reinforced high-density polyethylene composite: effect of fibre type and loading. *Ind Crops Prod* 28:63–72
59. Huang X, Netravai AN (2009) Biodegradable green composites made using bamboo micro/nano-fibrils and chemically modified soy protein resin. *Compos Sci Technol* 69:1009–1025
60. Lee BH, Kim HS, Lee S, Kim HJ, Dorgan JR et al (2009) Bio-composites of kenaf fibres in polylactide: role of improved interfacial adhesion in the carding process. *Compos Sci Technol* 69:2573–2579
61. Shih YF, Huang CC, Chen PW et al (2009) Biodegradable green composites reinforced by the fibre recycling from disposable chopsticks. *Mater Sci Eng* 527:1516–1521
62. Suryanegara L, Nakagaito AN, Yano H et al (2009) The effect of crystallization of PLA on the thermal and mechanical properties of microfibrillated cellulose-reinforced PLA composites. *Compos Sci Technol* 69:1187–1192

63. Wu CS (2009) Renewable resource-based composites of recycled natural fibres and maleated polylactide bioplastic: Characterization and biodegradability. *Polym Degrad Stab* 94:1076–1084
64. Ma X, Chang PR, Yu J, Stumborg M et al (2009) Properties of biodegradable citric acid-modified granular starch/thermoplastic pea starch composites. *Carbohydr Polym* 75:1–8
65. Netravali AN, Chabba S (2003) Composites get greener. *Mater Today* 6:22–29
66. Zhu H, Shen J, Feng X, Zhang H, Guo Y, Chen J et al (2010) Fabrication and characterization of bioactive silk fibroin/wollastonite composite scaffolds. *Mater Sci Eng* 30:132–140
67. Netravali AN, Huang X, Mizuta K et al (2007) Advanced green composites. *Adv Compos Mater* 16:16269–16282
68. Huang X, Netravali AN (2006) Characterization of Nano-clay reinforced phytagel modified soy protein concentrate. *Biomacromolecules* 7:2783–2789
69. Hill S (1997) Cars that grow on trees. *New Scientist* Feb 3–39
70. Suddell BC, Evans WJ (2005) Natural fibre composites in automotive applications. In: Mohanty AK, Misra M, Drzal LT (eds) *Natural fibres, biopolymers and biocomposites*. CRC, Boca Raton, p 37
71. Mohanty AK, Khan MA, Hinrichsen G et al (2000) Surface modification of jute and its influence on performance of biodegradable jute-fabric/Biopol composites. *Compos Sci Technol* 60:1115–1124
72. Leaño AL, Rowell R, Tavares N et al (1998) Applications of natural fibres in automotive industry in Brazil – thermoforming process. In: Prasad PN (ed) *Science and technology of polymers and advanced materials*. Plenum, New York
73. Alves C, Ferrão PMC, Silva AJ, Reis LG, Freita LB, Rodrigues M, Alves DE et al (2010) Ecodesign of automotive components making use of natural jute fibre composites. *J Clean Prod* 18:313–327
74. Singh B, Gupta M (2005) Natural fibre composites for building applications. In: Mohanty AK, Misra M, Drzal LT (eds) *Natural fibres, biopolymers and biocomposites*. CRC, Boca Raton, p 37
75. Singh B, Gupta M (2003) Proceedings of the advances in polymeric building materials. *Poly Build -2003*, Roorke, March 6–7: 5
76. Aziz MA, Paramasivam P, Lee SL et al (1981) Prospects for natural fibre reinforced concretes in construction. *Int J Cement Compos Lightweight Concrete* 3:123–132
77. Juárez C, Durán A, Valdez P, Fajardo G et al (2007) Performance of “Agave lecheguilla” natural fibre in Portland cement composites exposed to severe environment conditions. *Build Environ* 42:1151–1157
78. Savastano H Jr, Santos SF, Radonjic M, Soboyejo WO et al (2009) Fracture and fatigue of natural fibre-reinforced cementitious composites. *Cement Concr Compos* 31:232–243
79. Rahman WA, Tin SL, Razak RA et al (2008) Injection moulding simulation analysis of natural fibre composite window frame. *J Mater Process Technol* 197:22–30
80. Toledo FRD, Andrade SF, Fairbairn EMR, Melo FA et al (2009) Durability of compression molded sisal fibre reinforced mortar laminates. *Construct Build Mater* 23:2409–2420
81. Pillai MS (2006) Applications of natural coir fibre, proceedings, natural fibres vision 2020, New Delhi 8–9th December
82. Mwashia A (2009) Using environmentally friendly geotextiles for soil reinforcement: a parametric study. *Mater Des* 30:1798–1803
83. Bhattacharyya R, Fullen DK, Booth CA et al (2009) Utilizing of palm-leaf geotextile mats to conserve loamy sand soil in the United Kingdom. *Agric Ecosyst Environ* 130:50–58
84. Subaida EA, Chandrakaran S, Sankar N et al (2009) Laboratory performance of unpaved roads reinforced with woven coir geotextiles. *Geotextiles Geomembr* 27:204–210
85. Datye KR, Gore VN (1994) Application of natural geotextiles and related products. *Geotextiles Geomembr* 13:371–388
86. Alemdar A, Sain M (2008) Isolation and characterization of nanofibres from agricultural residues-wheat straw and soy hulls. *Bioresour Technol* 99:1664–1671

87. Cherian BM, Pothan LA, Nguyen-Chung T, Mennig G, Kottaisamy M, Thomas S et al (2008) A novel method for the synthesis of cellulose nanofibril whiskers from banana fibres and characterization. *J Agric Food Chem* 56:5617–5627
88. Mora'n JI, Alvarez VA, Cyras VP, Va'zquez A et al (2008) Extraction of cellulose and preparation of nanocellulose from sisal fibres. *Cellulose* 15:149–159
89. Wang B, Sain M, Oksman K et al (2007) Study of structural morphology of hemp fibre from the micro to the nanoscale. *Appl Compos Mater* 14:89–103
90. Zuluaga R, Putaux JL, Restrepo A, Mondragon I, Gan'a'n P et al (2007) Cellulose microfibrils from banana farming residues: isolation and characterization. *Cellulose* 14:585–592
91. Siro' I, David P (2010) Microfibrillated cellulose and new nanocomposite materials: a review. *Cellulose*. doi:[10.1007/s10570-010-9405-y](https://doi.org/10.1007/s10570-010-9405-y)
92. Ioelowich M (2008) Cellulose as a nano structured polymer: a short review. *Bioresources* 3(4):1403–1418
93. Henriksson M, Henriksson G, Berglund LA, Lindstro'm T et al (2007) An environmentally friendly method for enzyme assisted preparation of microfibrillated cellulose (MFC) nanofibres. *Eur Polym J* 43:3434–3441
94. Iwamoto S, Nakagaito AN, Yano H (2007) Nano-fibrillation of pulp fibres for the processing of transparent nanocomposites. *Appl Phys A-Mater Sci Process* 89:461–466
95. Klemm D, Schumann D, Kramer F, Hessler N, Hornung M, Schmauder HP, Marsch S et al (2006) Nanocelluloses as innovative polymers in research and application. *Polysaccharides* 205:49–96
96. Fahmy TYA, Mobarak F (2008) Nanocomposites from natural cellulose fibres filled with kaolin in presence of sucrose. *Carbohydr Polym* 72:751–755
97. Roohani M, Habibi Y, Belgacem NM, Ebrahim G, Karimi AN, Dufresne A et al (2008) Cellulose whiskers reinforced polyvinyl alcohol copolymers nanocomposites. *J Eur Polym* 44:2489–2498
98. Seydibeyog'lu MO, Oksman K (2008) Novel nanocomposites based on polyurethane and micro fibrillated cellulose. *J Compos Sci Technol* 68:908–914
99. Wang B, Sain M (2007) Isolation of nanofibres from soybean source and their reinforcing capability on synthetic polymers. *Compos Sci Technol* 67:2521–2527
100. Teixeira EM, Correã AC, Manzoli A, Leite FL, Oliveira CR, Mattoso LHC et al (2010) Cellulose nanofibres from white and naturally colored cotton fibres. *Cellulose*. doi:[10.1007/s10570-010-9403-0](https://doi.org/10.1007/s10570-010-9403-0)
101. Grande CJ, Torres FG, Gomez CM, Troncoso OP, Canet-Ferrer J, Martinez-Pastor J et al (2008) Morphological characterization of bacterial cellulose–starch nanocomposites. *Polym Compos* 16:181–185
102. Iguchi M, Yamanaka S, Budhiono A et al (2000) Bacterial cellulose – a masterpiece of nature's arts. *J Mater Sci* 35:261–270
103. Juntaro J, Pomet M, Kalinka G, Mantalaris A, Shaffer MSP, Bismarck A et al (2008) Creating hierarchical structures in renewable composites by attaching bacterial cellulose onto sisal fibres. *Adv Mater* 20:3122–3126
104. Nakagaito AN, Iwamoto S, Yano H et al (2005) Bacterial cellulose: the ultimate nano-scalar cellulose morphology for the production of high-strength composites. *Appl Phys A Mater Sci Process* 80:93–97
105. De Rodriguez NLG, Thielemans W, Dufresne A et al (2006) Sisal cellulose whiskers reinforced polyvinyl acetate nanocomposites. *Cellulose* 13:261–270
106. Bhatnagar A, Sain M (2005) Processing of cellulose nanofibres-reinforced composites. *J Reinf Plas Compos* 24:1259–1268
107. Gousse' C, Chanzy H, Cerrada ML, Fleury E et al (2004) Surface silylation of cellulose microfibrils: preparation and rheological properties. *Polymer* 45:1569–1575
108. Habibi Y, Vignon MR (2008) Optimization of cellouronic acid synthesis by TEMPO-mediated oxidation of cellulose III from sugar beet pulp. *Cellulose* 15:177–185

109. Dufresne A, Dupeyre D, Vignon MR et al (2000) Cellulose micro-fibrils from potato tuber cells: processing and characterization of starch–cellulose microfibril composites. *J Appl Polym Sci* 76:2080–2092
110. Bhattacharya D, Germinario LT, Winter WT et al (2008) Isolation, preparation and characterization of cellulose microfibrils obtained from bagasse. *Carbohydr Polym* 73:371–377
111. Malainine ME, Mahrouz M, Dufresne A et al (2005) Thermoplastic nanocomposites based on cellulose microfibrils from *Opuntia ficus-indica* parenchyma cell. *Compos Sci Technol* 65:1520–1526
112. Imai T, Putaux JL, Sugiyama J et al (2003) Geometric phase analysis of lattice images from algal cellulose microfibrils. *Polymer* 44:1871–1879
113. Nakagaito AN, Yano H (2004) Novel high-strength biocomposites based on microfibrillated cellulose having nano-order-unit web-like network structure. *Appl Phys A* 80:155–159
114. Dinand E, Chanzy H, Vignon MR et al (1999) Suspensions of cellulose micro-fibrils from sugar beet pulp. *Food Hydrocolloid* 13:275–283
115. Wan YZ, Hong L, Jia SR, Huang Y, Zhu Y, Wang YL et al (2006) Synthesis and characterization of hydroxyapatite–bacterial cellulose nanocomposites. *Compos Sci Technol* 66 (11–12):1825–1832
116. Svagan AJ, Samir MASA, Berglund LA et al (2008) Biomimetic foams of high mechanical performance based on nanostructured cell walls reinforced by native cellulose nano-fibrils. *Adv Mater* 20:1263–1269
117. Chakraborty A, Sain M, Kortschot M et al (2005) Cellulose microfibrils: a novel method of preparation using high shear refining and cryocrushing. *Holzforschung* 59:102–107
118. Menezes AJ, Siqueira G, Curvelo AAS, Dufresne A (2009) Extrusion and characterization of functionalized cellulose whiskers reinforced polyethylene nanocomposites. *Polymer* 50:4552–4563
119. Cherian BM, Leão AL, Souza SF, Thomas S, Pothan LA, Kottaisamy M (2010) Isolation of nanocellulose from pineapple leaf fibres by steam explosion. *Carbohydr Polym* 81:720–725

Chapter 2

Chemical Functionalization of Cellulose Derived from Nonconventional Sources

V. K. Varshney and Sanjay Naithani

Abstract Chemical functionalization of cellulose aims to adjust the properties of macromolecule for different purposes, particularly, as a chemical feedstock for production of cellulose derivatives for a variety of applications. The conventional sources of cellulose include cotton linters and wood pulp which now-a-days are discouraged on account of the cost of the former and environment conservative regulations associated with the latter. Further, renewable raw materials are gaining considerable importance because of the limited existing quantities of fossil supplies. In this regard, cellulose-rich biomass derived from the nonconventional sources such as weeds, fibers, bamboos, and wastes from agriculture and forests, etc. acquires enormous significance, as alternative chemical feedstock, since it consists of cellulose, hemicellulose, and lignin, which contain many functional groups suitable to chemical functionalization. Etherification of cellulose through methylation, carboxymethylation, cyanoethylation, hydroxypropylation, single or mixed, is one of the most important routes of cellulose functionalization. Chemical composition and rheological characteristics make possible the selection of the modified cellulose to serve special applications. Prompted by above facts, possibility for chemical functionalization of cellulose rich biomass derived from bamboo, *Dendrocalamus strictus* (DCS), and noxious weeds – *Lantana camara* (LC) and *Parthenium hysterophorus* (PH) for their utilization was examined and results are reported. Proximate analysis of these materials was conducted and processes were standardized for production of α -cellulose on 1 kg batch scale. The percent yield, Av. DP, and the percentage of α -cellulose content of the obtained celluloses were found in the range of 35–40, 400–825, >90 (Brightness 80% ISO), respectively. Processes were optimized for production of water-soluble carboxymethyl cellulose (DCS, LC, and PH), cyanoethyl cellulose (DCS) and water-soluble hydroxypropyl cellulose (DCS and PH). The optimized products were characterized by IR spectra. Rheological studies of 1% and 2% aqueous solutions of the optimized carboxymethyl celluloses and hydroxypropyl celluloses showed their non-Newtonian

V.K. Varshney (✉)

Chemistry Division, Forest Research Institute, Dehra Dun 248 006, India

e-mail: varshney2000@yahoo.com

pseudoplastic behavior. Thus, abundantly available biomass from *Dendrocalamus strictus* bamboo and the weeds – *Lantana camara* and *Parthenium hysterophorus* seem to be a potential feedstock for production of α -cellulose and its subsequent functionalization into cellulose derivatives for variety of applications. This was also demonstrated that these noxious weeds could also be managed by their utilization into products of commercial importance.

Keywords Bamboo · Cellulose · Cellulose ethers · Chemical functionalization · Lantana · Parthenium

Contents

2.1	Introduction	45
2.1.1	Cellulose and Its Sources	45
2.1.2	Chemical Functionalization of Cellulose	46
2.1.3	Applications of Cellulose Derivatives	48
2.2	Status of Research on Chemical Functionalization of Cellulose Derived from Nonconventional Sources	49
2.3	Chemical Functionalization of Cellulose Derived from Nonconventional Biomass <i>Dendrocalamus strictus</i> (DCS) and Noxious Weeds <i>Lantana camara</i> (LC) and <i>Parthenium hysterophorus</i> (PH)	50
2.3.1	Proximate Analysis of Biomass	51
2.3.2	Isolation of α -Cellulose	52
2.3.3	Etherification of α -Cellulose	53
2.3.4	Characterization and Rheology of the Optimized Derivatives	56
2.4	Conclusion	57
	References	58

Abbreviations

AGU	Anhydroglucose unit
AN	Acrylonitrile
CEC	Cyanoethylcellulose
CMC	Carboxymethyl cellulose
CMHEC	Carboxymethylhydroxyethylcellulose
DCS	<i>Dendrocalamus strictus</i>
DP	Degree of Polymerization
DS	Degree of Substitution
HDP	Hypochlorite/Chlorine dioxide/Peroxide
HEC	Hydroxyethylcellulose
HP	Hydroxypropoxyl content
HPC	Hydroxypropyl cellulose
HPMC	Hydroxypropylmethylcellulose
IR	Infra Red

ISO	International organization for standardization
LC	Lantana camara
MC	Methylcellulose
MCA	Monochloroacetic acid
MS	Molar Substitution
PH	Parthenium hysterophorus
PO	Propylene oxide

2.1 Introduction

2.1.1 Cellulose and Its Sources

Cellulose, the most abundant renewable and biodegradable polymer, is the promising feedstock for the production of chemicals for their applications in various industries. Annual production of cellulose in nature is estimated to be 10^{11} – 10^{12} t in two forms, partially in a pure form, for example seed hairs of the cotton plant, but mostly as hemicelluloses in cell wall of woody plants (Klemm et al. 1998). The versatility of cellulose has been reevaluated as a useful structural and functional material. The environmental benefits of cellulose have become even more apparent (Hon 1996a). Cellulose is revered as a construction material, mainly in the form of intact wood but also in the form of natural textile fibers like cotton or flax, or in the form of paper and board. The value of cellulose is also recognized as a versatile starting material for subsequent chemical transformation in production of artificial cellulose-based threads and films as well as of a variety of cellulose derivatives for their utilization in several industries such as food, printing, cosmetic, oil well drilling, textile, pharmaceutical, etc. and domestic life.

Cellulose can be derived from a variety of sources such as woods, annual plants, microbes, and animals. These include seed fiber (cotton), wood fibers (hardwoods and softwoods), bast fibers (flax, hemp, jute, ramie), grasses (bagasse, bamboo), algae (*Valonia ventricosa*), and bacteria (*Acetobacter xylinum*) (Nevell and Zeronian 1985). *A. xylinum* can synthesize extracellular pellicles of cellulose from glucose. Some simple marine animals such as tunicates deposit cellulose in their cell walls (Coffey et al. 1995). Besides cellulose, these materials also contain hemicelluloses, lignin, and a comparable small amount of lignin. Wood and cotton are the raw materials for commercial production of cellulose. Cellulose serves as a structural material within the complex architecture of the plant cell walls with variation in its content. In wood, it constitutes about 40–50%; in leaf fibers: sisal fibers (55–73%), in bast fibers: flax 70–75%, hemp 75–80%, jute 60–65%, ramie 70–75%, kenaf 47–57%, in canes: bamboo 40–55%, baggase 33–45%, and in cereal straw: barley 48%, oat 44–53%, rice 43–49%, rye 50–54%, wheat 49–54%. Cotton seed hairs, the purest source, contain 90–99% of cellulose (Hon 1996b; Han and Rowell 1996).

2.1.2 Chemical Functionalization of Cellulose

Among the polysaccharides, the structure of cellulose is unique and simple. However, this influences its chemical reactions significantly. Cellulose being rigid, highly crystalline, and insoluble in common organic solvents is an ideal structural engineering material (Hon 1996b; Mathur and Mathur 2001). Cellulose is a polydisperse, linear, syndiotactic polymer. Its basic monomeric unit is D-glucose (anhydroglucose unit, AGU), which links successively through a β -configuration between carbon 1 and carbon 4 of adjacent units to form a long chain 1,4 glucans (Mathur and Mathur 2001). Two glucose molecules react to form a cellobiose which is the basic chemical unit of a cellulose molecule. The pyranose rings are in the 4C_1 conformation, which means that the $-\text{CH}_2\text{OH}$ and $-\text{OH}$ groups as well as glycosidic bonds are all equatorial with respect to the mean planes of the rings. The hydroxyl groups at both ends of the cellulose chain show different behavior. The C-1 end has reducing properties, while the glucose end group with a free C-4 hydroxyl group is nonreducing.

When the cellulose molecule is fully extended it takes the form of a flat ribbon with hydroxyl groups protruding laterally and capable of forming both inter- and intramolecular hydrogen bonds. Intramolecular hydrogen bonding between adjacent anhydroglucose rings enhances the linear integrity of the polymer chain and affects the reactivity of the hydroxyl groups, particularly of the C-3 hydroxyl group, which hydrogen binds strongly to the ring oxygens on adjacent anhydroglucose units. The surface of ribbons consists mainly of hydrogen atoms linked directly to carbon and is therefore hydrophobic. These two features of cellulose are responsible for its supramolecular structure, and this in turn determines many of its chemical and physical properties. In the fully extended molecule adjacent chain units are oriented with their mean planes at an angle of 180° to each other. Thus the repeating unit in cellulose is the AGU and the number of repeating units per molecule is half the Degree of Polymerization (DP) (Nevell and Zeronian 1985).

The size of cellulose molecule occurring in nature is indicated by its chain length or DP, which is average value of the number of monomer units. The DP of cellulose can be determined by various physical methods such as intrinsic viscosity measurements, light scattering, etc. DP of cellulose is heavily dependent on source. For example, cellulose obtained from cotton fibers, cotton linters, baggase, and wood fibers have DP 8,000–14,000; 1,000–6,500; 700–900; and 8,000–9,000, respectively. The DP or molecular weight distribution in many cases profoundly influences the mechanical, solution, biological, and physiological properties of cellulose and has given very useful clues for the designing of effective cellulose derivatives (Hon 1996b).

The abundance of hydroxyl groups and concomitant tendency to form intra- and intermolecular hydrogen bonds results in the formation of linear aggregates. In the solid state, highly ordered crystalline areas are interspersed between less ordered amorphous zones. These amorphous zones are regions in which the hydroxyl groups are more readily available for reaction than in the more highly ordered crystalline areas, which are less reactive (Coffey et al. 1995). The ratio of amorphous cellulose to crystalline cellulose is called degree of crystallinity which depends upon the species

and pretreatment of the sample (Fink et al. 1995). For instance, the degree of crystallinity of cellulose derived from bacteria, cotton, and *Valonia* algae is about 75%, 40–45%, and 93%, respectively (Kulshreshtha and Dweltz 1973; Yamamoto and Horii 1993; Osullivan 1997).

Degree of crystallinity plays an important role in chemical functionalization of cellulose. Cellulose contains 31.48% by weight of hydroxyl groups (one primary and two secondary per AGU), accessibility of these present enormous opportunities for preparing useful derivatives. Reactivity of these hydroxyl groups varies according to the reaction medium in which functionalization is done. For example, the order of reactivity for etherification performed in an alkaline medium is $2 > 6 > 3$ while the primary hydroxyl group (OH-6) is the most active in esterification (Hon 1996b). The type, distribution, and uniformity of substituents groups determine the properties of derivatives. (Nicholson and Meritt 1985). The average number of hydroxyl groups replaced by the substituents is the degree of substitution (DS); the maximum is three. For example, in a cellulose ether with a DS 1.5, 50% of the hydroxyl groups are etherified and 50% are free, to average 1.5 substituent moieties per anhydroglucose unit. When the side chain formation is possible, as for example in hydroxypropylation, molar substitution (MS) is used to denote the length of the side chain, and the value can exceed three. If the DS value is known for a substitution, the average chain length of the ether side chain can be calculated from the ratio of MS to DS (Hon 1996b).

In 1838, Payen recognized cellulose as a definitive substance and coined the name cellulose (Zugenmaier 2008). The functionalization of cellulose was utilized extensively, even when its polymeric nature was not determined and understood, as evidenced from the discovery of cellulose nitrate by Schonbein (1846), the preparation of Schweizer's reagent, that is, a cuprammonium hydroxide solution, the first cellulose solvent (Schweizer 1857) in 1857, the synthesis of an organosoluble cellulose acetate by Schutzenberger in 1865 (Cross and Bevan 1907), and artificial fibers in 1892 (Menachem 2006). The partially nitrated ester of cellulose is well known among the first polymeric materials used as a "plastic" under the trade name of celluloid. Cellulose nitrates of higher N-content have been used extensively for military purposes. Cellulose nitrate is the only inorganic cellulose ester of commercial interest (Balsler et al. 1986). Other derivatives such as methyl-, ethyl-, hydroxyalkyl ethers, mixed ethers/esters like ethylhydroxyethyl, hydroxypropyl methyl cellulose, cellulose acetopropionates, and acetobutyrate are still important, many decades after their discovery.

Chemical functionalization of cellulose include reactions of hydroxyl groups such as esterification, etherification, intermolecular crosslinking reactions, and macrocellulosic free radical reactions, particularly in the formation of graft cellulose copolymers (Arthur 1986) to increase the usefulness of cellulose by altering its properties. These cellulose derivatives are grouped according to the processes and substituents, for instance, esters- cellulose acetate through esterification and ethers- methyl cellulose/cyanoethyl cellulose/carboxymethyl cellulose (CMC) via etherification. Chemical functionalization continue to play a dominant role in improving the overall utilization of cellulosic polymers. The accessibility to hydroxyl groups and their reactivity open prospects for preparation of specific molecular structures for

future applications. Broader and more specialized applications of advanced and trend setting materials based on this unique and renewable macromolecule will increase the demand for more diverse synthesis paths and derivatives (Heinze and Liebert 2001).

The esters of cellulose with inorganic and organic acids were the first chemically modified cellulose derivatives (Klemm et al. 1998). Among the more than 100 cellulose esters developed, only a few of them including nitrates, acetates, and mixed esters of acetic acid and propionic acid, acetic acid and butyric acid, and acetic acid and phthalic acid have industrial applications (Hon 1996b). Cellulose acetate is extensively used in fibers, plastics, and coatings and thus becomes the universally recognized and the most important organic ester of cellulose.

2.1.3 Applications of Cellulose Derivatives

Cellulose derivatives, being of natural origin, have diverse physicochemical properties because of the kind of substituents, DS, molecular weights and DP and are revered for their large scale use mainly as additives of fine/special chemicals in textile, pharmaceutical, cosmetic, food, and packaging industries (Balsler et al. 1986; Barndt 1986). Cellulose derivatives of commercial importance belong to water or organic solvents such as soluble ethers or esters (Table 2.1). Nevertheless, cross linked and graft copolymers of cellulose are also of significant industrial importance.

Despite the large variety of cellulose derivatives that have been made, there is continuous expansion in the worldwide market of cellulose ethers because of their availability, economic efficiency, easy handling, low toxicity, and great variety of types. Combined effects of flow control, stabilization, water retention, film formation, etc. provided by cellulose ethers are not generally obtainable by the use of fully synthetic polymers. Cellulose ethers such as CMC, hydroxypropyl cellulose (HPC), cyanoethylcellulose (CEC), ethylcellulose (EC), methylcellulose (MC), hydroxyethylcellulose (HEC), hydroxypropylmethylcellulose (HPMC), carboxymethylhydroxyethylcellulose (CMHEC), etc. have gained their position in the market due to their multifunctional properties. The worldwide annual production of cellulose ethers is estimated to be over 300,000 metric ton (Schweizer and Sorg 1995). They exhibit useful properties of thickening, thermal gelation, surfactancy, film formation, and adhesion. Further they are kinetically and thermodynamically more stable and appear easy to prepare and characterize. These characteristics earn them applications in areas such as pharmacy, cosmetics, food, oil drilling, paper, paint, textiles, construction, and adhesives (Davidson 1980; Whistler and BeMiller 1973; Nicholson and Meritt 1985). Among cellulose derivatives, cellulose ethers constitute the only food allowed group of modified celluloses.

Crosslinking of cellulose, in heterogeneous systems, with formaldehyde or formaldehyde adducts of urea, melamine, or carbamates impart dimensional stability to cellulosic textile and paper products (Nicholson and Meritt 1985). A range of polymers, to obtain a better balance of properties for the commercial application of

Table 2.1 Some commercially marketed cellulose esters and ethers (Arthur Jr 1986)

Cellulose derivatives	DS range	Solubility	Product applications
Cellulose esters			
Nitrate	1.5–3.0	MeOH, PhNO ₂ , ethanol-ether	Films, fibers, explosives
Acetate	1.0–3.0	Acetone	Films, fibers, coatings, heat and rot resistant fabrics
Cellulose ethers			
Methyl	1.5–2.4	Hot H ₂ O	Food additives, films, cosmetics, greaseproof paper
Carboxymethyl	0.5–1.2	H ₂ O	Food additives, fibers, coatings, oil-well drilling muds, paper size, paints, detergents
Ethyl	2.3–2.6	Organic solvents	Plastics, lacquers
Hydroxyethyl	Low DS	H ₂ O	Films
Hydroxypropyl	1.5–2.0	H ₂ O	Paints
Hydroxypropylmethyl	1.5–2.0	H ₂ O	Paints
Cyanoethyl	2.0	Organic solvents	Products with high dielectric constants, fabrics with heat and rot resistances

polymeric materials, can be synthesized by graft copolymerization of cellulose. By minimizing degradation, copolymerization reactions of cellulose could result in retaining of the desirable properties of the natural molecule giving it additional properties through the added polymer. Cellulose graft copolymers find a wide array of applications in construction (wood plastic composites), furniture and industrial parts, sporting goods, woodcarving, textiles, and pulp and paper. They are also used as thickeners, absorbents, and in making ion exchange fibers and extrudable composites (Hebeish and Guthrei 1981).

2.2 Status of Research on Chemical Functionalization of Cellulose Derived from Nonconventional Sources

Renewable raw materials are gaining considerable importance because of the limited existing quantities of fossil supplies, escalating cost and problem of nonbiodegradability of petroleum-based polymers, and the recent environment-conservative regulations. The chemical industry is estimated to meet about 10% of its raw material needs from the renewable raw materials (Clasen and Kulicke 2001). Natural polymers are of renewable nature, hence, environment-friendly and cost-effective technologies can be developed by functionalization of these polymers. In this regard, cellulose rich biomass acquires enormous significance as chemical feedstock, since it consists of cellulose, hemicellulose, and lignin, which contain many functional groups suitable to chemical functionalization (Barkalow and Young 1985). The limitation of insolubility of cellulose in water can be overcome and spectrum of its industrial applications can be widened by functionalized to water-soluble forms. Various polymer analogous reactions could be used to modify the cellulose and its derivatives can be used as substitutes of petrochemicals in getting some important polymers including thermoplastics.

The conventional sources of cellulose are wood pulp and cotton linters. However, global efforts are going on to search for cellulose biomass from other sources as a feedstock as an alternative to expensive cotton linters, and wood pulp which now-a-days are discouraged due to environment conservative regulations. Annual plants are considered as potential resource because of their higher yield of cellulose than wood (McDougall et al. 1993; Atchison 1996; Han 1998), lower lignin contents, looser fibril structure than wood, consumption of less pulping chemicals and energy (McDougall et al. 1993; Han and Rowell 1996; Oggiano et al. 1997), have same main chemical components as woody plants, i.e., cellulose, hemicellulose, lignin, and extractives, ease of cultivation, harvesting and transportation (McDougall et al. 1993). Under the consideration of the economical objective, the environment influence, the sufficient supply, and the higher yield of cellulose, annual plants are now gradually substituting woods as alternative resources of cellulosic products. Investigations have shown that annual plants such as *Miscanthus sinensis*, *Cynara cardunculus*, flax, hemp, jute, sisal, and abaca could be used as new alternative sources for production of methyl cellulose (Daiyong 2005).

Agricultural wastes, for example, rice straw, sugarcane bagasse, saw dust, cotton stables (Hebeish, et al. 1984), orange mesocarp (Akaranta and Osugi 1997), and weeds, *Eichoria crassipes* (Barai et al. 1997), have been used as a base material for production of CMC differing in their DS and properties using different set of reaction conditions depending upon the DP and composition of the cellulosic material. Reactivity of fibers of *Agave lechuguilla* and *Agave fourcroydes* toward chemical functionalization such as carboxymethylation, sulfation, acetylation, tritylation, and subsequent carboxymethylation as well as oxidation and grafting has been studied, which has demonstrated the suitability of the agave fibers as a potential feedstock for producing cellulose derivatives for a variety of applications (Vieira et al. 2002; Ramos et al. 2005; Cruz et al. 1999). Graft copolymerization of acrylonitrile and methyl methacrylate onto jute fibers and pineapple leaf fibers has been examined (Patra and Singh 1994; Patnaik et al. 1989; Ghosh and Ganguly 1994; Samal and Bhuyan 1994). Low-quality woods as well as industrial wastes of wood have been utilized to produce a thermoplastic material through cyanoethylation (Khalil and El-Wakil 2000). The goal of these functionalizations is to increase the utilization of this abundantly available cellulose biomass from nonconventional sources.

2.3 Chemical Functionalization of Cellulose Derived from Nonconventional Biomass *Dendrocalamus strictus* (DCS) and Noxious Weeds *Lantana camara* (LC) and *Parthenium hysterophorus* (PH)

Identification of biopolymers from different plant sources, their isolation, and subsequent chemical functionalization for varied applications has been one of the research programs of the Chemistry Division, Forest Research Institute, Dehra Dun

(Sharma 2003; Gupta 2005; Bhatt 2004; Bansal 2005; Rana 2006; Sharma 2007; Pandey 2008; Goyal 2008). A technology for production of α -cellulose of high DP (800–3,000), high purity (>95%), and high brightness (>80%) derived from cotton linters, bamboo, eucalyptus, and bagasse was developed.

L. camara L. (Verbenaceae) and *P. hysterophorus* L., (Helianthae: Asteraceae) are noxious weeds, which have imposed a great threat to land productivity, grazing livestock, human health, biodiversity, and consequently to the overall ecology (Sharma et al. 1988; Pass 1991; Evans 1997). Attempts to manage these weeds using mechanical, chemical, and biological means have been made but met with limited success on account of their inbuilt limitations such as high cost, impracticability, environmental safety, temporary relief, etc (Sharma 2004; Jayanth 1987; Jayakumar et al. 1989). Alternatively, luxuriant growth and vigorous survival make these weeds of potential economic value for utilization of their abundantly available biomass into value added products offering thereby an efficient and effective method for their management. During the last few years, research has been conducted to utilize the lantana biomass for development of furniture products, baskets, mulch, compost, drugs, and other biologically active agents (Sharma and Sharma 1989; Inada et al. 1997; Sharma 2004).

Bamboo, belonging to the grass family Poaceae, is an abundant renewable natural resource capable of producing maximum biomass per unit area and time as compared to counterpart timber species (Tewari 1995). The chemical composition of *D. strictus* has been studied, which was found to contain Cross and Bevan cellulose 68.0% and lignin 32.20% (Singh et al. 1991). Its hemicellulose (18.8%) has also been shown to consist of xylose 78.0%, arabinose 9.4%, and uronic acid 12.8% (Tewari 1995).

Driven by the challenges to explore and increase the usefulness of cellulosic biomass from nonconventional sources, possibility for chemical functionalization of cellulose rich biomass derived from bamboo, *D. strictus* (DS) and noxious weeds – *L. camara* (LC) and *P. hysterophorus* (PH) for their utilization was examined.

2.3.1 Proximate Analysis of Biomass

L. camara and *P. hysterophorus* used in the study were collected from the field of the institute's campus. All the chemicals used were of laboratory grade. Plant materials were reduced to chips of 1–2 in. size and air dried. Chips were reduced to dust, and the dust passing through 40 mesh and retained on 60 mesh were taken for studies. Proximate chemical composition of the plant material was studied using the standard methods to assess the quality and solubility of raw material for further processing and results of the analysis are presented in Table 2.2.

Table 2.2 Proximate chemical composition of *Lantana camara* (LC) and *Parthenium hysterophorus* (PH)

Sl. No.	Parameters	Value%		Method used
		LC	PH	
1	Hot water solubility	7.0	11.25	APPITA P 4 M-61
2	1% NaOH solubility	18.0	22.5	APPITA P 5 M-61
3	Alcohol–benzene solubility	4.45	5.89	APPITA P 7 M-70
4	Holocellulose	71.34	78.0	TAPPI 9 m-54
5	α -cellulose	64.91	65.0	TAPPI T-203 OM 88
6	Pentosans	13.0	15.86	TAPPI T-203 OM 84
7	Lignin	27.25	17.2	TAPPI T-222 OM 88
8	Ash	1.8	2.1	APPITA P3 M-69

2.3.2 Isolation of α -Cellulose

The air-dried chips were subjected to following treatments. The conditions at each stage were optimized and 1 Kg production of α -cellulose [yield 35% (DCS), 38.76% (LC), and 37.4% (PH) and Brightness 80% (DS), 81.0% (LC), and 80.0% (PH) ISO] was carried out under optimized conditions.

2.3.2.1 Water Prehydrolysis

The chips were prehydrolyzed in autoclave keeping bath ratio 1:4 at 100°C for 30.0 min (DCS and LC)/1:5 at 100°C for 30.0 min (PH). The yield after prehydrolysis was 96.5%, 95.5%, 92.2%, respectively.

2.3.2.2 Alkali Hydrolysis

Water prehydrolyzed chips were treated with 2% alkali as NaOH. The bath ratio was maintained 1:4 (DCS)/1:4 (LC)/1:5 (PH) and heated in autoclave to 130°C (DCS)/120°C (LC)/130°C (PH) for 60 min. The yield was 94.4%, 85.9%, and 87.4%, respectively.

2.3.2.3 Pulping

The pulping of alkali hydrolyzed chips was carried out with 20% (DCS)/20% (LC)/18% (PH) alkali as NaOH at 170°C for 120 min (DCS)/90.0 min (LC)/60 min (PH). The kappa number of the pulp was 24, 26, 23 and pulp yield was 45.8%, 48%, and 45.6% with 3.2–3.8%, 1.2% screen rejects, respectively.

2.3.2.4 Bleaching

Bleaching was carried out using HDP sequence.

Table 2.3 Characteristics of the cellulose isolated from *Dendrocalamus strictus* (DCS), *Lantana camara* (LC), and *Parthenium hysterophorus* (PH)

Characteristics of cellulose	Value (%)			Method used
	DCS	LC	PH	
α -cellulose	90.09	94.80	90.82	TAPPI T2003 OM-88
β -cellulose	3.9	2.5	3.2	
γ -cellulose (by difference)	5.0	1.42	1.2	
Lignin	0.44	0.80	4.0	TAPPI T-222
Ash	0.56	0.48	0.98	APPITA P3 M-69
Av. DP	816	430	661.5	SCAN 15

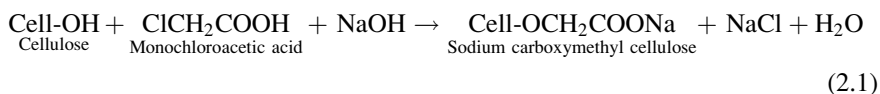
Cellulose obtained as above was characterized for its DP and composition and are presented in Table 2.3 DP was determined by CED viscosity method using following formula:

$$DP^{0.905} = 0.75 (\eta), \text{ where } \eta \text{ is intrinsic viscosity.}$$

2.3.3 Etherification of α -Cellulose

2.3.3.1 Carboxymethylation

A typical carboxymethylation method involving given below two competitive reactions was followed.



Carboxymethylation was conducted in two steps alkalization and etherification under heterogeneous conditions and the process was optimized with respect to DS by varying the reaction parameters such as concentration of NaOH, monochloroacetic acid (MCA), temperature, and duration of reaction. Each of these parameters was varied one by one keeping the remaining parameters constant as shown in Table 2.4. The alkalization consisted of addition of varied amount of aqueous NaOH to vigorously stirred slurry of α -cellulose (3 g) in iso-propanol (80 ml)/12.5% aq. iso-propanol (in case of PH) over a period of 30 min. Stirring was continued for another 60 min. Then varied amount of monochloro acetic acid dissolved in 10 ml iso-propanol was added under continuous stirring and the reaction mixture was heated upto the desired temperature and stirred at that temperature for fixed duration. After neutralizing the excess alkali with acetic acid, the CMC samples were filtered, washed with 70% aq. methanol, followed by absolute methanol, and dried at 60°C in oven. Yield: 110–124% (DCS), 110–133% (LC), and 140–150% (PH). Using the optimized set of reaction conditions as presented in Table 2.5,

Table 2.4 Reaction parameters for carboxymethylation of α -cellulose isolated from *Dendrocalamus strictus* (DCS), *Lantana camara* (LC), and *Parthenium hysterophorus* (PH)

Reaction parameters	DCS	LC	PH
Aq. NaOH concentration, temp. (°C)	2.5–12.5M 28	3.24 (mol/AGU); 10–40%; 25	3.89 (mol/AGU); 18–70% 25
MCA (mol/AGU)	1.80–2.55	1.55–2.30	0.98–2.48
Temperature of carboxymethylation (°C)	35–65	35–65	45–65
Duration of carboxymethylation (h)	1.5–5.5	1.5–4.5	3–6

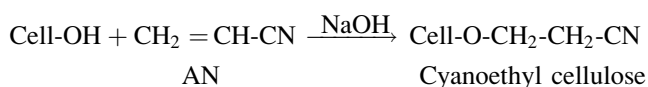
Table 2.5 Optimized reaction parameters for preparing CMC from α -cellulose isolated from *Dendrocalamus strictus* (DCS), *Lantana camara* (LC), and *Parthenium hysterophorus* (PH)

Reaction parameters	DCS	LC	PH
Aq. NaOH concentration, temp. (°C)	10M	3.24 (mol/AGU); 20%	3.89 (mol/AGU); 60%
MCA (mol/AGU)	1.80	2.05	1.98
Temperature of carboxymethylation (°C)	4.5	3.5	5.0
Duration of carboxymethylation (h)	55	55	55

water-soluble Na-CMC of degree of substitution 0.98 (DCS), 1.22 (LC), and 1.33 (PH) could be prepared (Varshney et al. 2005; Khullar et al. 2007).

2.3.3.2 Cyanoethylation

A typical cellulose etherification involving Michael addition of an activated C=C bond of acrylonitrile (AN) to a partially anionized cellulosic hydroxyls in an aqueous alkaline medium represented below was employed.

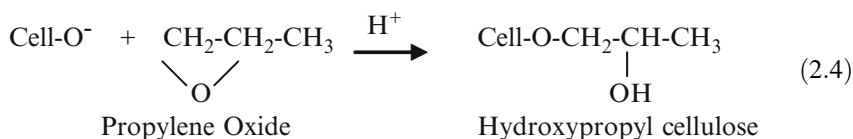
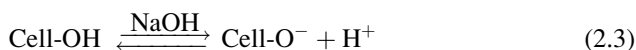


Cellulose (2 g) obtained from bamboo was cyanoethylated by first converting it into alkali cellulose using 20 ml of aqueous sodium hydroxide solution (8–14% by weight) for 1 h at temperature varying between 20 and 40°C followed by squeezing alkali from alkali cellulose up to three times the weight of the cellulosic material. The alkali cellulose was then dispersed in a large excess of acrylonitrile (70–90 mol/AGU) and reacted at a certain temperature for a fixed duration varying from 45 to 60°C and 0.5 to 1.25 h, respectively. During this reaction, the cyanoethylcellulose is dissolved in an excess of acrylonitrile to yield a homogenous solution. Each of these parameters was altered one by one keeping the remaining parameters constant in the reaction in order to optimize the reaction conditions for the production of CEC of maximum degree of substitution. The reaction was stopped by adding an excess of 10% aqueous acetic acid and was subsequently precipitated from this still

homogenous reaction mass by an excess of ethanol/water mixture (1:1, v/v), filtered, washed first with hot and then with cold water followed by drying in vacuum at 60°C (Yield: 124–145%). Using the optimized set of conditions, viz aqueous NaOH concentration 12%, alkalization temperature 20°C, acrylonitrile concentration 90 mol/AGU, cyanoethylation time 0.75 h, and temperature 55°C, an organosoluble CEC of DS 2.2 could be prepared (Khullar et al. 2008).

2.3.3.3 Hydroxypropylation

A typical hydroxypropylation reaction shown below was used.



The reaction was carried out in two steps – alkalization and etherification of cellulose under heterogeneous conditions and the process was optimized with respect to percent hydroxypropoxyl content (% HP) by varying the process parameters such as concentration of NaOH and propylene oxide (PO), temperature, and duration of reaction and studying their effect on the hydroxypropoxyl content. Each of these parameters was varied one by one keeping the remaining parameters constant in the reaction as shown in Table 2.6. The alkalization was carried out by adding varying amount of aqueous NaOH to slurry of finely pulverized cellulose (1.0 g) in iso-propanol (10 ml) at ambient temperature, with continuous stirring for 1 h (DS), while in case of PH for 0.5 h. Alkali cellulose thus formed was pressed to remove alkali and transferred to a three-necked round-bottom flask of capacity 250 ml, fitted with a coiled condenser and nitrogen inlet. Ice-cold water was circulated in the condenser throughout the reaction. Varied amount of propylene oxide (PO) in iso-propanol (50 ml) and water (2 ml) were added and the reaction was allowed to proceed at desired temperature for fixed duration. After neutralizing the excess alkali with acetic acid, the synthesized HPC samples were dissolved in water and precipitated in acetone, filtered and washed in acetone, and dried at 60°C in oven [Yield: 110–130% (DCS), 105–144% (PH)]. The standardized reaction

Table 2.6 Reaction parameters for hydroxypropylation of α -cellulose isolated from *Dendrocalamus strictus* (DCS) and *Parthenium hysterophorus* (PH)

Reaction parameters	DCS	PH
Aq. NaOH concentration (w/v%)	14–26	18 (0.5–2.0 mol/AGU)
Propylene oxide (mol/AGU)	11.6–29	11.6–38.9
Temperature of hydroxypropylation (°C)	30–60	60–80
Duration of hydroxypropylation (h)	2–5	2–4

Table 2.7 Optimized reaction parameters for hydroxypropylation of α -cellulose isolated from *Dendrocalamus strictus* (DCS) and *Parthenium hysterophorus* (PH)

Reaction parameters	DCS	PH
Aq. NaOH concentration (w/v%)	22	1.0 mol/AGU; 18%
Propylene oxide (mol/AGU)	17.4	34.77
Temperature of hydroxypropylation ($^{\circ}$ C)	50	70
Duration of hydroxypropylation (h)	4	3

conditions as shown in Table 2.7 afforded to produce water-soluble HPCs [soluble content 82%, 80.5% and hydroxypropoxyl content 65.89%, 67.75% (DCS and PH, respectively)] (Sharma et al. 2008).

2.3.4 Characterization and Rheology of the Optimized Derivatives

The IR spectra of all the optimized CMCs, CEC, and HPCs were recorded in KBr pellets. Typical absorptions of the cellulose backbone as well as bands at $1605\text{--}35\text{ cm}^{-1}$ [ν_{as} (COO $^{-}$); $1420\text{--}21\text{ cm}^{-1}$ ν_{s} (COO $^{-}$)] characterized for carboxymethyl ether group were observed in all the CMCs. Besides the typical signals of cellulose backbone (ν_{OH} $3,443\text{ cm}^{-1}$, ν_{CH} $2,862\text{ cm}^{-1}$, $1,415\text{ cm}^{-1}$, ν_{COC} $1,057\text{ cm}^{-1}$, ν_{β} -linkage 890 cm^{-1}), the IR spectra of the optimized CEC displayed a characteristic absorption band at $2,253\text{ cm}^{-1}$ for the nitrile group ($\text{--C}\equiv\text{N}$) introduced and the intensity of the band at $2,891\text{ cm}^{-1}$ characteristic for --CH_2 group is increased, furnishing thereby the evidence that cyanoethylation has occurred. The IR spectra of the optimized HPC displayed, besides the typical signals of cellulose backbone (ν_{OH} $3,398\text{ cm}^{-1}$, ν_{CH} $2,890\text{ cm}^{-1}$ and $1,419\text{ cm}^{-1}$, ν_{COC} $1,060\text{ cm}^{-1}$, ν_{β} -linkage 890 cm^{-1}), a shoulder at $2,974\text{ cm}^{-1}$, which was assigned to the --CH stretching of the methyl group characteristic for the hydroxypropyl group, furnishing thereby the evidence that hydroxypropylation has occurred. Further evidence of hydroxypropylation was revealed by comparing the Scanning Electron Microscope images for parent and the HPC obtained at magnification 1,000 and 5,000 (Sharma et al. 2008), which depicted the transformation in surface morphology of bamboo cellulose on hydroxypropylation. The parent bamboo cellulose exhibited a relatively smooth surface compared with HPC and deposition of PO on the surface and in the intercellular region of the bamboo cellulose fiber was clearly visible.

The DS of the CMC (LC and PH) samples determined by the standard method (Green 1963) was found to be 1.22 and 1.33, respectively, while in case of CMC derived from bamboo cellulose (DCS), this was calculated from its mole fractions after complete depolymerization of polymer chains by HPLC (Heinze et al. 1994) as 0.98. The DS of the optimized CEC sample was calculated from the N content using the equation $\text{DS} = 162 \times \%N/1,400 - (53 \times \%N)$ was 2.2. Nitrogen content was determined by the Kjeldahl's method. The percent hydroxypropoxyl content in HPCs determined by UV spectrophotometric method (Jhonson 1969) were found to be 65.89% (DCS) and 67.75% (PH).

One of the most important properties of CMC and HPC utilized in their wide range of practical applications is their ability to impart viscosity to the aqueous solutions. Each polymer chain in a dilute solution of CMC is hydrated and extended, and exhibits a stable viscosity. In aqueous solution, it represents a complex rheological system as it forms aggregates and associations, and hence higher-level structures (Kulicke et al. 1999). The viscosity is greatly influenced by polymer concentration, temperature, salt content, molecular structure, and the presence of surfactants (Edali et al. 2001; Kulicke et al. 1996; Ghannam and Esmail 1997). Consideration of the end uses for CMC and HPC make it immediately apparent that the rheological properties of the solutions of these cellulose derivatives are of prime importance. Rheological studies of the optimized CMCs and HPCs were, therefore, carried out by measuring apparent viscosity (η_{app}) of its 1% and 2% aqueous solutions using a Brookfield Digital Viscometer model “RVTD,” Stoughton, USA at different shear rates ranging from 3.4 to 34 s^{-1} at $25 \pm 10^\circ C$. The values of η_{app} (cps) of the solutions of the optimized products at both the concentrations [CMCs 75, 795 (DCS), 600, 7,500 (LC), 260, 2,255 (PH); HPCs 120–1,105 (DCS), 75, 745 (PH)] were observed to be dependent upon shear rate and decrease with increasing shear rate. No time effects were detected and the viscosity obtained with decreasing rate was identical with that obtained with increasing shear rate. Thus, the solutions of the optimized products exhibited non-Newtonian pseudoplastic behavior.

2.4 Conclusion

Continuously depleting limited fossil supplies, rising price, problem of nonbiodegradability of petroleum-based polymers, and the recent environment-conservative regulations have triggered search for nonconventional sources of cellulose biomass as feedstock for production of cellulose and its derivatives. Having initiated efforts in this direction, isolation and characterization of cellulose and its chemical functionalization to ethers from some nonconventional biomass were studied. The study contributed to find appropriate conditions for production of α -cellulose from bamboo, *D. strictus*, and two noxious weeds – *L. camara* and *P. hysterophorus* and its carboxymethylated, cyanoethylated, and hydroxypropylated derivatives. The present work demonstrated that these plants have the capacities to produce α -cellulose and its ethers for varied applications. The industry can utilize these biomass as an alternative feedstock to produce cellulose ethers. Therefore, a lot of wood will be saved. The work has also paved the way for management of these noxious weeds through their utilization into products of commercial importance.

Acknowledgments We duly thank the Director, Forest Research Institute, Dehra Dun, for encouragement and providing necessary facilities to carry out study. Financial support from the Indian Council of Forestry Research and Education (ICFRE), Dehra Dun, Department of Biotechnology (DBT), New Delhi, and World Bank under the KANDI IWDP (Hills II) scheme is gratefully acknowledged.

References

- Akaranta O, Osugi LC (1997) Carboxymethylation of orange mesocarp cellulose and its utilization in drilling mud formulation. *Cellulose Chem Technol* 31:195–198
- Arthur JC Jr (1986) In: Allen G, Bevington JC (eds) *Comprehensive polymer science*, Vol 6. Pergamon, Oxford
- Atchison JE (1996) Twenty-five years of global progress in nonwood plant fiber repulping. *TAPPI J* 79(10):87–95
- Balser K, Hoppe L, Eicher T, Wandel M, Astheimer HJ, Steinmeier H, Allen JM (1986) Cellulose esters. In: Gerhartz W, Stephen YY, Thomas CF, Pfefferkorn R, James F (eds) *Ullmann's encyclopedia of industrial chemistry*. Wiley, New York
- Bansal A (2005) Structural investigation of *Cassia tora* Linn. seed polysaccharides. Ph. D. thesis, Forest Research Institute, Deemed University, Dehradun, India
- Barai BK, Singhal RS, Kulkarni PR (1997) Optimization of a process for preparing carboxymethyl cellulose from water hyacinth (*Eichornia crassipes*). *Carbohydr Polym* 32:229–231
- Barkalow DG, Young RA (1985) Cellulose derivatives derived from pulp and paper mill sludge. *J Wood Chem Technol* 5:293–312
- Barndt L (1986) Cellulose ethers. In: Gerhartz W, Stephen YY, Thomas CF, Pfefferkorn R, James F (eds) *Ullmann's encyclopedia of industrial chemistry*. Wiley, New York
- Bhatt A (2004) Chemical investigation of *Kydia calysina* Rox. bark. Ph. D. thesis, Forest Research Institute, Deemed University, Dehradun, India
- Clasen C, Kulicke W-M (2001) Determination of viscoelastic and rheo-optical material functions of water soluble cellulose derivatives. *Prog Polym Sci* 26:1839–1919
- Coffey DG, Bell DA, Henderson A (1995) *Food polysaccharides and their application*. Marcel Dekker, New York
- Cross CF, Bevan EJ (1907) *Researches on cellulose*. Longman Green, London
- Cruz RA, Mendoza AM, Vieira MC, Heinze Th (1999) Studies on grafting of cellulosic materials isolated from *Agave lechuguilla* and *A. fourcroydes*. *Angew Makromol Chem* 273:86–90
- Daiyong Ye (2005) Preparation of methylcellulose from annual plants. Ph.D. Dissertation Graduate School of Rovira i Virgili University
- Davidson RL (1980) *Handbook of water soluble gums and resins*. McGraw-Hill, New York
- Edali M, Esmail MN, Vatistas GH (2001) Rheological properties of high concentrations of carboxymethyl cellulose solutions. *J Appl Polym Sci* 79:1787–1801
- Evans HC (1997) The potential of fungal pathogen as classical biological control agents for management of *Parthenium hysterophorus* L. In: Mahadevappa M and Patil VC (eds) *First international conference on Parthenium management*. Dharwad University of Agricultural Sciences, Dharwad, Karnataka, India
- Fink HP, Hofmann D, Philipp B (1995) Some aspects of lateral chain order in cellulose from X-ray scattering. *Cellulose* 2:51–70
- Ghannam MT, Esmail MN (1997) Rheological properties of carboxymethyl cellulose. *J Appl Polym Sci* 64:289–301
- Ghosh P, Ganguly PK (1994) Polyacrylonitrile (PAN)-grafted jute fibers: some physical and chemical properties and morphology. *J Appl Polym Sci* 52:77–84
- Goyal P (2008) Chemical modification of tamarind kernel powder. Ph. D. thesis, Forest Research Institute, Deemed University, Dehradun, India
- Green JW (1963) Carboxymethyl cellulose. In: Whistler RL (ed) *Methods in carbohydrate chemistry*, vol III. Academic, New York
- Gupta S (2005) Chemical modification of *Cassia occidentalis*. Ph. D. thesis, Forest Research Institute, Deemed University, Dehradun, India
- Han JS (1998) Properties of nonwood fibers. In: 1998 Proceedings of the Korean society of wood science and technology annual meeting 3–12
- Han JS, Rowell JS (1996) Chemical composition of fibers. In: Rowell RM, Young RA, Rowell J (eds) *Paper and composites from agrobased resources*. CRC, London

- Hebeish A, Guthrei JT (1981) The chemistry and technology of cellulosic copolymers. Springer, Berlin
- Hebeish A, Abou-Zied NY, Waly A, Higazy A (1984) Chemical modification of flax cellulose via etherification, esterification, and crosslinking reactions. *Cellulose Chem Technol* 22:591–605
- Heinze T, Liebert T (2001) Unconventional methods in cellulose fictionalization. *Prog Polym Sci* 26:1689–1762
- Heinze Th, Erler U, Nehls I, Klemm D (1994) Determination of the substitution pattern of heterogeneously and homogeneously synthesized carboxymethyl cellulose by using high-performance liquid chromatography. *Angew Makromol Chem* 215:93–106
- Hon DNS (1996a) Cellulose and its derivatives. In: Dumitriu S (ed) *Polysaccharides in medicinal applications*. Marcel Dekker, New York
- Hon DNS (1996b) Chemical modification of lignocellulosic material. Marcel Dekker, New York
- Inada A, Nakanishi T, Tokuda H, Sharma OP (1997) Antitumor activities of lantadenes on mouse skin tumors and mouse hepatic tumors. *Planta Med* 63:476–478
- Jayakumar R, Mahadevappa M, Joshi S, Prasad TG (1989) Dormancy studies in *Cassia sericea* seeds. *Seed Res* 17(2):118–121
- Jayanth KP (1987) Introduction and establishment of *Zygomma bicolorata* on *P. hysterophorus* at Bangalore, India. *Curr Sci* 56(7):310–311
- Jhonson DP (1969) Spectrophotometric determination of the hydroxypropyl group in starch ethers. *Anal Chem* 41:859–860
- Khalil EMA, El-Wakil NA (2000) Infrared absorption spectra of cyanoethylated cellulose fibers. *Cellulose Chem Technol* 34:473–479
- Khullar R, Varshney VK, Naithani S, Heinze T, Vieira-Nagel GPK, Naithani S, Soni PL (2007) Carboxymethylation of cellulose isolated from bamboo (*Dendrocalamus Strictus*) and its rheology. *Cellulose Chem Technol* 40(7):545–552
- Khullar R, Varshney VK, Naithani S, Soni PL (2008) Study of the influence of reaction conditions for production of cyanoethylcellulose from cellulosic material from bamboo (*Dendrocalamus strictus*). *J Nat Fibers* 5(2):138–147
- Klemm D, Phillip B, Heinze T, Heinze U, Wagenknecht W (1998) *Comprehensive cellulose chemistry*, vol 2. Wiley, Weinheim
- Kulicke WM, Kull AH, Thielking H, Engelhart J, Pannek JB (1996) Characterization of aqueous carboxymethylcellulose solutions in terms of their molecular structure and its influence on rheological behavior. *Polymer* 37(13):2723–2731
- Kulicke WM, Reinhardt Fuller UGG, Arendt O (1999) Characterization of the flow properties of sodium carboxymethylcellulose via mechanical and optical techniques. *Rheol Acta* 38:26–33
- Kulshreshtha AK, Dweltz NE (1973) Para crystalline lattice disorder in cellulose – 1. Reappraisal of the application of the two-phase hypothesis to the analysis of powder x-ray diffractograms of native and hydrolyzed cellulosic materials. *J Polym Sci* 11:487–497
- Mathur NK, Mathur V (2001) *Chemical Weekly*, July Edition, 155
- McDougall GJ, Morrison IM, Stewart D, Weyers JDB, Hillman JR (1993) Plant fibres: botany, chemistry and processing. *J Sci Food Agric* 62:1–20
- Menachem L (2006) *Handbook of fiber chemistry*. CRC, USA
- Nevell TP, Zeronian SH (1985) *Cellulose chemistry and its applications*. Ellis Horwood, Chichester York
- Nicholson MD, Meritt FM (1985) Cellulose ethers. In: Nevell TP, Zeronian SH (eds) *Cellulose chemistry and its applications*. Ellis Horwood, Chichester
- Oggiano N, Angelini LG, Cappelletto P (1997) Pulping and paper properties of some fibre crops. *Ind Crops Prod* 7(1):59–67
- Osullivan AC (1997) Cellulose: the structure slowly unravels. *Cellulose* 4:173–207
- Pandey N (2008) Chemical modification of alpha cellulose from *Lantana camara*. Ph. D. thesis, Forest Research Institute, Deemed University, Dehradun, India
- Pass MA (1991) Poisoning of livestock by Lantana plants. In: Keeler R, Tu AT (eds) *Handbook of natural toxins*, vol 6. Marcel Dekker, New York

- Patnaik S, Sarangi S, Mohanty AK, Singh BC (1989) Graft copolymerization of acrylonitrile onto jute fibers (Studies on Ce (IV)- hippuric acid redox system). *J Appl Polym Sci* 37: 2099–2107
- Patra CM, Singh BC (1994) Influence of N-acetylglycine on the kinetics of ceric ion-initiated graft-copolymerization of acrylonitrile and methyl-methacrylate onto jute fibers. *J Appl Polym Sci* 52:1557–1568
- Ramos LA, Frollini E, Heinze Th (2005) Carboxymethylation of cellulose in the new solvent dimethyl sulphoxide/tetrabutyl ammonium fluoride. *Carbohydr Polym* 60:259–267
- Rana V (2006) Chemical investigation of *Dalbergia sissoo* Rox. laef polysaccharides. Ph. D. thesis, Forest Research Institute, Deemed University, Dehradun, India
- Samal RK, Bhuyan BL (1994) Chemical modification of lignocellulosic fibers. 1. Functionality changes and graft polymerization of acrylonitrile onto pineapple leaf fibers – their characterization and behavior. *J Appl Polym Sci* 52:1675–1685
- Schweizer E (1857) Das Kupferoxyd-Ammoniak, ein Auflösungsmittel für die Pflanzenfaser. *J Prakt Chem* 72(1):109–111
- Schweizer D, Sorg C (1995) Cellulose ethers for cement extrusion. In: Kennedy JF, Phillips GO, Williams PA, Picullel L (eds) *Cellulose and cellulose derivatives: physico-chemical aspects and industrial applications*. Woodhead, England
- Sharma BR (2003) Chemical modification of polysaccharides for industrial applications. Ph. D. thesis, Forest Research Institute, Deemed University, Dehradun, India
- Sharma S (2004) Lantana-whose weed any way! Developing strategic directions for integrated utilization and control. In: Workshop on *Lantana camara*: Problems and Prospects (Volume of abstracts), organized by IIT, Delhi, HESCO, Dehra Dun and Department of Science & Technology (DST), Govt. of India at Dehra Dun from 10–11 Feb 2004
- Sharma R (2007) Studies on chemical modification of cellulose of different DP and their rheology. Ph. D. thesis, Forest Research Institute, Deemed University, Dehradun, India
- Sharma OP, Sharma PD (1989) Natural products of lantana plant – the present and prospects. *J Sci Ind Res* 48:471–478
- Sharma OP, Makkar HPS, Dawra RK (1988) A review of the poisonous plants *Lantana camara*. *Toxicon* 26:975–985
- Sharma R, Varshney VK, Naithani S, Chauhan GS, Soni PL (2008) Hydroxypropylation of cellulose (Av. DP 816) isolated from bamboo (*Dendrocalamus strictus*) with respect to hydroxypropoxyl content and rheological behavior of hydroxypropyl cellulose. *J Appl Polym Sci* 113(4):2450–2455
- Singh SV, Rai AK, Dhawan R (1991) *Advances in pulp and paper research in India*. ICFRE Publication 15, Dehra Dun
- Tewari DN (1995) A monograph on bamboo. International Book Distributors, Dehra Dun
- Varshney VK, Gupta PK, Naithani S, Khullar R, Bhatt A, Soni PL (2005) Carboxymethylation of α -cellulose isolated from *Lantana camara* with respect to degree of substitution and rheological behavior. *Carbohydr Polym* 63(1):40–45
- Vieira MC, Heinze Th, Antonio-Cruz R, Mendoza-Martinez AM (2002) Cellulose derivatives from cellulosic material isolated from *Agave lechuilla* and *A. fourcroydes*. *Cellulose* 9:203–212
- Whistler RL, BeMiller NJ (1973) *Industrial gum, polysaccharides and their derivatives*. Academic, New York
- Yamamoto H, Horii F (1993) CPMAS carbon-13 NMR analysis of the crystal transformation induced for Valonia cellulose by annealing at high temperatures. *Macromolecules* 26:1313–1317
- Zugenmaier P (2008) *Crystalline cellulose and derivatives: characterization and structures*. Springer, Berlin

Chapter 3

Production of Flax Fibers for Biocomposites

Jonn Foulk, Danny Akin, Roy Dodd, and Chad Ulven

Abstract Natural fibers for many and varied industrial uses are a current area of intense interest. Production of these fibers, furthermore, can add to farmer incomes and promote agricultural sustainability. Flax (*Linum usitatissimum* L.), which has been used for thousands of years, is unparalleled in supplying natural fibers for industrial applications as diverse as textiles and paper, providing high value linseed and fiber from a single plant, and maintaining sustainable agriculture in temperate and subtropical climates for summer or winter production, respectively. As a value-added replacement for glass fiber from a renewable resource, flax fiber is recyclable, biodegradable, and sustainable for the economy, ecology, and society. To the point, DaimlerChrysler reported that natural fibers for automotive components required 83% less energy and were 40% less expensive than glass fiber components. A better understanding of the fiber characteristics that influence composite performance could lead to the development of additives, coatings, binders, or sizing suitable for natural fiber and a variety of polymeric matrices. Stems of flax require retting to separate fiber from nonfiber components and rigorous mechanical cleaning to obtain industrial-grade fibers. Considerable work has been undertaken to improve the retting process using specific cell-free enzymes, especially pectinases, to control and tailor properties for industrial applications. Fiber processing and use in composites are affected by variables such as length, uniformity, strength, toughness, fineness, surface constituents, surface characteristics, and contaminants. One of the main concerns for the composite and other industries in incorporating natural fibers, such as flax, into production parts is the fiber variability resulting from crop diversity, retting quality, and different processing techniques. Standardized methods to assess flax fiber properties, therefore, are needed to maintain quality from crop to crop and provide a means to grade fibers for processing efficiency and applications. Other parts of the plant stalk, notably the waste shive and dust, can

J. Foulk (✉)

Cotton Quality Research Station, USDA-ARS, Ravenel Center room 10, Clemson, SC 29634, USA
e-mail: jonn.foulk@ars.usda.gov

potentially be utilized as coproducts to offset costs for producing the major products of fiber and seed.

Keywords Characteristics · Composites · Coproducts · Decortication · Flax fiber · Harvesting · Production · Quality · Retting · Textiles

Contents

3.1	Introduction	62
3.2	Characteristics of Flax Fibers	65
3.2.1	Physical characteristics	65
3.2.2	Chemical Characteristics	69
3.3	Processing of Flax Fibers	71
3.3.1	Production Techniques	71
3.3.2	Retting Methods	72
3.3.3	Harvesting Techniques	74
3.3.4	Decortication and Subsequent Processing	74
3.4	Fiber Characterization	77
3.5	Flax Coproducts	80
3.6	Fibers and Composite Formation	82
3.7	Conclusions	87
	References	87

3.1 Introduction

Flax (*Linum usitatissimum* L.) is grown predominantly in temperate climates and has been used by man since before it was a cultivated crop. Kavadze et al. (2009) identified 30,000-year-old wild-dyed flax fibers, indicating that prehistoric hunter-gatherers were making colorful cords for tools, baskets, or garments. Egyptian civilizations cultivated flax in the Nile Valley to produce fine fibers for textiles and industrial uses (Franck 1992). Koelkemoeck (1883) illustrated the antiquity of flax from the fine linen of Egypt to the purple and fine linen of Judea, reporting that linen manufacturing disappeared after the fall of the Roman Empire and reappeared in the tenth century due to the Flemish in the town of Ypres in Flanders. Throughout the Middle Ages and The Renaissance, flax and wool fibers were the major fibers in Europe, while hemp led in Japan and cotton in India (Franck 1992). Flax was an important commodity in Europe, and in 1531, Britain enacted a law requiring that for every 24 ha of land, one rood must be sown with flax or hemp (Bradbury 1920). Franck (1992) indicates that it was during the industrial revolution, where mechanical cotton spinning replaced hand spinning (flax spinning frames lagged behind those for cotton by ~40 years) and great quantities of inexpensive cotton produced by southern plantations in the US, that cotton ultimately replaced flax as the main vegetable fiber in the world.

In Europe, flax was traditionally grown, processed, and manufactured locally with the Baltic States known for linseed and fiber and Northern Ireland for fine linen

fabrics (Franck 1992). Fishler (1949) stated that Russia, Poland, and the Baltic countries accounted for 85–90% of the world's production. After World War II, European fiber flax growers adopted mechanical harvesters and processing machinery developed by USDA in Corvallis, Oregon (Ehrensing 2008). The largest area in the world under flax cultivation was the former Soviet Union which produced 3,788,000 tons of fiber (Mukhin 1992). According to Kozłowski (2009), the European Union presently supports flax with a subsidy of \$800/ha, and the leading producers of fiber flax are Belarus (78,500 ha), Belgium (12,030 ha), China (110,000 ha), France (67,000 ha), the Netherlands (2,500 ha), Russia (81,000 ha), and Ukraine (12,000 ha). Currently, European scutching facilities are located in Belgium, the Netherlands, France, Russian Federation, Ukraine, Belarus, and Poland, with leading spinning mills located in Italy, Belarus, and Russian Federation to supply flax fiber into cloth (54%), household goods (20%), technical applications (17%), and furniture coverings (9%) (Kozłowski 2009). The linen industry promotes its products with the Masters of Linen trademark (<http://www.purolino.it>) and the Irish Linen Guild trademark symbol (<http://www.irishlinen.co.uk>).

Flax is an agricultural crop that can provide food (Oomah 2001), fuel (Anonymous 1995), and fiber (Smeder and Liljedahl 1996) and is grown on 5 million ha worldwide (Myers 2000). Over the years, fiber and seed flax have been grown successfully across a large region of the U.S. (Stephens 1997a). Flax culture was brought to America by the early colonists, and flax fiber production was one of the earliest colonial industries encouraged on every person (Roland 1913). In 1638, Colonists established a textile mill in Massachusetts that produced linsey-woolsey, which was a coarse fabric consisting of linen and wool (Fisher 1981). In Connecticut, during the 1800s, the average yield was 224 kg of fiber ha⁻¹ with 15–20 bushels of seed ha⁻¹ (Stephens 1997a). Historically, flax of high quality (comparable to European grades) was commercially grown in eastern Michigan and in the Willamette Valley of Oregon, with smaller acreages grown in Washington, Minnesota, Wisconsin, and New York (Robinson and Hutcheson 1932). In 1915, the Oregon State legislature appropriated \$50,000 to create a flax-processing plant for developing a local flax industry that led to four additional mills built with private capital (Fishler 1949). In support of the effort for World War II, four other modern flax-processing mills were constructed in 1942, with two additional mills built in 1943 (Fishler 1949). Flax remained an important crop in Oregon (5,193 ha) and other areas of the US until withdrawal of government subsidies, improvements in cotton spinning, and introduction of synthetic fibers (Stephens 1997a). Presently, flax is grown primarily for its oilseed in North Dakota, South Dakota, and Minnesota, with some of the straw being used in papermaking (e.g., Schweitzer-Mauduit Inc., Alpharetta, GA), nonwoven production (e.g., FlexForm Technologies, Elkhart, IN), and composite applications (e.g., Composite America, Fargo, ND).

In the US, the commercial flax industry is located mostly in North Dakota and to a lesser extent in South Dakota and Minnesota. The flax is grown for seed in the summer. Several efforts, however, have been carried out to grow flax in the winter months (October to May) in the South Atlantic region of the US (Frederick et al. 1999 unpublished). Globally, the U.S. is the largest per capita consumer of flax

fiber, and all of the industrial grade fiber is imported. For example, in 2007, 2008, and 2009, the U.S. imported flax and linen (fiber, yarn, and fabric) with a customs value of \$184, \$224, and \$88 million dollars, respectively (<http://otexa.ita.doc.gov>, tariff and trade data from the US Department of Commerce). Commercially important flax fibers are historically known by two classes, namely oriented, long-line fiber for valued linen products and tow, or the short fiber by-product of long line production, for short staple textiles and composites. However, flax stems that are not grown specifically for high value linens may be processed to give “total fiber”, in which a single, nonoriented fiber product results. These cut fibers are usable in the short staple spinning and nonwoven units, which dominate North American textile mills, since no long-line flax fiber processing facilities operate in the US.

In contrast to the US, flax production in Canada is a large industry. Northwestern Canada is considered a great seed producing area with moderate rainfall, while Ontario is considered best for flax fiber due to increased precipitation (MacCracken 1916). According to MacCracken (1916), the beginnings of flax culture in Canada date back to the early pioneers and the ability for flax to produce textiles. Soon thereafter, flax processing facilities were built, and by 1891, 40 crude flax processing facilities existed that prospered under first and second generation immigrants from Ireland, Holland, and Germany (MacCracken 1916). Roland (1913) stated that in 1913, over 404,686 ha of flax (2 million tons of straw) were burned, but consideration should be given to the utilization of flax straw that exists in the same latitude as the best flax districts of Russia. Fiber flax was not seen as a permanent crop, and few operations felt the need for better agricultural operations, processing, mill improvement, or marketing improvements, and by 1910, only 15 mills existed for the 2,023 ha of fiber flax (MacCracken 1916).

In Canada, today, flax seed production for industrial, human, and animal consumption remains the main agricultural product produced from flax. Couture et al. (2004) evaluated reintroducing fiber flax production into eastern Canada. Depending on acreage planted and rainfall, the potential annual oilseed flax straw production in Canada is 500,000–1,000,000 tons, with fiber production approaching 250,000 tons (Anonymous 2006a). Schweitzer-Mauduit International in Canada produces the only flax fiber in North America from 100,000 to 200,000 tons annually of flaxseed straw purchased from farmers in Canada and the US for their hammer-mill decortication process (Hogue 2006). This flax fiber is known as Canadian tow and is baled into 136 kg bales for shipment to pulp mills for subsequent paper formation (Hogue 2006).

Renewed interest in flax is likely due in part to a worldwide environmental awareness (Mohanty et al. 2000), its historically recognized and excellent fiber properties (Morton and Hearle 1997), particularly as reinforcement for innovative industrial uses (Bogoeva-Gaceva et al. 2007), and the positive effects of its seed and oil on health (Muir and Westcott 2003). For example, feeding cattle a 10% flaxseed diet led to elevated levels of α -linolenic acid in muscle tissue, consequently producing positive health benefits to the consumer (Medeirosa et al. 2007). Chickens fed an enriched flaxseed diet provide eggs with omega-3 fatty acids and human health

benefits (Yannakopoulos 2007). As the nutritional benefits derived from flaxseed (omega-3 fatty acid, lignin, and dietary fiber content) have increased, the Mintel's Global New Products Database (<http://www.gnpd.com>) has reported 1,161 new US food products from 2003 to 2009 that contain flax. The importance of this latter point is emphasized by efforts by the U.S. Department of Agriculture and the US Food and Drug Administration to promote eating omega-3 fatty acids (Przybyla-Wilkes 2007). Ebskamp (2002) designated potential improvements for increasing fiber strength, softness, and hydrophobicity along with increasing yield and processing efficiency. Wrobel et al. (2004) indicate that the thermoplastic Poly- β -hydroxybutyrate (PHB) can be produced within the lumen of transgenic flax fibers, thus increasing its tensile strength. Lacoux et al. (2003) indicate that transgenic manipulation of pectin-related genes may lead to flax plants with improved retting capabilities. Flax stalks produce fibers that are lightweight, natural, renewable, and biodegradable for use in textiles, composites, or biocomposites, which produce valuable by-products including but not limited to industrial and food oils, waxes, pharmaceuticals, biofuels, and cosmetics. Indeed, the uses and new products from flax seem endless, fulfilling the scientific epithet *Linum usitatissimum* – linen most useful.

3.2 Characteristics of Flax Fibers

3.2.1 *Physical characteristics*

The flax plant is nature's composite with its strong bast fibers held together by matrix materials in bundles. These fiber bundles occur in the cortical region of the stem, located between the outermost cuticle–epidermis layer and the innermost, lignified tissues (shive). Flax fibers (3,000 times longer than its diameter) are considered strong and straight fibers without convolutions or crimp. Fiber dimensions greatly affect processing, and the multicellular flax fibers, which are bound together, consist of imprecise fiber dimensions and lengths. These fiber characteristics are highly variable and dependent upon many effects, such as species, maturity, growing location, retting, or extraction processes (Table 3.1). Shaw and Tabil (2007) estimate the physical properties of flax shives to have a geometric mean diameter of 0.64 mm ($\sigma = 0.37$ mm), bulk density of 108.0 kg/m³ ($\sigma = 22.0$ kg/m³), and particle density of 1,346.1 kg/m³ ($\sigma = 7.9$ kg/m³).

Zylinski (1964) reported younger and finer fibers at the top of the plant, with thicker fibers near the bottom of the stem. Soluble components in flax fiber impact the hygroscopic moisture handling characteristics (Table 3.2). Foulk et al. (2003) reports that late harvest stems are less easily retted than those harvested before full maturity while estimating the percent fiber contributed to total plant weight by the pedicel to be ~5% (Foulk et al. 2004). The plant stem has a diameter of 2–3 mm, which produces bast technical fibers with a diameter of 50–100 μ m composed of elementary fibers (single plant cells) with a diameter

Table 3.1 Fiber length, diameter, cell dimensions, density, electrical, frictional, and thermal properties

Fiber	Length (mm)	Diameter (μm)	Fineness (denier)	Cell length (mm)	Cell diameter (μm)	Density (g/cm^3)	Specific heat ($\text{cal}/\text{g}^\circ\text{C}$)	Porosity (%)	Coefficient of friction	Refractive index	Electrical resistance ($\log R_s$, 10% moisture) ($\Omega \text{ kg}/\text{m}^2$)	Shape
Cotton ^a	15–56	12–25	1–3.3	15–56	12–25	–	–	–	–	–	–	Round/oval
Cotton ^b	12–64	11.5–22	2.2	15–56	12–25	1.55	0.319	–	0.57	1.578	5.25	–
Cotton ^c	12.7–50.8	10–20	–	–	–	1.54	–	–	–	–	–	Flat ribbon
Cotton ^d	–	20–30	–	–	20–30	1.54–1.56	–	–	–	–	–	–
Cotton ^e	–	–	–	–	–	–	0.31	–	–	–	–	–
Flax ^a	20–140	40–62	1.7–17.8	4–77	5–76	1.5	–	10.7	–	–	–	Polygonal
Flax ^f	–	92–177	–	–	–	–	–	–	–	–	–	–
Flax ^b	200–1,400	12–20	1.9	4–66	12–76	1.50	0.322	–	–	1.596	5.78	–
Flax ^d	25–120	40–60	–	4–69	8–31	–	–	–	–	–	–	–
Flax ^e	1,000–1,270	15–18	–	–	–	1.52	–	–	–	–	–	–
Flax ^e	–	–	–	–	–	–	0.31	–	–	–	–	–
Flax ^g	–	–	–	–	–	–	–	–	0.27	–	–	–
Hemp ^a	100–300	–	3–20	5–55	10–51	1.48–1.50	–	–	–	–	–	Polygonal
Hemp ^b	1,000–3,000	10–51	3.0	5–55	16–50	1.48	0.323	–	–	–	7.02	–
Hemp ^h	1,500–2,500	–	–	5–100	15–50	–	–	–	–	–	–	–
Hemp ^d	100–400	5–50	–	5–55	16	–	–	–	–	–	–	–
Hemp ^e	760–1,800	18–25	–	–	–	1.48	–	–	–	–	–	Polygonal/oval
Hemp ^e	–	–	–	–	–	–	0.31	–	–	–	–	–

^aLewin and Pearce (1998)^bHarris (1954)^cBoltz and Tuve (1976)^dRowell et al. (1997)^eAnonymous (2010)^fKromer (2009)^gOpoku et al. (2007)^hFrank (2005)

Table 3.2 Fiber moisture content, moisture regain, heat of wetting, and swelling of fibers in water

Fiber	Moisture (%)	Moisture regain (%)	Heat of sorption 5% regain (cal/g)	Integral heat of sorption (cal/g)	Heat of wetting (J/g)	Axial swelling (%)	Transverse area swelling (%)
Cotton ^d	10	7–8	–	–	46	–	21,40,42
Cotton ^b	–	–	77	3.9	–	–	–
Cotton ^c	8	24	–	3.79	46.1	1.2	21
Cotton ^a	–	8.5–10.3	–	–	–	–	–
Cotton ^f	–	7.5–8.5	–	–	–	–	–
Flax ^d	10	7–12	–	–	55	0.1–0.2	47
Flax ^b	–	–	88	5	–	–	–
Flax ^c	9	–	–	4.59	–	–	47
Flax ^a	–	12	–	–	–	–	–
Flax ^f	–	12	–	–	–	–	–
Hemp ^d	10	8–12	–	–	–	–	–
Hemp ^c	8.76	–	–	–	–	–	–
Hemp ^e	–	8	–	–	–	–	–

^aLewin and Pearce (1998)^bGuthrie (1949)^cHarris (1954)^dHudson et al. (1993)^eBoltz and Tuve (1976)^fMorton and Hearle (1997)

of 10–25 μm (Bos et al. 2006). Flax fibers are specialized cells with extreme length and thick secondary walls forming a tripartite structure that encircle the vascular cylinder (Morvan et al. 2003). They contain oriented and highly crystalline cellulose microfibrils with high axial stiffness and strength (Andersons et al. 2009). These microfibrils produce fibers of high strength with fluctuating properties as seen in Table 3.3.

Dislocations perpendicular to the fiber axis, which are often called nodes or kinkbands, exist in fibers and fiber bundles from 40 to 200/cm (Khalili et al. 2002). Nodes perpendicular to the long axis of the fiber are visible (Akin 2003) along the fiber length and appear to occur naturally in flax fibers (Khalili et al. 2002) but can also be created by physical stresses (Bos et al. 2002). Hand decorticated, virtually defect-free elementary fibers demonstrated higher strength than commercially produced fibers that contain kink bands (Bos et al. 2002). Akin (2003) states bast fiber bundles consist of 10–40 individual fibers that Bledzki et al. (1996) indicate have a density of 1.5 g/cm^3 , an elongation to break of 2.4%, a tensile strength of 1,100 MPa, and a Young's modulus of 100 GPa. Flax fiber variable properties are presented in Tables 3.3 and 3.4. A principal reason that short-staple flax proves difficult to spin into yarn using traditional cotton processing methods is that flax fibers exhibit weak interfiber cohesive forces (Chen 2007). Coherence of card web, sliver, and roving, along with the strength and hairiness of yarn are affected by a fiber's crimp and cohesion (Shiloh 1965). The lack of cohesiveness typically requires a carrier fiber for processing and spinning. Surface morphology transformations may be required to improve the cohesion between fibers.

Table 3.3. Tensile properties of fibers

Fiber	Tenacity (g/den)	Breaking extension (%)	work factor	Elastic recovery 2% elongation (%)	Stiffness (g/tex)	Toughness (g/tex)	Work to rupture (mN/tex)	Initial modulus (N/tex)	Ratio tensile modulus over shear modulus	Breaking twist angle (α°)
Cotton ^a	2.1–5.1	5.6–7.1	0.46–0.49	–	–	–	5.1–14.9	3.9–7.3	3.9	37–34
Cotton ^b	3–5	–	–	75	–	–	–	–	–	–
Cotton ^c	2.1–6.3	8.0	0.48	74	570	14	–	–	–	–
Cotton ^d	2–5	5–11	–	–	–	–	–	–	–	–
Flax ^a	2.89–6.1	3.0	0.50	–	–	–	8.0	18	19	29.5–21.5
Flax ^e	5–10.8	1.63–2.48	–	–	–	–	–	–	–	–
Flax ^b	2.6–7.7	–	0.50	65	–	–	–	–	–	–
Flax ^c	5.82–6.29	3.0	0.50	63–66	2,700	0.6	–	–	–	–
Flax ^d	4–7	2–3	–	–	–	–	–	–	–	–
Hemp ^a	5.8–6.8	2.2	–	–	–	–	5.3	21.7	–	–
Hemp ^c	4.4–6.79	2.0	0.49–0.50	50	2,000	0.4	–	–	–	–
Hemp ^e	–	3.5	–	–	–	–	–	–	–	–

^aMorton and Hearle (1997)^bHudson et al. (1993)^cHarris (1954)^dBoltz and Tuve (1976)^eRowell et al. (1997)

Table 3.4 Elastic recovery of fibers

Fiber	Fineness denier	Elastic recovery			
		Stress (1g/denier)	Stress (4g/denier)	Strain 1%	Strain 2%
Cotton ^a	0.8	0.65	0.27	0.90	0.73
Cotton ^a	1.8	0.57	–	0.92	0.73
Cotton ^b	2.1	–	–	–	–
Flax ^a	2.6	0.76	0.60	0.71	0.63
Flax ^a	1.7	0.80	0.64	0.76	0.66
Flax ^b	16.5	–	–	–	–
Hemp ^a	3.1	0.64	0.49	0.55	0.50
Hemp ^b	12.75	–	–	–	–

^aMeredith (1945)^bHarris (1954)

3.2.2 Chemical Characteristics

Fiber processing and subsequent utilization could be affected by chemical fiber properties such as surface constituents, surface characteristics, and contaminants. Flax fibers consist of cellulose, lignin, and matrix polysaccharides (Focher 1992). Composition of noncellulosic polysaccharides and fiber morphology depends upon fiber position along the stem and fiber variety (Morvan et al. 2003). These fibers originate in the phloem (bast region) and provide an important food-conducting tissue for the plant. Diederichsena and Ulrich (2009) studied the fiber content of 1,177 seed and fiber flax accessions with fiber contents ranging from 9.0 to 35.0%. The chemical composition of flax fiber (Sharma et al. 1999) in wt.% is: 78.1 cellulose, 4.7 hemicellulose, 0.4 lignin, 1.9 lipids, 0.3 nitrogen, 6.2 hydrogen, 41.0 carbon, and 1.3 ash-yielding compounds (Table 3.5). Shaw and Tabil (2007) estimated the chemical properties of shives (lignified woody core). The outer epidermis layer accounts for 14–24% of total flax stem weight (Morrison and Akin 2001). Parenchyma cells are adjacent to fiber bundles, and retting degrades pectins and matrix polysaccharides, thus facilitating fiber separation (Akin et al. 2000a). The cuticle, composed of the waxy substance cutin, is a primary defense mechanism of the plant and protects the internal tissues from desiccation and pathogens (Morrison and Akin 2001). Unidirectional cellulose microfibrils are embedded in noncellulosic polysaccharides forming bundles that are bound together by pectins linked via calcium bridges (Morvan et al. 2003). Akin et al. (1996) stated that lignin found in flax is composed of polymerized guaiacyl/syringyl units.

Kolattukudy (1984) states that cutin is a network of interesterified hydroxyl fatty acids embedded in a layer of waxy material. Loss of a constituent of the cuticle (i.e., 16-dihydroxyhexadecanoic acid) may best provide an indication of the degree of retting (Morrison and Akin 2001). Wax evaluations of high and low quality flax fiber have indicated that an inverse relationship exists between the amount of palmitic acid, sinapylaldehyde, and sinapyl alcohol and fiber quality (Morrison and Archibald 1998). Some fiber characterization studies have been performed, which have created preliminary testing procedures for analyzing natural fibers

Table 3.5 Degree of polymerization, crystallinity, and chemical composition of fibers

Fiber	Degree of polymerization	Crystallinity (%)	Cellulose (%)	Hemicellulose (%)	Pectin (%)	Lignin (%)	Water solubles (%)	Fat and wax (%)	Ash (%)
Cotton ^a	2020	—	82.7	5.7	—	—	1.0	0.6	—
Cotton ^b	—	—	85–90	1–3 (Pentosan)	—	0.7–1.6	—	—	0.8–2
Cotton ^c	2,020	28.3–78.7	90	—	—	—	—	—	1
Cotton ^d	3,334	—	—	—	—	—	—	—	—
Flax ^a	—	—	64.1	16.7	1.8	2.0	3.9	1.5	—
Flax ^d	2,801	—	—	—	—	—	—	—	—
Flax ^e	1,505	91	79.0	—	—	—	—	—	—
Flax ^f	—	—	85.0	9	—	4.00	—	—	1.00
Flax ^g	—	—	—	3.7 (Pentosan)	—	6.2	—	—	1.40
Flax retted ^h	—	—	80.9	7.9	—	1.44	—	—	1.04
Flax alkali ^h	—	—	85.0	6.2	—	1.23	—	—	1.04
Flax alkali ^c	1,397	78	78.0	—	—	—	—	—	—
Flax bleached ^h	—	—	87.6	6.1	—	0.59	—	—	1.04
Seed Flax ^b	—	—	43–47	24–26 (Pentosan)	—	21–23	—	—	5.00
Flax ^c	2,190–2,420	—	—	—	—	—	—	—	—
Hemp ^a	2,200–2,300	—	67.0	16.1	0.8	3.3	2.1	0.7	—
Hemp ^b	—	—	57–77	14–17 (Pentosan)	—	9–13	—	—	0.80
Hemp ⁱ	4,800	—	78.3	4.15 (Pentosan)	—	2.9	—	—	0.53
Hemp ^c	2,200–2,300	—	77.07	—	—	—	—	—	0.82
Hemp ^j	—	—	57–77	9–14	—	5–9	—	—	—

^aLewin and Pearce (1998)^bRowell et al. (1997)^cHarris (1954)^dYueping et al. (2010)^eGassan and Bledzki (2001)^fFrank (2005)^gShishonok and Shadrina (2006)^hSoleimani et al. (2008)ⁱTimel (1957)^jGumuskaya et al. (2007)

(Nechwatal et al. 2003). Testing procedures have also been reported assessing biofiber applications in thermoplastic material by examining surface treatments and interfacial bonding components (Zafeiropoulos et al. 2002).

Frictional and wettability properties are likely related to fiber morphology, geometric features, static electrical forces, moisture, fiber surface roughness, and fiber surface components including pectin, hemicellulose, waxes, electrolytes, sugars, and metals. Theoretically, enzyme-retting is a process that is able to uniformly alter the surface of flax fibers, improve fiber properties, and strengthen interactions by affecting the fibers surface and wettability. Studies indicate that retted flax contains lignin levels of about 1–4% (Sharma et al. 1999). However, cleaned fibers could not be differentiated on quality using levels of crystalline cellulose, lignin, or aromatics (Morrison and Archibald 1998). Studies conducted by Morrison et al. (2003) demonstrated that only trace amounts of aromatic constituents were present to indicate the presence of lignin. Retting and mechanical processing typically does not remove all components such as the epidermis and shive, which leads to increased lignin levels (Morrison et al. 2003). These components serve as markers for near-infrared spectroscopy that allows researchers to estimate flax fiber cleanliness (Sohn et al. 2004).

Flax has often been described to be a natural fiber already having bacteriostatic characteristics (Cierpucha et al. 2004), and linen is sometimes described as being antibacterial (Anonymous 2006b). Fibers that contain lignin are more resistant to fungi and bacteria than fibers that do not contain lignin (Berkley 1949). Flax has been described as being more resistant to bacterial decomposition (Bose 1952) and more resistant to fungal growth than other natural fibers (Basu and Bhattacharyya 1951). Compounds associated with flax exhibit antibacterial properties (Akin et al. 2003). Results from the modified AATCC Test Method 100-1999 assay indicate that adding flax did not provide any additional bacteriostatic properties to flax denim against two challenging bacteria, *Staphylococcus aureus* and *Klebsiella pneumoniae* (Chun et al. 2009). With scouring removing loose/soluble components, Chun et al. (2010) indicate that the addition of flax does not impart bacteriostatic/antibacterial properties, and unscoured nonwoven felted mats contained substrate components that may support bacterial growth rather than inhibit it.

3.3 Processing of Flax Fibers

3.3.1 Production Techniques

Flax fibers can be obtained from plants grown primarily for fiber or from waste straw generated in flaxseed production. In North America, very little fiber flax is grown, with most flax straw production derived from the oilseed crop (Foulk et al. 2003). Fiber flax varieties are planted closer together than seed flax varieties so that only the main stem develops and the plants grow tall with fewer branches and seeds, thus producing long, fine, and strong fibers. Fatty acid composition of flax seeds is

influenced by the temperature and environment that plants are grown (Dybing and Zimmerman 1966; Green 1986). Finer fibers are obtained by harvesting the crop following a full bloom with the stem and leaves green or at medium fiber fineness when half to a third of seed bolls are yellow and brown with fully developed seeds (Robinson and Hutcheson 1932).

Fiber flax is an annual plant that grows for 90–180 days to a height of around 122 cm when sown in high density (Parks et al. 1993). Flax performs best during cool and moist weather on fertile silt to clay loams with proper crop rotation (Hocking et al. 1987). Cultivar selection and seeding density influence fiber properties of flax stems, while flax is best adapted for cool and moist climates (Sharma and Van Sumere 1992; Elhaak et al. 1999). Yields and production guidelines for several varieties from research in Connecticut are available (Stephens 1997a, b). A well-prepared field is required because flax grows from small seeds planted only 1.3–2.0 cm deep. Robinson (1934) indicated that superior fiber flax crops were grown when 84–96 kg seed/ha is planted at a proper planting time, while Parks et al. (1993) reported that 124 kg seeds/ha is the desired seeding rate. The growing practices for fiber and seed flax are comparable (Oelke et al. 1987), which allows use of flaxseed herbicide, pesticide, fertilizer, and insecticide recommendations (Anonymous 2002). To guard against diseases, a 4-year crop rotation of disease-resistant varieties is recommended along with seed treatment (Parks et al. 1993), while others state that to guard against disease requires a 7-year rotation with flax planted after wheat in rotation (Mark Van de Bilt et al. personal communication).

The quality, yield, and cross-sectional area of flax fibers grown in Egypt were reported to depend upon geographical locations, climatic conditions, and soil conditions (Elhaak et al. 1999). Sharma and Van Sumere (1992) reported that flax does not remove large quantities of nutrients from the soil but reduces the organic matter of the soil. Robinson and Hutcheson (1932) concluded that the South Atlantic region of the US had little land ideally suitable for summer flax production. Apparently, they did not evaluate production of winter-grown flax. Loadholt (1965), Parks et al. (1993), and Foulk et al. (2004b) established that winter-grown fiber flax could be grown in the South Atlantic region with stalk yields around 6,726 kg/ha. Flax can be grown in both temperate and subtropical climates of the US. Warm climates allow flax to be grown in the mild winters in southern parts of the US to produce flax on traditionally dormant fields or to double crop for high-value summer crops for higher economic benefits. Southern agricultural operations, designated Clemson Fiber Flax (CFF), involves carefully preparing the seedbed for planting between October and December, examining soil moisture and nutrients, planting, harvesting seed via a stripper header, drum-cutting stalks, field-drying stalks, raking stalks for even drying, and baling for enzymatic processing.

3.3.2 Retting Methods

Indigenous fungi and bacteria have traditionally been used to ret the stems of flax so that fine fibers can be removed from the straw for industrial applications. Retting

techniques and climatic conditions influence fiber quality (Sharma and Van Sumere 1992). Retting, which is the separation of bast fibers from the core tissues, is preeminent in flax fiber processing as it affects fiber quality and yield (Van Sumere 1992). Two traditional methods used commercially to ret flax are water- and dew-retting (Sharma and Van Sumere 1992). Today, fine bast fibers are commonly released from the stem by dew-retting. Processability of plant stalks into usable fiber requires retting to enhance separation and ease mechanical cleaning. Flax is dew-retted according to weather conditions and completed in a week (when weather is warm and moist) to months (when weather is cold and dry) (Robinson 1934). Traditionally, in Europe, specialized pullers and turners (e.g., Union Machines Inc., Beveren Leie, Belgium, <http://www.unionmachines.com>) have been used to create nonoverlapping, uniform, and parallel stalks that are equally turned for consistent retting and baling. According to the CFF process, flax is cut with a drum mower, producing random nonorganized stalks in the field that are left for dew-retting and subsequently raked into windrows for uniform dew-retting and baling. Mowing with relatively inexpensive, common equipment readily available on most farms provides a better economic situation to obtain whole plant fiber. Following dew-retting, in the CFF process, flax stalks are then dried for baling and further processing.

Stand-retting (Easson and Cooper 2002), chemical retting (Van Sumere 1992), enzyme-retting (Akin et al. 1997, 2000b), steam explosion techniques (Kessler and Kohler 1996), and sonication/cavitation techniques (Harwood et al. 2008) offer potential improvements in retting methods. Stand retting involves flax stems dehydrated by application of a desiccant herbicide and retted as a standing crop prior to cutting. Chemical retting can damage fibers, but if performed correctly, will shorten retting by removing noncellulosic components via degumming in alkali solution (remove pectic substances) and scouring via caustic soda (remove residual plant components). Enzymes, through selective biodegradation of the pectinaceous and matrix substances, facilitate the removal of fibers from the woody portion (i.e., shive) of a flax plant (Van Sumere 1992). Enzyme-retting produced fibers having fiber properties comparable to the best water-retted fiber (Van Sumere and Sharma 1991). Steam explosion (Kessler et al. 1998) requires that decorticated flax stalk be impregnated with sodium hydroxide under controlled conditions and then exposed to saturated steam with residuals extracted via alkaline scouring and water rinsing. Harwood et al. (2008) have developed a new method that cottonizes flax fibers immersed in water via the cavitation process (Fakin et al. 2006; Yachmenev et al. 2002) that produces the formation and violent collapse of small air bubbles, thus generating violent shock waves that produce many chemical and mechanical effects. Many of these processes require rinsing, drying, and opening of the fibers on textile equipment for baling.

The USDA Flax Pilot Plant (Flax-PP) contains a separate research component for enzyme-retting plant stalks to engineer fibers with desired properties, to optimize enzyme-retting, and to enhance processing. Pilot scale tests of commercially cleaned flax indicated that fiber strength, fineness, and yield could be varied by enzyme/chelator levels (Akin et al. 2001). Our proposed current method to enzymatically ret flax stalks includes commercial pectate lyases after chelator for high

yields and good retting efficiencies that maintain strength and fine fibers (Akin et al. 2007; Foulk et al. 2008b). Bioprep, a commercial pectate lyase, provides a potentially important enzyme for retting of flax due to its monocomponent nature, its commercial availability and price, and its ability to ret flax in combination with EDTA at high pH (Foulk et al. 2008b).

3.3.3 *Harvesting Techniques*

The time of harvest is influenced by climatic conditions and the crop's final use. Pullers and turners are used in Europe to harvest flax for long-line fibers (e.g., Dehondt Technologies (Notre Dame de Gravenchon, France) <http://www.dehondt-lin.com>; Depoortere (Beveren-Leie, Belgium) <http://www.depoortere.be>; Vlamalin nv (Tielt, Belgium) <http://www.vlamalin.be>; Union Machines (Beveren Leie, Belgium) <http://www.unionmachines.com>). Harvesting flax requires specially made, sole-purpose, and expensive equipment (Sultana 1992) manufactured overseas to pull and turn flax. Large acreages would require several pieces of equipment due to their low harvest rates (~1 ha/h). Bio-based agriculture includes environmentally friendly processing methods for new crops and value-added products needed to develop sustainable agriculture, boost farm economy, and improve global competitiveness.

In the US, flax is not harvested commercially for fiber, but experimental methods in South Carolina have been developed for short staple fiber with flax stalks cut using a drum-mower and then baled. New methods of harvest may obtain lower flax fiber yields than traditional methods, but the rate of harvesting is much higher and most agricultural operations currently have all required equipment. Drying, raking, and baling are required to provide a packaged lot of raw fiber for processing. At harvest, flax should be cut with a drum mower (e.g., Fella Werke, Feucht, Germany). For the late harvest of flax, seeds should be first removed from stalks with a stripper header (e.g., Shelbourne-Reynolds, Colby, Kansas) attached to a combine (e.g., CASE IH, International Harvester, Racine, WI) (Foulk et al. 2005). After stripping, the flax is mowed, allowed to dry, and evenly spread across the soil surface using a rake (e.g., HSR rake, JF Fabriken, Sonderborg, Denmark). Flax can be dried or dew-retted prior to baling. Flax straw should be raked into windrows and baled (e.g., CASE IH International Harvester, Racine, WI) using standard hay baling protocol such as straw dryness, baler setting, bale density, speed, and packaging. Linseed production is performed in North America, with Canada harvesting 524,000 ha and the US harvesting 141,235 ha in 2007 (<http://www.ag.ndsu.edu/agnic/flax/prodtables.htm>).

3.3.4 *Decortication and Subsequent Processing*

To obtain fibers, stems are harvested and dew-retted, and the fibers are then mechanically processed to extract fibers from the nonfiber woody materials

(shive) using an assortment of rigorous cleaning techniques. Long line mills are able to handle and maintain the orientation of long flax fiber bundles throughout breaking (break shive into fragments without damaging fibers), scutching (separates shive from fiber by beating the straw with dull blades), hackling, and combing (combing of flax to align long line fiber removing short fibers and extraneous matter) on specialized machinery that produce both long line linen and a by-product called tow (short fiber fraction). Tow is a by-product of long-line fiber production and used as short staple fibers in textile applications. Other facilities have embraced lower labor alternatives to this long line route that breaks the plant stalks into short bast fibers for uses including short staple textiles, nonwovens, and composites.

Anthony (2002) states that retting is the single most important issue for decortication and that properly retted flax allows for simplified decortication equipment while poorly retted or unretted material is difficult to detach and separate. Cotton cleaning equipment appears capable of decorticating seed flax stalks, especially if the stalks are retted properly (Anthony 2002). Foulk et al. (2007) demonstrated that selective pieces of traditional gin equipment can be utilized to generate textile grade fiber from various sources of properly retted flax stalks. Modification of gin equipment and processing stream flow are required for one to decorticate and efficiently separate retted flax stalks into high quality fiber and shive.

Typical equipment used in processing flax stalks include crushing rollers, scutchers, shakers (open fiber to facilitate shive removal), pin beaters (revolving cylinder covered with spikes/pins to open fiber and remove shive), metallic wire cylinders (revolving cylinder covered with wire to clean fibers), cards (revolving cylinder covered with wire to individualize and clean fibers), willowing cards (open and align long fibers using spiked workers and strippers), and hammer-mills (shred flax stalk bales using hammers that impact the stalks shredding them into fiber and expelled through screens). In 2009, there were numerous scutching mills in the world, with 60 in China, 55 in Belgium, 49 in Belarus, 31 in Egypt, 30 in France, 10 in Ukraine, 8 in The Netherlands, 3 in Latvia, and 3 in Lithuania (<http://www.saneco.com>). Commercial companies including but not limited to Demaitere BVBA (Moorsledge, Belgium), Temafa GmbH. (Bergisch Gladbach, Germany), Laroche (Cours La Ville, France), Charle and Co. BVBA (Bissegem-Kortrijk, Belgium), Van Dommele Engineering NV (Gullegem-Wevelgem, Belgium), Depoortere (Beveren-Leie, Belgium), N. Schlumberger (Guebwiller Cedex, France), and Czech Flax Machinery (Merin, Czech Republic) exist to produce long- and short-staple flax fiber while pilot plants can be found at the Biolin Research Inc. (Saskatoon, Canada), Institute of Agricultural Engineering (Potsdam-Bornim, Germany), USDA ARS CQRS (Clemson, SC), and Institute of Natural Fibers (Poznan, Poland). Commercial hammer milling is performed on flax seed straw by Schweitzer-Mauduit (Winkler, Manitoba, Canada).

To facilitate and integrate research on bast fiber retting and subsequent processing, a pilot plant was established to quickly and effectively evaluate processes (Akin et al. 2005; Foulk et al. 2008a, 2009). The USDA Flax Fiber Pilot Plant (Flax-PP), the only research facility of this type in the US, is able to process and extract bast fibers from retted and unretted plant stalks using commercial-type equipment.

This extraction process can be performed at the USDA Flax-PP using traditional crushing rollers, scutcher, shaker, pin beater, and card or using modified gin equipment that includes a three-cylinder cleaner followed by a saw-type cleaner. Work at the Flax-PP can produce fibers of specific properties for diverse grades of composites. This one-of-a-kind laboratory located at the USDA ARS federal facility in Clemson, SC, is available for collaborative research projects with individuals and other institutions to advance the utilization of natural fibers. Cooperative research and development agreements (CRADA) can be created that allows for federal and nonfederal parties to enter into agreements to conduct specified research and development related technology transfer activities that are consistent with the laboratory's mission. The benefit to the private sector include the opportunity to obtain exclusive rights to commercialization inventions conceived or first reduced to practice in the performance of work done under the CRADA, with access to federal expertise, equipment, facilities, and personnel.

The Flax-PP contains four customized modules that function as the commercial "Unified Line" (Czech Flax Machinery, Merin, Czech Republic). These modules are designed as standalone units, acting independently, rather than in a single line, to allow maximum flexibility for processing samples in any module, speed, direction, or order for research purposes (Akin et al. 2005). The components comprising the flax stalk processing of the Flax-PP are the following: a nine-roller crushing calender, top shaker, scutching wheel, and five-roller calender. Flax stalks are typically first processed through the nine-roller calender, which crushes and separates shive from fiber using a series of grooved and smooth rollers (Fig. 3.1). The top shaker uses top mounted metal prongs that vibrate rapidly within a fiber mat pulled along a pinned apron, thus opening and further separating the shive (Fig. 3.1). The final step in pilot plant processing is a repeat through the top shaker that is performed twice to remove residual shive, open the compact mat, and to some extent align the fibers. The scutching wheel, which is normally the third step in processing, aggressively strokes the fibers over a feed plate and through grid bars, further removing shive, opening fibers, shortening fibers, and enhancing the fiber softness (Fig. 3.1). A five-roller calender is subsequently used to crush, compact, and remove remaining shive (Fig. 3.1).

The second processing line has been set up with opening and cleaning machinery in our Flax-PP that allows continued research along the fiber cleaning stages. Opening and cleaning equipment progressively and uniformly separates fiber tufts to facilitate impurity removal and facilitate mixing for further processing. A guillotine can be used to control fiber length (Fig. 3.1). This opening and cleaning line consists of five modules in a continuous opening and cleaning process, which includes a fiber blender and opener, pin beater, condenser, card-evenfeed, and rollertop card (Fig. 3.2). The rollertop card is the final opening and cleaning machine that uses mechanical, gravitational, centrifugal, and pneumatic forces between feed roll, licker-in, main cylinder, workers, strippers, and doffer to remove fibers. Concurrently, a cotton pilot plant exists to test cotton/flax fiber and yarn properties, larger pilot plant studies, and miniature spinning. These pilot plants operate to provide a full evaluation of natural fibers.



Fig. 3.1 Enzymatic-retting, washing, and drying system as part of the Flax-PP (*top left*). Nine-roller calendar for initial crushing and breaking of retted flax stems. Photograph showing view of entry point for flax between top four (3 grooved and 1 smooth) and five bottom rollers (two grooved and three smooth) (*top right*). Top shaker to remove shive from fiber (*middle left*). Scutching wheel that strokes flax to shorten and clean fibers with condenser for fiber collection after processing (*middle right*). Five-roller, grooved calendar with three bottom rollers and two top grooved rollers (*bottom left*). Flax Cottonizing Line guillotine chopper for cottonizing flax fibers as part of the Flax-PP (*bottom right*)

3.4 Fiber Characterization

Major technical problems associated with establishing a flax fiber industry in the US are the efficiency of harvest methods, fiber extraction (retting), and the lack of standards for judging fiber quality. This latter problem has been noted for some time by researchers and users of flax fiber. Traditionally, grading systems have tested flax fiber for the following: fineness, length, impurities, color, stains, elasticity, divisibility, buttery feel, flexibility, elongation, strength, homogeneity, cuticle content, smell, roughness, adherence of shive to fiber, content of knots, and moisture content (Alvin Ulrich, personal communication). Grading of long line



Fig. 3.2 Flax Cottonizing Line fiber blender and opener that takes fiber tufts and continually opens them into smaller and lighter tufts for the pin beater (*top left*). Flax Cottonizing Line pin beater for fine flax fiber separation and cottonizing (*top right*). Flax Cottonizing Line card-evenfeeder forms a consistent mat of fibers that when delivered to the card has an even mass in longitudinal and lateral directions, well opened, and delivered in a consistent manner (*bottom left*). Flax Cottonizing Line rollertop card contains card cylinder along with “workers” and “strippers” to help open tufts, orient fibers, and remove short fibers, neps, dust, and trash (*bottom right*)

linen uses organoleptic methods and continues at companies such as Saneco (Nieppe, France) for fiber evaluation. Companies worldwide evaluate flax fibers by different albeit similar means, thus creating an assortment of grades for marketing. Without standard test methods, it is difficult to compare fiber samples from different parts of the world utilizing subjective and nonstandard test results. An optimized system of grading flax fibers would benefit the marketing of these fibers and promote sales and uses beyond current or conventional applications.

Uniform cotton standards were established in 1907 by international representatives from the cotton industry (United States Department of Agriculture 1995). The US Cotton Standards Act of 4 March 1923, authorized the Secretary of Agriculture to establish standards for the classification of cotton by which its quality could be

determined for commercial purposes. Prior to 1965, US cotton fibers were subjectively judged by cotton classers based on Universal Standards. Instrument systems to measure multiple fiber properties, later named High Volume Instruments (HVI™), came on-line in 1980. Flax standards in the long-term would help market decisions on the utilization of flax for various applications and thereby enhance and expand the industry. The USDA Agricultural Marketing Service (AMS) continues to use the HVI™ and classer to determine fiber properties on 13–20 million 227 kg cotton bales (<http://www.ams.usda.gov>). Uster Technologies (Knoxville, TN) manufactures HVI™ and Advanced Fiber Information System (AFIS) instruments that have both been evaluated for flax fiber measurements in coordination with IAF (Reutlingen, Germany) but not pursued due to costs, lack of industry support, and absence of standards at the time (Anja Schleth personal communication).

Developing a uniform classification system and standards for flax is confounded by the nature of flax fibers. Flax fibers consist of ultimate fibers in bundles of various sizes (Sharma and Van Sumere 1992). Research has been directed at an objective measure of fiber quality, utilizing for many years the various methods used in-house by research and industrial organizations (Sharma and Van Sumere 1992). In 1972, the International Organization for Standards (ISO) developed a standard to determine flax fiber fineness (ISO 2370). In 1999, an ASTM International subcommittee D13.17 (Flax and Linen) was officially created to develop objective flax standards for the textile industry. Strength, length, fineness, color, terminology (standard terms for clear communication), and trash (nonfibrous components) were immediate fiber parameters that were addressed by the subcommittee. Currently, one ISO and three ASTM International flax standards and one ASTM International flax terminology exist (Akin 2005; International Standard Organization 1980; ASTM International 2005a, b, c, d).

The method for trash (nonfiber) content is based on near-infrared spectroscopy verified by Sohn et al. (2003). Color standards provide objective data for fibers produced by various methods and for expanding markets (Epps and Akin 2003).

Fineness predicts a majority of mechanical properties and influences the quality of finished products. Different techniques exist for the measurement of fiber fineness including organoleptic, gravimetric, micrometric, airflow, and vibroscopic methods. The airflow method for cotton was modified for flax fibers using nine IFS (International Fineness Standards) long line calibration flax grades. These grades (determined internally) have a range of values and are available from Institut Textile de France, Lille (Villeneuve d'Ascq, France). Currently, in testing fiber strength, a modification of the HVI™ and/or Stelometer method of preparing fiber bundles is used to align fibers, and specialized grips are used in a testing load frame to break prepared fiber bundles. Fiber testing on a large number of samples is required for accurate determinations due to the natural variation of the flax fibers as well as diverse retting and processing techniques. The Fibrotest instrument (Textechno Herbert Stein GmbH & Co. KG, Mönchengladbach, Germany) is currently being assessed as a new device for flax fiber testing. It is considered a low volume instrument that prepares a fiber beard for testing, measures fiber length and length distribution, subsequently breaks the fibers, and automatically

determines sample size between the clamps enabling the calculation of the absolute value of tenacity.

Prospective flax fiber tests include a standard test method for flax fiber bundle strength and elongation similar to the Stelometer, fiber length and distribution, fineness distribution via image analysis, wax content via NIR, density measurement, and numerous flax mat characterization tests. Prior work has indicated that NIR spectroscopy has potential for determining wax content in flax fibers (Sohn et al. 2006). Potential standards could exist for farmers to predict fiber content in stems in the field by near-infrared spectroscopy (Barton et al. 2002). The Composites Innovation Center (CIC) in Winnipeg is working on a system to characterize flax fiber mats and subsequent composites.

3.5 Flax Coproducts

Waste streams generated during processing all become flax coproducts with prospective to improve profits and long term business stability. Various parts of the plant stalk (fiber, shive, and dust) and seed can potentially be utilized for commercial products including but not limited to bioenergy (e.g., <http://www.thepowerlog.com>), activated carbon, bioproducts, wax, industrial oils (e.g., <http://www.adm.com>), food additives, nutritional uses (e.g., <http://www.barleans.com>), aromatic extracts, and animal feed (e.g., <http://www.cargill.com>). By-product fiber (fiber lacking the correct length and fineness for main fiber stream) contains cellulose, the shive (lignified woody core) contains aromatics and cellulose, the cuticle (waxy defense mechanism of the plant) contains lipids, and the dust contains a mixture of components. Shive with its low density and absorption properties have been used as soil amendment, animal bedding, particle board, plastic compounds, fuel pellets, and as an alternative fuel source. Depending upon the end product, both fiber and shive by-products have potential applications in composite formation. Shive can be used to produce low-quality building materials such as shive-containing fiberboards/particleboards/chipboards (e.g., <http://www.sanopan.com>; <http://www.linopan.eu>). Shive waste by-products can be converted into useful products such as activated carbon or noncarbonized metal absorbers (Cox et al. 2005). Waste stream flax fibers could be used in the production of gypsum board (Dalmay et al. 2010) and fiber-reinforced concrete (Boghossian and Wegner 2008). Inferior flax straw bales could be burned for energy (carbon neutral fuel), with flax bales having a lower heat value (LHV) of 19.3–20.0 MJ/kg while flax shive LHV of 19.2 MJ/kg (Anonymous 1995). Brandenburg and Harmond (1956) have indicated that flax shive briquettes have a heat content of 17.6 MJ/kg.

At Schweitzer-Mauduit in Winkler, Manitoba, one semitruck load of shive (~17 tons) is produced in one hr from their hammermill process (Melitz 2005). Two thirds of flax straw that Schweitzer-Mauduit International purchases for processing is shive (Hogue 2006). New techniques and research for flax shive delignification along with complete identification of the assorted aromatics can

result in additional flax coproduct streams. Lignin and aromatic compounds have potential uses as antimicrobials, antioxidants, and resins (Lora and Glasser 2002). According to Himmelsbach and Holser (2008), fatty alcohols (policosanols) and long chain waxes (C40–C60 esters) can be extracted from waste fractions containing cuticular tissues and surface waxes for potential industrial, nutraceutical, and pharmaceutical applications recovered in emerging green separation techniques. Cellulosic material that remains following extraction has the potential to be saccharified and converted to ethanol via fermentation (Himmelsbach and Holser 2008). Flax shives as feed stocks for bio-fuels have the potential to be developed as an alternative energy source that will in turn increase the use of agricultural materials, create jobs, reduce dependence on foreign oil, and improve the environment. According to Kim and Mazza (2006), lignocellulose present in shive is a potential source of cellulosic ethanol (via fermentation) and other chemicals (phenolic compounds via hydrolysis of lignin) due to their abundance, renewability, and demand. University of Manitoba researchers and collaborations are looking for new ways to convert flax shives into biofuels and other products (<http://www.microbialrefinery.com>).

Flax seed is the main product with uses including both industrial and nutritional oil. Linseed oil (industrial grade is ~50% linolenic acid) is a major ingredient in paints, sealers, varnishes, polish, wax, and stains to preserve and protect both wood and concrete (Charlton and Ehrensing 2001). The product Dilulin (Cargill, Minneapolis, Minnesota) is a new linseed oil-based reactive diluent that reduces volatile organic compound (VOC) levels for VOC regulations. Other flaxseed oil products include Archer #1™ (Archer Daniels Midland Co., Decatur, Illinois), a coadhesive in fiberboard that replaces solvents and petroleum-based chemicals again reducing VOC levels. The economics of Biofuel production have been evaluated using flax seed as a feedstock (Jaeger and Siegel 2008). Linoleum flooring (30% linseed oil) is produced by oxidizing linseed oil to form a thick mixture called linoleum cement (<http://www.flaxcouncil.ca>). Flax varieties (e.g., Solin) have been developed to produce seeds with low levels of linolenic acid (~5%) that are suitable for human consumption that contain high levels of omega-3 fatty acids (Charlton and Ehrensing 2001). Flax seeds and its components have been shown to have a positive effect on health (Muir and Westcott 2003). The White House contacted the U.S. Department of Agriculture and the U.S. Food and Drug Administration to promote eating omega-3 fatty acids (Przybyla-Wilkes 2007). Feeding cattle a 10% flaxseed diet leads to elevated levels of α -linolenic acid in muscle tissue consequently producing positive health benefits to the consumer (Medeirosa et al. 2007). Chickens fed an enriched flaxseed diet provide eggs with omega-3 and human health benefits (Yannakopoulos 2007). As the nutritional benefits derived from flaxseed (omega-3 fatty acid, lignan, and dietary fiber content) have increased, the Mintel's Global New Products Database (<http://www.gnpd.com>) has reported 1,161 new US food products from 2003 to 2009 that contain flax. The health benefits of flax are not limited to the seed. Flax processing produces dust in which the cuticle is concentrated with nutraceutical potential (Morrison and Akin 2001). Such long chain alcohols have been suspected to

improve blood chemistry by lowering low-density lipoproteins (LDL) and increasing high-density lipoproteins (HDL) while lowering total cholesterol. Benefits of these phytochemical compounds include improved blood chemistry with fewer side effects (Taylor et al. 2003). Developing a flax fiber industry in the south would be expedited by the development of a flax seed industry with a ready outlet of flax seed for livestock and poultry feed, such as in states like Georgia, which produces more poultry and eggs than any other state (<http://www.farmland.org>).

3.6 Fibers and Composite Formation

Collectively, composites are light, stiff, strong, and allow both large- and small-scale production at lower energy costs. The lightweight nature of these composites also increases the energy efficiency for machinery and transportation. Flax fibers have been used to reinforce polymers in order to create biobased composites, thereby reducing the amount of nonbiodegradable materials (Mohanty et al. 2002). Emission and finite resource reductions may also occur because the fibers are derived from naturally renewable materials created through photosynthesis. The use of flax in biobased composites could help lessen dependence on fossil fuels today and into the future (Mohanty et al. 2002). In fact, DaimlerChrysler (2001) indicates that natural fiber automotive components require 83% less energy and are 40% less expensive to manufacture than glass fiber components. Natural fibers such as flax are being utilized in various composite applications due to their lower cost, low density, biodegradability, relatively high strength, low abrasiveness, abundance, renewability, nonhazardous nature, recyclability, reuse of production waste, and low equipment requirements. However, natural fibers continue to have drawbacks such as variable fiber quality, poor binding to matrix materials, chemical modification required for improved composite adhesion, lower strength than glass, and low processing temperatures. The European Union has established directives promoting the necessity of recyclability or degradability. One of these is the E.U.'s End-of-Life Vehicle (ELV) Directive, which has set a requirement for 95% of vehicles manufactured after January 2015 to be reused or recovered (European Parliament 2000). Another is the E.U.'s Landfill of Waste Directive, which severely restricts amounts of organic material that can be land-filled, which has caused the disposal of polymer composite materials illegal in many E.U. nations (European Parliament 1999).

Composite materials are combinations of two or more materials with different, often complementary properties (Cheremisinoff 1997). Polymeric natural fiber composites have traditionally been manufactured using short reinforcement fibers dispersed in a matrix (Van de Velde and Kiekens 2001) or compression molded from a nonwoven textile (Mueller and Krobjilowski 2003). These applications usually contain low fiber volume fractions and lack control of fiber angles, resulting in their primary use as nonload carrying components (Svensson 1997). The role of stiff and strong reinforcing fibers in a composite is to carry the load and improve mechanical properties of the matrix material. Regardless of fiber type (carbon,

glass, or natural fibers), they typically require surface treatment for good wetting and matrix adhesion. To combine hydrophilic flax fibers and hydrophobic polymers, an intermediate material is required for optimum properties.

Flax fiber components have ranged from interior to exterior parts (Wittig 1994). These plastic components reinforced with flax fiber have typically only been considered for parts exposed from low to middle levels of stress (Munker et al. 1998). Among plant fibers, flax fibers have the highest tensile strength and modulus of elasticity (Burger et al. 1995). Flax fibers are hydrophilic in nature, which means that in addition to matrix compatibility issues, moisture absorption and swelling will occur but can be controlled with physical and chemical treatments (Heijenrath and Peijs 1996). Several researchers have found stiffness values of flax fiber composites to be comparable to E-glass fiber composites and suited for low-cost engineering uses (Bledzki and Gassan 1997). As with glass fibers, increasing flax fiber content has been shown to improve mechanical properties of the composite (Hargitai et al. 1998). These fibers have also been shown to increase composite formability for manufacturing processes (Vila and Jabbur 2005).

The lack of fiber quality parameters, fiber standards, uncertainties of raw material supply, unpredictability of flax composite processing, possible long production cycles, and processing costs have likely limited a vast use of flax fibers in composites. From a performance perspective, flax fibers have lower strength than glass fibers; however, they have a lower density and cost, which reduces the overall load-bearing cost. Specifically, flax fibers exhibit nearly half the density of glass fibers, and therefore current technical data suggest that flax fibers can compete very easily with glass fibers when considering specific composite material properties (Wittig 1994). Lepsch and Horal (1998) have shown that flax-reinforced polypropylene composite shelf panel is a financially viable solution because of its acceptable strength properties and ease of processing. Bayer, BASF, Cannon, and Krauss-Maffei have all developed technology for producing natural fiber composites in the automobile industry (Mapleston and Smock 1998). Currently, the Lotus Eco Elise automobile project is intended to produce a greener automobile that contains flax and other natural fibers intended producible in the near future. Apart from the automotive market, progress is being made in making everyday products out of flax fiber biocomposites. A flax fiber-based tennis racket is currently available by Artengo (<http://www.artengo.com>) that incorporates flax and graphite in the frame to better absorb shocks. Several flax fiber-based bicycles are available through Museeuw (<http://www.museeuwbikes.be>) that are handcrafted in Europe containing 40–80% flax fiber and 3K HM carbon fiber.

In parallel with application development, a better understanding of flax fibers in terms of structure–property relationships has been ongoing. Charlet et al. (2007) reported that the chemical composition and mechanical properties of the fibers used to produce unidirectional composites were strongly influenced by their location in the stem. The interfacial strength of the composite can be assumed to correspondingly be a complex property arising from the complex nature of flax fibers. Flax fibers could be separately processed into individual fibers (i.e., highest achievable aspect ratio), industrial fibers (i.e., medium aspect ratio), or a trashy fiber and shive

mixture (i.e., low aspect ratio). The fiber extraction process has been shown to play a role in the variation found in flax fiber strength, fineness, color, and trash content (Van de Weyenberg et al. 2006). Retting flax stalks produces fibers with different surface components, while mechanically processing at different levels yields fibers with varying degrees of quality (Foulk et al. 2008a). The impact of flax fiber quality and its variability on composite performance through interfacial bonding has not been fully established.

Extremes in property variation were assessed between polymer matrix composites reinforced with long-line flax fiber versus linseed flax fiber (Fuqua et al. 2009). Varieties, growth, harvest, and processing of flax all impact manufacturability of flax fiber reinforced composites. Fuqua et al. (2009) analyzed both fiber architecture extremes and harvesting extremes. For one set of flax fiber-reinforced polymer composites, dew-retted, finely combed, long-line linen flax fiber was used to create unidirectional reinforced composite. For the second set of flax fiber-reinforced polymer composites, a combine harvested, minimal-retted, short oilseed flax fiber with a high percentage of shive was used to create a randomly oriented reinforced composite. The composite manufacturing technique and fiber surface treatments used were controlled resulting in good quality flax fiber-reinforced composites with minimal voids and fine surface appearance. The tensile and interlaminar shear strength properties obtained for the flax fiber-reinforced composites were drastically different (i.e., 61–93%). Conversely, flax fiber bundle pull-out tests proved that with appropriate cleaning, orientation, and combing, similar composite properties were obtained from samples.

In a study by Mekic et al. (2009), linseed flax fiber was investigated for its composite processability as compared to traditional fiberglass. Currently, liquid molding techniques [e.g., resin transfer molding (RTM) and vacuum-assisted resin transfer molding (VARTM)] can be used with a variety of synthetic fiberglass, aramid fibers, carbon fibers, etc. but have not necessarily been proven with flax or other natural fibers. O'Donnell et al. (2004) evaluated and characterized natural fiber permeability values. In a conventional, single-dimensional flow experiment, the in-plane permeability for a 20 oz. flax mat containing 85% fiber and 15% binder was measured to be $1.02 \times 10^{-10} \text{ m}^2$ (O'Donnell et al. 2004). In a study by Rodriguez et al. (2004), permeability of jute and sisal fiber preforms were measured to range between 0.25×10^{-8} and $1.5 \times 10^{-8} \text{ m}^2$. Rouison et al. (2006) determined that the permeability of hemp fiber preforms were an order of magnitude lower than a comparable fiberglass preform. These studies used a modeling approach widely accepted but recently found to provide inaccuracies if not used correctly (Mekic et al. 2009). Mekic et al. (2009) further determined that liquid flow through flax fiber preforms studied were similar to fiberglass preforms with the same porosity values under the identical processing conditions so that simulation software can be used without modifications.

It is well understood that proper fiber–matrix bonding is crucial to the performance of flax composites (Mustata 1997). This drawback is due to the hydrophilic nature of flax, caused by the hydroxyl groups in the fiber's cellulose and lignin (Nevel and Zeronian 1987), and resultant poor interaction with polymers, which

tend to be hydrophobic in nature. Physical methods do not change the chemical composition or structure, such as stretching, calendaring, thermotreatment, and electronic discharge (corona, cold plasma) (Bledzki and Gassan 1997). Some of the most successful chemical methods have been with coupling agents that react with the fiber surface and the polymer matrix, forming covalent and hydrogen bonds. This bonding has been accomplished through the use of isocyanates (Joseph et al. 1996), triazine (Oksman 2001), and silanes (Rong et al. 2001). Other treatment methods include acetylation (Mohanty et al. 2001), benzoylation (Joseph et al. 2000), enzyme with chelator treatment (Foulek et al. 2004), alkaline treatment (Van de Weyenberg et al. 2003), and peroxide treatment (Sreekala et al. 2000). Maleic acid anhydride grafted polypropylene (MAA-PP) has been demonstrated to be a successful coupling agent by creating polar interactions between the modified polymer and fiber (Van de Velde and Kiekens 2001). However, perhaps the most common method for chemically modifying the surface of natural fibers has been mercerization or the use of alkalis such as NaOH to improve the surface interaction between matrix and fiber (Baley et al. 2006). Alkali treatments lead to surface roughening, fibrillation, and the removal of natural and artificial impurities (Mishra et al. 2001). X-ray diffraction (XRD) analysis (Zafeiropoulos et al. 2002) has shown that acetylation treatments increase the crystallinity index of fibers significantly.

Huo et al. (2010b) utilized diverse fiber surface treatments to create fibers for a tailored VARTM method to process unidirectional composite laminates with high fiber volume fraction (i.e., 45–55%). They revealed that specific flexural strength and interfacial properties of acrylic acid treated flax/VE composites exhibited the best balance of property improvement compared with other flax/VE composites. Huo et al. (2010a) found that precoating the fiber's surface with VE prior to liquid molding with the same VE resin system increases the contact area between the fiber and matrix. In addition to using untreated VE, toluene- or tetra (hydro furan) (THF)-treated VE was also investigated because of their comparable polarities with acetone, previously established as an effective dispersion agent. Acrylic resins (AR) can potentially crosslink with VE (Stevanovic et al. 2002). Therefore, AR was used by Huo et al. (2010c) to modify the matrix for improved wetting of flax and to examine its effectiveness as a cross-linking agent and increase load transfer in the resulting biocomposite. The combination of fiber treatment and matrix modification improved interlaminar shear strength, tensile properties, and flexural properties of flax/VE biocomposites.

With or without fiber surface treatments, surface contaminants such as metals, waxes, and bacteria all further exacerbate the difficulties of interaction between the hydrophilic fiber surfaces and hydrophobic matrix polymers by acting as disconnects between the two phases. Density and fiber thickness have been demonstrated to be positively correlated to interfacial adhesion, while increased wax, bacteria, magnesium, and calcium content have shown correlation to decreases in interfacial strength (Foulek et al. 2010). Although bacteria were shown to correlate to a detrimental effect on fiber surface interfacial strength, bacteria play a fundamental role within the retting process. In water retting, anaerobic bacteria are considered the primary agent responsible for fiber release (Sharma et al. 1992). In dew retting,

rather than bacteria, fungi are mainly responsible for the production of pectinase enzymes (Sharma et al. 1992). Little is known regarding the influence of diverse forms of microorganisms on a fiber's surface to-date.

Flax fibers have recently been investigated as reinforcement in polymeric foam matrices for current components used in the transportation industry (Fuqua et al. 2010). Despite the fact that plywood bus floorboards are chemically treated to prevent decay, they still require repeated replacement over the lifecycle of a transit vehicle (Vaidya et al. 2004). Mechanical testing of both flexural performance and fastener pullout capabilities of flax-fiber/soy-based PU foam composites demonstrated that they could serve as a suitable flooring replacement in mass transit vehicles. Structures ranging from 55% to 70% renewable material by weight with an inexpensive lower quality flax mat (i.e., 40% shive content and 60% fiber) could produce flexural strength comparable to plywood with little environmental impact (Fuqua et al. 2010).

Hybrid composites by definition incorporate two different types of materials into one matrix (Cheremisinoff 1997). Hybrid textiles can be formed from blends of fibers, which can be processed on most short staple spinning and weaving machinery. Usually cottonized flax fibers are processed into a yarn (Czekalski et al. 2000) and then manufactured into a fabric for further composite formation. Hybrid textile preforms containing natural fiber directly impacts the composite because they (1) contain various fiber types via fiber or yarn blending, (2) possess fibers of longer length due to requirements in yarn formation (i.e., fibers are not chopped into fiber fragments), (3) control the fiber alignment via processing (e.g., spinning and weaving), and (4) control fiber volume via yarn size. It has been shown for thermoplastic composites that textile preforms can be saturated with polymer and processed into a final product, often by compression molding techniques (Pan 1996). Resulting properties of these short fiber discontinuous reinforcement composites (Cheremisinoff 1997) are, however, not as good as if long or continuous fiber would have been used. Properties of composites are best if their fibers are oriented in the primary load direction. A woven fabric consists of continuous fibers oriented in two directions (bidirectional). Therefore, continuous fibers are used for products requiring enhanced performance. Strips of parallel continuous fibers or continuous fibers woven, knitted, braided, etc. into a textile structure (i.e., preforms) can also be utilized for advanced composite products. Natural fibers are not continuous but have been processed to form yarns (i.e., a continuous package of short fibers) and fabric for textile preforms.

Flax fiber/recycled HDPE composites were prepared through compression molding using a textile perform (Foulk et al. 2006). These HDPE composites were formed with various levels of commercially available cotton and flax blended twill weave denim fabric. Straight and strong flax fibers present problems because they cannot be bound as tightly within yarns, thereby producing weaker and less elastic yarns that contain larger diameter variations and neps. Concurrently, as the blend percentage and mass of flax fibers increases, the fabric strength, density, and elongation generally decrease in value. Blends of cotton and flax fibers were randomly aligned in the yarn, fabric, and subsequently in the HDPE matrix.

Compared to recycled HDPE without fiber, physical properties of fiber composites demonstrated significant increases in tensile strength and modulus of elasticity. Additional research is needed to improve composite binding characteristics to allow the stronger flax fibers in the fabric to carry the composites load (Foulk et al. 2006).

3.7 Conclusions

Much research continues to develop renewable, recyclable, sustainable, and bio-based composites produced from agricultural feed stocks such as flax fiber. Primary requirements are sustainable production, low cost, and consistent and known quality. To better understand these bio-composites, research must continue to evaluate feed stock fibers, by-product fibers, fiber constituent makeup, processing requirements, and standards to judge fiber quality and consistency. Overall, replacement of glass fiber by natural fibers such as flax will be based not only on comparable specific composite mechanical properties but also on fiber consistency. While chemical surface treatments have been proven to be extremely beneficial when properly utilized, the growth of the natural fiber sector will likely be dictated by the ability to achieve consistent, low-cost improvements to mechanical bonding achieved by variation and control of the growing and harvesting methods. A better understanding of flax fibers has led to some manufacturers utilizing these natural fibers in everyday items, and future product growth is expected.

Acknowledgments We gratefully acknowledge and appreciate the help provided by producers, processors, and others. We gratefully acknowledge Nancy Carroll, Martha Duncan, Pat Fields, Don Gillespie, Robert Harrison, Curtis Heaton, Linda James, Jimmy Lewis, Judy Marcus, Mattie Morris, Brad Reed, and Debbie Sewell from USDA ARS CQRS. We gratefully acknowledge the manuscripts provided by Nahum Ben-Yehuda from Bar Ilan University. We gratefully acknowledge the research performed by Shanshan Huo, Sait Mekic, Michael Fuqua, Luke Gibbon, Amol Thapa, Lori Dionne, Martin Hanson, Derek Huotari, and Nathan Sailer at North Dakota State University. We gratefully acknowledge Mercedes Alcock, Stephen Meatherall, and Sean McKay from the Composites Innovation Center (CIC) for their development of flax fiber composites.

References

- Akin D (2003) Flax fiber. Kirk-Othmer encyclopedia of chemical technology. Wiley, New York, 33 pp. doi:10.1002/0471238961.0612012401110914.a01
- Akin D (2005) Standards for flax fiber. ASTM International Standard News, 22–25 Sept 2005
- Akin D, Gamble G, Morrison W, Rigsby L (1996) Chemical and structural analysis of fibre and core tissues from flax. *J Sci Food Agric* 72(2):155–165
- Akin D, Morrison W, Gamble G, Rigsby L (1997) Effect of retting enzymes on the structure and composition of flax cell walls. *Text Res J* 67(4):279–287
- Akin D, Dodd R, Perkins W, Henriksson G, Eriksson K (2000a) Spray enzymatic-retting: new method for processing flax fibers. *Text Res J* 70(6):486–494
- Akin D, Himmelsbach D, Morrison W (2000b) Biobased fiber production: enzyme-retting for flax/linen fibers. *J Polym Environ* 8(3):103–109

- Akin D, Morrison W, Rigsby L, Dodd R (2001) Plant factors influencing enzyme-retting of fiber and seed flax. *J Agric Food Chem* 49(12):5778–5784
- Akin D, Morrison W, Rigsby L, Evans J, Foulk J (2003) Influence of water presoak on enzyme-retting of flax. *Ind Crops Prod* 17(3):149–1159
- Akin D, Dodd R, Foulk J (2005) Pilot plant for processing flax fiber. *Ind Crops Prod* 21(3):369–378
- Akin D, Condon B, Sohn M, Foulk J, Dodd R, Rigsby L (2007) Optimization for enzyme-retting of flax with pectate lyase. *Ind Crops Prod* 25(2):136–146
- Andersons J, Sparmins E, Porike E (2009) Strength and damage of elementary flax fibers extracted from tow and long line flax. *J Compos Mater* 43(22):2653–2664
- Anonymous (1995) Using straw as a farm heating fuel. PAMI Research Update Pamphlet 719 Prairie Agricultural Machinery Institute Saskatchewan, Canada
- Anonymous (2002) Flax crop production. The Flax Council of Canada Winnipeg, Manitoba. <http://www.flaxcouncil.ca>. Accessed 20 April 2010
- Anonymous (2006a) Growing flax production management and diagnostic guide, 4th edn. Flax Council of Canada, Winnipeg, Manitoba, ISBN 0-9696073-4-2, 59 pp
- Anonymous (2006b) Flax yarns from Europe through Swicofil – The noble linen fiber. <http://www.swicofil.com/products/003flax.html>. Accessed 20 April 2010
- Anonymous (2010) Physical properties of materials. <http://www.ogdenmfg.com/pdf/tech9.pdf>. Accessed 20 April 2010
- Anthony W (2002) Separation of fiber from seed flax straw. *Appl Eng Agric* 18(2):227–233
- ASTM International (2005a) ASTM standard terminology relating to flax and linen (D6798), Annual Book of Standards, Section 7.02, Textiles. ASTM International, West Conshohocken, PA
- ASTM International (2005b) ASTM standard test method for color measurement of flax fiber (D6961), Annual Book of Standards, Section 7.02, Textiles. ASTM International, West Conshohocken, PA
- ASTM International (2005c) ASTM standard test method for assessing clean flax fiber fineness (D7025), Annual Book of Standards, Section 7.02, Textiles. ASTM International, West Conshohocken, PA
- ASTM International (2005d) ASTM standard test method for measurement of shives in retted flax (D7076), Annual Book of Standards, Section 7.02, Textiles. ASTM International, West Conshohocken, PA
- Baley C, Busnel F, Grohens Y, Sire O (2006) Influence of chemical treatments on surface properties and adhesion of flax fiber-polyester resin. *Compos A* 37(10):1626–1637
- Barton F, Akin D, Morrison W, Ulrich A, Archibald D (2002) Analysis of fiber content in flax stems by near-infrared spectroscopy. *J Agric Food Chem* 50(26):7576–7580
- Basu S, Bhattacharyya J (1951) Mildew of complex vegetable fibers. *J Sci Ind Res* 10B(4):91–93
- Berkley E (1949) Certain variations in the structure and properties of natural cellulose fibers. *Text Res J* 19(60):91–93
- Bledzki A, Gassan J (1997) Natural fiber reinforced plastics. In: Cheremisinoff N (ed) Handbook of engineering polymeric materials. Marcel Dekker, New York
- Bledzki A, Reihmane S, Gassan J (1996) Properties and modification methods for vegetable fibers for natural fiber composites. *J Appl Polym Sci* 59(8):1329–1336
- Boghossian E, Wegner L (2008) Use of flax fibers to reduce plastic shrinkage cracking in concrete. *Cement Concrete Comp* 30(10):929–937
- Bogoeva-Gaceva G, Avella M, Malinconico M, Buzarovska A, Grozdanov A, Gentile G, Errico M (2007) Natural fiber eco-composites. *Polym Compos* 28(1):98–107
- Boltz R, Tuve G (1976) CRC handbook of tables for applied engineering science. CRC, Cleveland, OH, 172 pp
- Bos H, Van den Oever M, Peters O (2002) Tensile and compressive properties of flax fibers for natural fiber reinforced composites. *J Mater Sci* 37(8):1683–1692

- Bos H, Mussig J, van den Oever M (2006) Mechanical properties of short flax fiber reinforced compounds. *Compos A Appl Sci* 37(10):1591–1604
- Bose R (1952) A comparative study of the microbiological decomposition of some cellulosic fibers. *Sci Cult India* 17(10):435–436
- Bradbury F (1920) Flax culture and preparation. Pittman's Textile Industries Series. Sir I Pitman, London, England, 213 pp
- Brandenburg N, Harmond N (1956) Development and testing of a forced air dryer for fiber flax. Agricultural Experiment Station, Oregon State College, Corvallis Technical Bulletin 37
- Burger H, Koine A, Maron R, Miecck K (1995) Use of natural fibers and environmental aspects. *Int Polym Sci Technol* 22(8):25–34
- Charlet K, Baley C, Morvan C, Jernot JP, Gomina M, Bréard J (2007) Characteristics of Hermes flax fibres as a function of their location in the stem and properties of the derived unidirectional composites. *Compos Part A Appl Sci* 38(8):1912–1921
- Charlton B, Ehrensing D (2001) Fiber and oilseed flax performance 2001 Annual Report. Oregon State University, Corvallis, OR, USA, pp 36–40
- Chen X (2007) Development of flax and natural protein fiber blend yarn. *Shanghai Text Sci Tech* 35(5):47–48
- Cheremisinoff N (1997) Handbook of engineering polymeric materials. Marcel Dekker, New York, NY, 888 pp
- Chun D, Foulk J, McAlister D (2009) Testing for antibacterial properties of cotton/flax denim. *Ind Crops Prod* 29(2–3):371–376
- Chun D, Foulk J, McAlister D (2010) Antibacterial properties of flax. *BioResources* 5(1):244–258
- Cierpucha W, Kozłowski R, Mankowski J, Wasko J, Mankowski T (2004) Applicability of flax and hemp as raw materials for production of cotton-like fibres and blended yarns in Poland. *Fibres Text East Eur* 12(3):13–18
- Couture S, DiTommaso A, Watson A (2004) Influence of seeding depth and seedbed preparation on establishment, growth and yield of fibre flax (*Linum usitatissimum* L.) in Eastern Canada. *J Agron Crop Sci* 190(3):184–190
- Cox M, El-Shafey E, Pichugin A, Appleton Q (2005) Sorption of precious metals onto chemically prepared carbon from flax shive. *Hydrometallurgy* 78(12):137–144
- Czekalski J, Jackowski T, Kruciska I (2000) Blends spinning with flax. *Text Asia* 31(6):34–39
- DaimlerChrysler (2001) Natural fibers replace glass fibers. *Umwelt-Umweltbericht 2001 Environmental Report*, 3 pp
- Dalmay P, Smith A, Chotard T, Sahay-Turner P, Gloaguen V, Krausz P (2010) Properties of cellulosic fiber reinforced plaster: influence of hemp or flax fibers on the properties of set gypsum. *J Mater Sci* 45(3):793–803
- Diederichsena A, Ulrich A (2009) Variability in stem fiber content and its association with other characteristics in 1177 flax (*Linum usitatissimum* L.) genebank accessions. *Ind Crops Prod* 30(1):33–39
- Dybing C, Zimmerman D (1966) Fatty acid accumulation in maturing flaxseeds as influenced by environment. *Plant Physiol* 41(9):1465–1470
- Easson D, Cooper K (2002) A study of the use of the trimesium salt of glyphosate to desiccate and ret flax and linseed (*Linum usitatissimum*) and of its effects on the yield of straw, seed and fiber. *J Agric Sci* 138(1):29–37
- Ebskamp M (2002) Engineering flax and hemp for an alternative to cotton. *Trends Biotechnol* 20(6):229–230
- Ehrensing D (2008) Oilseed crop flax. Publication No EM 8952-E Oregon State University Extension Service, OR, USA, 9 pp
- Elhaak M, El-Shourbagy N, El-Nagar R (1999) Effect of edaphic factors on technical properties of flax fibre. *J Agron Crop Sci* 182(2):113–120
- Epps H, Akin D (2003) The color gamut of undyed flax fiber. *AATCC Rev* 3(1):37–40
- European Parliament (1999) Council Directive 1999/31/EC of 26 April 1999 on the landfill of waste. <http://eur-lex.europa.eu/en/index.htm>. Accessed 20 April 2010

- European Parliament (2000) Council Directive 2000/53/EC of 18 September 2000 on end-of life vehicles. <http://eur-lex.europa.eu/en/index.htm>. Accessed 20 April 2010
- Fakin D, Golob V, Kleinschek K, Le Marechal A (2006) Sorption properties of flax fibers depending on pretreatment processes and their environmental impact. *Text Res J* 76(6): 448–454
- Fisher C (1981) History of natural fibers. *J Macromol Sci Chem A* 15(7):1345–1375
- Fishler D (1949) Fiber flax in Oregon. *Econ Bot* 3(4):395–406
- Focher B (1992) Physical characteristics of flax fiber. The biology and processing of flax. M publications, Belfast, UK
- Foulk J, Akin D, Dodd R (2003) Fiber flax farming practices in the southeastern United States. *Crop Manage*. doi:10.1094/CM-2003-0124-01-RS
- Foulk J, Chao W, Akin D, Dodd R, Layton P (2004) Enzyme-retted flax fiber and recycled polyethylene composites. *J Polym Environ* 12(3):165–171
- Foulk J, Akin D, Dodd R, McAlister D (2005) Harvesting and processing of flax in the USA. Recent progress in medicinal plants, vol 15 – Natural products. Studium, New Delhi, pp 563–580
- Foulk J, Chao W, Akin D, Dodd R, Layton P (2006) Analysis of flax and cotton fiber fabric blends and recycled polyethylene composites. *J Polym Environ* 14(1):15–25
- Foulk J, Dodd R, McAlister D, Chun D, Akin D, Morrison H (2007) Flax-cotton fiber blends: miniature spinning, gin processing, and dust potential. *Ind Crops Prod* 25(1):8–16
- Foulk J, Akin D, Dodd R (2008a) Processability of flax plants into functional bast fibers. *Compos Interf* 15(2–3):147–168
- Foulk J, Akin D, Dodd R (2008b) Influence of pectinolytic enzymes on retting effectiveness and resultant fiber properties. *BioResources* 3(1):155–169
- Foulk J, Akin D, Dodd R (2009) Miniature spinning enzyme-retted flax fibers. *J Nat Fibers* 6(1):1–13
- Foulk J, Fuqua M, Ulven C, Alcock M (2010) Flax fiber quality and influence on interfacial properties of composites. *Int J Sustain Eng* 3(1):1–8
- Franck R (1992) The history and present position of linen. In: The biology and processing of flax. M Publications, Belfast, UK, pp 1–9
- Frank R (2005) Bast and other plant fibres. CRC, Boca Raton, FL, 397 pp
- Fuqua M, Huo S, Thapa A, Gibbon L, Ulven C (2009) Challenges in manufacturing oilseed versus linen flax fiber reinforced composites. In: Proceedings of SAMPE 2009 technical conference: Changing times. New opportunities. Are you prepared? Baltimore, MD, 18–21 May 2009
- Fuqua M, Huo S, Chevali V, Ulven C (2010) Development of flax fiber/soy-based polyurethane composites for mass transit flooring application. In: Proceedings of Soc Auto Eng Int Congr Expt SAE Tech Paper 2010-01-0428, Detroit, MI, Warrendale, PA, 13–15 Apr 2010
- Gassan J, Bledzki A (2001) Thermal degradation of flax and jute fibers. *J Appl Polym Sci* 82(6):1417–1422
- Green A (1986) Effect of temperature during seed maturation on oil composition of low-linolenic genotypes of flax. *Crop Sci* 26(5):961–965
- Gumuskaya E, Usta M, Balaban M (2007) Carbohydrate components and crystalline structure of organosolv hemp (*Cannabis sativa* L.) bast fibers pulp. *Bioresour Technol* 98(3):491–497
- Guthrie J (1949) The integral and differential heats of sorption of water by cellulose. *J Text Inst* 40(8):T489–T504
- Hargitai H, Racz I, Czvikovsky T, Gaal J, Csukat G, Frojmovics G (1998) Development of natural fiber reinforced PP-composites for application in automobile industry. 5 International Tagung Stoffliche Nutzung nachwachsender Rohstoffe, Chemnitz Germany, 28–29 Oct 1998, pp 87–96
- Harris M (1954) Handbook of textile fibers. Harris Research Laboratories, Washington, DC, 356 pp

- Harwood R, Nusenbaum V, Harwood J (2008) Cottonisation of flax. In: 2008 International conference on flax and other bast plants, Saskatoon, Saskatchewan, Canada, 21-23 July 2008, pp 118–128 (ISBN #978-0-9809664-0-4)
- Heijenrath R, Peijs T (1996) Natural-fiber-mat reinforced thermoplastic composites based on flax fibers and polypropylene. *Adv Compos Lett* 5(3):81–85
- Himmelsbach D, Holser R (2008) Flax processing: use of waste streams for profit. In: 2008 International conference on flax and other bast plants, Saskatoon, Canada, pp 97–103
- Hocking P, Randall P, Pinkerton A (1987) Mineral nutrition of linseed and fiber flax. *Adv Agron* 41:221–296
- Hogue J (2006) What the buyer needs. Saskatchewan Flax Development Commission. <http://www.saskflax.com>. Accessed 20 April 2010
- Hudson P, Clapp A, Kness D (1993) Joseph's introductory textile science, 6th edn. Harcourt, Brace, and Jovanovich, New York, 417 pp
- Huo S, Chevali V, Ulven C (2010a) How to find an appropriate chemical modification for flax fibers in biocomposites? *Compos Sci Technol* (In Press)
- Huo S, Fuqua M, Chevali V, Ulven C (2010b) Effects of natural fiber surface treatments matrix modification on mechanical properties of their composites. In: Proceedings of Soc Automo Eng Int Congr Expt SAE Tech Paper 2010-01-0426, Detroit, MI, 13–15 Apr 2010, Warrendale, PA
- Huo S, Thapa A, Ulven C (2010c) Effect of surface treatments on interfacial properties of flax fiber reinforced composites. *Compos Sci Technol* (In Press)
- International Standard Organization (1980) 2370 Textiles – determination of fineness of flax fibres – permeametric methods. International Organization for Standardization, Geneva, 11 pp
- Jaeger W, Siegel R (2008) Economics of oilseed crops and their biodiesel potential in Oregon's Willamette Valley. Special Report 1081, Dept Agric Res Econ, Oregon State University, OR, USA, 50 pp
- Joseph K, Thomas S, Pavithran C (1996) Effect of chemical treatment on the tensile properties of short sisal fibre-reinforced polyethylene composites. *Polymer* 37(23):5139–5149
- Joseph K, Mattoso L, Toledo S, de Carvalho L, Pothen L, Kala S, James B (2000) Natural fiber reinforced thermoplastic composites. In: Frollini E, Leao A, Mattoso L (eds) Natural polymers and agrofibers composites. Embrapa, San Carlos, Brazil, pp 159–201
- Kessler R, Kohler R (1996) New strategies for exploiting flax and hemp. *Chemtech* 26(12):34–42
- Kessler R, Becker U, Kohler R, Goth B (1998) Steam explosion of flax a superior technique for upgrading fiber value. *Biomass Bioenerg* 14(3):237–249
- Khalili S, Akin D, Pettersson B, Henriksson G (2002) Fibernodes in flax and other bast fibers. *J Appl Bot Angew Bot* 76(5–6):133–138
- Kim J, Mazza G (2006) Optimization of extraction of phenolic compounds from flax shives by pressurized low-polarity water. *J Agric Food Chem* 54(20):7575–7584
- Koelkemoeck H (1883) Flax culture for the seed and the fiber in the United States. Hiram Sibley, MA, USA
- Kolattukudy P (1984) Biochemistry and function of cutin and suberin. *Can J Bot* 62(12): 2918–2933
- Kozlowski R (2009) EUROFLAX Newsletter Information Bulletin of the FAO/ESCORENA. *Eur Coop Res Netw Flax Other Bast Plants* 1(31):1–38
- Kromer K (2009) Physical properties of flax fibre for non-textile-use. *Res Agric Eng* 55(2):52–61
- Kvavadze E, Bar-Yosef O, Belfer-Cohen A, Boaretto E, Jakeli N, Matskevich Z, Meshveliani T (2009) 30, 000-Year-old wild flax fibers. *Science* 325(11):1359
- Lacoux J, Klein D, Domon JM, Burel C, Lamblin F, Alexandre F, Sihachakr D, Roger D, Balange AP, David A, Morvan C, Laine E (2003) Antisense transgenesis of *Linum usitatissimum* with a pectin methylesterase cDNA. *Plant Physiol Biochem* 41(3):241–249
- Lepsch D, Horal J (1998) Development of an integrated modular plastic electrical carrier and flax/polypropylene shelf panel for a vehicle rear shelf system. *Plastics: components, processes, and technology* (SP-1340), SAE technical paper series no 980727

- Lewin M, Pearce E (1998) Handbook of fiber chemistry, 2nd edn. Revised and Expanded. Marcel Dekker, New York, USA, 1083 pp
- Loadholt C (1965) The influence of nitrogen, phosphorus, potassium, and micronutrients on the yield and quality of fiber flax on two South Carolina coastal plain soils. Unpublished Masters Thesis, Clemson University, Clemson, SC
- Lora J, Glasser W (2002) Recent industrial applications of lignin: a sustainable alternative to nonrenewable materials. *J Polym Environ* 10(112):39–48
- MacCracken J (1916) A review of the status and possibilities of flax production and manipulation in Canada. Pub No 542-1 Ottawa Government printing bureau 38 pp
- Mapleston P, Smock D (1998) PUR processing goes au naturel with fibers. *Mod Plast* December 79 pp
- Medeirosa D, Hamptona M, Kurtzera K, Parelmana M, Al-Tamimia E, Drouillard J (2007) Feeding enriched omega-3 fatty acid beef to rats increases omega-3 fatty acid content of heart and liver membranes and decreases serum vascular cell adhesion molecule-1 and cholesterol levels. *Nutr Res* 27(5):295–299
- Mekic S, Akhatov I, Ulven C (2009) Analysis of a radial infusion model for in-plane permeability measurements of fiber reinforcement in composite materials. *Polym Compos* 30(12): 1788–1799
- Melitz S (2005) A framework for assessing the exchange costs in the flax fiber supply chain. Unpublished Masters Thesis, Department of Agricultural Economics University of Saskatchewan, Saskatoon, 154 pp
- Meredith R (1945) A comparison of tensile elasticity of some textile fibres. *J Text Inst* 36(7): T147–T164
- Mishra S, Misra M, Tripathy S, Nayak S, Mohanty A (2001) Potentiality of pineapple leaf fiber as reinforcement in PALF-Polyester composite: surface modification and mechanical performance. *J Reinf Plast Compos* 20(4):321–334
- Mohanty A, Misraa M, Hinrichsen G (2000) Biofibres, biodegradable polymers and biocomposites: an overview. *Macromol Mater Eng* 276/277(1):1–24
- Mohanty A, Misra M, Drzal L (2001) Surface modifications of natural fibers and performance of the resulting biocomposites: an overview. *Compos Interf* 8(5):313–343
- Mohanty M, Misra M, Drzal L (2002) Sustainable bio-composites from renewable resources: opportunities and challenges in the green materials world. *J Polym Environ* 10(1/2):19–26
- Morrison W, Akin D (2001) Chemical composition of components comprising bast tissue in flax. *J Agric Food Chem* 49(5):2333–2338
- Morrison W, Himmelsbach D, Akin D, Evans J (2003) Chemical and spectroscopic analysis of lignin in isolated flax fibers. *J Agric Food Chem* 51(9):2565–2568
- Morrison W, Archibald D (1998) Analysis of graded flax fiber and yarn by pyrolysis mass spectrometry and pyrolysis gas chromatography mass spectrometry. *J Agric Food Chem* 46(5):1870–1876
- Morton W, Hearle J (1997) Physical properties of textile fibers. The Textile Institute, Manchester, UK
- Morvan C, Andeme-Onzighi C, Girault R, Himmelsbach D, Driouch A, Akin D (2003) Building flax fibres: more than one brick in the walls. *Plant Physiol Biochem* 41(11):935–944
- Mueller D, Krobjilowski A (2003) New discovery in the properties of composites reinforced with natural fibers. *J Ind Text* 33(2):111–130
- Muir A, Westcott N (2003) Flax: the genus *Linum*. Taylor and Francis, London, UK, 320 pp
- Mukhin V (1992) Harvesting and retting of flax in the Soviet Union. In: The biology and processing of flax. M publications, Belfast, UK
- Munker M, Holtman R, Michaeli W (1998) Improvement of the fiber/matrix-adhesion of natural fiber reinforced polymers. In: Proceedings of 43rd international SAMPE symposium, 31 May–4 June 1998, pp 2123–2133
- Mustata A (1997) Factors influencing fiber-fiber friction in the case of bleached flax. *Cellul Chem Technol* 31(5–6):405–413

- Myers R (2000) Flax: a crop from America's past with renewed interest. Jefferson Agricultural Institute, Crop Production Guides, 601 West Nifong, Suite 1D, Columbia, MO 65203, 4 pp. <http://jeffersoninstitute.org/pubs/flax.shtml>. Accessed 20 April 2010
- Nechwatal A, Mieck K, Reußmann T (2003) Developments in the characterization of natural fibre properties and in the use of natural fibres for composites. *Compos Sci Technol* 63(9): 1273–1279
- Nevel T, Zeronian S (1987) Cellulose chemistry and its applications. Ellis Horwood, Chichester, England
- O'Donnell A, Dweib M, Wool R (2004) Natural fiber composites with plant oil-based resin. *Comp Sci Technol* 64(9):1135–1145
- Oelke E, Johnson S, Ehrhardt P, Comstock V (1987) From flax straw to linen fiber. Minnesota Exten Serv Fact Sheet AG-FS-3339
- Oksman K (2001) Mechanical properties and morphology of flax fiber reinforced melamine-formaldehyde composites. *Polym Compos* 22(4):568–578
- Oomah D (2001) Flaxseed as a functional food source. *J Sci Agric* 81(9):889–894
- Opoku A, Panigrahi S, Tabil L (2007) Frictional properties of natural and chemically treated flax fiber. In: 2007 ASABE Annual International Meeting, vol 13, Technical Paper Number: 076188 Minneapolis, MN, 17–20 June 2007
- Pan N (1996) An analysis on woven fabric strengths: prediction of fabric strength under uniaxial and biaxial extensions. *Compos Sci Technol* 56(3):311–327
- Parks C, Frederick J, Porter P, Murdock E (1993) Growing flax in South Carolina. Clemson University Cooperative Extension Service, Clemson, SC, 16 pp
- Przybyla-Wilkes A (2007) Flax heart health Flax use up as health benefits better realized. Prepared Foods BNP Publication April 1–7 pp
- Robinson B (1934) Flax-fiber production. Farmers Bull No 1728 United States Department of Agriculture, Washington, DC, pp 1–29
- Robinson B, Hutcheson T (1932) Adaptation of fiber flax to South Atlantic States. Circ 231 USDA, Washington, DC
- Rodriguez E, Giacomelli F, Vazquez A (2004) Permeability-porosity relationship in RTM for different fiberglass and natural reinforcements. *J Compos Mater* 38(3):259–268
- Roland C (1913) Possibilities for investment in the manufacture of Canadian flax fiber. Winnipeg Industrial Bureau, Winnipeg, Canada, 12 pp
- Rong M, Zhang M, Liu Y, Yang G, Zeng H (2001) The effect of fiber treatment on the mechanical properties of unidirectional sisal-reinforced epoxy composites. *Compos Sci Technol* 61 (10):1437–1447
- Rouison D, Couturier M, Panthapulakkal S, Sain M (2006) Measurement of the average permeability of natural fibre mats in resin transfer moulding application. *Polym Compos* 14 (3):229–238
- Rowell R, Young R, Rowell J (1997) Paper and composites from agro-based resources. CRC Lewis, Boca Raton, FL, 446 pp
- Sharma H, Van Sumere C (1992) The biology and processing of flax. M Publications, Belfast, UK, 576 pp
- Sharma H, Lefevre J, Boucaud J (1992) Role of microbial enzymes during previous term retting next term and their affects on fiber characteristics. In: Sharma HSS, Van Sumere CF (eds) The biology and processing of flax. M Publications, Belfast, UK, pp 157–198
- Sharma H, Faughey G, Lyons G (1999) Comparison of physical, chemical, and thermal characteristics of water- dew- and enzyme-retted flax fiber. *J Appl Polym Sci* 74(1):139–143
- Shaw M, Tabil L (2007) Compression, relaxation, and adhesion properties of selected biomass grinds. Agricultural Engineering International, CIGR Ejournal Manuscript FP 07 006 6:1-16
- Shiloh M (1965) Studies on cotton crimp. Part II: The recovery of crimp of cotton fibers after successive loadings. *Text Res J* 35(6):546–553
- Shishonok M, Shadrina V (2006) Recovery of wool from flax fibers using nitric acid. *Russ J Appl Chem* 79(9):1542–1545

- Smeder B, Liljedahl S (1996) Market oriented identification of important properties in developing flax fibres for technical uses. *Ind Crops Prod* 5(2):149–162
- Sohn M, Barton F, Morrison W, Archibald D (2003) Application of partial least squares regression to near-infrared reflectance spectroscopic determination of shive content in flax. *Appl Spectrosc* 57(5):551–556
- Sohn M, Barton F, Akin D, Morrison W (2004) A new approach for estimating purity of processed flax fiber by NIR spectroscopy. *J Near Infrared Spectrosc* 12(4):259–262
- Sohn M, Himmelsbach D, Morrison W, Akin D, Barton F (2006) Partial least squares regression calibration for determining wax content in processed flax fiber by near-infrared spectroscopy. *Appl Spectrosc* 60(4):437–440
- Soleimani M, Tabil L, Panigrahi S, Opuku A (2008) The effect of fiber pretreatment and compatibilizer on mechanical and physical properties of flax fiber-polypropylene composites. *J Polym Environ* 16(1):74–82
- Sreekala M, Kumaran M, Joseph S, Jacob M, Thomas S (2000) Oil plam fiber reinforced phenol formaldehyde composites: influence of fiber surface modifications on the mechanical performance. *Appl Compos Mater* 7(5–6):295–329
- Stephens G (1997a) Connecticut fiber flax trials 1994–1995. Connecticut Agricultural Experiment Station, New Haven, CT, USA, 946
- Stephens G (1997b) A manual for fiber flax production. Connecticut Agricultural Experiment Station, New Haven, CT, USA, 18 pp
- Stevanovic D, Lowe A, Kalyanasundaram S, Jar P, Otieno-Alego V (2002) Chemical and mechanical properties of vinyl-ester/ABS blends. *Polymer* 43(16):4503–4514
- Sultana C (1992) Growing and harvesting flax. In: Sharma H, Van Sumere C (eds) *Biology and processing of flax*. M Publications, Belfast, UK, pp 83–109
- Svensson N (1997) Development of textile structures for load carrying composites. In: *Niches in the world of textiles*, vol 1, 77th World conference of the textile institute, 22–24 May 1996, Tampere, Finland. The Textile Institute, Manchester, UK, pp 433–449
- Taylor J, Rapport L, Lockwood GB (2003) Octacosanol in human health. *Nutraceuticals* 19(2):192–195
- Timel T (1957) Some properties of native hemp, jute, and kapok celluloses. *Text Res J* 27(11):854–859
- United States Department of Agriculture (1995) *The classification of cotton*. Agricultural Handbook 566, Cotton Program, Agricultural Marketing Service, USDA, Washington, DC
- Vaidya U, Samalot F, Pillay S, Janowski G, Husman G, Gleich K (2004) Design and manufacture of woven reinforced glass/polypropylene composites for mass transit floor structure. *J Compos Mater* 38(21):1949–1972
- Van de Velde K, Kiekens P (2001) Thermoplastic polymers: overview of several properties and their consequences in flax fibre reinforced composites. *Polym Test* 20(8):885–893
- Van de Weyenberg I, Ivens J, De Coster A, Kino B, Baetens E, Verpoest I (2003) Influence of processing and chemical treatment of flax fibers on their composites. *Compos Sci Technol* 63(9):1241–1246
- Van de Weyenberg I, Truong T, Vangrimde B, Verpoest I (2006) Improving the properties of UD flax fibre reinforced composites by applying an alkaline fibre treatment. *Compos A Appl Sci* 37(9):1368–1376
- Van Sumere CF (1992) Retting of flax with special reference to enzyme retting. In: Sharma H, Van Sumere C (Eds) *Biology and processing of flax*. M Publications, Belfast, UK, pp 157–198
- Van Sumere C, Sharma H (1991) Analyses of fine flax fibre produced by enzymatic retting. *Aspects Appl Biol* 28:15–20
- Vila A, Jabbur F (2005) Sheet forming studies using low-cost composites. *J Thermoplast Compos* 18(1):5–22
- Wittig W (1994) The use of natural fibers in vehicle components. In: Haldenwanger H (ed) *Plastics in automotive engineering materials-components-systems*. Hanser -Gardner, Munich -Cincinnati

- Wrobel M, Zebrowski J, Szopa J (2004) Polyhydroxybutyrate synthesis in transgenic flax. *J Biotechnol* 107(1):41–54
- Yachmenev V, Bertoniere N, Blanchard E (2002) Intensification of the bio-processing of cotton textiles by combined enzyme/ultrasound treatment. *J Chem Technol Biotechnol* 77(5): 559–567
- Yannakopoulos A (2007) Egg enrichment in Omega-3 fatty acids. In: Huopalahti R, López-Fandino R, Anton M, Schade R (eds) *Bioactive egg compounds*. Springer, Berlin Heidelberg, pp 159–170
- Yueping W, Ge W, Haitao C, Genlin T, Zheng L, Feng X, Xiangqi Xiaojun H (2010) Structures of bamboo fiber for textiles. *Text Res J* 80(4):334–343
- Zafeiropoulos N, Williams D, Baillie C, Matthews F (2002) Engineering and characterization of the interface in flax fibre/polypropylene composite materials. Part I: Development and investigation of surface treatments. *Compos A Appl Sci* 33(8):1083–1093
- Zylinski T (1964) *Fiber science*. Office of Technical Services (OTS 60-21550) United States Department of Commerce, Washington, DC, 681 pp

Chapter 4

Cellulosic Bast Fibers, Their Structure and Properties Suitable for Composite Applications

Malgorzata Zimniewska, Maria Wladyka-Przybylak, and Jerzy Mankowski

Abstract A wide variety of natural fibers can be applied as reinforcement or fillers in composites. Bast fibers, such as flax and hemp, have a long history of cultivation and use. They are characterized by low weight and excellent range of mechanical properties. The properties of bast fibers are influenced by conditions of cultivation, retting, and processing. Pretreatment and surface modification of bast fibers is conducted for optimization of the interfacial characteristics between fiber and matrix as well as improvement of their mechanical properties. Application of bast fibers as reinforcement to replace the glass fibers to composite manufacture brings positive environmental benefits.

Keywords Bast fibers · Composite reinforcement · Fiber modification · Fiber properties · Fiber structure

Contents

4.1	Introduction	98
4.2	Classification of Cellulosic Bast Fibers	100
4.3	Key Issues of Cellulosic Bast Fibers	101
4.4	Structure of Cellulosic Bast Fiber	102
4.5	Cellulosic Bast Fibers Properties	105
4.5.1	Moisture Properties	106
4.6	Fiber Modification	107
4.6.1	Physical Methods	107
4.6.2	Chemical Methods	108
4.7	Natural Fibers as Reinforcement Material	112
4.8	Conclusions	117
	References	117

M. Zimniewska (✉)

Institute of Natural Fibres and Medicinal Plants, Wojska Polskiego 71b, 60-630 Poznan, Poland
e-mail: gosiaz@iwnirz.pl

4.1 Introduction

Cellulosic Bast Fibers constitute a significant part of the huge family of natural vegetable fibers. Generally, the term “natural vegetable fibers” is used for all types of fibers coming from plant material produced as a result of photosynthesis. Green lignocellulosic raw materials such as cotton, flax, jute, sisal, kenaf, and fibers of allied plants have served mankind for primitive tools, construction, goods for everyday life, or clothes manufacturing since more than 8000 BC. Flax and hemp fibers were used for fabric manufacturing in Europe about 4000 BC (Czerniak et al. 1998) (Fig. 4.1), and as a reinforcement of ceramics as early as 6500 BC (Kozłowski and Mackiewicz Talarczyk 2005). Ramie was used as a mummy clothes in Egypt during the period 5000–3300 BC. Hemp fiber implants have been found in over 10,000 years old pottery shards in China and Taiwan.

Nowadays, despite huge development of completely new fibrous raw materials – man-made fibers in the twentieth century – natural fibers still play an important role in world textile market.

Analysis of the world fibers supply since 1970 has showed that all fiber types suffered from demand reduction (Fig. 4.2). The established fibers like polyester, polyamide, polypropylene, and acrylic were down in volumes. The usage of cotton, wool, and silk also decreased by 10.1% to 25.2 million tonnes, and man-made fibers fell by 4.5% to 42.2 million tonnes.

Only the vegetable fibers section with kapok, ramie, flax, hemp, jute, sisal, and coir is anticipated to have stagnated at 5.9 million tonnes.

World production of three major bast fibers: flax, hemp, and ramie have kept the steady level since 2003, which is visible in Fig. 4.3. In time of growing concern for environment protection and counteracting global warming, the value of natural fibers significantly increased. As a renewable resource, natural fibers are used for manufacturing of recyclable “green” products in industrial processes, causing



Fig. 4.1 Images of flax threads dated to ap. 4000 BC found in Poland (Czerniak et al. 1998)

World Fibers Supply

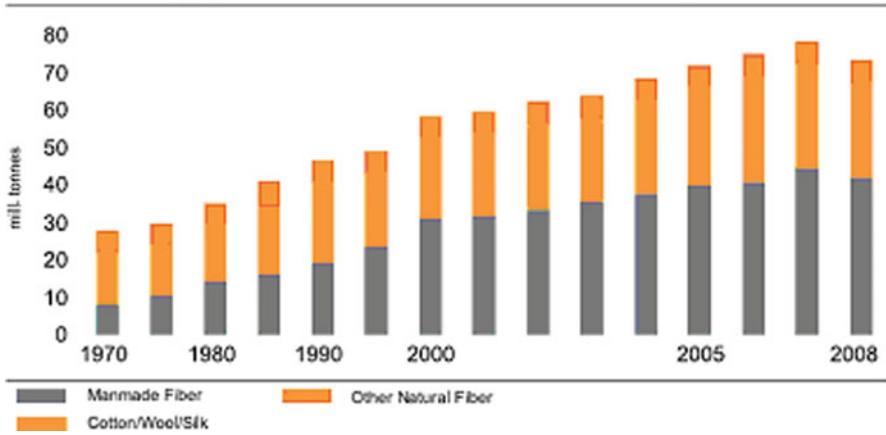


Fig. 4.2 World fiber supplies (Oerlikon Textile The Fibre Year 2008/09)

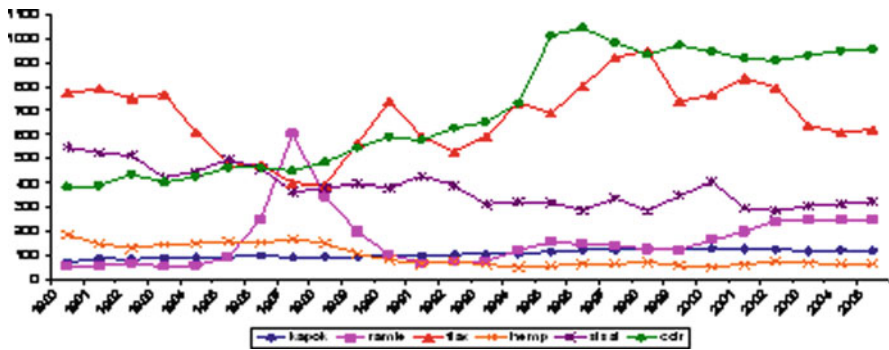


Fig. 4.3 Worldwide vegetable fiber production (Saurer Report 2006). Kapok, ramie, flax, hemp, sisal, coir

reduction of carbon emission and waste minimizing. Good example of action contributing to CO₂ reduction is fibrous plants cultivation. Cultivation of hemp *Cannabis sativa* on 1 ha area causes absorption of approximately 2.5 tonnes of CO₂ from atmosphere during the one growing period (Kolodziej et al. 2007) and jute absorbs as much as 2.4 tonnes of carbon per tonne of dry fiber. In contrast, producing 1 tonne of polypropylene emits into the atmosphere more than 3 tonnes of carbon dioxide. From the other side, properties of natural fibers such as mechanical strength, low weight, as well as low productions costs allow widening of their traditional utilization and applying them as reinforcement of composites in car industry. For example, DaimlerChrysler has developed flax-reinforced polyester composite, and in 2005, they produced an award-winning spare wheel well cover that incorporated abaca yarn from the Philippines. Vehicles in some BMW series contain up to 24 kg of flax and sisal. Released in July 2008, the Lotus Eco Elise

features body panels made with hemp, along with sisal carpets and seats upholstered with hemp fabric. Japan's carmakers, too, are "going green." In Indonesia, Toyota manufactures door trims made from kenaf and polypropylene, and Mazda is using a bioplastic made with kenaf for car interiors. For consumers, natural fiber composites in automobiles provide better thermal and acoustic insulation than fiberglass and reduce irritation of the skin and respiratory system. The low density of plant fibers also reduces vehicle weight, which cuts fuel consumption. For car manufacturers, the molding process consumes less energy than that of fiberglass and produces less wear and tear on machinery, cutting production costs by up to 30% (International Year of Natural Fibres 2009).

4.2 Classification of Cellulosic Bast Fibers

The classification system for vegetable fiber related to its anatomical origin contains the following main types of fibers:

- Seed fibers – represented by cotton and kapok
- Bast fibers – such as flax, hemp, kenaf, ramie, jute, and nettle
- Leaf fibers represented by agaves like sisal and henequen, pineapple, curaua, abaca (manila), cabuya, chambira, and pita
- Fruit fibers represented by coir
- Wood such as hardwood and softwood
- Grass and reed such as bamboo, wheat, rice, oat, barley, elephant grass, and others.

Fibrous plants can be classified from their purpose point of view. In this classification system, bast fibers are classified into group of fibrous plants cultivated just for fiber production. The second group of the system contains plants grown for other goods, for example, fruits – coconut production, and fibers constitutes only a by-product of the plant – coir (Pickering 2008). Another classification system indicates that most of the technically important bast fibers are obtained not only from plants cultivated in agriculture, such as flax, hemp, or ramie, but also from wild plants, such as nettle.

Geographic classification system covers information related to main location of fibrous plants cultivation. Flax for fiber production is cultivated mainly in France, Belgium, Netherlands, Eastern Europe, China, and Egypt. Small quantities are grown in other countries, for example, Brazil and Chile. Hemp is grown for fiber application mainly in Europe, Canada, and China. While more hemp is exported to the United States than to any other country, the United States' Government consistently does not distinguish between marijuana and the nonpsychoactive Cannabis used for industrial and commercial purposes (West 1998). Small quantity of hemp fibers characterized by low quality are extracted from plants *Cannabis sativa indica*, which are cultivated for medical drugs. Kenaf is cultivated for its fiber in India, China, Bangladesh, United States of America, Indonesia, Malaysia, South

Africa, Vietnam, Thailand, parts of Africa, and to a small extent in southeast Europe. India is the world's largest jute growing country. Jute is also grown in Bangladesh, China, Myanmar, Nepal, and Thailand. India, Pakistan, and China are the largest buyers of local jute, while Britain, Spain, Ivory Coast, Germany, and Brazil import raw jute from Bangladesh.

China leads in the production of ramie and exports mainly to Japan and Europe. The true ramie or China Grass, also called Chinese plant or white ramie, is the Chinese cultivated plant. Other producers include Japan, Taiwan, the Philippines, and Brazil. Only a small percentage of the ramie produced is available on the international market. Japan, Germany, France, and the UK are the main importers, and the remaining supply is consumed domestically. A second type of ramie is known as green ramie or rhea and is believed to have originated in the Malay Peninsula. This type has smaller leaves, which are green on the bottom, and it appears to be better suited to tropical conditions (Scruggs and Smith 2003).

Nettle, *Urtica dioica*, is a native to Europe but also occurs in Asia, northern Africa, and North America.

Isora occurs often gregariously throughout India, from Jamuna eastwards to Bihar and Bengal and southwards in central, western, and southern India and Andaman Islands.

4.3 Key Issues of Cellulosic Bast Fibers

Bast fiber is extracted from phloem surrounding the stem of fibrous plants, mainly dicotyledonous ones. Figure 4.4 presents cross section of fibrous plant stem. Bark or skin protects the plant against moisture evaporation, sudden temperature changes, as well as partly gives mechanical reinforcement to the stem. Fibers are located in the phloem and occur usually in bundles under the skin; they support the conductive

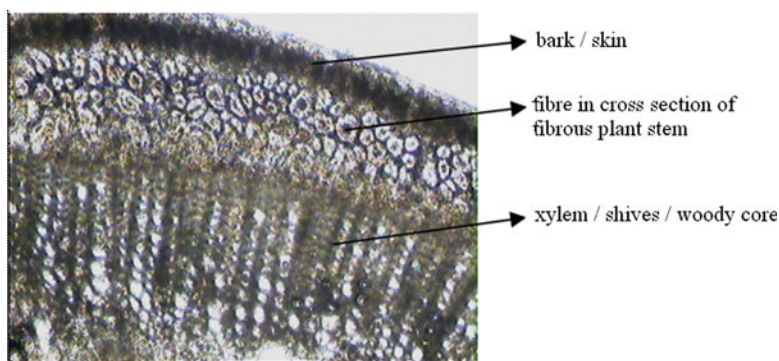


Fig. 4.4 Image of cross-section of fibrous plant (flax) stem (Prace wlasne INFMP)

Table 4.1 Fiber content by weight in straw (Urbanczyk 1985)

Fibrous plant	Phloem content in dry straw (%)	Fiber content in phloem (%)	Fiber content in dry straw (%)
Flax	36–42	47–54	17–22
Hemp	22–32	46–49	10–15
Ramie	20–35	24–48	4–21
Jute	30–48	–	19–20
Kenaf	23–28	48	16–17
Nettle ^a	–	–	16

^aBacci et al. (2009)

cells of the phloem and provide strength to the stem. Xylem material – woody core is in the middle part of the plant.


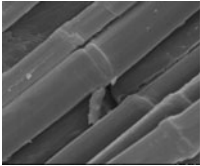
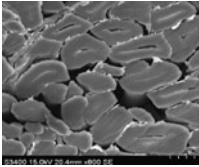

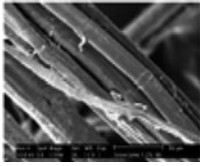
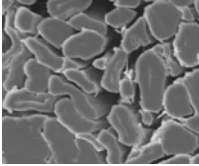

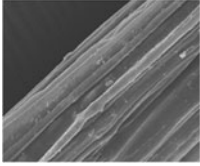
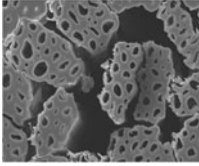

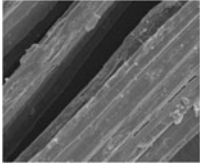
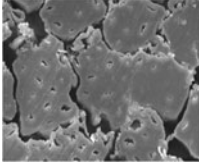

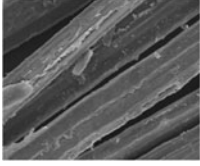
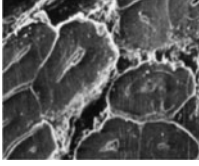

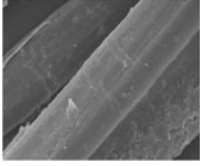
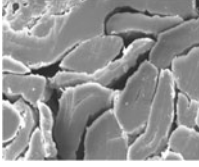

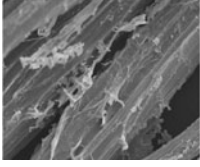
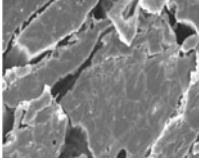
All parts of fibrous plant stem must be removed for proper fiber separation. Bast fiber extraction is usually conducted using special processes such as water and dew retting, degumming, or decortication, in which the separation of bundles containing elementary fibers joined together by pectin and calcium ions is also performed. Fiber content in the stem of fibrous plants is shown in Table 4.1.

Flax, the common fibrous plant is one of the oldest textile fiber used by mankind. Two main groups of flax plant varieties are cultivated: first for fiber production and second for linseed oil. Plants of flax fiber varieties grow up to 80–120 cm in height with stem diameter about 3 mm, but the oil varieties are smaller: 60–80 cm in height and thicker. Flax fiber varieties are utilized not only for textile application but also in composite and paper production. Seed extracted from *Linum usitatissimum* is used for production of diet food and pharmaceutical products based on linseed and linseed oil. Hemp *Cannabis Sativa* grows up to 1.2–5 m in height with stem diameter of 4–20 mm in approximately 140–145 days (Batra 2007). Ramie – *Boehmeria nivea* – is a perennial plant, growing to maturity in 45 days up to 1–2.5 m in height. Kenaf plant grows 1.5–3.5 m tall with woody base in 150–180 days of the growing cycle. The diameter of kenaf stems is 1–2 cm. Jute plant – *Corchorus Capsularis* – is known as a white jute and grows 2.5–3.5 m high (Pandey and Anantha Krishnan 1990). *Helicteres Isora* is a shrub or tree, growing around 1.8–5 m in height. Isora bast fibers are separated from the bark of the plant by retting process (Joshy and Mathew Lovely 2006). *Urtica Dioica* L. Stinging nettle is a dioecious herbaceous perennial, 1–2 m tall. Fiber nettle is a cultivated form of wild nettle. In over 30 years of breeding (Bredemann 1959), selected clones characterized by high fiber content (up to 16% compared to around 4–5% in wild nettle), long and not ramified stalks, and strong tillering (Table 4.2).

4.4 Structure of Cellulosic Bast Fiber

The structure of bast fibers is very similar to all types of fiber. Elementary fiber consists of cellulose fibrils held together by a lignin and hemicellulose. Typical phenomenon observed in bast fibers structure is occurrence of lumen with different

Table 4.2 Tabular presentation of bast fiber (Kicinska-Jakubowska 2009)

Fiber	Botanical name	Plant photo	Longitudinal view of fibers	Image of fiber cross section
Flax	<i>Linum usitatissimum</i>			
Hemp	<i>Cannabis sativa</i>			
Kenaf	<i>Hibiscus cannabinus</i>			
Jute	<i>Corchorus capsularis</i>			
Ramie	<i>Boehmeria nivea</i>			
Nettle	<i>Urtica dioica</i> L.			
Isora	<i>Helicteres isora</i>			

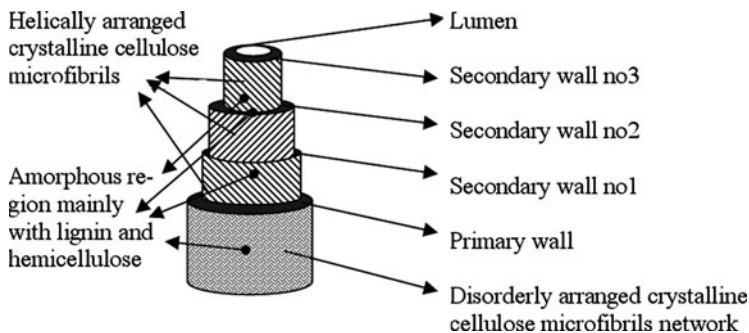


Fig. 4.5 Structure of natural fibers (Rong et al. 2001)

shape, located in central part parallel to fiber axis. The cell wall in a fiber is not a homogenous membrane (see Fig. 4.5). Each fiber has a complex, layered structure consisting of a thin primary wall, which is the first layer deposited during cell growth, encircling a secondary wall. The secondary wall is made of three layers, and the thick middle layer determines the mechanical properties of the fiber. The middle layer consists of a series of helically wound cellular microfibrils formed from long chain cellulose molecules. The angle between the fiber axis and the microfibrils is called the microfibrillar angle. The characteristic value of microfibrillar angle varies from one fiber to another. Such microfibrils have typically a diameter of about 10–30 nm and are made of 30–100 cellulose molecules in extended chain conformation and provide mechanical strength to the fiber. The amorphous matrix phase in a cell wall is very complex and consists of hemicellulose, lignin, and in some cases, pectin. The hemicellulose molecules are hydrogen bonded to cellulose and act as cementing matrix between the cellulose microfibrils, forming the cellulose–hemicellulose network, which is thought to be the main structural component of the fiber cell. The hydrophobic lignin network affects the properties of other network in a way that it acts as a coupling agent and increases the stiffness of the cellulose/hemicellulose composite (John and Anandjiwala 2008).

From the chemical composition view point, the main component of all bast fibers is cellulose that constitutes approximately 50–99% of their whole mass. Depending on the substance incrusting cellulose, different types of cellulose are present in fibers. Pectin–cellulose, a compound formed by cellulose and colloidal carbohydrates, is observed in flax or hemp, lignocellulose in jute or kenaf, and the clearest form of cellulose is found in ramie. Pectin occurs in secondary wall and glues together the elementary fibers and fiber bundles with cell of bark. Lignin is a substance incrusting cellulose, causing fiber fragility, and is collected on the fiber wall as well as in its central part. Waxes, fats, and other components occur in small amounts but have a negative effect on the technological process.

Chemical composition of bast fibers is presented in Table 4.3. Cellulose is the main component of vegetable fibers. The elementary unit of the macromolecule is anhydro D-glucose, containing three hydroxyl groups, which form hydrogen bonds

Table 4.3 Chemical composition of bast fibers by percentage mass

Fiber	Cellulose	Hemicellulose	Pectin	Lignin	Fat/wax
Flax	64–84	16–18	1.8–2.0	0.6–5.0	1.5
Hemp	67–78	16–18	0.8	3.5–5.5	0.7
Ramie	67–99	13–14	1.9–2.1	0.5–1.0	0.3
Jute	51–78	12–13	0.2–4.4	10.0–15.0	0.5
Kenaf	44–72	19	–	9–19	–
Nettle ^a	53–86	4–10	0.6–4.8	3.5–9.4	3.1–4.2
Isora	74	–	–	23	1.09

^aWurl and Vetter (1994)

Table 4.4 Characterization of bast fibers

Fiber	Density (g/m ³)	Length technical fibers (m)	Length elementary fibers (mm)	Diameter (μm)	Linear density (tex)
Flax	1.50	0.2–1.4	13–40	17–20	0.289
Hemp	1.48–1.49	1.0–3.0	15–25	15–30	0.333
Ramie	1.51–1.55	0.1–1.8	120–150	40–60	0.500
Jute	1.44–1.49	0.15–0.4	2–3	14–20	0.244
Kenaf	1.2	0.9–1.8	1.5–11	14–33	1.9–2.2
Nettle ^a	1.51	0.02–0.08	5.5	20–80	0.5 tex
Isora	1.2–1.3	–	–	–	–

^aDreyer et al. (2002)

inside the macromolecule itself (intramolecular) and between other cellulose macromolecules (intermolecular). Therefore, all vegetable fibers are hydrophilic in nature (Thomas 2002).

4.5 Cellulosic Bast Fibers Properties

There are many reports in scientific literature that present data determining physical–mechanical properties of bast fibers. The properties of the fiber are related to varieties of fibrous plants, condition of cultivation and retting, as well as the condition of measurement. Natural fibers are also characterized by the variability of individuals and from these reasons it is possible to find some differences between the fiber properties given by different authors in literature.

Properties related to bast fibers shape are shown in Table 4.4. Ramie, nettle, and flax are characterized by the highest density, but kenaf and isora show the lowest density. The longest technical fiber you can find is hemp, but ramie elementary fiber is the longest and the thickest.

The mechanical properties of bast fibers, especially flax, hemp, kenaf, and jute, are very good and may successfully compete with glass fiber. Their characteristics are strongly related to the structure and composition.

The structure, microfibrillar angle, cell dimensions, defects, and the chemical composition of fibers are the most important variables that determine the overall

properties of the fibers (Satyanarayana et al. 1986). Generally, tensile strength and Young's modulus of fibers increase with increasing cellulose content. The microfibrillar angle determines the stiffness of the fibers. Plant fibers are more ductile if the microfibrils have a spiral orientation to the fiber axis. If the microfibrils are oriented parallel to the fiber axis, the fibers will be rigid, inflexible, and have high tensile strength. Table 4.5 presents the important mechanical properties of natural fibers (Ray et al. 2005; Almeida et al. 2006).

4.5.1 Moisture Properties

Bast fibers show high ability for moisture sorption from surrounding area, similar to other hydrophilic materials. The amount of bonded water is strongly related to the humidity in air, which is shown in Table 4.6.

When a textile material is placed in a given atmosphere, it takes up or loses water at a gradually decreasing rate until it reaches equilibrium, when no further change takes place. This is a dynamic equilibrium, which occurs when the number of water molecules evaporating from the specimen in a given time becomes equal to the number condensing and being absorbed. From Table 4.7, it is visible that equilibrium moisture content is the highest for jute fibers.

Table 4.5 Mechanical properties of bast fibers (Hattallia et al. 2002; John and Anandjiwala 2008; Poradnik Inzyniera 1978)

Fiber	Tensile strength (MPa)	Tenacity of dry fibers (cN/tex)	Tenacity of wet fibers (% of dry tenacity)	Elongation of dry fibers (%)	Elongation at break (%)	Young's modulus (GPa)
Flax	345–1035	0.53	100–110	1.5–4.1	2.7–3.2	27.6
Hemp	690	0.57	100–115	1.5–4.2	1.6	70
Ramie	560	0.64	117–125	1.5–5.0	2.5	24.5
Jute	393–773	0.35	90–105	0.8–3.0	1.5–1.8	26.5
Kenaf	930	–	–	1.7–2.1	1.6	53
Nettle	650	–	–	1.7	1.7	38
Isora	500–600	–	–	5–6	5–6	–

Table 4.6 Effect of relative humidity of air on hygroscopicity of selected bast fibers

Fiber	Moisture content in different relative humidity of air (%)					
	30	40	50	60	70	100
Flax	7.5	8.3	9.1	9.9	10.7	23
Hemp	8.0	8.7	9.4	10.1	10.8	24
Jute	6.7	7.9	8.6	9.4	10.1	24

Table 4.7 Equilibrium moisture content of bast fibers at 65% relative humidity of air and 21°C

Fiber	Flax	Hemp	Jute	Ramie
EMC	7	9	12	9

Table 4.8 Swelling of fibers in water (Alexander et al. 1962)

Fiber	Transverse swelling diameter (%)	Transverse swelling area (%)	Axial swelling (%)
Flax	–	47	0.1; 0.2
Jute	20; 21	40	–

The plant cell walls of bast fibers consist mainly of cellulose, hemicellulose, and lignin. The uptake of water by a hygroscopic material as cellulose or hemicellulose is a hydration process involving accessible hydroxyl groups, or in this case $-\text{CH}_2\text{OH}$ groups of the host material. Water molecules absorbed by dry cellulose form a true cellulose hydrate, and the reaction is exothermic, which provides the driving force (Pizzi 1987).

Three different types of adsorbed water (Pott 2004) can be distinguished in lignocellulosic materials (Berthold et al. 1996): nonfreezing water, freezing water, and free water. The primary layer bound directly to the $-\text{CH}_2\text{OH}$ groups of the lignocellulose forms a relatively strong hydrogen bond and attracts other water molecules by weaker hydrogen bonding. This weaker bound layer may be several molecular layers thick and shows some order. It forms the freezing content, the fiber saturation point, and the adsorbed water may be considered as free water. In bast fibers, the fiber saturation point is at about 20% water content.

With water uptake in the cell walls, the fiber swell until the forces of water sorption are counterbalanced by the cohesive forces of the cell walls. Selected data of bast fiber swelling are shown in Table 4.8.

4.6 Fiber Modification

Reinforcing fibers can be modified by physical and chemical methods. Chemical and physical modifications of natural fibers are usually performed to correct the deficiencies (described above) of these materials, especially to impart bonding and adhesion, dimensional stability, and thermoplasticity. Surface modification of natural fibers can be used to optimize properties of the interface.

4.6.1 Physical Methods

Physical methods involve surface fibrillation, electric discharge (corona, cold plasma), etc. Cold plasma is already a very effective method to modify the surface of natural polymers without changing their bulk properties. This method has been used for increasing adhesion and compatibility between two polymers (Iorio et al. 1997; Petash et al. 1995; Tu et al. 1994). Physical treatments change structural and surface properties of the fiber and thereby influence the mechanical bonding with the matrix.

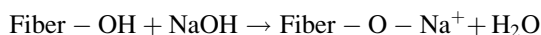
4.6.2 Chemical Methods

There are some treatment methods that are partially physical and chemical in nature, among which alkaline treatment (mercerization) (Kozłowski and Władysław-Przybylak 2004; Bledzki et al. 2000; Pauksta 2000) and liquid ammonia treatment (Yanai) should be mentioned.

4.6.2.1 Alkaline Treatment

Alkaline treatment or mercerization is one of the most used chemical treatments of natural fibers when used to reinforce thermoplastics and thermosets. Mercerization leads to the increase in the amount of amorphous cellulose at the expense of crystalline cellulose. The important modification expected here is the removal of hydrogen bonding in the network structure.

The following reaction proceeds as a result of treatment with alkalis:



As a result of sodium hydroxide penetration into crystalline regions of parent cellulose (cellulose I), alkali cellulose is formed. Then, after washing out unreacted NaOH, the formation of regenerated cellulose (cellulose II) takes place.

It is reported (Xue et al. 2007) that alkaline treatment has two effects on the fiber (1) it increases surface roughness resulting in better mechanical interlocking; and (2) it increases the amount of cellulose exposed on the fiber surface, thus increasing the number of possible reaction sites (Valadez-Gonzalez et al. 1999). Consequently, alkaline treatment has a lasting effect on the mechanical behavior of flax fibers, especially on fiber strength and stiffness (Jähn et al. 2002).

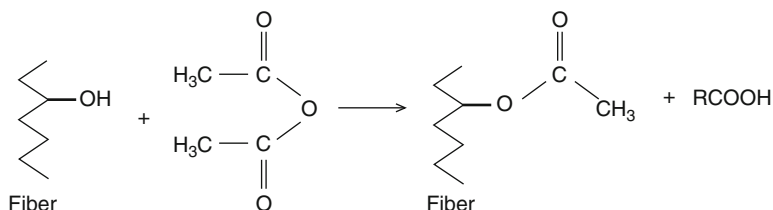
4.6.2.2 Liquid Ammonia Treatment

The treatment with liquid ammonia has been used mainly for cotton. Its development occurred since the late 1960s as an alternative to mercerization. Liquid ammonia, due to its low viscosity and surface tension, penetrates quickly the interior of cellulose fibers, forming a complex compound after the rupture of hydrogen bonds. The molecule of ammonia is relatively small and is able to increase distances between cellulose chains and penetrate crystalline regions. The original crystal structure of cellulose I changes to cellulose III after liquid ammonia treatment, and at the next stage, cellulose III changes to cellulose I again after hot water treatment (Pickering 2008). Liquid ammonia treatment of natural fibers results in their deconvolution and smoothing of their composites based on lignocellulosic raw materials' surfaces. At the same time, fiber cross-section becomes round and lumens decrease (Kozłowski et al. 2004).

4.6.2.3 Esterification

Conventional chemical modification is usually carried out through typical esterification and etherification reactions of lignocelluloses hydroxyl groups.

Esterification usually involves the reactions with organic acids or anhydrides. Many esters are possible depending on the nature of organic acid (anhydride) used in the reaction. Esters containing 1–4 carbon atoms are formate, acetate, propionate, and butyrate; laurate has 12 carbon atoms and stearate has 18 carbon atoms. Maleate and fumarate are esters of dicarboxylic acids containing double bonds in the carbon chain. Double bond-containing esters with longer chains confer thermoplasticity on the lignocellulosic materials (Young 1996). The most popular esterification method is acetylation, which has already been developed in commercial scale, first in the United States (Koppers 1961) and then in Russia (Otlesnov and Nikitina 1977). Within the UK, BP chemicals performed an economic appraisal of the process and built a small pilot plant to modify fibers but have now discontinued this work (Sheen 1992). Within Europe, several groups are working towards a scale up of the process (Beckers and Militz 1994; Militz et al. 1997; Rowell 2002). The reaction of acetic anhydride with fiber is shown as given below:



In Sweden, a continuous process of acetylation has been recently developed. The pilot plant for wood fiber or particles acetylation of capacity 500 kg/h is jointly owned by A-Cell and GEA Evaporation Technology AB and located in Kvarnorp.

Substitution of hydrophilic hydroxyl groups in lignocellulose by hydrophobic radicals alters properties of fibers, especially equilibrium moisture content (EMC), depending on the degree of substitution. Modification alters polarization of fibers and makes them more compatible to nonpolar matrix.

4.6.2.4 Silanization

Organosilanes are the main group of coupling agents for glass fiber-reinforced polymers. Silanization of natural fibers minimizes the disadvantageous effect of moisture on properties of composites and at the same time increases adhesion between fibers and polymer matrix, which results in upgrading composite strength. The effectiveness of the modification depends, among others, on the type of silane used, its concentration in solution, temperature, and time of fiber silanization, moisture content, and volume contribution of fibers to composite (Abdalla and Pickering 2002; Abdalla et al. 2002; Bledzki and Gassan 1997a, b).

4.6.2.5 Graft Copolymerization

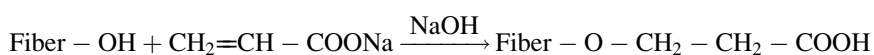
The surface of natural fibers can be modified by grafting copolymerization.

Grafting efficiency, grafting proportion, and grafting frequency determine the degree of compatibility of cellulose fibers with a polymer matrix. The grafting parameters are influenced by the type and concentration of the initiator, by the monomer to be grafted and the reaction conditions (Thomas 2002). The polymerization reaction is initiated at the surface of the fibers by the incorporation of peroxides or oxidation–reduction agents, or treatment with gamma radiation or cold plasmas.

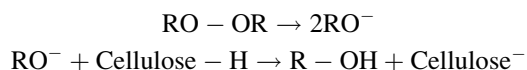
The cellulose is treated with an aqueous solution containing selected ions and is exposed to a high-energy radiation. Then, cellulose molecules crack and radicals are formed (Bledzki and Gassan 1997a, b). Afterwards, the radical sites of the cellulose are treated with a suitable solution (compatible with the polymer matrix), for example, vinyl monomer (Kroschwitz 1990), acrylonitrile (Mohanty et al. 1989), methyl methacrylate (Escamila et al. 1970), and polystyrene (Maldas et al. 1989). The resulting copolymer possesses properties characteristic of both fibrous cellulose and grafted polymer (Bredemann 1959). The lignin content in the fiber is a governing factor on the extent of acrylonitrile grafting. The accessibility of the monomer molecules to the active centers of cellulose is easier in water than in an organic solvent. It was found that without the presence of lignin, the grafting reaction could favorably proceed between cellulose and acrylonitrile.

4.6.2.6 Acrylation and Maleic Anhydride Treatment

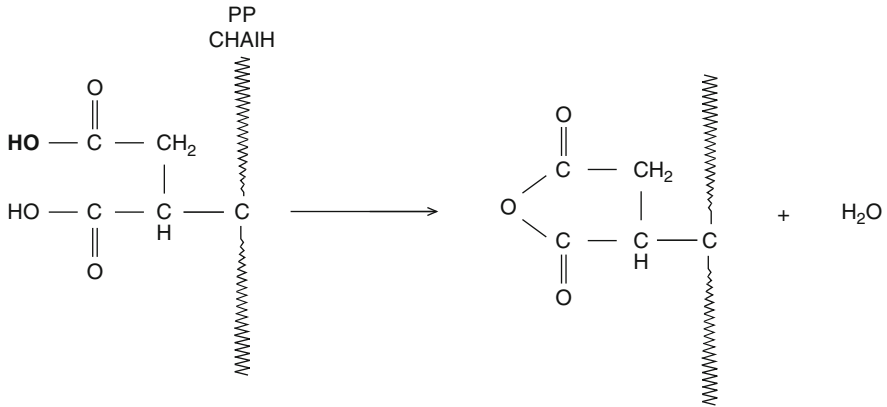
Acrylation reaction at hydroxyl groups of the fiber proceeds as follows



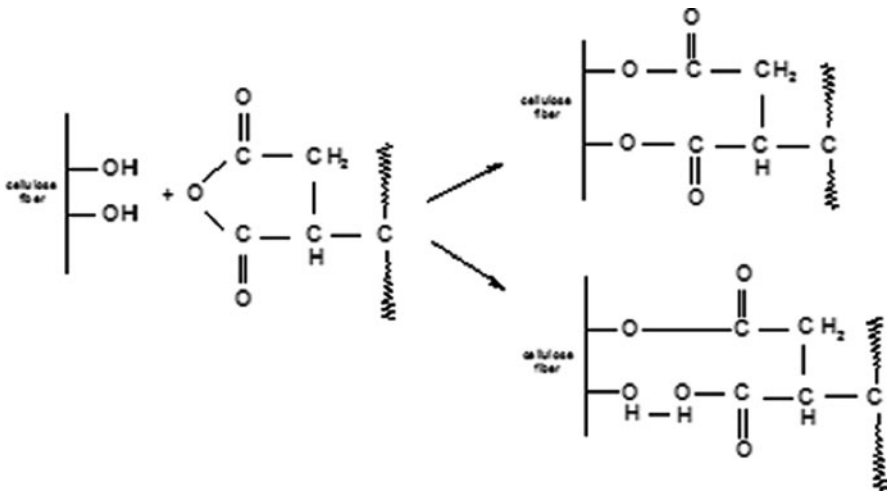
The decomposition of peroxide and subsequent reaction at the interface are expected at the time of curing of composites. Higher temperature is favored for the decomposition of peroxides. This can be shown as:



The treatment of cellulose fibers with hot polypropylene–maleic anhydride (MAPP) copolymers provides covalent bonds across the interface (Han et al. 1991). There are two ways of obtaining biocomposites from natural fibers and polymer. In the first one, pretreated fibers with maleated polymer are reinforced with desired polymer matrix.



In the second method, fibers, polymer, and maleic anhydride with the addition of peroxide initiator in one step processing are reactively extruded and then proceed with molding or injection to obtain a final composite.



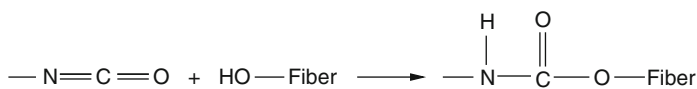
The effect of fiber surface modification on the mechanical performance of oil palm fiber is shown in Table 4.9.

4.6.2.7 Treatment with Isocyanates

Isocyanates have functional groups $-\text{N}=\text{C}=\text{O}$, which are very susceptible to reaction with the hydroxyl groups of cellulose and lignin in fibers. The reaction between fiber and isocyanate coupling agent is shown below:

Table 4.9 Mechanical performance of parent and modified oil palm fibers (Sreekala et al. 2000)

Fiber	Tensile strength (MPa)	Young's modulus (MPa)	Elongation at break (%)
Untreated	248	6700	14
Mercerized	224	5000	16
Acetylated	143	2000	28
Peroxide-treated	133	1100	24
Permanganate-treated	207	4000	23
γ -irradiated	88	1600	25
TDIC-treated	160	2000	22
Silane-treated	273	5250	14
Acrylated	275	11100	26
Acrylonitrile-grafted	95	1700	24
Latex-coated	98	1850	23



George et al. (1996) treated pineapple leaf fiber with polymethylene–polyphenyl–isocyanate (C₁₅H₁₀N₂O₂) solution at 50°C for 30 min to improve the fiber–matrix interfacial adhesion. Comparing silane and isocyanate-treated wood fiber–PS composites, it was reported that isocyanate treatment was more effective than silane treatment in enhancing the mechanical properties of cellulose fiber–PS composites (Maldas et al. 1989).

4.7 Natural Fibers as Reinforcement Material

Natural fibers are raw materials of growing importance as a reinforcing substance. This is due to their properties, especially low density at 1.2–1.4 g/cm³, and low production costs, this factor resulting from high yield of fibrous plants and relatively cheap labor in countries where such plants can be harvested a few times per year (e.g., Latin America countries) (Zuchowska 2000; Bledzki 1997). The above-mentioned factors cause that the cost of obtaining natural fibers is three times lower than that of glass fibers, four times lower than aramid fibers, and five times lower than the cost of carbon fibers (Zuchowska 2000; Bledzki 1997). With the low price and easy availability of various natural fibers, they may serve as a cheap and an ecological addition to the reinforcing fibers used in composite materials so far. The demand for new materials will stimulate economic growth of those countries and the whole world.

The polymeric materials, when compared to the traditional materials (metal, wood, stone, and glass), will prevail. Most global reports predict the development of advanced composite technologies, particularly those based on polymers and various kinds of reinforcement (also with bio-renewable plant fibers) (Czaplicka-Kolarz 2008a, b).

The development in producing composite materials with lignocellulosic fillers will be determined by issues related to the environment protection. The hazard of accumulating wastes from plastic materials is very likely. In order to avert this hazard, composite materials will contain natural reinforcing components of plant origin (Czaplicka-Kolarz 2008a, b). Thus, due to ecological reasons, growing interest in biodegradable polymers obtained from bio-renewable raw materials is observed. These materials comply with the requirements of after-use management of the composites that would not be harmful to the environment.

Further growth in the market share of the composites reinforced with natural fibers will affect the processing technologies and also will lead to decrease in the cost of fiber extraction (Mankowski et al. 2009). This reduction can be achieved by the use of decortication method. The method is based on mechanical separation of bast fibers from xylem without previous retting. Such extraction allows for a cost-effective and climate-independent technology of obtaining lignocellulosic raw material for reinforcing composites. The reduced costs of extraction, lowering the composite mass with the share of plant fibrous materials, the improvement of eco-impact of such composites, and the recyclability by biodegradation of wastes (from production and use) are all deciding factors in the development of applications of composites containing natural plant reinforcing substances (Kozłowski 1997).

The eco-friendliness of the natural fibrous materials applied for the composites is an important aspect of their obtaining, processing, and disposing. The agricultural production of natural plant fibers is efficient and ecological, prevent soil erosion, and can be carried out in the polluted postindustrial areas. The ecological aspect involves the CO₂ consumption during biomass formation. As claimed by Kozłowski, cultivation of 1 ha of hemp during the vegetation period accumulates circa 2,500 kg of atmospheric CO₂ (Kolodziej et al. 2007). This phenomenon has a positive result on the reduction of the glasshouse effect.

In case of utilization by combustion, polymeric composites reinforced with natural plant fibers emit less CO₂ than chemical fibers (Bledzki 1997). The composites based on natural fibers and synthetic polymers such as PE, PS, PP, etc. are called biocomposites, and being eco-friendly can contribute to solving numerous environmental problems.

The current trends in application of composites and their market share (%) are the following (Czaplicka-Kolarz 2008a Foresight):

- Construction – 30%
- Automotive industry – 25%
- Industrial equipment – 10%
- Electronics – 9%
- Sport – 8%
- Steel industry and shipbuilding – 6%
- Electrical engineering – 6%
- Aviation and space industries – 3%
- Medicine – 1%
- Railways – 1%
- Wind power plants – 1%

The trend watching in industry allows to assume that automotive and aviation industries are most likely to develop dynamically in terms of using composites reinforced with natural plant materials (Czaplicka-Kolarz 2008a). In the near future, it will be feasible to produce various parts for cars and aircrafts with the use of such materials. The elements containing natural fibers have better electrostatic properties, absorption of vibrations, thermal insulation, and sound attenuation as compared with traditional polymers. Lower weight of the composite affects the total weight of a vehicle, thus reducing the fuel consumption and consequently the costs of driving, and finally will have beneficial effect on the environment. Polymeric materials reinforced with natural fibers can be applied in the production of car parts such as bumpers, brake lining, and clutches (Fig. 4.6). Replacing chemical fibers (glass, carbon) with the natural ones enables to produce reinforcement of significantly less harmful for the environment and easier to recycle (Kozłowski 1997).

Car lining from flax or hemp fibers allow for creating a microclimate characterized with proper humidity, without dangerous substances and unpleasant odor that will absorb sound, noise, and vibrations, and provide insulation from heat. The replacement of glass fiber with natural fibers allows for reduction of their mass by 30% while maintaining the same mechanical parameters. It must be pointed out that the composites based on natural fibers have a high capacity of absorbing the impact energy, which is especially important in production of safe cars.

One might already say that the era of biopolymers is just beginning, as they can make up as much as 60 kg of mass in some car models. Some leaders in the automotive industry predict decrease in the use of glass fibers for the sake of natural ones such as wood, flax, hemp, bamboo, jute, and kenaf (Czaplicka-Kolarz 2008a).

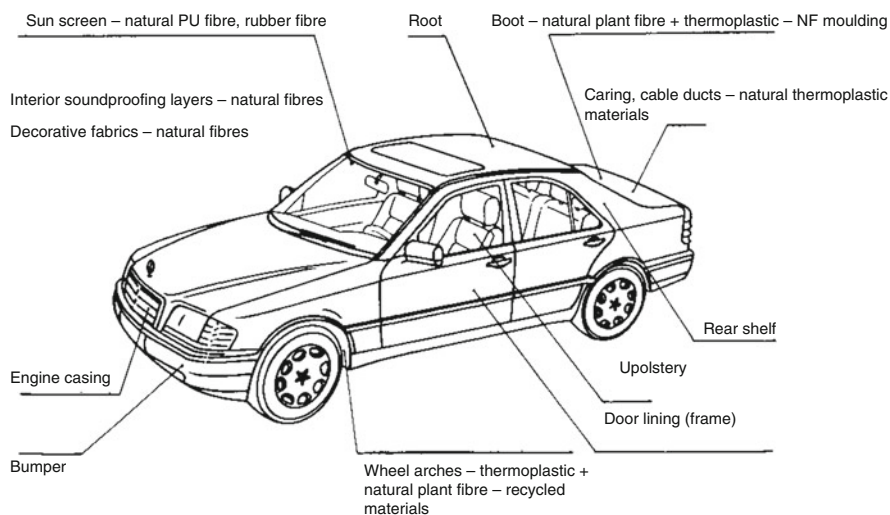


Fig. 4.6 Natural plant fiber used in company cars Daimler-Benz 65

This will result in higher safety due to the mechanical parameters of the fibers, which absorb energy very efficiently and do not break in a crash.

For production of light cars, construction composites are used, reinforced with carbon, aramid, glass, and graphite fibers as well as technically modified cellulosic fibers (often carbonized) with good mechanical properties (Czaplicka-Kolarz 2008a). The introduction of the latter composites is planned in Airbus A380 (see Fig. 4.7) aircrafts and the new version of Boeing 747 (see Fig. 4.8), which should result in lowering the weight of some elements even by 40%.

The aviation sector aims at obtaining composites that fulfill the mechanical requirements but also are easily recycled and utilized after use. These materials have found application as construction elements in the railway industry for production of railway cars and tramways and tube cars. Especially important are the



Fig. 4.7 Boeing 787 Dreamliner (Czaplicka-Kolarz 2008a, b)



Fig. 4.8 Airbus A380 (Czaplicka-Kolarz 2008a, b)

polymer composites used in the high-speed railway systems, e.g., TGV. As compared to the traditional public transport vehicles, those made partially of composites are about 30% lighter (Czaplicka-Kolarz 2008a). This implies reduction of the vehicle mass and thus the stress in the construction elements and raises the speed and reduces the noise. It is estimated that composites constitute more than 10% of the mass of a typical car with the new solutions increasing this share. Composites are found in military technology more and more often. The elements of military constructions must be characterized with low weight and high strength. They are applied in construction of military vehicles (cars), aircrafts, and helicopters. Equipping the army with the state-of-art floating and rescue paraphernalia is also of great importance (Czaplicka-Kolarz 2008a). Implementation of alternative energy production, using renewable resources, serves as an additional trigger for stimulating the progress in composites. One example of the new methods of producing bioenergy is construction of wind power plants. The technologies employed for the production of such power plants are based on modern 3D reinforcement, including carbonized cellulosic fibers (Czaplicka-Kolarz 2008a). Moreover, the composites reinforced with plant fibers are applied in other branches of economy, e.g., furniture and packaging, production, and construction. Because of special properties of these composites and their versatile applications, the growth in their production and demand for natural fibers is predicted. EU countries show an increase in use of vegetable raw materials for the reproducible production of biopolymers for different economic uses (Table 4.10) (Report on Bio-based Plastics and Composites 2009).

The composite materials reinforced with natural fibers will stimulate agriculture by the production of nonfood raw materials for the industry (Bledzki 1997) and by achieving high yields of raw materials derived from fibrous plants, thus leading to improvement in total yields of crops.

With yields at more than 10 t/ha of dry mass, hemp produces 3–5 times more biomass than in case of trees. This fact will contribute to creating new work places in agricultural processing sector, which is seriously affected by structural unemployment. Moreover, low quality soils, including contaminated soil, will be used for cultivation of nonfood crops. Finally, natural fibrous materials are eco-friendly at each stage of production, i.e., cultivation, processing, and also waste disposal.

Table 4.10 Biopolymer consumption in EU in 2009 (<http://www.renewable-resources.de>)

New biomaterials-technique	Quantities – region
Biodegradable bioplastics (mostly packing)	>80,000 tonnes
Bioplastics in permanent application	>60,000 tonnes
NF compression molding in the automotive industry	>40,000 tonnes
Wood fiber compression molding in the automotive industry	>50,000 tonnes
Cotton fiber compression molding	>100,000 tonnes
WPC injection molding and extrusion (construction, furniture, automobiles)	>120,000 tonnes
NF injection molding and extrusion	>5,000 tonnes
Total bio-based products	>450,000 tonnes

4.8 Conclusions

The chapter contains description of only selected vegetable fibers, bearing in mind that there are thousand different types of natural fibers in the world. However, presented fibers create a representative image of wide possibilities of their application, mainly as composite reinforcement. Many other applications such as nonwoven, filters, geotextiles, and technical textiles are possible using natural cellulosic fibers. Original features of the fibers such as good mechanical properties and low density predisposes them for use in multidirectional production. Additionally, natural fiber modification processes, such as alkaline treatment, mercerization, liquid ammonia treatment, esterification, silanization, graft copolymerization, acrylation and maleic anhydride, isocyanates treatment for improvement of their properties, and the reduction of moisture sensitivity, e.g., swelling, creates better synergy between fibers and polymer matrix.

Another strong aspect of vegetable fiber application in the industry is their ecological character with possibility of carbon dioxide reduction from the atmosphere during the fibrous plants' cultivation processes. Use of bast fibers ensures biodegradability of the end product, if natural polymer, e.g., PLA is applied as a matrix.

Summarizing, it is necessary to emphasize the increase of role of the renewable bast fibers in replacing inorganic filler and reinforcement materials, e.g., glass fibers in composites.

References

- Abdalla A, Pickering K (2002) The use of silane as a coupling agent for wood fibre composites. Proceedings of the 3rd Asian-Australasian Conference on Composite Materials (ACCM-3), Auckland, New Zealand
- Abdalla A, Pickering K, MacDonald AG (2002) Mechanical Properties of Thermoplastic Matrix Composites with Silane-Treated Wood Fibre. Proceedings of the 6rd International Conference on Flow Processes in Composite Materials, Auckland, New Zealand
- Alexander E, Lewin M, Litav Y, Peres H, Sholoh M (1962) Text Res J 32:898
- Almeida JRM, Aquino RCMP, Monteiro SN (2006) Compos A 37:1473
- Bacci L, Baronti S, Predieri S, di Virgilio N (2009) Fiber yield and quality of fiber nettle (*Urtica dioica* L.) cultivated in Italy. Ind Crops Prod 29(2–3):480–484
- Batra SK (2007) Other long vegetable fibres: abaca, banana, sisal, henequen, flax, ramie, hemp, sunn and coir. In: Lewin M (ed) Handbook of fiber chemistry, 3rd edn. Taylor and Francis, Boca Raton, FL, pp 453–520, Chapter 8
- Beckers EPJ, Militz H (1994). Acetylation of solid wood. Second Pacific Rim-Based Composites Symposium, Vancouver, Canada 125–134
- Berthold J, Rinaudo M, Salmen L (1996) Association of water to polar groups; estimation by an adsorption model for lignocellulose materials. Colloids Surf A 1996(112):117
- Bledzki A (1997) Recykling materialow polimerowych. Wydawnictwo Naukowo – Techniczne. Warszawa
- Bledzki AK, Gassan J (1997a) Natural fiber reinforced plastics. In: Cheremisinoff NP (ed) Handbook of engineering polymeric materials. Marcel Dekker Inc, New York

- Bledzki AK, Gassan J (1997b) Natural fiber reinforced plastics. In: Cheremisinoff NP (ed) Handbook of engineering polymeric materials. Marcel Dekker, New York
- Bledzki A, Gassan J, Lucka M. (2000) (in Polish) Renesans tworzyw sztucznych wzmocnionych włóknami naturalnymi. (Natural Fiber – Reinforced Polymers Come Back). *Polimery*, 45(2): 98–108
- Bredemann G (1959) Die große Brennessel *Urtica dioica* L. Forschung über ihren Anbau zur Fasergewinnung. Akademie-Verlag, Berlin
- Czaplicka-Kolarz K (2008a) Foresight technologiczny materialow polimerowych w Polsce – analiza stanu zagadnienia. Poznan
- Czaplicka-Kolarz K (2008b) Scenariusze rozwoju technologicznego materialow polimerowych w Polsce. Poznan
- Czerniak L, Kirkowski R, Kozłowski R, Zimmiewska M (1998) The earliest traces of flax textiles in central Europe, Kujawy (Poland). *Nat Fibres* 1:18–19, Special Edition
- Dreyer J, MüGssig J, Koschke N et al (2002) Comparison of enzymatically separated hemp and nettle fibre to chemically separated and steam exploded hemp fibre. *J Ind Hemp* 7(1):43–59
- Escamila G, Trugillo GR, Franco PJH, Mendizabal E, Puig JE (1970) *J Polym Sci* 66:339
- George J, Janardhan R, Anand JS, Bhagawan SS, Thomas S (1996) *Polymer* 37(24):5421–5431
- Han GS, Saka S, Shiraisi N (1991) Composites of wood and polypropylene. Morphological study of composites by TEM–EDXA. *Mokuzai Gakkaishi* 3:241
- Hattallia S, Benaboura A, Ham-Pichavant F, Nourmamode A, Castellan A (2002) *Polym Degrad Stab* 75:259
- International Year of Natural Fibres 2009 – <http://www.naturalfibres2009.org>
- Iorio I, Leone C, Nele L, Tagliaferri V (1997) Plasma treatments of polymeric materials and Al alloy for adhesive bonding. *J Mater Process Technol* 68:179–183
- Jähn A, Schröder MW, Fütting M, Schenzel K, Diepenbrock W (2002) *Spectrochim Acta A: Mol Biomol Spectrosc* 58:2271
- John MJ, Anandjiwala RD (2008) Recent developments in chemical modification and characterization of natural fiber-reinforced composites. *Polym Compos* 29:187–207
- Joshay MK, Mathew Lovely J (2006) Rani studies on short isora fibre-reinforced polyester composites. *Compos Interfaces* 13(4–6):377–390
- Kicinska-Jakubowska A, Bogacz E (2009) Private sources of INFMP
- Kolodziej J, Mankowski J, Kubacki A (2007) Wlasciwosci energetyczne odpadow z przerobu lnu i konopi w porownaniu z innymi surowcami roslinnymi. *Biuletyn Informacyjny PILiK Len i Konopie* nr 6 Poznan: 35–42
- Koppers' Acetylated Wood. *New Materials Technical Information No. (RDW-400), E-106* (1961)
- Kozłowski R (1997) The potential of natural fibres in Europe. *Industrial applications lignocellulosic – Plastics Composites* Sao Paulo
- Kozłowski R, Mackiewicz Talarczyk M (2005) Inventory of world fibres and involvement of FAO in fibre research. Institute of Natural Fibres, Poznan, Poland
- Kozłowski R, Władyka-Przybylak M (2004) Chapter 14 Uses of natural fiber reinforced plastics in book “natural fibers, plastics and composites” In: Wallenberger FT, Weston NE (ed) Kluwer Academic Publishers, Boston
- Kozłowski R, Władyka-Przybylak M, Helwig M, Kurzydłowski K (2004) Composites based on lignocellulosic raw materials. *Molecular crystal and liquid crystal. Proceedings of VIIth ICFPAM Molecular Crystals and Liquid Crystals. vol 415–418:301–321*
- Kroschwitz JI (1990) *Polymers: fibers and textiles*. Wiley, New York
- Maldas D, Kokta BV, Daneault C (1989) *J Appl Polym Sci* 37:751
- Mankowski J, Kaniweski R, Kubacki A (2001) Composite Elements for Automotive Industry. *Proceedings of Second Global Workshop Bast Plants in the New Millennium*
- Mankowski J, Kubacki A, Kolodziej J (2009) Efficient system of producing hemp fiber for industrial applications. *Natural fibres. Their attractiveness in multi directional applications*. Gdynia Cotton Association, Gdynia
- Militz H, Beckers EPJ, Homan WJ (1997). *Int. Res. Group Wood Pres., Doc. No. IRG = WP 97-40098*
- Mohanty AK, Patnaik S, Singh BC (1989) *J Appl Polym Sci* 37:1171–1181

- Oerlikon Textile The Fibre Year 2008/09 A World Survey on Textile and Nonwovens Industry, Issue 9 – May 2009 <http://www.oerlikontextile.com>
- Otlesnov Y, Nikitina N (1977) Latvijas Lauksaimniecības Akademijas Raksti: 130, 50
- Pandey SN, Anantha Krishnan SR (1990) Fifty years of research in jute 1939–1989. Jute Technology Research Laboratories, Hooghly Printing Co. Ltd., Calcutta, India
- Paukszta D (2000) The structure of modified natural fibers used for the preparation the composites with polypropylene. SPIE Int Soc Opt Eng 4240:38–41
- Petash W, Raüchle E, Walker M, Elsner P (1995) Improvement of the adhesion of low energy polymers by a short time plasma treatment. Surf Coat Technol 74–75:682–688
- Pickering LK (2008) Properties and performance of natural-fibre composites, Woodhead Publishing Limited: 3–66
- Pizzi A (1987) The structure of cellulose by conformation analysis. 5. The cellulose II water sorption isotherm, In: Macromol J (ed) Sci-Chem; A24(9): 1065–1084.
- Poradnik Inżyniera (1978) Włokiennictwo, WNT. Warszawa:11–27
- Pott GT (2004) Natural fibres with low moisture sensitivity, Chapter 8 of book: natural fibres, plastics and composites. In: Frederick T (ed) Wallenberger, Kluwer Academic Publishers, pp 106–110
- Ray AK, Moandal S, Das SK, Ramachandrarao P (2005) J Mater Sci 40:5249
- Report on Bio-based Plastics and Composites. Nova Institut 2009 <http://www.renewable-resources.de>
- Rong MZ, Zhang MQ, Liu Y, Yang GC, Zeng HM (2001) Compos Sci Technol 61:1437
- Rowell RM (2002) Chemical modification of natural fibres to improve performance. Wood Modification Thematic Network Newsletter, Issue 3 (April)
- Satyanarayana KG, Ravikumar KK, Sukumaran K, Mukherjee PS, Pillai SGK, Kulkarni AK (1986) J Mater Sci 21:57–63
- Saurer Report “The Fiber Year 2005/2006”, Issue 6, May 2006
- Scruggs B, Smith J (2003) “Ramie: Old Fibre – New Image” Ohio State University Extension Fact Sheet, HYG-5501-90
- Sheen AD (1992) The preparation of acetylated wood fibre on a commercial scale. Pacific Rim Bio-Based Composites Symposium; Chemical Modification of Lignocellulosics, FRI Bull: 176, 1–8
- Sreekala MS, Kumaran MG, Thomas S (2000) Effect of chemical modifications on the mechanical performance of oil palm fibre reinforced phenol formaldehyde composites. In natural polymers and composites. In: Capparelli Mattoso LH et al. (ed) Embrapa Instrumentacao Agropecuaria, Sao Carlos
- Thomas S (2002) Cellulose fiber reinforced composites: new challenges and opportunities. 4th International Wood and Natural Fibre Composites Symposium, Kassel Germany, April 10–11
- Tu X, Young RA, Denes F (1994) Improvement of bonding between cellulose and polypropylene by plasma treatment. Cellulose 1:87–106
- Urbanczyk G (1985) Nauka o Włoknie. WNT, Warszawa
- Valadez-Gonzalez A, Cervantes-Uc JM, Olayo R, Herrera-Franco PJ (1999) Compos B Eng 30:309–320
- Wurl and Vetter (1994), Faserinstitut Bremen
- West PD (1998) Hemp and Marijuana: Myths and Realities, North American Industrial Hemp Council
- Xue L, Tabil LG, Panigrahi S (2007) Chemical treatments of natural fiber for use in natural fiber reinforced composites: a review. J Polym Environ 15:25–33
- Yanai Y Non-resin shrink-proof process, Caltopia. Nisshinbo Industries Inc. Miai Plant, Aichi, Japan (unpublished)
- Young RA (1996) Utilization of natural fibers: characterization, modification and applications. In: Lea AL et al (eds) Lignocellulosic-plastics composites. UNESP, Sao Paulo
- Zuchowska D (2000) Polimery konstrukcyjne. Wydawnictwo Naukowe – Techniczne. Warszawa

Chapter 5

Potential Use of Micro- and Nanofibrillated Cellulose Composites Exemplified by Paper

Ramjee Subramanian, Eero Hiltunen, and Patrick A.C. Gane

Abstract Naturally abundant, biodegradable, and sustainable plant and wood fibres are composed of smaller and progressively mechanically stronger entities. These smaller structural load-bearing cellulosic fibrils, termed as micro- and nanocellulosic fibrils, can be separated by defibrillating the pulp fibres with either mechanical, chemical, enzymatic, and ultrasound sonication methods or a combination of these treatments. Engineered biopolymer, like cellulosic fibrils, and inorganic mineral composite structures have the potential to create new material properties and applications. This chapter deals with the production, characterisation, and application of cellulosic fibril-precipitated calcium carbonate structures in printing and writing paper. We enunciate a novel composite paper consisting of cellulosic fibrils and precipitated calcium carbonate as the backbone structure and reinforced with a minimal fraction of long fibres. However, recent research investigations show that cellulosic fibrils and their composites find wide application across different fields of manufacturing such as polymers and plastics, medicine, construction, and automotive industries.

Keywords Biopolymers · Calcium carbonate · Cellulosic fibrils · Composites · Coprecipitation · Micro- and Nanofibrillated cellulose · Morphology · Pigments · Properties

Contents

5.1	Introduction	122
5.2	Nanocellulosic Gel Composites	123
5.2.1	Cellulosic Fibrils	123
5.2.2	Mineral–Cellulosic Fibril Composites	126
5.3	Application of Nanocellulosic Fibrils–Mineral Pigment Composites in Paper	134
5.3.1	Need for and Means of Increasing Amount of Mineral Pigment in Paper	134
5.3.2	Formation of a Novel Composite Paper and Its Properties	135
5.3.3	Effect of PCC–Cellulosic Fibril Composites on Conventional Paper	146

R. Subramanian (✉)

Omya Development AG, Baslerstrasse 42, 4665 Oftringen, Switzerland

e-mail: ramjee.subramanian@gmail.com

5.4 Summary	150
References	150

Abbreviations

AmPCC	Amorphous PCC
BW	Bulk water
Co PCC	Colloidal PCC
c-PCC	Composite PCC
FBW	Freezing-bound water
FIB-SEM	Focussed ion beam SEM
FSP	Fibre saturation point
MFC	Microfibrillated cellulose
NBW	Nonfreezing bound water
NFC	Nanofibrillated cellulose
PCC	Precipitated calcium carbonate
r PCC	Rhombohedral PCC
ref-PCC	Conventional reference PCC
Sca PCC	Scalenoedral PCC
SEM	Scanning electron microscope
TMP	Thermomechanical Pulp

5.1 Introduction

This chapter discusses the potential and use of microfibrillated cellulose (MFC) and nanofibrillated cellulose (NFC) in papermaking. Cellulosic fibrils have many potential applications due to their structure.

In papermaking, delignified wood fibres (cellulose fibres) are widely applied. Paper and board are in most cases a network of complete fibres. This network is held together by forces affecting in the contact points between the fibres. The interfibre bonding is largely based on the chemical composition of fibres – hydrophilicity and hydrogen bonding capacity. In many paper grades, mineral filler is used as partial raw material in order to decrease the manufacturing costs and also to improve the print quality achievable. The amount of mineral filler in paper is limited by strength of paper – too high filler content for e.g., decreases tensile strength and promotes dusting.

If microfibrillated cellulose is used instead of complete fibres, the specific surface area increases dramatically. This is expected to compensate for the loss in interfibre bonding caused by mineral fillers. Thus, higher proportions of filler in paper are enabled. High filler content has a major effect toward lowering the raw materials costs in papermaking and also opens potential to develop novel engineered paper grades.

Already for some time, there have been studies about the nature of cellulosic fibrils, their superior strength and high surface area, and their application in different fields, including papermaking technology. In papermaking, these studies have dealt mostly with either understanding the phenomena in conventional papermaking or in trying to improve the current practise in small steps.

This chapter aims to introduce the concept of nanocellulosic–fibril and precipitated calcium carbonate (PCC) composites. The effect of cogrinding of lime and pulp fibres and different precipitation conditions on the production of PCC and modification of its morphologies are analysed in this chapter.

Finally, the impact of these new PCC–nanocellulosic fibril composites on paper properties is elucidated. In addition, we describe a novel and rather simple method to produce a new composite paper in laboratory scale. This paper based on cellulosic fibrils, which can be defined as the structural elements of the biopolymers, has radically higher filler proportion than conventional printing paper and exhibits superior quality.

Thus, the overall objective of this chapter is to introduce the concept of PCC–NFC composites to construct a novel and improved printing and writing paper by modifying or blending the structural elements of cellulosic pulp fibres and pigments, and to study the forming process and product properties.

5.2 Nanocellulosic Gel Composites

5.2.1 Cellulosic Fibrils

Natural, biodegradable, renewable, and sustainable plant and wood fibres have a hierarchical structure composed of smaller and progressively mechanically stronger entities. Cellulosic fibrils are the load-bearing constituents in plants. An elementary fibril in wood has a 30 nm^2 cross-sectional area, consisting of cellulose molecules (D-gluco-pyranose units linked by 1,2-glycoside bonds), and forming the smallest entity in a wood fibre structure. Lateral coaggregation and agglomeration of elementary and secondary nanofibrils lead to the formation of macrofibrils and fibres.

Fibrillar fines obtained from cellulosic fibres are known for their unique structure, material characteristics, and potential applications (Hubbe et al. 2008). An amorphous lignin and hemicellulose matrix separates the elementary nanofibrils in natural vegetable fibres. Based on raw material sources, pretreatment and subsequent defibrillation procedures will produce a broad spectrum of fibril structures as well as nomenclatures used to describe them. Thus, we find various terms adopted in the field, such as nanoscale-fibrillated cellulose, cellulosic fibrillar fines, cellulose aggregate fibrils, and microfibrillar cellulose.

Recently, various methods have been proposed to obtain nanocellulosic fibrils from cellulosic fibres. Chemical and enzymatic treatments followed by mechanical disintegration, homogenisation, or ultrasound sonication are being used extensively

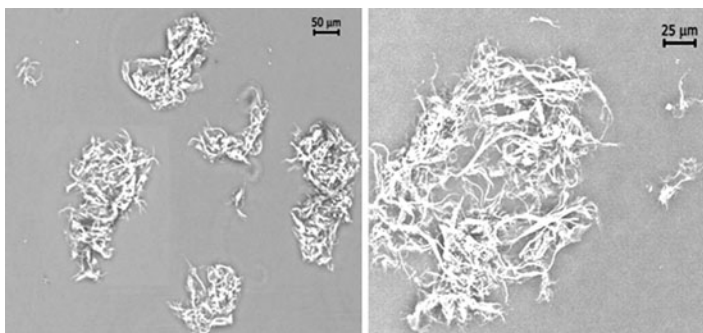


Fig. 5.1 Negative phase contrast image of fibrillar cellulosic fibrils obtained from bleached softwood kraft pulp; lower (*left*) and higher (*right*) magnification

to produce nanocellulosic fibrils. Physical treatments, such as grinding and homogenising, have become a major focus of development to separate the fibrillar bundles and produce micro- and nanofibrils (Matsuda et al. 2001; Pääkkö et al. 2007). Combination of acid hydrolysis and high shear pressure disintegration promotes isolation of free nanocrystalline cellulose particles with lengths of 100–200 nm and widths of 20–40 nm. Formation and characterisation of cellulosic fibrils obtained from dissolution (Liu and Hsieh 2002), cryocrushing (Chakraborty et al. 2005), and bacterial synthesis methods (Tokoh et al. 1998) have been described in detail in the literature.

Cellulosic fibril obtained from bleached softwood Kraft pulp by a grinding process at 3% consistency is illustrated in Fig. 5.1. The grinding was carried out with an ultrafine friction grinder (Super Masscolloider^{®1}). The grinder reduces the fibres into fines by mechanical shearing (Matsuda et al. 2001). The refining degree was increased by recirculating the pulp suspension. We find that the fibrils, thus produced, are intertwined to form a complex and flexible network capable of holding water in the interfibrillar space of the network. Nanocellulosic fibrillar particles in general, therefore, form highly viscous gels in water, with highly developed internal and external surfaces capable of holding a high amount of water in a semi-bound structure.

Rheological studies, carried out with softwood fibres, show that the storage modulus increases with increasing amounts of fibrils, as shown in Fig. 5.2. Increasing number of passes or recirculation of the exemplified nondried softwood pulp through such a grinder thus generates an ever greater amount of fibrils, and so, by significantly increasing the storage modulus at reduced volume occupancy of fibres, lowers the shear viscosity of the suspension, which, if allowed to reach rest equilibrium, leads to the formation of a hydrophilic gel. The suspension rheology of fibrils can vary depending on the raw material source (Subramanian et al.

¹Supermasscolloider[®] (Model MKZA 10-15J) is a trademark product of Masuko Sangyo Co. Ltd, Japan.

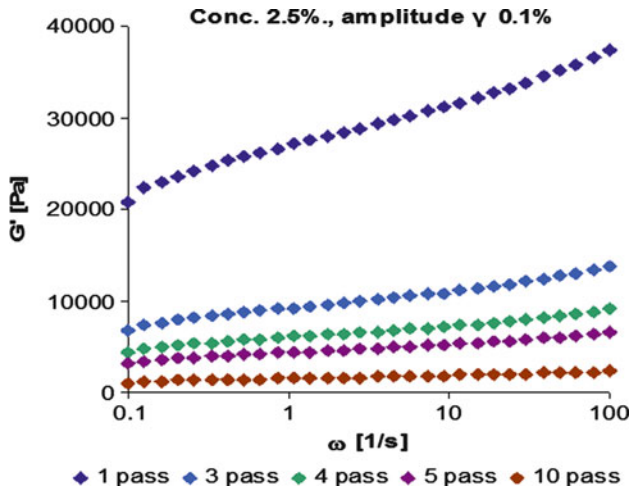


Fig. 5.2 Storage modulus with increasing amount of nanofibrils generated by grinding a cellulosic pulp suspension

Table 5.1 Rheology of different pulp fines suspensions

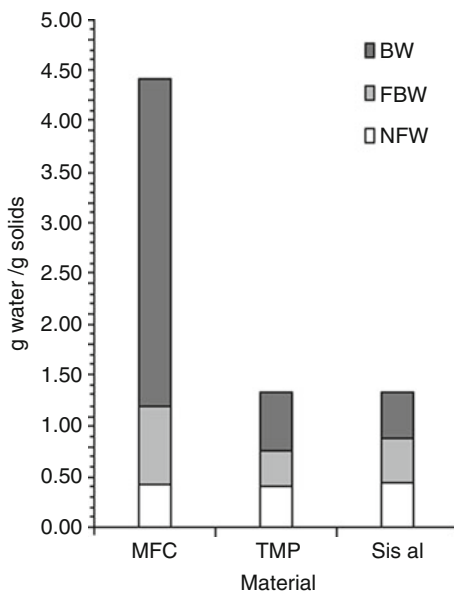
Sample	G'' (kPa)	Final bulk (cm^3/g)	Final solids (%)	Immobilisation time (s)	$\tan(\delta)$ ($= G''/G'$)	Consistency (g/l)
MFC	29	5.49	8.5	15.3	1.89	20
TMP	13	2.73	11.2	29.8	1.2	38
Sisal	16	5.15	17.3	14.4	1.16	32

2008), method of production (Wang and Sain 2007; Nakagaito and Yano 2006; Chakraborty et al. 2005; Lima and Borsali 2004; Pääkkö et al. 2007; Oksman and Sain 2006) or the concentration of the fibril suspension. Generally, hydrophilic nanocellulosic gels obtained by mechanically treating Kraft² chemical pulps are difficult to dewater, as shown by the solid content obtained at the immobilisation point (Table 5.1). However, mineral addition and chemical modifications can aid in increasing the dewatering ability of cellulosic fibrils.

Fibril–water interaction studies show that Kraft fibrils exhibit the highest fibre saturation point (FSP), defined as the maximum water uptake of a fibrillar mix before a free water layer is detectable. Measured FSP of Kraft fibrils is 4.3 g/g. The total water held inside the fibrous material is classified in terms of bulk water (BW), freezing-bound water (FBW), and nonfreezing bound water (NFW) (Maloney and Paulapuro 2001) (Fig. 5.3). Most of the water is held in the interfibrillar space, corresponding to the macropore level in Kraft nanofibrillated cellulose. This is illustrated by the higher bulk water (BW), as shown in Fig. 5.3. On the other hand, since the amount of nonfreezing water strongly associated with cell wall

²Kraft process (Kraft or sulphate pulping) describes a technology for conversion of wood into wood pulp consisting of almost pure cellulose fibres.

Fig. 5.3 Water absorption in the inter- and intrafibrillar matrix obtained with a differential scanning calorimetric technique and solute exclusion



constituents was similar for all the fines samples, their submolecular structure can be considered to be similar.

The fractional composition among studied fines can be obtained by passing the fraction through a 400-mesh sieve, having an aperture size of 36 μm . An example of such an analysis revealed that softwood chemical pulp fines have the highest percentage of cellulosic nanofibrils: 90% for softwood chemical nanofibrillar cellulose (NFC), >50% for TMP,³ and >30% for sisal. Rheological studies show that Kraft (NFC) fibril suspensions have the highest ability to store energy (elastic modulus G') and dissipate energy (viscous modulus G'') and highest loss modulus (G''') at the immobilisation point, as shown in Table 5.1.

5.2.2 Mineral–Cellulosic Fibril Composites

The ability to construct organised nanoscale, microscopic and bulky inorganic–mineral–biopolymer structures is of critical importance in various fields, such as paper, medicine, electronics, magnetism, and mechanical design. Pigment–biopolymer composites are formed by processing them together in nano/microscale to obtain a broad spectrum of structures. Engineering nanoscale components of biopolymers and pigments together have the potential to create new material properties

³TMP – thermomechanical pulp.

and applications. Typical examples of biomimetic structures, such as attempts to reproduce the famously quoted Abalone or Nacre (mother of pearl) shell, have long been sought after for their extraordinary strength and toughness properties.

A composite pigment–biopolymer structure with potential use in biocomposites can be formed by different techniques, such as precipitation, mixing, self-assembly, or hierarchical methods. There are many open questions about the production, use, and potential benefits of these filler–fibre complexes. In this chapter, we present some targeted work, which investigated biopolymer composites produced by in situ calcium carbonate precipitation and mixing techniques.

Study A: Formation and modification of the pigment crystal habits in coprecipitation of calcium carbonate (PCC) – biopolymeric structures.

Study B: Refining lime (calcium hydroxide) together with pulp and subsequently precipitating calcium carbonate.

5.2.2.1 Study A: Formation and Modification of the Pigment Crystal Habits in the Coprecipitation of Calcium Carbonate (PCC) – Biopolymer Structures

Elementary chlorine-free (ECF)-bleached unrefined softwood pulp obtained from a mill in southern Finland was ground in a Supermass colloidiser^{®4} to produce fines. The Bauer–McNett analysis of the fines showed that 92% of the fines passed through the 200 mesh. The consistency of the produced fines–PCC composite was in the range of 0.085–0.1%. Calcium hydroxide was mixed to obtain 2:1 PCC:nanofibrils and carbonised to crystallise PCCs with colloidal, rhombohedral, and scalenohedral morphologies.

Equivalent amounts of calcium hydroxide suspension were added to preformed fibrillated cellulosic gels, in order to obtain 2:1 and 1:1 PCC–pulp fibril mixtures, which were then carbonated to cocrystallise PCC with colloidal-, fine and coarse rhombohedral-, and scalenohedral-type structures. Reference PCC precipitates, composed of four different morphologies, were crystallised in the absence of cellulosic fibrils. The experimental precipitation conditions were similar for composite and reference PCC filler samples.

The carbonation was carried out using a mixture of 20% CO₂ and 80% air. PCC morphology was controlled through crystallisation of intermediary phases as described by Yamada and Hara (1987). This study details the phase changes that occur over a period of time during the carbonation process, with respect to the reaction of milk of lime and carbon dioxide. The reaction was monitored using electrical conductivity of the remaining milk of lime and pH.

To illustrate the observed changes in conductivity and pH during the composite PCC production (c-PCC), colloidal PCC composite crystallisation is shown in Fig. 5.4. The following mechanism can be proposed, similar to precipitation of PCC

⁴Supermass colloidiser is described in detail in Sect. 5.2.1.

from lime (Yamada and Hara 1987; Carmona et al. 2004), to explain the changes in the conductivity of lime during the precipitation of colloidal composite PCC.

1. In this process, the first descending curve of the conductivity value is related to the surface precipitation of very fine amorphous calcium carbonate (AmCC), which partially covers the surface of lime particles inhibiting its continued dissolution. Subsequently, when the density of the particles is high enough, the interparticle interactions become important and they aggregate in a line, probably by the charge polarisation of the particles. This aggregation can be seen on the surface of the fibrils in Fig. 5.5.
2. In the next zone of the diagram (Fig. 5.4), with ascending conductivity, the crystallisation of AmCC into chain-like calcite proceeds, being accompanied by its desorption from the lime surface, which enables a further dissolution period of $\text{Ca}(\text{OH})_2$.

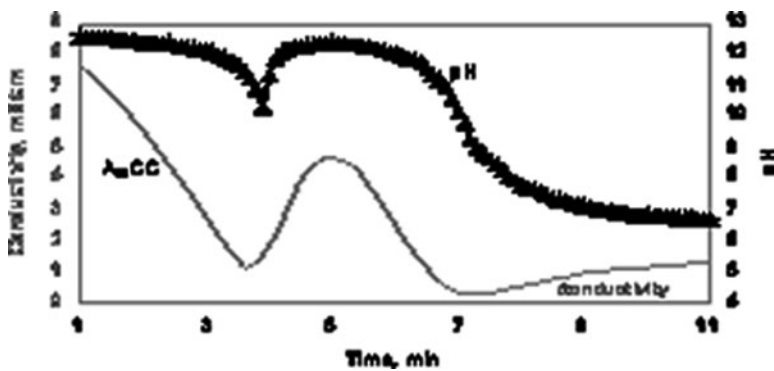


Fig. 5.4 Parameters observed during the crystallisation of composite calcium carbonate filler with colloidal morphology. *AmCC* amorphous calcium carbonate

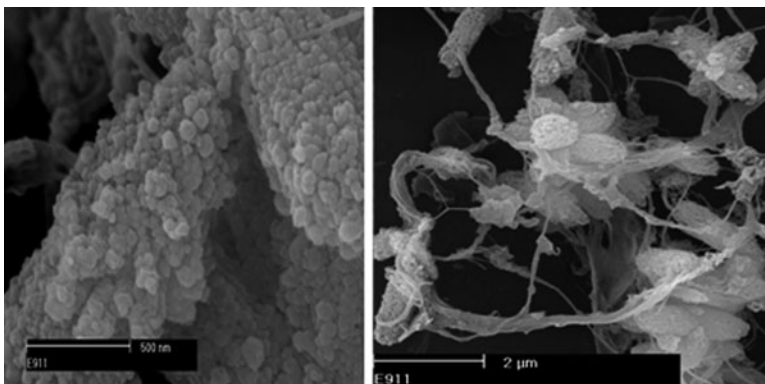


Fig. 5.5 Colloidal precipitated calcium carbonate composite (acronym: composite Co c-PCC)

3. With the growth of chain-like calcite, the solution is enriched with calcium and carbonate ions while $\text{Ca}(\text{OH})_2$ disappears. The conductivity starts to decrease until the complete consumption of the available calcium and carbonate ions in the form of CaCO_3 .
4. In the last ascending part of the curve, some of the interparticle material in the chain-like aggregates probably dissolves and separates into individual particles, which grow into nanometre-sized colloidal composite calcium carbonate.

Alternatively, due to differences in the nucleation mechanism, rhombohedral PCC (r-PCC) could be obtained through amorphous calcium carbonate (AmCC) and partially carbonated basic calcium carbonate (BCC), as shown below (Carmona et al. 2004).



Scalenohedral PCC (s-PCC) was precipitated onto cellulosic fibrils in similar conditions as described in the literature (Carmona et al. 2003; Meuronen 1997).

Analysis of Coprecipitated Composites

The particle size distribution was determined by sedimentation of the ash residue with a Sedigraph 5100. For calcium carbonate filler precipitated onto the surface of fibrils, the specific surface area was determined by oxidising the cellulosic fibres at low temperature (300°C) followed by oxidation for 1 h at 500°C. The specific surface area of the ash residue and reference PCC was determined with the Brunauer–Emmett–Teller (BET) nitrogen adsorption method. The measurement was carried out with a Micromeritics Gemini 2375 apparatus.

The particle size “75/25 ratio” is calculated from the Sedigraph as the measured value of the pigment particle size measured in micrometres at the 75 weight percentile, divided by the particle size measured in micrometres at the 25 weight percentile.

Coprecipitation Influence on PCC Morphology

The composite of nanofibrillar material formed with precipitated calcium carbonate (c-PCC), as described above in Sect. 5.2.2.1, seems to consist of precipitated nanocrystals aggregated into ellipsoidal shapes, as shown in Fig. 5.5. The precipitation occurs at random sites mostly on the end of fibrils and, hence, the fibrils are partially covered with calcium carbonate fillers. The particle size of the primary colloidal c-PCC particle is less than 100 nm.

The composite r-PCC is found in clusters forming a pearl necklace structure with the fibrils, as shown in Fig. 5.6 right-hand side scanning electron microscopy (SEM) micrograph. Some fibrils are covered by a PCC particulate surface.

In addition, films of microfibrils covering PCC surfaces are seen in the micrographs. The particle size of rhombohedral c-PCC is below 2 μm .

According to Alince, the scattering ability of a pigment is a function of its refractive index and size (Alince 1989), and in the case of agglomerates, also the particle spacing. Fibre surfaces contribute to light scattering due to areas of debonding having micrometre dimensions (Alince and Lepoutre 1985). The SEM pictures in Figs. 5.6 and 5.7, right-hand side, show that the width of some of the fibrils connecting the PCC particles is below 200 nm, and, hence, these fibrils may not contribute to improving the light scattering of paper.

Figure 5.8 illustrates a simple mixing of fines and reference structured s-PCC filler, with a mean particle size of 2 μm , and can be contrasted with the composite precipitations described above. The fibres were refined to nanofines and, subsequently, a defined amount of scalenohedral ref-PCC filler was added to this suspension and mixed thoroughly for 5 min. This fines–filler mixture was added

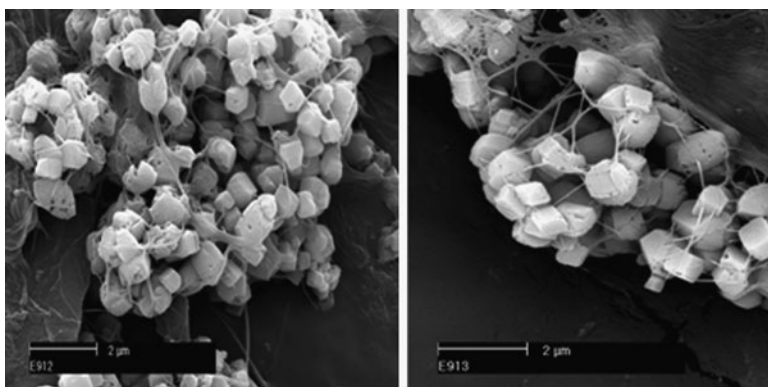


Fig. 5.6 Rhombohedral precipitated calcium carbonate composite (acronym: composite r c-PCC)

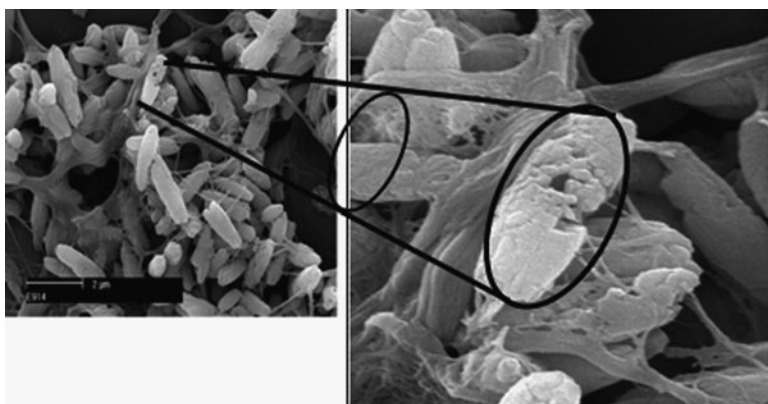


Fig. 5.7 Scalenohedral type of precipitated calcium carbonate composite (acronym: composite Sca c-PCC)

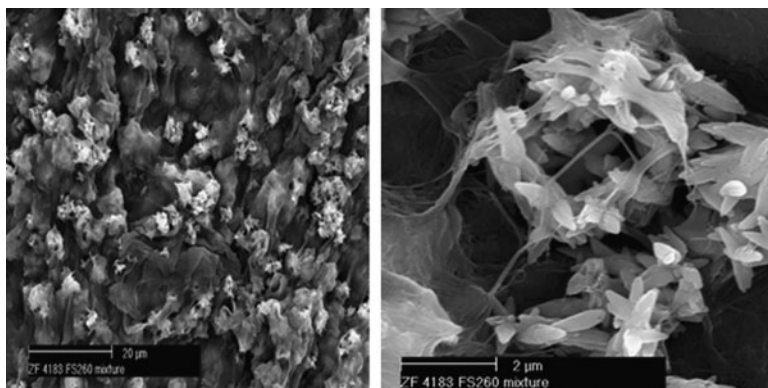


Fig. 5.8 Scalenohedral PCC mixed with fibrillar fines (acronym: reference Sca ref-PCC + nanofibril mixture)

Table 5.2 Characteristics of composite and reference calcium carbonate

Type of filler	BET surface area (m ² /g)	Weight median particle size (μm)	75/25 ratio
Co c-PCC	12.02	1.42	3.00
<i>Fine r</i> c-PCC	3.91	1.31	1.75
<i>Coarse r</i> c-PCC	3.36	1.73	1.82
Sca c-PCC	3.87	1.35	1.78
Co ref-PCC	20.76	1.32	2.74
<i>Fine r</i> ref-PCC	9.1	0.97	2.65
<i>Coarse r</i> ref-PCC	4.32	2.29	2.16
Sca ref-PCC	5.81	2.19	1.74

Note: Co colloidal, r rhombohedral, s scalenohedral morphologies

in required amounts to a copy paper furnish to form reference handsheets. From the micrographs, we observe that the filler is embedded into the fines network and partially covered by the fibrils. During mixing, the fibrillar network is pierced by the PCC particles, as seen on the right-hand side micrograph of Fig. 5.8. This will prevent the fibrils from merging together during drying of the handsheets.

The properties of the precipitated PCC–cellulosic fibril composites having different morphologies are compared with similar PCCs crystallised in the absence of cellulosic fibrils, denoted as reference PCC, in Table 5.2.

The particle size distributions of the composites and those of the reference PCCs were steep, as shown by the 75/25 ratio with the exception of colloidal PCC. The colloidal PCCs had the largest surface area, as measured with the nitrogen absorption technique, among the various crystal habits in both composite and reference fillers. Also, at the same particle size, colloidal composite and reference fillers show a significant difference in respect to their surface areas. Colloidal PCCs may thus be

described as small aggregates of nanosized crystals, which are also supported by the SEM investigation. The PCCs in fine and coarse rhombohedral composites do not differ significantly in size characteristics in comparison to the reference rhombohedral PCCs.

5.2.2.2 Study B: Refining Pulp and Calcium Hydroxide Together

In this investigation, two types of equipment are considered for refining together never dried bleached Kraft pulp, composed of pine and spruce, and milk of lime. They are as follows:

Supermass colloid[®] – as described earlier – is a type of grinder that reduces the fibres into fines by mechanical shearing (Matsuda et al. 2001). In this device, the grinding takes place between rotating and stationary abrasive stones made of silicon carbide. The gap between the stones, which had a grit size of 46, was adjusted to 230 μm (open gap setting). The treated pulp was discharged by centrifugal force. The refining degree was increased by recirculating the pulp suspension to a maximum of five times.

Laboratory Hollander refining – a Hollander beater design consists of a circular or ovoid water raceway with a beater wheel at a single point along the raceway. The beater wheel is made with multiple “blades” mounted on an axle-like shaft, similar to the construction of a water wheel. Under power, the blades rotate to beat the fibre into usable pulp slurry or highly fibrillated pulp suspension composed of cellulosic fibrils and fibres. In our study, we used a valley beater, and, hence, in this study the words Hollander and valley beater are used interchangeably. Co-refining of pulp fibre and lime was carried out to a maximum of 30 min in the Hollander beater.

The properties of the composite samples produced by each method are shown in Table 5.3. The particle size distribution and surface area of filler have been determined by the methods described earlier in Sect. 5.2.2.1.

For both refiners/grinders, the amount of filler attached to the fibrils increases with a higher degree of refining/grinding. Refining/grinding is believed to increase PCC attachment because it increases the cellulose surface area available for precipitation and also because it is more difficult to wash filler out of a more highly

Table 5.3 Properties of composite filler formed after milk of lime and pulp are refined together under different conditions

Refiner	Composite filler – time or passes in fibrillator	Total filler content (%)	Attached filler (%)	BET (m^2/g)	Weight median particle size (MPS) (μm)
Hollander	H- 0 min	61.6	11.6	11.00	2.27
	H- 15 min	63.0	12.4	10.70	1.15
	H- 30 min	63.0	19.0	11.50	0.98
Masuko	M- 1 pass	65.5	15.5	9.67	1.56
	M-3 pass	65.2	21.0	9.59	1.31
	M-5 pass	65.8	19.3	9.69	1.48
Reference	FR-180	100.0	–	5.10	2.62

Note: Reference PCC does not contain any fibrillar fines, and hence, attached filler is not indicated

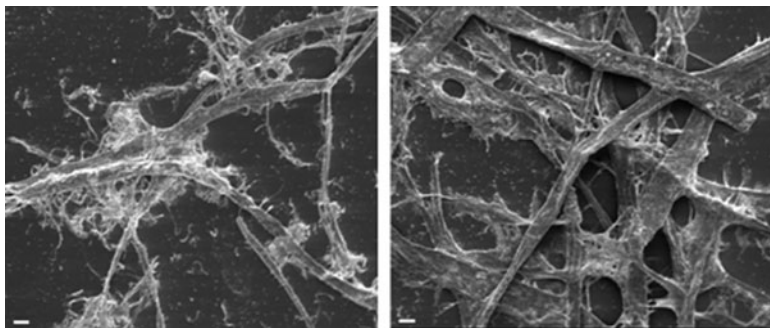


Fig. 5.9 Characteristics of the precipitated composite filler – Supermass colloid[®] (*left*) and Valley/Hollander beater (*right*). Scale bar: 20 μm

fibrillated network. All the precipitated filler samples have about the same surface area – around 9–11 m^2/g . This is somewhat higher than for the conventionally produced reference sample, but still in the range of ordinary fine paper PCC fillers. It is interesting to note that the refining has decreased the particle size of the composite filler somewhat compared to the unrefined one [Hollander at 0 min (H-0, Table 5.3)]. This may be due to grinding of the lime in the refiner.

The particle size distribution of the Hollander-refined composite filler becomes significantly narrower in refining. This indicates some changes in the filler distribution and state of agglomeration from refining together the milk of lime and pulp fibres.

Scanning electron microscopy (SEM) was used to determine the characteristics of the formed fillers, and their distribution in handsheets. Figure 5.9 represents the nature of the formed composite filler with the highest level of refining performed in this study. The pictures were taken after washing the composites two times in a dynamic drainage jar.⁵ It shows that increased fibrillation is obtained with the Supermass colloid[®]. In addition, a higher amount of filler is attached to the fibrils formed with the Supermass colloid[®] than Hollander beater.

Higher magnification of the washed composite fillers shows that filler is precipitated in the pits and surface of the pulp fibres (Fig. 5.10). Significant proportion of filler is agglomerated and patches of filler are observed on the surface of the fibres and fibrils with Supermass colloid[®] refined samples. Valley beater shows reduced agglomeration and retention of filler in the washed samples. Also, a minor fraction of calcium carbonate is precipitated inside the pits of fibres.

The beating of calcium hydroxide with pulp and subsequent precipitation leads to stronger attachment of smaller size PCC onto the pulp fibres. The smaller size and increased surface area of composites are shown in Table 5.3. SEM of washed composites shows that the Supermass colloid[®] refined composite had stronger adhesion of calcium hydroxide, and, hence, precipitated calcium carbonate onto the surface pulp fibres (Fig. 5.11).

⁵Washing is performed at 0.2% consistency and 800 rpm mixing in a dynamic drainage jar.

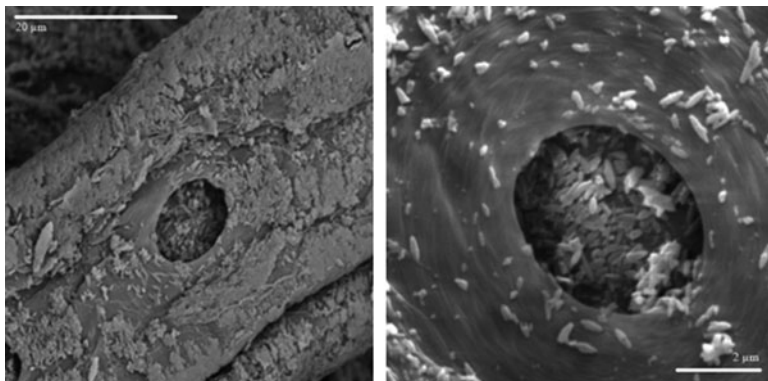


Fig. 5.10 Higher magnification of precipitated composite filler Supermass colloid[®] (*left*) and Valley/Hollander beaten (*right*)

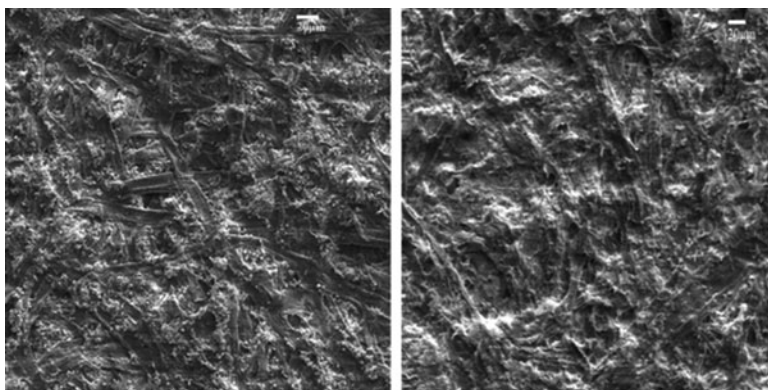


Fig. 5.11 Surface view of composite filled (*left*) and conventional reference (*right*) samples

5.3 Application of Nanocellulosic Fibrils–Mineral Pigment Composites in Paper

5.3.1 *Need for and Means of Increasing Amount of Mineral Pigment in Paper*

Mineral pigments have been an integral component of papermaking, with or without the papermaker's knowledge of their existence, since the beginning of papermaking in Europe. Filler pigments are incorporated into various grades of paper to decrease manufacturing costs, to improve brightness and light scattering properties, and to improve the quality of the printed image.

Today, there is a wide variety of fillers suited for acid, neutral, and alkaline papermaking conditions. The amount of pigment added to paper normally varies

from 5 to 35%, and considerable knowledge has been accumulated about the way in which pigments interact with fibres and other components in the papermaking system. There is a need to increase the mineral fraction in paper and to decrease paper grammage, while keeping critical paper properties at an acceptable level.

Different approaches have been proposed to increase filler contents in paper without impairing product quality, especially with respect to strength properties. Lumen loading, proposed by Green et al., aims to hold filler exclusively within the lumens of fibres (Green et al. 1982; Petlicki and van de Ven 1994). This gives higher fibre bonding than conventionally filled sheets. A modified approach to lumen loading has been suggested in order to make it an industrially viable process (Middleton et al. 2003). Allan and coworkers (Allan and Negri 1992; Allan et al. 1998) precipitated calcium carbonate in situ by treating pulp successively with calcium chloride and sodium carbonate ionic solutions. Klungness et al. (1994) developed a method to form PCC in a pulp refiner. Besides calcium carbonate, methods have been developed for incorporating aluminum (Siven and Manner 2003; Chauhan et al. 2007) and magnetic compounds inside the fibres (Rioux et al. 1992; Zakaria et al. 2004a, b). Preflocculation of filler (Mabee and Harvey 2000; Hak-Lae et al. 2006; Holm and Manner 2001) and coflocculation of filler and fines (Gavelin 1998; Lin et al. 2007) were examined to determine the feasibility of scaling up these processes as a means to increase the filler content in paper. Superfilled paper structures with high filler loadings were obtained by cationic wet-end starch addition, as reported by Lindström and Floren (1982).

Recently, Silenius (2002) has studied composites made from in situ precipitation of PCC onto pulp fines. The product was termed *superfill*. In his study, chemical pulp fines and heavily refined pulp, with a high proportion of fines, were used as substrates in both lab work and pilot experiments. Higher retention, improved strength and optical properties of paper, and cost savings were reported as the merits of using the *superfill* concept.

It has been shown earlier (Retulainen et al. 2002; Xu and Pelton 2005) that the weakening of paper by filler can be effectively compensated by augmenting the amount of microfines. Therefore, it is proposed that a microfines–filler base furnish should be more effective than a fibre–filler furnish in allowing an increased amount of filler pigments in paper. Thus, we envisioned a microfines–filler composite as the backbone structure for a new composite material – uncoated fine paper. In the new composite paper, the strength properties arise from the microfines and bulk and pores emerge from the filler surrounded by the microfines, while tear strength is provided by the minimal but essential fibre fraction in the composite.

5.3.2 Formation of a Novel Composite Paper and Its Properties

On the basis of the earlier studies (Przybysz and Czechowski 1985; Retulainen et al. 2002; Xu and Pelton 2005; Lin et al. 2007), the following conclusions can be drawn for filled papers:

- The weakening of the mechanical properties of paper by filler is largely compensated by the addition of cellulosic nanofines.
- Nanofines are effective strengthening agents because they are able to bridge the filler-induced void in the fibre–fibre bonding domain, acting as a glue strengthening the fibre–PCC and PCC–PCC contacts.

Thus, it can be deduced that acceptable strength for a fine paper can be obtained from cellulosic nanofines alone. Hence, the fines–filler matrix is envisioned as a base furnish when aiming to increase significantly the amount of filler in paper.

On this basis, a new composite paper structure is postulated, as depicted in Fig. 5.12. Since fibrils provide much higher strength per unit mass than fibres, the matrix structure consists of filler surrounded by nanofines. Fibres are interspersed in the matrix to reinforce the tear strength of the composite material. The objective of this paper is to investigate this new concept in the laboratory scale and to compare the product properties with laboratory and commercial reference samples. In addition, the following study aims to demonstrate the changes in structure–property relationships when we shift from fibres to pigment and fibrillar fines as the major papermaking furnish components.

The composite paper studied is a new combination of raw materials, consisting of the following components:

1. Precipitated calcium carbonate (PCC) for bulk, optical properties, porosity, and shrinkage reduction; proportion in the furnish – up to 60%.
2. Cellulosic fibrillar fines for tensile strength and bending resistance; proportion in the furnish – 15 and 30% fibres for tear; proportion in the furnish – 10 and 20%.

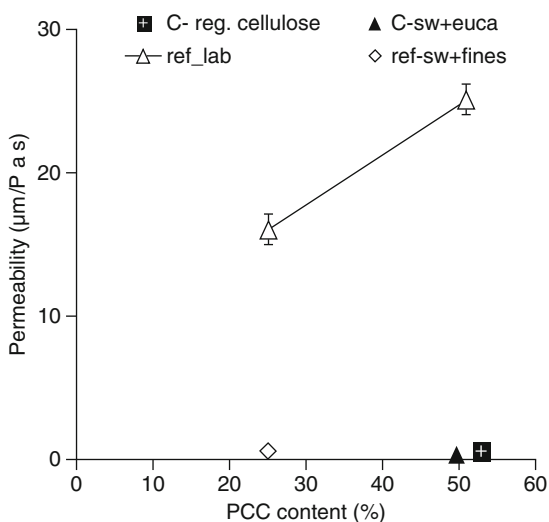


Fig. 5.12 Network structure of new composite paper-type material

5.3.2.1 Production and Analysis of Novel Composite and Reference Fine Paper

A suspension containing fibrillated cellulosic fines was produced from nondried ECF-bleached softwood pulp consisting of a mixture of pine and spruce in equal amounts, using the Masuko supermass colloid[®] (Kang and Paulapuro 2006). The refining degree is increased by recirculating the pulp suspension. The characteristics of the fibrillar fines produced by the grinder have been described in another publication in which they are referred as softwood bleached Kraft (swbk) fines (Ramjee Subramanian et al. 2008).

Dried softwood, made from 60% pine and 40% spruce, was refined to 23°SR and fractionated using a 30-mesh screen to obtain fractionated softwood fibres, used as long fibres in this study. Unrefined regenerated cellulose⁶ and unrefined eucalyptus fibres were also used as reinforcement fibres.

Conventional laboratory reference handsheets were formed from the above-mentioned nonfractionated softwood fibres and dried birch hardwood pulp refined to 28°SR. A 70:30 mixture of hardwood and softwood pulp was used as the base furnish. Standard commercial copy paper, composed of 70% birch and 30% mixed softwood of pine and spruce, was used as another reference.

Two-hundred and fifty grams per ton of C-PAM⁷ was used as retention aid in the forming of reference and 30% fines-containing long-fibre handsheets. Scalenohe-dral PCC with a weight median particle size of 2.4 µm was used as the mineral filler pigment in the paper.

After initial studies, an experimental plan was designed to produce new composite handsheets containing a minimum of 50% PCC, with a grammage of 80 g/m², as shown in Table 5.4.

The total volume of the stock suspension was 500 ml with a consistency of 0.43%. Handsheets were formed in a standard handsheet mould with a nylon fabric⁸ on top of the mesh in the sheet mould. Since the Nylon mesh, composed of nanoholes, was able to retain all the components, extra additives were not added during the forming of high-PCC-content handsheets. No extra water was added during forming. The dewatering time of the handsheets was 3–4 min. Pressing and drying were carried out according to standard methods.

The reference handsheets were formed by the ISO standard method (ISO 5269-1:2005). This handsheet was formed from a total stock suspension of 500 ml without any further water addition during the forming process. The standard method was slightly modified to form the handsheets containing long fibre and 30% fines.

Dried handsheets were conditioned (23°C; 50%RH). Relevant testing methods used in the analysis of handsheets are described in Table 5.5. In-plane tear strength was measured according to the procedure described by Gavelin (1998) and Kettunen

⁶Commercial regenerated cellulose fibres with the brand name Tencel were used in the experiments.

⁷Commercial C-PAM sold under the brand name of Fennopol was used in the experiment.

⁸Product name: SEFAR NITEX 03-10/2; mesh opening: 10 µm.

Table 5.4 Target compositions of reference and new composite samples

Test point	Precipitated calcium carbonate (PCC) fraction (%)	Nanofibrils fraction (%)	Base furnish
1 sw	23	0	Furnish: long fibres (softwood, sw)
2 sw + fibrils	23	30	Furnish: long fibres (softwood, sw)
3 C-euca+sw	50	30	10 (Eucalyptus, euca) 10 (softwood, sw)
4 C-sw	60	30	0 10 (softwood, sw)
5 C-reg. cellulose	–55	30	0 5 (Eucalyptus) and 10 (regenerated cellulose)
6 ref_lab	23	0	Furnish: 70:30 hardwood:softwood
7 ref_lab	50	0	Furnish: 70:30 hardwood:softwood

Note: The base furnish of conventional laboratory reference sheets consisted of a 70:30 mixture of hardwood and softwood pulp. Scandinavian softwood and birch hardwood pulps were refined to 23°SR and 21°SR, respectively

Table 5.5 Test methods used in the experiments and their standards

Test methods	Test standards
Grammage	ISO 536
Determination of thickness and bulk density or apparent sheet density	ISO 534:1998
Determination of air permeance	ISO 5636-3:1992
Determination of tensile strength – Part 2: Constant elongation method	ISO 1924-2:1994
Internal bond strength	T 569 pm-00
Fracture toughness and in-plane tear strength	Scan-P 77:95
Bending stiffness	ISO 2493:1992
Brightness	ISO 2470:1999
Light scattering	ISO 9416-1998
Ash content	ISO 1762:2001(E)

and Nikanen (2000). PCC content was measured by ashing the sample at 525°C in a muffle furnace.

5.3.2.2 Properties of Novel Composite and Reference Copy Paper

The grammage, PCC content and thickness of the sheets formed are shown in Table 5.6. The thicknesses of the handsheets formed in the laboratory were the same for both the high-filler-content and reference samples. Commercial copy paper has a lower thickness than the laboratory-made paper. Among the laboratory handsheets, softwood fibre samples exhibit higher thickness.

The bulk and bending stiffness of the samples at various PCC contents are compared in Fig. 5.13. Handsheets formed from long softwood fibres and 23% filler showed the highest bulk due to the open structure of the network. As expected, 30% addition of fines to this furnish significantly densifies the structure of paper (Retulainen 1997). Increasing filler addition to this network to form a fines–filler

Table 5.6 Basic properties of sheets formed with a high amount of PCC and of reference samples

Test point		Sheet grammage (g/m ²)	PCC content (%)	Thickness (μm)
1	Softwood fibre	87.8	24.20	164
2	Ref-softwood long fibre+finer	86.9	24.90	130
3	C-euca+sw	84.7	53.91	142
4	C-sw	84.9	49.68	140
5	C-reg. cellulose	82.1	60.50	139
6	Ref_lab	85.9	24.90	141
7	Ref_lab	85.9	50.80	146

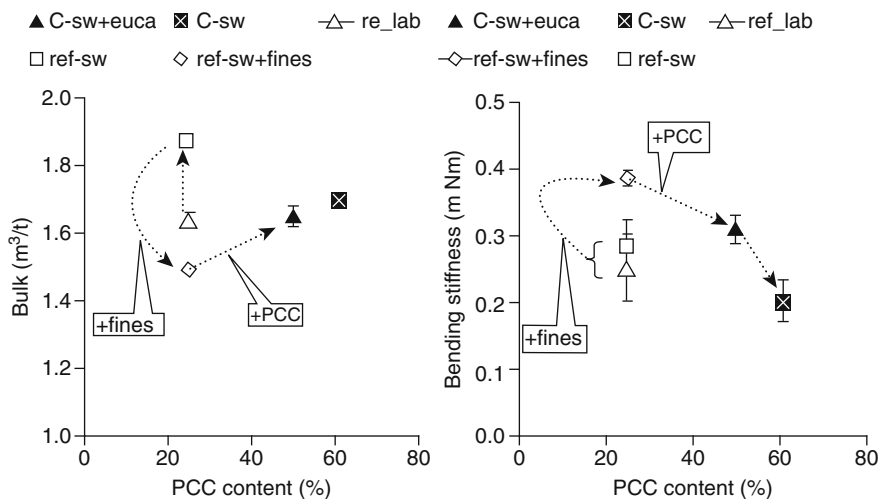


Fig. 5.13 Bulk and bending stiffness of the new composite and reference handsheets. Commercial copy – bending stiffness is a geometric mean value. *Abbreviations:* C new composite handsheets. Fibre components: euca eucalyptus unrefined, sw softwood fibres

contiguous structure partially opens up the structure by restricting the collapse of fibrillar fines, and, thus, improves the bulk of paper. The bulk of the fines–filler network is similar to that of a conventional paper formed, i.e., commercial copy, on an industrial scale. The bulk of the filler–fines matrix can be increased by decreasing the proportion of fines or probably by varying the type of filler in the matrix. For a conventional fibre furnish, doubling filler amounts results in a minimal, 5–6%, increase in bulk. Among all the samples, the commercial copy paper has the highest density due to differences in the forming process.

At constant filler content, addition of nanofibrillar fines to long fibre–fines matrix increases bending stiffness of paper significantly (Fig. 5.13). Augmenting filler in a filler–fines–fibre matrix decreases bending stiffness of paper to an almost similar level to that of the long fibre–fines matrix. Thus, the bending stiffness of the studied fibre–filler and fines–filler matrices are nearly the same. In addition, we find that the commercial copy and laboratory handsheets exhibit similar bending stiffness as that of the fines–filler composites. On the other hand, increasing filler in conventional

paper decreases its bending stiffness significantly. Among the fines–filler furnish-based samples, the results show that 50% of filler is a threshold value beyond which the bending stiffness of a paper decreases considerably.

The permeability of the handsheets as a function of filler content is shown in Fig. 5.14. An open network structure of fibres and filler has the highest permeability, above the range of the instrument. Addition of fines densifies and closes the network. Thus, the permeability decreases significantly. The permeability of the fines-added long fibre–filler samples is similar to that of the fines–filler matrix handsheets. Thus, increasing filler in handsheets composed of nanocellulosic fibrils does not act to decrease the permeability of paper. On the other hand, permeability is higher, and increases with higher proportions of filler, for conventional fibre-based laboratory reference sheets. Permeability of commercial copy paper is higher than filler–fines furnish samples but lower than commercial laboratory reference.

In Fig. 5.15, tensile strength is plotted against the PCC amount in the handsheets. Samples formed from long fibre and filler furnish exhibit the lowest tensile strength. Addition of fines to this furnish, increases the tensile strength significantly. Augmenting filler fraction in the fines–filler–fibre network decreases the tensile strength of paper. On the basis of our data, the filler content in a fine paper can be increased up to 50% using a fines–filler furnish. Above 50% filler, the tensile strength of PCC–fibrillar fines handsheets begins to decrease significantly compared to the laboratory reference.

Increasing filler addition to a standard fibre–filler matrix, as shown by the laboratory reference, decreases tensile strength significantly. The commercial copy paper produced with higher density, strength additives and machine draw shows the highest tensile index among the samples examined. Since there is no directionality in laboratory handsheets, the geometric mean of the machine-direction and

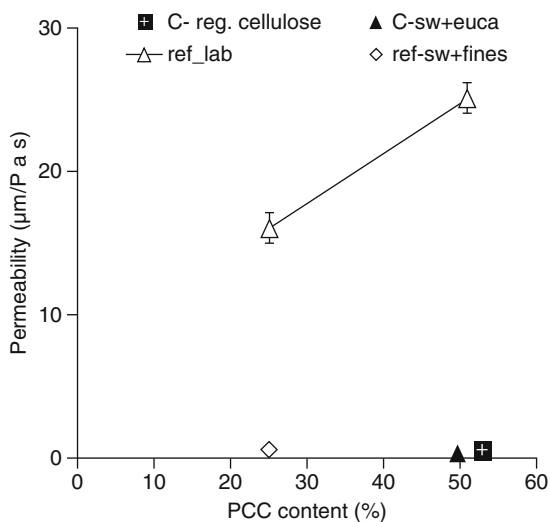


Fig. 5.14 Permeability against PCC content in the new composite and reference paper. Commercial copy is a geometric mean value. *Abbreviations:* C new composite handsheets. Fibre components: euca eucalyptus unrefined, sw fractionated refined softwood, reg. cellulose regenerated cellulose

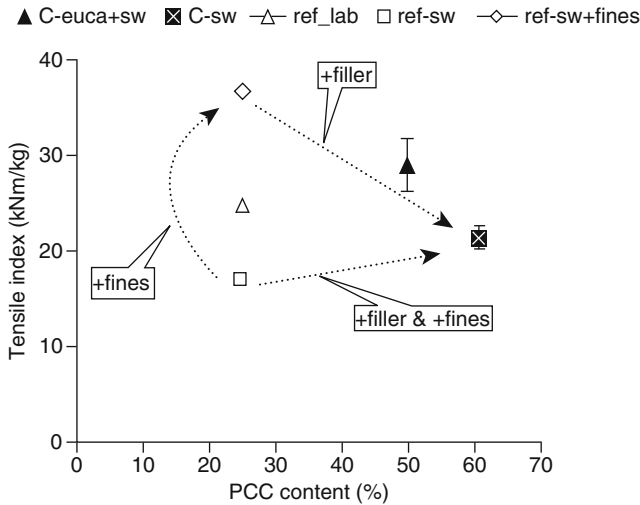


Fig. 5.15 Tensile index of the new composite and reference samples. Commercial copy is a geometric mean value. *Abbreviations:* C new composite handsheets. Fibre components: *euca* eucalyptus unrefined, *reg. cellulose* regenerated cellulose, *sw* fractionated refined softwood

cross-direction tensile indices of the commercial sheet was compared with that of the laboratory-made handsheets.

The internal bond strength of the new composite paper is significantly higher than that of the reference samples (Fig. 5.16). The internal bond strength of paper increases with increasing fines content and decreasing PCC content in the handsheets. In contrast to fibre–fines base furnish, the PCC–cellulose fibrils matrix gives the composite paper high internal bond strength.

The in-plane tear and fracture toughness are greatest for the commercial copy paper, followed by the new composite and laboratory reference handsheets (Fig. 5.17). The new composite handsheets containing PCC, cellulosic fibrillar fines and eucalyptus pulp exhibit similar or slightly lower tear strength and fracture toughness compared to the laboratory reference. Addition of 2% regenerated cellulose fibres does not have any significant impact on these properties. On the other hand, addition of 10% long fibres, either as regenerated cellulose fibres or fractionated softwood fibres, enhances the in-plane tear and fracture toughness of the new composite handsheets significantly. Addition of 10% refined and 30-mesh Bauer–McNett fractionated long fibres (Gooding and Olson 2001) to reinforce the new composite furnish significantly improves the in-plane tear strength and fracture toughness of the paper. A 10% increase of PCC, i.e., handsheet composed of 60% PCC, does not significantly change the in-plane tear index of the reinforced new composite paper.

Two different strength properties of the handsheets are compared in Fig. 5.18. According to the figure, an increased amount of fines significantly enhances the tensile strength of the new composite paper. Nanofibrillar cellulosic fines contribute

Fig. 5.16 Internal bond strength of new composite sheets and reference fine paper. *Abbreviations:* C new composite handsheets. Fibre components: *euca* eucalyptus unrefined, *sw* fractionated softwood

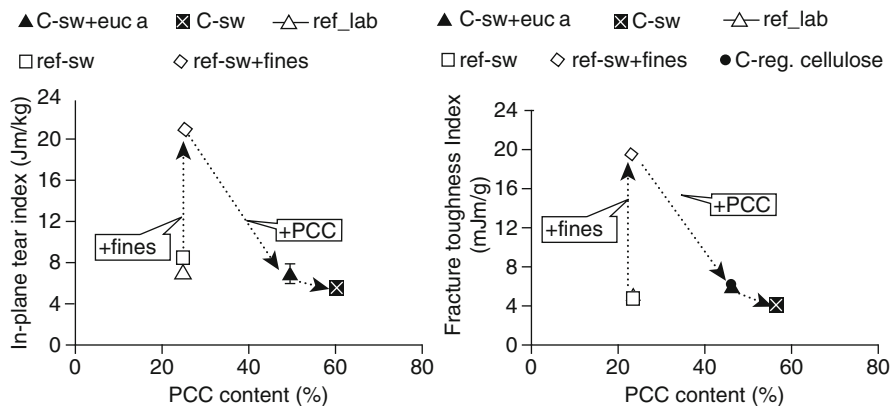
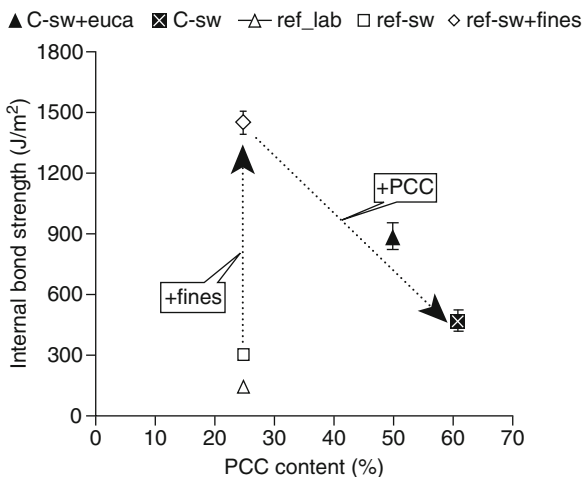


Fig. 5.17 In-plane tear and fracture toughness index against PCC content for the new composite and reference paper. Commercial copy is a geometric mean value. *Abbreviations:* C new composite handsheets. Fibre components: *reg.cellulose* regenerated cellulose, *euca* eucalyptus unrefined, *sw* fractionated refined softwood

to fibre segment activation and fibre straightening, thus enhancing the strength and fracture toughness of the composite material (Hiltunen 2003; Vainio 2007). From Fig. 5.18 (compare C-sw and C-sw+euca vs. ref_lab), we observe that the new long-fibre reinforced composite paper containing 60% PCC exhibits strength properties similar to those of the laboratory reference sample.

The fracture work (in-plane tear) of a medium consisting of small particles only, such as filler and nanofibrillated cellulose, is low. It can be considerably enhanced by adding reinforcement pulp fibres. Any particle crossing the rupture path must be released from the paper structure by bond failure, or it must be inactivated by fibre

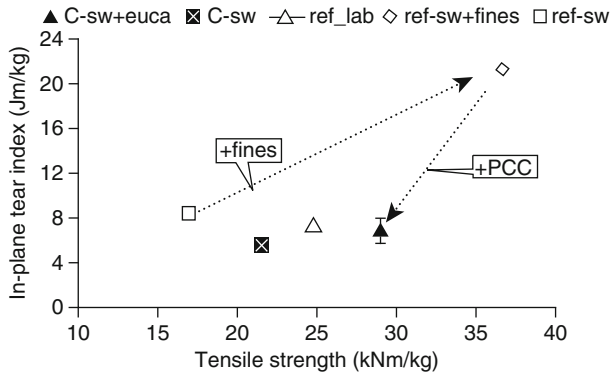


Fig. 5.18 Tensile strength as a function of in-plane tear strength for the new composite and reference paper. Commercial copy is a geometric mean value. *Abbreviations:* *C* new composite handsheets. Fibre components: *euca* eucalyptus unrefined, *reg.cellulose* regenerated cellulose, *sw* fractionated refined softwood

failure. This explains why the fracture work depends heavily on fibre length (Vainio 2007); with long fibres, many bonds must be broken to release a single fibre.

The fracture toughness of a composite material is a function of fibre length, bond density, fibre strength, and bonding strength. According to Kärenlampi (1996), Seth and Page (1992), the probability of fibre failure in a composite paper depends on the following:

1. For a fibrous matrix, the fracture resistance of a fibre depends linearly on the length of the fibre.
2. Given other properties of the fibre are constant, fibre strength directly contributes to the probability of fibre failure.
3. At constant fibre length and fibre strength, increased bonding, i.e., relative bonded area, contributes to higher fracture toughness.
4. Increased fibre length and beating contribute to enhancing the in-plane tear index.

In this study, initially, unrefined eucalyptus fibres were used to enhance the tear strength of paper. Because of their lower length, strength, and bonding degree, eucalyptus fibres did not contribute to increasing the tear strength of the pigment-based composite. In contrast, even though regenerated cellulose fibres had the maximum average length, they were not effective in enhancing the fracture toughness. This was probably due to the lower fibre strength and the absence of beating and deformation of these fibres in the network. At 2.3 mm, the average fibre length of beaten softwood pulp is greater than that of eucalyptus and lower than that of regenerated cellulose fibres. In addition, among reinforcement fibres, beaten softwood pulp has the highest fibre strength and bonding degree in the network. Thus, their reinforcing effect significantly improves the flaw-resisting ability of the PCC–cellulosic fibrillar fines matrix.

Figure 5.19 demonstrates a significant increase in light scattering and brightness obtained with high PCC contents in the new composite handsheets compared with the reference. The nanofibrillar cellulose and PCC matrix has a greater number of optically active pores, significantly increasing the light scattering of the handsheets.

Figure 5.20 shows a comparison of tensile and tear indices against light scattering of the handsheets. From the graphs, the following can be concluded:

- A fibrillar fines–PCC-based furnish significantly enhances the light scattering of paper compared to the reference samples.
- Comparing the laboratory-made handsheets, increased amounts of cellulosic fibrillar fines in the fines–PCC network contribute to enhancing the tensile strength and light scattering of the new composite paper.
- At constant in-plane tear, the new long-fibre reinforced composite samples exhibit higher light scattering compared to the laboratory reference paper.
- At constant light scattering, the tear strength of the new composite paper increases with increasing amounts of long fibres in the network structure.

The formation of the new composite and reference samples is illustrated in Fig. 5.21. It can be concluded that the formation improves with increasing amounts of nanofibrillar cellulose and PCC in the paper. Addition of 10% regenerated cellulose long fibres impairs the formation, while addition of softwood fibres results in a formation comparable to that of the reference handsheets. The handsheets were prepared from a suspension with a consistency of 4.3%. This combination of raw materials might also be suitable for higher consistencies, so the formation of handsheets at higher consistencies needs to be evaluated in detail.

The structure of the composite material studied with a focused ion beam-scanning electron microscope (FIB-SEM). In FIB-SEM microscopy, the composite paper sample is coated with a thin Pt layer (to give sharp edges) and then the sample

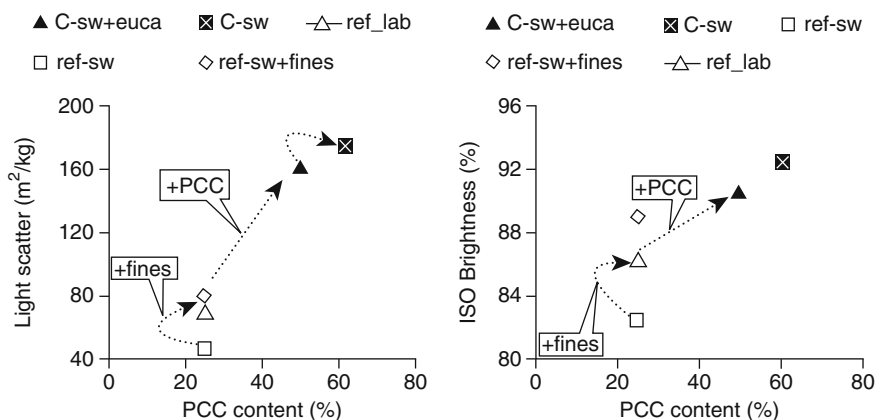


Fig. 5.19 ISO brightness and light scattering of handsheets with increasing PCC content. *Abbreviations:* C new composite handsheets. Fibre components: euca eucalyptus unrefined, sw fractionated refined softwood

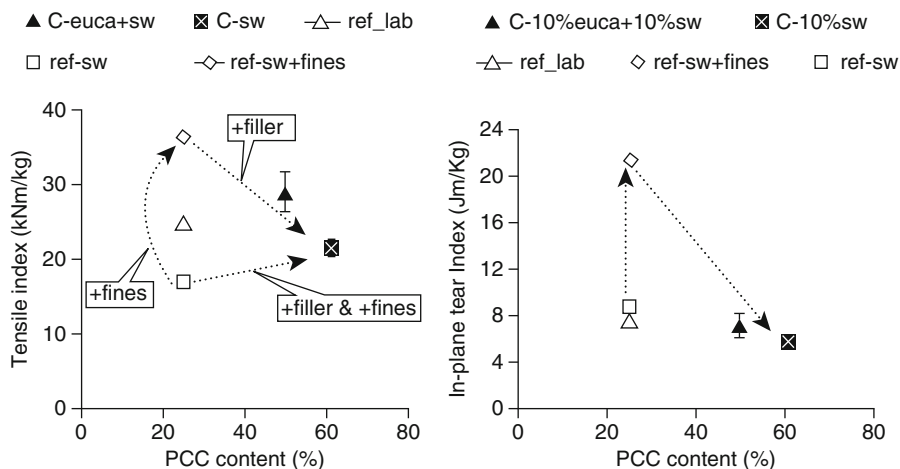


Fig. 5.20 In-plane tear and tensile indices as a function of light scattering of paper for the new composite and reference samples. *Abbreviations:* *C* new composite handsheets. Fibre components: *euca* eucalyptus unrefined, *sw* fractionated refined softwood

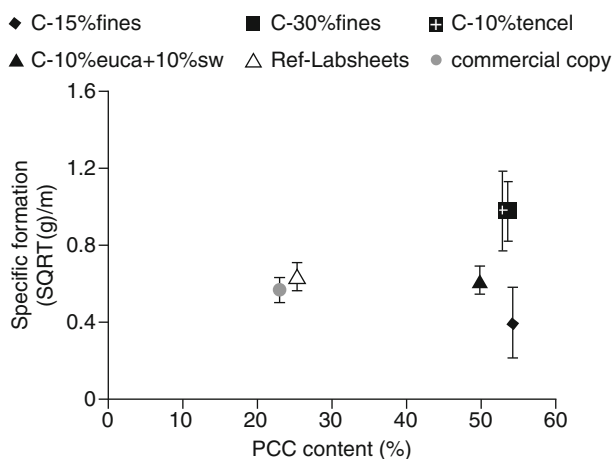


Fig. 5.21 Specific formation of the new composite and reference handsheets. *Abbreviations:* *C* new composite handsheets, *euca* eucalyptus unrefined, *tencel* regenerated cellulose, *sw* fractionated softwood, *SQRT(g)* square root(g)

is cut completely (distortionless) with a focused Ga-ion beam in the z -direction. The prepared sample is scanned and analysed using high-resolution imaging with an electronic beam. The z -directional SEM image is shown in Fig. 5.22. As seen from the image, the nanofibrils surround the PCC particles and form a network structure of PCC, fibrils, and pores. Typically, pores display a honeycomb-type structure with varying void volume.

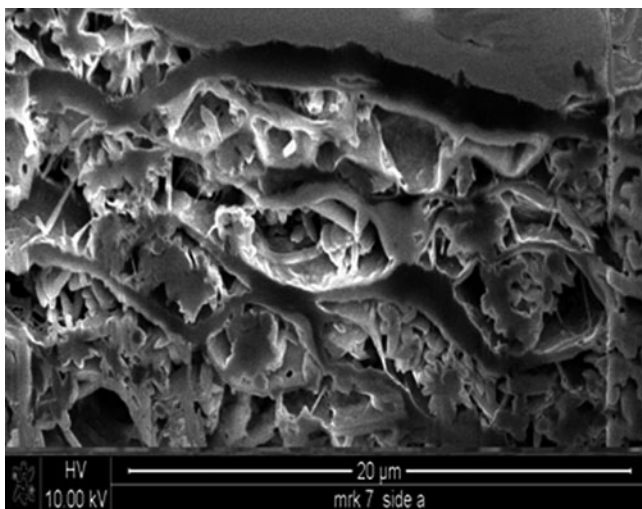


Fig. 5.22 z-directional SEM image of the new composite sample

The top surface SEM shows that the fibrils are firmly embedded into the filler matrix, as shown in Fig. 5.23. In addition, we find the films of cellulosic fibrils covering the filler surface on the surface of paper.

5.3.3 *Effect of PCC–Cellulosic Fibril Composites on Conventional Paper*

The objective of the following study was to investigate the impact of PCC–cellulosic fibril composites, described earlier in Sect. 5.2, on conventional printing and writing paper.

This section summarises the results of the impact of PCC–cellulosic fibril composites, the formation of which has also been described earlier in Sect. 5.2, on the properties of laboratory fine paper handsheets.

5.3.3.1 Production of Conventional Printing and Writing Paper

ECF-bleached unrefined pine pulp obtained from a mill in southern Finland was ground in the Supermass colloidizer[®] to produce fines. The Bauer–McNett analysis of the fines showed that 92% of the fines passed through the 200 mesh. The consistency of the produced fines–PCC composite was in the range of 0.085–0.1%.

The Supermass colloidizer[®] used in the formation of cellulosic fibrils has been described earlier in Sect. 5.2. The gap between the stones, which had a grit size of 46, was adjusted to 80 μm. Grinding was performed at room temperature and the

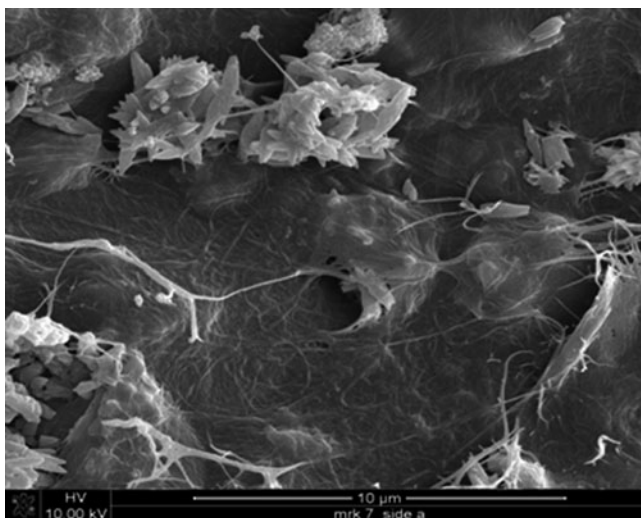


Fig. 5.23 Surface SEM scanning image of the new composite sample. This micrograph depicts the entrapment of filler inside the microfibrillar network structure

consistency of the treated pulps was 3%. The total treatment time for a 200 g dry sample was 800 s.

To compare the composite-formed sheets with standard products, a range of PCC morphologies available from the standard filler range were used in a further series of formed sheets. Refined pine softwood (23°SR) and birch hardwood pulp (18°SR) in a 30:70 ratio were used as the base furnish. C-PAM (250 g/t paper) was used as the retention aid in forming handsheets. No other additives were used. Conventional fillers were produced under similar conditions, in the absence of cellulosic fibrils, as the composite PCCs were used in the reference experiments.

Composite and reference handsheets (80 g/m²) were produced in a standard handsheet mould with the addition of retention aid. The samples were pressed twice in a material testing system (MTS) press at an impulse of 3.3 mPa/0.02 s with two blotting papers on each side. The handsheets were dried under standard conditions in a drum drier.

5.3.3.2 Properties of Conventional Printing and Writing Paper

Fine paper properties, as determined in studying the influence of PCC morphology, are shown in Fig. 5.24. Addition of fines, in the form of a PCC composite or as a mixture of filler and fibrillar fines, increases the density of paper. In contrast to reference PCC filler, a composite filler containing Kraft fines enhances Campbell's forces, and, thus, aids in forming a dense network structure (Retulainen 1997). Among the reference fillers, addition of s-PCC causes a significant increase in the

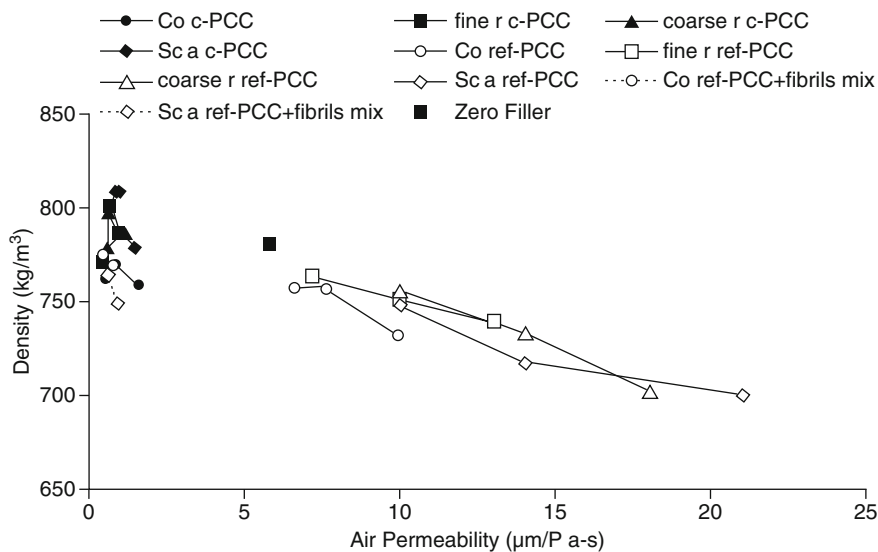


Fig. 5.24 Impact of PCC filler loading, as a function of PCC particle morphology, on the density and air permeability properties of paper. *Abbreviations:* *c* composite, *ref* reference, *Co* colloidal PCC, *r* rhombohedral PCC, *Sc a* scalenohedral PCC, *mix* mixture

air permeability and a decrease in density. Addition of reference c-PCC results in a minimal increase in the air permeability of paper.

Addition of fines improved the bending stiffness of handsheets, as shown in Fig. 5.25, due to stronger bonding and higher specific bond strength (Retulainen et al. 1993; Häggblom-Ahnger 1998). Addition of a mixture of each reference PCC and nanofines gives the highest bending stiffness resistance. Addition of reference r- and c-PCC gives the lowest bending stiffness, which decreases with increased addition of filler.

Comparing the internal bond strength and tensile index of various morphologies of PCC (Fig. 5.26), composites are found to give higher tensile strength than the reference fillers. These results correlate with earlier research findings (Xu and Pelton 2005), showing that fines contribute to strength by acting as a bridge that increases the bonding area in paper. Among composites, at all filler contents, papers filled with c-PCC and r-PCCs show minimum and maximum internal bond strength, respectively. Composite c-PCC imparts reduced tensile at low filler contents. This indicates that the PCC has acted to prevent bonding contact with the fibrillar fines.

Comparing the light scattering produced by composite fillers and reference blends, the composite material is found to give significantly better optical properties than a simple blend of PCC and fibrillated pulp.

However, even with increased density, composite fillers impart light scattering similar to that produced by conventional reference fillers (Fig. 5.27). This is due to

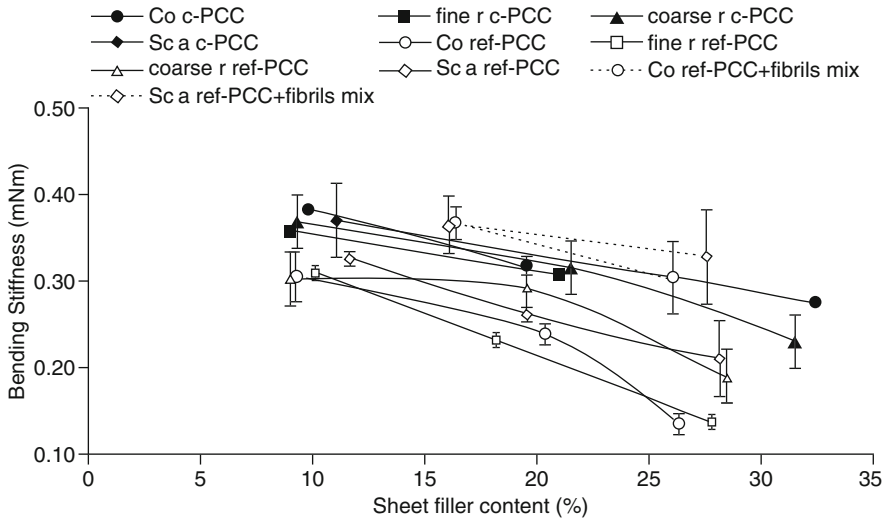


Fig. 5.25 Impact of PCC filler loading, as a function of PCC particle morphology, on the bending stiffness of paper. Abbreviations: *c* composite, *ref* reference, *Co* colloidal PCC, *r* rhombohedral PCC, *Sca* scalenohedral PCC, *mix* mixture

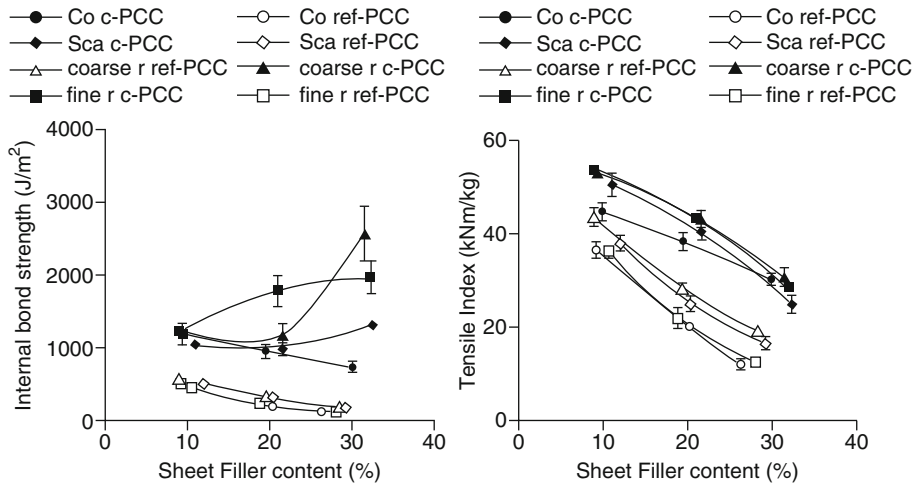
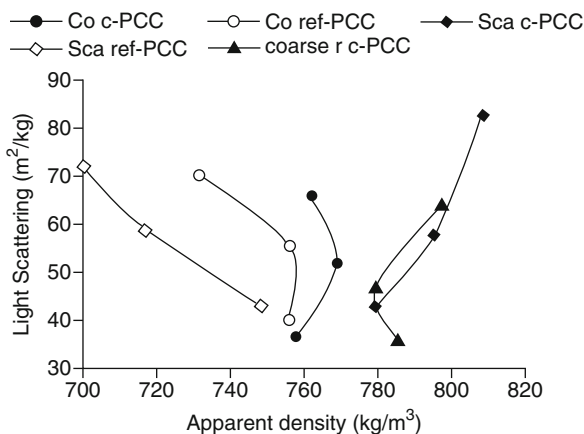


Fig. 5.26 Comparison of the strength properties of handsheets as a function of filler amount for composite and conventional PCC filler with three different morphologies. For abbreviations, refer to Fig. 5.23

the higher number of small-sized optical pores generated in the PCC composite network structure. The light scattering efficiency is directly related to the surface area associated with the optically active pores (Alince et al. 2002).

Fig. 5.27 Impact of PCC particle morphology on the light scattering properties of composite and conventional PCC filled handsheets. For abbreviations, refer to Fig. 5.23



5.4 Summary

Nanocellulose or nano/microfibrillar cellulose (NFC/MFC) is a material composed of nanosize cellulose fibrils with a high aspect ratio (length to width ratio). Typical dimensions are 100–200 nm long, width of 20–40 nm, and with pseudo-plastic characteristics. They can be produced by mechanical shearing, chemical and mechanical treatments, enzymatic degradations, and cryocrushing techniques. Nanofibrillar cellulose exhibits the property of certain gels or fluids that are viscous under normal conditions and develop a high storage modulus on standing. The fibrils have significantly high surface area and bonding ability.

Nanocellulosic fibrils can be used as a substrate for the production of precipitated calcium carbonate–nanocellulose composites. These, PCC–nanocellulose composites can contribute toward increasing the strength and optical properties of paper. We investigated formation and properties of a new composite paper composed of fibrillar fines and calcium carbonate as the base furnish in combination with cellulosic fibres as reinforcing elements.

This chapter illustrates the application of cellulosic fibrils in paper. However, research shows additionally that cellulosic fibrils find wide application across the manufacturing sector, in areas such as plastics, medical applications, and new novel product formulations.

References

- Alicine B (1989) Optimisation of pigment performance in paper. In: Baker CF (ed) Transactions of the fundamental research symposium, vol 1. Mechanical Engineering Publications, Cambridge, pp 495–510
- Alicine B, Lepoutre P (1985) Light scattering in filled sheets – separating the contribution of the pigment and of fibre debonding. *Tappi J* 68(4):122–123
- Alicine B, Porubska J, van de Ven TGM (2002) Light scattering and microporosity in paper. *J Pulp Pap Sci* 28(3):93–98

- Allan GG, Negri AR (1992) The microporosity of pulp. *Tappi J* 75(3):239–244
- Allan GG, Carroll JP, Jimenez G, Negri AR (1998) Enhancement of the optical properties of a bagasse newsprint furnish by fibre-wall-filler. *Cellulose Chem Technol* 32(3–4):339–347
- Carmona GJ, Morales GJ, Celmente RR (2003) Morphological control of precipitated calcite obtained by adjusting the electrical conductivity in the $\text{Ca}(\text{OH})_2\text{-H}_2\text{O-CO}_2$ system. *J Cryst Growth* 249(3–4):561–571
- Carmona GJ, Morales GJ, Sainz FJ, Loste E, Celmente RR (2004) The mechanism of precipitation of chain-like calcite. *J Cryst Growth* 262(1–4):479–489
- Chakraborty A, Sain N, Kortschort M (2005) Cellulose microfibrils: a novel method of preparation using high shear refining and cryocrushing. *Holzforschung* 59(1):102–107
- Chauhan VS, Singh SP, Bajpai PK (2007) Fibre loading of hardwood pulp by in-situ precipitation of aluminium silicate. *BioResources* 2(4):560–571
- Gavelin G (1998) A method and apparatus for manufacturing filler-containing paper. *Pat. EP 0270103*, Mo och domsjö ab., Sweden, 16p
- Gooding RW, Olson JA (2001) Fractionation in a Bauer–McNett Classifier. *J Pulp Pap Sci* 27(12):423–428
- Green HV, Fox TJ, Scallan AM (1982) Lumen-loaded paper pulp. *Pulp Pap Can* 83(7):T203–T207
- Hägglblom-Ahnger U (1998) Three ply office paper. Doctoral thesis, Åbo akademi University, ISBN 952-12-0288-2, Turku
- Hak-Lae L, Hye-Jung Y, Kyong-Ho L (2006) Effect of the size distribution of preflocculated GCC on the physical properties of paper. In: Zhan Huaiyu, Chen Fangang and Fu Shiyu (eds) *Proceedings of the third international conference on emerging technologies in pulping and papermaking*, South China University Press, pp 472–477
- Hiltunen E (2003) On the beating of reinforcement pulp. Doctoral thesis, Helsinki University of Technology, Reports, Series A16, Espoo
- Holm M, Manner H (2001) Increasing filler content in fine paper by using preflocculation. In: *Proceedings of the 28th DITP International annual symposium: Technical, technological and biological processes for the improvement of production, productivity, quality and ecology in papermaking*, Bled, Slovenia, pp 167–170
- Hubbe MA, Rojas OJ, Lucia LA, Sain M (2008) Cellulosic nanocomposites: a review. *BioResources* 3(3):929–980
- Kang T, Paulapuro H (2006) New mechanical treatment of chemical pulp. *J Process Mech Eng* 220(3):161–166
- Kärenlampi P (1996) Strength and toughness of paper: the effect of pulp fibre properties. Doctoral thesis, Helsinki University of Technology, Reports, Series A 4, Espoo
- Kettunen H, Nikanen KJ (2000) On the in-plane tear test. *Tappi J* 83(4):1–6
- Klungness JH, Caufield D, Sachs I, Tan F, Skyes M (1994) Fiber loading: a progress report. In: *Proceedings of Recycling symposium*, Boston, pp 283–290
- Lima MMD, Borsali R (2004) Rodlike cellulose microcrystals: structure, properties, and applications. *Macromol Rapid Commun* 25(7):771–787
- Lin L, Yin X, Retulainen E, Nazhad MM (2007) Effect of chemical pulp fines on filler retention and paper properties. *Appita J* 60(6):469–473
- Lindström T, Floren T (1982) The effects of cationic starch wet end addition on the properties of clay filled papers. *Svensk Papperstidning* 87(12):R99–R104
- Liu H, Hsieh Y-L (2002) Ultrafine fibrous cellulose membranes from electrospinning of cellulose acetate. *J Polym Sci B Polym Phys* 40(18):2119–2129
- Mabee S, Harvey R (2000) Filler flocculation technology – increasing sheet filler content without loss in strength or runnability parameters. In: *Proceedings of the 2000 Tappi papermakers conference*, Atlanta, pp 797–809
- Maloney TC, Paulapuro H (2001) Thermoporsimetry of pulp fibres. The science of papermaking. In: *Transactions of the 2001 Fundamental Research Symposium*, BPBMA, Oxford, pp 897–926
- Matsuda Y, Hirose M, Ueno K (2001) Super microfibrillated cellulose, process for producing the same and coated paper and tinted paper using the same. U.S. Pat. 6,214,163 B1, Tokushu Paper Mfg. Co. Ltd, 18 pp

- Meuronen J (1997) The precipitation of calcium carbonate to the fines fraction of chemical pulp and properties as a filler in papermaking. Master of Science thesis, Lappeenranta University of Technology, Finland
- Middleton SR, Desmeules J, Scallan AM (2003) Lumen loading with calcium carbonate fillers. *J Pulp Paper Sci* 29(7):241–246
- Nakagaito AN, Yano H (2006) Nanocomposites based on cellulose microfibril. Cellulose nanocomposites: processing, characterisation and properties. *ACS Symp Ser* 938:151–168
- Oksman K, Sain M (2006) Introduction to cellulose nanocomposites. Cellulose nanocomposites: processing, characterisation and properties. *ACS Symp Ser* 938:2–8
- Pääkkö M, Ankerfors M, Kosonen H, Nykänen A, Ahola S, Österberg J, Ruokolainen J, Laine J, Larsson PT, Ikkala O, Lindström T (2007) Enzymatic hydrolysis combined with mechanical shearing and high-pressure homogenization for nanoscale cellulose fibrils and strong gels. *Biomacromolecules* 8(6):1934–1941
- Petlicki J, van de Ven TGM (1994) Kinetics of lumen loading. *J Pulp Pap Sci* 20(12):J375–J382
- Przybysz K, Czechowski J (1985) The effect of pulp fines on the drying process and paper strength properties. *Cellulose Chem Technol* 19(2):197–209
- Retulainen E (1997) The role of fibre bonding in paper properties. Doctoral thesis, Helsinki University of Technology, Series A7, Espoo
- Retulainen E, Moss P, Nieminen K (1993) Effect of fines on the properties of fibre networks. In: *Transactions of the 1993 fundamental research symposium*. PIRA International, Oxford, pp 727–769
- Retulainen E, Luukko K, Fagerholm K, Pere J, Laine J, Paulapuro H (2002) Papermaking quality of fines from different pulps – the effect of size, shape and chemical composition. *Appita J* 50(6):457–460
- Rioux P, Ricard S, Marchessault RH (1992) The preparation of magnetic papermaking fibres. *J Pulp Pap Sci* 18(1):J39–J43
- Seth RS, Page DH (1992) Fibre properties and tearing resistance. *Tappi J* 75(1):172–174
- Silenius P (2002) Improving the combinations of critical properties and process parameters of printing and writing paper and paperboards by new paper-filling methods. Doctoral thesis, Helsinki University of Technology, Report Series A14, Espoo
- Siven SK, Manner H (2003) Fibre loading using an aluminium compound. *Appita J* 56(6):438–441
- Subramanian R, Kononov A, Kang T, Paltakari J, Paulapuro H (2008) Structure and properties of some natural cellulosic fibrils. *BioResources* 3(1):192–203
- Tokoh C, Takabe K, Fujita M, Saiki H (1998) Cellulose synthesised by *acetobacter xylinum* in the presence of acetyl glucomannan. *Cellulose* 5(4):249–261
- Vainio A (2007) Interfibre bonding and fibre segment activation in paper – observations on the phenomena and their influence on paper properties. Doctoral thesis, Helsinki University of Technology, Series A29, Espoo
- Wang B, Sain M (2007) Isolation of nanofibers from soybean source and their reinforcing capability on synthetic polymers. *Compos Sci Technol* 67(11–12):2521–2527 [No. 178]
- Xu Y, Pelton R (2005) A new look at how fines influence the strength of filled papers. *J Pulp Pap Sci* 31(3):147–152
- Yamada H, Hara N (1987) Synthesis of calcium carbonate by electrical conductivity monitoring. In: *Proceedings of the first international conference on ceramic powder processing science*, Florida, The American Ceramic Society, Ohio, pp 39–46
- Zakaria S, Ong BH, van de Ven TGM (2004a) Lumen loading magnetic paper I: flocculation. *Colloids Surf A Physicochem Eng Asp* 251(1–3):1–4
- Zakaria S, Ong BH, van de Ven TGM (2004b) Lumen loading magnetic paper II: mechanism and kinetics. *Colloids Surf A Physicochem Eng Asp* 251(1–3):31–36

Part II
Cellulosic Fiber-Reinforced Polymer
Composites and Nanocomposites

Chapter 6

Greener Surface Treatments of Natural Fibres for the Production of Renewable Composite Materials

Koon-Yang Lee, Anne Delille, and Alexander Bismarck

Abstract Natural fibres have been the prime candidate to replace synthetic fibres for the production of composite materials. Major advantages associated with natural fibres include low cost, low density, high toughness and biodegradability. However, these intriguing properties of natural fibres do come at a price. The hydrophilic nature of natural fibres often results in poor compatibility with hydrophobic polymer matrices. Various surface treatments of natural fibres using chemicals have been developed to improve the compatibility between the fibres and the matrix, but large amounts of solvents are usually involved. In this chapter, greener surface treatments without the use of hazardous chemicals are reviewed. These include plasma treatments, the use of enzymes and fungi for the extraction and surface treatment of raw fibres or natural fibres and the deposition of bacterial cellulose onto natural fibres. These treatments are aimed at improving the interfacial adhesion between the fibres and the matrix, thereby improving the stress transfer efficiency from the matrix to the fibre. The effects of these treatments on the properties of natural fibres are discussed. In addition to this, the overall impact of these treatments on the mechanical properties of the resulting natural fibre reinforced composites is also addressed.

Keywords Bacterial cellulose · Hierarchical composites · Mechanical properties · Natural fibres · Surface modification

Contents

6.1	Introduction	156
6.1.1	A Brief Introduction to Natural Fibres	156
6.1.2	Structure of Plant-Based Natural Fibres	157
6.2	Green Modifications of Plant-Based Natural Fibres	158
6.2.1	Plasma: A Brief Introduction	160

A. Bismarck (✉)

Department of Chemical Engineering, Imperial College London, Polymer and Composite Engineering (PaCE) Group, South Kensington Campus, London SW7 2AZ, UK
e-mail: a.bismarck@imperial.ac.uk

6.2.2	The Use of Enzymes for Natural Fibre Extraction and Surface Treatments	163
6.2.3	The Use of Fungi for Surface Treatments and Extraction of Natural Fibres	166
6.2.4	Coating Natural Fibres with Nanocellulose	169
6.3	Conclusion	172
	References	174

6.1 Introduction

Public's growing demand for more environmentally friendlier products, the search for greener sustainable technology, the ever-growing problem of global waste, environmental legislative pressure such as the end-of-life vehicle [1], the landfill of waste products [2] and waste electrical and electronic equipment regulations [3], as well as the depletion of fossil resources (and corresponding increase in raw materials prices), have initiated the interest of using renewable resources in the polymer industry [4, 5]. Polymer manufacturers are forced to consider the life cycle of their products and evaluate the environmental impact of these products throughout the products' lifetime. These include the selection of raw materials, polymer processing, recycling and disposal. Combining all these factors and the worldwide availability of plant-based natural fibres [6], research interest of using natural fillers to reinforce polymers is re-emerging in the field of composites engineering over the last three decades. The use of natural fibres in the production of composite materials is well developed [7–17]. Such extensive use of natural fibres as reinforcement for polymers is not surprising as natural fibres offer several advantages over conventional reinforcing fibres, such as lower cost, low density, high toughness and biodegradability [18, 19]. A big step towards the application of natural fibre reinforced composites can be found in door panels of *Mercedes-Benz E-class* [20]. Daimler AG replaced the door panels of *Mercedes-Benz E-class* with flax/sisal fibre mat embedded epoxy resin. A remarkable weight reduction of 20% and an improvement in the mechanical properties of the door panels were achieved. This further improves the protection of the passengers in an event of an accident. In addition to this, Rieter Automotive won the JEC Composites Award 2005 for their development in natural fibre reinforced thermoplastic composites for an under-floor module with integrated aerodynamic, thermal and acoustic functions [21].

6.1.1 A Brief Introduction to Natural Fibres

Natural fibres can be derived either from plants (such as flax or hemp), produced by animals (such as silk or spider silk) or from minerals (such as asbestos). Table 6.1 shows the comparison of selected physical properties between natural fibres and synthetic fibres. Although the mechanical properties of natural fibres are very much lower than those of conventional synthetic fibres, such as glass or carbon fibres,

Table 6.1 A comparison between the physical properties of selected natural fibres and synthetic fibres

Fibre	Density (g cm ⁻³)	Tensile strength (MPa)	Young's modulus (GPa)	Elongation at break (%)
Flax	1.5	345–1,500	27.6	2.7–3.2
Hemp	1.47	690	70	1.6
Jute	1.3–1.49	393–800	13–26.5	1.16–1.5
Ramie	1.55	400–938	61.4–128	1.2–3.8
Sisal	1.45	468–700	9.4–22	3–7
Cotton	1.5–1.6	287–800	5.5–12.6	7–8
Silk ^a		600	10	20
Spider silk ^b		800–1,000	7.2–9.2	30–60
Basalt ^c	2.66	3,050	92.5	
Asbestos ^c		550–750	1.0–3.5	
E-glass	2.55	3,400	73	2.5
Kevlar	1.44	3,000	60	2.5–3.7
Carbon	1.78	3,400 ^d –4,800 ^e	240 ^e –425 ^d	1.4–1.8

Source: Adapted from Bismarck et al. [22]. Further developed with Craven et al. [23], Brant [24], Perez-Rigueiro et al. [25] and Martiny et al. [26]

^aNatural fibre derived from animal sources (silkworm)

^bNatural fibre derived from mineral sources

^cNatural fibre derived from spider (*Argiope trifasciata*)

^dUltra high modulus carbon fibre

^eUltra high tenacity carbon fibre

significant research effort is still poured into the field of plant-based natural fibre reinforced composite materials due to its low cost and low environmental impact. On a “per weight” basis, flax, jute and hemp fibres have higher tensile moduli than E-glass fibres [27, 28] due to the low density of natural fibres (~1.4 g cm⁻³) compared to E-glass (~2.5 g cm⁻³). This is particularly important in applications where weight reduction is a priority. Therefore, it is not surprising that natural fibres are used as reinforcement for polymer matrices to replace conventional glass fibres.

6.1.2 Structure of Plant-Based Natural Fibres

Plant-based natural fibres are rigid and they are composed of cellulose, hemicellulose, lignin, pectin, waxes and water-soluble compounds, with cotton being the exception. Cotton is made up of nearly 90 wt% cellulose, 5.7 wt% hemicellulose, 1 wt% pectin and 0.6 wt% waxes [7]. Cellulose is the major constituent in plant-based natural fibres. It is a linear molecule consisting of repeating β-D-glucopyranose units linked together by 1 → 4 glycosidic bonds (Fig. 6.1). It has a degree of polymerisation of approximately 10,000 [29]. Strong hydrogen bonds exist between cellulose molecules due to the presence of hydroxyl groups, which governs the physical properties of cellulose. It has a semi-crystalline structure, consisting of crystalline and amorphous regions. Cellulose in natural fibres (such as cotton, flax and ramie) typically has a degree of crystallinity of between 65 and 70% [30].

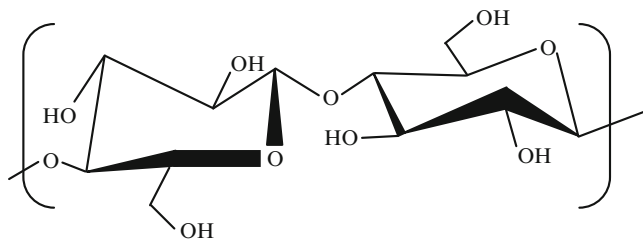


Fig. 6.1 Schematic diagram showing the structure of cellulose

The amorphous regions can be hydrolysed by acids to create short cellulose nanocrystals [31]. Nevertheless, cellulose is stable in most common organic solvents. It can only be dissolved in strong acidic solutions such as concentrated phosphoric acids and concentrated sulphuric acid [32] or ionic liquids such as *N*-ethylpyridinium [33] and lithium chloride/*N,N*-dimethylacetamide [34].

Hemicellulose is the other major constituent of plant-based natural fibres and it is made up of a combination of 5- and 6-ring carbon polysaccharides [22]. It is a branched polymer and has much shorter polymer chains (degree of polymerisation of between 50 and 300) compared to native cellulose. In addition to this, hemicellulose is very hydrophilic in nature [35], easily hydrolysed by acids and soluble in alkali. The role of hemicellulose in natural fibres is to form the supporting matrix for cellulose microfibrils.

Lignin is a phenolic compound that provides rigidity to the plant [22] and acts as a binder to consolidate the polysaccharide, holding cellulose and hemicellulose fibres together [36]. It was found that lignin has high carbon low hydrogen content and this implies that it is highly unsaturated or aromatic. Lignin can be produced by the dehydrogenation polymerisation of *p*-coumaryl, coniferyl and sinapyl alcohols [37]. It contains hydroxyl ($-OH$), methoxyl ($-O-CH_3$) and carbonyl ($C=O$) groups. Ethylenic and sulphur containing groups have also been identified in lignin [7]. Lignin is amorphous and hydrophobic in nature. It has been shown that lignin possesses a softening temperature of about $90^\circ C$ and a melt temperature of $170^\circ C$ [35].

6.2 Green Modifications of Plant-Based Natural Fibres

Although natural fibres are highly comparable to conventional glass fibres on a “per weight” basis, the major drawback arises from the inherent variability of natural fibres [22]. Natural fibres can vary in terms of their dimensions and mechanical properties, even within the same cultivation. This situation is different from synthetic fibres, which can be manufactured uniformly (e.g., Toray’s T700S carbon fibre has only a variability of $\pm 10\%$ in its tensile strength and modulus [Commercial documentation – No AQ.866-9 (September 2003), Personal communication], $\pm 3\%$ in its diameter). All natural fibres are hydrophilic in nature due to the presence

of large amounts of hydroxyl groups; their absorbed moisture content can be as high as 30% at 95% relative humidity [38]. This extremely hydrophilic nature of natural fibres often results in poor compatibility between natural fibres and hydrophobic polymer matrices, such as polypropylene or polylactide [14]. Another factor that limits the use of natural fibres is its low thermal stability. To avoid degradation of natural fibres during thermal processing, the temperature at which natural fibres are exposed to is usually limited to 200°C (shorter processing time is preferable) [39]. This further limits the choices of polymers that can be used as potential matrix for natural fibre reinforced composites. Figure 6.2 shows the reduction in the tensile strength of natural fibres with increasing processing temperature and time of the natural fibres.

To improve the compatibility between natural fibres and hydrophobic polymer matrices, various methods have been explored to increase the hydrophobicity of natural fibres [40–42]. Most of the chemical surface treatments of natural fibres involve silylation [43–46], acetylation [47], benzylation [48], maleated coupling agents [49], isocyanate treatment [50] and grafting polymers to natural fibres [51]. Although these methods alter the wettability of natural fibres, large quantities of hazardous chemicals were or are usually involved in the process of hydrophobising the natural fibres and the chemical waste must be handled and disposed of appropriately. This adds extra cost to the production of natural fibre reinforced composites, making the chemical treatments less attractive as a viable solution. Moreover, chemical treatments of natural fibres do not always result in improved composite performance. The main reason is the anisotropy of natural fibres. The transverse modulus of natural fibres is orders of magnitude lower than its axial modulus [52, 53]. Cichocki Jr et al. [52] showed that the axial modulus of jute fibres is 38.4 GPa, but its transverse modulus is only 5.5 GPa. [53] also showed that the axial modulus

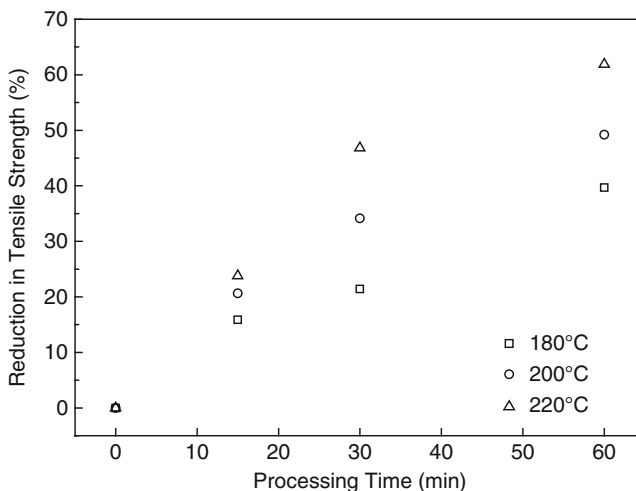


Fig. 6.2 Temperature and time dependency of natural fibre's tensile strength. Adapted from [39]

of flax fibres is seven times larger than its transverse modulus (axial modulus: 59 GPa, transverse modulus: 8 GPa). In addition to this, [54] also attributed the failure of natural fibres to deliver good performance in composites to the high linear thermal coefficient of expansion (LTCE) of natural fibres. The interfacial shear stress between the fibre and the matrix is the product of residual compressive stresses (σ_r) and the static friction coefficient at the fibre–matrix interface. Due to the high LTCE of natural fibres, σ_r will be lowered, leading to poor interfacial shear strength between the fibres and the matrix. Therefore, chemical modification of natural fibres might not be the next step forward. Instead, efforts should be focussed on environmental friendlier processes to increase the hydrophobicity of natural fibres and to avoid the shrinkage problem of natural fibres during thermal processing.

6.2.1 Plasma: A Brief Introduction

Plasma is known as the fourth state of matter. It is defined as a gaseous environment composed of charged and neutral species with an overall zero charge density. Plasma has been shown to modify the tribology of thermoplastics and synthetic fibres (such as carbon fibres) [55–58]. Further details regarding plasma treatments of various materials can be found in the literature [59–61]. Plasma treatments have the ability to change the surface properties of the fibres through the formation of free radicals, ions and electrons in the plasma stream [62]. During plasma treatment, the substrate is bombarded with high-energy particles travelling in the stream of plasma or vacuum UV (in low-pressure plasma). As a result, the surface properties such as the wettability, surface chemistry and surface roughness of the substrate can be altered without the need for any hazardous chemicals or solvents. Usually, plasma treatments modify the surface of natural fibres by [61] (1) removing weakly attached surface layers (i.e., cleaning and abrasion) and (2) forming new functional groups (functionalisation and cross-linking). The functional groups formed on the surface of natural fibres depend on the nature of the plasma feed gas. Therefore, plasma treatment minimises the environmental impact of natural fibre surface treatments. Different types of plasma sources are available [63] and they are summarised in Table 6.2.

6.2.1.1 Low-Pressure Plasma Treatment of Natural Fibres

The plasma discharge can be generated at atmospheric (see next section) or under vacuum conditions [42]. Essentially, the two types of plasmas generated are the same. The plasma produced can be used to modify the surface energy of natural fibres [64, 65], cross link the fibres [64], create free radicals to initiate polymerisation [51] or introduce functional groups onto the surface of the fibres [61]. A major advantage of employing low pressure plasma treatments is that such plasma can be generated at low power output. Atmospheric plasma treatments are usually carried out at a

Table 6.2 Comparison between different plasma sources

Plasma source	Gas temp (°C)	Electron temp (eV)	Applied voltage (kV)	Charge density (cm ⁻³)
Arc and torches	7,000–65,000	2.5–6.8	10–50	10 ¹⁶ –10 ¹⁹
Corona	50–400	4–6	10–50	10 ⁹ –10 ¹³
Dielectric barriers	50–400	2–10	5–25	10 ¹² –10 ¹⁵
Low-pressure discharge	10–500	1–10	0.2–0.8	10 ⁸ –10 ¹³
Atmospheric pressure discharge	25–200	1–2	0.05–0.2	10 ¹¹ –10 ¹²

Adapted from [63]

maximum power of 10 kW [64, 66]. Low pressure plasma treatments, on the other hand, are carried out at much lower power output of about 60–100 W [67, 68]. As aforementioned, the mechanical properties of natural fibres are highly dependent on the temperature at which the natural fibres are exposed to. By using a smaller power output, it is possible to minimise the thermal damage caused by plasma treatment on the natural fibres, thereby preserving the properties of natural fibres. However, there are disadvantages associated with low pressure plasma treatments. A well-designed plasma reactor system is required along with vacuum pumps and seals. In addition to this, low pressure plasma is also often used in small batch process only due to the limitation in the size of the vacuum chamber as a result of capital and operating costs.

Various researchers have investigated the use of low pressure plasmas to modify the surface of natural fibres [67–74]. Low pressure plasma has been used to treat wood fibres and sisal fibres, using argon and air as the plasma feed gas [67, 68]. Table 6.3 summarises the mechanical properties of untreated and plasma-treated natural fibre reinforced polypropylene (PP) composites. The plasma treatment of the fibres had a positive impact on the mechanical properties of the resulting wood fibre and sisal fibre reinforced PP composites when compared to the composites containing untreated natural fibres. The tensile strength was found to increase by as much as 16% for both wood fibres and sisal fibres reinforced PP composites. The tensile modulus improved by as much as 127% (wood fibre) and 93% (sisal fibre), respectively. When comparing neat PP to plasma-treated wood fibre or sisal fibre-reinforced PP composites, the tensile modulus improved by as much as 127% (wood fibre) and 113% (sisal fibre), respectively, and the tensile strength improved by as much as 17% (for both wood and sisal fibre). This is an indication of improved interfacial adhesion between the fibres and the matrix as a result of plasma treatment.

Jute fibres were treated in low pressure argon plasma [74]. The fibres were treated in argon plasma for 5 min, 10 min and 15 min, respectively. With longer plasma treatment, the fibres became rougher and the formation of pits on the fibre surface was observed when the fibres were plasma treated for 15 min. This is a result of plasma etching, which results in the degradation of the jute fibres [75]. The wettability of the plasma-treated jute fibres by water decreased with increasing treatment time (Table 6.4). This is also accompanied by an increase in the flexural strength of the plasma-treated jute fibre reinforced polyester composites. It was

Table 6.3 A comparison between untreated and plasma-treated wood fibre and sisal fibre reinforced PP composites. σ and E denote tensile strength and tensile modulus, respectively

Composites	Wood fibre		Sisal fibre	
	σ (MPa)	E (GPa)	σ (MPa)	E (GPa)
Neat PP	23	1.5	23	1.5
Untreated fibre	22	2.6	22	2.6
Argon plasma	25	3.0	24	3.2
Air plasma	27	3.4	27	2.9

All composites contain 20 wt% fibres. Adapted from [67, 68]

Table 6.4 A comparison between neat and plasma-treated jute fibres and the flexural strength of jute fibre reinforced polyester composites

Jute fibre treatment	Water/air contact angle	Polar surface energy (mJ m^{-2})	Flexural strength of polyester composites (MPa)
Neat jute fibres	81.6°	21.9	158.8
5 min plasma treated	84.1°	17.5	152.4
10 min plasma treated	86.9°	11.6	181.6
15 min plasma treated	90.0°	8.5	143.2

Adapted from [74]. The composites contain 15 wt% fibres loading fraction

found that the flexural strength of the composites improved by 14% (10 min plasma-treated jute fibres) compared to neat jute fibre reinforced polyester. This improvement was attributed to the increased roughness and hydrophobicity of the plasma-treated fibres, which results in better interfacial adhesion between the fibres and the matrix. However, composites reinforced with fibres treated in plasma for 15 min showed a 10% decrease in the flexural strength. This is a direct result of heavy degradation of the treated fibres during the prolonged plasma treatment [72].

6.2.1.2 Atmospheric Air Pressure Plasma Treatment of Natural Fibres

To improve the wettability and interfacial adhesion between natural fibres and a polymer matrix, atmospheric air pressure plasma (AAPP) treatment can be applied to natural fibres to remove non-cellulosic substances from the surface of these fibres. The advantages of using AAPP treatment for composite production are its low operating cost, short treatment time and greater flexibility, as no vacuum system is required [76–78]. It was reported that oxygen and nitrogen plasma led to a reduction of the critical surface tension¹ of lignocellulosic fibres as a result of etching effect [64]. Compressed air can be used as an alternative feed gas to overcome this negative impact generated by oxygen and nitrogen feed gases on lignocellulosic fibres.

As a general rule, good adhesion can be achieved when the surface tension of the substrate (natural fibres) is larger than that of the matrix. [64] have shown that the critical surface tension can be modified through AAPP treatment (Fig. 6.3). Different lignocellulosic fibres can be seen behaving differently if exposed to the same

¹The critical surface tension of a solid substrate corresponds to the surface tension of an imaginary liquid that will just wet the substrate completely.

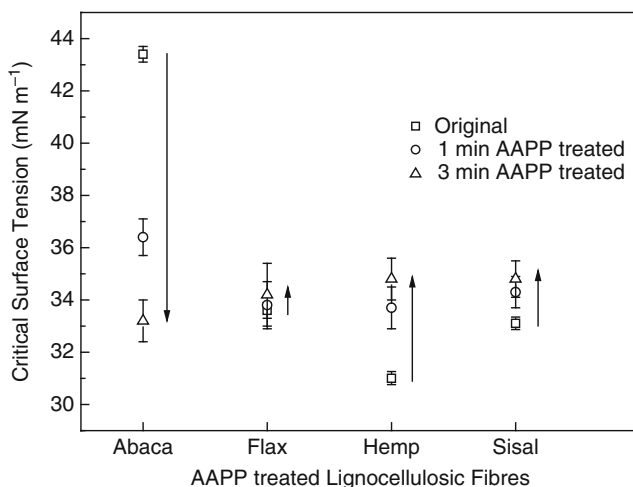


Fig. 6.3 Critical surface tension of lignocellulosic fibres after AAPP treatment at various times. Adapted from [64]

AAPP treatment. The critical surface tension of abaca fibres reduced with increasing treatment time. However, hemp and sisal fibres showed otherwise. With increasing AAPP treatment time, the critical surface tension increased. The authors hypothesised that longer treatment times of hemp and sisal fibres led to the cross-linking of the fibre surfaces (hemp fibres) and decomposition of hydrophobic groups. This might have led to the observed increase in the critical surface tension.

The effect of AAPP treatment on the properties of natural fibre reinforced cellulose acetate butyrate (CAB) composites was then further studied [66]. At a fibre loading fraction of 30 wt%, the storage modulus of the short fibre composites improved by as much as 370% (Fig. 6.4). This is due to the enhanced interfacial adhesion between the fibres and the matrix as a result of AAPP treatment (as measured by single fibre pull-out test) [79]. In addition to this, the increment in the mechanical glass transition temperature and a reduction in the height of $\tan \delta$ showed better fibre–matrix bonding and fibre-in-matrix distribution. It is evident that AAPP treatment is able to improve the fibre–matrix interface, resulting in composites with improved mechanical properties.

6.2.2 The Use of Enzymes for Natural Fibre Extraction and Surface Treatments

Retting is a process of the separation or loosening of bast fibres from its non-fibrous components [80]. Water-retting is performed by immersing the stalks of the fibre crops in water for a certain period of time. Water penetrates the central

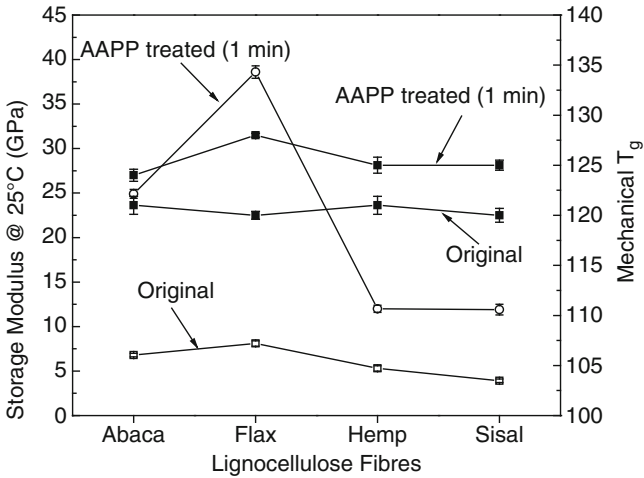


Fig. 6.4 Viscoelastic behaviour of AAPP-treated lignocellulosic fibre reinforced CAB composites. *Hollow icon* indicates storage modulus, *solid icon* indicates mechanical T_g . Adapted from [66]

stalk, swells the inner cells and bursts the outer most layers of the plant materials. This increases the absorption of moisture and decay-producing bacteria. Water-retting is able to produce high-quality fibres, but it also produces large amount of waste [81] and, therefore, this process was discontinued in many countries (apart from China and Hungary) [82]. Dew-retting, on the other hand, relies on fungi to colonise harvested fibre crop material in the fields. A combination of bacteria, air, sun and dew produces fermentation, which dissolves much of the stem materials surrounding the fibre bundles [80]. However, this method suffers from several disadvantages. Appropriate moisture and temperature conditions during dew-retting are needed [80]. This is a parameter that is very difficult to control as it is highly dependent on the region and the weather. In addition to this, the fibres extracted through dew-retting method have lower quality compared to water-retted fibres [80, 83].

Enzyme-retting is a natural fibre extraction method that refers to the separation of fibres from its non-fibre components through the use of enzymes [84]. This process generally uses pectin-degrading enzymes such as the commercially available Viscozyme L or Flaxzyme from Novozyme (Bagsvaerd, Denmark). The use of pectin-degrading enzymes promotes the selective degradation of pectinaceous substances [22]. Apart from this, the use of different types of enzymes such as cellulase, hemicellulase, laccase and peroxidase have also been reported [85, 86]. There are many advantages associated with enzyme-retting over conventional water-retting and dew-retting. Enzyme-retting is able to overcome the problems associated with dew- and water-retting as the fibres are treated in a well-controlled environment and the produced fibres possess the quality of water-retted fibres without large amount of fermentation waste. However, high cost

associated with enzymes and equipment have limited this technology to pilot scale only [87].

Foulk et al. [88, 89] compared dew-retted flax fibre reinforced high-density polyethylene (HDPE) composites with enzyme-retted flax fibre reinforced HDPE composites. Flax fibres were extracted with commercially available Viscozyme L (Novozymes, Bagsvaerd, Denmark) and a chelator, Mayoquest 200 (Callaway Chemical Co. Smyrna, GA). Mayoquest 200 is a chelator that contains about 36–38% sodium EDTA and 40% total dissolved salts [80]. The chelator is often used to improve the efficiency of enzyme-retting by sequestering calcium from the solution [90]. Figure 6.5 shows the effect of different flax fibre extractions (dew-retted, enzyme-retted at different enzyme/chelator concentration) on the mechanical properties of the randomly oriented flax fibre reinforced HDPE composites. The flax fibres treated with enzymes and chelators showed significant improvements in terms of tensile properties compared to raw flax fibre reinforced composites. Enzyme and chelators modified the surface of flax fibres by removing pectin and calcium, therefore enhancing the interfacial adhesion between the fibres and the matrix. The composites reinforced with dew-retted flax fibres showed worse properties compared to enzyme-retted flax fibres. This is most probably due to poor surface properties of dew-retted fibres (containing high levels of calcium and the inability of dew-retting to remove specific components such as pectin) compared to enzyme-retted fibres.

In addition to using enzymes for the extraction of natural fibres, they can also be used to treat post-extracted natural fibres. Enzyme treatments of natural fibres also have advantages over conventional alkaline-treated natural fibres. [91]

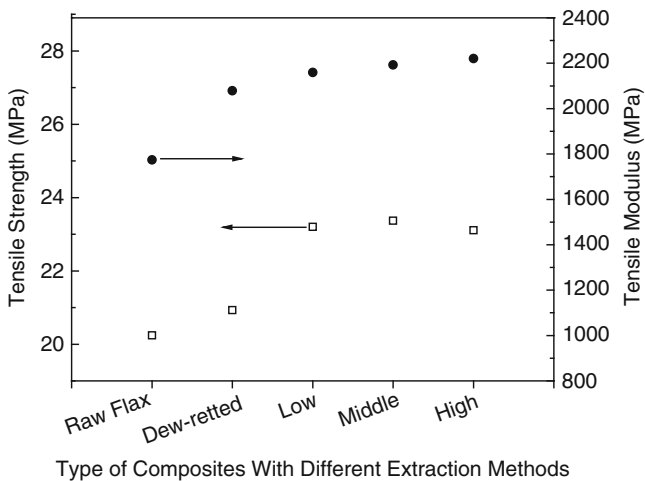


Fig. 6.5 A comparison between not-treated flax fibre, dew-retted flax fibre and enzyme-retted flax fibre reinforced HDPE composites. Adapted from [88]. Low indicates 0.05% enzyme and 5 mM chelator, medium indicates 0.1% enzyme and 10 mM chelator and high indicates 0.3% enzyme and 25 mM chelator

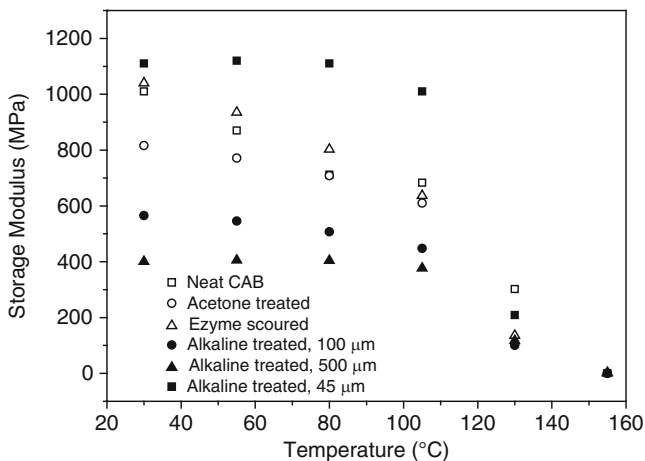


Fig. 6.6 Viscoelastic behaviour of flax fibre reinforced CAB composites. Adapted from [91]

compared the viscoelastic properties of neat, alkali-treated and enzyme-treated hemp fibre reinforced CAB composites. Hemp fibres were treated with Scourzyme L (Novozymes, Bagsvaerd, Denmark). Scourzyme is an alkaline pectinase that removes pectin without significant degradation of cellulose [92]. The enzyme-scoured hemp fibre reinforced CAB composites showed improvements over neat CAB, neat hemp fibre reinforced CAB and most of the alkaline-treated hemp fibre reinforced CAB. The composites reinforced with alkaline-treated hemp fibres (fibre length of 45 μm), however, possessed the highest storage modulus. Single fibre tensile tests indicated that the neat, alkaline-treated and enzyme-scoured hemp fibres possess Young's moduli of 42.8, 29.0, and 91.4 GPa, respectively [93, 94], with alkaline-treated fibres possessing the worst mechanical properties. Therefore, the observed better storage modulus of alkaline-treated hemp fibre reinforced composites (fibre length of 45 μm , Fig. 6.6) observed might be due to the greater control of fibre suspension in the polymer solvent prior to composite consolidation (solution casting method) [91]. Nonetheless, composites reinforced with enzyme-scoured hemp fibres possessed a toughness (area under the stress– strain curve) of 40% higher than that of untreated hemp fibre reinforced composites. This is an indication of the potential of enzyme treatment on natural fibre reinforced composites.

6.2.3 The Use of Fungi for Surface Treatments and Extraction of Natural Fibres

Enzyme-retting and treatments have been shown to be an effective method of treating natural fibres to improve the interface between the fibres and the matrix, leading to improved mechanical properties of the composites. However, it is

expensive and limited to pilot scale only. Another underexplored method of natural fibre surface treatment involves the use of fungi. The use of fungi can provide low-cost, highly efficient and environmentally friendly alternatives to natural fibre surface treatment [95]. Unlike dew-retting, fungal treatment is performed in a more controlled environment. The controlled parameters include the type of fungi, the temperature and the period of treatment.

Fungi can be classified into four categories: basidiomycetes, ascomycetes, zygomycetes and deuteromycetes, respectively. White rot fungus (basidiomycetes) is the only fungus that has been shown to degrade lignin, exposing cellulose and hemicellulose [95]. It has also been shown that white rot fungus can degrade the hydrophobic constituents of natural fibres such as triglycerides and fatty acids. In addition to this, white rot fungus can also degrade sitosterol, sitosterol esters and resin acid [96]. These compounds are known to be resistant towards microbial degradation [97–99]. Therefore, it is not surprising that white rot fungus is used to remove non-cellulosic compounds from natural fibres in order to improve the mechanical properties of the resulting natural fibre reinforced composites.

The use of white rot fungus in the treatment of natural fibres can be found in the literature [95, 100–102]. White rot fungi treated hemp fibres have higher crystallinity index as measured by X-ray diffraction when compared to untreated fibres [95]. This is a direct result of the fungi's ability to remove non-cellulosic compounds such as amorphous lignin, thereby increasing the crystallinity index. Zeta-potential measurements have also shown that non-cellulosic compounds were removed by the fungal treatment. A more negative zeta potential was obtained and this was due to the exposed hydroxyl groups from cellulose as a result of fungal treatment.

Table 6.5 shows the tensile strengths of hemp fibres and randomly oriented hemp fibre reinforced polypropylene (PP) composites. The fibres were treated with white rot fungi and/or alkali. The tensile strength of the composites improved by as much as 32% (combination of alkali and white rot fungi treatments) when compared to neat hemp fibre reinforced composites. Fungi treatments can provide extra benefits in addition to alkali treatment alone. This improvement seen in the composites is a result of improved fibre morphology and mechanical interlocking between the fibre and the matrix.

Table 6.5 Tensile strength of hemp fibre and its PP composites treated with white rot fungi

Treatment type	Lignin removal	Single fibre tensile strength (MPa)	Composites tensile strength (MPa)
Control	–	683	36.7
<i>Phanerochaete sordida</i>	Yes	576	41.5
<i>Pycnoporus</i> sp.	Yes	470	44.6
<i>Schizophyllum Commune</i>	Yes	354	45.0
Alkali	Yes	621	43.3
Alkali + <i>Phanerochaete sordida</i>	Yes	579	48.3

Adapted from [95]

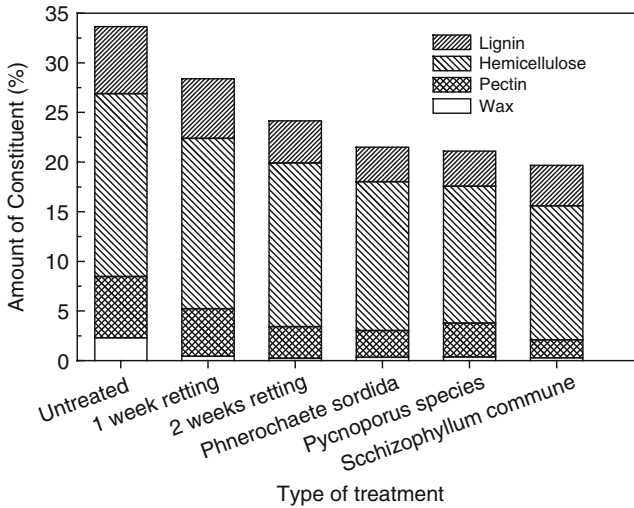


Fig. 6.7 A comparison between natural retting and white rot fungi treatment on the amount of non-cellulosic compound in hemp fibres. Adapted from [100]

White rot fungi have also been used to extract natural fibres [100]. Clarke et al. [103] reported a method for natural retting in which the hemp fibre bundles are separated from the plant by sealing the fibres in a bag for a fixed period of time. The microorganism present in the fibres will produce enzymes to remove non-cellulosic compounds. In a study by [100], natural retting was conducted by sealing non-retted hemp fibres in a bag under a controlled condition of 60% relative humidity for certain periods of time at room temperature. In another separate experiment, the authors treated non-retted hemp fibres with white rot fungi. It can be seen that fungal treatments removed more lignin compared to natural retting treatments (Fig. 6.7). The crystallinity index of the fibres increased from 66% to approximately 85%, due to the removal of non-cellulosic compounds from the fibres, which are generally amorphous. Figure 6.8 shows the tensile properties of single hemp fibres and randomly oriented hemp fibre reinforced polypropylene (PP) composites as a function of different types of treatments. Although the tensile strength of the fibres decreased when compared to neat hemp fibres, the composite strength improved by as much as 30% as a result of fungal treatment. This suggests improved fibre properties (crystallinity index) and interfacial adhesion (surface roughness) between fibres and the matrix, which was confirmed by scanning electron micrographs. Natural retted fibres does improve the composite's tensile strength (due to the removal of non-cellulosic compounds) when compared to unretted fibre reinforced composites but the increment in the observed tensile strength is less than that of white rot fungi treated hemp fibre reinforced PP composites. This might be a direct result of poor single fibre tensile strength due to long retting time.

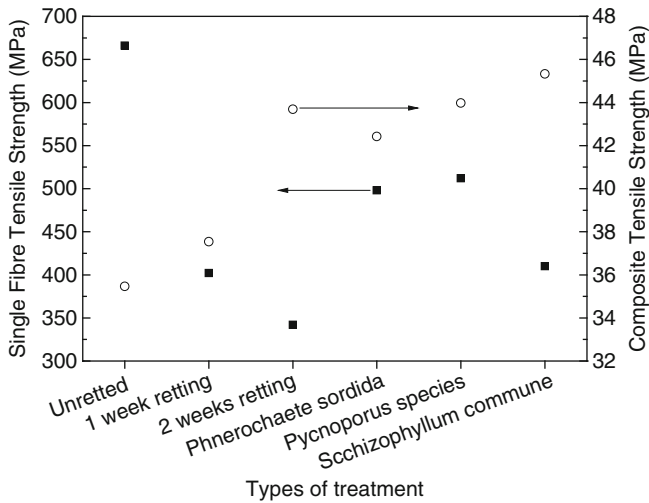


Fig. 6.8 Tensile properties of hemp fibres and hemp fibre reinforced PP composites treated with different methods. Adapted from [100]

6.2.4 Coating Natural Fibres with Nanocellulose

The previous three sections involved the treatment of natural fibres by removing substances from the natural fibres. This section, however, describes a new modification that does not involve the removal but the *addition* of new material onto the surface of natural fibres. This type of modification involves the deposition of nanosized cellulosic materials onto the surface of natural fibres to enhance the interfacial adhesion between the fibres and the matrix [9, 10, 14, 104]. By doing so, a hierarchical structure can be created. These works were inspired by nature. Nature maximises the efficiency of structural materials by creating hierarchical structures: the arrangement of the constituents at every level, from the molecular level to the macroscopic level. By applying this concept, composites that possess a hierarchical structure with improved mechanical properties can be manufactured.

In addition to plant-derived cellulose, cellulose can also be synthesised by bacteria such as from the *Acetobacter* species. By culturing cellulose-producing bacteria in the presence of natural fibres in an appropriate culture medium, bacterial cellulose is preferentially deposited *in situ* onto the surface of natural fibres. The introduction of bacterial cellulose onto natural fibres provides new means of controlling the interaction between natural fibres and polymer matrices. Coating of natural fibres with bacterial cellulose not only facilitates good distribution of bacterial cellulose within the matrix, but also results in an improved interfacial adhesion between the fibres and the matrix. This enhances the interaction between the natural fibres and the polymer matrix through mechanical interlocking.

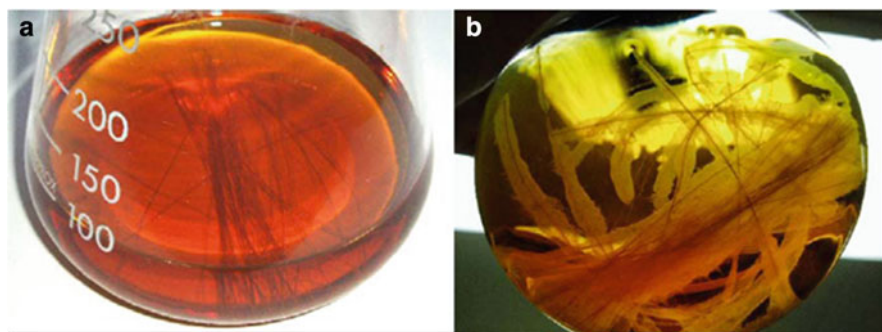


Fig. 6.9 Images showing (a) natural fibres immersed in a culture medium of *Gluconacetobacter xylinum* before bacteria culturing (b) the culture medium after 2 days. Reprinted from Pommet et al. [14] with permission from ACS publication

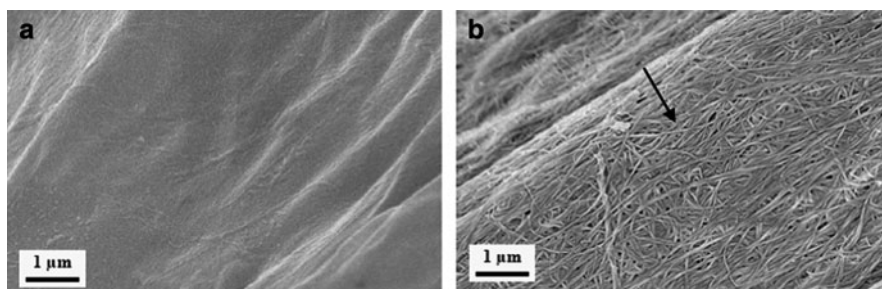


Fig. 6.10 SEM images showing (a) neat sisal fibre (b) sisal fibre coated with bacterial cellulose. Reprinted from Pommet et al. [14] with permission from ACS publication

Bacterial cellulose-coated natural fibres introduced nanocellulose at the interface between the fibres and the matrix, leading to increased stiffness of the matrix around the natural fibres. Figure 6.9 shows the images of the culture medium and natural fibres immersed in the culture medium before and 2 days after culturing. A layer of bacterial cellulose (BC) pellicles can be seen growing away from the surface of the natural fibres. Scanning electron micrographs of the BC-coated sisal fibres are shown in Fig. 6.10. A layer of bacterial cellulose nanofibrils can be seen attached onto the surface of sisal fibres (Fig. 6.10b). The coating of natural fibres with BC could also be a potential solution to the aforementioned shrinkage of natural fibres during thermal processing of the composites. Due to the low thermal expansion of BC ($0.1 \times 10^{-6} \text{ K}^{-1}$) [105], the BC coating could potentially bridge the gap that exists between the fibres and the matrix due to the high LCTE of natural fibres.

Simple weight gain measurements showed that approximately 5–6 wt% of BC was deposited onto the surface of these natural fibres. However, the mechanical properties of the natural fibres after bacterial cellulose modification depend on the

Table 6.6 The mechanical properties of natural fibres modified with bacterial cellulose nanofibrils

Natural fibres	Young's modulus (GPa)	Tensile strength (MPa)	Elongation at break (%)
Neat sisal fibre	15.0 ± 1.2	342 ± 33	2.9 ± 0.1
Bacterial cellulose-modified sisal fibre	12.5 ± 1.0	324 ± 33	4.5 ± 0.4
Bacterial cellulose-modified sisal fibre with purification ^a	12.0 ± 0.9	310 ± 32	4.1 ± 0.5
Neat hemp fibre	21.4 ± 2.0	286 ± 31	2.0 ± 0.2
Bacterial cellulose-modified hemp fibre	8.8 ± 0.7	171 ± 11	2.9 ± 0.2
Bacterial cellulose-modified hemp fibre with purification ^a	8.0 ± 0.6	130 ± 12	2.9 ± 0.2

Adapted from [14]

^aPurification indicates the extraction of post-bacterial cellulose-modified sisal fibres with NaOH at 80°C**Table 6.7** Interfacial shear strengths between modified natural fibres and CAB or PLLA

Natural fibres	Interfacial shear strength to CAB (MPa)	Interfacial shear strength to PLLA (MPa)
Neat sisal fibre	1.02 ± 0.06	12.1 ± 0.5
Bacterial cellulose-modified sisal fibre	1.49 ± 0.03	14.6 ± 1.2
Neat hemp fibre	0.76 ± 0.06	–
Bacterial cellulose-modified hemp fibre	1.83 ± 0.12	–

Adapted from [10] and [14]

type of natural fibres used. The modification process did not change the mechanical properties of sisal fibres, but the properties of hemp fibres were affected (see Table 6.6). The exposure of the hemp fibres to BC caused a drastic loss of fibre strength and Young's modulus. This might be due to a further separation of the bast fibres into smaller individual fibres making up the technical fibre as a result of the intrinsically non-cohesive structure of bast fibres. The interfacial shear strengths between sisal fibres and CAB and PLLA increased by 46 and 21%, respectively, and the interfacial shear strength between hemp fibres and CAB increased by as much as 140% (Table 6.7). It should be noted that the increment seen in the interfacial shear strength between hemp fibres and CAB could also be due to the combined effect of BC coating and the disintegration of the fibres. This improvement seen in the interfacial shear strengths indicates enhanced stress transfer between the fibres and the matrix, which is a direct result of improved interfacial adhesion due to the bacterial cellulose coating applied to natural fibres.

Bacterial cellulose-modified sisal and hemp fibres have also been used to produce unidirectional natural fibre reinforced CAB and polylactide (PLLA) model composites [9]. The mechanical properties of bacterial cellulose-coated sisal fibre reinforced polymers showed significant improvements over neat polymers (Table 6.8). The tensile strength and modulus for sisal/PLLA composites improved by as much as 68 and 49%, respectively. However, improvements were

Table 6.8 Mechanical properties of bacterial cellulose modified hemp and sisal fibres reinforced CAB and PLLA composites

Composites	Neat fibre		Modified fibre		Improvements	
	σ (MPa)	E (GPa)	σ (MPa)	E (GPa)	σ (%)	E (%)
CAB/Hemp ^a	98.1 ± 12.7	8.5 ± 1.3	86.7 ± 13.6	5.8 ± 0.5	-12	-35
PLLA/Hemp ^a	110.5 ± 27.2	11.8 ± 4.2	104.8 ± 9.1	7.9 ± 1.2	-5	-33
CAB/Sisal ^a	92.9 ± 9.3	5.5 ± 0.5	100.4 ± 7.0	8.8 ± 1.4	8	59
PLLA/Sisal ^a	78.9 ± 14.7	7.9 ± 1.3	113.8 ± 14.0	11.2 ± 1.2	44	42
CAB/Hemp ^b	15.8 ± 2.2	1.9 ± 0.1	13.4 ± 1.4	0.6 ± 0.2	-15	-69
PLLA/Hemp ^b	13.4 ± 3.6	3.2 ± 0.2	13.3 ± 2.5	2.3 ± 0.3	-1	-28
CAB/Sisal ^b	10.9 ± 1.7	1.6 ± 0.1	14.4 ± 3.7	1.8 ± 0.3	32	15
PLLA/Sisal ^b	10.0 ± 3.1	2.1 ± 0.1	16.8 ± 4.1	3.1 ± 0.2	68	49

Adapted from [9]

^aThe loading direction is parallel (0°) to the fibres

^bThe loading direction is perpendicular (90°) to the fibres

not observed for composites containing BC-coated hemp fibres. The tensile strength and modulus decreased by as much as 15 and 69%, respectively, for hemp/CAB composites. One should note that the fibres were damaged during bacteria culture and their tensile strength were only one third of that of the original fibres. The use of BC-coated sisal fibres has also led to some improvements in short fibre reinforced PLLA composites [104]. It was shown that the crystallinity of the matrix and the tensile and flexural properties improved through the addition of bacterial cellulose-coated sisal fibres to PLLA. The tensile and flexural properties of these composites were found to be higher than that of commercial polypropylene used in the automotive industry. This indicates the potential of hierarchical composites for applications in the automotive industry.

6.3 Conclusion

Natural fibres have significant advantages over conventional glass fibres. These include low cost, low density, high specific strength and, most importantly, biodegradability (this might, however, result in problems if the fibres degrade within inside the matrix). They are the prime candidates for the manufacturing of truly green composites. However, the extremely hydrophilic nature of these natural fibres often leads to poor compatibility between conventional thermoplastics, such as polylactide. Modification to the matrix is one of the possible solutions to this problem. Surface treatments of natural fibres to enhance the interface between the fibres and the matrix might be a viable solution. Chemical treatments have been explored extensively in this context but it is not the most desirable method; hazardous chemicals are often involved in the chemical treatment of natural fibres. Solvent waste disposal after chemical treatment is another problem associated with surface chemical treatment of natural fibres.

New and greener methods of surface treatment are emerging. Plasma treatments have been shown to be effective in increasing the critical surface tension of natural fibres, thereby improving the wettability between the fibres and the matrix. Enzyme-retting and treatments are also other emerging methods to extract or treat natural fibres. Non-cellulosic compounds such as pectin, lignin and hemicellulose can be removed by specific enzymes, exposing the main cellulose backbone of natural fibres, which was shown to result in increased surface tension. Enzyme-retting is favourable when compared to conventional water-retting and dew-retting methods. Water-retting produces vast amounts of fermentation waste, while dew-retting has the disadvantage of producing fibres that possess lower quality compared to enzyme-retting due to the inherent difficulties in controlling the retting parameters. However, enzyme-retting is limited to pilot scale only due to its high operating and capital cost when compared to water- and dew-retting methods.

White rot fungi have been shown to be effective in lignin removal. It has been used to remove non-cellulosic compounds from natural fibres, exposing the underlying cellulose and hemicellulose. A combination of alkali and fungal treatments showed the most improvement in the composites' mechanical properties. The surface of natural fibres can also be modified by coating them with a layer of (bacterial) cellulose nanofibrils, which allows the production of hierarchical composites. This can be done by immersing natural fibres in a culture medium containing cellulose-producing bacteria, such as the *Acetobacter* species. By using natural fibres as a substrate for cellulose-producing bacteria, the bacteria will deposit their cellulose preferentially onto the surface of natural fibres. This increases the effective area of the interface, enhances the interfacial adhesion through mechanical interlocking and improves the wettability of the fibres by the matrix, as bacterial cellulose possesses higher surface tension than natural fibres [106, 107]. The resulting polymers reinforced with bacterial cellulose-coated natural fibres have comparable properties with commercial polypropylene used in the automotive industry, indicating the potential of such surface treatment.

Public's demand for more environmentally friendly products and environmental legislations should motivate the composites industry (at least in parts) to move away from conventional synthetic materials such as synthetic glass fibres and polypropylene to greener materials such as natural fibres and biobased polymers. A combination of natural fibres as the reinforcing agent and greener surface treatments to enhance the interface and biobased polymers as the matrix should enable the production of truly green composite materials. The *ideal* truly green composite materials should be as follows: When the material is not at the end of its lifetime, it should be recyclable without significant loss of mechanical properties. When the material is at the end of its life cycle, it can be triggered to biodegrade in composting condition. Therefore, the next challenge in green composites would be the production of green composites with triggered biodegradability and good recyclability.

Acknowledgements The authors would like to thank the UK Engineering and Physical Science Research Council (EPSRC) for funding (EP/F032005/1).

References

1. Directive 2000/53/EC of the European Parliament And of the Council of 19 September 2000 on end-of-life vehicles: Official Journal of the European Communities (21/10/2000). p. L 269/34
2. Directive 1999/31/EC of The European Parliament And of The Council 26 April 1999 on The Landfill of Waste: Official Journal of the European Communities (16/7/1999). p. L 182/1
3. Directive 2002/96/EC of The European Parliament And of The Council of 27 January 2003 on waste electrical and electronic equipment (WEEE): Official Journal of the European Union (13/2/2003). p. L 32/24
4. Meier MAR (2009) Metathesis with oleochemicals: new approaches for the utilization of plant oils as renewable resources in polymer science. *Macromol Chem Phys* 210(13–14): 1073–1079
5. Flaris V, Singh G (2009) Recent developments in biopolymers. *J Vinyl Addit Technol* 15(1):1–11
6. Morton W, Hearle JWS (1993) Physical properties of textile fibres, 3rd edn. The Textile Institute, Manchester
7. Mohanty AK, Misra M, Hinrichsen G (2000) Biofibres, biodegradable polymers and biocomposites: an overview. *Macromol Mater Eng* 276(3–4):1–24
8. Oksman K, Skrifvars M, Selin JF (2003) Natural fibres as reinforcement in polylactic acid (PLA) composites. *Compos Sci Technol* 63(9):1317–1324
9. Juntaro J et al (2007) Nanocellulose enhanced interfaces in truly green unidirectional fibre reinforced composites. *Compos Interf* 14(7–9):753–762
10. Juntaro J et al (2008) Creating hierarchical structures in renewable composites by attaching bacterial cellulose onto sisal fibers. *Adv Mater* 20(16):3122–3126
11. Pickering KL et al (2007) Optimising industrial hemp fibre for composites. *Compos A Appl Sci Manuf* 38(2):461–468
12. Nishino T et al (2003) Kenaf reinforced biodegradable composite. *Compos Sci Technol* 63(9):1281–1286
13. Plackett D et al (2003) Biodegradable composites based on L-poly lactide and jute fibres. *Compos Sci Technol* 63(9):1287–1296
14. Pommet M et al (2008) Surface modification of natural fibers using bacteria: depositing bacterial cellulose onto natural fibers to create hierarchical fiber reinforced nanocomposites. *Biomacromolecules* 9(6):1643–1651
15. Castano VM et al (1995) Polyester resin reinforcement with natural grass. *J Reinforced Plast Compos* 14(8):866–888
16. Mohanty AK, Misra M (1995) Studies on jute composites – a literature-review. *Polym Plast Technol Eng* 34(5):729–792
17. Heijenrath R, Peijs T (1996) Natural-fibre-mat-reinforced thermoplastic composites based on flax fibres and polypropylene. *Adv Compos Lett* 5(3):81–85
18. Gindl W, Keckes J (2004) Tensile properties of cellulose acetate butyrate composites reinforced with bacterial cellulose. *Compos Sci Technol* 64(15):2407–2413
19. Karnani R, Krishnan M, Narayan R (1997) Biofiber-reinforced polypropylene composites. *Polym Eng Sci* 37(2):476–483
20. Schuh TG (2000) Renewable materials for automotive applications. Daimler-Chrysler AG, Stuttgart. p. <http://www.ienica.net/fibresseminar/schuh.pdf>
21. Ten Alps Communications Ltd t/a Sovereign Publications. (2008) Rieter Automotive Systems. p. <http://www.sovereign-publications.com/rieter.htm>
22. Bismarck A, Mishra S, Lampke T (2005) Plant fibers as reinforcement for green composites. In: Mohanty AK, Misra M, Drzal L (eds) *Natural fibers, biopolymers and biocomposites*. CRC, Boca Raton
23. Craven JP, Cripps R, Ciney V (2000) Evaluating the silk/epoxy interface by means of the microbond test. In: *Composites Part A – Applied Science and Manufacturing* 31(7):653–660
24. Brant AM (2009) *Cement-based composites: materials, mechanical properties and performance*. Taylor and Francis, New York

25. Perez-Rigueiro J, Elices M, Plaza GT, Real JL, Guinea GV (2006) The influence of anaesthesia on the tensile properties of spider silk. *J Exp Biol* 209(2):320–326
26. Mertiny P, Juss J, El Ghareeb MM (2009) Evaluation of glass and basalt fiber reinforcements for polymer composite pressure piping. *J Pres Ves* 131(6):061407-1
27. Riedel U, Nickel J (1999) Natural fibre-reinforced biopolymers as construction materials – new discoveries. *Angew Makromol Chem* 272:34–40
28. Saheb DN, Jog JP (1999) Natural fiber polymer composites: a review. *Adv Polym Technol* 18(4):351–363
29. Sjoström E (1981) *Wood chemistry: fundamentals and applications*. Academic, California
30. Franco PJH, Valadez-González A (2005) Fiber-matrix adhesion in natural fiber composites. In: Mohanty AK, Misra M, Drzal L (eds) *Natural fibers, biopolymers and biocomposites*. CRC, Boca Raton
31. Braun B, Dorgan JR, Chandler JP (2008) Cellulosic nanowhiskers. Theory and application of light scattering from polydisperse spheroids in the Rayleigh-Gans-Debye regime. *Biomacromolecules* 9(4):1255–1263
32. Bloch DR (1999) In: Brandrup J, Immergut EH, Grulke RA (eds) *Polymer handbook*, vol 2, 4th edn. Wiley Interscience, New York, pp VII/497-VII/545
33. Zhu SD et al (2006) Dissolution of cellulose with ionic liquids and its application: a mini-review. *Green Chem* 8(4):325–327
34. Dupont AL (2003) Cellulose in lithium chloride/N, N-dimethylacetamide, optimisation of a dissolution method using paper substrates and stability of the solutions. *Polymer* 44(15):4117–4126
35. Olesen PO, Plackett DV (1999) Perspectives on the performance of natural plant fibres. Plant Fibre Laboratory, Royal Veterinary and Agricultural University, Copenhagen. <http://www.ienica.net/fibresseminar/olesen.pdf>.
36. Kumar MNS et al (2009) Lignin and its applications with polymers. *J Biobased Mater Bioenergy* 3(1):1–24
37. Mohanty AK, Misra M, Drzal LT (2002) Sustainable bio-composites from renewable resources: opportunities and challenges in the green materials world. *J Polym Environ* 10(1–2):19–26
38. Hill CAS, Norton A, Newman G (2009) The water vapor sorption behavior of natural fibers. *J Appl Polym Sci* 112(3):1524–1537
39. Wielage B et al (1999) Thermogravimetric and differential scanning calorimetric analysis of natural fibres and polypropylene. *Thermochim Acta* 337(1–2):169–177
40. John MJ, Anandjiwala RD (2008) Recent developments in chemical modification and characterization of natural fiber-reinforced composites. *Polym Compos* 29(2):187–207
41. Li X, Tabil LG, Panigrahi S (2007) Chemical treatments of natural fiber for use in natural fiber-reinforced composites: a review. *J Polym Environ* 15(1):25–33
42. Kalia S, Kaith BS, Kaur I (2009) Pretreatments of natural fibers and their application as reinforcing material in polymer composites – a review. *Polym Eng Sci* 49(7):1253–1272
43. Valadez-Gonzalez A et al (1999) Chemical modification of henequen fibers with an organosilane coupling agent. *Compos B Eng* 30(3):321–331
44. Mehta G et al (2006) Effect of fiber surface treatment on the properties of biocomposites from nonwoven industrial hemp fiber mats and unsaturated polyester resin. *J Appl Polym Sci* 99(3):1055–1068
45. Ganan P et al (2005) Surface modification of sisal fibers: effects on the mechanical and thermal properties of their epoxy composites. *Polym Compos* 26(2):121–127
46. Pothan LA, Thomas S, Groeninckx G (2006) The role of fibre/matrix interactions on the dynamic mechanical properties of chemically modified banana fibre/polyester composites. *Compos A Appl Sci Manuf* 37(9):1260–1269
47. Tserki V et al (2005) A study of the effect of acetylation and propionylation surface treatments on natural fibres. *Compos A Appl Sci Manuf* 36(8):1110–1118
48. Nair KCM, Thomas S, Groeninckx G (2001) Thermal and dynamic mechanical analysis of polystyrene composites reinforced with short sisal fibres. *Compos Sci Technol* 61(16):2519–2529

49. Mishra S, Naik JB, Patil YP (2000) The compatibilising effect of maleic anhydride on swelling and mechanical properties of plant-fiber-reinforced novolac composites. *Compos Sci Technol* 60(9):1729–1735
50. George J et al (1996) Melt rheological behaviour of short pineapple fibre reinforced low density polyethylene composites. *Polymer* 37(24):5421–5431
51. Kaith BS, Kalia S (2008) Graft copolymerization of MMA onto flax under different reaction conditions: a comparative study. *Exp Polym Lett* 2(2):93–100
52. Cichocki FR, Thomason JL (2002) Thermoelastic anisotropy of a natural fiber. *Compos Sci Technol* 62(5):669–678
53. Baley C et al (2006) Transverse tensile behaviour of unidirectional plies reinforced with flax fibres. *Mater Lett* 60(24):2984–2987
54. Thomason JL (2009) Why are natural fibres failing to deliver on composite performance? In: Conference Proceedings of the 17th International Conference of Composite Materials, Edinburgh
55. Bismarck A, Kumru ME, Springer J (1999) Influence of oxygen plasma treatment of PAN-based carbon fibers on their electrokinetic and wetting properties. *J Colloid Interf Sci* 210(1):60–72
56. Bismarck A et al (2008) Effects of surface plasma treatment on tribology of thermoplastic polymers. *Polym Eng Sci* 48(10):1971–1976
57. Ho KKC et al (2007) Surface and bulk properties of severely fluorinated carbon fibres. *J Fluorine Chem* 128(11):1359–1368
58. Ho KKC, Lee AF, Bismarck A (2007) Fluorination of carbon fibres in atmospheric plasma. *Carbon* 45(4):775–784
59. Liston EM, Martinu L, Wertheimer MR (1993) Plasma surface modification of polymers for improved adhesion – a critical-review. *J Adhes Sci Technol* 7(10):1091–1127
60. Bismarck A et al (2000) Adhesion: comparison between physico-chemical expected and measured adhesion of oxygen-plasma-treated carbon fibers and polycarbonate. *J Adhes* 73(1):19–42
61. Bismarck A, Springer J (2006) Wettability of materials: Plasma treatment effects. In: Hubbard A, Somasundaran P (eds) *Encyclopedia of surface and colloids science*, 2nd edn. Taylor and Francis, Boca Raton
62. Morales J et al (2006) Plasma modification of cellulose fibers for composite materials. *J Appl Polym Sci* 101(6):3821–3828
63. Schutze A et al (1998) The atmospheric-pressure plasma jet: a review and comparison to other plasma sources. *IEEE Trans Plasma Sci* 26(6):1685–1694
64. Baltazar-Y-Jimenez A, Bismarck A (2007) Surface modification of lignocellulosic fibres in atmospheric air pressure plasma. *Green Chem* 9(10):1057–1066
65. Podgorski L et al (2000) Modification of wood wettability by plasma and corona treatments. *Int J Adhes Adhes* 20(2):103–111
66. Baltazar-Y-Jimenez A, Juntaro J, Bismarck A (2008) Effect of atmospheric air pressure plasma treatment on the thermal behaviour of natural fibres and dynamical mechanical properties of randomly-oriented short fibre composites. *J Biobased Mater Bioenergy* 2(3):264–272
67. Yuan XW, Jayaraman K, Bhattacharyya D (2004) Effects of plasma treatment in enhancing the performance of woodfibre-polypropylene composites. *Compos A Appl Sci Manuf* 35(12):1363–1374
68. Yuan XW, Jayaraman K, Bhattacharyya D (2004) Mechanical properties of plasma-treated sisal fibre-reinforced polypropylene composites. *J Adhes Sci Technol* 18(9):1027–1045
69. Yuan XW, Jayaraman K, Bhattacharyya D (2002) Plasma treatment of sisal fibres and its effects on tensile strength and interfacial bonding. *J Adhes Sci Technol* 16(6):703–727
70. Zanini S et al (2005) Modifications of lignocellulosic fibers by Ar plasma treatments in comparison with biological treatments. *Surf Coat Technol* 200(1–4):556–560
71. Couto E et al (2002) Oxygen plasma treatment of sisal fibers and polypropylene: effects on mechanical properties of composites. *Polym Eng Sci* 42(4):790–797

72. Marais S et al (2005) Unsaturated polyester composites reinforced with flax fibers: effect of cold plasma and autoclave treatments on mechanical and permeation properties. *Compos A Appl Sci Manuf* 36(7):975–986
73. Tu X, Young RA, Denes F (1994) Improvement of bonding between cellulose and polypropylene by plasma treatment. *Cellulose* 1(1):87–106
74. Sinha E, Panigrahi S (2009) Effect of plasma treatment on structure, Wettability of jute fiber and flexural strength of its composite. *J Compos Mater* 43(17):1791–1802
75. Kan CW et al (1998) Surface properties of low-temperature plasma treated wool fabrics. *J Mater Process Technol* 83(1–3):180–184
76. Tsai PP, Wadsworth LC, Roth JR (1997) Surface modification of fabrics using a one-atmosphere glow discharge plasma to improve fabric wettability. *Text Res J* 67(5):359–369
77. Noeske M et al (2004) Plasma jet treatment of five polymers at atmospheric pressure: surface modifications and the relevance for adhesion. *Int J Adhes Adhes* 24(2):171–177
78. Shenton MJ, Stevens GC (2001) Surface modification of polymer surfaces: atmospheric plasma versus vacuum plasma treatments. *J Phys D Appl Phys* 34(18):2761–2768
79. Baltazar-Y-Jimenez A et al (2008) Atmospheric air pressure plasma treatment of lignocellulosic fibres: Impact on mechanical properties and adhesion to cellulose acetate butyrate. *Compos Sci Technol* 68(1):215–227
80. Dodd RB, Akin DE (2005) Recent developments in retting and measurement of fiber quality in natural fibers: pros and cons. In: Mohanty AK, Misra M, Drzal L (eds) *Natural fibers, biopolymers and biocomposites*. CRC, Boca Raton
81. Sharma HSS, Sumere CFv (1992) Enzyme treatment of flax. *Genet Eng Biotechnol* 12(2):19–23
82. Anonymous (2009) Harvesting, retting and fiber separation, USDA. http://www.globalhemp.com/Archives/Government_Research/USDA/ages001Ee.pdf
83. Akin DE et al (2001) Enzyme-retting of flax and characterization of processed fibers. *J Biotechnol* 89(2–3):193–203
84. Pallesen BE (1996) The quality of combine-harvested fibre flax for industrial purposes depends on the degree of retting. *Ind Crops Prod* 5(1):65–78
85. Buschle-Diller G, Fanter C, Loth F (1999) Structural changes in hemp fibers as a result of enzymatic hydrolysis with mixed enzyme systems. *Text Res J* 69(4):244–251
86. Kenealy WR et al (2003) Modification of the physical properties of lignocellulosic materials by laccase. In: 225th National Meeting of the American-Chemical-Society, Washington DC
87. Dam JEGV (1999) Optimisation of methods of fibre preparation from agricultural raw materials. Department of fibres and cellulose, Agrotechnological Research Institute, Wageningen. <http://www.ienica.net/fibresseminar/vandam.pdf>
88. Foulk JA et al (2004) Enzyme-retted flax fiber and recycled polyethylene composites. *J Polym Environ* 12(3):165–171
89. Foulk JA et al (2006) Analysis of flax and cotton fiber fabric blends and recycled polyethylene composites. *J Polym Environ* 14(1):15–25
90. Adamsen APS, Akin DE, Rigsby LL (2002) Chelating agents and enzyme retting of flax. *Text Res J* 72(4):296–302
91. Ouajai S, Shanks RA (2009) Biocomposites of cellulose acetate butyrate with modified hemp cellulose fibres. *Macromol Mater Eng* 294(3):213–221
92. Scourzyme, Products and Solutions (2009) Novozyme Bagsvaerd, Denmark. <http://www.novozymes.com/en/MainStructure/ProductsAndSolutions/Textile+mill/Bio-preparation/Scourzyme/Scourzyme>
93. Ouajai S, Shanks RA (2005) Morphology and structure of hemp fibre after bioscouring. *Macromol Biosci* 5(2):124–134
94. Ouajai S, Hodzic A, Shanks RA (2004) Morphological and grafting modification of natural cellulose fibers. *J Appl Polym Sci* 94(6):2456–2465
95. Pickering KL et al (2007) Interfacial modification of hemp fiber reinforced composites using fungal and alkali treatment. *J Biobased Mater Bioenergy* 1(1):109–117

96. Gutierrez A et al (2001) The biotechnological control of pitch in paper pulp manufacturing. *Trends Biotechnol* 19(9):340–348
97. Leone R, Breuil C (1998) Filamentous fungi can degrade aspen steryl esters and waxes. *Int Biodeterior Biodegrad* 41(2):133–137
98. Martinez-Inigo MJ et al (1999) Biodegradability of extractives in sapwood and heartwood from Scots pine by sapstain and white rot fungi. *Holzforschung* 53(3):247–252
99. Martinez-Inigo MJ et al (2000) Time course of fungal removal of lipophilic extractives from *Eucalyptus globulus* wood. *J Biotechnol* 84(2):119–126
100. Li Y, Pickering KL, Farrell RL (2009) Analysis of green hemp fibre reinforced composites using bag retting and white rot fungal treatments. *Ind Crops Prod* 29(2–3):420–426
101. Schirp A et al (2006) Production and characterization of natural fiber-reinforced thermoplastic composites using wheat straw modified with the fungus *Pleurotus ostreatus*. *J Appl Polym Sci* 102(6):5191–5201
102. Gulati D, Sain M (2006) Fungal-modification of natural fibers: a novel method of treating natural fibers for composite reinforcement. *J Polym Environ* 14(4):347–352
103. Clarke AK et al (2004) Degumming of bast fibres. European Patent EP 1425440
104. Juntaro J (2009) Environmentally friendly hierarchical composites. PhD Thesis, Department of Chemical Engineering, Imperial College, London, 207 p
105. Nishino T, Matsuda I, Hirao K (2004) All-cellulose composite. *Macromolecules* 37(20):7683–7687
106. Baltazar-Y-Jimenez A, Bismarck A (2007) Wetting behaviour, moisture up-take and electrokinetic properties of lignocellulosic fibres. *Cellulose* 14(2):115–127
107. Heng JYY et al (2007) Methods to determine surface energies of natural fibres: a review. *Compos Interf* 14(7–9):581–604

Chapter 7

Nanocellulose-Based Composites

Kelley Spence, Youssef Habibi, and Alain Dufresne

Abstract When subjected to acid hydrolysis or mechanical shearing, lignocellulosic fibers yield defect-free, rod-like, or elongated fibrillar nanoparticles. These nanoparticles have particularly received great attention as reinforcing fillers in nanocomposite materials due to their low cost, availability, renewability, light weight, nanoscale dimension, and unique morphology. Preparation, morphological features, and physical properties of nanocelluloses are discussed in this chapter. Their incorporation in nanocomposite materials including processing methods and ensuing properties such as microstructure, thermal properties, mechanical performances, swelling behavior, and barrier properties are also presented.

Keywords Cellulose-based composites · Composite properties · Microfibrillated cellulose · Nanofibrillated cellulose · Production methods

Contents

7.1	Introduction	180
7.2	Hierarchical Structure of Cellulose Fibers	181
7.3	Top-to-Down Fiber Processing	182
7.4	Preparation of Nanocellulose Substrates	183
7.4.1	Preparation of Nanofibrillated Cellulose	183
7.4.2	Preparation of Cellulose Nanocrystals	185
7.5	Morphological Properties of Cellulose Nanoparticles	187
7.6	Processing of Cellulose Nanocomposites	190
7.6.1	Polymer Latexes	190
7.6.2	Hydrosoluble or Hydrodispersible Polymers	191
7.6.3	Nonaqueous Systems	191

A. Dufresne (✉)

Grenoble Institute of Technology, The International School of Paper, Print Media and Biomaterials (Pagora), BP 65, 38402 Saint Martin d'Hères cedex, France
and

Departamento de Engenharia Metalurgica e de Materiais, Universidade Federal do Rio de Janeiro (UFRJ), Coppe, Rio de Janeiro, Brazil
e-mail: alain.dufresne@pagora.grenoble-inp.fr

7.6.4	Long Chains Grafting	192
7.6.5	Extrusion and Impregnation	193
7.6.6	Electrospinning	194
7.6.7	Multilayer Films	196
7.7	Properties of Nanocellulose-Based Composites	196
7.7.1	Microstructure	196
7.7.2	Thermal Properties	198
7.7.3	Mechanical Properties	201
7.7.4	Swelling Properties	203
7.7.5	Barrier Properties	205
7.8	Conclusions and Outlooks	206
	References	206

7.1 Introduction

Over the last two decades, a significant amount of research has been dedicated to the use of lignocellulosic fibers as reinforcing elements in polymeric matrices, and for the potential of replacing conventional fibers, such as glass, by natural fibers in reinforced composites. However, one of the main drawbacks of lignocellulosic fibers is the significant variation of properties inherent to any natural product. Indeed, fiber properties are related to climatic conditions, maturity, and soil type. Disturbances during plant growth also affect the plant structure and are responsible for the enormous variation of mechanical plant fiber properties.

One of the basic ideas to further improve fiber and composite properties is to eliminate the macroscopic flaws by disintegrating the naturally grown fibers, and separating the almost defect-free, highly crystalline fibrils; this can be achieved by exploiting the hierarchical structure of the natural fibers. Aqueous suspensions of cellulose nanoparticles can be prepared by a mechanical treatment or acid hydrolysis of cellulosic biomass. The objective of the latter treatment is to dissolve regions of low lateral order, so that the water-insoluble, highly crystalline residue may be converted into a stable suspension by subsequent vigorous mechanical shearing action. The resulting nanocrystals occur as rod-like particles, known as whiskers, in which the dimensions depend on the nature of the substrate, but range in the nanometer scale. Because these whiskers contain only a small number of defects, their axial Young's modulus is close to the value derived from theoretical chemistry, potentially making them stronger than steel and similar to Kevlar. These highly stiff nanoparticles are, therefore, suitable for the processing of green nanocomposite materials.

Cellulosic nanoparticles, generally known as nanocellulose, have garnered interest from the scientific community because of their biodegradability, strength, and other characteristics. Sustainability and green issues continue as top priorities for many businesses and individuals, stimulating the search for nonpetroleum-based structural materials like bionanocomposites that are biodegradable, high performing, and lightweight.

7.2 Hierarchical Structure of Cellulose Fibers

Cellulose, discovered and isolated by Payen (1838), is considered to be the most abundant polymer on Earth. It is certainly one of the most important structural elements in plants, serving to maintain cell structure. Cellulose is also important to other living species such as bacteria, fungi, algae, amoebas, and even animals. It is a ubiquitous structural polymer that confers its mechanical properties to higher plant cells.

Cellulose is a high-molecular weight homopolysaccharide composed of β -1,4-anhydro-D-glucopyranose units. These units do not lie exactly in plane with the structure, rather they assume a chair conformation with successive glucose residues rotated through an angle of 180° about the molecular axis and hydroxyl groups in an equatorial position. This repeated segment is frequently taken to be the cellobiose dimer (Klemm et al. 2005).

In nature, cellulose chains have a degree of polymerization (DP) of approximately 10,000 glucopyranose units in wood cellulose and 15,000 in native cotton cellulose (Sjöström 1981). One of the most specific characteristics of cellulose is that each of its monomer bears three hydroxyl groups. These hydroxyl groups and their ability to hydrogen bond play a major role in directing crystalline packing and in governing important physical properties of these highly cohesive materials.

In plant cell walls, cellulose fiber biosynthesis results from the combined action of biopolymerization spinning and crystallization. These events are orchestrated by specific enzymatic terminal complexes (TCs) that act as biological spinnerets resulting in the linear association of cellulose chains to form cellulose microfibrils. Depending on the origin, the microfibril diameters range from approximately 2 to 20 nm with lengths that can reach several tens of microns. The cellulose obtained from nature is referred to as cellulose I, or native cellulose. In this type of cellulose, the chains within the unit cell are in a parallel conformation (Woodcock and Sarko 1980), making it an unstable form. Special treatments of native cellulose result in other forms of cellulose, namely cellulose II, III, and IV (Marchessault and Sundararajan 1983). This conversion also allows for the possibility of conversion from one form to another (O'Sullivan 1997).

The cellulose microfibril constitutes the basic structural unit of the plant cell wall; each microfibril can be considered as a string of cellulose crystallites, linked along the chain axis by amorphous domains (Fig. 7.1). Their structure consists of a predominantly crystalline cellulosic core which is covered with a sheath of paracrystalline polyglucosan material surrounded by hemicelluloses (Whistler and Richards 1970). These microfibrils are conjoined by other polymers like lignin and hemicelluloses and aggregate further to form lignocellulosic fibers. As they are almost defect free, the modulus of these sub-entities is close to the theoretical limit for cellulose.

The expectation placed on cellulose-based composites lies in the Young's modulus of the cellulose crystallite. This was first experimentally studied in 1962 from the crystal deformation of cellulose I using highly oriented fibers of bleached

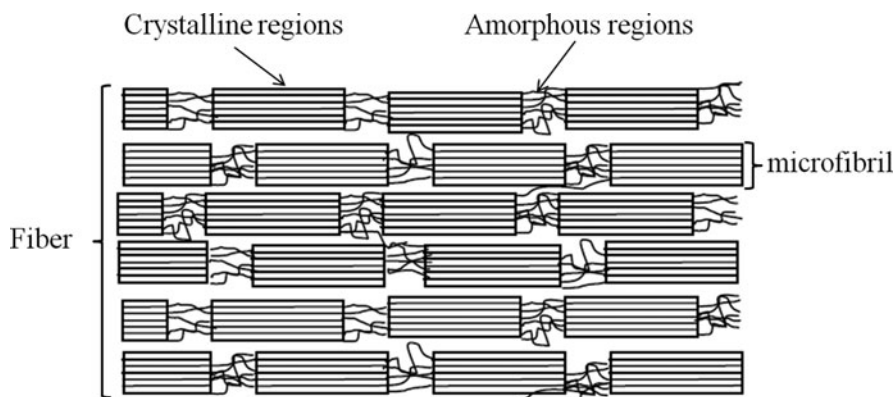


Fig. 7.1 Schematic diagram of the physical structure of a semicrystalline cellulose fiber

ramie (Sakurada et al. 1962); a value of 137 GPa was reported. This value differs from the theoretical estimate of 167.5 GPa reported by Tashiro and Kobayashi (1991). More recently, the Raman spectroscopy technique has been used to measure the elastic modulus of native cellulose crystals (Šturcova et al. 2005), with a reported value of approximately 143 GPa. The elastic modulus of a single microfibril from tunicate was measured by atomic force microscopy (AFM) using a three-point bending test (Iwamoto et al. 2009). Values of 145 and 150 GPa were reported for the single microfibrils prepared by 2,2,6,6-tetramethylpiperidinel-oxyl radical (TEMPO)-oxidation and sulfuric acid hydrolysis, respectively.

These impressive mechanical properties make nanocellulose substrates ideal candidates for reinforcing polymer-based composites. Incorporating these nanoparticles in a synthetic or natural polymeric matrix consists in mimicking nature.

7.3 Top-to-Down Fiber Processing

The major drawback of natural fibers for composite applications is the large variation in properties inherent to natural products. The properties could be impacted by climatic conditions, maturity, and soil type. Disturbances during plant growth also affect the plant structure and are responsible for the enormous variation of mechanical plant fiber properties. For instance, the number of knobby swellings and growth-induced lateral displacement present in plant fibers influence the tensile strength and elongation at break of the fibers obtained. One of the basic ideas to avoid this problem consists of decreasing the size of the natural particles from the micro to the nanoscale. Conceptually, nanoparticles refer to particles with at least one dimension less 100 nm.

When reducing the fibers into microfibrils, the hierarchical structure of natural fibers is exploited and important consequences occur. The first one is obviously an increase in the specific area of the particles, from values of approximately a few

square meter per gram to few hundred square meter per gram, resulting in an increase in the interfacial area with the polymeric matrix. There is also a decrease in the average inter-particle distance in the matrix as the particle size decreases. Thus, some particle–particle interactions can be expected. The homogeneous dispersion of nanoparticles in a continuous medium is generally difficult because the surface energy increases when decreasing the particle dimensions.

Another important feature of nanoparticles is the possibility to improve properties of the material for low filler content without detrimental effect on impact resistance and plastic deformation. A reduction of gas diffusion (a barrier effect) is also likely to occur. Moreover, cellulosic nanoparticles are distinguished by their liquid crystal behavior when suspended in water, presenting birefringence phenomena under polarized light.

Native cellulose fibers are formed by smaller and mechanically stronger entities, the cellulose fibrils. Fibrils contain both crystalline nanoparticles and noncrystalline domains; the latter being located at the surface and along the main axis. Noncrystalline domains form weak spots along the fibrils.

Different descriptors have been used in the literature to designate the crystalline rod-like nanoparticles. These particles are mainly referred to as whiskers, nano-whiskers, cellulose nanocrystals, NCC (nanocrystalline cellulose), monocrystals, microcrystals, or microcrystallites, despite their nanoscale dimensions. The terms microfibrils, microfibrillated cellulose (MFC), and nanofibrillated cellulose (NFC) are used to designate cellulosic nanoparticles obtained by a simple mechanical shearing disintegration process (Fig. 7.2) as described in the next section.

7.4 Preparation of Nanocellulose Substrates

7.4.1 Preparation of Nanofibrillated Cellulose

The process for isolating NFC consists of the disintegration of cellulose fibers along their long axis. They include simple mechanical methods or a combination of enzymatic or chemical pretreatments with mechanical processing. Two main technologies, e.g., Manton Gaulin Homogenizer and Microfluidizer, are commonly used for the mechanical treatment.

Homogenization, utilized most popularly in the food processing industry, particularly to homogenize milk, is estimated to consume approximately 4,000 kJ of energy per pass per kilogram of NFC (Spence et al. 2010). Materials are defibrillated utilizing rapid pressure drops and high shear and impact forces against a valve and an impact ring.

In comparison, microfluidization, utilized most commonly in the cosmetic and pharmaceutical industries, consumes approximately 200, 390, and 630 kJ/kg per pass at processing pressures of 10, 20, and 30 kpsi, respectively. Materials are defibrillated during processing using a large pressure drop and an interaction chamber that imposes shear and impact forces on the fibers.

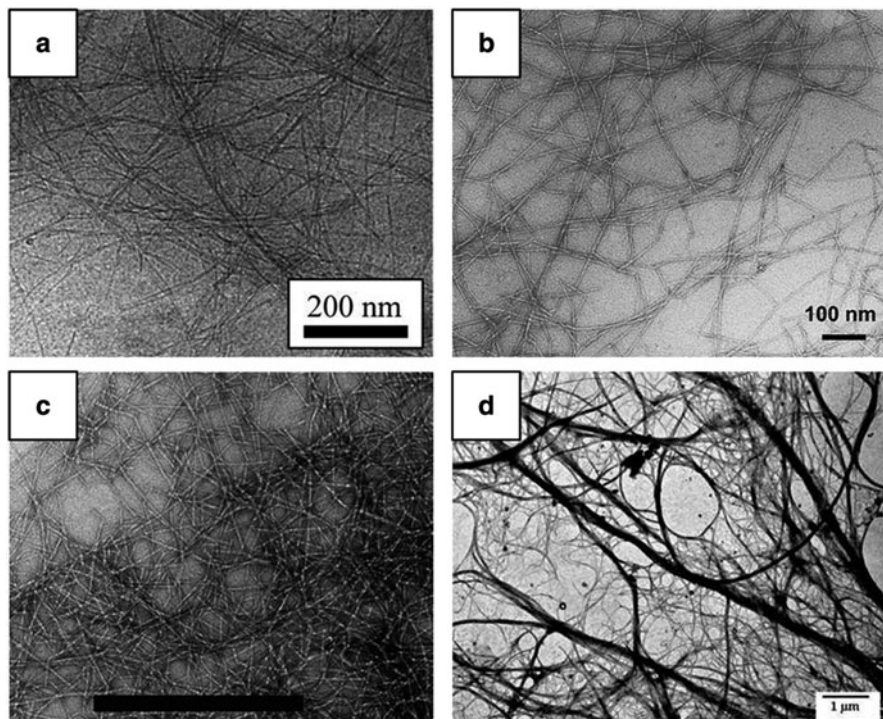


Fig. 7.2 Transmission electron micrographs from a dilute suspension of NFC obtained from wood fibers by mechanical processing combined to (a) enzymatic (Pääkkö et al. 2007), (b) TEMPO-mediated oxidation (Saito et al. 2007), (c) carboxymethylation pretreatment (Wågberg et al. 2008), (d) extracted from *Opuntia ficus-indica* (Malainine et al. 2005). (a, b, c) Reprinted with permission from copyright (2007) (2008) American Chemical Society (d) Reproduced by permission of Elsevier

The main issue with these processing methods is that the wood fibers tend to tangle during processing, causing equipment pluggage. Pretreatments are required for these methods to decrease the initial fiber length and to reduce energy consumption.

Another method, micro-grinding, is typically used in food processing. It is estimated to consume approximately 620 kJ/kg per pass to generate NFC. This method forces wood pulp through a gap between a rotary and a stator disks (Nakagaito and Yano 2004). These disks have patented bursts and grooves that contact the fibers.

NFC were first developed in by Turbak et al. (1983) using, as starting materials, purified cellulose fibers from wood pulp after high pressure mechanical homogenization. Cellulosic fibers were disintegrated into their substructural fibrils and microfibrils having lengths in the micron scale and widths ranging from ten to few hundred nanometers depending on the nature of the plant cell walls. The resulting aqueous suspensions exhibit gel-like characteristics in water with pseudoplastic and thixotropic properties even at low solid content.

The major obstacle for industrial production has been related to the very high-energy consumption involved in processing pure cellulosic fibers. Thus, chemical and/or enzymatic pretreatments were introduced in order to facilitate the fibrillation and mechanical shearing. NFC were produced by an environmentally friendly method by combining enzymatic hydrolysis and mechanical shearing of wood pulp (Henriksson et al. 2007; Lindström et al. 2007; Pääkkö et al. 2007). A cost-effective chemical pretreatment was also attempted prior to the mechanical shearing, by oxidizing cellulose fibers, using TEMPO-mediated oxidation, creating carboxyl groups on the fiber and microfibril surfaces. The TEMPO-oxidized cellulose fibers can be converted, utilizing mechanical shearing, to transparent and highly viscous dispersions in water, consisting of highly crystalline individual nanofibers (Saito et al. 2006, 2007; Fukuzumi et al. 2008). At pH 10 optimal conditions were reached, giving cellulose nanofibers with 3–4 nm in width and a few microns in length. Carboxymethylation was also successfully used to chemically pretreat cellulose fibers before the mechanical processing in order to generate NFC (Aulin et al. 2008; Wågberg et al. 2008). The processing of cellulosic materials extracted from primary cells such as parenchyma cells from sugar beet pulps (Dinand et al. 1996, 1999) or cactus cladodes (Malainine et al. 2005) and fruits (Habibi et al. 2009) were shown to be easier to mechanically process without any enzymatic or chemical pretreatment.

7.4.2 Preparation of Cellulose Nanocrystals

The extraction or isolation of crystalline cellulosic regions, in the form of rod-like nanocrystals, is a simple process based on acid hydrolysis that cleaves the cellulose fibers transversely.

The biomass is first subjected to purification and bleaching processes and, after the removal of noncellulosic constituents such as lignin and hemicelluloses, the bleached material is submitted to a hydrolysis treatment with acid under controlled conditions. The amorphous regions of cellulose act as structural defects and are responsible for the transverse cleavage of the cellulose fibers into short nanocrystals under acid hydrolysis. This transformation consists of the disruption of the amorphous regions surrounding the microfibrils, as well as those embedded between them while leaving the crystalline segments intact; this is ascribed to the faster hydrolysis kinetics of amorphous domains compared to crystalline ones. The hydronium ions penetrate the cellulosic material in the amorphous domains, promoting the hydrolytic cleavage of the glycosidic bonds and releasing individual crystallites. The resulting suspension is subsequently diluted with water and washed by successive centrifugations. Dialysis against distilled water is then performed to remove the free acid in the dispersion. Disintegration of aggregates and complete dispersion of the whiskers is obtained by a sonication step. These suspensions are generally more diluted because of the formation of a gel for low nanoparticle contents. The exact determination of the whisker content can be done by gravimetric methods before and after drying

suspension aliquots. The dispersions are stored in the refrigerator after filtration to remove residual aggregates. This general procedure has to be adapted depending on the nature of the substrate.

Dong et al. (1998) were among the first researchers to study the effect of hydrolysis conditions on the properties of the resulting cellulose nanocrystals. They proved that longer hydrolysis time leads to shorter monocystals and to an increase in surface charge. The acid concentration was also found to affect the morphology of whiskers prepared from sugar beet pulp as reported by Azizi Samir et al. (2004b). Beck-Candanedo et al. (2005) reported the properties of cellulose nanocrystals obtained by hydrolysis of softwood and hardwood pulp and investigated the influence of hydrolysis time and acid-to-pulp ratio. It was found that the reaction time is one of the most important parameters to consider in the acid hydrolysis of wood pulp. Moreover, it was observed that a too long reaction time will completely digest the cellulose to yield its component sugar molecules. On the contrary, lower reaction time will only yield large undispersable fibers and aggregates. It was reported that an increase in the hydrolysis time of pea hull fibers resulted in a decrease of both length and diameter, while the aspect ratio first increases and then decreases (Chen et al. 2009). The effect of the reaction conditions on cellulose nanocrystal surface charge and sulfur content was not significant and it was supposed to be controlled by factors other than hydrolysis conditions. However, chiral nematic pitch decreases when increasing the cellulose concentration and decreasing nanocrystals' length. An attempt to find optimized conditions to prepare cellulose nanocrystals from microcrystalline cellulose (MCC) derived from Norway spruce (*Picea abies*) was also reported (Bondeson et al. 2006). The processing parameters have been optimized by using a response surface methodology.

It was also shown that the hydrolysis of amorphous cellulosic chains can be performed simultaneously with the esterification of accessible hydroxyl groups to produce surface functionalized whiskers in a single step (Braun and Dorgan 2009). The reaction was carried out in an acid mixture composed of hydrochloric and an organic acid (acetic and butyric). Resulting nanocrystals are of similar dimensions compared to those obtained by hydrochloric acid hydrolysis alone. Narrower diameter polydispersity indices indicate that surface groups aid in the individualization of the nanowhiskers. The resulting surface-modified cellulose whiskers are dispersible in ethyl acetate and toluene, indicating increased hydrophobicity and presumably higher compatibility with hydrophobic polymers.

Cellulose nanoparticles are obtained as aqueous suspensions; the stability depends on the dimensions of the dispersed species, size polydispersity, and surface charge. The use of sulfuric acid to prepare cellulose nanocrystals leads to a more stable aqueous suspension than that prepared using hydrochloric acid (Araki et al. 1998). It was shown that the H_2SO_4 -prepared nanoparticles present a negatively charged surface while the HCl-prepared nanoparticles are not charged. During acid hydrolysis utilizing sulfuric acid, acidic sulfate ester groups are likely formed on the nanoparticle surface. This creates electric double-layer repulsion between the nanoparticles in suspension, which plays an important role in their interaction with a polymer matrix and with each other. The density of charges on the cellulose

nanocrystal surface depends on the hydrolysis conditions and can be determined by elementary analysis or conductimetric titration to exactly determine the sulfur content. The sulfate group content increases with acid concentration, acid-to-polysaccharide ratio, and hydrolysis time. Based on the density and size of the cellulose whiskers, Araki et al. (1998, 1999) estimated the charge density to be 0.155 e/nm^2 , where e is the elementary charge, for a nanocrystal with dimensions of $7 \times 7 \times 115 \text{ nm}^3$. With the following conditions: cellulose concentration of 10 wt% in 60% sulfuric acid at 46°C for 75 min, the charge coverage was estimated at 0.2 negative ester groups per nanometer (Revol et al. 1992). Other typical values of the sulfur content of cellulose whiskers prepared by sulfuric acid hydrolysis were reported (Marchessault et al. 1961; Revol et al. 1994). It was shown that even at low levels, the sulfate groups caused a significant decrease in degradation temperature and increase in char fraction confirming that the sulfate groups act as flame retardants (Roman and Winter 2004).

If the cellulose nanocrystals are prepared by hydrochloric acid hydrolysis, the resulting dispersability is limited and their aqueous suspensions tend to flocculate. Habibi et al. (2006) performed TEMPO-mediated oxidation of cellulose whiskers that were obtained from HCl hydrolysis of cellulose nanoparticles from tunicin to introduce negative charges on their surface. They showed that after hydrolysis and TEMPO-mediated oxidation, the nanoparticles kept their initial morphological integrity and native crystallinity, but at their surface, the hydroxymethyl groups were selectively converted to carboxylic groups, thus imparting a negative surface charge to the whiskers. When dispersed in water these oxidized cellulose nanocrystals did not flocculate, and their suspensions appeared birefringent.

7.5 Morphological Properties of Cellulose Nanoparticles

The origin of the cellulose fibers, mainly the nature of the plant cell wall, e.g., primary or secondary, determines the morphology of the generated NFC. They are elongated nanoparticles with widths ranging from 3 to 20 nm and lengths of few microns. NFC from primary cell walls, such as sugar beet pulps or *Opuntia ficus indica*, are generally thinner and longer and were much easier to produce compared to those extracted from secondary walls, such as wood. Figure 7.2 shows example of NFC extracted from primary or secondary cell walls.

Cellulose nanocrystals can be prepared from any botanical source containing cellulose. In the literature, different cellulosic sources have been used as shown in Fig. 7.3. Regardless of the source, cellulose nanocrystals occur as elongated nanoparticles. The persistence of the spot diffractogram when the electron probe is scanned along the rod during transmission electron microscopy (TEM) observation is evidence of the monocrystalline nature of the cellulosic fragment (Favier et al. 1995a); therefore, each fragment can be considered as a cellulosic crystal with no apparent defect. Their dimensions depend on several factors, including the source of the cellulose, the exact hydrolysis conditions, and ionic strength.

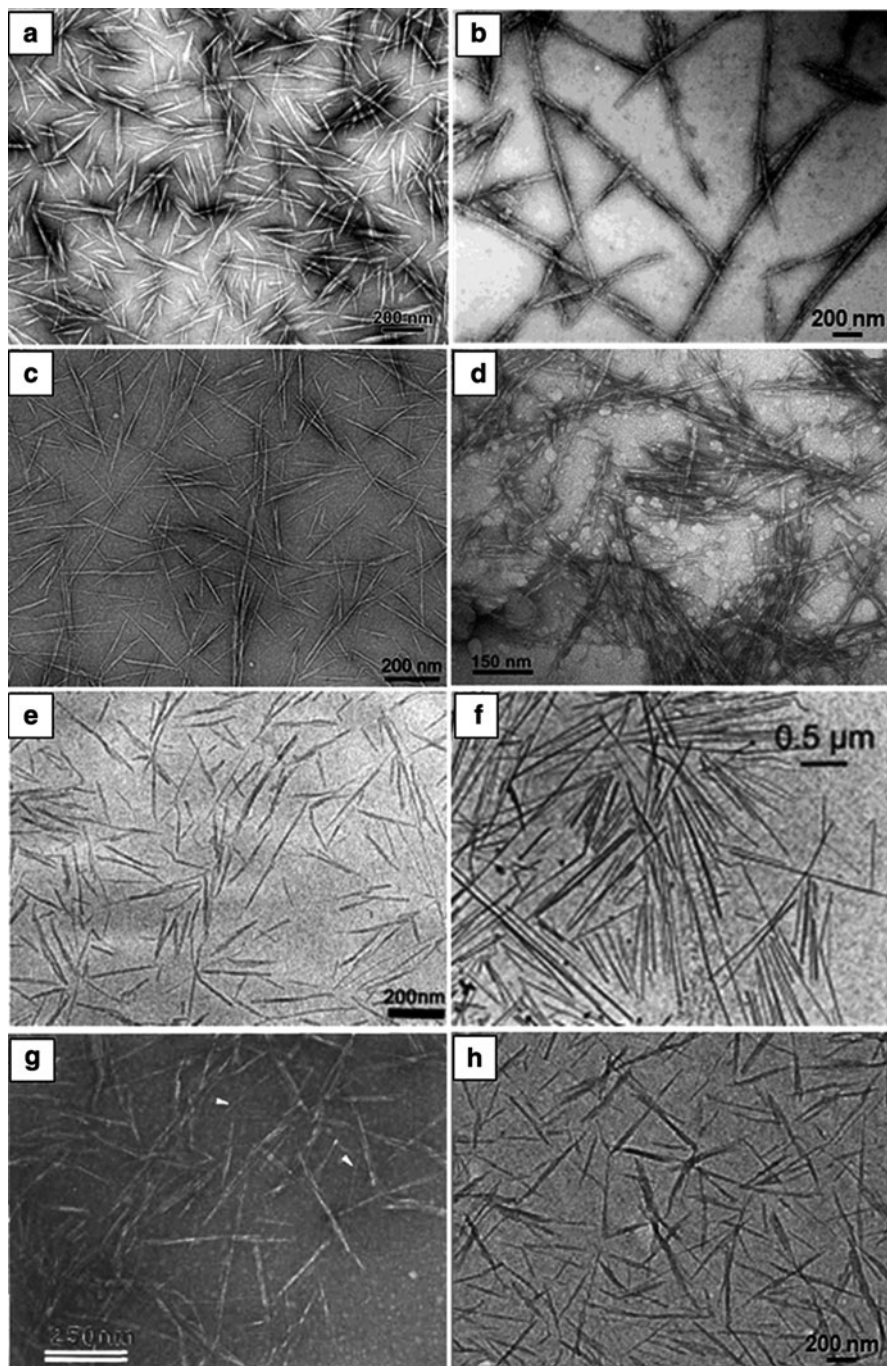


Fig. 7.3 Transmission electron micrographs from dilute suspension of cellulose nanocrystals from: (a) ramie (Habibi et al. 2008), (b) bacterial (Grunnert and Winter 2002), (c) sisal (Garcia de Rodriguez et al. 2006), (d) microcrystalline cellulose (Kvien et al. 2005), (e) sugar beet pulp

Table 7.1 Geometrical characteristics of cellulose nanocrystals from various sources: length (L) and cross section (D)

Source	L (nm)	D (nm)	Ref.
Alfa	200	10	Ben Elmabrouk et al. (2009)
Algal (Valonia)	>1,000	10–20	Revol (1982), Hanley et al. (1992)
Bacterial	100–several 1,000	5–10 × 30–50	Tokoh et al. (1998), Grunnert and Winter (2002), Roman and Winter (2004)
Cladophora	–	20 × 20	Kim et al. (2000)
Cotton	100–300	5–10	Fengel and Wegener (1983), Dong et al. (1998), Ebeling et al. (1999), Araki et al. (2000), Podsiadlo et al. (2005)
Cottonseed linter	170–490	40–60	Lu et al. (2005)
Flax	100–500	10–30	Cao et al. (2007)
Hemp	Several 1,000	30–100	Wang et al. (2007)
Luffa Cylindrica	242	5.2	Siqueira et al. (2010c)
MCC	150–300	3–7	Kvien et al. (2005)
Ramie	200–300	10–15	Habibi et al. (2007, 2008)
Sisal	100–500	3–5	Garcia de Rodriguez et al. (2006)
Sugar beet pulp	210	5	Azizi Samir et al. (2004b)
Tunicin	100–several 1,000	10–20	Favier et al. (1995a)
Wheat straw	150–300	5	Helbert et al. (1996b)
Wood	100–300	3–5	Fengel and Wegener (1983), Araki et al. (1998, 1999), Beck-Candanedo et al. (2005)

The typical geometrical characteristics for nanocrystals derived from different species and reported in the literature are collected in Table 7.1. Although, if often composed of few laterally bound elementary crystallites that are not separated by conventional acid hydrolysis and sonication process (Elazzouzi-Hafraoui et al. 2008), the length and width of hydrolyzed cellulose nanocrystals is generally in the order of few hundred nanometers and few nanometers, respectively. It was observed that the length polydispersity has a constant value, whereas the diameter polydispersity depends on the acid used for isolation (Braun et al. 2008). A smaller diameter polydispersity was obtained when using sulfuric acid instead of hydrochloric acid, because of electrostatic charges resulting from the introduction of sulfate ester groups when using the former.

← **Fig. 7.3** (continued) (Azizi Samir et al. 2004b), (f) tunicin (Anglès and Dufresne 2000), (g) wheat straw (Helbert et al. 1996a), and (h) cotton (Fleming et al. 2000). (a) Reproduced by permission of the Royal Society of Chemistry, (b, c) Reproduced by permission of Elsevier, (d, e, f, h). Reprinted with permission from copyright (2008) American Chemical Society and (g) Reproduced by permission of John Wiley & Sons Inc

An important parameter for cellulosic whiskers is the aspect ratio, defined as the ratio of the length to the width (Table 7.1). It determined the anisotropic phase formation and reinforcing properties. The average length ranges between 1 μm for nanocrystals prepared, for instance, from tunicate, and around 200 nm for cotton. The cellulose extracted from tunicate, a sea animal, is referred as tunicin. The diameter ranges between 15 nm for tunicin and 4–5 nm for sisal or wood. The high value reported for cottonseed linter corresponds to aggregates. The aspect ratio varies between 10 for cotton and 67 for tunicin. Relatively large and highly regular tunicin whiskers are ideal for modeling rheological and reinforcement behaviors and were extensively used in the literature. The shape and dimensions of cellulose whiskers can be accessed from microscopic observations or scattering techniques. The cross-sections of microfibrils observed by TEM are square, whereas their AFM topography shows a rounded profile due to convolution with the shape of the AFM tip (Hanley et al. 1992). AFM images of the surface of highly crystalline cellulose microfibrils showed periodicities along the microfibril axis of 1.07 and 0.53 nm that were supposed to correspond to the fiber and glucose unit repeat distances, respectively. Scattering techniques include small-angle light (de Souza Lima et al. 2003) and neutron (Orts et al. 1998) scattering.

7.6 Processing of Cellulose Nanocomposites

The main challenge with nanoparticles is related to their homogeneous dispersion within a polymeric matrix. The presence of sulfate groups resulting from the acid hydrolysis treatment when using sulfuric acid to prepare cellulose whiskers or nanocrystals induces the stability of the ensuing aqueous suspension. Water is therefore initially the preferred processing medium. A high level of dispersion of the filler within the host matrix in the resulting composite film is expected when processing nanocomposites in aqueous medium.

7.6.1 *Polymer Latexes*

The first publication reporting the preparation of cellulose nanocrystal reinforced polymer nanocomposites was carried out using a latex obtained by the copolymerization of styrene and butyl acrylate (poly(S-*co*-BuA)) and tunicin whiskers (Favier et al. 1995a). The same copolymer was used in association with wheat straw (Helbert et al. 1996a) or sugar beet (Azizi Samir et al. 2004b) cellulose nanocrystals. Other latexes such as poly (β -hydroxyoctanoate) (PHO) (Dubief et al. 1999; Dufresne et al. 1999, 2000), polyvinylchloride (PVC) (Chazeau et al. 1999a, b, c, 2000) waterborne epoxy (Matos Ruiz et al. 2001), natural rubber (NR) (Bendahou et al. 2009, 2010; Siqueira et al. 2010a), and polyvinyl acetate (PVAc) (Garcia de Rodriguez et al. 2006) were also used as a matrix. Recently,

stable aqueous nanocomposite dispersions containing cellulose whiskers and a poly(styrene-*co*-hexyl-acrylate) matrix were prepared via miniemulsion polymerization (Ben Elmabrouk et al. 2009). Addition of a reactive silane was used to stabilize the dispersion. Solid nanocomposite films can be obtained by mixing and casting the two aqueous suspensions followed by water evaporation. Alternative methods consist in freeze drying and hot pressing or freeze drying, extruding and hot pressing the mixture.

7.6.2 *Hydrosoluble or Hydrodispersible Polymers*

The preparation of cellulosic particle reinforced starch (Anglès and Dufresne 2000; Mathew and Dufresne 2002; Orts et al. 2005; Kvien et al. 2007; Mathew et al. 2008); (Svagan et al. 2009), silk fibroin (Noishiki et al. 2002), poly(oxyethylene) (POE) (Azizi Samir et al. 2004a, c, f, 2005b, 2006), polyvinyl alcohol (PVA) (Zimmerman et al. 2004a, 2005; Lu et al. 2008; Paralikar et al. 2008; Roohani et al. 2008a), hydroxypropyl cellulose (HPC) (Zimmerman et al. 2004a, 2005), carboxymethyl cellulose (CMC) (Choi and Simonsen 2006a), or soy protein isolate (SPI) (Wang et al. 2006) has been reported in the literature. The hydrosoluble or hydrodispersible polymer is first dissolved in water and this solution is mixed with the aqueous suspension of cellulose nanocrystals. The ensuing mixture is generally evaporated to obtain a solid nanocomposite film. It can also be freeze dried and hot pressed.

7.6.3 *Nonaqueous Systems*

Excluding the use of an aqueous polymer dispersion, or latex, an alternative way to process nonpolar polymer nanocomposites reinforced with cellulose nanocrystals consists of their dispersion in an adequate (with regard to matrix) organic medium. Coating with a surfactant or a surface chemical modification of the nanoparticles can be considered. The global objective is to reduce their surface energy in order to improve their dispersibility/compatibility with nonpolar media.

Coating of cotton and tunicin whiskers by a surfactant such as a phosphoric ester of polyoxyethylene (9) nonyl phenyl ether was found to lead to stable suspensions in toluene and cyclohexane (Heux et al. 2000) or chloroform (Kvien et al. 2005). Coated tunicin whisker reinforced atactic polypropylene (aPP) (Ljungberg et al. 2005), isotactic polypropylene (iPP) (Ljungberg et al. 2006), or poly(ethylene-*co*-vinyl acetate) (EVA) (Chauve et al. 2005) were obtained by solvent casting using toluene. The same procedure was used to disperse cellulosic nanoparticles in chloroform and process composites with poly lactic acid (PLA) (Kvien et al. 2005; Petersson and Oksman 2006). Nanocomposite materials were also prepared by dispersing cellulose acetate butyrate (CAB) in a dispersion of topochemically

trimethylsilylated bacterial cellulose nanocrystals in acetone and subsequent solution casting (Grunnert and Winter 2002).

Surface chemical modification of cellulosic nanoparticles is another way to decrease their surface energy and disperse them in organic liquids of low polarity. It generally involves reactive hydroxyl groups from the surface. Experimental conditions should avoid swelling media and the peeling effect of surface-grafted chains inducing their dissolution in the reaction medium. The chemical grafting has to be mild in order to preserve the integrity of the nanoparticle. Goussé et al. (2002) stabilized tunicin microcrystals in tetrahydrofuran (THF) by a partial silylation of their surface. Grunnert and Winter (2002) reported the preparation of bacterial cellulose nanocrystals topochemically trimethylsilylated. Resulting nanoparticles were dispersed in acetone to process nanocomposites with a cellulose acetatebutyrate matrix. Araki et al. (2001) prepared original sterically stabilized aqueous rod-like cellulose microcrystals suspensions by the combination of HCl hydrolysis, oxidative carboxylation, and grafting of poly(ethylene glycol) (PEG) having a terminal amino group on one end using water-soluble carbodiimide. The PEG-grafted microcrystals demonstrated drastically enhanced dispersion stability shown through resistance to the addition of 2 M sodium chloride. They also demonstrated ability to redisperse into either water or chloroform from the freeze-dried state. Alkenyl succinic anhydride (ASA) can be used for acylating the surface of cellulose nanocrystals. Surface chemical modification of tunicin whiskers with ASA was reported by Yuan et al. (2006). The acylated whiskers were found to disperse in medium- to low-polarity solvents. It was shown that by controlling the heating time, whiskers with different dispersibility could be obtained. Nogi et al. (2006a) and Ifuku et al. (2007) were among the first to use acetylated cellulosic nanofibers in the preparation of reinforced clear plastic.

Preparation of stable cellulose whisker suspensions in dimethylformamide (DMF) (Azizi Samir et al. 2004e; Marcovich et al. 2006) and dimethyl sulfoxide (DMSO) or *N*-methyl pyrrolidine (NMP) (van den Berg et al. 2007) without either addition of a surfactant or any chemical modification was also reported. From DMF, tunicin whiskers reinforced POE plasticized with tetraethylene glycol dimethyl ether (TEGDME) were prepared by casting and evaporation of DMF (Azizi Samir et al. 2004f). Cross-linked nanocomposites were also prepared by dispersing cellulose nanocrystals in a solution of an unsaturated linear polycondensate, addition of a photo-initiator, casting, evaporating the solvent, and UV curing (Azizi Samir et al. 2004d).

7.6.4 Long Chains Grafting

Long chain surface chemical modification of cellulosic nanoparticles consisting of grafting agents bearing a reactive end group and a long “compatibilizing” tail was also reported in the literature. The general objective is, of course, to increase the apolar character of the nanoparticle. In addition, it can yield some extraordinary

possibilities. The surface modifications can act as binding sites for active agents in drug delivery systems or for toxins in purifying and treatment systems. These surface modifications may also be able to interdiffuse, upon heating, to form the polymer matrix phase. The covalent linkage between reinforcement and matrix will result in near-perfect stress transfer at the interface with exceptional mechanical properties of the composite as a result.

Nanocomposite materials were processed from polycaprolactone (PCL)-grafted cellulose whiskers using the grafting “onto” (Habibi and Dufresne 2008) and grafting “from” (Habibi et al. 2008) approaches. The ensuing nanoparticles were used to process nanocomposites using PCL as a matrix and a casting/evaporation technique from dichloromethane. A co-continuous crystalline phase around the nanoparticles was observed. Cellulose whiskers were also surface grafted with PCL via microwave-assisted ring-opening polymerization yielding filaceous cellulose whisker-graft-PCL nanocrystals which were incorporated into PLA as matrix (Lin et al. 2009). Epoxy functionality was introduced onto the surface of cellulosic nanoparticles by oxidation by cerium (IV) followed by grafting of glycidyl methacrylate (Stenstad et al. 2008). The length of the polymeric chain was varied by regulating the amount of glycidyl methacrylate. The surface of cellulose whiskers was also chemically modified by grafting organic acid chlorides presenting different lengths of the aliphatic chain by an esterification reaction (de Menezes et al. 2009). These functionalized nanoparticles were extruded with low density polyethylene (LDPE) to prepare nanocomposite materials. Cellulose whisker reinforced waterborne polyurethane nanocomposites were synthesized via in situ polymerization using a casting/evaporation technique (Cao et al. 2009). The grafted chains were able to form a crystalline structure on the surface of the nanoparticles and induce the crystallization of the matrix. Cellulose nanoparticles were modified with *n*-octadecyl isocyanate (C₁₈H₃₇NCO) using two different methods with one consisting of an in situ solvent exchange procedure (Siqueira et al. 2010b). Phenol was also enzymatically polymerized in the presence of TEMPO-oxidized cellulosic nanoparticles to prepare nanocomposites under ambient conditions (Li et al. 2010).

7.6.5 *Extrusion and Impregnation*

Very few studies have been reported concerning the processing of cellulose nanocrystal reinforced nanocomposites by extrusion methods. The hydrophilic nature of cellulose causes irreversible agglomeration during drying and aggregation in non-polar matrices because of the formation of additional hydrogen bonds between amorphous parts of the cellulose nanoparticles. Therefore, the preparation of cellulose whisker reinforced PLA nanocomposites by melt extrusion was carried out by pumping the suspension of nanocrystals into the polymer melt during the extrusion process (Oksman et al. 2006). An attempt to use PVA as a compatibilizer to promote the dispersion of cellulose whiskers within the PLA matrix was reported (Bondeson and Oksman 2007). Organic acid chlorides-grafted cellulose whiskers



Fig. 7.4 Photographs of the neat LDPE film and extruded nanocomposite films reinforced with 10 wt% of unmodified and C18 acid chloride-grafted cellulose whiskers (de Menezes et al. 2009). Reproduced by permission of Elsevier

were extruded with LDPE (de Menezes et al. 2009). The homogeneity of the ensuing nanocomposite was found to increase with the length of the grafted chains (Fig. 7.4).

Another possible processing technique of nanocomposites using cellulosic nanoparticles in the dry state consists in the filtration of the aqueous suspension to obtain a film or dried mat of particles followed by immersion in a polymer solution. The impregnation of the dried mat is performed under vacuum. Composites were processed by filling the cavities with transparent thermosetting resins such as phenol formaldehyde (Nakagaito et al. 2004; Nakagaito and Yano 2004, 2008), epoxy (Shimazaki et al. 2007), acrylic (Yano et al. 2005; Nogi et al. 2005; Iwamoto et al. 2008), and melamine formaldehyde (Henriksson and Berglund 2007). Nonwoven mats of cellulose microfibrils were also used to prepare polyurethane composite materials using film stacking method (Seydibeyoğlu and Oksman 2008).

Water-redispersible NFC in powder form was recently prepared from refined bleached beech pulp by carboxymethylation and mechanical disintegration (Eyholzer et al. 2010). However, the carboxymethylated sample displayed a loss of crystallinity and strong decrease in thermal stability limiting its use for nanocomposite processing.

7.6.6 *Electrospinning*

Electrostatic fiber spinning, also known as electrospinning, is a versatile method to prepare continuous fibers with diameters ranging from several microns down to 100 nm through the action of electrostatic forces (Huang et al. 2003; Greiner and Wendorff 2007). Basically, the electrospinning process consists in the uniaxial

stretching of a viscoelastic solution by means of electrostatic forces. The desired polymer solution is held in a syringe, which is connected to a positive electrode from a power supply, by its surface tension. The other electrode is connected to a collector which can be static (plate) or dynamic (rotating drum). When the intensity of the electrical field increases, the resulting electrostatic forces overcome the surface tension of the polymer solution inducing a stretching of the solution and series of jets are ejected. As the solvent in the jet evaporates, it hits the collector which is no longer a solution but a collection of solvent-free fiber mats. Electrospinning has received great attention in the fabrication of polymer nanofibers and composites (Huang et al. 2003). It has recently been reported as an alternative processing method for nanocellulose-based polymer composites. However, the dispersion of cellulose nanoparticles discussed before can be challenging.

Bacterial cellulose whiskers were incorporated into POE nanofibers with a diameter of less than 1 μm by the electrospinning process to enhance the mechanical properties of the electrospun fibers (Park et al. 2007). The whiskers were found to be globally well embedded and aligned inside the fibers, even though they were partially aggregated. Likewise, electrospun PVA fiber mats loaded with cellulose nanocrystals (Fig. 7.5), with diameter in the nanoscale range and enhanced mechanical properties, were successfully produced (Medeiros et al. 2008; Peresin et al. 2010). “Core-in-shell” electrospinning approach in which cellulose nanoparticles constitute the discrete “core” component surrounded by a cellulose “shell” was reported (Magalhaes et al. 2009).

Electrospun polystyrene (PS) (Rojas et al. 2009) and PCL (Zoppe et al. 2009) micro or nanofibers reinforced with cellulose nanocrystals were obtained by electrospinning. Nonionic surfactant sorbitan monostearate was used to improve the dispersion of the particles in the hydrophobic PS matrix while surface grafting of long chains was used in the case of PCL.

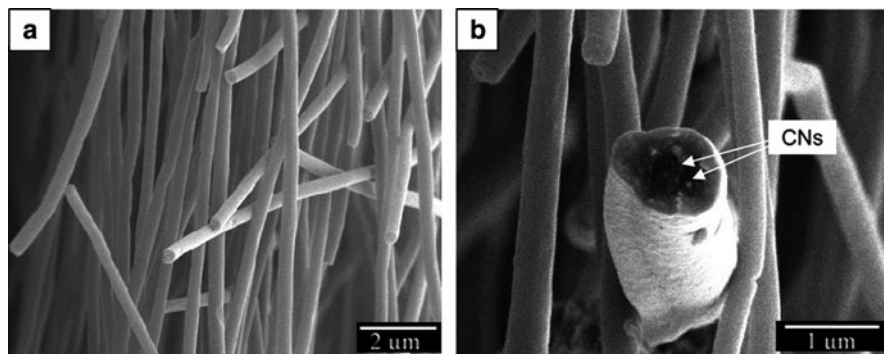


Fig. 7.5 Cryo-scanning electron microscopy micrographs of electrospun polyvinylalcohol loaded with 15% of cellulose nanocrystals (CNs) (Peresin et al. 2010) (copyright (2000) American Chemical Society)

7.6.7 *Multilayer Films*

The use of layer-by-layer (LBL) technique is expected to maximize the interaction between cellulose whiskers and a polar polymeric matrix, such as chitosan (de Mesquita et al. 2010). It also allows the incorporation of high amounts of cellulose whiskers, presenting a dense and homogeneous distribution in each layer.

Podsiadlo et al. (2005) reported the preparation of cellulose whisker multilayer composites with a polycation, poly-(dimethyldiallylammonium chloride) (PDDA), using LBL technique. The authors concluded that the multilayer films presented high uniformity and dense packing of nanocrystals. Orientated self-assembled films were also prepared using a strong magnetic field (Cranston and Gray 2006a) or spin coating technique (Cranston and Gray 2006b). The preparation of thin films composed of alternating layers of orientated rigid cellulose whiskers and flexible polycation chains was reported (Jean et al. 2008). Alignment of the rod-like nanocrystals was achieved using anisotropic suspensions of cellulose whiskers. Green composites based on cellulose nanocrystals/xyloglucan multilayers have been prepared using the nonelectrostatic cellulose–hemicellulose interaction (Jean et al. 2009). The thin films were characterized using neutron reflectivity experiments and AFM observations. More recently, biodegradable nanocomposites were obtained from the LBL technique using highly deacetylated chitosan and cellulose whiskers (de Mesquita et al. 2010). Hydrogen bonds and electrostatic interactions between the negatively charged sulfate groups on the nanoparticle surface and the ammonium groups of chitosan were the driving forces for the growth of the multilayered films. A high density and homogeneous distribution of cellulose nanocrystals adsorbed on each chitosan layer, each bilayer being around 7 nm thick, were reported. Self-organized films were also obtained using only charge-stabilized dispersions of cellulose nanoparticles with opposite charges (Aulin et al. 2010) from the LBL technique.

7.7 **Properties of Nanocellulose-Based Composites**

7.7.1 *Microstructure*

A visual examination is the simplest way to assess the dispersion of cellulosic nanoparticles within the host polymeric matrix. Because of the nanoscale dimensions of the reinforcing phase, the transparency of the nanocomposite film should remain if initially observed for the unfilled matrix. Opacity suggests the presence of aggregates of micrometric sizes (Ljungberg et al. 2005). Optical properties of UV-cured acrylic resin impregnated bacterial cellulose nanofibers were studied by Nogi et al. (2006b). Polarized optical microscopy was used by Azizi Samir et al. (2004c) to observe and follow the growth of POE spherulites in tunicin whisker reinforced films. For the unfilled POE matrix, birefringent spherulites were clearly

identified through the characteristic Maltese cross pattern indicating a spherical symmetry. For a 10 wt% tunicin whisker reinforced material, the supermolecular structure was found to be quite different. It was observed that the spherulites exhibited a less birefringent character, most probably due to a weakly organized structure. It was supposed that the cellulosic filler most probably interfered with the spherulite growth and that during growth, the whiskers are ejected and then occluded in interspherulitic regions. The high viscosity of the filled medium most likely restricts this phenomenon and limits the size of the spherulites.

Scanning electron microscopy (SEM) is generally employed for the more extensive morphological inspection of cellulose nanocrystals reinforced polymers. It consists of the observation of cryofractured surfaces. By comparing the micrographs showing the surface of fracture of the unfilled matrix and composites, the nanoparticles can be easily identified (Fig. 7.6). In fact, they appear like white dots in which concentration is a direct function of the particles content in the composite. These shiny dots correspond to the transverse sections of the cellulose whiskers, but their diameter determined by SEM microscopy is much higher than the whiskers diameter. This results from a charge concentration effect due to the emergence of cellulose whiskers from the observed surface (Anglès and Dufresne 2000).

The dispersion of nanoparticles in the nanocomposite film strongly depends on the processing technique and conditions. SEM comparison between either cast and evaporated or freeze-dried and subsequently hot-pressed composites based on poly (S-co-BuA) reinforced with wheat straw whiskers demonstrated that the former were less homogeneous and displayed a gradient of whiskers concentration between the upper and lower faces of the composite film (Helbert et al. 1996a; Dufresne et al. 1997). It was suggested that the casting/evaporation technique results in more homogenous films, where the whiskers have a tendency to orient randomly into horizontal planes. A two-dimensional in-plane random network of tunicin whisker reinforced epoxy was also reported from Raman spectroscopy experiments (Šturcova et al. 2005).

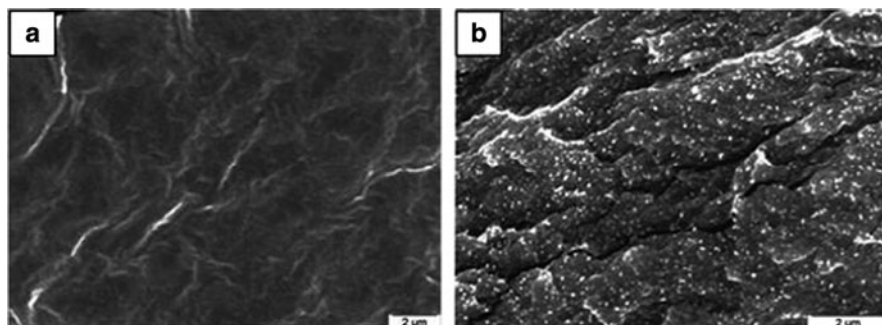


Fig. 7.6 Scanning electron micrographs from the fractured surfaces of (a) unfilled plasticized starch matrix and related composites filled with (b) 25 wt% tunicin whiskers (Anglès and Dufresne 2000) (copyright (2000) American Chemical Society)

TEM observations can be performed to investigate the microstructure and dispersion of the nanoparticles in the nanocomposite film. Casting/evaporation was reported to be an efficient processing technique to obtain a high dispersion level (Favier et al. 1995a; Matos Ruiz et al. 2001; Noishiki et al. 2002; Zimmerman et al. 2004b; Kvien et al. 2005). Small angle X-ray Scattering (SAXS) and small angle neutron scattering (SANS) are other ways to check the dispersion of cellulosic whiskers into the matrix. This latter technique was used to conclude to an isotropic dispersion of tunicin whiskers in plasticized PVC (Chazeau et al. 1999a). AFM imaging has been used to investigate the microstructure of cellulose nanocrystals reinforced polymer nanocomposites (Kvien et al. 2005; Zimmermann et al. 2005). A comparison between field emission (FE) SEM, AFM, and bright-field (BF) TEM for structure determination of cellulose whiskers and their nanocomposites with PLA was performed (Kvien et al. 2005). It was found that AFM overestimated the width of the whiskers due to the tip-broadening effect. FESEM allowed for a quick examination giving an overview of the sample but with limited resolution for detailed information. Detailed information was obtained from TEM, but this technique requires staining and suffers in general from limited contrast and beam sensitivity of the material.

7.7.2 *Thermal Properties*

The glass–rubber transition temperature, T_g , of cellulose whisker filled polymer composites is an important parameter, which controls different properties of the resulting composite such as its mechanical behavior, matrix chain dynamics, and swelling behavior. Its value depends on the interactions between the polymeric matrix and cellulosic nanoparticles. These interactions are expected to play an important role because of the huge specific area inherent to nanosize particles. For semicrystalline polymers, possible alteration of the crystalline domains by the cellulosic filler may indirectly affect the value of T_g .

No modification of T_g was reported for cellulose whiskers reinforced poly (*S-co*-BuA) (Favier et al. 1995a, b; Hajji et al. 1996; Dufresne et al. 1997), PHO (Dubief et al. 1999; Dufresne 2000), PVC (Chazeau et al. 1999a), POE (Azizi Samir et al. 2004a, c), PP (Ljungberg et al. 2005), and NR (Bendahou et al. 2009; Siqueira et al. 2010a). In glycerol plasticized starch-based composites, peculiar effects of tunicin whiskers on the T_g of the starch-rich fraction were reported depending on moisture conditions (Anglès and Dufresne 2000). For low loading level (up to 3.2 wt%), a classical plasticization effect of water was reported (Fig. 7.7). However, an antiplasticization phenomenon was observed for higher whiskers content (6.2 wt% and up). These observations were discussed according to the possible interactions between hydroxyl groups on the cellulosic surface and starch, the selective partitioning of glycerol and water in the bulk starch matrix or at whiskers surface, and the restriction of amorphous starch chains mobility in the vicinity of the starch crystallite coated filler surface. For glycerol plasticized starch reinforced with

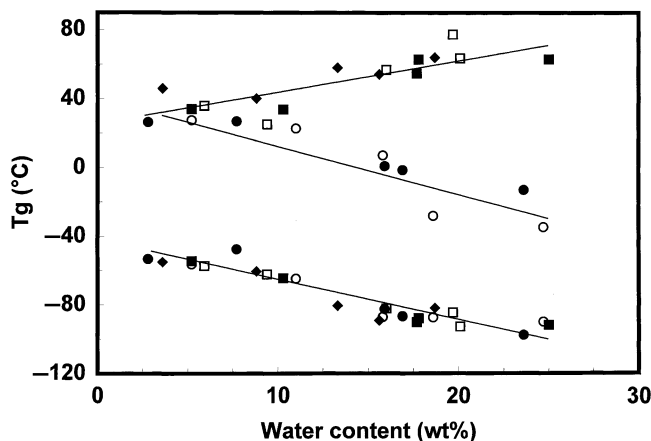


Fig. 7.7 Glass–rubber transition temperatures associated with the midpoints of the transitions versus water content for glycerol plasticized waxy maize starch filled with 0 (filled circle), 3.2 (circle), 6.2 (filled square), 16.7 (square), and 25 wt% (filled diamond) tunicin whiskers. Solid lines serve to guide the eye (Anglès and Dufresne 2000). Copyright (2000) American Chemical Society

cellulose crystallites prepared from cottonseed linter (Lu et al. 2005), an increase of T_g with filler content was reported and attributed to cellulose/starch interactions. For tunicin whiskers/sorbitol plasticized starch (Mathew and Dufresne 2002), T_g s were found to increase slightly up to about 15 wt% whiskers and to decrease for higher whisker loading. Crystallization of amylopectin chains upon whisker addition and migration of sorbitol molecules to the amorphous domains were proposed to explain the observed modifications. When using a PVA matrix, an increase of T_g was reported when the cellulose whiskers content increased (Garcia de Rodriguez et al. 2006; Roohani et al. 2008b). A similar observation was reported for CMC reinforced with cotton cellulose whiskers (Choi and Simonsen 2006b).

Melting temperature, T_m , values were reported to be nearly independent of the filler content in plasticized starch (Anglès and Dufresne 2000; Mathew and Dufresne 2002) and in POE-based materials (Azizi Samir et al. 2004a, c, e) filled with tunicin whiskers. The same observation was reported for CAB reinforced with native bacterial cellulose whiskers (Grunnert and Winter 2002). However, for the latter system, T_m values were found to increase when the amount of trimethylsilylated whiskers increased. The authors ascribed this difference to the stronger filler–matrix interaction in the case of chemically modified whiskers. A decrease of both T_m and degree of crystallinity of PVA was reported when adding cellulose nanocrystals (Roohani et al. 2008b). However, for electrospun cellulose whiskers reinforced PVA nanofibres, the crystallinity was found to be reduced upon filler addition (Peresin et al. 2010).

A significant increase in crystallinity of sorbitol plasticized starch (Mathew and Dufresne 2002) was reported when increasing the cellulose whiskers content. This phenomenon was ascribed to an anchoring effect of the cellulosic filler, probably

acting as a nucleating agent. For POE-based composites, the degree of crystallinity of the matrix was found to be roughly constant up to 10 wt% tunicin whiskers (Azizi Samir et al. 2004a, c, e) and to decrease for higher loading level (Azizi Samir et al. 2004c). It seems that the nucleating effect of cellulosic nanocrystals is mainly governed by surface chemical considerations (Ljungberg et al. 2006). It was shown from both X-ray diffraction and DSC analysis that the crystallization behavior of films containing unmodified and surfactant-modified whiskers displayed two crystalline forms (α and β), whereas the neat matrix and the nanocomposite reinforced with nanocrystals grafted with maleated polypropylene only crystallized in the α form. It was suspected that the more hydrophilic the whisker surface, the more it appeared to favor the appearance of the β phase. Grunnert and Winter (2002) observed from DSC measurements that native bacterial fillers impede the crystallization of the CAB matrix, whereas silylated ones help to nucleate the crystallization. The crystallinity of *N*-octadecyl isocyanate-grafted sisal whisker reinforced PCL was found to increase upon filler addition, whereas no influence of *N*-octadecyl isocyanate-grafted sisal MFC was reported (Siqueira et al. 2009). This difference was ascribed to the possibility of entanglement of MFC that tends to confine the polymeric matrix and restricts its crystallization.

For tunicin whisker-filled semi-crystalline matrices such as PHO (Dufresne et al. 1999) and glycerol plasticized starch (Anglès and Dufresne 2000), a transcrystallization phenomenon was reported. For glycerol plasticized starch-based systems, the formation of the transcrystalline zone around the whiskers was assumed to be due to the accumulation of plasticizer in the cellulose/amylopectin interfacial zones, improving the ability of amylopectin chains to crystallize. This transcrystalline zone could originate from a glycerol–starch V structure. In addition, the inherent restricted mobility of amylopectin chains was put forward to explain the lower water uptake of cellulose/starch composites for increasing filler content. Transcrystallization of PP at cellulose nanocrystal surfaces was evidenced and it was found to result from enhanced nucleation due to some form of epitaxy (Gray 2008).

The presence of sulfate groups introduced at the surface of the whiskers during hydrolysis with H_2SO_4 promotes their thermal decomposition (Roman and Winter 2004; Li et al. 2009). Thermogravimetric analysis (TGA) experiments were performed to investigate the thermal stability of tunicin whiskers/POE nanocomposites (Azizi Samir et al. 2004a, c). No significant influence of the cellulosic filler on the degradation temperature of the POE matrix was reported. Cellulose nanocrystal content appeared to have an effect on the thermal behavior of CMC plasticized with glycerol (Choi and Simonsen 2006b) suggesting a close association between the filler and the matrix. The thermal degradation of unfilled CMC was observed from its melting point (270°C) and had a very narrow temperature range of degradation. Cellulose nanocrystals were found to degrade at a lower temperature (230°C) than CMC, but showed a very broad degradation temperature range. The degradation of cellulose whisker reinforced CMC was observed between these two limits, but of interest was the lack of steps. Composites were reported to degrade as a unit.

7.7.3 Mechanical Properties

Nanoscale dimensions resulting in a very high surface area-to-volume ratio and impressive mechanical properties of rod-like cellulose whiskers have attracted significant interest in the last 15 years. These characteristics, along with the remarkable suitability for surface functionalization, make them ideal candidates to improve the mechanical properties of the host material.

The first demonstration of the reinforcing effect of cellulose whiskers in a poly (*S-co-BuA*) matrix was reported by Favier et al. (1995a, b). The authors measured, by dynamic mechanical analysis (DMA), a spectacular improvement in the storage modulus after adding tunicin whiskers even at low content into the host polymer. This increase was especially significant above the T_g of the thermoplastic matrix because of its poor mechanical properties in this temperature range. Figure 7.8 shows the isochronal evolution of the logarithm of the relative storage shear modulus ($\log G'_T/G'_{200}$, where G'_{200} corresponds to the experimental value measured at 200 K) at 1 Hz as a function of temperature for such composites prepared by water evaporation. In the rubbery state of the thermoplastic matrix, the modulus of the composite with a loading level as low as 6 wt% is more than two orders of magnitude higher than the one of the unfilled matrix. Moreover, the introduction of 3 wt% or more cellulosic whiskers provides an outstanding thermal stability of the matrix modulus up to the temperature at which cellulose starts to degrade (500 K). Since this pioneer work, many publications report the reinforcing capability of cellulose nanoparticles.

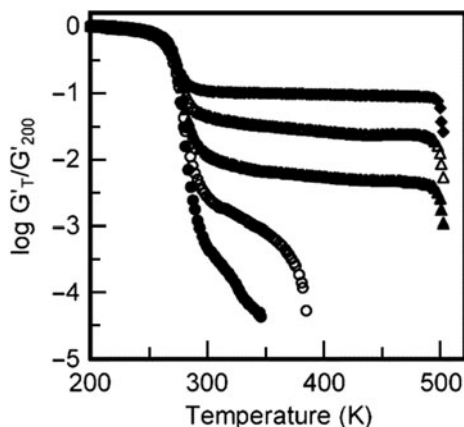


Fig. 7.8 Logarithm of the normalized storage shear modulus ($\log G'_T/G'_{200}$, where G'_{200} corresponds to the experimental value measured at 200 K) versus temperature at 1 Hz for tunicin whiskers reinforced poly(*S-co-BuA*) nanocomposite films obtained by water evaporation and filled with 0 (filled circle), 1 (circle), 3 (filled triangle), 6 (triangle), and 14 wt% (filled diamond) of cellulose whiskers (reprinted with permission from (Azizi Samir et al. 2005a). Copyright (2005) American Chemical Society

This outstanding reinforcing effect was ascribed to a mechanical percolation phenomenon (Favier et al. 1995a, b).

A good agreement between experimental and predicted data was reported when using the series-parallel model of Takayanagi modified to include a percolation approach. It was suspected that the stiffness of the material was due to infinite aggregates of cellulose whiskers. Above the percolation threshold, the cellulosic nanoparticles can connect and form a tri-dimensional continuous pathway through the nanocomposite film. For rod-like particles such as tunicin whiskers with an aspect ratio of 67, the percolation threshold is close to 1 vol% (Favier et al. 1997b). The formation of this cellulose network was supposed to result from strong interactions between whiskers, like hydrogen bonds (Favier et al. 1997a). This phenomenon is similar to the high mechanical properties observed for a paper sheet, which result from the hydrogen-bonding forces that hold the percolating network of fibers. This mechanical percolation effect explains both the high reinforcing effect and the thermal stabilization of the composite modulus for evaporated films. Any factor that affects the formation of the percolating whiskers network or interferes with it changes the mechanical performances of the composite (Dufresne 2006). Three main parameters were reported to affect the mechanical properties of such materials, viz. (1) the morphology and dimensions of the nanoparticles, (2) the processing method, and (3) the microstructure of the matrix and matrix/filler interactions.

1. For cellulose nanocrystals occurring as rod-like nanoparticles, the geometrical aspect ratio is an important factor because it determines the percolation threshold value. This factor is linked to the source of cellulose and whiskers preparation conditions. Higher reinforcing effect is obtained for nanocrystals with high aspect ratio. For instance, the rubbery storage tensile modulus was systematically lower for wheat straw whiskers/poly(S-co-BuA) composites than for tunicin whiskers-based materials (Dufresne 2006). Also, the flexibility and tangling possibility of the nanofibers plays an important role (Azizi Samir et al. 2004b; Bendahou et al. 2009; Siqueira et al. 2009). It was reported that entangled MFC induces a higher reinforcing effect than straight whiskers, whereas the elongation at break was lower.
2. The processing method conditions present the possibility of the formation of a continuous whiskers network and determine the final properties of the nanocomposite material. Slow processes such as casting/evaporation were reported to give the highest mechanical performance materials compared to freeze-drying/molding and freeze-drying/extruding/molding techniques. During slow water evaporation, because of Brownian motions in the suspension or solution (whose viscosity remains low, up to the end of the process when the latex particle or polymer concentration becomes very high), the rearrangement of the nanoparticles is possible. They have significant time to interact and connect to form a continuous network, which is the basis of their reinforcing effect. The resulting structure is completely relaxed and direct contacts between nanoparticles are then created. Conversely, during the freeze-drying/hot-pressing process, the nanoparticle arrangement in the suspension is first frozen, and then, during

the hot-pressing stage, because of the polymer melt viscosity, the particle rearrangements are strongly limited.

3. The microstructure of the matrix and the resulting competition between matrix/filler and filler/filler interactions also affect the mechanical behavior of cellulose nanocrystals reinforced nanocomposites. Classical composite science tends to favor matrix/filler interactions as a fundamental condition for optimal performance. But, for cellulose whisker-based composite materials, the opposite trend is generally observed when the material is processed via casting/evaporation method. This unusual behavior is ascribed to the originality of the reinforcing phenomenon of cellulosic nanoparticles resulting from the formation of a H-bonded percolating network. However, when using another processing route than casting/evaporation in aqueous medium, the dispersion of the hydrophilic filler in the polymeric matrix is also involved (de Menezes et al. 2009) and improved filler/matrix interactions generally lead to higher mechanical properties. In nonpercolating systems, for instance for materials processed from freeze-dried cellulose nanocrystals, strong matrix/filler interactions enhance the reinforcing effect of the filler (Ljungberg et al. 2005). The transcrystallization phenomenon reported for PHO (Dufresne et al. 1999) and plasticized starch (Anglès and Dufresne 2000) on cellulose whiskers resulted in a decrease of the mechanical properties (Anglès and Dufresne 2001) because of the coating of the nanoparticles with crystalline domains. When using unhydrolyzed cellulose microfibrils extracted from potato pulp rather than cellulose nanocrystals to reinforce glycerol plasticized thermoplastic starch, a completely different mechanical behavior was reported (Dufresne and Vignon 1998; Dufresne et al. 2000) and a significant reinforcing effect was observed. It was suspected that tangling effect contributed to this high reinforcing effect (Anglès and Dufresne 2001).

7.7.4 Swelling Properties

Swelling, or kinetics of solvent absorption, is a method that can highlight specific interactions between the filler and the matrix. It consists generally in first drying and weighing the sample, and then immersing it in the liquid solvent or exposing it to the vapor medium. The sample is then removed at specific intervals and weighed until an equilibrium value is reached. The swelling rate of the sample can be calculated by dividing the gain in weight by the initial weight. Generally, the short-time behavior displays a fast absorption phenomenon, whereas at longer times, the kinetics of absorption is low and leads to a plateau, corresponding to the solvent uptake at equilibrium. The diffusion coefficient can be determined from the initial slope of the solvent uptake curve as a function of time. For cellulosic particle reinforce composites, it is generally of interest to investigate the water absorption of the material because of the hydrophilic nature of the reinforcing phase. When a nonpolar polymeric matrix is used, the absorption of a nonaqueous liquid can be investigated.

A higher resistance of thermoplastic starch to water was reported when increasing the cellulose nanoparticle content (Anglès and Dufresne 2000; Lu et al. 2005; Svagan et al. 2009). Both the water uptake and the diffusion coefficient of water were found to decrease upon nanoparticle addition. These phenomena were ascribed to the presence of strong hydrogen bonding interactions between particles and between the starch matrix and cellulose whiskers. The hydrogen bonding interactions in the composites tend to stabilize the starch matrix when it is submitted to highly moist atmosphere. Moreover, the high crystallinity of cellulose also might be responsible for the decreased water uptake at equilibrium and diffusion coefficient of the material. A lower water uptake and dependence on cellulose whiskers content were reported when using sorbitol rather than glycerol as plasticizer for the starch matrix (Mathew and Dufresne 2002). An explanation was proposed based on the chemical structure of both plasticizers, more accessible end hydroxyl groups in glycerol being about twice those compared to sorbitol. Similar results were reported for cellulose whisker reinforced SPI (Wang et al. 2006) and CMC (Choi and Simonsen 2006b). Sisal whisker addition was found to stabilize PVA-based nanocomposites with no benefit seen when increasing the whisker content beyond the percolation threshold (Garcia de Rodriguez et al. 2006). A lower water uptake was observed when using MFC instead of cellulose whiskers as a reinforcing phase in NR (Bendahou et al. 2010). This observation was explained by the difference in the structure and composition of both nanoparticles, and in particular by the presence of residual lignin, extractive substances and fatty acids at the surface of MFC that limits, comparatively, the hydrophilic character of the filler. In addition, assuming that the filler/matrix compatibility was consequently lower for whiskers-based nanocomposites, one can imagine that water infiltration could be easier at the filler/matrix interface. For MFC-based nanocomposites, despite higher amorphous cellulose content, the higher hydrophobic character of the filler favors the compatibility with NR and restricts therefore the interfacial diffusion pathway for water.

Swelling experiments of PVC reinforced with tunicin whiskers were conducted in methyl ethyl ketone (MEK) (Chazeau et al. 1999b). A significant decrease in swelling was observed when increasing the cellulose whiskers content. It was assumed to be due to the existence of an interphase making a link between nanoparticles, thus allowing the formation of a flexible network. The swelling behavior in toluene of poly(S-co-BuA) reinforced with cellulose fibrils from *Opuntia ficus-indica* cladodes was reported by Malainine et al. (2005). They observed a strong toluene resistance even at very low filler loading. While the unfilled matrix completely dissolved in toluene, only 27 wt% of the polymer was able to dissolve when filled with only 1 wt% of cellulose microfibrils. This phenomenon was ascribed to the presence of a three-dimensional entangled cellulosic network which strongly restricted the swelling capability and dissolution of the matrix. For higher microfibrils content, no significant evolution was observed because of both the overlapping of the microfibrils restricting the filler-matrix interfacial area and the decrease of the entrapping matrix fraction due to the densification of the microfibrils network. Similar experiments were conducted

with cellulose microfibrils obtained from sugar beet pulp reinforced poly (S-co-BuA) (Dalmás et al. 2006). Toluene resistance of nanocomposites was found to be less significant than for microfibrils from *Opuntia ficus-indica* cladodes and to evolve with filler content. It was observed that the cohesion of composites prepared by evaporation was higher than the one of freeze-dried/hot-pressed materials. This difference was ascribed to the presence of a H-bonded network in the former samples. It was concluded that the solvent did not have any effect on the hydrogen bonds of the cellulose network present in evaporated composites. On the contrary, for freeze-dried/hot-pressed materials, lower interactions were supposed to create between fibrils and polymer chains were able to be more easily disentangled and dissolved by the solvent. The swelling behavior of cellulose whiskers reinforced NR in toluene was also reported (Bendahou et al. 2010). It was found to strongly decrease even with only 1 wt% of cellulose nanoparticles and to be almost independent of filler content and nature (MFC or whiskers).

7.7.5 Barrier Properties

Petrochemical-based polymers predominate in packaging of foods due to their easy processing, excellent barrier properties, and low cost. However, there is currently an increasing interest in replacing conventional synthetic polymers by more sustainable materials. One promising application area of cellulosic nanoparticles is barrier membranes, where the nano-sized fillers impart enhanced mechanical and barrier properties. Research in this area is burgeoning but is evolving rapidly to enhance the barrier properties and to overcome certain limitations. In addition, it is well known that molecules penetrate with difficulty in the crystalline domains of cellulose microfibrils. Moreover, the ability of cellulosic nanoparticles to form a dense percolating network held together by strong inter-particles bonds suggest their use as barrier films.

This suggestion, that the bond network has a significant effect on barrier properties, has been shown by comparing the water vapor transmission rate (WVTR) of cast films of NFC and hand sheets produced from the unprocessed pulps. The processing of bleached hardwood was shown to reduce the WVTR 4.6-fold, while the processing of bleached softwood reduced the WVTR 3.7-fold (Spence et al. 2010). The oxygen permeability of paper was considerably reduced when coated with MFC layer (Syverud and Stenius 2009). The WVTR of cotton nanocrystal reinforced CMC (Choi and Simonsen 2006b) and PVA (Paralikar et al. 2008) films were reported to decrease. Cellulose nanoparticles prepared by drop-wise addition of ethanol/HCl aqueous solution into a NaOH/urea/H₂O suspension of MCC were found to decrease the water vapor permeability of glycerol plasticized starch films (Chang et al. 2010). The water vapor barrier of mango puree-based edible (Azeredo et al. 2009) and chitosan films (Azeredo et al. 2010) were successfully improved by adding cellulose whiskers

7.8 Conclusions and Outlooks

The potential of nanocomposites in various sectors of research and application is promising and attracting increasing investment. Due to their abundance, high strength and stiffness, low weight and biodegradability, nanoscale cellulose fiber materials serve as promising candidates for the preparation of bionanocomposites. A broad range of applications of nanocellulose exists even if a high number of unknown remains to date. Tens of scientific publications and experts show its potential even if most of the studies focus on their mechanical properties as reinforcing phase and their liquid crystal self-ordering properties. Packaging is one area in which nanocellulose-reinforced polymeric films can be of interest because of the possibility to produce films with high transparency and improved mechanical and barrier properties. However, although there have been many promising achievements at the laboratory and pilot scale, there are several challenges to overcome in order to be able to produce cellulose-based nanocomposites at the industrial scale.

Two important programs have recently started on the production of nanocellulose. One is the creation in 2008 in Finland of the “Suomen Nanoselluloosakeskus” Centre or “Finnish Centre for Nanocellulosic Technologies.” One of the challenges is to produce large quantities of microfibrils of even quality. The forest industry in Finland is going through a major transition, and the utilization of new technologies is expected to provide a means for strengthening the competitiveness in the sector. The other program, supported by the Canadian government and represented by FPInnovations, is the creation of the ArboraNano network. The objective of this program for the valorization of nanocellulose (as cellulose nanocrystals) is also to revive the forestry sectors in Canada, strongly affected by the growing competition from emerging countries in Asia and South America.

However, it is worth noting that there are many safety concerns about nanomaterials, as their size allows them to penetrate into cells and eventually remain in the system. There is no consensus about categorizing nanomaterials as new materials.

References

- Anglès MN, Dufresne A (2000) Plasticized starch/tunicin whiskers nanocomposites. 1. Structural analysis. *Macromolecules* 33:8344–8353
- Anglès MN, Dufresne A (2001) Plasticized starch/tunicin whiskers nanocomposite materials. 2. Mechanical behavior. *Macromolecules* 34:2921–2931
- Araki J, Wada M, Kuga S et al (1998) Flow properties of microcrystalline cellulose suspension prepared by acid treatment of native cellulose. *Colloids Surf A* 142:75–82
- Araki J, Wada M, Kuga S et al (1999) Influence of surface charge on viscosity behavior of cellulose microcrystal suspension. *J Wood Sci* 45:258–261
- Araki J, Wada M, Kuga S et al (2000) Birefringent glassy phase of a cellulose microcrystal suspension. *Langmuir* 16:2413–2415

- Araki J, Wada M, Kuga S (2001) Steric stabilization of cellulose microcrystal suspension by poly (ethylene glycol) grafting. *Langmuir* 17:21–27
- Aulin C, Varga I, Claesson PM et al (2008) Buildup of polyelectrolyte multilayers of polyethyleneimine and microfibrillated cellulose studied by in situ dual-polarization interferometry and quartz crystal microbalance with dissipation. *Langmuir* 24:2509–2518
- Aulin C, Johansson E, Wågberg L et al (2010) Self-organized films from cellulose I nanofibrils using the layer-by-layer technique. *Biomacromolecules* 11:872–882
- Azeredo H, Henrique C, Mattoso L, Wood D et al (2009) Nanocomposite edible films from mango puree reinforced with cellulose nanofibers. *J Food Sci* 74:N31–N35
- Azeredo HMC, Mattoso HLC, Avena-Bustillos RJ et al (2010) Nanocellulose reinforced chitosan composite films as affected by nanofiller loading and plasticizer content. *J Food Sci* 75:N1–N7
- Azizi Samir MAS, Alloin F, Gorecki W et al (2004a) Nanocomposite polymer electrolytes based on poly(oxyethylene) and cellulose nanocrystals. *J Phys Chem B* 108:10845–10852
- Azizi Samir MAS, Alloin F, Paillet M et al (2004b) Tangling effect in fibrillated cellulose reinforced nanocomposites. *Macromolecules* 37:4313–4316
- Azizi Samir MAS, Alloin F, Sanchez J-Y et al (2004c) Cellulose nanocrystals reinforced poly (oxyethylene). *Polymer* 45:4149–4157
- Azizi Samir MAS, Alloin F, Sanchez J-Y et al (2004d) Cross-linked nanocomposite polymer electrolytes reinforced with cellulose whiskers. *Macromolecules* 37:4839–4844
- Azizi Samir MAS, Alloin F, Sanchez J-Y et al (2004e) Preparation of cellulose whiskers reinforced nanocomposites from an organic medium suspension. *Macromolecules* 37:1386–1393
- Azizi Samir MAS, Mateos AM, Alloin F et al (2004f) Plasticized nanocomposite polymer electrolytes based on poly(oxyethylene) and cellulose whiskers. *Electrochim Acta* 49:4667–4677
- Azizi Samir MAS, Alloin F, Dufresne A (2005a) Review of recent research into cellulosic whiskers, their properties and their application in nanocomposite field. *Biomacromolecules* 6:612–626
- Azizi Samir MAS, Chazeau L, Alloin F et al (2005b) POE-based nanocomposite polymer electrolytes reinforced with cellulose whiskers. *Electrochim Acta* 50:3897–3903
- Azizi Samir MAS, Alloin F, Dufresne A (2006) High performance nanocomposite polymer electrolytes. *Compos Interfaces* 13:545–559
- Beck-Candanedo S, Roman M, Gray DG (2005) Effect of reaction conditions on the properties and behavior of wood cellulose nanocrystal suspensions. *Biomacromolecules* 6:1048–1054
- Ben Elmabrouk A, Wim T, Dufresne A et al (2009) Preparation of poly(styrene-co-hexylacrylate)/cellulose whiskers nanocomposites via miniemulsion polymerization. *J Appl Polym Sci* 114:2946–2955
- Bendahou A, Habibi Y, Kaddami H et al (2009) Physico-chemical characterization of palm from Phoenix dactylifera-L, preparation of cellulose whiskers and natural rubber-based nanocomposites. *J Biobased Mater Bioenergy* 3:81–90
- Bendahou A, Kaddami H, Dufresne A (2010) Investigation on the effect of cellulosic nanoparticles' morphology on the properties of natural rubber based nanocomposites. *Eur Polym J* 46:609–620
- Bondeson D, Oksman K (2007) Polylactic acid/cellulose whisker nanocomposites modified by polyvinyl alcohol. *Compos Part A* 38A:2486–2492
- Bondeson D, Mathew A, Oksman K (2006) Optimization of the isolation of nanocrystals from microcrystalline cellulose by acid hydrolysis. *Cellulose* 13:171–180
- Braun B, Dorgan JR (2009) Single-step method for the isolation and surface functionalization of cellulosic nanowhiskers. *Biomacromolecules* 10:334–341
- Braun B, Dorgan JR, Chandler JP (2008) Cellulosic nanowhiskers. Theory and application of light scattering from polydisperse spheroids in the Rayleigh–Gans–Debye regime. *Biomacromolecules* 9:1255–1263
- Cao X, Dong H, Li CM (2007) New nanocomposite materials reinforced with flax cellulose nanocrystals in waterborne polyurethane. *Biomacromolecules* 8:899–904
- Cao X, Habibi Y, Lucia LA (2009) One-pot polymerization, surface grafting, and processing of waterborne polyurethane–cellulose nanocrystal nanocomposites. *J Mater Chem* 19: 7137–7145

- Chang PR, Jian R, Zheng P et al (2010) Preparation and properties of glycerol plasticized-starch (GPS)/cellulose nanoparticle (CN) composites. *Carbohydr Polym* 79:301–305
- Chauve G, Heux L, Arouini R et al (2005) Cellulose poly(ethylene-co-vinyl acetate) nanocomposites studied by molecular modeling and mechanical spectroscopy. *Biomacromolecules* 6: 2025–2031
- Chazeau L, Cavaillé JY, Canova G et al (1999a) Viscoelastic properties of plasticized PVC reinforced with cellulose whiskers. *J Appl Polym Sci* 71:1797–1808
- Chazeau L, Cavaillé JY, Terech P (1999b) Mechanical behaviour above T_g of a plasticised PVC reinforced with cellulose whiskers; a SANS structural study. *Polymer* 40:5333–5344
- Chazeau L, Paillet M, Cavaillé JY (1999c) Plasticized PVC reinforced with cellulose whiskers. I. Linear viscoelastic behavior analyzed through the quasi-point defect theory. *J Polym Sci Part B: Polym Phys* 37:2151–2164
- Chazeau L, Cavaillé JY, Perez J (2000) Plasticized PVC reinforced with cellulose whiskers. II. Plastic behavior. *J Polym Sci Part B: Polym Phys* 38:383–392
- Chen G, Dufresne A, Huang J et al (2009) A novel thermoformable bionanocomposite based on cellulose nanocrystal-graft-poly(ϵ -caprolactone). *Macromol Mater Eng* 294:59–67
- Choi Y, Simonsen J (2006) Cellulose nanocrystal-filled carboxymethyl cellulose nanocomposites. *J Nanosci Nanotechnol* 6:633–639
- Cranston ED, Gray DG (2006a) Formation of cellulose-based electrostatic layer-by-layer films in a magnetic field. *Sci Technol Adv Mater* 7:319–321
- Cranston ED, Gray DG (2006b) Morphological and optical characterization of polyelectrolyte multilayers incorporating nanocrystalline cellulose. *Biomacromolecules* 7:2522–2530
- Dalmas F, Chazeau L, Gauthier C et al (2006) Large deformation mechanical behavior of flexible nanofiber filled polymer nanocomposites. *Polymer* 47:2802–2812
- de Menezes JA, Siqueira G, Curvelo AAS et al (2009) Extrusion and characterization of functionalized cellulose whiskers reinforced polyethylene nanocomposites. *Polymer* 50:4552–4563
- de Mesquita JP, Donnici CL, Pereira FV (2010) Biobased nanocomposites from layer-by-layer assembly of cellulose nanowhiskers with chitosan. *Biomacromolecules* 11:473–480
- de Souza Lima MM, Wong JT, Paillet M et al (2003) Translational and rotational dynamics of rodlike cellulose whiskers. *Langmuir* 19:24–29
- Dinand E, Chanzy H, Vignon MR (1996) Parenchymal cell cellulose from sugar beet pulp: preparation and properties. *Cellulose* 3:183–188
- Dinand E, Chanzy H, Vignon R (1999) Suspensions of cellulose microfibrils from sugar beet pulp. *Food Hydrocolloids* 13:275–283
- Dong XM, Revol J-F, Gray DG (1998) Effect of microcrystallite preparation conditions on the formation of colloid crystals of cellulose. *Cellulose* 5:19–32
- Dubief D, Samain E, Dufresne A (1999) Polysaccharide microcrystals reinforced amorphous poly(beta-hydroxyoctanoate) nanocomposite materials. *Macromolecules* 32:5765–5771
- Dufresne A (2000) Dynamic mechanical analysis of the interphase in bacterial polyester/cellulose whiskers natural composites. *Compos Interfaces* 7:53–67
- Dufresne A (2006) Comparing the mechanical properties of high performance polymer nanocomposites from biological sources. *J Nanosci Nanotechnol* 6:322–330
- Dufresne A, Vignon MR (1998) Improvement of starch film performances using cellulose microfibrils. *Macromolecules* 31:2693–2696
- Dufresne A, Cavaillé JY, Helbert W (1997) Thermoplastic nanocomposites filled with wheat straw cellulose whiskers. Part II: effect of processing and modeling. *Polym Compos* 18:199
- Dufresne A, Kellerhals MB, Witholt B (1999) Transcrystallization in Mcl-PHAs/cellulose whiskers composites. *Macromolecules* 32:7396–7401
- Dufresne A, Dupuyre D, Vignon MR (2000) Cellulose microfibrils from potato tuber cells: processing and characterization of starch–cellulose microfibril composites. *J Appl Polym Sci* 76:2080–2092
- Ebeling T, Paillet M, Borsali R et al (1999) Shear-induced orientation phenomena in suspensions of cellulose microcrystals, revealed by small angle X-ray scattering. *Langmuir* 15:6123–6126

- Elazzouzi-Hafraoui S, Nishiyama Y, Putaux J-L et al (2008) The shape and size distribution of crystalline nanoparticles prepared by acid hydrolysis of native cellulose. *Biomacromolecules* 9:57–65
- Eyholler C, Bordeanu N, Lopez-Suevos F et al (2010) Preparation and characterization of water-redispersible nanofibrillated cellulose in powder form. *Cellulose* 17:19–30
- Favier V, Canova GR, Cavaillé JY et al (1995a) Nanocomposite materials from latex and cellulose whiskers. *Polym Adv Technol* 6:351–355
- Favier V, Chanzy H, Cavaillé JY (1995b) Polymer nanocomposites reinforced by cellulose whiskers. *Macromolecules* 28:6365–6367
- Favier V, Canova GR, Shrivastavas C et al (1997a) Mechanical percolation in cellulose whisker nanocomposites. *Polym Eng Sci* 37:1732–1739
- Favier V, Dendievel R, Canova G et al (1997b) Simulation and modeling of three-dimensional percolating structures: case of a latex matrix reinforced by a network of cellulose fibers. *Acta Mater* 45:1557–1565
- Fengel D, Wegener G (1983) *Wood, chemistry, ultrastructure, reactions*. Walter de Gruyter, New York
- Fleming K, Gray DG, Prasanna S et al (2000) Cellulose nanocrystals: a new and robust liquid crystalline medium for the measurement of residual dipolar couplings. *J Am Chem Soc* 122:5224–5225
- Fukuzumi H, Saito T, Iwata T et al (2008) Transparent and high gas barrier films of cellulose nanofibers prepared by TEMPO-mediated oxidation. *Biomacromolecules* 10:162–165
- Garcia de Rodriguez NL, Thielemans W, Dufresne A (2006) Sisal cellulose whiskers reinforced polyvinyl acetate nanocomposites. *Cellulose* 13:261–270
- Goussé C, Chanzy H, Excoffier G et al (2002) Stable suspensions of partially silylated cellulose whiskers dispersed in organic solvents. *Polymer* 43:2645–2651
- Gray DG (2008) Transcrystallization of polypropylene at cellulose nanocrystal surfaces. *Cellulose* 15:297–301
- Greiner A, Wendorff JH (2007) Electrospinning: a fascinating method for the preparation of ultrathin fibers. *Angew Chem Int Ed* 46:5670–5703
- Grunnert M, Winter WT (2002) Nanocomposites of cellulose acetate butyrate reinforced with cellulose nanocrystals. *J Polym Environ* 10:27–30
- Habibi Y, Dufresne A (2008) Highly filled bionanocomposites from functionalized polysaccharide nanocrystals. *Biomacromolecules* 9:1974–1980
- Habibi Y, Chanzy H, Vignon MR (2006) TEMPO-mediated surface oxidation of cellulose whiskers. *Cellulose* 13:679–687
- Habibi Y, Foulon L, Aguié-Béghin V et al (2007) Langmuir–Blodgett films of cellulose nanocrystals: preparation and characterization. *J Colloid Interface Sci* 316:388–397
- Habibi Y, Goffin A-L, Schiltz N et al (2008) Bionanocomposites based on poly(ϵ -caprolactone)-grafted cellulose nanocrystals by ring opening polymerization. *J Mater Chem* 18:5002–5010
- Habibi Y, Mahrouz M, Vignon M (2009) Microfibrillated cellulose from the peel of prickly pear fruits. *Food Chem* 115:423–429
- Hajji P, Cavaillé JY, Favier V et al (1996) Tensile behavior of nanocomposites from latex and cellulose whiskers. *Polym Compos* 17:612–619
- Hanley SJ, Giasson J, Revol JF et al (1992) Atomic force microscopy of cellulose microfibrils – comparison with transmission electron-microscopy. *Polymer* 33:4639–4642
- Helbert W, Cavaillé JY, Dufresne A (1996a) Thermoplastic nanocomposites filled with wheat straw cellulose whiskers. Part I: Processing and mechanical behavior. *Polym Compos* 17:604–611
- Helbert W, Cavaillé JY, Dufresne A (1996b) Thermoplastic nanocomposites filled with wheat straw cellulose whiskers. Part I: processing and mechanical behavior. *Polym Compos* 17:604–611
- Henriksson M, Berglund LA (2007) Structure and properties of cellulose nanocomposite films containing melamine formaldehyde. *J Appl Polym Sci* 106:2817–2824

- Henriksson M, Henriksson G, Berglund LA et al (2007) An environmentally friendly method for enzyme-assisted preparation of microfibrillated cellulose (MFC) nanofibers. *Eur Polym J* 43:3434–3441
- Heux L, Chauve G, Bonini C (2000) Nonflocculating and chiral-nematic self-ordering of cellulose microcrystals suspensions in nonpolar solvents. *Langmuir* 16:8210–8212
- Huang ZM, Zhang YZ, Kotaki M et al (2003) A review on polymer nanofibers by electrospinning and their applications in nanocomposites. *Compos Sci Technol* 63:2223–2253
- Ifuku S, Nogi M, Abe K et al (2007) Surface modification of bacterial cellulose nanofibers for property enhancement of optically transparent composites: dependence on acetyl-group DS. *Biomacromolecules* 8:1973–1978
- Iwamoto S, Abe K, Yano H (2008) The effect of hemicelluloses on wood pulp nanofibrillation and nanofiber network characteristics. *Biomacromolecules* 9:1022–1026
- Iwamoto S, Kai W, Isogai A et al (2009) Elastic modulus of single cellulose microfibrils from tunicate measured by atomic force microscopy. *Biomacromolecules* 10:2571–2576
- Jean B, Dubreuil F, Heux L et al (2008) Structural details of cellulose nanocrystals/polyelectrolytes multilayers probed by neutron reflectivity and AFM. *Langmuir* 24:3452–3458
- Jean B, Heux L, Dubreuil F et al (2009) Non-electrostatic building of biomimetic cellulose–xyloglucan multilayers. *Langmuir* 25:3920–3923
- Kim UJ, Kuga S, Wada M et al (2000) Periodate oxidation of crystalline cellulose. *Biomacromolecules* 1:488–492
- Klemm D, Heublein B, Fink H-P et al (2005) Cellulose: fascinating biopolymer and sustainable raw material. *Angew Chem Int Ed* 44:3358–3393
- Kvien I, Tanem BS, Oksman K (2005) Characterization of cellulose whiskers and their nanocomposites by atomic force and electron microscopy. *Biomacromolecules* 6:3160–3165
- Kvien I, Sugiyama J, Votruba M et al (2007) Characterization of starch based nanocomposites. *J Mater Sci* 42:8163–8171
- Li R, Fei J, Cai Y et al (2009) Cellulose whiskers extracted from mulberry: a novel biomass production. *Carbohydr Polym* 76:94–99
- Li Z, Rennecker S, Barone JR (2010) Nanocomposites prepared by in situ enzymatic polymerization of phenol with TEMPO-oxidized nanocellulose. *Cellulose* 17:57–68
- Lin N, Chen G, Huang J et al (2009) Effects of polymer-grafted natural nanocrystals on the structure and mechanical properties of poly(lactic acid): a case of cellulose whisker-graft-polycaprolactone. *J Appl Polym Sci* 113:3417–3425
- Lindström T, Ankerfors M and Henriksson G (2007) Method for treating chemical pulp for manufacturing microfibrillated cellulose. WO Patent, STFI-Packforsk AB: p 14
- Ljungberg N, Bonini C, Bortolussi F et al (2005) New nanocomposite materials reinforced with cellulose whiskers in atactic polypropylene: effect of surface and dispersion characteristics. *Biomacromolecules* 6:2732–2739
- Ljungberg N, Cavaillé J-Y, Heux L (2006) Nanocomposites of isotactic polypropylene reinforced with rod-like cellulose whiskers. *Polymer* 47:6285–6292
- Lu Y, Weng L, Cao X (2005) Biocomposites of plasticized starch reinforced with cellulose crystallites from cottonseed linter. *Macromol Biosci* 5:1101–1107
- Lu J, Wang T, Drzal LT (2008) Preparation and properties of microfibrillated cellulose polyvinyl alcohol composite materials. *Compos Part A* 39A:738–746
- Magalhaes WLE, Cao X, Lucia LA (2009) Cellulose nanocrystals/cellulose core-in-shell nanocomposite assemblies. *Langmuir*. doi:10.1021/la901928j
- Malainine ME, Mahrouz M, Dufresne A (2005) Thermoplastic nanocomposites based on cellulose microfibrils from *Opuntia ficus-indica* parenchyma cell. *Compos Sci Technol* 65:1520–1526
- Marchessault RH, Sundararajan PR (1983) Cellulose. In: Aspinall GO (ed) *The polysaccharides*. Academic, New York
- Marchessault RH, Morehead FF, Koch MJ (1961) Hydrodynamic properties of neutral suspensions of cellulose crystallites as related to size and shape. *J Colloid Sci* 16:327–344

- Marcovich NE, Auad ML, Bellesi NE et al (2006) Cellulose micro/nanocrystals reinforced polyurethane. *J Mater Res* 21:870–881
- Mathew AP, Dufresne A (2002) Morphological investigation of nanocomposites from sorbitol plasticized starch and tunicin whiskers. *Biomacromolecules* 3:609–617
- Mathew AP, Thielemans W, Dufresne A (2008) Mechanical properties of nanocomposites from sorbitol plasticized starch and tunicin whiskers. *J Appl Polym Sci* 109:4065–4074
- Matos Ruiz M, Cavaillé JY, Dufresne A et al (2001) New waterborne epoxy coatings based on cellulose nanofillers. *Macromol Symp* 169:211–222
- Medeiros ES, Mattoso LHC, Ito EN et al (2008) Electrospun nanofibers of poly(vinyl alcohol) reinforced with cellulose nanofibrils. *J Biobased Mater Bioenergy* 2:1–12
- Nakagaito AN, Yano H (2004) The effect of morphological changes from pulp fiber towards nano-scale fibrillated cellulose on the mechanical properties of high-strength plant fiber based composites. *Appl Phys A Mater Sci Process* 78:547–552
- Nakagaito AN, Yano H (2008) Toughness enhancement of cellulose nanocomposites by alkali treatment of the reinforcing cellulose nanofibers. *Cellulose* 15:323–331
- Nakagaito AN, Iwamoto S, Yano H (2004) Bacterial cellulose: the ultimate nano-scalar cellulose morphology for the production of high-strength composites. *Appl Phys A Mater Sci Process* 80:93–97
- Nogi M, Handa K, Nakagaito AN, Yano H (2005) Optically transparent bionanofiber composites with low sensitivity to refractive index of the polymer matrix. *Appl Phys Lett* 87:243110–243112
- Nogi M, Abe K, Handa K et al (2006a) Property enhancement of optically transparent bionanofiber composites by acetylation. *Appl Phys Lett* 89:233123/233121–233123/233123
- Nogi M, Ifuku S, Abe K et al (2006b) Fiber-content dependency of the optical transparency and thermal expansion of bacterial nanofiber reinforced composites. *Appl Phys Lett* 88:133124/133121–133124/133123
- Noishiki Y, Nishiyama Y, Wada M et al (2002) Mechanical properties of silk fibroin-microcrystalline cellulose composite films. *J Appl Polym Sci* 86:3425–3429
- O’Sullivan AC (1997) Cellulose: the structure slowly unravels. *Cellulose* 4:173–207
- Oksman K, Mathew AP, Bondeson D et al (2006) Manufacturing process of cellulose whiskers/poly(lactic acid) nanocomposites. *Compos Sci Technol* 66:2776–2784
- Orts WJ, Godbout L, Marchessault RH et al (1998) Enhanced ordering of liquid crystalline suspensions of cellulose microfibrils: a small-angle neutron scattering study. *Macromolecules* 31:5717–5725
- Orts WJ, Shey J, Imam SH et al (2005) Application of cellulose microfibrils in polymer nanocomposites. *J Polym Environ* 13:301–306
- Pääkkö M, Ankerfors M, Kosonen H et al (2007) Enzymatic hydrolysis combined with mechanical shearing and high-pressure homogenization for nanoscale cellulose fibrils and strong gels. *Biomacromolecules* 8:1934–1941
- Paralakar SA, Simonsen J, Lombardi J (2008) Poly(vinyl alcohol)/cellulose nanocrystal barrier membranes. *J Membr Sci* 320:248–258
- Park W-I, Kang M, Kim H-S et al (2007) Electrospinning of poly(ethylene oxide) with bacterial cellulose whiskers. *Macromol Symp* 249(250):289–294
- Payen A (1838) Mémoire sur la composition du tissu propre des plantes et du ligneux. *C R Hebd Seances Acad Sci* 7:1052–1056
- Peresin MS, Habibi Y, Zoppe JO et al (2010) Nanofiber composites of polyvinyl alcohol and cellulose nanocrystals: manufacture and characterization. *Biomacromolecules* 11:674–681
- Petersson L, Oksman K (2006) Biopolymer based nanocomposites: comparing layered silicates and microcrystalline cellulose as nanoreinforcement. *Compos Sci Technol* 66:2187–2196
- Podsiadlo P, Choi S-Y, Shim B et al (2005) Molecularly engineered nanocomposites: layer-by-layer assembly of cellulose nanocrystals. *Biomacromolecules* 6:2914–2918

- Revol JF (1982) On the cross-sectional shape of cellulose crystallites in *Valonia ventricosa*. *Carbohydr Polym* 2:123–134
- Revol JF, Bradford H, Giasson J et al (1992) Helicoidal self-ordering of cellulose microfibrils in aqueous suspension. *Int J Biol Macromol* 14:170–172
- Revol JF, Godbout L, Dong XM et al (1994) Chiral nematic suspensions of cellulose crystallites; phase separation and magnetic field orientation. *Liq Cryst* 16:127–134
- Rojas OJ, Montero GA, Habibi Y (2009) Electrospun nanocomposites from polystyrene loaded with cellulose nanowhiskers. *J Appl Polym Sci* 113:927–935
- Roman M, Winter WT (2004) Effect of sulfate groups from sulfuric acid hydrolysis on the thermal degradation behavior of bacterial cellulose. *Biomacromolecules* 5:1671–1677
- Roohani M, Habibi Y, Belgacem NM et al (2008) Cellulose whiskers reinforced polyvinyl alcohol copolymers nanocomposites. *Eur Polym J* 44:2489–2498
- Saito T, Nishiyama Y, Putaux J et al (2006) Homogeneous suspensions of individualized microfibrils from TEMPO-catalyzed oxidation of native cellulose. *Biomacromolecules* 7:1687–1691
- Saito T, Kimura S, Nishiyama Y et al (2007) Cellulose nanofibers prepared by TEMPO-mediated oxidation of native cellulose. *Biomacromolecules* 8:2485–2491
- Sakurada I, Nukushina Y, Ito T (1962) Experimental determination of the elastic modulus of crystalline regions oriented polymers. *J Polym Sci* 57:651–660
- Shimazaki Y, Miyazaki Y, Takezawa Y, Nogi M, Abe K, Ifuku S, Yano H (2007) Excellent thermal conductivity of transparent cellulose nanofiber/epoxy resin nanocomposites. *Biomacromolecules* 8:2976–2978
- Seydibeyoğlu ÖM, Oksman K (2008) Novel nanocomposites based on polyurethane and micro fibrillated cellulose. *Compos Sci Technol* 68:908–914
- Siqueira G, Bras J, Dufresne A (2009) Cellulose whiskers versus microfibrils: influence of the nature of the nanoparticle and its surface functionalization on the thermal and mechanical properties of nanocomposites. *Biomacromolecules* 10:425–432
- Siqueira G, Abdillahi H, Bras J et al (2010a) High reinforcing capability cellulose nanocrystals extracted from *Syngonanthus nitens* (Capim Dourado). *Cellulose* 17:289–298
- Siqueira G, Bras J, Dufresne A (2010b) New process of chemical grafting of cellulose nanoparticles with a long chain isocyanate. *Langmuir* 26:402–411
- Siqueira G, Bras J, Dufresne A (2010c) *Luffa cylindrica* as a lignocellulosic source of fiber, microfibrillated cellulose and cellulose nanocrystals. *BioResources* 5:0727–0740
- Sjöström E (1981) Wood chemistry: fundamentals and applications. Academic, New York
- Spence K, Venditti RA, Rojas OJ et al (2010) The effect of chemical composition on microfibrillar cellulose films from wood pulps: water interactions and physical properties for packaging applications. *Cellulose* 17:835–848
- Spence K, Venditti RA, Rojas OJ et al (2011) A comparative study of energy consumption and physical properties of microfibrillated cellulose produced by different processing methods. Submitted Cellulose
- Stenstad P, Andresen M, Tanem BS et al (2008) Chemical surface modifications of microfibrillated cellulose. *Cellulose* 15:35–45
- Šturcova A, Davies GR, Eichhorn SJ (2005) Elastic modulus and stress-transfer properties of tunicate cellulose whiskers. *Biomacromolecules* 6:1055–1061
- Svagan AJ, Hedenqvist MS, Berglund L (2009) Reduced water vapour sorption in cellulose nanocomposites with starch matrix. *Compos Sci Technol* 69:500–506
- Syverud K, Stenius P (2009) Strength and barrier properties of MFC films. *Cellulose* 16:75–85
- Tashiro K, Kobayashi M (1991) Theoretical evaluation of three-dimensional elastic constants of native and regenerated celluloses: role of hydrogen bonds. *Polymer* 32:1516–1526
- Tokoh C, Takabe K, Fujita M et al (1998) Cellulose synthesized by acetobacter xylinum in the presence of acetyl glucomannan. *Cellulose* 5:249–261
- Turbak A, Snyder F, Sandberg K (1983) Microfibrillated cellulose: a new cellulose product: properties, uses, and commercial potential. *J Appl Polym Sci: Appl Polym Symp* 37:815–827

- van den Berg O, Capadona JR, Weder C (2007) Preparation of homogeneous dispersions of tunicate cellulose whiskers in organic solvents. *Biomacromolecules* 8:1353–1357
- Wågberg L, Decher G, Norgren M et al (2008) The build-up of polyelectrolyte multilayers of microfibrillated cellulose and cationic polyelectrolytes. *Langmuir* 24:784–795
- Wang Y, Cao X, Zhang L (2006) Effects of cellulose whiskers on properties of soy protein thermoplastics. *Macromol Biosci* 6:524–531
- Wang B, Sain M, Oksman K (2007) Study of structural morphology of hemp fiber from the micro to the nanoscale. *Appl Compos Mater* 14:89–103
- Whistler RL, Richards EL (1970) *The Carbohydrates*. Academic, New York
- Woodcock C, Sarko A (1980) Packing analysis of carbohydrates and polysaccharides. 11. Molecular and crystal structure of native ramie cellulose. *Macromolecules* 13:1183–1187
- Yano H, Sugiyama J, Nakagaito AN, Nogi M, Matsuura T, Hikita M, Handa K (2005) Optically transparent composites reinforced with networks of bacterial nanofibers. *Adv Mat* 17:153–155
- Yuan H, Nishiyama Y, Wada M et al (2006) Surface acylation of cellulose whiskers by drying aqueous emulsion. *Biomacromolecules* 7:696–700
- Zimmerman T, Poehler E, Geiger T (2004a) Cellulose fibrils for polymer reinforcement. *Adv Eng Mater* 6:754–761
- Zimmerman T, Pöhler E, Geiger T (2004b) Cellulose fibrils for polymer reinforcement. *Adv Eng Mater* 6:754–761
- Zimmermann T, Pöhler E, Schwaller P (2005) Mechanical and morphological properties of cellulose fibril reinforced nanocomposites. *Adv Eng Mater* 7:1156–1161
- Zoppe JO, Peresin MS, Habibi Y et al (2009) Reinforcing poly(ϵ -caprolactone) nanofibers with cellulose nanocrystals. *ACS Appl Mater Interfaces* 1:1996–2004

Chapter 8

Dimensional Analysis and Surface Morphology as Selective Criteria of Lignocellulosic Fibers as Reinforcement in Polymeric Matrices

Kestur Gundappa Satyanarayana, Sergio Neves Monteiro, Felipe Perisse Duarte Lopes, Frederico Muylaert Margem, Helvio Pessanha Guimaraes Santafe Jr., and Lucas L. da Costa

Abstract In recent years, there has been a resurgence of interest for the use of renewable materials such as plant fibers, also called “lignocellulosic fibers”, due to increasing environmental concerns along with the unique characteristics of these fibers. These include abundant availability, renewability, biodegradability, as well as low wear and tear of equipments, particularly when processing their composites. In comparison with today’s most used synthetic fibers such as glass fiber, lignocellulosic fibers offer the advantage of lesser health hazards and of course lower cost. In addition, they help in generating employment, particularly in rural sector, by leading to better living standards of the rural population. Thus, the utilization of these fibers has both short-term objectives, through the synthesis and characterization of composites, and long-term objectives, to use them as alternates for synthetic fibers and possible substitute for wood. This has driven the researchers to bring out data on the source and availability of all the useful lignocellulosic fibers, cataloging their available information on morphology and properties as well as current uses. A sound knowledge of the morphology of these fibers helps the understanding of their observed properties in terms of structural parameters, such as number, size, and shape of cells, chemical constituents, as well as the fracture mechanism in these fibers. Further, a careful examination of various properties of these fibers indicates that they are inconsistent probably due to the nonuniformity in dimensions and the defects in these fibers. The latter may be present either inherently or due to their processing. As a consequence, highly scattered properties are observed, which may be one of the drawbacks for their use as engineering materials. These limitations could, in principle, be overcome through an individual selection of fibers with approximately the

K.G. Satyanarayana (✉)

Laboratory for Advanced Materials, LAMAV, State University of the Northern Rio de Janeiro, UENF, Av. Alberto Lamego 2000, Horto, Campos dos Goytacazes, Rio de Janeiro, Brazil

and UFPR, Curitiba, Paraná, Brazil

and

Acharya Institutes, BMS College of Engineering and Poornaprajna Institute of Scientific Research, Bangalore, India

e-mail: kgs_satya@yahoo.co.in

same dimensions and properties by knowing the nature of correlation of fiber dimensions with a given property whereby the strongest fibers based on selection of their diameters could be separated. However, this may pose some problem with tedious work. Development of a scientific methodology does become essential to the selection of these fibers particularly for their application as reinforcements in various matrices to render them reliable, similar to synthetic fiber products.

This chapter presents such a methodology involving some of the Brazilian fibers through statistical evaluation with the aim to select fibers of highest possible strength and to explain the strengthening mechanism responsible for the superior performance of these dimensionally selected fibers. Concluding remarks and suggestions are given at the end, indicating some future direction of work with a view to motivate the readers and researchers to explore the future potentials of these natural resources with proper selection of lignocellulosic fibers to develop new uses including composites for these fibers. In addition, this may help different industrial sectors, which are already using these fibers or may use them in the future.

Keywords Fractography · Morphology and properties · Plant fibers · Statistical evaluation · Weibull analysis

Contents

8.1	Introduction	216
8.1.1	Classification, Extraction, Availability, Morphology, and Properties of Lignocellulosic Fibers	218
8.2	Methodologies Used Including Weibull Analysis for Understanding and Explaining the Problem	222
8.2.1	Weibull Analysis	224
8.2.2	Artificial Neural Network Analysis	226
8.3	Discussions of Observations	227
8.3.1	Previous Studies	227
8.3.2	Recent Work by Authors	232
8.4	Concluding Remarks	236
8.5	Suggestions for Future Work	236
	References	237

8.1 Introduction

The world is looking towards the safety of the environment, taking into account the upsurge in the development of new materials underlying the need for improved performance and low cost. One of the methods suggested is utilization of renewable materials and work with these towards “no waste” concept [1]. This is more evident in composite materials, which have established themselves as more attractive materials having applications in both strategic and societal sectors. These materials consist of polymer or ceramic as matrix materials and synthetic or natural fibers as reinforcements or fillers. Natural fibers of vegetable origin are referred to as “plant fibers”, “vegetable fibers”, or “lignocellulosic fibers.” Some of these fibers are shown in Fig. 8.1.

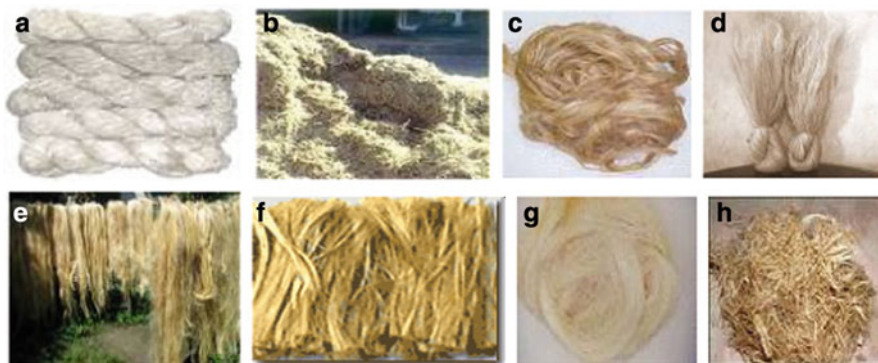


Fig. 8.1 Photographs of some lignocellulosic fibers (a) Banana; (b) Sugarcane Bagasse; (c) Curauá; (d) Flax; (e) Hemp; (f) Jute; (g) Sisal; (h) Kenaf

Since 1990 s, there is a growing interest in natural fibers, particularly in western countries, for the following reasons: (1) these fibers can replace the dwindling and expensive chemical-based feed stocks, (2) increasing quest for new materials, which support global sustainability, (3) intentional relook at agricultural industry through diversification of nonnutrient areas addressing global environment and stable economy, and the last, though not the least, (4) successful use of their composites in automotive, construction, and various engineering applications. In fact, the primary production of plant fibers was estimated at 2×10^{11} tons in 2000 compared to 1.5×10^8 tons of synthetic polymers [2, 3], while the estimated fibrous raw materials from agricultural crops is about 2.5×10^9 tons [4]. Further, these fibers are showing a steadily growing market. For example, the projection for North America is expected to grow from US\$ 155 million in 2000 to US\$ 1.38 billion by 2025 [1]. In addition, the availability of these fibers may lead not only to the production of consumer products with high durability that can be more easily recycled but also to the sustainable development underlying the importance of economic and technological aspects of lignocellulosic fibers [5].

Other characteristic and attractive features of natural fibers, besides the above-mentioned facts, include producing light weight materials of comparable specific properties with those of synthetic fibers due to their low density and the lower production cost as compared to the man-made synthetic fibers as well as their biodegradability contributing to a healthy ecosystem. Other attractive features with lignocellulosic fibers include renewable character and hence continued availability of these fibers, lack of any health hazards, good accoustical electrical and heat insulation properties, as well as lower abrasion and the advantage of providing a new source of income to the farmers.

These fibers also contribute significantly to the world economy not only through their accepted conventional usage in various sectors but also in new applications such as reinforcements in polymer/ceramic matrices. It is reported by many researchers [6–13] in the area of natural fiber–polymer composites that the possible substitutions of automotive parts is of particular interest. In fact, these composites favor the recycling of parts in addition to their low density and the consumption

along with reduction of emission of exhaust gasses. It is to be noted that the low cost of lignocellulosic fibers and their reasonable performance in new materials, such as composites, may raise economic interest in various industries. In view of these considerations, they also provide appropriate employment opportunities to both rural and urban populations. Thus, lignocellulosic fibers are gaining attention over synthetic fibers as reinforcement of polymer matrix composites owing to environmental, economical, societal, and technical advantages. However, one of the unsolved problems limiting the use of natural fibers is the high dispersion of the fibers' properties.

In view of the above, fiber characterization becomes important if the user industries define suitable quality aspects to obtain standardized quality products, as suggested by the European Commission on these fibers [14]. Towards this end, when a careful examination of various properties of these fibers is made, they are found to be inconsistent. This is probably due to the nonuniformity in dimensions of these fibers and their defects. The latter may be present either inherently or due to their processing. As a consequence, highly scattered properties are observed, which may be one of the drawbacks for their use as engineering materials. These limitations could, in principle, be overcome through an individual selection of fibers with approximately the same dimensions and properties. For this purpose, it is important to know the correlation of fiber dimensions with a given property. For example, if a correlation exists between the fiber diameter and its strength, then one could separate the strongest fibers based on selection of their diameters. Since this may pose some problem with tedious work, development of a scientific methodology becomes essential to the selection of these fibers, particularly for their application as reinforcements in various matrix materials to render them reliable, similar to synthetic fiber products. In fact, the well-known characteristic of natural fibers, viz. wide dispersion of fiber properties, has been analyzed by means of various methods including Weibull analysis [15–18] and a new advanced statistical approach based on neural network algorithms [19], which can provide a more accurate prediction of the behavior of lignocellulosic fibers. Furthermore, it is also mentioned by Peponi et al. [19] that while Griffith's theory is applied to understand the obtained (scatter) tensile strength of fibers and that thinner fibers contain strength-reducing defects (flaws) in small amount, Young's modulus may also follow a similar trend (inverse relation) with fiber diameter [20].

8.1.1 Classification, Extraction, Availability, Morphology, and Properties of Lignocellulosic Fibers

Since “defects”, both inherent (due to dimensional changes within the same fiber and among the fibers) and arising out of processing (extraction) of fibers, exist in lignocellulosic fibers, some discussions on the extraction, structure, and properties of lignocellulosic fibers will be made here. Readers are recommended to check

[1, 21–25] for more details on the above aspects as such details are outside the scope of this chapter. However, brief mention of these aspects is given below for the sake of continuity.

It is well known that the resources for lignocellulosic fibers are available in all parts of the world, with some of these being common to many countries, while others are specific to some countries only. For example, fibers such as banana, coconut, jute, pineapple, sugarcane bagasse, sisal, etc., are common to many countries. By contrast, fibers such as curaua, sponge gourde, malva, piassava, and buriti are specific to some South American countries such as Brazil. All the lignocellulosic fibers can be classified into main groups based on the parts from which they are extracted. Thus, banana, jute, ramie, sugarcane bagasse, etc., are called bast/bark/stem fibers; curaua, pineapple, sisal, etc., are called leaf fibers; coconut fiber (coir), cotton, kopak, etc., are called fruit/seed fibers. As a consequence, extraction methods for these fibers depend on the type of resource. Both manual and machine (“decorticators”) are used for this purpose. In the manual methods, an example is “retting”, wherein green pieces are kept under water for a few days and then fibers are extracted by beating the stems or husks as in the case of coir/jute/malva. Sometimes, even the leaf sheaths are scraped by knife and the fibers are extracted as in the case of banana and buriti fibers. On the other hand, fibers such as curaua, flax, pineapple, sisal, etc., are obtained using suitable machines. It is also known that manual method is time consuming, but good quality fibers are produced as in the case of Indian coir fibers [21]. Fibers produced by both methods always possess surface defects.

Morphological studies of various lignocellulosic fibers have shown that each fiber consists of a number of cells associated with filaments called ‘cellulose microfibrils’. These cells are arranged in a particular fashion depending on the type of fiber in a matrix consisting of lignin. There also exists a central hole called “lacuna” in each fiber to induct water and nutrients. Each cell in turn has a different size and shape arranged in some fashion with a central hole called “lumen.” Further, the structure of each type of fiber is different in the shape, size, and arrangements of cells and lacuna/lumen as well as the thickness of cell walls. These are illustrated in Fig. 8.2 for some of the fibers.

It is important to mention that the chemical composition of each type of fibers and the orientation of microfibrils about the fiber axis, called “microfibrillar angle” (Table 8.1), may significantly differ. Similarly, depending on the cellulose and lignin contents, crystallinity index of each type of fiber differs. In view of these, when lignocellulosic fibers are tested for their tensile properties, their fracture mode differs, which may be intercellular or intracellular or mixed modes of fracture. Accordingly, the tensile properties and fractographs are different for each type of fiber. These are also listed for some fibers in Table 8.1 and Fig. 8.3, respectively.

Taking the above facts into consideration, this chapter discusses methodologies to understand the observed scatter in tensile strength in natural fibers, particularly the lignocellulosic ones. While doing so, a methodology is presented to select fibers of highest possible strength and to explain the strengthening mechanism responsible for the superior performance of these dimensionally selected fibers, particularly

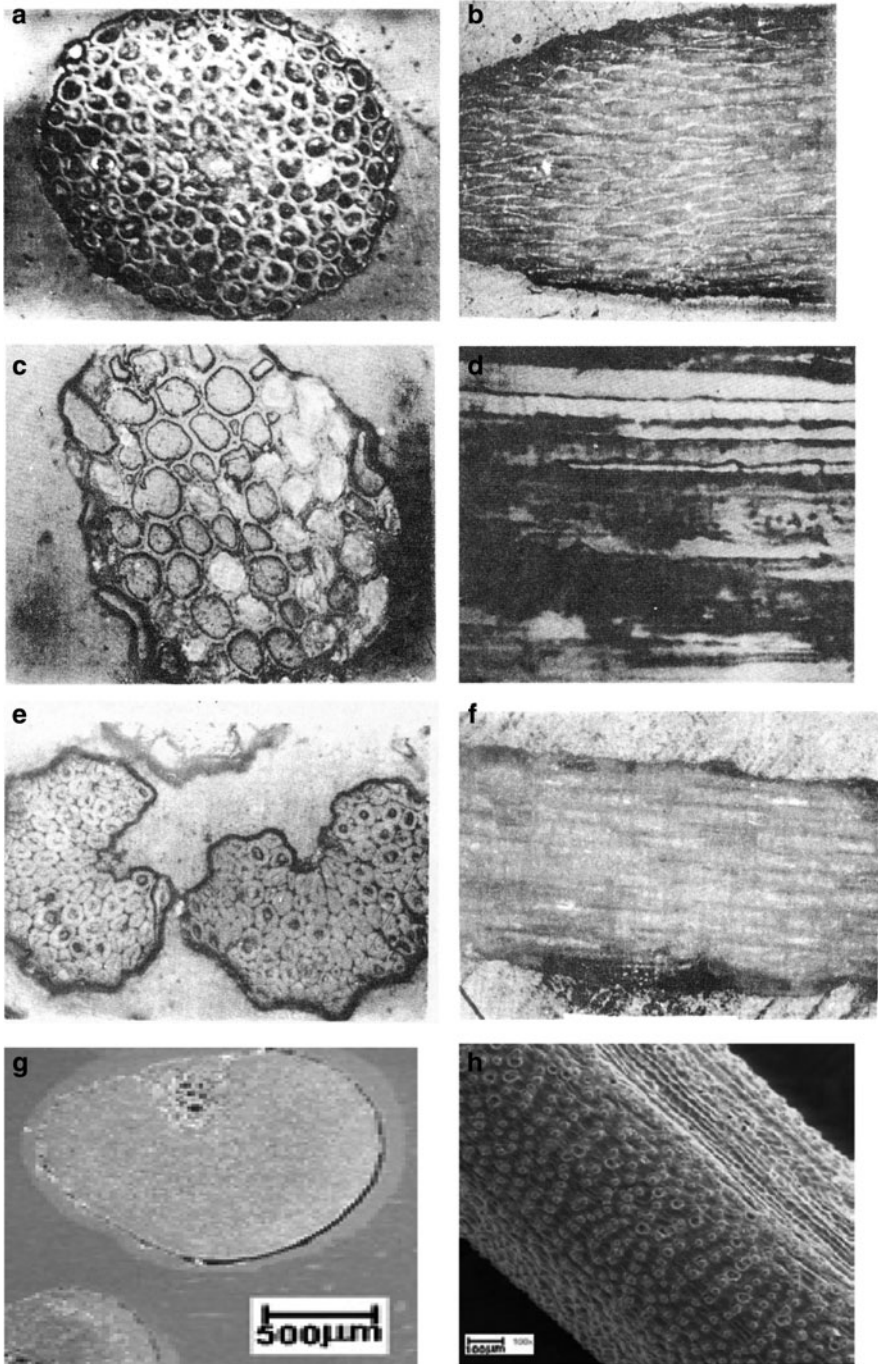


Fig. 8.2 Photomicrographs of longitudinal and cross sections of various lignocellulosic fibers (a and b) Coir; (c and d) Banana; (e and f) Sisal; (g and h) piassava (Adopted from [1, 21, 25])

Table 8.1 Physical/chemical and tensile properties of some lignocellulosic fibers used for biocomposites (Adopted from [1, 21, 25])

Fiber	Dimensions L (mm)/ D (μ m)	α -Cellulose (%)	Lignin (%)	Young's modulus (GPa)	Ultimate tensile strength (MPa)	Elongation at break (%)	Microfibrillar angle θ
Sugarcane bagasse	10–300/10–34	32–44	19–24	17.9 ^a –27.1	222	1.1	14–15
Banana	300–900/12–30	60–65	5–10	27–32	700–800	2.5–3.7	10–12
Jute	120/25–30	59–71	11.8–12.9	10–30	400–800	1.5–1.8	17.1
Ramie	900–1,200/20–80	80–85	0.5	44	500–870	1.2	7.2–12
Flax	750–900/50–150	62–72	2–5	60–80	780–1,500	1.2–2.4	10
Pineapple	900–1,500	80–83	12–	82	180	3.2	8–15
Curauá Wet	35/7–10	70.7–73.6	7.5–11.1	30–80 ^b	1,250–3,000 ^b	4.5–6 ^b	18.8
Curauá Dry				10.5	439–495 (MOR) ^c	1.3	
				27.1	117 (MOR) ^c /495	1.3–3.2	
				34–96 ^d	87–310 ^d	4–4.9 ^d	
Sisal	900/8–50	60–67	8–12	17–22	530–630	3.64–5.12	10–20
Cotton	35/10–45	90	<2	12	400		33–34
Coir	20–150/10–50	43.77	45	6	220	23.9–51.4	30–51
Lufia-cylíndrica – Brazil	25–60 (Diameter)	62	11.2	–	–	–	

^aCalculated^bDiameter: 30–60 μ m; Test length: 20 mm and Strain rate: 5 mm/min^cMOR: Modulus of rupture^dDiameter range 26–64 μ m

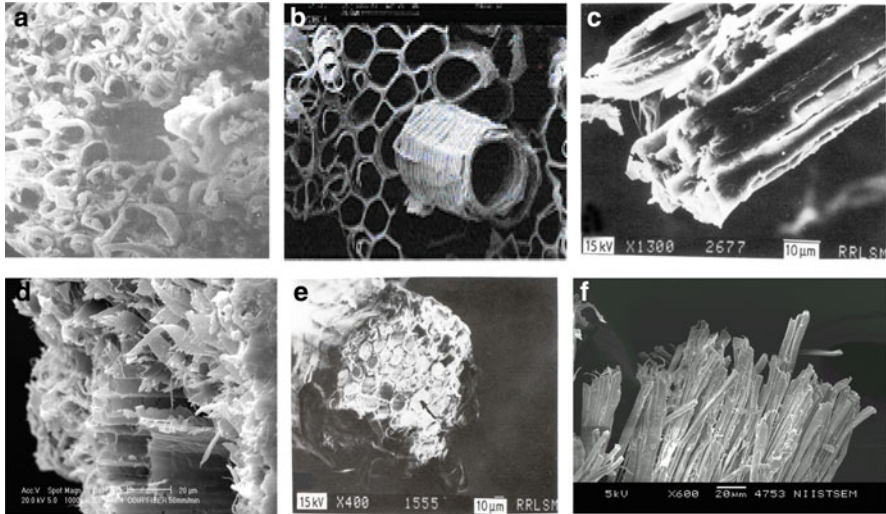


Fig. 8.3 Fractographs of some lignocellulosic fibers (a) Coir; (b) Coir fiber showing the helical spiral structure; (c) Pineapple; (d) Curaua; (e) Sisal; (f) American agave leaf (*Aechmea magdalenae*) fiber [a–e: Adopted from [1, 26, 29]]

with some of the Brazilian fibers through statistical evaluation. Concluding remarks and suggestions are given at the end, indicating some future direction of work with a view to motivate the readers and researchers to explore the potentials of these natural resources with proper selection of lignocellulosic fibers to develop new uses including composites reinforced with these fibers. In addition, this may help different industrial sectors that are already using these fibers or may use them in the future.

8.2 Methodologies Used Including Weibull Analysis for Understanding and Explaining the Problem

Quality of various types of materials, particularly of fibers, for their use in various applications is checked by their mechanical properties, which may also throw light on the “defects” in the fibers. It is well known now that many factors such as morphological structure, fiber dimensions, and its fracture mechanism contribute to the tensile behavior of the fiber. Whether the fiber is of synthetic or natural origin, the “defects” are supposed to be responsible for the large scatter in their properties. In both these type of fibers, there will be inherent defects related to internal structure–morphological factor. Moreover, one should also expect the existence of defects caused by the processing/extraction process, mainly in the case of natural fibers, which may be distributed nonuniformly and difficult to quantify. These are

termed as “weak links.” The inherent defects may be small, caused by the drastic change in the fiber cross section, or large, owing to changes in the sequence of cell growth, since the orientation of each cell varies with the fiber axis [15, 27]. In addition, variations exist in the diameter between fibers as well as within the same fiber, particularly the latter in natural fibers. Thus, there exist “weak links” in fibers due to internal structure, associated with morphological factors, or due to dimensional variations or a combination of both. It is also possible that the defects may decrease with increasing length of the fibers tested, whose number depends on both length and diameter, leading to the variation in fiber strength.

Limited studies have been reported on the evaluation of strength properties of some Brazilian fibers as function of fiber dimensions by selecting appropriate fibers for each evaluation [26, 28, 29]. When such fibers are subjected to tensile load, they may break at the “weak link”. In view of this, a considerable number of measurements have to be made with respect to the actual individual dimensions to account for the large scatter and so permitting a meaningful estimate of the fiber strength. In fact, breaking of fibers at “weak links” has been observed in the case of wool fibers where the diameter, due to dimensional variation, was minimum [30]. This concept of “weak link” proposed first by Pierce [31] in predicting the observed variation in strength in cotton fibers has been used to explain the strength variations in all types of fibers including geometrically uniform fibers such as synthetic or “classical” fibers [32–38], polymeric fibers including polyester yarns, and natural fibers such as coir and sisal [15–18]. In fact, it is necessary to use such an analysis for natural fibers since these fibers show greater scatter of properties than the synthetic ones. This has always been a drawback for their use as engineering materials, although some reliable data regarding these fibers became available in recent times [21]. In such cases, only the mean values are reported, and the nature of the variation in the tensile strength is disregarded. For example, when this is followed in the case of sisal fiber, its tensile strength was found to vary from 280 to 700 MPa with or without giving any standard deviation of the sampling. This range is considered too large [18], indicating that this simplified analysis is unable to fully characterize the fiber strength.

Accordingly, it has been proposed that both synthetic fibers [39–41] and some natural fibers [15–18] be characterized by strength–length correlations based on the Weibull type statistical analysis [42], using a linear equation correlating the test length, L , and the tensile strength, σ , of the fiber given by equation:

$$\sigma = mL \times L + \sigma_{L0} \quad (8.1)$$

where mL is the usually negative slope of the σ versus L plot [34]. Thus, one can determine the variations in tensile strength at varying test lengths and diameters of the fibers.

It was found that such an analysis not only revealed the “defects–strength” relationship but also helped in predicting the fiber strengths at very short lengths when there was no possibility to obtain them experimentally. Additionally, the analysis contributes to determine the flaw size distributions [15]. Further, using the

above method, the density of defects reported for pineapple fiber, coir, sisal, and banana fibers is about 4,461, 2,320, 2,368, and 1,376, respectively [43–47].

Knowing that Weibull distribution is a useful tool to explain the strength variation of fibers, attempts have been made to derive Weibull-weak link strength distribution of many independent unit links in fibers. This was based on the fact that the Weibull distribution is the most natural acceptable theory to interpret the fiber breaking event [48]. While the strength variations in synthetic fibers are considered as due to randomly distributed flaws and defects, they may also be caused by variations in diameter or combination of both. Following this, a number of researchers have investigated the correlations between the dimensions of lignocellulosic fibers and the mechanical properties [15, 49–54]. The fibers investigated include coir [15, 27], banana [49], sisal [16–18, 43], pineapple [47], palmyrah and talipot fibers [51], and wool fibers [52]. The two methodologies used in these investigations were (1) Weibull analysis and (2) artificial neural network, and both of them are based on statistical methods. In the case of Weibull analysis, two possibilities are available. The first one is a two-parameter analysis with simple numerical calculations, and the second is a three-parameter analysis, requiring laborious computer analysis. In the following sections, these methodologies will be discussed.

8.2.1 Weibull Analysis

This method is useful in a variety of applications, particularly as a model for the life of a product. For example, recently, this method is applied to arrive at the combination of service stress states and a requisite probability of survival for an Ingersoll-Rand microturbine rotor to determine Weibull distribution parameters for an arbitrary Si_3N_4 material [53]. Pairs of parameters (the Weibull modulus and the Weibull material characteristic strength) were plotted as “material performance curves”, which were then scaled to standard test coupons. Thus, a methodology was established for generating material performance curves/surfaces for any given component geometry – stress state combination by determining curves for standard test specimen geometries.

Weibull [42] proposed a failure statistics of a uniformly stressed fiber sample of length L of constant diameter. He represented this by an empirical equation associated with a unimodal distribution.

$$P = \exp\{-L(\sigma_f/\sigma_o)^m\} \quad (8.2)$$

where P is the probability of a survival at an applied stress of σ_f , σ_o is the normalizing stress at which $P = 0.368$, and “ m ”, called “Weibull parameter or modulus”, is regarded as the flaw frequency distribution factor. By suitably rewriting the above equation in logarithmic terms, one can plot $1/P$ versus σ_f . In this way,

a straight line is obtained for the experimental data for any specimen of length L , when the Weibull distribution is applicable. Further, for a fiber of constant diameter, but for another length L_1 , σ_f can be calculated by

$$\sigma_f = \sigma_1(L/L_1)^{-1/m} \quad (8.3)$$

where σ_f and σ_1 are the fiber strengths at gauge length L and gauge length L_1 , respectively.

It is a well known fact that the mechanical strength, particularly the tensile strength, of materials such as fibers, synthetic or natural, depends on their sizes and hence they follow a Weibull distribution. Slope and intercept on the x -axis of this straight line would then give the values of “ m ” and “ σ_o ”, respectively. In this unimodal distribution, m is also related to the coefficient of variation (CV), and therefore, one can obtain the values of m in two methods and compare them to understand the adequacy of the number of samples tested. For example, more scatter in the log plots of $1/P$ versus σ_f suggests that more number of samples should be tested. Furthermore, value of m will be the same for all gauge lengths in a homogeneous material, such as synthetic fibers, while the mean strength increases as the length of the fiber decreases. If the experimental values fall on a straight line, which distinctly changes the slope at any length, eventually becoming horizontal, one can infer that strength distributions in that fiber may not be characterized by identical unimodal Weibull distribution. In addition, histograms obtained from the plots of fiber strength versus gauge length for a number of samples suggest that different types of Weibull distribution appear at different gauge lengths [42]. In fact, increase in mean strength with decreasing test lengths has been reported in synthetic fibers as well as in natural fibers such as coir and jute [15, 27, 38, 54]. Some of these studies have shown (1) satisfactory application of unimodal Weibull distribution for scattered strength values at any length or diameter, (2) differing Weibull parameters obtained from such scattered strength values at different lengths, indicating a change in flaw distribution with the length of the tested fiber, and (3) close agreement of m values obtained from the Weibull plots and those from CV, suggesting a unimodal Weibull distribution of strengths [15].

When discrepancies between the strength predicted by the conventional Weibull model and the experimentally obtained data occur, then multimodal Weibull distributions have been used [18, 37]. Similarly, as mentioned earlier, the Weibull/weakest-link model can be utilized to predict the scale effect by combining the classical Weibull distribution with the “weakest link” theory. All these take into account the shape and scale of the distribution. Such models are reported to have shown improved accuracy of prediction including those for wool fibers [38].

It is reported that even equations, such as (8.3), showed greater deviation from the actual measured value when the gauge length effect was studied. Therefore, Weibull model was further modified [38] to include the effect of variation in

diameter among fibers as well as within the same fiber. In this case, the modified equation is:

$$P = 1 - \exp\left\{(-L/L_0)^\beta (\sigma_f/\sigma_o)^m\right\} \quad (8.4)$$

where L is the gauge length, L_0 is the length of the unit link of the fiber, and β is a parameter ($0 < \beta < 1$) to represent the diameter variations.

Thus, in recent years, (8.1) and (8.4) are being used for both uniformly brittle materials as well as polymeric fibers [38]. For instance, (8.4) for Weibull/weakest-link model was verified for wool fibers [38].

8.2.2 Artificial Neural Network Analysis

This method can be considered as an extension of the statistical approach to develop a comparative study of the behavior of different natural fibers. In this method, the density function of a quasi-stationary random process is estimated by means of an adaptive activation function neuron (FAN) endowed with a specific unsupervised learning theory with algorithms based on a neural network. The learning parameters could be chosen by carrying out several simulations. Here, one considers the values that provide a good trade-off between the convergence speed and the numerical stability of the algorithms [48].

Peponi et al. [19] have used this method of statistical analysis, with particular attention being paid to the dimensional characterization and tensile properties of some lignocellulosic fibers (flax, jute, abaca, and sisal and their polypropylene composites). With the help of semiparametric algorithms, drawn from neural network literature [48, 55], they have explicitly estimated the true distribution functions using a distribution of the geometrical properties and the mechanical behavior of the lignocellulosic fibers. It is known that artificial neural networks [56], which possess the necessary model flexibility and learning ability to match the available data [57], give classic semiparametric models for probability density functions (PDFs). An easy visualization of results is possible through such functional estimates, which enable to perform a more accurate interpolation of the missing data. One uses an adaptive activation neurons function to get the probability density function of a signal for which a basic idea of the new statistical model is adopted. It may be worth noting that adopting such techniques permits an estimation of the PDF of a stationary or quasi-stationary random process being repeatedly applied in the field of adaptive data processing, such as forecasting, linear regression, etc.

Peponi et al. [19] further extended the above-mentioned PDF estimation approach to the Halpin-Tsai equation in the case of PP-composites to predict their properties of random distribution of these fibers in PP matrix.

8.3 Discussions of Observations

8.3.1 Previous Studies

There are a number of studies on the application of Weibull analysis to synthetic fibers, while very limited studies on natural fibers. As this is not under the scope of this book, the former will not be covered. In the following section, some of the studies carried out in respect of natural fibers are discussed.

Kulkarni et al. [15] found that both the strength and elongation of these fibers were found to increase in the range of fiber diameters from 100 to 200 μm and then remain constant up to 450 μm . The fracture strength values of coir fiber showed large scatter (Fig. 8.4a), suggesting that more samples have to be tested to get meaningful result. On the other hand, when 20 samples were tested, the plot showed very low scatter (Fig. 8.4b).

By contrast, the initial modulus was found to gradually decrease with increasing diameter within the entire range investigated. Then, to understand the observed large scatter of strength values, two parameters associated with the Weibull distribution were applied to fibers of constant diameter (250 μm) but to a range of lengths

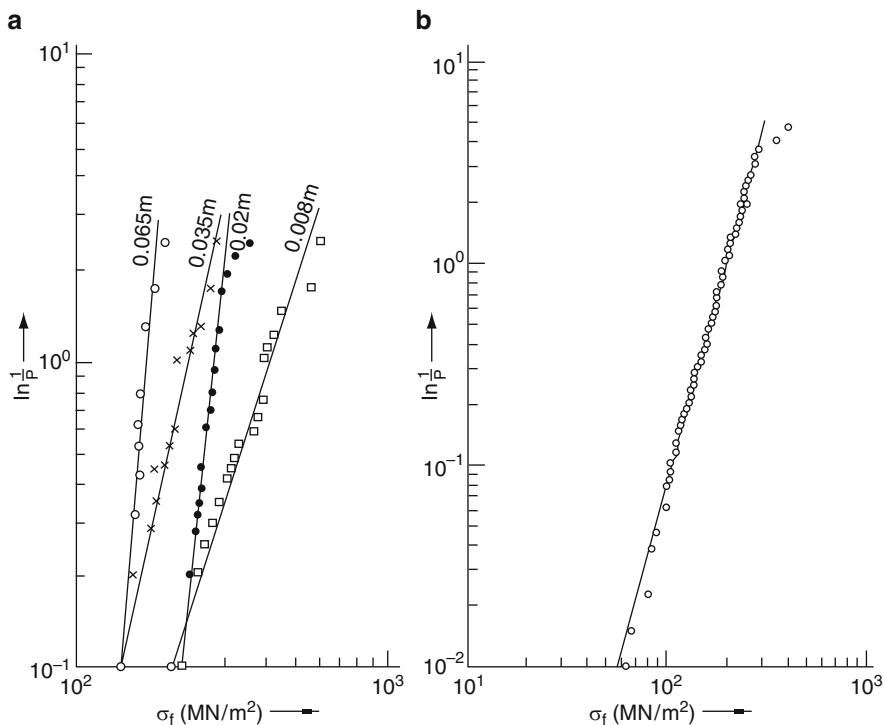


Fig. 8.4 Plot of fracture strength versus diameter for coir fiber (Reproduced with the kind permission of publishers of [15])

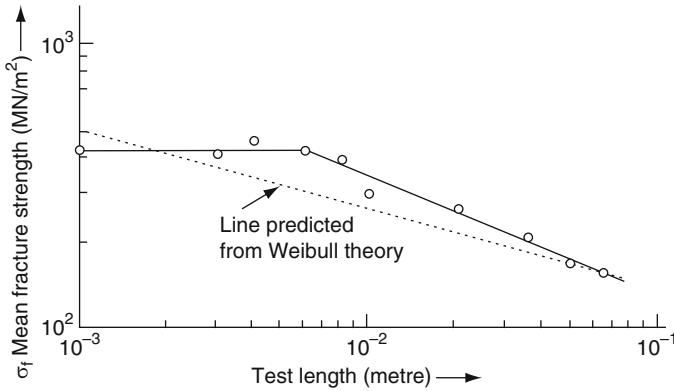
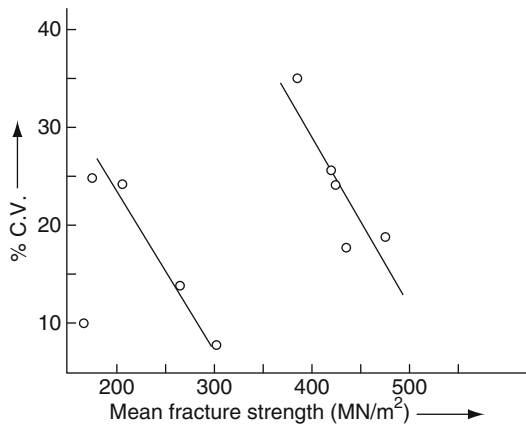


Fig. 8.5 Plots of mean fracture strength versus test lengths for fiber diameter of 250 μm (Reproduced from [15] with kind permission of the Publishers)

Fig. 8.6 Calculated the CV and plots of % of CV versus fracture strength for coir fibers (Reproduced from [15] with kind permission of the Publishers)



(150–350 mm) [15]. Plots on logarithmic coordinates of the mean fracture strength versus test lengths for fiber diameter of 250 μm showed (Fig. 8.5) a linear relationship between 0.065 m and 0.006 m, one straight line between 0.065 m and 0.006 m with a slope of 1.5 and the other between 0.006 m and 0.001 m, which is almost horizontal. Moreover, this relationship was found to be relatively independent of strength. Kulkarni et al. [15] also observed a distribution of flaws below this length (0.006 m) with the mean distance between the flaws of the order of 0.006 m. The researchers also calculated the CV and plots of percentage of CV versus fracture strength. The experimental points in these plots were found to fall in two parallel lines with discontinuity at a given strength corresponding to a length of about 0.006 m (Fig. 8.6), which is one of the shorter lengths studied. This also suggests that coir fiber might have two sizes of defects/flaws: one longer and the other shorter.

They also observed [15] nonuniform distribution of defects and their number decreasing with increasing gauge length. Furthermore, they contended that the population of large defect size determines fracture strength statistics at longer fiber lengths, while at shorter gauge lengths, it is the smaller defects population that rules. It was also considered that the larger defects could be due not only to the drastic variation in diameters in a given gauge length but also to the change in the central portion of the fiber called “lacuna.” It was suggested [15] that a change in the sequence of cell growth may be due to small defects in view of variation of orientation of each cell with the fiber axis. According to them, surface damages, which may also be called defects, might occur during processing of the fibers, for example, during extraction, which may also contribute to the scatter of fracture strength values. In fact, by microscopic studies, they observed change in lacuna sizes, surface defects, and cells grown in different directions but not aligned along the fiber axis.

Kulkarni et al. [15] also observed an increase in the Weibull modulus or parameter (m) with increasing diameter from the log plots of inverse of P versus fracture strength. This suggests a more uniform distribution of flaws in the case of fibers with large diameters. The values of m calculated from CV were found to be comparable. By these, the researchers concluded that unimodal Weibull distribution represents the fracture strength values for every diameter. Histograms of fiber strengths for different diameters were plotted, which were found to be in agreement with the uniform distribution of flaws.

Another relevant study on the application of the Weibull analysis was conducted by Amico et al. [16–18] by means of an investigation on the strength variation of sisal fibers with and without surface treatment (treatment with sodium hydroxide). The authors recognized that in the case of sisal fibers reporting only the mean value from very high variation of tensile strength, a range of 280–700 MPa, was not a proper procedure even when associated with the sampling standard deviation. Consequently, they used the Weibull distribution to evaluate the fracture strength. Moreover, they assumed a circular cross section for the sisal fiber as well as average values of the diameter at both fractured ends.

In the first instance, when the results were analyzed by simple mean and standard deviation analysis, Amico et al. [16–18] got large relative standard deviation, indicating limitation of this method for the proper characterization of the diameter. Then, they used Weibull probability density and cumulative distribution functions [20, 56, 58] to estimate two parameters, the characteristic life and a dimensionless positive pure number, which were supposed to determine the shape and scale of the distribution curve. For this, they adopted two methods, the maximum likelihood technique, which requires the solution of two nonlinear equations, and the analytical method using the probability plot as mentioned earlier for coir fibers.

In the first method, low coefficient of variation was observed, suggesting a poor Weibull distribution, and thus the use of statistical analysis for the diameter was not necessary or even justifiable for sisal fiber. The analytical method (W test) indicated that one should reject the Weibull distribution of diameters for both cases when all the diameters, for 100 fibers, or some of the largest diameters, were discarded.

Table 8.2 Influence of the chemical treatment on the Weibull distribution estimates [Adopted from [18]]

Treatment	α	β (MPa)	T_{50} (MPa)	Mean	Standard deviation
10% sol. NaOH	2.856	272.2	239.4	242.0	95.9
5% sol. NaOH	3.264	331.7	296.4	297.2	105.7
2% sol. NaOH	3.092	341.0	302.9	304.0	111.1
1% sol. NaOH	2.622	351.0	305.2	312.0	131.1
0.5% sol. NaOH	3.058	358.1	317.3	319.5	119.9
0.25% sol. NaOH	2.258	363.0	308.6	321.5	152.2
0% sol. NaOH	2.061	370.6	310.2	327.5	170.6
Untreated	1.938	372.8	308.5	329.5	180.9

The latter showed larger deviation from the regression plot. Then Weibull distribution of strength was carried out by histograms using mean single fiber diameter, for all the fibers (0.195 mm for the 100 fibers) and the actual fiber diameter along with the Weibull parameters obtained by the maximum likelihood method. Then, corrected fiber diameter decreased the scatter in strength values. This was tested by plotting the tensile strength values with both single fiber diameter of the actual fiber diameter with logarithm fitting. This fitting suggested smaller scatter in the corrected tensile strength values, thus showing the appropriateness of the model (Weibull probability) used. Values for the two parameters, viz. the characteristic life and T_{50} -the median, were obtained. Table 8.2 shows [18] the values of all the parameters (α , the shape determining factor, β , scale of distribution factor and T_{50} -the median) obtained by both maximum likelihood method and the probability plot techniques. It can be inferred from this table that α values are higher when actual diameters are used, while the second technique gives a slightly higher value for β , thus suggesting that both the methods give very close estimates for the tensile strength (308 MPa), which follows Weibull distribution, underlining the fact that the actual fiber diameter should be measured.

In the case of NaOH-treated fibers, irrespective of NaOH concentration, the possibility of occurrence of larger errors was felt when single fiber diameter was considered, while the scatter was low, when Weibull distribution was applied to each fiber treatment.

Application of the artificial neural network by Peponi et al. [19] to understand the mechanical behavior of flax fiber bundles with different lengths (5, 10, 20, and 30 mm) revealed the characteristic behavior in terms of the Weibull distribution of the measured tensile strength as a function of fiber length. Such strength-length dependency provides an insight into the homogeneity of the fiber and also to the amount of defects including voids. On the other hand, Weibull analysis of Young's modulus at different lengths was carried out for the four lignocellulosic fibers (abaca, flax, jute, and sisal) and for the first time revealed its nondependency on length in respect of flax fibers. Application of the Weibull method to analyze tensile strength of the four fibers mentioned for different diameters revealed that leaf fibers, such as abaca and sisal fibers, follow a rather similar behavior in respect of both Young's modulus and tensile strength. The stem fibers, such as flax and jute

fibers, show similar nature, but they were much thinner (diameter) and narrowly distributed (diameter) than those of leaf fibers.

The fibers taken from the same bundle showed a wide range of diameters, which is a typical drawback of natural fibers, justifying the need for the use of a more accurate statistical distribution function. In fact, all the fibers showed wide dispersion of strength with respect to diameter data, indicated by the dimensionless shape parameter of the Weibull equation. By contrast, the advanced statistical approach based on neural network algorithms (PDF estimation technique) mentioned above resulted in asymmetric curves of diameter distributions of four lignocellulosic fibers mentioned above (Fig. 8.7).

For the different diameters a shifting of most probable values of the distribution (MPV) to lower values occurs with respect to the Weibull dimensionless parameter. This is more accurate for the expected value regarding the traditional statistical function estimation approach. Thus, it is found that the fiber sample with a gauge length of 5 mm is much stronger than one with a gauge length of 30 mm. This new statistical approach, called “Statistical Model”, interpolates experimental data very well and correlates the geometrical properties (diameter and length) with the mechanical ones for each of the natural fiber studied. This is attributed to the morphological structure of these fibers that, as explained earlier (Sect. 8.1.1), are consisting of microfibrils along with larger presence of voids and/or defects in a long fiber. These results clearly underline the importance of a new statistical approach to explain satisfactorily the observed scatter of strength properties of all the natural materials, particularly those of lignocellulosic fibers.

On the other hand, the tensile properties of PP composites of these fibers analyzed through Halpin–Tsai equation revealed that the theoretical values of both Young’s modulus and tensile strength were higher than those of experimentally obtained values. The latter could be understood as due to the poor matrix–fiber interface as is generally explained in the case of most of polymer-based composites.

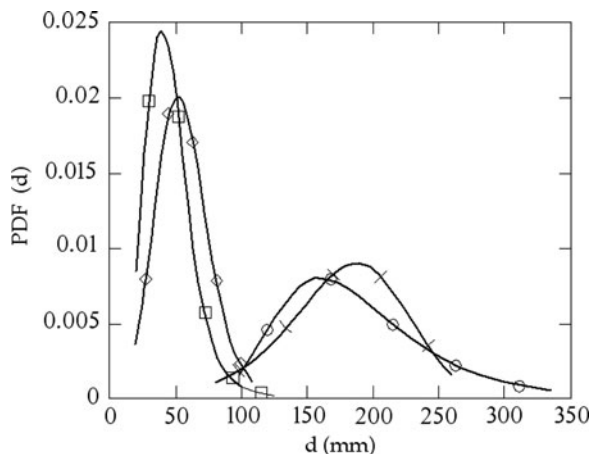


Fig. 8.7 PDF curves for diameters of natural fibers (*open square*) jute, (*open circle*) abaca, (*cross*) sisal, (*open diamond*) flax. (Reproduced from [19] with kind permission of the Publishers)

8.3.2 Recent Work by Authors

It is well known that a relevant difference between lignocellulosic and synthetic fibers is the dimensional uniformity. Lignocellulosic fibers have length and cross-section dimensions that are limited by anatomical restrictions. As mentioned earlier, this natural dispersion leads to scatter in fracture strength and thus resulting in different levels of strength. Unlike previous researchers, the authors of this chapter have analyzed the obtained fracture strength values for some of the Brazilian fibers using Weibull distribution based on the concept of “equivalent diameter”, which corresponds to the average between the larger and smaller diameters. This procedure takes into consideration the average of cross section width and thickness, which always displays an accentuated dispersion in values [59]. Brazilian fibers were tested for their strength properties and analyzed by Weibull distribution to understand the scatter of values obtained. The investigations included bamboo (*Bambusa vulgaris*) [60], coir (*Cocos nucifera*) [50], curaua (*Ananas erectifolius*) [61, 62], jute (*Corshorus capsularis*) [63], piassava (*Attalea funifera*) [64], ramie (*Boehmeria nivea*) [61, 65], sisal (*Agave sisalana*) [61, 66], and buriti (*Mauritia flexuosa*) [67].

Proper experimental procedure was followed as given below:

First, the as-received fibers were cleaned and dried. About 200 fibers were selected in each case and their diameters were measured using a profile projector at five distinct points, with a rotation of 90 °C at every point, to obtain a final value of the average diameter for each fiber. All fibers were then tensile tested in an Instron universal machine at a constant strain rate (10^{-3} s^{-1}). In all cases, a special grip was used to allow the fiber to be firmly held without any damage. Morphology studies were carried out on both as-received and tensile fractured fiber samples using scanning electron microscope (SEM) using appropriate preparation of samples without any thermal damaging and testing conditions. Then histograms of fiber diameters were prepared for each of the fibers studied. Figure 8.8 presents the statistical distribution of the equivalent diameters of six fibers studied in this investigation measured along the fiber length in five distinct locations in each case.

It can be seen that the diameters vary from 0.3 to 0.9 mm for bamboo, from 0.1 to 0.8 mm for coir, from 30 to 150 μm for curaua, from 0.04 to 0.18 mm for jute, from 0.20 to 2.45 mm for piassava, from 0.019 to 0.209 mm for ramie, and from 0.04–0.22 mm for sisal fibers. Their mean diameters were found to be 0.56 mm, 0.28 mm, 90 μm , 0.082 mm, 1.00 mm, 0.114 mm, and 0.17 mm, respectively. Based on these, several diameter intervals for each fiber were considered, ranging from 5 to 12 intervals, depending on the fiber. Then, about 20 fibers from each interval were tested for fracture strength.

First, simple statistical analysis (arithmetic average and standard deviation) was applied to three fibers, namely curaua, ramie, and sisal fibers. In other studies, Weibull analysis program was used to analyze the obtained fracture strength values of different diameters. In both the cases, the results indicated that two types of variation of strength of fibers could be possible. Thinner fibers showed increased

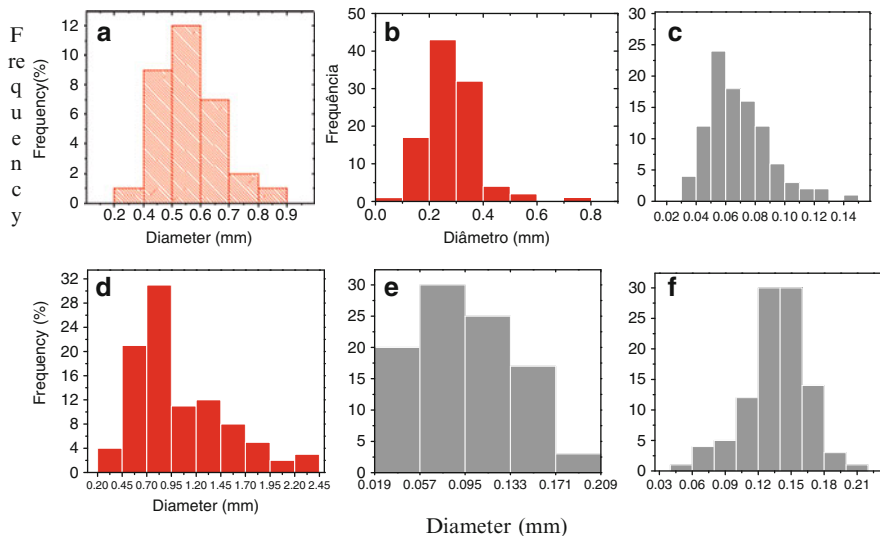


Fig. 8.8 Statistical distribution of diameters for the as-received fibers of (a) bamboo, (b) coir, (c) curaua, (d) piassava, (e) ramie, (f) sisal. (Adopted from [60–62], with kind permission of the Publishers)

(highest) strength, while for thicker fibers, it decreased. Further, from the first method, it was possible to predict very high strength values (above 1,000 MPa) for curaua, ramie, and sisal fibers, when their diameters were less than certain values (<60 μm , 50 μm , and 40 μm in the case of curaua, sisal, and ramie fibers, respectively).

In the second case, the analysis showed that all the fibers followed a unimodal distribution as illustrated by the plots of tensile strength versus diameter on logarithmic scale. Typical plots for coir fibers are shown in Fig. 8.9. Also, both methods showed an inverse relation between the diameter and the tensile strength for each fiber represented by a hyperbolic equation. These equations are shown in Table 8.3.

Based on scanning electron microscopic (SEM) studies, the mechanism responsible for the higher strength of thinner fibers was associated with a more uniform rupture of the fiber filaments, which has a greater statistical probability of having less structure defects. For example, Fig. 8.10 shows fractographs of some of these fibers for two different diameters. An analysis of these fractographs statistically supports a mechanism of premature rupture in thicker fibers due to the relatively larger distribution of fibril compared to thinner fibers. Also, thicker fibers, with more fibrils, would have a comparative larger distribution of both weaker and stronger fibrils. Consequently, during the tensile test of single fibers, there will be a higher probability of a weaker fibril in the thicker fiber breaking at lower stress than the weaker fibril in the thinner fiber. Once the first fibril is broken in such fibers, it acts as a flaw in the fiber structure, which then propagates until total rupture. In other words, statistically, many fibrils of a thicker fiber tend to have one

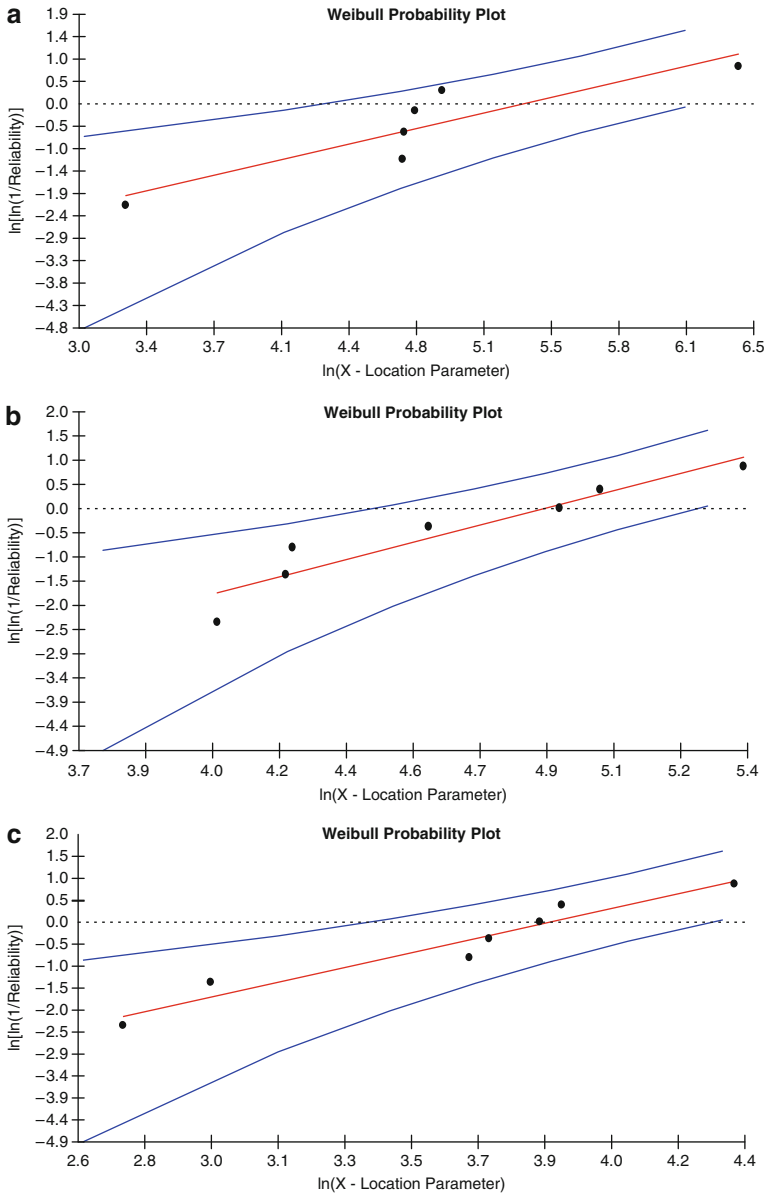


Fig. 8.9 Typical Graphs of the probability of Weibull for some diameter intervals for coir fibers (a) $d < 0.148$ (b) $0.529 < d < 0.593$ (c) $d > 0.656$. (Reproduced from [62] with kind permission of the Publishers)

of them breaking early during the application of load compared to any of the fewer fibrils of a thinner fiber. Thus, one can expect the fiber with smaller diameter to be stronger than the one with larger diameter.

Table 8.3 Relationship between tensile strength and diameter of various fibers

Fiber	Equation	Correlation coefficient (%)	Reference
Bamboo	$\sigma_c = 54/d_c + 49$	98	[60]
Coir	$\sigma_c = 13/d_c + 68$	74	[50]
Curaua	$\sigma_c = 67/d_c - 196$	95	[61, 62]
Jute	$\sigma_c = 19/d_c - 64$	99	[63]
Piassava	$\sigma_c = 620/d_c - 349$	92	[64]
Ramie	$\sigma_r = 21/d_r + 389$	88	[61, 65]
		72	
Sisal	$\sigma_s = 39/d_s + 209$	93	[61, 66]
		84	
Buriti	$\sigma_c = 96/d_c + 15$	99	[67]

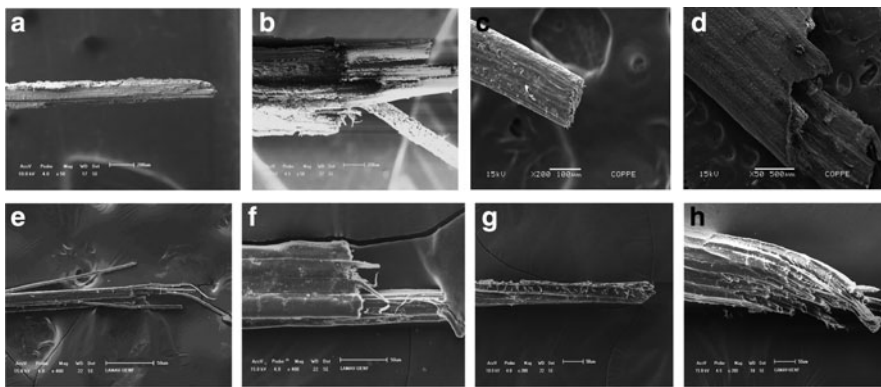


Fig. 8.10 Fractographs of tensile ruptured of various fibers for different diameters: Curaua- (a) thinner, $d = 80 \mu\text{m}$ and (b) thicker, $d = 120 \mu\text{m}$; Coir-(c) thinner, $d = 0.14 \text{ mm}$, and (d) thicker, $d = 1.7 \text{ mm}$; Jute-(e) thinner, $d = 0.02 \text{ mm}$ and (f) thicker, $d = 0.19 \text{ mm}$; Sisal-(g) thinner, $d = 0.05 \text{ mm}$ and (h) thicker, $d = 0.15 \text{ mm}$. (Reproduced from [60, 62, 63, 66], with kind permission of the Publishers)

Considering the possibility to select stronger fibers following the above-mentioned methods and thus the possibility of fabricating polymer-based composites with improved mechanical properties by reinforcement with these thinner fibers, polyester-based composites were prepared with some of these selected fibers and their flexural strengths were determined. In most of the cases, 30 wt. % selected fibers were incorporated into polyester resin in a continuous and aligned way, and composites were produced by compression molding technique. For example, in the case of curaua, sisal, and ramie fibers containing polymer composites, the level of the flexural strength attained (Fig. 8.11) was more than 30% of the corresponding values recently obtained for identical composites reinforced with randomly selected respective fibers, curaua [68], sisal [69], and ramie [70] fibers. It is interesting to note that the strengths shown in Fig. 8.11 are one of the highest reported for polymeric composites reinforced with lignocellulosic fibers.

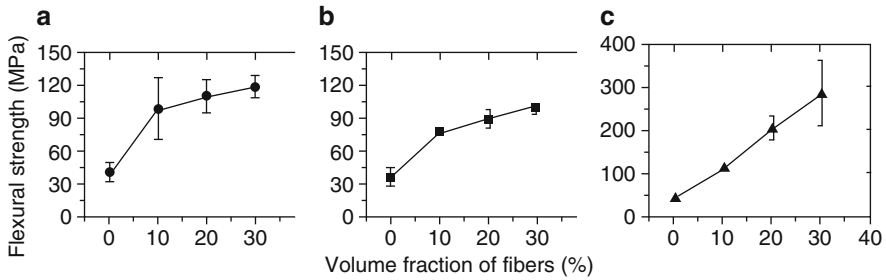


Fig. 8.11 Flexural strength of polyester composites versus the amount of continuous and aligned fibers of (a) Curaua, (b) Sisal (c) Ramie fibers (Reproduced from [61] with kind permission of the Publishers)

8.4 Concluding Remarks

Natural fibers such as lignocellulosic fibers show scatter in their properties, particularly mechanical properties, due to their condition of possessing both types of defects, namely inherent and those introduced by processing. In order to understand such scatter in some of the fibers, either average arithmetic averages and corresponding standard deviations or statistical analysis through Weibull distribution or even artificial neural network have been successfully used. Fractographic studies of some of the fibers have substantiated such analysis. This type of analysis helps in selecting any of the natural fibers of highest possible strength and to explain the strengthening mechanism responsible for the superior performance of these dimensionally selected fibers.

8.5 Suggestions for Future Work

In order to use the lignocellulosic fibers in various applications including in structural components, selection of suitable fibers with consistent strength values with given dimensions (diameter and length) should be selected. For this purpose, the most advanced statistical technique such as artificial neural network should be applied. Hence, it is necessary to revisit the characterization of all the lignocellulosic fibers and analyze the corresponding extensive data generated so far in respect of mechanical properties, particularly tensile strength and modulus. If sufficient data is not available for any fiber, they should be evaluated afresh for different diameters and lengths so that they can be analyzed with advanced statistical approaches to get dependable values for intended applications. This should be applied to the specific case of composite reinforcement. Further, it is necessary to include more parameters in the statistical model (Weibull analysis or artificial neural network) in order to determine the quality of the matrix–fiber interface.

Acknowledgments The authors sincerely acknowledge the Publishers (Elsevier Publishers, Wiley InterScience Publishers and Brazilian Association for Metallurgy and Materials (ABM) and TMS-ABM Organizers) for their kind permission to reproduce some of the Figures and Tables used in this chapter. They also thank Mr. Huluriah, Technician, Acharya Institute of Technology, Bangalore, for his help in drawing some of the figures used here. One of the authors (Dr. KGS) also acknowledges the support and encouragement provided during the preparation of this chapter by the three Institutions in Bangalore (Acharya Institutes, Poornapragna Institute of Scientific Research, and BMS College of Engineering) with whom he is associated presently.

References

1. Satyanarayana KG, Gregorio GC, Fernando W (2009a) Biodegradable composites based on lignocellulosic fibers – an overview. *Prog Polym Sci* 34:982–1021
2. Hon DNS (1988) Cellulose: a wonder material with promising future. *Polym News* 13:34–140
3. Hon DNS (1992) Chemical modification of lignocellulosic materials: old chemistry, new approaches. *Polym News* 17:102–107
4. Kozolowski R, Rawluk M, Barriga J (2004) State of the art-production, processing and applications of fibrous plants. In: *Proceedings of 2nd international conference on textiles (SINTEX-II)*, Natal, Brazil (in CD)
5. Corbière-Nicollier T, Laban BG, Lundquist L, Leterrier Y, Manson JA, Joliet O (2001) Life cycle assessment of biofibres replacing glass fibres as reinforcement in plastics. *Res Conserv Rec* 33:267–287
6. Zapeiropoulos NE, Baillie CA, Matthews FL (2001) A study of transcrystallinity and its effect on the interface in flax fibre reinforced composite materials. *Compos A* 32(3):525–543
7. Hagstrand PO, Oksman K (2001) Mechanical properties and morphology of flax fiber reinforced melamine-formaldehyde composites. *Polym Comp* 22(4):568–578
8. Vázquez A, Dominguez V, Kenny JM (1999) Bagasse-fiber-polypropylene based composites. *J Therm Compos Mater* 12:477–497
9. Stamboulis A, Baillie CA, Peijs T (2001) Effects of environmental conditions on mechanical and physical properties. *Compos A* 32(8):1105–1115
10. Karmaker AC, Youngquist JA (1996) Injection molding of polypropylene reinforced with short jute fibers. *J Appl Polym Sci* 62:1147–1151
11. Kaveline KG, Ermolaeva NS, Kandachar PV (2006) Investigation of stochastic properties of the natural fiber mats. *Compos Sci Technol* 66(2):160–165
12. Yan L, Yiu-Wing M (2006) Interfacial characteristics of sisal fiber and polymeric matrices. *J Adhes* 82(5):527–554
13. Morales J, Olayo MG, Cruz GJ, Herrera-Franco P, Olayo R (2006) Plasma modification of cellulose fibers for composite materials. *J Appl Polym Sci* 101:3821–3828
14. European Commission (1994) Science Research Development. Agricultural Division, European Commission, Brussels, Belgium
15. Kulkarni AG, Satyanarayana KG, Rohatgi PK (1983) Weibull analysis of strength of coir fibers. *Fibre Sci Technol* 19:59–76
16. Amico SC, Costa THS, Silva PS (2001a) Tensile strength of sisal fibers I: The Weibull distribution. In: *Proceedings of 11th international molecular colloquium and 6th Brazil polymers Congress*, Gramado, pp 1537–1540
17. Amico SC, Costa THS, Monachnacz S (2001b) Tensile strength of sisal fibers II: Influence of chemical treatment from the point of view of a Weibull distribution. In: *Proceedings of 11th international molecular colloquium and 6th Brazil polymers congress*, Gramado, pp 1541–1544

18. Amico SC, Sydenstricker THD, da Silva PSCP (2005) Evaluation of the influence of chemical treatment on the tensile strength of sisal fibres by a Weibull distribution analysis. *Met Mater Proc* 17:233–242
19. Peponi L, Biagiotti J, Torre L, Kenny JM, Mondragòn I (2008) Statistical analysis of the mechanical properties of natural fibers and their composite materials. I: Natural fibers. *Poly Compos* 29(3):313–320; II: 322–325
20. Biagiotti J, Fiori S, Torre L, López-Manchado MA, Kenny JM (2004) Mechanical properties of polypropylene matrix composites reinforced with natural fibers: a statistical approach. *Polym Compos* 25(1):26–36
21. Satyanarayana KG, Luiz PR, Fernando W (2009b) Comparative study of Brazilian natural fibers and their composites with others. In: Thomas S, Pothan LA (eds) *Natural fibre reinforced polymer composites*, vol 1. Old City, Philadelphia, pp 473–522. ISBN: 978-1-933153-09-4
22. Beldzki AK, Gassan J (1999) Composites reinforced with cellulose based fibers. *Prog Polym Sci* 24:221–274
23. Eichhorn SJ, Baillie CA, Zafeiropoulos N, Mwaikambo LY, Ansell MP, Dufresne A, Entwistle KM, Herrera-Franco PJ, Escamilla GC, Groom L, Hughes M, Hill C, Rials TG, Wild PM (2001) Current international research into cellulosic fibres and composites – Review. *J Mater Sci* 36:2107–2131
24. Joshi VS, Drzal TL, Mohanty KA, Arora S (2004) Are natural fiber composites environmentally superior to glass fiber reinforced composites? *Compos A* 35:371–376
25. Satyanarayana KG, Fernando W (2007) Characterization of natural fibers. In: Fakirov S, Bhattacharyya D (eds) *Engineering biopolymers: homopolymers, blends and composites*, Auckland, New Zealand, vol 1. Hanser, Munich, pp 03–47
26. Satyanarayana KG, Guimarães JL, Fernando W (2007) Studies on lignocellulosic fibers of Brazil. Part I: Source, production, morphology, properties and applications. *Compos A* 38:1694–1709
27. Kulkarni AG, Satyanarayana KG, Sukumaran K, Rohatgi PK (1981) Mechanical behavior of coir fibers under tensile load. *J Mater Sci* 16:905–914
28. Fábio T, Thais HDS, Satyanarayana KG (2007a) Studies on lignocellulosic fibers of Brazil. Part II: Morphology and properties of Brazilian coconut fibers. *Compos A* 38:1710–1721
29. Fábio T, Thais HDS, Satyanarayana KG (2007b) Studies on lignocellulosic fibers of Brazil: Part III – Morphology and properties of Brazilian curauá fibers. *Compos A* 38:2227–2236
30. Orwin DFG, Woods JL, Elliott KH (1980) Proceedings of 6th international wool textile research conference, vol II, Pretoria, p 193
31. Peirce FT (1926) *J Text Inst* 17:T355
32. Bader MG, Priest AM (1982) Proceedings of ICCM-IV, Tokyo, p 1129
33. Gurvich MR, Dibenedetto AT, Pegoretti A (1997) Evaluation of the statistical parameters of a Weibull distribution. *J Mater Sci* 32:3711–3716
34. Patankar SN (1991) Weibull distribution as applied to ceramic fibres. *J Mater Sci Lett* 10:1176–1181
35. Wu HF, Netravali AN (1992) Weibull analysis of strength-length relationships in single Nicalon SiC fibres. *J Mater Sci* 27:3318
36. Amaniampong G, Burgoyne CJ (1994) Statistical variability in strength and failure strain of aramid and polyester yarns. *J Mater Sci* 29:5141
37. Pan N, Chen HC, Thompson J, Inglesby MK, Khatua S, Zhang XS, Zeronian SH (1997) The size effects on the mechanical behaviour of fibres. *J Mater Sci* 32:2677
38. Zhang Y, Wang X, Pan N, Postle R (2002) Weibull analysis of the tensile behavior of fibers with geometrical irregularities. *J Mater Sci* 37(7):1401–1406
39. Metcalfe AG, Schmitz GK (1964) The effect of length on the strength of glass fibers. *Proc ASTM* 64:1075–1093
40. Street KN, Forte JP (1976) On the strength-length dependence of boron fibers. *Proc ICCM (AIME)* 1:137–163

41. Hutchinson JW, Phillips DC (1979) The dependence of strength of carbon fibers on length. *Fiber Sci Technol* 12:217–233
42. Weibull W (1951) A statistical distribution function of wide applicability. *J Appl Mech Trans ASME* 18:293–297
43. Mukherjee PS, Satyanarayana KG (1984) Structure and properties of some vegetable fibers – Part 1: Sisal fiber. *J Mater Sci* 19:3925–3934
44. Satyanarayana KG, Pillai CKS, Sukumaran K, Pillai SGK, Vijayan K, Rohatgi PK (1982) Structure and properties of fibres from various parts of coconut palm. *J Mater Sci* 17: 2453–2462
45. Satyanarayana KG, Mangalakumari C, Kulkarni AG, Koshy P (1984) Microscopic studies of natural fibres. *Bull Electron Micr Soc India* 7:179–186
46. Sahu NC, Das C, Satyanarayana KG (1986) Investigations of submicroscopic structure in fibers of jute, mesta and coir. *J Optics* 15:48–53
47. Mukherjee PS, Satyanarayana KG (1986) Structure and properties of some vegetable fibers – Part 2: Pineapple fiber. *J Mater Sci* 21:51–56
48. Fiori S, Bucciarelli P (2001) Probability density estimation using adaptive activation function neurons. *Neural Process Lett* 13:31–42
49. Kulkarni AG, Satyanarayana KG, Rohatgi PK, Vijayan K (1983) Mechanical properties of banana fibers. *J Mater Sci* 18:2290–2296
50. Santafe HPG Jr, Monteiro SN, Costa LL et al (2009) Weibull distribution as an instrument of statistical analysis for coir fiber tensile tests (in Portuguese). Proceedings of the 64 rd international congress of the Brazilian association for metallurgy and materials. Belo Horizonte-MG, Brazil, 13–17 July 2009, pp 1–12
51. Satyanarayana KG, Ravikumar KK, Sukumaran K, Mukherjee PS, Pillai SGK, Kulkarni AG (1986) Structure and properties of some vegetable fibers – Part 3: Talipot and palmyrah fibers. *J Mater Sci* 21:57–63
52. Zhang Y, Wang X (2001) The minimum diameter distribution and strength variation of top dyed wool. *Wool Technol Sheep Breed* 49(3):212–221 (Wool Research Organisation of New Zealand, New Zealand)
53. Steve D, Eric B, Jim K, Andy W, Curt J (2003) Weibull strength parameter requirements for Si3N4 Turbine rotor reliability. Paper presented at the environmental barrier coatings workshop, Gaylord Opryland Resort & Convention Center, Nashville, TN, USA, 18–19 Nov 2003 http://www.ornl.gov/sci/de_materials/documents/DuffyEBC2003_000.pdf. Accessed on 18 May 2010
54. Lavaste V, Besson J, Bunsell AR (1995) Statistical analysis of strength distribution of alumina based single fibres accounting for fibre diameter variations. *J Mater Sci* 30:2042–2048
55. Fiori S (2001) Probability density function learning by unsupervised neurons. *Int J Neural Syst* 11:399–417
56. Nelson W (1982) *Applied life data analysis*. Wiley, New York
57. Bishop C (1995) *Neural networks for pattern recognition*. Oxford University Press, Oxford. ISBN 0-19-853864-2
58. Wadsworth HM (1998) *Handbook of statistical methods for engineers and scientists*. McGraw-Hill, New York
59. Monteiro SN, Lopes FPD, Ferreira AS, Nascimento DCO (2009) Natural fiber polymer matrix composites: cheaper, tougher and environmentally friendly. *JOM* 61:17–22
60. Costa LL, Loiola RL, Monteiro SN (2010) Tensile strength of bamboo fibers: Weibull analysis to characterize the diameter dependence. In: Proceedings of biomaterials symposium, First TMS-ABM international materials congress, Rio de Janeiro, Brazil, 26–30 July 2010, pp 1–10 (to be published in CD)
61. Monteiro SN, Satyanarayana KG, Lopes FPD (2010) High strength natural fibers for improved polymer matrix composites. *Mater Sci Forum* 638–642:961–966
62. Ferreira AS, Monteiro SN, Lopes FPD et al. (2009) Curaua fiber mechanical properties evaluation by the Weibull analysis (in Portuguese). In: Proceedings of 64 rd international

- congress of the Brazilian association for metallurgy and materials. Belo Horizonte, Brazil, pp 1–12
63. Bevitori AB, Silva ILA, Felipe PDL, Monteiro SN (2010) Weibull analysis of the tensile strength variation with diameter for jute fibers. In: Proceedings of biomaterials symposium, First TMS-ABM international materials congress, Rio de Janeiro, Brazil, 26–30 July 2010, pp 1–10. (To be published in CD)
 64. Nascimento DCO, Motta LC, Monteiro SN (2010) Weibull analysis of tensile tested piassava fibers with different diameters. In: Proceedings of characterization of minerals, metals and materials – TMS 2010, Seattle, USA, 21–25 Feb 2010, pp 1–8
 65. Margem FM, Bravo Neto J, Monteiro SN (2010) Ramie fibers mechanical properties evaluation by the Weibull analysis (in Portuguese). In: Proceedings of the Brazilian congress on materials science and engineering. Campos do Jordão, Brazil, pp 1–10
 66. Inacio WP, Lopes FPD, Monteiro SN (2010) Tensile strength as a function of sisal fiber diameter through a Weibull analysis. In: Proceedings of biomaterials symposium, First TMS-ABM international materials congress, Rio de Janeiro, Brazil, pp 1–10 (to be published in CD)
 67. Portela TGR, Costa LL, Lopes FPD et al (2010) Characterization of fibers from different parts of the buriti palm tree. In: Proceedings of characterization of minerals, metals and materials – TMS 2010, Seattle, USA, pp 1–7
 68. Monteiro SN, Aquino RCMP, Lopes FPD, Carvalho EA, d’Almeida JRM (2006) Proceedings of the 61th congress of the Brazilian association for metallurgy and materials, pub. ABM, July 2006, Rio de Janeiro, Brazil, pp 1–10 (in CD-Rom)
 69. Inácio WP, Monteiro SN, Lopes FPD (2009) Proceedings of the 64th congress of the Brazilian association for metallurgy and materials, pub. ABM, July 2009, Belo Horizonte, Brazil, pp 1–9 (in CD-Rom)
 70. Monteiro SN, Santos LFL Jr, Margem FM (2009b) Proceedings of the characterization of minerals, metals and materials – TMS Conference, pub. TMS, February 2009, San Francisco, USA, Feb 2009, pp 1–6 (in CD-Rom)

Chapter 9

Interfacial Shear Strength in Lignocellulosic Fibers Incorporated Polymeric Composites

Sergio Neves Monteiro, Kestur Gundappa Satyanarayana,
Frederico Muylaert Margem, Ailton da Silva Ferreira,
Denise Cristina Oliveira Nascimento, Helvio Pessanha Guimarães Santafé Jr,
and Felipe Perissé Duarte Lopes

Abstract Lignocellulosic fibers have been recognized as attractive fillers for different types of matrices in polymeric composites. Their advantages such as recyclability and renewability are unique characteristics for composites used as automobile components and building structural panels. In view of the hydrophobic behavior of most polymers and the hydrophilic nature of lignocellulosic fibers, poor adhesion is observed between lignocellulosic fibers and the polymeric matrix, which results in lower mechanical properties. Pullout tests have been successfully used to determine the interfacial shear stress in synthetic fiber-reinforced composites, but little has been reported in the case of lignocellulosic fiber–polymer composites. This chapter presents an overview on the determination of the interfacial strength of lignocellulosic fibers–polymer matrix composites including some obtained by the authors on Brazilian fibers such as curaua, ramie, and piassava, considered as reinforcement for composites. Concluding remarks and suggestions indicate some future works.

Keywords Interfacial shear strength · Lignocellulosic fiber · Microbond test · Polymer composite · Pullout test · Single fiber fragmentation test

Contents

9.1 Introduction	242
9.2 Single Fiber Pullout Test	244
9.2.1 Fundamental Considerations	244

K.G. Satyanarayana (✉)

Laboratory for Advanced Materials, LAMAV, State University of the Northern Rio de Janeiro, UENF, Av. Alberto Lamego 2000, Horto, Campos dos Goytacazes, Rio de Janeiro, Brazil

and UFPR, Curitiba, Paraná, Brazil

and

Acharya Institutes, BMS College of Engineering and Poornapragna Institute of Scientific Research, Bangalore, India

e-mail: kgs_satya@yahoo.co.in

9.2.2	Examples of SFP Tests Results	246
9.3	Critical Length Pullout Curve	246
9.3.1	Fundamental Considerations	246
9.3.2	Interpretation of CLP Curves	248
9.3.3	IFSS of Lignocellulosic Fiber Composites by CLP Curves	249
9.3.4	Examples of CLP Curve Results	249
9.4	Single-Fiber Fragmentation Test	252
9.4.1	Fundamental Considerations	252
9.4.2	Examples of SFF Test Results	254
9.5	Microbond Test	255
9.5.1	Fundamental Considerations	255
9.5.2	Example of Microbond Test Results	256
9.6	Other Proposed Methods to Measure the IFSS	257
9.7	Concluding Remarks	258
	References	259

9.1 Introduction

Fiber-reinforced composites emerged in the last century as a successful class of material and has been extensively used in a wide range of applications from sport and leisure to aerospace and defense systems, owing to superior mechanical properties [1–3]. Today, synthetic fibers such as glass, carbon, and aramid are the main reinforcing phase in these composites. However, the fabrication of synthetic fibers as well as their processing in composites requires a relatively large amount of energy. As a consequence, the quality of the environment suffered because of the pollution generated during the production and recycling of these synthetic materials [4]. In fact, carbon dioxide and other gasses associated with the energy consumption and processing methods during synthetic fiber and related composites' fabrication are responsible for the atmospheric greenhouse effect, which causes global warming [5].

The possibility of substituting the traditional energy-intensive synthetic materials for natural ones is therefore gaining attention in recent years. A typical example is the case of natural fibers, especially those obtained from cellulose-based plants, also known as lignocellulosic fibers. These fibers have been extensively investigated in the past decades as possible substitutes for synthetic fibers, especially the glass fiber, traditionally used as reinforcement of polymeric composites [6–11]. According to Kalia et al. [4], the renewed interest in natural fibers has resulted in a large number of modifications to bring them at par and even superior in some properties to synthetic fibers. Moreover, due to such tremendous changes in the quality of natural fibers, they are fast emerging as a reinforcing phase in composite materials.

Lignocellulosic fibers offer relative advantages such as low cost and density as well as renewability and biodegradability. In addition, their life cycle and processing conditions make them neutral with respect to carbon dioxide emission, and so they are considered as an environmentally friendly material. By contrast to synthetic fibers

extensively fabricated in industrialized countries, lignocellulosic fibers are cultivated mainly in rural areas of developing countries [12]. This is of societal relevance since the market of lignocellulosic fibers represents a major source of income to populations in South Asia, Africa, and Latin America. For instance, relatively unknown fibers such as piassava [13–16], curaua [17–20], sponge gourde [21, 22], and buriti [23, 24], which have traditionally been used, mainly for simple domestic items, in the Amazon and other regions of South America, are currently being investigated and already applied as composite reinforcement with higher economic value in industrial products. The cost effectiveness, lightness, and some superior properties such as the impact resistance are attractive advantages related to the use of lignocellulosic fiber composites in building panels and automobile components [25]. The car industry, especially in Europe, is successfully using composites reinforced with several types of lignocellulosic fibers in components such as head rests, interior panels, and seat cushions originally made of glass mat composites, common plastics, or polymeric foams [26–30]. Technical reasons justify this preference. A lignocellulosic fiber composite is associated with less damage to industrial molding equipment as well as a relatively better finishing. Additionally, a high degree of flexibility, which makes a lignocellulosic fiber to bend rather than fracture, contributes to a significantly greater toughness of an automobile composite part, which is then able to absorb the impact energy in case of an accident crash.

Contrary to these advantages, it is recognized [6–11] that lignocellulosic fibers present drawbacks related to dimensional irregularities, structural defects, and weak adhesion to most polymers, such as polyester, vinyl esters, and epoxy, normally used as composite matrices. In particular, a weak fiber/matrix adhesion may result in lower mechanical performance of the composite even if a high strength fiber is used as reinforcement. In the case of a lignocellulosic fiber, the hydrophilic tendency to absorb water onto its surface causes a weak bonding to be formed in contact with a hydrophobic polymer. This fiber/matrix bonding condition can be analyzed through the resistance at the interface region between the fiber and the matrix by means of the interfacial shear strength (IFSS) [1–3]. The experimental evaluation of the IFSS can be done by different methods [31–36]. These include the single fiber pullout test, the critical length pullout (CLP) curve, the single fiber fragmentation (SFF) test, the microbond test, and others that may employ similar experimental conditions but receive distinct denomination such as the push-out, the microdebond, the microindentation, and the microcompression tests. The IFSS can also be calculated using theoretical modeling and even undirected estimation by inferred critical length values from mechanical tests.

As further discussed, a relevant point regarding the experimental evaluation of the IFSS is the representativeness of the samples. Synthetic fibers such as glass, carbon, and aramid are usually cylindrical and uniform not only in dimensions but also in surface finishing, as illustrated in Fig. 9.1.

On the other hand, lignocellulosic fibers are never perfect cylinders. Furthermore, they possess naturally nonuniform shape and dimensions, particularly at their cross sections. Even if an average equivalent diameter is considered, lignocellulosic fibers display significant changes in diameters from one fiber to another as well as

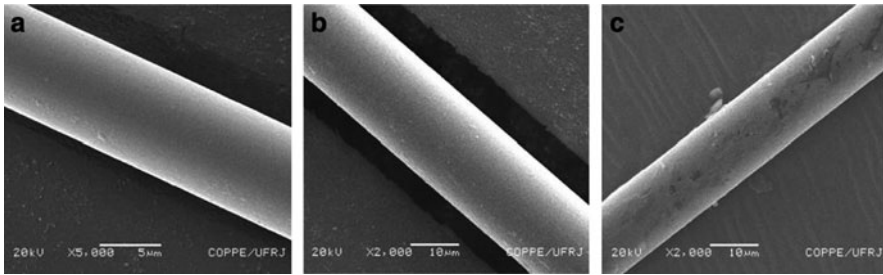


Fig. 9.1 The uniform aspect of synthetic fibers (a) carbon, (b) glass, and (c) aramid

along the axis of the same fiber. Moreover, as exemplified in Fig. 9.2, the relatively rough surface of any lignocellulosic fiber has natural protrusions and reentrances. These irregularities can be associated with defects and weak points that may strongly affect the mechanical resistance of the fiber [25].

As a consequence of their nonuniform morphology, Fig. 9.2, lignocellulosic fibers are difficult to be evaluated in terms of micromechanical properties such as the single fiber pullout or microbond tests. In fact, any experimental method to determine the IFSS has to take into account that diameters and cross-section areas can only be estimated with a relatively low precision. The only way to comply with this difficulty is to conduct a large number of tests under the same condition and then interpret the results using reliable statistic methods such as the Weibull analysis. Additionally, a bundle of fibers from separate climatic regions or distinct vegetal subspecies may show marked different micromechanical properties with respect to the same polymeric matrix. This is certainly not the case of almost perfect and defect-free synthetic fibers, Fig. 9.1, for which IFSS evaluation has been the subject of many works. These works, however, are of marginal interest to the scope of this overview.

The following sections of this chapter deal with fundamentals (backgrounds) of the major methods that are being used to evaluate the IFSS of lignocellulosic fibers in polymeric matrices. A few experimental examples will be presented to illustrate each method. Advantages, limitations, and shortcoming will be pointed out.

9.2 Single Fiber Pullout Test

9.2.1 Fundamental Considerations

A simple and direct micromechanical method to evaluate the IFSS is based on a tensile test in which a partially embedded single fiber is pulled out from a block of matrix material. This simulates the stress constraints acting on a fiber/matrix

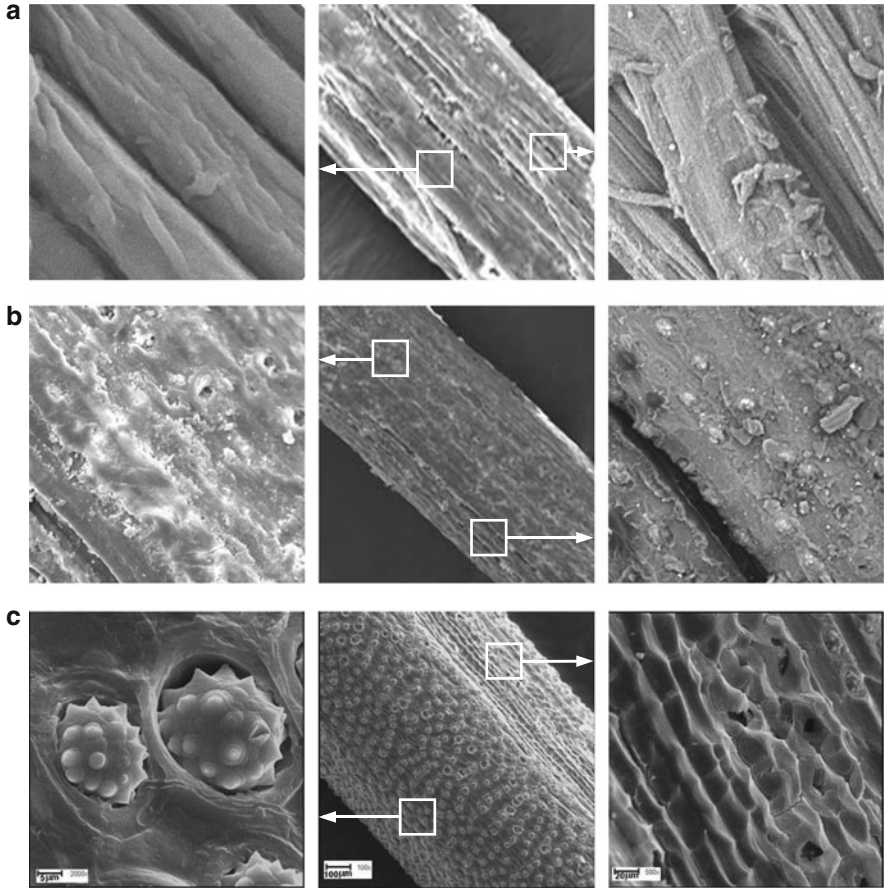


Fig. 9.2 The nonuniform aspect of lignocellulosic fibers (a) curaua, (b) coir, and (c) piassava, with surface details inside *white squares*

elemental part of a composite under a tensile loading. Researchers have applied the single fiber pullout (SFP) test to determine the IFSS in lignocellulosic fibers associated with polymeric matrices [37–39]. In this method, the IFSS (τ) can be obtained by means of:

$$\tau = \frac{F}{\pi dL} \tag{9.1}$$

where d is the fiber diameter, F , the pullout tensile force, and L , the partially embedded length. Park et al. [39], recognized that it is more difficult to get statistically meaningful information from SFP tests using this method since natural fibers are more nonuniform. As mentioned in the previous section of this chapter, irregularities, defects, and weak points, Fig. 9.2, are always expected to exist in lignocellulosic fibers.

Table 9.1 Sisal fiber/polyester interfacial shear strength measured by single fiber pullout test. Reproduced with kind permission of the publishers of [38]

Fiber treatment	IFSS (MPa)
Untreated	2.6 ± 0.6
0.25% NaOH	4.5 ± 1.3
0.50% NaOH	5.2 ± 1.3
1.00% NaOH	5.9 ± 1.0
2.00% NaOH	6.9 ± 1.1
5.00% NaOH	6.7 ± 1.6
10.0% NaOH	6.3 ± 1.4
1% <i>N</i> -isopropyl acrylamide	5.9 ± 1.7
2% <i>N</i> -isopropyl acrylamide	6.8 ± 1.5
3% <i>N</i> -isopropyl acrylamide	5.8 ± 1.9

9.2.2 Examples of SFP Tests Results

Sydenstricker et al. [38] evaluated the IFSS of sisal fibers, both untreated and subjected to different surface chemical treatments, by SFP tests. The sisal fibers were inserted at a constant 3 mm depth in polyester blocks. The authors found [38] that the values of IFSS that are given in Table 9.1 showing treated sisal fibers, up to a certain level of surface chemical treatment, present better IFSS with polyester as possible composite matrix. It can also be inferred from Table 9.1 that the value for both the untreated and treated fibers are markedly lower when compared to synthetic fibers with polymeric matrix. For instance, Tanaka et al. [40] reported an IFSS of 20 MPa for aramid fiber embedded in epoxy matrix.

9.3 Critical Length Pullout Curve

9.3.1 Fundamental Considerations

The influence of the fiber length and the efficiency of its adhesion to a matrix are of well-known importance to the strength and stiffness of a composite [1–3]. Fibers that are not long enough fail to provide an effective reinforcement to the matrix. Kelly and Tyson [41] proposed that a critical length (ℓ_c) should be exceeded in order to allow for an effective matrix reinforcement. Under an applied load, which eventually leads to the rupture of the composite, a long and continuous fiber, $\ell \gg \ell_c$, will break without being pulled out of the matrix. Below ℓ_c , a short and discontinuous fiber does not provide an efficient matrix to fiber load transference. In this case, the matrix deforms around the fiber in such a way that virtually no stress transference and little reinforcement by the fiber occur [42]. Moreover, since the fiber fails to break, the composite rupture is determined either by the matrix strength or the interface resistance, whichever is smaller. A possible microstructural

consequence of $l < l_c$ is a crack formation at the interface due to the fiber/matrix debonding.

According to Kelly and Tyson [41], the critical length can be evaluated by the following equation

$$l_c = \frac{d\sigma_f}{2\tau} \tag{9.2}$$

where d is the fiber diameter, σ_f , the fiber tensile strength, and τ , the fiber/matrix interfacial shear strength, IFSS, or the matrix shear strength. As shown along this chapter, for lignocellulosic fibers incorporated to polymeric matrices, the value of IFSS is always lower and, consequently, corresponds to τ in Equation (9.2). Actually, this equation was the first proposed for the critical length. Later, Hull and Clyne [43] derived another version, in which l_c was reduced to half of its value of Equation (9.2)

$$l_c = \frac{r\sigma_f}{2\tau} \tag{9.3}$$

where r is the fiber radius considered as half of the equivalent diameter. Equation (9.2) has been used in most works related to lignocellulosic fiber composites.

In their original publication, Kelly and Tyson [41] also proposed an experimental procedure to evaluate l_c and, by the Equation (9.2), to determine the IFSS. This became known as the pullout test and was the basis for some more elaborated versions presented in this chapter. In the original version, Fig. 9.3, a single long fiber with part of its length, L , embedded in a block made of the same material of the matrix, Fig. 9.3a, is tensile tested. The test simulates the stress condition acting on the fiber/matrix elemental part of the composite. By decreasing the embedded length L , a threshold should be found, below which the fiber would slip away, i.e., pull out of the block without breaking. A curve corresponding to the variation of the tensile stress with L , Fig. 9.3b, presents a horizontal part associated with embedded lengths large enough to prevent fiber pullout. In this case, rupture is

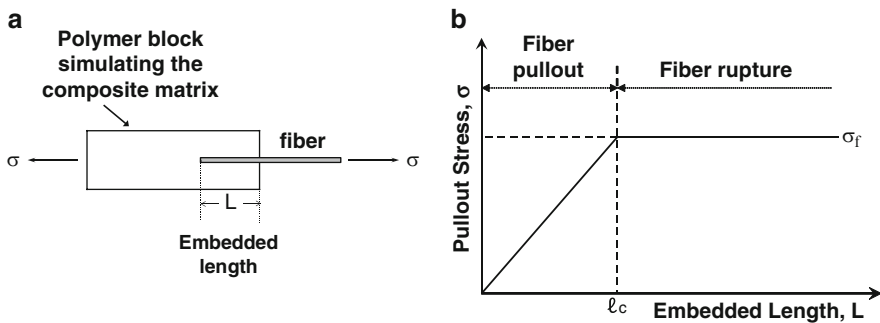


Fig. 9.3 Schematic of the pullout test (a) and corresponding pullout curve (b)

expected to occur at the fiber by its typical tensile fracture. Small embedded length causes the fiber to partially or totally be pulled out of the block, at continuous lowering stresses with decreasing L , until the obvious condition of $\sigma_f = 0$ for $L = 0$, as schematically shown in Fig. 9.3b. The transition point where the horizontal part meets the second decreasing part is considered the critical length ℓ_c .

The major advantage of this method is the intrinsic statistical support to the determination of ℓ_c based on intersection of straight line (linear regression) plots from many experimental points. Moreover, the aspect of the fiber after the test, as well as the serrations and drops (stick–slip) in the tensile loading graph, serves as a clear indication that the pullout had occurred . A limitation may exist when the critical length is very small, for instance, below 3 mm, which brings greater uncertainty due to specimen fabrication and testing.

9.3.2 Interpretation of CLP Curves

Experimentally, it is difficult to obtain straightforward pullout curves such as the one in Fig. 9.3b. In particular, lignocellulosic fibers embedded in polymeric blocks display a considerable dispersion in stress values, both when pulling out (first part) or breaking (second part) the fiber. In fact, the σ versus L curve usually has experimental points that do not adjust to two single straight lines with ℓ_c at the intersection [36]. A more realistic result could conceive an intermediate stage in which both pullout and break of the fiber take place. Kelly [44] suggested that an inclined straight line exists relating the strength σ and the embedded length L .

$$\sigma = \sigma_0 + kL/d \tag{9.4}$$

where σ_0 and k are constant, while d is the fiber diameter. This can only happen in association with an intermediate stage since the strength $\sigma = \sigma_0$ for $L = 0$ does not fit Equation (9.4). In other words, the more realistic pullout curve would have three linear stages [36] as schematically shown in Fig. 9.4a.

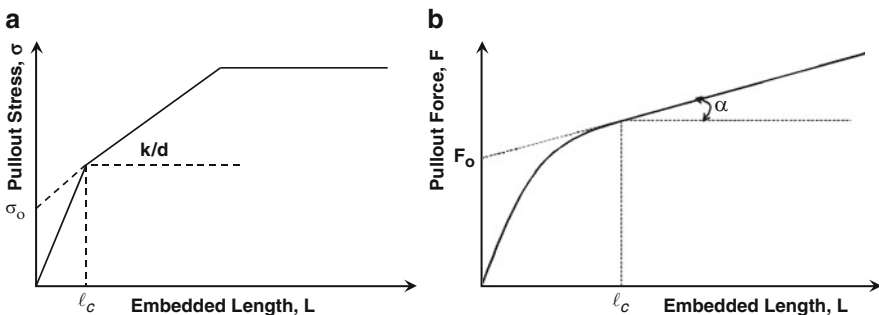


Fig. 9.4 Possible interpretation of experimental results associated with CLP curves proposed in (a) [36] and (b) Reproduced with the kind permission of the publishers of [45, 46]

Another interpretation proposed by Yue et al. [45] considered an initial nonlinear stage from the origin to ℓ_c , as shown in Fig. 9.4b. This initial stage is followed by an ascending linear stage with a slope α that could be used to calculate the IFSS [46]

$$\tau(2\pi rN^{-1}) = F_0 + \alpha\ell_c \quad (9.5)$$

where r is the fiber radius and N is a parameter dependent on the physical properties of the fiber and matrix as well as the specimen geometry. Since the pullout curve, Fig. 9.4b, suggested by Yue et al. [45, 46] was only applied to synthetic fibers, it will not be discussed in this chapter.

In both interpretations of pullout curves shown in Fig. 9.4, the first linear, Fig. 9.4a, or nonlinear, Fig. 9.4b, part would be associated with debonding of the fiber with respect to the block. For long enough embedded L , the pullout stress would correspond to ultimate (breaking) stress of the fiber constant.

9.3.3 IFSS of Lignocellulosic Fiber Composites by CLP Curves

The interfacial shear strength of polymer composites reinforced with lignocellulosic fibers has been evaluated using (9.2) for the critical length obtained in CLP curves. Transformation of this equation provides a simple way to determine the IFSS of a system composed of a given lignocellulosic fiber embedded into a polymeric matrix.

$$\tau = \frac{d\sigma_f}{2\ell_c}. \quad (9.6)$$

This simple method requires, however, a precise value of d and σ_f for the fiber. Owing to the heterogeneous characteristics of any lignocellulosic fiber, one is never sure that correct values of d and σ_f are used. The fiber diameter, even when carefully measured by profile projector technique, varies within a range from one fiber to another as well as along the length of any given fiber. This also requires the determination of the tensile strength, which needs the cross-section area values of the fiber. Statistical analysis of diameter variation and the application of Weibull method for the tensile strength helped to reduce the uncertainty in d and σ_f . This subject has been detailed in another chapter of this book and will here be discussed only for specific cases.

9.3.4 Examples of CLP Curve Results

Using the pullout test methodology described in Fig. 9.4, the critical length ℓ_c and corresponding IFSS, τ in Equation (9.6), for several lignocellulosic fibers and

polymeric matrices were evaluated. These are piassava fiber/polyester [14], curaua fiber/polyester [47], curaua fiber/epoxy [48], coir fiber/polyester [36], coir fiber/epoxy [49], ramie fiber/polyester [50], and sisal fiber/polyester [51].

Figure 9.5 illustrates typical CLP curves for different lignocellulosic fiber embedded in polyester matrices.

Examples of load versus elongation curve characteristics of the pullout tests are shown in Fig. 9.6 for different lignocellulosic fibers embedded in thermoset polymeric matrices.

The aspect of the flow curves in Fig. 9.6 indicates the predominant condition of the test. For instance, Fig. 9.6a shows uniform serrations (stick–slip) associated with a continuous, step-by-step process of fiber slipping away off the polymeric block. This exclusive pullout mechanism occurred only in the first part of the curve depicted in Fig. 9.5c. In this case, the fiber was intact after the test and, in some cases, covered with a layer of polyester. By contrast, Fig. 9.6d shows a smooth curve up to fracture. In this case, no pullout process occurred, and the fiber had undergone tensile rupture in association with the last horizontal part of the curve. The intermediate condition of both pullout and fiber rupture are shown in Fig. 9.6b, c.

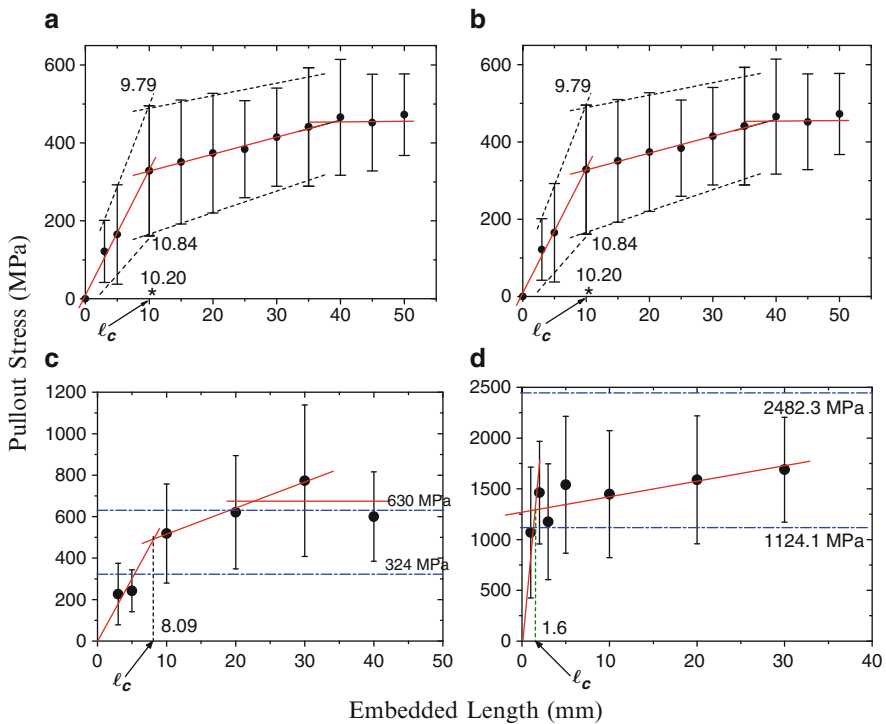


Fig. 9.5 Critical length pullout curves for (a) curaua fiber/polyester; (b) coir fiber/polyester; (c) sisal fiber/polyester; and (d) ramie fiber/polyester

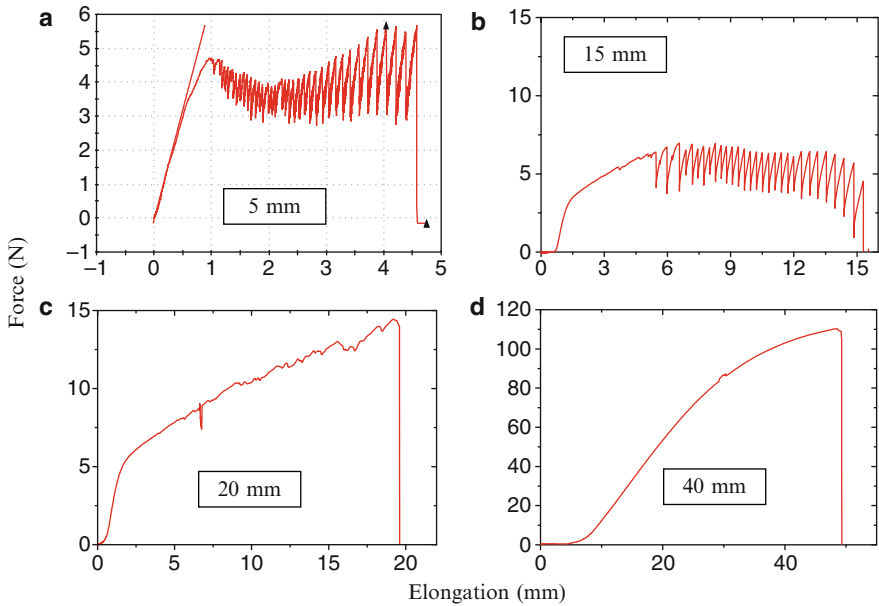


Fig. 9.6 Load versus elongation curves directly obtained from a digital acquisition data of the tensile machine (a) sisal fiber/polyester – 5 mm; (b) coir fiber/epoxy – 15 mm; coir fiber/polyester – 20 mm; and (d) piassava fiber/polyester – 40 mm

Another point worth mentioning is the fact that CLP curves are given as stress versus L [41, 44]. Therefore, a careful measurement of the fiber diameter is needed to calculate the stress. The difficulty of performing this calculation was already discussed in terms of the nonuniform characteristics of any lignocellulosic fiber. In spite of the dispersion in stress values experimentally obtained for embedded length L in Fig. 9.5, the resisting area to the applied load has to be evaluated according to the test condition. For a test like the one in Fig. 9.6a, in which only pullout occurs, the area should be $2\pi rL$. This corresponds to the points in the first part of the CLP curve associated with the shortest L . By contrast, for conditions involving rupture of the fiber, the area should be πr^2 .

The pullout condition can be confirmed by observing the fiber, usually on a scanning electron microscope (SEM), after the test. This is illustrated in Fig. 9.7 for coir fiber/epoxy. In this figure, a short embedded length, Fig. 9.7a, was pulled out without rupture and left patches of resin, Fig. 9.7b, impregnating the surface. For longer embedded length, Fig. 9.7c, the fiber was tensile ruptured without slipping away from the epoxy block.

It is relevant to mention that the method of obtaining the IFSS based on the CLP curve provides not only interfacial information but also the critical length ℓ_c , which is important for composite design. For instance, fiber for which the natural length is greater than $15\ell_c$ are considered continuous [42]. In this case, the composite equations (rule-of-mixtures) for the strength and stiffness give maximum values.

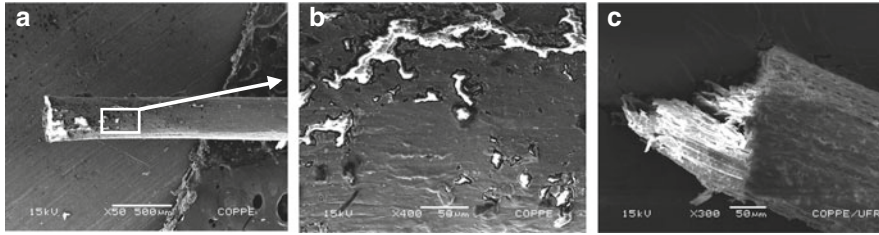


Fig. 9.7 After test surface conditions of coir fibers (a) complete pullout; (b) epoxy vestiges on fiber surface; and (c) ruptured point of a non-pulled out fiber

Table 9.2 Critical length, ℓ_c , and corresponding interfacial shear strength of lignocellulosic fibers in polymeric matrices

Lignocellulosic fiber/polymeric matrix	ℓ_c (mm)	IFSS (MPa)	Reference
Piassava/polyester	15.3	2.4 ± 0.5	Aquino et al. [14]
Curaua/polyester	10.2	3.4 ± 1.2	Monteiro et al. [47]
Curaua/epoxy	3.0	6.5 ± 6.7	Monteiro et al. [48]
Coir/polyester	5.4	3.8 ± 1.1	Monteiro and d'Almeida [36]
Coir/epoxy	5.6	3.4 ± 1.0	da Costa et al. [49]
Ramie/polyester	1.6	6.2 ± 2.3	Monteiro et al. [50]
Sisal/polyester	8.1	7.3 ± 2.0	Monteiro et al. [51]

Table 9.2 presents the critical length evaluated by CLP curves and corresponding IFSS, calculated by the Kelly and Tyson equation, for different lignocellulosic fibers embedded in thermoset polymeric matrices.

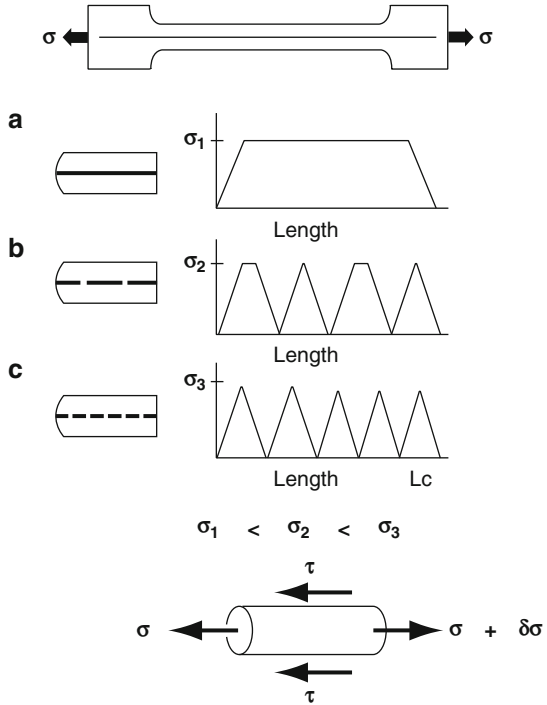
As an additional comment, Yue et al. [45] indicated that, apart from the failure by debonding followed by fiber pulling out, specimens sometimes exhibit failure through fiber fracture or matrix yielding. The authors suggested a restrained-top loading test condition as more convenient to ensure specimen failure via interfacial debonding, leading to pullout.

9.4 Single-Fiber Fragmentation Test

9.4.1 Fundamental Considerations

This is another micromechanical method for single fiber simulation of a composite fiber/matrix behavior. According to Herrera-Franco and Drzal [34], the single-fiber fragmentation (SFF) is a simple test with fewer parameters involved in its characterization. Figure 9.8 shows a schematic representation of the SFF test. In this figure, different stages, (a) to (c), of the test are presented together with the typical specimen (top) and the modeling of stresses acting on a fragment of fiber (bottom).

Fig. 9.8 Schematic of a single fiber fragmentation test. Reproduced with the kind permission of the publishers of [37]



The SFF test begins with a specimen composed of a single fiber embedded in a dumbbell-shaped tensile coupon, top of Fig. 9.8.

The schematic testing sequence shown in Fig. 9.8 indicates that, initially, a SFF specimen containing a continuous fiber (see Fig. 9.8a), is tensile tested until the fiber strength is reached. The fiber then fractures at some point where the stress concentration is high enough. As the tensile loading continues to increase, other ruptured points occur, Fig. 9.8b, in a process of fiber fragmentation. Finally, the fiber fragments, Fig. 9.8c, are so small that the applied load no longer reaches the fiber strength, and the fragmentation process ceases. This final unchanged fragment is associated with the fiber critical length, l_c . From the value of l_c , the IFSS can then be calculated by the Equation (9.2) developed by Kelly and Tyson [41] or Equation (9.3), of Hull and Clyne [43]. Another proposed relationship by Valadez-Gonzalez et al. [37] recognized that the distribution of fragments fits a two-parameter Weibull distribution, and then the IFSS (τ) could be calculated as

$$\tau = \frac{\sigma_f \Gamma}{2\beta} \left(1 - \frac{1}{\alpha}\right) \tag{9.7}$$

where α (shape) and β (scale) are Weibull parameters, while Γ is the gamma function.

Although simple, Herrera-Franco and Drzal [34] indicate that the SFF test has several shortcomings:

- The matrix must have a strain limit, at least three times greater than that of the fiber
- The matrix should have sufficient toughness to avoid fiber fracture-induced failure
- The fiber strength should be known at the critical length
- Transverse normal stresses could be higher due to Poisson's effects, resulting in a higher interfacial shear strength
- The state of stress at the fiber break is highly complicated by the presence of the penny-shaped crack, which could affect the failure mode of the interface, thus affecting the obtained values of interface strength
- Despite the sophisticated statistical techniques used to characterize the fiber fragment length distribution, the shear strength is calculated using an over-simplified representation of the state of stress occurring at the interface

9.4.2 Examples of SFF Test Results

The work of Valadez-Gonzalez et al. [37] was the only study reported so far to compare two methods, the SFP and the SFF, using a lignocellulosic fiber. In their work, the IFSS of henequen fibers embedded in polyethylene was separately evaluated by means of both SFP and SFF tests. The fibers were previously subjected to different surface chemical treatments aiming at improving the fiber/matrix adhesion. Table 9.3 shows the probable results obtained as a composition of Fig. 11 and Table 4 of Valadez-Gonzalez et al. [37] article.

Valadez-Gonzalez et al. [37] concluded that the IFSS for natural fibers embedded in thermoplastic matrices can be improved by morphological modifications caused by surface chemical treatments. Moreover, from the fiber fragmentation tests, higher IFSS were obtained than those with the single fiber pullout tests, Table 9.3. The authors attributed such discrepancies to the differences in the experimental configurations and mechanical solicitation in both arrangements. Additionally, differences in the mechanical behavior of the fibers that had been impregnated with the matrix

Table 9.3 Comparison between the IFSS of henequen fiber/polyethylene obtained by single fiber pullout (SFP) and single fiber fragmentation (SFF) tests for several fiber treatments. Reproduced with the kind permission of the publishers of [37]

Fiber condition	Single fiber pullout (SFP) test		Single fiber fragment (SFF) Test	
	By the fiber diameter	By the fiber perimeter	By the fiber diameter	By the fiber perimeter
No fiber treatment	2.4 ± 0.6	1.6 ± 0.3	4.4 ± 1.2	3.0 ± 0.9
Aqueous alkaline solution (AAS)	3.4 ± 1.0	2.2 ± 0.6	6.2 ± 1.3	4.3 ± 1.0
AAS + silane coupling agent	4.7 ± 0.6	3.1 ± 0.4	16.0 ± 1.8	11.0 ± 1.5
AAS and impregnated with diluted matrix solution	8.4 ± 0.4	4.1 ± 0.3	8.4 ± 1.4	5.8 ± 1.0

could also be responsible for the discrepancies. Finally, they stated that the results obtained from the fiber fragmentation test seem to be in better agreement with the effective mechanical properties measured for the laminated material.

9.5 Microbond Test

9.5.1 Fundamental Considerations

Still another micromechanical method for single fiber simulation of a polymer composite interfacial adhesion is the microbond test. This method was developed by Miller et al. [52] and initially applied for synthetic fibers. As mentioned by Craven et al. [53], the microbond test is suitable for any fiber that can carry only low loads. This is the particular case of silk, a strong natural fiber but with limited load bearing capacity due to diameters that can be finer than 50 μm . This could be the case of some lignocellulosic fibers such as the ramie with diameters of the order of 10 μm .

The microbond test is also mentioned as the microdroplet test [39] and believed to possess some of the characteristics of fiber pullout in composites [34]. The test consists of a microdroplet of still fluid polymeric resin deposited onto a fiber, as shown in the schematic diagram of Fig. 9.9 [53].

After the resin is cured, a steady increasing force is applied to the free end of the fiber (top in Fig. 9.9) in order to pull it out of the microdroplet. Load and displacement are monitored as the fiber is pulled axially until either complete pullout occurs or the fiber fractured [34]. The IFSS (τ) can be calculated from the force required to pull the fiber out of the microdroplet by means of Equation (9.1). According to Herrera-Franco and Drzal [34], the IFSS can also be calculated to a first approximation by

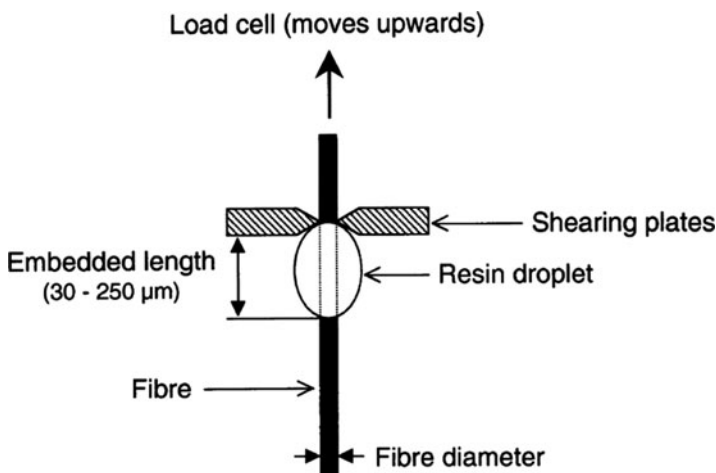


Fig. 9.9 Schematic diagram of the microbond test. Reproduced with the kind permission of the publishers of [53]

$$\tau = \frac{\sigma_f d}{2L} \quad (9.8)$$

where σ_f is the fiber tensile stress, d the fiber diameter, and L , the embedded length of the fiber, Fig. 9.9, inside the microdroplet.

It is recognized that the microbond test has the advantage of permitting almost any fiber/polymer matrix combination with a pullout force measurement at the moment of debonding. However, Herrera-Franco and Drzal [34] indicate serious inherent limitations:

- The debonding force is a function of the embedded length. When using very fine reinforcing fibers with diameters ranging from 5 to 50 μm , the maximum embedded length is of the range 0.05–1.0 mm. Longer embedded lengths cause fiber fracture.
- The meniscus that is formed on the fiber by the resin makes the measurement of the embedded length somewhat inaccurate.
- The small microdrop size makes the failure process difficult to observe.
- Most important, the state of stress in the droplet can vary both with size and with variations in the location of points of contact between the blades and the microdrop.
- The presence of a meniscus has a large effect on the interfacial stresses, which oscillate along the embedded fiber, thus making the practice of calculating an average shear strength value questionable. Also, premature failure of the meniscus region due to tensile stresses could lead to premature microdrop debonding of the fiber.
- Furthermore, it has been shown by Rao et al. [33] that the mechanical properties of the microdrop may vary with size because of variations in concentration of the curing agent.
- For a given fiber/matrix combination, a relatively large scatter in the test data is obtained from the microdrop test. Such wide distribution of shear strengths have been attributed mainly to testing parameters such as position of the microdrop in the loading fixture, droplet gripping, faulty measurement of fiber diameters, etc.

In addition, variation in the chemical, physical, or morphological nature of the fiber along its length will affect the results of interfacial shear strength measurements, which only consider very small sections.

9.5.2 Example of Microbond Test Results

Parks et al. [39] applied the microbond (or microdroplet) test to measure the IFSS of NaOH-treated ramie and kenaf fibers with different lengths embedded into an epoxy microdroplet as in Fig. 9.9. These lignocellulosic fibers/epoxy microdroplet specimens were fixed by a microdevice and tested to obtain the pullout force F and

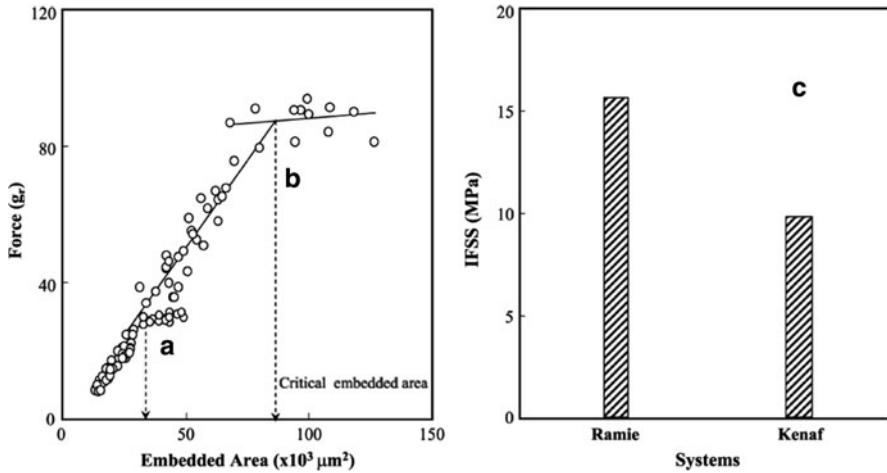


Fig. 9.10 Plots of pullout force versus embedded area for (a) untreated ramie fiber; (b) untreated kenaf fiber; and (c) corresponding IFSS for both. Reproduced with the kind permission of the publishers of [39]

then calculate the interfacial shear strength τ through Equation (9.1). Using different embedded areas, the authors obtained plots of F versus the embedded area and determined the corresponding IFSS, as in Fig. 9.10 [39].

In Fig. 9.10a, b, the critical embedded area was obtained by intersection of two linear regression lines: one associated with the fiber pullout, whereas the other with the fiber fracture linear regression line. The corresponding IFSS were given as par plots, Fig. 9.10c, from which apparently values of 15.7 MPa for ramie fiber/epoxy and 9.7 MPa for kenaf fiber/epoxy may be found.

9.6 Other Proposed Methods to Measure the IFSS

Other methods to evaluate the IFSS have been proposed mainly for synthetic fibers. Among these, the microbond, also known as the microindentation test, first proposed by Mandell et al. [54], has been theoretically investigated [34, 35] and applied to synthetic and metallic fibers. To the knowledge of the authors of this chapter, the microindentation test has not yet been used to measure the IFSS of lignocellulosic fibers embedded in polymeric resins. In spite of advantages listed by Herrera-Franco and Drzal [34], they also emphasized the following drawbacks for this test:

- The failure mode or locus of failure cannot be observed
- There exists the possibility of inducing artifacts by the surface preparation procedure
- The assumptions made to calculate the IFSS may not be valid
- Crushing of fibers is observed very frequently, limiting the variety of fibers to be tested

This last one, in particular, represents a strong limitation to test lignocellulosic fibers by the microindentation method.

For an extended review on current trends to characterize the fiber/matrix interphase as well as both direct and less direct methods for measuring the interfacial level of adhesion, the reader is referred to the work of Herrera-Franco and Drzal [34]. In this work, apart from the four methods and techniques already discussed (SFP, CLP, SFF, and microbond), all others have not been applied for lignocellulosic fibers.

Finally, a possible method for estimation of IFSS in lignocellulosic fiber composites could be based on the evaluation of the critical length ℓ_c at the condition of maximized mechanical properties [55, 56]. According to Nair et al. [56], as the fiber length increases, there is a chance for better orientation that may lead to an improvement in mechanical properties of the composites. Based on this assumption, critical lengths of 6 mm for sisal fibers in polyethylene [55] and 10 mm for sisal fibers in polystyrene composites were reported [56]. Even though the authors have not attempted to calculate the IFSS, these reported critical length values are comparable to those obtained for sisal fibers in polyester matrix [51, 57]. As earlier mentioned in this chapter, with the value of ℓ_c , the IFSS could then be calculated by means of Equation (9.6).

9.7 Concluding Remarks

It is unquestionable that the fiber/matrix interface is a region that uniquely affects a composite mechanical behavior. Drzal et al. [58] indicated that this region has different structures and compositions within a three-dimensional (3D) extension. This includes the 2D contact surface between fiber and matrix but also incorporates some finite thickness, making this interface region a complex interphase. The evaluation of adhesion and interfacial shear strength (IFSS) are, consequently, associated with a level of complexity. In principle, a simple pullout test using a piece of fiber with any small enough part of its length (L) embedded in a polymer block would suffice to determine the IFSS and, hence, the adhesion strength, by means of Equation (9.1). However, many factors such as the fiber's surface condition (chemical treatment), the structure and composition of the fiber/matrix interphase, as well as the 3D state of stress make the result of a single fiber pullout unreliable [34].

In the case of lignocellulosic fibers, this is even more critical, owing to the nonuniform characteristics as previously discussed in this chapter. That is the reason why so many methods based on sophisticated procedure and statistical analysis has been proposed and are still under investigation. Most of them have been applied to synthetic fibers. As shown throughout this chapter, only few methods: single fiber pullout test, critical length pullout curve, single fiber fragmentation test, and microbond test have directly been dedicated to lignocellulosic fibers embedded in polymeric matrices. Surprisingly, in spite of the above-mentioned complexity of the fiber matrix interphase, all results obtained so far for

lignocellulosic fibers agreed with relatively low values for the IFSS. In fact, these values in Tables 9.1–9.3 ranges from 2.4 to 7.3 MPa for untreated fibers. This corroborates the expected weak adhesion between lignocellulosic fibers and the common (commercially available) polymeric matrices.

Another relevant comment is that the research efforts to improve the fiber/matrix adhesion by surface chemical treatment of the lignocellulosic fiber are showing promising results. IFSS values above 15 MPa [37, 39] were found and represent, in some cases, more than three times the interfacial strength of corresponding untreated fibers. In principle, substantial improvement in the performance of lignocellulosic fibers adhesion to polymer matrix might be achieved with further investigation. This is a necessary condition in the current effort towards matching the mechanical behavior of synthetic fiber composites, especially the “fiberglass.” The IFSS of synthetic fiber/polymer matrix systems are still comparatively higher than the corresponding ones of lignocellulosic fibers. For instance, carbon fiber/epoxy systems [34] may reach values of IFSS above 50 MPa for all common pullout methods and 95.28 MPa in the Iosipescu shear test.

As reviewed in this chapter, for lignocellulosic fibers, the development of stronger interfaces with polymeric matrices has already given the first steps. The world expectation that natural materials assume a greater participation in industrialized products is a motivation for future works on the possibility of lignocellulosic fibers replacing synthetic fibers in polymer composites. With improved IFSS, this will certainly become a reality and hopefully will contribute to the quality of our environment.

Acknowledgments The authors sincerely acknowledge the Publishers: Elsevier Publishers, Wiley InterScience Publishers, SpringerLink Com and Brazilian Association for Metallurgy and Materials (ABM) for their kind permission to reproduce some of the Figures and Tables used in this chapter. The authors thank the support to this investigation by the Brazilian agencies CNPq, CAPES, FINEP, and FAPERJ. The collaboration of Lucas L. da Costa, Jarbas Bravo Neto, Wellington P. Inacio, Romulo L. Loiola, Tammy G. Portela, Isabela L.A. da Silva, and Alice B. Bevitore is also acknowledged. One of the authors (Dr.KGS) acknowledges the encouragement and interest shown by the three Institutions with which he is presently associated with.

References

1. Agarwal BD, Broutman LJ (1990) Analysis and performance of fiber composites. Wiley, New York
2. Ashbee KHG (1993) Fundamental principles of fiber reinforced composites. Technomic, Lancaster
3. Mallick PK (1993) Fiber-reinforced composites – materials, manufacturing, and design. Marcel Dekker, New York
4. Kalia S, Kaith BS, Kaur I (2009) Pretreatment of natural fibers and their application as reinforcing materials in polymer composites – a review. *Polym Eng Sci* 49:1253–1272
5. Houghton JT (2004) Global warming – the complete briefing. Cambridge University Press, Cambridge

6. Nabi-Sahed D, Jog JP (1999) Natural fiber polymer composites: a review. *Adv Polym Technol* 18:221–274
7. Bledzki AK, Gassan J (1999) Composites reinforced with cellulose-based fibers. *Prog Polym Sci* 4:221–274
8. Mohanty AK, Misra M, Hinrichsen G (2000) Biofibers, biodegradable polymers and biocomposites: an overview. *Macromol Mater Eng* 276(277):1–24
9. Mohanty AK, Misra M, Drzal LT (2002) Sustainable biocomposites from renewable resources: opportunities and challenges in the green material world. *J Polym Environ* 10:9–26
10. Eichhorn SJ, Baillie CA, Zafeiropoulos N et al (2001) Review of current international research into cellulosic fibres and composites. *J Mater Sci* 36:2107–2113
11. Wambua P, Ivens I, Verpoest I (2003) Natural fibers: can they replace glass and fibre reinforced plastics? *Compos Sci Technol* 63:1259–1264
12. Satyanarayana KG, Guimarães L, Wypych F (2007) Studies on lignocellulosic fibers of Brazil. Part I: Source, production, morphology, properties and applications. *Compos A* 38:1694–1709
13. Aquino RCMP, d'Almeida JRM, Monteiro SN (2001) Flexural mechanical properties of piassava fibers (*Attalea funifera*)-resin matrix composites. *J Mater Sci Lett* 20:1017–1019
14. Aquino RCMP, Monteiro SN, d'Almeida JRM (2003) Evaluation of the critical fiber Plength of iassava (*Attalea funifera*) fibers using the pullout test. *J Mater Sci Lett* 22:1495–1497
15. de Deus JF, Monteiro SN, d'Almeida JRM (2005) Effect of drying, molding pressure, and strain rate on the flexural mechanical behavior of piassava (*Attalea funifera Mart*) fiber-polyester composites. *Polym Test* 24:750–755
16. d'Almeida JRM, Aquino RCMP, Monteiro SN (2006) Tensile mechanical properties, morphological aspects and chemical characterization of piassava (*Attalea funifera*) fibers composites. *Compos A* 37:1473–1479
17. Leão AL, Tan IH, Caraschi JC (1998) Curaua fiber – a tropical natural fiber from Amazon – potential and applications in composites. In: Proceedings of the internacional conference on advanced composites, Hurghada, Egypt, pp 557–564
18. Monteiro SN, Aquino RCMP, Lopes FPD et al (2006) Mechanical behavior and structural characteristics of polymeric composites reinforced with continuous and aligned curaua fibers (in Portuguese). *Rev Mater* 11:197–203
19. Monteiro SN, Ferreira AS, Lopes FPD (2008a) TMS Rupture mechanisms in composites reinforced with curaua fibers. In: Proceedings of the TMS 137th annual meeting and exhibition, New Orleans, LA, USA, pp 117–123
20. Silva RV, Aquino EMF (2008) Curaua fiber: a new alternative to polymeric composites. *J Reinf Plast Comp* 27:103–112
21. d'Almeida JRM, Boynard CA (2000) Morphological characterization and mechanical behavior of sponge gourd (*Luffa-cylindrica*)-polyester composite materials. *Polym Plast Technol Eng* 39:489–499
22. Boynard CA, Monteiro SN, d'Almeida JRM (2003) Aspects of alkali treatment of sponge Gourd (*Luffa cylindrica*) fibers on the flexural properties of polyester matrix composites. *J Appl Polym Sci* 87:1927–1932
23. Santos RS, Silveira ELC, Souza CML (2007) Study of the mechanical properties of thermoset polymeric matrix composites reinforced with buriti fibers (in Portuguese). In: Proceedings of the 30th Annual Meeting of the Brazilian Chemistry Society, Águas de Lindoia, Brazil, p 1
24. Monteiro SN, Lopes FPD, Costa LL et al (2008b) Study of the buriti waste fiber as a possible reinforcement of polyester composites. In: Proceedings of REWAS 2008: Global symposium on recycling, waste treatment and clean technology, Cancun, Mexico, pp 517–522
25. Monteiro SN, Lopes FPD, Ferreira AS, Nascimento DCO (2009) Natural fiber polymer matrix composites: cheaper, tougher and environmentally friendly. *JOM* 61:17–22
26. Suddell BC, Evans WJ, Isaac DH et al (2002) A survey into the application of natural fibre composites in the automobile industry. In: Proceedings of the 4th international symposium on natural polymers and composites – ISNAPol, São Pedro, SP, Brazil, pp 455–461

27. Marsh G (2003) Next step for automotive materials. *Mater Today* 6:36–43
28. Hill S (1997) Cars that grow on trees. *New Scientist* 153:36–39
29. Zah R, Hischier R, Leão AL et al (2007) Curaua fibers in automobile industry – a sustainability assessment. *J Clean Prod* 15:1032–1040
30. Mercedes-Benz (2008) web page <http://www.mercedes-benz.com.br>. Accessed 30 August 2008
31. Piggot MR (1987) The effect of interface/interphase on fiber composites properties. *Polym Comp* 8:291–297
32. Désarmont G, Favre JP (1991) Advances in pull-out testing and data analysis. *Comp Sci Technol* 42:151–181
33. Rao V, Herrera-Franco P, Ozello AD et al (1991) A direct comparison of the fragmentation test and the microbond pullout test for determining the interfacial shear strength. *J Adhes* 34:65–67
34. Herrera-Franco PJ, Drzal LT (1992) Comparison methods for the measurement of fibre/matrix adhesion in composites. *Composites* 23:2–27
35. Kim JK, Lu S, Mai Y (1994) Interfacial debonding and fibre pull out stresses. *J Mater Sci* 29:554–561
36. Monteiro SN, d’Almeida JRM (2006) Pullout test in lignocellulosic fiber – a methodology of analysis. *Rev Mater* 11:189–196 (in Portuguese)
37. Valadez-Gonzalez A, Cervantes-Uc JM, Olayo R, Herrera-Franco PJ (1999) Effect of fiber surface treatment on the fiber – matrix bond strength of natural fiber reinforced composites. *Compos B* 30:309–320
38. Sydenstricker THD, Mochnaz S, Amico SC (2003) Pull-out and other evaluations on sisal-reinforced polyester biocomposites. *Polym Test* 22:375–380
39. Park J-M, Son TQ, Jung J-G et al (2006) Interfacial evaluation of single ramie and kenaf fiber/epoxy resin composites using micromechanical test and nondestructive acoustic emission. *Comp Interf* 13:105–129
40. Tanaka K, Minoshima, KM, Grela V et al (2002) Characterization of the aramid/epoxy interfacial properties by means of pull-out test and the influence of water absorption. *Comp Sci Technol* 62:2169–2177
41. Kelly A, Tyson WR (1965) *High strength materials*. Wiley, New York
42. Callister WD Jr (2007) *Materials science and engineering – an introduction*, 7th edn. Wiley, New York
43. Hull D, Clyne TW (1981) *An introduction to composite materials*. Cambridge University Press, Cambridge
44. Kelly A (1966) *Strong solids*. University Press, London
45. Yue CY, Looi HC, Quek MY (1995) Assessment of fibre-matrix adhesion and interfacial properties using the pullout test. *Int J Adhes Adhes* 15:73–78
46. Yue CY, Cheung WL (1992) Interfacial properties of fibrous composites: Part I. Model for the debonding and pullout processes. *J Mater Sci* 27:3173–3180
47. Monteiro SN, Aquino RCM P, Lopes FPD (2008) Performance of curaua fibers in pullout tests. *J Mater Sci* 43:489–493
48. Monteiro SN, Ferreira AS, Lopes FPD (2009b) Pullout tests of curaua fibers in epoxy matrix for evaluation of interfacial strength. In: *Proceedings of the TMS 138th annual meeting and exhibition, San Francisco, USA*, pp 1–7
49. da Costa LL, Santafé Jr HPG, Monteiro SN et al (2008) Pullout tests of coir fibers embedded in epoxy matrix. (in Portuguese). In: *Proceedings of the 63th annual congress of the Brazilian association for metallurgy and materials, Santos, São Paulo*, pp 1–10
50. Monteiro SN, Margem FM, Bravo Neto J (2010) Evaluation of the interfacial strength of ramie fibers in polyester matrix composites. In: *Proceedings of the TMS 139th annual meeting and exhibition, Seattle, USA*, pp 1–8
51. Monteiro SN, Inacio WP, Lopes FPD et al (2009c) Characterization of the critical length of sisal fibers for polyester composite reinforcement. In: *Proceedings of the TMS 138th annual meeting and exhibition, San Francisco, USA*, pp 1–8

52. Miller B, Muri P, Rebenfeld LA (1987) Microbond method for determination of the shear strength of a fiber/resin interface. *Compos Sci Tech* 28:17–32
53. Craven JP, Cripps R, Viney C (2000) Evaluating the silk epoxy interface by means of the microbond test. *Compos A* 31:653–660
54. Mandell JF, Grande DH, Hong KCCT (1989) Fibre-matrix bond strength studies of glass, ceramic and metal matrix composites. *J Mater Sci* 23:311–328
55. Joseph K, Thomas S, Pavithran C et al (1993) Tensile properties of short sisal fiber-reinforced polyethylene composites. *J Appl Polym Sci* 47:1731–1739
56. Nair KCM, Diwan SM, Thomas S et al (1996) Tensile properties of short sisal fiber-reinforced polystyrene composites. *J Appl Polym Sci* 60:1483–1497
57. Chand N, Rohtgi PK (1986) Adhesion of sisal fibre-polyester system. *Polym Commun* 27:157–160
58. Drzal LT, Rich MJ, Lloyd PF (1982) Adhesion of graphite fibers to epoxy matrices. I. The role of fiber surface treatment. *J Adhes* 16:1–30

Chapter 10

The Structure, Morphology, and Mechanical Properties of Thermoplastic Composites with Lignocellulosic Fiber

Slawomir Borysiak, Dominik Paukszta, Paulina Batkowska,
and Jerzy Mańkowski

Abstract This chapter discusses the supermolecular structure and interphase phenomenon in composite-reinforced natural fibers. We analyzed the formation of the polymorphic forms in polypropylene (PP) matrix. It was found that in the composites with natural fibers, the hexagonal form arises when the fibers are in motion in relation to the polymeric matrix. of Moving temperature of the natural fibers was found to have a strong influence on the content of the hexagonal modification. If the temperature of the moving fibers is low, then the amount of β -PP significantly increases. The content of β -PP also depends on the rate of the moving of fibers; however, the chemical modification of the natural fiber's surface reduces the content of this form. Also, the processing conditions play an important role for structural changes in PP matrix.

Further, this chapter provides a survey about the formation of a transcrystalline layer in the composite system. The occurrence of transcrystallization was found to strongly depend on the type of chemical treatment of the fiber surface. Predominant nucleation ability was found for unmodified fibers. However, chemical modification of fiber surface slightly depressed the nucleation of polypropylene matrixes.

The influence of physical and chemical treatment methods of natural fibers on mechanical properties was analyzed also. Additionally, the mechanical and other physical properties of the composite are generally dependent on the length, content, and dispersion of fibrous filler and processing parameters.

Keywords Composites · Mechanical properties · Natural fibers · Supermolecular structure · Transcrystalline layer

S. Borysiak (✉)

Poznan University of Technology, Institute of Chemical Technology and Engineering, Skłodowskiej-Curie 1, 60-965 Poznan, Poland

e-mail: Slawomir.Borysiak@put.poznan.pl

Contents

10.1	Introduction	264
10.2	Polymorphism in Isotactic Polypropylene Used as Composite Matrix	265
10.3	Analysis of Pseudo-hexagonal Form Created in Composites Containing Fibers	265
10.3.1	Influence of Fibers Pulling in Polypropylene Matrix	265
10.3.2	Influence of Processing Parameters	271
10.4	Interphase Phenomenon in Fiber/Polypropylene Composites	272
10.4.1	Formation of the Transcrystalline Layer in Composite Materials	272
10.4.2	Transcrystallization of Isotactic Polypropylene on the Surface of Lignocellulosic Fillers	274
10.4.3	Effect of Chemical Modification on Transcrystalline Layer Formation	276
10.4.4	Influence of Lignocellulosic Fibers on the Nucleation and Polypropylene Crystallization Process	277
10.5	The Analysis of Various Factors on Mechanical Properties of Composite Polypropylene–Natural Fibers	281
10.5.1	Effect of Improvement of an Interphase Adhesion on the Mechanical Properties of Composites	281
10.5.2	The Effect of Length, Content, and Dispersion of Fibrous Filler and Processing Parameters on the Mechanical Properties of Composites ...	284
10.6	Conclusions	285
	References	286

10.1 Introduction

It is well established that the supermolecular structure of semicrystalline matrix is of pivotal importance to the mechanical and physical behavior of composite materials. We analyzed the formation of the polymorphic forms in polypropylene composites with natural fibers. Moreover, analysis of the effect of processing conditions, during preparation of the composites, on the structure of polymer matrix is a focal issue because polymorphic changes in polypropylene can be stimulated by the temperature of processing and the shearing forces applied.

In thermoplastic/fiber systems, the fiber may act as a series of nucleating sites for the polymer, resulting in a transcrystalline region around the fiber. In this chapter, a large number of factors have been demonstrated to contribute to the interactions across the interface. The effect of various conditions such as the chemical modification of natural fibers and nucleation ability of semicrystalline matrix on the formation of transcrystallinity was investigated.

Moreover, obtaining composites filled with the lignocellulosic component with desired strength properties require consideration of many factors having an effect on the final macroscopic properties. The objectives of this study is to analyze the effect of the following factors such as the adhesion between the components, filler content, fiber length of fibrous filler, filler distribution, and the effect of processing parameters on the mechanical properties of composites.

10.2 Polymorphism in Isotactic Polypropylene Used as Composite Matrix

Polymorphism, which means existence of different crystalline forms, is a phenomenon observed in many organic and inorganic compounds. Also, natural (e.g., cellulose) and synthetic polymers show numerous polymorphic forms. Among synthetic semicrystalline polymers, which can be a matrix in composites with lignocellulosic materials, the isotactic polypropylene is the one to take a close look on this phenomenon.

In polypropylene composites containing lignocellulosic materials, one can expect two forms, α and β , because the conditions required to create for the third form – γ are not existing when forming and processing composites containing lignocellulosic materials. The most stable form is the α phase, crystallizing in a monoclinic unit. The form β , also known as hexagonal or pseudo-hexagonal [1, 2], is in fact a higher energetic form, crystallizing in triclinic unit. This phase used to be called a hexagonal due to the relation of network constants $a = b$ and an angle between them – 120° . This choice of an elementary cell is characteristic for hexagonal and trigonal units. However, the location of polypropylene helices in elementary cell shows that it lacks the elements of symmetry typical for these systems.

The mechanical properties of the α phase polypropylene are generally better than that of β form, except for impact resistance. Therefore, in products specially exposed to impact, the matrix containing the pseudo-hexagonal form is a better choice [3].

All lignocellulosic materials contain no active nucleants that can initiate forming the hexagonal form. Therefore, this form can be present in composites under shearing forces in a temperature interval typical for these forces to appear. β phase cannot be found in products made by press molding. The structural analyses of polymers and composites are very important as the structure of these materials is determined, to a high extent, by molecular and supermolecular structure.

10.3 Analysis of Pseudo-hexagonal Form Created in Composites Containing Fibers

10.3.1 Influence of Fibers Pulling in Polypropylene Matrix

As reported earlier by Varga and Karger-Kocsis [4, 5] and Hoecker and Karger-Kocsis [6], the movement of glass or carbon fibers in PP matrix causes forming the β polypropylene. So, the question was asked: does the movement of natural fibers affect the formation of polypropylene matrix crystalline structure? These kinds of interactions are present in manufacturing and processing of polymers. Solving this

problem may offer the way to change the polypropylene structure and consequently the properties of the final products.

To solve the problem outlined above, it is necessary to analyze the following problems and find answers to the following questions:

- How does the movement of natural fibers affect the formation of polypropylene matrix?
- How does the temperature in which the fiber is moved, the type of fiber, the modification, and the speed of fiber movement fibers affect the formation of polypropylene matrix?
- What is the range of the structural changes in the matrix in function of the distance on which the fiber is moved?

By trying to answer the above questions, the trials were made in which the polypropylene-containing fibers were heated up to 220°C. Then the samples were cooled to the predefined temperature in which the fiber was pulled at a predefined speed. The structure analysis was carried out by the WAXS technique.

We tested a stationary system and a system where flax fiber was pulled at $w = 0.62$ mm/s for different temperatures in the range 180–130°C [7, 8].

Obtained results showed clearly that the presence of the flax fiber itself, in the crystallizing polypropylene, causes no formation of hexagonal phase (Fig. 10.1). For samples where fiber was moved, the X-ray patterns revealed the diffraction maximum at 2θ 16.2°, which proves the presence of β form. The amount of this form was calculated from the diffractograms according to the well-known Turner-Jones formula [1]. It was shown that the formation and the amount of this form in composite matrix depend on the temperature at which the fiber is moved in

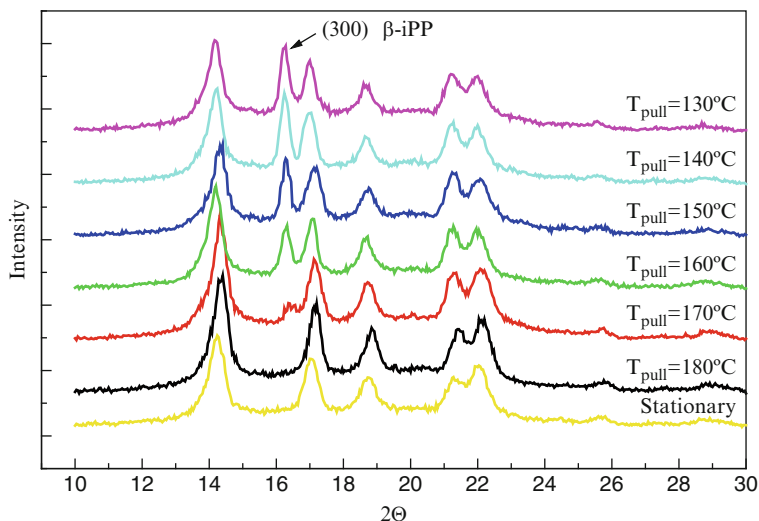


Fig. 10.1 The X-ray diffraction pattern of iPP/flax composites, where fibers were pulled with speed 0.62 mm/s in the temperature range 130–180°C [8]

the matrix. However, there is a critical temperature value of 180°C above which the hexagonal form is not induced. Thus, the formation of the polymorphic β form is connected with forced macromolecular orientation during crystallization.

Further research showed that the same effect can be obtained when using other natural fibers, for instance, hemp or sisal.

Further studies investigated the effect of earlier chemical modification of natural fibers on arising of hexagonal form of polypropylene. For these studies, it was important to consider the content of induced hexagonal phase in crystalline phase of the polypropylene matrix. Figure 10.2 shows how the content of β form changes upon the temperature in which modified and unmodified hemp fiber is moved. It is worth to mention that the curves course of modified and unmodified flax fiber is very similar to that of hemp [8, 9].

It was shown that crude natural fibers and fibers modified by mercerization process induce much better creation of polymorphic β form than fibers modified to improve adhesion with nonpolar polypropylene. It was found that the lower the temperature of the matrix during fiber movements, the higher the content for hexagonal form. Over 180°C , the hexagonal phase is not formed and polypropylene crystallizes only in a monoclinic α form. However, in the range $150\text{--}180^{\circ}\text{C}$, the content of hexagonal form decreases as the temperature of polypropylene matrix rises. It was also found that chemical modification of fibers causes reduction of hexagonal form generation that is formed as a result of moving the fibers. For flax fibers, this reduction is estimated to be about 25%. A similar tendency is observed for hemp fibers modified by an acetic anhydride (Fig. 10.2).

In the analysis of the induction of β form creation by lignocellulosic fibers moving in relation to the matrix, a question should be answered: does the change

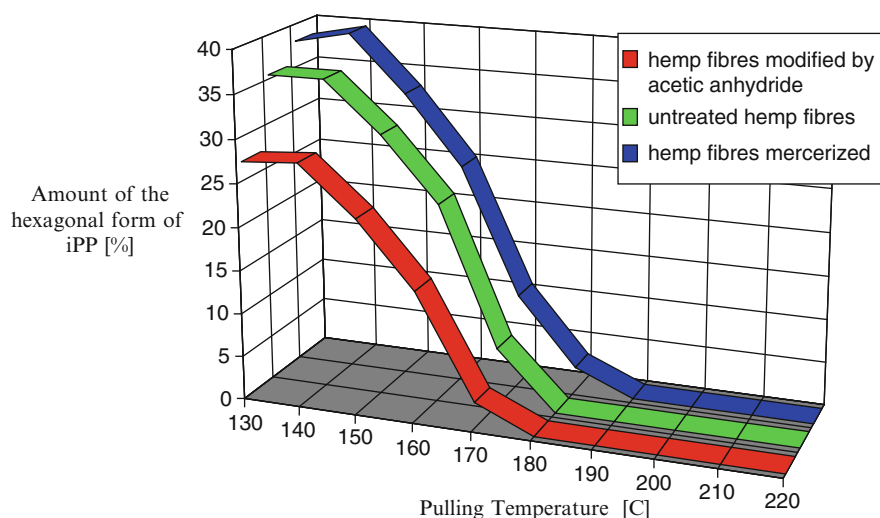


Fig. 10.2 The amount of hexagonal form of iPP versus pulling temperature for hemp fibers [8]

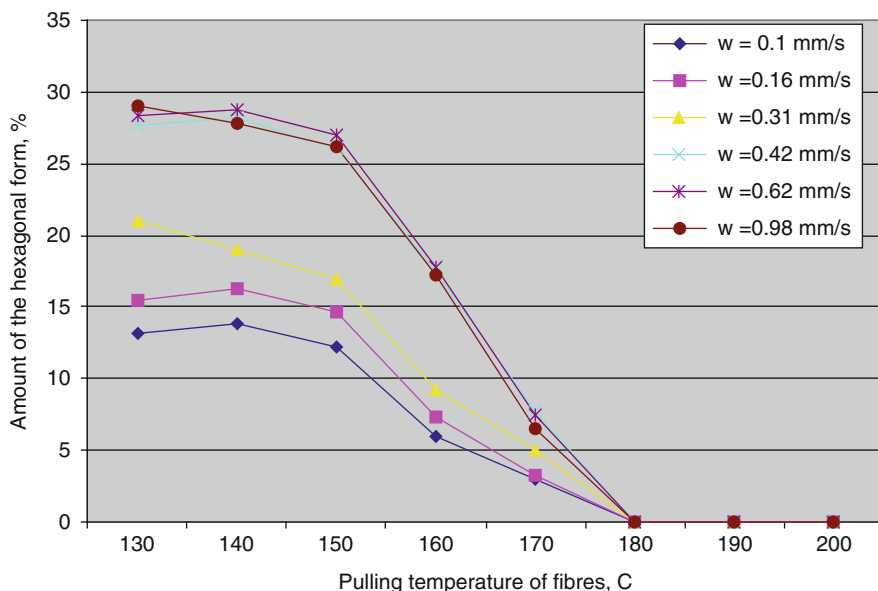


Fig. 10.3 The amount of hexagonal form versus pulling temperature of flax fibers for different speed of fiber pulling

of the speed of fiber movement in the polypropylene matrix have an effect on the observed phenomenon?

The studies were focused on unmodified flax fibers and fibers modified with an acetic anhydride. The speed of fibers moved in the matrix was from 0.10 up to 0.98 mm/s.

Figure 10.3 shows that the amount of induced hexagonal form reaches the optimum value at the speed of 0.42 mm/s. The content of β form does not increase nor decrease at higher speeds of fiber pulling. In the case of modified fibers, the dependences are similar; however, the amount of form that is being created does not exceed 25%. Additionally, the optimum speed of fiber moving, over which the content of the form β does not increase, is higher – 0.62 mm/s. Earlier findings referring to not inducing the crystalline phase above 180°C were also confirmed.

It would seem that modified fibers, in the aspect of adhesion improvement, should induce creation of polymorphic β form to a higher degree. Moreover, the experiments conducted on carbon and polypropylene fibers confirmed the adverse dependence between the adhesion and generation of hexagonal form in the surroundings of moving fiber. Thus, the alternation of interphase interactions caused by the increase of adhesion in the system polypropylene with lignocellulosic fibers is not the only factor having the effect on the polymorphism phenomenon in composite matrix.

The parallel research conducted at our laboratory by DSC, PLM, and SEM [7] techniques were to explain why the chemical modification with agents promoting adhesion decreases the nucleation activity of hexagonal form crystallization

process. Mercerization of fibers only causes inducing of form β in the amount comparable to that achieved with unmodified fibers. Native flax fibers and hemp have embossment – roughness and considerable number of pores on the surface. Mercerization, to some extent, “smoothens” the surface of the cuticle, but on the other hand, it causes fiber to split. Chemical modification, e.g., with acetic anhydride, causes binding of elementary fibers in bigger strands with uniform surface. That is why moving of modified fibers is ultimately moving polypropylene chains bonded to the flax fiber by adhesion in relation to polypropylene chains of the matrix. Such movement causes no creation of such strong shearing forces as in the case of native and mercerized fiber movement – where the surface of the lignocellulosic fiber is moved against the matrix.

Thus, the topography of the outer surface of modified fibers, having higher specific surface, can be an important factor influencing the creation of β form during the fiber movement in the matrix.

Another objective of β form induction analysis, besides α form that is most often observed, is to investigate in what distance from the moved fiber the form β is present. The range of structural changes caused by moving fibers has not only a cognitive importance but also a practical dimension for composite manufacture.

Figure 10.4 shows the dependence between the content of hexagonal form and the distance from moving unmodified flax fiber. It is clearly visible that interaction is very intense in the range up to 2 mm, while in the range over 2 mm from the surface of moved fiber, the content of β form reduces drastically. In the range up to 7 mm, the amount of this form is only identified by traces, while in range over 7 mm cannot be observed at all.

It is worth mentioning an interesting analogy of increasing the crystalline degree of polypropylene matrix with the increasing presence of hexagonal form in analyzed

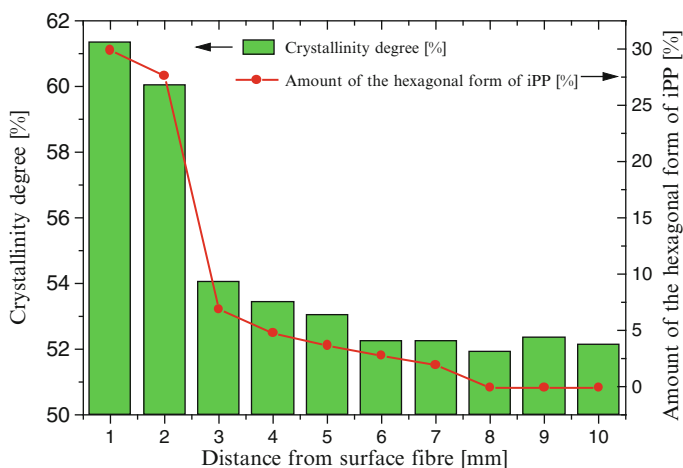


Fig. 10.4 Degree of crystallinity of iPP and the amount of the hexagonal form of iPP versus distance from surface fibers [8]

samples. The degree of matrix crystallinity increases with the reduction of temperature at which the fiber is moved. Additionally, at the nearest range from the moved fiber, the content of β form is not only the highest one but the degree of crystallinity of polymeric matrix is also much higher, which has been presented in Fig. 10.4.

Figure 10.5 shows morphology in flax fiber/polypropylene composites after crystallization in dynamic conditions. Microscopic investigations confirmed the presence of both phases (α and β) in the polypropylene layer exposed to shearing forces.

As we can seen in Fig. 10.5b, the morphology of the composite after selective melting at 150°C was observed.

It is visible that after remelting, the β -form is not present and in consequence the α phase exist only. No presence of distinct thin layer of row-nuclei was found on

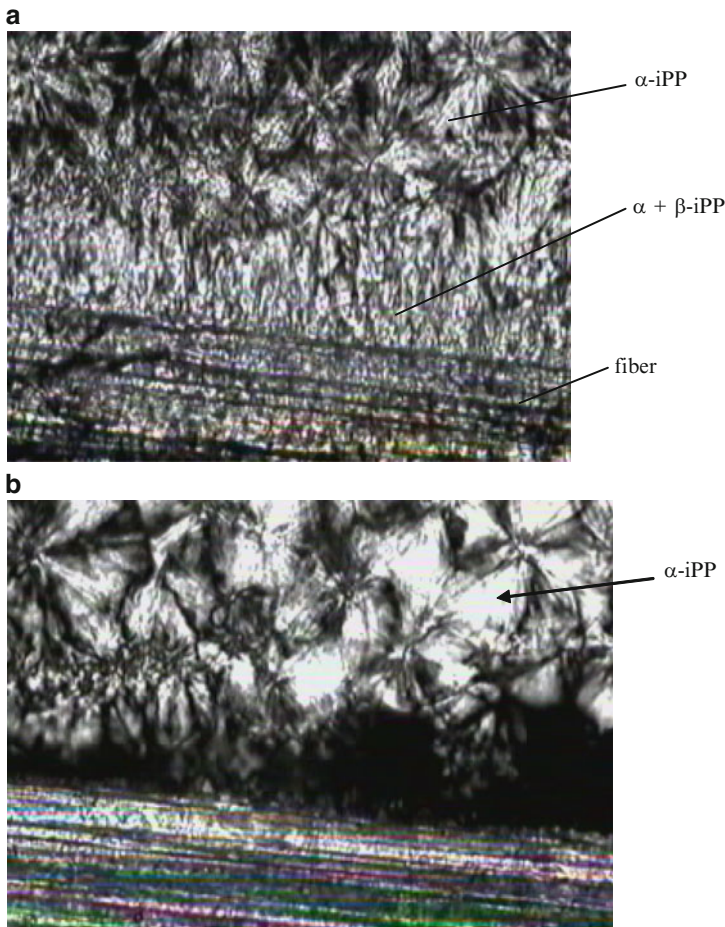


Fig. 10.5 Optical micrographs showing the transcristallization in flax fiber/polypropylene composites. (a) crystallization temperature -130°C , speed of fibers pulling -0.42 mm/s, (b) after selective melting in temperature -150°C of sample showed in Fig. 10.5a

the surface of the fibers. According to Varga and Karger-Kocsic [4], the layer of row-nuclei forms in the close neighborhood of pulled fiber is built of form α crystallites having the ability to nucleation of hexagonal form on their surface. Our experiments do not contradict the previously mentioned considerations but we believe that topography of lignocellulosic materials results in the deterioration of the nucleation and crystallization of the polypropylene matrix. It is known that surface roughness of different fillers is one of the possible causes of development of transcrystalline layers. Transcrystallization phenomena will be described in second chapter.

10.3.2 Influence of Processing Parameters

10.3.2.1 Extrusion Process

During extrusion process, especially in the extruding die, shearing forces (similar to the model studies described above) can be the reason of structural changes in polypropylene matrix. The investigations on extrusion process of polypropylene composite containing short flax fiber, conducted at different nozzle temperatures, confirmed that at temperatures of 180–200°C no β phase can be found in the extrudate. As the processing temperature reduces, beginning from 180°C, the process of inducing form β commences. The content increase of this form in the extrudate is connected first of all with decreasing the temperature in the extruding die as well as with increasing of fiber content in the composite.

In case of obtaining composites in the form of granulate, the phase variability is not very important as the composite is meant for further processing to obtain a desired element. However, in the case of extrusion, the continuous profiles such as pipes or troughs and the presence of hexagonal phase can considerably influence the properties of the final products.

10.3.2.2 Injection Molding

The hexagonal form of polypropylene in molds can be observed more often than in extrudate due to the fact that the polymer is injected into the form of much lower temperature than the temperature at which the fibers were pulled, over which no polymorphic form of polypropylene is formed [10]. Analyzing the earlier described structural studies, this temperature was called the critical temperature of hexagonal form of isotactic polypropylene forming.

Additionally, besides the movement of fibers occurring in a whole bulk of molten polymer, the phenomenon of shearing is also present, which occurs between polypropylene chains and injection mold. It was found that a small amount (5% by weight) of flax or hemp fibers in injected polymer already causes the presence of hexagonal form in molds. As the content of fibers in the composite increases (by weight), the amount of induced β form increases and exceeds 25% at 10% fiber content in the composite. Further increasing of short fiber content

in the composite causes no considerable increase of hexagonal form amount, which is in accordance with earlier described model studies conducted for single fibers pulled in the mass of the composite. It was confirmed that unmodified fibers initiate the creation of form β to a higher degree. It was also observed that in layers adjacent to walls of the injection form, i.e., where the shearing forces are stronger, the amount of polymorphic form is significantly higher than inside the molds [10].

10.3.2.3 Fiber Pulling During Press Molding

Industrial application of fiber pulling inside the crystallizing polypropylene matrix can be a method for manufacturing products characterized by a higher impact resistance and elasticity; however, the advantages of the products are the result of the presence of hexagonal form [9].

The forming method has it that isotactic polypropylene is formed as a board on which one or more parallel layers of fibers are applied. Additionally, on one side, the ends of fibers must reach out over the edge of the board to be caught and pulled. Next, the second polypropylene board is applied. The boards are heated to 175–285°C at a constant or increased pressure, and then the set is cooled down. Below 150°C, the fibers are moved to the distance up to few millimeters at 0.01–0.1 m/s. Having obtained the desired shape, the product is cooled down to the ambient temperature [3]. The technique presented in the cited patent description ensures high content of β form in the polypropylene composite reinforced with natural fiber.

10.4 Interphase Phenomenon in Fiber/Polypropylene Composites

The results of research conducted during the last decade confirm the nucleating character of lignocellulosic filler in polymeric composites. Natural fibers added to polymeric composites are the active source of creating a nucleus of crystallization. The addition of the filler reduces the interphase energy semicrystalline polymer-filler and consequently makes the crystallization process easier. A “foreign” surface as the filler structure, by its presence, makes it possible.

10.4.1 Formation of the Transcrystalline Layer in Composite Materials

A transcrystalline layer (TCL) is the supermolecular crystalline structure, induced by an oriented growth in the presence of the foreign surface. Transcrystallization occurs when the nucleation density of a solid filler that is in contact with melted

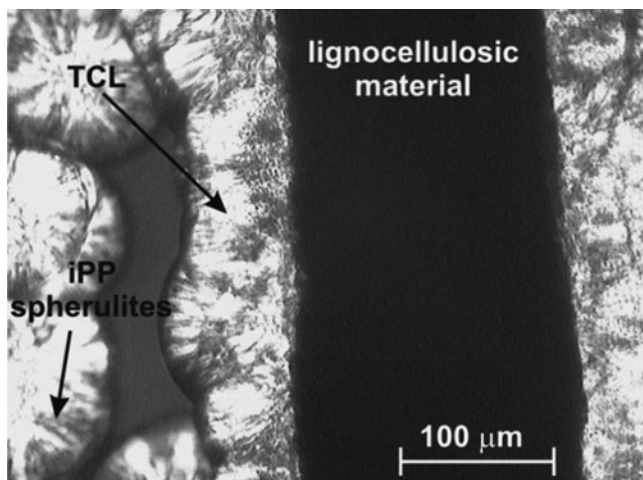


Fig. 10.6 Transcrystalline layer formed as a result of crystallization of iPP with lignocellulosic material

polymer is clearly higher on the surface than the density of nucleation in the bulk of melt.

Transcrystallization is influenced by many factors:

- Matrix topography
- Crystallization initiated by shearing
- Matrix surface energy
- Adsorption on small particles

High density of nuclei on foreign surface causes disturbance in spherulites growth, which results in the only possible growth – perpendicularly to the surface. As a result, transcrystalline front will emerge parallel to the surface. Transcrystallization is possible when nucleation energy conditions are more favorable on the surface than in the bulk of the melt. The microscopic photograph of TCL is shown in Fig. 10.6.

Presence of TCL changes the properties of crystalline matrix. Transcrystallization of isotactic polypropylene in the presence of different fibers has been thoroughly analyzed. Gray as the first one provided detailed description of isotactic polypropylene behavior in the presence of wood fibers using polarized light microscopy. He observed that when melted polymer is cooled down, it crystallizes in spherulite forms in nonisothermal and isothermal conditions, creating additionally a TCL.

Results of many researches confirm the presence of TCL as the effect of nucleation ability of different substances. Among the factors inducing transcrystallization in polyolefin matrix, the following fillers can be listed:

- Lignocellulosic material:
 - Kenaf fibers [11]
 - Wood fibers [12–14]

- Thermomechanical pulp [15]
- Flax fibers [16, 17]
- Spanish Broom (*Spartium junceum*) [18]
- Bamboo fibers [19]
- Cotton fibers [20]
- Cellulose nanocrystals from ramie and flax [21]
- Glass fibers [22]
- Aramid fibers [22, 23]
- Carbon fibers [22, 24]
- Carbon nanotubes [25]
- Talc [26]
- Nylon-6 fibers [27]
- PET fibers [28]
- Isotactic PP fibers [29].

Observations of polypropylene crystallization by polarized light microscopy helped to understand phenomena on interphase of polymer-filler. When analyzing the influence of the filler, many researchers noted transcrystallization of the polypropylene as a result of high enough nucleation density on the filler's surface and also in the presence polypropylene fibers. The addition of both mineral substances and natural composites containing lignocellulosic material can induce formation of TCL.

10.4.2 Transcrystallization of Isotactic Polypropylene on the Surface of Lignocellulosic Fillers

Most results of research on addition of unmodified chemically lignocellulosic filler confirm the presence of the TCL on the interphases in the composite. In this aspect, the results showing no significant effect of chemical modification on TCL forming are interesting. An example of such modification is the use of polypropylene grafted with maleic anhydride as the compatibilizing agent.

Sanadi and Caulfield [11] tested the effect of kenaf presence, with the addition of an agent improving adhesion, on the interphase – polypropylene grafted with maleic anhydride (MAPP). The tests using polarized light microscopy with a heating device showed that composites containing both MAPP fibers and unmodified fibers had a transcrystalline structure. Dynamic mechanical analysis justified a suggestion that TCL contains many defects. This could be caused not only by the presence of MAPP in TCL but also by the presence of solid body surface, which limited the crystallization process.

The PP molecular weight and amount of MAPP-grafted polypropylene has been considered an important factor influencing the adhesion. Longer PP macromolecules and smaller amounts of maleic anhydride may result in crystal defects. On the other hand, longer molecules make the physical interaction between TCL as well as spherulites and fiber surface easier [11].

Interesting results were reported by Mi et al. [19]. They analyzed polypropylene filled with bamboo fibers with the addition of polypropylene grafted with maleic anhydride. The use of the agent promoting the adhesion was aimed at improving interactions between the components. In case of systems polypropylene/bamboo fibers/compatibilizer, the TCL has been formed. This was explained by higher ability to nucleation of bamboo fibers in relation to MAPP-grafted polypropylene as compared to pure polymeric matrix.

Similar results were obtained by Son et al. [13], who treated cellulose fibers with NaOH solution and additionally modified by cellulase enzyme. He also used MAPP as an additional compatibilizing agent. It was noticed that both the unmodified cellulose and NaOH-modified cellulose have equal nucleating ability. The TCL formed around both kinds of fibers; however, it was higher for unmodified fibers. In modified fibers, the TCL around the filler was also observed. The highest layer growth of TCL was noted for the system with fibers modified by cellulase. It was explained by probable increase of TCL growth rate by the increase of surface roughness and unhomogeneity by cellulase action.

Felix and Gatenholm [20] were among the first researchers who showed results confirming the presence of TCL on the surface of lignocellulosic filler. In the manufacturing of polypropylene composites containing cotton fibers, they observed the presence of TCL around fibers. An interesting observation was that the presence of formed TCL improves the shear transfer between filler fiber and the matrix.

Sangyeob et al. [15] conducted research on heterogenic nucleation of semicrystalline polymers in the fiber surface. Using the analysis of polarized light microscopy, he noted the nucleating ability of thermomechanical pulp with the formation of TCL. The tests were conducted using fibers modified by dichloromethane extraction and rinsing with water. Modification of fibers by extraction resulted in the reduction of nucleating ability. Changes in fiber topography were noted as the result of the elimination of low molecular compounds extracted from the surface that caused the reduction of nucleating ability of lignocellulosic material. Similar observations were made by Borysiak [30] who found that applying the extraction of the lignocellulosic component results in considerable reduction of nucleating ability of the polymeric matrix. He also noted that chemical modifications, by the application of numerous acid anhydrides, are responsible for filler surface activity reduction.

Gray [21] obtained a new, interesting type of polymeric–cellulose composites. The matrix filler he used was cellulose nanocrystals extracted from cotton and ramie fibers and, next, isolated with the help of bacteria. He conducted microscopic analyses for two variants of samples. The first sample was built like a “sandwich” composite, while the other was composed of evaporated nanocrystals of cellulose covered with polypropylene disc. Gray observed the formation of TCL in both samples and explained it as a result of some kind of epitaxy. Increased nucleation was noted on the edges of the layer. It was suggested that nucleation goes better at the ends of fibers as compared to longitudinal surface.

10.4.3 Effect of Chemical Modification on Transcrystalline Layer Formation

Chemical modification to improve compatibility of composite components is very often connected with the effect of lack of TCL. The effect of filler modification on TCL formation inhibition was presented by numerous studies. Quillin et al. [29] explained the lack of TCL as a result of fiber modification by “covering” the ordered crystalline structure of cellulose chains by particles of modifiers. Gray [31], on the other hand, said that crystalline cellulose, called the cellulose II, unlike the cellulose I, causes no formation of TCLs. He explained that by the differences in crystalline structures of both types of cellulose. The results contradictory to those presented earlier were presented by Son et al. [32] – the cellulose II did initiate the transcrystallization in polypropylene matrix.

The effect of chemically modified lignocellulosic filler on the formation of TCL was thoroughly investigated by Borysiak and Doczekalska [33]. They conducted a number of pine wood modifications using different acid anhydrides: maleic, phthalic, propionic, crotonic, and succinic. The filler was also subjected to mercerization and extraction. It was found that the presence of TCL is strongly connected with chemical structure of used anhydrides. The system of the best nucleating ability was polypropylene with unmodified pine wood. It was found that mercerization and extraction slightly reduces the nucleating ability of the matrix. Unexpectedly, it was noted that wood modified with acid anhydrides may strengthen the effect of transcrystallization of polymeric matrix. The fact that the lignocellulosic filler subjected to succinic anhydride action caused no transcrystallization remained unexplained.

Lenes and Gregersen [14] found out that, analyzing the effect of cellulose fiber modification from sulphite softwood, chemical modification inhibits formation of TCL. Wood was first subjected to mercerization and next esterification with hexane and benzoic acid. Another portion of samples was knife milled sulphite fiber. All these modifications aimed at changing the fiber surface topography. Unmodified fibers showed ability to form the TCL. Even higher degree of transcrystallization was observed in composites with addition of mechanically modified fibers. The growth of TCL was noted after fibrillation. Additionally, it was observed that the differences in transcrystalline phase growth for systems containing fibers esterified with different reagents. It was explained by different degree of filler hydroxyl group substitution.

The effect of flax fiber modification and the effect on the presence of TCL were also studied by Arbelaiz et al. [17]. In his studies, fibers were subjected to maleic anhydride, vinyltrimetoxy silane, and alkali with addition of MAPP-grafted polypropylene. All applied modifications produced improvement in the thermal stability of lignocellulosic material. Analysis of the crystalline structure showed the increase of crystallinity as a result of filler addition. Nucleation density around unmodified fibers was higher than around fibers modified with maleic anhydride. Surfaces of unmodified fibers had the surface active for initialization of transcrystallization, which, in the case of modified fibers, did not occur. Son et al. [32] explained this phenomenon as

the result of penetration of the MAPP molecules into the interphase areas. This blocked and inhibited the development of TCL or reduced it to trace amounts. The results obtained by Arbelaiz et al. [17] were similar to those obtained by Son et al. [32]. Transcrystallization around fibers occurred to a small degree. It was found that modifying the filler with maleic anhydride causes changes in the nucleation ability, which resulted in the formation of TCL with a low density. It was also observed that the thickness of this layer depends on the temperature of crystallization. The increase of temperature caused the reduction of the layer thickness.

Studies on lignocellulosic material modification were also conducted by Nekkaa et al. [18]. The cellulose fibers obtained from Spanish broom (*Spartium junceum*) were subjected to silane's action to improve adhesion between composite components. Thermal analysis confirmed the nucleating effect upon the addition of unmodified fibers, while the addition of modified fibers did not significantly influence the crystallinity of polypropylene matrix.

Zafeiropoulos et al. [16] used four types of flax fiber when studying the crystallization of isotactic polypropylene in the presence of fibers: unmodified, dew-retted (pectin removed), flax modified by esterification with stearic acid and flax modified by high temperature in autoclave. It was interesting to see that transcrystallization occurred in both chemically and hydrothermally modified fibers. Zafeiropoulos also found that the rate of cooling may have an effect on the morphology of TCL.

Modification by stearic acid, similar to that used by Zafeiropoulos et al. [16], was conducted also by Quillin et al. [29]. He found, however, that treating fibers with this acid inhibits development of TCL. Different results can be explained by the fact that Quillin, unlike Zafeiropoulos, used a new technique where no solvent was used, which turned out to be an advantage in terms of TCL formation. The TCL formed around particular fibers varied. The structure formed around unmodified fiber was asymmetric and had different thicknesses at different places. It also showed different optical properties from the layer formed on modified fibers in autoclave.

10.4.4 Influence of Lignocellulosic Fibers on the Nucleation and Polypropylene Crystallization Process

The aspect that is indispensably connected with polymer composites containing lignocellulosic materials is the modification of both the filler and polymeric matrix. In the last few years, intensive research has been conducted aimed at optimization of lignocellulosic composites manufacturing. General methods used to improve polymer and filler adhesion are based on chemical and physical modifications. In manufacturing composites based on polypropylene and lignocellulosic fibers, the mixing process is the important problem in preparation of composite materials. Numerous studies aiming at improvement of mixing of hydrophobic polypropylene with hydrophilic lignocellulosic filler resulted in a number of helpful modifications. Application of these modifications on lignocellulosic material has significant effect on the characteristics of temperatures and kinetic parameters.

A very commonly used method to investigate thermal properties of polymeric materials is differential scanning calorimetry (DSC). Many studies were conducted based on thermal analysis. The DSC is defined as a method in which the rate of heat flow, to which the sample is exposed, is measured in function of time or temperature, while the sample temperature (in defined atmosphere) is programmed. The DSC method allows for obtaining measurable information regarding phase transition and kinetic parameters of composite materials.

Joseph et al. [34] thermally analyzed the polypropylene composites reinforced with sisal fibers. He applied the following modifications: 10% NaOH, polypropylene glycol urethane derivative (PPG/TDI), and potassium permanganate (KMnO_4). He additionally investigated composites in which polymeric matrices were MAPP-grafted polypropylene.

DSC was used to determine the melting and crystallization temperatures, melting enthalpy, and the degree of crystallinity. The results showed the increase of polypropylene crystallization temperature and degree of crystallinity upon addition of sisal fibers. It was explained by the nucleating effect of fibers. Also, dependence between the amount of added filler and changes in the degree of crystallinity and melting point were observed. The addition of chemically modified sisal caused a stronger increase of crystallization temperature as compared to composites containing unmodified fibers.

Studies on a similar group of materials – polymeric composites reinforced with sisal fibers – were conducted by Manchado et al. [35]. They analyzed the presence of different fibers, such as sisal, on crystallization of polypropylene. The composites were prepared in special chamber for mixing where the matrix was plastified at 190°C. Obtained materials were subjected to thermal analysis by DSC. The analysis of thermograms allowed for a similar finding like in Joseph's studies [34]. The presence of sisal fibers, as well as other fibers used in the study, accelerated crystallization of polypropylene. This was explained by the nucleating effect of sisal filler. Also, the half-time crystallization ($t_{1/2}$) decrease was observed for polypropylene with the addition of sisal fibers in comparison with unfilled polypropylene. The analysis of nonisothermal crystallization showed that the degree of polypropylene crystallinity is higher for the composites filled with sisal fibers than for unfilled polymer.

Similar observations were made by Arbelaiz et al. [17]. Flax fibers were subjected to action of maleic anhydride, vinyltrimethoxy silane, and alkali. As an additional compatibilizing agent, a MAPP-grafted polypropylene was used. The modifications had an effect on shaping the TCL. Addition of MAPP-grafted polypropylene caused formation of TCL of lower density as compared to the systems with unmodified fibers. Calorimetric analyses of composites containing flax fibers revealed a visible increase of crystallization rate as compared to the matrix without any additives. Addition of fibers had no significant effect on the melting point, unlike the degree of crystallization and the temperature of matrix crystallization. These parameters increased together with the increase of flax fiber amount content.

The nucleating effect of lignocellulosic filler was also investigated by Yang et al. [36]. They used thermal analysis to test polypropylene composites filled with

rice husks and wood flour. They used maleic anhydride-grafted polypropylene as a compatibilizer. They analyzed crystallization of the matrix in nonisothermal conditions. The analysis showed a slight effect of addition of the filler on glass transition of the matrix. The authors suggested that this proved the lack of chemical bonds between the matrix and the filler. Melting temperatures of composites showed no significant differences. No effect of filler on polypropylene melting was observed.

The consequence of lignocellulosic material addition, not only in the form of fibers but also in the form of wood flour or wood particles, is the nucleating effect. Numerous reports prove that the presence of wood origin lignocellulosic filler has an influence on crystallization of polymeric matrix.

Qiu et al. [37] observed comparable melting points of PP regardless of the amount of lignocellulosic fibers added. This refers to both the systems in which the matrix was the polyethylene with no additives and MAPP-grafted polypropylene. Different observations were made for crystallization temperature of polymeric matrix. The increase of the crystallization temperature occurred in both systems with MAPP-grafted polypropylene and in PP without additives. Modification of the filler by 1,6-diisocyanatohexane caused reduction of PP melting point and crystallization temperature, reducing also nucleating effect of wood.

Also, Amash and Zugenmaier [38] observed an increase in the crystallization temperature of polymeric matrix with the addition of cellulose fibers and MAPP, used as a compatibilizing agent. The DSC results clearly show that the addition of small amounts of cellulose fibers to PP increases the crystallization temperature of the polymer matrix. The effects observed can be explained by the assumption that the cellulose fibers act as efficient nucleating agents for the crystallization of PP.

Mucha and Królikowski [39], studying the kinetics of isothermal crystallization of polypropylene, noticed that addition of a filler, e.g., wood flour, efficiently reduces the time of crystallization. This is desirable in the processing of composites as it reduces the injection-forming cycle and forms small spherulites improving the mechanical properties of composites. Transcrystalline structures are formed during polymer crystallization in the presence of lignocellulosic filler.

Harper and Wolcott [40] conducted research aiming at the analysis of interactions between adhesion promoters and lubricants in polypropylene composites with wood. Based on calorimetric tests results, the crystallization and melting kinetics of systems with isotactic polypropylene with wood, containing adhesion promoter (MAPP-grafted polypropylene) and lubricants (e.g., zinc stearate), were analyzed. Analyses by DSC confirmed the nucleating effect of wood on polypropylene crystallization. The increase of crystallization temperature was observed. The results revealed occurrence of transcrystalline structure around cellulose fibers. The presence of wood caused increase of crystallization nuclei density in normal direction in reference to the filler surface. An interesting observation was the analyse of the presence of adhesion promoters and lubricants in amorphous areas of the polypropylene matrix. According to the authors, deposition of lubricants in amorphous areas influenced the mechanical strength of polymer and lignocellulosic materials composites.

Polymer and lignocellulosic material composites can be analyzed by wide angle X-ray scattering (WAXS) due to a character of the matrix. The necessary condition for diffraction is the fact that the wavelength of X-rays must be of the same order of magnitude as the distance between the lattice planes in polymer crystals. The most often used matrix polymers for composites containing lignocellulosic materials are thermoplastic polymers. Among the most studied ones are the systems with isotactic polypropylene. Besides PP, polyethylene (recycled and nonrecycled) is also used.

Lei et al. [41] manufactured composites from recycled high-density polyethylene, reinforced with sugarcane and wood. As a compatibilizer, the MAPP-grafted polyethylene, carboxylated polyethylene, and titanium-derived mixture (TDM) were used. Obtained composites were analyzed by the following methods: wide angle X-ray scattering, DSC, and dynamical mechanical analysis. WAXS analyses allowed for crystallinity comparison of sugarcane composite and pure matrix. The reflection plane and the degree of crystallinity were analyzed. Obtained diffractograms showed crystalline structures of cellulose present in sugarcane and wood cell walls. The peak corresponding to cellulose was visible on the diffractogram at angle $2\theta = 22^\circ$. Peaks for planes (110) and (200) corresponding to the crystalline structure of recycled high density polyethylene (RHDPE) were changed as a results of adding fibers and one of the compatibilizing agents. In the case when intensity of peaks changed, authors observed differences in crystallinity of particular samples. Comparison of DSC and WAXS analyses showed that the addition of lignocellulosic material results in increasing the crystallization temperature of the polyethylene matrix. Moreover, it was observed that the addition of the compatibilizing agent causes a slight decrease of crystallinity degree as compared to the material in which no compatibilizers were used.

Also, Lei et al. [42] tested composites manufactured of rice straw fibers and recycled high-density polyethylene using WAXS method. As fillers, they used fibers coming from different parts of the plant: leaves, husks, stem, and mixture of all these fibers. The filler and the two types of matrices – RHDPE and the polyethylene that is not recycled – were placed in the mixer. Obtained mixtures were pressed under 30 tons at 175°C . The WAXS technique was used to analyze the effect of the presence of fibers on polymeric matrix crystallization. The filler caused the increase of crystallinity degree of tested materials. This was explained similarly as earlier cited reports, namely that single fibers play the role of heterogenic nucleating agents.

The results of research described above prove univocally that the presence of lignocellulosic material in polymeric composites influences the crystallization process, altering the kinetic parameters, such as induction time, degree of crystallinity, conversion degree, etc., and characteristic temperatures. Using modification of the filler is not without the effect on crystallization of the matrix. An interesting phenomenon that has not been explained completely so far is the transcrystallization. Both the formation of transcrystallization and its effect on mechanical properties remain a disputable question among researchers.

10.5 The Analysis of Various Factors on Mechanical Properties of Composite Polypropylene–Natural Fibers

Within many past years, the research on polymers has concentrated, among others, on how to prolong the durability and stability. In time, this approach was supplemented by the materials that would degrade within a certain time after their life. Even if synthetic polymers make only 7% of total amount of wastes by weight, their volume share is over 30%. Therefore, for over a decade, a strong interest can be observed in using materials that are able to degrade. Among materials characterized by a partial degradability are a system of polypropylene and natural cellulose fibers. Introduction of a biodegradable component (a cellulose fiber) into a polymer causes its assimilation by microorganisms during a decomposition process, while the remaining part of a composite is safely dispersed in the environment. Additionally, such materials can be successfully recycled in terms of both material and energy.

Another important aspect that makes a wide application of such materials in industry is obtaining interesting physicochemical properties. The strength and Young's modulus parameters of natural fibers are similar to those of glass fiber [43–47], which may make them an alternative for fillers in polymers. When comparing mechanical properties of composites PP/lignocellulosic component with a system PP/glass fiber, one can notice very similar strength parameters [48]. The main advantage of introducing natural fibers into PP matrix is obtaining a material that shows a better stiffness, which is a crucial parameter in higher temperature applications.

Nevertheless, obtaining composites filled with the lignocellulosic component with desired strength properties requires to consider many factors having an effect on the final macroscopic properties. According to information from the literature, the following factors should be taken into account when designing a composite: adhesion between the components, filler content, fiber length of fibrous filler, filler distribution, the effect of processing parameters, etc. [49–53]. Achieving a good interphase adhesion between polymer matrix and fibers is necessary to transmit stress from the matrix to the fibers and finally for improvement of a material strength.

10.5.1 *Effect of Improvement of an Interphase Adhesion on the Mechanical Properties of Composites*

One of the most important problems occurring in composite manufacture is a low adhesion between the components, which significantly limits the application of such materials in a broader scale. Finding effective methods of improving adhesion and description of interphase interactions are the topics of numerous studies.

Literature studies showed that the most often method for improving the adhesion between the composite components is using a MAPP. This compatibilizer can be an effective adhesion promoter for a system cellulose fibers–polypropylene matrix

[54–61]. Creating covalence bonds between the cellulose –OH groups and anhydride groups of MAPP grafted to the PP chain is one of the reasons for achieving a better strength of composites [57, 62]. Obtaining a cross bond between MAPP and PP is responsible for transmission of stresses from the polymer matrix to the fiber.

Literature also reports the effect of MAPP content. The results show a certain optimum necessary for improving the mechanical properties [49]. It is also known that the content of the anhydride grafted on the polypropylene chains at the level of 0.2% is enough to obtain a positive strength effect [49]. Gauthier [63], using a microbond test, found that composites containing MAPP-modified cellulose fiber shows approximately 70% better adhesion as compared to a system with a nonmodified fiber. Oksman et al. [64] noticed that 2% addition of MAPP causes a considerable improvement of mechanical properties. In composites PP–sisal fibers, the increase of tensile strength was from 40 to 79 MPa while for the system PP–flax fiber – from 46 to 75 MPa. Similar relations were observed for Young’s modulus. An addition of 10% sisal fiber into the PP matrix (in presence of MAPP) resulted in Young’s modulus increase by 150% and in tensile strength increase by about 10% [65]. Bengtsson et al. [66] also noticed that the application of MAPP is responsible for the improvement of tensile strength for composites made of polypropylene and Kraft cellulose fibers. Similar observations were made for PP composites with flax fibers [53, 67, 68] and systems PP–kenaf fibers [69], where application of MAPP caused improvement of mechanical properties.

Hornsby et al. [70] noticed improvement of tensile strength, Young’s modulus, and impact resistance in composites PP–flax fibers containing 5% of the MAPP compatibilizer. Also, Kim et al. [71] noticed considerable improvement of PP/cotton fiber composite tensile strength when using the MAPP as a compatibilizer.

The research results confirm that the application of silica-organic compounds for modification of cellulose fiber surface considerably improves strength properties of composites [50, 51, 72–75]. Raj et al. [72] found that the modification of cellulose fibers with silanes as well as with isocyanate caused improvement of mechanical properties of composites based on polypropylene matrix. However, studies conducted by Hornsby et al. [76] do not confirm that. His results prove that processing flax fibers with silanes has no effect on mechanical properties of composites based on polypropylene matrix. These contradictory conclusions are probably the effect of a complex anatomical structure of cellulose fiber and/or application of suitable conditions of modification reaction.

Another way to improve the adhesion is by using the process of natural fiber acetylation. Acetylation reduces the jute fiber water sorption by about 50% [77]. Liu et al. [77] investigated the effect of acetylation on cotton and rayon fibers and found that the strength of composites improved. [78] noticed the increase of fiber surface energy upon acetylation, which was explained by forming ester bonds.

Studies on acetylation as one of the methods for modification of lignocellulosic materials are conducted at our research center [7–9, 30, 33, 79–81]. Tables 10.1 and 10.2 show the values of strength of composites based on polypropylene matrix and long flax or hemp fibers. These components were obtained by compression molding according to a procedure described in a patent [82]. The developed method

ensures processing of polymers containing natural fibers that are 10 cm in length and longer ones, which is not possible by extrusion and press molding methods.

Based on the results reported above, one can notice that chemical modification of natural fibers using acetic anhydride caused significant improvement of composite mechanical properties. It is also worth to emphasize that the content of lignocellulosic filler has considerable effect on mechanical parameters. The tensile strength for polypropylene composites containing 20% and 30% of unmodified fiber is comparable to polymer matrix. Only introduction of 40% of filler has caused the increase of tensile strength (by about 15%). Application of chemical modification of lignocellulosic component is responsible for the increase of tensile strength at already 20% content of natural fibers. Further increase of amount of flax or hemp fiber causes significant increase of tensile strength. The results in Tables 10.1 and 10.2 confirm that the introduction of any amount of a filler leads to the increase of Young's elasticity modulus as compared to polypropylene matrix. It is worth emphasizing that application of acetylation of lignocellulosic fibers caused the increase of the Young's modulus by about 30% as compared to unmodified composites. A very interesting observation is reduction of elongation at break for composites containing modified fibers. This situation can be a result of increasing of interphase adhesion between the polymer and hydrophobicized natural fibers that were treated by acetic anhydride. The presence of ester groups was confirmed by IR testing.

Also isocyanates were used as adhesion modifiers. These compounds are efficient compatibilizers ensuring a significant improvement of tensile strength [50, 51, 72, 83–86]. Qiu et al. [37] showed that the application of hexamethylenedi-isocyanate causes increase of tensile strength by about 45% and bending strength by 85%, as compared to unmodified composites. Raj et al. [50, 72] noticed that application

Table 10.1 Mechanical properties of long flax/PP composites

	Mechanical properties of flax/PP composites						
	PP	PP + unmodified flax fibers			PP + flax fibers modified by acetic anhydride		
		20%	30%	40%	20%	30%	40%
R_m (MPa)	29.9	28.7	30.4	35.7	31.2	34.9	38.1
ϵ (%)	342	26.2	22.3	15.8	24.1	14.4	9.4
E (MPa)	639	789	845	1,200	921	1,079	1,469

Table 10.2 Mechanical properties of long hemp/PP composites

	Mechanical properties of hemp/PP composites						
	PP	PP + unmodified hemp fibers			PP + hemp fibers modified by acetic anhydride		
		20%	30%	40%	20%	30%	40%
R_m (MPa)	29.9	28.4	31.3	34.9	32.1	36.5	39.8
ϵ (%)	342	24.4	19.9	12.32	20.7	13.8	7.73
E (MPa)	639	802	913	1,169	1,084	1,211	1,662

of isocyanates and silanes can be an effective method to improve adhesion in composites PP–cellulose fibers, which is demonstrated by improvement of mechanical properties and better dimensional stability.

The literature reports also other methods for modification of lignocellulosic components to improve interphase adhesion. These comprise reactions with triazine derivatives [87], *n*-octadecyl vinyl-sulfone [87], potassium permanganate [86, 88], as well as dicumil or benzoyl peroxides ([89]; Jayamol [90]). Processing with peroxides in addition to significant improvement of mechanical properties of composites is also responsible for making processing of composite materials easier [86, 91, 92].

10.5.2 The Effect of Length, Content, and Dispersion of Fibrous Filler and Processing Parameters on the Mechanical Properties of Composites

Another important factor having an effect on strengthening of polymer matrix is the fiber length [89, 93, 94]. When using composites containing “short” fibers, there is a critical length that is necessary to achieve the desired mechanical parameters [52, 58, 88]. When the length of fibers is shorter than the critical value, the composites show worsening of mechanical properties. Based on a report by Joseph et al. [88], one can observe that tensile strength is increasing with increase of fiber length. It is also known that the strength of composites is higher when decreasing the critical length of fibers [52]. Those authors also noticed that the strength of composites is dependent on fiber orientation. It was found that the strength of fibers oriented unidirectionally is higher than randomly distributed ones.

Obtaining a composite with maximum high filler content is economically justified. It is known that as the content of filler increases, the price of the composite is decreasing. It is worth to mention, however, that increasing the content of fibers in the matrix causes higher stiffness of the composite [95]. Pukanszky [95] reports that mechanical properties are strongly dependent on filler particle characteristics. Composites containing a filler of spherical shape are characterized by decrease of tensile strength as the content of the filler is increased in the matrix. Oksman et al. [64] observed higher strengths of composites as the content of sisal, jute, and flax fibers increased in the matrix. The key factor responsible for improvement of mechanical properties is achieving very good dispersion of the filler in the matrix [96].

Obtaining the composite with high strength parameters is determined also by conditions of processing. It is necessary to optimize the technological processes of extrusion, injection molding, or press molding. The parameters that should be optimized are temperature plasticity, mold temperature, temperature of molded piece, rate of cooling, and process pressure. These factors are crucial for thermal

resistance of lignocellulosic component, distribution and shape of the filler, and shaping the supermolecular structure of polymer matrix.

Joseph et al. [88] noticed that mechanical properties depend on the time of mixing the composite components. At shorter times, the strength and Young's modulus were lower, which can be explained by less thorough mixing and insufficient dispersion of filler in the matrix. Longer time of mixing increases the dispersion. It was also found [88] that higher temperature of processing (over 70°C) leads to decrease of strength, which can be explained by thermal degradation of cellulose component. Additionally, poorer fiber dispersion was observed, which was caused by decrease of viscosity in higher temperature.

Medina et al. [97] investigated the effect of pressure during processing on the mechanical properties. He found that a pressure of 15–60 bar results in composites of higher tensile strength as compared to higher pressures (80–200 bar). The SEM analyses explained that by occurrence of fractures in fibers at higher pressures.

10.6 Conclusions

It was found that in the composites with natural fibers the hexagonal form arises when the fibers are in motion in relation to the polymeric matrix. The processing conditions play an important role for structural changes in PP matrix. Moving temperature of natural fibers was found to have a strong influence on the content of hexagonal modification. If the temperature of the moving of fibers is low, then the amount of β -PP significantly increases. The content of β -PP also depends on the rate of moving of fibers; however, the chemical modification of the natural fiber surface reduces the content of this form.

Many factors such as adhesion between components, fiber topography, and kinetic parameters of crystallization of semicrystalline matrix have been reported to influence transcrystallinity. The transcrystallinity phenomenon in the natural fibers/polypropylene system is affected by the different type of chemical treatment of lignocellulosic materials. Moreover, the ability of natural filler to induce nucleation in polypropylene matrix is also dependent on the kind of chemical modification of surface fibers. Predominant nucleation ability was found for unmodified fibers. However, chemical modification of fiber surface slightly depressed the nucleation of polypropylene matrixes.

The mechanical and other physical properties of the composite are generally dependent on the length, content, and dispersion of fibrous filler and processing parameters.

Acknowledgments This research was supported by University Grant of Poznan University of Technology 32-171/11-DS.

The authors are grateful to Professor Józef Garbarczyk for inspiration and valuable discussion of the material presented in this manuscript.

References

1. Turner-Jones A, Aizlewood JM, Beckett DR (1964) Crystalline forms of isotactic polypropylene. *Makromol Chem* 75:134–158
2. Garbarczyk J (1985) A study on the mechanism of transition $\beta \rightarrow \alpha$ in isotactic polypropylene. *Makromol Chem* 186:2145–2151
3. Borysiak S, Garbarczyk J, Paukszta D (2007) Polish Patent P-348,342
4. Varga J, Karger-Kocsis (1993) Direct evidence of row-nucleated cylindrical crystallization in glass fiber-reinforced polypropylene composites. *J Polym Bull* 30:105–110
5. Varga J, Karger-Kocsis J (1994) The difference between transcrystallization and shear-induced cylindrical crystallization in fibre-reinforced polypropylene composites. *J Mater Sci Lett* 13:1069–1071
6. Hoecker F, Karger-Kocsis J (1995) On the effects of processing conditions and interphase of modification on the fiber/matrix load transfer in single fiber polypropylene composites. *J Adhes* 52:81–100
7. Borysiak S (2000) PhD Thesis, Faculty of Chemical Technology, Poznan University of Technology, CT PUT
8. Garbarczyk J, Borysiak S (2004) Influence of the pulling of embedded natural fibres on the crystal structure of polypropylene matrix. *Int J Polym Mater* 53:725–733
9. Garbarczyk J, Paukszta D, Borysiak S (2002) Polymorphism of isotactic polypropylene in presence of additives, in blends and in composites. *J Macromol Sci Part B Phys B* 41:1267–1278
10. Paukszta D, Borysiak S (2005) Structure of isotactic polypropylene in composites with natural fibres obtained in various processing methods. *Fibres & Textiles in Eastern Europe* 13:107–109
11. Sanadi R, Caulfield DF (2000) Transcrystalline interphases in natural fiber – PP composites: effect of coupling agent. *Compos Interface* 7:31–43
12. Suzhou Y, Rials TG, Wolcott MP (1999) Crystallization behavior of polypropylene and its effect on woodfiber composite properties. pp. 139–146. *Proceedings of 5th International Conference on Wood-Plastic Composites.*, Forest Products Society (Eds) Madison, WI, USA
13. Son SJ, Lee YM, Im SS (2000) Transcrystalline morphology and mechanical properties in polypropylene composites containing cellulose treated with sodium hydroxide and cellulose. *J Mater Sci* 35:5767–5778
14. Lenes M, Gregersen W (2006) Effect of surface chemistry and topography of sulphite fibers on transcrystallinity of polypropylene. *Cellulose* 13:345–355
15. Sangyeob L, Shupe TF, Groom LH, Chung YH (2007) Thermomechanical pulp fiber surface modification for enhancing the interfacial adhesion with polypropylene. *Wood Fiber Sci* 39:424–433
16. Zafeiropoulos NE, Baillie CA, Matthews FL (2001) A study of transcrystallinity and its effect on the interface in flax fibre reinforced. *Composites* 32:525–543
17. Arbelaiz A, Fernandez B, Ramos JA, Mondragon I (2006) Thermal and crystallization studies of short flax fibre reinforced polypropylene matrix composites: effect of treatments. *Thermochim Acta* 440:111–121
18. Nekkaa S, Guessoum M, Chebira F, Haddaoui N (2008) Effect of fibre content and chemical treatment on the thermal properties of *Spartium junceum* fiber-reinforced polypropylene composites. *Int J Polym Mater* 57:771–784
19. Mi Y, Chen X, Guo Q (1997) Bamboo fiber-reinforced polypropylene composites: crystallization and interfacial morphology. *J App Polym Sci* 64:1267–1273
20. Felix JM, Gatenholm P (1994) Effect of transcrystalline morphology on interfacial adhesion in cellulose/polypropylene composites. *J Mater Sci* 29:3043–3049
21. Gray DG (2008) Transcrystallization of polypropylene at cellulose nanocrystal surfaces. *Cellulose* 15:297–301
22. Yi C, Petermann J, Wittich H (1997) Transcrystallization in fiber-reinforced isotactic polypropylene composites in temperature gradient. *J App Polym Sci* 65:67–75

23. Thomason JL, Rooyen AA (1992) Transcrystallized interphase in thermoplastic composites. *J Mater Sci* 27:889–896
24. Grozdanov A, Bogoeva-Gaceva G (2003) Transcrystallization of maleated polypropylene In the presence of various carbon fibers. *Polym Bull* 50:397–404
25. Zhang S, Minus ML, Zhu L, Wong CP, Kumar S (2008) Polymer transcrystallinity by carbon nanotubes. *Polymer* 49:1356–1364
26. Naiki M, Fukui Y, Matsumura T, Nomura T (2001) The effect of talc on the crystallization of isotactic polypropylene. *J Appl Polym Sci* 79:1693–1703
27. Huihui L, Liu J, Wang D, Yan S (2003) A comparison study on the homogeneity and heterogeneity fiber induced crystallization of isotactic polypropylene. *Colloid Polym Sci* 281:973–979
28. Huihui L, Liu J, Wang D, Yan S (2003) Optical microscopic study on the morphologies of isotactic polypropylene induced by its homogeneity fibers. *Macromolecules* 36:2802–2807
29. Quillin DT, Canfield DF, Koutsky JA (1993) Crystallinity in the polypropylene/cellulose system. I nucleation and crystalline morphology. *J App Polym Sci* 50:1187–1194
30. Borysiak S (2007) Determination of nucleation ability of wood for non-isothermal crystallisation of polypropylene. *J Therm Anal Calorim* 88:455–462
31. Gray D (1974) Polypropylene transcrystallization at the surface of cellulose fibre. *J Polym Sci* 12:509–515
32. Son SJ, Lee YM, Im SS (2002) Transcrystalline morphology and mechanical properties in polypropylene composites containing cellulose treated with sodium hydroxide and cellulose. *J Mater Sci* 35:5767–5778
33. Borysiak S, Doczekalska B (2009) The influence of chemical modification of wood on its nucleation ability in polypropylene composite. *Polymers* 54:820–827
34. Joseph PV, Joseph K, Thomas S, Pillai CKS, Prasad VS, Groeninckx G, Sarkissova M (2003) The thermal and crystallisation studies of short sisal fibre reinforced polypropylene composites. *Composites* 34:253–266
35. Manchado MAL, Blagiotti J, Torre L, Kenny JM (2000) Effects of reinforcing fibers on the crystallization of polypropylene. *Polym Eng Sci* 40:2194–2204
36. Yang HS, Gardner DJ, Kim HJ (2009) Viscoelastic and thermal analysis of lignocellulosic material filled polypropylene bio-composites. *J Therm Anal Calorim* 98:553–558
37. Qiu W, Zhang F, Endo T, Hirotsu T (2005) Isocyanate as a compatibilizing agent on the properties of highly crystalline cellulose/polypropylene composites. *J Mater Sci* 40:3607–3614
38. Amash A, Zugenmaier P (2000) Morphology and properties of isotropic and oriented samples of cellulose fibre–polypropylene composites. *Polymer* 40:1589–1596
39. Mucha M, Królikowski Z (2003) Application of DSC to study crystallization kinetics of polypropylene containing fillers. *J Therm Anal Calorim* 74:549–557
40. Harper D, Wolcott M (2004) Interaction between coupling agent and lubricants in wood–polypropylene composites. *Composites* 35:385–394
41. Lei Y, Wu Q, Yao F, Xu Y (2007) Preparation and properties of recycled HDPE/natural fiber composites. *Composites* 38:1664–1674
42. Lei Y, Wu Q, Yao F, Xu Y (2008) Rice straw fiber-reinforced high-density polyethylene composite: effect of fiber type and loading. *Ind Crops Prod* 28:63–72
43. Folster T, Michaeli W (1993) Flachs-eine nachwachsende Verstärkungsfaser für Kunststoffe. *Kunststoffe* 83:687–691
44. Mieck KP, Reubmann T (1995) Flachs versus Glas. *Kunststoffe* 85:366–370
45. Heijenrath R, Peijs T (1996) Natural-fibre-mat-reinforced thermoplastic composites based on flax fibres and polypropylene. *Adv Compos Lett* 5:81–85
46. Peijs T, Garkhail S, Heijenrath R, Van den Oever M, Bos H (1998) Thermoplastic composites based on flax fibres and polypropylene: influence of fibre length and fibre volum fraction on mechanical properties. *Macromol Symp* 127:193–203
47. Mieck KP (1999) Natural fibre/polypropylene composites: an A–Z reference. Chapman & Hall, London

48. Bisanda ETN, Mwaikambo LY (1997) Potential of Kapok fibre as a substitute of cotton in textiles. *J Agric Sci Technol* 1:66–71
49. Miwa M, Nakayama A, Ohsawa T, Hasegawa A (1979) Temperature dependence of the tensile strength of glass fiber-epoxy and glass fiber-unsaturated polyester composites. *J Appl Polym Sci* 23:2957
50. Raj RG, Kokta BV, Maldas D, Daneault C (1989) Use of wood fibers in thermoplastics VII. The effect of coupling agents in polyethylene–wood fiber composites. *J Appl Polym Sci* 37:1089
51. Maldas D, Kokta BV, Daneault C (1989) Influence of coupling agents and treatments on the mechanical properties of cellulose fibre–polystyrene composites. *J Appl Polym Sci* 37:751–775
52. Fu SY, Lauke B (1996) Effects of fiber length and fiber orientation distribution on the tensile strength of short-fiber-reinforced polymers. *Compos Sci Technol* 56:1179–1190
53. Arbelaz A, Fernandez B, Ramos JA, Retegi A, Llano-Ponte R, Mondragon I (2005) Mechanical properties of short flax fibre bundle/polypropylene composites: influence of matrix/fibre modification, fibre content, water uptake and recycling. *Comp Sci Technol* 65:1582–1592
54. Fung KL, Li RK, Tjong SC (2002) Interface modification on the properties of sisal fibre reinforced polypropylene composites. *J Appl Polym Sci* 85:169–176
55. Tjong SC, Xu Y, Meng YZ (1999) Composites based on maleated polypropylene and methyl cellulosic fiber: mechanical and thermal properties. *J Appl Polym Sci* 72:1647–1653
56. Li TQ, Ng CN, Li RKY (2001) Impact behavior of sawdust/recycled-PP composites. *J Appl Polym Sci* 81:1420–1428
57. Karmaker AC, Youngquist JA (1996) Injection moulding of polypropylene reinforced with short jute fibres. *J Appl Polym Sci* 62:1147–1151
58. Sanadi AR, Caulfield DF, Jacobsaon RE, Rowell RM (1995) Renewable agricultural fibres as reinforcing fillers in plastics: mechanical properties of kenaf fibre–polypropylene composites. *Ind Eng Chem Res* 34:1889–1896
59. Felix JM, Gatenholm P (1991) The nature of adhesion in composites of modified cellulose fibres and polypropylene. *J Appl Polym Sci* 42:609–620
60. Chuai C, Almdal K, Poulsen L, Plackett D (2001) Conifer fibres as reinforcing materials for polypropylene-based composites. *J Appl Polym Sci* 80:2833–2841
61. Olsen DJ (1991) Effectiveness of maleated polypropylenes as coupling agents for wood flour/polypropylene composites. *Proceedings of the ANTEC Conference*, Society of Plastics Engineers (Eds) Montreal, Canada
62. Rana AK, Mandal A, Mitra B, Jacobson R, Rowell R, Banerjee AN (1998) Short jute fiber-reinforced polypropylene composites: effect of compatibilizer. *J Appl Polym Sci* 69:329–338
63. Joly C, Kofman M, Gauthier R (1996) Polypropylene/cellulosic fiber composites: chemical treatment of the cellulose assuming compatibilization between the two materials. *J Mol Sci Pure Appl Chem* 12:1981–1996
64. Oksman K, Mathew AP, Langstrom R, Nystrom B, Joseph K (2009) The influence of fibre microstructure on fibre breakage and mechanical properties of natural fibre reinforced polypropylene. *Compos Sci Technol* 69:1847–1853
65. Fung KL, Xing XS, Li RKY, Tjong SC, Mai YW (2003) An investigation on the processing of sisal fibre reinforced polypropylene composites. *Compos Sci Technol* 63:1255–1258
66. Bengtsson M, Baillif M, Oksman K (2007) Extrusion and mechanical properties of highly filled cellulose fibre–polypropylene composites. *Compos Part A* 38:1922–1931
67. Arbelaz A, Cantero G, Fernandez B, Ganan P, Kenny JM, Mondragon I (2005) Flax fiber surface modifications. Effect on fibre physico mechanical and flax/polypropylene interface properties. *Polym Compos* 26:324–332
68. Van den Oever MJA, Bos HL, Van Kemenade JM (2000) Influence of the physical structure of flax fibres on the mechanical properties of flax fibre reinforced polypropylene composites. *Appl Compos Mater* 7:387–402

69. Sanadi AR, Feng D, Caulfield DF (1997) Highly filled lignocellulosic reinforced thermoplastic: effect on interphase modification. Proceedings of the 18th Riso International Symposium on Materials Science: Polymeric Composites-Expanding the Limits.; SI Andersen, P Brondsted, H Lilholt, A Lystrup, JT Rheinlander, BF Sorensen H (Eds) Toftegaard, Roskilde, Denmark
70. Hornsby PR, Hinrichsen E, Tarverdi K (1997) Preparation and properties of polypropylene composites reinforced with wheat and flax straw fibres. *J Mater Sci* 32:1009–1015
71. Kim SJ, Moon JB, Kim GH, Ha CS (2008) Mechanical properties of polypropylene/natural fiber composites: comparison of wood fiber and cotton fiber. *Polym Test* 27:801–806
72. Raj RG, Kokta D, Daneault C (1989) Effect of chemical treatment of fibers on the mechanical properties of polyethylene–wood fiber composites. *J Adhes Sci Technol* 3:55–64
73. Królikowski W (1998) Tworzywa wzmocnione i włókna wzmocniające. Warsaw, Poland
74. Bataille P, Ricard L, Sapieha S (1989) Effects of cellulose fibers in polypropylene composites. *Polym Compos* 10:103–108
75. Schneider MH, Brebner KI (1985) Wood–polymer combinations: the chemical modification of wood by alkoxysilane coupling agents. *Wood Sci Technol* 19:67–73
76. Hornsby PR et al (1997) Preparation and properties of polypropylene composites reinforced with wheat and flax straw fibres: Part II analysis of composite microstructure and mechanical properties. *J Mater Sci* 32:1009–1015
77. Liu FP, Wolcott MP, Gardner DJ, Rials GT (1994) Characterization of the interface between cellulose fibers and a thermoplastic matrix. *Compos Interface* 2:419–432
78. Zafeiropoulos NE, Williams DR, Baillie CA, Matthews FL (2002) Engineering and characterization of the interface in flax fibre/polypropylene composite materials. Part I. Development and investigation of surface treatments. *Compos Part A* 33:1083–1093
79. Borysiak S (2010) Supermolecular structure of wood/polypropylene composites: I. The influence of processing parameters and chemical treatment of the filler. *Polym Bull* 64:275–290
80. Borysiak S, Doczekalska B (2006) Influence of chemical modification of wood on the crystallisation of polypropylene. *Holz Roh-Werkst* 64:451–454
81. Borysiak S, Paukszta D (2008) Mechanical properties of lignocellulosic/polypropylene composites. *Mol Cryst Liq Cyst* 484:379
82. Borysiak S et al (2005) Method of preparation of board composites. Poland Patent No 190,405
83. George J, Sreekala MS, Thomas S (2001) A review on interface modification and characterization of natural fiber reinforced plastic composites. *Polym Eng Sci* 41:1471
84. Bledzki AK, Reihmane S, Gassan J (1998) Thermoplastics reinforced with wood fillers: a literature review. *Polym Plast Technol Eng* 37:451–468
85. Joly C, Gauthier R, Escoubes M (1996) Partial masking of cellulosic fiber hydrophilicity for composite applications. Water sorption by chemically modified fibers. Water sorption by chemically modified fibers. *J Appl Polym Sci* 61:57–69
86. Joseph K, Thomas S, Pavithran C (1996) Effect of chemical treatment on the tensile properties of short sisal fibre-reinforced polyethylene composites. *Polymer* 37:5139–5149
87. Zadorecki P, Flodin P (1986) Surface modification of cellulose fibers III. Durability of cellulose–polyester composites under environmental aging. *J Appl Polym Sci* 31:1699–1707
88. Joseph PV, Joseph K, Thomas S (1999) Effect of processing variables on the mechanical properties of sisal-fiber-reinforced polypropylene composites. *Compos Sci Technol* 59:1625–1640
89. Kuruvilla J, Sabu C, Pavithran C (1996) Effect of chemical treatment on the tensile properties of short sisal fibre-reinforced polyethylene composites. *Polymer* 37:5139–5149
90. George J et al (1996) Melt rheological behaviour of short pineapple fibre reinforced low density polyethylene composites. *Polymer* 37:5421–5431
91. Subramanian RV, Hoffmann R (1983) Study of the kinetic of in situ polymerization in wood by dynamic mechanical measurements. *J Polym Sci Polym Chem Ed* 12:105–109
92. Kalinski R, Galeski A, Kryszewski M (1981) Low-density polyethylene filled with chalk and liquid modifier. *J Appl Polym Sci* 26:4047

93. Thomason JL (1999) Mechanical and thermal properties of long glass fiber reinforced polypropylene. In: Karger-Kocsis J (ed) *Polypropylene: An A-Z reference*. Kluwer Academic Publishers, Dordrecht, The Netherlands
94. Hine PJ, Davidson N, Duckett RA, Ward IM (1995) Measuring the fibre orientation and modelling the elastic properties of injection-molded long-fibre-reinforced nylon. *Compos Sci Technol* 53:125–131
95. Pukanszky B (1999) Particulate filled polypropylene composites. In: Karger-Kocsis J (ed) *Polypropylene: An A-Z reference*. Chapman & Hall, London
96. Amash A, Zugenmaier P (2000) Morphology and properties of isotropic and oriented samples of cellulose fibre–polypropylene composites. *Polymer* 41:1589–1596
97. Medina L, Schledjewski R, Schlarb A (2009) Process related mechanical properties of press molded natural fiber reinforced polymers. *Compos Sci Technol* 69:1404–1411

Chapter 11

Isora Fibre: A Natural Reinforcement for the Development of High Performance Engineering Materials

Lovely Mathew, M.K. Joshy, and Rani Joseph

Abstract In this chapter, the technical potential of a natural fibre namely “ISORA” has been examined as an effective reinforcing material to design and manufacture high performance eco friendly composites in various polymers like natural rubber, polyester, epoxy resin, etc.; “Isora” a bast fibre separated from the bark of *Helicteres isora* plant is an important raw material can be used for the preparation of cost-effective and eco friendly composites. Morphology and physical properties of these fibres have been studied. Density and microscopic methods are used to determine the cross-sectional area and diameter of fibre bundles. Surface modification by alkali treatment and silane treatment were tried. Tensile properties of the treated and untreated fibres were determined by density method. The thermal characteristics, crystallinity index, reactivity, and surface morphology of the untreated and treated fibres have been studied by TGA, DSC, DTA, WAXRD, FTIR, and SEM. Average tensile strength of the fibre decreased and density increased to some extent on treatment with alkali and silane. Chemical constituents of the fibre were determined according to ASTM standards. SEM studies showed that as a result of chemical treatment fibre surface becomes rough promoting the fibre matrix adhesion which in turn improves the mechanical performance of the composites. Thermal analysis showed that chemical modification improves the thermal stability of the fibre. The strength of the fibre was theoretically calculated. For the successful design of a composite material using isora fibre and various polymers like natural rubber and thermosets (polyester and epoxy resin) several parameters like fibre aspect ratio, fibre orientation, fibre loading, chemical modification of fibre surface, fibre matrix adhesion that influences the performance of a short fibre composite were studied and optimised.

Keywords Adhesion · Bonding agent · Interface · Isora fibre · Natural fibre · Polymers · Reinforcement

L. Mathew (✉)

Department of Chemistry, Newman College, Thodupuzha, Kerala, India
e-mail: lovely.mathew@gmail.com

Contents

11.1	Introduction	292
11.2	Isora Fibre: Characterisation	295
11.2.1	Materials and Experimental Techniques	295
11.2.2	Chemical Composition and Mechanical Property Studies	295
11.2.3	Surface Morphology Studies	297
11.2.4	Chemical Reactivity of the Fibre	299
11.2.5	Thermal Analysis	300
11.2.6	Wide Angle X-Ray Diffraction Studies	302
11.3	Isora: Polymer Composites	303
11.3.1	Isora: Natural Rubber Composites	303
11.3.2	Isora: Polyester Composites	315
11.4	Conclusions	322
11.4.1	Fibre Characterisation	322
11.4.2	Isora: Rubber Composites	323
11.4.3	Isora: Polyester Composites	323
	References	324

11.1 Introduction

Nature is endowed with abundant quantity of natural fibres and now industrialists have focused on the development of natural fibre composites primarily to explore value added application avenues. Natural fibres do have a number of techno-economical and ecological advantages over synthetic fibres. The combination of interesting mechanical and physical properties together with environment friendly character has triggered a number of industrial sectors to consider these fibres as potential candidates to replace synthetic fibres in environmentally safe products. Composites fabricated with these natural fibres have the potential to be an attractive alternative to synthetic fibre composites. Interest in using natural fibres as reinforcement in polymer matrices and also in certain application as partial replacement of glass fibres has grown up significantly in recent years for making low-cost building materials and automobile components. Composites, the wonder material with light weight, high strength to weight ratio, and stiffness properties have come a long way in replacing the conventional materials like metals and woods. In this context, we have made efforts in search for some natural materials that can be effectively used as reinforcement for composites. There have been several attempts to utilise the abundant and renewable resources of plant fibres in composite materials with a view to replace the use of expensive synthetic fibres. Their application is diversified into engineering end uses such as building materials and structural part of motor vehicles where lightweight is required. The attractive features of natural fibres are their low cost, lightweight, high specific modulus, renewability and biodegradability. Low cost and less tool wear during processing are among the known advantages of plant fibres and ease of recycling makes them eco friendly. There are at least 1,000 types of plant that bear useful fibres. However

factors like lack of wettability and interfacial bonding between natural fibres and the well-known commercial polymers are the major problems that usually encountered with many of the applications. Experimental studies have shown that control of the fibre matrix interfacial bond strength is a critical factor in obtaining the best mechanical properties for the composites [1]. Hence studies have been focused on the treatment of fibres to improve bonding with the polymer matrix [2–4]. A wide variety of natural fibres like coir, sisal, oil palm, flax, banana, jute, pineapple, bamboo, etc. have been studied by several researchers [5–11]. However the use of “isora” has not yet been investigated by other researchers. Isora is a bast fibre separated from the bark of *Helicteres isora* plant by retting process. Two varieties of the plant are distinguished: *tomentosa* and *glabrescens* in which in the former the under side of the leaves is glabrous and in the latter both sides of the leaves are glabrous. The plant occurs as undergrowth especially as a secondary growth in forests. It coppices well, shooting up rapidly when cut or burnt. Seed sown during the rainy season easily propagates it. Roots, leaves and fruits of the plant are used for medicinal applications (Fig. 11.1). The stem bark is exploited for the fibre. Retting the stem in water and removing the fibre, which is pale yellow to light brown in colour, extract the fibre. The best type of fibre is obtained when the plants are 1–1.5 years old; plants older than 2 years yield coarse and brittle fibre. Stalks can be harvested annually for fibre extraction from regenerated shoots [12]. Fibre of good quality and colour is obtained when retting is effected in running water. Properties of natural fibres depend mainly on the nature and age of the plant, and the extraction method used. Isora fibre resembles jute in appearance, with comparable strength and better durability [13]. The fibre is used for making cordages,

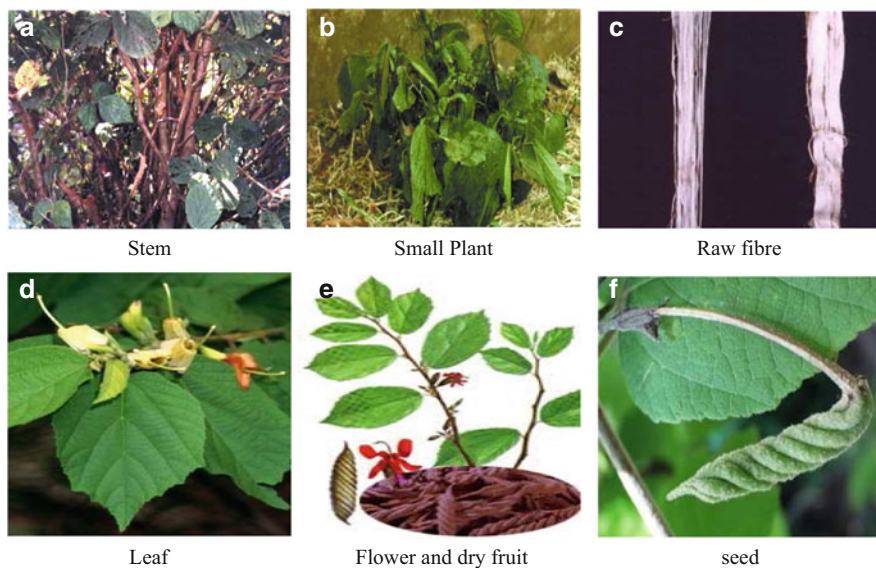


Fig. 11.1 *Helicteres isora* plant and its various parts

bags, fancy items, canvas, etc. Ropes and cordages made of the fibre are better and smoother than coir products. Recently we have reported about the possibilities of using isora fibre as a potential reinforcement in natural rubber and polyesters [14, 15]. The mechanical properties of these matrices are greatly improved by incorporation of this fibre. The resultant composite product will be a cost-effective and value added material for various components of machines like conveyor belts, v belts, and automobile parts. Use of biodegradable matrix and natural fibres as reinforcement has open new potential applications to these composites as they are eco friendly materials. To date no systematic work has been taken undertaken to study the properties of isora fibre from other researchers. This chapter reports on the physical, chemical, mechanical, thermal, and morphological characteristics of isora fibre and its utilisation as reinforcement in the development of polymer composites.

Short fibre reinforced rubber composites is a rapidly growing class of materials because of their improved physical and mechanical properties, easy process ability, and economic advantages. These materials bridge the gap between elastomers and fibres by combining the strength and stiffness of short fibres with the elasticity of rubber [1, 16]. Complex shaped engineering components may be developed using short fibre reinforced elastomers. The most important parameters that affect the short fibre reinforcement are fibre aspect ratio, fibre dispersion and orientation, fibre loading, fibre length, and adhesion between the fibre and the matrix [2, 17]. Use of biodegradable matrix and natural fibres as reinforcement has open new potential applications to these composites as they are eco friendly materials. Nowadays natural fibre is getting more attention from researchers. Natural cellulosic fibres when used as reinforcement imparts mechanical properties comparable to those of synthetic fibres like glass. Composites fabricated using these natural fibres have the potential to be an attractive alternative to synthetic fibre composites and are currently being explored in sectors like automobiles and buildings. In addition, these fibres offer an excellent opportunity to utilise an abundant source of such materials. These fibres, however, exhibit large variation in quality and are sensitive to moisture. The main problems that are usually encountered while using natural fibres as reinforcement are that the incorporation of a hydrophilic fibre into a hydrophobic polymer leads to a heterogeneous system with the result that they exhibit properties inferior to those of the unfilled system due to the poor adhesion at the fibre matrix interface. The surface characteristics of the reinforcing fibres are therefore important in transferring stresses from the matrix to the fibre. In the past, many attempts have been made to modify the surface properties of natural fibres in order to enhance adhesion with the polymer. Various methods such as corona treatment, plasma treatment, mercerisation, heat treatment, graft co polymerisation, and silane treatment have been reported to enhance the compatibility in natural fibre composites [18–24]. Unsaturated polyester is one of the thermoset matrices most frequently employed in the production of fibre reinforced composites, as it is available in liquid form, easily processed and cured, low in cost, easily available and has good mechanical properties when reinforced. Fibres are known to confer strength and rigidity to the weak and brittle matrix [25, 26].

11.2 Isora Fibre: Characterisation

11.2.1 Materials and Experimental Techniques

Isora fibre was separated from the bark of *H. isora* plant by retting process. Fibre presented in the inner part of the bark was peeled off, washed, and dried. The photographs of the stem, small plant, and the raw fibre are given in Fig. 11.1. Fibre surface was modified using alkali and silane treatments. For alkali treatment, fibres were dipped in 5% NaOH for about 4 h, then washed with water containing little acetic acid, washed well with water, and dried in an air oven. For silane treatment (Silane A 172), the alkali treated fibres were dipped in 1% silane solution in alcohol water mixture (60:40) for 2 h. The pH of the solution was maintained between 3.5 and 4. The fibres were washed with water and dried.

11.2.2 Chemical Composition and Mechanical Property Studies

Chemical composition of the fibre was estimated according to the following ASTM procedures: lignin-ASTM D1106, holocellulose-ASTM D1104, ash content-ASTM D1102, alcohol benzene solubility-ASTM D1107, ether solubility-ASTM D1108, 1% caustic soda solubility-ASTM D1109, and water solubility-ASTM D1110. Metal ions present were estimated using ICP AES analyser model IRIS INTREPID II XSP. For mechanical property studies, the cleaned isora fibres were cut into 70 mm, weighed, and finally mounted on a manila paper card mounts with a central cut out using a strong adhesive and the tensile test was then conducted according to ASTM 2256. Tensile strength was then calculated using cross-sectional area obtained from the weight and density of the fibre as shown in the equation. $\sigma_T = F_{\max}/A$, $\sigma_T = (\rho \cdot F_{\max} \cdot l_f)/m_f$, where F is the maximum force, ρ the density of the fibre, and l_f the length of the fibre. The bulk density of the fibre was determined using a liquid of lower density (benzene) than the fibre.

From Table 11.1 it is clear that isora is a cellulose rich fibre with comparatively low lignin content which contributes to better performance of the fibre as reinforcement in polymers. The fine structure of cellulose materials is composed of crystalline and amorphous regions. The amorphous regions easily absorb chemicals such as dyes and resins, whereas the compactness of the crystalline regions make it difficult for chemical penetration. The physical characteristics and chemical constituents of the fibre are given in Table 11.1. The bulk density includes all the solid material and pores within the fibre which is always less than the absolute density. The absolute density of most plant fibres is between 1.4 and 1.5 g/cm³. The fibre density is assumed to be closely related to the mechanical properties, moisture absorption, homogeneity, and degree of order of the fibre. After chemical treatment there is a slight positive change in the bulk density which normally signifies cell wall densification. The nature and texture of the fibres obtained from different

Table 11.1 (a) Chemical constituents of isora fibre, (b) Physical and mechanical properties of the fibre

(a)			
Chemical constituents (%)		Solubility in various solvents (%)	
Cellulose	74.8	Alcohol–benzene	6.3
Lignin	14.0	Ether	5.7
Ash	0.92	1% Caustic soda	14
Fat	1.09	Cold water	10
Moisture content	6–7	Hot water	12
Ca (ppm)	713.45	Acetone	5.6
Mg (ppm)	37.93		
Fe (ppm)	16.10		
K (ppm)	10.54		
Na (ppm)	10.42		
(b)			
Properties	U	A	Si
Tensile strength (MPa)	561	500	474
Young's modulus (GPa)	19	22	20
Elongation break (%)	5	4	4
Diameter (μm)	10	–	–
Density (gm cm^{-3})	1.39	1.42	1.51
Crystallinity index (%)	70.9	80.6	77.8
Micro fibrillar angle ($^{\circ}$)	20–26	–	–
Intrinsic strength (g/denier)	0.987	–	–
Length to diameter ratio	99	–	–

U Untreated, A Alkali treated, Si Silane treated

plants may not be the same. Hence this will affect the properties of the fibre; therefore, there is a large variation in the observed properties. An average value of the properties is reported. The tensile properties like tensile strength and elongation at break of the fibre change slightly after chemical treatment. Tensile strength of the treated fibre is less than that of the untreated fibre. Lignin, the binding material that binds the three-dimensional cellulose structures as well as the fibrils, get partially removed on chemical treatment and hence tensile strength decreases. Elongation at break remains more or less same even after chemical treatment. The modification of plant fibres may involve the removal of the surface impurities, the swelling of the crystalline region, and the removal of the hydrophilic hydroxyl group of the cellulose. The effective reinforcement of composites with plant fibres is dependent on the moisture content, fibre matrix adhesion, crystalline, and cellulose content.

11.2.2.1 Theoretical Prediction of Microfibrillar Angle and Strength of the Fibre

Strength properties of the fibre are dependent mainly on the fibrillar structure, microfibrillar angle, and the cellulose content. There is a correlation between percentage elongation ε and microfibrillar angle θ as follows:

$$\epsilon = -2.78 + 7.28 \times 10^{-2}\theta + 7.7 \times 10^{-3}\theta^2, \tag{11.1}$$

$$\sigma = -334.005 - 2.830\theta + 12.22W, \tag{11.2}$$

where W is the cellulose content of the fibre and σ the fibre strength [27].

The theoretical strength of the fibre was found to be 520 MPa which is in close agreement to the experimental value (568 MPa).

11.2.3 Surface Morphology Studies

The surface morphology of the fibre was studied using scanning electron microscopic studies (SEM). The SEM photographs of the fibre surface and cross section of the untreated and treated fibres were taken using a JEOL JSM 35 C model SEM. To avoid electron charging effects, the samples were gold coated in a Polaron SEM coating unit SC515. Figure 11.2 is the SEM photographs revealing the morphology of untreated isora fibres. The scanning electron micrograph of a single fibril and the cross section of isora fibre are given in Fig. 11.2a, b. The diameter of the fibre was found to be 10 μm . The cross section is polygonal with a circular or oval lumen. The fibres are arranged in a reticulate pattern in a series of zones alternating with zones of soft tissue in the phloem region. The fibre consists of cells embedded in a matrix; the cells are the crystalline cellulose arranged in a matrix consisting of noncrystalline cellulose–lignin complex. The cell wall of the fibre elements is thick and lignified. The central core is referred to as “lacuna” can also be seen in Fig. 11.2b. For the alkali treated fibre (Fig. 11.2d), it was observed that the size of the central lacuna

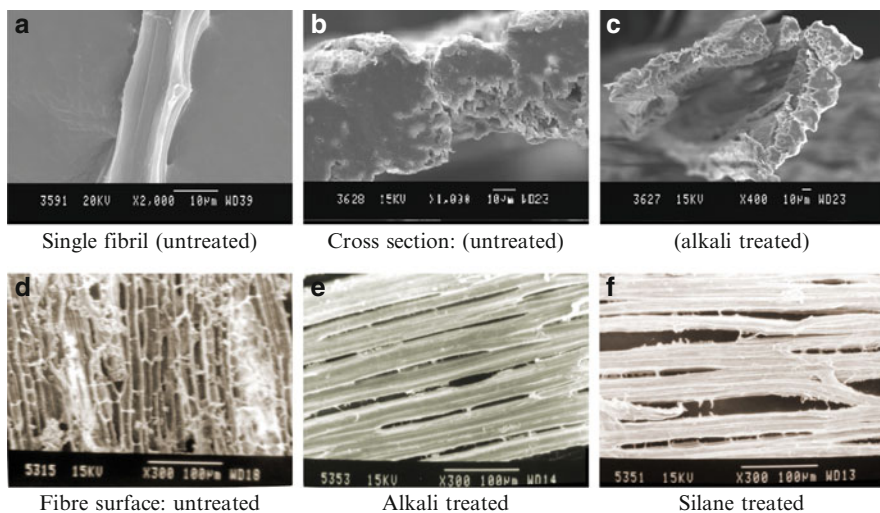


Fig. 11.2 SEM photographs of untreated and chemically treated fibres

is less than that of the untreated fibre indicating cell wall thickening and shrinkage of fibres during alkali treatment. From these pictures, it was found that isora fibres consisted of aligned fibrils with materials cementing the fibres together. Based on the results of FTIR and the structure of the natural fibre, the cementing material would be expected to be hemicellulose and lignin. It is well known that hemicellulose is a branched amorphous polymer with a low degree of polymerisation, which always associated with cellulose by hydrogen bonding. Therefore isora fibres should thought of as a composite material with fibrous reinforcement and a mixture of hemicellulose and lignin as matrix. SEM photographs of the alkali treated fibre were given in Fig. 11.3a–f. When the soaking time of the fibre in alkali was increased, it can be seen that the materials in the interfibrillar region were obviously etched away and the fibrous region becomes more pronounced as interfibrillar region is removed. SEM picture of the untreated isora fibre (Fig. 11.2d) shows that the fibre surface is very smooth. A series of globular particles can be seen to be embedded in the fibre surface at regular intervals. They are identified as tyloses which covers the pits on the cell walls. When the fibres are soaked for 4–12 h, most of the tyloses are intact, but at a few isolated places, it was removed creating holes as shown in Fig. 11.3b. When the soaking time was increased to 24–48 h, a much greater proportion of the tyloses appeared to be removed. At still higher soaking time, the SEM pictures show complete exposure of the fibrils indicating the leaching of the intercellular binding material and the cuticle layer (Fig. 11.3c–f). Fibre modification by alkali and silane treatment renders roughness to the fibre surface as evident from the SEM photographs (Fig. 11.2e, f). This will enhance the interlocking with the matrix, thereby the property of the composite increases [14, 15] by the incorporation of treated fibres.

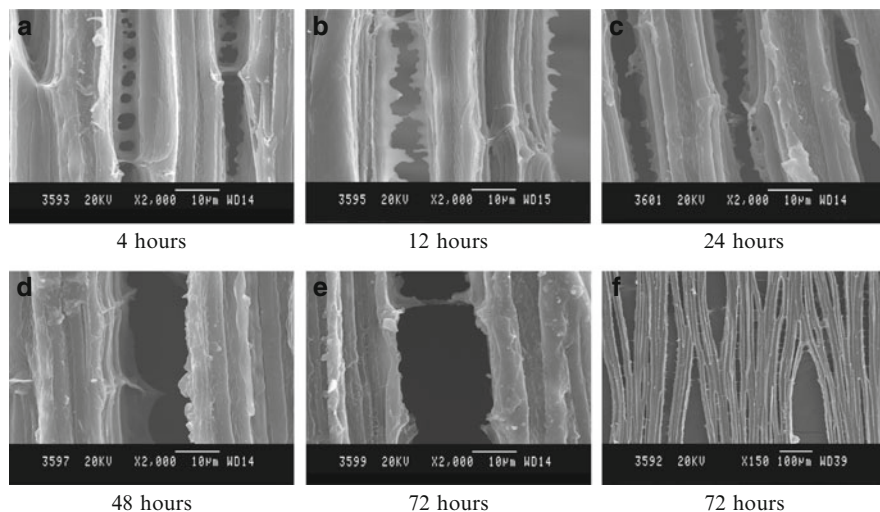


Fig. 11.3 SEM photographs of alkali treated fibres (at different intervals of soaking in NaOH) at 2,000× magnification

11.2.4 Chemical Reactivity of the Fibre

The chemical reactivity of the fibre was clearly evident from the IR spectra. The IR spectra of the raw and chemically modified isora fibres were taken using a Shimadzu IR 470 Infra red spectrophotometer, by the KBr pellet technique. The IR spectra of untreated and treated fibres are given in Fig. 11.4. It can be understood from the spectra that some chemical reactions are occurred during different treatments. Major changes are observed in the IR absorbance of alkali and silane treated fibres. By alkali treatment, a peak at $1,730\text{ cm}^{-1}$ due to the C=O stretching frequency of the carboxylic acid or ester present at the surface of the untreated fibre was disappeared due to the partial removal of lignin and hemicellulose. Also alkali treatment reduces the hydrogen bonding in the cellulosic hydroxyl groups, which is evident from the increased intensity of the -OH peak ($3,350\text{ cm}^{-1}$) in the alkali treated fibre. In the case of silane treated fibres, an additional peak at $3,400\text{ cm}^{-1}$ indicated intermolecular hydrogen bonding between the silanol -OH and that of cellulosic -OH of the fibres. The peak at $1,525\text{ cm}^{-1}$ in the untreated fibre is shifted to $1,600\text{ cm}^{-1}$ upon silane treatment. This may be due to the C=C stretching of the vinyl group. Additionally a peak at $2,900\text{ cm}^{-1}$ belonging to the CH stretching vibration in the cellulose and hemicellulose decreased after alkali treatment indicating the partial removal of lignin and hemicellulose.

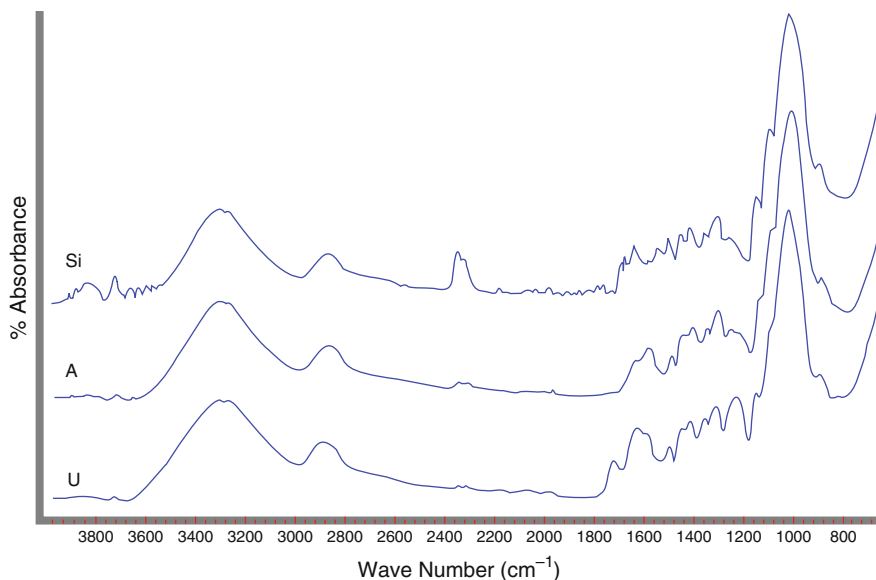


Fig. 11.4 IR spectra of various chemically treated fibres (*U* untreated; *A* alkali treated; *Si* silane treated)

11.2.5 Thermal Analysis

TGA and DSC studies of the fibres were carried out using a TGA Q-50 (TA Instruments) and a Mettler Toledo model DSC 822 thermal analyser with a heating scheme of 30–550°C and at a heating rate of 10°C min⁻¹ in nitrogen atmosphere purged at 25 ml min⁻¹. DTA and TGA studies were also carried in an oxygen atmosphere using a Perkin Elmer model diamond TGA/DTA thermal analyser.

Thermal degradation pattern of untreated, alkali treated, and silane treated fibres are shown in Figs. 11.5–11.7 (DTG, DSC, and DTA). Figure 11.5 shows the DTG curves for the fibre with different treatments. Around 100°C an initial weight loss was observed due to the removal of sorbed moisture from the fibres. The initial degradation temperature is higher for the alkali treated fibre. Major weight losses of the untreated and silane treated fibres take place at between 360 and 370°C. Alkali treatment raises this temperature to 380°C. The DTA curve (Fig. 11.6) in oxygen shows a major peak between 300 and 350°C that may be due to the thermal depolymerisation of hemicelluloses and the cleavage of the glycosidic linkages of cellulose. This is an exothermic process. At the first stage of the degradation, the DTA curve shows an endothermic peak in all cases around 100°C (Fig. 11.6). This peak may be due to the removal of moisture. Breakage of the decomposition products of the second stage (second peak) leads to the formation of charred residue. The third exothermic peak present in DTA curve is due to this oxidation and burning of the high molecular weight residues. In alkali treated fibre, the second peak is not prominent and broadening of the DTA peak was observed. In DTA (oxygen), the initial degradation temperature is higher for the untreated fibre. The DSC studies in nitrogen also show a similar trend (Fig. 11.7). A broad endotherm in the temperature range of 75–120°C was observed. The peak of maximum weight

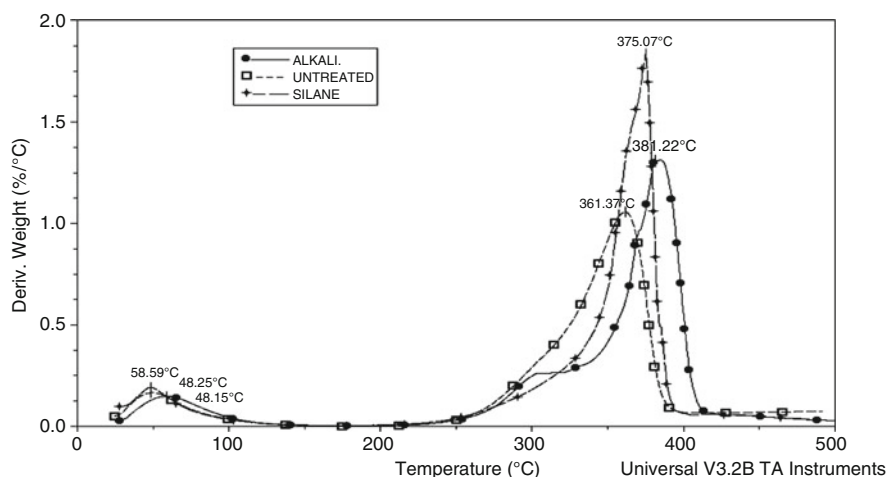


Fig. 11.5 DTG curves of untreated, alkali, and silane treated fibres in nitrogen atmosphere

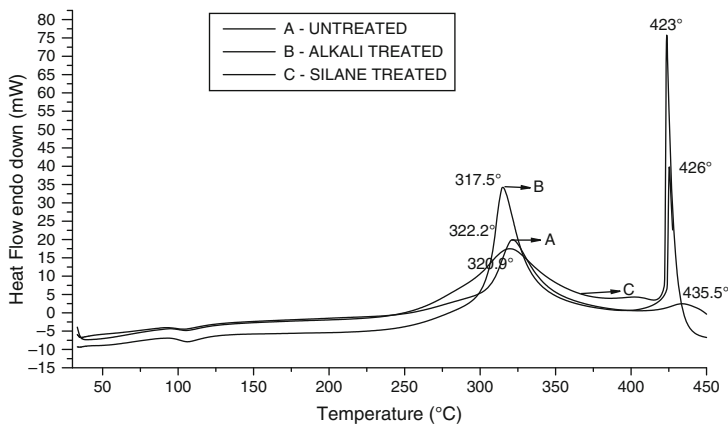


Fig. 11.6 DTA curves of the untreated, alkali, and silane treated fibres in oxygen atmosphere

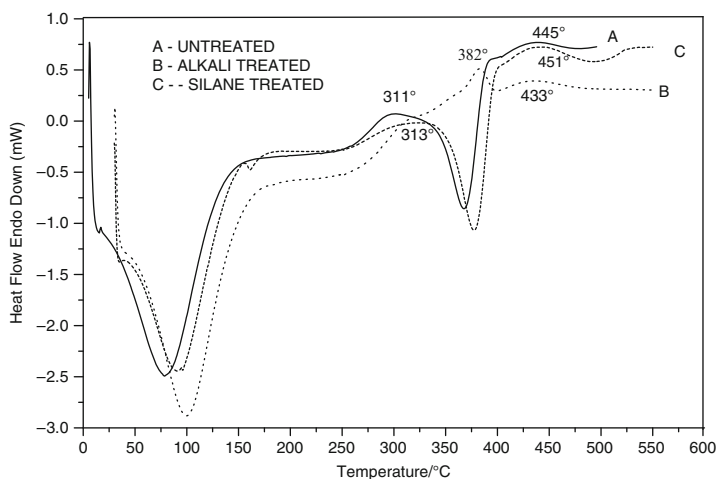


Fig. 11.7 DSC curves of untreated, alkali treated, and silane treated fibres in nitrogen atmosphere

loss was observed for untreated and treated fibres between 300 and 350°C. Fibre treatment slightly increased the thermal stability of the fibres in nitrogen atmosphere. This is evident from the DSC curves (Fig. 11.7) which is an indication of the increase in the crystalline cellulose, which is known to have good thermal resistance. Two and three exothermic peaks are observed for the untreated and treated fibres, respectively. In cellulose fibres, lignin degrades at a temperature around 200°C [28]. While the other polysaccharides such as cellulose degrade at higher temperatures. Therefore these exothermic peaks which were higher than 200°C indicate the decomposition temperature of the cellulose in the fibres. The region between 150 and 270°C shows no exothermic or endothermic reactions which suggest that the fibres are stable between these temperatures. From the first

exothermic peak, it can be deduced that the alkali treated fibre is more thermally stable compared to the untreated and silane treated fibre. Similar observations have also been reported in the case of other natural fibres [29]. It was reported that alkali and silane treatment increase the thermal stability of the fibres [6].

11.2.6 Wide Angle X-Ray Diffraction Studies

The crystallinity index of the fibres was studied using a wide angle X-ray diffractometer Bruker model D8 Advance, equipped with a scintillation counter and a linear amplifier was used. The diffraction intensities were recorded between 5 and 60° (2θ angle range). The crystallinity index was determined using the equation:

$$I_c = \frac{[(I_{002} - I_{am}) \times 100]}{I_{002}},$$

where I_c is the crystallinity index, I_{002} is the counter reading at peak intensity at a 2θ angle close to 22° representing crystalline material, and I_{am} is the counter reading at peak intensity at a 2θ angle close to 18° representing amorphous material in the fibre.

From Table 11.1 and Fig. 11.6, it is clear that the treated fibres show an overall initial increase in the crystallinity index, with maximum for alkali treated fibres which is an indication of the improvement in the order of crystallites as the cell wall thickens upon chemical treatment. The use of wide angle X-ray diffraction studies (WAXRD) counts offers a simple and quick method of determining the crystallinity index, and the minimum between 101 and 002 peaks (Fig. 11.8) is an indication of the reflection intensity of the amorphous material. Alkalisiation and silane treatment increases the crystallite packing order. Crystallinity index is a measure of the order of the crystallites rather than the crystallinity of the crystallites.

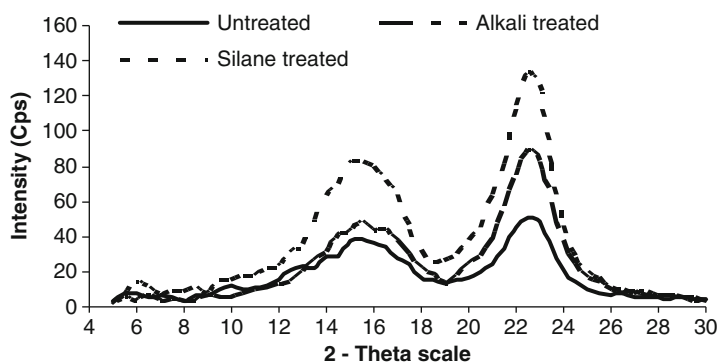


Fig. 11.8 WAXRD spectra of untreated, alkali treated, and silane treated fibres

11.3 Isora: Polymer Composites

11.3.1 Isora: Natural Rubber Composites

11.3.1.1 Preparation and Characterisation of Isora/Natural Rubber Composites

Fibre, separated from the bark of *H. isora* plant by retting process, was chopped almost accurately to different lengths of 6, 10, and 14 mm using a fibre chopper on which the length of fibre cuttings can be adjusted and washed with water to remove the undesirable impurities and dried. Treated fibre was prepared from raw fibre by immersing it in 5% aqueous NaOH for 4 h. Washing with water was done several times followed by drying in an air oven.

The composites were prepared by incorporating short isora fibres of different lengths 6, 10, and 14 mm (15 phr) and different loadings 10, 20, 30, 40 phr (10 mm) both for treated and untreated fibres into natural rubber matrix as per the formulation given in Tables 11.2 and 11.3. Mixes were prepared in a laboratory (150 × 300 mm) two roll mixing mill as per ASTM standards D 3184-80 at a nip gap of 1.3 mm. The samples were milled for sufficient time to disperse the fibres in the matrix. The final sheeting was done by passing the compound through a tight nip gap of 0.8 mm. The bonding agent (resorcinol, hexa, and silica) was incorporated

Table 11.2 Mixes with varying fibre length (phr^a)

Ingredients	Gum	L ₁	L ₂	L ₃
Natural rubber	100	100	100	100
Zinc oxide	5.0	5.0	5.0	5.0
Stearic acid	2.0	2.0	2.0	2.0
TDQ	1.0	1.0	1.0	1.0
CBS	0.6	0.6	0.6	0.6
TMTD	0.1	0.1	0.1	0.1
S	2.5	2.5	2.5	2.5
Untreated isora fibre	0	15	15	15
Fibre length (mm)	0	6	10	14

^aparts per hundred rubber

Table 11.3 Mixes (phr)^a with varying fibre loading and bonding agent

Mixes	Gum	X ₁₀	X ₂₀	X ₃₀	X ₄₀	Y ₁₀	Y ₂₀	Y ₃₀	Y ₄₀
Fibre (untreated)	0	10	20	30	40	–	–	–	–
Fibre (treated)	0	–	–	–	–	10	20	30	40
Mixes	–	X _{10b}	X _{20b}	X _{30b}	X _{40b}	Y _{10b}	Y _{20b}	Y _{30b}	Y _{40b}
Resorcinol	0	2.5	5.0	7.5	10	2.5	5.0	7.5	10
Hexa	0	1.6	3.2	4.8	6.4	1.6	3.2	4.8	6.4
Silica	0	1	2	3	4	1	2	3	4
Fibre (untreated)	0	10	20	30	40	–	–	–	–
Fibre (treated)	0	–	–	–	–	10	20	30	40

^aBasic recipe: NR-100, ZnO-5, Stearic acid-2,TDQ-1, CBS-0.6, TMTD-0.1, S-2.5

along with the other ingredients. The fibre was incorporated at the end of mixing process taking care to maintain the direction of compound flow, so that majority of fibres followed the direction of flow. In order to study the extent of fibre breakage, which occurs during milling operations, the fibres were extracted from the green compound by dissolving it in toluene, and their length and diameter were measured by using a travelling microscope. The cure characteristics were studied by an oscillating disc rheometer (Goettfert Elastograph). The samples were vulcanised at 150°C in a hydraulic press up to their respective optimum cure time t_{90} as measured on a Goettfert Elastograph.

11.3.1.2 Evaluation of Fibre Breakage

Mixes L_1 , L_2 , and L_3 are the NR mixes containing fibres of lengths 6, 10, and 14 mm, respectively (Table 11.2). The control of fibre length and aspect ratio of fibres in rubber matrix is difficult because of fibre breakage during processing. The severity of fibre breakage depends mainly on the type of fibre, the initial aspect ratio and the magnitude of stress and strain experienced by the fibres during processing [20]. Shear force during mixing orients most of the fibres along the mill grain direction. It may cause breakage of fibres also. The average diameter (10 μm) of the fibre remained unchanged after mixing. The results of the fibre breakage analysis are given in Table 11.4. From the data it is seen that the compound L_2 contained a total of 52.3% of the fibre in the range of 2–6 mm length and 63.3% of fibre in the range of 4–8 mm length after mixing and the aspect ratio remains higher than 200 which is generally required for effective stress transfer in short fibre elastomer composites [30]. From Table 11.7 it is clear that the reinforcement is high for the compound L_2 which contained fibres having an original length of 10 mm before mixing as evident from the high tensile strength, modulus, and tear strength of the compound L_2 compared to that of L_1 . The tensile strength and modulus of the compound L_3 are comparable to those of L_2 , even though it contained almost the same level of fibres (48.9%) having a length in the range 2–6 mm as that of the compound L_1 (48.3%). This is likely to be due to the presence of 39.7% of fibres having a final length in the range of 6–10 mm in L_3 , which is almost comparable to that present in L_2 (38.7%). These observations indicate that an original fibre length

Table 11.4 Distribution of fibre length after mixing

Length of fibre after mixing (mm)	Percentage available in the mix after mixing		
	L_1	L_2	L_3
0–2	51.7	9.0	11.4
2–4	27.9	22.0	23.3
4–6	20.4	30.3	25.6
6–8	–	33.0	32.7
8–10	–	5.7	7.0

Mixes L_1 , L_2 , and L_3 contain fibres of length 6, 10, and 14 mm before mixing

of 10 mm is the critical fibre length which is essential for getting better reinforcement in short isora fibre natural rubber composites.

11.3.1.3 Cure Characteristics

Tables 11.5 and 11.6 show the variation of cure characteristics of composites with varying fibre length and loading, respectively. The maximum torque is a measure of cross link density and stiffness in the rubber. In general, for all the mixes, the torque initially decreases, then increases, and finally levels off. The initial decrease in torque to a minimum value is due to the softening of the rubber matrix while the increase in torque is due to the cross linking of rubber. The levelling off is an indication of the completion of curing. It is found that the addition of fibres into the mix generally increases the torque values. It also shows that the torque increases with increase in fibre length and reaches a maximum at 10 mm fibre length. This increase is due to the presence of longer fibres, which imparts more restriction to deformation. However, the maximum torque was slightly higher for 10 mm than 14 mm. This may be due to the fact that longer fibres undergo fibre entanglement and breakage during mixing. The maximum torque also increases with increase in fibre loading. This is due to the increase in the stiffness and hardness of the composite. These torque values are also increased by alkali treatment as the treated fibre may provide a better surface for reinforcement. It is observed that the curing time is not very much affected by the modification of fibre surface. The optimum cure time is found to increase with addition of bonding agent. The longer curing time is due to the better bonding between the fibre and the matrix when bonding agent is used. Maximum and minimum torque values also increase in the presence of bonding agent. This is due to the strong bonding at the fibre/rubber interface and consequently the composite becomes stronger, harder, and stiffer.

Table 11.5 Vulcanisation parameters for mixes with varying fibre length

Mixes	Gum	L ₁	L ₂	L ₃
Min. torq. (Nm)	0.01	0.03	0.02	0.02
Max. torq. (Nm)	0.21	0.24	0.30	0.28
Scorch time	2.36	1.8	1.76	1.76
Cure time <i>t</i> ₉₀	4.32	4.62	5.42	5.46

Table 11.6 Vulcanisation parameters for mixes with varying fibre loading and bonding agent

Mixes	Gum	X ₁₀	X ₂₀	X ₃₀	X ₄₀	Y ₁₀	Y ₂₀	Y ₃₀	Y ₄₀
Curetime <i>t</i> ₉₀ (min)	4.32	5.4	5.5	5.7	5.85	4.61	4.91	5.22	5.64
Max. torq. (Nm)	0.22	0.29	0.32	0.35	0.40	0.32	0.34	0.40	0.51
Mixes		X _{10b}	X _{20b}	X _{30b}	X _{40b}	Y _{10b}	Y _{20b}	Y _{30b}	Y _{40b}
Curetime <i>t</i> ₉₀ (min)	4.32	7.24	7.76	8.12	8.36	6.9	7.0	7.32	7.68
Max. torq (Nm)	0.22	0.33	0.35	0.52	0.64	0.35	0.47	0.58	0.69

11.3.1.4 Extent of Fibre Orientation from Green Strength Measurements

The green strength of short fibre-reinforced composites depends on the degree of fibre orientation. The extent of fibre orientation can be calculated by using the following equation:

$$\text{Orientation \%} = \frac{S_L/S_{G,L}}{S_L/S_{G,L} + S_T/S_{G,T}},$$

where S is the green strength and subscripts G, L, and T denote gum, longitudinal, and transverse, respectively. The effect of fibre loading on the percentage orientation is shown in Fig. 11.9. At low fibre loading, the percentage orientation is the lowest as the fibres can randomly move around leading to increased chaoticity and decreased levels of orientation. As fibre loading increases, percentage orientation increases with the maximum value for composite containing 30 phr fibre. At 40 phr fibre loading, the percentage orientation decreases indicating that the fibres cannot orient themselves due to the entanglement caused by the increased content of fibres.

11.3.1.5 Mechanical Properties

Dumb bell and crescent-shaped tensile and tear specimens with longitudinal and transverse fibre orientations were punched from the vulcanised sheets. Stress–strain measurements were carried out at a crosshead speed 500 mm min^{-1} on a Schimadzu Model AG1 universal testing machine. Tensile and tear strengths were measured according to ASTM D 412-68 and D 624-54, respectively. Compression set of the specimens was measured in accordance with ASTM D 395-86 (method B). Abrasion resistance of the samples was tested using a DIN 53516. The hardness was measured using the Shore A type Durometer according to ASTM 2240-81. The SEM photographs of the fibres and the fractured surfaces were taken using a JEOL

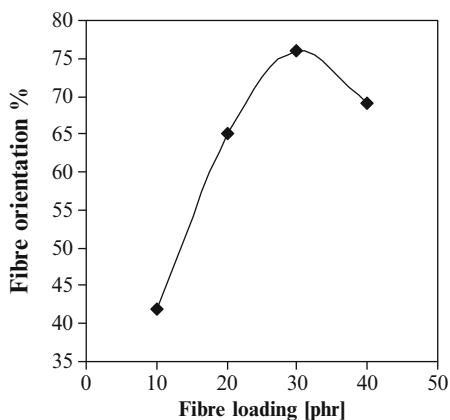


Fig. 11.9 Effect of fibre loading on percentage of fibre orientation of the composites

JSM 35 C model SEM. The fibre and the fracture surfaces were sputter coated with gold within 24 h of testing by using a fine coat JFC-1100.

Effect of Fibre Length

The effect of fibre length and orientation on the properties of the composites is given in Table 11.7. The properties are found to increase with increase in fibre length. The increase in the strength with increase in fibre length is attributed to the fact that the extent of load transmittance is a function of fibre length and magnitude of fibre matrix interfacial bond [31]. In fibre reinforced composites, there exists a critical fibre length at which the load transmittance from the matrix to the fibre is maximum. Critical fibre length is that length which is required by the fibre to develop its fully stressed condition in the matrix. Longer fibres impart more restriction to deformation while shorter fibres create friction and heat generation due to the increased number of fibre ends. Tensile and tear strengths show a maximum value for the composite with fibres having an original length of 10 mm before mixing. The interaction between the fibre and the matrix reaches its maximum at this fibre length and the effect of fibre length decreases with longer fibres because of fibre entanglement and breakage. At higher fibre length, the dispersion of fibres in rubber matrix is difficult. Hence a further increase in fibre length beyond 10 mm decreases the mechanical properties like tensile strength and tear strength. These observations indicate that an original fibre length of 10 mm is the critical fibre length which is essential for getting better reinforcement in short isora fibre natural rubber composites.

Effect of Fibre Orientation

Fibre orientation affects composite properties. During milling of rubber composites, majority of the fibres tend to orient along the flow direction, causing the mechanical properties to vary in different directions. In case of short fibre reinforced composites, longitudinal and transverse orientations are possible. In longitudinal orientation, the fibres are aligned along the mill grain direction and in transverse one the fibres are aligned across the grain direction. Properties like tensile modulus, tensile strength,

Table 11.7 Mechanical properties of vulcanisates with varying fibre length

Properties	O	Gum	L ₁	L ₂	L ₃
Tensile modulus (300% E) MPa	L	2.3 (0.28)	2.71 (1.18)	2.95 (0.55)	2.80 (1.05)
	T	2.3 (0.22)	2.30 (0.95)	2.40 (0.73)	2.30 (0.91)
Tensile strength (MPa)	L	25.9 (0.48)	14.0 (1.02)	16.2 (0.87)	15.9 (0.90)
	T	25.0 (0.39)	12.1 (0.98)	13.8 (0.97)	14.0 (0.95)
Elongation break (%)	L	1,050 (0.29)	700 (1.15)	625 (0.45)	695 (0.77)
	T	1,045 (0.31)	725 (1.06)	650 (0.88)	715 (1.11)
Tear strength (kN m ⁻¹)	L	35.1 (0.42)	37.5 (0.92)	42.0 (0.65)	42.5 (0.61)

L₁, L₂, and L₃ are mixes with fibre length 6, 10, and 14 mm, respectively. Figures given in the parentheses are standard deviations

O Orientation, L longitudinal, T transverse

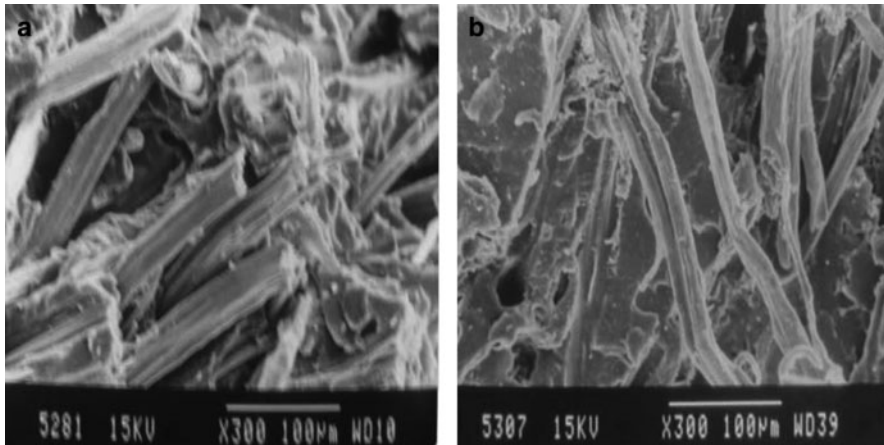


Fig. 11.10 SEM photographs showing (a) longitudinal and (b) transverse orientation of fibres in the composite X_{30}

and tear strength of the composites with longitudinal orientation are always higher than the composites with transverse fibre orientation (Table 11.7). The extent of fibre orientation can also be understood qualitatively from the examination of the SEM photographs. Figure 11.10a, b are tensile fracture surfaces of the longitudinally and transversely oriented composite (X_{30}). The broken fibre ends protruding from the fracture surface (Fig. 11.10a) indicate that the fibres are well aligned longitudinally in the direction of applied force. While in transverse orientation, the fibres are aligned across the direction of applied force (Fig. 11.10b). The tensile strength of the composites depends on the fibres, which obstruct the progress of the fracture front. In longitudinal orientation, the crack progresses in the direction perpendicular to the fibre alignment causing greater obstruction by the fibres and hence tensile strength increases. Breakage and pulling out of fibres take place when fibres are oriented longitudinally, whereas in transverse orientation crack progresses in the direction of fibre alignment experiencing a lower resistance by the fibres. The increase in tear strength in longitudinal orientation is due to the obstruction caused to the tear path by the short fibres.

Effect of Chemical Treatment and Fibre Loading

Good interfacial strength between the fibre and rubber is the essential factor to achieve good fibre reinforcement. The interfacial strength depends on the surface topology of the fibre. The cellulose fibres even though possess hydroxyl groups on its surface, the lignin and other waxy contents make it a less effective reinforcement. Hence to improve adhesion between isora fibre and rubber, it should be subjected to some chemical treatment to remove the lignin and other waxy impurities. So the mixes Y_{10} , Y_{20} , Y_{30} , and Y_{40} are prepared using alkali treated fibres. The surface

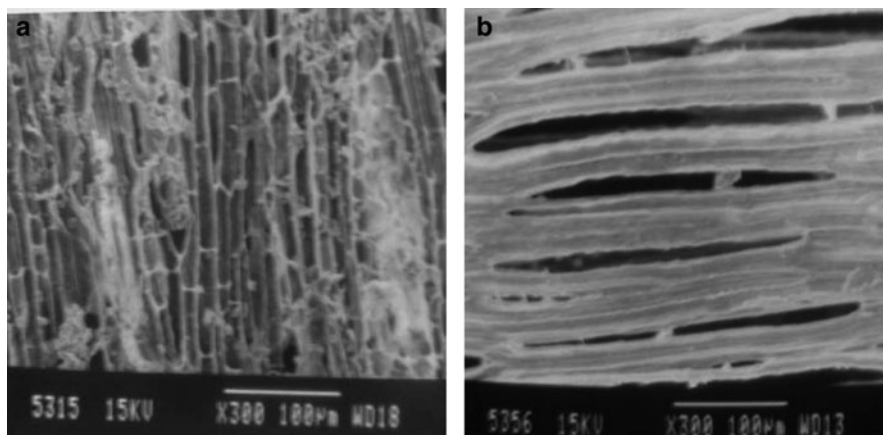


Fig. 11.11 SEM photographs of (a) raw fibre (b) alkali treated fibre

topology of isora fibre was studied by SEM, as shown in Fig. 11.11a, b. In Fig. 11.11a, the multicellular nature of the raw fibre is seen. The fibrillar nature and porosity of the fibre is revealed from the fibre topography. The porous surface morphology is useful to have better mechanical interlocking with the matrix for composite fabrication. The SEM of alkali treated fibre (Fig. 11.11b) gives strong evidence for the physical microcellular structural changes occurred to the fibre surface on mercerisation. Here pores become clearer and fibre becomes thinner, also fibres undergo fibrillation as shown in the figure. This may be due to the dissolution and leaching out of fatty acids and lignin components of the fibre. This renders roughness to the fibre, thereby enhancing the mechanical interlocking at the interface. The development of a rough surface topography offers better fibre rubber interface adhesion and increase in mechanical properties. Table 11.8 shows the mechanical properties of the composites containing treated and untreated fibres for varying fibre loadings. The tensile properties (tensile modulus, tensile strength, tear strength, etc.) of the composites filled with treated fibres are higher than those with untreated fibres at similar loadings. To obtain good fibre reinforcement in rubber composites, the adhesion between the rubber and the fibre is very important. From these results it is clear that the aqueous alkali treatment of isora fibre has improved the fibre adhesion to rubber matrix. It is reported that the surface of fibres can be modified by aqueous alkali treatment at elevated temperatures, and this was found to improve the adhesion properties significantly [32]. Fibre treatment can be used to prevent the debonding at the fibre interface since it can form covalent bonds between the rubber matrix and fibre. Strong adhesion between treated fibre and rubber leads to higher shear strength at fibre rubber interface. Stronger force must be used to overcome the shear strength, which resulted in higher tensile strength. The elongation at break for composites with treated fibres is lower than composites with untreated fibre at similar loading. This is due to the better strength and stiffness achieved from strong adhesion between fibre and rubber. Consequently,

Table 11.8 Mechanical properties of vulcanisates with varying fibre loading

Properties	O	Gum	X ₁₀	X ₂₀	X ₃₀	X ₄₀	Y ₁₀	Y ₂₀	Y ₃₀	Y ₄₀
Modulus (300% elongation) (MPa)	L	2.3 (0.32)	2.8 (0.19)	2.9 (0.41)	3.2 (0.92)	3.0 (0.65)	3.1 (1.12)	3.3 (0.84)	3.8 (0.64)	3.5 (1.05)
	T	2.3 (0.30)	2.0 (0.89)	2.1 (0.16)	2.2 (1.25)	2.4 (2.18)	2.5 (0.14)	2.6 (0.78)	2.8 (0.55)	2.9 (1.12)
Tensile strength (MPa)	L	25.9 (0.96)	20.9 (0.88)	14.0 (1.01)	9.8 (1.28)	9.0 (0.77)	21.1 (0.32)	15.2 (0.28)	10.7 (1.31)	9.8 (0.68)
	T	25.0 (0.93)	13.2 (0.82)	10.1 (1.44)	6.8 (1.05)	6.2 (0.79)	15.2 (0.59)	11.5 (1.34)	8.2 (1.28)	7.8 (0.37)
Elongation at break (%)	L	1050 (0.88)	860 (0.96)	615 (0.16)	437 (0.83)	380 (0.75)	790 (2.04)	605 (1.16)	400 (0.81)	310 (0.95)
	T	1045 (0.86)	900 (1.08)	690 (0.28)	480 (0.84)	425 (1.17)	612 (0.93)	625 (0.48)	412 (2.03)	395 (0.19)
Tear strength (kN m ⁻¹)	L	35.1 (0.68)	36.5 (0.96)	42.8 (0.77)	46.8 (0.18)	40.9 (0.99)	38.1 (0.83)	44.6 (1.52)	47.9 (1.17)	43.1 (0.31)
	T	34.5 (0.74)	35.5 (1.11)	40.1 (1.41)	43.9 (0.32)	39.5 (0.53)	37.5 (1.00)	41.9 (0.86)	44.2 (0.56)	40.8 (0.57)
Hardness (shore A)	-	45	50	63	69	72	55	65	73	76

Figures given in parentheses are standard deviations

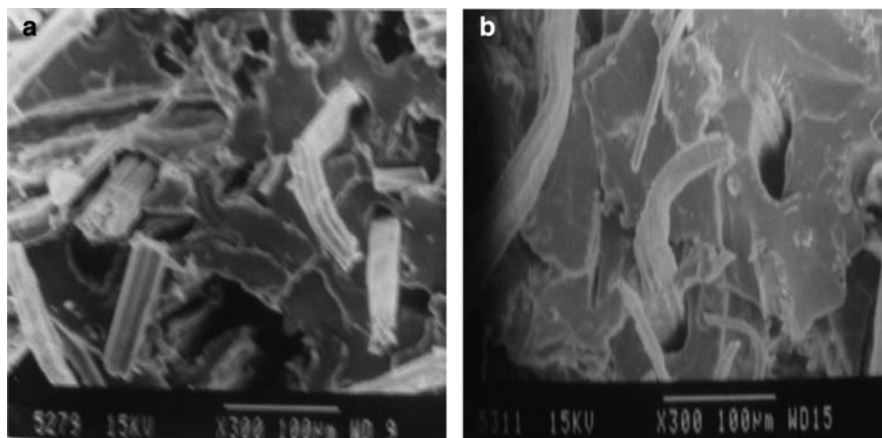


Fig. 11.12 SEM of the fractured surface containing (a) untreated (b) alkali treated fibres of the composites X_{30} and Y_{30}

the toughness of the composites is reduced resulting in lower elongation at break. Higher toughness is obtained from weak interfacial adhesion as shown by higher elongation at break for composites filled with untreated fibres. Figure 11.12a, b are the SEM of the tensile fracture surfaces of composites with untreated and treated fibres (X_{30} and Y_{30}). In the case of untreated fibre composites, due to the weak interfacial adhesion between the fibre and rubber, fibre pull out may take place leaving holes on the surface when stress is applied (Fig. 11.12a). Figure 11.12b shows the presence of broken fibres on the fracture surface which is due to the strong adhesion between the fibre and rubber matrix for composites with treated fibres. Composites containing treated fibres show enhancement in modulus compared to the untreated ones for similar fibre loading.

Natural rubber inherently possesses high tensile strength due to strain-induced crystallisation. When fibres are incorporated into NR, the regular arrangement of rubber molecules is disrupted and hence the ability of crystallisation is lost. Hence the fibre reinforced natural rubber composites possess lower tensile strength than gum compounds. When fibre reinforced rubber composites are subjected to a load, the fibres act as carriers of load and stress is transferred from matrix along the fibres which results in a composite having good mechanical properties. The uniform distribution of stress is dependant on the population and orientation of fibres. At low levels of fibre loading, the orientation of fibres is poor and the fibres are not capable of transferring load to one another and stress get accumulated at certain points of composite, leading to low modulus. From Table 11.8, it is clear that modulus shows a continuous increase up to 30 phr fibre loading in the case of longitudinal orientation. At higher levels of fibre loading, the increased population of fibres leads to agglomeration, and stress transfer gets partially blocked. On transverse orientation, the modulus increases gradually but with a lower value than longitudinal orientation. Also with the increase of fibre loadings, tensile strength of the

composites shows an abrupt decrease up to a loading of 30 phr and there afterwards a gradual decrease both in longitudinal and in transverse orientations. At intermediate levels of loading (30 phr), the population of fibres is just sufficient for maximum orientation and fibres actively participate in stress transfer. As fibre loading increases tear strength gradually increases and reaches a maximum at 30 phr fibre loading. When the fibre loading increased further, tear strength again decreases as the increased strain in the matrix between closely packed fibres increases tearing and reduces the tear strength. Maya and Thomas [33] also have observed similar results. There is a reduction for elongation at break with increasing fibre loading. Increased fibre loading in the rubber matrix resulted in composites becoming stiffer and harder. This will reduce the composite's resilience and lead to lower elongation at break. The elongation at break for composites with treated fibres is lower than composites with untreated fibre at similar loading. This is due to the better strength and stiffness achieved from strong adhesion between fibre and rubber. Consequently, the toughness of the composites is reduced resulting in a still lower elongation at break. Higher toughness is obtained from weak interfacial adhesion as shown by higher elongation at break for composites filled with untreated fibres.

Effect of Bonding Agent

Further increase in properties is seen by the incorporation of bonding agent to the system. It has already been established that a tricomponent system consisting of hexamethylene tetramine, resorcinol, and fine particle of silica can be used as a bonding agent for most rubber and fibre combinations [34]. Presence of bonding agent in the mixes improved the mechanical properties like modulus, tensile strength, and tear strength. Alkali treatment of fibres further enhances the effect of bonding agent as seen from the higher modulus, tensile strength, tear strength, etc. from Figs. 11.13–11.15. The treated fibre provides a better surface for strong adhesion between fibre and matrix, and the stress transfer becomes more efficient and consequently better enhancement in the properties. Elongation at break for composites with bonding agent has a lower value than composites without bonding agent. Again treated fibres show a lower elongation at break than untreated fibres (Fig. 11.16). The variation of compression set, abrasion loss, and hardness with fibre loading for the treated and untreated fibre composites with bonding agent are given in Figs. 11.17–11.19. Compression set increased steadily with increase in fibre loading. The rate of increase in set, however, decreased as loading was increased. But the set was lower for the composites having alkali treated fibres (Fig. 11.17). It has been reported that this behaviour is due to the buckling of the fibre, taking place invariably when the closely packed fibres are compressed in the direction of their alignment [35]. Due to the strong adhesion between the treated fibres and rubber, the extent of buckling is reduced in treated fibre composites resulting in a low value for the set. Abrasion loss decreased with increase in fibre concentration in the composite (Fig. 11.18). Here also the treated fibre composites

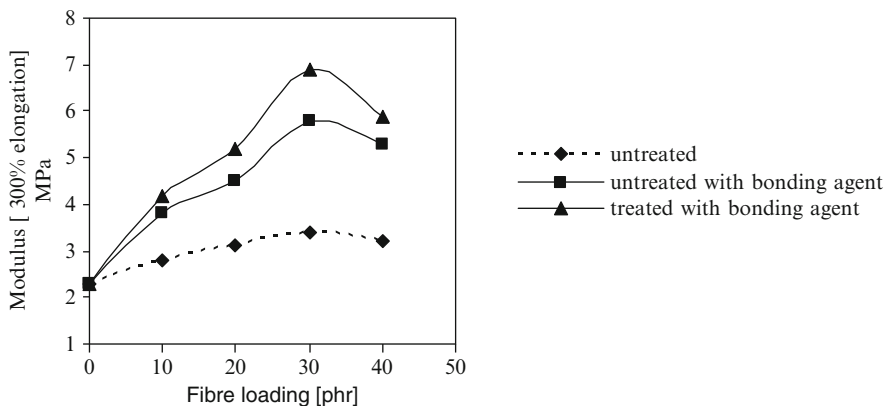


Fig. 11.13 Effect of fibre loading on modulus of the composites

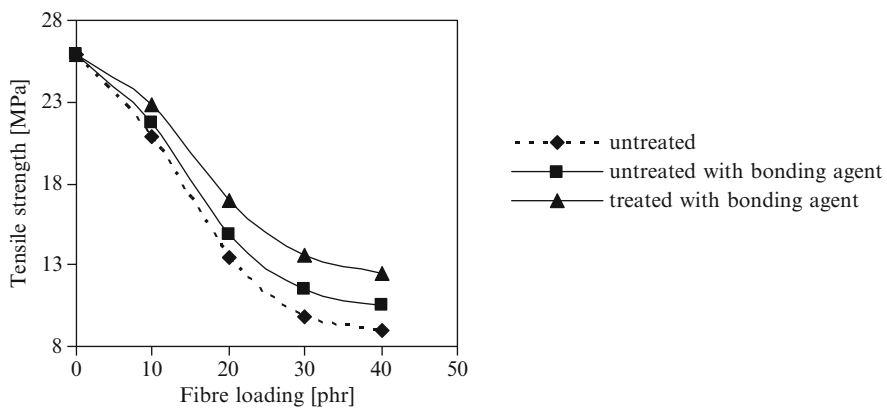


Fig. 11.14 Effect of fibre loading on tensile strength of the composites

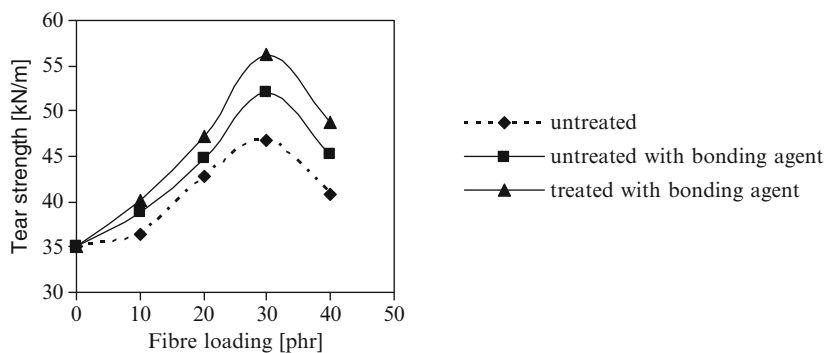


Fig. 11.15 Effect of fibre loading on tear strength of the composites

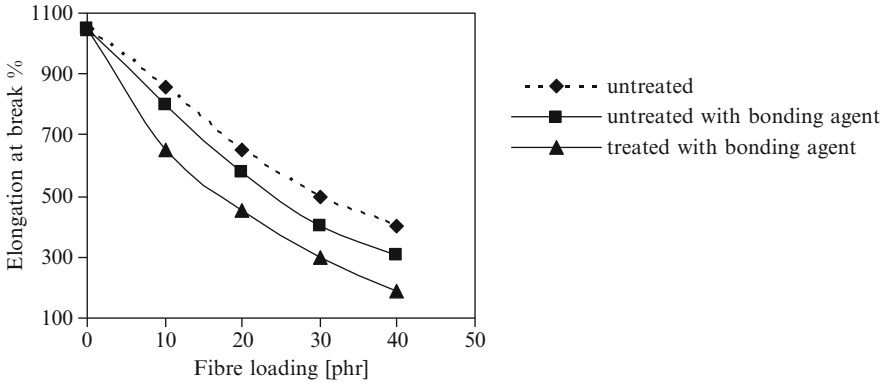


Fig. 11.16 Effect of fibre loading on elongation at break of the composites

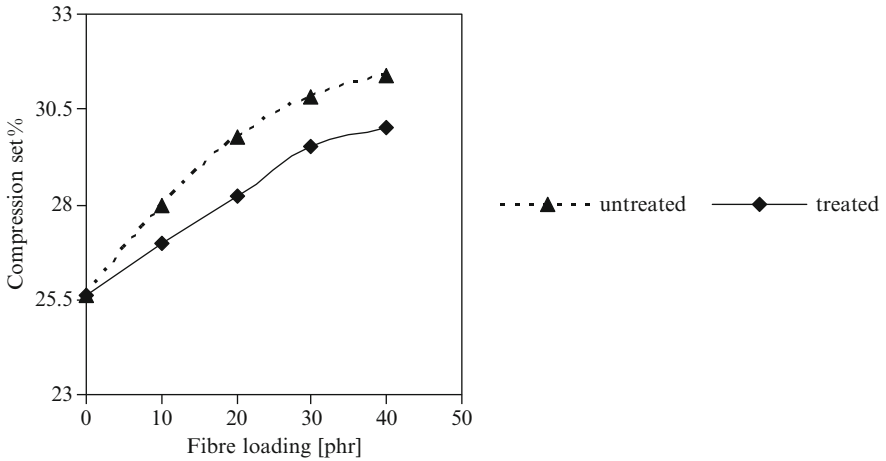


Fig. 11.17 Variation of compression set with fibre loading for the composites with bonding agent

showed better resistance to abrasion compared to those containing untreated fibres. The better abrasion resistance of the treated fibre composites may be resulting from the combination of higher tear strength, tensile strength, and modulus achieved through better bonding with the rubber matrix. The hardness of the composites also increases in the presence of bonding agent (Fig. 11.19). The SEM studies revealed the indications of high interfacial adhesion. Figures 11.20a, b and 11.21a, b are the SEM of the tensile and tear fracture surfaces of composites (X₃₀ and Y_{30b}) with and without bonding agent. SEM studies also revealed that for composites without bonding agent, failure occurred at the weak fibre/rubber interface while for composites containing treated fibre and bonding agent failure occurred at the fibre due to strong adhesion between fibres and matrix.

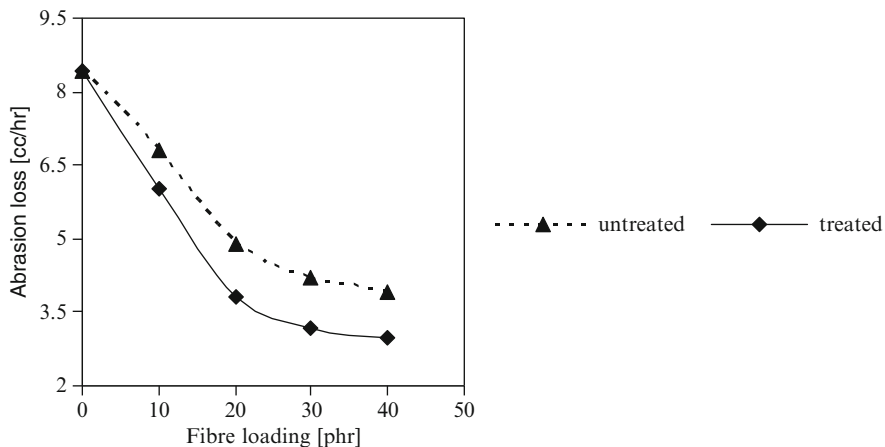


Fig. 11.18 Variation of abrasion loss with fibre loading for the composites with bonding agent

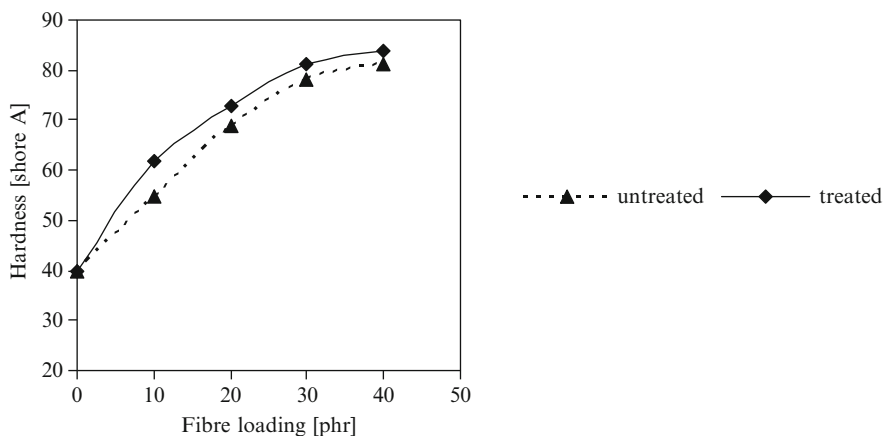


Fig. 11.19 Variation of hardness with fibre loading for the composites with bonding agent

11.3.2 Isora: Polyester Composites

11.3.2.1 Composite Preparation

Unidirectional isora fibre–polyester composites containing varying fibre volume fractions were prepared by hand lay up technique using a three-piece stainless steel mould having dimensions $150 \times 70 \times 2 \text{ mm}^3$. Prior to the composite preparation, the mould surface was polished well and a mould releasing agent (waxpol) was applied on the surface. A weighed amount of the polyester resin was thoroughly mixed with 0.5% by wt. Cobalt naphthenate accelerator and 0.5% by wt. MEKP

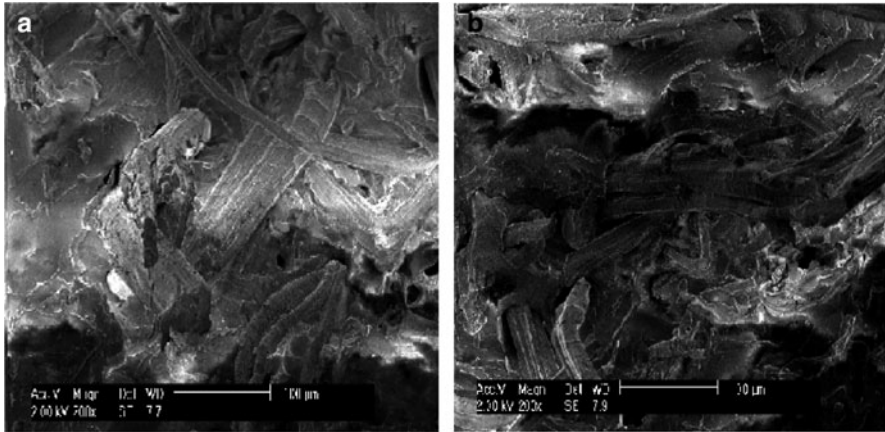


Fig. 11.20 SEM of the tensile fractured surfaces containing (a) untreated fibre without bonding agent and (b) treated fibre with bonding agent of the composites X₃₀ and Y_{30b}

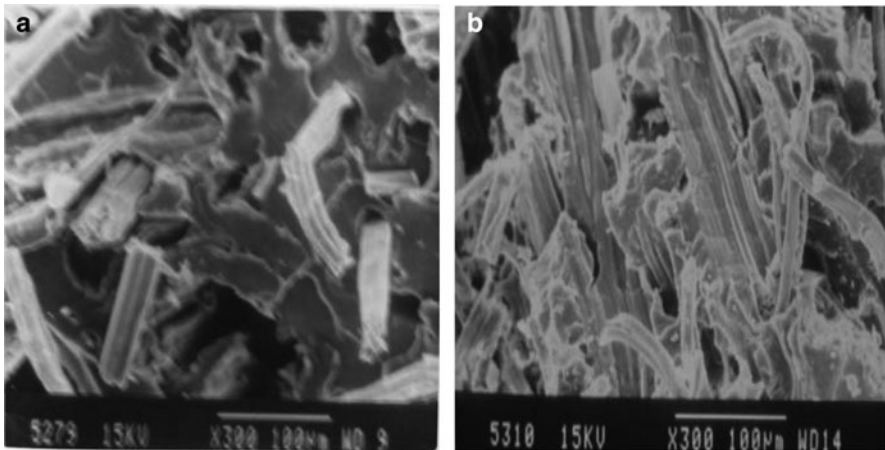


Fig. 11.21 SEM of the tear fractured surfaces containing (a) untreated fibre without bonding agent and (b) treated fibre with bonding agent of the composites X₃₀ and Y_{30b}

catalyst. Using a brush, the resin was applied evenly on the fibre lamina and were stacked one above the other in the mould and the mould was closed. The mould was pressed in a hydraulic press at room temperature and the excess resin was allowed to flow out as “flash.” The pressure was increased very slowly taking care to avoid the slippage of the fibre sheets, so that the unidirectional nature of the fibre is not lost. The pressure was held constant during curing. Mylar film was placed on both sides of the stack for easy release and to obtain superior surface finish of the pressed laminates. The composite sheet was post-cured at 80°C for 4 h. From the sheet, samples were cut for measuring tensile and flexural properties according to

ASTM standards. Composites containing varying fibre loading were prepared using untreated and alkali treated fibres.

The mould with dimensions $120 \times 60 \times 4 \text{ mm}^3$ was used for preparing samples to determine the impact strength. Composites were prepared in a similar manner described above, using untreated and alkali treated fibres.

11.3.2.2 Characterisation of the Composites

The SEM photographs of the fractured surfaces of the composites were taken using a JEOL JSM 840 SEM. Dynamic mechanical analysis of the composites was carried out using rectangular specimens of size $60 \times 10 \times 3 \text{ mm}^3$. The dynamic moduli and mechanical damping ($\tan \delta$) were measured using a dynamic mechanical thermal analyser DMA Q80, TA instruments. The temperature range over which properties were measured ranged from 30 to 130°C at a heating rate of 3°C min^{-1} . The test was carried out at a frequency of 1 Hz.

Tensile testing of the composite specimens was carried out according to ASTM D5083 on a Shimadzu Model AG1 50 kN universal testing machine at a cross head speed of 20 mm min^{-1} and a gauge length of 50 mm. Rectangular specimens of dimensions $150 \times 10 \times 2 \text{ mm}^3$ were used for testing. The tensile strength and Young's modulus were determined from the stress–strain curves.

Flexural tests were performed according to ASTM D790 with rectangular strips of size $75 \times 20 \times 2 \text{ mm}^3$ at a cross head speed of 2 mm min^{-1} and lower support 32 mm. Flexural strength and flexural modulus were determined from the stress–strain curves.

Izod impact strength of unnotched sample of the composite was determined according to ASTM D256 using Tinius Olsen Model 503.

11.3.2.3 Dynamic Mechanical Analysis of the Composite

Dynamic mechanical thermal analysis was carried out on the cured neat resin and composite samples. The DMA curves of storage modulus (E') versus temperature of neat resin (cured) and composites containing raw (UT) and alkali treated (AT) fibres are given in Fig. 11.22a. It is evident from the figure that the E' values of the composites are higher than that of neat resin. Also the alkali treated fibre composite has higher E' value compared to untreated one. The higher E' value of the treated long isora fibre reinforced polyester composite is due to greater interfacial adhesion and bond strength between matrix resin and fibre as reported by several authors [36, 37].

Figure 11.22b shows $\tan \delta$ versus temperature plots of neat resin (cured) and composites containing UT and AT fibres. It has been reported by other researchers that incorporation of stiff fibres reduced the $\tan \delta$ peak by restricting the movement of polymer molecules [36, 38]. From Fig. 11.22b it can be observed that the height of the $\tan \delta$ peaks of the composites lie far below that of the neat resin. It can also be noted that the peak height of the UT and AT fibre composites are almost same, indicating the same damping capabilities of the composites. Similar results have been reported

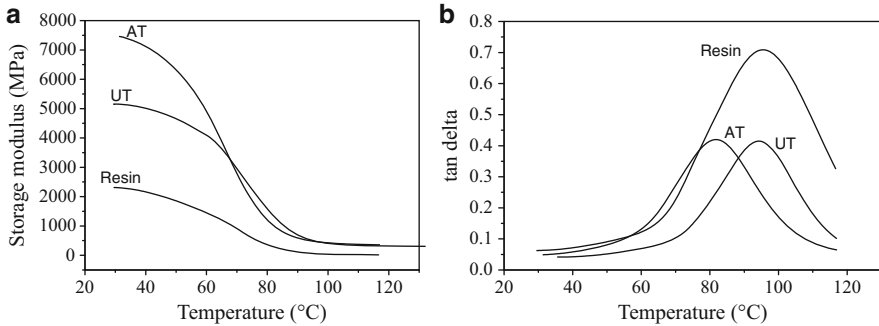


Fig. 11.22 (a) Variation of storage modulus with temperature of neat resin (cured) and composites containing untreated and alkali treated fibres. (b) Variation of $\tan \delta$ with temperature of neat resin (cured) and composites containing untreated and alkali treated fibres

for hemp fibres by Aziz and Ansell [37]. This is also supported by the impact strength of the UT and AT fibre composites.

11.3.2.4 Mechanical Properties of the Composite

(a) *Tensile properties.* The effect of alkali treatment of the fibre on tensile strength of the composite with fibre loading is given in Fig. 11.23. Tensile strength for the UT and AT fibre composite increased regularly with fibre loading. For UT fibre composite the tensile strength showed maximum value at 45% fibre loading. AT fibre composites showed higher tensile strength values at all fibre loadings indicating enhanced adhesion in the composite. The optimum fibre loading is increased from 45 to 66%, which is again an indication of enhancement in fibre/matrix adhesion in the composite. At higher fibre loadings, the tensile strength values showed a gradual decrease. Young's modulus values for the treated and untreated fibre composites varied in a similar way (Fig. 11.24).

At the optimum fibre loading, there is maximum wetting of the fibre and effective stress transfer at the fibre/matrix interface occurred. The decrease in tensile properties at higher loadings may be due to improper wetting and adhesion between fibre and matrix resulting in inefficient stress transfer.

(b) *Flexural properties.* The effect of alkali treatment on the flexural strength with fibre loading of UT and AT fibre composites is given in Fig. 11.25. The flexural strength of the UT and AT fibre composite increased regularly with fibre loading, the latter values being always higher than the former at all loadings. UT fibre composite showed maximum flexural strength at 56% loading and AT fibre composite at 66% loading, after which the values decreased. So the optimum fibre loading for flexural properties of the untreated fibre composite is 56%. Increase in flexural strength with fibre loading is due to better interaction between fibre and matrix, whereas the decrease of flexural strength at higher fibre loading is due to increased fibre to fibre interaction and also due to dispersion problems. Alkali treatment enhances the

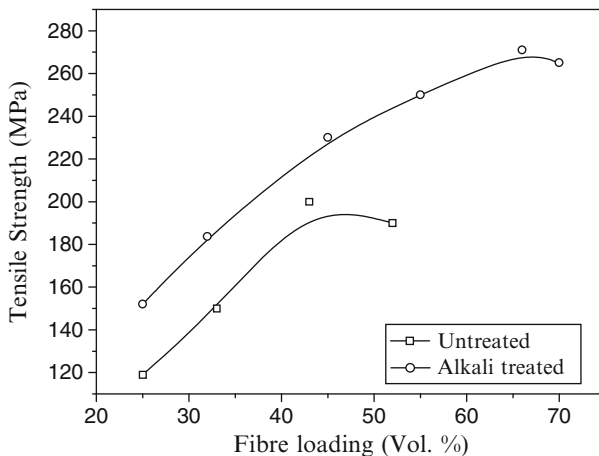


Fig. 11.23 Effect of alkali treatment on the tensile strength of the composite

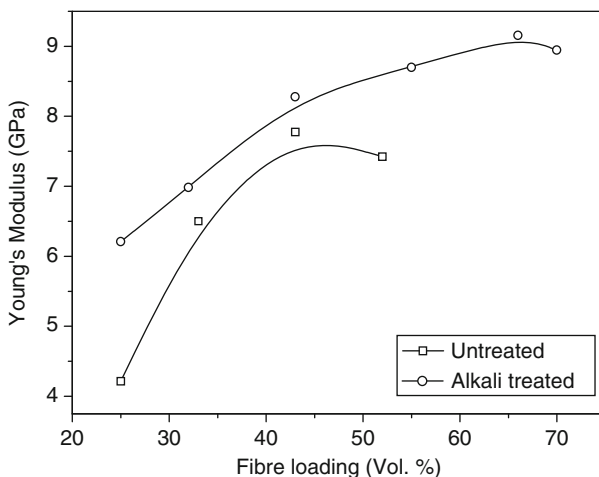


Fig. 11.24 Effect of alkali treatment on the Young's modulus of the composite

optimum fibre loading for flexural properties from 56 to 66% which indicates enhanced fibre/matrix adhesion in the composite. Flexural modulus of the treated and untreated fibre composites varied in the same manner (Fig. 11.26).

11.3.2.5 Impact Strength

Figure 11.27 shows the variation of impact strength of the untreated fibre composite as a function of fibre loading. Impact strength increases with fibre loading, reached

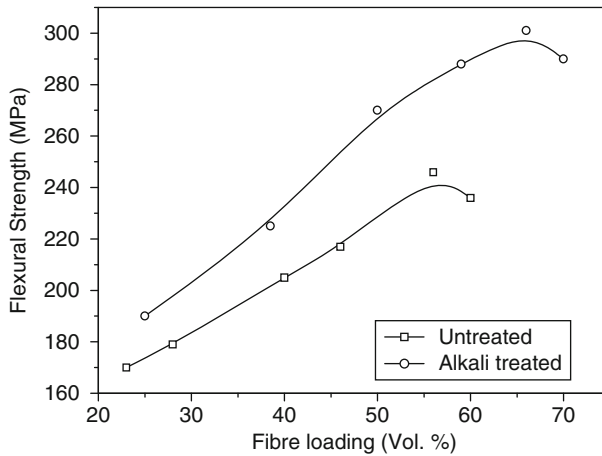


Fig. 11.25 Effect of alkali treatment on the flexural strength of the composite

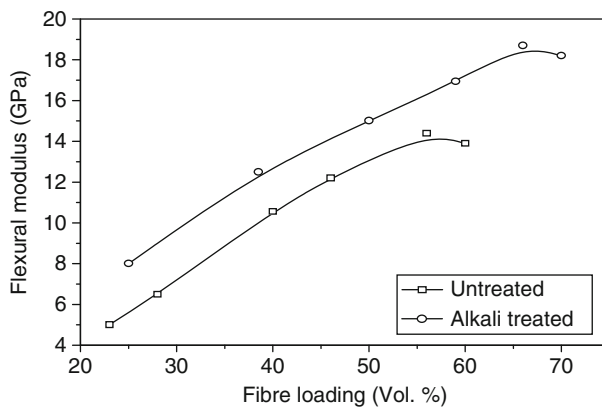


Fig. 11.26 Effect of alkali treatment on the flexural modulus of the composite

a maximum at 57% by volume of fibre. With further increase in fibre loading, there is no significant increase in impact strength. There is only a nominal increase in impact strength on alkalisation of the fibre (Fig. 11.28). This is supported by the DMA analysis. The fibres play an important role in the impact resistance of the composites as they interact with the crack formation in the matrix and act as stress transferring medium.

On alkali treatment, lignin and hemicellulose, the cementing materials present in the fibre, get dissolved. This makes the interfibrillar region less dense and less rigid as a result of which the fibrils become more capable of orienting themselves along the tensile deformation [39]. Other authors have also reported on the change in crystallinity of alkali treated fibre because of the removal of the cementing

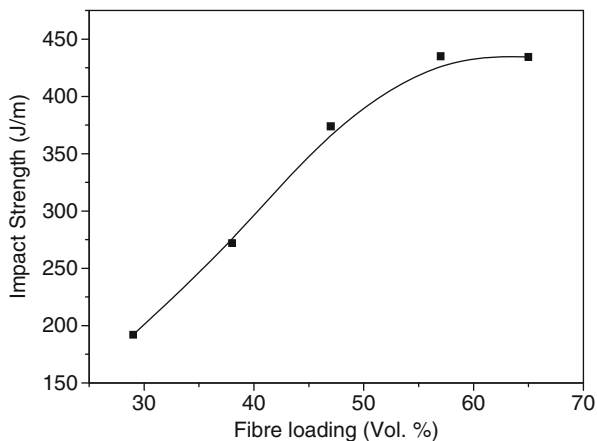


Fig. 11.27 Variation of impact strength of the untreated fibre composite with fibre loading

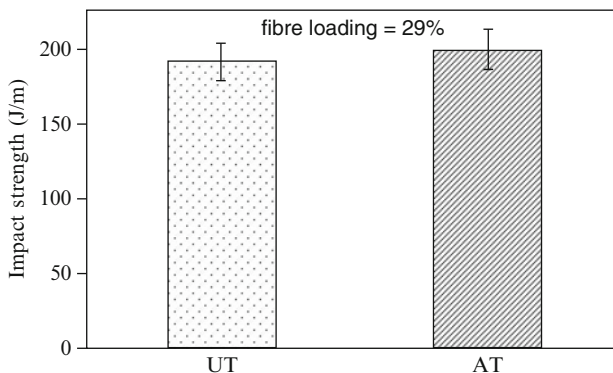
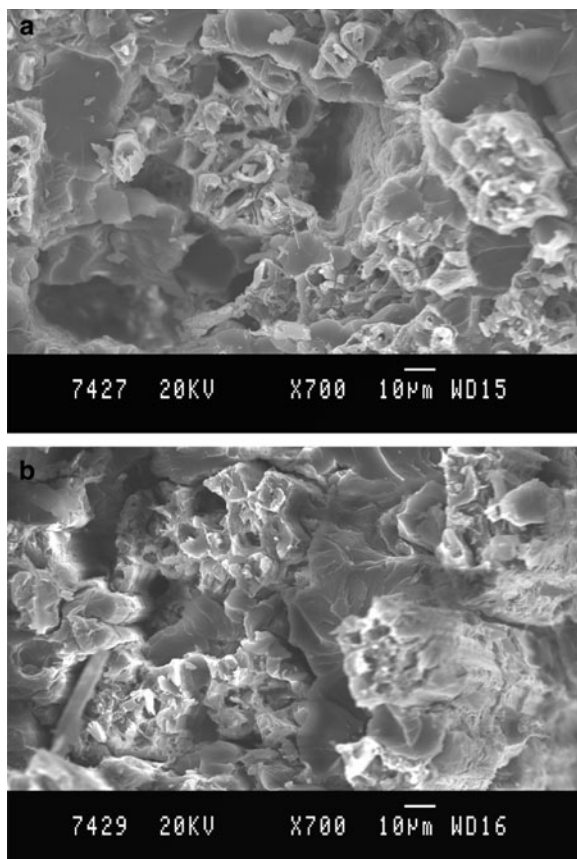


Fig. 11.28 Effect of alkali treatment on the impact strength of the composite

materials which leads to a better packing of cellulose chains [40, 41]. More than that increase in surface area of the fibre occurs due to the dissolution of lignin, hemicellulose, and alien substances associated with the fibre. Alkali treatment cleans the surface debris and develops microporosity with many pits and holes on the fibre surface by the removal of globular protrusions of fibre surface present in the untreated fibre. This leads to a larger area of contact and greater mechanical interlocking between fibre and matrix, making the interfacial adhesion stronger and the mechanical properties higher.

SEM micrographs of the tensile fractured surfaces of the composites containing untreated and alkali treated fibres (Figs. 11.29a, b) were investigated to evaluate the fibre/matrix adhesion which again indicates a better fibre–matrix interfacial adhesion for the alkali treated fibre composite.

Fig. 11.29 (a) SEM photograph of the tensile fractured surface of untreated fibre composite. (b) SEM photograph of the tensile fractured surface of alkali treated fibre composite



11.4 Conclusions

11.4.1 Fibre Characterisation

Isora is found to be a cellulosic rich fibre with comparatively less lignin content.

A small positive change in the fibre density was observed for the treated fibres indicating cell wall densification. Isora fibre contains a higher percentage of hot water soluble and caustic soda soluble matter.

Chemical treatment slightly reduced the tensile strength of the fibre as the binding component of the fibrils gets removed on alkali treatment. Elongation at break more or less same even after the treatment.

WAXRD studies indicate an increase in the crystallinity index after chemical treatment.

FTIR spectroscopy has provided additional information on the reactivity of the fibres following treatment with alkali and silane

SEM studies revealed that chemical treatment modified the fibre surface. Fine structural changes of the fibres can be seen from the respective SEM photographs.

Thermal stability and degradation characteristics of the fibre was investigated by TGA/DTG, DTA, and DSC which indicate that thermal stability of the fibres was increased upon treatment with alkali and silane. Fibres are stable up to 300°C without any considerable weight loss.

Finally, it is important to mention that properties of isora fibre are comparable to other natural fibres and therefore they could be successfully used as a potential reinforcing material for polymer matrices.

11.4.2 Isora: Rubber Composites

The mechanical properties of short isora fibre reinforced natural rubber composites are enhanced by chemical treatment on the fibre surface and by the use of bonding agent. Longitudinally oriented fibre composites have superior properties than transversely oriented ones.

The optimum length and loading of isora fibre in NR composite are found to be 10 mm and 30 phr, respectively, to achieve good reinforcement.

The surface morphology of isora fibre is modified by alkali treatment. SEM analysis revealed that better adhesion is observed between alkali treated isora fibre and NR in the composites.

Presence of bonding agents in the composites prolonged curing time.

SEM studies also revealed that for the control compound (untreated fibre without bonding agent), failure occurred at the weak fibre/rubber interface, while for composites containing treated fibre and bonding agent, failure occurred in the fibre due to the strong adhesion at the fibre/rubber interface.

11.4.3 Isora: Polyester Composites

The optimum fibre loading for untreated fibre composite for tensile and flexural properties were found to be 45 and 49 vol.%, respectively.

On alkali treatment, the optimum fibre loading for tensile and flexural properties was increased to 66 vol.%, indicating enhanced fibre–matrix adhesion.

Impact strength of the composite increased with increase in fibre loading and remained constant at a loading of 57 vol.%.

Alkali treatment has only a marginal effect on the impact strength.

DMA analysis revealed that treated fibre composite has higher storage modulus (E'), equal $\tan \delta$, and impact strength indicating greater interfacial bond strength and adhesion between the matrix and the fibre compared to untreated fibre composites.

SEM studies of the tensile fractured surface of the composites gave evidence for the enhanced interfacial adhesion between the fibre and the matrix on alkalisation of the fibre.

References

1. Scola DA (1974) In: Broutman LJ, Krock RH (eds) *Composite materials*, vol 6. Academic, New York, pp 239–245
2. Ismail H, Rosnah N (1997) *Polym International* 43:223–230
3. Edyham MR, Ismail H (2002) *Eur Polym J* 38:39–47
4. Ray D, Sarkar BK, Rana AK (2001) *Bull Mater Sci* 24(2):129–135
5. Geethamma V, Joseph R, Thomas S (1995) *J Appl Polym Sci* 55:583–594
6. Sreekala M, Kumaran M, Thomas S (1997) *J Appl Polym Sci* 66:821–835
7. Liu C, Cuculo J, Allen T (1991) *J Appl Polym Sci Polym Phys* 29:181–196
8. Pothan L, Neelakandan NR, Thomas S (1997) *J Reinf Plast Comp* 16(8):744–765
9. Ansell M, Mwaikambo LY (2002) *J Appl Polym Sci* 84(12):2222–2223
10. Devi L, Bhagawan S, Thomas S (1997) *J Appl Polym Sci* 64:1739–1748
11. Chen X, Guo Q, Mi Y (1998) *J Appl Polym Sci* 69:1891–1899
12. Punnoose T (1953) *Plant fibres. Indian Text J* 63:388–400
13. Krishnamurthy T (1993) *Minor forests products of India*. Oxford & IBH, New Delhi
14. Lovely M, Joseph KU, Rani J (2004) *Prog Rubb Plast Recyc Technol* 20(4):337–351
15. Joshy MK, Lovely M, Rani J (2005) *Compos Interf* 13(4–6):370
16. Ismail H, Rosnah N, Rozman HD (1997) *Polymer* 38(16):4059
17. Geethamma VJ, Thomas S, Kuriakose B (1995) *J Appl Polym Sci* 55:583
18. Belgacem MN, Baille P (1994) *J Appl Polym Sci* 53:379
19. Felix JM, Carlson CMG (1994) *J Adhes Sci Technol* 8(2):163
20. Geethamma VJ, Thomas S (1998) *Polymer* 39:1483
21. Sapiha S, Pupo JF (1989) *J Appl Polym Sci* 37:233
22. Felix JM, Gatenholm P (1991) *J Appl Polym Sci* 42:609
23. Bisanda BTN, Ansell MP (1991) *Comp Sci Technol* 41:167
24. Ismail H, Edyham MR, Shuhelmy S (2002) *Eur Polym J* 38:39
25. Uma Devi L, Bhagavan SS, Thomas S (1997) *J Appl Polym Sci* 64:1739–1748
26. Dash BN, Rana AK, Mishra HK (2004) *Polym Comp* 20(1):62–71
27. Satyanarayana KG, Pilli CKS, Sukumaran K (1982) *J Mater Sci* 17:2453
28. Akita K, Kase M (1967) *J Polym Sci A* 5:833–848
29. Aziz SH, Ansell M (2004) *Comp Sci Technol* 64:1219–1230
30. Goettler LA, Shen KS (1983) *Rubb Chem Technol* 56:619
31. Chakraborty SK, Setu DK (1982) *Rubb Chem Technol* 55:1286
32. Czvikovszky T, Kovacs I (1985) *J Appl Polym Sci* 30:1827
33. Maya J, Thomas S (2004) *Comp Sci Technol* 64:955
34. Varghese S, Kuriakose B, Thomas S (1994) *J Adhes Sci Technol* 8(3):235
35. Murthy VM, De SK (1982) *Rubb Chem Technol* 55:287
36. Ray D, Sarkar BK, Das S, Rana AK (2002) *Comp Sci Technol* 62:911–917
37. Aziz SH, Ansell MP (2004) *Comp Sci Technol* 63:283–293
38. Saha AK, Das S, Bhatta D, Mitra BC (1999) *J Appl Polym Sci* 71:1505–1513
39. Gassan J, Bledzki AK (1999) *Comp Sci Technol* 59:1303–1309
40. Varma DS, Varma M, Varma IK (1984) *J Text Res* 54:349
41. Sharma HSS, Fraser TW, Mc Call D, Lyons G (1995) *J Text Inst* 86:539

Chapter 12

Pineapple Leaf Fibers and PALF-Reinforced Polymer Composites

S.M. Sapuan, A.R. Mohamed, J.P. Siregar, and M.R. Ishak

Abstract Pineapple leaf fibers (PALF) have long been known as textile materials in many countries. Despite being mechanically excellent and environmentally sound, PALF are the least-studied natural fibers, especially for reinforcing composites. This article presents a survey of research works carried out on PALF and PALF-reinforced composites. It reviews PALF extraction, fiber characterization, and PALF applications, modification of PALF, and manufacture and properties of PALF-reinforced composites. With increasing importance of pineapple and pineapple plantation area, value-added applications of PALF as reinforcing fibers in polymer composites must be developed in order to increase “resource potential” of pineapple and consequently energize the utilization of PALF.

Keywords *Ananas comosus* · PALF-reinforced composites · Pineapple leaf fibers

Contents

12.1	Introduction	326
12.2	Pineapple Leaf Fibers	327
12.2.1	PALF Applications	327
12.2.2	PALF Extraction	328
12.2.3	PALF Characterization	330
12.2.4	PALF Modifications	332
12.3	PALF-Reinforced Polymer Composites	334
12.3.1	PALF-Thermoplastics Composites	334
12.3.2	PALF Thermoset Polymer Composites	336
12.3.3	Other Matrices Reinforced with PALF	337
12.3.4	Hybrid PALF-Reinforced Composites	338
12.4	Conclusions	338
	References	339

S.M. Sapuan (✉)

Department of Mechanical and Manufacturing Engineering, Universiti of Putra Malaysia, 43400 UPM Serdang, Selangor, Malaysia
e-mail: sapuan@eng.upm.edu.my

12.1 Introduction

Polymer composites represent a class of versatile materials, each comprising a matrix binding a filling or reinforcing phase(s) resulting in a material with more desirable properties than those of the constituents taken individually (Mallick 1993). Matrices and synthetic fibers made from petroleum-based resources or produced using energy-intensive processes have been the standard constituents in making polymer composites until recently. Depletion of natural resources and serious environmental problems has spurred the search for renewable and more environment-friendly materials. The scientific community has since taken a serious relook at using natural plant fibers to reinforce composites like they used to be utilized during the early days.

Natural plant fibers have become popular among the scientific community as viable alternatives to glass fibers in fiber-reinforced plastics. These lignocellulosic fibers have lower densities, cost relatively lower to produce, consume lesser energies during production, pose no abrasion to machines and have no health risk when inhaled; in addition to being widely available, they are renewable and biodegradable and are CO₂ neutral (Wambua et al. 2003). To make it even more attractive, many of the fiber sources are at present agricultural wastes (Abdul Khalil et al. 2006).

One such fiber source known for a long time is pineapple leaves from which pineapple leaf fibers (PALF) may be extracted. Pineapple (*Ananas comosus*) is the third most important tropical fruit in the world after banana and citrus (Bartholomew et al. 2002). While reportedly having some of the highest mechanical properties (Bismarck et al. 2005), PALF are still the least-studied fibers, and pineapple leaves are mainly wasted through composting and burning. It is high time that value-added applications of PALF are identified as industrial significance and plantation area of pineapple in many countries increase (Anon 2008b). Development of PALF as reinforcing fibers in polymer composites shall improve the utilization of “resource potential” of pineapple (Benjamin and van Weenen 2000).

The properties of a composite are dictated by the intrinsic properties of the constituents which may be summarized as fiber architecture and fiber–matrix interface (Fowler et al. 2006). The reinforcing efficiency of natural fibers depends on their physical, chemical, and mechanical properties. Major shortcomings of natural plant fibers include fiber nonuniformity, property variation even between individual plants, low degradation temperature, low microbial resistance, and susceptibility to rotting. In addition to naturally occurring nonuniformity, fiber extraction and processing techniques also have major impacts on final fiber quality, not to mention fiber costs and yield (Munder et al. 2005).

Another serious drawback of using natural fibers with polymeric matrices is poor fiber–matrix interfacial adhesion, thus impairing composite mechanical and other properties. Optimization of interfacial adhesion between natural fibers and thermoplastic and thermoset matrices has been the focus of a large amount of research conducted during the past two decades (John and Anandjiwala 2008). Various

means of modification applied on either the fibers or the matrix change not only the fiber–matrix interface, but also the fibers themselves.

12.2 Pineapple Leaf Fibers

PALF are obtained from the leaves of pineapple plant (*A. comosus*) from the family of Bromeliaceae (Anon 2008a) as shown in Fig. 12.1. Mwaikambo stated that pineapple plants are largely grown in tropical America, Africa, and Far-East Asian countries (Mwaikambo 2006). Thailand and the Philippines are the biggest pineapple fruit producers in the world (Anon 2008c). The Food and Agriculture Organization (FAO) has reported that most of the world pineapple fruit production in 2001 amounting to about 13.7 million tons of fresh fruits are produced in Asia (Anon 2008d). Pineapple leaves from the plantations are being wasted as they are cut after the fruits are harvested before being either composted or burnt. Ahmad et al. concluded that the practices of decomposing and burning the leaves in situ did not contribute to the improvement of plantation yield (Ahmed et al. 2002, 2004). Additionally, burning of these beneficial agricultural wastes causes environmental pollution.

12.2.1 PALF Applications

PALF have been traditionally used for making threads and textile fabrics in many countries. In the Philippines, PALF have been used for commercial products such as dresses, table linens, bags, mats, and other clothing items (Anon 2008b). PALF are also being utilized as textile materials in Indonesia, while works on using PALF for this application have just started in Malaysia (Mohamed et al. 2009). The use of



Fig. 12.1 Pineapple plant

chemically treated PALF in making industrial textiles, V-belt cord, conveyor belt cord, transmission cloth, air-bag tying cords, and shoe laces was reported in Basu et al. (2003). PALF can be blended with polyester fibers to replace jute for making needle-punched nonwovens for technical textiles (Hayavadana et al. 2003). The spinning, weaving, and processing of PALF were examined in Kumar et al. (1997), where the authors reported the use of PALF in making carpets and urged further studies on chemical processing, dyeing behavior, strength losses, and fiber degradation of PALF. PALF were blended with polyester fibers and silk, resulting in esthetically pleasing fabric and nonwovens (Anon 1992). The use of PALF to reinforce composites, the main focus of this review, shall be explained in the coming sections. Using PALF as textiles involves elaborate processes to increase the fiber fineness, blendability, and dyeing-ability. PALF dresses are known to be very costly understandably due to tedious manual processes involved. In contrast, the use of PALF as reinforcements in polymer composites may not involve such processes.

12.2.2 PALF Extraction

Pineapple leaves from which PALF are extracted are about 70–90 cm in length and 5–7.5 cm in width. Figure 12.2a shows the sword-shaped, dark green pineapple leaves, while Fig. 12.2b shows the extracted PALF bundles from the leaves. Manual extraction process can extract at least 3–4% of fibers from the leaves (Paul 1980). PALF are strong, white, and with a silky luster (Fig. 12.2c) and they are usually used to produce rope, broom, mat, nets, and cloths (Bhaduri et al. 1983).

Like other natural fibers, PALF vary in their properties according to species, geographical regions, age, locations in each plant, and weather conditions among others (Bismarck et al. 2005). There are many different species under the genus of *A. comosus*, while in the works on PALF and PALF-reinforced polymer composites reviewed, specific species of pineapple from which PALF were extracted were barely mentioned. Only in Bhaduri et al. (1983) the chemical compositions

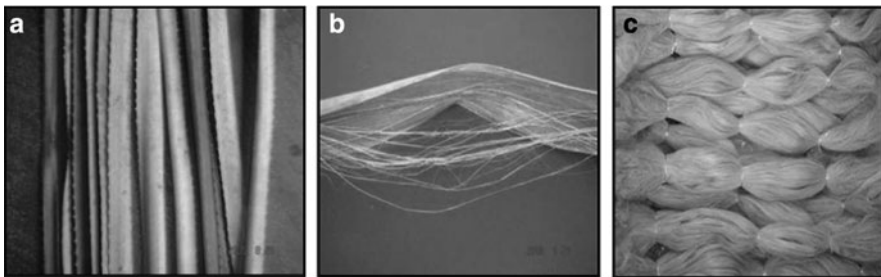


Fig. 12.2 Pineapple leaf fibers (PALF) obtained from pineapple leaves

of PALF extracted from the leaves of three different varieties of the plant, viz. Giant Kew, Queen, and Mauritius were reported. It was reported in (Anon 1992) that various species of pineapple especially those with inedible fruits produced useful fibers for the textile industry. In light of species–property variability and lack of previous studies, Mohamed et al. (2009) carried out characterization of PALF extracted from three most popular species in Malaysia namely Queen (Moris Gajah), Smooth Cayenne (Sarawak), and Spanish (Josapine). They determined Josapine as the most appropriate species for PALF extraction considering potential fiber quantity, ease of extraction, fiber fineness, mechanical, and thermal properties.

Ways of obtaining PALF from the leaves have been crude and they continue to be hand-separated as the use of machines is generally slower than the manual process though it facilitates production processes (Mwaikambo 2006). Though simpler and more cost-effective, mechanical processes induce damage to natural fibers through breaking, scotching, and hackling actions leading to tensile strength of the elementary fibers to be only marginally higher than that of the technical fibers (Joffe et al. 2003). Manual extraction allows two types of fibers (Bartholomew et al. 2002) to be obtained from the leaves: 75 wt% of large vascular bundles present in the top lamina and 25 wt% of fine fiber strands in the bottom lamina (Mohamed 2010). Unlike bast fibers, PALF are readily available as distinct fiber bundles once they are separated from the leaf tissues. Large bundles are made up of loosely bound technical fibers which consist of elementary fibers with diameters less than 10 μm .

A simple PALF separation technique using abrasive-combing in which large vascular bundles were pulled between #100 sandpapers was experimented in Mohamed et al. (2010a). Large bundles easily separated into two finer bundles reducing the mean PALF vascular bundle diameter by 50.3% ($p = 0.01$). Subsequent defibrillation using this technique was more difficult as experienced during manual separation of these bundles. The vascular bundles may therefore be visualized as being made up of two loosely bound parallel bundles, relatively speaking. The two bundles were made up of finer bundles not easily separated unless they were extracted with other mechanical or chemical means (Bismarck et al. 2005), and the smallest single bundles were expected to be those present in the bottom-most epidermal layer in the leaf.

Usually, plant fibers are retted to separate the fiber bundles from cementing materials resulting in finer bundles. Bacteria retting of PALF produced cleaner fibers with good tensile strength and reduced nonfibrous constituents as retting process converted much of the hemicellulose to α -cellulose (Palmario et al. 1976; Cueto et al. 1978). However, the problems associated with retting of natural fibers are limiting their competitiveness and range of applications (Hepworth et al. 2000). Hepworth et al. discovered that lack of retting did not significantly change the reinforcing capabilities of hemp fibers and the same may be reasonably assumed with PALF. Meanwhile they urged further study on possible degradation of unretted tissue over time after it has been embedded in resin for any serious effects on the useful life of the composites.

12.2.3 PALF Characterization

12.2.3.1 PALF Physical Properties

The average length of PALF bundles is approximately 1 m as reported in (Sharma 1981), while lower lengths (0.6–0.7 m) were noted in Mohamed et al. (2009). In Mohamed et al. (2010a) the authors measured PALF diameters in two perpendicular directions and, unlike the previous practice of assuming fiber circularity, used an ellipse as the chosen shape. They found an almost constant ratio of major to minor axis, hence the appropriateness of using ellipse to describe both large bundles and fine strands.

Majority of the previous works on PALF and PALF-reinforced composites utilized fine bundles with diameters less than 100 μm . Mohamed et al. differentiated large vascular bundles and fine strands and determined that the former had a mean diameter of 241.9 μm and was less varying, while the latter had a mean diameter of 72.7 μm and a larger diameter variation as confirmed by visual observation (Mohamed et al. 2010a). They observed that PALF vascular bundles were present and extracted in one lamina, while fine fiber strands were present in a few bottom layers. The diameters of fine fiber strands were decreasing toward the bottom face of the leaf.

12.2.3.2 PALF Chemical Compositions and Structure

Table 12.1 shows PALF chemical composition obtained from previous studies. It can be seen that the content of cellulose was in the range of 67.12–82%; hemicelluloses 9.45–18.80%, hollocellulose 80–87.56%, lignin 4.4–15.4%, pectin 1.2–3%, fat and wax 3.2–4.2%, and ash 0.9–2.7%. Differing composition may be attributed to factors including source of fibers, age of fibers, climate conditions, and the process to obtain the fibers. Chemical composition, lignin distribution, and cell wall structure of PALF were analyzed in Abdul Khalil et al. (2006). Using transmission electron microscopy the authors confirmed that PALF cell wall structure

Table 12.1 Chemical compositions of PALF

Chemical composition (%)	Source						
	Bhaduri et al. (1983)	Mohanty et al. (2000)	Abdul Khalil et al. (2006)	Saha et al. (1990)	Rowell and Han (2000)	Munirah et al. (2007)	Siregar et al. (2008)
Cellulose	69.5	70–82	73.4	68.5	80–81	78.11	67.12–69.34
Hemicellulose	–	–	–	18.80	16–19	9.45	–
Hollocellulose	–	–	80.5	–	–	87.56	82.3–85.5
Lignin	4.4	5–12.7	10.5	6.04	4.6–12	4.78	14.5–15.4
Pectin	1.2	–	–	1.10	2–3	–	–
Fat and wax	4.2	–	–	3.2	–	–	–
Ash	2.7	–	2	0.9	–	–	1.21
Extractive	–	–	5.5	–	–	–	3.83–0.97

may be described in terms of classical cell wall structure of a primary (P) and secondary (S1, S2, and S3) layers.

PALF have a multicellular structure with noncellulosic constituents like lignin and hemicelluloses holding the ultimate fibers together (Saha et al. 1990). The elementary unit of cellulose macromolecules is anhydro-D-glucoseopyranose, which contains three hydroxyls (–OH) per unit (Bledzki and Gassan 1999). These hydroxyls form intramolecular and intermolecular hydrogen bonds with each other as well as with hydroxyl groups from moist air (Mishra et al. 2001). Therefore, PALF are hydrophilic in nature and this feature affects the mechanical properties of PALF-reinforced composites (Abdul Khalil et al. 2007). The molecular chains of cellulose lie parallel and in three-dimensions in the crystalline region of PALF, while the other portions of the molecular chains are believed to lie in a less-ordered state in the amorphous regions (Mishra et al. 2004). Through X-ray diffraction (XRD) and thermogravimetric analyses, Mohamed et al. (2010a) concluded that the large PALF vascular bundles and fine fiber strands were chemically and structurally the same. XRD curves obtained resemble closely that of cellulose I (Nishino et al. 2003).

12.2.3.3 PALF Mechanical, Thermal, and Other Properties

Recently, the research community has shown growing interest in using PALF as to reinforce polymer composites due to their excellent mechanical properties compared to those of other natural fibers (Bismarck et al. 2005). Table 12.2 provides PALF mechanical properties obtained from previous studies. The tensile strength of PALF is in the range of 170–1,627 MPa, the tensile modulus is from 6.26 to 82.5 GPa, while the elongation at break 0.8–3.37%. Ultimately, high cellulose content and low microfibrillar angle of 14° (Bismarck et al. 2005) result in excellent PALF mechanical properties. Both flexural and torsional rigidity of PALF are comparable with jute fibers, while wet bundle strength of PALF decreases by 50% but the yarn strength increases by about 13% (Mishra et al. 2004).

Table 12.2 Mechanical and physical properties of PALF

Mechanical and physical properties	Source				
	Mohanty et al. (2000)	George et al. (1993)	Luo and Netravali (1995)	Arib et al. (2006)	Mohamed et al. (2009)
Tensile strength (MPa)	413–1,627	170	445	126.6	293.08
Young's modulus (GPa)	34.5–82.5	6.26	13.21	4.405	18.934
Elongation at break (%)	1.6	0.8–1.6	3.37	2.2	1.41
Diameter (μm)	20–80	5–30	–	–	105–300
Density (g cm ⁻³)	–	1.44	1.36	1.07	–
Moisture content (%)	11.8	–	–	–	–
Microfibrillar angle (°)	14	12	–	–	–

PALF tensile strength and Young's modulus decrease while elongation at break was not affected as fiber diameter increased (Mohamed et al. 2009, 2010a). Similar characteristics were also reported for another study on PALF (Mukherjee and Satyanarayana 1986). Unlike Mukherjee et al., Mohamed et al. differentiated large vascular bundles and fine fiber strands and tested them separately. The results suggested that it was not the absolute fiber diameter which dictated the mechanical properties but the number of individual fiber bundles making up larger bundles that did (Mohamed et al. 2010a). Fine PALF strands had high tensile strength and modulus and by linear regression gave strength and modulus values at 20 and 50 μm of approximately 1800 MPa and 30 GPa and 750 MPa and 12 GPa, respectively. The strength and modulus of fine strands were very similar and within range of the values given in Bismarck et al. (2005) and Payae and Lopattananon (2009).

Normalizing mean strength of fine fiber strands at the mean diameter of large vascular bundles indicated that the vascular bundles were effectively stronger than the finer bundles (Mohamed 2010). This may be attributed to added strength of noncellulosic substances such as pectin and gums (Bel-Berger et al. 1999). Abrasive-combed PALF had 51.5% higher tensile strength and 48.6% greater moduli, while elongations at break did not differ much compared to those of nontreated PALF ($p = 0.01$) (Mohamed et al. 2010a). Linear regression analysis on data of fiber strands of diameters ranging 50–125 μm , however, suggested that the mean tensile strength was not much affected while modulus and elongation at break were reduced. This may be explained by possible introduction of defects on the defibrillated bundles through the action of the abrasives causing fraying and breaking of elementary fibers.

PALF mechanical properties are expected to decrease with temperature unless treated and modified. Most natural fibers lose their strength at about 160°C (George et al. 1996a). Removal of water present in natural fibers caused an increase in stiffness (Tomczak et al. 2007). The age of the pineapple plant is also expected to have some effects on fiber tensile strength and modulus, toughness, and elongation as found previously with sisal (Chand and Hashmi 1993). In Mohamed et al. (2009) thermal analysis of PALF from Josapine, Moris, and Sarawak cultivars gave curves similar in shape to that reported in George et al. (1996a). Major decomposition occurred at a temperature of approximately 340°C for Sarawak PALF and 320°C for Josapine and Moris PALF indicating higher thermal stability of Sarawak PALF. Interestingly, these decomposition temperatures were also higher than that reported on jute felt (Dash et al. 2002). In a more detailed study on Josapine PALF (Mohamed 2010), the authors concluded that large PALF vascular bundles and fine strands were thermally the same.

12.2.4 PALF Modifications

Good fiber–matrix interface is essential in the use of natural fibers as reinforcement in plastics to ensure performance and stability (Mwaikambo and Ansell 1999).

The works on treatments and modifications of these hydrophilic lignocellulosic fibers were reviewed in John and Anandjiwala (2008). Various physical and chemical methods have been applied in order to overcome shortcomings of natural fibers like PALF which include low strength, fiber–matrix incompatibility, undesirable water uptake, and poor fiber–matrix adhesion. These include using chemical treatment (Joseph et al. 1996), surface modification (Mohanty et al. 2000; Danyadi et al. 2010), coupling agents (Araujo et al. 2008; Keener et al. 2004), and compatibilizing agent (Siregar et al. 2009).

12.2.4.1 PALF Pretreatments

The effects of simple pretreatments on the properties of PALF were studied in Mohamed (2010) and Mohamed et al. (2010a). The authors observed that washing PALF with water to remove leaf juices and dirt was found to be adequate but necessary in ensuring minimum fiber–matrix adhesion, while prolonged soaking was unnecessary unless retting with microorganisms (Palmario et al. 1976) is employed. Bleaching PALF with sodium hypochlorite (NaOCl) degraded the fibers mechanically and thermally as well as destroying PALF crystalline structure while PALF–vinyl ester adhesion was not improved. Hydrogen peroxide (H₂O₂) bleach improved PALF fineness by 5–6% but reduced the tensile strength by 40–45% (Ghosh et al. 1988). Bleached fibers when spun into yarns produced a more uniform and extensible but lower strength yarns than unbleached raw fibers.

12.2.4.2 Chemical Treatments

Alkali treatment or mercerization using sodium hydroxide (NaOH) is the most commonly used treatment for bleaching and cleaning the surface of natural fibers to produce high-quality fibers (Rahman and Khan 2007). Modifying natural fibers with alkali has greatly improved the mechanical properties of the resultant composites (Gomes et al. 2007; Van de Weyenberg et al. 2006). Additionally, alkali treatment leads to fiber fibrillation, thus increasing the effective surface area available for wetting by the matrix. Increasing fiber aspect ratio caused by reducing fiber diameter and producing a rough surface topography offer better fiber–matrix adhesion and increase in mechanical properties (de Albuquerque et al. 2000; George et al. 1998a). NaOH reacts with hydroxyl groups of the cementing materials in natural fibers and brings on the destruction of the cellular structure, thereby splitting the fibers into filaments (Cao et al. 2006).

Structural features and fracture morphology of raw and chemically treated PALF were studied by Saha et al. (1990) using scanning electron microscopy. Upon gradual removal of lignin and hemicellulose by alkali treatment, surface morphology progressively changed. Uniform sharing of the load in the ultimate fibers of raw PALF was observed, whereas treated fibers showed irregular fractures characterized by the slippage of ultimate fibers. Alkali treatment, nitration, dinitrophenylation, benzylation, and benzylation–acetylation of PALF have been reported

in Samal and Bhuyan (1994). Reduction in PALF percent moisture regain was significant upon dinitrophenylation and benzylation–acetylation but low upon nitration, while higher mechanical strength was registered for all chemically modified fibers except for benzyolated PALF. NaOH treatment of PALF was also found to increase tensile modulus and strength by 25% and 19%, respectively, in addition to a 100% increase of PALF-epoxy interfacial shear strength (IFSS) (Payae and Lopattananon 2009). The authors observed even higher IFSS between epoxy-treated PALF and the matrix even though this treatment only increased PALF stiffness and not strength.

12.2.4.3 Chemical Coupling

Chemical coupling method utilized a compound to treat fiber surface to improve fiber–matrix interfacial adhesion through formation of a bridge of chemical bonds between the fiber and matrix. The interaction between silane coupling agents with natural fibers may be divided into four steps (a) hydrolysis, (b) self condensation, (c) adsorption, and (d) grafting (Xie et al. 2010). The effect of two different silane treatments namely, γ -(aminopropyl) trimethoxy silane (Z-6011) and γ -methacrylate propyl trimethoxy silane (Z-6030), on the mechanical properties of PALF-polycarbonate composites was studied in Threepopnatkul et al. (2009). The modulus PALF/Z-60011-PC composites have higher modulus compared to PALF/Z-60030-PC composites due to stronger interfacial adhesion between PALF/Z-6011.

Graft copolymerization of acrylonitrile (AN) onto chemically modified PALF has been studied in Mohanty et al. (1996) using Ce(IV) and *N*-acetylglycine (NAG) combination as an initiator in the temperature range 40–60°C. Tripathy et al. studied the Cu(II)–IO₄[−] initiated graft copolymerization of MMA from defatted PALF and investigated the effects of variation of time and temperature, concentration of Cu(II), KIO₄, and MMA, the amount of PALF, and also the effects of some inorganic salts and organic solvents on the percentage of graft yield (Tripathy et al. 1999). It has been shown that grafting improved the thermal stability of PALF. Graft copolymerization of AN and MMA onto PALF, using ceric ion as an initiator at varying concentrations of monomer, initiator, and mineral acid at a number of temperatures for various time intervals, was studied in Samal et al. (1994). Tensile data revealed a moderate increase in PALF tensile modulus when grafted with AN. Cyanoethylated PALF-graft-PAN samples had higher percentage of grafting but the increase in tensile modulus was not high.

12.3 PALF-Reinforced Polymer Composites

12.3.1 PALF-Thermoplastics Composites

Thermoplastics, especially commodity resins like polyethylene (PE) and polypropylene (PP), account for majority of the matrices used with PALF. Understandably,

these commodity resins are inexpensive, widely available, and recyclable. Processing methods of natural fiber-reinforced thermoplastic composites include melt-mixing and injection molding (George et al. 1996b; Abu-Sharkh and Hamid 2004; Threepopnatkul et al. 2009; Bledzki et al. 2010), sandwiching with compression molding (Luo and Netravali 1995; Arib et al. 2006; Mukhopadhyay and Srikanta 2008), melt mixing and compression molding (Antich et al. 2006; Kim et al. 2008), and extrusion and compression molding (Nair et al. 2001). Mixing natural fibers with thermoplastic matrices must be carried out at less than 200°C as most natural fibers lose their strength at temperature of 160°C (George et al. 1996a).

George et al. carried out systematic studies on PALF-reinforced low-density polyethylene (LDPE) composites investigating the effects of PALF addition on composite viscoelastic properties (George et al. 1993), thermogravimetric and dynamic mechanical characteristics (George et al. 1996a), melt rheological behavior (George et al. 1996b), and electrical properties (George et al. 1997). They also evaluated the environmental effects on the properties of PALF-LDPE (George et al. 1998b), stress relaxation behavior of short PALF-LDPE composites (George et al. 1998c), and the effects of strain rate and temperature on the tensile failure of PALF-LDPE composites (George et al. 1999). In studying short PALF-LDPE composites the authors determined the optimum parameters for melt mixing process to be 6 min of mixing at rotor speed of 60 rpm and mixing temperature of 130°C (George et al. 1995). Fiber length of 6 mm was the most suitable length for enhanced properties in solution mixing.

Incorporating PALF in LDPE in increasing amount caused increased water uptake and decreased mechanical properties (George et al. 1998b), increased dynamic storage and loss modulus (George et al. 1993, 1996a), lowered degradation temperature (George et al. 1996a), increased viscosity (George et al. 1996b), increase in dielectric constants and decreased volumetric resistivity and dielectric dissipation factor values (George et al. 1997), decreased rate of relaxation (George et al. 1998c), and better strength retention at higher temperature (George et al. 1999). Fiber treatments using NaOH, silane A-172, isocyanate (PMPPIC), and benzoyl peroxide carried out in the above studies improved fiber–matrix adhesion, and in many instances enhanced the positive gains or reduced the undesirable properties as a result of PALF addition.

The effect of fiber loading on mechanical properties of unidirectional PALF-reinforced PP composites produced by compression molding was investigated in Arib et al. (2006). Tensile modulus and strength increased with increasing fiber volume fraction with maximum values obtained at 10.8% PALF before decreasing slightly at 16.2%. Increases in flexural modulus and stress were relatively low attributed to fiber–fiber interaction, voids, and dispersion problems. Injection-molded polycarbonate (PC) reinforced with PALF pretreated with NaOH and modified with two types of silane was studied in Threepopnatkul et al. (2009). The authors observed that composite mechanical properties were better than neat PC, while silanized composites have lower mechanical property than NaOH-treated composites due to the formation of flexible polysiloxane. Siregar and Sapuan (2009) studied the mechanical properties of PALF-reinforced high impact polystyrene (HIPS)

composites utilizing ground PALF fibers of 10–40, 40–60, and 60–80 meshes. They observed that adding PALF of various sizes at different fiber loadings resulted in increases in composite tensile and flexural moduli and hardness. However, tensile and flexural strengths and notched and un-notched impact strength of the composites decreased. Increase in fiber content caused increase in the moduli while strength decreased.

12.3.2 PALF Thermoset Polymer Composites

Polyester, epoxy, phenol formaldehyde (PF), and vinyl ester are typical thermosets used in natural fiber-reinforced composites, with polyester being the most widely used (Sanadi et al. 1986). Compression molding is a common and convenient method to make these composites regardless of fiber length (Mishra et al. 2004), though in the case of PALF-reinforced thermoset composites, no indication of high consolidation pressure had been observed. Polyester composites reinforced with unidirectional natural fibers including PALF were studied in Pavithran et al. (1987), and the composite toughness of the composites was observed to increase with the fiber microfibrillar angle. The influence of fiber length, fiber loading, and coupling agents on tensile, flexural, and impact properties of PALF-reinforced polyester composites was investigated in Uma Devi et al. (1997). With optimum fiber length of 30 mm, composite tensile strength, Young's modulus, flexural strength, and impact strength increased linearly with fiber weight fraction. In the case of flexural strength, however, a leveling off beyond 30% was observed. This trend was also observed in another study of PALF–polyester composites (Mishra et al. 2001). 30 wt% of PALF seemed to result in maximum tensile, flexural, and impact strengths with corresponding decreases thereafter. In another study, thermal conductivity of PALF/PF composites decreased with the increasing fiber content (Mangal et al. 2003). The addition of varying PALF content (10–50%) to reinforce PF composites cannot improve composite thermal conductivity due to low PALF thermal conductivity.

Recently Payae and Lopattananon (2009) studied the use of epoxy as the matrix for PALF even though they stopped short of studying PALF-reinforced epoxy composites. The use of PALF to reinforce vinyl ester was studied by Mohamed (2010) and Mohamed et al. (2010b). Vinyl esters are in between polyester and epoxy in terms of cost, ease of processing, and performance (Li 1998) and are tough, resilient, and less susceptible to water degradation (Joffe et al. 2003). Liquid compression molding of PALF with vinyl ester was tried in Mohamed et al. (2010b). It was observed that the reinforcing capability of PALF stored for 6 months under hot and humid ambient conditions was not degraded (Mohamed 2010). The authors noted that PALF may be utilized at random from different parts of the leaves without affecting composite flexural properties. Utilizing large vascular bundles and fine fiber strands separately at 20 wt% and low consolidating pressure suggested that fiber diameter hardly affects flexural strength and modulus.

Table 12.3 Selected tensile, flexural, and impact strengths of PALF-reinforced thermoset composites

Property	Unit	PALF–polyester ^a	PALF–polyester ^b	PALF–vinyl ester ^c	PALF–vinyl ester ^d
Untreated PALF					
Tensile strength	(MPa)	52.9	42	73.2	–
Flexural strength	(MPa)	80.2	86.28	98.9	122
Impact strength	(kJ m ⁻²)	24.2	–	19.2	105 ^e
Treated PALF					
Tensile strength	(MPa)	73.5 ^f	43.6 ^g	–	–
Flexural strength	(MPa)	85.6 ^f	117 ^g	–	–
Impact strength	(kJ/m ²)	–	102.4 ^{e,f}	–	–

Values either categorically stated or inferred from the figures.

^aRandomly oriented 30 mm PALF (30 wt%) (Uma Devi et al. 1997)

^bRandom nonwoven PALF mat (30 wt%) (Mishra et al. 2001)

^cCompression molded, randomly oriented nonwoven PALF mat (28.4 wt%) (Mohamed et al. 2010b)

^dHand laid, unidirectional PALF (20 wt%) (Mohamed 2010)

^e(J/m)

^fSilane A-172

^gCyanoethylated PALF

Using fine fiber strands, however, significantly improved the toughness of PALF–vinyl ester composite due to greater number of interfaces generated. Composites reinforced with abrasive-combed PALF though finer than large vascular bundles were less tough than those using coarser bundles due to defects present on them, thereby highlighting the importance of fiber integrity.

Effects of fiber treatments and modifications on the properties of PALF-thermoset composites were also studied by the above workers. The effects of dewaxing, alkali treatment, cyanoethylation, and grafting of AN onto dewaxed PALF on composite mechanical properties were studied in Mishra et al. (2001). Amongst all the modifications, 10% AN-grafted PALF composites exhibited maximum tensile strength, whereas cyanoethylated PALF composite exhibited better flexural and impact strengths. In another study, a significant increase in the strength of the composites was observed using PALF treated with silane A-172 (Uma Devi et al. 1997). Table 12.3 provides a summary of selected tensile, flexural, and impact strengths of PALF-reinforced thermoset composites.

12.3.3 Other Matrices Reinforced with PALF

Mechanical properties of PALF-reinforced natural rubber composites were studied in Bhattacharya et al. (1986) in which PALF addition increased hardness, compression set, tear resistance, and Mooney viscosity. However, elongation at break, mill shrinkage, and Mooney scorch time decreased. The use of resorcinol, hexamethylenetetramine, and silica is essential for PALF–rubber adhesion. PALF-reinforced

natural rubbers filled with carbon black have high hardness, low elongation, moderate tensile strength, and moderate flex resistance.

Ideally, natural polymer matrices are used with PALF to make totally green composites. Currently, performance limitations and high cost of biopolymers are major barriers for their widespread acceptance as substitutes to traditional petroleum-based polymers (Mohanty et al. 2005). The low value interfacial shear stress of PALF/poly(hydroxybutyrate-co-valerate) (PHBV) reported in Luo and Netravali (1999) gave a clue of the performance limitations of biopolymers. Many of them are still being developed using elaborate chemical reactions in laboratories. In Luo and Netravali (1995) the authors utilized PALF to reinforce PHBV composites prepared by sandwiching three layers of PALF fibers between four layers of PHBV films and compression molding them with temperature and pressure of 180°C and 140 MPa respectively. Their study showed that adding 20 wt% unidirectional PALF enhanced the composite tensile and flexural strength by 75% and 32%, respectively. Tensile and flexural strengths increased by 100% and 60%, respectively, with 30 wt% PALF addition. Other matrices used with PALF include biodegradable polymers such as petroleum-based polyester amide (BAK 1095) (Mishra et al. 2002) and corn-based poly(lactic), PLA (Liu et al. 2005).

12.3.4 Hybrid PALF-Reinforced Composites

Hybrid biocomposites are formed by incorporating two or more fibers into a single matrix resulting in an apparent synergistic improvement in composite properties and favorable balance between the inherent advantages and disadvantages of individual components (John et al. 2009). Mishra et al. (2003) evaluated the mechanical properties of PALF/glass fiber-reinforced polyester composites and observed improvement in tensile, flexural, and impact strengths of the composites through incorporation of a small amount of glass fibers indicating positive hybrid effects. An optimum glass fiber loading of 8.6 wt% was noted. The PALF/glass fiber-reinforced polyester composites also showed significant reduction in water uptake compared to unhybridized samples. Thermophysical properties of PALF/glass fiber-reinforced polyester composites were also studied in Idicula et al. (2006). Varying hybrid effects may be calculated for the mean values of thermal conductivity, diffusivity, specific heat, and density obtained.

12.4 Conclusions

PALF are environmentally sound and mechanically excellent materials to reinforce polymer composites for making industrial goods. As the industrial importance and plantation area of pineapple increase, it makes environmental and economical sense to energize the research and development to enhance PALF as reinforcing fibers. Developmental works must be carried out to mechanize PALF extraction and

separation techniques in order to cost-effectively produce good quality fibers. Polymer composite applications using PALF as reinforcing or filling phase must be quickly developed and commercialized in order to increase pineapple “resource potential” and consequently push the development and utilization of PALF and subsequently reduce wastage and environmental degradation. Systematic studies must be carried out to determine the most influential factors dictating the quality of PALF-reinforced polymer composites and allow optimization to be further carried out. Proper balance of performance and costs may then be achieved with the final aim to contribute positively toward the environment and well-being of the people. Hybridization of PALF with other biofibers or synthetic fibers in order to obtain “net positive hybrid effect” may still be explored. The use of biopolymers or blends of matrices in conjunction with PALF must also be given adequate attention.

Acknowledgments The authors would like to thank Universiti Putra Malaysia for the assistance received under the Fundamental Research Grant Scheme (grant number 5523413).

References

- Abdul Khalil HPS, Siti Alwani M, Mohd Omar AK (2006) Chemical composition, anatomy, lignin distribution and cell wall structure of Malaysian plant waste fiber. *Bioresources* 1:220–232
- Abdul Khalil HPS, Issam AM, Ahmad Shakri MT, Suriani R, Awang AY (2007) Conventional agro-composites from chemically modified fibres. *Ind Crops Prod* 26:315–323
- Abu-Sharkh BF, Hamid H (2004) Degradation study of date palm fibre/polypropylene composites in natural and artificial weathering: mechanical and thermal analysis. *Polym Degrad Stab* 85:967–973
- Ahmed OH, Husni MH, Anuar AR, Hanafi MM (2002) Effect of residue management practices on yield and economic viability of Malaysian pineapple production. *J Sustain Agric* 20:83–94
- Ahmed OH, Husni MH, Anuar AR, Hanafi MM (2004) Towards sustainable use of potassium in pineapple waste. *Sci World J* 4:1007–1013
- Anon (1992) A guide to unusual natural fibers: pineapple leaf fiber (PALF). *Textiles* 21:21
- Anon (2008a) <http://en.wikipedia.org/wiki/Pineapple>. Accessed 1 July 2008
- Anon (2008b) www.mpib.gov.my. Accessed 28 Feb 2008
- Anon (2008c) <http://www.uga.edu/fruit/pinapple.html>. Accessed 1 July 2008
- Anon (2008d) <http://www.fao.org/ag/AGL/aglw/cropwater/pineapple.stm>. Accessed 28 July 2008
- Antich P, Vazquez A, Mondragon I, Bernal C (2006) Mechanical behavior of high impact polystyrene reinforced with short sisal fibers. *Compos A* 37:139–150
- Araujo JR, Waldman WR, De Paoli MA (2008) Thermal properties of high density polyethylene composites with natural fibres: coupling agent effect. *Polym Degrad Stab* 93:1770–1775
- Arib RMN, Sapuan SM, Ahmad MMHM, Paridah MT, Khairul Zaman HMD (2006) Mechanical properties of pineapple leaf fiber reinforced polypropylene composites. *Mater Des* 27:391–396
- Bartholomew DP, Paull RE, Rohrbach KG (2002) *The pineapple: botany, production and uses*. CAB International, United Kingdom
- Basu A, Chellamani KP, Kumar PR (2003) Jute and pineapple leaf fibres for the manufacture of technical textiles. *Asian Text J* 12:94–96
- Bel-Berger P, Von Hoven T, Ramaswamy GN, Kimmel L, Boylston E (1999) Textile technology. *J Cotton Sci* 3:60–70
- Benjamin Y, van Weenen H (2000) *Design for sustainable development: crops for sustainable enterprise*. European Foundation for the Improvement of Living and Working Conditions, Ireland

- Bhaduri SK, Sen SK, Dasgupta PC (1983) Structural studies of an acidic polysaccharide isolated from the leaf fibre of pineapple (*Ananas comosus* MERR). *Carbohydr Res* 121:211–220
- Bhattacharya TB, Biswas AK, Chatterjee J, Pramnck D (1986) Short pineapple leaf fibre reinforced rubber composites. *Plast Rubb Process Appl* 6:119–125
- Bismarck A, Mishra S, Lampke T (2005) Plant fibers as reinforcement for green composites. In: Mohanty AK, Misra M, Drzal LT (eds) *Natural fibers, biopolymers and biocomposites*. Taylor & Francis, FL, Boca Raton
- Bledzki AK, Gassan J (1999) Composites reinforced with cellulose based fibres. *Prog Polym* 24:221–274
- Bledzki AK, Mamun AA, Volk J (2010) Barley husk and coconut shell reinforced polypropylene composites: the effect of fibre physical, chemical and surface properties. *Compos Sci Technol* 70:840–846
- Cao Y, Shibata S, Fukumoto I (2006) Mechanical properties of biodegradable composites reinforced with bagasse fibre before and after alkali treatments. *Compos A* 37:423–429
- Chand N, Hashmi SAR (1993) Mechanical properties of sisal fibre at elevated temperatures. *J Mater Sci* 28:6724–6728
- Cueto CU, Quintos AG, Peralta CN, Palmario MS (1978) Pineapple fibres: the retting process II. *NSDB Technol J* :73–79
- Danyadi L, Moczo J, Pukanszky B (2010) Effect of various surface modifications of wood flour on the properties of PP/wood composites. *Compos A* 41:199–206
- Dash BN, Sarkar M, Rana AK, Mishra M, Mohanty AK, Tripathy SS (2002) A study on biodegradable composite prepared from jute felt and polyesteramide (BAK). *J Reinf Plast Compos* 21:1493–1503
- de Albuquerque AC, Joseph K, de Carvalho LH, d'Almeida JRM (2000) Effect of wettability and ageing conditions on the physical and mechanical properties of uniaxially oriented jute-roving-reinforced polyester composites. *Compos Sci Technol* 60:833–844
- Fowler PA, Hughes JM, Elias RM (2006) Biocomposites: technology, environmental credentials and market forces. *J Sci Food Agric* 86:1781–1789
- George J, Joseph K, Bhagawan SS, Thomas S (1993) Influence of short pineapple fiber on the viscoelastic properties of low-density polyethylene. *Mater Lett* 18:163–170
- George J, Bhagawan SS, Prabhakaran N, Thomas S (1995) Short Pineapple-leaf-fiber-reinforced low-density polyethylene composites. *J Appl Polym Sci* 57:843–854
- George J, Bhagawan SS, Thomas S (1996a) Thermogravimetric and dynamic mechanical thermal analysis of pineapple fiber reinforced polyethylene composites. *J Therm Anal* 47:1121–1140
- George J, Janardhan R, Anand JS, Bhagawan SS, Sabu T (1996b) Melt rheological behaviour of short pineapple fibre reinforced low density polyethylene composites. *Polymer* 37:5421–5431
- George J, Bhagawan SS, Thomas S (1997) Electrical of pineapple fiber reinforced polyethylene composites. *J Polym Eng* 17:383–404
- George J, Bhagawan SS, Thomas S (1998a) Improved interactions in chemically modified pineapple leaf fibre reinforced polyethylene composites. *Compos Interf* 5:201–223
- George J, Bhagawan SS, Thomas S (1998b) Effects of environment on the properties of low-density polyethylene composites reinforced with pineapple fibers. *Compos Sci Technol* 58:1471–1485
- George J, Sreekala MS, Thomas S, Bhagawan SS, Neelakantan NR (1998c) Stress relaxation behavior of short pineapple fiber reinforced polyethylene composites. *J Reinf Plast Compos* 17:651–672
- George J, Thomas S, Bhagawan SS (1999) Effects of strain rate and temperature on tensile failure of pineapple fiber reinforced polyethylene composites. *J Thermoplast Compos Mater* 12:443–464
- Ghosh SK, Dey SK, Dey A (1988) Tensile behaviour and processing of bleached yarn from pineapple leaf fibre. *Indian J Text Res* 13:17–20
- Gomes A, Matsuo T, Goda K, Ohgi J (2007) Development and effect of alkali treatment on tensile properties of curaua fiber green composites. *Compos A* 38:1811–1820

- Hayavadana J, Jacob M, Sampath G (2003) Diversified product of pine apple leaf fibres. *Man Made Text India* 46:301–305
- Hepworth DG, Hobson RN, Bruce DM, Farrent JW (2000) The use of unretted hemp fibre in composite manufacture. *Compos A* 31:1279–1283
- Iidicula M, Boudenne A, Umadevi L, Ibos L, Candau Y, Thomas S (2006) Thermophysical properties of natural fibre reinforced polyester composites. *Compos Sci Technol* 66:2719–2725
- Joffe R, Andersons J, Wallstrom L (2003) Strength and adhesion characteristics of elementary flax fibers with different surface treatments. *Compos A* 34:603–612
- John MJ, Anandjiwala RD (2008) Recent developments in chemical modification and characterization of natural fiber-reinforced composites. *Polym Compos* 29:187–207
- John MJ, Anandjiwala RD, Thomas S (2009) Hybrid composites. In: Thomas S, Pothan LA (eds) *Natural fiber reinforced polymer composites: macro to nanoscale*. Old City, Philadelphia, pp 315–328
- Joseph K, Thomas S, Pavithran C (1996) Effect of chemical treatment on the tensile properties of short sisal fibre-reinforced polyethylene composites. *Polymer* 37:5139–5149
- Keener TJ, Stuart RK, Brown TK (2004) Maleated coupling agents for natural fibre composites. *Compos A* 35:357–362
- Kim SJ, Moon JB, Kim GH, Ha CS (2008) Mechanical properties of polypropylene/natural fiber composites: Comparison of wood fiber and cotton fiber. *Polym Test* 27:801–806
- Kumar KBK, Prabhakaran G, Muruganandam R, Raghu P, Namasivayam N, Rajendran K, Durairaj V, Kannan G (1997) Study on pineapple fiber processing. *Colourage* 44:27–30
- Li H III (1998) Synthesis, characterization and properties of vinyl ester matrix resins. PhD Thesis, Virginia Polytechnic Institute and State University, Blacksburg, VA
- Liu W, Misra M, Askeland P, Drzal LT, Mohanty AK (2005) ‘Green’ composites from soy based plastic and pineapple leaf fiber: fabrication and properties evaluation. *Polymer* 46:2710–2721
- Luo S, Netravali AN (1995) Mechanical and thermal properties of environment-friendly “green” composites made from pineapple leaf fibres and poly(hydroxybutyrate-co-valerate) resin. *Polym Compos* 57:843–854
- Luo S, Netravali AN (1999) Interfacial and mechanical properties of environment-friendly “green” composites made from pineapple fibers and poly(hydroxybutyrate-co-valerate) resin. *J Mater Sci* 34:3709–3719
- Mallick PK (1993) *Fiber-reinforced composites: materials, manufacturing, and design*. Dekker, New York
- Mangal R, Saxena NS, Sreekala MS, Thomas S, Singh K (2003) Thermal properties of pineapple leaf fiber reinforced composites. *Mater Sci Eng A* 339:281–285
- Mishra S, Misra M, Tripathy SS, Nayak SK, Mohanty AK (2001) Potentially of pineapple leaf fibre as reinforcement in PALF-polyester composite: surface modification and mechanical performance. *J Reinf Plast Compos* 20:322–334
- Mishra S, Tripathy SS, Misra M, Mohanty AK, Nayak SK (2002) Novel eco-friendly biocomposites: biofiber reinforced biodegradable polyester amide composites-fabrication and properties evaluation. *J Reinf Plast Compos* 21:55–70
- Mishra S, Mohanty AK, Drzal LT, Misra M, Parija S, Nayak SK, Tripathy SS (2003) Studies on mechanical performance of biofibre/glass reinforced polyester hybrid composites. *Compos Sci Technol* 63:1377–1385
- Mishra S, Mohanty AK, Drzal LT, Misra M, Hinrichsen G (2004) A review on pineapple leaf fibers, sisal fibers and their biocomposites. *Macromol Mater Eng* 289:955–974
- Mohamed AR (2010) Physical, mechanical and thermal properties of pineapple leaf fibers (PALF) and PALF-reinforced vinyl ester composites. PhD Thesis, Universiti Putra Malaysia
- Mohamed AR, Sapuan SM, Shahjahan M, Khalina A (2009) Characterization of pineapple leaf fibers from selected Malaysian cultivars. *J Food Agric Environ* 7:235–240
- Mohamed AR, Sapuan SM, Shahjahan M, Khalina A (2010a) Effects of simple abrasive combing and pretreatments on properties of pineapple leaf fibers (PALF) and PALF-vinyl ester composite adhesion. *Polym Plast Technol Eng* 49:972–978

- Mohamed AR, Sapuan SM, Shahjahan M, Khalina A (2010b) Selected properties of hand-laid and compression molded pineapple leaf fiber (PALF)-reinforced vinyl ester composites. *Int J Mech Mater Eng* 5:68–73
- Mohanty AK, Parija S, Misra M (1996) Ce(IV)-*N*-acetyl glycine initiated graft copolymerization of acrylonitrile onto chemically modified pineapple leaf fibers. *J Appl Polym Sci* 60:931–937
- Mohanty AK, Khan MA, Hinrichsen G (2000) Surface modification of jute and its influence on performance of biodegradable jute-fabric/Biopol composites. *Compos Sci Technol* 60:1115–1124
- Mohanty AK, Misra M, Drzal LT, Selke SE, Harte BR, Hinrichsen G (2005) Natural fibers, biopolymers and biocomposites: an introduction. In: Mohanty AK, Misra M, Drzal LT (eds) *Natural fibers, biopolymers and biocomposites*. Taylor & Francis, FL, Boca Raton
- Mukherjee PS, Satyanarayana KG (1986) Structure and properties of some vegetable fibres: Part 2 pineapple fiber. *J Mater Sci* 21:51–56
- Mukhopadhyay S, Srikanta R (2008) Effect of ageing of sisal fibres on properties of sisal: polypropylene composites. *Polym Degrad Stab* 93:2048–2051
- Munder F, Furl C, Hempel H (2005) Processing of bast fiber plants for industrial application. In: Mohanty AK, Misra M, Drzal LT (eds) *Natural fibers, biopolymers and biocomposites*. Taylor & Francis, FL, Boca Raton
- Munirah M, Rahmat AR, Hassan A (2007) Characterization and treatment of pineapple leaf fibre thermoplastic composite for construction application. Research Report, Department of Polymer Engineering, Faculty Chemical and Faculty Natural Resources, Universiti Teknologi Malaysia, pp 1–63
- Mwaikambo LY (2006) Review of the history, properties and application of plant fibres. *Afr J Sci Technol* 7:120–133
- Mwaikambo LY, Ansell MP (1999) The effect of chemical treatment on the properties of hemp, sisal, jute and kapok fibre for composite reinforcement. In: 2nd International wood and natural fibre composites symposium, Kassel, Germany
- Nair MKC, Thomas S, Groeninckx G (2001) Thermal and dynamic mechanical analysis of polystyrene composites reinforced with short sisal fibres. *Compos Sci Technol* 61:2519–2529
- Nishino T, Hirao K, Kotera M, Nakamae K, Inagaki H (2003) Kenaf reinforced biodegradable composite. *Compos Sci Technol* 63:1281–1286
- Palmario MS, Cueto CU, Imperial ZS, Tayco SA, Soriaga RP, Buenaventure RV, De Guzman MC (1976) Pineapple fibres: the retting process. *Sci Rev* 17(4):8–16
- Paul NG (1980) Some methods for the utilisation of waste from fibre crops and fibre waste from other crops. *Agric Waste* 2:313–318
- Pavithran CPS, Mukherjee M, Brahmakumar DAD (1987) Impact properties of natural fibre composites. *J Mater Sci Lett* 6:882–884
- Payae Y, Lopattananon N (2009) Adhesion of pineapple-leaf fiber to epoxy matrix: the role of surface treatments. *Songklanakarin J Sci Technol* 31:189–194
- Rahman MM, Khan MA (2007) Surface treatment of coir (*Cocos nucifera*) fibers and its influence on the fibers' physico-mechanical properties. *Compos Sci Technol* 67:2369–2376
- Rowell RM, Han JS (2000) Characterization and factors effecting fibre properties. In: Frolini E, Leao AL, Mattosso LHC (eds) *Natural polymers and agrofibres composites*. San Carlos, Brazil, pp 115–127
- Saha SC, Das BK, Ray PK, Pandey SN, Goswami K (1990) SEM studies of the surface fracture morphology of pineapple leaf fibres. *Text Res J* 60:726–731
- Samal RK, Bhuyan BL (1994) Chemical modification of lignocellulosic fibers I. Functionality changes and graft copolymerization of acrylonitrile onto pineapple leaf fibers; their characterization and behavior. *J Appl Polym Sci* 52:1675–1685
- Samal RK, Giri G, Bhuyan BL (1994) Chemical modification of lignocellulosic fibers II. Functionality changes and graft copolymerization of methyl methacrylate onto pineapple leaf fibers. *J Polym Mater* 11:113–119
- Sanadi AR, Prasad SV, Rohatgi PK (1986) Sunhemp fibre-reinforced polyester – Part 1. Analysis of tensile and impact properties. *J Mater Sci* 21:4299–4304

- Sharma U (1981) Investigations on the fibers of pineapple [*Ananas comosus* (L). MERR.] leaves. *Carbohydr Res* 97:323–329
- Siregar JP, Sapuan SM (2009) Mechanical properties of pineapple leaf fibre (PALF) reinforced high impact polystyrene (HIPS) composites. In: Sapuan SM (ed) *Research in natural fibre reinforced polymer composites*. UPM, Serdang, Selangor, Malaysia
- Siregar JP, Sapuan SM, Rahman MZA, Zaman HMDK Characterization and chemical composition of short pineapple leaf fibres (PALF). In: SM Sapuan (ed) *Proceeding of postgraduate seminar on natural fibre composites*, Faculty of Engineering, Universiti Putra Malaysia, Serdang, Selangor, 10 June 2008, pp 19–24
- Siregar JP, Sapuan SM, Rahman MZA, Zaman HMDK (2009) The effect of compatibilising agent and surface modification on the physical properties of short pineapple leaf fibre (PALF) reinforced high impact polystyrene (HIPS) composites. *Polym Polym Compos* 17:379–384
- Threepopnatkul P, Kaerkitcha N, Athipongarporn N (2009) Effect of surface treatment on performance of pineapple leaf fiber-polycarbonate composites. *Compos B* 40:628–632
- Tomczak F, Satyanarayana KG, Sydenstricker THD (2007) Studies on lignocellulosic fibres of Brazil: Part III – morphology and properties of Brazilian curauá fibres. *Compos A* 38:2227–2236
- Tripathy PC, Misra M, Parija S, Mishra S, Mohanty AK (1999) Studies of Cu(II)-IO_4^- initiated graft copolymerization of methyl methacrylate from defatted pineapple leaf fibres. *Polym Int* 48:868–872
- Uma Devi L, Bhagawan SS, Thomas S (1997) Mechanical properties of pineapple leaf fiber-reinforced polyester composites. *Appl Polym Sci* 64:1739–1748
- Van de Weyenberg I, Chi Truong T, Vangrimde B, Verpoest I (2006) Improving the properties of UD flax fibre reinforced composites by applying an alkaline fibre treatment. *Compos A* 37:1368–1376
- Wambua P, Ivens J, Verpoest I (2003) Natural fibres: can they replace glass in fiber reinforced plastics? *Compos Sci Technol* 63:1259–1264
- Xie Y, Hill CAS, Xiao Z, Militz H, Mai C (2010) Silane coupling agents used for natural fiber/polymer composites: a review. *Compos A* 41(7):806–819

Chapter 13

Utilization of Rice Husks and the Products of Its Thermal Degradation as Fillers in Polymer Composites

S.D. Genieva, S.Ch. Turmanova, and L.T. Vlaev

Abstract Rice husks are an important by-product of the rice milling process and are a major waste product of the agricultural industry. Rice husks contain nearly 20 mass% silica, which is present in hydrated amorphous form. They have now become a great source of raw biomass material for manufacturing value-added silicon composite products, including silicon carbide, silicon nitride, silicon tetrachloride, magnesium silicide, pure silicon, zeolite, fillers of rubber and plastic composites, cement, adsorbent, and support of heterogeneous catalysts. The controlled burning or thermal degradation of the rice husks in air or nitrogen leads to the production of white rice husk ash (WRHA) or black rice husk ash (BRHA), respectively.

The present review is an attempt to consolidate and critically analyze the research work carried out so far on the processing, properties, and application of rice husks and the products of its thermal degradation in various laboratories and also highlight some results on the processing and characterization of rice husk ashes (RHAs) and reactive silica obtained in the author's laboratory. In this connection, the composition, structure, and morphology of the raw rice husks (RRHs) and the products obtained from its thermal degradation in an oxidative or inert atmosphere are described in detail. The controlled burning or pyrolysis of the RRHs in a fluidized-bed reactor is shown to be the most perspective method. The products obtained might successfully be used as fillers of polypropylene (PP) and tetrafluoroethylene-ethylene copolymer (TFE-E) composites, rubbers, and other polymer composites and to replace the expensive synthetic additive as Aerosil, for instance. The physicochemical and physicomachanical characteristics of the obtained composites are described. The RHA-polymer composites can lead to the futuristic "organic-inorganic hybrid materials" with specific properties. Due to the high pozzolanic activity, the rice husk silica also finds application in high strength concrete as a substitute for silica fume.

S.D. Genieva (✉)

Department of Inorganic Chemistry, Assen Zlatarov University, 8010 Burgas, Bulgaria
e-mail: sgenieva@btu.bg

The abundance of waste from paddy milling industry as well as its interesting complex of behaviors are prerequisites for success in obtaining cheap and valuable products and stipulate new alternatives for its applications. The production of value added materials from rice husks not only facilitates utilization of an abundantly available agro waste but also reduces the environmental pollution and solves a serious ecological problem.

Keywords Fillers · Polymer and rubber composites · Pyrolysis · Rice husks · White and black rice husk ash

Contents

13.1	Introduction	346
13.2	Disposal of Rice Plants and Chemical Constituent, Structure, and Properties of Raw Rice Husks	347
13.3	Technologies Available for Rice Husks Thermal Degradation	350
13.4	Key Factors for the Production of Amorphous Silica from Rice Husks	351
	13.4.1 Uniform Temperature Distribution	351
	13.4.2 Lower Operating Temperature Range	351
	13.4.3 Rapid Reaction Time	352
	13.4.4 High Carbon Conversion Efficiency	352
	13.4.5 Ash Composition and Its Removal	352
	13.4.6 Other Factors	353
13.5	Physicochemical Characteristics of Rice Husk and the Products of Its Thermal Degradation	359
13.6	Utilization of the Rice Husks and the Products of Its Thermal Degradation as Fillers of Polymers	367
	13.6.1 Rice Husk Ashes as Fillers in Rubbers	368
	13.6.2 Other Applications	369
13.7	Conclusions	369
	References	370

13.1 Introduction

A number of reviews and monographs [1–11] have been dedicated to rice husks and the products obtained from its thermal degradation at different conditions. The production of rice, one of the major food crops in the world, generates one of the major wastes of the world, namely rice husks (RH). It is one of the agricultural “waste” materials, which is amenable for value addition, available in large amounts in rice producing countries. It is reported that about 0.23 tons of RH are generated per ton of rice produced. Efforts to utilize it have been handicapped by their tough, woody, abrasive nature, low nutritive properties, and resistance to degradation, great bulk, and high ash content. Such efforts have resulted in minor usage, mostly in low-value applications in agricultural areas or as fuel. Little advantage is taken of the RH, and pollution is caused in such disposal processes. However, because of the high silicon content in RH, its utilization has been significantly widened in the past

few decades. At present, RH and especially rice husk ashes (RHAs) obtained after controlled burning of rice husks are the raw materials for the production of a series of silicon-based materials [3], including silica [12–15], activated carbon [16, 17], sodium silicate [18], silicon tetrachloride [19, 20], sodium silicofluoride [3], and silanes [21]. The high reactivity and purity of RHA makes it an ideal starting material/silica source for preparing advanced materials like sialon [3, 22], silicon carbide [23–25], silicon nitride [26, 27], cordierite [3, 28], forsterite [3], gehlenite [3, 29], pure elemental silicon [3, 30], magnesium silicide, [31], Si–O–C fibers [3, 32], zeolites [33, 34], etc. Recently, RHA has been successfully used as a sorbent of heavy metal ions, dyes, and pigments from aqueous solutions [35–37] and as a support of Ni, Cu, Cr, or V containing catalysts for various organic reactions, and it was found to be preferable over silica gel [38–41].

In the last two decades, RH and the products of its thermal degradation are often used as fillers in paper, paint [5], polymers [42, 43], polymeric composites [44–47], rubber [48–50], cement [51, 52], adhesives, and fertilizers [5]. By the addition of fillers, the mechanical, thermal, chemical, and other properties of the material are improved. Controlled burning of RH in air or inert atmosphere yields two grades of fillers, namely white rice husk ash (WRHA) and black rice husk ash (BRHA). Both these RHA have been used as fillers in polyethylene [53–55], polypropylene [56–61], polystyrene [62, 63], etc. [64, 65]. Tremendous opportunities exist in more exhaustive research on the RHA-polymer composites, which can lead to the futuristic “organic–inorganic hybrid materials” with specific properties. In this respect, the aim of the present work is to describe the possibility for utilization of RRHs and the products of its thermal degradation as fillers in different polymer plastic composites.

13.2 Disposal of Rice Plants and Chemical Constituent, Structure, and Properties of Raw Rice Husks

Lifefood for billions of people, rice is one of the major crops grown throughout the world, sharing equal importance with wheat as the principal staple food and a provider of nourishment for the world’s population. Covering 1% of the earth’s surface, rice is now a way of life, being grown on every continent, and it is deeply embedded in cultures, rituals, and myths. Generally, rice is a cereal foodstuff grown as a monocarp annual plant and can survive as a perennial, producing ratio crop for up to %. Practically, domesticated rice comprises two species of food crops in the *Oryza* genus of the Poaceae family, namely *Oryza sativa* (Asian rice), which contains two major subspecies: the sticky, short-grained japonica or sinica variety, and the nonsticky, long-grained indica variety, and *Oryza glaberrima* (African rice) that is native to the West Africa. According to the statistical data of Food and Agriculture Organization (FAO), the global annual paddy production in 2003 was reported to be 582 million tons, cultivated in 171 million hectares of land.

Concomitant with the rigorous development of the rice milling industries, rice husks (or rice hulls), an abundantly available by-product, the fibrous, hard, outermost covering of the grain of rice, is generated at 145 million tons per year, accounting for about one-fifth of the annual gross rice production throughout the world [66]. Global paddy production reached 628 million tons in 2005 with an additional 1% increase in 2006 [67]. These large quantities of rice husks are available as waste from rice milling industry. These husks are not of commercial interest and cause serious pollution problems. It is necessary, then, to consider the use of this residue in polymer formulations with a clear positive effect to the environment. In nature, rice husk is tough, insoluble in water, woody, and characterized by its abrasive inherent resistance behavior and silica–cellulose structural arrangement. Its major constituents are cellulose, hemicellulose, lignin, hydrated silica, and ash content. The exterior of rice husks is composed of dentate rectangular elements, mostly silica coated with a thick cuticle and surface hairs, while the mid region and inner epidermis usually contain a small amount of silica. The chemical constituents are found to vary from sample-to-sample, which may be due to the different geographical conditions, type of paddy, climatic variation, soil chemistry, and fertilizers used in the paddy growth [14, 68, 69]. In an extensive review, [1] has analyzed all the data reported on the chemical composition of rice husks from various countries, including western world and Asia, and has given an average composition of dry basis as organic matter 80% and ash 20%. The organic part is composed approximately of 42.8% α -cellulose, 22.5% lignin, 32.7% hemicellulose, and about 2% other organic matter. Hemicellulose (xilan) is a mixture of D-xylose – 17.52%, L-arabinose – 6.53%, methylglucuronic acid – 3.27%, and D-galactose – 2.37% [5, 69]. The chemical analyses of the inorganic part in rice husks showed that the main component is amorphous silica and small amounts of some oxides of alkali, alkali earth metals, aluminum, and iron. There are significant variations in the last mentioned compounds, due to the use of different chemical fertilizers in the paddy field in addition to the difference in the soil chemistry. The nature of silica is mainly amorphous and has been termed *Opaline silica* [5, 68]. The silicon atoms are concentrated in the protuberances and hairs on the outer and inner epidermis of the husks in the predominant form of silica gel. Because of its high silica and lignin content, the rice husks are insoluble in water, tough, woody, and abrasive in nature with low nutritive properties and resistance to weathering [69]. It is well known that the rice husks have a high calorific value (12–15 MJ kg⁻¹), high (20–22 mass%) ash content [5, 8, 68, 69], and is sufficient to promote sustainable combustion process, thus reducing the cost of fuel required for the conversion process. Figure 13.1 shows that milling of 1 ton of paddy produces about 220 kg rice husks, which are equivalent to approximately 150 kWh of potential power [11].

The energetic balance shows that utilization of the rice husks as a fuel may convert paddy milling process from a consumer to a producer of energy. The ash obtained contains nearly 95% silica and is an important renewable source of silica. Burning is a cheap method of extracting the silica from rice husks for possible commercial use, but it brings up the associated problems of uncontrolled particle

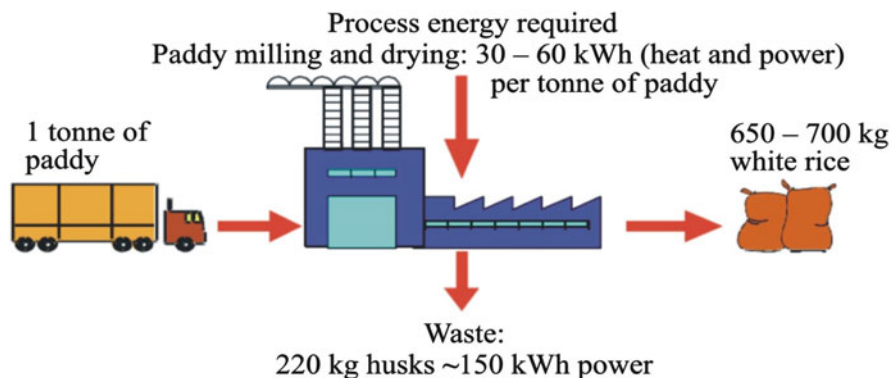


Fig. 13.1 Power generation potential from rice husk mills

size and variable impurity levels, mainly in the form of intimately mixed carbon. Because of growing environmental concern and the need to conserve energy and resources, efforts have been made to burn the husks under controlled conditions and to utilize the residual ash in a variety of end products.

The controlled burning of the RRHs in air atmosphere [70, 71] can actually reduce the greenhouse effect by converting emissions that would have been methane into greenhouse gas less potent than carbon dioxide and can lead to the production of white rice husk ash (WRHA) or the so-called “white ash” containing almost pure ($\geq 95\%$) silica in a hydrated amorphous form, similar to silica gel, with high porosity and reactivity. This silica can be used as an excellent starting material for synthesis of advanced materials such as silicon tetrachloride, magnesium silicide, sodium silicate, zeolites, etc. This silica is an excellent source of very high purity elemental silicon, useful for manufacturing solar cells for photovoltaic power generation and semiconductors. White rice husk ash can also be used in the cement and fertilizer industries (as a pozzolone and as anticaking component, respectively).

The controlled pyrolysis of RRHs in nitrogen or inert atmosphere leads to the production of black rice husk ash (BRHA) or the so-called “black ash,” which contains different amounts of carbon and silica [72, 73]. This material has very high porosity and may be used as a starting material for the synthesis of silicon carbide and silicon nitride. Properties such as high surface area and porosity give additional advantage to the WRHA and BRHA for their possible use as adsorbents for adsorption of dyes, pigments, and heavy metal ions from aqueous solutions and catalytic support. In the recent years, the RRH and rice husk ash have been used as fillers in rubber and plastic composites. Thermoplastic composites filled with low cost reinforcing natural fillers are widely used in construction and automobile industries and in many consumer goods. The interest toward natural fillers is stipulated by their immanent advantages such as availability, high filling levels, low cost, renewability, biodegradability, low density, high specific strength, and nonabrasiveness [42, 54].

13.3 Technologies Available for Rice Husks Thermal Degradation

Four thermal treatment technologies have been widely used to produce amorphous silica from rice husks: muffle furnace, rotary kiln, stepped grate furnace, and inclined grate furnace. According to the literature data [11, 74–76], the thermal degradation of rice husks may be carried out under static or dynamic conditions. A photograph of raw and thermally degraded rice husks in air or nitrogen atmosphere at 680°C in muffle furnace under static conditions is presented on Fig. 13.2.

The products obtained are brittle, amorphous, and porous. The major disadvantages of this method for thermal degradation of rice husks are its high energy consumption (electrical power), batch-like process, absence of mixing amongst the reactants, low production rate, long reaction time, and the risk of explosion. To maintain the temperature in the range of 600–700°C for the conversion process to take place, substantial amount of heat need to be supplied through electrical heating. It is impossible to mix the reactants (rice husks and oxygen) aiming to increase the rates of mass and heat transfer and, therefore, the rice husks feed has to be spread as a very thin layer inside the furnace to ensure sufficient oxygen transfer on microlevel. This in turn limits the amount of rice husks that could be processed in any one time.

The absence of mixing also results in the formation of ash with intact skeleton-like shape, which tends to entrap any unburnt carbon and makes it difficult to be oxidized. Since the process is taking place in a closed system, the absence of free-flowing oxygen results also in incomplete oxidation of carbon in the husks. To prevent the risk of crystallization, the furnace needs to be operated at a lower temperature range (such as 400–600°C), which in turn requires longer treatment periods (3–6 h) in order to achieve high carbon conversion efficiency. Rice husks contain a high amount of volatiles (in the excess of 60 mass%, wet basis) and the



Fig. 13.2 Appearance of raw rice husks (a), black rice husk ash (b), and white rice husk ash (c)

sudden release of these volatiles upon exposure to high temperature in a closed system such as that of the muffle furnace might pose the risk of explosion.

Detailed analysis of literature data showed that products of high quality and economic advantage may be obtained under dynamic conditions using bubbling fluidized bed reactor for burning or pyrolysis of RRHs [11, 17, 73, 77–89]. The fluidized bed technology is selected as preferable for the production of amorphous silica from rice husks.

13.4 Key Factors for the Production of Amorphous Silica from Rice Husks

13.4.1 Uniform Temperature Distribution

The bubbling action in the fluidized bed provides a high degree of turbulence and mixing in the bed region, which results in high heat transfer rates within the bed region. Therefore, the heat evolved during the combustion process is distributed uniformly within the bed, with temperature variation within the bed region typically not exceeding 5–8°C [11, 75]. The high level of turbulence in the bed also eliminates the formation of hot-spots and leads to uniform temperature distribution within the bed region. The presence of hot-spots in the combustion zone poses the risk crystallizing the silica in the RHA. In addition, the high rates of heat transfer also leads to high combustion efficiency. So far as combustion temperatures are concerned, they can be kept low (typically in the range of 600–700°C) while allowing autogenous combustion to take place compared to other types of combustors (e.g., the inclined grate system).

13.4.2 Lower Operating Temperature Range

The lower range of operating temperatures in the fluidized bed is also very important for the following reasons: first, operating at temperatures above 700°C might expose the silica in the ash to the risk of crystallization; second, the formation of nitrogen oxides (NO_x) can be minimized. The rate of formation of thermal NO_x is highly temperature sensitive, becoming rapid only at flame temperatures (in range of 1,350–1,950°C); and third – to prevent slagging and fouling problems. In the presence of alkali metals in RHA, particularly potassium and sodium compounds (K_2O and Na_2O), the ash remains sticky at temperature much lower than the melting point of ash. Sodium and potassium salts react with silica in the ash to form eutectic mixtures having low melting point. The melting point of these eutectic mixtures might be as low as 600–700°C at high concentration of sodium

or potassium [11, 89]. The low ash fusion temperature results in the adhesion of particles, which can lead to excessive slagging and fouling problems.

13.4.3 Rapid Reaction Time

When the rice husk particles are introduced into the hot bubbling fluidized bed region, their drying and devolatilization reactions (both endothermic) occur instantaneously. Most of the volatile constituents in rice husks are released while the remaining char particles are oxidized within the bed to provide heat source for the endothermic reactions. The intense abrasive action of the turbulent bubbling bed tends to remove any surface deposits (char or ash) from the rice husk particles, thus continuously exposing a “clean” reaction surface to the surrounding hot gasses. Due to the change in the bulk density, the char particles are entrained into the freeboard region where they spend a few seconds undergoing further oxidation process. Besides, the char and ash particles are brittle and are easily broken down into smaller fragments by the abrasive action of the bubbling bed, making them more easily entrained to the freeboard region. As a result, the time rice husks reside in the fluidized bed is only in the order of a few minutes compared to hours for other types of thermal treatment systems. Such rapid reaction time increases the throughput value of rice husks in the combustor and, subsequently, the production rate of ash [11].

13.4.4 High Carbon Conversion Efficiency

The residual carbon content in the RHA after being thermally treated in fluidized bed combustor gives the highest carbon conversion efficiency, i.e., as high as 99%. According to Rozainee [11, 85, 86], the combustion efficiency in a fluidized bed is approximately 7.5 times higher than the maximum possible combustion efficiency in a grate type furnace per unit grate area. In addition, the combustion intensity in a fluidized bed increased with bed height due to increase in bed volume.

13.4.5 Ash Composition and Its Removal

RHA has a rigid skeleton-like structure due to its high silica content, resulting in a considerable amount of carbon being trapped in the skeleton that cannot be burned or gasified. Due to its high silica content, carbon in rice husks char is located at points that are interlaced with silica so that access to carbon is difficult. In order to obviate this problem, rice husks could be pulverized prior to thermal treatment, but this in turn would definitely increase the operation costs, health risk

associated with the handling of powdered rice husks, and operational hazard in the form of dust explosion. In a fluidized bed, the turbulence due to fluidization in the bed can break the rigid ash skeleton to make the trapped carbon available for conversion [11, 90]. Simultaneous attrition of ash particles in the fluidized bed gives smaller ash particles compared to these obtained from a grate type furnace. The ash produced is fine with sizes less than 400 μm , which means that it can be easily elutriated out of bed even by a low fluidization velocity of about 0.55 m s^{-1} [11, 91]. Therefore, the ash can be removed from the fluidized bed by entrainment in the gas stream and then separated by a particle separating system, such as cyclone. When rice husks are burned in fluidized bed reactor under controlled conditions, the resulting ash is undoubtedly the cheapest bulk source of highly reactive silica with high specific surface area. Since the ash is obtained as a fine powder, it does not require further grinding, which makes it the most economical source of nanoscale silica.

13.4.6 Other Factors

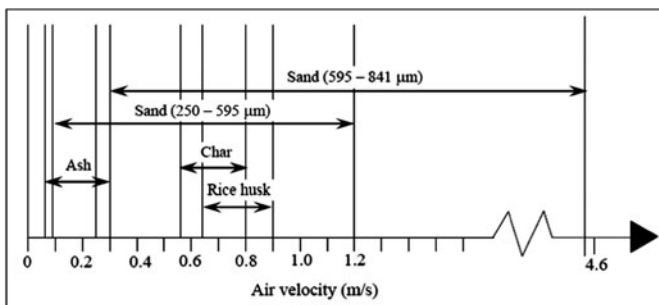
The fluidized bed technology is capable to provide high carbon conversion efficiency at moderate temperatures (below the crystallization point of silica in RHA) in short reaction times, which are the characteristics necessary to overcome the major concerns in heat treatment of rice husks. It offers a continuous and self-sustaining process without the need for auxiliary fuel, except during the brief start-up period. In fact, the combustion of rice husks in fluidized bed offers an added bonus of heat recovery. The reaction time is also very short (in the order of minutes), thus significantly increasing the production rate. Using this method, energy may be produced rather than consumed. The energy produced could be recovered in the form of heat or electricity. The turbulent bubbling action in the sand bed provides a high degree of mixing between the reactants and, more importantly, aids in breaking down the rigid skeleton-like structure of the ash [11].

The fluidization or bubble formation characteristics affect the degree of mixing in the fluidized bed. The mixing behavior, in turn, affects the combustion efficiency, which is promoted by good mixing since it provides turbulence and higher contact time between the reactants. Thus, two of the three fundamental requirements for the combustion reaction (temperature, turbulence, and residence time) can be fulfilled. Depending on the combustor operating conditions, particle combustion may be controlled either by chemical reaction or by transport phenomena. At low temperatures, the chemical reactions are the dominant factor rather than at high temperatures, where chemical kinetics are fast. At high temperatures, intra- and extra-particle mass transfer resistance of the oxidizing agent plays a major role in the determination of the combustion rate. Combustion at these high temperature regimes, therefore, is diffusion limited. In fluidized bed combustion, the combustion process was widely believed to be limited by the char oxidation state, as the conversion of carbon to CO_2 generates three times the heat released in comparison to its conversion to CO . Chars

from rice husks belong to the most reactive among technical carbon materials due to their porous and highly disordered carbon structure [92]. Therefore, the temperature regime for diffusion-limited combustion of biomass chars such as rice husk chars is expected to be in lower range. The speculation that combustion of rice husk chars is diffusion limited at temperatures beyond 650°C is further supported by the thermogravimetric analysis (TGA) of rice husks. As Mansaray and Ghaly reported in their studies on the thermal degradation of rice husks in air atmosphere [73, 78], it was observed through the mass loss profile that the char oxidation stage took place in the temperature range of 300–500°C. This showed that the combustion of rice husks should be kinetically controlled at temperatures below 500°C. Under conditions whereby the combustion is diffusion-limited, the importance of turbulence and residence time is significantly enhanced. Higher degree of turbulence increases the contact between reactants (rice husks and air) and the heat source (high temperature), thereby increasing the rates of heat and mass transfer to the reactants at microlevel. In addition, the turbulence in the bubbling sand bed is also responsible for the breaking of the rigid char skeleton, which is formed after the devolatilization of the rice husks, thereby making the entrapped carbon more readily available for further oxidation process. Due to their specific shape (like boat), however, it is almost impossible to maintain a stable regime of the fluidized bed. Besides, it is quite difficult to ignite and burn pure rice husks because of their low heat conductivity and heat capacity. All this indicates that auxiliary techniques and original approaches should be sought to solve the problem. The most effective way to overcome it turned out to be the use of quartz sand of suitable granulometric composition as heat carrier in the fluidized bed reactor. Its choice is stipulated by its high thermal resistance and chemical inertness, as well as its availability and low price. With the use of a same distributor design, the bubble formation characteristics and thus the mixing in the fluidized bed is governed by the fluidization parameters. For effective performance of the fluidized bed reactors, very important parameters are the fluidizing velocity of air, sand size fraction, and static bed height of sand [11].

13.4.6.1 Fluidizing Velocity

The choice of sand grain size to be used for the operation of the fluidized bed reactor affects the amount of air input required to maintain certain fluidizing conditions. A material is in its fluidizing state when the velocities lay within the range of its minimum fluidizing velocity (U_{mf}) and its terminal velocity (U_t). It was reported by Rozainee [11, 85, 86] that a fluidization number (U_t/U_{mf}) of 3 was necessary to produce the turbulence regime crucial in attaining good mixing behavior in a fluidized bed. He found in his study that incineration was stable at a fluidization number of 3 and that at fluidization number of 5, the combustion efficiency was similar to that of fluidization number of 3. The velocity ranges experimentally obtained for the fluidizing state of rice husks, its char and ashes, as well as sand samples are compared in Fig. 13.3 [11].



Reprinted with permission from Rozainee, M., Production of amorphous silica from rice husk in fluidized bed system, 2007, Faculty of Chemical Engineering and Natural Resource Engineering, Universiti Teknologi Malaysia., ref. 11.

Fig. 13.3 Experimental values of velocities range for the fluidizing state of raw rice husks, rice husk char, or ash and sand samples



Fig. 13.4 Sand fraction sizes 500–830 μm and 350–420 μm , respectively

13.4.6.2 Sand Size

According to Bhattacharya et al. [77], the optimal operating velocity of air for combustion of rice husks in a fluidized bed with sand particle sized 350–420 μm was 0.185–0.37 m s^{-1} at room temperature and pressure. After some trial runs with different sand sizes, they concluded that this sand size was deemed the most suitable for the combustion of rice husks in fluidized bed as there was considerable sand entrainment with sand size much smaller than 350 μm . On the other hand, too large sand particles would not mix well with rice husks, resulting in poor combustion behavior. This was found to be consistent with other studies, which reported the use of sand with sizes less than 830 μm , mostly in the range 300–500 μm . Photographs of sand with different fraction sizes are presented in Fig. 13.4.

Rice husks have very low bulk density (approximately 100 kg m^{-3}) and low terminal velocity (1.1 m s^{-1}) [11, 85, 86]. During the combustion of rice husks, the

bed consists of a mixture of rice husks, char, and ash in addition to the inert bed material (sand). There is a delicate balance to maintain in order to ensure good mixing by introducing fluidizing air at fluidizing velocity much higher than the minimum (namely $3\text{--}5 U_{mf}$), whilst ensuring that the rice husks would not be elutriated prior to being burnt to completion. Using sand with particle size in the range of $710\text{--}850\ \mu\text{m}$ is considered to be the upper limit for sand size to maintain the fluidizing velocity at $3 U_{mf}$ (the minimum fluidization number required to promote good mixing in the bed); it will result in a superficial velocity of approximately $1.0\ \text{m s}^{-1}$, which is sufficient to elutriate the rice husk particles. Some authors [11, 86] recommended a superficial fluidizing velocity of $0.65\text{--}1.0\ \text{m s}^{-1}$ to achieve good fluidization of sand, rice husks, and its char and ash mixture. On other hand, if the sand size is too small, the sand particles might be trapped in the voids of the ash skeleton, resulting in significant sand contamination of the ash product. In addition, since a large volume of the sand is required for the operation of the fluidized bed (for topping up and replacing used sand), commercially available sand source is necessary. Fluidization experiments showed that the U_{mf} for the $595\text{--}840$ and $250\text{--}595\ \mu\text{m}$ sand samples were 0.30 and $0.09\ \text{m s}^{-1}$, respectively. Maintaining the fluidizing number as high as $5 U_{mf}$ for the sand size of $250\text{--}595\ \mu\text{m}$ will only result in a superficial velocity of $0.45\ \text{m s}^{-1}$, less than half of the terminal velocity of rice husks. The use of sand size of $595\text{--}840\ \mu\text{m}$ operating at $5 U_{mf}$ will result in a fluidizing velocity of $1.50\ \text{m s}^{-1}$, which might be sufficient to elutriate the sand particles. Further, Rao and Ram [92] reported that the minimum fluidizing velocities for binary mixtures of particles with different densities and sand (such as rice husks and sand) differ upon the mass fractions of the mixture materials. For example, increasing the mass fraction of rice husks in a bed of sand particles from 2 to $15\ \text{mass}\%$ would let an increase of in the minimum fluidizing velocities of the mixture U_{mf} by up to 2.6 times. This phenomenon could lead to a poorer mixing behavior of the mixture material as the U_{mf} number was computed based on the U_{mf} of the bed material. However, the drastic increase in the value of U_{mf} was only observed at higher mass fractions, when the mass fraction of rice husks in the bed was increased from 10 to $15\ \text{mass}\%$. The increase of U_{mf} was found to be less than 60% when the mixture fraction of rice husks was kept below $10\ \text{mass}\%$. Hence, it was hypothesized that when operating at fluidizing velocity of $3\text{--}5 U_{mf}$, sand with particle size ranging from 250 to $850\ \mu\text{m}$ could give good mixing of rice husks in the fluidized bed while preventing excessive elutriation of the low-density rice husk particles. It was also necessary to limit the amount of rice husks present in the bed to less than $10\ \text{mass}\%$ of the weight of the entire bed materials to prevent significant difference between the minimum fluidizing velocity of the bed material and the minimum fluidizing velocity of the mixture materials.

13.4.6.3 Static Bed Height

The static bed height in the fluidized bed is usually expressed in terms of the ratio of the static height of bed materials (H) to the column diameter (D). A bed height

of $1D$ means that H is equal to D . Existing literary sources reported using a sand bed height from 0.15 – $1.25 D$ for the combustion of rice husks [11, 80]. The combustion intensity depended on the bed height, with the intensity being higher for higher bed height due to the increase in bed volume. In addition, since the bed acts as a thermal “fly-wheel,” namely temporarily storing and then transferring the heat evolved during the combustion process to the feed materials, it is preferable to use a bed of bigger height to increase the thermal capacity of the bed. However, several drawbacks are associated with the use of higher beds, such as the higher pressure drop incurred (which translates to higher investment cost for compressed air source) and the higher fuel cost for start-up of the bed. Rozainee [11, 85, 86] concluded that a sand bed height of $0.5 D$ (in an 80 mm inner diameter fluidized bed combustor) was optimum due to the following reasons: easier start-up of bed via preheating with premixed LPG-air combustion compared to higher beds (i.e., 0.75 – $1 D$). The entire bed could be preheated at $0.5 D$ up to a temperature of 900°C in less than 8 min, whereas for the 0.75 and $1.0 D$ bed heights, the bed could only reach a temperature of up to 750°C even after being preheated more than 10 and 20 min, respectively. The second reason is easier control of bed temperature. Thicker beds result in bigger bubbles as they rise to the bed surface. Eruption of such big bubbles makes it very difficult for the LPG flame to remain inside the bed, and finally, better mixing behavior in the absence of slugging or channeling as observed in beds with height of 0.75 and $1.0 D$.

A laboratory installation for the thermal degradation of rice husks, equipped with quartz fluidized-bed reactor [93], is presented in Fig. 13.5.

The fluidized bed reactor (6), presented in Fig. 13.5, is with inner diameter 7.5 cm and height 110 cm. The static bed height is 3.5 cm with the sand size of 250 – $630 \mu\text{m}$. Operating at $4 U_{\text{mf}}$ for this sand size resulted in a fluidizing velocity of 0.4 m s^{-1} . This velocity is less than half the terminal velocity of whole rice husk particles, thus enabling them to reach the bed region. To achieve stable fluidized bed, the air volume is about $110 \text{ dm}^3 \text{ min}^{-1}$ (standard temperature and pressure). The mass ratio sand/rice husk is $10/1$. The optimal bed temperature for the combustion of rice husks is maintained at approximately 700°C . Under these conditions, a considerable amount of rice husks is observed to mix within the bed. Only a small amount of the rice husks, mostly fine fragments, is elutriated into the freeboard region. There are many publications [11, 73, 77–96] in which different types and constructions of fluidize bed combustor system for thermal degradation of rice husks is described.

The WRHA obtained under these conditions has a good quality and may be used as adsorbent, filler of polymers, rubbers, cement, and concrete, or for other purposes. In conclusion, it may be stated that as the high ash content, low bulk density, poor flow characteristic, and low ash melting point makes the other conventional types of reactors unsuitable for rice husks utilization, fluidized bed reactors seem to be a suitable choice. The study of published reports indicates that it is technically feasible to successfully burn the rice husk in a fluidized bed reactor, and combustion intensity of about $530 \text{ kg h}^{-1} \text{ m}^{-3}$ can be achieved.



Fig. 13.5 A photograph of the laboratory equipment setup for combustion of raw rice husks in fluidized bed reactor (1) air compressor *Black & Decker*; (2) tank for liquid petroleum gas (LPG); (3) distributor for gasses; (4) manometer; (5) air Rota meter; (6) quartz fluidized bed reactor; (7) gas burner; (8) asbestos insulator; (9) porous quartz diaphragm; (10) electrical heater; (11) electrical transformer; (12) voltmeter; (13–15) thermo couples; (16) economizer; (17) separator; (18) temperature recorder; (19, 20) thermo regulators; and (21) PC



Fig. 13.6 A photograph of the pilot plant for rice husks pyrolysis

Based on the results, obtained from the carried out studying with the laboratory equipment was build pilot plant for pyrolysis of RRHs with productivity of 100 kg h^{-1} rice husks, which shape is presented on Fig. 13.6.

Metal serpentines are installed in the volume of the two hot cyclones and in the volume of the uppermost part of the fluidized bed combustor. Inside them, deionized water flows in reverse direction to the exhaust fumes. The water gets heated and vaporizes, which results in high temperature steam. Thus a triple effect is achieved: the ecological problem of the utilization of waste rice husks is solved and black or white rice husk ash, which is a commercial product, and technological steam are obtained.

13.5 Physicochemical Characteristics of Rice Husk and the Products of Its Thermal Degradation

The main physicochemical characteristics of the rice husks and the products of its thermal degradation in different atmosphere used as fillers of polymers are morphology, crystalline, or amorphous state, surface reactivity functional groups, thermal stability, and pore structure. Some of them are presented in Table 13.1, and compared with those of Aerosil A200 (AR), Degussa AG, Germany.

The typical morphology of RRH and black and white rice husk ash was examined by a scanning electron microscopy. SEM micrographs of RRH, after combustion in air and after pyrolysis in nitrogen atmosphere at 700°C, are presented in Fig. 13.7.

The main components of rice husk are in lemma and palea form, which tightly interlock with each other [5, 13, 69, 99]. Figure 13.7 shows the outer epidermis of RRH, which is well organized and has a corrugate structure. The outer surface of lemma is highly ridged, and the ridged structures have a linear profile. The epidermal cells of lemma are arranged in linear ridges and furrows, and the ridges

Table 13.1 Physicochemical characteristics of the RH, WRHA, BRHA, and AR [97]

Parameter	RH	WRHA	BRHA	AR
SiO ₂ , mass%	20.2	94.2	54.0	100
Moisture, mass%	7.1	0.8	0.6	–
Mean particle size, μm	800	15	20	5
Surface area, m ² g ⁻¹	<1	228	241	273
True density, g cm ⁻³	1.47	2.2	1.8	2.2

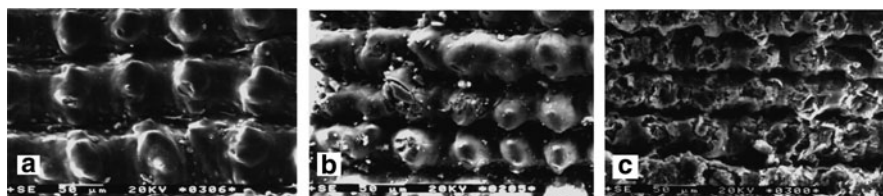


Fig. 13.7 SEM micrographs of ungrounded RRH (a), WRHA (b), and BRHA (c) at 700°C [98]

are punctuated with prominent globular protrusions [98]. The outer surface of lemma also contains papillae and hairs of varying sizes, but they were often broken at their bases in the material examined and therefore are not illustrated. As can be seen in Fig. 13.7a, the structure of RRH was globular. The relatively stable Si–O carcass and biomass assembled around it formed the structure of rice hull. The silicon atoms are presented all over, but they are concentrated in the protuberances and hairs (trichomes) on the outer and inner epidermis, adjacent to the rice kernel. After combustion of rice husk in air (Fig. 13.7b), the morphology tended to maintain its original shape, although the product is brittle and loose when carefully pinched with the fingers. The only difference that can be observed was that the globules were shrunk and compacted due to the release of the volatile products. The hard residue was formed of almost pure SiO₂ (96.8%). As it has been pointed out [100], the rate of combustion process depends strongly on the vapor diffusion rate from the bulk of the spherical globules. The structure of the pyrolysis product obtained in nitrogen medium was also globular (Fig. 13.7c), but due to the lower percentage of volatile products released, the solid residue contained significantly more carbon (42.6%). In this case, therefore, the initial globular structure of rice husk was also preserved due to the high thermal stability of SiO₂. The last two SEM micrographs showed that many residual pores are distributed within the ash samples, indicating that WRHA and BRHA are highly porous materials with large internal specific surface area. The rice husk might have become broken up during thermal decomposition of organic matter, thus obtaining highly porous structure. By comparison of these micrographs, it is observed that the surface of RRH is relatively nonporous, whereas burned or pyrolyzed rice husk exhibit porous surface, as indicated by the pore structure analysis (nitrogen adsorption).

The pyrolysis of rice husks caused decomposition of organic part and breaking of the bonds with Si atoms. The XRD patterns of the RRHs, pyrolyzed and combusted rice husks, as well as Aerosil A200, which is nonporous highly dispersed silica, are shown on Fig. 13.8 for comparison [98].

Figure 13.8 shows X-ray diffraction analysis on the rice husk before and after thermal decomposition in nitrogen or air medium. All the three samples were amorphous, although a broad diffused peak centered at about $2\theta = 22.5^\circ$ was observed. No reflexes, characterizing cristobalite or tridymite phase, were noticed in the samples studied, indicating the absence of any crystalline phases. Curve (a) from Fig. 13.8 represents the X-ray diffraction of the RRH. A broad hump around $2\theta = 22^\circ$ was noticed, indicating the presence of amorphous silica (disordered cristobalite). The same results were obtained for the BRHA and WRHA, as well as for Aerosil Degussa (curve c) used for comparison. The maxima of the diffused peaks were found to vary from $2\theta = 22^\circ$ for RRHs to $2\theta = 20.7^\circ$ for white ash. The pyrolyzed rice husks showed an almost flat maximum spreading from $2\theta = 21^\circ$ to $2\theta = 26^\circ$. This could be attributed to a gradual change in the bonding of silicon with organic material in RRHs to silica–silica bonding in white ash. According to Liou [7, 14], Rozainee [11], Real et al. [13], Rahnman and Saleh [22], Hanafi et al. [101], and Ibrahim et al. [102], the partially crystalline cellulose in naturally aged RRHs shows an XRD peak at $2\theta = 26.7^\circ$. The XRD pattern for the RRHs,

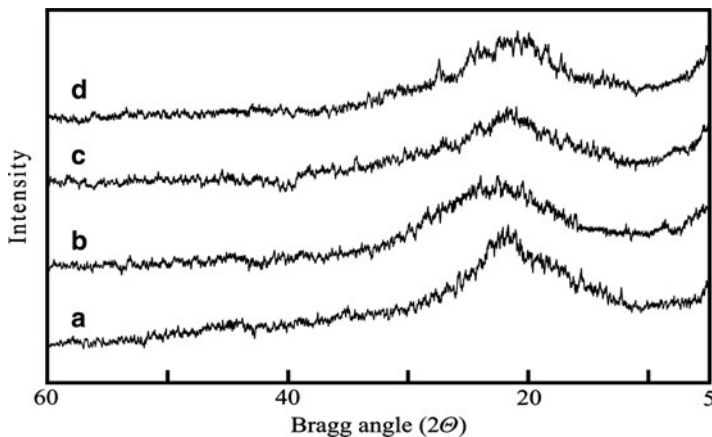


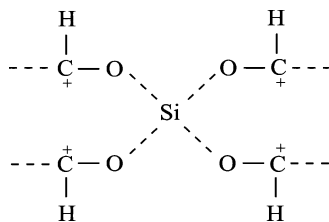
Fig. 13.8 X-ray diffraction patterns of grounded RRH (a), BRHA (b), WRHA (c), and Aerosil A200 Degussa (d) [98]

presented on Fig. 13.8, with its maximum at $2\theta = 23^\circ$ suggests that the silicon in RRH is bonded with organic material.

Going a little deeper into the structure of the organic compounds present in rice husks, the concept of the bonding of silicon with organic molecules can be confirmed. About the bonding of silicon with organic molecules, it may be assumed that cellulose ($C_6H_{10}O_5)_n$, being a polysaccharide and the main component of rice husk, does not seem to possess considerable bonding ability. Lignin, which coexists with cellulose, is mostly inert and therefore is not expected to be suitable for bonding. The remaining four organic components included in hemicellulose are aldehydes (monosaccharides), which polarize due to an electrometric effect. In the aldehyde group, the electrometric effect occurs as shown below [100]:



This type of electron transfer is brought into play only under the influence of an attacking reagent. The nature of silicon bonding in rice husk is complex and it appears to be bonded with the carbohydrates only. The possible bonding of silicon with four aldehyde residues in the RRH, as indicated above, may be illustrated with the following scheme [100, 103]:



The pyrolysis of RRH causes the decomposition of the organic material and breaking of the bonds between silicon and the organic material. The Si–O groups attach to each other to produce a low form of cristobalite. The resulting carbon and amorphous silica in the white ash showed an XRD pattern with a broad maximum. Upon complete burning, the single phase amorphous silica shows a diffused XRD peak with a maximum at about $2\theta = 21.8^\circ$. Thus, the X-ray diffraction patterns of rice husk ash showed a curve resembling that of silica gel without any characteristic peak. For both thermally treated samples, peaks characterizing cristobalite and tridymite phases were not registered. Cristobalite was detected at temperature above 727°C , while at $1,150^\circ\text{C}$, both cristobalite and tridymite were present. These results are in consistence with those obtained in other studies [101, 102]. Aerosil Degussa used as reference has also amorphous structure similar to that of WRHA.

The different groups in which silicon exists, e.g., siloxane Si–O–Si and silanol Si–OH, are best observed in IR spectra. Figure 13.9 presents IR absorption spectra of RRHs and after pyrolysis in nitrogen or combustion in air at 700°C and for comparison – Aerosil Degussa [98].

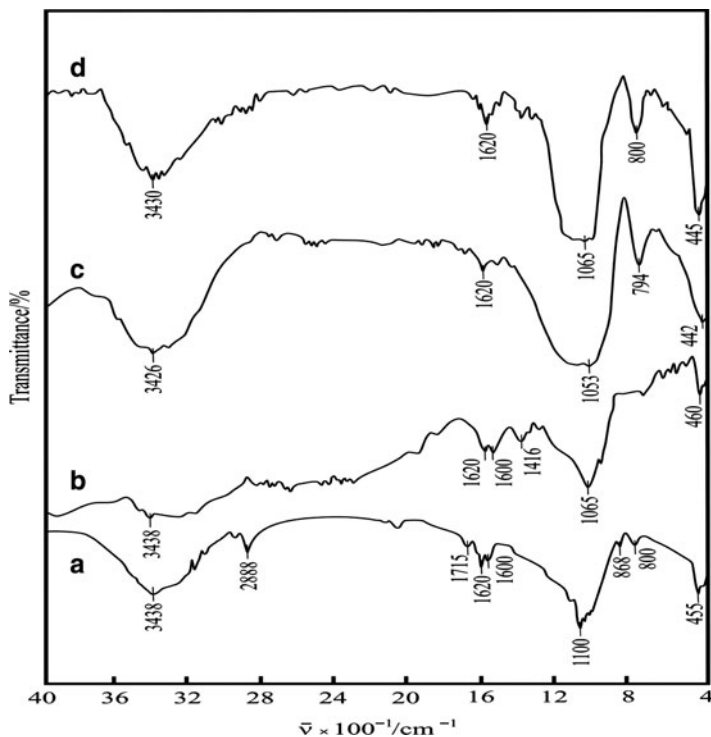
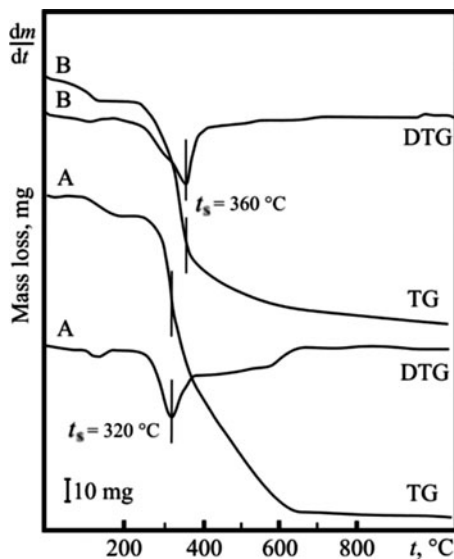


Fig. 13.9 IR spectra of RRH (a), BRHA (b), WRHA (c), and Aerosil A200 Degussa (d) [98]

Fig. 13.10 TG and DTG curves of the samples: combustion in air flow of grounded rice husks (a) and pyrolysis in nitrogen flow (b)



Infrared spectroscopy provides information on the chemical structure and surface functional groups of the samples. The IR spectra of rice husk gave typical bands of Si–O–Si stretching (very strong at $1,096\text{ cm}^{-1}$ and strong at 798 cm^{-1}) and bending vibrations (very strong at 466 cm^{-1}). The bands at $3,437$ and $1,633\text{ cm}^{-1}$ correspond to the O–H vibrations [14, 68, 69, 98–102, 104]. It can be seen from Fig. 13.10 (spectrum a) that RRHs are characterized by broad band between $3,750$ and $2,800\text{ cm}^{-1}$. The O–H stretching mode of hexagonal groups and adsorbed water can be assigned to this band. The position and asymmetry of this band at lower wave numbers indicate the presence of strong hydrogen bonds. A very weak band at $3,750\text{ cm}^{-1}$ can be assigned to isolated O–H groups. The adsorption band observed at $2,920\text{ cm}^{-1}$ was related to aliphatic C–H groups, and the very small peak near $1,720\text{ cm}^{-1}$ was attributed to the C=O stretching vibrations of ketones, aldehydes, lactones, or carboxyl groups. The weak bands at $1,600\text{ cm}^{-1}$ and $1,500\text{ cm}^{-1}$ correspond to bending vibration of H_2O molecules physically adsorbed onto rice husks and C–H deformation vibrations, respectively. The weak band at $1,400\text{ cm}^{-1}$ corresponds to a C–O stretching vibration of carboxylate groups. The predominant absorbance peak at $1,320\text{ cm}^{-1}$ was due to stretching vibrations, and the one at 450 cm^{-1} was due to bending vibration of siloxane bonds (Si–O–Si). The peaks between $1,200$ and 700 cm^{-1} are attributed to vibration modes of the Si–O network.

After the pyrolysis of rice husk in nitrogen medium, the IR spectrum of the black ash obtained did not differ significantly from that of RRHs, except for the quite higher intensities of the bands at $1,045$ and 450 cm^{-1} . This can be explained with

the decrease of organic matter content and its transformation into active carbon. The thermal treatment of rice husk in air, however, resulted in very different IR spectrum (Fig. 13.9, spectrum c). Wide, highly intense peak was observed with maximum at $3,420\text{ cm}^{-1}$, attributed to the stretching vibrations of silanol groups. The bands at $1,050\text{--}1,150$ and 790 cm^{-1} correspond to the Si–O stretching vibration, and the bending vibration at 450 cm^{-1} appeared sharper as the organic matter was no longer present. The positions of this feature are the same as those observed for commercial grade silica. Probably, the silicon atom was initially attached to the oxygen atom in RRH and, after the thermal decomposition, the combination of silicon and oxygen atoms lead to the formation of amorphous silica. In addition, it can be also observed that the peak for the white ash sample was sharper than that of the black ash sample, indicating that the percentage of silica contents increased when the rice husk is burnt in air. The IR spectrum of white rice husk ash silica is the same as those of Aerosil A200 Degussa. This means that both products have a similar nature.

The overall decomposition behavior of rice husks was reported to be due to decomposition of hemicellulose, cellulose, and lignin [7]. Mansaray and Ghaly [72, 73] reported that the hemicellulose and cellulose components of the rice husks were the main contributors to the evolution of the volatile compounds, while lignin is mainly responsible for the char portion of the products. In the present study on the carbonization or combustion behavior of rice husks, it can be deduced from these observations that decomposition of hemicellulose starts first, followed by the cellulose and finally by the lignin. The gaseous volatiles were released from organic materials during thermal decomposition. The final solid product of the carbonization process in nitrogen atmosphere is composed of a mixture of carbon and silica, and for the combustion process in air, it is a pure silica powder.

According to the data obtained from the TGA, the thermal decomposition of rice husks in air medium occurred in three main stages of mass loss, namely removal of moisture (drying), release of organic volatile matters (devolatilization), and oxidation of fixed carbon (slow combustion) [7, 65, 103]. The TG and DTG curves of studied samples are presented in Fig. 13.10 [70].

As can be seen from Fig. 13.10 (curve a), the mass loss in the first stage took place in the range $77\text{--}150^\circ\text{C}$ and is accompanied with small endothermic effect. The mass loss is about 7% and is associated with the evolution of adsorbed water in the sample and external water bonded by surface tension. The observed features of the thermal decomposition of rice husks can be explained on the basis of the decomposition behaviors of its major constituents: cellulose, hemicellulose, lignin, and ash. According to Stefani et al. [66], hemicellulose is degraded first at temperatures between 150 and 350°C , cellulose from 275 to 380°C , and finally lignin from 350 to 550°C . The second and major mass loss of nearly 50 wt% is attributed to the breakdown of the cellulose constituent to combustible volatiles, water, carbon dioxide, and char. Using a pycnometer as described previously, the true densities of the white and black rice husk ash were measured to be $2,200$ and $1,800\text{ kg m}^{-3}$, respectively. It is considerably more than the true density of grounded RRH. The lower density of the latter was due to the high content of active carbon in it ($\geq 40\%$).

Table 13.2 Kinetic characteristics of rice husk thermal degradation in air or nitrogen atmosphere [70]

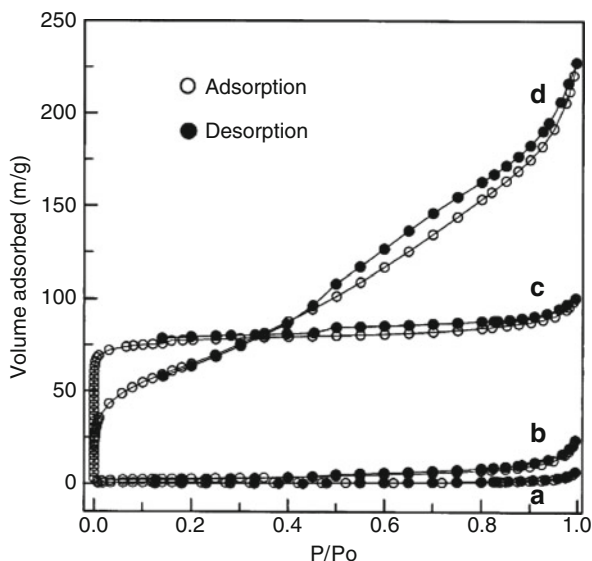
Parameter	Sample			
	A		B	
	$T < T_p$	$T > T_p$	$T < T_p$	$T > T_p$
T_p (exp.), K	593		633	
T_p (calc.), K	597		634	
E , kJ mol ⁻¹	187.1	23.1	175.1	5.3
A , min ⁻¹	3.45×10^{14}	2.04×10^{-1}	1.78×10^{13}	5.60×10^{-3}
k , min ⁻¹	1.14×10^{-24}	1.85×10^{-3}	6.32×10^{-2}	2.05×10^{-3}
$-\Delta S^\ddagger$, J mol ⁻¹ K ⁻¹	14.7	306.4	39.9	336.6
P	0.171	9.88×10^{-17}	8.3×10^{-3}	2.60×10^{-18}
ΔH^\ddagger , kJ mol ⁻¹	182.2	18.2	169.8	0.04
ΔG^\ddagger , kJ mol ⁻¹	190.9	199.9	195.1	213.1
R^2	0.9899	0.9950	0.9988	0.9822

The kinetic mechanism and kinetic parameters of nonisothermal degradation of rice husks in nitrogen or air medium have been described in detail in [70]. The smaller kinetic parameters obtained in the third stage, compared to these obtained in second stage, may be due to the fact that lignin, which has lower decomposition rates than cellulose and hemicellulose components in rice husk, was condensed to char.

On the basis of TG-curves, Coats–Redfern calculation procedure and the equation of Ginstling–Brounshtein calculated the kinetics parameters, characterizing nonisothermal degradation of rice husks in air or nitrogen atmosphere [70], and the obtained data are summarized in Table 13.2.

As can be seen from Table 13.2, the kinetic curves have two linear regions: the first one at temperatures lower than T_p (peak temperature in DTG curve) is steeper and the second one at higher temperatures has a smaller slope. For a detailed study of the mechanisms of both stages, the values of the activation energy E , frequency factor A in Arrhenius equation, change of entropy ΔS^\ddagger , enthalpy ΔH^\ddagger , Gibbs free energy ΔG^\ddagger for the formation of the activated complex from the reagent, and the steric factor $P = \exp(\Delta S^\ddagger/R)$ were calculated. Besides the value of the correlation coefficient of the linear regression analysis R^2 , the second criterion used was $T_{p(\text{calc})}$. This temperature was calculated from the cross point between the corresponding straight lines and was compared to the experimentally determined reference temperature $T_{p(\text{exp})}$, which in turn corresponds to the peak temperature in the DTG curve. As can be seen from the table, the difference between these two temperatures was less than 4°C. It means that the equation of Ginstling–Brounshtein was selected correctly and that a study on the kinetics of pyrolysis of rice husk should take into account the diffusion of volatile products from inside layers of the biomass. The higher values of E observed at $T < T_p$ show that the initial release of volatile products occurs under kinetic-diffusion control while the much lower values of E at $T > T_p$ indicate that pyrolysis takes place under typical diffusion control. The similar values of activation energy found that for the first stages,

Fig. 13.11 Adsorption-desorption isotherms of water-rinsed rice husks (a), acid-leached rice husks (b), BRHA (c), and WRHA (d)



sample B shows the release of volatile products during burning in air, or pyrolysis in nitrogen medium occurs by similar mechanisms. For monomolecular reactions of decomposition taking place within the solid phase, values of the frequency factor A of the order of 10^{14} show that the rotations of the activated complex and the reagent do not change during the reaction. At values of ca. 10^{11} , the reagent can rotate freely, while the active complex cannot rotate. The negative values of the change of entropy mean that the activated complex can be characterized by a much higher “degree of arrangement.” Besides, higher degree of “arrangement” was observed in the second stage (higher value of ΔS^\ddagger). The significantly lower than unity values of the steric factor P in the second stage give enough grounds to classify this stage as “slow.” For the first stage, however, the values of P are much closer to unity, so the first stage may be considered as “fast” [70].

The pore structure of rice husks and the products of its thermal degradation was studied in [7, 14, 104]. The typical nitrogen adsorption–desorption isotherms of samples obtained both before and after heating the rice husks in air or nitrogen atmosphere [7] are shown in Fig. 13.11.

For water-rinsed and acid-leached rice husks, Fig. 13.11a, b shows lower nitrogen capacity and no apparent desorption hysteresis loop, indicating that the porosity of the two raw materials is relatively lower than that of heat-treated rice husks samples. For carbonized in nitrogen and burned in air atmosphere husk samples, Fig. 13.11c, d shows that the isotherms are of type I according IUPAC classification. The hysteresis loops (associated with capillary condensation) found in both samples are of various shapes. According to these observations, BRHA is mainly microporous with narrow pore size distribution while WRHA contains both micro- and mesopores.

13.6 Utilization of the Rice Husks and the Products of Its Thermal Degradation as Fillers of Polymers

Using RHA as filler in certain polymers gives composites with better physical, thermal, and moisture resistance, as well as processing properties, and better economics [3, 105]. The addition of fillers to polymers is a fast and cheap method to modify the properties of the base polymer. Each filler brings its own characteristics to the matrices and, consequently, to the properties of the composite. The effect of the fillers on the preparation and properties of the composite materials is stipulated by the nature and quantity of the filler and some of its physicochemical properties such as particles size, hydrophobicity or hydrophilicity, specific area and surface functional groups, as well as coefficient of distribution in matrix volume. Therefore, composites based on the same filler may have quite different properties depending on the nature, physical and chemical composition, and compounding conditions [42–44]. As early as the 1970s, researchers began performing studies on rice husk flour (RHF) and RHAs as fillers in rubbers and plastics. In this respect, there are many publications in the literature reporting the use of natural fibers (rice husks or rice straw fiber) as replacement to man-made fiber in fiber-reinforced composites [3, 5, 42, 60, 99, 105, 106]. Yang et al. [60, 106, 107] studied the morphological and mechanical properties of flour polypropylene composites filled with 10–40% rice husks at different testing rates and temperatures. The authors observed decreased tensile strengths and increased tensile modules with the increase of the degree of filling. The composites showed brittleness at break at high testing rates and plastic deformation at higher temperatures. Advantages of natural fibers over man-made fibers include low density, low cost, recyclability, and biodegradability [106]. These advantages make rice husks a potential replacement for glass fiber in composite materials, which can be applied in the plastics, automobile, and packaging industries to cut down on material cost. A serious problem with rice husk fibers is their polar character, which creates incompatibility with most polymer matrices and the relatively high moisture sorption. Therefore, chemical treatments should be employed to modify the fiber surface properties. The treatments aimed at improving the adhesion between the fiber surface and the polymer matrix may not only modify the fiber surface but also increase fiber strength, improve their mechanical properties, and reduce water sorption of the composites. A better understanding of the chemical composition and surface adhesive bonding of natural fiber is necessary for developing natural fiber-reinforced composites. As it has been mentioned above, RRHs contain cellulose, hemicellulose, lignin, waxes, and water-soluble substances. Cellulose is semicrystalline polysaccharide containing D-glucopyranose units linked together by β -(1-4)-glucosidic bonds. The large amount of hydroxyl groups in cellulose imparts hydrophilic properties to natural fibers when used to reinforce hydrophobic matrices; the result is very poor interface and poor resistance to moisture absorption. Hemicellulose is strongly bound to cellulose fibrils presumably by hydrogen bonds. Hemicellulose polymers are branched, fully amorphous, and have significantly lower molecular weight than

cellulose. Because of its open structure containing many hydroxyl and acetyl groups, hemicellulose is partly soluble in water and hygroscopic. Lignin polymers are amorphous, highly complex, and mainly aromatic compounds built of phenylpropane units, but they have the least water sorption among the natural fiber composites. Since the poor properties of the interface between the fiber and polymer matrix often reduce their potential as reinforcing agents due to the hydrophilic nature of natural fibers, chemical modifications are considered to optimize the fiber surface. Chemicals may activate hydroxyl groups or introduce new moieties that can effectively interlock with the matrix. Generally, chemical coupling agents are molecules possessing two functions. In this case, the first function is to react with hydroxyl groups of cellulose and the second is to react with the functional groups of the matrix. In this respect, silanes, maleated ethylene, maleated propylene, and a few acrylic-grafted linear polymers [55, 60, 106, 107] are very often used as coupling agents. They may reduce the number of cellulose hydroxyl groups in the fiber–matrix interface. In the presence of moisture, hydrolysable alkoxy group leads to the formation of silanols. The silanol then reacts with the hydroxyl group of the fiber to form stable covalent bonds to the cell wall that are chemisorbed onto the fiber surface. Therefore, the hydrocarbon chains provided by the application of silane restrain the swelling of the fiber by creating a crosslinked network due to covalent bonding between the matrix and the fiber. Yet most chemical treatments have achieved various levels of success in improving fiber strength, fiber fitness, and fiber–matrix adhesion in natural fiber-reinforced components, but this additional operation leads to a negative impact on economics. This problem may be partially overcome using the products of thermal degradation of rice husks.

13.6.1 Rice Husk Ashes as Fillers in Rubbers

RHA can also be used as a filler in natural rubber, styrene butadiene rubber, nitrile butadiene rubber, butyl rubber, etc. [3, 5, 48–50, 53]. Especially in epoxidized natural rubber, the addition of WRHA can increase the tensile strength, tear strength, and hardness of the rubber. As WRHA is predominantly silica, it responds effectively to silane-coupling agents in improving the properties of rubber compounds. WRHA modified by silane-coupling agents not only can effectively improve epoxidized natural rubber's mechanical properties, such as tensile and tear strength, but also can improve its cure characteristics. The cure characteristics of WRHA-filled vulcanizates show a close resemblance to those of carbon black. This can be attributed to the similarities of filler-related parameters such as surface area, surface reactivity, particle size, and metal oxide content. Generally, WRHA is not as good as fumed silica and carbon black, especially in terms of tensile strength and tear strength, but it can replace or partially replace fumed silica and carbon black on some occasions [108–110]. In addition, WRHA can sometimes be combined with other fillers, especially with reinforcing blacks. The properties obtained are linear functions of the amount of the particular filler present in the blend.

BRHA has a lower silica content, typically about 54 mass% and a substantial carbon content of about 44 mass%. It can be also used as a filler for rubber, but the effect is not as good as can be obtained with WRHA [110, 111].

13.6.2 Other Applications

Because of high energy consumed in cement production, some countries short of energy often incorporate some other components into cement [3, 5]. The micro silica in RHA produced by controlled burning of rice husks has been recently used instead of the more expensive silica fume for achieving high strength lightweight concrete [50–52]. In all these studies, RHA has been reported as a source for silica in cement manufacture. This pozzolanic material is used to prevent or minimize cracking in concrete due to the expansive gel formation by the alkali–silica reaction. The results indicate that the use of RHA leads to enhanced resistance to segregation of fresh concrete and to increased strength compared to a control mixture with Portland cement alone. When RHA is used as filler in concrete blocks, the strength is enhanced due to its pozzolanic property.

The chemical reactivity of RHA with lime and water imparts the pozzolanic property, and a number of publications/patents are available [112–116]. In fact, the incorporation of RHA into cement can not only decrease the cost but can also improve certain properties of the cement. The incorporation of RHA into cement paste does not increase its compressive strength, but if the RHA is filled in mortar or concrete, the compressive strength of both the mortar and concrete increase. The reason might lie in the reduced porosity, reduced $\text{Ca}(\text{OH})_2$ content, and reduced area of the interface zone between the paste and the aggregate when RHA is present [114]. In addition to compressive strength, RHA can also increase concrete's resistance to acid and sulfate, flexural strength, carbonation, penetration, etc. [110, 114]. RHA will affect the volume changes of the concrete, but the volume changes will be within the limit specified in the American standards [3]. When expansive cement was partly replaced by RHA, its compressive strength substantially increased and its chloride permeability decreased significantly, whereas its total expansion decreased slightly. Because RRH can react with lime and water, RHA is sometimes mixed with lime first and then filled into cement [113, 114]. The properties of lime- RHA cement are acceptable. It can be used as the replacement of Portland cement in some application. Sometimes, RHA has even been directly blended with lime and then used as a construction material.

13.7 Conclusions

Rice husks are an important by-product of the rice milling process and are a major waste product of the agricultural industry. They have now become a great source as a raw biomass material for manufacturing of value-added silicon composite

products. Currently, the use of the RRHs and the products of its thermal degradation is an object of intense studies. More of these studies have been carried out at the laboratory level. Tremendous opportunities exist for further research and development activities to convert all the laboratory findings into commercial production with appropriate technologies. Development of economically viable processes for getting rice husk silica with specific properties gathers importance at this juncture. Economy of the manufacturing process improves if the fuel value of the material is also utilized. The method of controlled thermal treatment of RRHs helps solving the disposal and pollution problems of the rice milling industry and gives an excellent starting material for preparation of advanced high-quality ceramic powders, such as silicon carbide, silicon nitride, and magnesium silicide, which are good for application in high temperature material engineering. In addition, small scale of pure silica powder can be widely used for production of high purity elemental silicon for electronic, adsorbents, catalyst support, as tixotropic agents, and thermal insulators. Some of the novel applications of the RHAs are as fillers of rubbers, plastics, and cement. They may successfully replace the more expensive condensed silica fume. The laboratory obtained results were considered enough to conclude that the cheap RRHs and the products of its thermal degradation (BRHA and WRHA), after vigorously grounding and mixing, can successfully be used as fillers for polypropylene and tetrafluoroethylene-ethylene copolymer to replace the expensive synthetic additive Aerosil in the preparation of different polymer composites. The RHA-polymer composites can lead to the futuristic “organic–inorganic hybrid materials” with specific properties.

The abundance of waste from paddy milling industry as well as its interesting complex of behaviors is a prerequisite for success in obtaining cheap and valuable products and gives new alternatives for its applications. Hence, production of value added materials from rice husks not only facilitates utilization of an abundantly available agro waste but also reduces the environmental pollution.

Acknowledgments This work has been financially supported by the European Union Program 2007BG161PO003 and Bulgarian Project SIP-02-4 for supporting and development of starting innovation enterprises.

References

1. Govindarao VMH (1980) Utilization of rice husk: a preliminary analysis. *J Sci Ind Res* 39:495–515
2. Bailey SE, Olin TJ, Bricka RM, Adrian DD (1999) A review of potentially low-cost sorbents for heavy metals. *Water Res* 33:2469–2479
3. Sun L, Gong K (2001) Silicon-based materials from rice husks and their applications. *Ind Eng Chem Res* 40:5861–5877
4. Kaushik V, Sharma HK, Prasad KM, Bera B (2001) Utilization of husk ash from rice milling industry: a review. *J Ind Pollut Contr* 17:201–205
5. Chandrasekhar S, Satyanarayana KG, Pramada PN, Raghavan P, Gupta TN (2003) Processing, properties and applications of reactive silica from rice husk: an overview. *J Mater Sci* 38:3159–3168

6. Babel S, Kurniawan TA (2003) Low cost adsorbents for heavy metals uptake from contaminated water: a review. *J Hazard Mater* B97:219–243
7. Liou TH (2004) Evolution of chemistry and morphology during the carbonization and combustion of rice husk. *Carbon* 42:785–794
8. Chuah TG, Jumariah A, Aznu I, Katayon S, Thomas Choong SY (2005) Rice husks as a potentially low-cost biosorbent for heavy metal and dye removal: an overview. *Desalination* 175:305–316
9. Crini G (2006) Non-conventional low-cost adsorbents for dye removal: a review. *Bioresour Technol* 97:1061–1085
10. Muthadhi A, Anitha R, Kothandaraman S (2007) Rice husk ash – properties and its use: a review. *IE(I) Journal-CV* 88:50–56
11. Rozainee M (2007) Production of amorphous silica from rice husk in fluidized bed system. Faculty of Chemical Engineering and Natural Resource Engineering, Universiti Teknologi Malaysia. Research VOT 74526
12. Mishra P, Chakraverty A, Banerjee HD (1986) Studies on physical and thermal properties of rice husk related to its industrial application. *J Mater Sci* 21:2129–2132
13. Real C, Alcalá MD, Criado JM (1996) Preparation of silica from rice husk. *J Am Ceram Soc* 79:2012–2016
14. Liou TH (2004) Preparation and characterization of nano-structured silica from rice husk. *Mater Sci Eng A* 364:313–323
15. Umeda J, Kondoh K, Michiura Y (2007) Process parameters optimization in preparing high-purity amorphous silica originated from rice husks. *Mater Trans* 48(12):3095–3010
16. Watari T, Nakata A, Kiba Y, Torikai T, Yada M (2006) Fabrication of porous SiO₂/C composite from rice husk. *J Eur Ceram Soc* 26:797–801
17. Kalderis D, Bethanis S, Paraskeva P, Diamadopoulos E (2008) Production of activated carbon from bagasse and rice husk by single-stage chemical activation method at low retention times. *Bioresour Technol* 99:6809–6816
18. Sekar N, Virutha Giri T (2005) Preparation of sodium silicate from waste rice husk. *Chem Eng World* 40:81–85
19. Basu PK, King CJ, Lynn S (1973) Manufacture of silicon tetrachloride from rice hulls. *AIChE J* 19:439–445
20. Seo ESM, Andreoli M, Chiba R (2003) Silicon tetrachloride production by chlorination method using rice husk as raw material. *J Mater Process Tech* 141:351–356
21. Nandi KC, Mukherjee D, Biswas AK, Acharia HNA (1991) A novel and inexpensive method of production of silanes from rice husk and their gas chromatographic analyses. *Sol Energy Mater* 22:161–164
22. Rahman IA, Saleh MI (1995) Formation of β -sialon in the carbothermal reduction of digested rice husks. *Mater Lett* 23:157–161
23. Rodriguez-Lugo V, Ribio E, Gomez I, Torres-Martinez L, Castano VM (2002) Synthesis of silicon carbide from rice husk. *Int J Environ Pollut* 18:378–387
24. Adylov GT, Faiziev ShA, Paizullakhanov MS, Mukhsimov S, Nodirmatov E (2003) Silicon carbide materials obtained from rice husk. *Tech Phys Lett* 29:221–223
25. Sujirote K, Leangsuwan P (2003) Silicon carbide formation from pretreated rice husks. *J Mater Sci* 38:4739–4744
26. Kumar B, Godkhindi MM (1996) Studies on the formation of SiC, Si₃N₄, and Si₂N₂O during pyrolysis of rice husks. *J Mater Sci Lett* 15:403–405
27. Real C, Alcalá MD, Criado JM (2004) Synthesis of silicon nitride from carbothermal reduction of rice husk by the constant-rate-thermal-analysis (CRTA) method. *J Am Ceram Soc* 87:75–78
28. Kurama S, Kurama H (2008) The reaction kinetics of rice husk based cordierite ceramics. *Ceram Int* 34:269–272
29. Han H-W, Huang C-Y, Liu HS (1999) Formation of gehlenite (Ca₂Al₂SiO₇) by carbothermal reduction of carbonized rice hulls. *J Ceram Soc Jpn* 107:1115–1120

30. Hunt LP, Dismukes JP, Amick JA, Schei A, Larsen KK (1984) Rice husk as a raw material from producing silicon. *J Electrochem Soc* 131:1683–1686
31. Ghosh TB, Nandi KC, Acharya HN, Mukherjee D (1991) XPS studies of magnesium silicide obtained from rice husk. *Mater Lett* 11:6–9
32. Shimokawa K, Sekiguchi I, Suzuki Y, Ueda Y (1992) Synthesis of Si-O-C fibers from rice husk carbide-explanation of formation condition. *J Ceram Soc Jpn* 100:1111–1119
33. Gokhal KVGK, Dalai AK, Rao MS (1986) Thermal characteristics of synthetic sodium zeolites prepared with silica from rice-husk ash. *J Term Anal* 31:33–39
34. Paul H, Wang HP, Lin KS, Huang YJ, Li MC, Tsaur LK (1998) Synthesis of zeolite ZSM-48 from rice husk ash. *J Hazard Mater* 58:147–152
35. Mohanty K, Naidu JT, Meikap BC, Biswas MN (2006) Removal of crystal violet from wastewater by activated carbons prepared from rice husk. *Ind Eng Chem Res* 45: 5165–5171
36. Srivastava VC, Mall ID, Mishra IM (2008) Removal of cadmium(II) and zinc(II) metal ions from binary aqueous solution by rice husk ash. *Colloid Surf A* 312:172–184
37. Lakshmi UR, Srivastava VC, Mall ID, Lataye DH (2009) Rice husk ash an effective adsorbent: evaluation of adsorptive characteristics for Indigo Carmine dye. *J Environ Manag* 90:710–720
38. Tsai MT, Chang FW (2000) Characterization of rice husk ash-supported nickel catalysts prepared by ion exchange. *Appl Catal A Gen* 203:15–22
39. Chang FW, Kuo WY, Yang H (2005) Preparation of Cr₂O₃-promoted copper catalysts on rice husk ash by incipient wetness impregnation. *Appl Catal Gen* 288:53–61
40. Chang FW, Yang H, Roselin L, Kuo W (2006) Ethanol dehydrogenation over copper catalysts on rice husk ash prepared by ion exchange. *Appl Catal Gen* 304:30–39
41. Renu P, Radhika T, Sugunan S (2008) Characterization and catalytic activity of vanadia supported on rice husk silica promoted samaria. *Catal Commun* 9:584–589
42. Saheb DN, Jog JP (1999) Natural fiber polymer composites: a review. *Adv Polymer Tech* 18 (4):351–363
43. Chaudhary DS, Jollands MC, Cser F (2002) Understanding rice hull ash as fillers in polymers: a review. *Silicon Chem* 1:281–289
44. Chaudhary DS, Jollands MC, Cser F (2004) Recycling rice husk ash: a filler material for polymeric composites. *Adv Polym Technol* 23:147–155
45. Siriwardena S, Ismail H, Ishiaku US (2001) White rice husk ash filled ethylene-propylene-diene terpolymer/polypropylene blends: effect of dynamic vulcanization and filler loading. *Polym Plast Technol Eng* 40:519–538
46. Premalal HGB, Ismail H, Baharin A (2003) Effect of processing time on the tensile, morphological and thermal properties of rice husk powder-filled polypropylene composites. *Polymer Plast Tech Eng* 42:827–851
47. Kim HS, Yang HS, Kim HJ, Park HJ (2004) Thermogravimetric analysis of rice husk flour filled thermoplastic polymer composites. *J Therm Anal Cal* 76:395–404
48. Ismail H, Chung FL (1999) The effect of partial replacement of silica by white rice husk ash in natural rubber composites. *Int J Polym Mater* 43:301–312
49. Ismail H, Mega L, Khalil HPS (2001) Effect of a silane coupling agent on the properties of white rice husk ash-polypropylene/natural rubber composites. *Polym Int* 50:606–611
50. Arayaprane W, Naranong N, Rempel GL (2005) Application of rice husk ash as fillers in the natural rubber industry. *J Appl Polym Sci* 98:34–41
51. Jauberthie R, Rendell F, Tamba SE, Cisse IK (2003) Properties of cement-rice husk mixture. *Constr Build Mater* 17:239–243
52. Basha EA, Hashim R, Mahmud HB, Muntohar AS (2005) Stabilization of residual soil with rice husk ash and cement. *Constr Build Mater* 19:448–453
53. Ismail H, Nizam JM, Khalil HPS (2001) The effect of a compatibilizer on the mechanical properties and mass swell of white rice husk ash filled natural rubber/linear low density polyethylene blends. *Polym Test* 20:125–133

54. Panthapulakkal S, Law S, Sain M (2005) Enhancement of process ability of rice husk filled high-density polyethylene composite profiles. *J Thermoplastic Compos Mater* 18: 445–458
55. Panthapulakkal S, Sain M, Law S (2005) Effect of coupling agents on rice-husk-filled HDPE extruded profiles. *Polym Int* 54:137–142
56. Fuad MYA, Jamaludin M, Ishak ZAM, Omar AKM (1993) Rice husk ash as filler in polypropylene: Preliminary study. *Int J Polym Mater* 19:75–92
57. Fuad MYA, Mustafah J, Mansor MS (1995) Thermal properties of polypropylene/rice husk ash composites. *Polym Int* 38:33–43
58. Fuad MYA, Ismail Z, Mansor MS, Ishak ZAM, Omar AKM (1995) Mechanical properties of rice husk ash/polypropylene composites. *Polym J* 27:1002–1015
59. Siriwardena S, Ismail H, Ishiaku US (2003) A comparison of the mechanical properties and water adsorption behavior of white rice husk and silica filled polypropylene composites. *J Reinforc Plast Compos* 22:1645–1666
60. Yang HS, Kim HJ, Son J, Park HJ, Lee BJ, Hwang TS (2004) Rice-husk flour filled polypropylene composites; mechanical and morphological study. *Compos Struct* 63:305–312
61. Toro P, Quijada R, Murillo O, Yazdani-Pedram M (2005) Study of the morphology and mechanical properties of polypropylene composites with silica or rice-husk. *Polym Int* 54:730–734
62. Ismail H, Ishiaku US, Arinab AR, Izhak Z (1997) The effect of rice husks ash as filler for epoxidized natural rubber compounds. *Int J Polym Mater* 36:39–44
63. Ismail H, Mohamad Z, Bakar AA (2003) A comparative study of processing, mechanical properties, thermo-oxidative aging, water adsorption, and morphology of rice husk powder and silica fillers in polystyrene/styrene butadiene rubber blends. *Polymer Plast Tech Eng* 42 (1):81–103
64. Siriwardena S, Ismail H, Ishiaku US (2001) A comparison of white-rice husk ash and silica as a fillers of ethylene-propylene-diene terpolymer vulcanizates. *Polym Int* 50:707–713
65. Siriwardena S, Ismail H, Ishiaku US (2002) Water adsorption behaviour and its effect on tensile properties of ethylene-propylene-diene-terpolymer/polypropylene/filler ternary composites: a preliminary study. *Polym Plast Technol Eng* 41(3):419–433
66. Stefany PM, Garcia D, Lopez J, Jimenez A (2005) Thermogravimetric analysis of composites obtained from sintering of rice husk-scrap tire mixtures. *J Therm Anal Calorim* 81:315–320
67. Yao F, Wu Q, Lei Y, Xu Y (2008) Rice straw fiber-reinforced high-density polyethylene composite: effect of fiber type and loading. *Ind Crops Prod* 28:63–72
68. Chaudhary DS, Jollands MC (2004) Characterization of rice hull ash. *J Appl Polym Sci* 93:1–8
69. Daifullah AAM, Girgis BS, Gad HMH (2003) Utilization of agro-residues (rice husk) in small waste water treatment plants. *Mater Lett* 57:1723–1731
70. Vlaev LT, Markovska IG, Lyubchev LA (2003) Non-isothermal kinetics of pyrolysis of rice husk. *Therochim Acta* 406:1–7
71. Tsai WT, Lee MK, Chang YM (2007) Fast pyrolysis of rice husk: product yields and compositions. *Bioresour Technol* 98:22–28
72. Mansaray KG, Ghaly AE (1999) Kinetics of the thermal degradation of rice husk in nitrogen atmosphere. *Energy Sources* 21:773–784
73. Ghaly AE, Mansaray KG (1999) Comparative study on the thermal degradation of rice husk in various atmospheres. *Energy Sources* 21:867–881
74. Petro F, Anthony EJ, Disea DL, Friedrich FD (1987) Combustion trials of rice husk in a pilot-scale fluidized bed. In: *Proceeding of the 9th international conference on fluidized bed combustion* 2:1123–1127
75. Niessen WR (1995) *Combustion and incineration processes: applications in environmental engineering*, 2nd edn. Marcel, New York
76. Natarajan E, Nordin A, Rao AN (1998) Overview of combustion and gasification of rice husk in fluidized bed reactor. *Biomass Bioenergy* 14(5/6):533–546

77. Bhattacharya SC, Shah N, Alikhani Z (1984) Some aspects of fluidized bed combustion of paddy husk. *Appl Energy* 16:307–316
78. Mansaray KG, Ghaly AE, Al-Taweel AM, Hamdullahpur F, Ugursal VI (1999) Air gasification of rice husk in a dual distributor type fluidized bed gasifier. *Biomass Bioenergy* 17:315–332
79. Huang S, Jing S, Wang J, Wang Z, Jin Y (2001) Silica white obtained from rice husk in a fluidized bed. *Power Technol* 117:232–238
80. Armesto L, Bahillo A, Veijonen K, Cabanillas A, Otero J (2002) Combustion behaviour of rice husk in a bubbling fluidized bed. *Biomass Bioenergy* 23:171–179
81. Skrifvars B-J, Yrjas P, Kinni J, Stiefen P, Hupa M (2005) The fouling behavior of rice husk ash in fluidized-bed combustion. 1. Fuel characteristics. *Energy Fuels* 19:1503–1511
82. Skrifvars B-J, Yrjas P, Lauren T, Kinni J, Tran H, Hupa M (2005) The fouling behavior of rice husk ash in fluidized-bed combustion. 2. Pilot-scale and full-scale measurements. *Energy Fuels* 19:1512–1519
83. Yusof IM, Farid NA, Zainal ZA, Azman M (2008) Characterization of rice husk for cyclone gasifier. *J Appl Sci* 8(4):622–628
84. Singh RI, Mohapatra SK, Gangacharyulu D (2008) Studies in an atmospheric bubbling fluidized-bed combustor 10 MW power plant based on rice husk. *Energy Convers Manage* 49:3086–3103
85. Rozainee M, Ngo SP, Salema AA, Tan KG (2008) Fluidized bed combustion of rice husk to produce amorphous siliceous ash. *Energy for Sustainable Development* 12(1):33–42
86. Rozainee M, Ngo SP, Salema AA, Tan KG, Ariffin M, Zainura ZN (2008) Effect of fluidizing velocity on the combustion of rice husk in a bench-scale fluidized bed combustor for the production of amorphous rice husk ash. *Bioresour Technol* 99:703–713
87. Janvijitsakul K, Kuprianov VI (2008) Major gaseous and PAN emissions from fluidized-bed combustor firing rice husk with high combustion efficiency. *Fuel Process Technol* 89:777–787
88. Estevez M, Vargas S, Castano VM, Rodriguez R (2009) Silica nano-particles produced by worms through a bio-digestion process of rice husk. *J Non Cryst Solids* 355:844–850
89. Kulasekaran S, Linjewile TM, Agarwal PK, Biggs MJ (1998) Combustion of a porous char particle in an incipiently fluidized bed. *Fuel* 77:1549–1560
90. Mansaray KG, Ghaly AE (1998) Agglomeration characteristics of silica sand-rice husk mixture s at elevated temperatures. *Energy Sources* 20:631–652
91. Mansaray KG, Ghaly AE (1998) Thermogravimetric analysis of rice husk in an air atmosphere. *Energy Sources* 20:653–663
92. Rao TR, Ram JV (2001) Minimum fluidization velocities of mixtures of biomass and sand. *Energy* 26:633–644
93. Turmanova S, Genieva S, Vlaev L (2009) Thermal degradation of rice husks: structure, morphology, thermal and kinetics characteristics – review. *Chem Technol Ind J* 18:754–769
94. Fang M, Yang L, Chen G, Shi Z, Luo Z, Cen K (2004) Experimental study on rice husk combustion in a circulating fluidized bed. *Fuel Proc Technol* 85:1273–1282
95. Galgano A, Salatino P, Grescitelli S, Scala F, Maffettone P (2005) A model of the dynamics of a fluidized bed combustor burning biomass. *Combust Flame* 140:371–384
96. Qiaoqun S, Huilin L, Wentie L, Yurong H, Lidan Y, Gidaspow D (2005) Simulation and experiment of segregating/mixing of rice husk-sand mixture in a bubbling fluidized bed. *Fuel* 84:1739–1748
97. Turmanova S, Dimitrova AS, Vlaev LT (2008) Study of polypropene composites filled with rice husk ash. *Oxidation Commun* 31:465–481
98. Genieva SD, Turmanova S, Dimitrova AS, Vlaev LT (2008) Characterization of rice husks and the products of its thermal degradation in air or nitrogen atmosphere. *J Therm Anal Calorim* 93:387–396
99. Park BD, Wi SG, Lee KH, Singh AP, Yoon TH, Kim YS (2003) Characterization of anatomical features and silica distribution in rice husk using microscopic and micro-analytical techniques. *Biomass Bioenergy* 25:319–327

100. Patel M, Karera A, Prasanna P (1987) Effect of thermal and chemical treatments on carbon and silica contents in rice husk. *J Mater Sci* 22:2457–2464
101. Hanafi S, Abo-El-Enein SA, Ibrahim DM, El-Hemaly SA (1980) Surface properties of silicas produced by thermal treatment of rice husk ash. *Thermochim Acta* 37:137–143
102. Ibrahim DM, El-Hemaly SA, Abdel-Kerim FM (1980) Study of rice husk ash silica by infrared spectroscopy. *Thermochim Acta* 37:307–314
103. Amorim JJ, Elizariro SA, Gouveia DS, Simoes ASM, Santos JCO, Conceicao MM, Souza AG, Trindade MFS (2004) Thermal analysis of the rice and by-products. *J Therm Anal Calorim* 75:393–399
104. Kennedy LJ, Vijaya JJ, Sekaran G (2004) Effect of two-stage process on the preparation and characterization of porous carbon composite from rice husk by phosphoric acid activation. *Ind Eng Chem Res* 43:1832–1838
105. Moreland J (1979) The first decade of inorganic and organic surface modification. In: Society of the plastics industry, reinforced plastics/composites industries, proceedings of the 34th annual conference, Society of Plastics Industry, New York, Section 14-A, 30 Jan–2 Feb 1979
106. Li X, Tabil LG, Panigrahi S (2007) Chemical treatments of natural fiber for use in natural fiber-reinforced composites: a review. *J Polym Environ* 15:25–33
107. Yang HS, Kim HJ, Park HJ, Park HJ, Lee BJ, Hwang TS (2007) Effect of compatibilizing on rice-husk flour reinforced polypropylene composites. *Compos Struct* 77:45–55
108. Ishak ZAM, Baker AA (1995) An the investigation on the potential of rice husk ash as fillers for epoxidized natural rubber (ENR). *Eur Polym J* 31:259–269
109. Ismail H, Ishaku US, Arinab AR, Ishak ZAM (1998) Epoxidized natural rubber composites: effect of vulcanization systems and fillers. *Polym Plast Technol Eng* 37:469–474
110. Ismail H, Chung FL (1998) Partial replacement of silica by white rice husk ash in natural rubber composites: the effect of bonding agents. *Iran Polym J* 7:255–261
111. Costa HMD, Visconte LLY, Nunes RCR, Furtado CRG (2000) The effect of coupling agent and chemical treatment on rice husk ash-filled natural rubber composites. *J Appl Polym Sci* 76:1019–1027
112. Mehta PK (1977) Properties of blended cements made from rice husk ash. *J Am Concr Inst* 74:440–446
113. James J, Rao MS (1986) Reaction product of lime and silica from rice husk ash. *Cem Concr Res* 16:67–73
114. Zhang MH, Lastra R, Malhorta VM (1996) Rice-husk ash paste and concrete: some aspects of hydration and the microstructure of the interfacial zone between the aggregate and paste. *Cem Concr Res* 26:963–977
115. Rodrigues FA, Monteiro PJM (1999) Hydrothermal synthesis of cements from rice hull ash. *J Mater Sci Lett* 18:1551–1552
116. Ajiwe VIE, Okeke CA, Akigew FC (2000) A preliminary study of manufacture of cement from rice husk ash. *Bioresour Technol* 73:37–39

Chapter 14

Polyolefin-Based Natural Fiber Composites

Santosh D. Wanjale and Jyoti P. Jog

Abstract The development of high performance natural fiber composites (NFC) in the last few decades saw a significant growth in the industries as well as academia. These natural fiber reinforced composites exhibit numerous advantages such as high mechanical properties, low weight, low cost, low density, high specific properties, good thermal and acoustic insulating properties when compared with other composites. There has been a dramatic increase in the use of natural fibers for composites based on thermoplastics polymers such as polyvinyl chloride (PVC), polypropylene (PP), and high-density polyethylene (HDPE). A large number of natural fibers including flax, hemp, jute, kenaf, and sisal are being used for this purpose. In development of these composites, incompatibility between the natural fibers and polymer matrix and the tendency of the fibers to form aggregates are the two important issues. Additionally, the composites exhibit poor dimensional stability due to moisture absorption. Some of these issues/problems can be solved by the use of coupling agents, use of compatibilizer and treatments of fibers using peroxide, permanganate, and plasma.

In this chapter, the preparation and properties of polyolefin-based NFC with special reference to the types of fibers, compatibilization, processing methods, mechanical properties, and some applications will be discussed.

Keywords Compatibilization · Composites · Natural Fiber · Polyolefin

Contents

14.1 Introduction	378
14.2 Natural Fibers	379
14.3 Compatibilization	379

J.P. Jog (✉)

Polymer Science and Engineering Division, National Chemical Laboratory, Dr. Homi Bhabha Road, Pashan, Pune 411008, India

e-mail: jp.jog@ncl.res.in

14.3.1	Modification of Natural Fibers	381
14.3.2	Polymer Modification	383
14.4	Natural Fiber Composites	383
14.4.1	Bast Fibers	383
14.4.2	Leaf Fibers	386
14.4.3	Seed Fibers	389
14.4.4	Wood Fiber	390
14.4.5	Fruit Fibers	392
14.5	Applications	393
14.6	Conclusions	393
	References	394

14.1 Introduction

Natural fibers are now emerging as a feasible alternative to glass fibers for various applications. The advantages of natural fibers over synthetic fibers such as glass are their relatively high stiffness, lower density, recyclability, biodegradability, renewability, and lower cost [1–5]. The abundance of natural fibers combined with the ease of their processability is an attractive feature, which makes them a desirable substitute for synthetic fibers that are potentially toxic [6].

Importantly, there are some pros and cons in using these natural fibers. Natural fibers give less health problems for the people producing the composites, does not cause skin irritations, and they are not suspected of causing lung cancer [2]. The disadvantages include their moisture sensitivity and variability of diameter and length. In addition, most of these fibers degrade at temperatures around 250°C and hence the use of natural fibers is limited to low melting polymers, which can be processed at low temperatures. Thus, most of the reported work is on thermoset polymers and polyolefins [7–66], which can be processed at low temperatures.

The properties of thermoplastic composites containing fibers as fillers are dependent on a number of parameters, which include the properties of the matrix material, the size and aspect ratio of the fibers, dispersion of the fibers and the interface. In development of these composites, two important issues need to be addressed, namely, the incompatibility between the natural fibers and polymer matrix, and the tendency of the fibers to form aggregates [67]. Additionally, the composites exhibit poor dimensional stability due to moisture absorption. The orientation of the fibers is also important. In short-fiber reinforced composites, the orientation of the fibers is usually random and therefore the properties of such composites are not as superior as those containing continuous fibers. Optimization of processing conditions and use of coupling agents/compatibilizers and treatment of fibers can enhance the properties of these composites.

We present here an overview of the reported work on polymer-based natural fiber composites (NFC) with special reference to thermoplastic polymers such as polyolefins.

14.2 Natural Fibers

Natural fibers derived from plants are grouped based on the origin of the fibers as follows:

1. Bast fibers – Flax, Jute, Hemp, Kenaf
2. Leaf fibers – Sisal, Pineapple, Henequen
3. Seed fibers – Cotton
4. Cereal fibers – Rice straw, Corn, Wheat
5. Grass fibers – Bamboo, Switch grass
6. Fruit fiber – Coconut

The bast and leaf fibers give mechanical support to the plant's stem and leaf, respectively. Bast consists of a wood core surrounded by stem, and within the stem, there are a numbers of fiber bundles, each containing individual fiber cells or filaments. The bast fibers such as, hemp, flax, jute, kenaf, and ramie are usually grown in warm climates. The leaf fibers, such as sisal, abaca, banana, and henequen, are coarser than bast fibers. The seed-hair fibers, such as cotton, coir, and milkweed, are attached to the plant's seeds [68].

Natural fibers are composed of cellulose, hemicellulose, lignin, and waxes. A well-defined structure of the natural fiber is given by Kalia et al. [69]. Basically these are multicellular in nature consisting of a number of continuous, mostly cylindrical honeycomb cells having various sizes and shapes and the arrangements. These cells are cemented together by an intercellular substance, which is isotropic, noncellulosic, and ligneous in nature with a lacuna. There is a central cavity in each cell called the lumen. The microfibrils in the central walls form a constant angle for each type of fiber with the fiber axis, so that the crystallites are arranged in a spiral form. Thus, the properties of single fiber depend on the crystallite content, its size, shape, orientation, aspect ratio (L/D) of cells, and the thickness of cell walls. Mechanical properties of natural fibers vary significantly depending on the processing method used to break them down to the fiber level. Table 14.1 depicts properties of some natural fibers.

Humans have used all these natural fibers for textiles because of their wide availability, long fiber geometries, chemical stability, and favorable mechanical properties. The coarse texture and high mechanical properties of many bast and leaf fibers have been utilized in making common cordage fibers for rope, twine, and string [68].

14.3 Compatibilization

Despite the significant advantages, use of natural fibers as reinforcement or filler in thermoplastics such as polyolefins is not as simple as expected. The main issues include limited thermal stability during processing, poor dispersion in the thermoplastic melt due to limited compatibility with the matrix, strong fiber–fiber

Table 14.1 Properties of natural fibers

Natural fiber	Type of fiber	Density	Composition (%)			Degradation peak temperature (°C) (First derivative) (Ref.)	Tensile strength (MPa)	Young's modulus (GPa)
			Cellulose	Hemicellulose	Lignin			
Coconut	Fruit	1.2	32–43	0.15–0.25	40–45	190 [70]	140–225	3–5
Pineapple	Leaf	1.44	81	13.4	12.7	350 [71]	413–1,627	35–83
Hemp	Bast	1.48	68	15	10	220 [41]	690	35
Flax	Bast	1.5	71	18.6–20.6	2.2	250 [72]	45–1,100	27.6
Jute	Bast	1.3	61–71	14–20	12–13	300 [73]	393–773	13–26.5
Sisal	Leaf	1.5	65	12	9.9	350 [74]	468–640	9.4–22
Curaua	Leaf	1.4	73.6	9.9	7.5	250 [75]	500–1,150	11.8
Henequen	Leaf	1.2	60	28	8	320 [76]	372	10

interactions (fiber agglomeration) resulting from hydrogen bonding, and poor toughness and stress transfer efficiency due to poor interfacial properties. Physical and chemical methods are used to modify the surface properties of the fibers as well as polymer matrices to improve the interactions between fiber and matrix as well as dispersion of fibers in the matrix.

14.3.1 Modification of Natural Fibers

Various physical and chemical methods have been employed to modify the natural fibers [77–92]. In this section we discuss few of these methods.

14.3.1.1 Physical Methods

The physical methods of fiber modification include corona discharge and cold plasma treatments. These treatments change the surface as well as structural properties of the fiber and thus improve the mechanical bonding between fiber and matrix. Cold plasma treatment generally modifies the fiber surface through roughening by the sputtering effect. The roughened surface enhances the contact area between fiber and the matrix. Since the treatment is carried out at low gas temperature (as low as room temperature in most of the cases), the surface modification is achieved without loss of the mechanical properties of the fibers.

Plasma modification of the surface of the fibers results in the following events, in various degrees, which have profound effect on adhesion.

1. Surface cleaning that promotes adhesion and action of coupling agents
2. Etching or ablation of materials that results in rougher surface
3. Cross linking or branching of materials at the surface, which may strengthen surface layer
4. Modification of surface chemical structure and introduction of free radicals

14.3.1.2 Chemical Methods

To improve the adhesion between natural fiber and polymer matrix, chemical modification of natural fibers was investigated by a number of researchers. The mechanism and utilization of selected chemical treatments is discussed in this section. There are many different methods to improve the interfacial adhesion between fiber and matrix by modifying fiber surface such as acetylation, benzoylation, acrylation, permanganate, and isocyanate treatment. These treatments are described in detail by Kalia et al. [69].

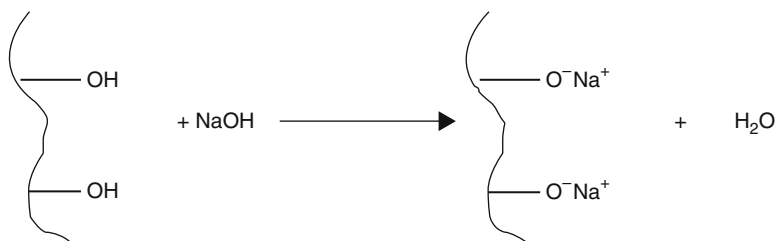
Here we discuss the alkali treatment and the silane treatment, which are the most common treatments used for fiber modification. Effect of various treatments on the mechanical properties of the polymer matrix is shown in Table 14.2.

Table 14.2 Effect of various treatments on the elastic modulus of polymer matrix

System	Treatment	Improvement in elastic modulus (%)	References
PP/cellulose	Corona	40	Belgacem et al. [78]
PE/cellulose	γ -Mercaptopropyl-trimethoxy silane	35	Abdelmouleh et al. [7]
	γ -Methacryloxypropyl-trimethoxy silane	15	
HDPE/Bamboo	Maleic anhydride	112	Han et al. [26]
LDPE/Sisal	Alkali	8	Joseph et al. [33]
	Isocyanate	32	

Alkaline Treatment

In alkali treatment, the fibers are treated with NaOH, KOH, LiOH, etc. and the following reaction takes place.



In this technique, the fiber swells and the type of the alkaline treatment and the concentration influence the degree of swelling and thus the degree of lattice transformation. It is reported that Na^+ has got a favorable diameter and is able to widen the smallest pores in between the lattice planes and able to penetrate into them. Therefore, sodium hydroxide (NaOH) treatment results in a higher amount of swelling. The alkali solution is reported to influence not only the cellulosic components inside the plant fiber but also the noncellulosic components (hemicellulose, lignin, and pectin) [69].

Silane Treatment

Silanes are coupling agents used to improve the adhesion between fibers and matrix. In silane treatment, one end group attached to silicon reacts with hydrophilic fiber and the other with matrix. Thus, it improves the degree of cross-linking in the interface region and hence leads to perfect bonding between matrix and fiber. It has been shown that alkaline pretreatment of the fibers is essential to improve the efficiency of the silane coupling agents. The hydrocarbon chains in silane groups can also influence the wettability of the fibers and thus chemical affinity toward the nonpolar polymer matrices [69].

14.3.2 Polymer Modification

14.3.2.1 Physical Methods

The effects of air or oxygen plasma on polymer films have been reported. In a comparative study with polypropylene (PP) and polyethylene (PE), higher levels of oxygen incorporation were achieved in PP than with PE. In this method, the initial step involves formation of radicals on the top of the layer of the polymer surface. These can react with each other to initiate cross linking or branching or result in surface oxidation. The use of nonthermal plasma treatment to polymer surfaces to enhance wettability and adhesion has been reported. The use of Corona discharge and dielectric discharge has also been reported for polymer modification [78].

14.3.2.2 Use of Compatibilizers

Compatibilizers are mostly functionalized polyolefins, which are incorporated to lower the interfacial tension and to improve the interfacial interactions between the polymer and the fibers. It must be noted that the inherent properties of functionalized polyolefins as described below significantly influence their effectiveness as a compatibilizer. For example the chemical structure and molecular weight affect the miscibility and entanglement with the base resin and the degree of grafting determines the level of functionality present in the compatibilizer. Thus choice of a suitable compatibilizer is an important issue in developing polyolefin composites. Maleic anhydride grafted PP (MA-g-PP) and PE (MA-g-PE) have been used widely for the compatibilization. Acrylic acid grafting is also been reported [85].

14.4 Natural Fiber Composites

14.4.1 Bast Fibers

14.4.1.1 Flax

Flax fibers are stronger, crisper, and stiffer to handle, and more easily wrinkled due to their crystalline nature. Flax fibers are about 12–16 μm in diameter. Effect of various treatments such as maleic anhydride (MAH), maleic anhydride–PP copolymer (MAPP), and vinyl trimethoxy silane (VTMOS) have been studied on flax fibers (natural flax and flax pulp) and PP composites. These composites were characterized by FTIR to study the effect of treatment and by dynamic contact angle (long fibers) and capillary rise (pulp) to determine the surface energy values. All these three treatments reduced the polar component of the surface energy of the fibers. The composites prepared with MAPP treated PP exhibited highest

mechanical properties, while the MA and VTMO treated fibers did not show enhanced values when compared with those of the untreated ones [24].

Effects of modification method (fibers and polymer matrix) on mechanical properties of short flax fiber bundle/PP composites have been reported. Modification of fibers was carried out by two different amounts of coupling agent Epolene – E43 (MA-g-PP), whereas PP matrix was modified using several amounts of maleic anhydride-polypropylene copolymer (MAPP) as compatibilizer. The effects of fiber bundle loading and the use of MAPP modification on both water sorption and mechanical properties were evaluated. Results showed that using MA-g-PP as coupling agent, the mechanical properties of composites improved and water uptake rate decreased. However, long period of water immersion resulted in drastically decreased mechanical properties. The mechanical recycling of flax fiber bundle/PP composites was also shown to be feasible [9].

The structure of the composites of PP with natural fibers such as flax and hemp was investigated. Effect of processing techniques such as injection and press molding and the size of the natural fibers was studied. The composites prepared by injection molding showed beta form (hexagonal) along with alpha (monoclinic), whereas the composites prepared by press molding PP crystallized in monoclinic form only as there were no shear forces present. The amount of beta form was found to be dependent on the content and on the type of fibers. The composites with flax fibers exhibited higher amount of beta form when compared with the composites with hemp fiber [42].

14.4.1.2 Jute

Jute fibers are long, soft, and shiny, with a length of 1–4 m and a diameter in the range of 17–20 μm . The fibers exhibit high insulating and antistatic properties, moderate moisture regain and low thermal conductivity.

Figure 14.1 shows the scanning electron micrograph of the Jute fiber and inset in figure depicts the surface structure. Figure 14.2 shows the dispersion of Jute fibers in PP matrix. Jute fibers were found to be well dispersed in the PP matrix. There are certain regions in which debonding is observed.

Effects of fiber content, matrix molecular weight, and presence or absence of matrix modifier (MAH grafted PP) were studied for short fiber reinforced injection molded jute fiber PP composites. An increase in moisture absorption was observed with increase in the fiber content and the modified PP (MA-g-PP) composites absorbed less moisture compared with unmodified PP composites. This was because of presence of MA-g-PP, which reduces number of hydrophilic fiber surface moieties. It was also observed that the moisture uptake did not deteriorate the mechanical properties of the composites at the same level of fiber content [55].

Two different approaches were used to modify the fiber surface. In the first, the jute fibers were surface treated with 1% solution of MA-g-PP dissolved in toluene at 100°C. Then the fibers were washed in Toluene and dried at 60°C. After drying, these fibers were mechanically mixed with PP and then compression molded into

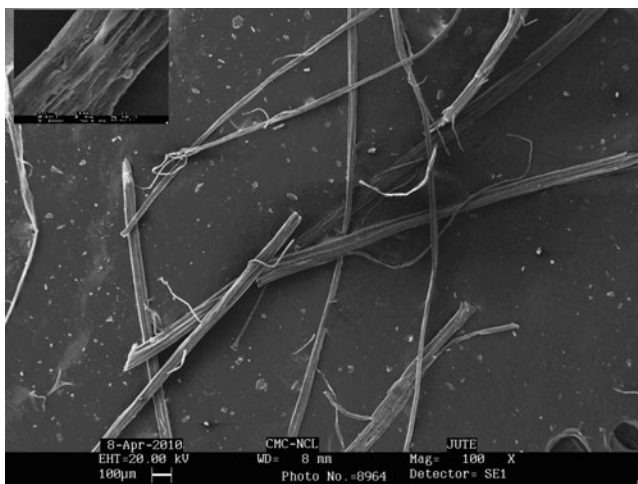


Fig. 14.1 Scanning electron micrograph for jute fiber

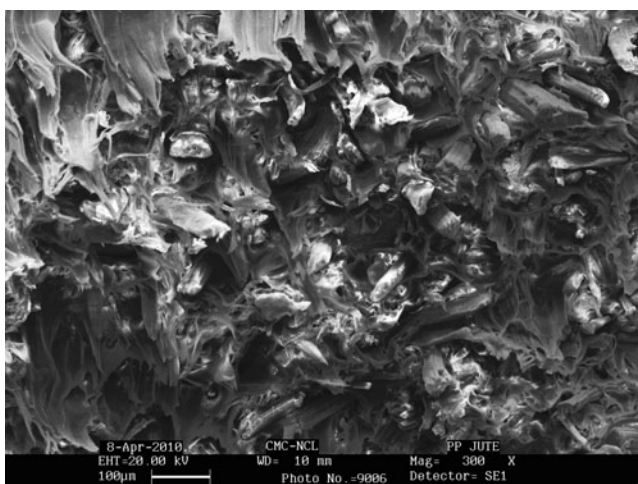


Fig. 14.2 Scanning electron micrograph for PP/jute fiber composite

sheets. In the second approach, 1 wt% MA-g-PP was added during melt mixing of jute fiber with PP at 170°C in a two roll mixer and the samples were prepared by compression molding. The use of coupling agent resulted in better wear resistance compared with unmodified fibers. It was also noted that the addition of MA-g-PP coupling agent during melt mixing gave better wear resistance when compared with the jute PP composites having MA-g-PP solution-treated jute fibers [46].

Effect of fiber treatment (untreated and alkali treated), fiber size (1, 2, and 4 mm), and fiber content (5, 10, and 15% by weight) was investigated for jute fiber composites

prepared by hot compression molding technique. The results showed that tensile strength increased with increase in the fiber size and fiber percentage; however, after a certain size and percentage, the tensile strength decreased again. No significant changes in tensile strength were observed for treated jute fiber reinforced PP composites when compared with composites with untreated fibers [50].

14.4.1.3 Hemp

Hemp fibers are obtained from the bast of the plant. These fibers exhibit natural antibacterial properties and conduct heat. Because of the low lignin content; hemp fibers are mainly used in the paper industry.

Composites of isotactic PP with Hemp fibers with various compatibilizers (PP-g-GMA, SEBS, SEBS-g-GMA) were studied. All modified composites showed improved fiber dispersion in the polyolefin matrix and higher interfacial adhesion when compared with the unmodified system (PP/Hemp) as a consequence of chemical bonding between fiber and polymer. The spherulitic morphology and crystallization behavior of PP were changed in the composites due to the nucleating effect of Hemp fibers. All composites displayed higher tensile modulus (about 2.9 GPa) and lower elongation at break compared with plain PP [41].

Interfacial evaluation of the untreated and treated Hemp fibers reinforced polypropylene-maleic anhydride polypropylene copolymer (PP/MA-g-PP) composites was investigated by micromechanical technique combined with acoustic emission (AE) and dynamic contact angle measurement. The acid–base parameter on the interfacial shear strength of the NFC was characterized by calculating the work adhesion (W_a). The effect of alkaline, silane coupling agent on natural fibers was obtained with varying MA-g-PP content in PP/MA-g-PP matrices. The surface energy was higher for alkaline treatment because of the removal of the weak boundary layers and thus increasing the surface area, whereas the surface energy of silane treated Hemp fibers was decreased because of blocked high energy sites. MA-g-PP in the PP/MA-g-PP matrix caused the surface energy to increase due to introduced acid–base sites. Microfailure modes for the composites were observed and consistent results were also shown by nondestructive AE analysis indirectly [34].

14.4.2 Leaf Fibers

14.4.2.1 Sisal

Sisal fibers are hard, strong, durable, and stretchable fibers with a diameter of 200–400 μm . These fibers do not absorb moisture easily, resist saltwater deterioration, and have a fine surface texture that accepts a wide range of dyes.

Effects of various chemical treatments such as sodium hydroxide, isocyanate, permanganate, and peroxide on the tensile properties of sisal fiber-reinforced low-density polyethylene (LDPE) composites were investigated. Sodium hydroxide treated fiber composites showed better tensile properties than untreated composites, and the enhancement was attributed to their rough surface topography and increased aspect ratio. It was reported that long chain structured cardanol derivative of toluene diisocyanate (CTDIC) treatment reduces the hydrophilic nature of the sisal fiber resulting in improved compatibility and dispersion. It was also reported that peroxide treatment of fiber showed maximum interfacial interactions [33].

Effect of ageing of Sisal fibers on the properties of PP/sisal composites was studied. Fresh Sisal fibers showed better tenacity, breaking strength, and elongation compared with the fibers aged for about 1 year, while in composites, the aged fiber composites exhibited better mechanical properties than the composites with fresh fibers. These results were explained on the basis of improved adhesion between aged fiber and matrix due to less moisture absorption in the fibers. It was also proposed that the reduced moisture content resisted the degradation of fibers resulting in better strength [44].

The effects of water immersion treatment on tensile and impact fracture of sisal fiber reinforced PP were investigated. The specimens were immersed in hot water (90°C) for various time periods. The apparent weight gain and weight loss have been reported. It was noted that the tensile modulus and strength decreased with increasing water immersion time. The impact strength improved initially with increasing immersion time until it reached to maximum value. After reaching the maximum value, impact strength decreased with increase in immersion time. This contradictory behavior of the tensile and impact properties was explained on the basis of the plasticization of the interface and the swelling of the sisal fibers [16].

14.4.2.2 Curaua

Curaua is a lignocellulosic fiber extracted from the plant *Ananus erectifilius*. The plants leaves are hard, straight, and have flat surfaces. The leaves are 4–5 cm wide and about 1 m long. It is one of the important natural fibers.

High-density polyethylene (HDPE) composites with curaua fibers were prepared using two different types of coupling agents. The thermal stability of the composites prepared with MAH grafted polyethylene affected the composite stability more significantly compared with the composites prepared using poly (ethylene-co-vinyl acetate). However, oxidation induction times (OITs) were found to be similar for composites with and without coupling agents. The results for OIT show no significant influence of the curaua fiber on the oxidative stability of the composites in comparison with pure HDPE. This was an important observation because it indicated that no further stabilization is required when producing the composites on a large scale.

It was shown that higher fiber–matrix interaction in the composites prepared using coupling agents prohibit the crystallinity enhancement caused by the fiber

while increased crystallinity due to transcrystallinity was noted for the composites without any coupling agent. The thermo-gravimetric analysis of the composites showed decreased T_{max} in comparison with that expected relative to the fiber content. A higher char residue formation was observed when using PE-g-MA as coupling agent [8].

14.4.2.3 Henequen

Henequen (*Agave fourcroydes*) fibers are hard, strong, and long similar to sisal fiber family. These fibers are obtained from long leaves of Agave plants, which are mainly used for making twines, ropes, carpets, and cordages. When compared with other natural fibers, these fibers are of relatively lower cost and density for biocomposites.

In a study of mechanical behavior of HDPE reinforced with continuous henequen fibers, the interfacial adhesion between fiber and matrix was improved by fiber surface modifications using an alkaline treatment and a matrix preimpregnation together with a silane coupling agent. The strength and stiffness of the composite was found to be dependent on the amount of silane deposited on the fiber. A maximum value for the tensile strength was obtained for a certain silane concentration but at higher concentrations, the tensile strength did not increase. The modulus of the composite did not increase with the fiber surface modification. The elastic modulus in the longitudinal fiber direction obtained from the tensile and flexural measurement was lower than the values calculated using the rule of mixtures. From the analysis of the failure surfaces, it was concluded that the failure mode changed from interfacial failure to matrix failure with increasing fiber matrix interaction [29].

In another study of Henequen fiber-PP composites prepared by compression molding technique, the fiber surface was treated (soaked) with tap water and sodium hydroxide and ultrasonicated. It was noted that the soaking and ultrasonication treatments significantly influenced the interfacial, flexural, and dynamic mechanical properties. The alkali treatment was found to be more effective than the water treatment for randomly oriented chopped Henequen-PP biocomposites. This treatment might be useful in practical applications with advantages such as low cost, environmentally benign properties, easy handling and processing [30].

14.4.2.4 Pineapple Leaf

The leaves of the pineapple plant yield strong, white fine silky fibers. Pineapple leaf fibers have a potential to form composites because they are rich in cellulose, relatively inexpensive, and available abundantly.

Melt mixing and solution mixing methods were used to prepare short pineapple leaf fiber-LDPE composites. Effects of fiber length, content, and orientation on the mechanical properties have been studied. The mechanical properties were improved while the elongation at break was found to be reduced. Longitudinally oriented composites describe better properties compared to transversely and

randomly oriented composites. It was showed that 6 mm was the optimum fiber length for the reinforcement. Authors also stated that the PALF-LDPE composites exhibited better properties compared to other cellulose fiber-LDPE composites [22].

The tensile and flexural behaviors of pineapple leaf fiber-PP composites as a function of volume fraction were investigated. The tensile modulus and tensile strength of the composites were found to increase with fiber content in accordance with the rule of mixtures. The flexural modulus and stress of the composites increased with the content of fiber but these values were lower than the reported values by other researchers. The lower values for flexural modulus and stress were ascribed to the presence of fiber-fiber interactions, voids, and dispersion level [10].

14.4.3 Seed Fibers

14.4.3.1 Cotton

The fiber is composed of about 90% cellulose and about 6% moisture and the rest as natural impurities. Each fiber is a single elongated cell that is generally flat, twisted, and has a ribbon-like structure. The fiber has a wide inner hollow. The outer surface of the fiber is covered with a protective wax like coating, giving the fiber an adhesive like quality. Cotton fiber can be easily spun into a yarn. The biodegradability, softness, absorbency, and breathability make them useful in fabrics.

The mechanical properties of PP/cotton fiber were compared with those of wood fiber composites. To improve the interfacial interaction between the hydrophilic natural fibers and the hydrophobic matrix PP, MAH grafted PP (PP-g-MAH) was used as a compatibilizer. The tensile strength of the PP/wood fiber composites decreases with increasing wt% of the wood fibers, whereas that of the PP/cotton fiber composites displays different behavior. With the addition of 10 wt% cotton fiber, the tensile strength decreases, but with the addition of 20 and 30 wt% cotton fibers it increases because of the entanglement of the cotton fibers. For the PP/wood fiber composites, the melt flow index (MI) of PP was also found to be a key factor governing the mechanical properties (tensile and flexural strengths). The use of PP-g-MAH was helpful to increase the tensile and flexural strengths of the PP/cotton fiber and PP/wood fiber composites, due to the increased interaction between the fiber and PP matrix [36].

In this study, PP and textile cotton fibers were commingled and fabricated to composite laminates. Process variables such as temperature, pressure, and holding time affect the mechanical properties such as impact strength and tear resistance. Fiber content and winding pattern or fiber orientation were also important for the optimization of the mechanical properties. The modification of the interface by chemical treatments of the matrix or reinforcement with reagents like potassium permanganate, benzoyl peroxide, and MAH modified PP enhanced some mechanical properties like tear strength of cotton fiber-reinforced PP commingled composite systems [56].

14.4.4 Wood Fiber

14.4.4.1 Bamboo

Bamboo fibers – alkaline hydrolysis and multiphase bleaching is carried out to produce starchy pulp from bamboo stems and leaves. Further chemical processes produce bamboo fibers. These fibers have strong durability, stability, and tenacity. Because of their antibacterial activity, these fibers find applications in fabrics.

Bamboo fiber–PP composites were prepared. The adhesion between fiber and matrix, MA-g-PP (MAH content was 0.5%) was used as a compatibilizer. A significant improvement was observed in the mechanical properties such as tensile modulus, tensile strength, and impact strength [15].

PP composites were prepared using bamboo as reinforcement and PP, and two maleated PP as matrices. The addition of bamboo to the PP matrices induces higher crystallization rates. It was interesting to note that a considerable amount of beta-form crystals was found along with alpha-form crystals in the composite while the pristine PP was devoid of beta-form crystals. A synergistic effect was observed as the bamboo fiber acted as reinforcement as well as beta nucleator for PP matrices. In maleated PP, the nucleation density was significantly higher than pure PP because of improved interfacial adhesion. In maleated PP composites, a trans-crystalline growth was observed on the bamboo surface [63].

HDPE/bamboo composites with different nanoclay and maleated polyethylene (MAPE) contents were fabricated by melt compounding. The compounding characteristics, clay dispersion, HDPE crystallization, and mechanical properties of the composites were studied. The X-ray diffraction (XRD) data showed that the clay was exfoliated only when 1% clay was added to pure HDPE without MAPE. For HDPE/bamboo systems, MAPE was necessary to achieve clay exfoliation. For the HDPE/bamboo fiber composites, tensile strength, bending modulus, and strength were improved with the use of MAPE; however, the use of the clay in the system led to reduced mechanical properties [27].

The rheological behavior of wood fiber (hardwood, high cellulose fiber)/polyethylene composites made of corona treated constituents was investigated. Corona treatment of one or both of the constituents resulted in decreased melt viscosities relative to compounds containing untreated materials. The reduction of melt viscosity was explained on the basis of formation of low molecular weight moieties on the surfaces of both polyethylene and cellulose during corona treatment, which acts as lubricants at interfaces. Also it was found that the corona treatment of fibers leads to higher packing volumes due to a reduction in fiber length during processing under high shear conditions. As a result, in these fibers, the normal flow pattern in the melt was perturbed to a lesser degree than the longer fibers of untreated cellulose. Both these factors contributed to the observed reduction in the melt viscosity [20].

14.4.4.2 Aspen

Aspen wood has a relatively low lignin content when compared with other pulped hardwoods, which makes the pulp easier to bleach. Typical aspen hardwood kraft pulp fibers have length 1.0–1.3 mm and width about 18–19 μm . The wall thickness is around 2–3 μm .

The mechanical properties of aspen fiber–polypropylene composites (APC) at the temperatures and humidity conditions that are typical for domestic housing applications were investigated. Variable temperature and humidity conditions were applied to see the environmental effects on the mechanical properties of APCs with two different fiber-loadings. As the fiber content increased, the tensile moduli, flexural moduli, and the flexural strength were increased while the tensile strength decreased. A slight improvement in the tensile strength was seen after addition of coupling agents [59].

Aspen fibers were incorporated into recycled HDPE with a corotating intermeshing twin-screw extruder and tensile, impact, and flexural strengths were measured as functions of fiber concentration. The composites containing untreated fibers and acetylated fibers yielded higher strength than those of heat treated fibers. The enhanced tensile strength and flexural strength of composites observed for untreated fiber when compared with those from heat-treated fibers were attributed to the better dispersion of the fibers. The presence of lignin and natural waxes facilitated the dispersion of the fibers in the nonpolar HDPE matrix. The mechanical properties and fiber length were found to be sensitive to screw configuration and compounding temperature [60].

Kokta et al. studied the effect of independent variables on mechanical properties of aspen–PP composites. The objective of the study was to protect or increase the impact strength without sacrificing the tensile strength. Additives such as MA-g-PP, dicumyl peroxide (DCP), nanoclay (NC), and aspen fibers were used. The optimum concentration of additives was determined using central composite design of Statgraphic plus to maximize both impact and tensile strength of PP. The mechanical properties of the composite were found to be decreased by the addition of DCP and NC. The impact and tensile strength was improved by adding MA-g-PP with high content of MAH grafted to fiber. It has also been shown that the modulus of the composite increased linearly with the content of fiber without any extra additives [51].

Grafting of polyethylene on the aspen fibers was carried out by radical initiation in the presence of MAH. LLDPE – aspen fiber (in the form of chemi-thermo-mechanical pulp) composites were prepared by melt mixing polymer with fiber in a roll-mill. Composites were treated by immersion in boiling water, heat exposure at 105°C for 7 days and cooling at –40°C, and the effect of these treatments on the mechanical properties was studied. These composites exhibited significant improvement in properties such as secant modulus, tensile strength, energy, and strain compared with wood flour, mica, or glass-fiber filled LLDPE. Water uptake was found to be about 0.61–3.97% (2 days to 5 weeks) for 40% fiber content. Importantly, it was noted that the dimensional stability (immersion in boiling water

for 4 h) of aspen–LLDPE composite was better than that of mica or glass fiber–LLDPE composite [37].

14.4.4.3 Cellulose Fiber

Effects of fiber length and maleated polymers on the mechanical properties and foaming behavior of cellulose fiber reinforced HDPE composites were investigated. The results of mechanical testing revealed that higher flexural and impact properties were obtained for composites with long fibers when compared with short fibers. It was also shown that the use of maleated HDPE increased the flexural strength of the composites significantly, whereas use of maleated thermoplastic elastomer increased the notched Izod impact strength. Although the composites with long and short fibers exhibited similar cell morphology in terms of average cell size and cell size distribution in extrusion foaming, the addition of maleated HDPE increased the average cell size and cell size distribution in the composites [38].

Composites based on LDPE with four different cellulose fibers were prepared and characterized for the mechanical and thermal properties as well as water absorbance behavior. Four different cellulose fibers with different average lengths were used, namely, avicel ($L = 70 \mu\text{m}$), technocel ($L = 2.5 \text{ mm}$ and $50 \mu\text{m}$), alfa fibers ($L = 500 \mu\text{m}$), and pine fibers ($L = 3.5 \text{ mm}$). Cellulose fibers were incorporated into the polymer matrix after chemical surface modification using three types of silane coupling agents, namely γ -methacryloxypropyltrimethoxy (MPS), γ mercaptoproyltrimethoxy (MRPS), and hexadecyltrimethoxy-silanes (HDS). The mechanical properties of the composites showed increase with increasing average fiber length, and the composites with MPS and MRPS treated fibers exhibited good mechanical properties. The fibers treated with HDS showed modest enhancement on composite properties, which was attributed to the inefficiency of HDS to form covalent bonding with matrix [7].

14.4.5 Fruit Fibers

14.4.5.1 Coconut

These are lignin-rich fibers with diameters ranging from 150 to 250 μm . The high lignin content results in tougher and stiffer fibers with high failure strain (15–40%) and thus are important as reinforcement for polymer matrix.

Coconut fiber possesses a thin continuous surface layer of an aliphatic compound (Waxy layer), which is reported to provide a good fiber–matrix bond and also exhibited a stronger effect on interfacial bonding. The mechanical properties of fibers were found to be better than the wax free and the C-15 long-chain alkyl molecule grafted wax-free fiber [14].

Lai et al. evaluated the suitability of coconut coir fibers to prepare fiber composites prepared by compression method. The fibers were treated using alkali, stearic acid, etc. to improve the interfacial bonding between fiber and matrix. The composites based on chemically treated fibers exhibited superior mechanical properties compared with composites prepared using untreated fibers. Authors conclude that the superior properties are due to improved adhesion and enhanced polar interactions along the fiber–matrix interface [39].

14.5 Applications

The NFC finds applications in various areas such as automotive interiors, households, ornaments, buildings, and packaging.

Automotive applications represent the best opportunity for natural fiber-filled thermoplastics due to some distinctive advantages over glass fiber composites. With the use of natural fibers, lighter composites can be prepared when compared with the glass fibers used in automobiles (vehicle weight reduces by about 40%). These are low-cost and have better crash absorbance and sound insulation [49]. The curaua fibers have almost similar properties to that of glass fibers, so that the glass fibers can be replaced by these fibers easily. A study has shown that the replacement of glass fibers by natural fibers is a small step toward the sustainability of the automobile industry [64].

There are many applications of wood fiber/plastic composites in everyday life. Wood fiber/PP composites are used in cars behind the vinyl carpeting on the doors, consoles, and seat backs. Many window and door manufacturers are looking at wood fiber/plastic composites as an alternative to solid wood in clad components.

The ballistic properties of high performance fibers such as ultra high molecular weight polyethylene (UHMWPE) and aramid and their composites are very well known. The ballistic properties of flax, hemp, and jute fabric reinforced PP composites processed by hot compression molding have also been investigated. It has been shown that flax composites exhibited better properties when compared with hemp and jute composites [48].

14.6 Conclusions

Based on the literature discussed in this chapter, it seems that surface modification of natural fibers is absolutely necessary to improve their thermal stability, dispersion in the polymer matrix, and compatibility with the polymer matrix. Physical and chemical methods reported have significantly modified the surface properties of the fibers as well as polymer matrices to improve the dispersion of the fibers and hence various properties of the polymers. Use of silane coupling agents and acetylation

are the most commonly employed surface modification techniques. However, it has also been noted that the presence of covalent bonding was necessary to obtain enhancement in the properties. It has been observed that the presence of natural waxy layer of the coconut fiber provided a good fiber/matrix bond and also exhibited a stronger effect on interfacial bonding.

The incorporation of natural fibers in polymer matrix in general results in improvement in tensile and flexural modulus as well as flexural strength. A strong interface between polymer matrix and fiber helps in increasing the flexural strength but has adverse effect on the impact strength of the composites. It is important to note that the mechanical properties of the composites not only rely upon the fiber strength but also on the interfacial adhesion (interaction) between fiber and matrix. Also the extent of enhancement in the properties is dependent on the fiber properties, its dispersion, and interfacial properties. The mechanical properties show nonlinear dependence on the fiber content and show maximum enhancement at some intermediate composition. The processing parameters also have found to influence the properties of NFC.

As reported the aged sisal fiber composites exhibited better mechanical properties than the composites with fresh fibers. Although the aging of other fibers is seldom reported, it could be of great interest to investigate the effect of aging on the properties of fibers as well as their composites.

Natural fibers also act as nucleating agents and enhance the crystallization rate of polymer as reported for PP. The fiber surface roughness of the fiber and thermal stresses were found to facilitate the growth of transcrystallinity on cotton fibers, whereas bamboo fibers induced significant amount of beta form crystals and transcrystalline growth of maleated PP.

Presently there is a huge potential market for recyclable, energy efficient, and more environmentally friendly composite materials. The utilization of natural fiber can thus lead to the reduction of waste disposal problems and environmental pollution. These NFC find applications in various engineering, electronic and automotive fields once the issues such as moisture sensitivity, compatibility, dispersion are addressed in a proper way. Green, environmentally friendly, sustainable, renewable, biodegradable, composites from natural fibers are most desired materials for future.

References

1. Baiardo M, Zini E, Scandola M (2004) Flax fibre-polyester composites. *Compos A Appl Sci Manuf* 35:703–710
2. Lee BH, Kim HJ, Yu WR (2009) Fabrication of long and discontinuous natural fiber reinforced polypropylene bio composites and their mechanical properties. *Fibers Polym* 10 (1):83–90
3. Mohanty AK, Misra M (2000) Biofibers, biodegradable polymers and biocomposites: an overview. *Macromol Mater Eng* 276/277:1–24
4. Park JM, Quang ST, Hwang BS, Devries KL (2006) In terfacial evaluation of modified jute and hemp fibers/polypropylene (PP)-maleic anhydride polypropylene copolymers

- (PP-MAPP) composites using micromechanical technique and nondestructive acoustic emission. *Compos Sci Technol* 66:2686–2899
5. Rana AK, Mandal A, Bandyopadhyay S (2003) Short jute fiber reinforced polypropylene composites: effect of compatibiliser, impact modifier and fiber loading. *Compos Sci Technol* 63:801–806
 6. Pothan C, Thomas S, Groeninckx G (2006) The role of fibre/matrix interactions on the dynamic mechanical properties of chemically modified banana fibre/polyester. *Compos A* 37:1260–1269
 7. Abdelmouleh M, Boufi S, Belgacem MN, Dufresne A (2007) Short natural-fibre reinforced polyethylene and natural rubber composites: effect of silane coupling agents and fibres loading. *Compos Sci Technol* 67:1627–1639
 8. Araujo JR, Waldman WR, De Paoli MA (2008) Thermal properties of high density polyethylene composites with natural fibres: coupling agent effect. *Polym Degrad Stab* 93:1770–1775
 9. Arbelaez A, Fernandez B, Ramos JA, Retegi A, Llano RP, Mondragon I (2005) Mechanical properties of short flax fibre bundle/polypropylene composites: influence of matrix/fibre modification, fibre content, water uptake and recycling. *Compos Sci Technol* 65:1582–1592
 10. Arib RMN, Sapuan SM, Ahmad MMHM, Paridah MT, Hairul ZHMD (2006) Mechanical properties of pineapple leaf fibre reinforced polypropylene composites. *Mater Des* 27:391–396
 11. Askargorta IA, Lampke T, Bismarck A (2003) Wetting behavior of flax fibers as reinforcement for polypropylene. *J Colloid Interf Sci* 263:580–589
 12. Barone JR, Schmidt WF, Liebner CFE (2005) Compounding and molding of polyethylene composites reinforced with keratin feather fiber. *Compos Sci Technol* 65:683–692
 13. Bengtsson M, Oksman K (2006) The use of silane technology in crosslinking polyethylene/wood flour composites. *Compos A* 37:752–765
 14. Brahmakumar M, Pavithran C, Pillai RM (2005) Coconut fibre reinforced polyethylene composites: effect of natural waxy surface layer of the fibre on fibre/matrix interfacial bonding and strength of composites. *Compos Sci Technol* 65:563–569
 15. Chen X, Qipeng G, Yongli M (1998) Bamboo fiber-reinforced polypropylene composites: a study of the mechanical properties. *J Appl Polym Sci* 69:1891–1899
 16. Chow CPL, Xing XS, Li RKY (2007) Moisture absorption studies of sisal fibre reinforced polypropylene composites. *Compos Sci Technol* 67:306–313
 17. Demir H, Atikler U, Balkose D, Tihminlioglu D (2006) The effect of fiber surface treatments on the tensile and water sorption properties of polypropylene-luffa fiber composites. *Compos A* 37:447–456
 18. Demir H, Balkose D, Ulku S (2006) Influence of surface modification of fillers and polymer on flammability and tensile behaviour of polypropylene-composites. *Polym Degrad Stab* 91:1079–1085
 19. Dominik P, Slawomir B (2005) Structure of isotactic polypropylene in composites with natural fibers obtained in various processing methods. *Fiber Text East Eur* 13(5):107–109
 20. Dong S, Sapiieha S, Schwber HP (1992) Rheological properties of corona modified cellulose/polyethylene composites. *Polym Eng Sci* 32:1734–1739
 21. Dong S, Sapiieha S, Schwber HP (1993) Mechanical properties of corona-modified cellulose/polyethylene composites. *Polym Eng Sci* 33:343–346
 22. George J, Bhacawan SS, Prabhakaran N, Thomas S (1995) Short pineapple-leaf-fiber-reinforced low-density polyethylene composites. *J Appl Polym Sci* 57: 843–854
 23. George J, Joseph K, Bhagawan SS, Thomas S (1993) Influence of short pineapple fiber on the viscoelastic properties of low-density polyethylene. *Mater Lett* 18:163–170
 24. Guillermo C, Aitor A, Rodrigo LP, Inaki M (2003) Effects of fibre treatment on wettability and mechanical behaviour of flax/polypropylene composites. *Compos Sci Technol* 63:1247–1254
 25. Han SY, Wolcott MP, Kim HS, Kim S, Kim HJ (2007) Effect of different compatibilizing agents on the mechanical properties of lignocellulosic material filled polyethylene bio-composites. *Compos Struct* 79:369–375

26. Han G, Lei Y, Wu Q, Kojima Y, Suzuki S (2008) Bamboo-fiber filled high density polyethylene composites: effect of coupling treatment and nanoclay. *J Polym Environ* 16:123–130
27. Han G, Lei Y, Wu Q et al (2008) Bamboo-fiber filled high density polyethylene composites: effect of coupling treatment and nanoclay. *J Polym Environ* 16:123–130
28. Herrera PJ, Gonzalez AV (2004) Mechanical properties of continuous natural fibre-reinforced polymer composites. *Compos A* 35:339–345
29. Herrera-Franco PJ, Valadez-Gonzalez A (2004) Mechanical properties of continuous natural fiber-reinforced polymer composites. *Compos A* 35:339–345
30. Hyun SL, Donghwan C (2008) Effect of natural fiber surface treatments on the interfacial and mechanical properties of henequen/polypropylene biocomposites. *Macromol Res* 16:411–417
31. Jose CC, Alcides LL (2000) Characterization of curaua fiber. *Mol Cyr Liq Cryst* 353:149–152
32. Joseph K, Thomas S (1996) Effect of chemical treatment on the tensile properties of short sisal fibre-reinforced polyethylene composites. *Polymer* 37:5139–5149
33. Joseph K, Thomas S, Pavithran C (1996) Effect of chemical treatment on the tensile properties of sisal-fiber reinforced polyethylene composites. *Polymer* 37(23):5139–5149
34. Joung MP, Son TQ, Byung SH, Lawrence KD (2006) Interfacial evaluation of modified jute and hemp fibers/polypropylene (PP)-maleic anhydride polypropylene copolymers (PP-MAPP) composites using micromechanical technique and nondestructive acoustic emission. *Compos Sci Technol* 66:2686–2699
35. Keener TJ, Stuart RK, Brown TK (2004) Maleated coupling agents for natural fibre composites. *Compos A* 35:357–362
36. Kim S, Moon J, Kim G et al (2008) Mechanical properties of polypropylene/natural fiber composites: comparison of wood fiber and cotton fiber. *Polym Test* 27(7):801–806
37. Kokta BV, Daneault C (1986) Use of grafted aspen fibers in thermoplastic composites:IV. Effect of extreme conditions on mechanical properties of polyethylene composites. *Polym Compos* 7:337–348
38. Kuboki T, Lee YH, Park CB, Sain M (2009) Mechanical properties and foaming behavior of cellulose fiber reinforced high-density polyethylene composites. *Polym Eng Sci* 49: 2179–2188
39. Lai CY, Sapuan SM, Ahmad M, Yahya N, Dahlan KZHM (2005) Mechanical and electrical properties of coconut coir fiber-reinforced polypropylene composites. *Polym Plast Technol Eng* 44:619–632
40. Li F, Larock R (2005) Synthesis, properties, and potential applications of novel thermosetting biopolymers from soybean and other natural oils. In: Mohanty A et al (eds) *Natural fibers, biopolymers, and biocomposites*. CRC, Boca Raton, FL, pp 727–751
41. Mariano P, Donatella C, Irene A, Zbigniew K, Ewa P (2006) Functionalization, compatibilization and properties of polypropylene composites with hemp fibres. *Compos Sci Technol* 66:2218–2230
42. Matyjas-Zgondek E, Bacciarelli A, Rybicki E, Szykowska MI, Kołodziejczyk M (2008) Antibacterial properties of silver-finished textiles. *Fiber Text East Eur* 16:101–107
43. Migneault S, Koubaa A, Erchiqui F, Chaala A, Englund K, Krause C, Wolcott M (2008) Effect of fiber length on processing and properties of extruded wood-fiber/hdpe composites. *J Appl Polym Sci* 110:1086–1092
44. Mukhopadhyay S, Srikanta R (2008) Thermal properties of high density polyethylene Composites with natural fibres: coupling agent effect. *Polym Degrad Stab* 93:2048–2051
45. Naik JB, Mishra S (2005) Studies on electrical properties of natural fiber, HDPE composites. *Polym Plast Technol Eng* 44:687–693
46. Navin C, Dwivedi UK (2006) Effect of coupling agent on abrasive wear behaviour of chopped jute fibre-reinforced polypropylene composites. *Wear* 261:1057–1063
47. Panthapulakkal S, Sain M (2007) Agro-residue reinforced high-density polyethylene composites: fiber characterization and analysis of composite properties. *Compos A* 38:1445–1454
48. Paul W, Bart V, Stepan L, Ignaas V (2007) The response of natural fiber composites to ballistic impact by fragment simulating projectiles. *Compos Struct* 77:232–240

49. Pervaiz M, Sain M (2003) Sheet-molded polyolefin natural fiber composites for automotive applications. *Macromol Mater Eng* 288(7):553–557
50. Rashed HMMA, Islam MA, Rizvi FB (2006) Effects of process parameters on tensile strength of jute fiber reinforced thermoplastic composites. *J Nav Arch Mar Eng* 3:1–6
51. Ruijun GU, Bohuslav KV (2008) Effect of independent variables on mechanical properties and maximization of aspen–polypropylene composites. *J Thermoplast Compos Mater* 21:27–50
52. Sapiaha S, Caron M, Schreiber HP (1986) Kinetics and equilibria of water sorption in LLDPE-cellulose composites. *J Appl Polym Sci* 32:5661–5663
53. Seung-H L, Siqun W, George M, Pharr M, Haitao X (2007) Evaluation of interphase properties in a cellulose fiber-reinforced polypropylene composite by nanoindentation and finite element analysis. *Compos A* 38:1517–1524
54. Singleton ACN, Baillie CA, Beaumont PWR, Peijs T (2003) On the mechanical properties, deformation and fracture of a natural fibre/recycled polymer composite. *Compos B* 34: 519–526
55. Doan TTL, Hanna B, Edith M (2007) Jute fibre/polypropylene composites II. Thermal, hydrothermal and dynamic mechanical behavior. *Compos Sci Technol* 67:2707–2714
56. Tomlal EJ, Thomas P, George K et al (2009) Impact, tear, and dielectric properties of cotton/polypropylene commingled composites. *J Reinforc Plast Compos*. doi:[10.1177/0731684409338748](https://doi.org/10.1177/0731684409338748)
57. Tomlal JE, Aju J, Mikael S, Thomas S, Kuruvilla J (2010) Thermal and crystallization behavior of cotton-polypropylene commingled composite systems. *Polym Compos* 31:1487–1494
58. Wang W, Sain M, Cooper PA (2005) Hygrothermal weathering of rice hull/HDPE composites under extreme climatic conditions. *Polym Degrad Stab* 90:540–545
59. Xue Y, Veazie DR, Glinsey C, Horstemeyer MF, Rowell RM (2007) Environmental effects on the mechanical and thermomechanical properties of aspen fiber–polypropylene composites. *Compos B* 38:152–158
60. Yam KB, Gogol K, Lai CC, Selke SE (1990) Composites from compounding wood fibers with recycled high density polyethylene. *Polym Eng Sci* 30:693–699
61. Yang HS, Wolcott MP, Kim HS, Kim S, Kim HJ (2007) Effect of different compatibilizing agents on the mechanical properties of lignocellulosic material filled polyethylene biocomposites. *Compos Struct* 79:369–375
62. Wang Y, Yeh FC, Lai SM, Chan HC, Shan HF (2003) Effectiveness of functionalized polyolefins as compatibilizers for polyethylene/wood flour composites. *Polym Eng Sci* 43:933–945
63. Yongli M, Xiaoya C, Qipeng G (1997) Bamboo fiber-reinforced polypropylene composites: crystallization and interfacial morphology. *J Appl Polym Sci* 64:1267–1273
64. Zah R, Hirschier R, Leao AL, Braun I (2007) Curaua fibers in the automobile industry a sustainability assessment. *J Clean Prod* 15:1032–1040
65. Zampaloni M, Pourboghraat F, Yankovich S, Rodgers B, Moore J, Drzal LT, Mohanty AK, Misra M (2007) Kenaf natural fiber reinforced polypropylene composites: a discussion on manufacturing problems and solutions. *Compos A* 38:1569–1580
66. Zang YH, Sapiaha S (1991) A differential scanning calorimetric characterization of the sorption and desorption of water in cellulose/linear low-density polyethylene composites. *Polymer* 32(3):489–492
67. Nabi Saheb D, Jog JP (1999) Natural fiber polymer composites: a review. *Adv Polym Technol* 18(4):351–363
68. Rials T, Wolcott M (1997) Physical and mechanical properties of agro-based fibers. In: Rowell RM et al (eds) *Paper and composites from agro-based resources*. CRC, Boca Raton, FL, pp 63–82
69. Kalia S, Kaith B, Kaur I (2009) Pretreatments of natural fibers and their application as reinforcing material in polymer composites: a review. *Polym Eng Sci* 49(7):1253–1272

70. Rosa M, Chiou B, Medeiros E, Wood D, Mattoso L, Orts W, Imam S (2009) Biodegradable composites based on starch/EVOH/glycerol blends and coconut fibers. *J Appl Polym Sci* 111:612–618
71. George J, Bhagawan SS, Thomas S (1996) Thermogravimetric and dynamic mechanical thermal analysis of pineapple fiber reinforced polyethylene composites. *J Therm Anal* 47:1121–1140
72. Susan W, Robert S, Alma H (2004) Interfacial improve ments in poly(3-hydroxybutyrate)-flax fibre composites with hydrogen bonding additives. *Compos Sci Technol* 64:1321–1330
73. Alvarez V, Rodriguez E, Vázquez A (2006) Thermal degradation and decomposition of jute/vinylester composites. *J Therm Anal Calorim* 85:383–389
74. Joseph PV, Joseph K, Thomas S, Pillai CKS, Prasad VS, Groeninckx G, Mariana S (2003) The thermal and crystallisation studies of short sisal fibre reinforced polypropylene composites. *Composites* 34:253–266
75. Claudio J, Caraschi ALL (2003) Characterization of curaua fiber. *Mol Cryst Liq Cryst* 353:149–152
76. Han Y, Han S, Cho D, Kim H (2006) Henequen unsaturated polyester biocomposites: electron beam Ir radiation treatment and alkali treatment effects on the henequen fiber. *Macromol Symp* 245–246:539–548
77. Andersson M, Tillman AM (1989) Acetylation of jute: effects on strength, rot resistance and hydrophobicity. *J Appl Polym Sci* 37:3437–3447
78. Belgacem MN, Bataille P, Sapieha S (1994) Effect of corona modification on the mechanical properties of poly propylene/cellulose. *Compos J Appl Polym Sci* 53:379–385
79. Bledzki AK, Reihmane S, Gassan J (1996) Properties and modification methods for vegetable fibers for natural fiber composites. *J Appl Polym Sci* 59:1329–1336
80. Bogoeva-Gaceva G, Avella M, Malinconico M, Buzarovska A, Grozdanov A, Gentile G, Errico M (2007) Natural fiber eco-composites. *Polym Compos* 28(1):98–107
81. Huque MM, Habibuddowla M, Mohamood AJ, Jabbar MA (1980) Graft copolymerization onto jute fiber: ceric ion-initiated graft copolymerization of methyl methacrylate. *J Polym Sci Polym Chem* 18:1447–1458
82. Liao B, Huang Y, Cong G (1997) Influence of modified wood fibers on the mechanical properties of wood fiber-reinforced polyethylene. *J Appl Polym Sci* 66:1561–1568
83. Mani P, Satyanarayan KG (1990) Effects of the surface treatments of lignocellulosic fibers on their debonding stress. *J Adhes Sci Technol* 4:17–24
84. Mannan KH, Latifa BL (1980) Effects of grafted methyl methacrylate on the microstructure of jute fibres. *Polymer* 21:777–780
85. McDowall D, Gupta B, Stannett V (1982) The ceric Ion method of grafting acrylic acid to cellulose. *ACS Symposium Series* 187, Chapter 4, pp 45–55
86. Mohanty AK, Singh BC (1987) Redox-initiated graft copolymerization onto modified jute fibers. *J Appl Polym Sci* 34:1325–1327
87. Rowell RM (1992) Opportunities for lignocellulosic materials and composites. *ACS Proc Polym Mater Sci Eng* 476:12–27
88. Sahoo PK, Samantaray HS, Samal RK (1986) Graft copolymerization with new class of acidic peroxy salts as initiators. I. Grafting of acrylamide onto cotton-cellulose using potassium monopersulfate, catalyzed by CO(II). *J Appl Polym Sci* 32:5693–5703
89. Samal RK, Ray MC (1997) Effect of chemical modification on FTIR-spectra and physico-chemical behavior of pineapple bead fibre. *J Polym Mater* 14:183–188
90. Samal RK, Samantaray HS, Samal RN (1986) Graft copolymerization with a new class of acidic peroxy salts as initiator. V. Grafting of methyl methacrylate onto jute fiber using potassium monopersulfate catalyzed by Fe(II). *J Appl Polym Sci* 37:3085–3096
91. Samal RK, Sahoo PK, Samantaray HS (1986) Graft copolymerization of cellulose, cellulose derivatives, and lignocellulose. *J Macromol Sci Rev Macromol Chem Phys* 26:81–141
92. Yap MG, Chia SLHL, Teoh SH (1990) Wood-Polymer composites from tropical hardwoods I. WPC properties. *J Wood Chem Technol* 10:1–19

Chapter 15

All-Cellulosic Based Composites

J.P. Borges, M.H. Godinho, J.L. Figueirinhas, M.N. de Pinho,
and M.N. Belgacem

Abstract The use of cellulosic fibers as load bearing constituents in composite materials has increased over the last decade due to their relative cheapness compared to conventional materials such as glass and aramid fibers, their ability to recycle, and because they compete well in terms of strength per weight of material. All-cellulosic based composites prepared from cellulose derivatives based matrices and micro-crystalline cellulosic fibers made by direct coupling between fibers and matrix present interesting mechanical and gas permeation properties, thus being potential candidates for packaging materials. Both the cellulosic matrix and the reinforcing fibers are biocompatible and widely used in the pharmaceutical industry, which is very important for the envisaged application. In addition to their biocompatibility, cellulosic systems have the ability to form both thermotropic and lyotropic chiral nematic phases, and the composites produced from the latter show improved mechanical properties due to fiber orientation induced by the anisotropic matrix. The preparation and characterization (morphological, topographical, mechanical, gas barrier properties) of all-cellulosic based composites are described in this chapter.

Keywords Cellulose fibers · Composites · Hydroxypropylcellulose · Liquid crystals

Contents

15.1	Introduction	400
15.2	All-Cellulosic Based Composites Preparation Methodology	402
15.3	Microstructural Properties	402
15.4	Mechanical Properties	408
	15.4.1 Modeling of Mechanical Properties	410
15.5	Gas Barrier Properties	415
15.6	Further Developments	418
15.7	Conclusion	419
	References	419

J.P. Borges (✉)

Departamento de Ciência dos Materiais and CENIMAT/I3N, FCT, Universidade Nova de Lisboa,
2829-516 Caparica, Portugal

e-mail: jpb@fct.unl.pt

15.1 Introduction

The important feature of composite materials is that they can be designed and tailored to meet different requirements, since the overall mechanical properties of a starting material (the matrix) can be improved by the addition of a reinforcing agent [1]. Owing to increasing environmental concerns, the use and removal of traditional polymeric composite structures, usually made of epoxy, unsaturated polyester or phenolic resins reinforced with glass, carbon, or aramid fibers has been criticized. Recently, composite materials based on cellulose and/or its derivatives have been the subject of intense research [2–12]. The reason for this resides in the renewable and biodegradable character of cellulose, and also in the fact that (a) it is abundant and inexpensive; (b) nature provides a large variety of cellulosic fibers in terms of morphology, geometry, and surface properties, depending on the source and/or separation process; and (c) in terms of specific strength, cellulosic fibers can be compared with the extensively used glass fibers. Moreover, cellulose-based composites are easy to recycle at the end of their life cycle, either by reprocessing (thermoplastic matrices) or by energy recovery (combustion of thermoset composites), which does not leave any residue since they are based on two organic components.

The major drawback of cellulose fibers in the present context resides in their highly polar and hydrophilic character, which make them both poorly compatible with commonly used non-polar matrices, such as polyolefins, and subject to loss of mechanical properties upon atmospheric moisture absorption. That is why they should be submitted to specific surface modifications in order to obtain an efficient hydrophobic barrier and to minimize their interfacial energy with the often non-polar polymer matrix, and thus generate optimum adhesion. Further improvement of this interfacial strength, which is a basic requirement for the optimized mechanical performance of any composite, is attained by chain entanglement between the matrix macromolecules and the long chains appended to the fiber surface (brushes) or, better still, by the establishment of a continuity of covalent bonds at the interface between the two components of the composite.

Several fiber treatments are reported in literature [9], namely (a) physical treatments, such as solvent extraction; (b) physico-chemical treatments, like the use of corona and plasma discharges or laser, γ -ray and UV bombardment and (c) chemical modifications, both by the direct condensation of the coupling agents onto the cellulose surface and by various grafting strategies calling upon polycondensations and free-radical or ionic polymerizations.

Another approach to enhance interfacial bonding was proposed by Borges et al. [10], and deals with the direct coupling between the matrix and the reinforcing fibers. The elaboration of the composite is based on using a cellulose derivative based matrix and diisocyanates as coupling agents. To the best of our knowledge, this was the first attempt to the production of all-cellulosic based composites. These soft materials (sub-ambient glass transition temperature) are insoluble, meaning that the isocyanates also promote a cross-linking reaction between the anhydroglucose units of the matrix (see Fig. 15.1) [13]. These properties along with mechanical and

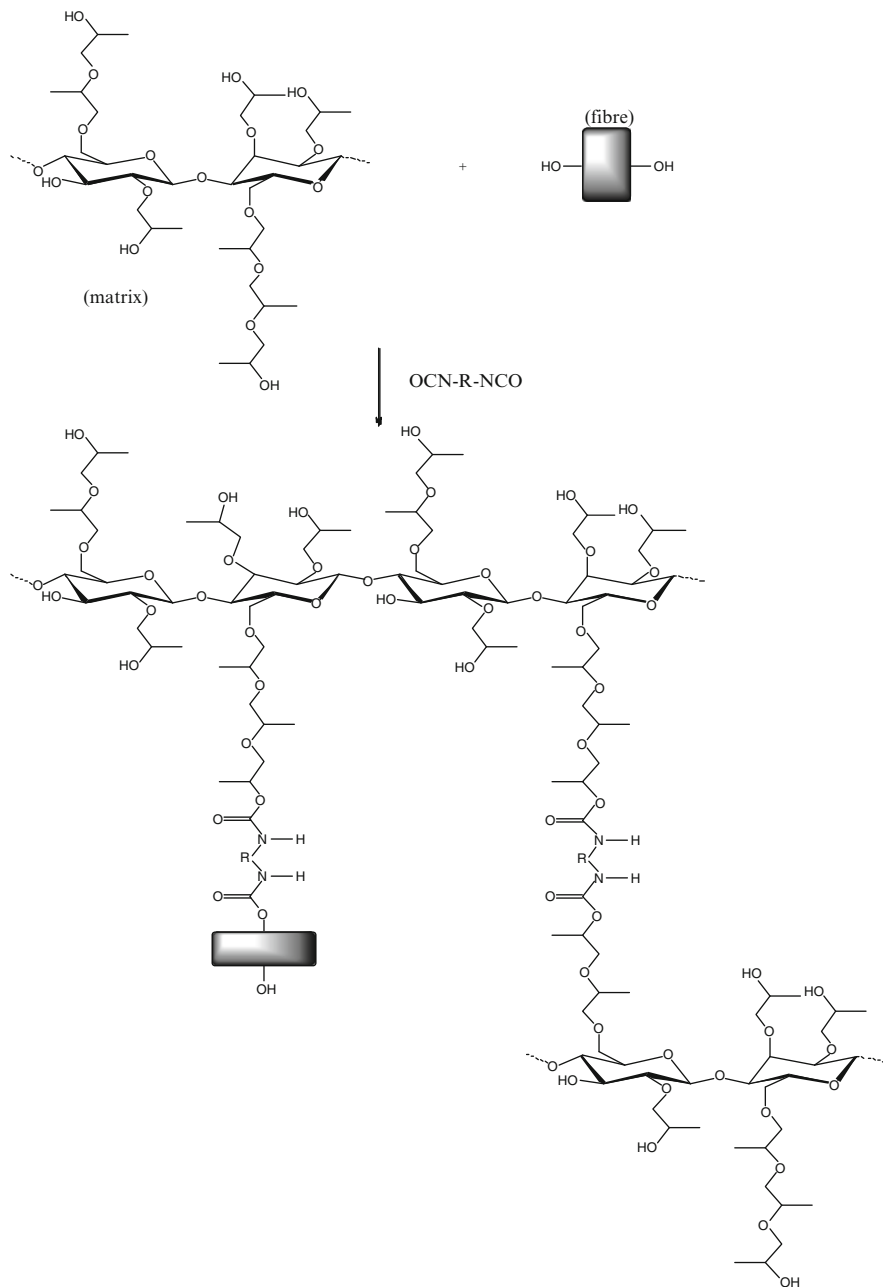


Fig. 15.1 Schematics of competitive chemical bonds promoted by diisocyanates in all-cellulosic based composites. Chemical coupling between fibers and matrix and cross-linking between anhydroglucose units of the matrix are shown. R refers to an aliphatic or aromatic group. The matrix is hydroxypropylcellulose (HPC)

gas barrier properties, which are analyzed in this chapter, make these materials suitable for packaging applications.

The designation “all-cellulosic based composites” is used throughout this chapter that focuses on the production and characterization of these materials.

15.2 All-Cellulosic Based Composites Preparation Methodology

An ester of cellulose, the hydroxypropylcellulose (HPC), was chosen among the several cellulosic derivatives which can be used as matrix materials. HPC is readily available, inexpensive and soluble in a wide variety of common organic solvents. As reinforcement, Avicel fibers ($l = 30 \mu\text{m}$ and $l/d = 5$) were used. Cross-linking was achieved using several aliphatic or aromatic diisocyanates [13]. It is worth mention that general trends concerning the mechanical and gas barrier properties were similar for all cross-linked composites, and for that reason we refer to those that have been cross-linked with 1,4-butyldiisocyanate (BDI).

The all-cellulosic based composites were prepared in the form of dense films (thickness: 20–60 μm). Clear composite films were obtained either from isotropic or liquid crystalline solutions of HPC (chiral nematic) by a casting method.

Isotropic solutions of HPC (10–12% wt HPC) were prepared by mixing acetone with HPC at room temperature. Avicel fibers were added (0, 2, 4, 10, 15, 20 and 30% w/w HPC) to these solutions and the mixture was left to homogenize, by magnetic stirring, for 24 h. Two sets of isotropic composite films were obtained from these solutions. In the first set, the films were cast and sheared over a teflon substrate with a knife edge moving at a calibrated speed. In the second set, the cross-linked films were obtained by first promoting the reaction of BDI (7% w/w HPC) under nitrogen atmosphere with HPC-Avicel. After the cross-linking the films were obtained as described above.

Anisotropic solutions of HPC (60% wt HPC) were prepared by mixing *N,N*-dimethylacetamide (DMAc) with HPC at room temperature. Avicel fibers were added (0, 2, 4, 6, 10 and 12% w/w HPC) to these solutions and the mixture was left to homogenize, by mechanical stirring, for 24 h. Anisotropic composite films were obtained by the above mentioned method. In this case cross-linked films were not produced.

15.3 Microstructural Properties

Microstructural evaluation of the composite films was accomplished using two different microscopy techniques: POM and AFM. These two techniques gave information at different levels about the texture (morphology), uniformity and topography of the composites. Birefringence measurements and SALS gave complementary information about the degree of molecular orientation in the matrix and fiber orientation in the composites, respectively.

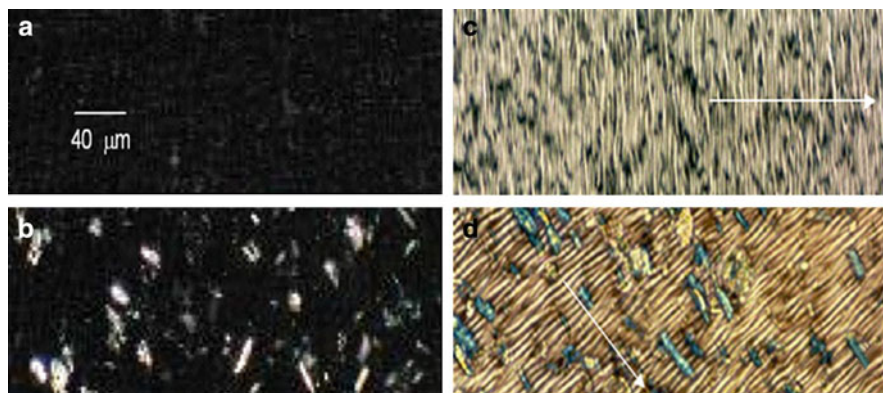


Fig. 15.2 POM photographs of isotropic (b) and anisotropic (d) all-cellulosic based composites with 4% w/w HPC of Avicel fibers [birefringent rods in images (b) and (d), respectively]. Images (a) and (c) are the POM photographs of the isotropic (a) and anisotropic (c) HPC matrix. *White arrows* in images (c) and (d) indicate the shear direction. All images were taken under crossed polars. Images were obtained from references [12] (a and b) and [14] (c and d)

POM images (taken on an Olympus BH2 microscope) of isotropic and anisotropic all-cellulosic based composites are shown in Fig. 15.2.

POM shows that solid films cast from 10 to 12% wt HPC are isotropic (Fig. 15.2a) (dark field under crossed polars). In contrast, solid films cast from a chiral nematic solution of HPC (60% HPC/40% DMAc, w/w) are clearly birefringent (anisotropic) and present a characteristic banded texture perpendicular to the shear direction, observed for thermotropic and lyotropic liquid crystalline phases of HPC after shear.

The formation of banded textures in thin-film samples of solutions of liquid crystalline polymers (LCPs), subjected to shear, has been reported in the literature since 1979 [15]. Because of the symmetrical properties of the liquid crystal solutions, large domains of well-oriented polymer chains are formed during shear flow, while defects are squeezed into small regions. The shear accounts for an additional energy stored in the solution. When the shear is stopped, the system will first relax with a characteristic time t_b to a transient state. In this state the distortion energy is minimized, and the orientational order is kept, resulting in a banded structure.

This behavior is observed only if two conditions are fulfilled [16]:

1. If the shear rate, $\dot{\gamma}$, is higher than a critical shear rate, $\dot{\gamma}^c$, with $\dot{\gamma}^c$ being strongly dependent on the molecular weight, M , of the polymer and slightly sensitive to the polymer concentration, C , according to the relation $\dot{\gamma}^c \propto C^{-1}M^{-7} \log M$.
2. If the shearing time, t_s , is longer than a critical time, that depends on the shear rate. This means that there is a minimum deformation, γ^c , below which the periodic structure was not observed. The general dependency of the band formation time, t_b , on the experimental parameters is known [16] (e.g., in the first approximation $t_b \sim t_s^{-2}$, t_b increases with the molecular weight M), but no analytical expression was yet deduced, due to the complexity of the dynamic behavior of LCPs under shear.

Band structure may be characterized by the band spacing (typically 4–10 μm) [17] and is energetically very stable, but it only persists during a characteristic time t_d (typically $t_d \sim 10$ min). The thermal agitation may be sufficient for the system to overcome the energy barrier between the band texture (local minimum) and the nondistorted state (overall minimum). The bands begin to lose their parallel orientation; they form elongated domains and finally collapse, giving rise to an equilibrium texture near the undeformed state. As expected, the time t_d is found to be strongly dependent [16] on the molecular weight (t_d increases with increasing M) and on the shear rate (t_d increases with increasing $\dot{\gamma}$).

The HPC lyotropic solutions are, regarding the ability to form band texture, among the most studied systems and thoroughly described in the literature [16, 18]. The formed periodic structures can be locked within the polymer after the solvent evaporation, if the evaporation time is shorter than the relaxation time t_d , and the topography can be tuned by control of the processing conditions [19]. In the case of the anisotropic all-cellulosic based composites this was attained due to the small thickness of the films (20–60 μm).

Another interesting feature of these anisotropic composites is their ability to orient the fibers (see Fig. 15.2d) in contrast to isotropic homologues, where no overall orientation of the fibers is achieved (see Fig. 15.2b), which means that this orientation is due to a competition between the alignment promoted by the matrix and the shear.

Fiber alignment in short fiber composites (SFCs) is very difficult to achieve, however the results obtained with anisotropic all-cellulosic based composites point out for a simple and new way of producing fiber aligned SFCs with enhanced mechanical properties, as discussed later on.

Small angle light scattering and birefringence experiments showed a direct correlation between the director alignment in the anisotropic matrix and the orientation of the cellulosic fibers in these composites.

From SALS patterns an order parameter, $S = \frac{1}{2} \langle 3\cos^2\theta - 1 \rangle$, was determined. This parameter gives the degree of orientation of the fibers in the composites. It is expressed as the average ($\langle \rangle$) of the second Legendre polynomial of the cosine function of the angle in between the fibers axes and the shear direction (θ). The order parameter is 0 for a random orientation of the fibers and 1 for its total alignment with the shear direction.

Figure 15.3 presents the variation of the order parameter as a function of HPC concentration in the precursor solutions for the composites made with 2% w/w HPC of Avicel fibers. Similar trends are observed for other fiber contents.

As expected, results in Fig. 15.3 show that significant fiber orientation is only achieved when the matrix is anisotropic. Similar conclusions can be drawn from birefringence measurements (made by the compensation method, using a Berek compensator) on composite films, as shown in Fig. 15.4. The birefringence is a measure of the degree of order of the matrix and therefore the good agreement between these data and those obtained from SALS (S) reveal the excellent compatibility between the matrix and the fibers, which results from a similarity between the chemical structure of both components of the composites.

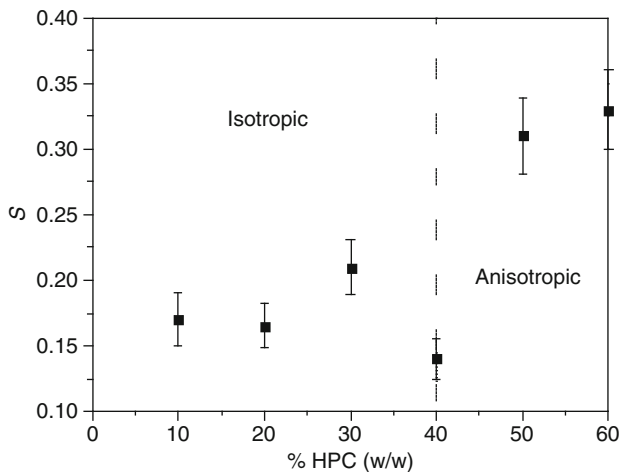


Fig. 15.3 Plot of the order parameter, S , for all-cellulosic based composites (2% w/w HPC of Avicel fibers), as a function of the HPC content. Isotropic and anisotropic composites are marked [13]

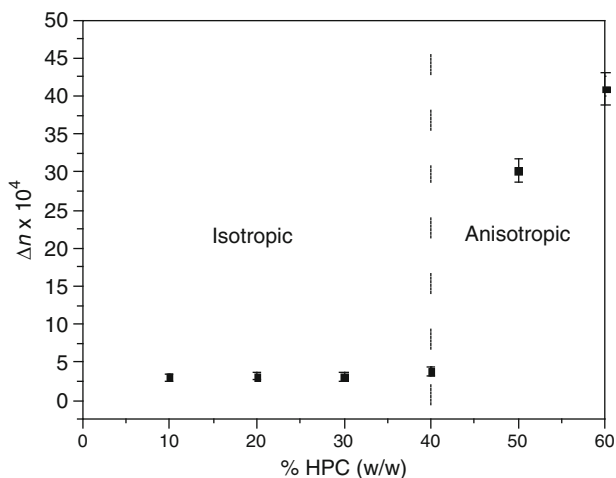


Fig. 15.4 Variation of the birefringence, Δn , of all-cellulosic based composites (2% w/w HPC of Avicel fibers) with the HPC content. Isotropic and anisotropic composites are marked [13]

The surface topography of the films was analyzed using an atomic force microscope from Digital Instruments, Multimode Scanning Probe Microscope with a Nanoscope IIIa Controller. The film surface was scanned in intermediate contact (tapping mode) with an oscillating tip. This eliminates shear forces, which can damage soft samples and reduce the image resolution. At first the tip is far from the sample surface, bouncing up and down with “free vibration” amplitude. The tip then approaches the

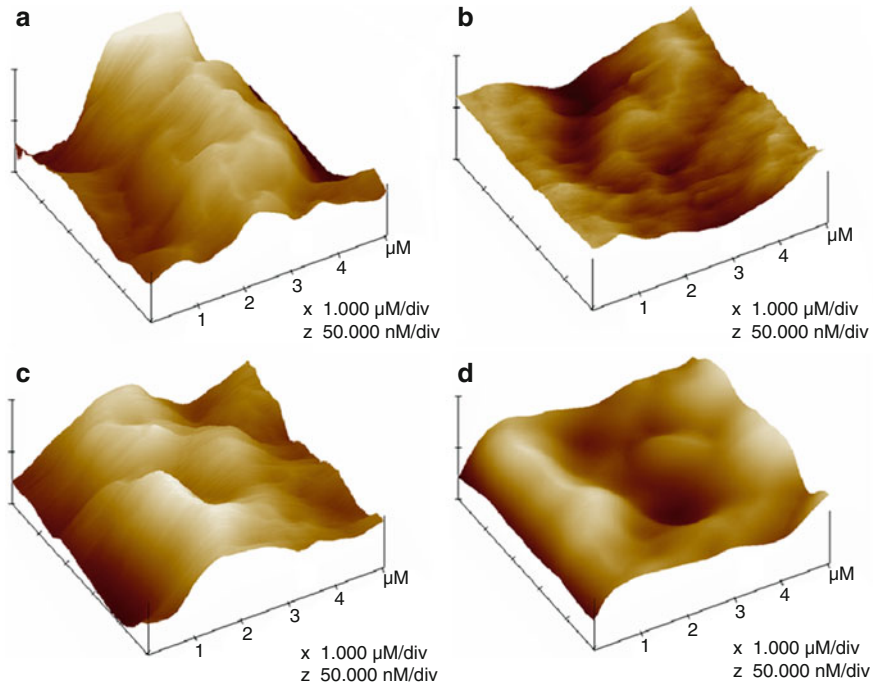


Fig. 15.5 Typical AFM images of uncross-linked (**a** and **b**) and cross-linked (**c** and **d**) isotropic composites with 10% w/w HPC of Avicel fibers: **a** and **c** – bottom surface; **b** and **d** – top surface [12]

sample surface, and because of the tip–surface interaction, the vibration amplitude decreases. During the scanning procedure the vibration amplitude of the tip is kept constant by changing the scanner’s height.

Small pieces were cut from each film, glued onto metal discs and attached to a magnetic sample holder located on top of the scanner tube. All the AFM images were taken at 25°C. Typical AFM images are presented in Fig. 15.5. Images of the surfaces of cross-linked and uncross-linked isotropic composite films with 10% (w/w HPC) of fibers are presented, as an example.

Differences in the film-surface morphologies can be expressed in terms of various roughness parameters, such as:

1. The difference between the highest and the lowest points within the given area, z
2. The standard deviation of the z values within the given area (R_q). This parameter is calculated as

$$R_q = \sqrt{\frac{\sum (Z_i - Z_{\text{avg}})^2}{N_p}}, \quad (15.1)$$

where Z_i is the current z value, Z_{avg} the average of the z values within the given area and N_p the number of points within the given area.

3. The mean roughness (R_a). This parameter represents the mean value of the surface relative to the center plane, that is, the plane for which the volumes enclosed by the image above and below this plane are equal. It is calculated as

$$R_a = \frac{1}{L_x L_y} \int_0^{L_x} \int_0^{L_y} |f(x, y)| \, dx dy, \quad (15.2)$$

where $f(x, y)$ defines the surface relative to the center plane and L_x and L_y the dimensions of the surface in the x and y directions.

The surface roughness parameters were calculated from the AFM images obtained at several points of each film sample by using an AFM software program.

The roughness parameters depend on the curvature and size of the tip, as well as on the treatment of the captured surface data (plane fitting, flattening, etc.). Therefore, these parameters should not be considered as absolute roughness values. However, in the present study the same tip was used for all films and all captured surfaces were treated in the same way. Tables 15.1 and 15.2 display the roughness parameters calculated from the respective AFM images of both surfaces (top and

Table 15.1 Roughness parameters calculated from the respective AFM images of the uncross-linked isotropic all-cellulosic based composites [12]

Fiber content (% w/w HPC)	Surface	R_q (nm)	z (nm)	R_q (nm)
0	Top	4.70	37.04	5.80
	Bottom	4.99	34.55	7.91
4	Top	3.4	28.76	4.28
	Bottom	14.96	108.1	18.5
10	Top	4.86	43.96	6.24
	Bottom	18.77	167.09	23.59
20	Top	4.50	38.77	5.74
	Bottom	17.19	122.73	20.87
30	Top	9.27	83.86	11.83
	Bottom	22.89	149.99	27.05

Table 15.2 Roughness parameters calculated from the respective AFM images of the cross-linked isotropic all-cellulosic based composites [12]

Fiber content (% w/w HPC)	Surface	R_a (nm)	z (nm)	R_q (nm)
0	Top	1.97	16.52	2.56
	Bottom	2.24	17.95	2.82
4	Top	4.64	48.57	6.06
	Bottom	15.09	119.57	18.59
10	Top	7.85	72.29	10.06
	Bottom	12.04	86.20	15.07
20	Top	9.48	79.48	12.01
	Bottom	18.10	144.81	23.47
30	Top	12.17	132.32	15.63
	Bottom	17.48	199.73	22.96

bottom) of some of the uncross-linked and cross-linked isotropic composites produced.

As seen from Fig. 15.5, all-cellulosic based composites are asymmetric. Bottom surface has a more pronounced roughness, as evidenced by the results presented in Tables 15.1 and 15.2.

The films without fibers have very low values of the parameters R_a and z , revealing relatively uniform structures of the top and bottom surfaces of both uncross-linked and cross-linked films. The very slight differences between the two surfaces can be attributed to the different natures of the air-casting solution and of the Teflon[®] plate-casting solution interfaces. In contrast to that, the films incorporating fibers display very different values of the roughness parameters for the top and bottom surfaces. In fact, for the uncross-linked composite films the R_a parameter of the bottom surface is nearly four times higher than the corresponding value of the top surface. This is valid up to 20% w/w HPC of fiber incorporation. For 30% w/w HPC of fibers the R_a value of the bottom surface is approximately twice the value of the top surface. These results lead to the conclusion that the fibers are probably preferentially distributed at the bottom of the films.

In the case of the cross-linked composite films, R_a and z parameters of both surfaces of the films seem to increase gradually with the increase of the fiber content, with the bottom surfaces showing always higher values than those of the corresponding top surfaces.

In the cross-linked films, the difference between the roughness parameters of the two surfaces is smaller than that observed in the case of the uncross-linked ones, as shown also in Fig. 15.5. This means that the effect of fiber settling at the bottom surfaces is less pronounced for the cross-linked films, suggesting a better distribution of the fibers over the cross section. This influences the mechanical properties of isotropic all-cellulosic based composites, as discussed later. Also, the asymmetry between top and bottom surfaces will have an impact in gas barrier properties of these composites.

15.4 Mechanical Properties

The mechanical properties (Young's modulus, E , yield stress, σ_y , tensile stress, σ_u , tensile strain, ε_u) of the films were determined using a tensile testing machine from Rheometric Scientific (Minimat-Firmware 3.1). For each composition, three films were obtained and ten samples of 5×2 cm were cut from each film and stretched uniaxially at a speed of 5 mm min^{-1} at room temperature. Half of the samples were cut in the shear direction (0°) and the rest perpendicularly to it (90°). Therefore, 30 samples (15 in each direction) of each composition were tested in order to take into account the inherent variability of these systems. All the parameters were calculated for a 95% confidence interval for the mean.

Mechanical parameters of isotropic all-cellulosic based composites are invariant regardless of the direction of measurement (0° or 90°). It has been shown [12] that

the inclusion of fibers in a HPC matrix produces composites with superior mechanical properties, which can be improved by cross-linking. Mechanical data seem to indicate that the elastic deformation of the isotropic cross-linked composites is predominantly dominated by the fiber content, while the cross-linking affects mainly the plastic deformation.

Mechanical properties of anisotropic all-cellulosic based composites are presented in Table 15.3.

In all cases the composite films were found to be more resistant in the shear direction and consequently less deformable. The high anisotropy of the mechanical properties is evident from the results of Table 15.3, where it can be seen that Young's modulus, yield stress and ultimate tensile strength are higher in the shear direction.

For comparison, Table 15.4 presents the mechanical properties of anisotropic and uncross-linked isotropic all-cellulosic based composites.

Table 15.4 clearly shows that anisotropic composite films present better mechanical properties. It is worth noting that anisotropic composites also have higher Young's modulus, yield stress and ultimate tensile strength than cross-linked isotropic homologues [13]. This, along with results presented in Table 15.4, seems to indicate that the mechanical properties of these all-cellulosic based composites depend on matrix anisotropy and fiber orientation rather than on cross-linking.

In fact, due to the same chemical nature of fibers and matrix, an efficient matrix-fiber stress transfer will probably be ensured by hydrogen bonds between the two components.

Table 15.3 Mechanical properties of anisotropic all-cellulosic based composite films, measured in the shear direction (0°) and perpendicular to it (90°)

Fiber content (% w/w HPC)	E (MPa)		σ_y (MPa)		σ_u (MPa)		ϵ_u (%)	
	0°	90°	0°	90°	0°	90°	0°	90°
0	274	130	7.7	4.1	12.8	5.1	28.0	54.0
2	350	150	9.3	6.2	14.0	7.9	14.0	40.4
4	431	160	9.9	6.6	18.0	7.5	16.0	35.6
6	470	214	12.7	6.2	28.7	9.1	15.5	20.0
10	481	240	12.0	7.8	19.7	10.4	17.0	16.6
12	441	193	12.4	7.9	19.1	10.0	18.0	15.5

Presented results are average values with an error of about 10% [14]

Table 15.4 Comparison of the mechanical properties of uncross-linked isotropic (I) and anisotropic (A) all-cellulosic based composite films

Fiber content (% w/w HPC)	E (MPa)		σ_y (MPa)		σ_u (MPa)	
	I	A	I	A	I	A
0	109	274	3.5	7.7	5.2	12.8
2	145	350	4.8	9.3	5.9	14.0
4	155	431	5.3	9.9	6.4	18.0
6	–	470	–	12.7	–	28.7
10	213	481	6.1	12.0	8.1	19.7
12	–	441	–	12.4	–	19.1

Presented results are average values obtained in the shear direction with an error of about 10% [14]

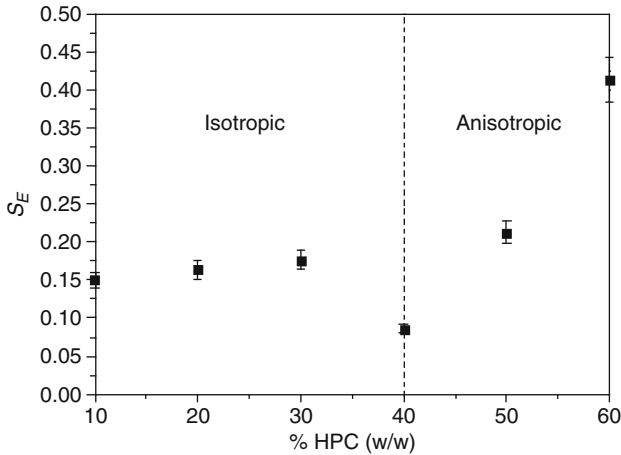


Fig. 15.6 Plot of the order parameter, S , of all-cellulosic based composites (2% w/w HPC of Avicel fibers), as a function of HPC content. Isotropic and anisotropic composites are marked [13]

From the mechanical properties of all-cellulosic based composites, an order parameter, S_E , was calculated using (15.3) [20]:

$$S_E = \frac{((E_{0^\circ}/E_{90^\circ}) - 1)}{((E_{0^\circ}/E_{90^\circ}) + 2)} \quad (15.3)$$

The variation of S_E with HPC concentration in the precursor solutions for composites preparation is shown in Fig. 15.6. Results presented refer to composites with 2% w/w HPC of Avicel fibers, but similar trends are observed for the other fiber contents.

This order parameter is a macroscopic measure of the anisotropy of the composites but it, nevertheless, reflects the microstructural organization of the all-cellulosic based composites. The variation of S_E with HPC content is similar to that observed for S (Fig. 15.3) and Δn (Fig. 15.4). Table 15.3 (and also Fig. 15.2c) shows that HPC matrix (0% w/w HPC of fibers) is clearly anisotropic and therefore the anisotropy in these composites arises from the synergy between the liquid crystalline character of the matrix and the fiber orientation.

15.4.1 Modeling of Mechanical Properties

In this section the mechanical properties (Young's modulus) and the strength of the fiber–matrix interface (quality of the interface) of isotropic all-cellulosic based composites will be analyzed using theoretical models existing in literature. For the anisotropic composites such an approach was not performed. The anisotropy in these composites arises mainly from the liquid crystalline character of the matrix,

which in turn induces fiber orientation. Liquid crystalline materials have complex structure and dynamics and there are no available theoretical models for composites with this kind of matrices.

Two theoretical models were used to predict Young's modulus of isotropic all-cellulosic based composites:

1. Cox "shear-lag" model [21] that takes into account the geometrical arrangement of the fibers.
2. Modified Halpin–Tsai equations [22, 23], which are dependent on fiber packing efficiency.

When SFCs are stressed, the stresses are transferred to the fibers by shear at the fibers surface, which causes fiber deformation. To estimate the Young's modulus of SFCs, Cox [21] proposed a model that assumes a completely elastic transfer of stresses from the matrix to the fiber. By averaging the stress distribution within the fibers, the theory predicts the Young's modulus for aligned SFCs, in the direction of alignment, to be equal to:

$$E = \chi_2 v_f E_f + (1 - v_f) E_m, \quad (15.4)$$

where v_f refers to the volume fraction of fibers; E_f and E_m to the Young's modulus of fibers and matrix, respectively. The parameter χ_2 is a fiber-length correction factor that depends on fiber aspect ratio, fiber packing (center-to-center distance), matrix shear modulus and fibers' Young modulus. When the fiber length is not uniform (as in the case of isotropic all-cellulosic based composites) χ_2 can be obtained as a weighted sum, with the weights determined by the fiber-length distribution [24].

When fibers are not perfectly aligned with the direction of the modulus estimate, an orientation-efficiency factor, χ_1 , is added to (15.4) [25] and Young's modulus will be then deduced from (15.5).

$$E = \chi_1 \chi_2 v_f E_f + (1 - v_f) E_m, \quad 0 < \chi_1 < 1 \quad (15.5)$$

The orientation-efficiency factor was theoretically determined by Krenchel [26]. For in-plane uniformly distributed fiber orientations, the factor is 3/8 and for 3D uniform fiber orientation distribution is 1/5. In practice, the determination of fiber orientation distribution is normally done by image analysis of different sections of the composites [27]. In the case of all-cellulosic based composites this would be impossible, due to their thickness. In this case, the value of the orientation-efficiency factor was taken as the value of the order parameter, S , determined by SALS.

The most used materials property model, particularly in engineering design applications, is the Halpin–Tsai model [28] or Halpin–Tsai equations as they are often termed. Although the model has limitations with respect to its rigor and accuracy, its main advantage is the simple universal form of expressions in its formulation, and its applicability to a number of different material forms and their *moduli*. The general form of Halpin–Tsai equations is given by:

$$\frac{M}{M_m} = \frac{1 + ABv_f}{1 - Bv_f} \wedge B = \frac{(M_f/M_m) - 1}{(M_f/M_m) + A}, \tag{15.6}$$

where M is the composite modulus (plane strain bulk modulus, longitudinal and transverse shear modulus or longitudinal and transverse Young modulus), M_f the corresponding fiber modulus and M_m the corresponding matrix modulus. A is a measure of the reinforcement geometry and loading and for longitudinal Young’s Modulus and it will take the value of $2l/d$ (l/d is the fiber aspect ratio, which for Avicel fibers as the value of 5). Halpin–Tsai equations have been found to be inaccurate at higher volume fraction of fibers, because it does not take into account the limit in maximum packing fraction in a real system. The problem was addressed by Nielsen [22] who produced the amended form of the generalized equation, presented in expression (15.7).

$$\frac{M}{M_m} = \frac{1 + ABv_f}{1 - B\psi v_f} \wedge \psi = \frac{1 - \phi_m}{\phi_m^2} v_f \tag{15.7}$$

The introduction of the parameter ψ takes into account the maximum packing fraction ϕ_m . For cubic packing $\phi_m = 0.785$, whilst for hexagonal packing $\phi_m = 0.907$ [23]. For SFCs, where fibers are generally more random in their arrangement, ϕ_m can take significantly lower values. Because of the uncertainty of the maximum packing fraction and its dependence on both alignment and aspect ratio, ϕ_m is used as an empirical fitting factor in the materials modeling process.

The results of Young’s modulus prediction, according to (15.5) and (15.7), for uncross-linked isotropic all-cellulosic based composites are presented in Figs. 15.7 and 15.8. The modeling parameters used for (15.5) are listed in Table 15.5.

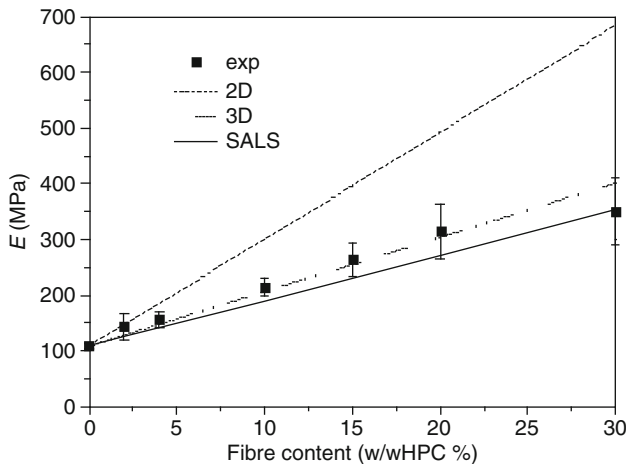


Fig. 15.7 Variation of the Young’s modulus of uncross-linked isotropic all-cellulosic based composites with fiber content. Experimental values (exp) are compared to those obtained from (15.5) using different values of χ_1 as explained in Table 15.5

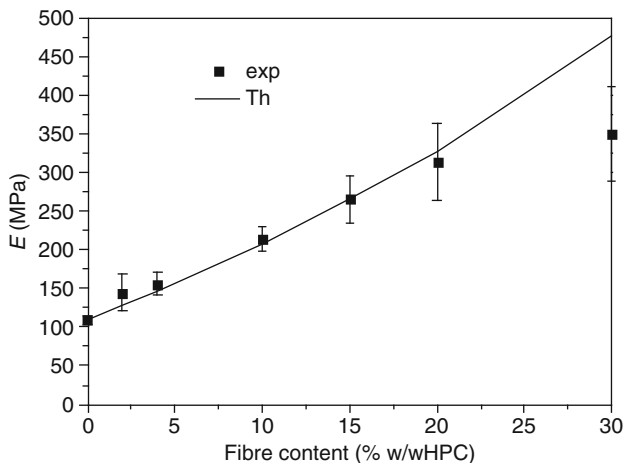


Fig. 15.8 Variation of the Young’s modulus of uncross-linked isotropic all-cellulosic based composites with fiber content. Experimental values (exp) are compared to theoretical predictions (Th) obtained from (15.7). Note that fiber content is presented in wt% but all calculations were made using the volume fraction of fibers [13]

Table 15.5 Fitting parameters used in (15.5) [13]

Fitting parameters	Observations
$E_f = 25 \text{ GPa}$	Value of E_f from [29]
$E_m = 109 \text{ MPa}$	Values of the orientation efficiency factor, χ_1 , are given for (a) in-plane fiber orientation (2D) [26], (b) 3D uniform fiber orientation (3D) and (c) fiber orientation parameter determined by light scattering (SALS)
$\chi_2 = 0.23$	
$\chi_1 = \begin{cases} 0.375 & \text{(2D)} \\ 0.20 & \text{(3D)} \\ 0.17 & \text{(SALS)} \end{cases}$	

Figure 15.7 displays the dependence between the Young’s modulus of uncross-linked isotropic composites and their fiber content and shows that an in-plane distribution of the fibers in the composites is highly improbable. The same conclusion was drawn from the fit of the experimental data of the cross-linked composites. The predicted values of the Young’s modulus for a 3D uniform distribution of the fibers are closer to that of the average values determined experimentally. Avicel fibers are not perfect rod objects (low aspect ratio: $l/d \sim 5$), being this the probable justification for a preferred 3D arrangement.

Results obtained using the order parameter determined by SALS, as the value of the orientation efficiency factor, are always closer to the lower bound values of the Young’s modulus of the composites. The order parameter is determined as a function of the angle of the fibers to the shear direction, meaning that its value will be more accurate for an in-plane distribution of the fibers. This would probably be the case if the fibers had higher aspect ratio. Nevertheless, SALS seems to be a promising

technique in order to determine the orientation efficiency parameter for composite systems like these, i.e., thin composite materials.

The fit of the Young's modulus experimental values using (15.7) allowed the determination of the maximum packing fraction of fibers, ϕ_m . The results of this fit for the uncross-linked composites are presented, as an example, in Fig. 15.8. From the fits, values of 0.81 and 0.51 for ϕ_m were obtained for uncross-linked and cross-linked isotropic all-cellulosic based composites, respectively.

High values of ϕ_m for the uncross-linked composites may be related to the preferred 3D packing of the fibers. Lower value of the maximum packing fraction in cross-linked composites confirms the more uniform distribution of the fibers over its cross section, as deduced from AFM measurements. The more efficient packing of the fibers in cross-linked composites is most probably the main reason for the better mechanical performance of these materials.

The second reason for the better mechanical properties of cross-linked composites is the higher quality of the fiber–matrix interface which improves the stress transfer efficiency between these two components.

The strength of the interaction was quantitatively characterized for isotropic uncross-linked and cross-linked all-cellulosic based composites with the help of a semi-empirical model taken from literature [30, 31].

The model describes the composition dependence of tensile yield stress or tensile strength of particulate filled polymers. The expression for yield stress takes the form:

$$\sigma_y = \sigma_{y0} \frac{1 - v_f}{1 + 2.5v_f} \exp(Bv_f), \quad (15.8)$$

where σ_y and σ_{y0} are the yield stresses of the composite and that of the polymer matrix, respectively, v_f is the volume fraction of the filler in the composite and B the parameter characterizing fiber–matrix interaction.

The term $(1 - v_f)/(1 + 2.5v_f)$ takes into account the decrease of the effective load-bearing cross-section owing to the introduction of the filler into the polymer matrix.

Equation (15.8) can be rearranged to take the linear form

$$\ln\left(\frac{\sigma_y}{(1 - v_f)/(1 + 2.5v_f)}\right) = \ln(\sigma_{y0}) + Bv_f, \quad (15.9)$$

where the term $\sigma_y/((1 - v_f)/(1 + 2.5v_f))$ is a reduced yield stress.

A semi-log plot of the reduced yield stress versus fiber content for uncross-linked and cross-linked composites is presented in Fig. 15.9. A maximum of 15% (w/w HPC) of fibers was considered since, as seen from Fig. 15.8, an efficient packing (in terms of mechanical performance of the composites) is attained up to 15–20% (w/w HPC) of fibers.

The values of B and σ_{y0} , obtained from the fit of the experimental data with (15.9) are presented in Table 15.6.

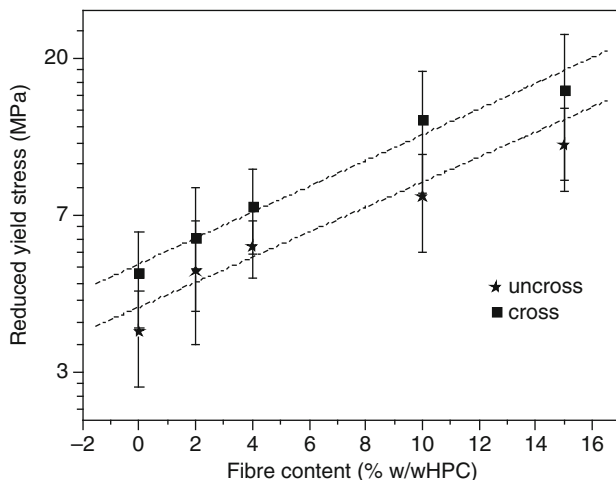


Fig. 15.9 Semi-log plot of the reduced yield stress versus fiber content for uncross-linked (uncross) and cross-linked (cross) isotropic all-cellulosic based composites. *Dash lines* represent the linear fit, according to (15.9). Note that fiber content is presented in wt% but all calculations were made using the volume fraction of fibers

Table 15.6 Values of B and σ_{y0} for isotropic all-cellulosic based composites obtained from the linear fits of (15.9)

	B	σ_{y0} (MPa)	R^2
Uncross-linked	1.66 ± 0.04	3.80 ± 0.31	0.985
Cross-linked	2.16 ± 0.06	4.95 ± 0.40	0.991

The corresponding correlation coefficients (R^2) are presented

Values obtained for the matrix yield stress, σ_{y0} , are very close to those obtained experimentally (uncross = 3.51 ± 0.4 MPa; cross = 5.10 ± 0.6 MPa), which confirms the validity of the model to these composites. Higher B values for cross-linked isotropic all-cellulosic based composites show that the interface is stronger in these materials, which is a consequence of the possibility of establishing covalent linkages between fibers and matrix.

15.5 Gas Barrier Properties

Gas barrier properties were evaluated to access the potential of isotropic all-cellulosic based composites for packaging applications. The mechanical properties, flexibility and biocompatibility of these materials can be useful, in particular, for food packaging. Due to the nature of the envisaged application insoluble materials are required. This requisite is only fulfilled by cross-linked composites and, therefore, we have decided to subject only cross-linked films for gas permeation measurements.

Gas permeation experiments were carried out for carbon dioxide, oxygen and nitrogen. The method used to measure the gas permeability was the constant pressure or variable volume method. For the measurements a home-made system was used [32]. It comprised a two-compartment flat sheet permeability cell. The feed stream circulates in the bottom compartment tangentially to the composite films and permeates through them to be collected in the top compartment where a flowmeter is connected. Due to the asymmetry of the composites the permeation experiments were carried out both for the top and bottom surfaces of the composite films facing the feed stream.

The feed pressure used ranged from 1 to 4 bar and the effective membrane surface area was 9.07 cm². The gas permeability was determined by the following equation:

$$P = \frac{qL}{(P_1 - P_2)At}, \quad (15.10)$$

where P is the gas permeability (cm³ (STP) cm cm⁻² s⁻¹ cm Hg⁻¹), q/t the volumetric flow rate of the gas permeation, L the membrane thickness, P_1 and P_2 the pressures and A the effective membrane area.

As an example, the permeability to carbon dioxide of the isotropic HPC matrix is shown in Fig. 15.10, as a function of feed pressure. It was observed that the permeabilities decrease in the order of $P(\text{CO}_2) > P(\text{O}_2) > P(\text{N}_2)$. The higher CO₂ permeability is probably due to the relative high solubility of this gas in the HPC matrix when compared with O₂ and N₂. The permeability of CO₂, O₂ and N₂ increases linearly with the upstream pressure and it is always higher for the bottom surface. The data collected in Table 15.2 show that HPC matrix (0% w/w HPC) has

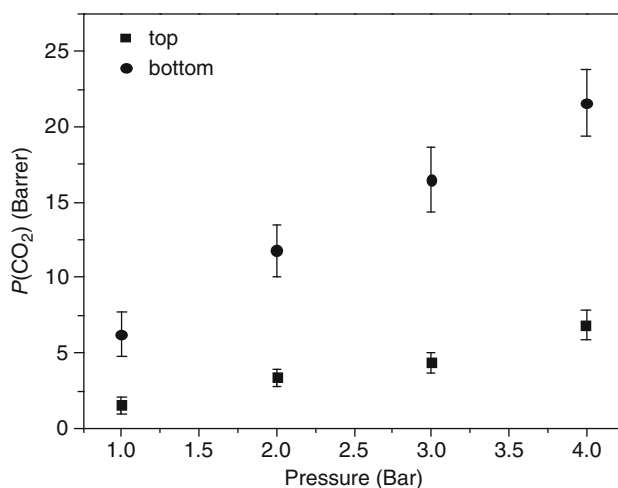


Fig. 15.10 Carbon dioxide permeability of the isotropic HPC matrix versus feed pressure [13]

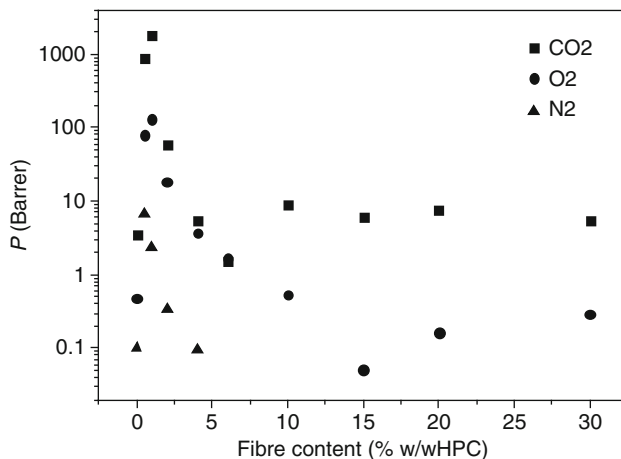


Fig. 15.11 Variation of gas permeability (CO₂, O₂ and N₂) of the cross-linked isotropic all-cellulosic based composites with fiber content [13]

relatively uniform structures of the top and bottom surfaces. However, roughness parameters are slightly higher for the bottom side, and this is probably the cause for the observed surface higher permeability to the three gases.

The permeability of the composites towards the three gases is higher than that of the matrix, as shown in Fig. 15.11. The introduction of 0.5–1% (w/w HPC) of fibers promotes a two to three orders of magnitude increase in top surface permeability to the three gases. For the bottom surface a similar trend was observed and, as for the HPC matrix, higher values of the permeabilities were obtained. The explanation of such behavior lies probably in the molecular structure of these materials. In polymeric systems, the gas permeability is related to the mobility of the macromolecules [33]. Therefore, lower permeability values of the HPC matrix should be related to the low mobility of the polymeric chains, induced by cross-linking. As referred before, the diisocyanates promote cross-linking of the matrix and fiber–matrix covalent bonds. In the presence of fibers part of the diisocyanate in the system will be consumed in fiber–matrix coupling, which will locally increase the mobility of the HPC macromolecules.

The density of the cross-links and the fiber–matrix covalent links are dictated by the amount of diisocyanate used. It's also important to notice that –OH groups of HPC are more accessible, therefore most of the diisocyanate is consumed in cross-linking of HPC. The maximum permeability obtained for 0.5–1% (w/w HPC) of fibers is probably related to the maximum density of fiber–matrix covalent links allowed in the system, which is likely dependent on the amount of diisocyanate used. The increase of the fiber content leads firstly to the settling of fibers at the bottom surface and then to its distribution over the volume of the composites. Such fiber packing mode may be responsible for the decrease in the diffusivity of the gases, which in turn causes the decrease in permeability.

Table 15.7 Oxygen permeability of selected polymers used in food packaging [34]

	PET	LDPE	HDPE	PP	PS
$P(O_2)$ /Barrer	0.01–0.013	0.85–1.18	0.34–0.68	0.51–0.85	0.85–1.35

PET poly(ethylene terephthalate), *LDPE* low-density polyethylene, *HDPE* high-density polyethylene, *PP* polypropylene, *PS* polystyrene

Table 15.8 Oxygen permeability of cross-linked isotropic all-cellulosic based composites

Fiber content (% w/w HPC)	0	0.5	1	2	4	6	10	15	20	30
$P(O_2)$ /Barrer	0.48	78.1	131	18.2	3.64	1.66	0.54	0.05	0.16	0.29

The permeability of the packaging material is one of the most critical features of the package. In particular, oxygen can promote oxidation reactions, altering the quality of the food and its shelf life. Any candidate for food packaging material should therefore be an oxygen high barrier. In Tables 15.7 and 15.8 oxygen permeability for selected polymers [34] used in food packaging and for cross-linked isotropic all-cellulosic based composites, respectively, are presented.

The cross-linked HPC matrix and composites with 10–30% of fibers have similar or even lower oxygen permeabilities than those of most common polymers used in food packaging (LDPE, HDPE, PP and PS), which makes these materials good candidates for that application.

15.6 Further Developments

All-cellulosic based composite films can be prepared from either isotropic or anisotropic cellulosic derivatives solutions. However, these composites cannot compete with mechanical properties of cellulose nanofiber reinforced composites. Pioneering studies reported by Favier et al. [35, 36], showed that small amounts of cellulose tunicate whiskers resulted in dramatic improvements in modulus above the glass transition temperature of an amorphous polymer matrix, due to the percolation of the cellulose nanofibers. Also recently, a completely new route to cellulose-based composites was proposed by Nishino and Arimoto [37], Soykeabkaew et al. [38–40]. They focused on approaches following self-reinforcing polymer concepts [41, 42] to create composites that often outperform traditional nanofiber reinforced composites [38, 40].

The use of cellulosic nanofibers in the production of all-cellulosic based composites can greatly improve the mechanical performance of these composites. With these nanofibers and a cellulosic anisotropic matrix a synergy between the percolation of the nanofibers and its matrix-induced orientation can lead to composites with enhanced mechanical properties.

A better mechanical performance of the all-cellulosic composites reported here could also be achieved taking advantage of liquid crystalline properties of aqueous suspensions of acid hydrolysed microcrystalline cellulose (MCC) [43, 44]. A chiral ordering of MCC aqueous suspensions was observed for various cellulose origins

such as wood, cotton, ramie, and bacterial cellulose. The authors also reported the conservation of this structure after water evaporation. Orts et al. [45] also verified that these cellulose microfibrils can be oriented by shear. This may lead to the future development of high-performance composites, fully anisotropic and highly ordered, based on liquid crystalline phases of both cellulosic derivative and cellulose fibers.

15.7 Conclusion

All-cellulosic based composites exhibit very interesting mechanical and gas barrier properties along with biocompatibility, making them promising candidates for applications in food packaging. The mechanical properties can be tuned in function of the anisotropy of the matrix. Future developments towards high-strength materials can be envisaged by taking full advantage of the orientational liquid crystalline properties of both the matrix and the fibers.

Acknowledgments This work was partially sponsored by Portuguese Science and Technology Foundation through project PTDC/CTM/099595/2008.

References

1. Manson JA, Sperling LH (1976) Polymer blends and composites. Plenum, New York
2. Eichhorn SJ, Dufresne A et al (2010) Review: current international research into cellulose nanofibers and nanocomposites. *J Mater Sci* 45:1–33
3. Berglund LA, Peijs T (2010) Cellulose biocomposites—from bulk moldings to nanostructured systems. *MRS Bull* 35:201–207
4. Ly B, Thielemans W et al (2008) Surface functionalization of cellulose fibers and their incorporation in renewable polymeric matrices. *Compos Sci Technol* 68:3193–3201
5. Peijs T, Baillie C (eds) (2003) Eco-composites. *Compos Sci Technol* 63:1223–1336
6. Mohanty AK, Misra M et al (2000) Biofibers, biodegradable polymers and biocomposites. An overview. *Macromol Mater Eng* 276(277):1–24
7. Gassan J, Bledzki AK (1999) Composites reinforced with cellulose based fibers. *Prog Polym Sci* 24:221–274
8. Lu JZ, Wu Q et al (2000) Chemical coupling in wood fiber and polymer composites: a review of coupling agents and treatments. *Wood Fiber Sci* 32:88–108
9. Belgacem MN, Gandini A (2005) The surface modification of cellulose fibers for use as reinforcing elements in composite materials. *Compos Interf* 12:41–75
10. Borges JP, Godinho MH et al (2001) New bio-composites based on short fiber reinforced hydroxypropylcellulose films. *Compos Interf* 8:233–241
11. Borges JP, Godinho MH et al (2001) Cellulose-based composite films. *Mech Compos Mater* 37:257–264
12. Borges JP, Godinho MH et al (2004) Tensile properties of cellulose fiber reinforced hydroxypropylcellulose films. *Polym Compos* 25:102–110
13. Borges JP (2004) PhD Thesis, FCT-UNL
14. Borges JP, Godinho MH (2008) Cellulose-based anisotropic composites. *Mater Sci Forum* 587–588:604–607

15. Aharoni SM, Walsh EK (1979) Rigid backbone polymers. 4. Solution properties of two lyotropic mesomorphic poly(isocyanates). *Macromolecules* 12:271–276
16. Ernst B, Navard P (1989) Band textures in mesomorphic (hydroxypropyl) cellulose solutions. *Macromolecules* 22:1419–1422
17. Viney C, Putnam W (1995) The banded microstructure of sheared liquid-crystalline polymers. *Polymer* 36:1731–1741
18. Riti JB, Cidade MT et al (1997) Shear induced textures of thermotropic acetoxypolypropylcellulose. *J Rheol* 41:1247–1259
19. Godinho MH, Fonseca JG et al (2002) Atomic force microscopy study of hydroxypropylcellulose films prepared from liquid crystalline aqueous solutions. *Macromolecules* 35:5932–5936
20. Schätzle J, Finkelmann H (1987) State of order in liquid crystalline elastomers. *Mol Cryst Liq Cryst* 142:85–100
21. Cox HL (1952) The elasticity and strength of paper and other fibrous materials. *Br J Appl Phys* 3:72–79
22. Nielsen LE (1970) Generalized equation for the elastic moduli of composite materials. *J Appl Phys* 41:4626–4627
23. Nielsen LE, Landel RF (1994) *Mechanical properties of polymers and composites*. Dekker, New York
24. Piggott MR, Ko M et al (1993) Aligned short-fiber reinforced thermosets: experiments and analysis lend little support for established theory. *Compos Sci Technol* 48:291–299
25. Hull D (1981) *An introduction to composite materials*. Cambridge University Press, London
26. Krenchel H (1964) *Fiber reinforcement*. Akademisk Forlag, Copenhagen
27. De SK, White JR (eds) (1996) *Short fiber-polymer composites*. Woodhead, Cambridge, England
28. Halpin JC, Kardos JL (1976) The Halpin-Tsai equations: a review. *Polym Eng Sci* 16:344–352
29. Eichhorn SJ, Young RJ (2001) The Young's modulus of a microcrystalline cellulose. *Cellulose* 8:197–207
30. Turcsányi B, Pukánszky B et al (1988) Composition dependence of tensile yield stress in filled polymers. *J Mater Sci Lett* 7:160–162
31. Pukánszky B (1990) Influence of the interface interaction on the ultimate tensile properties of polymer composites. *Composites* 21:255–262
32. Queiroz DP, de Pinho MN (2005) Structural characteristics and gas permeation properties of polydimethylsiloxane/poly(propylene oxide) urethane/urea bi-soft segment membranes. *Polymer* 46:2346–2353
33. Mulder M (1996) *Basic principles of membrane technology*. Kluwer, London
34. Delassus P (1997) Barrier properties. In: Brody A, Marsh K (eds) *The Wiley encyclopedia of packaging technology*, 2nd edn. New York, Wiley
35. Favier V, Canova GR et al (1995) Nanocomposite materials from latex and cellulose whiskers. *Polym Adv Technol* 6:351–355
36. Favier V, Chanzy H et al (1995) Polymer nanocomposites reinforced by cellulose whiskers. *Macromolecules* 28:6365–6367
37. Nishino T, Arimoto N (2007) All-cellulose composite prepared by selective dissolving of fiber surface. *Biomacromolecules* 8:2712–2716
38. Soykeabkaew N, Arimoto N et al (2008) All-cellulose composites by selective dissolution of aligned lingo-cellulosic fibers. *Compos Sci Technol* 68:2201–2207
39. Soykeabkaew N, Sian N et al (2009) All-cellulose nanocomposites by surface selective dissolution of bacterial cellulose. *Cellulose* 16:435–444
40. Qin C, Soykeabkaew N et al (2008) The effect of fiber volume fraction on the properties of all-cellulose composites. *Carbohydr Polym* 71:458–467
41. Alcock B, Cabrera NO et al (2006) Low velocity impact performance of recyclable all-polypropylene composites. *Compos Sci Technol* 66:1724–1737

42. Alcock B, Cabrera NO et al (2007) The effect of temperature and strain rate on the mechanical properties of highly oriented polypropylene tapes and all-polypropylene composites. *Compos Sci Technol* 67:2061–2070
43. Revol JF, Bradford H et al (1992) Helicoidal self-ordering of cellulose microfibrils in aqueous suspension. *Int J Biol Macromol* 14:170–172
44. Habibi Y, Lucia LA et al (2010) Cellulose nanocrystals: chemistry, self-assembly and applications. *Chem Rev.* doi:[10.1021/cr900339w](https://doi.org/10.1021/cr900339w)
45. Orts WJ, Godbout L et al (1998) Enhanced ordering of liquid crystalline suspensions of cellulose microfibrils: a small angle neutron scattering study. *Macromolecules* 31:5717–5725

Part III
Biodegradable Plastics and Composites
from Renewable Resources

Chapter 16

Environment Benevolent Biodegradable Polymers: Synthesis, Biodegradability, and Applications

B.S. Kaith, Hemant Mittal, Rajeev Jindal, Mithu Maiti, and Susheel Kalia

Abstract The increasing amount of synthetic polymers above the permissible limits is causing a lot of environmental pollution and is one of the greatest threats to the modern world. There is a growing demand for biodegradable polymeric materials derived from nature and is being seen as a solution for solid waste management. Biodegradable materials have been found to show a pronounced impact in case of environmental protection. Such biodegradable and eco-friendly materials have got diversified applications including sustained drug delivery devices, gene therapy, soft-tissue engineering, biomedical engineering, pharmaceuticals, artificial organ design, etc. Biodegradable materials have been found to possess good elasticity and impact strength because of which they have got potential applications in replacement of heart valves and kidneys. Moreover, such materials have been found to exhibit selective absorption toward saline water and are of great importance in petroleum industry as well as in desalination of water. Recently, such materials have been found to show electrical stimulus sensitivity both under the influence of AC and DC. These polymers have been found to be stimuli responsive and could be of great significance for drug and pesticide/fungicide delivery devices. Such materials are also pH sensitive toward different media and are of potential industrial usage in packaging and nursery plantation as well as in tissue culturing.

Keywords Biodegradation · Characterization · Composites · Fiber · Polysaccharides

Contents

16.1 Introduction	426
16.2 Biodegradable Polymers	427

B.S. Kaith (✉)

Department of Chemistry, Dr. B.R. Ambedkar National Institute of Technology (Deemed University), Jalandhar 144 011, Punjab, India
e-mail: bskaith@yahoo.co.in

16.2.1	Chemically Synthesized Plastics	428
16.2.2	Natural Polysaccharides	433
16.3	Biodegradability, Its Mechanism and Methods of Biodegradation	440
16.4	Applications of Biodegradable Polymers	441
16.4.1	Packaging	442
16.4.2	Agriculture	442
16.4.3	Medical Applications	442
16.4.4	Automotive Sector	443
16.4.5	Food	443
16.4.6	Other Applications	444
16.5	Environmental Impact	444
16.5.1	Recycling Impact	444
16.6	Microorganism Degradation of Plastics	445
16.7	Conclusion	445
	References	446

16.1 Introduction

In the past three decades, a variety of synthetic polymers have been reported to degrade in the environment within acceptable time periods. The term “degradation” is difficult to define exactly because of conflicting and reiterated definitions. Recently, Wang and coworkers have summarized different views concerning degradation and especially the biodegradation of polymeric materials. Biodegradation is defined by Albertsson and Karlsson as an event which takes place through the action of enzymes and/or chemical decomposition associated with living organisms (bacteria, fungi, yeasts, and insects) or their secretion products. It is also of prime concern to consider anaerobic reactions involving chemical (oxidation and hydrolysis), physical (photo-degradation and thermal-degradation), and environmental factors that alter the polymer structure prior to biodegradation. These factors may produce a synergistic effect resulting in fragmentation of the polymer leading to the degradation of macromolecules and their conversion into low-molecular-weight compounds. Therefore, biodegradation of a polymer is defined as the deterioration of its physical and chemical properties and a reduction of its molecular mass due to its conversion into CO_2 , H_2O , and CH_4 along with other low-molecular-weight products under the influence of microorganisms in both aerobic and anaerobic conditions. Moreover, the residue eventually be incorporated into the natural geochemical cycle biomass should be nontoxic [1–5].

Development of advanced materials took a long time to enter in a new era, by developing artificial, cheap, bio-stable, and versatile polymers based on petroleum chemistry, when people started looking for equivalent polymeric systems that can be degraded or biodegraded. In the last two decades, polymer industry has seen a remarkable rise in the marketing and development of biodegradable materials. Biodegradable polymers were regarded as a source of environment-friendly materials and seen at first glance as a major improvement with respect to the management of the wastes like plastic bags and packaging [6–10]. Biodegradable materials have

a pronounced effect on the human health care industry. They have a number of biomedical applications including drug delivery devices, gene therapy, soft-tissue engineering, biomedical engineering applications, pharmaceuticals, etc. In recent years, hydrogels have been used as one of the most important biodegradable material because they can absorb a significant amount of water. Moreover, hydrogels are as flexible as soft tissue, which reduces the chance of irritation of surrounding tissues.

Some of the synthetic polymers like aliphatic polyesters have attracted considerable attention because they have the features like biodegradability, biocompatibility, and possess physical or chemical properties comparable with the traditional and nonbiodegradable polymers. Such polymers have a variety of applications like films, packaging, and agriculture applications. Aliphatic polyesters, derived from aliphatic diols and dicarboxylic acids, are considered to be the most preferable among a number of biodegradable polymers because of ecological reasons like balance between physical properties and cost-effectiveness. Most of the polyesters produced are low melting and is difficult to produce high melting polyesters. Production of high-molecular-weight polyesters is one of the essential criteria with appropriate processibility and acceptable mechanical properties [11–17].

16.2 Biodegradable Polymers

Composite materials from the annually renewable natural fibers and biodegradable matrices have been developed in the past decade with an attempt to find alternatives to the fossil fuel-based polymeric materials in the automotive and packaging industries. One of the problems associated with biodegradable composites is the price, which limits investigation of these materials to a laboratory scale. With the new economic and climate turning attention, a wide variety of agro-based resources for the manufacture of new composite materials including geo-textiles, filters, sorbents, structural/nonstructural composites, molded products, and combination of other materials made it possible to explore new application areas such as packaging, housing, and automotive products [18].

Biodegradable thermoplastic materials that currently dominate as matrices for natural fibers are PP, PE, and PVC, while thermosets, such as phenolics and polyesters are common matrices. Biodegradable polymers are yet to become popular as “green” substitutes for synthetic polymers. Besides, the use of biodegradable plastics appears as an attractive alternative for enhancing sustainable and environment-friendly agricultural activities, especially in mulching and cultivation [19]. The increasing global interest on the agro-based structural materials from the natural, annually renewable, and biodegradable sources was also driven by the conservation of forests and forest resources. With a view to replace the wooden fittings, fixtures, and furniture, natural composites reinforced with jute, kenaf, sisal, coir, straw, hemp, banana, pineapple, rice husk, bamboo, etc. can be used in place of the conventional polymer composites reinforced with man-made fibers such as glass.

Development of new composite products from the existing resources has a strong potential to deliver a novel, biodegradable, and/or readily recyclable material suitable for the automotive and packaging industry. Lignocellulosic bio-fibers, when rightly combined with the recyclable thermoplastics, can possess an outstanding potential to produce environment-friendly composite materials possessing specific properties favorably comparable with those of glass fiber-based composites. Complete matrix fusion to facilitate thorough fiber impregnation, formation of strong fiber/matrix interfacial bonding, and matrix-to-fiber stress transfer efficiency are vital requirements for the manufacture of reliable and eco-friendly composites that can possess better mechanical properties and withstand environmental attacks. Mohanty et al. carried out a detailed review work on jute fiber-reinforced thermosets, thermoplastics, and rubber-based composites. Jute-based composites, an alternative to wood products, are not severely affected by mites, moisture and are generally considered to be fire-retardant. Due to its insulating characteristics, jute may find areas of applications in automotive door/ceiling panels and panels separating the engine and passenger compartments. With the increasing popularity of natural fibers in polymer composites, it is more important to study the natural fiber-based composites [20–44].

16.2.1 Chemically Synthesized Plastics

16.2.1.1 Polylactic Acid

Poly(lactic acid) (PLA) has been extensively used for making systems for controlled delivery of therapeutic substances including contraceptive steroids, anticancer drugs, antimalarial agents, and peptide hormones. The drugs can be imbibed either as dissolved or dispersed phase into polymeric matrix which degrades in contact with the biological fluids and allows a sustained release of the drug content. Various configurations of drug-release devices including microspheres, rods, films, and nanoparticles have been fabricated from PLA to control the drug release with suitable modification in polymer composition, crystallinity, molecular weight, and structure. Three mechanisms for controlling drug release from these systems have been proposed (1) Fickian diffusion through the polymer matrix, (2) diffusion through water-filled pores created upon swelling of the matrix, and (3) delivery by erosion of the polymer matrix. A combination of these mechanisms with contribution of surface burst effect has also been claimed to explain the release profile. It was reported that polymer–drug interaction plays a significant role on the drug-release behavior. In case of acidic drugs, faster hydrolysis of ester bond is expected due to acid catalysis, whereas in case of basic drugs two effects can be observed: base catalysis of the ester bond cleavage and neutralization of carboxyl end groups of polymer chains which restricts the autocatalytic effect of acidic chain ends. Thus, degradation can be accelerated or retarded by a base, depending on the relative contribution of the above two effects [45–55].

Polymeric carriers such as hydroxylpropylmethyl cellulose (HPMC) and nanoparticles made of poly- ϵ -caprolactone (PCL), poly(lactide-*co*-glycolide) (PLGA), or ethylcellulose were used for the preparation of systems which could control the release profile and to provide more effective therapies. Controlled drug administration through PLGA, HPC, ethyl cellulose, and chitosan provides sustained release of diclofenac and reduces the localized gastrointestinal disturbances. Diclofenac shows the following two important characteristics. First, its solubility depends on the pH of the surrounding solution and, secondly, it undergoes an intramolecular cyclization under the acidic conditions found in gastric liquids, which can cause its inactivation [56–61]. Salicylic acid, an acidic drug, is the key additive in many skin-care products for the treatment of acne, keratosis pilaris, and warts. The controlled release of salicylic acid has been studied using different types of formulations, such as PLA tablets, poly(ethylene oxide) (PEO) hydrogels, micro-balloons, and films made of chitosan and polyalkyleneoxide maleic acid copolymer [62–65]. Sulfasalazine is an acidic drug used to treat colon disease, such as irritable bowel syndrome, Crohn's disease, and ulcerative colitis. For the treatment of inflammatory bowel disease, regular intake of anti-inflammatory drugs and daily administration of high drug doses are required. Therefore, controlled-release devices such as capsules, tablets, and micro-particles have been developed and these devices are capable of delivering the drug specifically to the colon in order to reduce the total administered dose to the patient and to decrease their possible adverse effects [66, 67].

A lactic acid-based polymer can't be referred as "biopolymer" not as "biodegradable." It is actually degradable or hydrodegradable, and partly bioassimilable and biomineralizable [68–70]. Devices made of L-lactic acid-rich stereo copolymers can be seen as compostable. Bioresorbable polymeric devices made up of degradable or biodegradable materials derived from lactic and glycolic acids are successfully exploited in the biomedical field with applications in surgery and in pharmacology as well as in packaging. Another polymer currently regarded as an environment-friendly polymer is poly(ϵ -caprolactone) (PCL) [71]. This petrochemical-based polymer is definitely biodegradable but only under outdoor conditions. In the human body, it is slowly hydrolytically degradable.

Copolymers of the aliphatic polyester-type combining hydroxyl caproic acid with lactic acid are basically of interest for outdoor applications because their degradation involves both hydrolysis of lactic acid-based segments and biodegradation of hydroxycaproic acid-based molecules [72, 73]. The range of properties can be enhanced by taking advantage of the chirality of lactic acid to include stereocopolymer segments of L- and D-lactic acid in the chains. These copolymers and stereo-copolymers are industrially compostable.

16.2.1.2 Polyglycolic Acid

Polyglycolide or polyglycolic acid (PGA) is a simplest linear aliphatic polyester. It is a biodegradable thermoplastic polymer which can be prepared from glycolic acid

through polycondensation or ring-opening polymerization (ROP). Since 1950s, PGA has been known as a tough fiber-forming polymer. However, due to its hydrolytic instability, its utilization was limited. Recently, polyglycolide and its copolymers with lactic acid, ϵ -caprolactone, and poly trimethylene carbonate are widely used as materials for the preparation of absorbable sutures. Moreover, these polymers have got applications in biomedical fields. Polyglycolides have been found to possess glass transition temperature between 35 and 40°C and melting point in the range of 225–230°C. PGA exhibits about 45–55% degree of crystallinity thus resulting in water insolubility. Due to high molecular weight polyester is insoluble in almost all common organic solvents including acetone, dichloromethane, chloroform, ethyl acetate, and tetrahydrofuran. However, low-molecular-weight oligomers differ in their physical properties and exhibit more solubility. Polyglycolides are soluble in highly fluorinated solvents like hexafluoroisopropanol (HFIP) and hexafluoroacetone sesquihydrate. These solvents are used for the preparation of high-molecular-weight polymers which can be used for melt spinning and film preparation [74, 75, 139]. Fibers of PGA with stiff and high modulus (7 GPa) along with better mechanical strength.

Though polycondensation of glycolic acid is the simplest process, it is not an efficient process as it yields the low-molecular-weight products. Initially, glycolic acid is heated at atmospheric pressure and a temperature of about 175–185°C until water ceases to distill. Subsequently, pressure is reduced to 150 mmHg and keeping the temperature unaltered for about 2 h. In this way low-molecular-weight polyglycolide is obtained. The most common synthesis used to produce a high-molecular-weight PGA is ROP. ROP of glycolide can be catalyzed using different catalysts like antimony trioxide or antimony trihalides, stannous octoate, or tin alkoxides. Other catalysts used are aluminum isopropoxide, calcium acetylacetonate, and several lanthanide alkoxides like yttrium isopropoxide. Under ring-opening process, a catalytic amount of initiator is added to the glycolide under nitrogen atmosphere at 195°C. The reaction is allowed to proceed for about 2 h followed by rise in temperature to 230°C for about half an hour. After solidification, the resulting high-molecular-weight polymer is collected [76, 77, 138].

16.2.1.3 Polyhydroxyalkanoates

Polyhydroxyalkanoates (PHAs) are the biopolymers possessing the material properties ranging from rigid and highly crystalline to flexible, amorphous, and elastomeric. Because of such properties and inherent biodegradability, PHAs have attracted the world-wide attention of scientists and researchers as environment-friendly alternative to the conventional petroleum-based polymers. Polyhydroxybutyrate (PHB) and polyhydroxyoctanoate (PHO) have been found to possess biocompatibility in mammalian systems. Such biomaterials have got great potential as medical implantation devices [78–81].

Many microorganisms synthesize PHAs under conditions of nutrient stress with an excess of environmental carbon. PHAs function primarily as intracellular

reserves of carbon and energy. PHA biosynthesis pathways are highly versatile and can be used to synthesize a wide range of PHAs with a large number of monomeric units. Researchers have prepared the neutral synthetic hybrid copolymer of PHO-*b*-PEG which exhibited similar thermal crystalline properties to PHO but possessed molecular weight less than 50% that of its nonhybridized counterpart [82–85]. Such hybrid copolymers have been characterized with small-angle neutron scattering (SANS) technique and incorporation of comparatively small hydrophilic PEG groups at the end of the hydrophobic PHA chains were characterized. Thus PEG groups were found to have an influence on chain organization.

16.2.1.4 Polycaprolactone

Polycaprolactone polymers, because of their biodegradability and biomedical applications, are receiving the attention of scientists from all over the world. PCL have got wide applications in the biomedical area. Pure strains of microorganisms isolated from industrial compost have the capability of biodegrading the PCL and can induce the weight reduction to about 95% after 200 h of incubation [86]. Moreover, derivatives obtained by chain extension reaction of PCL (Fig. 16.1) were found to exhibit biodegradation behavior. Most of such derivatives have got potential application in surgery and as drug delivery devices.

Because of the presence of hydroxyl end groups, diol derivatives of PCL (Fig. 16.2) have the great potential for chain extension and can undergo reaction with different functional groups [87–94].

The more convenient method for the synthesis has been found to be the ROP of ϵ -caprolactone (CL) using catalyst-like derivatives of Ge, Nd, Bi, Sn, Zn, and Al [87–93].

Fig. 16.1 Structure of polycaprolactone

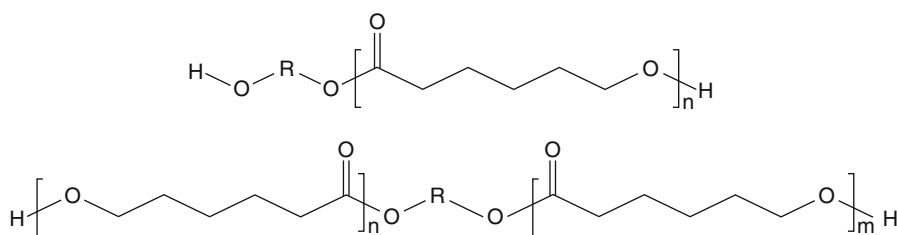
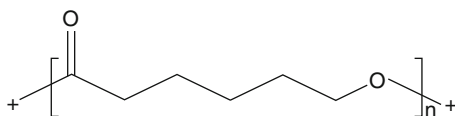


Fig. 16.2 Structure of diol derivatives of polycaprolactone

16.2.1.5 Polyvinyl Alcohol

Polyvinyl alcohol is a synthetic biodegradable polymer which is susceptible to biodegradation on action of *Fusarium lini*. PVA being highly soluble in water involves the random endocleavage of the polymer chains in aqueous medium. The initial step during biodegradation is associated with the specific oxidation of methane carbon bearing hydroxyl group in the presence of enzymes like oxidase and dehydrogenase and gives rise to β -diketone moieties. The later groups are able to facilitate the carbon-carbon bond cleavage which is promoted by specific β -diketone hydrolase leading to the formation of carboxylic and methyl ketone as end groups. Many bacterial PVA-oxidases are constitutive, whereas some PVA-dehydrogenases are inducible enzymes which require essential co-factors like pyrroloquinoline quinone (PQQ) and bivalent cations for their enhanced activity [94–97].

16.2.1.6 Polyesters

Polyesters, a category of polymers containing ester functional groups in the main chain, are thermoplastic or thermoset in nature. However, most of the polyesters are thermoplastics. Natural polyesters and a few synthetic one are biodegradable in nature. But most of the synthetic polymers are nonbiodegradable. Naturally occurring chemicals like cutin of plant cuticles are biodegradable natural polyesters. Synthetic polyesters can be obtained through step growth polymerization, e.g., polycarbonate and polybutyrate.

Polyesters refer to the various polymers in which the backbones are formed by the esterification condensation of polyfunctional alcohols and acids. Polyesters chemically are divided into two types: saturated and unsaturated polyesters. Saturated polyesters refer to the polyesters with saturated backbones. Such polyesters are unreactive and consist of low-molecular-weight liquids which are used as plasticizers and reactants in forming urethane polymers and linear, high-molecular-weight thermoplastics such as polyethylene terephthalate. Unsaturated polyesters refer to the polyesters with vinyl unsaturation. Most of them are used in reinforced plastics and are widely used as economically class resins.

Polyester fabrics are extensively used in apparel, home furnishing, conveyer belts, safety belts, jackets, hats, bed sheets, blankets, and as reinforcement in tires. Polyester fibers are used as cushioning and insulating materials for pillows. Synthetic polyesters provide some specific advantages over natural polyesters, e.g., improved wrinkle resistance, durability, and high color retention. Because of such properties polyester fibers are spun with natural fibers for the preparation of blend possessing the desired properties. They are also used in finishing high-quality wood products. Thixotropic properties of spray applicable polyesters make them ideal for use in open grain timbers.

16.2.2 Natural Polysaccharides

16.2.2.1 Starch

Starch is a linear or cross-linked polysaccharide made up of repeating glucose groups with α -1,4 glycosidic linkages in giving rise to a chain length of 500–2,000 glucose units. Starch consists of two major compounds: amylose (Fig. 16.3) and amylopectin (Fig. 16.4).

Amylose is both flexible and digestible. It is a main component of cereal grains and roots. It has increased functionality for food use after chemical, physical, or enzymatic modifications, e.g., amylolytic enzymes hydrolyze parts of starch molecules into low-molecular-weight ingredients like maltodextrin or dextrin. Physical modification of starch involves pre-gelatinization and heat-treatment.

Different kinds of chemically modified starches have been developed with diversified applications like food, paper, interior decoration of vehicles and houses, textile industries, and biomedical applications. With an increase in starch content of a polymer, there is an increase in biodegradability.

Starch-Based Biodegradable Polymers

Biodegradation of starch-based polymers due to enzymatic attack on glycosidic linkages leads to decrease in chain length. Separation of low-molecular-weight

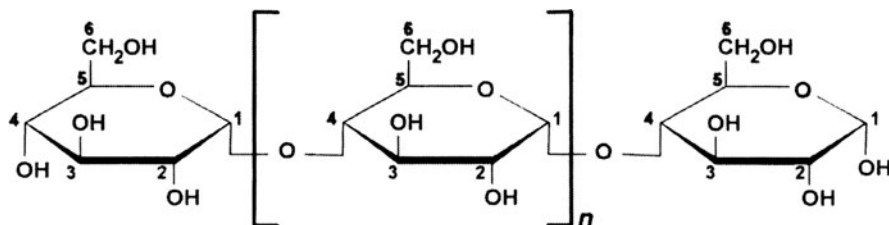


Fig. 16.3 Structure of amylose

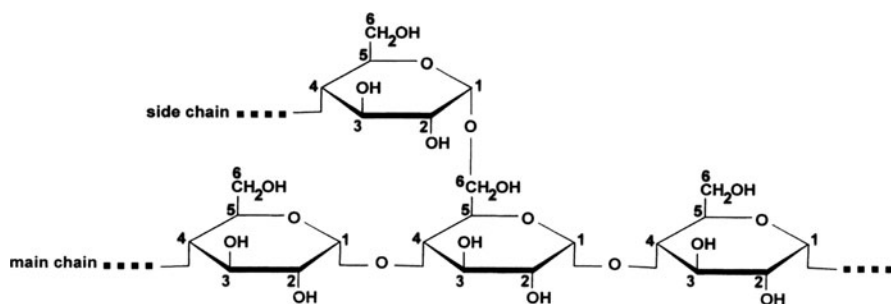


Fig. 16.4 Structure of amylopectin

sugar units such as monosaccharides, disaccharides, and oligosaccharides takes place which can readily be used in biochemical pathways. Different workers have investigated biodegradable starch-based polymers for their potential use in several biomedical applications, e.g., development of materials with mechanical strength comparable to that of bones and such polymers are suitable for bone-replacement implants, bone cements, drug-delivery systems, and tissue-engineering scaffolds [98–102].

Thermoplastic-Starch Products

Thermoplastics with good performance properties are produced by combining biodegradable thermoplastic starch plastics with specific plasticizing solvents and such materials possess inherent biodegradability. The hydrophilic nature of high-starch content plastics can be overcome through blending and chemical modification like acetylation, esterification, and etherification. Blending is always carried out with high-performance polymers like aliphatic polyesters and polyvinyl alcohols that provide useful mechanical properties.

Starch-Aliphatic Polyester Blends

High-quality sheets and films for packaging are prepared as blends of biodegradable starch and aliphatic polyesters (Fig. 16.5). About 50% of synthetic polyester could be replaced with starch with better market economy and biodegradability. Moreover, polyesters can be modified by incorporating different functional groups like hydroxy, amine, and carbonyl that are capable of reacting with natural starch. Several starch-based plastic products are available commercially and these include shopping bags, bread bags, overwraps, materials for “flushable” sanitary products, and mulch films. “Biobag” which is produced from Italy-based Novamont resin has been around since 1994. It consists of cornstarch combined with fully biodegradable PLA.

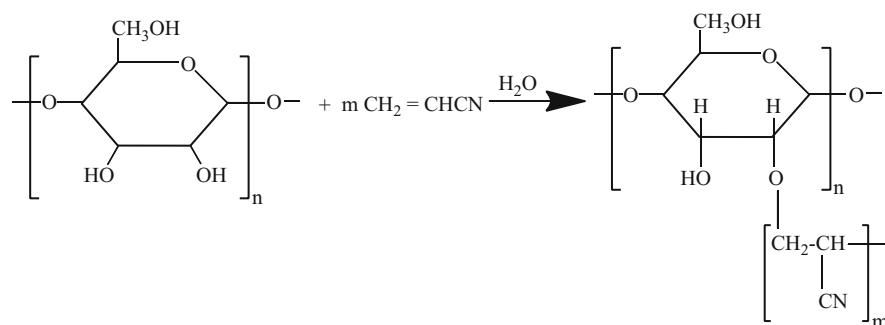


Fig. 16.5 Copolymer of cellulose and acrylonitrile

Water-soluble beads made from potato starch can replace polystyrene-foam packaging beads. Starch-based beads are readily water soluble and biodegradable, which could create an early market for biodegradable plastics.

Starch and PBS/PBSA Polyester Blends

In order to improve the mechanical properties of the materials, polybutylene succinate (PBS), polybutylene succinate adipate (PBSA), and other polyesters can be blended with starch. Starch and PBS or PBSA blends produce biodegradable plastic sheets with diversified applications like trays and other film products. Though with increase in starch content, there is decrease in tensile strength but biodegradability of the product keeps on increasing. Plasticizers are added to avoid the brittleness of the products and to increase the flexibility and end uses.

Starch-Based Superabsorbent Polymers

Superabsorbents are a unique group of materials that can absorb water more than a hundred times of their own weight. In addition, superabsorbents do not easily release the water, even under pressure. During 1970s first superabsorbent was developed by U.S. Department of Agriculture. They prepared starch/acrylonitrile/acrylamide-based polymers, which were originally used in agricultural/horticultural markets as hydrogels in order to retain moisture in soil during the growing and shipping of crops and other plants. Starch-graft copolymers are prepared by graft-copolymerizing acrylonitrile onto a starch substrate. Saponification of a starch-graft polymer with an alkali yields a final product with more hydrophilicity. Hydrophilic groups on the final product can be adjusted by controlling the amount of sodium hydroxide and reaction time during the saponification process [103–105]. Cross-linking during polymerization yields a networked polymer that is not only insoluble in water but is also able to absorb and retain water under low load. Typical cross-linking agents are trimethylolpropane triacrylate and ethylene-glycol diglycid ether.

In 2003, global demand for superabsorbents was 1.05 million tones and was found to increase at an average of 3.6% per annum. Out of the total demand, baby diapers account for about 81%, feminine hygiene products about 5%, adult incontinence about 8%, and other 6%. Other applications of superabsorbents are in removal of toxic heavy metal ions from industrial effluents, as drying agents, and removal of colloidal particles from potable water [106].

16.2.2.2 Cellulose

Cellulose (Fig. 16.6) is the most common organic compound. It consists of formula $(C_6H_{10}O_5)_n$. It is a polysaccharide containing a linear chain of several hundred $\beta(1 \rightarrow 4)$ linked D-glucose units [107, 108]. It is the structural component of the primary cell wall of green plants, algae and oomycetes. Some species of bacteria

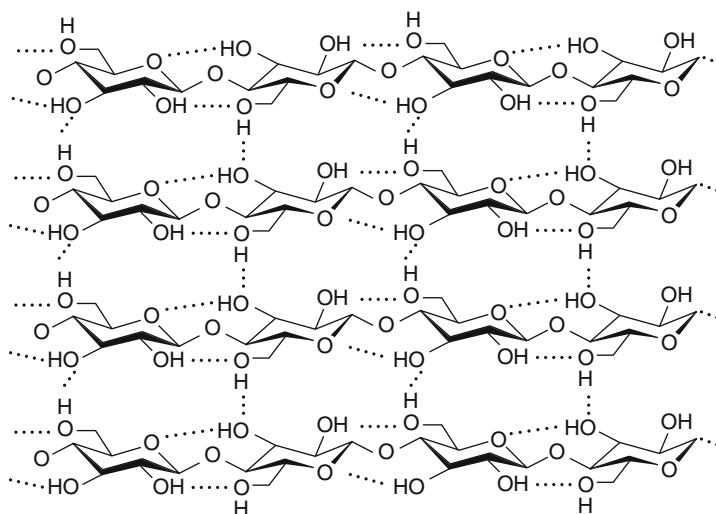


Fig. 16.6 Structure of cellulose

have been found to secrete it to form biofilms. About 33% of all plant matter is cellulose. The cellulose content of cotton is about 90% and that of wood is 50% [4]. For industrial applications, cellulose is mainly extracted from wood pulp and cotton. Mostly it is used to produce cardboard and paper. It is also converted into a wide variety of products such as cellophane and rayon. Currently, people are working on conversion of cellulose into biofuels, i.e., cellulose as green and alternative fuel source. Certain organisms like ruminants and termites can digest cellulose with the help of symbiotic microorganisms that live in their guts. Cellulose is not digestible by humans and is often used as “dietary fiber,” which acts as a hydrophilic bulking agent for feces.

Cellulose is tasteless, odorless, and hydrophilic in nature. It is insoluble in water and most organic solvents. It is chiral and is biodegradable. On treatment with concentrated acids it can be broken into its glucose units. Cellulose is a straight chain polymer. Unlike starch, there occurs no coiling or branching and the molecule adopts an extended and stiff rod-like conformation, aided by the equatorial conformation of the glucose residues. The hydroxyl groups present on the glucose units of one chain undergo hydrogen bonding with oxygen molecules of the same or a neighbor chain, thereby holding the chains firmly together side-by-side and forming microfibrils with high tensile strength. Such strength is important in cell walls, where the microfibrils are meshed into a carbohydrate matrix, giving rigidity to plant cells. Cellulose exhibits crystallinity and requires a temperature of 320°C and pressure of 25 MPa to become amorphous in water [109]. Most of the properties of cellulose depend on the degree of polymerization, i.e., the number of glucose units that make up one polymer molecule. For example, cellulose from wood pulp has typical chain lengths between 300 and 1,700 units, whereas cotton

and other plant fibers as well as bacterial celluloses have chain lengths ranging from 800 to 10,000 units [110].

The portion of cellulose containing material that does not dissolve in 17.5% NaOH at 20°C is the cellulose, known as true cellulose. On acidification of the extract β -cellulose gets precipitated out, whereas the portion that dissolves in base but does not precipitate out on acidification is a γ -cellulose.

Derivatives of Cellulose

Hydroxyl groups present on 2, 3, and 6 positions are the sites where derivatization can be carried out. Cellulose esters and ethers are the most important commercial materials. Among the esters, cellulose acetate and cellulose triacetate are film- and fiber-forming materials and have wide range of applications. The inorganic ester nitrocellulose was initially used as an explosive and as a film-forming material.

Ethyl cellulose is mainly used as a thin-film coating material [111] and is also used as a food additive in the form of emulsifier.

Methylcellulose has got a large number of applications like thickeners and emulsifiers. It is also used in the treatment of constipation, as artificial tears and saliva and nutritional supplement capsules. It has got applications in construction industry as glue and binders with wide range uses in textile and paper industries.

Hydroxypropyl cellulose (HPC) is used for the preparation of artificial tears, treat medical conditions characterized by insufficient tear production such as keratoconjunctivitis sicca, recurrent corneal erosions, decreased corneal sensitivity, exposure, and neuroparalytic keratitis. It is also used as a disintegrant and a binder in tablets, sieving matrix for DNA separations by capillary and microchip electrophoresis and lubricant for artificial eyes, food additive, thickener, and as an emulsion stabilizer [111, 112].

Carboxymethyl cellulose (CMC) plays an important role in food industry. Because of high viscosity, nontoxicity, and nonallergic nature, it is used as a viscosity modifier or thickener and to stabilize emulsions in various products including ice cream. It is also a constituent of many nonfood products, such as jellies, toothpaste, laxatives, diet pills, water-based paints, detergents, textile, and various paper products. In laundry detergents, CMC is used as a soil suspension polymer which creates a negatively charged barrier to soils in the wash solution. CMC is also used as a lubricant in nonvolatile eye drops.

It is also used in the oil drilling industry as an ingredient of drilling mud, where it acts as a viscosity modifier and water retention agent. In this field, it is referred to as poly-anionic cellulose (PAC). Insoluble microgranular CMC is used as a cation-exchange resin in ion-exchange chromatography for the purification of proteins [111].

Hypromellose or hydroxypropylmethylcellulose (HPMC) is a semisynthetic, inert, viscoelastic polymer, which is used as an ophthalmic lubricant, an excipient and controlled delivery component in oral medicaments and is found in a variety of commercial products [111]. Hypromellose is used as an alternative to animal gelatin and as an emulsifier, thickener, and suspending agent.

Applications

Major constituent of paper, cardboards, and textiles is the cellulose. Some of the products of cellulose are cellophane, rayon fiber, nitrocellulose, water-soluble adhesives, and binders. Powdered cellulose is used as inactive fillers in tablets and as a thickener and stabilizer in processed foods. In the laboratories, cellulose is used in TLCs as a stationary phase, liquid filtration, as highly hydrophilic and absorbent sponges. These days cellulose insulation made from recycled paper is becoming popular as an environment-friendly material. On treatment with boric acid cellulose can be used as a fire retardant.

16.2.2.3 Hemicellulose

Hemicellulose is a branched polysaccharide consisting of shorter chains of around 200 sugar units. Twenty percent of the biomass contains hemicelluloses and is derived from different sugars like glucose, xylose, mannose, galactose, rhamnose, and arabinose (Fig. 16.7).

16.2.2.4 Natural Oil Polyols

Natural oil polyols (NOPs) are bio-polyols which are derived from vegetable oils using different techniques. The primary use of these NOPs is in the production of polyurethanes. Most of the NOPs qualify as bio-based products, as defined by United States Secretary of Agriculture in the Farm Security and Rural Investment Act 2002.

NOPs are clear liquids ranging from colorless to medium yellow. The viscosity of NOPs is versatile and usually depends upon the molecular weight and the number of hydroxyl groups per molecule. Odor is the most characteristic property of the NOPs which differentiate one NOP from other. Most of the NOPs are proven to become rancid, which involves the autoxidation of fatty chains containing carbon-carbon

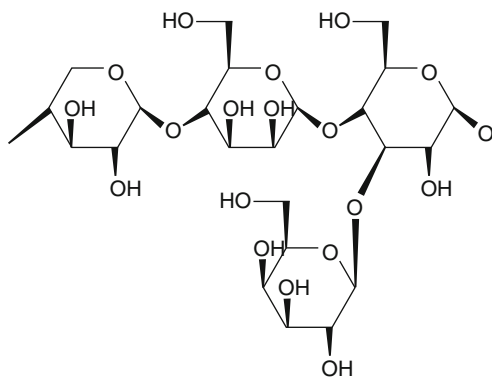


Fig. 16.7 Structure of hemicellulose

double bonds and formation of odoriferous low-molecular-weight aldehydes, ketones, and carboxylic acids. Limited number of naturally occurring vegetable oils (triglycerides) contains the type of hydroxyl groups that account for both the name and important reactivity of NOPs.

Castor oil is the only commercially available NOP which can be obtained directly from the source, whereas other NOPs require chemical modifications after their extraction from the plants. Ninety percent of the fatty acids that make up castor oil are ricinoleic acid containing hydroxyl group at C-12 along with a carbon-carbon double bond.

Other vegetable oils like soy bean oil and peanut oil do not contain hydroxyl groups but possess carbon-carbon double bonds. Chemical processes like oxidation of C-C double bond are used for introduction of hydroxyl groups onto the carbon chains of fatty acids. Autoxidation of oils which results in the drying of oils gives increased molecular weight and introduces hydroxyl groups. In fact such a process which involves free radical mechanism gives rise to a mixture of cross-linked and oxidized triglycerides. Chemical reaction of vegetable oils with peroxides gives rise to epoxides which on further reaction with nucleophiles result in the introduction of hydroxyl groups. Acid-catalyzed ring opening of epoxidized soybean can be used for the preparation of polyurethane foams. Triglycerides of unsaturated fatty acids or methyl esters of such acids on treatment with carbon monoxide and hydrogen in presence of a metal catalyst can introduce -CHO (formyl) groups to the chain which on further hydrogenation result in the addition of hydroxyl groups in the chain^{1,2} [112, 137].

16.2.2.5 Soy Plastics

One of the promising class of biodegradable and green materials is soy-protein-based plastics. Soy protein plastics are made from casein and soy protein and have got applications in biomedical. Soybeans were introduced in USA from Asia during 1800s. In 1930, patents were filed in Britain and France for the preparation of plastics from soy proteins. First US patent for soy protein plastic was issued to Sadakichi Satow in 1917. In United States, soy protein provides over 60% of the fats and oils used in food industry. Soy beans contain about 20% oils and 40% proteins. In some species protein levels are as high as 55%. Since soy beans consist of discrete groups of proteins with abroad range of molecular sizes and are composed of approximately 38% of non-polar and non-reactive amino-acid residues while 58% are polar and reactive, therefore, taking into account the water solubility and reactivity of these soy protein based biopolymers have been prepared. Injection and compression molding techniques are used for soy plastic processing [113-117]. Soy proteins have a large number of applications including automobile parts and

¹US Patent 2,006,041,156.

²US Patent 4,742,087.

have got adhesive properties. Dried soy plastics display 50% higher modulus than that of epoxy engineering plastics.

Wet process was used for the preparation of soy protein-based plastics. However, it involved a long hardening period in formaldehyde. The final products were found susceptible to warping, shrinkage, porosity, and water absorption, because of which the soy-based plastic products could not be commercialized. A process for the preparation of water-resistant and chemically-stable plastics using soy bean meal containing 48% proteins, formaldehyde, and phenolic resins has been developed. These thermoset phenolic-soy-formaldehyde plastics were filled with 30% wood flour. Other way of decreasing water absorption is to denature the proteins prior to processing. The denatured soy protein is not water soluble and cannot be plasticized by water. However, if it is plasticized with formamide the material could be successfully molded and retains its mechanical strength and displays little swelling or distortion when submerged in water for 48 hours. Thus denatured water insoluble protein is a promising raw material for the preparation of water resistant plastic materials.

16.3 Biodegradability, Its Mechanism and Methods of Biodegradation

According to the American Society for Testing of Materials (ASTM) and the International Standards Organization (ISO), the degradable plastics are those which undergo a significant change in chemical structure under specific environmental conditions. Materials must meet specific criteria set out by the ASTM and ISO in order to be classified as biodegradable. These changes result in a loss of physical and mechanical properties. Biodegradable plastics undergo degradation under the action of naturally occurring microorganisms such as bacteria, fungi and algae. Depending upon the type of degradation, plastics may be classified as photodegradable, oxidatively degradable, hydrolytically degradable, or those which may be composted.³ Conventional plastics are resistant to biodegradation, as the surfaces in contact with the soil are smooth and hydrophobic [118]. Microorganisms within the soil are unable to consume a portion. This group of materials usually has an impenetrable petroleum-based matrix, which is reinforced with carbon or glass fibers. The second class of polymer materials under consideration is partially degradable. Production of this class of materials typically includes natural fiber reinforcement within the petroleum-based matrix. When disposed of, microorganisms are able to consume the natural macromolecules within the plastic matrix which leaves a weakened material, with rough and open edges and further degradation gets accelerated. The third class of polymer materials is currently attracting a great deal of attention from researchers and industry. These plastics are designed to be completely biodegradable. The polymer matrix is derived from natural sources like starch or microbially

³Canadian Patent No 2,350,112.

grown polymers and the fiber reinforcements are of agro-based origin. Microorganisms are able to consume such materials leaving behind carbon dioxide and water as by-products. In fact microbial attack on a material is dependent on the framework structure of the polymer. Moreover, in polymer materials from a scientific standpoint, certain ingredients like starch and cellulose must be present in order for biodegradation to occur.

The organism type determines the appropriate degradation temperature, which usually falls between 20 and 60°C. The disposal site must contain oxygen, moisture, and mineral nutrients along with neutral or slightly acidic pH. Biodegradation of materials involves the digestible macromolecules, which join to form a chain and experience a direct enzymatic scission. This is followed by metabolism of the split portions, leading to a progressive enzymatic dissimilation of the macromolecules from the chain ends. Oxidative cleavage of the macromolecules leading to metabolization of the fragments may take place. Thus, the chain fragments become short enough to be degraded easily. Biodegradable polymers begin their lifecycle as renewable resources, usually in the form of starch or cellulose. Many biopolymers are designed to be discarded in landfills, composts, or soil. The materials are broken down by the microorganisms in presence of appropriate pH [118–120].

In the case of materials where starch is used as an additive to a conventional plastic matrix, the polymer in contact with the soil and/or water is easily attacked by the microbes. The microbes digest the starch, leaving behind a porous sponge-like structure with a high interfacial area and low structural strength. After the depletion of starch the polymer matrix begins to be degraded by an enzymatic attack. Enzymatic reaction results in the scission of the molecular chain thereby, slowly reducing the weight of the matrix till the entire material gets digested. Another method of microbial degradation of biopolymers involves growing microorganisms for the specific purpose of digesting polymer materials. But this process is more intensive and costs more. Moreover, it circumvents the use of renewable resources as biopolymer feedstocks. Microorganisms under consideration are designed to target and breakdown petroleum-based plastics. Though this method reduces the volume of waste, it does not aid in the preservation of nonrenewable resources [120–125].

Polyolefins are the polymers susceptible to photodegradation and addition of additive-like benzophenone further accelerate the photochemical degradation. Modification of the composition of the polymer with the incorporation of more UV absorbing groups accelerates the rate of photo degradation. Synthesizing new polymers with light-sensitive groups are the examples of photodegradable polymers.

16.4 Applications of Biodegradable Polymers

Biopolymers are used in diversified sectors including medicine, packaging, agriculture, and automotive industry. With advancement, choice of materials, and environmental awareness, some of the materials are replaced whereas the others are complimented. Biodegradable plastic films may be used as garbage bags, disposable

cutlery and plates, food packaging, and shipping materials. Depending upon the application, biodegradable materials can be classified in different categories.

16.4.1 Packaging

It is estimated that approximately two-fifths of the total plastics is used in packaging and about 50% of that is used in food industry as a packaging material. Since large volume of the inert materials is disposed of as waste-land fillers, therefore, people all over the world are trying to use the biodegradable packaging materials so as to reduce the volume of waste materials.

16.4.2 Agriculture

At the end of the life cycle, the biopolymers are used in agriculture as soil regenerators. For example, ecoflex as a thin film can be used to cover frost susceptible plants during winter season and at the end of life cycle gets mixed up with the soil as a nutrient-rich fertilizer. Biopolymers which are compostable supplement the current nutrient cycle in the soil and are important from agriculture point of view. Application of a plastic mulch cover for less than 40 days, immediately after seeding is found to increase the yield of spring wheat and is an ideal material as a crop mulcher. Applications of biopolymers are not limited to film covers as mulchers, other areas of more interest are plant pots, disposable composting containers, and bags. The plants along with pots are seeded directly into the soil where the biodegradable plastic breaks down as the plant begins to grow. In order to avoid the disposal problem, material scientists are also carrying out research on biodegradable fertilizer and chemical storage bags [125, 126].

16.4.3 Medical Applications

The classification of bioactive materials includes all biopolymers used for medical applications. BASF, a world leader in the chemical and plastic industry, introduced ecoflex as a fully biodegradable material in 2001. The material has been found to be resistant toward water and grease, making it suitable for its application as a hygienic disposable wrapping material and at the end it gets decomposed in normal composting systems. Polyvinyl alcohol is designed for extrusion, injection molding, and blow molding possessing features user-controlled solubility in water. Dissolution of this product occurs at a preset temperature, thereby, allowing its applications in diversified fields like hospital laundry bags, disposable food service items, agricultural products, and catheter bags. Biodegradable loose-fill packaging

materials can be developed from renewable material like starch. The starch is treated by an acetylation process followed by other chemical treatments and post-extrusion steaming. Mechanical properties of such materials have been found to be adequate and true biodegradability can be achieved.

Since today's medical world is constantly and rapidly changing, therefore, the materials required also need recurrent adjustments. The biopolymers used in medical applications must have tissue compatibility. Moreover, they may or may not be expected to break down after a given time period. Researchers working all over the world on tissue engineering are attempting to develop organs from polymeric materials, which could be transplanted into humans. The plastics with growth factor injections are required for growth of cell and blood vessel in the new organ. Biopolymers with adhesion sites that act as cell hosts in giving shapes and can mimic different organs have been developed, e.g., artificial bone material which adheres and integrates onto bone in the human body. The most commonly employed material is bioglass. Other application of biopolymers is in controlled release delivery of medications. The bioactive materials release drugs at a rate determined by its enzymatic degradation over a long period. PLA materials have been developed as medical devices such as resorbable screws, sutures, and pins. These materials are neutral and reduce the risk of tissue reactions to the devices and have short recovery times and decreased number of doctor visits needed by patients [127–130].

16.4.4 Automotive Sector

This sector is constantly responding to societal and governmental demands for environmental responsibility. Research and development activities in the area of automobiles using natural fibers as reinforcing materials in plastic parts continues to be enthusiastic, especially in European countries. Bio-based cars are lighter with better mileage, making them a more economical choice for consumers. Being biodegradable natural fibers are the best substituents for glass fibers as reinforcement materials in plastic parts of automobiles and commercial vehicles [131]. At the end of life cycle such biodegradable polymer materials can be composted. Natural fibers like flax, jute, ramie, and hemp are being used in interior parts as reinforcing agents. Since the components do not need load-bearing capacities and the dimensional stability is more important, the application of natural fibers as reinforcing materials is more effective.

16.4.5 Food

One of the novel applications of biopolymers, which do not fit into any of the previous categories, is its use in modifying the food textures, e.g., gelatin-based biopolymer starch fat replacers possess fat-like characteristics with smoothness and short plastic textures that remain highly viscous after melting. Research is

continuing to manipulate biopolymers into food products. The eventual goals have improved physical characteristics such as foaming, gelling, and water- or fat-binding abilities [132].

16.4.6 Other Applications

Nowadays, biopolymer materials are finding their applications in other fields such as adhesives, paints, engine lubricants, and construction materials. Biodegradable golf materials and fishing hooks are also available.

16.5 Environmental Impact

Biopolymers are of great importance in environment-friendly management because of their applications in diversified fields. For example, formulation of biodegradable mulching films to be used for agriculture crops and such films do not need to be taken off the fields as they do not have any environmental impact. Moreover, these bioplastic films possess specific mechanical and optical properties similar to those of the traditional plastics used in films, agriculture, e.g., like polyethylene and poly[ethylene-*co*-(vinylacetate)]. However, biodegradable mulch films are made to be biodegraded in soil at the end of crop cycle, therefore, durability cannot be compared with traditional mulch films. In case of agriculture, resistance to photo-oxidation is more important characteristic of films so as to enhance the durability of the materials. Researchers have processed a biodegradable polymer in the presence of small amount of UV stabilizing systems, added during the melt process, which could improve the photo-oxidation resistance [133, 134].

16.5.1 Recycling Impact

In order to protect the environment, scientists are attempting to integrate environmental considerations directly into material selection processes. The use of renewable resources in the production of biopolymers achieves it through: the feed-stocks being used can be replaced either through natural cycles or through intentional intervention by humans or use of renewable feed-stocks for biopolymer development is biodegradable as the end product and can prevent the potential pollution which can be due to the disposal of equivalent volume of traditional plastics. At the end of their life cycle, biopolymeric materials are generally used as land fillers or are composted. In case of plastic materials recycling is encouraged but effective recycling is very less, e.g., in United States, less than 10% of plastic products are recycled at the end of their life cycle. For material development, recycling has to be recognized as a disposal technique but not as a final goal. Since the return on

investment in recycling is positive under economic situation, therefore, in underdeveloped countries plastics are almost completely recycled.

No doubt it appears to be positive at the onset but the open systems by which the plastics are recycled emits toxic gases in the environment. Though recycling appeared to be a viable way to reduce pollution and environmental damage when it was first introduced as a waste reduction technique but the emission of toxic gases in the environment has diverted the attention of researchers and environmentalists toward the use of plastic-based renewable feed-stocks that are biodegradable and the end products are organic matter. In this way toxic emission can be avoided and the growth of easily compostable and biodegradable plastics is encouraged [135].

16.6 Microorganism Degradation of Plastics

Microbial degradation of polymers is a two-step process. Initially, microorganisms bind to the polymer substrate followed by the catalyzed hydrolytic cleavage. Degradation of polymers can be monitored through roughening of the surface, formation of holes or cracks, defragmentation or change in color. Various characterization techniques used for the confirmation of different stages of biodegradation are scanning electron microscopy (SEM), atomic force microscopy (AFM), FT-IR, and thermal analysis [136]. CO₂ evolution/O₂ consumption is the laboratory method for the measurement of biodegradation of polymers. Anaerobic microorganisms produce predominantly a mixture of CO₂ and methane as an extracellular product of their metabolic reactions. Use of biodegradable plastic goods in daily life is common and is increasing day by day in the developed countries. Now the trend is going to change and dependency is increasing on biodegradable plastics in comparison to synthetic polymeric materials because of their complete biodegradability in the natural environment after disposal. Moreover, selected strains can be characterized and used in defined degradation tests. Biological degradation of polymers is generally influenced by a number of factors, such as, the kind of organisms involved in the biodegradation and the environmental conditions.

16.7 Conclusion

Biopolymers are being used in diversified fields like packaging, agriculture, medicals, automobile sector, and food industry. Because of environment friendliness, biopolymers are replacing the synthetic polymers at a fast pace. Biodegradation of plastic materials is of prime importance and is a process occurring through the intervention of bacteria and other living organisms like fungi, yeasts, and insects. Biodegradation of biopolymers is regarded as a green process because it leaves CO₂ and H₂O molecules along with organic materials as the end products, thereby

adding no pollution load to the environment. Moreover, the amount of CO₂ released at the end of life cycle is much lower than the amount of CO₂ consumed by the plants throughout the life cycle. Rate of use of biopolymers is higher in case of developed and developing countries, whereas underdeveloped countries are still dependent upon synthetic plastics because of their cost-effectiveness.

References

1. Wang XL, Yang KK, Wang YZ (2003) Properties of starch blends with biodegradable polymers. *J Macromol Sci Part C* 43:385–409
2. Albertsson AC, Karlsson S (1994) Chemistry and technology of biodegradable polymers. Blackie, Glasgow
3. Suvorova AI, Tyukova IS, Trufanova EI (2000) Biodegradable starch-based polymeric materials. *Russ Chem Rev* 69:451–459
4. Decriaud AC, Maurel VB, Silvestre F (1998) Standards methods for testing the aerobic biodegradation of polymeric materials. In: Albertsson AC (ed) *Review and perspectives: advanced polymer science*, vol 135. Berlin, Springer
5. Nayak PL (2000) Natural oil-based polymers: opportunities and challenges. *JMS Rev Macromol Chem Phys* 40:1–21
6. Barenberg SA, Brash JL, Narayan R et al (1990) Degradable materials: perspectives, issues and opportunities. CRC, Boca Raton
7. Vert M, Feijen J, Albertson A et al (1992) Biodegradable polymers and plastics. The Royal Society of Chemistry, Cambridge
8. Scholz C, Gross RA (2000) Polymers from renewable resources: biopolyesters and biocatalysts. ACS Symposium Series, Washington, DC
9. Chiellini E, Gil H, Braunegg G et al (2001) Biorelated polymers: sustainable polymer science and technology. Kluwer Academic/Plenum Publishers, New York
10. Stevens ES (2002) Green plastics: an introduction to the new science of biodegradable plastics. Princeton University Press, Princeton
11. Guillet J (1995) Degradable polymers, principles and applications. Chapman & Hall, London
12. Bikiaris D, Panayiotou C (1998) LDPE/starch blends compatibilized with PE-g-MA copolymers. *J Appl Polym Sci* 70:1503–1521
13. Ferre T, Franco L, Rodriguez-Galan A et al (2003) Poly(ester amide)s derived from 1, 4-butanediol, adipic acid and 6-aminohexanoic acid. Part-II: composition changes and fillers. *Polymer* 44:6139–6152
14. Aburto J, Thiebaud S, Alric I et al (1997) Properties of octanoated starch and its blends with polyethylene. *Carbohydr Polym* 34:101–112
15. Bikiaris D, Aburto J, Alric I et al (1999) Mechanical properties and biodegradability of LDPE blends with fatty-acid esters of amylase and starch. *J Appl Polym Sci* 71:1089–1100
16. Chandra R, Rustgi R (1998) Biodegradable polymers. *Prog Polym Sci* 23:1273
17. Carothers WH (1929) Studies on polymerization and ring formation I. An introduction to the general theory of condensation polymers. *J Am Chem Soc* 51:2548–2549
18. Rowell RM (1996) Composites from agri-based resources. Proceedings No. 7286 of the conference entitled In: *The Use of Recycled Wood and paper in Building Applications*, USDA Forest Services and the Forest Products Society, Madison, Wisconsin
19. Briassoulis DJ (2004) An overview on the mechanical behavior of biodegradable agricultural films. *Polym Environ* 12:65–81
20. Wambua P, Ivens I, Verpoest I (2003) Natural fibers: can they replace glass in fiber reinforced plastics. *Compos Sci Technol* 63:1259–1264
21. Netravali AN, Chabba S (2003) Composites get greener. *Mater Today* 6:22–29

22. Mohanty AK, Misra M, Hinrichsen G (2000) Biofibers, biodegradable polymers and bio-composites: an overview. *Macromol Mater Eng* 276(277):1–24
23. Leao AL, Rowell R, Tavares N (1998) Applications of natural fibers in automotive industry in Brazil-thermoforming process. In: Prasad PN (ed) *Science and technology of polymers and advanced materials*. Plenum, New York
24. Biswas S, Srikanth G, Nangia G (2001a) Development of natural fiber composites in India. In: *Proceedings of annual convention & trade show, Composites, Composites Fabricator's Association at Tampa, Florida*
25. Biswas S, Mittal A, Srikanth G (2001) Composites – the future building material. *J Indian Build Congress* 8:199–206
26. Biswas S, Mittal A, Srikanth G (2001) Gujarat earthquake – composite materials towards re-building & rehabilitation. *J Indian Build Congress* 8:383–390
27. Biswas S, Mittal A, Srikanth G (2002) Composites: a vision for the future. In: *ICERP Conference, IIT, Madras*
28. Karnani R, Krishnan M, Narayan R (1997) Bio-fibers reinforced polypropylene composites. *Polym Eng Sci* 37:476–487
29. de Albuquerque AC, Joseph K, de Carvalho LH et al (2000) Effect of wettability and ageing conditions on the physical and mechanical properties of uniaxially oriented jute-roving-reinforced polyester composites. *Compos Sci Technol* 60:833–844
30. Nangia S, Mittal A, Srikanth G, Biswas S (2000) Towards faster trains – role of composites. *Sci Tech Entrepreneur* 8:63–68
31. Nangia S, Biswas S (2000) Jute composites: technology business opportunities. In: *Proceedings of international conference on advances in composites, IISc & HAL, Bangalore*
32. Rowell RM, Sanadi AR, Caulfield DF et al (1997) Utilization of natural fibers in plastic composites: problems and opportunities. In: Leao et al (Ed) *Lignocellulosic-plastic composite, USP, UNESP, Sao Paulo*
33. Al-Qureshi HA (2001) The application of jute fiber reinforced composites for the development of a car body. In: *UMIST Conference, UK*
34. Karus M, Kaup M (2002) Natural fibers in the European automotive industry. *J Indus Hemp* 7:119–131
35. Singh B, Gupta M, Verma A (2000) The durability of jute fiber-reinforced phenolic composites. *Compos Sci Technol* 60:581–589
36. Gassan J (2002) A study of fiber and interface parameters affecting the fatigue behaviour of natural fiber composites. *Compos Part A* 33:369–374
37. Gassan J, Bledzki A (1997) The influence of fiber-surface treatment on the mechanical properties of jute–polypropylene composites. *Compos Part A* 28:1001–1005
38. Wollerdorfer M, Bader H (1998) Influence of natural fibers on the mechanical properties of biodegradable polymers. *Ind Crops Prod* 8:105–112
39. Li Y, Mai YW, Ye L (2000) Sisal fibers and its composites: a review of recent developments. *Compos Sci Technol* 60:2037–2055
40. Karmaker AC, Youngquist JA (1996) Injection molding of polypropylene reinforced with short jute fibers. *J Appl Polym Sci* 62:1147–1151
41. Rana AK, Mandal A, Bandyopadhyay S (2003) Short jute fiber reinforced polypropylene composites: effect of compatibiliser, impact modifier and fiber loading. *Compos Sci Technol* 63:801–806
42. Jayaraman K (2003) Manufacturing sisal–polypropylene composites with minimum fiber degradation. *Compos Sci Technol* 63:367–374
43. Corden TJ, Jones IA, Rudd CD et al (2000) Physical and biocompatibility properties of poly-ε-caprolactone produced using in situ polymerization: a novel manufacturing technique for long-fiber composite materials. *Biomaterials* 21:713–724
44. Sakaguchi M, Nakai A, Hamada H et al (2000) Mechanical properties of thermoplastic unidirectional composites using microbraiding technique. *Compos Sci Technol* 60:717–722

45. Baras B, Benoit MA, Gillard J (2000) Parameters influencing the antigen release from spray-dried poly(DL-lactide) microparticles. *Int J Pharm* 200:133–145
46. Sendil D, Wise DL, Hasirci V (2002) Assessment of biodegradable controlled release rod systems for pain relief applications. *J Biomater Sci* 13:1–15
47. Gumusderelioglu M, Deniz G (2000) Sustained release of mitomycin-C from poly(DL-lactide)/poly(DL-lactide-co-glycolide) films. *J Biomater Sci* 11:1039–1050
48. Xiong XY, Tam KC, Gan LH (2005) Release kinetics of hydrophobic and hydrophilic model drugs from pluronic F127/poly(lactic acid) nanoparticles. *J Control Release* 103:73–82
49. Jalil R, Nixon JR (1990) Biodegradable poly(lactic acid) and poly(lactide-co-glycolide) microcapsules: problems associated with preparative techniques and release properties. *J Microencapsul* 7:297–325
50. Shah SS, Cha Y, Pitt CG (1992) Poly (glycolic acid-co-DL-lactic acid): diffusion or degradation controlled drug delivery. *J Control Release* 18:261–270
51. Kissel T, Brich Z, Bantle S et al (1991) Parenteral depot-systems on the basis of biodegradable polyesters. *J Control Release* 16:27–42
52. Li S, Girod-Holland S, Vert M (1996) Hydrolytic degradation of poly(DL-lactic acid) in the presence of caffeine base. *J Control Release* 40:41–53
53. Miyajima M, Koshika A, Okada J et al (1998) Factors influencing the diffusion-controlled release of papaverine from poly(L-lactic acid) matrix. *J Control Release* 56:85–94
54. Proikakis CS, Mamouzelos NJ, Tarantili PA et al (2003) Stability of DL-poly(lactic acid) in aqueous solutions. *J Appl Polym Sci* 87:795–804
55. Proikakis CS, Mamouzelos NJ, Tarantili PA et al (2006) Swelling and hydrolytic degradation of poly(D,L-lactic acid) in aqueous solutions. *Polym Degrad Stab* 91:614–619
56. Takka S, Rajbhandari S, Sakr A (2001) Effect of anionic polymers on the release of propranolol hydrochloride from matrix tablets. *Eur J Pharm Biopharm* 52:75–82
57. Ubrich N, Bouillot P, Pellerin C et al (2004) Preparation and characterization of propranolol hydrochloride nanoparticles: a comparative study. *J Control Release* 97:291–300
58. Tuncay M, Calis S, Kas HS et al (2000) Diclofenac sodium incorporated PLGA (50:50) microspheres: formulation considerations and in vitro/in vivo evaluation. *Int J Pharm* 195:179–188
59. Palomo ME, Ballesteros MP, Frutos P (1999) Analysis of diclofenac sodium derivatives. *J Pharm Anal* 21:83–94
60. Liu CH, Kao YH, Chen SC et al (1995) In vitro and in-vivo studies of the diclofenac sodium controlled release matrix tablets. *J Pharm Pharmacol* 47:360–364
61. Dangprasirt P, Ritthidej GC (1997) Development of diclofenac sodium controlled release solid dispersion tablet using optimization strategy. *Drug Dev Ind Pharm* 23:843–848
62. Andreopoulos AG, Hatzl E, Doxastakis M (2001) Controlled release of salicylic acid from poly(DL-lactide). *J Mater Sci: Mater Med* 12:233–239
63. Savas H, Guven O (2001) Investigation of active substance from poly(ethylene oxide) hydrogels. *Int J Pharm* 224:151–158
64. Sato Y, Kawashima Y, Takeuchi H (2003) Physicochemical properties to determine the buoyancy of hollow microspheres (microballoons) prepared by the solvent diffusion method. *Eur J Pharm Biopharm* 55:297–304
65. Yoshizawa T, Shin-ya Y, Hong KJ (2005) pH- and temperature-sensitive release behaviors from polyelectrolyte complex films composed of chitosan and PAOMA copolymer. *Eur J Pharm Biopharm* 59:307–313
66. Lamprecht A, Torres HR, Schafer U et al (2000) Biodegradable microparticles as a two-drug controlled release formulation: a potential treatment of inflammatory bowel disease. *J Control Release* 69:445–454
67. Clemett D, Markham A (2000) Prolonged-release Mesalazine: a review of its therapeutic potential in ulcerative colitis and Crohn's disease. *Drugs* 59:929–956
68. Jarerat A, Tokiwa Y, Tanaka H (2003) Poly(L-lactide) degradation by *Kibdelosporangium aridum*. *Biotechnol Lett* 25:2035–2038

69. Li S, Tenon M, Garreau H et al (2000) Enzymatic degradation of stereocopolymers derived from L-, DL-and meso-lactides. *Polym Degrad Stab* 67:85–90
70. Torres A, Li SM, Roussos S et al (1999) Biopolymers utilizing nature's advanced materials, vol 723. ACS Symposium Series, ACS, Washington, DC
71. Rutkowska M, Dereszewska A, Jastrzebska JH (1998) Biodegradation of poly(ϵ -caprolactone) in plant treatment active sludge. *Macromol Symp* 130:199–204
72. Tsuji H, Suzuyoshi K (2002) Environmental degradation of biodegradable polyesters 2. Poly(ϵ -caprolactone), poly[(R)-3-hydroxybutyrate], and poly(L-lactide) films in natural dynamic seawater. *Polym Degrad Stab* 75:357–365
73. Asrar J, Gruys KJ (2002) Biopolymers: biology, chemistry, biochemistry, applications, polyesters III applications and commercial products. Wiley-VCH, Weinheim
74. Gilding DK, Reed AM (1979) Biodegradable polymers for use in surgery – polyglycolic/poly(lactic acid) homo- and copolymers: 1. *Polymer* 20:1459–1464
75. Schmitt E (1973) Polyglycolic acid in solutions. US Patent 3,737,440
76. Lowe CE (1954) Preparation of high molecular weight polyhydroxyacetic ester. US Patent 2,668,162
77. Stridsberg KM, Maria R, Ann-Christine A (2002) Controlled ring-opening polymerization: polymers with designed macromolecular architecture. *Adv Polym Sci* 157:41–65
78. Dawes EA, Senior PJ (1973) The role and regulation of energy reserve polymers in microorganisms. *Adv Microbiol Physiol* 10:135–266
79. Brandl H, Gross RA, Lenz RW et al (1990) Advances in biochemical engineering/biotechnology. Springer, Berlin
80. Foster LJ, Tighe RBJ (1995) Enzymatic assay hydroxybutaric acid monomer formation in poly(β -hydroxybutyrate) degradation studies. *Biomaterials* 16:341–343
81. Foster LJR (2000) Polymers from renewable resources: biopolyesters and biocatalysis. ACS Books, Washington, DC
82. Steinbuechel A (1996) Biotechnology. Wiley, Weinheim, Germany
83. Doi Y (1990) Microbial polyesters. VCH Publishers, New York
84. Sanguanchaipaiwong V, Gabelish CL, Hook J et al (2002) Biosynthesis of natural synthetic hybrid copolymers: polyhydroxyoctanoate-diethylene glycol. *Biomacromolecules* 5: 643–649
85. Sanguanchaipaiwong FLJR, VC GL et al (2004) A natural–synthetic copolymer of polyhydroxyoctanoate–diethylene glycol: biosynthesis and properties. *Polymer* 46:6587–6594
86. Lefevre C, Tidjani A, Vander Wauven C et al (2002) The interaction mechanism between microorganisms and substrate in the biodegradation of polycaprolactone. *J Appl Polym Sci* 83:1334–1340
87. Kricheldorf HR, Langanke D (2002) Polylactone 54: ring-opening and ring-expansion polymerizations of caprolactone initiated by germanium alkoxides. *Polymer* 43:1973–1977
88. Guillaume SM, Schappacher M, Soum A (2003) Polymerization of ϵ -caprolactone Initiated by $\text{Nd}(\text{BH}_4)_3(\text{THF})_3$: synthesis of hydroxytelechelic poly(ϵ -caprolactone). *Macromolecules* 36:54–60
89. Kricheldorf HR, Hachmann-Thiessen H, Schwarz G (2004) Di-, tri- and tetrafunctional poly(ϵ -caprolactone)s by $\text{Bi}(\text{OAc})_3$ -catalyzed ring-opening polymerizations of ϵ -caprolactone. *Macromolecules* 37:6340–6345
90. Kricheldorf HR, Behnken G, Schwarz G (2006) Ring opening polymerization of ϵ -caprolactone via the bismuth-2-mercaptoethanol complex. *J Polym Sci Part A Polym Chem* 44: 3175–3183
91. Yu F, Zhuo R (2004) Synthesis and characterization of OH-Terminated poly(trimethylene carbonate)s by alcohol-initiated ring-opening polymerization in melt bulk without using any catalyst. *Polym J* 36:28–33
92. Kricheldorf HR, Thieben HH (2005) Telechelic polylactones functionalized with trimethylsilyl groups. *Polymer* 46:12103–12108

93. Dubois P, Zhang J, Jerome XR et al (1994) Macromolecular engineering of polylactones and poly lactides: 13. Synthesis of techelic polyesters by coupling reactions. *Polymer* 35: 4998–5004
94. Chiellini E, Corti A, D'Antone S et al (2003) Biodegradation of poly(vinyl alcohol) based materials. *Prog Polym Sci* 28:963–1014
95. Sakai K, Hamada N, Watanabe Y (1986) Studies on the poly(vinyl alcohol)-degrading enzyme. Part VI. Degradation mechanism of poly(vinyl alcohol) by successive reactions of secondary alcohol oxidase and b-diketone hydrolase from *Pseudomonas* sp. *Agric Biol Chem* 50:989–996
96. Shimao M, Yamamoto H, Ninomiya K et al (1984) Pyrroloquinoline quinone as an essential growth factor for a poly(vinyl alcohol)-degrading symbiont, *Pseudomonas* sp. VM15C. *Agric Biol Chem* 48:2873–2876
97. Nakasaki K, Ohtaki A, Takano H (2000) Biodegradable plastic reduces ammonia emission during composting. *Polym Degrad Stab* 70:185–188
98. Reis RL, Cunha AM, Bevis MJ (1997) Structure development and control of injection-molded hydroxylapatite-reinforced starch/EVOH composites. *Adv Polym Technol* 16:263–277
99. Reis RL, Mendes SC, Cunha AM et al (1997) Processing and in vitro degradation of starch/EVOH thermo-plastic blends. *Polym Int* 43:347–352
100. Reis RL, Cunha AM (1995) Characterisation of two biodegradable polymers of potential application within the biomaterials field. *J Mater Sci* 6:786–792
101. Malafaya PB, Elvira C, Gallardo A et al (2001) Porous starch-based drug delivery systems processed by a microwave route. *J Biomater Sci Polym Ed* 12:1227–1241
102. Gomes ME, Ribeiro AS, Malafaya PB et al (2001) A new approach based on injection moulding to produce biodegradable starch-based polymeric scaffolds: morphology, mechanical and degradation behaviour. *Biomaterials* 22:883–889
103. Yamaguchi M, Watamoto H, Sakamoto M (1987) Super-absorbent polymers from starch–polyacrylonitrile graft copolymers by acid hydrolysis before saponification. *Carbohydr Polym* 7:71–82
104. Smith T (1972) Water absorbing alkali metal carboxylate salts of starch–polyacrylonitrile graft copolymers. US Patent 3,661,815
105. Wu J, Wei Y, Lin J et al (2003) Study on starch-graft-acrylamide/mineral powder superabsorbent composite. *Polymer* 44:6513–6520
106. Farrar D, Flesher P, Skinner M et al (1995) Water absorbing polymers. US Patent 5,384,343
107. Crawford RL (1981) Lignin biodegradation and transformation. Wiley, New York
108. Updegraff DM (1969) Semimicro determination of cellulose in biological materials. *Anal Biochem* 32:420–424
109. Young R (1986) Cellulose structure modification and hydrolysis. Wiley, New York
110. Weiner ML, Lois AK (1999) Excipient toxicity and safety. Dekker, New York
111. de Silva DJ, Olver JM (2005) Hydroxypropyl methylcellulose (HPMC) lubricant facilitates insertion of porous spherical orbital implants. *Ophthal Plast Reconstr Surg* 21:301–302
112. Narayan R, Phuong T, Daniel GJ (2005) Ozone-mediated polyol synthesis from soybean oil. *Am Oil Chem Soc* 82:653–659
113. Satow S (1917) US Patent 1,245,975,976,980
114. Ly YTP, Johnson LA, Jane J (1998) Soy Protein as Biopolymer. In: Kaplan DL (ed) *Biopolymers from renewable resources, macromolecular systems-materials approach*. Springer, Berlin
115. Huang SJ (1994) Plant proteins as materials. In: Baumel CP, Johnson LA, Greiner CA (Eds) *Identifying new industrial uses of soybean protein*. Special Rep 95, Iowa Agriculture and Home Economics Experiment Station, Iowa State University, Ames, IA, USA
116. Thames SF (1994) Soybean polypeptide polymers. In: Baumel CP, Johnson LA, Greiner CA (Eds) *Identifying new industrial uses of soybean protein*. Special Rep 95, Iowa Agriculture and Home Economics Experiment Station, Iowa State University, Ames, IA, USA
117. Jane J, Wang S (1996) US Patent 5,523,293

118. Aminabhavi TM, Balundgi RH, Cassidy PE (1990) A review on biodegradable plastics. *Polym Plast Technol Eng* 29:235–262
119. Huang JC, Shetty AS, Wang MS (1990) Biodegradable plastics: a review. *Adv Polym Technol* 10:23–30
120. Lorcks J (1998) Properties and applications of compostable starch-based plastic materials. *Polym Degrad Stab* 59:245–249
121. Fredrik-Selin J (2002) Lactic acid formed into biodegradable polymer. *Adv Mater Proc* 160: 13–16
122. Andreopoulos AG (1994) Theophandies, degradable plastics – a smart approach to various applications. *J Elast Plast* 24:308–326
123. ASTM Standards (1998) Vol 08.01. D883-96: standard terminology relating to plastics. New York, NY: ASTM
124. Leaversuch R (2002) Biodegradable polyesters; packaging goes green. *Plast Technol* 8: 66–83
125. Chau H, Yu P (1999) Production of biodegradable plastics from chemical wastewater: a treatment. *Water Sci Technol* 39:273–280
126. Fomin VA, Guzeev VV (2001) Biodegradable polymers, their present state and future prospects. *Prog Rub Plast Technol* 17:186–204
127. Li FM, Guo AH, Wei H (1999) Effects of clear plastic film mulch on yield of spring wheat. *Field Crop Res* 63:79–86
128. Mukhopadhyay P (2002) Emerging trends in plastic technology. *Plast Eng* 58:28–35
129. Kokubo T, Kim H, Kawashita M (2003) Novel bioactive materials with different mechanical properties. *Biomaterials* 24:2161–2175
130. Sakiyama-Elbert S, Hubbell J (2001) Functional biomaterials: design of novel biomaterials. *Annu Rev Mater Res* 31:183–210
131. Lammers P, Kromer K (2002) Competitive natural fiber used in composite materials for automotive parts. ASAE Paper No. 026167, Illinois, ASAE, Chicago
132. Griffin GJL (1994) Chemistry and technology of biodegradable polymers. Blackie Academic & Professional, London
133. Scott G, Gilead D (1995) Degradable polymers. Chapman & Hall, London
134. Copinet A, Bertrand C, Longieras AY et al (2003) Photodegradation and biodegradable study of a starch and poly(lactic acid) coextruded material. *J Polym Environ* 11:169–176
135. Thurston D, Lloyd S, Wallace J (1994) Considering consumer preferences for protection in material selection. *Mater Des* 15:203–209
136. Kaith BS, Jindal R, Jana AK et al (2010) Development of corn starch based green composites reinforced with Saccharum spontaneum L fiber and graft copolymers – evaluation of thermal, physio-chemical and mechanical properties. *Biores Technol* 101:6843–6851
137. Babb D, Phillips J, Keillor C (2006) soy-based polyol for flexible slabstock foam. Alliance for the Polyurethanes Industry, Salt Lake City
138. Bero M, Piotr D, Kasperczyk J (1999) Application of calcium acetylacetonate to the polymerization of glycolide and copolymerization of glycolide with ϵ -caprolactone and L-lactide. *Macromolecules* 32:4735–4737
139. Middleton J, Tipton A (2006) Synthetic biodegradable polymers as medical devices. *Medical Plastics and Biomaterials Magazine*

Chapter 17

Biocomposites Based on Biodegradable Thermoplastic Polyester and Lignocellulose Fibers

Luc Avérous

Abstract In the recent years, biobased products have raised great interest since sustainable development policies tend to expand with the decreasing reserve of fossil fuel and the growing concern for the environment. Consequently, biopolymers, i.e., biodegradable polymers, have been the topic of many researches. They can be mainly classified as agro-polymers (starch, protein, etc.) and biodegradable thermoplastic homo or copolyesters (polyhydroxyalkanoates, poly(lactic acid), etc.). These latter, also called biopolyesters, can be synthesized from fossil resources but main productions are obtained from renewable resources. Unfortunately for certain applications, biopolyesters cannot be fully competitive with conventional thermoplastics because some of their properties are too weak. Therefore, to extend their applications, these biopolymers have been formulated and associated with lignocellulose fillers, which could bring a large range of improved properties (stiffness, crystallinity, thermal stability, etc.). The resulting “biocomposites” have been the subject of many recent publications.

This chapter is dedicated to this class of materials, which are elaborated from different natural fibers and biopolyesters. These systems based on renewable resources nowadays show strong developments in different fields, including automotive and packaging industries.

Keywords Biocomposite · Biodegradable · Lignocellulose fiber · Polyester

Contents

17.1	Introduction	454
17.2	Biodegradable Polymers and Biopolyesters	455
17.2.1	Biodegradable Polymers Classification	455
17.2.2	Biopolyesters	456

L. Avérous
LIPHT-ECPM, EAC (CNRS) 4375, University of Strasbourg, 25 rue Becquerel, 67087 Strasbourg
Cedex 2, France
e-mail: luc.averous@unistra.fr

17.3	Biocomposites Based on Biodegradable Thermoplastic Polyester and Lignocellulose Fibers	463
17.3.1	Generalities	463
17.3.2	The Case of Biocomposites Based on Copolyesters	464
17.4	Conclusion	474
	References	475

17.1 Introduction

In the last years, biopolymers, i.e., biodegradable polymers, have attracted more and more interest due to the increasing environmental concern and the decreasing fossil resources. This recent evolution incites researchers and industrials to develop novel materials labeled as “environmentally friendly,” i.e., materials produced from alternative resources, with lower energy consumption, biodegradable, and nontoxic for the environment. Since the biopolymers are biodegradable and the main productions are obtained from renewable resources such as agro-resources, they represent an interesting alternative route to common nondegradable polymers for short-life range applications (packaging, agriculture, etc.). Nevertheless, till now, most biopolymers are costly compared to conventional thermoplastic and their properties are sometimes too weak for certain end-uses. Therefore, it appears necessary to improve these biopolymers to make them fully competitive towards common thermoplastics.

To overcome these weaknesses, during the last decades different strategies were elaborated. Chemical copolymerization or modification has been carried out. But, this strategy is strongly limited as far as toxicity and diversity of by-products obtained during the chemical reactions are concerned. Another limitation lies in the cost of the modification. Yet, for various decades another more promising strategy has developed the association with other biodegradable compounds to obtain compostable multiphase materials. We can obtain different structures (blends, composites, etc.) with corresponding properties to fulfill various applications. This approach induces some problematics linked with the quality of the interfaces, i.e., concerning the continuity between the phases and the compatibility between the different materials.

Biocomposites (biodegradable composites) are a special class of composite materials. They are obtained by blending biodegradable polymers with biodegradable and biobased fillers (e.g., lignocellulose fibers). Since main components are biodegradable, the composite, as the integral part, is also expected to be biodegradable.

Tailoring new composites within a perspective of eco-design or sustainable development is a philosophy that is applied to more and more materials. Ecological concerns have resulted in a resumed interest in renewable resources-based and/or compostable products. It is the reason why material components such as natural fibers, biodegradable polymers can be considered as “interesting” – environmentally safe – alternatives.

Table 17.1 Chemical composition (wt.%) of vegetable fibers

	Cellulose	Hemicellulose	Pectin	Lignin	Ash
Bast fibers					
Flax	71	19	2	2	1–2
Hemp	75	18	1	4	1–2
Jute	72	13	>1	13	8
Ramie	76	15	2	1	5
Leaf fibers					
Abaca	70	22	1	6	1
Sisal	73	13	1	11	7
Seed-hair fibers					
Cotton	93	3	3	–	1
Wheat straw	51	26	–	16	7
LCF ₀₋₁	58	8	–	31	3
LCF _{0-0.1}	56	7	–	31	6
LCF _{0.1-1}	59	8	–	31	2

Reproduced with permission (Averous and Le Digabel 2006). Copyright of Elsevier

Lignocellulose-based fibers are the most widely used, as biodegradable filler. Intrinsically, these fibers have a number of interesting mechanical and physical properties (Gatenholm et al. 1992; Avella et al. 1993, 2007a, b; Bledzki and Gassan 1999; Mohanty et al. 2000; Shanks et al. 2004; Cyras et al. 2007; Barkoula et al. 2010). These renewable materials present strong variations according to the botanical origin. With their environmentally friendly character and some techno-economical advantages, these fibers motivate more and more different industrial sectors (automotive) to replace, e.g., common fiberglass. Intrinsically, the agro-fibers have a number of interesting mechanical and physical properties. The structure and the organization of such agro-materials have been largely described in different publications. But till now, the macromolecular architectures in the fiber cell walls still remain partially unknown. Main macromolecular elements are cellulose, hemicellulose, and lignin. The chemical composition of different lignocellulose fibers is given in Table 17.1. According to the botanical source, these renewable fillers present large variations in their composition. The different contents can vary according to the conditions of the fibers pretreatment (e.g., fractionation process and surface treatment).

17.2 Biodegradable Polymers and Biopolyesters

17.2.1 Biodegradable Polymers Classification

A vast number of biodegradable polymers (biopolymers) are chemically synthesized or biosynthesized during the growth cycles of all organisms. Some microorganisms and enzymes capable of degrading them have been identified (Kaplan et al. 1993; Chandra and Rustgi 1998; Kaplan 1998; Steinbuchel 2003). Depending on the synthesis process, Fig. 17.1 shows a classification with four different categories

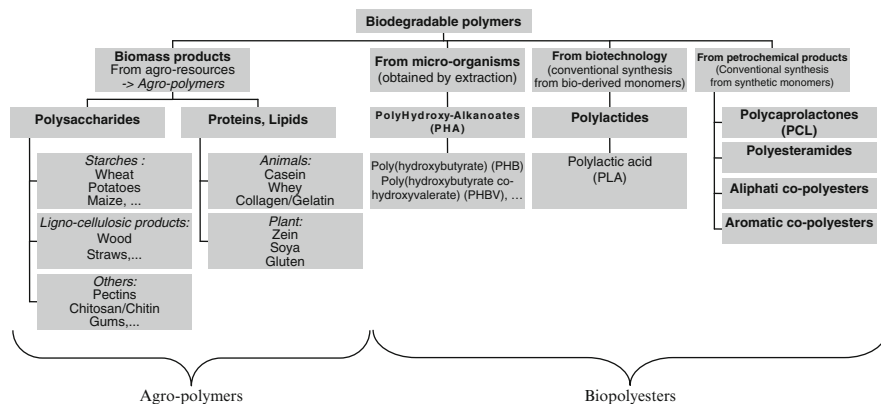


Fig. 17.1 Classification of the main biodegradable polymers. Reproduced with permission (Bordes et al. 2009). Copyright of Elsevier

(Averous and Boquillon 2004) (1) polymers from biomass such as the agro-polymers from agro-resources (e.g., starch and cellulose), (2) polymers obtained by microbial production, e.g., the polyhydroxyalkanoates, (3) polymers chemically synthesized using monomers obtained from agro-resources, e.g., the poly(lactic acid), and (4) polymers whose monomers and polymers are both obtained by chemical synthesis from fossil resources. Only, three categories (1–3) are obtained from renewable resources. We can sort these different biodegradable polymers into two main families, the agro-polymers (category 1) and the biodegradable polyesters (categories 2–4), also called as biopolyesters.

17.2.2 Biopolyesters

Table 17.2 and Fig. 17.2 show the chemical structures, trade names, and main properties of commercially available biopolyesters.

17.2.2.1 Polyesters Based on Agro-Resources

Poly(lactic acid)

Lactic acid is a chiral molecule existing as two stereoisomers, L- and D-lactic acid which can be produced by different ways, i.e., biologically or chemically synthesized (Averous 2008).

In the first case, lactic acid is obtained by fermentation of carbohydrates from lactic bacteria, belonging mainly to the genus *Lactobacillus*, or fungi (Garlotta 2001; Wee et al. 2006). This fermentative process requires a bacterial strain but also

Table 17.2 Physical data of some commercial biopolyesters

	PLA Dow-Cargill (Nature Works)	PHBV Monsanto (Biopol D400G – HV = 7 mol%)	PCL Solvay (CAPA (680)	PEA Bayer (BAK 1095)	PBSA Showa (Bionolle 3000)	PBAT Eastman (Eastar bio 14766)
Density	1.25	1.25	1.11	1.07	1.23	1.21
Melting point (°C) ^a	152	153	65	112	114	110–115
Glass transition (°C) ^a	58	5	–61	–29	–45	–30
Crystallinity ^b (in percentage)	0–1	51	67	33	41	20–35
Modulus (MPa) (NFT 51-035)	2,050	900	190	262	249	52
Elongation at break (%) (NFT 51- 035)	9	15	>500	420	>500	>500
Tensile stress at break or max. (MPa) (NFT 51-035)	–	–	14	17	19	9
Biodegradation ^c (Mineralization in percentage)	100	100	100	100	90	100
Water permeability WVTR at 25°C (g/m ² /day)	172	21	177	680	330	550
Surface tension (γ) (mN/m)	50	–	51	59	56	53
γ _d (dispersive component)	37	–	41	37	43	43
γ _p (polar component)	13	–	11	22	14	11

Reproduced with permission (Bordes et al. 2009). Copyright of Elsevier

^aMeasured by DSC

^bDetermined on granules, before processing

^cAfter 60 days in controlled composting according to ASTM 5336

a carbon source (carbohydrates), a nitrogen source (yeast extract, peptides, etc.), and mineral elements to allow the growth of bacteria and the production of lactic acid. The lactic acid as-formed exists almost exclusively as L-lactic acid and leads to poly(L-lactic acid) (PLLA) with low molecular weight by polycondensation reaction. However, Moon et al. (2000, 2001) have proposed an alternative solution to obtain higher molecular weight PLLA by the polycondensation route.

In contrast, the chemical process could lead to various ratio of L- and D-lactic acid. Indeed, the chemical reactions leading to the formation of the cyclic dimer, the lactide, as an intermediate step to the production of PLA, could lead to macromolecular chains with L- and D-lactic acid monomers. This mechanism of ring-opening polymerization (ROP) from the lactide explains the formation of two enantiomers. This ROP route has

	Trade Name	Company
Agro-resources based polyesters:		
<i>Poly(lactic acid) (PLA)</i>		
	Natureworks Lacty Lacea Heplon CPLA PLA Eco Plastic Treofan PDLA Ecoloju Biomer L	Cargill (USA) Shimadzu (Japan) Mitsui Chemicals (Japan) Chronopol (USA) Dainippon Ink Chem. (Japan) Galactic/Total (Belgium) Toyota (Japan) Treofan (Netherland) Purac (Netherland) Mitsubishi (Japan) Biomer (Germany)
<i>Polyhydroxyalkanoate (PHA)</i>		
	(PHBV, PHB) (PHBV, PHB) (PHB, PHBV) (PHB, PHBV) (PHB, PHBV) (PHBHx, PHBO, PHBOd)	Biopol Mirel Biocycle Biomer P Enmat Nodax Monsanto (USA)* Metabolix/ADM (USA) PHB Industrial (Brazil) Biomer (Germany) Tianan (China) Procter & Gamble (USA)*
Petroleum-based polyesters:		
<i>Polycaprolactone (PCL)</i>		
	CAPA Tone	Solvay (Belgium) Union Carbide (USA)
<i>Polyesteramide (PEA)</i>		
	BAK	Bayer (Germany)*
<i>Aliphatic copolyesters (e.g., PBSA)</i>		
	Bionolle EnPol Skygreen Lunare SE	Showa Highpolymer (Japan) Ire Chemical Ild (Korea) SK Chemicals (Korea) Nippon shokubai (Japan)
<i>Aromatic copolyesters (e.g., PBAT)</i>		
	Eastar Bio Ecoflex Biomax Origo-Bi	Eastman Chemical (USA)* BASF (Germany) Dupont (USA) Novamont (Italy)

(*) These polyesters productions have been stopped.

Fig. 17.2 Structure, trade names, and suppliers of main commercially and available biodegradable polyesters. Reproduced with permission (Bordes et al. 2009). Copyright of Elsevier

the advantage of reaching high molecular weight polymers (Kaplan et al. 1993; Garlotta 2001; Albertsson and Varma 2002; Okada 2002) and allows the control of the PLA final properties by adjusting the proportions and the sequencing of L- and D-lactic acid units.

At present, due to its availability on the market and its low price (Vert et al. 1995; Sinclair 1996; Lunt 1998; Auras et al. 2004), PLA has one of the highest potential among biopolyesters, particularly for packaging (Sinclair 1996; Auras et al. 2004) and medical applications. For instance, Cargill has developed processes that use corn and other feedstock to produce different PLA grades (NatureWorks[®]) (Lunt 1998; Steinbuechel and Doi 2002). For this company, the actual production is estimated to be 50–60 kTons per year although the production capacity is given at 140 kTons. However, presently, it is the highest and worldwide production of biodegradable polyester. Its price was around €2/kg in 2010, but nowadays the cost has slightly increased. Different companies such as Mitsui Chemicals (Japan), Mitsubishi (Japan), Biomer (Germany), Shimadzu (Japan), Galactic-Total (Belgium), Toyota (Japan), Purac (Netherlands), Treofan (Netherlands), and Dainippon Ink Chemicals (Japan) produce smaller PLA outputs with different D/L ratios. Commercially available, we can find 100% PLLA which present a high crystallinity (C-PLA) and copolymers of PLLA and poly(D,L-lactic acid) (PDLLA) which are rather amorphous (A-PLA) (Bigg 1996; Perego et al. 1996; Steinbuechel and Doi 2002). The PLA can show crystalline polymorphism (Cartier et al. 2000) which can lead to different melting peaks (Martin and Averous 2001) with a main endotherm at 152°C for the PDLLA (see Table 17.2). Furthermore, PLA can be plasticized using oligomeric lactic acid (o-LA) (Martin and Averous 2001), citrate ester (Labrecque et al. 1997), or low molecular weight polyethylene glycol (PEG) (Jacobsen and Fritz 1999; Kranz et al. 2000; Martin and Averous 2001; Ljungberg et al. 2003). The effect of plasticization increases the chains mobility and then favors the PLA organization and crystallization. After plasticization, we obtain a crystallinity ranging between 20% and 30%. The PLA presents a medium water and oxygen permeability level (Van Tuil et al. 2000; Auras et al. 2004) comparable to polystyrene (Lehermeier et al. 2001). These different properties associated with its tunability and its availability favor its actual developments in different packaging applications (trays, cups, bottles, films, etc.) (Sinclair 1996; Steinbuechel and Doi 2002; Auras et al. 2004). McCarthy et al. (1999) showed that A-PLA presents a soil degradation rate much slower compared to PBSA. The PLA is presumed to be biodegradable although the role of hydrolysis vs. enzymatic depolymerization in this process remains open to debate (Bastioli 1998a, b). Regarding biodegradation in compost, adequate conditions are only found in industrial units with a high temperature (above 50°C) and a high relative humidity (RH%) to promote chain hydrolysis. According to Tuominen et al. (2002), PLA biodegradation does not exhibit any eco-toxicological effect.

Polyhydroxyalkanoates

Polyhydroxyalkanoates (PHAs) are naturally produced by microorganisms from various carbon substrates as a carbon or energy reserve. A wide variety of prokaryotic organisms (De Koning 1993; Madison and Huisman 1999) accumulate PHA from 30% to 80% of their cellular dry weight. Biotechnological studies revealed that

PHB is produced under balanced growth conditions when the cells become limited for an essential nutrient but are exposed to an excess of carbon (Doi 1990). Depending on the carbon substrates and the metabolism of the microorganism, different monomers, and thus (co)polymers, could be obtained (Zinn et al. 2001). The main polymer of the polyhydroxyalkanoates family is the polyhydroxybutyrate homopolymer (PHB), but different poly(hydroxybutyrate-*co*-hydroxyalkanoates) copolyesters exist such as poly(hydroxybutyrate-*co*-hydroxyvalerate) (PHBV) (see Fig. 17.2) or poly(hydroxybutyrate-*co*-hydroxyhexanoate) (PHBHx), poly(hydroxybutyrate-*co*-hydroxyoctanoate) (PHBO) and poly(hydroxybutyrate-*co*-hydroxyoctadecanoate) (PHBOD). With the progress in biotechnology, it is possible not only for recombinant bacteria (Madison and Huisman 1999), but also plants (Madison and Huisman 1999; Valentin et al. 1999; Poirier 2002) to produce such polymers. However, the recovery process, i.e., the extraction and purification steps, is decisive to obtain a highly pure PHA and often explains why such polymers are still expensive. Pure synthetic PHA can be produced by the ROP from butyrolactone and other lactones (Hori et al. 1993a, b; Kobayashi et al. 1995; Hori and Hagiwara 1996; Nobes et al. 1996; Juzwa and Jedlinski 2006). Thus, according to the synthesis route, we obtain different structures, isotactic with random stereosequences for the bacterial copolyesters and with partially stereoregular block for the synthetic copolyesters. Recently, Monsanto has developed genetic modification of plants to make them produce small quantities of PHB (Valentin et al. 1999; Asrar et al. 2000, 2001).

The PHB is a highly crystalline polyester (above 50%) with a high melting point, $T_m = 173\text{--}180^\circ\text{C}$, compared to the other biodegradable polyesters. Glass transition temperature (T_g) is around 5°C . The homopolymer shows a narrow window for the processing conditions. To ease the transformation, PHB can be plasticized with citrate ester, but the PHBV copolymer is more adapted for the process. A large range of bacterial copolymer grades had been industrially produced by Monsanto under the Biopol[®] trade mark, with HV contents reaching 20%. The production was stopped at the end of 1999. Metabolix bought Biopol[®] assets in 2001. Presently, Telles[™], a joint venture between Metabolix and Archer Daniels Midlands Company (ADM), has marketed the Mirel[™] product as a new biobased biodegradable plastic from corn sugar. ADM has begun to build the first plant in Clinton, Iowa (US) which will be able to produce 50,000 tons of resin per year. The startup is scheduled for late 2010.

Different small companies currently produce bacterial PHA, e.g., PHB Industrial (Brazil) produces PHB and PHBV (HV = 12%) 45% crystalline from sugar cane molasses (El-Hadi et al. 2002). The Biocycle[®] production is planned to be 4,000 tons/year in 2008 and then to be extended to 14,000 tons/year. In 2004, Procter & Gamble (US) and Kaneka Corporation (Japan) announced a joint development agreement for the completion of R&D leading to the commercialization of Nodax, a large range of polyhydroxybutyrate-*co*-hydroxyalkanoates (PHBHx, PHBO, PHBOD) (Noda et al. 2005). Although the industrial production was planned for 2006 with a target price around $\text{€}2/\text{kg}$, the production was stopped (Philip et al. 2007).

The production of PHA is intended to replace synthetic nondegradable polymers for a wide range of applications (Philip et al. 2007): packaging, agriculture, and also medicine (Williams et al. 1999; Zinn et al. 2001) because PHA are biocompatible. Figure 17.2 and Table 17.2 show the chemical structure and the properties of some PHBV, respectively. Material properties can be tailored by varying the HV content. An increase of the HV content induces an increase of the impact strength and a decrease of the melting temperature and glass transition (Amass et al. 1998), the crystallinity (Shogren 1997), the water permeability (Shogren 1997), and the tensile strength (Kotnis et al. 1995).

Besides, PHBV properties can evolve when plasticization occurs, e.g., with citrate ester (triacetin) (Kotnis et al. 1995; Shogren 1995). The polyhydroxyalkanoates, like the PLAs, are sensitive to the processing conditions. Under extrusion, we obtain a rapid diminution of the viscosity and the molecular weight due to macromolecular chain cleavage by increasing the shear level, the temperature, and/or the residential time (Ramkumar and Bhattacharya 1998). Regarding the biodegradable behavior, the kinetic of enzymatic degradation is variable according to the crystallinity, the structure (Karlsson and Albertsson 1998; El-Hadi et al. 2002), and then to the processing history (Parikh et al. 1998). Bacterial copolyesters biodegrade faster than homopolymers (Dos Santos et al. 2004) and synthetic copolyesters (Chiellini and Solaro 1996).

17.2.2.2 Petroleum-Based Polyesters

A large number of biodegradable polyesters are based on petroleum resources, obtained chemically from synthetic monomers (Vert et al. 1995; Bigg 1996; Sinclair 1996; Lunt 1998; Albertsson and Varma 2002; Okada 2002; Steinbuchel and Doi 2002). According to the chemical structures (see Fig 17.2), we can distinguish (see Table 17.2) homopolymers (polycaprolactone, etc.), aliphatic or aromatic copolyesters. All these polyesters are soft at room temperature.

Polycaprolactone

Poly(ϵ -caprolactone) (PCL) is usually obtained by ring opening polymerization (ROP) of ϵ -caprolactone in the presence of metal alkoxides (aluminum isopropoxide, tin octoate, etc.) (Chiellini and Solaro 1996; Albertsson and Varma 2002; Okada 2002). The PCL is widely used as a PVC solid plasticizer or for polyurethane applications, as polyols. But, it also finds some applications based on its biodegradable character in domains such as biomedicine (e.g., drugs controlled release) and environment (e.g., soft compostable packaging). Different commercial grades are produced by Solvay (CAPA[®] – Solvay has sold this activity in 2008 to Perstorp AB – Sweden), Union Carbide (Tone[®] – Union Carbide has transferred this activity to Dow Chemicals. Then, the production has been stopped), and Daicel (Celgreen[®]). Figure 17.2 and Table 17.2 show, the chemical structure and the properties of this

polyester, respectively. The PCL shows a very low T_g (-61°C) and a low melting point (65°C), which could be a handicap in some applications. Therefore, PCL is generally blended (Bastioli et al. 1995; Bastioli 1998a, b; Avérous et al. 2000) or modified [e.g., copolymerization, crosslinking (Koenig and Huang 1994)]. Tokiwa and Suzuki (1977) have discussed the hydrolysis of PCL and biodegradation by fungi. They have shown that PCL can be easily enzymatically degraded. According to Bastioli (1998a, b), the biodegradability can be clearly claimed but the homopolymer hydrolysis rate is very low. The presence of polysaccharides can significantly increase the biodegradation rate of PCL (Bastioli et al. 1995).

Biodegradable Aliphatic Copolyesters

A large number of aliphatic copolyesters are biodegradable copolymers based on petroleum resources. They are obtained by the combination of diols such as 1,2-ethanediol, 1,3-propanediol, or 1,4-butanediol and dicarboxylic acids like adipic, sebacic, or succinic acid. Showa Highpolymer (Japan) has developed a large range of polybutylene succinate (PBS) obtained by polycondensation of 1,4-butanediol and succinic acid. Polybutylene succinate/adipate (PBSA), shown in Fig. 17.2, is obtained by addition of adipic acid. These copolymers are commercialized under the Bionolle[®] trademark (Steinbuchel and Doi 2002). Table 17.2 shows the properties of such biopolyesters. Ire Chemical (Korea) commercializes exactly the same kind of copolyesters under EnPol[®] trademark. Skygreen[®], a product from SK Chemicals (Korea), is obtained by polycondensation of 1,2-ethanediol, 1,4-butanediol with succinic and adipic acids (Lee et al. 2002). Nippon Shokubai (Japan) also commercializes an aliphatic copolyester under Lunare SE[®] trademark. These copolyesters' properties depend on the structure (Muller et al. 1998), i.e., the combination of diols and diacids used. These products' biodegradability depends also on the structure. The addition of adipic acid, which decreases the crystallinity (Yokota and Marechal 1999) tends to increase the compost biodegradation rate (Fujimaki 1998). According to Ratto et al. (1999), the biodegradation results demonstrate that although PBSA is inherently biodegradable, the addition of starch filler significantly improves the rate of degradation.

Biodegradable Aromatic Copolyesters

Compared to totally aliphatic copolyesters, aromatic copolyesters are often based on terephthalic acid. Figure 17.2 and Table 17.2 show, the chemical structure and the properties of such products, respectively. (e.g., Eastar Bio[®] from Eastman). Besides, BASF and DuPont commercialize aromatic copolyesters under Ecoflex[®] (Steinbuchel and Doi 2002) and Biomax[®] trademarks, respectively. Biomax[®] shows a high terephthalic acid content that modifies some properties such as the melting temperature (200°C). But, according to Muller et al. (1998), an increase of terephthalic acid content tends to decrease the degradation rate. Ecoflex[®] biodegradation has been analyzed by Witt et al. (2001). They concluded that there is no

indication for an environmental risk (ecotoxicity) when aliphatic–aromatic copolyesters of the Ecoflex[®] type are introduced into composting processes.

17.3 Biocomposites Based on Biodegradable Thermoplastic Polyester and Lignocellulose Fibers

17.3.1 Generalities

Biocomposites are obtained by the association of macrofillers (mainly lignocellulose fibers) into a biomatrix. For short-term applications, biocomposites based on biodegradable polymers present strong advantages and a large number of papers have been published on this topic. Although, few publications are based on agro-polymer matrices such as plasticized starch or proteins, most of the published studies on biocomposites are based on biopolyesters (biodegradable polyesters) matrices, for instance, with PHA. One of the main advantages of PHA for biocomposite applications is its polar character, because PHA shows better adhesion to lignocellulose fibers compared to conventional polyolefins (Shanks et al. 2004). Also, we can find a large number of papers based on PHA biocomposites. The addition of cellulose fibers and different fillers has often been proposed as a solution for increased mechanical performance and toughness of PHB and PHBV (Gatenholm et al. 1992; Avella et al. 1993, 2007a, b; Mohanty et al. 2000; Shanks et al. 2004; Cyras et al. 2007; Barkoula et al. 2010). In terms of crystallization and thermal behavior, no significant effect of cellulose on PHB crystallinity was reported. A slight increase of T_g (glass-transition temperature) and delay in the crystallization process was observed (Avella et al. 1993). The presence of cellulose filler fibers increased the rate of PHBV crystallization, due to a nucleating effect, while the thermal parameters such as crystallinity content remained unchanged. Studies on the crystallization behavior of PHB/kenaf fiber biocomposites showed that the nucleation of kenaf fibers affected the crystallization kinetics of the PHB matrix (Avella et al. 2007a, b). Differences in the effect of cellulose fibers on the crystallization process have been attributed to the lignin content at the surface/interface of the cellulose fiber. The increase of the HV content, the addition of compatibilizers, and the rise of fiber content on PHA-based composites influenced the mechanical performance of the corresponding biocomposites. The addition of HV led to a reduction in the stiffness of the PHB but to an increased elongation at break. In reinforced PHBV, a 50–150% enhancement in tensile strength, 30–50% in bending strength, and 90% in impact strength have been reported (Mohanty et al. 2000). The addition of varying HV content to PHB polymers improved the toughness of the natural fiber composites and increased the ductility, but lowered the crystallization rate. It has been suggested, however, that the combination of coupling agents and HV improved the storage modulus and led to a reduction in the $\tan \delta$ (Shanks et al. 2004) due to an improvement in the interfacial bonding between PHB and the fibers

and an increase in transcrystallinity near the fiber interfaces. The addition of cellulose fibers led to some improvement in tensile strength and stiffness, but the composites remained brittle (Gatenholm et al. 1992). At low content, the incorporation of cellulose fibers lowered the stiffness; however, higher amounts of cellulose fibers greatly improved the mechanical properties of PHB. For biocomposites based on cellulose fibers and PHB, the effect of fiber length, surface modification on the tensile and flexural properties have been investigated. Results on PHB reinforced with straw fibers have been published (Avella et al. 1993). Fracture toughness values of composite materials containing 10–20 wt.% straw fibers were higher than those of pure PHB, while biocomposites containing 30–50 wt.% straw fibers presented almost the same values as neat PHB. With the addition of interface modifiers, the interfacial shear strength has also been improved (Wong et al. 2007). The PHB with wood flour and plasticizers presents modest increase in tensile strength, while some improvement in terms of thermal stability was demonstrated.

The PLA has been associated with a great number of lignocellulose fillers such as paper waste fibers, wood flour, kenaf (Nishino et al. 2003), bamboo (Lee et al. 2004), papyrus (Nishino et al. 2007), jute (Plackett et al. 2003), or flax fibers (Van de Velde and Kiekens 2002).

Some authors have also tested flax (Van de Velde and Kiekens 2002) or sisal (Ruseckaite and Jimenez 2003) with PCL.

Aliphatic copolyesters have been used with several cellulosic fibers (Wollerdorfer and Bader 1998), bamboo fibers (Nakamura et al. 2006) or flax, oil palm, jute, or ramie fibers (Wollerdorfer and Bader 1998).

Aromatic copolyesters have been associated with wheat straw fillers. Some results on such systems are presented in previous publications on biodegradable polymers (Le Digabel et al. 2004; Averous and Le Digabel 2006; Le Digabel and Averous 2006). These authors have shown a good compatibility between the lignocellulose fillers and the biodegradable matrix without compatibilizers or special fillers treatment. This last system and the main corresponding results will be developed in the next chapter.

17.3.2 The Case of Biocomposites Based on Copolyesters

17.3.2.1 Framework

This section is focused on the presentation of results based on biocomposites which have been elaborated with different lignocellulose fillers displaying various lignin contents, different lengths and contents. These fillers are combined with biodegradable aromatic copolyester, polybutylene adipate-*co*-terephthalate (PBAT). The lignocellulose fillers (LF) are a by-product of an industrial wheat straw fractionation based on the extraction and the recovery of most of the hemicellulose sugars. Table 17.1 shows that, compared to wheat straw, LF present higher lignin content (30%)

and a lower cellulose/lignin ratio, 1.9 compared to 3.2 for wheat straw. These low cost fillers (LF) are treated to reduce the lignin content and then to increase the cellulose concentration with the aim to analyze the impact of the lignin content variation on the biocomposites properties. By varying the extraction conditions, several fillers fractions displaying different lignin contents are obtained. To elaborate the biocomposites, the treated lignocellulose fillers (TLF) are mixed with polybutylene adipate-*co*-terephthalate (PBAT), a biodegradable aromatic copolyester. The influence of the lignin extraction method and the impact of the lignin content on the fillers–matrix compatibility and on the final properties of these materials have been investigated. In this case, the lignocellulosic fillers (LCF) are by-products of an industrial fractionation of wheat straw. The use of low cost biofillers is a way to reduce the cost of the end product with improved properties.

17.3.2.2 Materials and Biocomposites Processing

The matrix is a biodegradable and aromatic copolyester (polybutylene adipate-*co*-terephthalate, PBAT), from Eastman (EASTAR BIO Ultra Copolyester 14766). Copolyester chemical structure is given in Table 17.2. This copolyester is soluble at room temperature in different solvents such as THF, CH₂Cl₂, or CHCl₃. Determined by ¹HNMR, PBAT composition is 43% of butylene terephthalate and 57% of butylene adipate. Determined by size exclusion chromatography (SEC), molecular weight (M_w) and polydispersity index (IP) are 48,000 and 2.4, respectively. Melt flow index (MFI) is 13 g/10 min at 190°C/2.16 Kg. PBAT density is 1.27 g/cm³ at 23°C.

The lignocellulosic materials used as fillers are a by-product of an industrial fractionation process of wheat straw (ARD, Pomacle – France). This product is obtained from a multistep process. Two hundred and fifty kilograms of chopped wheat straw (10–15 cm) are introduced into a 1 m³ reactor under high shearing to promote fibers fragmentation. Wheat straw is hydrolyzed in acid medium (H₂SO₄, 0.1 N) under pressure (3.5 bars) at 130°C, during 90 min. The soluble fraction (mostly hemicellulose sugars) is filtered and refined for further applications. The insoluble fraction, the by-product called lignocellulose filler (LCF) is neutralized, washed, and dried with a turbo-dryer (Alpha Vomm – Italy). The process yield from the wheat straw to the LCF is 33%. The dried LCF filler is sieved with a 1-mm grid to eliminate the biggest fillers (20 wt.%). This product is named LCF₀₋₁. According to Fig. 17.3, this last fraction is sieved with a 0.1-mm grille and then two fractions are obtained, LCF_{0.1-1} and LCF_{0-0.1}.

Prior to blending, fillers and thermoplastic granules are dried in an air-circulating oven at 80°C, for up to 4 h and 1 h, respectively. PBAT and varying amounts of LCF are directly added in the feeding zone of a single screw extruder (SCAMIA S 2032, France) equipped with a specific designed torpedo-like element to promote high shearing and mixing. The screw diameter (D) and the L/D ratio are 30 mm and 26/1, respectively. Typically, for technical reasons due to the quality of the filler dispersion, the maximum LCF content is 30–40 wt.%. Extrusion temperature is 135°C.

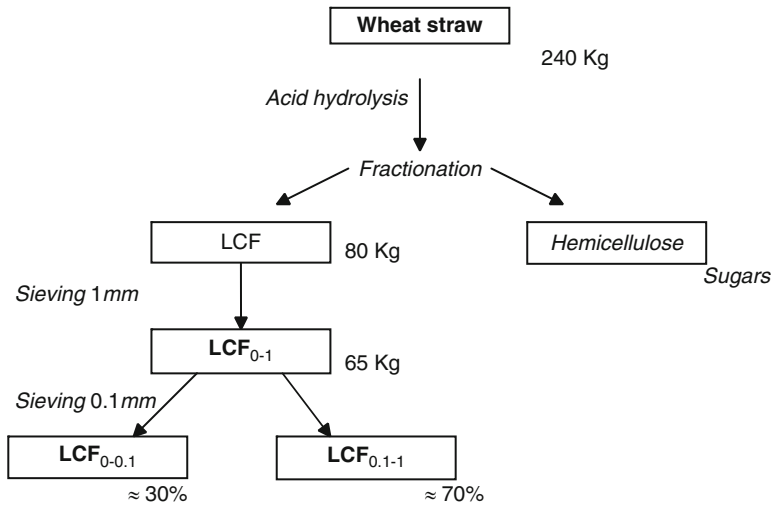


Fig. 17.3 Elaboration of lignocellulose fillers fractions: wheat straw fractionation schema. Reproduced with permission (Averous and Le Digabel 2006). Copyright of Elsevier

Three-millimeter-diameter strands are pelletized after air cooling. These granules are extruded once again in the same condition to improve the filler dispersion into the matrix.

Standard dumbbell specimens (NFT 51-034-1981) are molded with an injection molding machine (DK codim NGH 50/100) in a temperature range between 115°C and 130°C, with an injection pressure and speed of 500 bars and 50 mm/s. Holding pressure and times are 500 bars and 12 s (PBAT) or 14s (biocomposites), respectively. Mold temperature is 30°C. The total cooling time is 22 s (neat PBAT) and 24 s. The injection-molded specimens are approximately 10-mm wide and 4-mm thick on the central part (NFT 51-0.34 1981).

17.3.2.3 Analysis of the Lignocellulose Fillers

Wheat straw is composed of different tissues that are more or less destroyable during the process. Leaves, internodes, and the parenchyma (see Fig. 17.4) are more particularly destroyable. The sclerenchyma and the fibers networks are more resistant.

Table 17.1 presents the chemical composition of different vegetable fibers. Compared to the other fibers, wheat straw shows rather low cellulose content, a high lignin composition, but also a high ash content linked to a high silica fraction. Silica is mainly located on the leaves, 12% of ash in the leaves compared to, for example, 6% in the internodes. Average value is 7–8% of ash in the straw.

Table 17.1 also shows the compositions of the different LCF fractions. We can show the effect of the wheat straw treatment. The LCF shows higher lignin content.

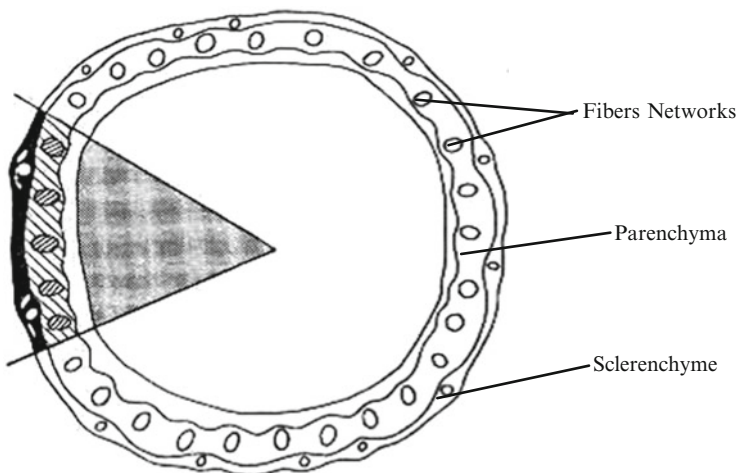


Fig. 17.4 Cross-section of a wheat straw stem with the corresponding tissues

Assuming that the lignin which is insoluble is poorly affected by the hydrolysis process, the lignin quantity (in weight) stays constant from the initial wheat straw to the LCF_{0-1} . Cellulose and hemicellulose contents have been decreased under the hydrolysis treatment. Around 40% of the total cellulose and 85% of the hemicellulose have been eliminated during the process and collected mostly in the soluble fraction (see Table 17.1). We can notice that the process yield of hemicellulose sugars recovery is not total. By HPLC analysis, the hemicellulose composition can be given. Hemicellulose is composed with 96% of xylose, 3% of arabinose, and 1% of mannose.

In Table 17.1, $LCF_{0-0.1}$ shows intermediate values between $LCF_{0-0.1}$ and $LCF_{0.1-1}$. Comparing $LCF_{0-0.1}$ and $LCF_{0.1-1}$, we can notice that silica (ash) is more particularly present in the finest fraction. Then, $LCF_{0-0.1}$ must be composed more particularly by pieces of chopped leaves, which present higher silica content.

Figure 17.5 shows the size distributions of the different fractions (LCF_{0-1} , $LCF_{0-0.1}$, and $LCF_{0.1-1}$). The fillers size distributions have been determined by light scattering with a particles size analyzer. LCF_{0-1} presents a double granulometric distribution, a population centered on 50 μm and another one on 700 μm . After sieving, we obtain two log-normal curves, i.e., two homogeneous populations. A first distribution is centered on 50 μm and another one on 630 μm .

17.3.2.4 Biocomposites Thermal Properties

The TGA has been carried out to evaluate the thermal behavior of different biocomposites with filler content from 0 to 40 wt. Table 17.3 shows the main results. Till more than 10 wt.%, we cannot observe a transition linked to the fillers. At 300°C, the variations of weight losses are due to the water uptake at equilibrium,

Fig. 17.5 Granulometric distributions of the different fillers (LCF_{0-1} , $LCF_{0-0.1}$, and $LCF_{0.1-1}$). Reproduced with permission (Averous and Le Digabel 2006). Copyright of Elsevier

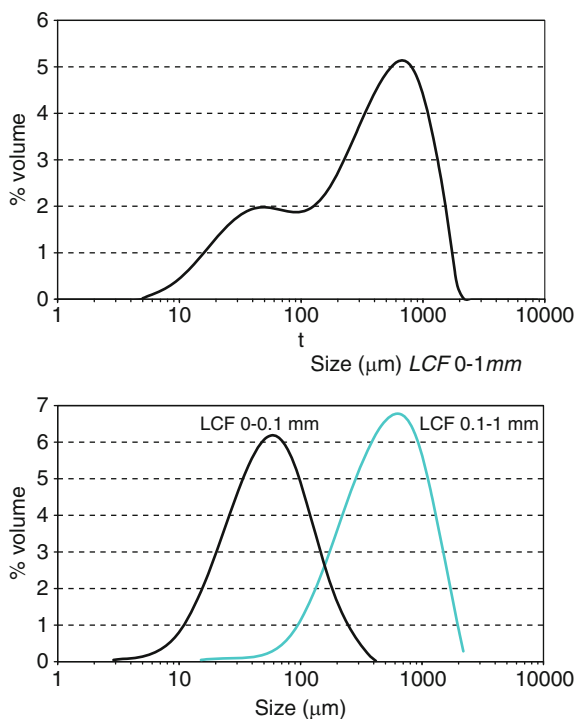


Table 17.3 Main TGA results

	Transition 1 -Filler-		Transition 2 -Matrix-		Loss of weight at 300°C
	Onset 1	Degradation temperature Maximum 1 of DTG	Onset 2	Degradation temperature Maximum 2 of DTG	
PBAT	No visible “transition”		382°C	410°C	1%
LCF-10%			15%	60%	3%
			384°C	411°C	
LCF-30%	323°C	364°C	15%	59%	5%
	6%	17%	398°C	413°C	
LCF-40%	324°C	357°C	61%	63%	7%
	10%	22%	401°C	421°C	
			48%	70%	

Reproduced with permission (Averous and Le Digabel 2006). Copyright of Elsevier
The weight losses (%) are given below the corresponding temperatures

which is higher for lignocellulosic fillers compared to PBAT. Then the weight loss increases with the filler content. This result can be obtained by the addition of the matrix water uptake (1%) and the filler water uptake (13–14%) corrected with the corresponding contents. Table 17.3 shows the matrix degradation temperature and

the corresponding onset increase with the filler content. These latter results are in agreement with Ruseckaite and Jimenez (2003) studies based on PCL matrix (Ruseckaite and Jimenez 2003) or with a previous work based on plasticized starch (Averous and Boquillon 2004). In the same way, the filler degradation temperature (around 360°C) is consistent with values obtained by various authors on lignocellulosic fillers (Ruseckaite and Jimenez 2003; Averous and Boquillon 2004). Besides, we can show that LCF fillers are thermally stable up to 200°C. The degradation behavior of these fillers is then compatible with the plastic processing temperatures.

Table 17.4 gives the main thermal characteristics. Compared to most thermoplastics, T_g and T_f are rather low and then processing temperature are not high, around 130°C. We can notice that this copolymer presents a single transition for T_g , T_c , and T_m due to the repartition of the different sequences. These temperatures are intermediate between the data of both homopolymers, polybutylene adipate and polybutylene terephthalate (Chang and Tsai 1994). At room temperature, PBAT is on the rubber plateau, i.e., between T_g and T_f . Without knowing the theoretical enthalpy for 100% crystalline PBAT, we have used the approach presented by Herrera et al. (2002). Theoretical enthalpy is calculated by the contribution of the different chain groups. The contributions of ester, methylene, and *p*-phenylene groups are -2.5 kJ/mol, 4.0 kJ/mol, and 5.0 kJ/mol, respectively. The calculated value ($\Delta H_{100\%}$) is equal to 22.3 kJ/mol, i.e., 114 J/g. The degree of crystallinity (in percentage) is estimated with (17.3). PBAT crystallinity is rather low, around 12%. We can notice that the ΔC_p gap at the glass transition is rather small. The different thermodynamic values are consistent with data obtained by other authors (Herrera et al. 2002).

Table 17.4 presents the different values obtained by DSC determinations on PBAT with increasing fillers contents. As shown in Table 17.4, the addition of increasing amounts of LCF results in a slight but significant increase in T_g of PBAT, from -39.3 to -35.7°C. According to Avella et al. (2000), this trend may be explained by intermolecular interactions between the hydroxyl groups of the fillers and the carbonyl groups of the PBAT ester functions. These hydrogen bonds would probably reduce the polymer mobility and then increase T_g values. The PBAT/LCF biocomposites do not show any significant variation of T_f , in agreement with the data of Avella et al. (2000). We have shown by SEC that the molecular weight variation is insignificant. We have not detected any chain degradation phenomena under the thermo-mechanical treatment. We can notice that crystallization and fusion heats decrease. This is due to a dilution effect linked to the fillers incorporation into the matrix. But, when the enthalpy is corrected by the filler content these values stay rather constant, e.g., $\Delta H_c'$ data (Table 17.4). The corrected heats of crystallization and fusion are equivalent; we have not significant crystallization during the second scan. The heats of crystallization and fusion are equal to 13–14 J/g, i.e., around 2.6 kJ/mol. The dilution effect seems also to affect ΔC_p which tends to decrease with fillers incorporation. We can notice that an increase in the amount of LCF does not affect the degree of PBAT crystallinity which stays constant, at around 12%. The incorporation of LCF induces a slight but significant

Table 17.4 Main DSC results

Samples	T_g (°C)	ΔC_p (W, g^{-1})	T_c (°C)	T_i (°C)	ΔH_c (J, g^{-1})	$\Delta H_c'$ (J, g^{-1})	T_f (°C)	ΔH_f (J, g^{-1})	X_c (%)
PBAT	-39.3 ± 0.3	0.038 ± 0.001	68.0 ± 1.0	84 ± 1	13.5 ± 0.2	13.5 ± 0.2	113.9 ± 0.5	13.9 ± 0.3	12
PBAT-10%	-38.2 ± 0.2	0.028 ± 0.002	68.0 ± 0.4	87 ± 1	11.3 ± 0.1	12.6 ± 0.1	113.2 ± 0.7	11.7 ± 0.2	11
PBAT-20%	-36.6 ± 0.2	0.020 ± 0.001	71.0 ± 0.3	90 ± 1	11.4 ± 0.2	14.2 ± 0.3	113.8 ± 0.5	11.2 ± 0.4	12
PBAT-30%	-35.7 ± 0.2	0.010 ± 0.001	70.7 ± 0.3	91 ± 1	9.3 ± 0.5	13.3 ± 0.7	114.2 ± 0.6	10.0 ± 0.3	12

Reproduced with permission (Averous and Le Digabel 2006). Copyright of Elsevier

increase in T_c . This is probably linked to the reduction of the polymer mobility. The beginning of the crystallization (T_i) during the cooling tends to increase with increasing fillers content. The fillers modify the crystallization by increasing the number of nucleating sites.

17.3.2.5 Biocomposites Mechanical Properties

Figure 17.6 shows the tensile mechanical properties of biocomposites based on different fillers (LCF_{0-1} , $LCF_{0-0.1}$, and $LCF_{0.1-1}$) with different content (from 0 to 30 wt.%). Stress–strain evolutions show that PBAT is at room temperature a ductile material with a high elongation at break (ϵ_b), more than 200%. This is consistent with T_g and T_f values.

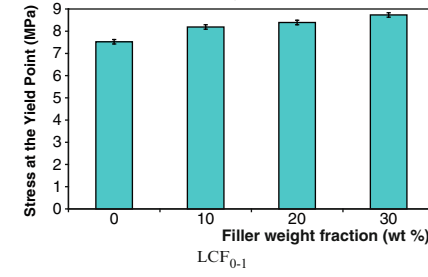
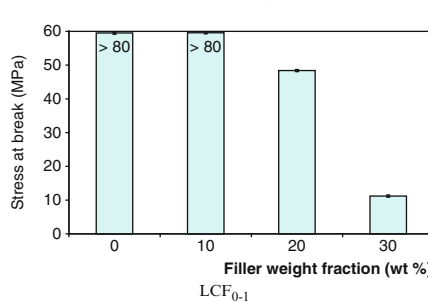
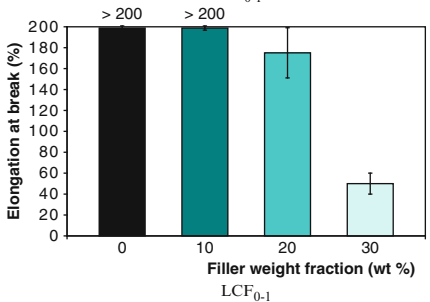
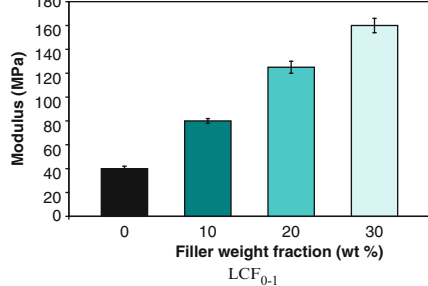
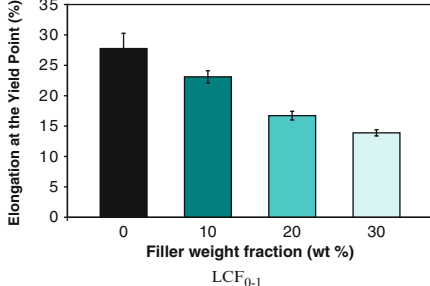
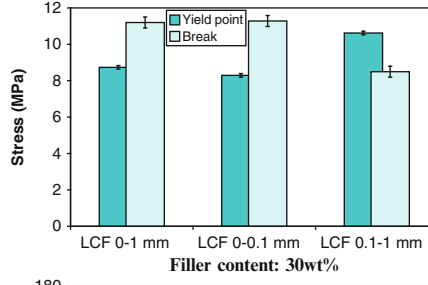
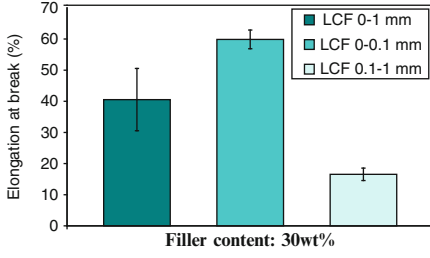
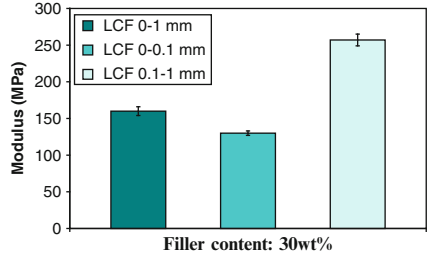
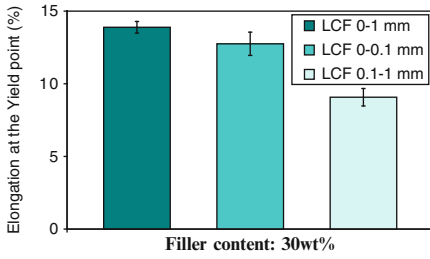
Concerning the modulus evaluation of the fillers is always problematic. The modulus has been evaluated. Different composites had been processed with increasing LCF_{0-1} content. The fillers modulus has been estimated by fitting a semiempirical Halpin-Tsai model on the evolution of the composites Young's modulus as a function of fillers volume fraction. By extrapolation at 100% of fillers, we obtain the filler modulus which is estimated at 6.7 GPa. This value is coherent with wheat straw data given in the literature (Hornsby et al. 1997; Kronbergs 2000).

Effect of the Fillers Size

Figure 17.6 shows, the variation of the modulus and the true values of ϵ_Y , ϵ_b , σ_Y , and σ_b respectively ($Y =$ at the yield point, $b =$ at break) for the different fillers, fractions, and contents. The first four graphs present the mechanical behavior of LCF_{0-1} , $LCF_{0-0.1}$, and $LCF_{0.1-1}$ based biocomposites reinforced at 30 wt.%. These composites show a common behavior compared to equivalent reinforced thermoplastics. The LCF fractions act as reinforcing materials. By adding fillers, we obtain strong evolutions of the mechanical properties compared to the neat matrix, e.g., we increase the moduli of a magnitude order between 3.3 and 6.4 times. We can see that by increasing the filler size, we obtain both modulus and yield stress increases but also a decrease of ϵ_Y , ϵ_b , and σ_b . Concerning the modulus and the elongation at break, LCF_{0-1} shows intermediate values between $LCF_{0-0.1}$ and $LCF_{0.1-1}$ data. The smallest fraction ($LCF_{0-0.1}$) which is not the major fraction seems to drive LCF_{0-1} properties for the elongation at the yield point and the different tensile stresses. In any case, the biggest fraction ($LCF_{0.1-1}$) fully drives the LCF_{0-1} tensile properties.

Effect of the Fillers Content

To estimate the effect of the fillers, composite/matrix ratios are calculated from tensile tests results. In Fig. 17.6 are shown, with the last five graphs, different



variations of mechanical parameters versus the fillers volume fraction for LCF_{0-1} . Volume fractions (ϕ) are determined from the fractions in weight (ww) according to (17.1), using the density of each component (d). The LCF density is 1.45 g/cm^3 . This value has been determined by pycnometry measurements on 10, 20, and 30 wt.% LCF_{0-1} biocomposites. This data is in agreement with cellulose and lignin densities.

$$\varphi_i = \frac{ww_i/d_i}{\sum_i ww_i/d_i}. \quad (17.1)$$

Percolation Effect and Moduli Modeling

Figure 17.7 shows that the moduli slope increases with the filler content. According to the literature, the percolation threshold obtained by 2D/3D simulations (Favier et al. 1997) for such filler length is around 10 wt.%. But the influence on the modulus of this percolation threshold is too low to be taken into account on a model contrary to, e.g., nanocomposite systems (Favier et al. 1997) where the impact of the threshold on the modulus is higher.

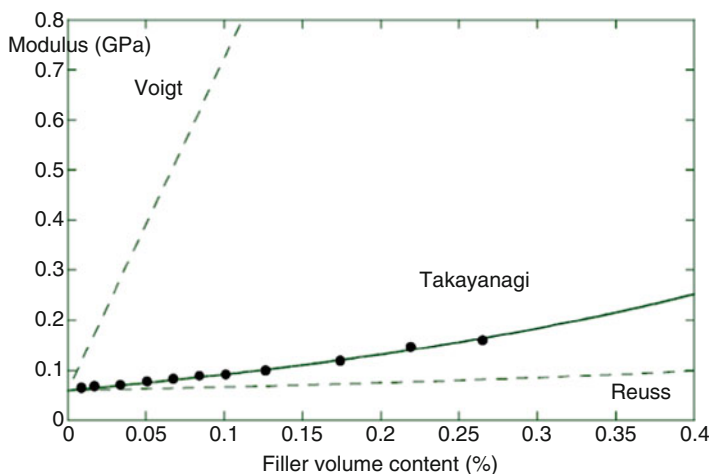


Fig. 17.7 Fittings on the evolution of the modulus of LCF_{0-1} -based biocomposites versus filler volume fraction content (Takayanagi, Voigt and Reuss models). Reproduced with permission (Averous and Le Digabel 2006). Copyright of Elsevier

Fig. 17.6 Tensile mechanical properties – Impact of the filler (LCF_{0-1} , $LCF_{0-0.1}$, and $LCF_{0.1-1}$) with different content (from 0 to 30 wt.%). Reproduced with permission (Averous and Le Digabel 2006). Copyright of Elsevier

To fit and to estimate the modulus evolution, different simple models have been tested such as the models of Voigt (17.2), Reuss (17.3), and Takayanagi (17.4). The composite modulus (E_c) is determined from E_f and E_m which are the filler and the matrix moduli, respectively.

The lowest and the highest moduli estimations are given by the serial model from Reuss ($E_{c(R)}$) and by the parallel model from Voigt ($E_{c(V)}$), respectively. The modulus value should be comprised between these two boundaries.

$$E_{c(V)} = \varphi_m E_m + \varphi_f E_f, \quad (17.2)$$

$$\frac{1}{E_{c(R)}} = \frac{\varphi_m}{E_m} + \frac{\varphi_f}{E_f}. \quad (17.3)$$

Takayanagi's model is a phenomenological model obtained by combination of serial and parallel models. The composite modulus ($E_{c(T)}$) is determined by (17.4) with λ , an adjustment parameter.

$$E_{c(T)} = (1 - \lambda)E_m + \frac{\lambda}{\frac{1-\varphi_f}{E_m} + \frac{\varphi_f}{E_f}}. \quad (17.4)$$

Figure 17.7 shows that Takayanagi's equation seems to be an excellent model to predict the modulus evolution, on the range 0–30 wt.% of filler. The parameter (λ) has been determined by adjustment at 4.5. Reuss and Voigt's models are not well adapted to estimate correctly the composite moduli. This is because the matrix and the fillers mechanical characteristics are too different. But, we can show that the composite moduli are comprised between both boundaries, $E_{c(R)}$ and $E_{c(V)}$.

17.4 Conclusion

Biocomposites usefulness is no longer in question and more and more reports are focused on applicative aspects in the environment, packaging, agriculture devices, biomedical fields, etc. Moreover, because industrials were concerned about sustainable developments and a controlled end of life, production cost of biopolymers goes on decreasing which will allow strong developments of biopolymer-based materials. Therefore, these materials will be technically and financially competitive towards synthetic polymer-based composites. Then, this class of material opens a new dimension for plastic industry for a better sustainable development.

Future research will address some actual issues such as the difficulty sometimes to disperse the natural filler with some biopolyesters, to achieve excellent filler/matrix compatibility, and to decrease the impact of the thermo-mechanical treatment on the compounds.

References

- Albertsson A-C, Varma IK (2002) Aliphatic polyesters: synthesis, properties and applications. *Adv Polym Sci* 157:1–40
- Amass W, Amass A, Tighe B (1998) A review of biodegradable polymers: uses, current developments in the synthesis and characterization of biodegradable polyesters, blends of biodegradable polymers and recent advances in biodegradation studies. *Polym Int* 47:89–144
- Asrar J, Mitsky TA, Shah DT (2000) Polyhydroxyalkanoates of narrow molecular weight distribution prepared in transgenic plants. Monsanto Company, St Louis, MO
- Asrar J, Mitsky TA, Shah DT (2001) Polyhydroxyalkanoates of narrow molecular weight distribution prepared in transgenic plants. Monsanto Company, St Louis, MO
- Auras R, Harte B, Selke S (2004) An overview of polylactides as packaging materials. *Macromol Biosci* 4:835–864
- Avella M, Martuscelli E, Pascucci B et al (1993) A new class of biodegradable materials: poly-3-hydroxy-butyrates/steam exploded straw fiber composites. I. Thermal and impact behavior. *J Appl Polym Sci* 49:2091–2103
- Avella M, Rota GL, Martuscelli E et al (2000) Poly(3-hydroxybutyrate-co-3-hydroxyvalerate) and wheat straw fibre composites: thermal, mechanical properties and biodegradation behaviour. *J Mater Sci* 35:829–836
- Avella M, Bogoeva-Gaceva G, Buzǎrovska A et al (2007a) Poly(3-hydroxybutyrate-co-3-hydroxyvalerate)-based biocomposites reinforced with kenaf fibers. *J Appl Polym Sci* 104: 3192–3200
- Avella M, Bogoeva-Gaceva G, Buzǎrovska A et al (2007b) Poly(3-hydroxybutyrate-co-3-hydroxyvalerate)-based biocomposites reinforced with kenaf fibers. *J Appl Polym Sci* 104: 3192–3200
- Averous L (2008) Poly(lactic acid): synthesis, properties and applications. In: Belgacem N, Gandini A (eds) *Monomers, oligomers, polymers and composites from renewable resources*. Elsevier, Amsterdam
- Averous L, Boquillon N (2004) Biocomposites based on plasticized starch: thermal and mechanical behaviours. *Carbohydr Polym* 56:111–122
- Averous L, Le Digabel F (2006) Properties of biocomposites based on lignocellulosic fillers. *Carbohydr Polym* 66:480–493
- Averous L, Moro L, Dole P et al (2000) Properties of thermoplastic blends: starch-polycaprolactone. *Polymer* 41:4157–4167
- Barkoula NM, Garkhail SK, Peijs T (2010) Biodegradable composites based on flax/polyhydroxybutyrate and its copolymer with hydroxyvalerate. *Ind Crops Prod* 31:34–42
- Bastioli C (1998a) Biodegradable materials – present situation and future perspectives. *Macromol Symp* 135:193–204
- Bastioli C (1998b) Properties and applications of mater-bi starch-based materials. *Polym Degrad Stab* 59:263–272
- Bastioli C, Cerutti A, Guanella I et al (1995) Physical state and biodegradation behavior of starch-polycaprolactone systems. *J Environ Polym Degrad* 3:81–95
- Bigg DM (1996) Effect of copolymer ratio on the crystallinity and properties of poly(lactic acid) copolymers. *J Eng Appl Sci* 2:2028–2039
- Bledzki AK, Gassan J (1999) Composites reinforced with cellulose based fibres. *Prog Polym Sci* 24:221–274
- Bordes P, Pollet E, Averous L (2009) Nano-biocomposites: Biodegradable polyester/nanoclay systems. *Prog Polym Sci* 34:125–155
- Cartier L, Okihara T, Ikada Y et al (2000) Epitaxial crystallization and crystalline polymorphism of polylactides. *Polymer* 41:8909–8919
- Chandra R, Rustgi R (1998) Biodegradable polymers. *Prog Polym Sci* 23:1273–1335
- Chang SJ, Tsai HB (1994) Copolyesters. 7. Thermal transitions of poly(butylene terephthalate-co-isophthalate-co-adipate)S. *J Appl Polym Sci* 51:999–1004

- Chiellini E, Solaro R (1996) Biodegradable polymeric materials. *Adv Mater* 8:305–313
- Cyras VP, Comisso MS, Mauri AN et al (2007) Biodegradable double-layer films based on biological resources: polyhydroxybutyrate and cellulose. *J Appl Polym Sci* 106:749–756
- De Koning GJM (1993). Prospects of bacterial poly[(R)-3-hydroxyalkanoates]. Center for Polymers and Composites (CPC), Eindhoven University of Technology, Eindhoven
- Doi Y (1990) *Microbial polyesters*. Wiley, New York
- Dos Santos RD, Calil MR, Fassina Guedes CDG et al (2004) Biodegradability of thermally aged PHB, PHB-V, and PCL in soil compostage. *J Polym Environ* 12:239–245
- El-Hadi A, Schnabel R, Straube E et al (2002) Correlation between degree of crystallinity, morphology, glass temperature, mechanical properties and biodegradation of poly(3-hydroxyalkanoate) PHAs and their blends. *Polym Test* 21:665–674
- Favier V, Dendievel R, Canova G et al (1997) Simulation and modeling of three-dimensional percolating structures: case of a latex matrix reinforced by a network of cellulose fibers. *Acta Mater* 45:1557–1565
- Fujimaki T (1998) Processability and properties of aliphatic polyesters, 'Bionolle', synthesized by polycondensation reaction. *Polym Degrad Stab* 59:209–214
- Garlotta D (2001) A literature review of poly(lactic acid). *J Polym Environ* 9:63–84
- Gatenholm P, Kubát J, Mathiasson A (1992) Biodegradable natural composites. I. Processing and properties. *J Appl Polym Sci* 45:1667–1677
- Herrera R, Franco L, Rodriguez-Galan A et al (2002) Characterization and degradation behavior of poly(butylene adipate-co-terephthalate)s. *J Polym Sci A Polym Chem* 40:4141–4157
- Hori Y, Hagiwara T (1996) Ring-opening polymerisation of *b*-butyrolactone catalysed by distannoxane complexes: study of the mechanism. *Int J Biol Macromol* 25:235–247
- Hori Y, Suzuki M, Yamaguchi A et al (1993a) Ring-opening polymerization of optically active *b*-butyrolactone using distannoxane catalysts: synthesis of high-molecular-weight poly(3-hydroxybutyrate). *Macromolecules* 26:5533
- Hori Y, Takahashi Y, Yamaguchi A et al (1993b) Ring-opening copolymerization of optically active *b*-butyrolactone with several lactones catalyzed by distannoxane complexes: synthesis of new biodegradable polyesters. *Macromolecules* 26:4388
- Hornsby PR, Hinrichsen E, Tarverdi K (1997) Preparation and properties of polypropylene composites reinforced with wheat and flax straw fibres. 2. Analysis of composite microstructure and mechanical properties. *J Mater Sci* 32:1009–1015
- Jacobsen S, Fritz HG (1999) Plasticizing polylactide – the effect of different plasticizers on the mechanical properties. *Polym Eng Sci* 39:1303–1310
- Juzwa M, Jedlinski Z (2006) Novel synthesis of poly(3-hydroxybutyrate). *Macromolecules* 39:4627
- Kaplan DL (1998) *Biopolymers from renewable resources*. Springer, Berlin
- Kaplan DL, Mayer JM, Ball D et al (1993) Fundamentals of biodegradable polymers. In: Ching C, Kaplan DL, Thomas EL (eds) *Biodegradable polymers and packaging*. Technomic, Lancaster
- Karlsson S, Albertsson A-C (1998) Biodegradable polymers and environmental interaction. *Polym Eng Sci* 38:1251–1253
- Kobayashi T, Yamaguchi A, Hagiwara T et al (1995) Synthesis of poly(3-hydroxyalkanoate)s by ring-opening copolymerization of (R)-*b*-butyrolactone with other four-membered lactones using a distannoxane complex as a catalyst. *Polymer* 36:4707–4710
- Koenig MF, Huang SJ (1994) Evaluation of crosslinked poly(caprolactone) as a biodegradable, hydrophobic coating. *Polym Degrad Stab* 45:139–144
- Kotnis MA, O'Brien GS, Willett JL (1995) Processing and mechanical properties of biodegradable poly(hydroxybutyrate-co-valerate)-starch compositions. *J Environ Polym Degrad* 3:97–105
- Kranz H, Ubrich N, Maincent P et al (2000) Physicomechanical properties of biodegradable poly(D, L-lactide) and poly(D, L-lactide-co-glycolide) films in the dry and wet states. *J Pharm Sci* 89:1558–1566
- Kronbergs E (2000) Mechanical strength testing of stalk materials and compacting energy evaluation. *Ind Crops Prod* 11:211–216

- Labrecque LV, Kumar RA, Dave V et al (1997) Citrate esters as plasticizers for poly(lactic acid). *J Appl Polym Sci* 66:1507–1513
- Le Digabel F, Averous L (2006) Effects of lignin content on the properties of lignocellulose-based biocomposites. *Carbohydr Polym* 66:537–545
- Le Digabel F, Boquillon N, Dole P et al (2004) Properties of thermoplastic composites based on wheat-straw lignocellulosic fillers. *J Appl Polym Sci* 93:428–436
- Lee S-R, Park H-M, Lim H et al (2002) Microstructure, tensile properties, and biodegradability of aliphatic polyester/clay nanocomposites. *Polymer* 43:2495–2500
- Lee SH, Ohkita T, Kitagawa K (2004) Eco-composite from poly(lactic acid) and bamboo fiber. *Holzforschung* 58:529–536
- Lehermeier HJ, Dorgan JR, Way JD (2001) Gas permeation properties of poly(lactic acid). *J Membr Sci* 190:243–251
- Ljungberg N, Andersson T, Wesslen B (2003) Film extrusion and film weldability of poly(lactic acid) plasticized with triacetin and tributyl citrate. *J Appl Polym Sci* 88:3239–3247
- Lunt J (1998) Large-scale production, properties and commercial applications of polylactic acid polymers. *Polym Degrad Stab* 59:145–152
- Madison LL, Huisman GW (1999) Metabolic engineering of poly(3-hydroxyalkanoates): from DNA to plastic. *Microbiol Mol Biol Rev* 63:21–53
- Martin O, Averous L (2001) Poly(lactic acid): plasticization and properties of biodegradable multiphase systems. *Polymer* 42:6209–6219
- Mccarthy SP, Ranganthan A, Ma W (1999) Advances in properties and biodegradability of co-continuous, immiscible, biodegradable, polymer blends. *Macromol Symp* 144:63–72
- Mohanty AK, Misra M, Hinrichsen G (2000) Biofibres, biodegradable polymers and biocomposites: an overview. *Macromol Mater Eng* 276–277:1–24
- Moon SI, Lee CW, Miyamoto M et al (2000) Melt polycondensation of L-lactic acid with Sn(II) catalysts activated by various proton acids: a direct manufacturing route to high molecular weight poly(L-lactic acid). *J Polym Sci A Polym Chem* 38:1673–1679
- Moon S-I, Lee C-W, Taniguchi I et al (2001) Melt/solid polycondensation of L-lactic acid: An alternative route to poly(L-lactic acid) with high molecular weight. *Polymer* 42:5059–5062
- Muller R-J, Witt U, Rantze E et al (1998) Architecture of biodegradable copolyesters containing aromatic constituents. *Polym Degrad Stab* 59:203–208
- Nakamura M, Sahoo S, Ishiaku US et al (2006) Interfacial adhesion in bamboo fiber/biodegradable polymer composites. *Design Manuf Appl Compos* 52–58:443
- Nishino T, Hirao K, Kotera M et al (2003) Kenaf reinforced biodegradable composite. *Compos Sci Technol* 63:1281–1286
- Nishino T, Hirao K, Kotera M (2007) Papyrus reinforced poly(L-lactic acid) composite. *Adv Compos Mater* 16:259–267
- Nobes GaR, Kazlauskas RJ, Marchessault RH (1996) Lipase-catalyzed ring-opening polymerization of lactones: a novel route to poly(hydroxyalkanoate)s. *Macromolecules* 29:4829
- Noda I, Green PR, Satkowski MM et al (2005) Preparation and properties of a novel class of polyhydroxyalkanoate copolymers. *Biomacromolecules* 6:580–586
- Okada M (2002) Chemical syntheses of biodegradable polymers. *Prog Polym Sci* 27:87–133
- Parikh M, Gross RA, Mccarthy SP (1998) The influence of injection molding conditions on biodegradable polymers. *J Inject Mold Technol* 2:30
- Perego G, Cella GD, Bastioli C (1996) Effect of molecular weight and crystallinity on poly(lactic acid) mechanical properties. *J Appl Polym Sci* 59:37–43
- Philip S, Keshavarz T, Roy I (2007) Polyhydroxyalkanoates: biodegradable polymers with a range of applications. *J Chem Technol Biotechnol* 82:233–247
- Plackett D, Andersen TL, Pedersen WB et al (2003) Biodegradable composites based on L-poly(lactide) and jute fibres. *Compos Sci Technol* 63:1287–1296
- Poirier Y (2002) Polyhydroxyalkanoate synthesis in plants as a tool for biotechnology and basic studies of lipid metabolism. *Prog Lipid Res* 41:131–155

- Ramkumar DHS, Bhattacharya M (1998) Steady shear and dynamic properties of biodegradable polyesters. *Polym Eng Sci* 38:1426–1435
- Ratto JA, Stenhouse PJ, Auerbach M et al (1999) Processing, performance and biodegradability of a thermoplastic aliphatic polyester/starch system. *Polymer* 40:6777–6788
- Ruseckaite RA, Jimenez A (2003) Thermal degradation of mixtures of polycaprolactone with cellulose derivatives. *Polym Degrad Stab* 81:353–358
- Shanks RA, Hodzic A, Wong S (2004) Thermoplastic biopolyester natural fiber composites. *J Appl Polym Sci* 91:2114–2121
- Shogren RL (1995) Poly(ethylene oxide)-coated granular starch-poly(hydroxybutyrate-co-hydroxyvalerate) composite materials. *J Environ Polym Degrad* 3:75–80
- Shogren R (1997) Water vapor permeability of biodegradable polymers. *J Environ Polym Degrad* 5:91–95
- Sinclair RG (1996) The case for polylactic acid as a commodity packaging plastic. *J Macromol Sci Pure Appl Chem* 33:585–597
- Steinbuechel A (2003) *Biopolymers, general aspects and special applications*. Wiley-VCH, Weinheim, Germany
- Steinbuechel A, Doi Y (2002) *Polyesters III – Applications and commercial products*. Wiley-VCH, Weinheim, Germany
- Tokiwa Y, Suzuki T (1977) Hydrolysis of polyesters by lipases. *Nature* 270:76–78
- Tuominen J, Kylma J, Kapanen A et al (2002) Biodegradation of lactic acid based polymers under controlled composting conditions and evaluation of the ecotoxicological impact. *Biomacromolecules* 3:445–455
- Valentin HE, Broyles DL, Casagrande LA et al (1999) PHA production, from bacteria to plants. *Int J Biol Macromol* 25:303–306
- Van De Velde K, Kiekens P (2002) Biopolymers: overview of several properties and consequences on their applications. *Polym Test* 21:433–442
- Van Tuil R, Fowler P, Lawther M et al (2000). Properties of biobased packaging materials. In: *Biobased packaging materials for the food industry – status and perspectives*. KVL, Frederiksberg, Denmark
- Vert M, Schwarch G, Coudane J (1995) Present and future of PLA polymers. *J Macromol Sci Pure Appl Chem* A32:787–796
- Wee Y-J, Kim J-N, Ryu H-W (2006) Biotechnological production of lactic acid and its recent applications. *Food Technol Biotechnol* 44:163–172
- Williams SF, Martin DP, Horowitz DM et al (1999) PHA applications: addressing the price performance issue I. *Tissue engineering*. *Int J Biol Macromol* 25:111–121
- Witt U, Einig T, Yamamoto M et al (2001) Biodegradation of aliphatic-aromatic copolyesters: evaluation of the final biodegradability and ecotoxicological impact of degradation intermediates. *Chemosphere* 44:289–299
- Wollerdorfer M, Bader H (1998) Influence of natural fibres on the mechanical properties of biodegradable polymers. *Ind Crops Prod* 8:105–112
- Wong S, Shanks RA, Hodzic A (2007) Effect of additives on the interfacial strength of poly(l-lactic acid) and poly(3-hydroxy butyric acid)-flax fibre composites. *Compos Sci Technol* 67:2478–2484
- Yokota Y, Marechal H (1999). Processability of biodegradable poly(butylene) succinate and its derivatives. A case study. *Biopolymer Conference*, Wurzburg, Germany.
- Zinn M, Witholt B, Egli T (2001) Occurrence, synthesis and medical application of bacterial polyhydroxyalkanoate. *Adv Drug Deliv Rev* 53:5–21

Chapter 18

Man-Made Cellulose Short Fiber Reinforced Oil and Bio-Based Thermoplastics

Johannes Ganster and Hans-Peter Fink

Abstract The present chapter considers the possibilities of reinforcing thermoplastic matrix materials with cellulose man-made fibers, in particular high performance rayon tire cord yarn. Mechanical properties of the composites such as tensile strength, stiffness, and impact properties are in the focus of interest. Composite and fracture surface morphology is accessed by scanning electron microscopy (SEM) and the quality of fiber–matrix adhesion is revealed. Advantages and disadvantages of using coupling agents are discussed. Thermoplastics both from fossil and from renewable resources are used as matrix materials. From the first group, polypropylene is the most important example and is considered in detail while polyethylene, polybutene-1, impact modified polystyrene, ABS are briefly sketched. On the bio-based side, the emphasis is on poly(lactic acid) (PLA) as the most easily commercially accessible inexpensive bioplastic. Polyhydroxyalkanoates (PHA) are also considered but in less detail. Composites are manufactured by a specially developed melt compounding method on twin screw extruders and shaped by injection molding. In general, rayon reinforcement proves to be superior to natural fiber reinforcement, in particular in terms of impact strength. For PP–rayon the properties are even comparable to those of short glass fiber reinforced polypropylene (GFPP) and PC/ABS with advantages in terms of impact strength compared to GFPP. With 30% rayon in PP, tensile strength is tripled, modulus is doubled, and notched impact strength is doubled at room temperature and quadrupled at -18°C . For the bio-based thermoplastics, rayon is an ideal reinforcement since the bio-based character is preserved. Strength and modulus always increase, and at the same time, impact strength is increased dramatically for brittle products such as PLA. This is true in particular for a specially designed fiber–matrix interphase using a decoupling agent.

Keywords Bioplastics · Cellulose fiber · Composite · Coupling · Decoupling · Fiber-matrix interphase · PLA · PP · Reinforcement

J. Ganster (✉)

Fraunhofer Institute for Applied Polymer Research IAP, Geiselbergstr. 69, 14476 Potsdam, Germany

e-mail: johannes.ganster@iap.fraunhofer.de

Contents

18.1	Introduction	480
18.2	Rayon and Other Man-Made Cellulose Fibers	481
	18.2.1 Mechanical Properties	481
	18.2.2 Structural Features	482
	18.2.3 Rayon Versus Glass Fiber for Reinforcement	484
18.3	Compounding Methods	484
	18.3.1 Two-Stage Method	484
	18.3.2 Free Flowing Rayon Pellets	487
18.4	Rayon Composites with Oil-Based Matrices	489
	18.4.1 Polypropylene	489
	18.4.2 Other Oil-Based Matrices	496
18.5	Composites with Bio-Based Matrices	498
	18.5.1 Poly(Lactic Acid)	498
	18.5.2 Polyhydroxyalkanoates	502
18.6	Conclusions	504
	References	505

18.1 Introduction

The reinforcement of thermoplastics, notably polypropylene (PP) and polyamide (PA), with short glass fibers is a classical method to improve polymer mechanical properties. Fibers are dispersed more or less homogeneously in the polymer by melt compounding techniques such as twin screw extrusion to produce compounds ready for injection molding. Molded parts benefit from the better mechanical properties of the reinforcing fibers as the fibers bear a considerable part of the load applied to the composite structure.

Successful as they are in this kind of application, glass fibers have a series of disadvantages. First, they have the relatively high density of approx. 2.5 g/cm^3 compared to matrix densities of, e.g., 0.9 g/cm^3 for PP or 1.13 g/cm^3 for PA6. This might be counterproductive for light weight construction purposes unless the improved properties allow for thinner walls in mold design. Second, glass fibers are prone to breakage so that in composite recycling their length is reduced considerably with detrimental effects on the properties. Third, incineration as a useful end of life option is impaired by the presence of the glass fiber phase which is often 30, sometimes even 40 weight percent. Finally, glass fibers are abrasive to the processing equipment such that the service life of screws, cutting tools, and molds is reduced.

Attempts have been and are being made to overcome these problems with lignocellulosic reinforcement also in view of environmental and sustainability aspects. There is a vast scientific literature on this topic (cf. [1–3] for recent reviews) which cannot be reviewed here. By and large, it can be said that lignocellulosic fibers such as bast (e.g., flax, hemp, jute, ramie, kenaf, bamboo), leaf (e.g., sisal, abacá) or wood fibers can be used as reinforcement with advantages over glass reinforcement in price, density (approx. 1.5 g/cm^3 or less), and renewability. Compared to the pristine matrix, stiffness is increased considerably while strength

usually remains the same, at best. Problems occur in terms of uniformity, quality assessment, thermal degradation and smell during the compounding process, discoloration and smell as well as a lack of impact strength or toughness in the molded body. Nevertheless, considerable progress has been made, say, in the last 10 years. Injection molding compounds (mostly based on PP and wood fibers) can be purchased today from a series of companies such as JER Envirotech Ltd., Canada, AD Majoris, France, FuturaMat, France, Kareline Oy Ltd., Finland, or Transmare Compounding B.V., Netherlands.

Apart from naturally occurring wood and plant fibers, being associated with varying amounts of lignin and hemicelluloses, cellulose can be obtained industrially in pure form from the viscose or the NMMO process as man-made fibers. Yarns are used in textile applications (e.g., as viscose, Modal[®], Tencel[®]) or for reinforcing rubber goods such as tires or hoses (rayon tire cord yarn, e.g., Cordenka[®]). The potential of these fibers to be used as thermoplastic reinforcement has been recognized some years ago [4, 5]. In the present chapter this topic will be presented in detail both for oil and bio-based matrix materials mostly based on own work. It will become apparent that many of the problems encountered with natural and wood fibers can be overcome with cellulose man-made fibers. In particular, strength and impact strength will be shown to benefit from this kind of reinforcement without compromising the bio-based nature of the reinforcement. This is of particular interest in combination with bio-based and biodegradable matrix polymers.

In the present chapter, rayon and other man-made cellulose fibers will be introduced in terms of properties and structure. The compounding method to obtain the composites will be described briefly. PP–rayon composites will be considered in more detail as the practically most relevant class of this type of material at present arousing interest from the automotive industry. In another section rayon composites with poly(lactic acid) (PLA) and polyhydroxyalkanoates (PHA) will be studied as a promising bio-based and biodegradable alternative to conventional materials in durable applications, transport, and automotive industry. Finally, some concluding remarks will be given concerning future prospects of rayon reinforced thermoplastics and the problems to be tackled in future work.

18.2 Rayon and Other Man-Made Cellulose Fibers

18.2.1 *Mechanical Properties*

Man-made cellulose fibers are spun from high quality, the so-called dissolving pulp with complete dissolution of cellulose either without chemical modification of the chains (direct methods, e.g., Lyocel process) or as a derivative (e.g., cellulose xanthogenate in the viscose process) with subsequent regeneration of the pure cellulose. A more detailed account is given, e.g., in Ganster and Fink [6]. Fibers are sold as staple with lengths in the cm range for textile applications and as

Table 18.1 Mechanical properties of typical man-made cellulose fibers from single fiber measurements

Fiber	Strength [MPa]	Elongation [%]	Modulus [GPa]
Cordenka [®] RT 700	830 ± 60 ^a	13 ± 2	20 ± 1
Enka viscose [®]	308 ± 15	24 ± 1	11 ± 0.4
Viscose sliver	338 ± 45	12 ± 4	11 ± 1
NewCell [®]	603 ± 30	9 ± 1	31 ± 4
Tencel [®] sliver	552 ± 45	11 ± 2	23 ± 2
Carbamate	366 ± 15	8 ± 1	22 ± 1

Data from Ganster and Fink [7]

^aStandard deviation

continuous filament yarns resembling glass fiber rovings for technical and textile uses. Cross sectional dimensions are in the range of 10–20 μm .

Tensile properties of typical man-made cellulose fibers are shown in Table 18.1. Cordenka[®] RT 700 is a rayon (filament) yarn spun by a special variant of the viscose process and produced by Cordenka GmbH Obernburg, Germany. This standard yarn comes with 1,350 filaments and is used mainly to manufacture tire cord for reinforcing the carcass of high speed and run flat tires. It has the highest strength of cellulose man-made fibers commercially available and is used as the standard fiber in the present investigations. Despite the high strength there is a fair elongation which is exploited for the improvement of impact properties of the composites as shown later. For a viscose fiber the modulus is comparatively high.

The following two entries in Table 18.1 are viscose fibers for textile applications and display much lowered strengths and moduli accompanied with increased elongation for Enka viscose[®]. NewCell[®] and Tencel[®] are manufactured with a direct method, the NMMO or Lyocell process (see, e.g., Ganster and Fink [6]) as filament and staple, respectively. Medium strength and high modulus are characteristic for the filament yarn which is no longer produced at present. The staple fiber Tencel[®] is used in textile applications and is a trademark of Lenzing Co., Austria. Finally, Carbamate is a cellulose fiber spun in this institute via the CARBACELL process, an environmental-friendly alternative to the viscose process using urea as the derivatizing agent [8].

18.2.2 Structural Features

Structural parameters crystallinity x_c , crystallite dimensions D_{1-10} , D_{110} , and D_{004} as well as crystalline orientation factor f_c as determined by wide angle X-ray scattering [9] for selected cellulose man-made fibers are shown in Table 18.2 [from Rihm [10]].

Both viscose fibers have the lowest crystallinities and the shortest crystallites in chain direction (D_{004}) with a tendency to form oblate crystallites for the tire cord. High orientation f_c in combination with low crystallinity accounts for the medium

Table 18.2 Crystallinity x_c , crystallite dimensions D_{1-10} , D_{110} , and D_{004} , and crystalline orientation factor f_c from X-ray diffraction for selected man-made cellulose fibers

Fiber	x_c [%]	D_{1-10} [nm]	D_{110} [nm]	D_{004} [nm]	f_c
Cordenka [®] RT 700	28	6.6	3.9	9.7	0.963
Enka viscose [®]	31	5.1	4.5	9.8	0.943
NewCell [®]	35	4.4	3.3	17.5	0.961
Carbamate	40	3.9	4.6	12.4	0.944

Data from Rihm [10]

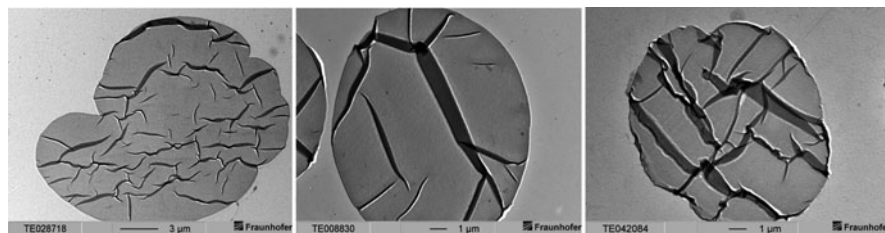


Fig. 18.1 Cross sections of rayon tire cord (*left*), Lyocell (*middle*), and cellulose carbamate fibers as obtained by transmission electron microscopy

stiffness, very good strength, and fair elongation for Cordenka[®] RT 700. The same orientation is displayed for NewCell[®]; however, the higher crystallinity and the oblong crystal shape with 17.5 nm long crystallites are likely to cause the higher modulus. Carbamate has a similar crystal orientation as textile viscose. The higher modulus is probably due to the higher crystallinity and larger crystal dimension in chain direction.

As shown in Fig. 18.1, fiber cross sections clearly differ between viscose (including rayon tire cord as shown) on the one hand and Lyocell (NMMO) and Carbamate fibers on the other, as demonstrated in the transmission electron micrographs of ultra thin cuts (60 nm).

Rayon (left) has a lobed cross section which is typical for fibers spun industrially by the viscose process. In contrast, Lyocell (middle) displays a round shape similar to the cellulose carbamate example (right). (In all the micrographs, the dark streaks are overlaps of sample material caused by the cutting movement of the ultra microtome knife.) Cross sectional shape and pore structure are strongly dependent on the precipitation conditions. For NMMO fibers [11] it was shown that harsh precipitation with water gave dense, round structures while softer precipitation into alcohols lead to a skin-core structure with dense skin and a porous inner region. Still, cross sections are round in contrast to viscose-type fibers.

In principle, all the fiber types described above can be used advantageously for reinforcing thermoplastic matrix materials to improve their mechanical and thermomechanical properties. This has been demonstrated for PP as matrix material [7]. In what follows, however, the focus is put on rayon tire cord yarn, as it has favorable properties (cf. Table 18.1) and is commercially available as a technical (endless) filament yarn with suitable yarn titre.

18.2.3 Rayon Versus Glass Fiber for Reinforcement

Rayon offers a series of advantages compared to glass fibers if it can be successfully used for reinforcing thermoplastics. Obviously, with about 1.5 g/cm^3 , the density is less than the glass density of approx. 2.5 g/cm^3 opening up possibilities for light weight construction. Being “softer” than glass, rayon fibers are less abrasive to the processing equipment, such as screws, pelletizers, and molds. This is due to their anisotropic nature with high strength and stiffness in the fiber direction and moderate properties in the cross direction. Moreover, this gives improved recycling properties since fiber breakage at repeated processing is much less severe than for glass. Additionally, for incineration as an energy generating end of life option for the composite, there will be no troublesome residue.

Being 100% cellulose, rayon is completely bio-based and biodegradable. Thus, it is an obvious choice for bio-based and/or biodegradable matrices such as PLA or PHA. Compared to natural fibers, the compact structure and the well-defined and constant properties as well as the availability on an industrial scale and ease of handling are advantageous.

On the down side, there is definitely the lower stiffness of 20 GPa versus, say, 70 GPa for glass fibers and the reduced thermal processing window, excluding higher melting polymers such as polyethylene terephthalate, for instance. However, for most bioplastics with melting points below 200°C , this is usually not a problem. Thirdly, but less critically, composite preparation is affected by the hydrophilic nature of rayon.

18.3 Compounding Methods

In contrast to glass fibers, where established methods for incorporating the fibers into the polymer melt exist, the feeding of organic fibers, in the present case of rayon filaments, is not straightforward. On the one hand, direct feeding of the endless fiber rovings (Fig. 18.2) into a twin screw extruder equipped with suitable mixing and kneading elements is not successful owing to the high toughness of the fibers compared to glass fibers which are much more prone to breakage. On the other hand, rayon fibers which are cut prior to feeding into the extruder tend to be very fluffy and pose dosage problems due to the very low bulk density and for not being free-flowing.

18.3.1 Two-Stage Method

To overcome these problems, a two-stage compounding method has been developed [4] as shown schematically in Fig. 18.3. In a first step, the fibers are taken from

Fig. 18.2 Cellulose rayon tire cord yarn rovings (Cordenka[®] RT 700, 1,350 filaments, filament titre 1.8 dtex)

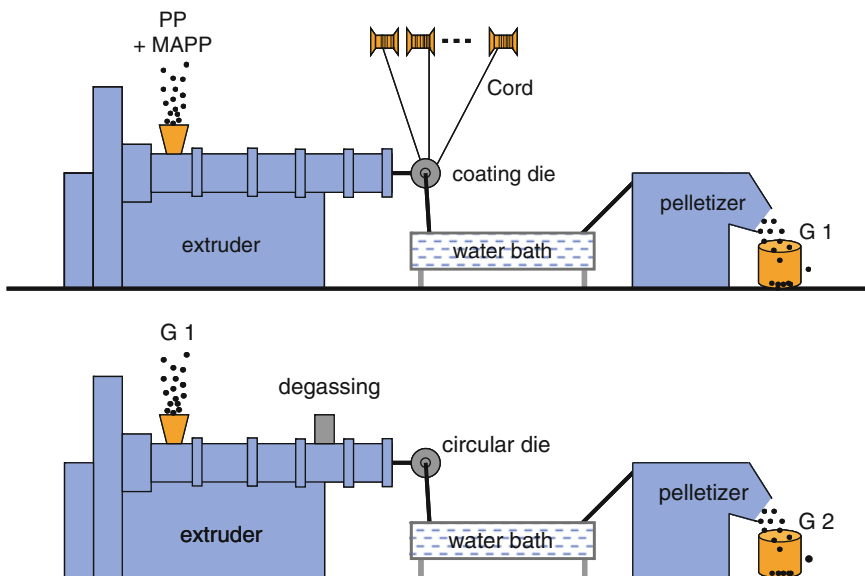


Fig. 18.3 Two-stage compounding with coating step (*above*) and homogenization step (*below*)

a creel and fed into a coating die covering the fiber bundles with thermoplastic matrix material. After cooling in a water bath, the strand is cut with a commercial pelletizer to give pellets G1.

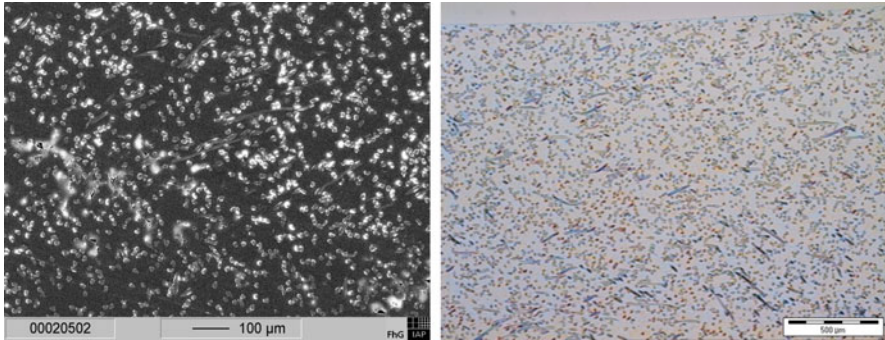


Fig. 18.4 Homogeneity of fiber distribution in rayon reinforced PP: SEM (*left*) and optical (*right*) micrographs (from Ganster et al. [12] with permission from Elsevier)

After drying, these pellets are fed into a twin screw extruder with optimized screw configuration (mixing and kneading elements) for homogenization and final water removal to give the pellets G2 which are then used, after drying, for injection molding.

The quality of fiber distribution obtained by this method is demonstrated in Fig. 18.4, where an SEM micrograph (*left*) and an optical micrograph of a 10 μm thick slice cut through an injection molded rayon reinforced PP sample perpendicular to the molding direction are shown.

In the SEM picture, the light spots represent the fibers while in the optical micrograph the fibers are shown as dark spots. Besides the even distribution, a preferred orientation of the fibers along the molding direction is visible since fibers are preferentially cut perpendicular to their axis.

As it is well known from glass fiber reinforcement, fiber length in the final molded parts is a critical factor influencing the mechanical and thermomechanical properties of the composites to a large extent [13]. The fiber length distribution originating from the two-stage method described above has been investigated for two different cutting lengths in the pelletizing steps (Fig. 18.3), viz. 3 and 5 mm [12]. The distribution in injection molded test bars from pellets cut to 3 mm both in the coating and the homogenization steps is displayed in Fig. 18.5. A severe length reduction is visible with a maximum in the distribution between 250 and 500 μm . This reduction is caused by the second pelletizing and the action of the kneading and mixing elements in the homogenization step.

Increasing the cut length in both steps to 5 mm gives a distribution shifted to higher lengths with a maximum in the range of 0.5–1 mm. However, the mechanical properties are not improved appreciably. Thus the fiber aspect ratio (length to diameter) is high enough to accomplish fibrous reinforcement (as opposed to particular reinforcement) already for the distribution shown in Fig. 18.5. This-distribution gives an average length of 820 μm and with the fiber diameter of 12 μm an average aspect ratio of approximately 70 which is, obviously, well above the critical ratio [14].

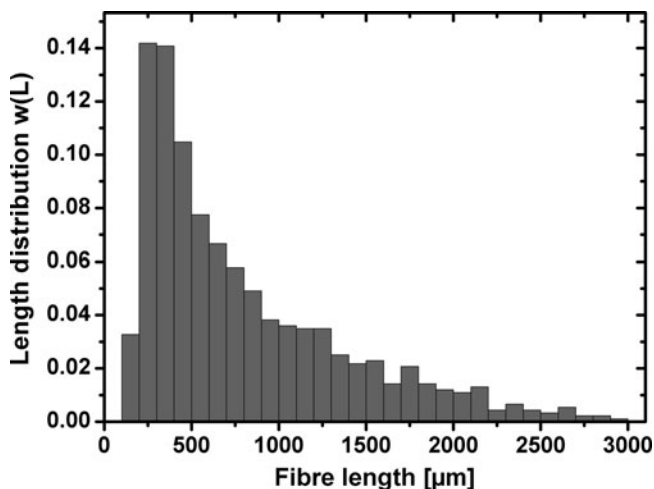


Fig. 18.5 Fiber length distribution in rayon-PP composite injection molded test bar with 25% fiber content, 3 mm cut length during processing

18.3.2 Free Flowing Rayon Pellets

In order to simplify the procedure above, a one-stage technology has been developed together with the fiber producing company Cordenka based on direct feeding of short cut fiber pellets into the extruder [15]. The actual novelty in this respect is presented by the pellets themselves, since pure short cut rayon fibers cannot be fed into the extruder by usual techniques due to their wadding-like structure and thus low bulk density. Therefore, the fibers were coated with a special sizing to provide fiber adherence and pellet formation.

This sizing has to comply with a series of partly contradicting requirements (a) fiber adherence as to provide pellet formation, (b) pellet opening during compounding down to the single filament level, and (c) avoiding negative effects on composite properties. Moreover, due to technological reasons, only water borne systems were reasonably taken into consideration.

Successful experiments were performed with starch/starch derivatives, cellulose derivatives, polyvinyl acetate, polyvinyl alcohol, and mixtures of the same. As an example, the morphology of 4 mm pellets with a polyvinyl acetate sizing is shown in Fig. 18.6. Suchlike pellets can easily be fed into the extruder with common screw feeding systems. The pellet opening down to the filament level during extrusion is demonstrated in Fig. 18.7 showing a scanning electron microscopy (SEM) micrograph of a cryo fracture surface for an injection molded PP test bar reinforced with polyvinyl acetate coated rayon pellets. Obviously, also the fiber distribution is quite homogeneous. Fiber lengths are in the same range as for the two-stage method above.



Fig. 18.6 Free flowing pellets from Cordenka[®] rayon with 4 mm cut length

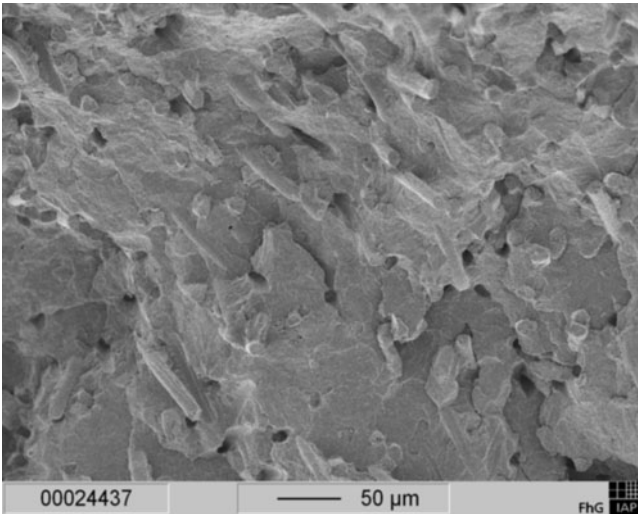


Fig. 18.7 Dispersion of rayon fibers after pellet opening during compounding – SEM cryo fracture surface of injection molded test specimen

Other methods for feeding loose or fluffy material can be found in the patent literature, ranging from air flow supported variants of side-feeding [16] over densifiers [17] up to special designs for chopped fibers [18]. In the latter, forced feeding by a screw is supported by inclined conveyer belts transporting the chopped fibers to the screw and pressing the fibers into the screw flights.

The results presented in the following are obtained, if not stated otherwise, with composites manufactured by the two-stage technique described above.

18.4 Rayon Composites with Oil-Based Matrices

18.4.1 Polypropylene

PP is one of the most important thermoplastic polymers for the automotive industry and other sectors using injection molding for producing large quantities of goods. Purely aliphatic, it has favorable properties in terms of chemical resistance, ease of processing, and low density (0.9 g/cm^3). Its higher thermal stability (melting point 160°C , heat distortion temperature HDT-A of 62°C) makes it often preferable to high density polyethylene (PE), which has a melting point of 130°C and an HDT-A of 50°C [19]. On the other hand, with its relatively low strength (20–30 MPa), stiffness (1–1.5 GPa), and price it is a good candidate for improving its properties with fibrous reinforcements and other fillers. For successfully reinforcing with the hydrophilic cellulosic fibers, however, a sufficient coupling to the extremely hydrophobic matrix must be accomplished.

18.4.1.1 Fiber–Matrix Coupling

Coupling of cellulose fibers to a PP matrix can be accomplished by an esterification reaction between the cellulose hydroxyl groups on the fiber surface and an anhydride function grafted to PP according to the scheme in Fig. 18.8.

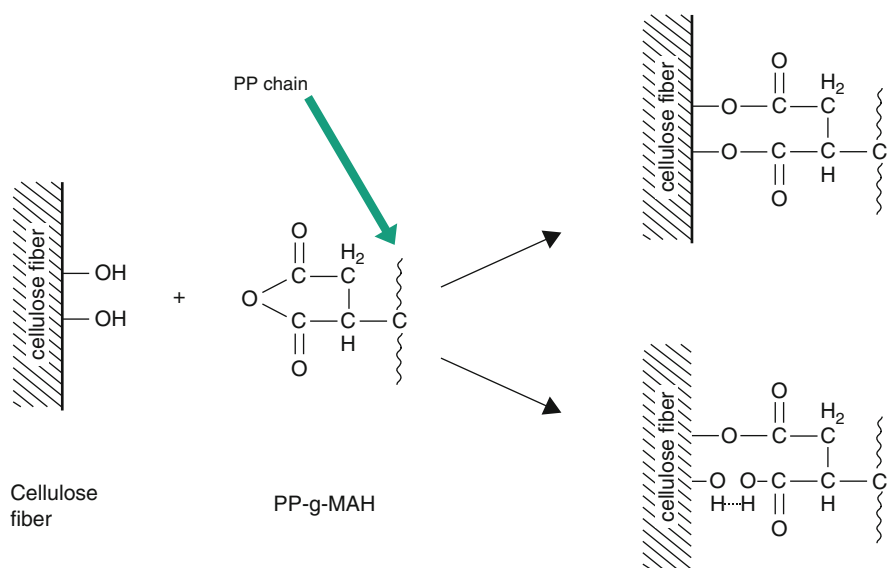


Fig. 18.8 Coupling scheme between cellulose fiber and maleic anhydride grafted polypropylene according to Felix and Gatenholm [20] (with permission from Wiley)

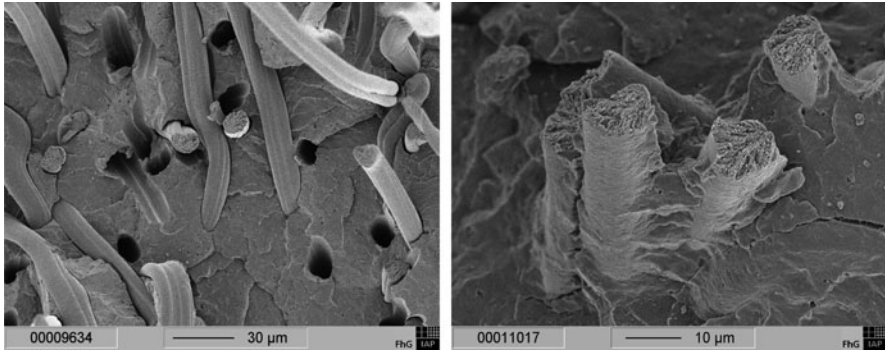


Fig. 18.9 SEM cryo fracture micrographs for uncoupled (*left*) and coupled (*right*) rayon-PP composites [3 wt% PP-g-MAH coupling agent, from Ganster and Fink [7]]

Maleic anhydride (MAH) grafted PP is used as a coupling agent (CA) which under extrusion conditions forms ester linkages to the cellulose OH-groups on the one hand and entanglements with PP chains on the other. Commercial products are available with graft levels between 0.5% and 1.5% MAH and various PP chain lengths to give melt flow indices between 120 and 450 g/10 min at 190°C and 21.6 N load [12]. Rather low concentrations of the CA are sufficient to couple the fibers to the matrix, as demonstrated in Fig. 18.9 with cryo fracture SEM micrographs of uncoupled (*left*) and coupled (*right*) PP composites with 25% rayon.

In contrast to the system without CA, where the bare fibers pulled out from the matrix and the corresponding holes are visible, already 3 wt% of CA suffice to cover the fibers with the PP matrix and produce short fiber stumps after the fracture event. Obviously, in terms of morphological features, the coupling scheme from Fig. 18.8 works exceptionally well. Similar results were obtained by Paunikallio et al. [21]. Implications for mechanical properties of the composites will be discussed in the next sections.

18.4.1.2 Tensile and Bending Properties

Tensile strength and modulus as well as three-point bending strength (stress at 3.5% strain) and modulus of rayon-PP composites coupled with 3 wt% PP-g-MAH are shown in Fig. 18.10 as a function of fiber volume fraction. For details see Ganster et al. [12]. The improvements are considerable. With already 15 vol% of fiber the strength is more than tripled and the modulus is doubled. The increase is not linear probably due to an increasing mutual influence of the fibers at higher percentages in obtaining an optimal orientation along the injection molding direction.

Bending properties (triangles) of the reinforced samples do not reach values as high as for their tensile counterparts. This is in particular true for stiffness and has to do with the compression components in the bending experiment. For compressive

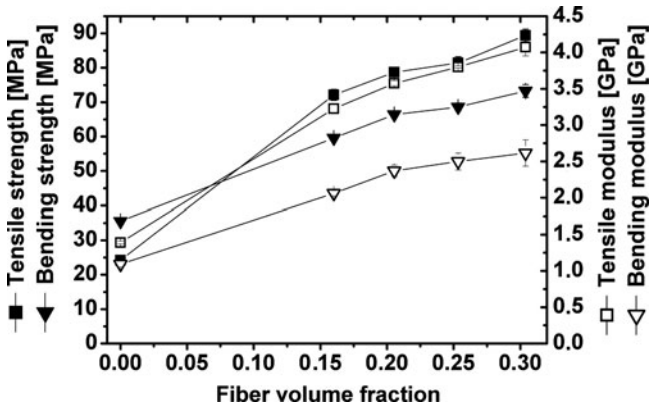


Fig. 18.10 Tensile and bending strengths and moduli of rayon-PP composites coupled with 3 wt% PP-g-MAH

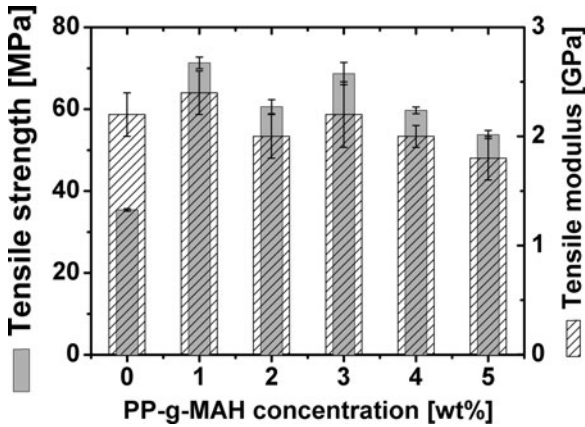


Fig. 18.11 Tensile strength and modulus for rayon-PP composites with 20% rayon as a function of coupling agent PP-g-MAH concentration

loads, the ductile fibers do not contribute much to the composite’s stiffness: the reinforcing action is rope-like, in contrast to glass fibers which act more like reinforcing rods.

A concentration of 3 wt% CA has been chosen in these experiments based on data given in Fig. 18.11, where the implications of CA concentration on tensile strength and modulus have been investigated for a composite with 20 wt% rayon fibers.

Already 1 wt% of CA is sufficient to improve the strength by 100%. Therefore, 3% is a secure choice also for composites with higher fiber fractions, since rigorously, CA concentration should be adapted to the amount of fibers (or fiber surface) present in the composite, according to Fig. 18.8.

The modulus, on the other hand, is basically unaffected by the CA concentration. Apparently, the fibers are embedded tightly in the matrix such that they are able to contribute to the stiffness which is measured at very small elongations between 0.05% and 0.25%. For higher elongations encountered in measuring the strength, the coupling becomes important and the uncoupled composite falls short behind the coupled counterparts.

Moreover, for higher concentrations of the CA (above 3 wt%) the properties decrease somewhat, displaying the action of the short chain PP-g-MAH which is acting like a plasticizer.

Similar experiments have been performed by Paunikallio et al. [22] for viscose fibers of unspecified mechanical properties and a fiber fraction of 40%. Their observations are similar: the modulus is not changed at all while tensile strength is increased by the PP-g-MAH CA up to 6% CA with respect to the fiber fraction, which corresponds to 4% CA relative to the matrix weight.

18.4.1.3 Impact Properties

Besides strength and stiffness, impact properties of a material are of great practical relevance. Here the time scale of loading is in the order of milliseconds, while strength properties are tested in seconds or even minutes. Therefore, elongation from tensile experiments, which is often used as a measure of ductility, can only be of limited interest and standard impact experiments, like Izod or Charpy pendulum methods, have been developed.

Unnotched and notched Charpy impact strengths at room temperature and at -18°C for rayon-PP composites coupled with 3 wt% PP-g-MAH are shown in Figs. 18.12 and 18.13, respectively, as a function of fiber volume fraction.

A high level of unnotched impact resistance is seen in Fig. 18.12 both at room temperature and at -18°C virtually independently from the fiber concentration. Unreinforced PP is soft enough to slide through the sample holder and not to break at all. Both crack initiation and propagation is tested in this experiment in contrast to the notched experiment in Fig. 18.13, where crack propagation plays the major role. Here, the impact resistance increases approximately linearly with the fiber content.

As to the different behavior in the unnotched and notched experiments, it seems that the layer of pure and ductile PP, visible on the surface of the injection molded specimen, masks the differences in crack propagation seen in the notched experiments and leveling off the effects of fiber concentration.

The use of CAs has important consequences for the impact properties of the composites as demonstrated for the PP matrix in comparison to a PP composite with 30 wt% rayon without and with 3% CA in Fig. 18.14. Strength and modulus are changed as in Fig. 18.11, but unnotched impact strength is improved by the CA while notched impact strength is reduced.

This point will be discussed in more detail for PLA composites where it will become clear that a frictional pull out is responsible for large energy absorption and thus increases the notched impact strength.

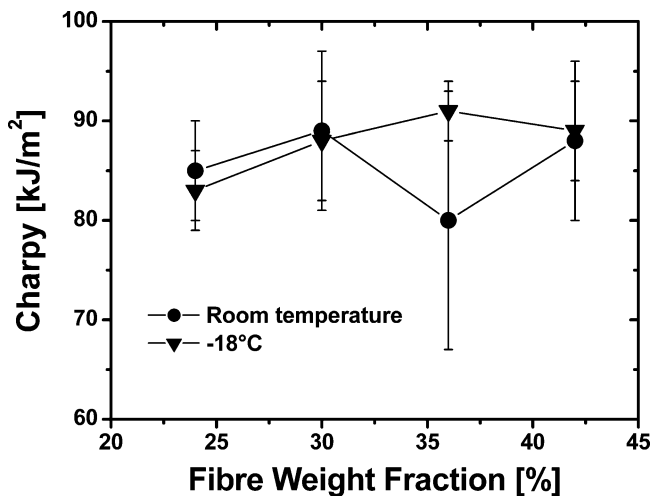


Fig. 18.12 Unnotched Charpy impact strength of rayon-PP composites coupled with 3 wt% PP-g-MAH at room temperature and at -18°C (from Ganster et al. [12] with permission from Elsevier)

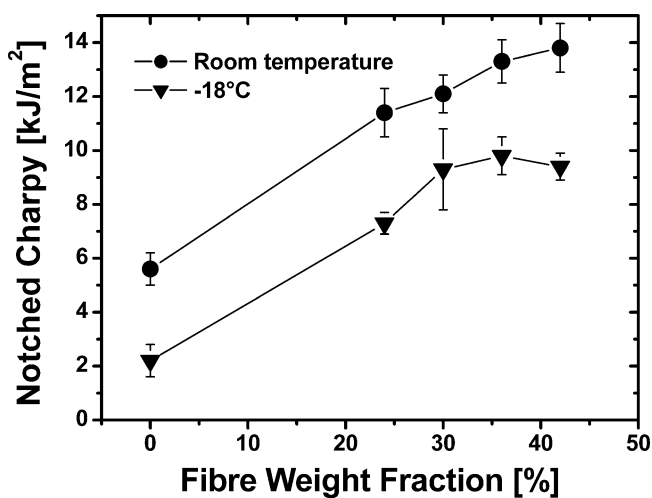


Fig. 18.13 Notched Charpy impact strength of rayon-PP composites coupled with 3 wt% PP-g-MAH at room temperature and at -18°C (from Ganster et al. [12] with permission from Elsevier)

18.4.1.4 Heat Stability

In the automotive industry and other areas of application, a polymer material is often required not to change its shape at elevated temperatures. For estimating this ability, a three point bending test with constant load (1.8 MPa) and increasing

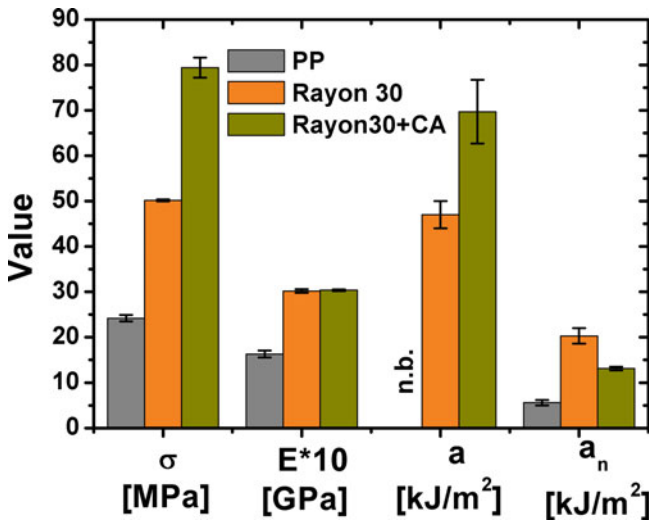


Fig. 18.14 Tensile strength and modulus, Charpy unnotched and notched impact strength for PP, and PP–rayon composites without and with 3% CA

Table 18.3 Tensile strength and modulus, unnotched Charpy impact strength, and heat distortion temperature (HDT-A) for PP-man-made cellulose fiber composites showing ways to increase HDT

Material	Strength [MPa]	Modulus [GPa]	Charpy [kJ/m ²]	HDT-A [°C]
PP	23	1.4	n.b.	55
PP + 25% rayon	72	2.7	85	80
PP + 25% Lyocell	66	3.6	36	134
PP + 22% rayon + 8% jute	70	3.1	76	106
PP + 18% rayon + 7% Lyocell	65	2.8	80	105
PP + 25% rayon + 10% talcum	68	3.2	71	117

From Ganster and Fink [23]

temperature is usually carried out giving the so-called heat distortion temperature HDT-A, at which a certain deflection (0.2%) is attained. For pure PP, this temperature is rather low (55°C) and an increase is highly desirable.

With 25% pure rayon, a moderate increase to 80°C can be obtained, as shown in Table 18.3. In this table, the HDT-A values for pure PP and cellulose man-made fiber-based composites are given together with other important mechanical characteristics. In order to increase the HDT to more than 100°C, three routes were pursued (1) change the cellulose fiber type from rayon to Lyocell, (2) use fiber mixtures with natural fibers or Lyocell, and (3) add organic fillers (like talcum) to the matrix.

Compared to the rayon composite the Lyocell reinforcement leads to a 30% increase in tensile modulus and to a shift in HDT to 134°C. These two values are the best in the whole series of tested composites. However, undesired effects are that the unnotched Charpy impact strength drops to one-half and the strength is reduced.

Mixtures of rayon with jute or Lyocell show the desired balance of high HDT and a high level of the other properties. HDT values are shifted to above 100°C, stiffness is increased slightly and the losses in impact strength remain below 10%. As compared to Lyocell, rayon again proves to be an excellent impact modifier.

Also specific modifications of the matrix lead to the desired effect. The second best values for stiffness and HDT are found for the sample with 10% talcum. The impact strength decreases by approximately 15% but stays on a high level of 71 kJ/m².

A more systematic study on jute admixtures to PP–rayon composites has been performed by Khan et al. [24]. Coupled PP composites with an overall fiber content of 25 wt% and varying proportions of native and NaOH-treated (mercerized) jute fibers mixed to rayon were produced and tested. Generally, mercerized jute fibers showed better performance and a jute fraction of 20 wt% produced the most favorable properties.

Thus, appropriate fiber mixtures on the one hand, and specific matrix modifications by inorganic fillers on the other can be utilized to obtain a well-balanced property profile for rayon-based PP composites.

18.4.1.5 Rayon and PP-Type Variation

Correlations between rayon fiber properties, such as strength, modulus, and elongation, and PP composite properties (3% CA) including impact strength have been studied in some detail [25]. It turned out that fiber and composite strength are not directly correlated. Neither is modulus in a straightforward manner. Rather tensile elongation of the composite follows the elongation of the fiber as shown in Fig. 18.15 giving a correlation coefficient of 0.93.

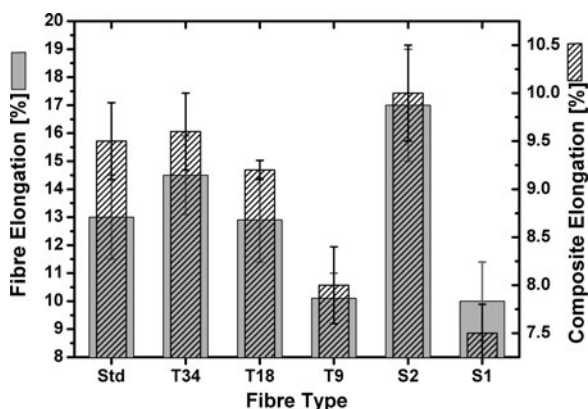


Fig. 18.15 Correlation between single fiber elongation (*left*) and coupled PP–rayon composite elongation at break (*right*) from Ganster et al. [25]

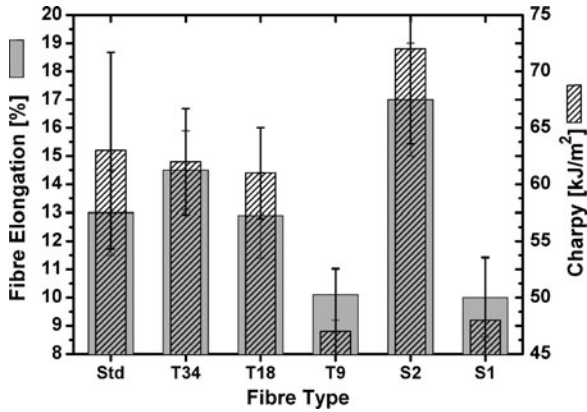


Fig. 18.16 Correlation between single fiber elongation (*left*) and coupled PP-rayon composite unnotched Charpy impact strength (*right*) from Ganster et al. [25]

It seems that composite failure is an elongation controlled process such that a high fiber elongation can increase the composite elongation for this ductile PP matrix (elongation of 40%). This view is in accord with the excellent fiber matrix coupling from Fig. 18.9 (right).

More important for practical applications is the impact behavior of the composite. The correlation of unnotched impact strength with fiber elongation is depicted in Fig. 18.16. A correlation coefficient as high as 0.97 is found, which is the best value in this series. A slightly lower correlation (coefficient 0.82) is found for single fiber elongation and notched Charpy impact strength.

In other words, a high fiber elongation is decisive for high impact strength in this kind of composite material. Moreover, there is a clear correlation between composite tensile elongation (low testing speed) and impact strength (high testing speed).

Various PPs with MFIs ranging from 15 to 150 g/10 min and notched impact strengths from 2 to 9 kJ/m² have been tested as matrix materials for coupled rayon composites with 30 wt% fiber content (unpublished results). Resulting composite properties are fiber-dominated, i.e., differences in the matrix properties are smoothed out in the composites all having tripled strengths of around 75 MPa, at least doubled moduli of approximately 3 GPa and notched impact strengths often four times improved to between 10 and 13 kJ/m². One exception in terms of impact strength is an extremely viscous PP (MFI 1.8 g/cm³) with a notched Charpy value of as high as 40 kJ/m². This value was reduced by the presence of the fibers to 14 kJ/m². Only at -18°C, notched Charpy was doubled to 7 kJ/m².

18.4.2 Other Oil-Based Matrices

The potential of rayon for reinforcing other oil-based matrix materials has been tested for a series of polymers with suitable melting or softening points, as a rule

below 200°C to avoid fiber degradation. The coupling scheme used for PP (Fig. 18.8) can be used in many cases; however, the carrier chain for MAH must be adapted to the chemical composition of the matrix in order to guarantee the formation of entanglements with the matrix and avoid phase separation. As an example, the mechanical properties of a high density PE composite with 25% rayon and 3% PE-g-MAH as the CA are shown in Fig. 18.17 [data from Ganster et al. [12]].

Rayon reinforcement works exceptionally well. The results are similar to those for PP (Fig. 18.14) while the effects are generated here with only 25 wt% of fibers. Uncoupled composites have not been investigated.

Table 18.4 gives further examples. For a soft matrix material like Polybutene-1, strength is roughly tripled and modulus quadrupled. In the other cases, strength is doubled and the increase in modulus is between 50% and 100%. As to

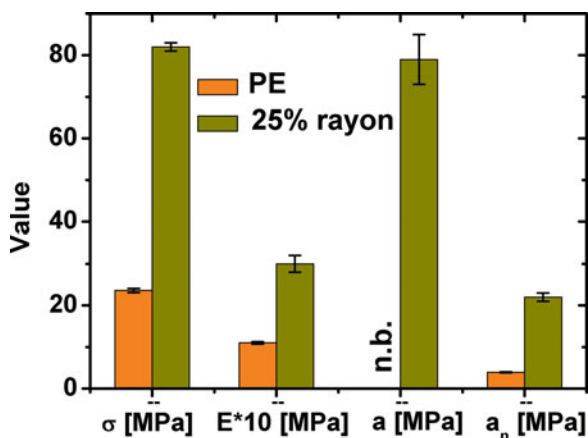


Fig. 18.17 Tensile strength and modulus, Charpy unnotched and notched impact strength for high density PE, and a PE–rayon composite with 3% PE-g-MAH

Table 18.4 Tensile and impact properties of selected matrix materials and the corresponding rayon composites

Material	Strength [MPa]	Modulus [GPa]	Charpy [kJ/m ²]	Charpy(n) [kJ/m ²]
Polybutene-1	20.5 ± 0.5	0.500 ± 0.003	n.b. ^a	63 ± 3
with 30% rayon ^b	73 ± 2	2.30 ± 0.05	80 ± 5	16 ± 1
High impact PS	28.9 ± 0.2	2.0 ± 0.1	58 ± 15	12.3 ± 0.5
with 25% rayon ^c	58 ± 3	3.1 ± 0.4	45 ± 6	10.8 ± 0.4
ABS	42.2 ± 0.2	2.1 ± 0.1	n.b.	20.5 ± 0.3
with 30% rayon	74 ± 2	4.0 ± 0.1	38 ± 6	12 ± 1
PA12	43 ± 1	1.31 ± 0.01	n.b.	4.8 ± 0.3
with 30% rayon	75 ± 2	3.10 ± 0.05	40 ± 2	9 ± 1

^aNot broken

^bCoupled with PB-1-g-MAH

^cCoupled with Poly(styrene-co-MAH)

unnotched impact properties, all samples break when reinforced, but Charpy impact strength remains on a high (polybutene-1) or fair level. Notched Charpy increases (doubles) only for PA12, while the other materials, having a high level from the start, show reasonably good impact values above 10 kJ/m² in the composite.

In general it can be stated that rayon reinforcement provides a good bio-based option to increase strength and modulus of thermoplastic materials with a melting or softening point below, say, 200°C preserving or often increasing the impact properties of the matrix materials while very tough polymers retain a good impact level.

18.5 Composites with Bio-Based Matrices

Bio-based thermoplastic polymers or bioplastics, produced from renewable raw materials, have attracted much attention in recent years as a possible alternative to oil-based thermoplastics. Reinforcing those polymers with cellulosic fibers offers the possibility to improve their properties without compromising their bio-based nature. Using cellulose man-made fibers instead of wood or annual plant fibers offers the advantages mentioned in the Introduction and will be shown to give composites with high strength, stiffness, and impact strength.

18.5.1 *Poly(Lactic Acid)*

PLA [e.g., see Södergård and Stolt [26]] is one of the most important bio-based and biodegradable thermoplastic polymers commercially available today with some molecular weights and optical purities. First attempts to reinforce PLA with man-made cellulose fibers have been reported in [12], followed by papers of other groups [27–29]. Results are in full agreement with each other and will be reported on the basis of own work in this field [30, 31].

18.5.1.1 Tensile and Impact Properties

Compared to PP, PLA has a higher strength and a higher stiffness which are further increased by rayon reinforcement without any CA as shown in Fig. 18.18 for NatureWorks PLA 7000D. A higher fiber fraction generates higher strength and modulus, while the latter seems to be affected by reduced fiber distribution due to entanglements for concentrations above 25%. In similar composites, however, reinforced with thermo-mechanical pulp fibers, an increase in strength could not be observed [30] pointing out again the beneficial properties of rayon.

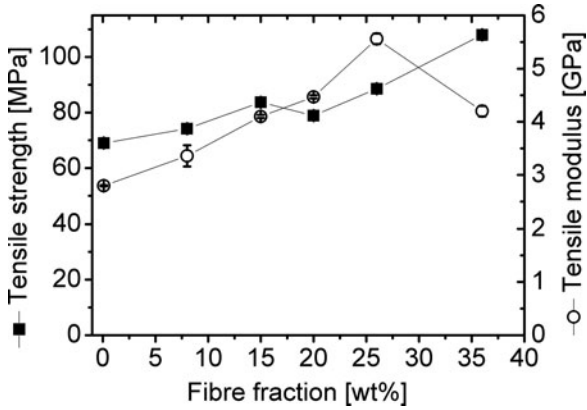


Fig. 18.18 Tensile properties of uncoupled PLA-rayon composites as a function of fiber content (from Ganster and Fink [30] with permission from CRC press)

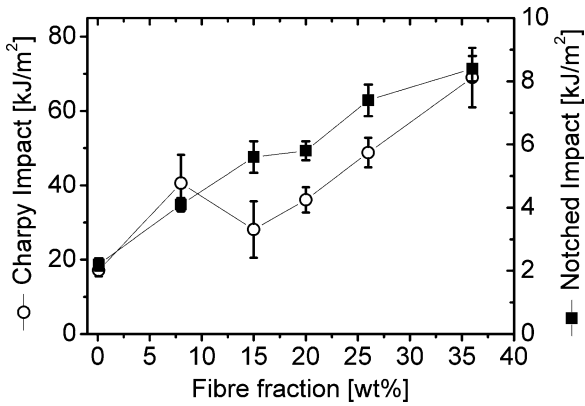


Fig. 18.19 Impact properties of uncoupled PLA-rayon composites as a function of fiber content (from Ganster and Fink [30] with permission from CRC press)

One of the disadvantages of PLA for many applications is its brittleness (20 kJ/m² and 2 kJ/m² for unnotched and notched Charpy, respectively). Instead of using common impact modifiers which reduce strength and stiffness, rayon fibers generate improved impact properties both in the unnotched and notched testing modes, as demonstrated in Fig. 18.19. Again, with wood or natural fibers, such a behavior cannot be generated [30].

Notched Charpy impact at reduced temperature (−18°C) is quite similar to the values for that property at room temperature [30]. There is no glass transition in between and PLA itself is not embrittled as, e.g., PP.

18.5.1.2 Fiber–Matrix Coupling and Decoupling

The results in the preceding paragraph were obtained without the use of any CA but from the experience with PP (Fig. 18.14) it can be assumed that further improvements are possible. Since MAH grafted PLA could not be synthesized, an alternative coupling mechanism was developed based on a bifunctional isocyanate, i.e., hexamethylene diisocyanate (HMDI). As shown in Fig. 18.20, the HMDI-cyanate groups can react with the cellulose surface hydroxyl groups to form amide linkages on the one hand, and react with the PLA end hydroxyls or carboxyls to form amide or urethane links, respectively, on the other.

That this mechanism leads to successful bonding indeed is demonstrated with the SEM cryo fracture micrographs in Fig. 18.21 of composites with 20% rayon and 1 wt% HMDI produced on a 100 g scale using a kneader. Three cases are shown: the

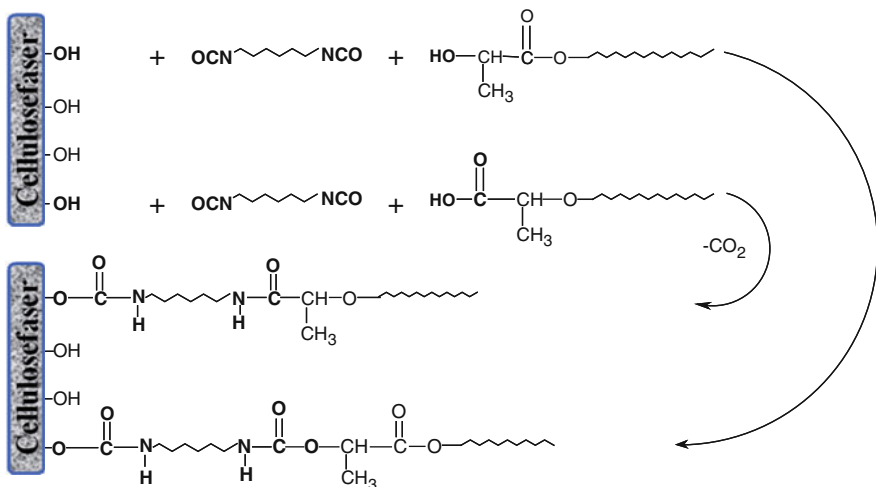


Fig. 18.20 Possible mechanisms of fiber–matrix coupling through a reaction with hexamethylene diisocyanate

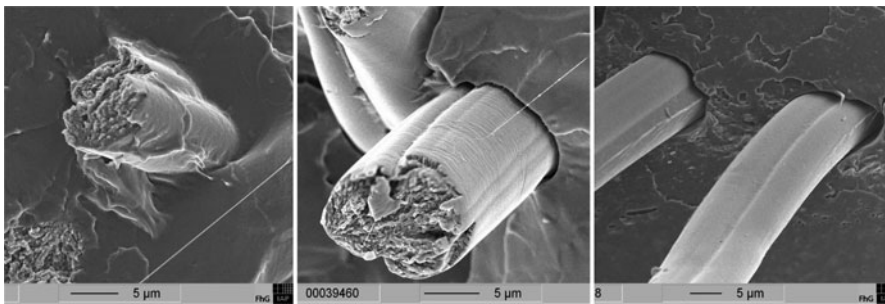


Fig. 18.21 SEM cryo fracture micrographs of PLA–rayon composites with strong (*left*), moderate (*middle*), and weak (*right*) interphase

HMDI-coupled composite on the left, the one without coupling in the middle, and a composite with a decoupling interface on the right (see below).

The effects might be even more obvious in Fig. 18.22, where a lower magnification of cryo fracture surfaces of the same composites is presented. Almost no fiber stumps are detected for the strong, HMDI-coupled interphase (left) while medium length stumps/pullouts are found for the “normal” case without CA (middle), and extremely long pullouts are visible for the so-called weak interphase (right).

The latter was designed by impregnating the fibers with PP-g-MAH by reactive extrusion in the mixing step during compounding. A concentration of 3 wt% PP-g-MAH was used, analogous to the PP case. In that way fibers become covered with PP-g-MAH and thus a hydrophobic surface is generated which does not attach to the polyester matrix and so, long pullouts are produced during fracture.

The consequences of the interphase design on mechanical properties are shown in Fig. 18.23. In contrast to the PP case, the tensile strength is not increased much by

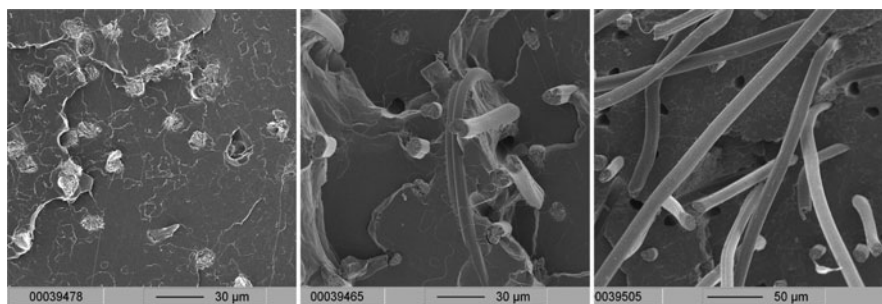


Fig. 18.22 Same as Fig. 18.21 but with lower magnification

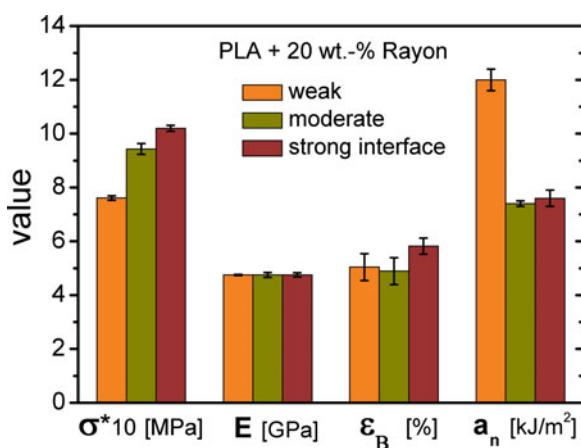


Fig. 18.23 Selected mechanical properties of PLA–rayon composites with designed interphases

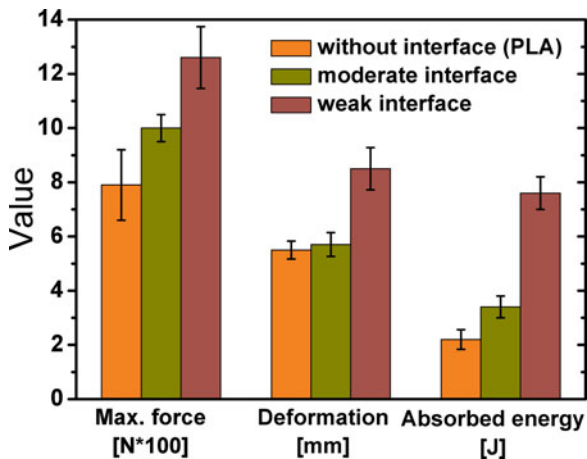


Fig. 18.24 Results of the dart drop test showing the increased energy absorption due to decoupling with a hydrophobic fiber surface (weak interphase)

the action of the CA. Elongation and modulus are not changed by both the weak and strong interphase. However, the weak interphase acts as a means to improve the notched impact strength considerably [32]. Obviously, a frictional mechanism is activated allowing a long fiber pullout which is absorbing an appreciable amount of fracture energy.

This effect is fully corroborated by a dart drop test (DIN EN ISO 6603-2) with a 100 J dart and injection molded plates of 2 mm thickness, as shown in Fig. 18.24. In particular, the absorbed energy during the puncture event for the weak PP-g-MAH interphase is more than doubled compared to the “normal” composite without decoupling (moderate interphase).

A summarizing comparison for composites produced on a kilogram-scale with the two-step method described above including unnotched Charpy values and data for glass fiber reinforced PP is given in Fig. 18.25.

It is evident that excellent Charpy values both for the unnotched and notched experiments are obtained when using the decoupling agent. Slight decrease in strength must be accepted, but with over 75 MPa, tensile strength is still on a level exceeding glass fiber reinforced PP.

18.5.2 Polyhydroxyalkanoates

PHA constitute a whole class of microbially synthesized polyesters [33], of which polyhydroxybutyrate (PHB) and the copolymer with valerate (PHBV) have attracted much attention as possible replacements of oil-based thermoplastics. To serve as a useful injection moldable plastic with reasonable ductility, PHA

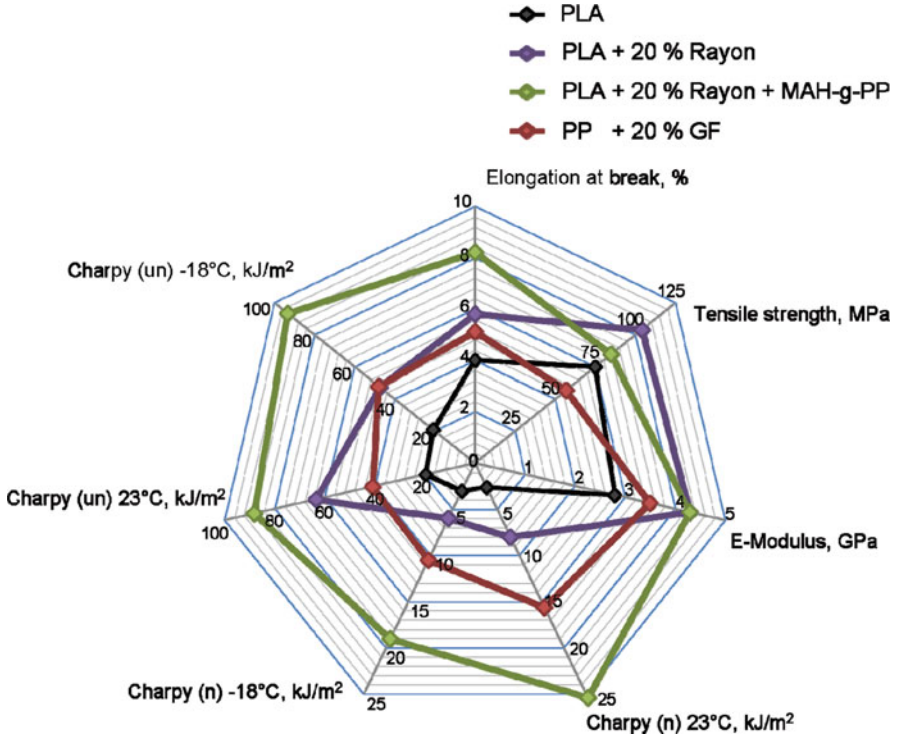


Fig. 18.25 Selected mechanical properties of PLA (black) and its rayon composites with standard (blue) and weak (green) interphase in comparison to glass fiber reinforced PP (red)

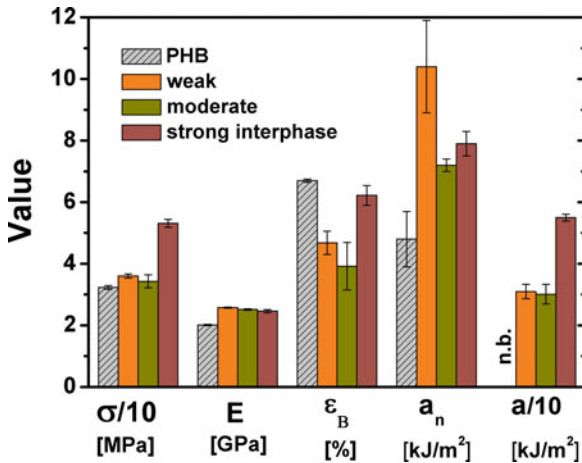


Fig. 18.26 Selected mechanical properties of PHB and PHB-rayon composites with designed interphases

has to be compounded with suitable cocomponents [34]. In the work presented here, a commercial product, Biomer P226 (Biomer Co., Krailling, Germany) was used, again with 1% HMDI-coupling (strong interface), without coupling (moderate interphase), and 3% PP-g-MAH decoupling (weak interphase) with mechanical results presented in Fig. 18.26 for a fiber fraction of 20 wt%.

In contrast to the high-strength PLA, the strong interphase leads to a significant increase in tensile strength in the present case of a weaker matrix which is roughly half as strong. The modulus (all values taken after 7 days of storage to allow for crystallization) is increased only slightly from 2 to 2.5 GPa. Again, the weak interphase leads to the best improvement in notched impact strength from 5 to 10 kJ/m². A fairly high unnotched impact strength of 55 kJ/m² is obtained as the best value of the reinforced samples.

18.6 Conclusions

Cellulose man-made fibers, in particular rayon tire cord yarn, can advantageously be utilized for the reinforcement of thermoplastics. By melt mixing with 30 wt% fibers or less, matrix properties such as modulus, strength, or impact strength are increased significantly, often doubled, sometimes quadrupled.

For strength and modulus, this is true in particular for matrix materials with comparatively low modulus, such as, e.g., PP, PE, and certain PHB formulations. For stiff and strong polymers, such as PLA, the effects are similar, but less pronounced.

Impact strength is increased significantly for brittle materials (PLA) and materials with low notched impact strength (e.g., PP) in particular at reduced temperatures when a matrix glass transition is passed (e.g., PP). Impact strength of very tough matrix materials cannot be improved; however, values remain on a high level.

Rayon fibers represent an ideal reinforcement for bioplastics, since the composite material remains bio-based and/or biodegradable. With PLA and PHB, the fiber–matrix interphase can be designed to be weak (decoupling), moderate (without CA), and strong (HMDI coupling). A decoupled interphase results in much improved notched impact values by activating a frictional, fracture energy absorbing fiber pull out.

The cellulosic nature of the rayon fibers entails certain limitations in terms of processing temperature and discoloration. These effects have to be further studied and the nature of degradation (oxidative vs. hydrolytic) has to be elucidated. Experience with bio-based PA11 shows that specific interactions of cellulose and spurious compounds present in the matrix must be taken into account. If remedies can be found either by adjusting processing conditions or adding inhibitors, higher melting polymers, in particular bio-based PAs such as PA6.10 and PA10.10 might be used as matrix materials.

The ground is laid for industrial use of man-made cellulose fibers for reinforcing a series of thermoplastics. Specific recipes, including processing aids, stabilizers, color master batches, etc., remain to be developed for possible applications in various sectors of the plastics industry.

References

1. Malkapuram R, Kumar V, Negi YS (2009) Recent development in natural fiber reinforced polypropylene composites. *J Reinf Plast Compos* 28:1169–1189
2. Kalia S, Kaith BS, Kaur I (2009) Pretreatments of natural fibers and their application as reinforcing material in polymer composites – a review. *Polym Eng Sci* 49:1253–1272
3. John MJ, Thomas S (2008) Review – biofibers and biocomposites. *Carbohydr Polym* 71:343–364
4. Weigel P, Ganster J, Fink H-P, Gassan J, Uihlein K (2002) Polypropylene-cellulose compounds. High strength cellulose fibers strengthen injection molded parts. *Kunststoffe Plast Eur* 92(5):35–37
5. Fink H-P, Weigel P, Geiger O, Busch M (2004) Neue Commodity-Verbundmaterialien unter Verwendung von Cellulose regeneratfasern. *Technische Textilien* 47:126–130
6. Ganster J, Fink H-P (2009) The structure of man-made cellulosic fibres. In: Eichhorn S, Hearle JWS, Jaffe M, Kikutani T (eds) *Handbook of textile fibre structure*, vol 2, Natural, regenerated, inorganic, and specialist fibres. CRC, Boca Raton, FL
7. Ganster J, Fink H-P (2006) Novel cellulose fibre reinforced thermoplastic materials. *Cellulose* 13:271–280
8. Voges M, Brück M, Gensrich J, Fink H-P (2002) The CARBACELL process – an environmentally friendly alternative for cellulose man-made fibre production. *ipw/Das Papier*, Issue 4, T74
9. Hofmann D, Fink H-P, Philipp B (1989) Lateral crystallite size and lattice distortions in cellulose II samples of different origin. *Polymer* 30:237–241
10. Rihm R (2003) Röntgen-Strukturuntersuchungen an Cellulose regeneratfasern. PhD thesis, TU Berlin, p. 90. http://deposit.d-nb.de/cgi-bin/dokserv?idn=969224958&dok_var=d1&dok_ext=pdf&filename=969224958.pdf. Assessed 4 February 2010
11. Fink H-P, Weigel P, Purz HJ, Ganster J (2001) Structure formation of regenerated cellulose materials from NMMO-solutions. *Prog Polym Sci* 26:1473–1524
12. Ganster J, Pinnow M, Fink H-P (2006) High tenacity man-made cellulose fibre reinforced thermoplastics – injection moulding compounds with polypropylene and alternative matrices. *Compos A* 37:1796–1804
13. Thomason JL (2002) The influence of fiber length and concentration on the properties of glass fiber reinforced polypropylene: 5. Injection molded long and short fiber PP. *Compos A* 33:1641–1652
14. Bader MG, Hill AR (1993) Short fiber composites. In: Chou T-W (ed) *Material science and technology – a comprehensive treatment*, vol 13: structure and properties of composites. VCH, Weinheim, Germany, pp 291–338
15. Fink H-P, Ganster J, Uihlein K, Zengel A, Zimmerer B (2006) Flowable pellets based on cellulose textile fibers and a method for the production thereof. WO2006/032406
16. Bayer R (2003) Feed system for continuous supply of loose materials to an extruder comprises a side screw feeder through which material is drawn by an air flow and then separated from the air by a screen. DE10201869
17. N.N. to Kreyenborg (1982) Stopfwerk für Kunststoffextruder. DE3031201
18. Busch M, Stache P (2009) Device for feeding short fibers. DE102007047548

19. Dominginghaus H (2005) Polyolefine (PO). In: Eyerer P, Elsner P, Hirth T (eds) Die Kunststoffe und ihre Eigenschaften, 6th edn. Springer, Heidelberg, p 453 ff
20. Felix JM, Gatenholm P (1991) The nature of adhesion in composites of modified cellulose fibers and polypropylene. *J Appl Polym Sci* 42:609–620
21. Paunikallio T, Suvanto M, Pakkanen TT (2004) Composition, tensile properties, and dispersion of polypropylene composites reinforced with viscose fibers. *J Appl Polym Sci* 91:2676–2684
22. Paunikallio T, Kasanen J, Pakkanen TT (2003) Influence of maleated polypropylene on mechanical properties of composite made of viscose fiber and polypropylene. *J Appl Polym Sci* 87:1895–1900
23. Ganster J, Fink H-P (2003) Wärmeformbeständige Commodity-Verbundwerkstoffe. Fraunhofer IAP Jahresbericht. p 20
24. Khan MA, Ganster J, Fink H-P (2009) Hybrid composites of jute and man-made cellulose fibers with polypropylene by injection molding. *Compos A Appl Sci Manuf* 40:846–851
25. Ganster J, Fink H-P, Uihlein K, Zimmerer B (2008) Cellulose man-made fibre reinforced polypropylene – correlations between fibre and composite properties. *Cellulose* 15:561–569
26. Södergård A, Stolt M (2002) Properties of lactic acid based polymers and their correlation with composition. *Prog Polym Sci* 27:1123–1163
27. Bax B, Müssig J (2008) Impact and tensile properties of PLA/Cordenka and PLA/flax composites. *Compos Sci Technol* 68:1601–1607
28. Graupner N, Herrmann AS, Müssig J (2009) Natural and man-made cellulose fibre-reinforced poly(lactic acid) (PLA) composites: an overview about mechanical characteristics and application areas. *Compos A Appl Sci Manuf* 40:810–821
29. Beldzki AK, Jaskiewicz A, Scherzer D (2009) Mechanical properties of PLA composites with man-made cellulose and abaca fibres. *Compos A* 40:404–412
30. Ganster J, Fink H-P (2009) PLA-based bio- and nanocomposites. In: Lau AK-T, Hussain F, Lafdi K (eds) Nano- and biocomposites. CRC, Boca Raton, FL
31. Ganster J, Rihm R, Erdmann J, Fink H-P (2010) Cellulose man-made fiber reinforced bioplastics – structure and mechanical properties. ACS Spring Meeting, San Francisco, CA, 21–25 Mar 2010
32. Erdmann J, Ganster J (2010) Verfahren zur Hydrophobierung von cellulosischen Fasern mit dem Effekt der Schlagzähverbesserung in Bioverbunden. German patent application AZ102010008780.7
33. Chen G-Q (2009) A microbial polyhydroxyalkanoates (PHA) based bio- and materials industry. *Chem Soc Rev* 38:2434–2446
34. El-Hadi A, Schnabel R, Straube E, Müller G, Henning S (2002) Correlation between degree of crystallinity, morphology, glass temperature, mechanical properties and biodegradation of poly(3-hydroxyalkanoate) PHAs and their blend. *Polym Test* 21:665–674

Chapter 19

Degradation of Cellulose-Based Polymer Composites

J.K. Pandey, D.R. Saini, and S.H. Ahn

Abstract The primary objective for development of cellulose-based polymer composites is to create a material with acceptable environmental degradability in order to reduce the increasing ecological risk by so-called nonbiodegradable polymers. It is believed that cellulose may act as biodegradable part in the composite, which is preferably consumed by microorganism leaving behind disintegrated polymer fraction that may enter in bio-cycle in a systematic manner and ultimately convert into biomass and carbon dioxide. The present chapter is focused on the biodegradation behavior of cellulose-based composites under different circumstances.

Keywords Biocomposites · Biodegradation · Biopolymers · Cellulose · Photo-degradation

Contents

19.1	Introduction	508
19.2	Biodegradation	509
19.2.1	Process of Biodegradation	509
19.2.2	Measurement of Degradation	511
19.3	Degradation of Cellulose	513
19.4	Biodegradation of Cellulose-Based Composites	513
19.5	Conclusions	516
References	517

S.H. Ahn (✉)

School of Mechanical and Aerospace Engineering, Seoul National University, Kwanak-Ro 599,
Seoul 151-742, South Korea
e-mail: ahnsh@snu.ac.kr

19.1 Introduction

Polymer composites from renewable resources offer an answer to maintain the sustainable development of economically and ecologically attractive technology. Nature's litter is acceptable because it is biodegradable, even though it may take several years to be bioassimilated completely into the ecosystem, whereas plastics (particularly polyolefins) are normally considered as a nonbiodegradable material when discarded after the end of its useful life in comparison to the time scale when the nature's materials are assimilated into biosystem. The mixing of biopolymers in the matrix of polymers has been recognized as a relevant way to get rid of plastic waste. However, this blending may lead to phase separation and reduction in mechanical properties due to the lack of compatibility between hydrophilic biopolymer and generally hydrophobic thermoplastic. In the family of the polymers of renewable resources, cellulose has been considered as the most promising material for this purpose as it exists abundantly and may form a cost-effective end product [1, 2]. Light weight, low price, wide availability in a variety of forms, low density, comparable material properties, high molding flexibility, and particularly biodegradable nature makes cellulosic material a conceivable option to traditional fillers like mica, calcium carbonate, and glass [2].

In plant cell walls, stiff semicrystalline cellulose microfibrils are embedded in a pliable amorphous matrix. The modulus of elasticity of the homopolymer cellulose is approximately 134 GPa in the axial direction under moist conditions [3, 4]. Chemically, cellulose is a hydrophilic glucan polymer consisting of linear chain of 1,4- β -bonded anhydroglucose units, which contains alcoholic hydroxyl groups. These hydroxyl groups form inter- and intra-molecular hydrogen bonds inside the macromolecule itself and among other cellulose macromolecules as well as with hydroxyl groups from the air [3]. It has been hypothesized that the orientation of the cellulose microfibrils during deposition is controlled by geometrical constraints of the cell and the number of cellulose synthase complexes [4]. The specific chain orientation, extended chain conformation with morphology of least defect provides them a significant load carrying capability around order of 10 GPa strength [5]. The tensile strength of flax ranges from 254 to 390 N mm⁻² [6] to 1,100 N mm⁻² [7] and that of jute varies between 187 N mm⁻² [8] and 533 N mm⁻² [7]. Cellulose fibrils of 5–20 nm diameter and length of 100 nm to several micrometers depend upon origin, linked together by disordered region (amorphous domains) and stabilized laterally by intra- and intermolecular electrostatic bondings; they are recently being used to develop cellulose-based nanocomposites [4, 9].

After resolving the incompatibility and dispersion issues between hydrophilic cellulose and mostly hydrophobic matrix in order to increase the mechanical performance of resulting composites up to a satisfactory level (not equal to glass fiber-reinforced engineering plastic composites) [10], mainly through surface chemistry, it appears essential to evaluate the fate of product at the end of its use or start of disposal [11]. It has been addressed during the comparison of synthetic and bio-fibers in more detail, that the total replacement of glass fibers

with cellulosic material (e.g., flax fibers) was difficult, and that glass fibers were more competitive as polymer fillers [10]. The present chapter is aimed to discuss the biodegradation of cellulose composites which is probably a key factor to enhance the industrial and social acceptance of cellulose-based material.

19.2 Biodegradation

19.2.1 Process of Biodegradation

In general, degradation is the process where the deterioration in the properties of the polymer takes place due to different factors like light, heat, UV rays, mechanical, etc. As a consequence of degradation, the resulting smaller fragments do not contribute effectively to the mechanical properties and the article becomes brittle and the life of the material becomes limited [2]. There are several means of polymer degradation such as thermal, photo, X-rays, γ , rays, mechanical, and biodegradation [12]. Polymer chains containing ester, amide, and acetal functional groups in their backbone may undergo degradation by the hydrolysis at a particular pH. Many high-molecular-weight elastomers can be attacked by ozone where they form ozonides. The definition of biodegradation is not always clear and is open to a large diversity of interpretations as it has to cover duration, mechanism, circumstances, and most importantly the nature of residual waste after the process. In a biodegradable plastic, degradation results from the action of naturally occurring microorganisms such as bacteria, fungi, and algae, whereas biodegradability is the ability of material to be utilized as a carbon source by microorganisms and converted safely into carbon dioxide, biomass, and water (ASTM's definitions). In case of polyolefin, microbial attack starts after functionalization of polymer chains [12, 13]. A carbonyl group is generated in the polymer during photo-oxidation process. Photodegradation begins with the production of macro-radical (P^{\cdot}), preferentially in the amorphous regions of polymer substrate. This radical rapidly reacts with oxygen to give a macroperoxy radical (POO^{\cdot}), which abstracts a hydrogen atom from the polymer backbone to produce a hydroperoxide group ($POOH$) [10, 11]. The hydroperoxide group is photolytically cleaved to produce the highly reactive radicals, which continue the chain degradation in the polymer, irreversibly [12–14]. The tentative cycle of degradation and stabilization is illustrated in Fig. 19.1. Carbonyl groups may convert into ester functionality as represented in Fig. 19.2. Additional functionalization may generate by cleavage of carbonyl group through Norrish type-I and -II mechanisms (Fig. 19.3). The manner and rate of degradation of these plastics are dependent on the mechanism and acceleration of process. The degradation process may cause erosion on the surface and photodegradation generates several small chains with hydroxyl groups as could be evidenced by increasing the area under FTIR analysis (Fig. 19.4) [14]. In the biodegradation experiment with PE wax where its MW distribution peaked at

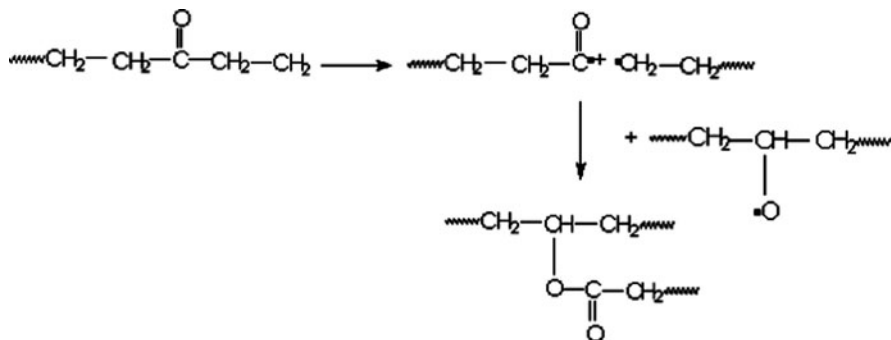


Fig. 19.3 Norrish Type First (NI I) and Norrish type second (NI II) reactions during photodegradation of polyethylene

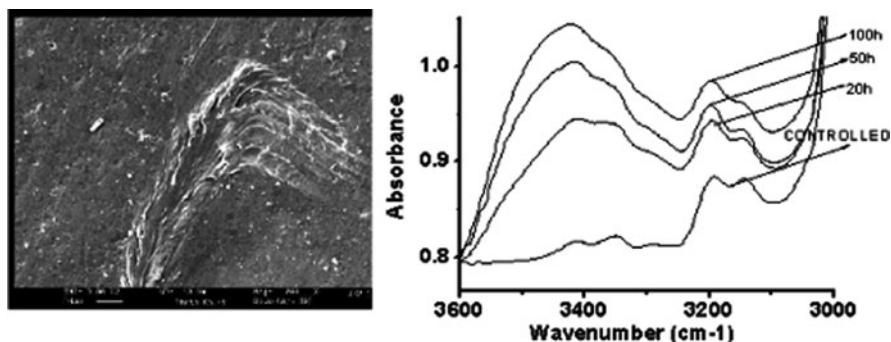


Fig. 19.4 SEM of degraded samples of cellulose polypropylene composites (a) and changes in the FT-IR spectra (hydroxyl region) of GFC of PP upon irradiation after different hours. (b) From Pandey [15]

and water releases after entering the citric acid cycle from these carboxylic acid containing short chains. The terminal carboxylic groups may also be formed by breaking the ester bonds, generated during degradation by other factors [14, 16]. The consumption of these functionalized chains in polymer was ascertained through FT-IR analysis [15] where a decrease in the carbonyl region (1,850–1,550 cm⁻¹) was observed after composting and attributed to the release of short chains in the form of degradation products during the biotic step as in the case of paraffin. Here it is worth recalling that nature and process of degradation also depend on the type of microorganism and measurement parameters such as temperature, humidity, duration, etc.

19.2.2 Measurement of Degradation

The International Organization for Standardization (ISO) is a worldwide federation of national standard bodies. Table 19.1 described the methods for aerobic

Table 19.1 ISO/DIS methods for the evaluation of biodegradability

Standard	Description
ISO/DIS 14851	Evaluation of the ultimate aerobic biodegradability in an aqueous medium – method by determining the oxygen demand in a closed respire-meter
ISO/DIS 14852	Evaluation of the ultimate aerobic biodegradability in an aqueous medium – method by analysis of released carbon dioxide
ISO/DIS 14855	Evaluation of the ultimate aerobic biodegradability and disintegration of plastics under controlled composting conditions – method by analysis of released carbon dioxide

Table 19.2 Evaluation of environmental degradability of polymers

Composting environments	
Standard	Description
[D 5338]	Standard test method for determining the aerobic biodegradation of plastic materials under controlled composting conditions
[D 5209]	Standard test method for determining the aerobic biodegradation of plastic materials in the presence of municipal sewage sludge
[D 5512]	Standard practice for exposing plastics to a simulated compost environment using an externally heated reactor
[D 5509]	Standard practice for exposing plastics to a simulated compost environment
[D 5988]	Standard test method for determining the aerobic biodegradation in soil of plastic materials or residual plastic materials after composting
[D 6340]	Standard test for determining aerobic biodegradation of radiolabeled plastic materials in compost environment
[D 5152]	Standard practice for water extraction of residual solids from degraded plastics for toxicity testing
<i>Anaerobic digestion/processes</i>	
[D 5271]	Standard test method for assessing the aerobic biodegradation of plastic materials in an activated-sludge-wastewater-treatment system
[D 5210]	Standard test method for determining the anaerobic biodegradation of plastic Materials in the presence of municipal sewage sludge
[D 5526]	Standard test method for determining anaerobic biodegradation of plastic materials under accelerated landfill conditions
<i>Photodegradation environment</i>	
[D 3826]	Practice for determining degradation end point in degradable polyolefins using a tensile test
[D 5071]	Practice for operating xenon arc-type exposure apparatus with water for exposure of photodegradable plastics

biodegradation those that have recently advanced to Draft of International Standard (DIS) stage. ISO/DIS 14851, 14852, and 14855 are recognized as useful screening tests for establishing the aerobic biodegradability or compostability of plastics. Some other test methods are DIN (Deutsches Institut für Normung)-54900-Draft for evaluation of the compostability and CEN (Comité Européen de Normalisation)-TC 261/SC4/WG2 for evaluation of the compostability, biodegradability, and disintegration of plastics. American Society of Testing of Materials (ASTM) has established many standards for the measurement of environmental degradability of polymers as has been tabulated in Table 19.2. ASTM D 5247 is used for

determining the aerobic biodegradability of degradable plastics by specific microorganisms, whereas photodegradation in plastic may be evaluated by ASTM D 5208, which is a practice for operating Fluorescent UV and Condensation Apparatus for Exposure of Photodegradable Plastics.

19.3 Degradation of Cellulose

Because of the highly crystalline microfibrils embedded inside the matrix of cellulosic polymers, the penetration of degradative enzymes become restricted and make the cellulose less degradable toward enzymatic hydrolysis. Chemically, β -glucosidic linkage between the cellulose base units hydrolyzes in acidic and basic media [17]. An additional degradation reaction taking place in alkaline media is the so-called peeling reaction. In the course of this reaction, which even takes place at temperatures well below 100°C, the cellulose chain molecules are degraded step-by-step, beginning at the reducing end and proceeding in a “zipper-like” reaction [18].

Cellulose biodegradation by fungi has generally been considered to involve only three types of hydrolytic enzymes: endoglucanases (EGs), cellobiohydrolases (CBHs), and β -glucosidase (BGL). EGs randomly cleave the internal β -1,4-glucosidic links, CBHs act on the free ends of cellulose polymer chains, and BGL hydrolyzes cellobiose and other water-soluble cellodextrins to glucose [19]. A study by Yoon and Kim [20] demonstrated that the brown rot basidiomycete *Fomitopsis palustris* was able to degrade crystalline cellulose (Avicel). This fungus could also produce the three major cellulases (exoglucanases, endoglucanases, and glucosidase) when the cells were grown on 2.0% Avicel. Avicel degraded by *F. palustris* showed a decrease in relative crystallinity from 83 to 78.5% after 14 days of incubation. Hydrolysis of Avicel by the crude enzyme from *F. palustris* yielded 1.6 mg ml⁻¹ of glucose after 43 h, which corresponded to a cellulose conversion degree of 3.2%. Therefore, this study revealed for the first time that the brown rot basidiomycete *F. palustris* produces cellulases capable of yielding soluble sugars from crystalline cellulose. Factors such as the abundance and variety of microorganisms that can degrade cellulosic materials, the general adaptability of microbes to their environment, available carbon sources, and the long regulatory time period have been proven to play key role for the degradation of cellulose in the environments.

19.4 Biodegradation of Cellulose-Based Composites

The cellulose addition in the synthetic polymers is primarily focused to incorporate biodegradability. These biodegradable materials can be completely degraded into natural ecosystems such as active sludge, soil, lake, and marine. Accordingly, the

biodegradability of polymers corresponds to the ability to be chemically transformed by the action of biological enzymes or microorganisms.

Polypropylene and polyethylene are the most applicable polymers for commodity applications and have attracted major attention for their degradability. The pre-oxidized polymeric chains undergo simultaneous photolysis, hydrolysis, and biodegradation. Pandey and Singh [21] studied the biodegradability of polypropylene, polyethylene, and their copolymer under composting and culture environments. Weight loss is one of the most valuable data indicating the actual biodegradation of polymeric material after composting whenever validated by parallel monitoring of the neat respirometric microbial activity bound to the carbon content of the sample under testing. The weight loss UV irradiated, compost buried, polymer samples was measured periodically from 1 to 6 months. Among all the samples, longer hours irradiated sample showed much more weight loss after 5 months and was unrecoverable. Specimens of PP were showing comparatively high linear increase in degradation than observed for PE after 6 months, indicating the more susceptibility of PP to microorganisms of compost during degradation process. Furthermore, this fact was supported by more weight loss in PP (in both forms irradiated and unirradiated) in comparison with other samples. In the case of E-P copolymers, degradation rate was increased rapidly after 4-month incubation and both copolymer samples (EPF and EPQ, the molar percentages of ethylene content in copolymer samples was 7.7 and 15.1% for EPF and EPQ, respectively) were not recoverable after 6 months, suggesting that initially the degradation rate was slow due to comparatively less degradable ethylene component.

The effect of UV irradiation on the biodegradation of cellulose-based composites from PP, PE, and its copolymers has also been studied under composting and culture environments [22]. The polymers were blended with cellulose by two methods, first by melt mixing (direct method) and other by solvent mixing methods. The effect of compatibility was also studied on the degradation behavior of polymers. Photodegradation study shows that composites prepared from direct mixing method were more photodegradable than commercial polymers and composite prepared by grafting method. Biodegradability was increased with the increasing time of UV treatment. In compost incubation, weight loss of unirradiated samples for directly prepared composites was more than composite prepared by grafting method. This behavior was attributed to the additional degradation which had already taken place during preparation through peroxide-initiated photo-oxidation; consequently, there was generation of more active sites for microbial attack by providing functional groups. Kaczmarek and Oldak [23] studied the degradation of LDPE and its blend with cellulose in soil up to 1 year after treating under UV with different doses. The course of photo- and biodegradation was monitored by estimation of average molecular weights and polydispersity, gel amount, changes of PE crystallinity, and mechanical properties. It was found that biodegradation of PE with cellulose is hampered by intermolecular crosslinking of both components. Composting of preirradiated blend somewhat reduces its crosslinking (41.7% gel) compared with the effect observed in UV-irradiated (49.3% after 20 h UV) sample.

Attempts have been made to blend the cellulose with biodegradable polymers [biodegradable polymers may be defined [2] as those that undergo microbial induced chain scission, leading to mineralization, photodegradation, oxidation, and hydrolysis, which can alter the polymer during the degradation process]. The composites of cellulose and biodegradable polymers may be considered as a safe option for complete mineralization of end product mainly because both matrix and reinforcing phases are biodegradable in nature.

Ki et al. [24] investigated the biodegradability of composites from poly(butylene succinate) (PBS) and bio-flour in natural and aerobic compost soil. It could be observed that the biodegradability of PBS initially commences with surface erosion, followed by random chain scission of the PBS main chain from the attached soil microbes. The decreased molecular weight of PBS may be attributed to the hydrolysis of the aliphatic ester linkage of PBS, as well as to the changed low-molecular-weight materials such as oligomer and monomer. Research by Barkoula et al. [25] focuses on flax fiber-reinforced composites based on polyhydroxybutyrate (PHB) and its copolymer with hydroxyvalerate (HV). The biodegradability of the composites is expressed as weight, stiffness, and strength loss as a function of burrier time. Composites manufactured through injection molding exhibited lower impact strength than those manufactured through compression molding. Based on the biodegradation study of PHB/HV composites, it was found that the tensile properties drop significantly in the initial stage of degradation and become more gradual in the later stages of biodegradation process.

The composites of aliphatic polyesters [poly(ϵ -caprolactone) (PCL), poly(3-hydroxybutyrate-*co*-3-hydroxyvalerate) (PHBV), PBS, and poly(lactic acid) (PLA)] with 10 wt% untreated or acetic anhydride-treated (AA-) abaca fibers have been prepared and tested during soil-burial test by Teramoto et al. [26]. The addition of abaca fibers caused the acceleration of weight loss in case of PHBV and PBS composites. Especially, when untreated abaca was used, the PHBV and PBS composite specimens were crumbled within 3 months. Although no weight loss was observed for neat PLA and PLA and treated abaca composite, the PLA and untreated abaca composite exhibited 10% weight loss at 60 days, which was caused by the preferential degradation of the fiber. The result was a marked contrast to the fact that neat PHBV and PBS specimens retain the original shape even after 6 months. Raberg and Hafren [27] made an attempt to show the biodegradability in relation to the properties of plastic and solid wood. This study describes the biodegradation of two wood species in combination with a biodegradable and a nonbiodegradable plastic. Wood blocks of Scots pine and English Oak were treated with biodegradable aliphatic polyester, polycaprolactone, and a nonbiodegradable aromatic thermoplastic, polystyrene. The effect of brown rot on wood was analyzed by the loss of cellulose birefringence as a result of the decay. The fungal cellulases degrade the crystalline cellulose in the outer secondary cell wall of the wood fibers. Scots pine showed the biggest improvement of resistance to fungal attack after impregnation, presumably because it is also the easier wood specie to impregnate. An environmentally friendly wood-based product composed of waste wood and poly(vinyl alcohol) (PVA) modified by phthalic anhydride, which possesses

mechanical properties and weight loss liable to be controlled by reactants ratio, was produced by Ozaki et al. [28]. Biodegradation in soil and mechanical properties were evaluated to establish a correlation between different parameters. When wood flour was added to PVA/phthalic anhydride reaction medium, crosslinking occurred between cellulose fibrils and PVA during the hot-pressing step. The presence of phthalic anhydride has proved to be a decisive factor in this system, promoting the reaction of crosslinking between fibrils and microfibrils through PVA chains. It was correlated that weight loss was higher in the composites with higher phthalic anhydride content.

Whatever the application, a natural concern often arises regarding the durability or degradability of polymeric materials, partly because of their useful lifetime and the requirement for maintenance and replacement. There are numerous reports in literature describing preparation, characteristics, and properties of cellulose-based composites. Commonly cellulose-based composites are called green/biodegradable/ecofriendly composites due to the presence of polymers from the nature. However, the literature on the biodegradability of these composites under different conditions is comparatively less available. The research on the development and characterization of cellulose-based composites should be assisted with the testing of biodegradability under defined circumstances

19.5 Conclusions

The need of biodegradable plastics has been increased during the past decades not only due to the increasing environmental concerns but also for its biomedical applications. It is appeared from the available literature that the mixing of cellulose in polymer matrix enhances the biodegradability of material under specified environmental conditions. However, the terms “biodegradation” and “compostability” are very common but are frequently misused. In general, during biodegradation the enzymes of the biosphere essentially take part at least in one step during cleavage of the chemical bonds of the material. Notably, biodegradation does not ensure that a biodegradable material will always degrade. In fact, degradation will only occur in a favorable environment and the biodegradable material will not necessarily degrade within a short time. It is, therefore, important to couple the term biodegradable with the specification of the particular environment where the biodegradation is expected to happen, and of the time-scale of the process. Advantages of natural fibers are low cost, low density, high specific properties, biodegradable, and nonadhesive characteristics. However, their inherent disadvantages such as the relatively low tensile property, high water absorbency, poor solubility, and processability have limited wider applicability of cellulose-based material. The design of an optimum model that can effectively balance biodegradability, mechanical properties, and cost of resulting hybrids is an essential requirement for the future.

Acknowledgment This work was supported by the Second Stage of Brain Korea 21 at Seoul National University. This project was part of the Practical Application Project in the Advanced Microsystems Packaging Program at Seoul Technopark (Grant 10029790), funded by the Ministry of Commerce, Industry, and Energy.

References

1. Kalpan DL (1998) In: Biopolymers from renewable resources. Springer, Germany
2. Mohanty A, Misra M, Hinrichsen G (2000) Biofibre, biodegradable polymer and bio-composites. *Macromol Mater Eng* 266:1–24
3. Mariam B (2008) *Nat Rev Genet* 9:433–443
4. Baker AA, Helbert W, Sugiyama J, Miles MJ (2000) *Biophysical Journal* 79:1139–1145
5. Samir MASA, Alloin F, Dufresne A (2005) *Biomacromolecules* 6:612–617
6. Fölster T, Michaeli W (1993) Flachs – eine nachwachsende Verstärkungsfaser für Kunststoffe. *Kunststoffe* 83:687–691
7. Flemming M, Ziegmann G, Roth S (1995) *Faserverbundbauwesen – Fasern und Matrices*. Springer, Berlin
8. Hinrichsen G, (1991) Herstellung und Charakterisierung von Naturfaser-Thermoplast-Verbund-Werkstoffen am Beispiel von Jutefaser-Polyolefin-Compositen. In: Congress reprint for the seminar ‘Flachs – ein nachwachsender Faserrohstoff, 2–3 May 1991, Bonn, Germany, pp 285–295
9. Kohler R, Nebel K (2006) *Macromol Symp* 244:97–106
10. Mohanty AK, Misra M, Drzal LT (2005), In: Natural fibers, biopolymers and biocomposites. CRC, Chicago
11. Pandey JK, Reddy RK, Kumar AP, Singh RP (2005) *Polym Degrad Stab* 88:234–250
12. Scott G, Gilead D (1995) Degradable polymers in waste and litter control. In: *degradable polymers: principles and applications*, Chapman & Hall, London
13. Koutny M, Lemaire J, Delort A (2006) *Chemosphere* 64:1243–1252
14. Albertsson AC, Andersson S, Karlsson SS (1987) *Polym Degrad Stab* 18:73–87
15. Pandey JK (2007) Degradability of polymer composites from renewable resources. PhD Thesis
16. Scott G (1994) Environmental biodegradation of hydrocarbon polymers. In: Doi Y, Fukuda K (eds) *Biodegradable plastics and polymers*. Elsevier Science BV, Amsterdam
17. Lai YJ (1981) “Kinetics of base catalyzed cleavage of glucosidic linkages.” In: *The Ekman Days 1981, vol 2 Int. Symp. Wood Pulp Chem*, Stockholm, p 26
18. Lindberg B (1956) *Sven Papperstidn* 59:42–49
19. Beguin P, Aubert J (1994) *FEMS Microbiol Rev* 13:25–58
20. Yoon J, Kim Y (2005) *J Microbiol* 53:487–492
21. Pandey JK, Singh RP (2001) *Biomacromolecules* 3:880–885
22. Pandey JK, Ahmed A, Singh RP (2003) *J Appl Polym Sci* 90:1009–1017
23. Kaczmarek H, Oldak D (2006) *Polym Degrad Stab* 91:2282–2291
24. Ki HS, Kim HJ, Lee JW, Choi IG (2006) *Polym Degrad Stab* 91:1117–1127
25. Barkoula NM, Garkhail SK, Peijs T (2010) *Ind Crops Prod* 31:34–42
26. Teramoto N, Urata K, Ozawa K, Shibata M (2008) *Polym Degrad Stab* 86:401–409
27. Raberg U, Hafren J (2008) *Int Biodeterior Biodegradation* 62:210–213
28. Ozaki SK, Monteiro MBB, Yanoc H, Imamura Y, Souza YM (2005) *Polym Degrad Stab* 87:293–299

Chapter 20

Biopolymeric Nanocomposites as Environment Benign Materials

Pratheep Kumar Annamalai and Raj Pal Singh

Abstract In the twenty-first century, major changes are coming and materials will be a key enabling technology. Fuel economy, consumption, and demand for high-performance light-weight materials are pressurizing the industrialists. The maximum possible use of renewable resources is gaining attention as an alternative to petroleum resources. On the other hand, reinforcement of polymers with nanoscale particulates has gained a massive attraction from the researchers in academia and industries, because of the exponential improvement in physical, mechanical, and thermal properties with smaller amount of incorporation. For a global commercialization of these materials, the environmental concerns such as raw materials, energy use, recycling, and disposal (especially via biodegradation) are also to be envisioned. Thus, this chapter is intended to review the recent research activities in the area of nanocomposites using biopolymers that include polymers derived from renewable resources. General preparation methods, structure–property relationships, and biodegradability of these nanocomposites have been discussed in the context of environmental benignness.

Keywords Biodegradation · Biopolymer · Cellulose · Composites · Nanocomposites · Renewable resources

Contents

20.1	Introduction	520
20.1.1	Polymers	520
20.1.2	Environmental Aspects	520
20.1.3	Biodegradation and Environmental Benignness	521

P.K. Annamalai (✉)

Division of Polymer Science and Engineering, National Chemical Laboratory, Dr. Homi Bhabha Road, Pune 411 008, India

and

Laboratoire Génie des Procèdes d'élaboration des Bioproduits (GPEB), Université Montpellier II, Place Eugène Bataillon, 34095 Montpellier, France

e-mail: pkannama@univ-montp2.fr

20.1.4	Biodegradable Polymers and Biopolymers	521
20.2	Bio-/Nano-Composites	523
20.2.1	Nanoscale Particle Reinforcement	523
20.2.2	Growth and Importance of Polymer Nanocomposites	524
20.2.3	Nanocomposites of Biodegradable Polymers	524
20.2.4	Biopolymer–Biopolymer Nanocomposites	528
20.3	Environmental Advantages of Biopolymeric Nanocomposites	530
20.4	Future Perspectives	531
20.4.1	New Materials for Existing Applications	531
20.4.2	Novel or Renewable Green Methods: Use of “Ionic Liquids”	531
20.4.3	Importance	532
20.5	Conclusion	532
	Reference	532

20.1 Introduction

20.1.1 *Polymers*

The polymer industry has revolutionized the quality of life through the generation of new materials that have transformed everything. Almost in every application from agriculture to transport and from aerospace to food packaging, the use of polymeric materials has become an integral part of our modern daily living and it is difficult to imagine our society without polymers. However, the growth of polymers and plastics has had remarkable parallels to the growth of the environmental movement.

20.1.2 *Environmental Aspects*

The evolution and the success of the chemical industry have intimately been related to the introduction of fossil feedstocks as a basis for synthesis. Today, fossil feedstocks are the most important raw materials for the chemical industry, accounting for more than 90% of their use. The success of plastics based on petroleum resources can be attributed not only to the reliable raw materials basis and to their versatile applications properties, but also to their melt processability (Mecking 2004). However, their real problem is disposal. In landfills, they occupy the land for indefinite amounts of time due to very slow degradation. As a result of the fossil fuel crisis, alternative energy and raw materials sources such as biomass are propagated and investigated intensely. The low production cost (labor and energy) of plastic materials from crude oil is attributed to their ease of processability and production. The processing of conventional materials (metal, glass, wood, and paper) requires more energy than that needed for plastics. Thus, as far as energy for the processing is concerned, the plastics make their use as a positive contribution

to the environmental resources. However, the long life and desirability of plastics, which have made them a material of choice for many applications, are seemingly a disadvantage when it comes to their disposal. The disposal of items made of petroleum-based plastics, such as fast-food utensils, packaging containers, and trash bags, also creates an environmental problem. Open burning of plastics is even more dangerous. Ultimately, polymer waste if dumped or discarded haphazardly will pose serious problems (litter, toxic, and blocking of sewage/drainage) (Maiti and Jana 2005).

20.1.3 Biodegradation and Environmental Benignness

Figure 20.1 shows the relationship of environmental benignness in the process of making polymeric materials. While developing any materials, environmental concerns such as minimal use of energy and solvents, reduced or no waste generation and recycling are to be considered. Polymer is affected by environmental conditions and proceeds over a time comprising of one or more steps. *In biodegradation, process is mediated at least one step/partially by a biological system* (Ottenbrite et al. 1992). It is a natural process by which organic chemicals in the environment are converted to simpler compounds, mineralized and redistributed through elemental cycles such as carbon, nitrogen, and sulfur cycles (Chandra and Rustgi 1998). It is believed to be an environment friendly method of disposal. Because the biodegradability of polymers will be independent of their resources and derivation methods. So, it should be differentiated from the polymers of renewable resources in the context of environmental friendliness.

20.1.4 Biodegradable Polymers and Biopolymers

In recent decades, polymer waste management through biodegradation and bioconversion has become more important. It has also motivated the development and

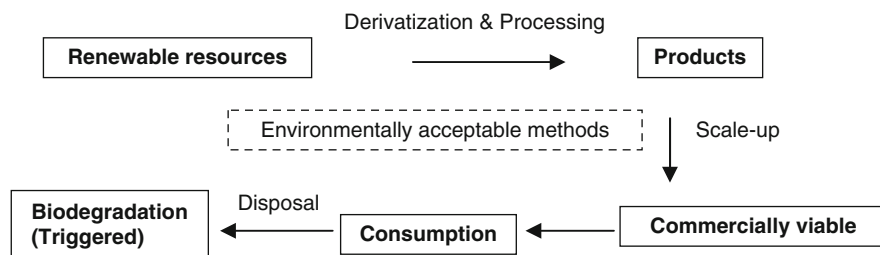


Fig. 20.1 Concept for environmental benignness

manufacture of polymers from biomass. Biodegradable polymers are designed to degrade by the action of living organism. They can be derived from both petroleum and renewable resources. However, petroleum resources are finite and prices are likely to continue to rise in the future (Patel 2003). It is necessary to find new ways to secure sustainable world development. Renewable biomaterials, which can be used for both bioenergy and bioproducts, are a possible alternative to petroleum-based synthetic products. The biodegradability is an added advantage for the polymers derived from renewable resources which are also called as “biopolymers”. However, there are also many biobased materials that do not exhibit inherent biodegradability (Steinbchel 2005).

The biobased polymers can be derived in three ways (Fig. 20.2). Firstly, the polymers, which are most commonly available in nature, are derived/extracted from marine and agricultural animals and plants. They are produced naturally during the growth cycles of organisms. Examples are polysaccharides such as cellulose, starch, chitin, and gums, proteins such as soya, gelatin, and lipids. Secondly, a wide range of polymers is synthesized by classical chemical synthesis method using biobased monomers (Lindblad et al. 2002), for example, polyesters, polyurethanes, polyamides, etc. They can also be called as “semisynthetic polymers”. To date, polylactic acid (PLA) has been proved to be commercially viable and successful in this category because of its potential for major scale production (Drumright et al. 2000). Its monomer, lactic acid, can be easily produced by fermentation of carbohydrate feedstock (corn, maize, and wheat). Thirdly, polymers are generated by microorganisms as a byproduct of their biochemical cycles, for example, polyhydroxyalkanoates (PHAs) and bacterial cellulose. The PHAs are polyesters that accumulate as inclusions in a wide variety of bacteria.

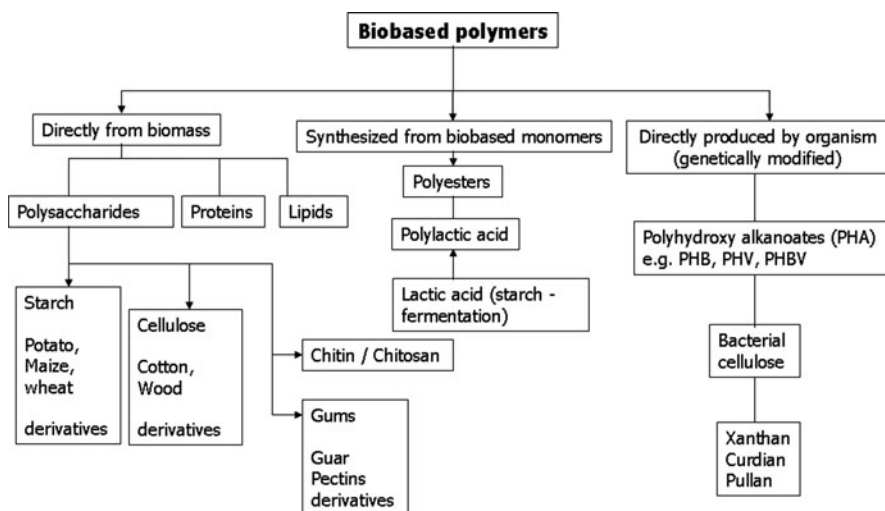


Fig. 20.2 Schematic representation of origin and method of production of biobased polymers

20.2 Bio-/Nano-Composites

20.2.1 Nanoscale Particle Reinforcement

The composite materials that combine one or more separate components in order to improve performance properties, for which at least one dimension of the dispersed particles is lesser than 100 nm (Kumar et al. 2009). As shown in Fig. 20.3, nanoscale particles are classified into three categories depending on their dimensions as follows: (a) *Nanoparticles*: When the three dimensions of particulates are in the order of nanometers, they are referred to as equi-axed (isodimensional) nanoparticles, nanogranules, or nanocrystals, for example, silica, titania, calcium carbonate, and magnesium oxide; (b) *Nanotubes*: When the two dimensions of particulates are in the nanometer scale and the third is larger, forming an elongated structure, they are generally referred to as “nanotubes” or nanofibers/whiskers, for example, carbon nanotubes (CNTs) and cellulose whiskers; (c) *Nanolayers*: The particulates that are characterized by only one dimension in nanometer scale are nanolayers/nanosheets, for example, clay (layered silicates) and layered double hydroxides (LDH). These particulates are present in the form of sheets of one to a few nanometers thick to hundreds to thousands nanometers long.

In principle, any kind of material can be produced to appear in a nanoscaled shape and size, but in the last few decades, none of these particles have gained as

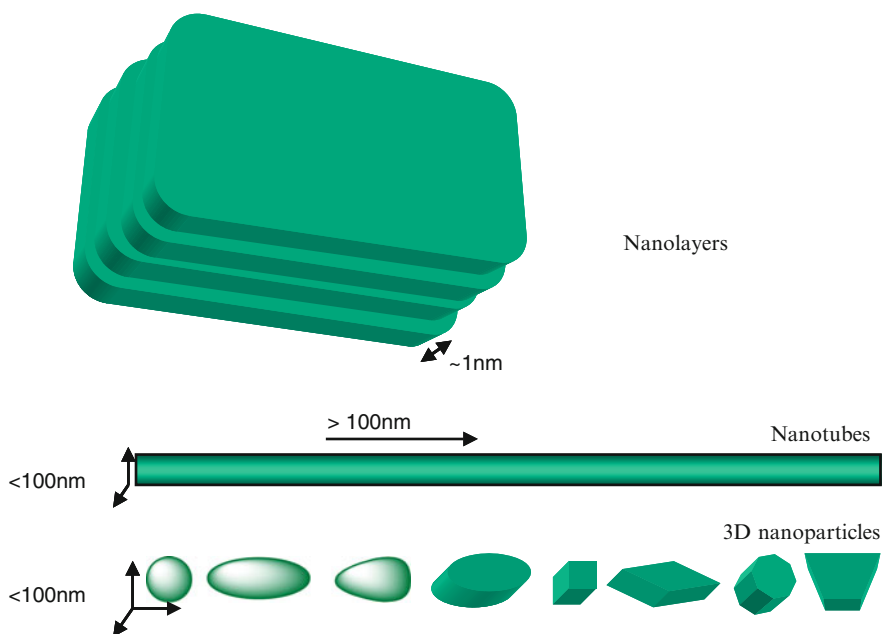


Fig. 20.3 Schematic representation of various shapes and dimensions of nanoscale materials

much attention as clay (especially layered silicates) and carbon nanotubes. This is because of the fact that they can simultaneously improve both physical, mechanical properties and flammability. Unlike conventional fillers, these nanosized particles have exhibited tremendous improvement in properties with very low amount of loading (up to 10 wt%).

20.2.2 Growth and Importance of Polymer Nanocomposites

Recently, a big window of opportunities has opened for polymer nanocomposites just to overcome the limitations of traditional microcomposites. Although, the chemistry of clay minerals and composites based on some nanoscale particles is known for several decades, the research and development of nanoscale-filled polymers has been skyrocketed in recent years, for numerous reasons. First, unprecedented combinations of properties have been observed in some polymer nanocomposites. For example, incorporation of isodimensional nanoparticles into thermoplastics increases the modulus, the yield stress, and the ultimate tensile strength (Sumita et al. 1983).

20.2.3 Nanocomposites of Biodegradable Polymers

Biodegradable polymers have great commercial potential for bioplastics, but in comparison to synthetic polymers, some of the properties, such as brittleness, low heat distortion temperature, high gas permeability, low melt viscosity for further processing, etc., restrict their use in a wide range of applications. On the other hand, nanoreinforcement of polymers has already proven to be an effective way to improve these properties concurrently (Ray and Bousmina 2005). Therefore, preparations to processing of biodegradable polymer-based nanocomposites, i.e., *green nanocomposites* are the wave of the future and considered as the next generation materials.

20.2.3.1 Cellulose-Based Nanocomposites

From the current point of view, cellulose is the most common organic polymer, representing about 1.5×10^{12} tons of the total annual biomass production, and is considered an almost inexhaustible source of raw material for the increasing demand for environmentally friendly and biocompatible products (Kaplan 1998).

The nanocomposites based on cellulose can be made in two ways: (a) the disintegrated microfibrils/nanoscale whiskers can be used for reinforcing polymers and (b) cellulose or cellulose derivatives can be reinforced by other nanoscale particles. In nanoscience and nanotechnology, cellulose and its derivatives are used as templates and surfactants for synthesizing inorganic nanoparticles for many industrial and biomedical applications.

Cellulose ester powders in the presence of different plasticizers and additives are extruded to produce various grades of commercial cellulose plastics in pelletized form. The nanoscale fillers can be mixed with these thermoplastic cellulose derivatives with the aid of plasticizers. Recently, Park et al. (2004) successfully used melt intercalation technique for the fabrication of cellulose nanocomposites from cellulose acetate (CA), triethylcitrate (TEC, as plasticizers), and organically modified clay.

20.2.3.2 Starch-Based Nanocomposites

Starch is not truly a thermoplastic as are most synthetic polymers, but it can be melted/processed using conventional plastic processing equipment with the addition of water and/or other plasticizers (generally polyols, such as glycerol) and made to flow at high temperatures under pressure and shear. De Carvalho et al. (2001) reported the first preparation of TPS/kaolin hybrids by melt intercalation technique using a twin screw extruder. Then, Park et al. (2002) reported the preparation of TPS/sodium montmorillonite (MMT) nanocomposites by melt intercalation in detail. They showed an intercalation of TPS in the silicate layer due to the matching of the surface polarity and interactions of the Cloisite Na⁺ and the TPS, which exhibited higher tensile strength and better barrier properties to water vapor than other TPS/organoclay hybrids as well as the pristine TPS. This indicates the potential of bionanocomposites with minimum possible processing.

20.2.3.3 Chitin/Chitosan-Based Nanocomposites

Chitin is a nitrogen-rich polysaccharide that is abundant in crustaceans, mollusks, insects, and fungi and is the second most abundant organic material found in nature next to cellulose. Chitosan, the *N*-deacetylated derivative of chitin, is environmentally friendly, nontoxic, biodegradable, and antibacterial. When the intrinsically beneficial effects of chitosan are combined with the enhanced properties of nanofibrous mats, applications arise in a wide range of fields, including medical, packaging, agricultural, and automotive. Unlike cellulose, it is easier to process or dissolve in acidic medium. Initially, Wang et al. (2005a, b) have successfully prepared chitosan nanocomposites with multiwalled carbon nanotubes (MWNTs) and clay by a simple solution–evaporation method. Similarly, using many other inorganic nanoparticulates, environmentally and biologically important nanocomposites were prepared (Huang et al. 2005a).

20.2.3.4 Other Polysaccharide Nanocomposites

Pectin is a linear macromolecule constituted of $\alpha(1 \rightarrow 4)$ linked D-galacturonic acid. This monomer unit could be partially replaced by $\alpha(1 \rightarrow 2)$ -linked L-rhamnose leading to a new structure named rhamnagalacturonan I. A third pectin structural

type is rhamnogalacturonan II, which is a less frequent complex and highly branched polysaccharide. Only few systems of nanobiocomposites have been elaborated, studied, and reported in the literature with MMT-Na or OMMT-OH2 (Mangiacapra et al. 2006). Pectin and clay nanocomposites were prepared just by dissolving milled pectin/clay powder in distilled water and casting. With OMMT-OH2, the results pointed out the major effect of the residence milling time on the resulting clay dispersion, a complete destructuration of the clay lamellar morphology being observed for high residence time. In similar condition, exfoliation state was also obtained with MMT-Na.

20.2.3.5 Protein-Based Nanocomposites

Proteins can be derived from animals (casein, whey, and collagen) and plants (zein, soy, and gluten). The proteins that have found applications as materials are, for the most part, neither soluble nor fusible without degradation, so they are used in the form in which they are found in nature. Because proteins can be used in applications where biocompatibility with the cells is required, most of the nanocomposites based on proteins are prepared with biologically important nanoparticles for biomedical applications (Wong et al. 1998). Initially, Lu et al. (2004) have successfully developed environmentally friendly thermoplastic nanocomposites using a colloidal suspension of chitin whiskers as a filler to reinforce soy protein isolate (SPI) plastics. According to Zhang et al. (2007), by dispersing nanoclay particles into plasticized protein systems, nanocomposites can be produced under thermal processing conditions. The exfoliation of the nanoparticles in wheat gluten (WG) has resulted in significant enhancement of the mechanical properties for both deamidated proteins and vital gluten systems under 50% relative humidity (RH). Such strength improvement was also pronounced for WG systems under a high humidity condition (RH = 85%). A similar level of further strength enhancement was obtained for the WG systems that had been strengthened by blending with poly(vinyl alcohol) (PVA) and cross-linking with glyoxal. The interactions between the gluten matrix and the nanoparticles were predominant in all of these nanocomposites for the enhancement of properties.

20.2.3.6 Polylactic Acid (PLA) Nanocomposites

The commercially successful biopolymer using biobased monomer is PLA. Its monomer, lactic acid, can be easily produced by fermentation of carbohydrate feedstock (corn, maize, and wheat). The properties of PLA are highly related to the D/L mesoform ratio. It can be plasticized using its monomer or oligomer. It can be processed into blown films, molded objects, and coatings. First, Ogata et al. (1997) prepared PLA/organically modified layered silicates (OMLS) blends by dissolving polymer and found that the silicate layers forming the clay could not be intercalated in the PLA/MMT blends. After that Bandyopadhyay et al. (1999) reported the preparation of intercalated PLA/OMLS nanocomposites with much

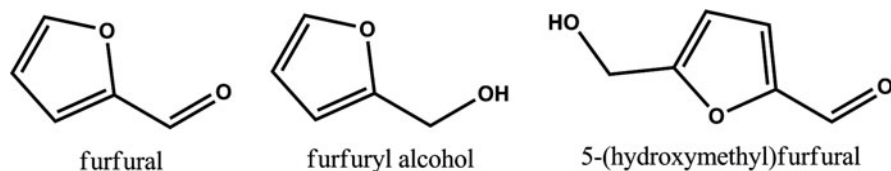


Fig. 20.4 Chemical structure of furan monomers

improved mechanical and thermal properties. Then, Ray et al. (2002a, b) have made many reports on PLA/clay nanocomposites.

In the category polymers from biobased monomers, next successful monomer is furfural. Furan resin can be derived from biomass (wood) through biotechnological transformation. In a peculiar version of a biorefinery, two first-generation furan derivatives (Fig. 20.4), furfural (F) and 5-hydroxymethylfurfural (HMF), readily prepared from ubiquitous C5 and C6 carbohydrate resources, respectively, represent the precursors to the rich array of monomer structures, suitable for any type of polymerization process. The vast majority of F is converted into furfuryl alcohol (FA), a well-established industrial commodity, which has found growing applications as a source of a variety of materials, with notable recent progress (Gandini and Belgacem 2008).

Using furfuryl alcohol, recently Pranger and Tannenbaum (2008) employed an in situ polymerization approach to produce polyfurfuryl alcohol (PFA) nanocomposites without the use of solvents or surfactants. On the one hand, furfuryl alcohol (FA) has a dual function, serving both as an effective dispersant for MMT clay nanoparticles and as the matrix precursor for the in situ polymerization.

20.2.3.7 Natural Oil-Based Nanocomposites

Many seed crops and some plants like flax also contain fatty acids and oils in which linoleic acid, oleic acid, and β -linolenic acids are major components. These unsaturated fatty acids are of interest for application in coatings and paintings and others utilizing air drying process (Höfer et al. 1997). Oleochemicals have long been recognized as useful precursors in preparing polymeric materials (polyesters and polyamides) (Hill 2007). Initially, Uyama et al. (2003) have synthesized new green nanocomposites consisting of plant oils and clay with much improved properties. They used epoxidized soybean oil (ESO) as an organic monomer. It triggered the use of natural oil for developing nanocomposites research. Later, Miyagawa et al. (2005) prepared nanocomposites with enhanced properties from functionalized vegetable oil [anhydride-cured epoxidized linseed oil (ELO)] and OMLS clay.

20.2.3.8 Other Biopolymer Nanocomposites

Natural polyhydroxyalkanoates are typically produced by different types of microorganisms as an energy storage product. Different approaches have been developed

to create highly versatile, sustainable, environment-friendly polyhydroxybutyrates (PHB) plastics either from plant or from bacteria. The PHB is a rare example of hydrophobic polymer that is truly biocompatible and biodegradable with high melting temperature and crystallinity. It has the potential to replace petroleum-based plastics in packaging, agricultural, and biomedical applications. Maiti et al. (2003, 2007) reported the first preparation of PHB/clay nanocomposites (PHBCNs) by melt intercalation method. The nanocomposites have shown significant improvement in thermal and mechanical properties of the matrix as compared to the neat polymer. The silicate particles were shown to act as a strong nucleating agent for the crystallization of PHB, which may be an added feature to improve the mechanical and optical properties. Similarly, the biodegradable nanocomposites based on other aliphatic polyesters are also prepared.

20.2.4 Biopolymer–Biopolymer Nanocomposites

Biopolymeric nanocomposites can be easily made using nanoparticles that are derived from biobased polymers. This is an added advantage in terms of reducing inorganic content in the nanocomposites with improved mechanical properties and without affecting inherent biodegradability.

20.2.4.1 Cellulose Whiskers as Nanoscale Fillers

The biosynthesis of cellulose has led to highly crystalline microfibrils, which are defect free, with the consequence of axial physical properties approaching perfect crystals. The research group at CERMAV-CNRS has shown that these microfibrils can be disintegrated and used as nanoscale fillers for reinforcing polymers (Favier et al. 1995). The microfibrils (10–50 nm width) are typically disintegrated from an edible tunicate (a sea animal) and parenchyma cells of sugar beet and potato tuber. They have presented numerous studies based on cellulose whisker-reinforced nanocomposites, which is separately discussed in this book in Chapter 7. Cellulose whiskers were used to obtain bionanocomposites/“green composites” natural polymers such as starch, cellulose derivatives, natural rubber, etc. A review of the recent research into cellulosic whiskers, their properties, and their application in nanocomposite field has been presented by the same group (Azizi Samir et al. 2005). Similarly, bacterial or microbial cellulose (BC) have also found their way as reinforcement in composites. Using low-cost plant primary cell walls, Bruce et al. (2005) prepared the high performance composites, which gave the best tensile properties. The control over properties (e.g., wettability, chemical resistance, biocompatibility, etc.) of the resultant composite materials can be achieved by surface coating the layer-by-layer assembly of polyelectrolytes (Huang et al. 2005b). Cao et al. (2007) have reported nanocomposite materials reinforced with flax cellulose nanocrystals in waterborne polyurethane. The films showed a significant increase in

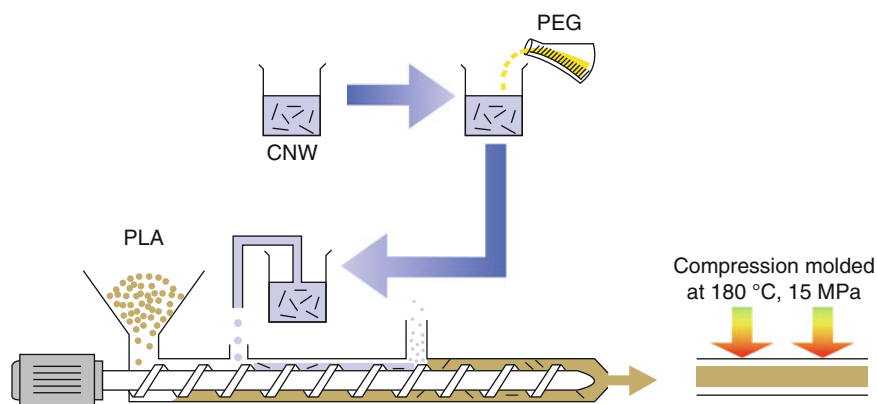


Fig. 20.5 Schematic of compounding process of PLA–nanocellulose composites

Young’s modulus and tensile strength from 0.51 to 344 MPa and 4.27 to 14.96 MPa, respectively, with increasing filler content from 0 to 30 wt%, with better dispersion.

Generally, the main challenge in developing nanocomposites with biopolymers is scaling-up by conventional melt processing methods. To achieve well-dispersed nanoreinforcements in the polymer matrix, Oksman et al. (2006) have encountered several compromises while making bionanocomposites based on cellulose nanowhiskers by melt compounding. Recently, they demonstrated the manufacturing process for cellulose whiskers/PLA nanocomposites. The composite materials were compounded using a corotating twin screw extruder as shown in Fig. 20.5.

As mentioned earlier, furyl alcohol can serve as both dispersants and matrices for polar nanoscale particles, cellulose whiskers were used to obtain PFA nanocomposites without the use of solvents or surfactants (Pranger and Tannenbaum 2008). Nowadays, the various sources (e.g., coconut husk and pea hull fibers) of cellulose whiskers are being explored (Chen et al. 2009; Rosa et al. 2010).

20.2.4.2 Starch Nanocrystal-Based Bionanocomposites

By analogy with works on cellulose whiskers, starch microcrystals can be processed by partial acid hydrolysis of the amorphous domains of starch granules into nanocrystals (Dufresne et al. 1996). The objective of this treatment is to dissolve away regions of low lateral order so that the water-insoluble and highly crystalline residue may be converted into a stable suspensoid by subsequent vigorous mechanical shearing action. It has been incorporated into natural polymers such as polyhydroxyalkanoates and natural rubber later (Angellier et al. 2005). In addition, starch nanocrystals were incorporated into starch itself to obtain all-starch “green nanocomposites” with remarkable improvements in the properties (Angellier et al. 2006).

20.2.4.3 Chitin Whisker-Based Bionanocomposites

Similarly, the chitin whiskers are made by partial hydrolysis, and incorporated biopolymers such as polycaprolactone (Morin and Dufresne 2002), natural rubber (Nair and Dufresne 2003), and SPI (Lu et al. 2004). Nowadays, different sources of chitin are treated to obtain nanocrystals (Goodrich and Winter 2007).

20.3 Environmental Advantages of Biopolymeric Nanocomposites

An interesting and exciting aspect of biopolymeric nanocomposites is the retained or enhanced biodegradability. A major problem with neat PLA is the slow rate of degradation as compared to the rate of waste accumulation. Ray et al. (2002a, b) have demonstrated improvement in materials properties and crystalline behavior with a simultaneous enhancement in biodegradability (by measuring CO₂ evolution under composting environment at $58 \pm 2^\circ\text{C}$) as compared to neat PLA by incorporating nanoscale filler, clay. Figure 20.6 shows the time dependence of the degree of biodegradation of neat PLA and its nanocomposites (PLACN4), indicating that the biodegradability of PLA in PLACN4 was enhanced significantly.

Thellen et al. (2005) observed about 48% and 50% improvement in oxygen and water vapor barrier with PLA/MMT nanocomposites in comparison to the neat PLA, which is an advantage for majority of packaging materials. Interestingly, their biodegradation rates in soil were slightly greater for the nanocomposites than the pure PLA.

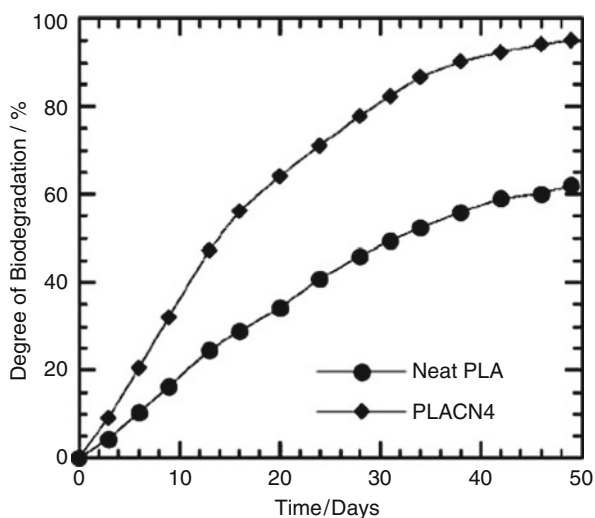


Fig. 20.6 Biodegradability of PLA nanocomposites measured by respirometry

Table 20.1 Global projection for materials demand in a “*business-as-usual*” scenario

	Total global demand (Mt/Year)					Of which from biomass in 2100	
	2000	2020	2030	2050	2100	%	Mt
Wood	306	530	670	1,010	1,620	100	1,620
Paper	320	600	760	1,110	1,750	100	1,750
Polymers	180	370	490	820	1,880	10–100	190–1,880
Total	806	1,500	1,920	2,940	5,250	68–100	3,560–5,250

20.4 Future Perspectives

Considering the demand and applications of biodegradable polymers, the shortage of landfill availability and petroleum resources and CO₂ neutrality, development of polymeric materials from renewable resources has revived research interests around the world. Table 20.1 shows the global projection for materials demand in a “*business-as-usual*” scenario (Chateau et al. 2005; Lysen 2001). It can be understood that the portion of biobased polymeric materials has to be increased according to the projected materials demand and considering the environmental balance.

20.4.1 New Materials for Existing Applications

Thus, it is necessary to develop research activities on exploring maximum possible use of various renewable resources for materials in new and more environmental friendly pathways. In essence, while current research on natural fibers focuses much on cellulosic fibers, Poole et al. (2009) highlighted that protein fibers regenerated from waste or byproduct sources should also be considered. For example, feather keratin and wheat gluten may both be suitable. They are annually renewable, commercially abundant, of consistent quality, and have guaranteed supply. They contain useful amino acids for fiber making, with interchain cross-linking possible via cysteine residues or through the metal-catalyzed photocrosslinking of tyrosine residues. Contemporary nanoparticle and cross-linking technology has the potential to overcome poor wet strength of conventional fibers, allowing commercial production to resume. This would bring together two existing large production and processing pipelines, agricultural protein production and textile processing, to divert potential waste streams into useful products.

20.4.2 Novel or Renewable Green Methods: Use of “Ionic Liquids”

Ionic liquids (ILs) are composed only of ions where at least one ion (usually the cation) is organic and whose melting points are below or not far above room temperature. ILs are designated as green solvents because they have extremely

low vapor pressure, nonflammable, and thermally and chemically stable. Therefore, many of them can be, in principle, recycled into the process indefinitely. Recently, El Seoud et al. (2007) have discussed the use of ILs in carbohydrate chemistry, in particular, dissolution and functionalization of simple sugars, cyclodextrins, cellulose, starch, and chitin/chitosan. Thus, the use of ionic liquid in preparing biopolymer–inorganic nanohybrids is also an environmentally friendly method (Mumalo-Djokic et al. 2008).

20.4.3 Importance

Nanocomposites have a high potential for the benefit of society through applications, for example, food packaging. They can be made into cheaper products with more efficiency. However, any new technology carries an ethical responsibility for wise application and the recognition that there are potential unforeseen risks that may come with the tremendous positive potential. In parallel to the technical evolution of nanotechnologies, it is expected that there will be new regulatory directives and guidelines to accommodate nanotechnology-based products. To date, very few studies have investigated the toxicological and environmental impacts of direct and indirect exposure of nanomaterials. However, there is no clear data and guidelines available to quantify these effects. Thus, it becomes important in the present scenario to focus on environmental and toxicological effects of nanomaterials.

20.5 Conclusion

Recent research on nanomaterials has demonstrated its potential on utilizing the biobased polymers, as their mechanical, thermal, optical, and physical properties are dramatically improved. Nanoparticles are found to be incorporated in biopolymers via conventional melt processing as well as modern methods. Possible environment friendly methods such as use of water and ionic liquids are also shown as a significant way of developing nanocomposites. The retained or enhanced biodegradability is an added advantage in terms of biological recycling of resources especially in case of using clay. Hence, the research on the processability, biodegradability and toxicity of biopolymeric nanocomposites in environment will give an insight to their applications as well as limitations.

Reference

- Angellier H, Molina-Boisseau S, Lebrun L et al (2005) Processing and structural properties of waxy maize starch nanocrystals reinforced natural rubber. *Macromolecules* 38:3783–3792
- Angellier H, Molina-Boisseau S, Dole P et al (2006) Thermoplastic starch–waxy maize starch nanocrystals nanocomposites. *Biomacromolecules* 7:531–539

- Azizi Samir MAS, Alloin F, Dufresne A (2005) Review of recent research into cellulosic whiskers, their properties and their application in nanocomposite field. *Biomacromolecules* 6:612–626
- Bandyopadhyay S, Chen R, Giannelis EP (1999) Biodegradable organic inorganic hybrids based on poly(L-lactic acid). *Polym Mater Sci Eng* 81:159–160
- Bruce DM, Hobson RN, Farrent JW et al (2005) High-performance composites from low-cost plant primary cell walls. *Compos A* 36:1486–1493
- Cao X, Dong H, Li CM (2007) New nanocomposite materials reinforced with flax cellulose nanocrystals in waterborne polyurethane. *Biomacromolecules* 8:899–904
- Chandra R, Rustgi R (1998) Biodegradable polymers. *Prog Polym Sci* 23:1273–1335
- Chateau B et al (2005) Very long-term energy environmental model (VLEEM) 2. Enerdata, Grenoble, France
- Chen Y, Liu C, Chang PR et al (2009) Bionanocomposites based on pea starch and cellulose nanowhiskers hydrolyzed from pea hull fibre: effect of hydrolysis time. *Carbohydr Polym* 76:607–615
- De Carvalho AJF, Curvelo AAS, Agnelli JAM (2001) A first insight of thermoplastic starch and kaolin. *Carbohydr Polym* 45:189–194
- Drumright RE, Gruber PR, Henton DE (2000) Polylactic acid technology. *Adv Mater* 12:1841–1846
- Dufresne A, Cavaille J-Y, Helbert W (1996) New nanocomposite materials: microcrystalline starch reinforced thermoplastic. *Macromolecules* 29:7624–7626
- El Seoud OA, Koschella A, Fidale LC et al (2007) Applications of ionic liquids in carbohydrate chemistry: a window of opportunities. *Biomacromolecules* 8:2629–2647
- Favier V, Chanzy H, Cavaille JY (1995) Polymer nanocomposites reinforced by cellulose whiskers. *Macromolecules* 28:6365–6367
- Gandini A, Belgacem MN (2008) Furan derivatives and furan chemistry at the service of macromolecular materials. In: Belgacem MN, Gandini A (eds) *Monomers, polymers and composites from renewable resources*. Elsevier, Amsterdam
- Goodrich JD, Winter WT (2007) α -Chitin nanocrystals prepared from shrimp shells and their specific surface area measurement. *Biomacromolecules* 8:252–257
- Hill K (2007) Industrial development and application of biobased oleochemicals. *Pure Appl Chem* 79:1999–2011
- Höfer R, Daute P, Grützmacher R et al (1997) Oleochemical polyols: a new raw material source for polyurethane coatings and floorings. *J Coat Technol* 69:65–72
- Huang H, Yuan Q, Yang X (2005a) Morphology study of gold–chitosan nanocomposites. *J Colloid Interf Sci* 282:26–31
- Huang J, Ichinose I, Kunitake T (2005b) Nanocoating of natural cellulose fibers with conjugated polymer: hierarchical polypyrrole composite materials. *Chem Commun* 13:1717–1719
- Kaplan DL (1998) Introduction to biopolymers and renewable resources. In: Kaplan DL (ed) *Biopolymers from renewable resources*. Springer, Berlin
- Kumar AP, Depan D, Tomer NS et al (2009) Nanoscale particles for polymer degradation and stabilization-trends and future perspectives. *Prog Polym Sci* 34:479–515
- Lindblad MS, Liu Y, Albertsson A-C et al (2002) Polymers from renewable resources. *Adv Polym Sci* 157:139–161
- Lu Y, Weng L, Zhang L (2004) Morphology and properties of soy protein isolate thermoplastics reinforced with chitin whiskers. *Biomacromolecules* 5:1046–1051
- Lysen EH (2001) Global restrictions on biomass availability import to the Netherlands, Project Report, Utrecht Centre for Energy Research, Utercht, The Netherlands
- Maiti S, Jana S (2005) Biodegradable polymers, polymer recycle and waste management. Anusandhan, Midnapore
- Maiti P, Batt CA, Giannelis EP (2003) Renewable plastics: synthesis and properties of PHB nanocomposites. *Polym Mater Sci Eng* 88:58–59
- Maiti P, Batt CA, Giannelis EP (2007) New biodegradable polyhydroxybutyrate/layered silicate nanocomposites. *Biomacromolecules* 8:3393–3400

- Mangiacapra P, Gorrasi G, Sorrentino A et al (2006) Biodegradable nanocomposites obtained by ball milling of pectin and montmorillonites. *Carbohydr Polym* 64:516–523
- Mecking S (2004) Nature or petrochemistry? Biologically degradable materials. *Angew Chem Int Ed* 43:1078–1085
- Miyagawa H, Misra M, Drazal LT et al (2005) Novel biobased nanocomposites from functionalized vegetable oil and organically-modified layered silicate clay. *Polymer* 46:445–453
- Morin A, Dufresne A (2002) Nanocomposites of chitin whiskers from riftia tubes and poly (caprolactone). *Macromolecules* 35:2190–2199
- Mumalo-Djokic D, Stern WB, Taubert A (2008) Zinc oxide/carbohydrate hybrid materials via mineralization of starch and cellulose in the strongly hydrated ionic liquid tetrabutylammonium hydroxide. *Cryst Growth Des* 8:330–335
- Nair KG, Dufresne A (2003) Crab shell chitin whisker reinforced natural rubber nanocomposites. 1. Processing and swelling behavior. *Biomacromolecules* 4:657–665
- Ogata N, Jimenez G, Kawai H et al (1997) Structure and thermal/mechanical properties of poly (l-lactide)-clay blend. *J Polym Sci B Polym Phys* 35:389–396
- Oksman K, Mathew AP, Bondeson D et al (2006) Manufacturing process of cellulose whiskers/poly(lactide) acid nanocomposites. *Compos Sci Technol* 66:2776–2784
- Oksman K, Mathew AP, Sain M (2009) Novel bionanocomposites: processing, properties and potential applications. *Plast Rubb Compos* 38:396–405
- Ottenbrite RM, Albertsson AC, Scott G (1992) Discussion on degradation terminology. In: Vert M, Feijen J, Albertsson AC, Scott G, Chiellini E (eds) *Biodegradable polymers and plastics*, 1st edn. Royal Society of Chemistry, Cambridge
- Park HM, Li X, Jin CZ et al (2002) Preparation and properties of biodegradable thermoplastic starch/clay hybrids. *Macromol Mater Eng* 287:553–558
- Park HM, Misra M, Drzal LT et al (2004) “Green” nanocomposites from cellulose acetate bioplastic and clay: effect of eco-friendly triethyl citrate plasticizer. *Biomacromolecules* 5:2281–2288
- Patel M (2003) Do biopolymers fulfill our expectations concerning environmental benefits? In: Chiellini E, Solaro R (eds) *Biodegradable polymers and plastics*. Kluwer/Plenum, New York
- Poole AJ, Church JS, Huson MG (2009) Environmentally sustainable fibers from regenerated protein. *Biomacromolecules* 10:1–8
- Pranger L, Tannenbaum R (2008) Biobased nanocomposites prepared by in situ polymerization of furfuryl alcohol with cellulose whiskers or montmorillonite clay. *Macromolecules* 41:8682–8689
- Ray SS, Bousmina M (2005) Biodegradable polymers and their layered silicate nanocomposites: in greening the 21st century materials world. *Prog Mater Sci* 50:962–1079
- Ray SS, Yamada K, Ogami A, Okamoto M, Ueda K (2002a) New poly(lactide)/layered silicate nanocomposite: nanoscale control over multiple properties. *Macromol Rapid Commun* 23:943–947
- Ray SS, Yamada K, Okamoto M, Ueda K (2002b) Poly(lactide)-layered silicate nanocomposite: a novel biodegradable material. *Nano Lett* 2:1093–1096
- Rosa MF, Medeiros ES, Malmonge JA et al (2010) Cellulose nanowhiskers from coconut husk fibers: effect of preparation conditions on their thermal and morphological behavior. *Carbohydr Polym* 81:83–92
- Steinbchel A (2005) Non-biodegradable biopolymers from renewable resources: perspectives and impacts. *Curr Opin Biotechnol* 16:607–613
- Sumita M, Tsukumo Y, Miyasaka K et al (1983) Tensile yield stress of polypropylene composites filled with ultrafine particles. *J Mater Sci* 18:1758–1764
- Thellen C, Orroth C, Froio D et al (2005) Influence of montmorillonite layered silicate on plasticized poly(l-lactide) blown films. *Polymer* 46:1716–1727
- Uyama H, Kuwabara M, Tsujimoto T et al (2003) Green nanocomposites from renewable resources: plant oil–clay hybrid materials. *Chem Mater* 15:2492–2494
- Wang SF, Shen L, Zhang WD et al (2005a) Preparation and mechanical properties of chitosan/carbon nanotubes composites. *Biomacromolecules* 6:3067–3072

- Wang SF, Shen L, Tong YJ et al (2005b) Biopolymer chitosan/montmorillonite nanocomposites: preparation and characterization. *Polym Degrad Stab* 90:123–131
- Wong KKW, Douglas T, Gider S et al (1998) Biomimetic synthesis and characterization of magnetic proteins (magnetoferritin). *Chem Mater* 10:279–285
- Zhang X, Do MD, Dean K et al (2007) Wheat-gluten-based natural polymer nanoparticle composites. *Biomacromolecules* 8:345–353

Part IV
Applications of Cellulose Fiber-Reinforced
Polymer Composites

Chapter 21

Cellulose Nanocomposites for High-Performance Applications

Bibin Mathew Cherian, Alcides Lopes Leao, Sivoney Ferreira de Souza, Sabu Thomas, Laly A. Pothan, and M. Kottaisamy

Abstract Cellulose nanofibers and their composites offer a highly attractive research line in recent times. Cellulose nanofibers have generated a great deal of interest as a source of nanometer-sized fillers because of their sustainability, easy availability, and the related characteristics such as a very large surface-to-volume ratio, outstanding mechanical, electrical, and thermal properties. This chapter describes the many processes to produce nanocellulose from different cellulosic sources and how to increase the compatibility between cellulosic surfaces and a variety of plastic materials. Furthermore, it provides knowledge of different nanocelluloses and nanocomposites and provides updated information on their properties and also deals with fascinating high-tech applications, especially in the medical field.

Keywords Cardiovascular tissues · Cosmetic tissues · Medical applications · Meniscus implant · Nanocelluloses · Nanocomposites · Veterinary medicine

Contents

21.1	Introduction	540
21.1.1	Crystalline Forms of Cellulose	541
21.1.2	Nanocellulose	544
21.1.3	Types of Nanocelluloses	545
21.2	Isolation of Nanocellulose	555
21.3	Chemical Modifications of Nanocellulose	558
21.4	Cellulose Nanocomposites	561
21.5	Application of Nanocellulose in Medicine	564
21.5.1	Nanocellulose Microvessel Endoprosthesis	564
21.5.2	Nanocellulose for Artificial Cardiovascular Tissues	567
21.5.3	Bone Graft	567

B.M. Cherian (✉)

Department of Natural Science, College of Agricultural Sciences, São Paulo State University (UNESP), Botucatu 18610-307, São Paulo, Brazil
e-mail: bmcherian@gmail.com

21.5.4	Nanocellulose Meniscus Implant	568
21.5.5	Nanocellulose in the Treatment of Chronic Wounds and Burns	571
21.5.6	Cosmetic Tissues	573
21.5.7	Nanocellulose in Veterinary Medicine	574
21.6	Concluding Remarks	577
	References	578

21.1 Introduction

The incorporation of small amounts of high-stiffness, high-aspect-ratio nanometer-sized fillers into polymers is a design approach that has rapidly emerged as a broadly exploited framework for the creation of new materials with tailored mechanical properties (Whitesides 2005; Hussain et al. 2006). Cellulose is one of the most abundant and ubiquitous polymers on the planet, given its widespread industrial use not only in the present age, but also in the past for housing, paper, ropes, sails, timber, and for many other applications. Crystalline cellulose nanofibers are attracting significant interest in this context, mainly due to their intriguing mechanical properties and the abundance of cellulose in the biomass. These fiber-like crystals, often referred to as nanowhiskers, display an elastic modulus of 120–150 GPa and are readily obtained from renewable biosources such as bacteria, wood, cotton, and sessile sea creatures called tunicates (Dufresne 2006).

The recent interest in using stiff nanometric particles as reinforcement materials in polymeric matrixes, composites, or nanocomposites has been increasing. Two good examples of these types of particles are carbon nanotubes and cellulose nanofibers. Cellulose nanofibers, also reported in the literature as whiskers, nanocrystals, cellulose crystallites, or crystals, are the crystalline domains of cellulosic fibers, isolated by means of acid hydrolysis, and are called in this way due to their physical characteristics of stiffness, thickness, and length (Souza and Borsali 2004).

Samir et al. (2005) report that cellulose whiskers are regions growing under controlled conditions, which allows individual high-purity crystals to form. Their highly ordered structure may not only impart high resistance, but also make significant changes to some important properties of materials, such as electrical, optical, magnetic, ferromagnetic, and dielectric nature, as well as concerning conductivity.

Since cellulose is classed as a carbohydrate (a substance containing carbon, hydrogen, and oxygen), it is necessary to point out that although this term applies to a large number of organic compounds, cellulose is unique in that it can be either synthesized from, or hydrolyzed to, monosaccharides (Khadem 1988). The repeat unit of the cellulose polymer is known to comprise two anhydroglucose rings joined via a β -1,4 glycosidic linkage from this unit (Klemm et al. 1998) (called cellobiose) as shown in Fig. 21.1.

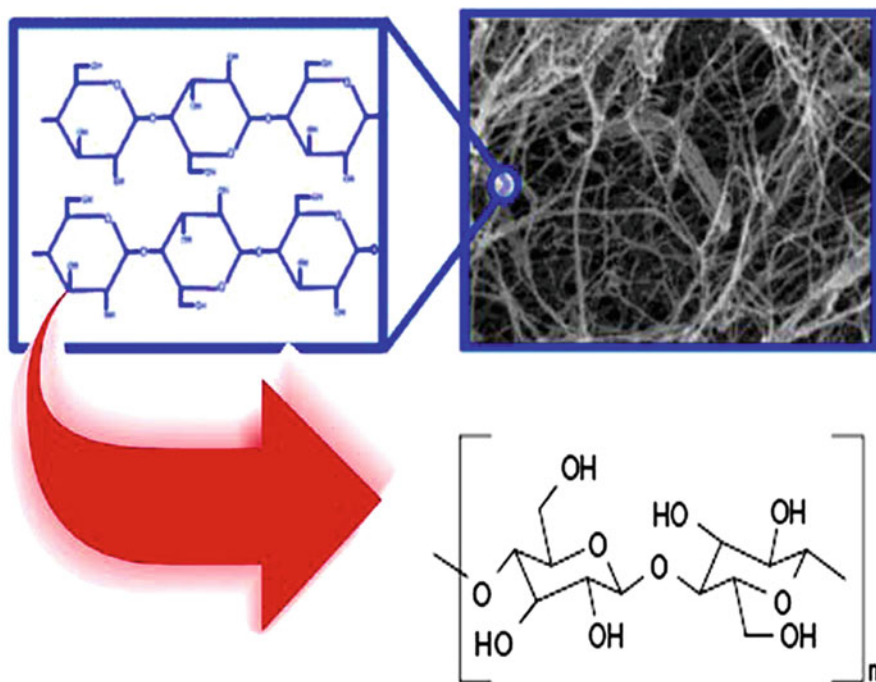


Fig. 21.1 The repeat unit of cellulose

21.1.1 Crystalline Forms of Cellulose

Cellulose is a semicrystalline polymer and its crystallinity depends on the origin and on the isolation and processing methods. The complex structural hierarchy of cellulose, due to profuse hydrogen bonding, is manifested by the existence of several polymorphs (crystalline forms). The crystalline forms that exist in native cellulose is typically called cellulose I. This cellulose I crystal form, or native cellulose, also comprises two allomorphs, namely cellulose I α and I β (Atalla and Vanderhart 1984). The ratio of these allomorphs is found to vary from plant species to species, but bacterial and tunicate forms are I α and I β rich, respectively. The crystal structures of cellulose allomorphs I α and I β have been determined with great accuracy, particularly the complex hydrogen bonding system (Nishiyama et al. 2002, 2003a).

Less organized (amorphous) cellulose is also present along with the crystalline cellulose. The crystalline forms I α and I β differ by their crystalline unit cell structure and overall hydrogen bonding pattern, but the main intermolecular hydrogen bond is the same for both, i.e., O6-H \rightarrow O3 (Fig. 21.2). The intramolecular hydrogen bond of O3-H \rightarrow O5, which is partly responsible for the cellulose chain stiffness and contributes to load transfer along the chain, is also shown in Fig. 21.2. Other crystalline forms of cellulose include cellulose II, cellulose III, and cellulose

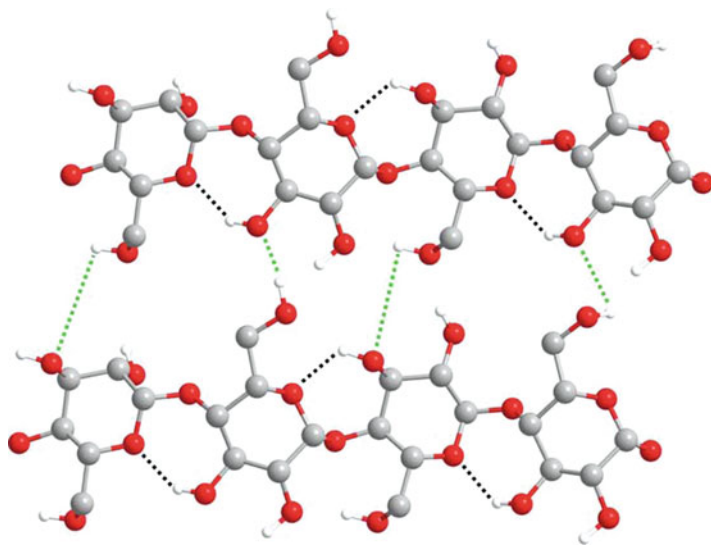


Fig. 21.2 Supramolecular structure of the cellulose I polymorph showing the main intermolecular O6-H \rightarrow O3 (green) and intramolecular O3-H \rightarrow O5 (black) hydrogen bonding patterns

IV that are not native forms of cellulose but formed upon chemical processing. Cellulose III and IV are mainly of scientific interest, but cellulose II is of technical relevance because it is formed in the mercerization and the regeneration processes of cellulose. Cellulose II differs from cellulose I by O6-H \rightarrow O2 intermolecular hydrogen bonding and by antiparallel chain orientation (Nishiyama et al. 2002, 2003a; Dumitriu 2005; Hofstetter et al. 2006). The hydrogen bond network makes cellulose a relatively stable polymer, which does not readily dissolve in typical aqueous solvents and has no melting point. This network also gives the cellulose chains a high axial stiffness (Kroonbatenburg et al. 1986).

The projections of the crystal structures of cellulose I α and I β (Fig. 21.3) down the chain axes are remarkably similar. As the projection perpendicular to the chain axis and in the plane of the hydrogen-bonded sheets shows, the main difference between I α and I β is the relative displacement of the sheets in the chain direction. In both I α and I β , the second sheet, designated II, is shifted in the “up” direction by $\sim c/4$ relative to the first sheet, designated I. The third sheet, designated III, is similarly shifted with respect to II by $\sim c/4$ in I α but in I β it is shifted by $a \sim c/4$ in the “down” direction. There is a relative difference of $\sim c/2$ in the position of III with respect to II in I α and I β . Because there exists an approximate molecular 2_1 screw axis, this difference is equivalent to stacking opposite faces of III on II.

The most likely route for solid-state conversion of cellulose I α \rightarrow I β is the relative slippage of the cellulose chains past one another. This movement does not require the disruption of the hydrogen-bonded sheets (along the 100 planes for cellulose I β and 110 planes for cellulose I α) but slippage by $\sim c/2$ at the interface of sheets of type II and III is shown in Fig. 21.3. The possibility of rotation of the

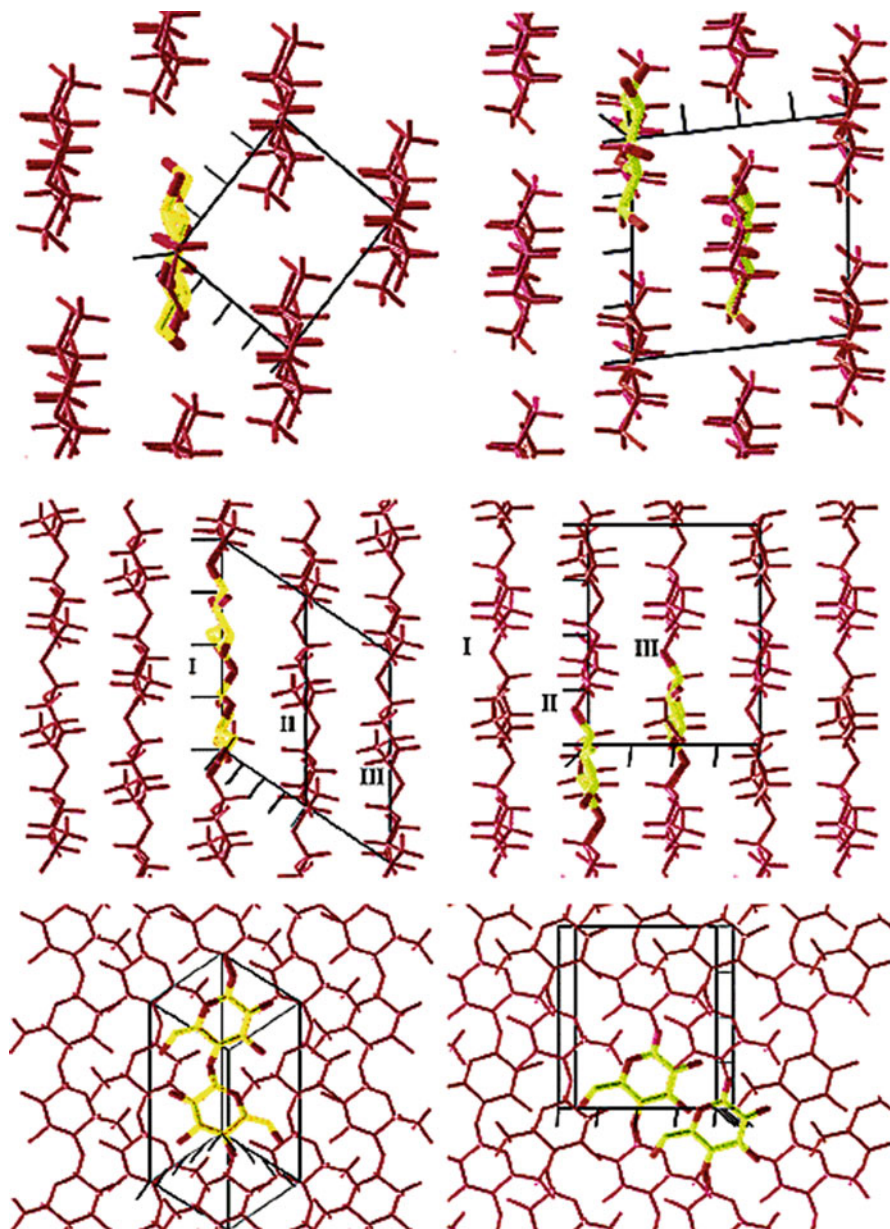


Fig. 21.3 Projections of the crystal structures of cellulose IR (*left*) and I α (*right*) down the chain axes (*top*), perpendicular to the chain axis and in the plane of the hydrogen bonded sheets (*middle*), and perpendicular to the hydrogen bonded sheets (*bottom*). The cellulose chains are represented by *red* skeletal models. The asymmetric unit of each structure is also represented in thicker lines with carbons in *yellow*. The unit cell of each structure is shown in *white*. Reproduced with permission from Nishiyama et al. (2003a). Copyright © 2003, American Chemical Society

chains in III around their axes could also be observed, because a slippage of $\sim c/2$ is equivalent to a rotation of 180° around a 2_1 molecular axis which seems to be improbable (Nishiyama et al. 2003a).

21.1.2 Nanocellulose

Generally, cellulose-based biofibers, including banana, pineapple leaf, coir, cotton, flax, hemp, jute, kenaf, sisal, and wood fibers are used to reinforce plastics due to their relative high strength, high stiffness, and low density. Because of their annual renewability, agricultural crops' residues can be a valuable source of natural fibers. Biocomposites have future commercial application that would unlock the potential of these underutilized renewable materials and provide a non-food-based market for agricultural industry. In addition, they are biodegradable and offer potential advantages over unmanageable synthetic plastics in disposable applications (Alemdar and Sain 2006). Recent advances in producing biofibers, microfibrillated or nano-sized fibers with high strength and surface area offer manufacturing high-performance composites from these biofibers (Dufresne and Vignon 1998; Nakagaito and Yano 2005; Chakraborty et al. 2006).

The study of cellulosic nanofibers as a reinforcing phase in nanocomposites started 15 years ago (Favier et al. 1995a). Since then a large amount of literature has been devoted to cellulose nanofibers and it is becoming an increasingly topical subject. Different descriptors of these nanofibers are often referred to in the literature. These include "nanowhiskers" (or just simply "whiskers"), "nanocrystals," or even "monocrystals." These crystallites have also often been referred to in literature as "microfibrils," "microcrystals," or "microcrystallites," despite their nanoscale dimensions. The term "whiskers" is used to designate elongated crystalline rod-like nanoparticles, whereas the designation "nanofibrils" should be used to designate long flexible nanoparticles consisting of alternating crystalline and amorphous strings.

In quintessence, the principal reason to utilize cellulose nanofibers in composite materials is because one can potentially exploit the high stiffness of the cellulose crystal for reinforcement. This can be done by breaking down the hierarchical structure of the plant into individualized nanofibers of high crystallinity, therefore reducing the amount of amorphous material present. Since plant fibers are hierarchically fibrous it is possible to do this by yielding a fibrous form of the material (nanowhiskers and nanofibrils), which due to their aspect ratio (length/diameter) and therefore reinforcing capabilities are potentially suitable for composite materials. A high aspect ratio to the fibers is desirable as this enables a critical length for stress transfer from the matrix to the reinforcing phase. It is however not clear what the true crystal modulus of cellulose is, nor whether this stiffness is really obtainable from plants, bacteria, or tunicates. Establishing a true value of the crystal modulus of cellulose sets an upper limit to what is achievable in terms of reinforcing potential.

Against this background and in view of broadening the range of cellulose use, including the development of novel materials with ground-breaking new features,

it is important to have access to various types of celluloses of miscellaneous provenance, supramolecular structure, exceptional properties, different availability, and expanded application areas. The dominant pathway to cellulose material is its production from plants. In the seed hairs of cotton, cellulose is available in an almost pure state. In contrast, wood cellulose forms a native composite with lignin and other carbohydrates (hemicelluloses) from which it is isolated by large-scale chemical pulping, separation, and purification processes. Wood pulp (Koch 2006) remains the most important industrial feedstock for the production of paper and cardboard, for cellulose regenerate fibers and films, as well as for the industrial-scale synthesis of the palette of cellulose esters and ethers. These derivatives are used as very important and well-known active components in coatings, optical films, sorption media, and additives in building materials, drilling techniques, pharmaceuticals, foodstuffs, and cosmetics. Numerous novel applications of cellulose also take advantage of its biocompatibility and chirality. Apart from plants, certain bacteria, algae, and fungi produce cellulose as well. Amongst the cellulose-forming bacteria, *Acetobacter* strains – reclassified as the genus *Gluconacetobacter* – are especially suitable for the formation of cellulose. They are not pathogenic, are commonly found on fruits and fruit products, and can be cultivated under laboratory conditions. One of the first applications of the natural product bacterial cellulose (BC) was the use of it as a calorie-free dessert called “Nata de Coco,” today a common Asian food, mainly in Philippines.

In terms of the molecular formula, BC is identical to cellulose of plant origin. However, important structural features and properties significant for practical application of BC are quite different from wood cellulose: high purity, high degree of polymerization (up to 8,000), high crystallinity (of 70–80%), high water content to 99%, and high mechanical stability.

These specific parameters are caused by the subsequently outlined biosynthetic formation of the BC and the resulting particular supramolecular structure as a network of nanofibers formed during self-assembly of the cellulose molecules in the aqueous culture medium, free from potential composite partners as in wood biosynthesis.

The main aim of this contribution is to present various approaches to the preparation of nanocellulosic materials from plant sources. The focus is on the extraction and investigation of microfibrillated cellulose (MFC) in particular; however, to put this topic in context, cellulose whiskers and bacterial cellulose are also discussed in particular sections of the text and applications of nanocelluloses in the animal body for the development of medical devices such as artificial blood vessels, and the application of bacterial nanocellulose as animal wound dressings and cosmetic tissues. Therefore, this chapter has brought together a variety of areas from chemistry, medicine, and biotechnology.

21.1.3 Types of Nanocelluloses

Nanocellulose prepared from the nearly inexhaustible source of feedstock and wood using chemical treatments and controlled mechanical disintegration procedures to produce the favored product properties belong to the first classification.

Another type of nanocellulose is formed directly as the result of biosynthesis of special bacteria. An extremely pure product with subsequently reported important properties is formed that necessitates challenging biosynthesis/biotechnological handling and the development of large-scale production.

21.1.3.1 Nanocellulose from Wood

The enormous abundance of wood has been considered as an attractive starting material for making nanomaterials. However, isolation of cellulosic nanofibers, crystalline whiskers, or other relatively pure cellulosic structures having minimum dimensions in the range of 1–100 nm usually requires a multistage process involving vigorous chemical and/or mechanical operations. In the last 25 years, there have been efforts to reduce wood fibers in nanodimension. As an initial step, nanofibers isolated from wood by mechanical process dates back to the 1980s when Turbak et al. (1983) and Herrick et al. (1983) produced MFC from wood pulp using cyclic mechanical treatment in a high-pressure homogenizer. The homogenization process resulted in disintegration of the wood pulp and a material in which the fibers were opened into their sub-structural microfibrils (Andresen et al. 2006). The resulting MFC gels consisted of strongly entangled and disordered networks of cellulose nanofiber. Today, there are different ways to produce these materials with controlled fiber diameters.

Bleached kraft pulp has often been used as the starting material for research on MFC production (Bhatnagar and Sain 2005; Iwamoto et al. 2005; Janardhnan and Sain 2006; Saito et al. 2006, 2007, 2009; Iwatake et al. 2008).

Nakagaito and Yano (2004, 2005) developed MFC, which consists of mechanically fibrillated pulp into nano to submicron wide fibers forming a web-like network (Fig. 21.4), shows much promise as reinforcement of composites. The pulp has a smooth surface with 30–50 μm in diameter, refiner-treated pulp has a fibrillated surface with a diameter similar to pulp and MFC is completely disintegrated into nano to submicron wide fibers forming a network.

There have also been some investigations into the properties of nanocellulose from wood, which has an amazing waterstorage capacity, similar to BC. A dispersion of

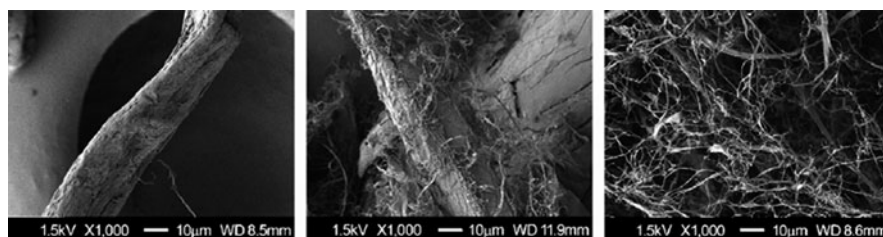


Fig. 21.4 Filler morphology of Needle-leaf Bleached Kraft Pulp (NBKP), refiner-treated (eight passes) NBKP, and MFC. Reproduced with permission from Iwatake et al. (2008). Copyright © 2008, Elsevier Ltd



Fig. 21.5 Photograph of microfibrillated cellulose (MFC)

these cellulose fibers in water with a solid content of only 2% leads to a mechanically stable transparent gel (Fig. 21.5).

The wood nanocellulose fibers are suitable for solidification of emulsion paints and filter aids, useful for both primary rough filtration and precision filtration. Moreover, nanocellulose from wood is used in paper making as a coating and dye carrier in paper tinting (Matsuda 2000; Matsuda Y et al. 2001). Additionally, wood nanocellulose can be employed in the food industry as a thickening agent, a gas barrier, and in moisture resistant paper laminate for packaging (Ioelovich and Leykin 2004).

In medicine, these nanocelluloses can be utilized as excipients such as binders, fillers, and/or disintegrants in the development of solid dosage forms. In cosmetics, wood nanocellulose is suitable as an additive in skin-cleansing cloths and as part of disposal diapers, sanitary napkins, and incontinence pads (Kumar 2002).

Besides application in its pure form, it is possible to use nanocellulose from wood in polymer composites. The tensile strength of such composites was five times higher than that of the original polymers.

Yano and Nakahara (2004) used accessory polysaccharides to form composites with wood MFC/nanocelluloses. The disintegrated wood celluloses were mixed with starch as a binder and then hot pressed between porous metal plates. Using a starch content of 2 wt%, the bending strength reached 310 MPa, compared to 250 MPa for unmodified fibers. Concurrently, the Young's modulus decreased from 16 to 12.5 GPa. When the starch content was 20 wt%, the bending strength decreased to 270 MPa.

Nyström et al. (2010) demonstrated the coating of individual fibers of wood-based nanocellulose with polypyrrole using in situ chemical polymerization to obtain an electrically conducting continuous high surface area composite. The researchers were successful in fabricating an electronically conductive high surface area composite material composed of MFC and polypyrrole by direct chemical polymerization of pyrrole on wood derived nanofibers in hydrogels without the need for sophisticated, time-consuming drying techniques such as solvent exchange



Fig. 21.6 Luminescence of an organic light-emitting diode deposited onto a flexible, low CTE and optically transparent wood–cellulose nanocomposite. Reproduced with permission from Okahisa et al. (2009). Copyright © 2009, Elsevier Ltd

drying or lyophilization. The air-dried composite sheets exhibited a conductivity of 1.5 S/cm and a specific surface area of 89 m²/g. Since the material was found to be electroactive with an ion-exchange capacity for Cl⁻ of 289 C/g (i.e., a specific charge of 80 mAh/g), this finding consequently gave rise to new exciting possibilities regarding large-scale production of inexpensive paper-based materials for energy storage as well as electrochemically controlled extraction and separation of biologically interesting compounds.

Okahisa et al. (2009) fabricated an organic light-emitting diode on flexible, low coefficient of thermal expansion and optically transparent wood–cellulose nanocomposites (Fig. 21.6). At the same fiber content, the nanocomposites using lower Young's modulus matrix resin exhibited lower coefficient of thermal expansion values than using higher Young's modulus matrix resins. It led to the development of nanocomposites with a very low coefficient of thermal expansion while having high flexibility and ductile properties which open up many possibilities for the application of OLEDs in flexible, transparent displays.

21.1.3.2 Nanocellulose from Agricultural Crops and By-Products

Although wood is certainly the most important industrial source of cellulosic fibers, competition from different sectors such as the building products and furniture industries and the pulp and paper industry, as well as the combustion of wood for energy, makes it challenging to supply all users with the quantities of wood needed at reasonable cost. Besides this, many regions do not have wood available, turning its options to nonwood cellulose. For this reason, fibers from crops such as flax, hemp, sisal, and others, especially from by-products of these different plants, are

likely to become a matter of increasing interest. These nonwood plants generally contain less lignin than wood and therefore bleaching processes are less chemical demanding. Other examples of agricultural by-products that might be used to derive nanocellulose include those obtained from the cultivation of corn, wheat, rice, sorghum, barley, sugar cane, pineapple, banana, and coconut crop. These agricultural by-products are either burned, used for low-value products such as animal feed, or used in biofuel production. The renewable nature of crop residues and immense availability of these raw materials can be utilized as valuable sources of natural nanofibers (Reddy and Yang 2005). In addition, when by-products, such as pulps after juice extraction, are used as raw materials, fewer processing steps are required to obtain cellulose (Bruce et al. 2005). The cellulose microfibrils in these agricultural fibers are less tightly wound in the primary cell wall than in the secondary wall in wood, thus fibrillation to produce nanocellulose should be less energy demanding (Dinand et al. 1996).

Researchers have reported the isolation of cellulose nanoparticles from diverse nonwood sources. Cellulose nanoparticles have been synthesized in spherical form (Pu et al. 2007; Zhang et al. 2007, 2008), rod-like highly crystalline nanocrystals (Souza and Borsali 2004; Samir et al. 2005; Dufresne 2008) which are obtained by acid hydrolysis of cellulosic fibers, and MFC resulting from disintegration of cellulose fibers under high shearing and impact forces. For the latter, a network of interconnected microfibrils with dimensions of 10–100 nm thick and several microns long are obtained (Cherian et al. 2008; Pääkkö et al. 2007; Gardner et al. 2008). The degree of crystallinity of MFC or cellulose microfibrils is usually low because the amorphous domains of cellulose remain intact (Pääkkö et al. 2007).

Cellulose nanostructures from agricultural residues such as banana farming (Cherian et al. 2008; Zuluaga et al. 2007, 2009), wheat straw and soy hulls (Alemdar and Sain 2008), and pineapple leaf (Cherian et al. 2010) have already been reported. Nanocellulose isolated from pineapple leaf fiber (PALF) has unique characteristics such as high hygroscopicity, high cross-linking, uncomplicated chemical structure, and nontoxic desired for various biomedical applications. For biomedical applications, physical cross-linking has the advantages of not leaving residual amounts of the toxic cross-linking agent. Our group reported that due to the unique nanostructure and properties of PALF nanocellulose it can be utilized as a natural candidate for numerous medical and tissue-engineered applications because it is both durable and biocompatible. The nonwoven ribbons of these nanocelluloses closely resemble the structure of native extracellular matrices, suggesting that it could function as a scaffold for the production of many tissue-engineered constructs (Cherian et al. 2010).

21.1.3.3 Animal Nanocellulose

Some of the largest of all known nanocelluloses are obtained from animals of the Subphylum *Urochordata*, commonly known as tunicates or sea squirts. The cellulose reinforces proteins in a protective tunic. Nanocellulose can be obtained by

bleaching and dissolving the protein, disintegrating the cellulosic mass in a homogenizer, and hydrolyzing the particles in sulfuric acid. The nanocelluloses are parallelepiped rods, typically $>1\ \mu\text{m}$ long and 10–20 nm wide (Elazzouzi-Hafraoui et al. 2008). In 1995, Favier et al. published a paper, where they presented data on composites based on tunicin cellulose whiskers in a copolymer acrylate latex film (Favier et al. 1995a). The cellulose suspension is mixed with a styrene (35w/w), butyl acrylate (65w/w) latex containing small amounts of acrylic acid. Two-millimetre-thick films are solution cast, with an evaporation time of 1 month. In the following, this matrix is often termed as acrylate latex.

This paper and numerous subsequent studies using other matrices have renewed the interest in composites based on cellulose microfibrils. Although cellulose whiskers from tunicin are of little commercial interest, this work provides an inspiring demonstration of the reinforcing potential of high aspect ratio cellulose microfibrils. The paper presents a model nanocomposite based on unusually well-defined cellulose whiskers. The widths are 10–20 nm and the average aspect ratio is typically 70–100. The whiskers are disintegrated from an edible tunicate, a sea animal of around 5–10 cm in diameter. The animal contains a 1-cm-thick cellulose tunic. This is cut into smaller pieces and is deproteinized by bleaching treatments. The bleached mantles are disintegrated in dilute water suspension in a blender and then in many passes through a laboratory homogenizer. The aqueous tunicin suspension is then hydrolyzed by sulfuric acid, sonicated, neutralized, and washed. The presence of surface sulfate groups is critical, because agglomeration or sedimentation is avoided. An AFM micrograph of the tunicin cellulose whiskers is shown in Fig. 21.7, where the high aspect ratio is apparent, having an average thickness of $10.6 \pm 2.3\ \text{nm}$. The isolated tunicin whiskers showed that the height could typically vary from 6 to 14 nm (Elazzouzi-Hafraoui et al. 2008).

The relative purity as well as the potential to produce nearly defect-free cellulosic “whiskers” was some of the reasons that certain animal products became amongst the first materials studied as a potential source of cellulosic nanomaterials for use in composites (Favier et al. 1995b). Subsequent studies have evaluated the use of tunicate-derived whiskers in a variety of ways (Favier et al. 1995b, 1997; Terech et al. 1999; Angle’s and Dufresne 2000, 2001; Ruiz et al. 2001; Mathew and Dufresne 2002; Dufresne 2003, 2006; Schroers et al. 2004; Azizi Samir et al. 2004a, 2006; Samir et al. 2005; Kimura et al. 2005; Yuan and Ding 2006; Podsiadlo et al. 2007; Van den Berg et al. 2007a, b; Elazzouzi-Hafraoui et al. 2008).

21.1.3.4 Algal Nanocellulose

Some green algae reinforce their cell walls with crystalline cellulose. Particularly, large nanocelluloses have been found in algae of the class *Chlorophyceae*. Nanocellulose can be obtained, e.g., by treating cell walls in 0.1 M aqueous NaOH at 100°C for 2 h, then in 0.05 M HCl at room temperature overnight, washing, homogenizing, freeze-drying, then partly hydrolyzing in 66% (by weight) aqueous H₂SO₄ for 3 h, washing, and partly hydrolyzing with either cellulose or 2.5 M HCl

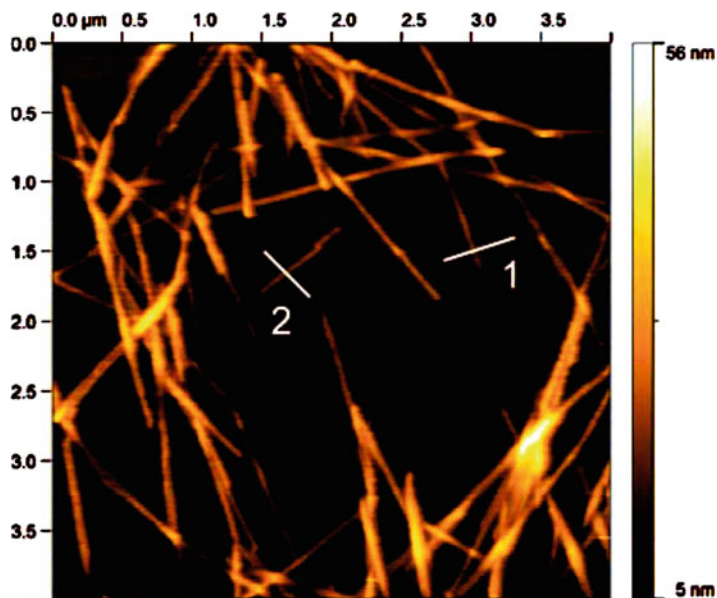


Fig. 21.7 AFM images (topography mode, $2.1 \times 2.1 \mu\text{m}^2$) of cellulose from tunicin spread onto a freshly cleaved mica surface. Reproduced with permission from Elazzouzi-Hafraoui et al. (2008). Copyright © 2008, American Chemical Society

at 100°C for several hours (Hayashi et al. 2005). Typical nanocelluloses are 10 nm wide and 350 nm long.

21.1.3.5 Bacterial Nanocellulose

Cellulose is produced from some bacteria and *Acetobacter xylinum*, vinegar or acetic acid bacteria are the most widely studied. The bacteria that secrete cellulose extracellularly belong to the genera *Acetobacter*, *Agrobacterium*, *Alcaligenes*, *Pseudomonas*, *Rhizobium*, or *Sarcina* (El-Saied et al. 2004). The most efficient producer of bacterial cellulose (BC) is *A. xylinum* (or *Gluconacetobacter xylinus*), a Gram-negative strain of acetic acid producing bacteria (Brown 2004; Klemm et al. 2006). Bacterial or microbial cellulose is an extracellular product that is excreted into the culture medium and special care and handling is necessary to maintain optimal production. Acetic acid bacteria are not photosynthetic but can convert glucose, sugar, glycerol, or other substances to pure cellulose. A typical single cell can convert up to 108 glucose molecules per hour into cellulose. The activities in a single cell are numerous. Each cell acts as a spinneret and produces a bundle of submicroscopic fibrils fetching polymer aggregates through a row of pores (Iguchi et al. 2000). The bacteria produce a membrane of pure cellulose, which is very strong in its never dried state. It also has an extremely large absorbance of water.

There are important structural differences between BC and plant cellulose. The BC is secreted as a ribbon-shaped fibril (Fig. 21.8), less than 100 nm wide, which is composed of much finer 2–4 nm nanofibrils (Iguchi et al. 2000; Brown and Laborie 2007). In contrast to the existing methods for obtaining nanocellulose through mechanical or chemo-mechanical processes, BC is produced by bacteria through cellulose biosynthesis and the building up of bundles of microfibrils.

Bacterial cellulose (BC) is frequently studied in order to clarify the mechanism for biosynthesis of cellulose (Tokoh et al. 2002a). Details of mechanisms for biopolymerization and simultaneous crystallization in long parallel rows of extended chains are understood fairly well. As an example of the nature of such studies, effects of pectin and xylan medium on the crystallite morphology have been demonstrated (Tokoh et al. 2002b).

Bacterial cellulose nanofibril bundles have excellent intrinsic properties due to their high crystallinity (up to 84–89%) (Czaja et al. 2004), including a reported elastic modulus of 78 GPa (Guhados et al. 2005), which is higher than that generally recorded for macro-scale natural fibers (Mohanty et al. 2000) and is of the same order as the elastic modulus of glass fibers (70 GPa) (Juntaro et al. 2007). Compared with cellulose from plants, BC also possesses higher water holding capacity, higher degree of polymerization (up to 8,000), and a finer web-like network. In addition, BC is produced as a highly hydrated and relatively pure cellulose membrane and

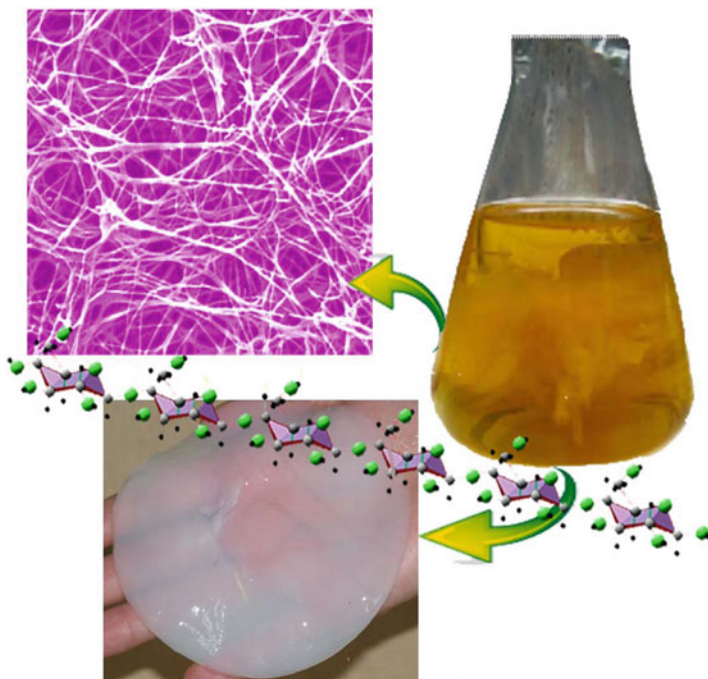


Fig. 21.8 Appearance and structure of nanofiber network of bacterial nanocellulose from common static culture

therefore no chemical treatments are needed to remove lignin and hemicelluloses, as is the case for plant cellulose (Barud et al. 2008; Wan et al. 2006).

Researchers have studied the potential of BC as reinforcement in nanocomposites. Nogi and Yano (2008) succeeded in depositing an electroluminescent layer on these transparent BC nanocomposites, as shown in Fig. 21.9. However, these nanocomposites, although of sufficiently low coefficient of thermal expansion (CTE), required 60–70 wt% cellulose nanofibers of high Young's modulus, 138 GPa (Nishino et al. 1995), resulting in BC nanocomposites with a modulus on the order of 21 GPa. They also developed foldable and ultra-low CTE (4 ppm/K) transparent BC nanocomposites (Fig. 21.10). Their foldable properties and high thermal stability are achieved by reinforcing a low-Young's-modulus transparent resin with 5 wt% of low CTE and high-Young's-modulus cellulose nanofibers, taking advantage of the layered structure of planar BC nanofiber networks.

A web-like network of bacterial nanofibers has been demonstrated by Yano et al. (2005) which exhibits very promising characteristics as a reinforcement material for optically functional composites (Fig. 21.11). They reported that due to the size effect, the nanofiber network in a variety of resins led to a very low loss of transparency of the original resin, even at a high fiber content and offering higher mechanical strength and significantly lower thermal expansion coefficients.

Sanchavanakit et al. (2006) reported the responses of human skin keratinocytes and fibroblasts on bacterial cellulose (BC) film. The results suggest that BC film can promote the reepithelialization process. This may be a biological mechanism by which BC film facilitates wound healing. Therefore, BC film holds a high potential for therapeutic application for skin wounds, which is suitable for partial thickness dermal loss wounds such as donor site skin graft wound or post abrasive laser

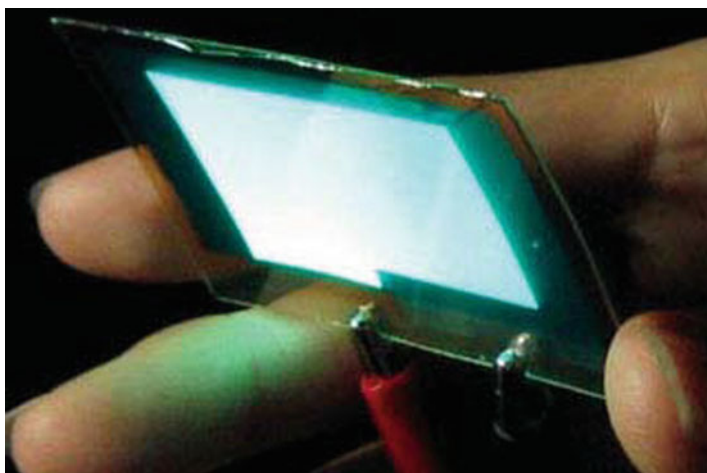


Fig. 21.9 Luminescence of an organic light-emitting diode deposited onto a transparent BC nanocomposite. Reproduced with permission from Nogi and Yano (2008). Copyright © 2008 Wiley-VCH Verlag GmbH & Co. KGaA, Weinheim



Fig. 21.10 Foldable transparent nanocomposites reinforced with bacterial cellulose nanofibers. Reproduced with permission from Nogi and Yano (2008). Copyright © 2008 Wiley-VCH Verlag GmbH & Co. KGaA, Weinheim

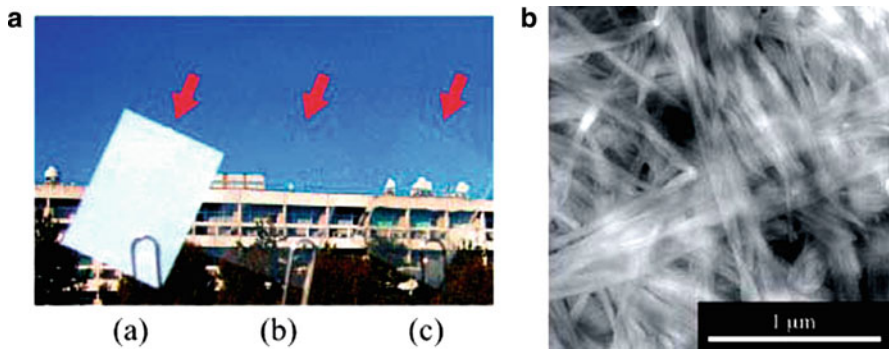


Fig. 21.11 (A) Appearance of a 65- μm -thick BC sheet: (a) with no added resin, (b) with acrylic resin, (c) with epoxy resin, and (b) tapping mode AFM image of a bacterial cellulose/epoxy resin sheet. Reproduced with permission from Yano et al. (2005). Copyright © 2005 Wiley-VCH Verlag GmbH & Co. KGaA, Weinheim

wound. Nonpromoting fibroblast adhesion may promote the inhibition of hypertrophic scars. The BC may be applied as a long-term soft tissue augmentation material. More detailed discussion of BC preparation and use is presented by Wan et al. (2006), Brown (2004), Ifuku et al. (2007), Iguchi et al. (2000), Juntaro et al. (2007, 2008), El-ceSaied et al. (2004), Grande et al. (2008), Brown and Laborie (2007), and Shoda and Sugano (2005).

21.2 Isolation of Nanocellulose

The main process for the isolation of nanocellulose from cellulose fibers is based on acid hydrolysis. Disordered or paracrystalline regions of cellulose are preferentially hydrolyzed, whereas crystalline regions that have a higher resistance to acid attack remain intact (Ruiz et al. 2000). Thus, following an acid treatment that hydrolyzes the cellulose (leading to removal of the microfibrils at the defects), rod-like nanocelluloses are produced. The obtained nanocellulose has a morphology and crystallinity similar to the original cellulose fibers. The actual occurrence of the acid cleavage event is attributed to differences in the kinetics of hydrolysis between amorphous and crystalline domains. In general, acid hydrolysis of native cellulose induces a rapid decrease in its degree of polymerization (DP), to the so-called level-off of DP (LODP). The DP subsequently decreases much more slowly even during prolonged hydrolysis times (Håkansson and Ahlgren 2005; Yachi et al. 1983). The LODP has been thought to correlate with crystal sizes along the longitudinal direction of cellulose chains present in the original cellulose before the acid hydrolysis. This hypothesis was based on the reasonable assumption that disordered or paracrystalline domains are regularly distributed along the microfibrils and therefore, they are more susceptible to acid attack (in contrast to crystalline regions that are more impervious to attack). Also, homogeneous crystallites were supposed to be generated after acid hydrolysis. It was shown that the LODP values obtained by acid hydrolysis of cellulose correlated well with the periodic crystal sizes along cellulose chains. The value of LODP has been shown to depend on the cellulose origin, with typical values of 250 being recorded for hydrolyzed cotton (Battista 1950), 300 for ramie fibers (Nishiyama et al. 2003b), 140–200 for bleached wood pulp (Battista et al. 1956), and up to 6,000 for the highly crystalline *Valonia* cellulose (from the cell wall of *Valonia ventricosa*) (Kai 1976). However, a wide distribution of DPs is typically observed for different cellulose sources, even at the LODP. In fact, the acid hydrolysis of bacterial, tunicate, algae, or cotton results in a higher polydispersity in the molecular weight, without any evidence of the LODP, probably because these cellulosic materials have no regular distribution of the less organized domains.

Typical procedures currently employed for the production of nanocellulose consist of subjecting pure cellulosic material to strong acid hydrolysis under strictly controlled conditions of temperature agitation, and time. The nature of the acid and the acid-to-cellulosic fibers ratio are also important parameters that affect the preparation of nanocellulose. A resulting suspension is subsequently diluted with water and washed with successive centrifugations. Dialysis against distilled water is then performed to remove any free acid molecules from the dispersion. Additional steps such as filtration (Elazzouzi-Hafraoui et al. 2008), differential centrifugation (Bai et al. 2009), or ultracentrifugation (using a saccharose gradient) (de Souza Lima and Borsali 2002) have also been reported.

Another technique developed for the preparation of nanocellulose is dilute acid coupled steam treatment (Cherian et al. 2008, 2010). This technique involves the

process of saturating the cellulosic material with steam at elevated pressure and temperature followed by sudden release of pressure, during which the flash evaporation of water exerts a thermo-mechanical force causing the material to rupture. By this method, noncellulosic compounds that cement the fiber aggregates were removed and the cellulose fibers are liberated from the bundles as individual entities in nano dimension, offering increased efficiency as composite reinforcements. This method is effective for the synthesis of high pure and high crystalline nanocellulose, especially for biomedical applications.

Specific hydrolysis and separation protocols have been developed that depend on the origin of the cellulosic fibers. Most common sources include among others, cellulose fibers from cotton (Teixeira et al. 2010; Dong et al. 1998; Araki et al. 2000), ramie (Habibi and Dufresne 2008; Habibi et al. 2008), hemp (Cao et al. 2008a), flax (Cao et al. 2007, 2008b), sisal (Siqueira et al. 2009; Garcia de Rodriguez et al. 2006), wheat straw (Helbert et al. 1996), palm (Bendahou et al. 2009), bleached softwood (Araki et al. 1999) and hardwood (Beck-Candanedo et al. 2005) pulps, cotton linters pulp (Roohani et al. 2008; Cao et al. 2009), microcrystalline cellulose (Bondeson et al. 2006a; Pranger and Tannenbaum 2008; Capadona et al. 2009) sugar beet pulp (Azizi Samir et al. 2004b), bacterial cellulose (Grunnert and Winter 2002; Hirai et al. 2009), and tunicates, sulfuric and hydrochloric acids have been extensively used for nanocellulose preparation, but phosphoric (Koshizawa 1960) and hydrobromic acids (Filpponen 2009) have also been reported for such purposes. If the nanocellulose is prepared by hydrolysis in hydrochloric acid, their ability to disperse is limited and their aqueous suspensions tend to flocculate (Araki et al. 1998). On the other hand, when sulfuric acid is used as a hydrolyzing agent, it reacts with the surface hydroxyl groups of cellulose to yield charged surface sulfate esters that promote dispersion of the nanocellulose in water (Revol et al. 1992). However, the introduction of charged sulfate groups compromises the thermostability of the nanocellulose (Roman and Winter 2004). Also, differences in the rheological behavior have been shown between suspensions obtained from sulfuric acid hydrolysis and those obtained from hydrochloric acid.

Figure 21.12 shows the STEM and AFM images of cellulose nanofibers extracted from white and naturally colored cotton fibers by sulfuric acid treatment. In fact, the sulfuric acid treated suspension has shown no time-dependent viscosity, whereas the hydrochloric acid-treated suspension showed a thixotropic behavior at concentrations above 0.5% (w/v) and antithixotropic behavior at concentrations below 0.3%. Post-treatment of nanocellulose generated by hydrochloric acid hydrolysis with sulfuric acid has been studied to introduce, in a controlled fashion, sulfate moieties on their surfaces (Araki et al. 1999, 2000). Nanocellulose generated from hydrochloric acid hydrolysis and then treated with sulfuric acid solution had the same particle size as those directly obtained from sulfuric acid hydrolysis; however, the surface charge density could be tuned to given values by sulfuric acid hydrolysis. With respect to the morphology of the particles, a combination of both sulfuric and hydrochloric acids during hydrolysis steps appears to generate spherical nanocellulose instead of rod-like nanocellulose when carried out under ultrasonic treatment

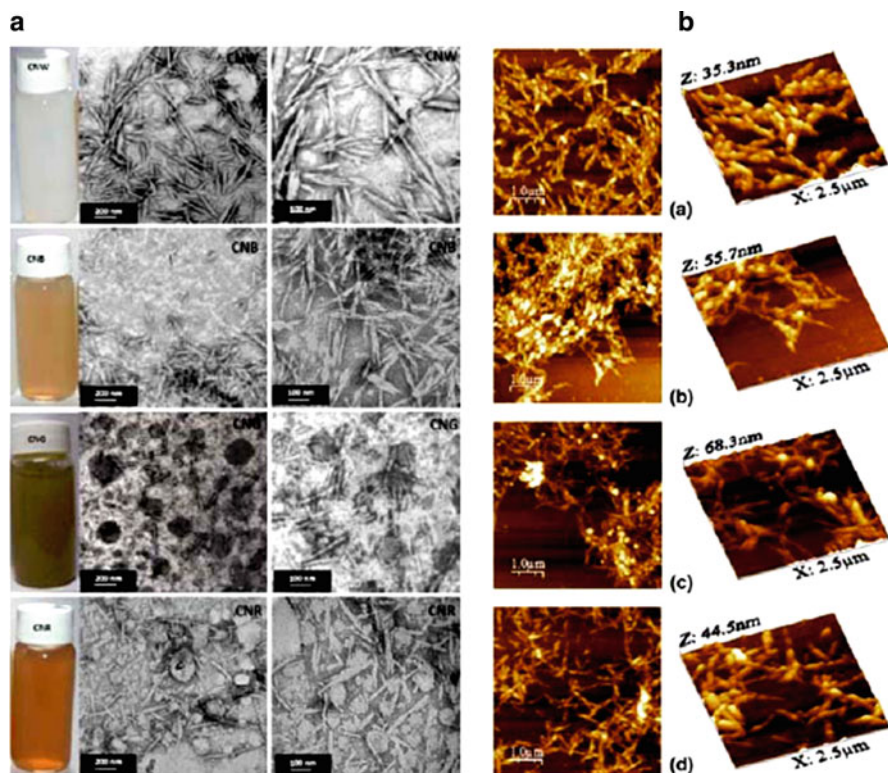


Fig. 21.12 Suspensions of cellulose nanofibers (on the left) and (a) scanning transmission electron micrographs of nanofibers (at two magnifications), (b) atomic force micrographs of cellulose nanofibers extracted from white and naturally colored cotton fibers by sulfuric acid treatment. Reproduced with permission from Teixeira et al. (2010). Copyright © 2010 Springer Science + Business Media B.V.

(Wang et al. 2007a, 2008). These spherical nanocelluloses demonstrated better thermal stability mainly because they possess fewer sulfate groups on their surfaces (Wang et al. 2007a). The concentration of sulfuric acid in hydrolysis reactions to obtain nanocellulose does not vary much from a typical value of ca. 65% (wt); however, the temperature can range from room temperature up to 70°C and the corresponding hydrolysis time can be varied from 30 min to overnight depending on the temperature. In the case of hydrochloric acid catalyzed hydrolysis, the reaction is usually carried out at reflux temperature and an acid concentration between 2.5 and 4 N with variable time of reaction depending on the source of the cellulosic material. Bondeson et al. (2006b) investigated optimizing the hydrolysis conditions by an experimental factorial design matrix (response surface methodology) using microcrystalline cellulose that was derived from Norway spruce (*Picea abies*) as the cellulosic starting material. The factors that were varied during the process were the concentrations of microcrystalline cellulose and sulfuric acid, the hydrolysis time

and temperature, and the ultrasonic treatment time. The responses that were measured were the median size of the cellulose particles and the yield of the reaction. The authors demonstrated that with a sulfuric acid concentration of 63.5% (w/w) over a time of approximately 2 h, it was possible to obtain nanocellulose having a length between 200 and 400 nm and a width less than 10 nm with a yield of 30% (based on initial weight). Prolongation of the hydrolysis time induced a decrease in nanocellulose length and an increase in surface charge (Dong et al. 1998). Reaction time and acid-to-pulp ratio on nanocellulose obtained by sulfuric acid hydrolysis of bleached softwood (black spruce, *Picea mariana*) sulfite pulp was investigated by Beck-Candanedo et al. (2005). They reported that shorter nanoparticles with narrow size polydispersity were produced at longer hydrolysis times.

Recently, Elazzouzi-Hafraoui et al. (2008) studied the size distribution of nanocellulose resulting from sulfuric acid hydrolysis of cotton treated with 65% sulfuric acid over 30 min at different temperatures, ranging from 45 to 72°C. By increasing the temperature, they demonstrated that shorter crystals were obtained; however, no clear influence on the width of the crystal was revealed.

The geometric properties of the nanocellulose structures (shape, length, and diameter) depend mainly on the origin of the cellulose and the extraction process (acid hydrolysis, shearing and high-pressure homogenization, biosynthesis by bacteria or electrospinning). Several sources of cellulose have been used to obtain cellulose nanostructures, not necessarily needle-shaped, which have high crystallinity. Examples include tunicin (Angle's and Dufresne 2000, 2001) wheat straw (Alemdar and Sain 2008), bacterial cellulose (Nakagaito et al. 2005), sisal (Garcia de Rodriguez et al. 2006; Morán et al. 2008), banana residues (Zuluaga et al. 2007), hemp (Janardhnan and Sain 2006), and microcrystalline cellulose (Wang et al. 2007b). Recently, cellulose nanoparticles have also been synthesized in spherical form (Pu et al. 2007; Zhang et al. 2007, 2008).

21.3 Chemical Modifications of Nanocellulose

Different chemical modifications have been attempted on cellulose nanofibers because of a natural advantage of an abundance of hydroxyl groups at the surface, including esterification, etherification, oxidation, silylation, polymer grafting, etc. Noncovalent surface modification, including the use of adsorbing surfactants and polymer coating, has also been studied. All chemical functionalizations have been mainly conducted to (1) introduce stable negative or positive electrostatic charges on the surface of nanocellulose to obtain better dispersion (cellulose nanofibers obtained after sulfuric acid hydrolysis introduce labile sulfate moieties that are readily removed under mild alkaline conditions); and (2) tune the surface energy characteristics of nanocellulose to improve compatibility, especially when used in combination with nonpolar or hydrophobic matrices in nanocomposites. The main challenge for the chemical functionalization of cellulose nanofibers is to conduct the process in such a way that it only changes the surface of nanofibers, while avoiding any polymorphic

conversion, preserving the original morphology and to maintain the integrity of the fibers.

Although the intention of nanocellulose modification is usually to enhance compatibility with nonpolar polymers, thus to improve mechanical properties, chemical modification may also add extra functionality to nanocellulosic materials. For example, positively charged amine functionalized nanocellulose is reported to be antimicrobially active in biomedical applications (Thomas et al. 2005). Andresen et al. (2007) also introduced extra functionality to nanocellulose film by covalently grafting the cellulose with octadecyldimethyl (3-trimethoxysilylpropyl) ammonium chloride (ODDMAC). The surface-modified nanocellulose films showed antibacterial activity against both Gram-positive and Gram-negative bacteria, even at very low concentrations of antimicrobial agent on the surface, killing more than 99% of *Escherichia coli* and *Staphylococcus aureus* when the atomic concentration of ODDMAC nitrogen on the film surface was 0.14% or higher.

Heux et al. (2000) and Heux and Bonini (2000) introduced the attempt on the noncovalent surface modifications of nanocellulose which are made via adsorption of surfactants. They employed surfactants consisting of the mono and diesters of phosphoric acid bearing alkylphenol tails. The obtained surfactant coated nanocellulose disseminated very well in nonpolar solvents. The nonionic surfactants coated nanocellulose in polystyrene-based nanocomposites have been studied by Kim et al. (2009) and Rojas et al. (2009). Anionic surfactant modified nanocellulose was used by Bondeson and Oksman (2007a) to enhance the dispersion in poly lactic acid (PLA). Surface cationization was done by weak or strong ammonium containing groups, such as epoxypropyltrimethylammonium chloride (EPTMAC), grafted onto the nanocellulose surfaces (Hasani et al. 2008). Zhou et al. (2009) recently reported a new and elegant way of nanocellulose surface modification based on the adsorption of saccharide-based amphiphilic block copolymers. By mimicking lignin-carbohydrate copolymers, they adsorbed xyloglucan oligosaccharide-poly(ethylene glycol)-polystyrene triblock copolymer onto the surface of nanocellulose. The resulting nanocellulose showed excellent dispersion abilities in nonpolar solvents.

Esterification of nanocellulose by reacting organic fatty acid chlorides, having different lengths of the aliphatic chain (C12–C18), has also been reported with a grafting density high enough that the fatty acids with backbones of 18 carbons were able to crystallize on the surface of the nanocellulose (Junior de Menezes et al. 2009). An environmentally friendly nanocellulose surface acetylation route was recently developed by Yuan et al. (2006) involving a low reagent consumption and uncomplicated procedure. The method used alkyenyl succinic anhydride (ASA) aqueous emulsions as a template. Berlioz et al. (2009) have reported recently a new and highly efficient synthetic method for an almost complete surface esterification of nanocellulose, leading to highly substituted nanocellulose esters. The reaction of fatty acid chains was carried out on dried nanocellulose via a gas-phase process. Gousse et al. (2002) reported the partial silylation of cellulose whiskers resulting from the acid hydrolysis of tunicate by a series of alkyl dimethylchlorosilanes, with the carbon backbone of the alkyl moieties ranging from a short carbon length of

isopropyl to longer lengths represented by *n*-butyl, *n*-octyl, and *n*-dodecyl. Surface trimethyl silylation of nanocellulose from bacterial cellulose and their resulting cellulose acetate butyrate (Roman and Winter 2006) or polysiloxane (Grunnert and Winter 2000) based nanocomposites was also investigated by Roman and Winter. Finally, coupling nanocellulose with *N*-octadecyl isocyanate, via a bulk reaction in toluene, has also been reported to enhance their dispersion in organic medium and compatibility with polycaprolactone, which significantly improved the stiffness and ductility of the resultant nanocomposites (Siqueira et al. 2009).

TEMPO-mediated oxidation of nanocellulose, obtained from HCl hydrolysis of cellulose fibers, was first reported by Araki et al. (2001) as an intermediate step to promote grafting of polymeric chains. Habibi et al. (2006) performed TEMPO-mediated oxidation of nanocellulose obtained from HCl hydrolysis of cellulose fibers from tunicate and showed that it did not compromise the morphological integrity of nanocellulose or their native crystallinity. The authors demonstrated on the basis of the morphology, supramolecular structure, and crystallographic parameters of the nanocellulose, that various degrees of oxidation can be predicted and attained by using specific amounts of the primary oxidizing agent (Fig. 21.13(I)), TEMPO-oxidized or carboxylated nanocellulose suspensions display birefringence patterns (Fig. 21.13(II)) and do not flocculate or sediment when dispersed in water owing to the polyanionic character imparted by the negative charges on the nanocellulose surfaces.

The surface of nanocellulose is grafted by polymers. The polymer grafting of nanocellulose has been done using two main strategies, namely the “grafting-onto” and “grafting-from” (Zhao and Brittain 2000). The grafting onto approach involves

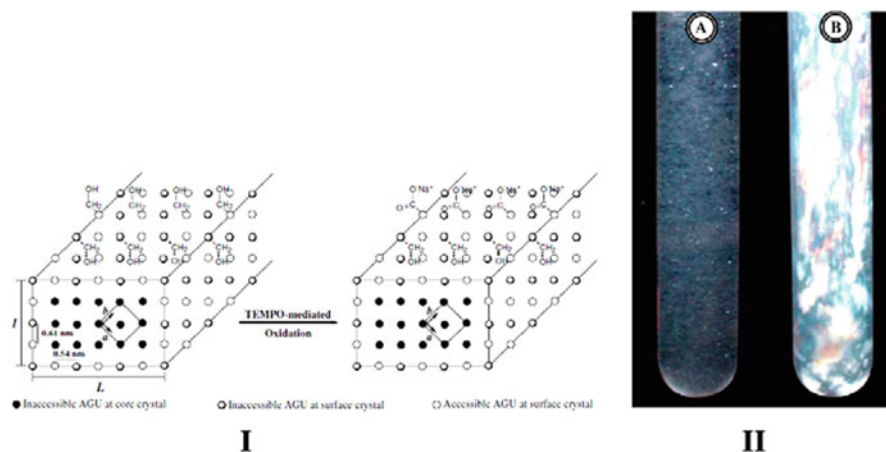


Fig. 21.13 (a) Scheme of cross-sectional representation of cellulose nanocrystal indicating the occurrence of the surface TEMPO-mediated oxidation of available hydroxyl groups (surface crystal representations), (b) aqueous 0.53% (w/v) suspensions of cellulose whiskers observed between crossed polarizer's: (a) before and (b) after TEMPO-mediated oxidation. Reproduced with permission from Habibi et al. (2006). Copyright © 2006 Springer

attachment onto the hydroxyl groups at the cellulose surface of presynthesized polymer chains by using a coupling agent. In the “grafting from” approach, the polymer chains are formed by in situ surface initiated polymerization from immobilized initiators on the substrate.

The “grafting onto” approach was implemented by Mangalam et al. (2009) who grafted DNA oligomers on the surface of nanocellulose. The grafting of polycaprolactone having different molecular weights on the surface of nanocellulose has been achieved by using isocyanate-mediated coupling (Habibi and Dufresne 2008). Similar attempts were made by Cao et al. (2009) who reported the isocyanate-catalyzed grafting of presynthesized waterborne polyurethane polymers via a one-pot process. Such crystallization provoked cocrystallizations of the free chains of the respective polymer matrices during nanocellulose-based nanocomposite processing and also induced the formation of a co-continuous phase between the matrix and filler, which significantly enhanced the interfacial adhesion and consequently contributed to a highly improved mechanical strength of the resulting nanocomposites. Ljungberg et al. (2005) used “grafting onto” approach to graft maleated polypropylene (PPgMA) onto the surface of tunicate-extracted nanocellulose. The resulting grafted nanocellulose showed very good compatibility and high adhesion when dispersed in atactic polypropylene. Araki et al. (2001) and Vignon et al. (2004) studied the grafting of amine-terminated polymers on the surface of TEMPO-mediated oxidized nanocellulose by using a peptide coupling process catalyzed by carbodiimide derivatives in water.

Habibi et al. (2008) first reported the “grafting from” approach applied to nanocellulose. In this work, they grafted polycaprolactone onto the surface of nanocellulose via ring-opening polymerization (ROP) using stannous octoate ($\text{Sn}(\text{Oct})_2$) as a grafting and polymerization agent. Yi et al. (2008) and Morandi et al. (2009) propagated polystyrene brushes via atom transfer radical polymerization (ATRP) on the surface of nanocellulose with ethyl 2-bromoisobutyrate as the initiator agent. Similarly, Chen et al. (2009) and Lin et al. (2009) conducted grafting reactions under microwave irradiation to enhance the grafting efficiency. In situ polymerization of furfuryl alcohol from the surface of cellulose whiskers was studied by Pranger and Tannenbaum (2008). Mattoso et al. (2009) developed grafting of polyaniline from nanocellulose, accomplished by in situ polymerization of aniline onto nanocellulose in hydrochloric acid aqueous solution, via an oxidative polymerization using ammonium peroxydisulfate as the initiator. Zoppe et al. (2009) polymerized vinyl monomers, mainly acrylic monomers such as *N*-isopropylacrylamide from the surface of nanocellulose to produce thermo responsive substrates.

21.4 Cellulose Nanocomposites

Nanocelluloses have attracted a great deal of interest in the nanocomposites field due to their appealing intrinsic properties such as nanoscale dimensions, high surface area, unique morphology, low density [which is estimated to be 1.61 g/cm^3

(Nishiyama et al. 2002) for pure crystalline cellulose I β], and mechanical strength. In addition, they are easily (chemically) modified, readily available, renewable, and biodegradable. The first publication related to the use of nanocellulose as reinforcing fillers in poly(styrene-*co*-butyl acrylate) (poly(S-*co*-BuA)) based nanocomposites was by Favier et al. (1995a). Nakagaito and Yano (2004, 2005) impregnated microfibrillated Kraft pulp with a phenol formaldehyde resin and then compressed the resulting material under high pressure to produce high strength cellulose nanocomposites. Hayashi and Shimo (2006) reported the use of MFC in phenolic resin for the preparation of car fenders. More recently, they employed aqueous sodium hydroxide treated nanocellulose and phenolic resin to produce nanocomposites (Nakagaito and Yano 2008). Nogi and Yano (2008) prepared a foldable and ductile transparent nanocomposite film by combining low Young's modulus transparent acrylic resin with 5 wt% of low Coefficient of Thermal Expansion and high-Young's modulus bacterial cellulose. The same researchers reported that transparent cellulose nanofiber sheets prepared from MFC and coated with acrylic resin have low CTEs of 8.5–14.9 ppm/K and a modulus of 7.2–13 GPa (Nogi and Yano 2009; Nogi et al. 2009).

Nogi et al. (2005, 2006a, b) obtained transparent composites by reinforcing various acrylic resins with BC at loadings up to 70 wt%. Bruce et al. (2005) prepared composites based on swede root (rutabaga) MFC and different resins including four types of acrylic and two types of epoxy resins. Dalmas et al. (2007) dispersed cellulose nanofibrils obtained from sugar beet pulp in the same poly(styrene-*co*-butyl acrylate) latex. In a study by Malainine et al. (2005), nanocomposite materials were prepared by solution casting from an aqueous suspension of cellulose microfibrils obtained from *Opuntia ficus-indica cladodes* (i.e., modified stems) and a latex of poly(styrene-*co*-butyl acrylate). Seydibeyoglu and Oksman (2008) prepared PU-cellulose nanofiber composite materials using a film stacking method in which the PU films and nonwoven cellulose fibril mats were stacked and compression molded. Auad et al. (2008) reported that MFC was utilized to reinforce shape memory polyurethanes. Shape memory polymers (SMPs) are capable of fixing a transient shape and of recovering their original dimensions by the application of an external stimulus (Tobushi et al. 1996a, b).

Hassan and Peppas (2000) worked on poly(vinyl alcohol)–nanocellulose which acts as an ideal candidate for biomedical applications including tissue reconstruction and replacement, cell entrapment and drug delivery, soft contact lens materials and wound covering bandages for burn victims. Leitner et al. (2007) also prepared PVOH nanocomposites with a range of nanocellulose contents (0–90 wt%). At a cellulose content of 50 wt%, the modulus of elasticity of PVOH increased by a factor of 20 and tensile strength increased by a factor of 3.5. Bhatnagar and Sain (2005) reported blend containing 10% cellulose nanofibers obtained from various sources, such as flax bast fibers, hemp fibers, kraft pulp, or rutabaga, and 90% poly(vinyl alcohol) was used for making nanofiber-reinforced composite material by a solution casting procedure. Soybean stock-based nanofiber reinforced PVOH films were reported by Wang and Sain (2007a, b) and Zimmermann et al. (2004), dispersed MFC into PVOH and generated fibril-reinforced PVOH nanocomposites

(fibril content 20 wt%) with up to three times higher E -modulus and up to five times higher tensile strength when compared to the reference polymer. Bacterial cellulose/poly(ethylene oxide)-nanocomposites were studied by Brown and Laborie (2007). By tailoring the composition and morphology of BC/PEO nanocomposites, it is further hypothesized that physical, thermal, and mechanical properties might be fine-tuned. Poly(ethylene oxide) is a highly biocompatible, biodegradable, hydrophilic, and flexible polymer which has recognized many different applications in drug delivery, mucoadhesive, dispersant, surfactant, hydrogel, electrolyte solvent in lithium polymer cell, flocculation, and rheology control agents.

Cheng et al. (2007) fabricated PP composites from filtered mats of regenerated cellulose (Lyocell) fibril aggregates and PP fibers using compression molding. Nanocellulose with PLA, Okubo et al. (2005, 2009) reported an effective technique for improving the mechanical properties of PLA-based bamboo fiber composites by adding MFC up to 20 wt%. Mathew et al. (2006) reported a nonuniform dispersion of cellulose fillers in PLA matrix when nanocomposites of PLA with 5 wt% cellulose nanowhiskers and MFC were prepared by twin-screw extrusion. Fabrication of MFC/PLA nanocomposites based on a papermaking like process has been presented as an industrially practical method. Wang and Sain (2007c) used chemically treated cellulose nanofibers extracted from hemp to prepare PLA and PHB nanocomposites. Suryanegara et al. (2009) demonstrated that crystallization of PLA increases the storage modulus as well as the strength and Young's modulus of PLA/MFC nanocomposites without significant reduction in the strain at break.

Nanocellulose was successfully grafted with different molecular weights of poly(ϵ -caprolactone) in order to improve compatibility with a PCL matrix (Lönnerberg et al. 2008). Siqueira et al. (2009) applied *N*-octadecyl isocyanate as a grafting agent for modifying the surface of two types of cellulose nanofillers. In this study, the reinforcing capacity of nanowhiskers and MFC in PCL matrix was compared. Wågberg et al. (2008), for example, successfully prepared polyelectrolyte multilayers (PEMs) by combining different types of polyelectrolytes and carboxylated MFC. Thus, nanocellulose has been incorporated into a wide range of polymer matrices, including polysiloxanes (Grunnert and Winter 2000), polysulfonates (Noorani et al. 2006), poly(caprolactone) (Habibi and Dufresne 2008; Habibi et al. 2008) styrenebutyl acrylate latex (Paillet and Dufresne 2001), poly(oxyethylene) (Azizi Samir et al. 2004c, 2005a, b), poly(styrene-*co*-butyl acrylate) (poly(*S-co*-BuA)) (Favier et al. 1995a), cellulose acetate butyrate (Grunnert and Winter 2002; Petersson et al. 2009), carboxymethyl cellulose (Choi and Simonsen 2006), poly(vinyl alcohol) (Paralikar et al. 2008), poly(vinyl acetate) (Garcia de Rodriguez et al. 2006), poly(ethylene-vinyl acetate) (EVA) (Chauve et al. 2005), epoxides (Ruiz et al. 2000), polyethylene (Junior de Menezes et al. 2009), polypropylene (Bonini 2000), poly(vinyl chloride) (Chazeau et al. 1990, 1999a, b, 2000), polyurethane (Marcovich et al. 2006), and waterborne polyurethane (Cao et al. 2009). Their incorporation into biopolymers, such as starch-based polymers (Cao et al. 2008a; Angle's and Dufresne 2001; Lu et al. 2005, 2006), soy protein (Wang et al. 2006), chitosan (Li et al. 2009) or regenerated cellulose (Qi et al. 2009), biopolymer like poly(lactic acid) (Bondeson and Oksman 2007b; Petersson et al. 2007), poly

(hydroxyoctanoate) (Dubief et al. 1999; Dufresne 2000), and polyhydroxybutyrates (Jiang et al. 2008) have also been reported.

21.5 Application of Nanocellulose in Medicine

Recent advances in the field of biomaterials and their medical applications indicate the significance and potential of various nanocellulose in the development of novel classes of medical devices and applications in healthcare and veterinary medicine. The physical and mechanical properties of nanocellulose are attributes that enable nanocellulose membranes to function as effective temporary wound dressings. On the other hand, because implantable biomaterials (i.e., scaffolds) are also needed, a new approach has been undertaken to apply cellulose as a material entirely integrated into the body, either as a bone or skin graft.

Nanocellulose product Gengiflex[®] has intended applications within the dental industry. It was developed to aid periodontal tissue recovery (Novaes and Novaes 1997). A description was given of a complete restoration of an osseus defect around an IMZ implant in association with a Gengiflex[®] therapy. The benefits included the reestablishment of esthetics and function of the mouth and that a reduced number of surgical steps were required. A recent trial on mongrel dogs, however, showed that negligible improvements were gained from using Gengiflex[®] (Novaes et al. 2003).

A more successful product, called Biofill[®], is used as a bandage that can be applied to cases of second and third degree burns and ulcers. Biofill[®] is ideal as a temporary substitute for human skin. The greatest drawback of the product was the limited elasticity when applied to areas of great mobility. In contrast, the benefits included immediate pain relief, close adhesion to the wound bed, diminished postsurgery discomfort, and reduced infection rate. The transparent cellulose made wound inspection easy while Biofill[®] detached when new skin formed. By reducing treatment time and costs, Biofill[®] has potentially financial viability (Fontana et al. 1990).

21.5.1 Nanocellulose Microvessel Endoprosthesis

A team of chemists, biologists, and surgeons developed a product called BASYC[®] (BACTERIAL SYNTHESISED CELLULOSE). BASYC[®] is a statically produced tube to be used as replacement blood vessel. Tubes of 1 mm inner diameter and 5 mm length were produced, which could be used as replacement blood vessels. Another benefit was that the inner surface of the BASYC[®] tube was smoother than other synthetic materials used for similar purposes. To test the product, a BASYC[®] tube was inserted as an endoprosthesis into a white rat. A histological exam showed that the

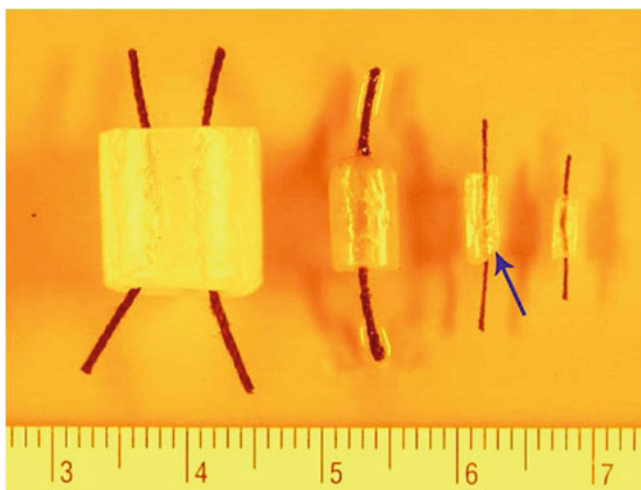


Fig. 21.14 BASYC[®] tubes sufficient for experimental microsurgical applications with different inside diameter, different wall thickness, and different length. Reproduced with permission from Klemm et al. (2001). Copyright © 2001, Elsevier Science Ltd

microvessel had become covered with well-orientated endogenous cells indicating a regular vascular wall had formed inside the cellulose wall (Klemm et al. 2001).

Using a patented matrix technique, *A. xylinum* is able to build up cellulose network as very regularly formed tubes of different length, wall thickness, and inner diameter (Fig. 21.14). The marked BASYC[®] tube has an inner diameter of 1 mm, length of about 5 mm, and wall thickness of 0.7 mm. These parameters are sufficient for experimental microsurgical requirements.

For the BASYC vessel implants, the low roughness of the inner surface (feature variations of ~15 nm) is especially significant and can be obtained with the matrix reservoir technique. This degree of roughness is within the order of magnitude of that for typical blood vessels in rats. The BASYC tubes also meet other significant demands for microvessel replacement: they have a constant shape, are sufficiently stable against internal and external pressure, are flexible and elastic, and are capable of handling a tight microsurgical suture. Figure 21.15a shows an example of the microsurgical work with shaped cellulose material. Results of investigations of the microsurgery of nerves and vessels of the rat as an experimental model are shown in Fig. 21.15b–f.

Upon dissection of the nervus ischiadicus and subsequent reconnection by a microsurgical suture, a protective cover (cuff) of BASYC prevents connective tissue from growing into the nerve gap, and favors the adhesion of the fascicles, which facilitates early regeneration of the nerve and a rapid return of muscle function. The good incorporation of bacterial cellulose-forming connective tissue and new blood vessels on the surface of the protective cover is worthy of particular emphasis (Klemm et al. 2005).

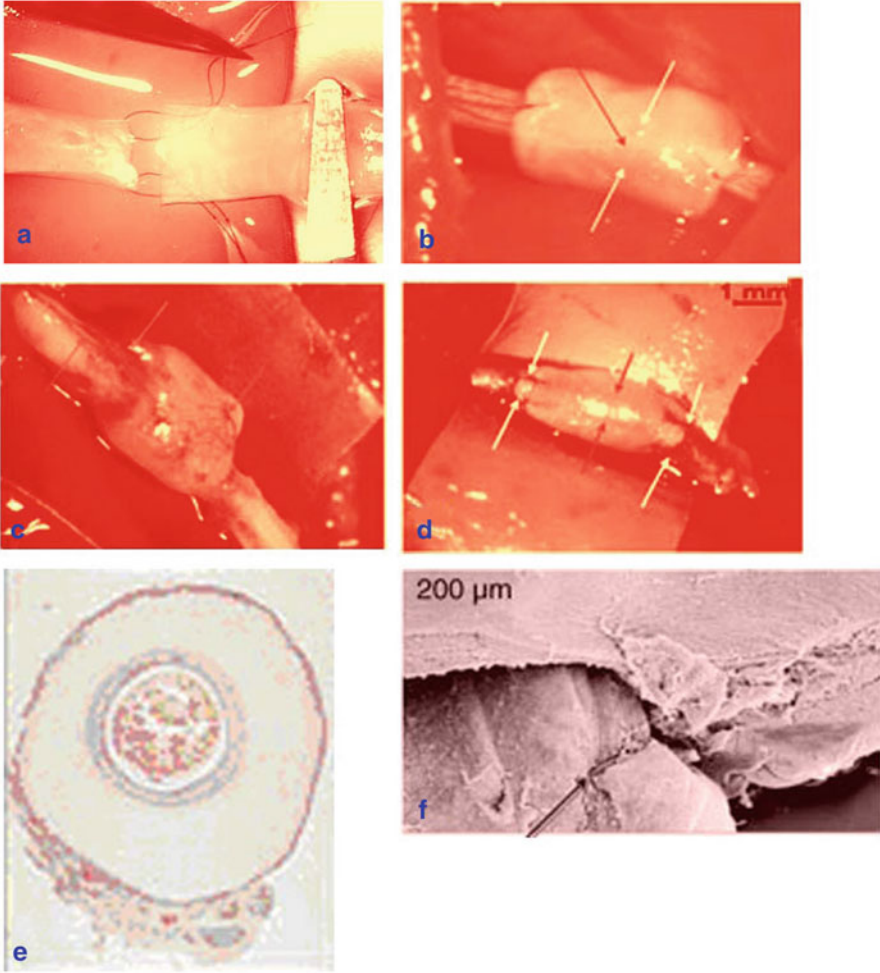


Fig. 21.15 Application of bacterial cellulose tubes (BASYC) for training in microsurgical techniques and for animal experimental microsurgery on nerves and vessels: (a) end-in-end connection (anastomosis) of BASYC tubes; (b) nervus ischiadicus of the rat directly after operation of the dissected nerve (*white arrows*: anastomosis, *black arrow*: suture) with BASYC protective cover; (c) operating field 10 weeks after the nerve dissection (*arrows*: new connective tissue and new blood vessels); (d) BASYC implant in the carotid artery of the rat directly after operation (*white arrows*: anastomosis, *black arrows*: free blood flow, visible through the cellulose tube); (e) cross-section of the middle part of a BASYC implant from the carotid artery of the rat after 4 weeks of residence time in the body as a histological preparation (H/E staining); (f) SEM image of a longitudinally cut BASYC implant with a homogeneous surface in the cellulose (left) and natural vessel region (*arrow*: remaining suture material). Magnification: 10 \times : (a, b, c); 6 \times : (d); and 32 \times : (e). Reproduced with permission from Klemm et al. (2005). Copyright © 2001, Elsevier Science Ltd

Upon reconnection of a dissected carotid artery (in a rat model) with a BASYC tube, the internal surface of the BASYC material becomes completely covered by an endothelial cell layer after a residence time of 4 weeks, as determined by histological examination of the preparation along with a specific test for endothelial cells (Fig. 21.15e). Blood remnants can be found in the lumen. As observed by electron microscopy, the complete colonization of the BASYC region with endothelial cells covering both parts of the suture (Fig. 21.15f) can be substantiated. Apparently, the BASYC material is a good substrate for the anchoring of autologous cells. Upon coverage of longitudinally cleaved tubes with bovine endothelial cells in cell culture tests, a distinct sprouting of the initially spherical cells takes place within 24 h.

21.5.2 Nanocellulose for Artificial Cardiovascular Tissues

One of the greatest advantages of microbial cellulose is its ability to be molded into almost any size and shape during its synthesis without causing any significant alteration of its physical properties. Because of recent developments in implant technologies and microsurgical techniques, small, versatile, microbial cellulose objects may prove to be quite useful in this area of biomedical research. Roberts et al. described and patented one of the first production methods for the creation of shaped (molded) objects (Czaja et al. 2007a, b). The method developed by Roberts and co-workers involves inoculating *A. xylinum* into a suitable liquid medium, which is then transferred into a mold consisting of an oxygen-permeable polymer, such as polyvinyl chloride. One of the sides of this fermentation vessel stays in contact with oxygen while the other side remains in contact with the liquid medium, where the cellulose is produced (Roberts et al. 1986). With this stationary culture technique, various three-dimensional objects of potential biomedical importance can easily be synthesized (Fig. 21.16).

Schumann et al. (2009) reported the positive results of the application of long bacterial nanocellulose grafts in the porcine carotid artery (Fig. 21.17). They demonstrated the possibility to fabricate nanocellulose as in vitro scaffold and implant it as a substitute for a small diameter artery. The biocompatibility of nanocellulose is good and the material has a potential to be used as a scaffold in tissue engineering process with a highly attractive approach to in vivo tissue engineered blood vessels as part of programs in cardiovascular surgery.

21.5.3 Bone Graft

Intensive investigations on preparation, characterization, and application experiments of bacterial nanocellulose tubes are also reported by Helenius et al. (2006) and Bodin et al. (2007a). As part of investigations on bone repair, Hutchens et al. (2006) demonstrated by combination of hydroxyapatite and bacterial nanocellulose that bacterial nanocellulose provides a template for the ordered formation of calcium-deficient hydroxyapatite (CDHAP), the natural mineral component of bone. An

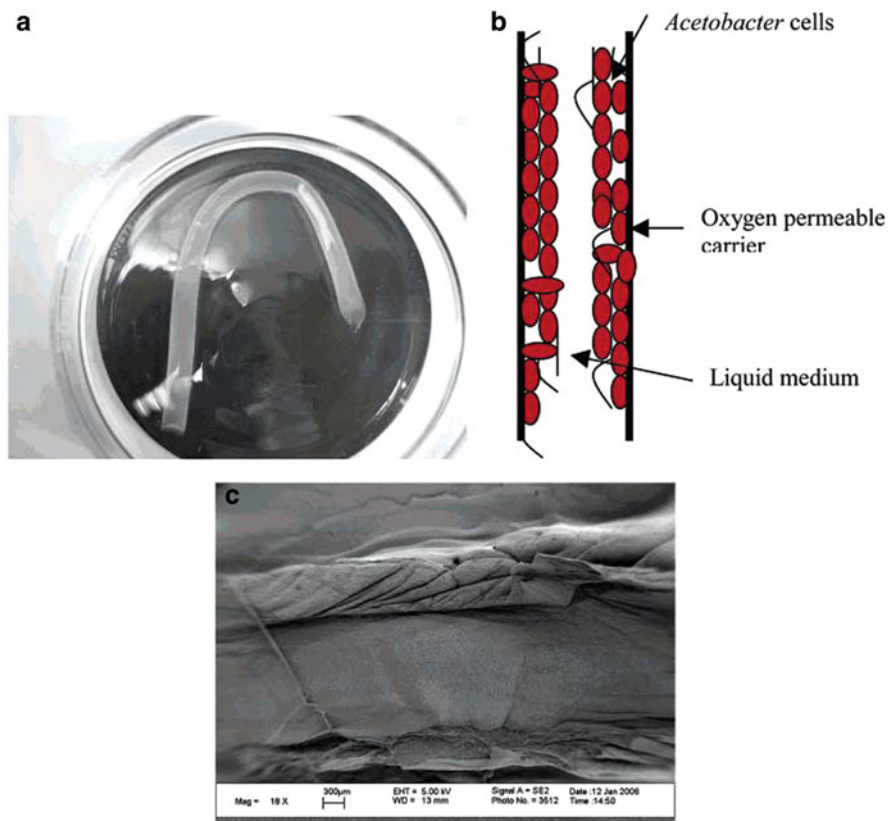


Fig. 21.16 Hollow tube made from microbial cellulose, using a silicon tube as a mold (a). *Acetobacter* cells that are highly aerobic organisms tend to gather in the oxygen-rich zones near the inner wall of the silicon tube where they produce and deposit cellulose (b). The inner surface (lumen) of the cellulose tube can be made very smooth and highly homogeneous (c). Reproduced with permission from Czaja et al. (2007a, b). Copyright © 2007, American Chemical Society

application as bone graft seems promising because CDHAP promotes bone colonization when implanted in osseous defects and degrades over time to be replaced by new bone (Fig. 21.18). The bioactivity of CDHAP and the biocompatibility of bacterial nanocellulose substantiate these composites as a new potential orthopedic biomaterial. The composites were formed by alternating incubation cycles of bacterial nanocellulose pellicles with calcium and phosphate solutions.

21.5.4 Nanocellulose Meniscus Implant

Traumatic or degenerative meniscal lesions are a frequent problem. The meniscus cannot regenerate after resection. These lesions often progress and lead to osteoarthritis. Collagen meniscal implants have been used in clinical practice to regenerate

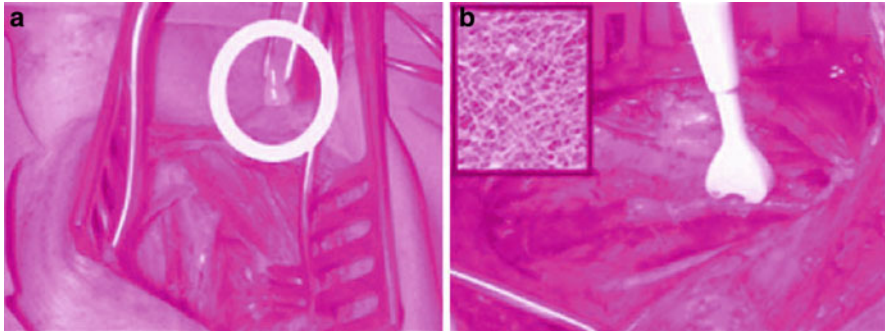


Fig. 21.17 (a) Intraoperative situs of the carotid artery, BC tube in the forceps, (b) nanocellulose graft implanted in the porcine carotid artery (7-0 monofilament prolene). Patency was subsequently controlled by flow measurement. The small picture is showing the ultra fine network structure of cellulose in the tube. The matrix did not contain cells and required no preclotting. Reproduced with permission from Schumann et al. (2009). Copyright © 2008 Springer Science + Business Media B.V

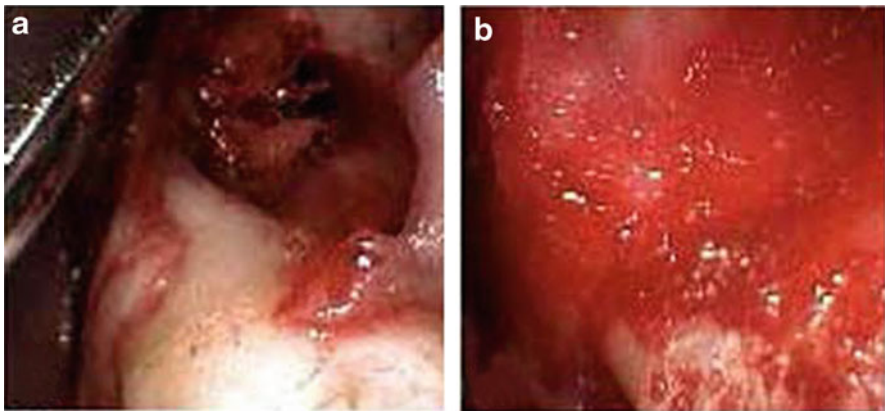


Fig. 21.18 (a) The large osseous defect in bone, (b) The bone defect is packed with a freeze-dried bone graft

meniscal tissue after partial meniscectomy. Nanocellulose from bacteria can be utilized to regenerate meniscal tissue. Bacterial cellulose, grown statically in corn steep liquid medium was molded into a half-moon shape with dimensions similar to those of a meniscus (Fig. 21.19). The wedge character of the meniscus was created by introducing a silicone support in the middle of the fermentation vessel, which was successively lowered during production, tilting the cellulose network on the surface. Shortly after resection of the lateral meniscus, the cellulose implant was transplanted and secured with sutures (PDS 6.0; Ethicon) to the remaining capsular tissue. Young's modulus of bacterial cellulose was measured to be 1 MPa, 100 times

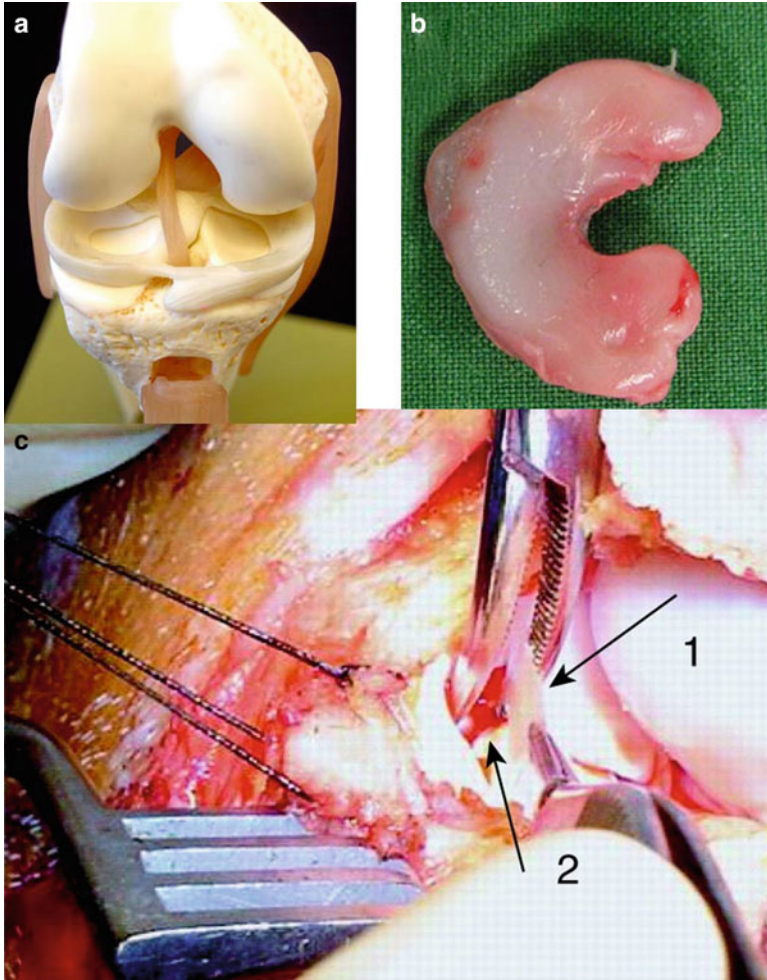


Fig. 21.19 (a) Model of a semi-circular cartilaginous disk (Meniscus) that resides in the knee joint, (b) Molded bacterial cellulose meniscus. (c) Implantation of the construct into a created meniscal lesion in vivo. The traction sutures are visible on the outer third of the meniscus. The seeded implant (Arrow 1) is inserted into the created meniscal lesion with an Adson forcep. The insertion of the implant is facilitated by the use of a hemostat, opening the lesion (arrow 2)

less for the collagen material, 0.01 MPa in tensile load. The Young's modulus of bacterial cellulose and meniscus are similar in magnitude under a compression load of 2 kPa and with five times better mechanical properties than the collagen material (Bodin et al. 2007b). The bacterial cellulose is inexpensive, can be produced in a meniscus shape, and promotes cell migration which makes it an attractive material for consideration as a meniscus implant.

21.5.5 Nanocellulose in the Treatment of Chronic Wounds and Burns

Burns are very complex injuries, causing extensive damage to skin tissues. Burns are classified according to depth and identified by three degrees (Latarjet 1995): first-degree burn – usually superficial, affects only the outer layer of skin (epidermis); second-degree burn – either superficial, with damage to the epidermis layer of the skin (second-degree A), or deep when penetrating into the dermis (second-degree B); third-degree burn – a total destruction of all the epidermis and dermis, extending into subcutaneous tissue (skin grafting is recommended). The healing process involves the regeneration of the epidermis and the repair of the dermis, both of which result in the formation of scar tissue (Balasubramani et al. 2001). The major goal during treatment of burn patients is to quickly accomplish effective wound closure to increase the rate of healing and significantly reduce pain (Demling and DeSanti 1999; Jones et al. 2002; Prasanna et al. 2004). In addition, proper wound management must prohibit the wound from becoming infected and dehydrated (Gallin and Hepperle 1998). Despite the fact that many different biological and synthetic wound dressings have already been developed, the search for an ideal wound dressing is still in progress. According to the modern approaches in the field of wound healing, an ideal wound dressing system must be structurally and functionally similar to autograft skin (Quinn et al. 1985).

Because of its unique properties, nanocellulose has been shown to be a highly effective wound dressing material. In fact, the results of various studies indicate that topical applications of nanocellulose membranes improve the healing process of burns and chronic wounds. Recent study conducted in Poland used never-dried cellulose membranes in order to treat patients with severe second-degree burns (Czaja et al. 2007a, b). This study showed that the skin of the patients whose burns were covered with never-dried cellulose membranes healed faster (faster reepithelialization) than the wounds of patients who received a conventional wound dressing (such as wet gauze and ointments). The Polish study also found that cellulose membranes actually performed better than conventional wound dressings in (1) conforming to the wound surface (excellent molding to all facial contours and a high degree of adherence even to the contoured parts such as nose, mouth, etc. were observed), (2) maintaining a moist environment within the wound, (3) significantly reducing pain, (4) accelerating reepithelialization and the formation of granulation tissue, and (5) reducing scar formation. These nanocellulose membranes can be created in any shape and size, which is beneficial for the treatment of large and difficult to cover areas of the body (Fig. 21.20).

In studies conducted by Fontana et al. (1990) and Mayall et al. (1990) on nanocellulose product called BioFill[®], it proved to be a very successful wound covering for skin problems such as burns and chronic ulcers. BioFill[®] was also shown to be more effective than other skin treatments. Another nanocellulose product called XCell, which is manufactured by Xylos Corporation, was used in a



Fig. 21.20 A deep second-degree facial burn caused by the exposure to flame (a); a highly conformable mask of the MC dressing with holes on eyes, nose, and mouth was tightly applied on the wounded face (b); the epithelialization in the regions of wound edges and from the deep epidermal appendages has been clearly observed at 17 days upon burning (c); the entirely healed face after next 28 days (d); examination after about 20 months upon burning showed the shallow, nonhypertrophic scar tissues on the facial surface where third-degree burn occurred (front) (e); and the lack of tissue fragments on the right ear (f). Reproduced with permission from Czaja et al. (2007a, b). Copyright © 2007 Springer

study conducted by Alvarez et al. (2004). In this study, the XCell dressing was used to treat patients suffering from chronic venous ulcers. Nanocellulose proved to be very effective in promoting autolytic debridement, reducing pain, and accelerating granulation, all of which are important for proper wound healing.

21.5.6 Cosmetic Tissues

Nanocellulose due to its special properties, such as high wetness (water content 95%), high purity, and mechanical stability, finds applications in the cosmetics as a moistening mask, as well as an ingredient of moistening cream. For instance, two cosmetic tissue products are successful on the market: a series of masks based on BioCellulose and the mask basis material NanoMasque[®]. Both tissues are produced from pure bacterial cellulose and alternatively impregnated with active substances applied in cosmetics such as plant extracts, extracts from algae, essential oils, and panthenol. The additives are bound inside the cellulose matrix, e.g., by hydrogen bonds. These bonds are selective enough to localize the substances in the matrix as well as to allow their migration into the skin during application (Fig. 21.21).

Several randomized studies with humans have been realized: a human patch test for 72 h and a repetitive epicutaneous test for 6 weeks, as well as tests on the influence of nanocellulose on the moistness of the skin after short-term treatment (20 min, measuring of moistness up to 12 h after treatment). The results demonstrate that the applied nanocellulose will not cause any unwanted skin reactions due to irritating, sensitizing, or early allergic effects and the moistness of the treated



Fig. 21.21 Example of cosmetic application of NanoMasque[®]. (a) Treatment of the skin, (b) microscopic structure and NanoMasque[®], (c) facial mask pack, and (d) microscopic structure and BioCellulose.

skin was significantly higher than in untreated areas proving the safe and prevalent application of these nanocellulose in the field of cosmetic treatment.

21.5.7 Nanocellulose in Veterinary Medicine

In veterinary medicine, the reports consulted about the use of biocellulose produced by the *A. xylinum* refer to applications for: conduit for isolation in reconstruction of peripheral nerves; healing of experimental wounds of bovine mammary teats; healing of experimental tegument wounds in equine and swine; prophylaxis of the formation of membrane post laminectomy in dogs; and healing of incisional experimental lesions of the cornea in dogs. Clinically, gross (brute) membrane was used in healing of natural wounds of dogs.

Biosynthesized nanocellulose membrane was utilized (Iamaguti et al. 2008) in experimental trochleoplasty in dogs and it was found that the use of this biomaterial has advantages instead of the conventional treatment for osteochondral injuries. The cellulose membrane was applied in the tissue formation of fibrocartilage ripe obtaining good integration of the newly formed tissue and the adjacent cartilage, allowing its clinical use in dogs.

The membranes were tested through a lateral parapatellar skin incision 5–7 cm, followed by incision of the retinaculum and articular capsule, until the exposure of the knee joint. With the limb in extension the patella was displaced by promoting the exposure of the femoral trochlea (Fig. 21.22a) (Iamaguti et al. 2008).

Iamaguti et al. conducted a bent knee and trochleoplasty through the deepening of the trochlear groove with the aid of gouge forceps (Fig. 21.22b). The nanocellulose membrane, the base of cellulose with 5 μm thick, was applied inside the limb of the dogs, after the deepening of the groove and fixed with 4–5 simple points separated the edge normal cartilage, with the use of synthetic absorbable suture thread 6-0 (Fig. 21.22c). The patella was repositioned after the extension of the limb, performing the synthesis of the articular capsule and retinaculum in type of points of suture, with 3-0 monofilament nylon thread (Fig. 21.22d) (Iamaguti et al. 2008). After the inclusion of the membrane, a link was obtained between the subcutaneous tissue in simple continuous pattern and skin, using 3-0 monofilament nylon, with simple stitches apart (Fig. 21.22e).

The cartilage that covers the trochlear groove is composed of chondrocytes embedded in a matrix and has the surface layer formed by flattened chondrocytes, Fig. 21.23b shows bigger quantity of chondrogenic cells than in control group (Fig. 21.23a), which demonstrates the facility produced by the cellulose membrane in the chondrogenic migration of cells. The repaired tissue that covers the region of trochleoplasty consisted of more organized tissue, with higher thickness compared to the previous period.

The nanocellulose membranes were used to repair defects of the abdominal wall in humans or animals. Nanocellulose may be used as treatment of great abdominal

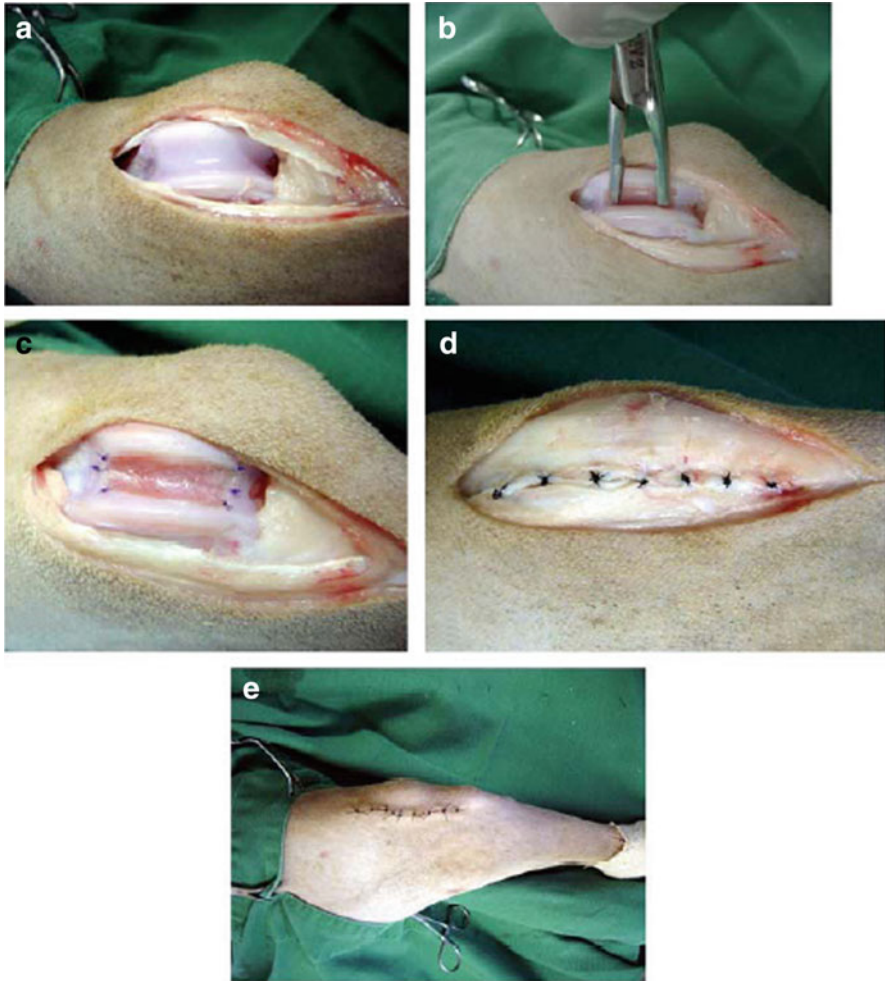


Fig. 21.22 (a) Dislocation of the patella to expose the trochlear groove, (b) deepening of the groove trochlear with the aid of gouge forceps, (c) fixing the biosynthesized cellulose membrane with 6-0 synthetic absorbable sutures, (d) suturing the joint capsule and retinaculum in type of points of suture, with 3-0 monofilament nylon thread, and (e) suture the skin with simple stitches apart

wall defects to avoid tension during repair. Falcão et al. (2008) investigated the incorporation type by host tissue of membranes of nanocellulose, produced by the bacteria and of polytetrafluoroethylene (ePTFE) in abdominal wall defects of rats (Fig. 21.24). The cellulose membrane was sutured at the level of the muscle-aponeurotic defect with Prolene[®] and continuous suture, anchored at the four angles of the rectangle. Then the skin was closed with thread of Mononylon[®] through an interrupted suture.

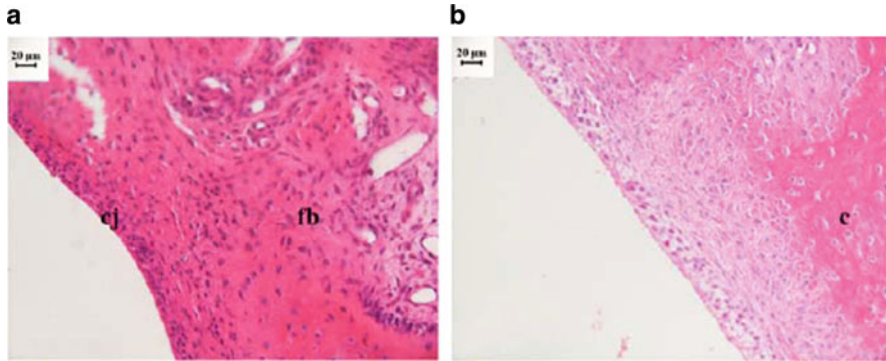


Fig. 21.23 (a) Cutting of central trochleoplasty at 60 days. Juxtaped cells (cj) in the surface region, and many fibroblasts (fb) in the region deeper; fibrosis (Magnification: 40 \times), (b) Cutting of central trochleoplasty 60 days of nanocellulose treatment. Greater number of cells shaped chondrocyte (c), vascularization and cell juxtaped less evident (Magnification: 40 \times)

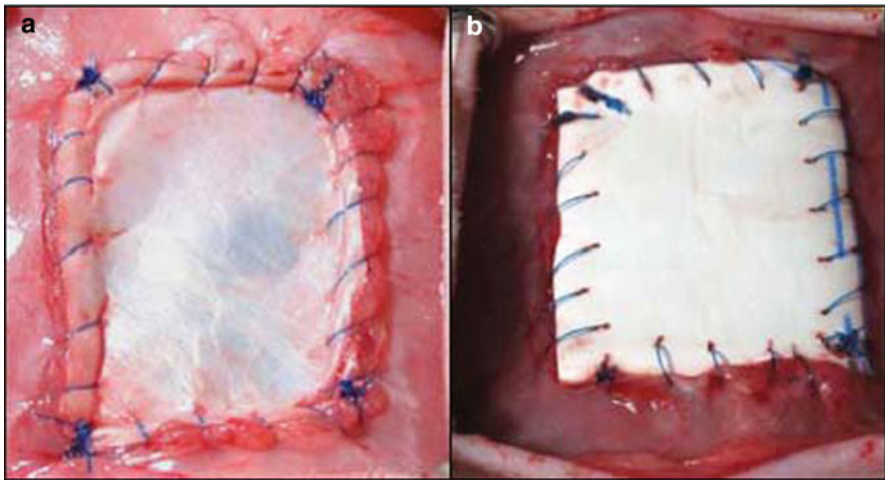


Fig. 21.24 Suture placed on microbial cellulose (a) and polytetrafluoroethylene (b) membranes

The use of nanocellulose has been suggested in different areas of medicine as substitute of blood vessels and linfatics (Yamanaka et al. 1990; Klemm et al. 2003); substitute of hollow internal organs as ureter, trachea, and digestive tract (Yamanaka et al. 1990; Klemm et al. 2003; Ono et al. 1989); cuff for reconstruction of nerves (Klemm et al. 2003); substitute of duramater (Oster et al. 2003; Damien et al. 2005); substitute of the abdominal wall, skin, subcutaneous tissue, articulation, cartilage, and reinforcement of areas of decreased resistance in the abdominal wall, esophagus, and intestinal tube (Ono et al. 1989); threads (Roberts et al. 1986); and agent for increases in soft tissue, reconstruction of the pelvic

floor, suspension of bladder, repair of hernias and patch for inguinal hernias (Oster et al. 2003). In humans, nanocellulose has been used on lesions of tegument [serious burns, skin graft (in the donor and receiving areas), facial peeling, infectious dermolysis, abrasion of tattoos, chronic ulcers], Hanseníase of the distal members (Fontana et al. 1990, 1991). Experimental studies for clinical application have been accomplished with membrane produced by the *A. xylinum* in several conditions as protective cover for reconstruction of nerves; duraplasty (Mello et al. 1997); healing of epithelial lesions of cornea; healing of duodenal lesions; substitute of blood vessels; cuffs for reconstruction of micronerves; reconstruction of the retroperitoneum; and technical training in microsurgery (Klemm et al. 2001).

21.6 Concluding Remarks

Nanocellulose is a material with unlimited applications, made from one of the most abundant natural polymer available in nature, cellulose. The biobased nanoparticles can improve the composite final properties in many aspects like thermal stability, mechanical properties, improved biological protection, toughness, barrier, electrical, etc. The nanotechnology is bringing new challenges to attend the demands for the twenty-first century: medicine, computer science, automotive, power industry, biotechnology, transportation, agriculture, packaging, military, cosmetics, and textile sectors, with intelligent fabrics.

In this chapter, different methods of isolation of nanocellulose from different cellulosic sources and methods to increase the compatibility in nanocomposites were demonstrated. The technology developed in the use of cellulose has shown big advantages in medicine because of their compatibility with the human and animal bodies. The nanocellulose as framework has great potential in some applications like it was demonstrated for the case of tissues, where the cells grow faster than conventional procedures.

There are attractive opportunities of nanocellulose application for the tissue regeneration and calcium formation, demonstrated in the case of the meniscus and in the formation of calcium in the bones through the template provided by the nanocellulose. The nanocellulose membrane is very effective in the burn treatment reducing pain, accelerating granulation, increasing the rate of healing, all of which are significant for proper wound healing. For the cosmetics, the nanocellulose has been used as a vehicle for important additives, facilitating and enhancing the absorption of cosmetic through the skin at deeper layers.

Application of traditional materials on nanoscale leads to nanomodifiers of structure that will result in new materials with new and more perfect properties; new kinds of materials with higher resistance, cheaper and lighter, definitively an edge material for the twenty-first century.

References

- Alemdar A, Sain M (2006). Biodegradable nanocomposites from wheat straw. In: Proceedings of the AIChE 2006 Annual Meeting, San Francisco, CA November 12–17
- Alemdar A, Sain M (2008) Isolation and characterization of nanofibres from agricultural residues – wheat straw and soy hulls. *Bioresour Technol* 99:1664–1671
- Alvarez O, Patel M, Booker J et al (2004) Effectiveness of a biocellulose wound dressing for the treatment of chronic venous leg ulcers: results of a single center randomized study involving 24 patients. *Wounds* 16:224–233
- Andresen M, Johansson LS, Tanem BS et al (2006) Properties and characterization of hydrophobized microfibrillated cellulose. *Cellulose* 13:665–677
- Andresen M, Stenstad P, Moretro T et al (2007) Nonleaching antimicrobial films prepared from surface-modified microfibrillated cellulose. *Biomacromolecules* 8:2149–2155
- Angle's MN, Dufresne A (2000) Plasticized starch/tunicin whiskers nanocomposites. 1. Structural analysis. *Macromolecules* 33:8344–8353
- Angle's MN, Dufresne A (2001) Plasticized starch/tunicin whiskers nanocomposites materials. 2. Mechanical behavior. *Macromolecules* 34:2921–2931
- Araki J, Wada M, Kuga S et al (1998) Flow properties of microcrystalline cellulose suspension prepared by acid treatment of native cellulose. *Colloids Surf A* 142:75–82
- Araki J, Wada M, Kuga S et al (1999) Influence of surface charge on viscosity behavior of cellulose microcrystal suspension. *J Wood Sci* 45:258–261
- Araki J, Wada M, Kuga S et al (2000) Birefringent glassy phase of a cellulose microcrystal suspension. *Langmuir* 16:2413–2415
- Araki J, Wada M, Kuga S (2001) Steric stabilization of a cellulose microcrystal suspension by poly(ethylene glycol) grafting. *Langmuir* 17:21–27
- Atalla RH, Vanderhart DL (1984) Native celluloses: a composite of two distinct crystalline forms. *Science* 223:283–285
- Auad ML, Contos VS, Nutt S et al (2008) Characterization of nanocellulose-reinforced shape memory polyurethanes. *Polym Int* 57:651–659
- Azizi Samir MAS, Alloin F, Sanchez JY et al (2004a) Preparation of cellulose whiskers reinforced nanocomposites from an organic medium suspension. *Macromolecules* 37:1386–1393
- Azizi Samir MAS, Alloin F, Paillet M et al (2004b) Tangling effect in fibrillated cellulose reinforced nanocomposites. *Macromolecules* 37:4313–4316
- Azizi Samir MAS, Mateos AM et al (2004c) Plasticized nanocomposites polymer electrolytes based on poly(oxyethylene) and cellulose whiskers. *Electrochim Acta* 49:4667–4677
- Azizi Samir MAS, Chazeau L, Alloin F et al (2005a) POE-based nanocomposite polymer electrolytes reinforced with cellulose whiskers. *Electrochim Acta* 50:3897–3903
- Azizi Samir MAS, Alloin F, Sanchez JY et al (2005b) Nanocomposite polymer electrolytes based poly(oxyethylene) and cellulose whiskers. *Polymeros: Ciência e Tecnologia* 15:109–113
- Azizi Samir MAS, Alloin F, Dufresne A (2006) High performance nanocomposite polymer electrolytes. *Compos Interface* 13:545–559
- Bai W, Holbery J, Li K (2009) A technique for production of nanocrystalline cellulose with a narrow size distribution. *Cellulose* 16:455–465
- Balasubramani M, Kumar TR, Babu M (2001) Skin substitutes: a review. *Burns* 27:534–544
- Barud HS, Barrios C, Regiani T et al (2008) Selfsupported silver nanoparticles containing bacterial cellulose membranes. *Mater Sci Eng C-Biomim Supramol Syst* 28:515–518
- Battista OA (1950) Hydrolysis and crystallization of cellulose. *Ind Eng Chem* 42:502–507
- Battista OA, Coppick S, Howsmon JA et al (1956) Level-off degree of polymerization. Relation to polyphase structure of cellulose fibres. *Ind Eng Chem* 48:333–335
- Beck-Candanedo S, Roman M, Gray DG (2005) Effect of reaction conditions on the properties and behavior of wood cellulose nanocrystal suspensions. *Biomacromolecules* 6:1048–1054

- Bendahou A, Habibi Y, Kaddami H et al (2009) Physico-chemical characterization of palm from phoenix dactylifera-1, preparation of cellulose whiskers and natural rubber-based composites. *J Biobased Mater Bioenergy* 3:81–90
- Berlioz S, Molina-Boisseau S, Nishiyama Y et al (2009) Gas-phase surface esterification of cellulose microfibrils and whiskers. *Biomacromolecules* 10:2144–2151
- Bhatnagar A, Sain M (2005) Processing of cellulose nanofibre-reinforced composites. *J Reinf Plast Compos* 24:1259–1268
- Bodin A, Bäckdahl H, Fink L et al (2007a) Influence of cultivation conditions on mechanical and morphological properties of bacterial cellulose tubes. *Biotechnol Bioeng* 97:425–434
- Bodin A, Concaro S, Britberg M et al (2007b) Bacterial cellulose as a potential meniscus implant. *J Tissue Eng Regen Med* 1:406–408
- Bondeson D, Oksman K (2007a) Dispersion and characteristics of surfactant modified cellulose whiskers nanocomposites. *Compos Interface* 14:617–630
- Bondeson D, Oksman K (2007b) Poly(lactic acid)/cellulose whisker nanocomposites modified by poly(vinyl alcohol). *Compos Part A* 38:2486–2492
- Bondeson D, Mathew A, Oksman K (2006a) Optimization of the isolation of nanocrystals from microcrystalline cellulose by acid hydrolysis. *Cellulose* 13:171–180
- Bondeson D, Kvien I, Oksman K (2006b) ACS symposium series, vol 938. American Chemical Society, Washington, DC
- Bonin C (2000) PhD Thesis, Joseph Fourier University, Grenoble, France
- Brown RM (2004) Bacterial cellulose: its potential for new products of commerce. *Abstr Pap Am Chem Soc* 227:U303–U303
- Brown EE, Laborie MPG (2007) Bioengineering bacterial cellulose/poly(ethylene oxide) nanocomposites. *Biomacromolecules* 8:3074–3081
- Bruce DM, Hobson RN, Farrent JW et al (2005) High-performance composites from low-cost plant primary cell walls. *Compos Part A Appl Sci Manuf* 36:1486–1493
- Cao X, Dong H, Li C (2007) New nanocomposite materials reinforced with flax cellulose nanocrystals in waterborne polyurethane. *Biomacromolecules* 8:899–904
- Cao X, Chen Y, Chang PR et al (2008a) Green composites reinforced with hemp nanocrystals in plasticized starch. *J Appl Polym Sci* 109:3804–3810
- Cao X, Chen Y, Chang PR et al (2008b) Starch-based nanocomposites reinforced with flax cellulose nanocrystals. *Exp Polym Lett* 2:502–510
- Cao X, Habibi Y, Lucia LAJ (2009) One-pot polymerization, surface grafting, and processing of waterborne polyurethane-cellulose nanocrystal nanocomposites. *J Mater Chem* 19:7137–7145
- Capadona JR, Shanmuganathan K, Trittschuh S et al (2009) Polymer nanocomposites with nanowhiskers isolated from microcrystalline cellulose. *Biomacromolecules* 10:712–716
- Chakraborty A, Sain M, Kortschot M (2006) “Cellulose microfibrils as reinforcing agents for structural materials”, cellulose nanocomposites: processing, characterization, and properties. *ACS Symp Ser* 938:169–86
- Chauve G, Heux L, Arouini R et al (2005) Cellulose poly(ethylene-co-vinyl acetate) nanocomposites studied by molecular modeling and mechanical spectroscopy. *Biomacromolecules* 6:2025–2031
- Chazeau L, Cavaille JY, Terech P (1990) Mechanical behaviour above T_g of a plasticized PVC reinforced with cellulose whiskers. A SANS structural study. *Polymer* 40:5333–5344
- Chazeau L, Cavaille JY, Canova G et al (1999a) Viscoelastic properties of plasticized PVC reinforced with cellulose whiskers. *J Appl Polym Sci* 71:1797–1808
- Chazeau L, Paillet M, Cavaille JY (1999b) Plasticized PVC reinforced with cellulose whiskers I. Linear viscoelastic behavior analyzed through the quasi-point defect theory. *J Polym Sci Part B: Polym Phys* 37:2151–2164
- Chazeau L, Cavaille JY, Perez J (2000) Plasticized PVC reinforced with cellulose whiskers II. Plastic behavior. *J Polym Sci Part B: Polym Phys* 38:383–392
- Chen G, Dufresne A, Huang J et al (2009) A novel thermoformable bionanocomposite based on cellulose nanocrystal-graft-poly(epsilon-caprolactone). *Macromol Mater Eng* 294:59–67

- Cheng Q, Wang SQ, Rials TG et al (2007) Physical and mechanical properties of polyvinyl alcohol and polypropylene composite materials reinforced with fibril aggregates isolated from regenerated cellulose fibres. *Cellulose* 14:593–602
- Cherian BM, Pothan LA, Nguyen-Chung T et al (2008) A novel method for the synthesis of cellulose nanofibril whiskers from banana fibres and characterization. *J Agric Food Chem* 56:5617–5627
- Cherian BM, Leão AL, Souza SF et al (2010) Isolation of nanocellulose from pineapple leaf fibres by steam explosion. *Carbohydr Polym* 81:720–725
- Choi Y, Simonsen J (2006) Cellulose nanocrystal-filled carboxymethyl cellulose nanocomposites. *J Nanosci Nanotechnol* 6:633–639
- Czaja W, Romanovicz D, Brown RM (2004) Structural investigations of microbial cellulose produced in stationary and agitated culture. *Cellulose* 11:403–411
- Czaja WK, David JY, Kawecki M et al (2007a) The future prospects of microbial cellulose in biomedical applications. *Biomacromolecules* 8:1–12
- Czaja W, Krystynowicz A, Kawecki M et al (2007) Biomedical applications of microbial cellulose in burn wound recovery. In: Brown Jr. RM, Saxena IM (eds) *Cellulose: Molecular and Structural Biology: Selected Articles on the Synthesis, Structure, and Applications of Cellulose*. Springer, Dordrecht, The Netherlands
- Dalmas F, Cavaillé JY, Gauthier C et al (2007) Viscoelastic behavior and electrical properties of flexible nanofibre filled polymer nanocomposites. Influence of processing conditions. *Compos Sci Technol* 67:829–839
- Damien C, Heather AB, Oster GA et al (2005) Dura substitute and a process for producing the same. United State Patent US20050042263A1
- de Souza Lima MM, Borsali R (2002) Static and dynamic light scattering from polyelectrolyte microcrystal cellulose. *Langmuir* 18:992–996
- Demling RH, DeSanti L (1999) Management of partial thickness facial burns (comparison of topical antibiotics and bio-engineered skin substitutes). *Burns* 25:256–261
- Dinand E, Chanzy H, Vignon MR (1996) Parenchymal cell cellulose from sugar beet pulp. *Cellulose* 3:183–188
- Dong XM, Revol JF, Gray DG (1998) Effect of microcrystallite preparation conditions on the formation of colloid crystals of cellulose. *Cellulose* 5:19–32
- Dubief D, Samain E, Dufresne A (1999) Polysaccharide microcrystals reinforced amorphous poly (beta-hydroxyoctanoate) nanocomposite materials. *Macromolecules* 32:5765–5771
- Dufresne A (2000) Dynamic mechanical analysis of the interphase in bacterial polyester/cellulose whiskers natural composites. *Compos Interface* 7:53–67
- Dufresne A (2003) Interfacial phenomena in nanocomposites based on polysaccharide nanocrystals. *Compos Interface* 10:369–387
- Dufresne AJ (2006) Comparing the mechanical properties of high performance polymer nanocomposites from biological sources. *J Nanosci Nanotechnol* 6:322–330
- Dufresne A (2008) Polysaccharide nano crystal reinforced nanocomposites. *Can J Chem* 86:484–494
- Dufresne A, Vignon M (1998) Improvement of starch film performances using cellulose microfibrils. *Macromolecules* 31:2693–2696
- Dumitriu S (2005) *Polysaccharides: structural diversity and functional versatility*. Marcel Dekker, New York
- Elazzouzi-Hafraoui S, Nishiyama Y, Putaux JL et al (2008) The shape and size distribution of crystalline nanoparticles prepared by acid hydrolysis of native cellulose. *Biomacromolecules* 9:57–65
- El-Saied H, Basta AH, Gobran RH (2004) Research progress in friendly environmental technology for the production of cellulose products (bacterial cellulose and its application). *Polym Plast Technol Eng* 43:797–820
- Falcão SC, Neto JE, Coelho ARB (2008) Incorporation by host tissue of two biomaterials used as repair of defects produced in abdominal wall of rats. *Acta Cir Bras* 23:78–83
- Favier V, Chanzy H, Cavaillé JY (1995a) Polymer nanocomposites reinforced by cellulose whiskers. *Macromolecules* 28:6365–6367

- Favier V, Canova GR, Cavaille JY et al (1995b) Nanocomposite materials from latex and cellulose whiskers. *Polym Adv Technol* 6:351–355
- Favier V, Canova GR, Shrivastava SC et al (1997) Mechanical percolation in cellulose whisker nanocomposites. *Polym Eng Sci* 37:1732–1739
- Filpponen I (2009) PhD Thesis, North Carolina State University, Raleigh, NC
- Fontana JD, Souza AM, Fontana CK et al (1990) Acetobacter cellulose pellicle as a temporary skin substitute. *Appl Biochem Biotechnol* 24–25:253–264
- Fontana JD, Franco VC, Souza SJ et al (1991) Nature of plant stimulator in the production of *Acetobacter xylinum* (“Tea Fungus”) biofilm used in therapy. *Appl Biochem Biotechnol* 28–29:341–351
- Gallin WJ, Hepperle B (1998) Burn healing in organ cultures of embryonic chicken skin: a model system. *Burns* 24:613–620
- Garcia de Rodriguez NL, Thielemans W, Dufresne A (2006) Sisal cellulose whiskers reinforced polyvinyl acetate nanocomposites. *Cellulose* 13:261–270
- Gardner DJ, Oporto GS, Mills R et al (2008) Adhesion and surface issues in cellulose and nanocellulose. *J Adhes Sci Technol* 22:545–567
- Gousse C, Chanzy H, Excoffier G et al (2002) Stable suspensions of partially silylated cellulose whiskers dispersed in organic solvents. *Polymer* 43:2645–2651
- Grande CJ, Torres FG, Gomez CM et al (2008) Morphological characterisation of bacterial cellulose–starch nanocomposites. *Polym Polym Compos* 16:181–185
- Grunnert M, Winter WT (2000) Progress in the development of cellulose reinforced nanocomposites. *Polym Mater Sci Eng* 82:232–238
- Grunnert M, Winter WT (2002) Nanocomposites of cellulose acetate butyrate reinforced with cellulose nanocrystals. *Polym Environ* 10:27–30
- Guhados G, Wan WK, Hutter JL (2005) Measurement of the elastic modulus of single bacterial cellulose fibres using atomic force microscopy. *Langmuir* 21:6642–6646
- Habibi Y, Dufresne A (2008) Highly filled bionanocomposites from functionalized polysaccharide nanocrystals. *Biomacromolecules* 9:1974–1980
- Habibi Y, Chanzy H, Vignon MR (2006) TEMPO-mediated surface oxidation of cellulose whiskers. *Cellulose* 13:679–687
- Habibi Y, Goffin AL, Schiltz N et al (2008) Bionanocomposites based on poly(epsilon-caprolactone)-grafted cellulose nanocrystals by ring-opening polymerization. *J Mater Chem* 18:5002–5010
- Håkansson H, Ahlgren P (2005) Acid hydrolysis of some industrial pulps of hydrolysis conditions and raw materials. *Cellulose* 12:177–183
- Hasani M, Cranston ED, Westmana G et al (2008) Cationic surface functionalization of cellulose nanocrystals. *Soft Mater* 4:2238–2244
- Hassan CM, Peppas NA (2000) Structure and applications of poly(vinyl alcohol) hydrogels produced by conventional crosslinking or by freezing/thawing methods. *Biopolym/PVA Hydrogels/Anionic Polym Nanocompos* 153:37–65
- Hayashi H, Shimo T (2006) Automobile outside plates with good surface smoothness from cellulose fibre prepregs. *Jpn Kokai Tokkyo Koho* 2005–136053:9
- Hayashi N, Kondo T, Ishihara M (2005) Enzymatically produced nano-ordered short elements containing cellulose I_c crystalline domains. *Carbohydr Polym* 61:191–197
- Helbert W, Cavaille JY, Dufresne A (1996) Thermoplastic nanocomposites filled with wheat straw cellulose whiskers Part I: processing and mechanical behavior. *Polym Compos* 17:604–611
- Helenius G, Bäckdahl H, Bodin A et al (2006) In vivo biocompatibility of bacterial cellulose. *J Biomed Mat Res Part A* 76:431–438
- Herrick FW, Casebier RL, Hamilton JK et al (1983) Microfibrillated cellulose: morphology and accessibility. *J Appl Polym Sci: Appl Polym Symp* 37:797–813
- Heux L, Bonini C (2000) Microfibrillated and/or microcrystalline dispersion, in particular of cellulose, in an organic solvent. International Patent WO/2000/077088
- Heux L, Chauve G, Bonini C (2000) Nonfloculating and chiral-nematic self-ordering of cellulose microcrystals suspensions in nonpolar solvents. *Langmuir* 16:8210–8212

- Hirai A, Inui O, Horii F et al (2009) Phase separation behavior in aqueous suspensions of bacterial cellulose nanocrystals prepared by sulfuric acid treatment. *Langmuir* 25:497–502
- Hofstetter K, Hinterstoisser K, Salmén L (2006) Moisture uptake in native cellulose – the roles of different hydrogen bonds: a dynamic FT-IR study using deuterium exchange. *Cellulose* 13:131–145
- Hussain F, Hojjati M, Okamoto M et al (2006) Review article: polymer–matrix nanocomposites, processing, and application: an overview. *Compos Mater* 40:1511–1575
- Hutchens SA, Benson RS, Evans BR et al (2006) Biomimetic synthesis of calcium-deficient hydroxyapatite in a natural hydrogel. *Biomaterials* 27:4661–4670
- Iamaguti LS, Brandão CVS, Minto BW et al (2008) Utilização de membrana biossintética de celulose na troclectomia experimental em cães. Avaliações clínica, radiográfica e macroscópica. *Vet e Zootec* 15:160–168
- Ifuku S, Nogi M, Abe K et al (2007) Surface modification of bacterial cellulose nanofibres for property enhancement of optically transparent composites: dependence on acetyl-group DS. *Biomacromolecules* 8:1973–1978
- Iguchi M, Yamanaka S, Budhiono A (2000) Bacterial cellulose – a masterpiece of nature's arts. *J Mater Sci* 35:261–270
- Ioelovich M, Leykin A (2004) Nano-cellulose and its applications. *Sci Israel – Technol Adv* 6:17–24
- Iwamoto S, Nakagaito AN, Yano H et al (2005) Optically transparent composites reinforced with plant fibre-based nanofibres. *Appl Phys A-Mater Sci Process* 81:1109–1112
- Iwatake A, Nogi M, Yano H (2008) Cellulose nanofibre-reinforced polylactic acid. *Compos Sci Technol* 68:2103–2106
- Janardhnan S, Sain M (2006) Isolation of cellulose microfibrils – an enzymatic approach. *Bioresources* 1:176–188
- Jiang L, Morelius E, Zhang J et al (2008) Study of the poly(3-hydroxybutyrate-co-3-hydroxyvalerate)/cellulose nanowhisker composites prepared by solution casting and melt processing. *J Compos Mater* 42:2629–2645
- Jones I, Currie L, Martin R (2002) A guide to biological skin substitutes. *Br J Plast Surg* 55:185–193
- Junior de Menezes A, Siqueira G, Curvelo AAS et al (2009) Extrusion and characterization of functionalized cellulose whiskers reinforced polyethylene nanocomposites. *Polymers* 50:4552–4563
- Juntaro J, Pommet M, Mantalaris A et al (2007) Nanocellulose enhanced interfaces in truly green unidirectional fibre reinforced composites. *Compos Interface* 14:753–762
- Juntaro J, Pommet M, Kalinka G et al (2008) Creating hierarchical structures in renewable composites by attaching bacterial cellulose onto sisal fibres. *Adv Mater* 20:3122–3126
- Kai A (1976) The fine structure of Valonia microfibril. Gel permeation chromatographic studies of Valonia cellulose. *Sen-i Gakkaishi* 32:T326–T334
- Khadem HS (1988) Carbohydrate chemistry: monosaccharides and their oligomers. Academic, New York
- Kim J, Montero G, Habibi Y et al (2009) Dispersion of cellulose crystallites by nonionic surfactants in a hydrophobic polymer matrix. *Polym Eng Sci* 49:2054–2061
- Kimura F, Kimura T, Tamura M et al (2005) Magnetic alignment of the chiral nematic phase of a cellulose microfibril suspension. *Langmuir* 21:2034–2037
- Klemm D, Philipp B, Heinze T, Heinze U, Wagenknecht W (1998) *Comprehensive cellulose chemistry*. Wiley VCH, Chichester
- Klemm D, Schumann D, Udhart U et al (2001) Bacterial synthesized cellulose – artificial blood vessels for microsurgery. *Prog Polym Sci* 26:1561–1603
- Klemm D, Udhardt U, Marsch S et al (2003) Method and device for producing shaped microbial cellulose for use as a biomaterial, especially for microsurgery. United State Patent US2003/0013163
- Klemm D, Heublein B, Fink H-P et al (2005) Cellulose: fascinating biopolymer and sustainable raw material. *Angew Chem Int Ed* 44:3358–3393

- Klemm D, Schumann D, Kramer F et al (2006) Nanocelluloses as innovative polymers in research and application. *Polysaccharides* 205:49–96
- Koch G (2006) Raw Material for Pulp. In: Sixta H (ed) *Handbook of pulp*. Wiley-VCH Verlag GmbH & Co. KGaA, Weinheim
- Koshizawa T (1960) Degradation of wood cellulose and cotton linters in phosphoric acid. *Kami Pa Gikyoshi* 14:455
- Kroonbatenburg LMJ, Kroon J, Northolt MG (1986) Chain modulus and intramolecular hydrogen-bonding in native and regenerated cellulose fibres. *Polym Commun* 27:290–292
- Kumar V (2002) Powdered/microfibrillated cellulose. WO Patent WO/2002/022172
- Latarjet J (1995) A simple guide to burn treatment. *Burns* 21:221–225
- Leitner J, Hinterstoisser B, Wastyn M et al (2007) Sugar beet cellulose nanofibril-reinforced composites. *Cellulose* 14:419–425
- Li Q, Zhou J, Zhang L (2009) Structure and properties of the nanocomposite films of chitosan reinforced with cellulose whiskers. *J Polym Sci Part B: Polym Phys* 47:1069–1077
- Lin N, Chen G, Huang J et al (2009) Effects of polymer-grafted natural nanocrystals on the structure and mechanical properties of poly(lactic acid): a case of cellulose whisker-graft-polycaprolactone. *J Appl Polym Sci* 113:3417–3425
- Ljungberg N, Bonini C, Bortolussi F et al (2005) New nanocomposite materials reinforced with cellulose whiskers in atactic polypropylene: effect of surface and dispersion characteristics. *Biomacromolecules* 6:2732–2739
- Lönnerberg H, Fogelström L, Malström E et al (2008) Microfibrillated cellulose films grafted with poly(ϵ -caprolactone) – for biocomposite applications. *Nordic Polymer Days, Stockholm*, 11–13 June
- Lu Y, Weng L, Cao X (2005) Biocomposites of plasticized starch reinforced with cellulose crystallites from cottonseed linter. *Macromol Biosci* 5:1101–1107
- Lu Y, Weng L, Cao X (2006) Morphological, thermal and mechanical properties of ramie crystallites-reinforced plasticized starch biocomposites. *Carbohydr Polym* 63:198–204
- Malainine ME, Mahrouz M, Dufresne A (2005) Thermoplastic nanocomposites based on cellulose microfibrils from *Opuntia ficus-indica* parenchyma cell. *Compos Sci Technol* 65:1520–1526
- Mangalam AP, Simonsen J, Benight AS (2009) Cellulose/DNA hybrid nanomaterials. *Biomacromolecules* 10:497–504
- Marcovich NE, Auad ML, Bellesi NE et al (2006) Cellulose micro/nanocrystals reinforced polyurethane. *J Mater Res* 21:870–881
- Mathew AP, Dufresne A (2002) Morphological investigation of nanocomposites from sorbitol plasticized starch and tunicin whiskers. *Biomacromolecules* 3:609–617
- Mathew AP, Chakraborty A, Oksman K et al (2006) The structure and mechanical properties of cellulose nanocomposites prepared by twin screw extrusion. In: Oksman K, Sain M (eds) *Cellulose nanocomposites: processing, characterization, and properties*. American Chemical Society, Washington, DC
- Matsuda Y (2000) Properties and use of microfibrillated cellulose as papermaking addition. *Sen'i Gakkaishi* 56:192
- Matsuda Y, Hirose M, Ueno K (2001) Super microfibrillated cellulose, process for producing the same, and coated paper and tinted paper using the same. US Patent 6183596
- Mattoso LHC, Medeiros ES, Baker DA et al (2009) Electrically conductive nanocomposites made from cellulose nanofibrils and polyaniline. *J Nanosci Nanotechnol* 9:2917–2922
- Mayall RC, Mayall AC, Mayall LC et al (1990) Tratamento das úlceras troficas dos membros com um novo substituto da pele. *Rev Bras Cir* 80:257–283
- Mello LR, Feltrin LT, Fontes Neto PT et al (1997) Duraplasty with biosynthetic cellulose: an experimental study. *J Neurosurg* 86:143–50
- Mohanty AK, Misra M, Hinrichsen G (2000) Biofibres, biodegradable polymers and biocomposites: an overview. *Macromol Mater Eng* 276:1–24
- Morán JI, Alvarez VA, Cyras VP et al (2008) Extraction of cellulose and preparation of nanocellulose from sisal fibres. *Cellulose* 15:149–159

- Morandi G, Heath L, Thielemans W (2009) Cellulose nanocrystals grafted with polystyrene chains through surface-initiated atom transfer radical polymerization (SI-ATRP). *Langmuir* 25:8280–8286
- Nakagaito AN, Yano H (2004) The effect of morphological changes from pulp fibre towards nano-scale fibrillated cellulose on the mechanical properties of high-strength plant fibre based composites. *Appl Phys A* 78:547–552
- Nakagaito AN, Yano H (2005) Novel high-strength biocomposites based on microfibrillated cellulose having nano-order-unit web-like network structure. *Appl Phys A Mater* 80: 155–159
- Nakagaito AN, Yano H (2008) Toughness enhancement of cellulose nanocomposites by alkali treatment of the reinforcing cellulose nanofibres. *Cellulose* 15:323–331
- Nakagaito AN, Iwamoto S, Yano H (2005) Bacterial cellulose: the ultimate nano-scalar cellulose morphology for the production of high-strength composites. *Appl Phys A Mat Mater Sci Process* 80:93–97
- Nishino T, Takano K, Nakamae K (1995) Elastic modulus of the crystalline regions of cellulose polymorphs. *J Polym Sci Part B* 33:1647–1651
- Nishiyama Y, Langan P, Chanzy H (2002) Crystal structure and hydrogen-bonding system in cellulose I β from synchrotron X-ray and neutron fibre diffraction. *J Am Chem Soc* 124:9074–9082
- Nishiyama Y, Sugiyama J, Chanzy H et al (2003a) Crystal structure and hydrogen bonding system in cellulose I α from synchrotron X-ray and neutron fibre diffraction. *J Am Chem Soc* 125:14300–14306
- Nishiyama Y, Kim UJ, Kim DY et al (2003b) Periodic disorder along ramie cellulose microfibrils. *Biomacromolecules* 4:1013–1017
- Nogi M, Yano H (2008) Transparent nanocomposites based on cellulose produced by bacteria offer potential innovation in the electronics device industry. *Adv Mater* 20:1849–1852
- Nogi M, Yano H (2009) Optically transparent nanofibre sheets by deposition of transparent materials: a concept for roll-to-roll processing. *Appl Phys Lett* 94:1–3
- Nogi M, Handa K, Nakagaito AN et al (2005) Optically transparent bionanofibre composites with low sensitivity to refractive index of the polymer matrix. *Appl Phys Lett* 87:1–3
- Nogi M, Abe K, Handa K et al (2006a) Property enhancement of optically transparent bionanofibre composites by acetylation. *Appl Phys Lett* 89:1–3
- Nogi M, Ifuku S, Abe K et al (2006b) Fibre-content dependency of the optical transparency and thermal expansion of bacterial nanofibre reinforced composites. *Appl Phys Lett* 88:1–3
- Nogi M, Iwamoto S, Nakagaito AN et al (2009) Optically transparent nanofibre paper. *Adv Mater* 21:1595–1598
- Noorani S, Simonsen J, Atre S (2006) In cellulose nanocomposites: processing, characterization and properties. In: Oksman K, Sain M (eds) ACS symposium series, vol 938. American Chemical Society, Washington, DC
- Novaes AB, Novaes AB (1997) Soft tissue management for primary closure in guided bone regeneration: surgical technique and case report. *Int J Oral Maxillofac Implants* 12:84–87
- Novaes AB Jr, Marcaccini AM, Souza SL et al (2003) Immediate placement of implants into periodontally infected sites in dogs: a histomorphometric study of bone-implant contact. *Int J Oral Maxillofac Implants* 18:391–398
- Nyström G, Mihranyan A, Razaq A et al (2010) A nanocellulose polypyrrole composite based on microfibrillated cellulose from wood. *J Phys Chem B* 114:4178–4182
- Okahisa Y, Yoshida A, Miyaguchi S et al (2009) Optically transparent wood-cellulose nanocomposite as a base substrate for flexible organic light-emitting diode displays. *Compos Sci Technol* 69:1958–1961
- Okubo K, Fujii T, Yamashita N (2005) Improvement of interfacial adhesion in bamboo polymer composite enhanced with micro-fibrillated cellulose. *JSME Int J Series A-Solid Mech Mater Eng* 48:199–204

- Okubo K, Fujii T, Thostenson ET (2009) Multi-scale hybrid biocomposite: processing and mechanical characterization of bamboo fibre reinforced PLA with microfibrillated cellulose. *Compos Part A-Appl Sci Manuf* 40:469–475
- Ono E, Watabe O, Yamanaka S (1989) Substitution material for living body texture. Japanese Patent JP03165774A2
- Oster GA, Lentz Y, Koehler K et al (2003) Xylus Corporation, assignee. Solvent dehydrated microbially-derived cellulose for in vivo implantation. United State Patent US6599518
- Pääkkö M, Ankerfors M, Kosonen H et al (2007) Enzymatic hydrolysis combined with mechanical shearing and high-pressure. *Biomacromolecules* 8:1934–1941
- Paillet M, Dufresne A (2001) Chitin whisker reinforced thermoplastic nanocomposites. *Macromolecules* 34:6527–6530
- Paralakar AS, Simonsen J, Lombardi J (2008) Poly(vinyl alcohol)/cellulose nanocrystal barrier membranes. *J Membr Sci* 320:248–258
- Petersson L, Kvien I, Oksman K (2007) Structure and thermal properties of poly (lactic acid)/cellulose whiskers nanocomposite materials. *Compos Sci Technol* 67:2535–2544
- Petersson L, Mathew AP, Oksman K (2009) Dispersion and properties of cellulose nanowhiskers and layered silicates in cellulose acetate butyrate nanocomposites. *J Appl Polym Sci* 112: 2001–2009
- Podsiadlo P, Sui L, Elkasabi Y et al (2007) Layer-by-layer assembled films of cellulose nanowires with antireflective properties. *Langmuir* 23:7901–7906
- Pranger L, Tannenbaum R (2008) Biobased nanocomposites prepared by in situ polymerization of furfuryl alcohol with cellulose whiskers or montmorillonite clay. *Macromolecules* 41: 8682–8687
- Prasanna M, Mishra P, Thomas C (2004) Delayed primary closure of the burn wounds. *Burns* 30:169–175
- Pu YQ, Zhang JG, Elder T et al (2007) Investigation into nanocellulosics versus acacia reinforced acrylic films. *Compos Part B Eng* 38:360–366
- Qi H, Cai J, Zhang L et al (2009) Properties of films composed of cellulose nanowhiskers and a cellulose matrix regenerated from alkali/urea solution. *Biomacromolecules* 10:1597–1602
- Quinn KJ, Courtney JM, Evans JH et al (1985) Principles of burn dressings. *Biomaterials* 6:369–377
- Reddy N, Yang Y (2005) Biofibres from agricultural by products for industrial applications. *Trends Biotechnol* 23:22–27
- Revol JF, Bradford H, Giasson J et al (1992) Helicoidal self-ordering of cellulose microfibrils in aqueous suspension. *Int J Biol Macromol* 14:170–172
- Roberts EM, Hardison LK, Brown Jr. RM (1986) Production of Microbial Cellulose. European Patent No. 0186495
- Rojas OJ, Montero GA, Habibi YJ (2009) Electrospun nanocomposites from polystyrene loaded with cellulose nanowhiskers. *Appl Polym Sci* 113:927–935
- Roman M, Winter WT (2004) Effect of sulfate groups from sulfuric acid hydrolysis on the thermal degradation behavior of bacterial cellulose. *Biomacromolecules* 5:1671–1677
- Roman M, Winter WT (2006) Cellulose nanocomposites: processing, characterization, and properties. In: Oksman K, Sain M (eds) ACS symposium series 938. American Chemical Society, Washington, DC
- Roohani M, Habibi Y, Belgacem NM et al (2008) Cellulose whiskers reinforced polyvinyl alcohol copolymers nanocomposites. *Eur Polym J* 44:2489–2498
- Ruiz MM, Cavaille JY, Dufresne A et al (2000) Processing and characterization of new thermoset nanocomposites based on cellulose whiskers. *Compos Interface* 7:117–131
- Ruiz MM, Cavaille JY, Dufresne A et al (2001) New waterborne epoxy coatings based on cellulose nanofillers. *Macromol Symp* 16:211–222
- Saito T, Nishiyama Y, Putaux JL et al (2006) Homogeneous suspensions of individualized microfibrils from TEMPO-catalyzed oxidation of native cellulose. *Biomacromolecules* 7:1687–1691

- Saito T, Kimura S, Nishiyama Y et al (2007) Cellulose nanofibres prepared by TEMPO-mediated oxidation of native cellulose. *Biomacromolecules* 8:2485–2491
- Saito T, Hirota M, Tamura N et al (2009) Individualization of nano-sized plant cellulose fibrils by direct surface carboxylation using TEMPO catalyst under neutral conditions. *Biomacromolecules* 10:1992–1996
- Samir MASA, Alloin F, Dufresne A (2005) Review of recent research into cellulosic whiskers, their properties and their application in nanocomposite field. Review. *Biomacromolecules* 6:612–626
- Sanchavanakit N, Sangrungraungroj W, Kaomongkolgit R et al (2006) Growth of human keratinocytes and fibroblasts on bacterial cellulose film. *Biotechnol Prog* 22:1194–1199
- Schroers M, Kokil A, Weder C (2004) Solid polymer electrolytes based on nanocomposites of ethylene oxide-epichlorohydrin copolymers and cellulose whiskers. *J Appl Polym Sci* 93:2883–2888
- Schumann DA, Wippermann J, Klemm DO et al (2009) Artificial vascular implants from bacterial cellulose: preliminary results of small arterial substitutes. *Cellulose* 16:877–885
- Seydibeyoglu MO, Oksman K (2008) Novel nanocomposites based on polyurethane and microfibrillated cellulose. *Compos Sci Technol* 68:908–914
- Shoda M, Sugano Y (2005) Recent advances in bacterial cellulose production. *Biotechnol Bioprocess Eng* 10:1–8
- Siqueira G, Bras J, Dufresne A (2009) Cellulose whiskers versus microfibrils: influence of the nature of the nanoparticle and its surface functionalization on the thermal and mechanical properties of nanocomposites. *Biomacromolecules* 10:425–432
- Souza LMM, Borsali R (2004) Rod like cellulose microcrystals: structure, properties, and applications. *Macromol Rapid Commun* 25:771–787
- Suryanegara L, Nakagaito AN, Yano H (2009) The effect of crystallization of PLA on the thermal and mechanical properties of microfibrillated cellulose-reinforced PLA composites. *Compos Sci Technol* 69:1187–1192
- Teixeira EM, Corrêa AC, Manzoli A et al (2010) Cellulose nanofibres from white and naturally colored cotton fibres. *Cellulose* 17:595–606
- Terech P, Chazeau L, Cavaille JY (1999) A small-angle scattering study of cellulose whiskers in aqueous suspensions. *Macromolecules* 32:1872–1875
- Thomas H, Heine E, Wollseifen R et al (2005) Nanofibres from natural and inorganic polymers via electrospinning. *Int Nonwovens J* 14:18
- Tobushi H, Hara H, Yamada E et al (1996a) Thermomechanical properties in a thin film of shape memory polymer of polyurethane series. *Smart Mater Struct* 5:483–491
- Tobushi H, Hayashi S, Ikai A et al (1996b) Thermomechanical properties of shape memory polymers of polyurethane series and their applications. *J de Phys IV* 6:377–384
- Tokoh C, Takabe K, Sugiyama J et al (2002a) Cp/MAS 13c NMR and electron diffraction study of bacterial cellulose structure affected by cell wall polysaccharides. *Cellulose* 9:351–360
- Tokoh C, Takabe K, Fujita M (2002b) Cellulose synthesized by *Acetobacter xylinum* in the presence of plant cell wall polysaccharides. *Cellulose* 9:65–74
- Turbak AF, Snyder FW, Sandberg KR (1983) Microfibrillated cellulose, a new cellulose product: properties, uses, and commercial potential. *J Appl Polym Sci: Appl Polym Symp* 37:815–827
- Van den Berg O, Capadona JR, Weder C (2007a) Preparation of homogeneous dispersions of tunicate cellulose whiskers in organic solvents. *Biomacromolecules* 8:1353–1357
- Van den Berg O, Schroeter M, Capadona JR et al (2007b) Nanocomposites based on cellulose whiskers and (semi)conducting conjugated polymers. *J Mater Chem* 17:2746–2753
- Vignon MR, Montanari S, Habibi Y (2004) Crystalline polysaccharide derivatives in the form of water-insoluble aggregates of microcrystals, for use e.g. as viscosity modifiers or super-absorbers, manufactured by controlled oxidation of primary alcohol groups. Centre National de la Recherche Scientifique (CNRS), France, FR 2003/5195

- Wågberg L, Decher G, Norgren M et al (2008) The build up of polyelectrolyte multilayers of microfibrillated cellulose and cationic polyelectrolytes. *Langmuir* 24:784–795
- Wan WK, Hutter JL, Millon LE et al (2006) Bacterial cellulose and its nanocomposites for biomedical applications. In: Oksman K, Sain M (eds) *Cellulose nanocomposites. Processing characterization and properties*. American Chemical Society, Washington, DC
- Wang B, Sain M (2007a) Dispersion of soybean stock-based nanofibre in a plastic matrix. *Polym Int* 56:538–546
- Wang B, Sain M (2007b) Isolation of nanofibres from soybean source and their reinforcing capability on synthetic polymers. *Compos Sci Technol* 67:2521–2527
- Wang B, Sain M (2007c) The effect of chemically coated nanofibre reinforcement on biopolymer based nanocomposites. *Bioresources* 2:371–388
- Wang Y, Cao X, Zhang L (2006) Effects of cellulose whiskers on properties of soy protein thermoplastics. *Macromol Biosci* 6:524–531
- Wang N, Ding E, Cheng R (2007a) Thermal degradation behaviors of spherical cellulose nanocrystals with sulfate groups. *Polymer* 48:3486–3493
- Wang B, Sain M, Oksman K (2007b) Study of structural morphology of hemp fibre from the micro to the nanoscale. *Appl Compos Mater* 14:89–103
- Wang N, Ding E, Cheng R (2008) Preparation and liquid crystalline properties of spherical cellulose nanocrystals. *Langmuir* 24:5–8
- Whitesides GM (2005) Nanoscience, nanotechnology, and chemistry. *Small* 1:172–179
- Yachi T, Hayashi J, Takai M et al (1983) Supermolecular structure of cellulose: stepwise decrease in LODP and particle size of cellulose hydrolyzed after chemical treatment. *J Appl Polym Sci Appl Polym Symp* 37:325–343
- Yamanaka S, Ono E, Watanabe K et al (1990) Hollow microbial cellulose, process for preparation thereof, and artificial blood vessel formed of said cellulose. European Patent EP0396344A2
- Yano H, Nakahara S (2004) Bio-composites produced from plant microfibril bundles with a nanometer unit web-like network. *J Mater Sci* 39:1635–1638
- Yano H, Sugiyama J, Nakagaito AN et al (2005) Optically transparent composites reinforced with networks of bacterial nanofibres. *Adv Mater* 17:153–155
- Yi J, Xu Q, Zhang X et al (2008) Chiral-nematic self-ordering of rodlike cellulose nanocrystals grafted with poly(styrene) in both thermotropic and lyotropic states. *Polymer* 49:4406–4412
- Yuan XP, Ding EY (2006) Synthesis and characterization of storage energy materials prepared from nano-crystalline cellulose polyethylene glycol. *Chin Chem Let* 17:1129–1132
- Yuan H, Nishiyama Y, Wada M et al (2006) Surface acylation of cellulose whiskers by drying aqueous emulsion. *Biomacromolecules* 7:696–700
- Zhang JG, Elder TJ, Pu YQ et al (2007) Facile synthesis of spherical cellulose nanoparticles. *Carbohydr Polym* 69:607–611
- Zhang J, Jiang N, Dang Z et al (2008) Oxidation and sulfonation of cellulose. *Cellulose* 15:489–496
- Zhao B, Brittain WJ (2000) Polymer brushes: surface-immobilized macromolecules. *Prog Polym Sci* 25:677–710
- Zhou Q, Brumer H, Teeri TT (2009) Self-organization of cellulose nanocrystals adsorbed with xyloglucan oligosaccharide-poly(ethylene glycol)-polystyrene triblock copolymer. *Macromolecules* 42:5430–5432
- Zimmermann T, Pohler E, Geiger T (2004) Cellulose fibrils for polymer reinforcement. *Adv Eng Mater* 6:754–761
- Zoppe J, Habibi, Y, Efimenko K et al (2009) ATRP modification of nanocellulose substrates, *Abstr Pap ACS Natl Meet* 237: Cell-46
- Zuluaga R, Putaux JL, Restrepo A et al (2007) Cellulose microfibrils from banana farming residues: isolation and characterization. *Cellulose* 14:585–592
- Zuluaga R, Putaux JL, Cruz J et al (2009) Cellulose microfibrils from banana rachis: effect of alkaline treatments on structural and morphological features. *Carbohydr Polym* 76:51–59

Chapter 22

Sisal Fiber Based Polymer Composites and Their Applications

Mohini Saxena, Asokan Pappu, Ruhi Haque, and Anusha Sharma

Abstract The natural resources of the World are depleting very fast due to the high rate of exploitation and low rate of restoration, leading to an increase in global warming and pollution hazards. In recent years, there has been increasing interest in the substitution of synthetic fibers in reinforced plastic composites by natural plant fibers such as jute, coir, flax, hemp, and sisal. Sisal is one of the natural fibers widely available in most parts of the world; it requires minimum financial input and maintenance for cultivation and is often grown in wastelands, which helps in soil conservation. Advantages of sisal fiber are: low density and high specific strength, biodegradable and renewable resource, and it provides thermal and acoustic insulation. Sisal fiber is better than other natural fibers such as jute in many ways, including its higher strength, bright shiny color, large staple length, poor crimp property, variation in properties and quality due to the growing conditions, limited maximum processing temperatures. In recent years, there has been an increasing interest in finding innovative applications for sisal fiber-reinforced composites other than their traditional use in making ropes, mats, carpets, handicrafts, and other fancy articles. Composites made of sisal fibers are green materials and do not consume much energy for their production.

The characteristics of composites depend on different parameters such as extraction of fiber, surface modification and the synthesis of composites. During synthesis, fiber length, orientation, concentration, dispersion, aspect ratios, selection of matrix, and chemistry of matrix have to be considered to achieve the required strength. Inorganic fibers have several disadvantages, including their nonbiodegradability, the abrasion in processing equipments, high cost and density, and the health problems caused to workers during processing and handling. Commonly used composites, these days are, glass, aramid, carbon, and asbestos fibers filled in thermoplastic, thermoset, or cement composites. Yet natural fiber composites with equivalent characteristics to synthetic fibre composites are not

M. Saxena (✉)

Building Materials Development Group, Advanced Materials and Processes Research Institute (AMPRI), CSIR, HabibGanj Naka, 462064, Bhopal, India
e-mail: mohinisaxena@yahoo.com; saxenamohini@hotmail.com

available. Most of the plant fibers are hydrophilic in nature and water absorption may be very high. This may be controlled by different methods of interfacial surface modification. Because of the low density and high specific strength and modulus. Sisal fiber is a potential resource material for various engineering applications in the electrical industry, automobiles, railways, building materials, geotextiles, defense and in the packaging industry. Present chapter discuss about the research work on sisal cultivation, fiber extraction, processing, sisal fiber characteristics, and the use of sisal fiber in thermoplastic and thermoset polymer composites for various engineering applications.

Keywords Characterization · Chemical treatment · Engineering applications · Fibre extraction · Sisal fibre · Surface modification · Thermoset and thermoplastic composites

Contents

22.1	Introduction	592
22.2	Sisal Fiber Plant	592
22.2.1	Variety, Availability, Volume and Yield	593
22.2.2	Cultivation and Harvesting	594
22.2.3	Fiber Extractions and Processing	598
22.3	Sisal Fiber Composition, Structure and Properties	600
22.3.1	Composition	600
22.3.2	Structure	600
22.3.3	Properties	601
22.4	Fiber Surface Modification Methods	601
22.4.1	Physical Methods of Modification	602
22.4.1	Chemical Methods of Modification	603
22.4.2	Physico-Chemical and Mechanical Properties of Sisal Fiber and Its Comparison with Other Natural Fiber	611
22.5	Sisal Fiber Reinforced Polymer Composite	617
22.5.1	Natural Fiber Reinforced Polymer Composite	617
22.5.2	Fiber Matrix Adhesion in Natural Fiber Reinforced Polymer Composite ...	617
22.5.3	Making of Sisal Fiber Reinforced Polymer Composite	618
22.6	Application of Sisal Fiber-based Composites	637
22.6.1	Applications of Sisal Fiber Composites in Building Materials	638
22.6.2	Automotive Applications of Sisal Fiber	644
22.6.3	Electrical Application of Sisal Fiber	647
22.6.4	Application of Sisal Fiber in Railways	648
22.6.5	Application of Sisal Fiber in Geotextiles	648
22.6.6	Defense Applications of Sisal Fiber	649
22.6.7	Application of Sisal Fiber in Packaging Industry	649
22.6.8	Other Applications of Sisal Fiber	649
22.7	Conclusions and Future Prospects	651
	References	653

Abbreviations

AMPRI	Advanced Materials and Processes Research Institute
Aq	Aqueous
BMC	Bulk Molding Compound
BPO	Benzoyl Peroxide
CBRI	Central Building Research Institute
CRIJAF	Central Research Institute for Jute and Allied Fibers
CSIR	Council of Scientific and Industrial Research
DSC	Differential Scanning Calorimetry
DTA	Differential Thermal Analyser
DCP	Dicumyl Peroxide
FSP	Fiber Saturation Point
GCL	Geosynthetic Clay Liners
HDPE	High Density Polyethylene
HC ₅	Hostaprim
L	Longitudinal
LS	Longitudinal Section
LDPE	Low Density Polyethylene
IPIRTI	Indian Plywood Industries Research and Training Institute
MA-g-PP	Maleic Anhydride-Grafting Polypropylene
MAPP	Maleic Anhydride Polypropylene
MMA	Methylmethacrylate
NIRJAFT	National Institute of Research on Jute and Allied Fiber Technology
PE	Polyethylene
PEEK	Polyether Ether Ketone
PP	Polypropylene
PS	Polystyrene
PVC	Polyvinyl Chloride
R	Randomly
R&D	Research and Development
RTM	Resin Transfer Molding
SEM	Scanning Electron Microscope
TGA	Thermal Gravimetric Analysis
TIFAC	Technology Information, Forecasting and Assessment Council
TPA	Tons Per Annum
UFR	Urea-Formaldehyde Resin
UNIDO	United Nation Industrial Development Organization

22.1 Introduction

Natural fibers are classified based on their origins, whether they are plant, animal or mineral fibers. All plant fibers are composed of cellulose while animal fibers consist of proteins (hair, silk, and wool). Plant fibers include bast (or stem or soft sclerenchyma) fibers, leaf or hard fibers, seed, fruit, wood, cereal straw, and other grass fibers [1]. Over the last few years, a number of researchers have been involved in investigating the exploitation of natural fibers as load bearing constituents in composite materials. The use of such materials in composites has increased due to their relative cheapness, their ability to be recycled, and because they can compete well in terms of strength per weight of material [2]. Provided below is the classification of natural fibers based on origin:

- Vegetable (Cellulose) fiber: Fibers obtained from various parts of plants are known as vegetable fibers. These fibers are classified as (a) bast or stem fibers, (b) leaf fiber, and (c) fruit fiber
- Bast fibers: flax, hemp, jute, and ramie which are obtained from the bast tissue of bark
- Leaf fibers: sisal, pineapple, banana, and henequen obtained from the leaves
- Seed hair fibers: cotton, kapok, and coir which are obtained from seeds and the inner wall of fruits
- Animal (Protein) fiber: wool, silk
- Mineral (Asbestos) fiber

22.2 Sisal Fiber Plant

The sisal plant is shown in Fig. 22.1. Sisal fiber is a very strong and important leaf fiber [3]. It is extracted from the leaves of the sisal plant (*Agave sisalana*) and is very hard [5].



Fig. 22.1 Sisal plant

22.2.1 Variety, Availability, Volume and Yield

Variety

Sisal fibers are mainly obtained from *Agave sisalana*, which belongs to the genus *Agave* of the family of *Agavaceae* in which there are also other species such as *A. cantala*, *A. veracruz*, *A. americana*, *A. angustifolia*, *A. foucroydes*.

Availability

In India, sisal plant is not cultivated in an organized way; it is mostly grown on embankments, bunds, and roadsides, serving the purpose of soil conservation and for protection as hedge plantation. They are not optimally utilized and commercially exploited.

The sisal plant was introduced into East Africa (Tanganyika now Tanzania) in 1893 by Dr. Richard Hindorf. However, it originated in Central America, confined particularly to a zone between latitudes 10° and 25°N mainly in Mexico. Brazil is the largest world producer of sisal fiber. The Portuguese introduced sisal fiber in India around 1825. Sisal is the only crop that resists the semi arid climate and which is economically feasible in the unfertile and wasteland regions of the country.

Sisal is usually planted on the bunds or along the cattle proof trench-cum-mound structures for the basic purpose of either soil conservation or protection of the forested/cultivated lands against predatory animals or both. Sisal plants in India can be found mainly in the states of Orissa, Madhya Pradesh, Chhattisgarh, Andhra Pradesh, Bihar, Jharkhand, Maharashtra, Karnataka, and Tamilnadu [6]. In India, sisal is called *Ketki* and *RamBaan* in Hindi. A high yielding sisal hybrid *Bamrabum* was introduced in 1985 in all the sisal growing tracts of India by the Sisal Research Station of CRIJAF, Bamra (Near Sambalpur), Orissa.

Worldwide, there are more than 275 agaves present in different continents. Other agaves apart from *Agave Sisalana* prevalent in India include *Agave vera-cruz* (Elephant aloe, Gray aloe, and Railway aloe), *Agave cantala* (Maguey, Cantala/Cantula, Bombay aloe), *Agave fourcryodes* (Henequen, Mexican sisal), *Agave augustifolia* (Dwarf aoe), *Agave americana* (Century plant, American aloe), and *Agave mexicana*. Each of these species yields fiber of varying nature and properties.

Volume

Sisal is the sixth most commonly produced fiber globally and accounts for 2% of the world's plant fiber production [7]. According to the year 2007 data, the major sisal producers are [153]

Brazil – 130,000 tons
Mexico – 45,000 tons
China – 40,000 tons
Tanzania – 37,000 tons
Kenya – 27,000 tons
Madagascar – 15,000 tons

Other producers of sisal fiber include South Africa, Mozambique, Haiti, Venezuela, and Cuba.

Yield

Sisal plant produces 200–250 commercially usable leaves during its life cycle. The dried fiber represents only 4% of the total weight of the leaf. The dry fiber yield of the sisal plant varies between 2.5 and 4.0 ton/ha depending upon the plant population and management practices. Fibers (*Agave sisalana*) are extracted from the sisal plant leaves in the form of long fiber bundles called technical fibers [8]. The sisal leaf has a sandwich structure. Each leaf contains approximately 700–1,400 technical fibers with a length of 0.5–1 m. Every technical fiber contains numerous individual fibers about 3–8 mm in length and 10–30 mm in diameter [8, 9] and the total sisal leaf mass contains 2–4% technical fibers [150].

22.2.2 Cultivation and Harvesting

Sisal Propagation Mechanism

Sisal is a monocarpic perennial plant that produces a terminal tight rosette of narrow tapering spine after 6–9 years before it poles (flowers) and subsequently dies. Bulbils form on the elongated flowering inflorescence and when they become full-sized, they generally fall off. On average, a sisal plant generates 500–2,000 bulbils. These bulbils are collected and grown in nurseries. Sisal also produces suckers, which can be used for propagation. Suckers that begin to emerge from the second year of planting can be dug out and removed to be raised in a nursery [10, 11].

Sisal Nursery Raising

Sisal bulbils are raised in nursery beds with a spacing of about 25×25 cm². Bulbils may be preferred over suckers for planting. Bulbils or suckers can be collected about 6–8 months prior to the planting. The growth of bulbils is improved by mulching sisal nurseries with grass, paper or polythene. The sisal nursery needs

irrigation throughout and weeding in nursery beds as necessary. The nursery incubation period is about 8 months depending upon the growth and vigor of the bulbils/suckers. The area of nursery to main plantation field may be approximately 1:10. Before plantation, the roots should be trimmed slightly and the withered leaves pulled off. Avoid plants with a damaged bole; it may pose the risk of rot.

The size of bulbils or suckers should be 40–50 cm in length and weigh about 600–1,000 g at the time of planting. Reliable quality sisal plantation materials (bulbils/suckers/plants) in India can be obtained on prior request from the Sisal Research Station of CRIJAF, Bamra (Near Sambalpur), Orissa, India [10, 11].

Sisal Growth and Climate Suitability

The sisal plant is drought resistant and tolerant of a variety of soils and climates, hence can flourish even in the arid and semiarid regions and subhumid tracts covering major parts of India. The sisal plant prefers well-drained and aerated soils because it is extremely sensitive to water logging and intolerant to marshy lands. Sisal can thrive in prolonged drought conditions and can survive at a low annual rainfall of 40–300 cm also. Sisal can withstand temperatures up to 40–50°C [12].

Land Preparation

Like any other plantation crop, proper land preparation is essential for commercial sisal plantations, where crops are planted in rows with a specified plant-to-plant distance. Land clearance, removal of boulders and rubble, ploughing of land, and digging out pits are the basic requirements of such plantations. Soil conservation contour bunds or field bunds can be utilized for sisal plantations with the excavated soil serving as support. Placing the excavated soil along cattle proof trenches can also serve as support to sisal plants. Arrangement of lines should be kept across the soil slopes and as parallel to contours as possible for effective soil and water conservation and better survival of sisal plants.

Sisal Spacing and Plantation

The right time for sisal planting is 20–30 days ahead of the rainy season. Sisal plantation can be done either in single rows or in double rows. A spacing of $2 \times 1 \text{ m}^2$ corresponding to 5,000 plants/ha in a single row system is convenient and economical. The grown bulbils can be planted in the main field at the rate of 5,000 plants/ha with a double row system ($1 \times 2 \times 1 \text{ m}^3$), where spacing of plant to plant is 1 m and row to row is 2 m. The most suitable spacing suggested is $2.5 \text{ m} + (1 \times 1 \text{ m}^2)$ and $3.0 \text{ m} + (1 \times 0.8 \text{ m}^2)$, which gives about 5,700 and 6,250 plants/ha respectively. The depth of plantation may be kept at 6–8 cm and enough care should

be taken to ensure that the base of the spike is not buried in the soil; this will prevent rotting. Irrigation to the transplanted sisal saplings is essential if a severe and prolonged drought follows immediately after transplantation. About 2–3% of the total sisal planted should be available for gap filling in the event of initial mortality.

Intercropping

Intercropping can be done safely in the initial 2 years of the establishment of sisal plantations. Rainfed crops such as fodders, horse gram (kulthi, *Macrotyloma uniflorum*), castor (erandi, *Ricinus communis*), jowar (*Sorghum Bicolor*), bajra (*Pennisetum glaucum*) etc. can be raised as intercrops. Wherever irrigation water is unavailable, crop like beans (*Phaseolus coccineus* L), soybean (*Glycine max*), moong (*Vigna radiata*), urad (*Vigna mungo*), groundnut (*Arachis hypogaea*), etc. can be raised in the rabi season. The extent of intercropping in subsequent seasons depends on the growth of the sisal plants and their lateral spread. It is not advisable to raise water-intensive crops such as paddy, sugarcane, etc. that may cause drainage problems.

Fertilizers and Manuring

Under normal conditions, sisal does not require commercial fertilizers. But sisal responds very well to nitrogen, phosphorus, and potassium. In general, an application of 60–100 kg nitrogen, 30–35 kg phosphorus, and 60–100 kg potassium per ha per year is recommended.

Irrigation and Drainage

Sisal plantations require moderate irrigation in the first year immediately after plantation for proper establishment in case of severe drought or if the rains are interspersed with prolonged dry periods. Once established, sisal plantations do not require irrigation. However, irrigation in the winter and summer is beneficial for the growth of the plants and fetches healthy leaves of proportionately higher quantity.

Sisal plantations may not tolerate water logging and hence require proper drainage during continuous heavy rains and floods. Hence sisal plantations are established on the upper side of bunds and provision should be made for drainage of the entire field.

Weed Control

Removal of weeds and obnoxious plants, especially during the initial stage of plant growth, is advised as weeds compete for survival with sisal. Excessive weed

competition leads to pale sisal due to nutrient deficiency. Hand weeding may be done depending upon the intensity of weed infestation and growth.

Harvesting of Sisal Leaves

The sisal plant normally yields up to 100 leaves and is ready for harvest after 2–3 years of planting. A sisal leaf is considered to be mature for harvest when it attains a length of about 1.0 m and forms an angle of about 60° with the main spike or when the color of the terminal spine changes to ash brown. A typical sisal plant yields 200–250 effective leaves in its lifetime in a period of about 10 years. Each sisal leaf contains 1,000–1,200 fibers. The plant matures fully after 3–4 years of growth.

A straight knife with a wooden handle is generally used to cut sisal leaves. It is better to nip the terminal spines before cutting the leaves. Harvesting should be initiated always from the lowermost whorls to the upper side; about 25 leaves are spared after the first cut and about 20 leaves at each subsequent cut. Where growth is unsatisfactory, more leaves are left after each cut. Each leaf is cut at a point about 3 cm from the bole through the upper part of its bulbous base, or just below the neck. Depending upon the growth, vigor, and maturity of the leaves, 2–3 cuttings per year may be undertaken. Care should be taken to avoid excessive cutting of the plants.

After cutting, the spike at the tip of the leaf is removed and leaves are bundled for transportation to the decortication site. This must be carried out as soon as possible since the cut leaves soon deteriorate if left exposed to the sun and decortication will become difficult. Sisal plantations in India yield about 2.5 ton dry fiber per hectare per year, with an annual net profit of Rs. 45,000 per ha. The fiber is usually obtained from sisal leaves by decortication in a machine called Raspador. The lustrous strands, usually creamy white, average from 80 to 120 cm in length and 0.2–0.5 mm in diameter.

Sisal-Production and Consumption Scenario

In 2007, sisal occupied sixth place among fibrous plants. The world's largest producer of sisal is Brazil (130,000 ton), followed by Mexico (45,000 ton) China (40,000 ton), Tanzania (37,000 ton), Kenya (27,000 ton), and Madagascar (15,000 ton). Smaller quantities of sisal fiber are also produced in South Africa, Mozambique, Haiti, Angola, Uganda, Malawi, Venezuela, Jamaica, Puerto Rico, France, Indonesia, Cuba, and India. Experts opine that the current worldwide demand for sisal fiber is about one million tons. Currently, high prices are being offered for the crop in the global market, in which the sisal fiber now fetches between 650 and 900 US\$/ton up from 150 US\$/ton in the 1990s.

India needs about 25,000 ton of sisal fiber of annually for internal consumption, whereas production is less (5,000 ton). The fiber was priced at Rs. 9,000–10,000 per

ton in 1988–1989, which rose to Rs. 27,000 per ton in 1996–1997, showing a phenomenal rise in its price. The current price is about Rs. 35,000 per ton, indicating the decadal growth in price.

22.2.3 Fiber Extractions and Processing

Sisal fiber can be extracted from its leaves by the following methods [13].

Retting

Water retting is a traditional biodegradation process involving microbial decomposition (breaking of the chemical bonds) of sisal leaves, which separates the fiber from the pith. The fibers are washed and processed further. This process takes 15–21 days for a single cycle of extraction and degrades the quality of fiber. Retting is a very slow, water intensive process, unhygienic, and not eco-friendly. Fiber extracted by this method is poor in quality [14, 15].

Boiling

In this method leaves of sisal plant are boiled, subsequently beating is done then after washing and sun drying we may get the usable clean fiber. This method is not suitable for large-scale extraction [15].

Mechanical Method

Mechanical extraction involves inserting leaves into the Raspador machine and pulling the raw material out. The mechanical extraction method is safe, this process does not deteriorate the fiber quality and is suitable for small-scale operations. The Raspador, run by an electric motor, is efficient, versatile, safe for labor, and cost-effective; it takes minimum time and is an eco-friendly process. In addition, residues are available after extraction of fiber of which about 96% is useful for other applications, such as biogas generation, composting, and isolation of a steroid hecogenin. The residue is also used for making paper, paperboard, and biodegradable polymer, wax, etc. [8, 16–19]. The extraction of sisal fiber using Raspador machine is shown in Fig. 22.2.

Fig. 22.2 Extraction of fiber from sisal leaf



Fibre extraction using Raspador machine



Harvested sisal leaves



Sisal fibre

22.3 Sisal Fiber Composition, Structure and Properties

22.3.1 *Composition*

A sisal plant can produce about 200–250 leaves. Each leaf composed of 3–4% fiber, 0.75% cuticle, 8% dry matter and 87.25% water [20]. Normally, the weight of a leaf is about 600 g and it will yield about 3% by weight of fiber. Each leaf contains about 1,000 fibers [21], and each fiber has a longitudinal approximately cylindrical shape. Physically, each fiber cell has four main parts: the primary wall, the thick secondary wall, the tertiary wall, and the lumen [3]. Its microstructure consists of parallel cells and a cuticle interface in the form of a continuous network around each cell. It is tough and strong because of its flexible interface and solid cells [22].

Sisal varies in quality. The large variations in its chemical compositions are because of its different sources, age, extraction methods, etc. [23]. For example, Wilson [13] indicated that sisal fiber contains 78% cellulose, 8% lignin, 10% hemicelluloses, 2% waxes, and about 1% ash by weight, whereas Rowell et al. [24] found that sisal contains 43–56% cellulose, 7–9% lignin, 21–24% pentosan, and 0.6–1.1% ash. The work carried out by Chand and Hashmi [25] showed that the cellulose and lignin contents of sisal vary from 49.62 to 60.95% and 3.75 to 4.40%, respectively, depending on the age of the plant.

According to Mohanty et al. [26] sisal fiber contain around 66–78% cellulose, 10–14% hemicellulose, 10–11% lignin, 10% pectin, 10–22% moisture content, and 2% waxes.

22.3.2 *Structure*

All natural fibers are cellulosic in nature. The major constituents of natural fibers are cellulose and lignin. During the biological synthesis of plant cell walls, polysaccharides such as cellulose and hemicellulose are produced simultaneously. Lignin fills the space between the polysaccharide fibers, cementing them together. This lignification process causes a stiffening of cell walls and the carbohydrate is protected from chemical and physical damage.

Cellulose forms slender rod-like crystalline microfibrils. The crystal structure of naturally occurring cellulose is known as cellulose I. Lignin is a high molecular weight phenolic compound but the exact chemical nature of lignin still remains obscure. Its associated hydroxyl and methoxy groups characterize lignin. It is believed that the structural units of the lignin molecule are derivatives of 4-hydroxy-3-methoxyphenylpropane, and the composition of the external surface of the cell wall is a layer of ligninaceous material and waxy substances that bond the cell to its adjacent neighbors. Hence, this surface does not form strong bonds with a polymer matrix [26].

22.3.3 Properties

Cellulose is a hydrophilic glucon polymer consisting of a linear chain of 1,4- β anhydroglucose units, which contain alcoholic hydroxyl groups. These hydroxyl groups form intermolecular and intramolecular hydrogen bonds with the macromolecule itself and also with other cellulose macromolecules or polar molecules. Therefore, all natural fibers are hydrophilic in nature. Although the chemical structure of cellulose from different plants fiber is the same, the degree of polymerization varies. The mechanical properties of a fiber are significantly dependent on the degree of polymerization.

Lignin is a biochemical polymer that functions as a structural support material in plants. Lignin is a high molecular weight phenolic compound, generally resistant to microbial degradation. Lignin is believed to be linked with the carbohydrate moiety through two types of linkages, one alkali sensitive and other alkali resistant. The alkali sensitive linkage forms an ester type combination between lignin hydroxyls and carboxyls of hemi-cellulose uronic acid. The ether type linkage occurs through the lignin hydroxyl combining with the hydroxyl of cellulose [26]. The plant fibers absorb moisture as the cell wall polymers contain hydroxyl and other oxygenated groups that attract moisture through hydrogen bonding. The hemicelluloses are mainly responsible for moisture absorption in the plant fiber, but the other noncrystalline cellulose, lignin, also plays a major role in this. In general, plant fibers absorb moisture up to a certain level – the Fiber Saturation Point (FSP). Absorption above or below the FSP causes swelling and shrinking of the fiber respectively, and this leads to dimensional instability in the final composite product made of the natural fiber as a reinforcing element. When plant fibers are exposed to the outdoors, they undergo photochemical degradation caused by ultraviolet radiation. The degradation takes place primarily in the lignin component, which is responsible for the characteristic color changes. As the lignin degrades, the surface becomes richer with cellulose content – this results in the rough surface of the composite and also accounts for a significant loss in surface fibers [27].

22.4 Fiber Surface Modification Methods

Research and engineering interests have been shifting from monolithic materials to fiber-reinforced polymeric materials because the latter offer many advantages: they are lightweight, have low abrasiveness, are combustible, do not cause much wearing of the machine or health hazards during processing and application, and are eco friendly, making disposal easy. However, the most important problem with these plants fiber composites is the poor fiber–matrix adhesion; insufficient adhesion between hydrophobic polymers and hydrophilic fibers results in poor mechanical properties of the natural fiber-reinforced polymer composites. However, surface

modification of the fiber by various physical and chemical treatments improves these properties [21, 28].

22.4.1 Physical Methods of Modification

A physical treatment changes the structural and surface properties of the fiber and thereby treated fibre influences the mechanical properties of composites. Physical methods involve heat treatment, cold plasma treatment, surface fibrillation, electric discharge, and gamma radiation treatment.

Low Temperature Plasma Treatment

Plasma treatment of the surface of plant fiber can be done without changing its bulk properties. The plasma discharge can be generated by cold plasma treatment. In plasma treatment, ionized gases with an equivalent number of positive and negatively charged molecules are used and these charged molecules react with the surface of the present material. The distinguishing feature between the two categories of plasmas is the frequency of the electric discharge. High-frequency cold plasma can be produced by microwave energy, whereas a lower frequency alternating current discharge at atmospheric pressure produces corona plasma [29].

Low temperature plasma treatment mainly causes chemical implantation, etching, polymerization, free radical formation, and crystallization; whereas sputter etching brings physical changes such as surface roughness which in turn leads to increased adhesion [30]. Low temperature plasma is a useful technique to improve surface characteristics of the fiber and polymeric materials by utilizing ingredients such as electrons, ions, radicals, and excited molecules produced by electric discharge. Low temperature plasma can be generated under atmospheric pressure in the presence of helium. The action of these plasma involves the removal of protons and creation of unstable radicals that convert functional groups such as alcohols, aldehyde, ketone, and carboxylic acids [30]. Corona treatment changes the surface energy of the cellulosic fibers, which in turn affects the melt viscosity of the composites. Corona treatment modifies surface composition resulting in an improvement in the surface properties of the composite [149].

Electric Discharge

Electric discharge methods are used for cellulose fiber modification to increase the melt viscosity of the fiber and to improve its mechanical properties [31].

Gamma Treatment

Fibers were treated with NaOH or just washed with water. They were then dried for 48 h at 75°C. The sample was irradiated by integral doses up to 10, 25, 50, 60, and 70 kGy with a dose rate of 4.8 kGy/h in an oxygenated atmosphere and at room temperature [32]. Albano et al. [32] reported the mechanical, thermal, and morphological behavior of blends of polypropylene filled with wood flour and sisal fiber composite with different doses of gamma irradiation (10, 25, 30, 50, 60 and 70 kGy) at room temperature and in the presence of oxygen. It was found that low irradiation doses improved the mechanical behavior of the compound or composites and the thermal study was acceptable [148]. Gamma irradiation is therefore a promising technology to modify composites [32, 148].

Chemical Methods of Modification

To modify the fiber surface and its internal structure various treatments have been carried out, including alkalization, acetylation, acrylation, permanganate, cyanoethylation, and the use of silane coupling agents. In general, fiber treatments can increase interphase adhesion and also lead to penetration of the matrix resin into the fibers and influence the mechanical properties of fiber reinforced composites [33].

Alkali Treatment

Alkali treatment improves the surface structure of sisal fiber and decreases its diameter. Due to the removal of cementing substances from the inner surface of lumen, polymer can easily penetrate into the cavities of sisal fiber. Moreover, alkali treatment improves the fiber wetting. Extensive work has been done by several researchers who reported that sisal fiber was treated with different concentrations of NaOH (% w/w 0.25, 0.5, 1.0, 2.0, 5.0, 10) solution for a fixed time period, washed with water, and dried in an air oven or vacuum dried [34–40]. This process is known as alkalization or mercerization.

Surface modification processes usually affect the morphology, mechanical properties, and thermal degradation of natural fiber or plant fiber. The surface of the sisal fiber was wrapped with some cementing substances before alkali treatment, a the epidermal cells of sisal fiber combined closely with the neighboring cells. Due to mercerization, fibrillation occurs in which the fiber bundle splits into separate fibrils. The reduced diameter of the fiber increases the aspect ratio which leads to the development of a rough topography which further results in better fiber–matrix interface adhesion and an increase in mechanical properties [41]. Alkali reagents affect the chemical composition of the fiber, the degree of polymerization, and the molecular orientation of the cellulose crystallite because the cementing substances

such as lignin and hemicelluloses are removed during the treatment process [42]. Sydenstricker et al. [35], found that the tensile strength of sisal fiber increases after 0.25–2% alkali treatment for the duration of 60 min but on further increasing the concentration, these properties show a decrease as reported in the Table 22.1. Garcia et al. also reported that 2% alkali treatment for 90 s at 1.5 MPa pressure was suitable for degumming and defibrillation of individual fibers [43]. Many researchers have reported that alkali treatment can increase amorphous cellulose and decrease crystalline cellulose and network hydrogen bonding [41, 44–47].

Acetylation

Acetylation is mainly applied to stabilize the cell wall against moisture absorption for improving its stability and environmental degradability [48–52]. In acetylation, acetic anhydride substitutes the hydroxyl group of the cellulose with acetyl groups that modify the properties of fibers so that they become hydrophobic [50]. Moisture absorption of fiber reduces after acetylation, which is beneficial for composites application. It was reported that after acetylation reduction in moisture uptake was found to be around 50–65% [53].

It is reported that in acetylation treatment, sisal fiber was soaked in glacial acetic acid at room temperature, decanted, and then soaked in acetic anhydride containing a few drops of concentrated sulfuric acid [34]. In another method, sisal fiber was treated with NaOH for 5 min, washed with distilled water and treated with glacial acetic acid containing a few drops of sulfuric acid as neutralizing agent, then dried and soaked in acetic acid solution, and then washed and air dried. Fiber treated in this manner showed an enhancement in tensile strength (423 MPa) [38]. Mishra et al. have done the acetylation of dewaxed–mercerized sisal fiber. They soaked alkaline treated fiber in glacial acetic acid for 1 h at 300°C and after 1 h it was decanted and soaked for 5 min in acetic anhydride containing one drop of concentrated sulfuric acid [54].

Permanganate Treatment

In permanganate treatment, mercerized fiber was treated with acetone solution of KMnO_4 for 1–5 min and air-dried after separation from solution [3, 4, 44, 55–59]. Kalaprasad and Thomas [34] studied the uses of permanganate-treated sisal fiber for making composites with a polyethylene matrix. In a polyethylene matrix, MnO_4^- ion is responsible for initiating permanganate-induced grafting of polyethylene into sisal fiber [34]. Joseph et al. studied permanganate treatment and found that the tensile strength of permanganate-treated sisal was around 38.80 MPa which was found to be higher than that of the untreated sisal fiber composites [3]. Paul et al. soaked alkaline-treated sisal fibers in different solutions of acetone containing 3.3 g, 6.25 g, and 12.5 g KMnO_4 in 100 ml acetone. It resulted in reduction of

Table 22.1 Effect of different chemical treatments on sisal tensile strength

S. No.	Treatments	Concentration (%)	Density (g/cm ³)	Tensile strength (MPa)	References
1.	Alkali (60 min)	0.25	–	350	Sydenstricker et al. [35]
		0.5	–	372	
		1	–	366.2	
		2	0.19	375.4	
		5	–	328.0	
2.	Alkali (4 h) (60°C) Acrylation – <i>N</i> -isopropyl acryl amide (60 min)	10	1.16	296.9	Rong et al. [38] Sydenstricker et al. [35]
		2	1.27	391	
		1	1.18	331.2	
		2	1.18	347.8	
		3	1.18	256.4	
		50% aq acetic acid solution	1.32	423 ± 27.3	
		4% NaOH saturated solution with sodium-thiocyanate	–	375.8 ± 31.4	
		2	–	387.5 ± 34.5	
		–	1.31	535 ± 42.3	
		5	–	612.75	
3.	Acrylonitrile grafting (10 min) (50–70°C)	10	–	602.61	Rong et al. [38] Rong et al. [38] Rong et al. [38] Rong et al. [38]
		25	–	589.15	
		(10/5)	–	522.5 ± 155.9	
		–	–	764.9 ± 162.2	
		5	–	859.2 ± 121.7	
4.	NaOH + ethyl Alcohol Hot water treatment (100°C) NaOH (10 min)	(10/5)	–	549.4 ± 139.9	Present study by authors Present study by authors Present study by authors
		–	–	809.1 ± 122.5	
		5	–	512.1 ± 150.8	
5.	Polyethylene glycol Ethyl acetate + acetic acid + water	10	–	–	Present study by authors Present study by authors
		(5/1/4)	–	–	

hydrophilicity of the fiber –the water absorption of fiber-reinforced composite is reduced. The hydrophilic tendency of sisal fiber decreases with increasing KMnO_4 concentration. But at a higher concentration of permanganate, degradation is observed which results in the formation of polar groups between fiber and matrix [56, 57].

Stearic Acid Treatment

It is reported that a solution of stearic acid in ethyl alcohol (4% by weight of fiber) was used to treat sisal fiber and the results showed that stearic acid-treated sisal showed better compatibility between sisal fiber and matrix [34].

Silane Treatment

Coupling agents can enhance the degree of cross-linking at the interface and improve bonding. Silane was found to be the most effective among many coupling agents to modify the natural fiber–matrix interface. The efficiency of silane treatment was high for the alkaline-treated fiber than for untreated fiber because more reactive sites can be generated for silane reaction [33].

After silane treatment, the number of cellulose hydroxyl groups in the fiber–matrix interface may reduce. In the presence of moisture, alkoxy groups convert into silanols, and after that the silanol reacts with the hydroxyl group of the fiber, forming stable covalent bonds to the cell wall on the fiber surface [62]. After silanation, swelling of fiber decreases because a cross-linked network of covalent bonding between the matrix and the fiber is created [33]. Silanes were effective in enhancing the interface properties [63–66]. Alkoxy silanes can easily form bonds with hydroxyl groups. After hydrolysis, silanes can form a polysiloxane structure by reaction with hydroxyl groups of fiber [44]. After silane application, hydrocarbon chains allow the fibers to absorb more water, which means that its chemical affinity to the polymer matrix is improved [33].

Earlier too, several researchers studied silane treatment. One reported that sisal fiber was mixed with a mixture of silane, CCl_4 and dicumyl peroxide and heated and dried in an oven [34]. In other experiment, sisal fiber was soaked in a solution of amino silane and alcohol at pH range up 4.5 to 5.5, and the fiber was oven dried after separation [34, 39, 67]. Some researchers treated the surface of the fiber with 1% silane and 0.5% dicumyl peroxide, in a mix of methanol/water (90/10 w) at pH 3.5 with acetic acid, under agitation [39]. Another study showed that silane treatments were done using silane [Fluoro silane (F8261)], amino propyl tri-ethoxy silane, and vinyl triethoxy silane mixed with an ethanol/water mix (of ratio 6:4) for 1 h at pH 4 in acetic acid [25]. The general formula for silane coupling agent is $\text{YR}_1\text{Si}(\text{OR}_2)_3$, where Y is the polymerizable vinyl group of silane and OR_2 is a hydrolyzable group. During silane treatment, the OR_2 group of the silane may

hydrolyze to some extent to form silanols. The resulting –OH groups of silanol or –OR₂ groups of unhydrolyzed silane interact with cellulose through their –OH groups by the formation of hydrogen bonds. Results showed that 2% silane treated sisal shows tensile strength 387.5 MPa [34, 114].

Peroxide Treatment

Many researchers treat cellulose fiber with peroxide because the process is simple and the mechanical properties of the fiber improve. In peroxide treatment, organic peroxide easily decomposes into peroxide free radicals, which can easily react with the hydrogen group of the matrix and cellulose fiber.

In one experiment, fibers were treated with a solution of benzoyl peroxide and dicumyl peroxide in acetone for about half hour after alkali treatment [44, 55–57]. High temperature favors decomposition of peroxides [74]. Studies on sisal fiber treatment were performed and composites were developed using benzoyl peroxide and dicumyl peroxide and toluene solvent with polyethylene at the time of mixing with fiber. The peroxide-treated matrix showed higher viscosity than untreated composites because of the grafting of polyethylene onto sisal fiber in the presence of peroxide [34]. Benzoyl peroxide-treated sisal fiber showed a tensile strength of 40.90 MPa [60, 61].

Acrylation

Acrylation of fiber is initiated by free radicals of the cellulose molecule [44, 68, 69]. The surface energy of fibers was increased after chemical treatment, providing better wettability and high interfacial adhesion [33].

Sisal fiber was treated at different percentage (1, 2, 3% w/w) of *N*-iso propyl acryl amide aqueous solution at room temperature [35]. It was observed that the treatment with *N*-iso propyl acryl amide 1, 2, and 3% gradually affected the fiber, exposing its inner layers. However, the 3% treatment significantly altered its surface. Pull-out tests in polyester resin were performed and found effective in improving interfacial adhesion [35]. Sreekala et al. used acrylic acid for acrylation [44]. The 2% acryl amide treatments showed optimum strength (347.8 MPa) because it showed higher tensile strength in 1% and 3% [44].

Dewaxing

It is very important to dewax the sisal fiber to improve its properties. One of the researchers studied the dewaxing of sisal fiber with a 1:2 mix of ethanol and

benzene at 72 h at 50°C. The fiber was then washed in distilled water and air dried [36, 37].

Bleaching

In bleaching fiber is usually treated with sodium chlorite and links are developed between lignin and carbohydrates. Removal of noncellulosic compounds by chemical treatments resulted in improvement of mechanical and physical characteristics as well as of fiber strength [33].

The bleaching of sisal fiber was done with sodium chlorite solution with a liquor ratio 25:1 at 75°C for 2 h. Further, the fiber was washed with distilled water, then treated with a 2% solution of sodium sulfite, and then vacuum dried. Zahran et al. developed a bleaching process in which activation of sodium chlorite was done by hexamethylene tetramine in the presence of a nonionic wetting agent [70]. The results revealed that bleached sisal fiber showed less tensile strength due to the loss of the cementing material. But the composite with bleached sisal shows enhanced flexural strength because of less stiffness and more flexible character of fiber after delignification. Moreover, high impact strength was achieved which may be due to the better bonding between the bleached fiber and the matrix [36, 37].

Cyanoethylation

Efforts were made to improve the strength of the sisal fiber for its value addition in engineering applications. The earlier work showed that the defatted fiber were refluxed with acrylonitrile, where pyridine was used as catalyst at a temperature range of 50°C–70°C for 2 h. The washed fiber using acetic acid and acetone followed by washing was vacuum dried to get cyanoethylated fibers at three different temperatures [36, 37]. Cyanoethylated sisal fiber showed a tensile strength of about 375.8 MPa [36, 37].

Isocyanate Treatment of Sisal Fiber

Isocyanate is very susceptible to reaction with the hydroxyl group of cellulose and lignin in the fibers and forms strong covalent bonds, hence increases fiber–matrix interface adhesion. In isocyanate treatment, the isocyanate group acts as a coupling agent [71, 72], and fiber is treated with the polymethylene–polyphenyl–isocyanate (C₁₅H₁₀N₂O₂) solution at 50°C for 30 min duration [72].

Benzoylation of Sisal Fiber

In benzoylation, benzoyl chloride is used for fiber treatment. The benzoyl group interacts with the hydroxyl group of fibers and decreases the hydrophilic nature of the fiber.

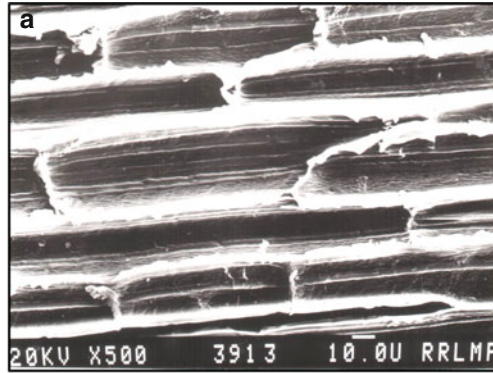
Joseph et al. [41] have done benzoylation of fiber, in which fiber was soaked in 18% NaOH solution followed by filtration, washing, and drying. Treated fiber was agitated in a solution of 10% NaOH and 50 ml benzoyl chloride. The reaction between hydroxyl of cellulose and benzoyl groups takes place, resulting in decreased hydrophilicity [41, 73]. In one experiment, alkali treatment of fiber was done before benzoylation for the activation of fiber. After benzoylation extra benzoyl chloride can be removed by the treatment of fiber with ethanol for 1 h and finally washed with water and dried in oven at 80°C for 24 h [74].

Polymeric Coating on Sisal Fiber

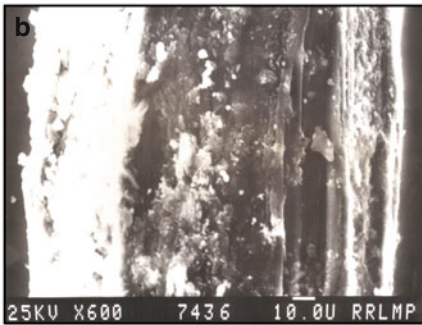
The strength of composites mainly depends on the interfacial bonding of fiber with the matrix and tensile modulus of fiber. Research work has been carried out to improve interfacial bonding of pretreated fiber with different polymer coatings (acrylic and polystyrene). Improvement in interfacial bonding between the fiber and matrix is clearly visible in SEM micrographs Fig. 22.3. To impart hydrophobicity and improve the interfacial bonding, sisal fibers were coated with acrylic resin and polystyrene resin. NaOH treated fibers were dipped in 3%, 5%, and 7% acrylic resin and polystyrene resin followed by air drying. The polymeric coatings on sisal fiber were done to overcome the hydrophilic nature of sisal fiber and improving the mechanical properties and interfacial bonding.

Tensile test machine is shown in Fig. 22.4 (Make AMETEK LLYOD/LRX, UK). The tensile strength of sisal fiber treated with 3%, 5%, and 7% acrylic coated NaOH-treated sisal fiber is shown in Fig. 22.5. Results revealed that the tensile strength of treated fiber was found to be increased maximum in NaOH-treated fiber with 5% acrylic coating (Fig. 22.5) [75].

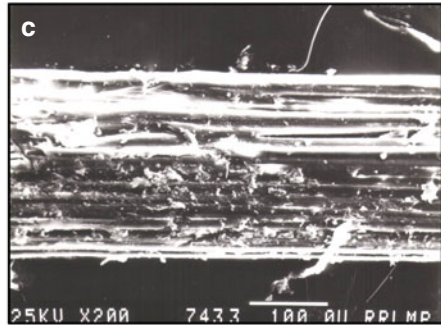
The effect of different chemical treatments on the tensile properties of sisal fiber is shown in Table 22.1. However, there is a wide variation in the tensile strength of the treated fiber. And the prime factors responsible for such variations are the age of the fiber; climatic condition under which it is grown; the technique of extracting fiber from the sisal leaf; precision and treatment handling techniques; and finally the untreated fibers being not of the same properties to compare with the treated fiber, especially where the work was conducted in different parts of the world. Nevertheless, the tensile strength of untreated sisal fiber, cultivated at AMPRI Bhopal, Central India, over a period of 5 years, and after harvest extracted using the Raspador machine was 501.3 ± 119.5 MPa (Table 22.2).



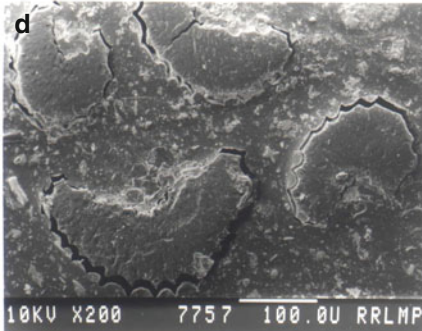
Uncoated Sisal fibre (LS)



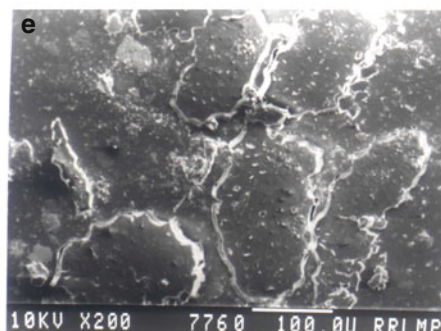
5% Acrylic Coated Sisal fibre (LS)



5% Polystyrene Coated Sisal fibre (LS)



Cross Section of Uncoated Sisal fibre



Cross Section of Polymer Coated Sisal fibre

Fig. 22.3 SEM microstructure of sisal fiber

It is apparent from the work done by the various researchers that the tensile strength of the sisal fiber after different chemical treatment varies from 256 to 612 MPa [35, 38]. In fact, under NaOH treatment, the tensile strength of sisal fiber was as high as 859.2 ± 121.7 MPa.

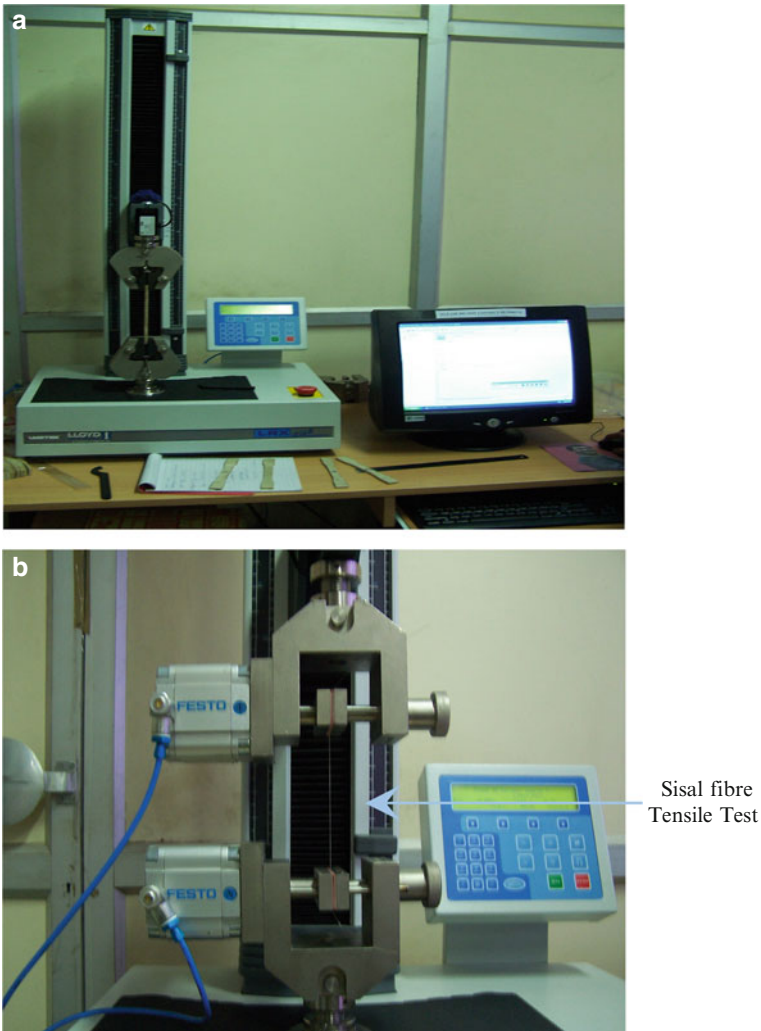


Fig. 22.4 Fiber testing machine

22.4.2 *Physico-Chemical and Mechanical Properties of Sisal Fiber and Its Comparison with Other Natural Fiber*

The chemical composition and cell structure of plant fiber is very interesting as each fiber is a composite in which rigid cellulose micro fibrils are reinforced with soft lignin and hemicellulose matrix. Also, the micro fibrils are helically wound along the fiber axis. Sisal fiber is equipped with high content of cellulose (60–80%), hemicellulose (10–25%), and lignin (7–14%) with high tensile strength and modulus in comparison with other natural fibers. This has led to a great interest among the

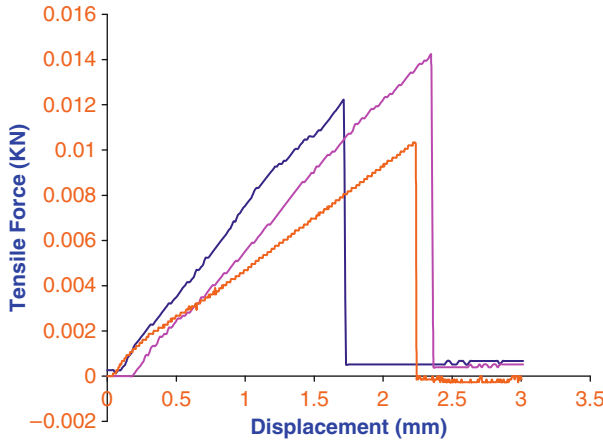


Fig. 22.5 Tensile strength of 3%, 5% and 7% acrylic coated NaOH treated sisal fiber

researchers as its properties make sisal suitable for reinforcement in composites for various applications [38]. The chemical composition of sisal fibers is reported in Table 22.3.

Properties of Sisal Fibers

Sisal is a strong fiber traditionally used for making rope, cordage, and twine. It is also used to manufacture coarse fabric, rugs, carpets, handicrafts, mats, fishing nets, etc. The sisal pulp left after fiber extraction is used for making paper/paperboards [17], hecogenin (a cortioco steroid) [17], wax [17], biodegradable polymer [81], biogas [82], and vermicompost [83].

The mechanical, thermal, and dielectric properties of sisal fiber have been studied in detail. X-ray diffraction, Infrared Spectroscopy, Thermal Gravimetric Analysis, Scanning Electron Microscopy, Differential Scanning Calorimetry, Dynamic Mechanical Analysis etc., have been used to determine the characteristics of sisal fiber and provide theoretical support for processing and application of the fiber.

The mechanical properties of sisal fiber tested by several researchers have been compiled and shown in Table 22.2. The results show that the tensile strength of sisal fiber varies from 100 to 700MPa, tensile modulus is in the range of 9–40 GPa, and elongation at break in the range of 2–14%. It may be noted that the tensile properties of sisal fiber may not be uniform along its length. The fibers extracted from the lower part of the leaf may exhibit a lower tensile strength and modulus but a higher fracture strain. The fiber becomes stronger and stiffer at midspan and the fibers extracted from the tip have moderate properties. It is reported that the tensile strength, modulus, and toughness of sisal fibers decrease with increasing temperature [26].

Silva et al. [84] studied the monotonic tensile behavior of a high performance sisal fiber. Tensile tests were performed on a micro force testing system using four

Table 22.2 Mechanical properties of Sisal fiber

S. No.	Tensile strength (MPa)	Tensile modulus (GPa)	Elongation at break (%)	References
1.	550 ± 100	24 ± 0.4	2.4 ± 0.4	Oksman et al. [9]
2.	400–700	7–20	2–14	Oksman et al. [9]
3.	400–700	9.0–38.0	2.0–14	Li et al. [76]
4.	400–700	9.0–20	5–14	Joseph et al. [77]
5.	530–630	17–22	3–7	Jacob et al. [40]
6.	400–700	9–20	5–14	Paul et al. [56, 57]
7.	434	17.5	–	Ganan et al. [78]
8.	580	–	4.3	Joseph et al. [3, 4]
9.	100–700	25–50	3–6	Li et al. [76]
10.	511–635	9.4–22.0	2.0–2.5	Shibata et al. [95]
11.	500 ± 70	13.2 ± 3.1	4.8 ± 1.1	Gonzalez et al. [150]
12.	450–700	7–13	4–9	Nair et al. [79]
13.	511–700	3.0–98	2.0–2.5	Bogoeva et al. [94]
14.	340 ± 7	12.8	6–7	Idicula and Boudenne [80]
15.	501.3 ± 119.5	50.57 ± 3.27	0.78 ± 0.41	Present study by authors

Table 22.3 Chemical composition of sisal fibers

S. No.	Cellulose (%)	Hemicellulose (%)	Lignin (%)	Ash (%)	References
1.	47–78	10–24	7–11	0.6–1	Li et al. [76]
2.	85–88	4	4–5	1	Joseph et al. [77]
3.	78	10	8	–	Jacob et al. [40]
4.	66–72	12	14–10	–	Paul et al. [56, 57]
5.	70	12	–	–	Joseph et al. [58, 59]
6.	60	28	8	0.5	Gonzalez et al. [150]
7.	73	10.1	7.6	3.1	Sydenstricker et al. [35]
8.	65	12	9.9	–	Idicula and Boudenne [80]

different gauge lengths and the results show that the gauge length does not seem to influence the modulus of the fiber. The variability in modulus, for a given gauge length, is likely due to the variability in the microstructure of the sisal fiber and possible damage that occurred during the extraction process [84]. Over the last few decades, several studies have been reported on the use of sisal fiber as reinforcements in polymer matrices [85–91]. Due to various advantages the use of sisal fiber and its composites is becoming a great area of interest amongst scientists and engineers.

Thermal Properties

The thermal property of sisal fiber was studied at AMPRI Bhopal using the Mettler Toledo STAR^e System by thermo gravimetric curve and differential thermo gravimetric curve, as shown in Fig. 22.6a, b. The temperature range used for analysis was from 500°C to 800°C. Results revealed that in the temperature range of 50°C–200°C, dehydration as well as degradation of lignin occurred. But, at

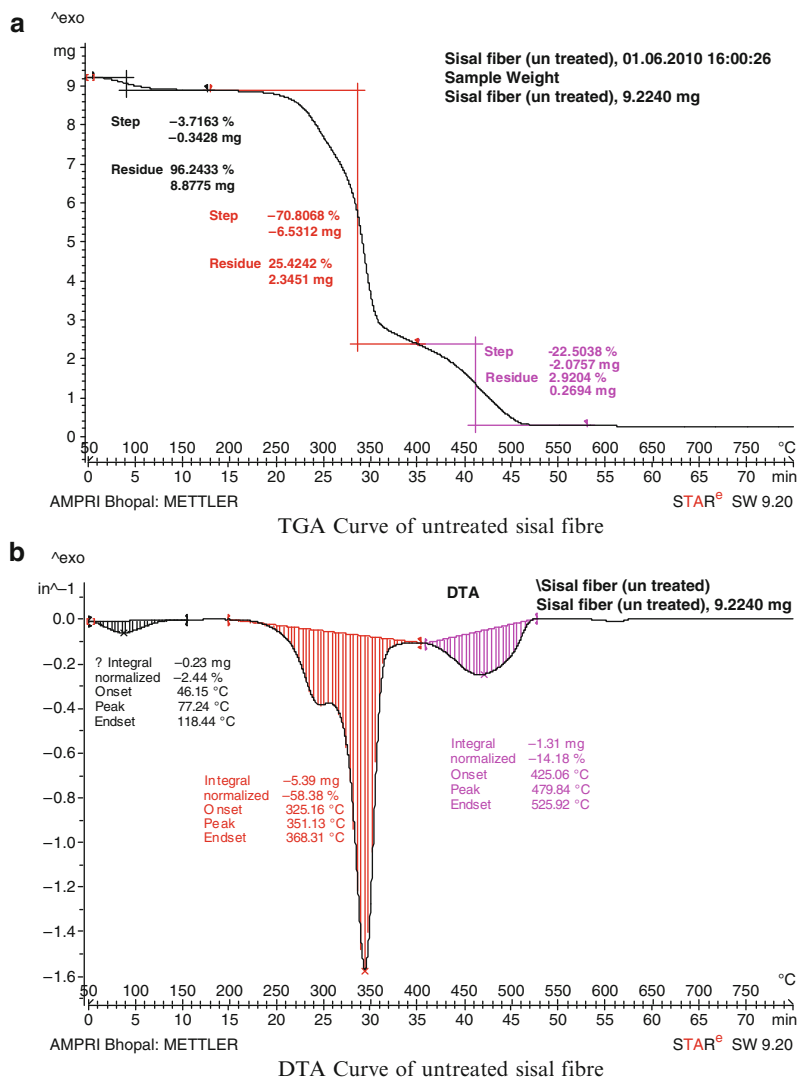


Fig. 22.6 Thermal properties (a) TGA (b) DTA of untreated sisal fiber

350°C most of the cellulose decomposed and released energy, which is shown in the Differential Scanning Calorimetry (DSC) curves. In the DTA curves, the peak observed at 78°C for sisal fiber corresponds to the heat of evaporation of water from the fiber (stage 1). The second peak of sisal at about 350°C was due to the thermal depolymerization of the hemicellulose and the cleavage of the glycosidic linkage of cellulose (stage 2). The third peak (at about 450°C) for sisal fiber may be due to the further breakage of the decomposition products of stage 2.

Earlier, Yi et al. studied the thermal properties of sisal fiber by thermo gravimetric curves and thermo gravimetric differential curves in thermal process. The temperature used for the analysis by this author was 30–600°C. It is reported that dehydration as well as degradation of lignin occurs in the temperature range from 60 to 200°C. As reported in the present study carried out by AMPRI, Bhopal, almost similar thermal properties of sisal fiber were recorded [92, 151].

Comparison of Sisal Fiber with Other Natural Fiber

The density of sisal fiber varies from 1.35 to 1.45 g/cm². Literature shows that sisal fiber exhibits tensile strength in the range of 400–700 MPa, which is nearly similar to many commercially used natural fiber such as jute, flax, banana, and sun hemp. Therefore, we can use sisal for commercial application as we can use jute, flax, banana, pineapple leaf fiber, etc. The mechanical properties of some of the natural fibers and other mineral fibers are shown in Table 22.4.

It is evident from Table 22.4 that flax fiber demonstrates higher tensile strength and modulus than sisal fiber due to its smaller lumen and smaller micro fibril angle. A literature review showed that there are large variations in both Young's modulus and tensile strengths of sisal fibre [20, 21, 53, 58, 59, 86]. This variation is due to various factors including the methods of testing. Mukherjee and Satyanarayana showed that different fiber test lengths and strain rates result in different tensile properties for sisal fibers. Increased test length decreases the strength of the fibers because the number of defects is increased. It was also observed that the strength of natural/sisal fibers is not uniform along the length of the fiber bundle. The reason is that the probability of finding significant defects is much larger in a natural/sisal technical fiber than in a single fiber. In addition, the load distribution is much more inhomogeneous in technical fiber [9].

In India, a wide variety of natural fibers is available such as sisal, coir, jute, banana, and sun hemp. These fibers are either the primary products of cultivation such as jute and sun hemp or the byproducts of crops raised for other purposes such as banana and coconut. However, sisal is not cultivated commercially in India. In recent years, considerable developmental activities in the science and technology of composite materials have been undertaken. Polymer matrix composites reinforced with glass fiber, carbon fiber, kevlar fiber, etc. have been among the forefront in the development and are already well-established materials. It is a well-known fact that composite materials offer many advantages over the use of conventional materials. In India, fiber-reinforced composite materials invaded the building construction area and started establishing itself in the mid 1980s in the form of natural fiber composites. The Advanced Materials and Processes Research Institute, CSIR, Bhopal had started its activities in the area of natural fiber composites and now this has grown exponentially in other laboratories and industries.

Natural fibers such as sisal, coir, jute, banana and sun hemp are vital renewable resources that can be used in many applications. Natural fibers are cheaper and easily available resources. As compared to manmade fibers, natural fibers have low specific

Table 22.4 Physico-chemical and mechanical properties of different fibers

Fiber	Density	Cellulose (%)	Hemi cellulose (%)	Lignin (%)	Moisture content (%)	Ash (%)	Micro fibriller angle(e)	Wax (%)	Tensile strength (MPa)	Young's modulus (GPa)	Elongation at break (%)	Reference
Sisal	-	67-78	10.0-14.2	8.0-11.0	11.0	-	20.0	-	468-640	9.4-22	3-7	Bismarck et al. [93]
Coir	-	36-43	0.15-0.25	41-45	8.0	-	41-45	-	568-640	-	3-7	George et al. [4]
Oil Palm	-	65	19	-	-	2	46	-	131-175	-	15-40	Bismarck et al. [93]
Jute	1.3 - 1.46	61-71	13.6-20.4	12-13	12.6	-	8.0	0.5	248	6.7	14	Bismarck et al. [93]
Cotton	1.5	82.7	5.7	-	-	-	-	-	393-800	10-30	1.5-1.8	Bogoeva-Gaceva et al. [94]
							0.6	-	226	-	1.3	George et al. [4]
							-	-	287-597	-	7.0-8.0	Bogoeva-Gaceva et al. [94]
							-	-	200-400	-	6-7	George et al. [4]
Flax	1.4-1.5	71-78	18.6-20.6	2.2	10.0	1.5	10.0	1.7	345-1,500	-	2.7-3.2	Bogoeva-Gaceva et al. [94]
	14-1.5	-	-	-	-	-	-	-	600-1,100	45-100	1.5-2.4	Li et al. [76]
	-	-	-	-	-	-	-	-	780	-	2-4	George et al. [4]
Hemp	1.48	70.2-74.2	17.9-22.4	3.7-5.7	10.8	2.6	6.2	0.8	270-900	-	2.7-3.2	Bogoeva-Gaceva et al. [94]
Bamboo	0.8	-	-	-	-	-	-	-	391-100	48-89	-	Bogoeva-Gaceva et al. [94]
Soft wood	1.5	-	-	-	-	-	-	-	10,000	400	-	Bogoeva-Gaceva et al. [94]
Ramie	1.5	-	-	-	-	-	-	-	400-938	44-128	-	Bogoeva-Gaceva et al. [94]
Banana	1.350	63-64	19	5	10-11	-	11	-	559 ± 6.7	20	5-6	Idicula and Boudenne [80]
Pineapple leaf fibre	1.526	81	-	12.7	13.5	-	14	-	54-754	-	1-4	George et al. [4]
									413+8	-	3-4	Idicula and Boudenne [80]
									413-1,627	-	0.8-1	George et al. [4]
Aramid (PALF)	-	-	-	-	-	-	-	-	3,000-3,150	-	3.3-3.7	George et al. [4]
Abaca	-	-	-	-	-	-	-	-	756	31.1	2.9	George et al. [4]
Sun hemp	2.56	-	-	-	-	-	-	-	760	-	2-4	George et al. [4]
Glass	1.5 ± 5.8	-	-	-	-	-	-	-	2,000-3,400	-	1.8-3.2	Li et al. [76]
Carbon	-	-	-	-	-	-	-	-	2,500 ± 8	56-72	3	Idicula and Boudenne [80]
									4,000	230-240	1.4-1.8	Shibata et al. [95]

weight and thus higher specific strength and stiffness, their extraction requires less energy, and also their thermal recycling is possible and they have good thermal and acoustic insulating properties. Universally, the demand for natural fibers is increasing day by day. The properties of natural fibers not only provide environmental benefits, but there are other price and physical advantages over synthetic alternatives. Intensive efforts are being made worldwide for the development of natural fiber-based composites for various applications. Advanced composites are used as primary load carrying structural elements, as they are lightweight and result in higher stiffness. Therefore there is a need for understanding the full characteristics of different natural and manmade fibers as they exhibit significant variation in their properties and possess a huge potential to be used in a variety of applications.

22.5 Sisal Fiber Reinforced Polymer Composite

Natural fibers are preferred to synthetic fiber in composites because of the many benefits of the latter: it requires less energy for fiber processing, it is a nonhazardous, replenishable resource, is biodegradable, and has low density and high specific strength, and is cost effective. As plant fibers are hydrophilic, the adhesion between the fibers and hydrophobic polymer matrices is not adequate. To achieve sufficient interfacial bonding, either surface modification of the fiber or plasticization of the fibers is required [18, 58, 59, 96].

The matrices used in sisal fiber-reinforced composites include thermoplastics (polyethylene, polypropylene, polystyrene, PVC, etc.), thermosets (epoxy, polyester, and phenol–formaldehyde resin, etc.), rubber (natural rubber, styrene-butadiene rubber, etc.) gypsum, and cement. The effects of fiber length, fiber orientation, processing methods, fiber volume fraction and fiber surface treatment on the mechanical and physical properties of sisal fiber reinforced composites have been studied.

22.5.1 Natural Fiber Reinforced Polymer Composite

Sisal fiber can be added as reinforcement in thermosets, thermoplastics, rubbers, cement, and gypsum and their composites are similarly classified as thermosets, thermoplastics, rubbers, and cement and gypsum according to their matrices.

22.5.2 Fiber Matrix Adhesion in Natural Fiber Reinforced Polymer Composite

Fiber matrix adhesion refers to the extent of bonding and anchoring between fiber and matrix. The presence of a large number of hydroxyl groups is responsible for

the hydrophilic nature of sisal fiber. Several fiber surface-treatment methods have been studied to improve the adhesion properties between sisal fibers and the surrounding matrix and to simultaneously reduce water absorption.

22.5.3 Making of Sisal Fiber Reinforced Polymer Composite

Applications of reinforced composites vary with the methodology adopted for manufacturing. The method of production also affects the cost of the product. As glass fiber-reinforced composites are made by various methods, similarly sisal fiber (natural fiber)-reinforced composites can be manufactured by hand lay-up/spray-up, resin transfer molding (RTM), compression molding, injection molding, filament winding, and pultrusion [81–83, 97]. Each processing method is described here in brief.

1. *Hand Lay-up/Spray up*: Spray up and open contact molding (hand lay-up) in one-sided molds is one of the cheapest and most common process for making fiber composite products. Typical products are boat hulls and decks, truck cabs and fenders. In a typical open mold application, the mold is first waxed and sprayed with gel coat and cured in a heated oven at about 49°C. In the spray up process, after the gel coat is cured, catalyzed resin (usually polyester or vinyl ester at 500–1,000 cP viscosity) is sprayed into the mold, along with chopped fiber. A secondary spray up layer imbeds the core between the laminates (sandwich construction). Then it is cured, cooled, and removed from the reusable mold. In hand layup processing, continuous fiber strand mat and other fabrics such as woven roving are manually placed in the mold. Each ply is sprayed with catalyzed resin (1,000–1,500 cP) and the resin is worked into the fiber with brush rollers to wet-out and compact the laminate.
2. *Resin Transfer Molding (RTM)*: The RTM system gives high quality surface on both the sides. A relatively low pressure (vacuum to 100 psi) process, RTM makes perfect shapes in 30 min to 1 h. The fabricator generally gel coats one or both mold halves, then lays continuous or chopped strand mat and the core, if used, into the bottom half, and closes the mold. The resin transfers into the mold through injection pressure, vacuum pressure, or both. Cure temperature depends on the resin system used. Heater blankets can heat the mold up to 202°C, if the matrix allows sensors to detect resin flow position in the mold and monitor resin and cure data [98].
3. *Compression Molding*: Compression molding is a molding technique for making composite materials under specific temperature and pressure. The unit cost is reduced by the faster cycle times that are possible when compression molding/sheet molding compounds (SMC) are made. SMC is a sheet that sandwiches chopped fiber between two layers of resin paste. Chopped fiber drop onto the paste and a second film carrier faces another layer of resin down on top of the fiber. Rollers compact the sheet to saturate the fiber with resin and to squeeze out

entrapped air. When the SMC is ready for molding, it is cut into sheets and is assembled on a mold with the required temperature. The mold is closed, clamped, and between 500 and 1,200 psi pressure is applied. Material viscosity drops and the SMC flows to fill the mold cavity. After curing, the mold is opened and the component removed manually or through an integral injector system.

4. *Injection Molding*: Automated injection molding of thermoset bulk molding compound (BMC) has increasingly taken over markets previously held by thermoplastics for application in electrical and automotive components, housing appliances, and motor parts. BMC is a low-profile (nearly zero shrinkage) formulation of a thermoset resin mix with 15–20% chopped fiber. Injection molding is a fast, high volume, low pressure, and closed process. Injection speeds are typically 1–5 s and nearly 2,000 small parts can be produced per hour. A ram or screw type plunger forces a material shot through the machine's heated barrel and injects it into a closed, heated mold. Heat build-up is carefully controlled to minimize curing time. After cure and injection, parts need only minimal finishing [99].
5. *Filament Winding*: Filament winding is an automated, high volume process that is ideal for manufacturing pipe, tank, shafts and tubing, pressure vessels, and other cylindrical shapes. The winding machine pulls dry fibers from supply racks through a resin bath and winds the wet fiber around a mandrel.
6. *Pultrusion*: Pultrusion is the continuous, automated closed-molding process that is cost effective for high volume production of constant cross sectional parts. Pultruded custom profiles include standard shapes such as channels, angles, beams, rods, bars, tubing and sheets.

Sisal Fiber-Reinforced Thermoset Polymer Composite

Thermoset composites are made up of thermoset resin-like polyester; epoxy and phenol–formaldehyde resin composites with varying fiber volume fractions and fiber length were prepared by following one of the techniques. Among polyester epoxy and phenol–formaldehyde composites, a phenolic-type resin performed as a better matrix than epoxy and polyester resins with respect to tensile and flexural properties due to the high interfacial bonding in phenolic composites [58, 59, 100].

In natural fiber composites, polyester is the most widely used thermosetting polymer with natural fiber. Irrespective of fiber length, the compression molding method is the most widely used and most convenient method to make these composites.

Physical and Mechanical Properties of Sisal Fiber-Reinforced Thermoset Polymer Composite

Variation in tensile, impact, and flexural properties of thermoset composites, viz. sisal–polyester, sisal–epoxy, and sisal–phenol–formaldehyde is explained here, with the change in length of the fiber (5–30 mm), fiber volume, etc.

Sisal Fiber-Reinforced Epoxy Composites

Considerable work has been done on the sisal fiber-reinforced epoxy composites. It is reported that the fractured cross sections of the sisal–epoxy composites, showed no epoxy resin in the fiber lumen. The total lumen area in the fiber cross-section was found to be 15% and the total void content was about 17%. In sisal, total leaf mass contains only 2–4% sisal fibers; other cells take care of the water distribution. Oksman et al. [9] studied the thermoplastic fiber composites and showed that lumen was filled with the polymer matrix. Fibers therefore have distribution channels between the single wood cells. It is possible that the absence of such channels in sisal, due to the different function of sisal fibers, is the reason for lack of polymer in the lumen. At several locations in the sisal fiber, a gap between the fiber and matrix can be observed. The gaps indicate weak fiber–matrix adhesion [9, 58, 59].

Mechanical Properties of Sisal Fiber-Reinforced Epoxy Composites

Earlier work showed that sisal fibers incorporation significantly increased the tensile strength and Young's modulus of the epoxy resin; a composite with 46% by volume of sisal fibers has a Young's modulus of about 20 GPa. The tensile strength of the same material is 210 MPa. Moreover, Bisanda and Ansell [86] reported that the flexural modulus for unidirectional sisal epoxy composites showed 16 GPa at 40% fiber volume. The flexural strength was 266 MPa [9].

The tensile modulus of sisal fiber was 24 GPa. The tensile modulus of the sisal fiber made from the bundles of technical fibers was found to be lower than the real fiber (single fibril) since the individual fibrils are not loaded uniformly. The effective fiber modulus in the composite was 40 GPa. This point demonstrates a more favorable stress distribution in the sisal fibers in the composite material.

Oksman et al. [9] assumed that all fiber fracture happens at the same critical stress and this corresponds to the final fracture. For volume fraction of fiber 0.28, 0.35, and 0.46, the effective fiber strength obtained was 420, 400, and 390 MPa respectively. Effective fiber strength around 400 MPa was also reasonably compared with measured average fiber strength of 550 MPa. The earlier researchers recorded that poor interfacial adhesion leads to fiber–matrix debonding close to fracture sites and corresponding load redistribution from fractured fibers to neighboring fibers. The results from mechanical testing demonstrate that sisal fiber shows higher modulus when embedded in a matrix material as compared to a material without matrix. On the other hand, the effective fiber strength in the composite is lower than the measured fiber strength. This indicates that the low strength fraction of the fiber population controls composite strength. However, more uniform fiber distribution and improved fiber–matrix adhesion may improve the strength of sisal–epoxy composites [9].

In a natural fiber polymer composite, natural fiber is incorporated in a definite volume in the polymer matrix. Mechanical properties can be enhanced by increasing the fiber volume in a composite, but after a certain level, it may start decreasing due to the poor bonding between fiber and matrix. Oksman et al. [9] studied the effect of fiber loading with epoxy polymer. As shown in the Table 22.5, sisal fiber

Table 22.5 Effect of fiber loading on tensile properties of sisal fiber reinforced epoxy thermoset composite

S. No.	Fiber volume (wt%)	Density (g/cm ³)	Tensile strength (MPa)	Tensile modulus (GPa)	Elongation at break (%)	Reference
1.	0	1.15	76	3.10–3.20	7.3	Oksman et al.
2.	28	1.16	169 ± 23	14.2 ± 1.6	2.3	[9]
3.	35	1.17	183 ± 16	14.5 ± 1.6	2.2	
4.	46	1.17	211 ± 12	19.7 ± 1.5	1.9	

significantly increased the tensile strength and Young's modulus of the epoxy resin. The composite with 46% by sisal fiber volume has a Young's modulus 20 GPa and a tensile strength of 210 MPa. But Bisanda and Ansell [86] attained a flexural strength about 266 MPa. In general, the mechanical properties of thermoset composites increased with the fiber length. It is interesting to note that at a fiber length of 5 mm, the tensile and flexural properties of phenolic composites was about 20% higher than those of epoxy composites. But by increasing the length of the fiber from 5 to 20 mm, the tensile and flexural strength of the epoxy resin composite are increased as compared to other composites. Polyester composites did not show any significant enhancement in its tensile and flexural strength with the change in fiber length in the range of 5–30 mm. It can be noticed that the mechanical properties of epoxy polyester composites showed a marginal decrease with an increase of fiber length from 20 to 30 mm [58, 59].

Sisal Fiber-Reinforced Polyester Composite

The tensile and flexural behavior of sisal fiber-reinforced polyester composites were investigated as a function of fiber length and fiber content by Sreekumar et al. [101]. Resin transfer molding and compression molding techniques were used for composite making. From the studies, it was found that mechanical properties increased with an increase in fiber loading in both cases [101].

Tensile and Impact Strength

Neat polyester composite showed tensile strength around 41 MPa, Young's modulus around 9.68 GPa, and flexural strength around 61 MPa. After reinforcement with fiber, mechanical properties were enhanced and some of the important properties are explained below. Singh et al. [102] reported that sisal–polyester composites from nonwoven sisal mats with fiber content 50% by volume showed a tensile strength of 30 MPa and a tensile modulus of 1.15 GPa. The composites were manufactured by impregnation of the nonwoven sisal mats under compression molding for 2 hrs [9, 102].

Effect of Fiber Length

Results showed that tensile strength and Young's modulus increased with increase in fiber length which was maximum at fiber length of 30 mm. On further increasing the fiber length, the strength reduced. Thus, fiber having length of

5–30 mm was found to be suitable for effective reinforcement in polyester composites [101].

Effect of Fiber Loading

As fiber volume increased, tensile strength and Young's modulus for the composite also increased up to a fiber loading of 42–43% volume fraction, respectively, but after that a decreasing trend in properties was reported [101]. This may be due to the higher fiber volume because there is a strong tendency for fiber–fiber interaction at lower fiber loading, dispersion of fiber is very poor and thus stress transfer may also be poor. In sisal fiber-reinforced polyester composite, therefore, both lower fiber volume and higher fiber volume are responsible for downright properties because of poor wetting and dispersion of fiber [101].

Mishra et al. [46] studied the effect of fiber volume on different mechanical properties of sisal–polyester composite. They found that while increasing fiber volume up to 30%, the tensile, flexural, and impact properties increased, but on further increment in fiber volume, they showed unqualified properties. Addition of 30 wt% fiber increased the tensile and flexural strength of composite to about 198% and 122% compared to that of neat polyester composite. Like tensile and flexural strength, impact strength also increased while loading fiber volume up to 30%, as shown in Table 22.6, but after increasing fiber loading, there was a downfall in the impact properties by about 46% as compared to 30% wt fiber content composite. This may be due to less fiber–matrix interaction. At high ratio of fiber in the composite, polymer would infiltrate it poorly [46].

Flexural Properties

It is observed that flexural strength and flexural modulus increased with increase in fiber length. Composites having fiber length 30 mm showed a maximum flexural strength and flexural modulus; beyond that limit a decreasing trend was observed [101].

Water Absorption

The slightest amount of water can significantly affect the mechanical properties of natural fiber-reinforced composites. Water absorption in a fibrous composite is dependent on many factors such as temperature, fiber loading, orientation of fibers, permeability of fibers, surface protection, area of the exposed surfaces, diffusivity, void content, hydrophilicity of the individual components, etc.

Table 22.6 Effect of fiber loading on impact properties of sisal fiber reinforced polyester composite

S. No.	Fiber volume (wt%)	Impact strength (J/m)	References
1.	0	14.76	Mishra et al. [46]
2.	10	76.52	
3.	20	109.19	
4.	30	163.58	
5.	40	88.23	
6.	30	261	Present study by authors

The neat polyester resin showed very low water uptake due to the three dimensionally cross-linked network structure after curing. The $-OH$ group in the chain end of polyester and oxygen of the ester linkage influences the formation of hydrogen bonds. However it absorbs 0.05 mol% of water due to the presence of micro cracks and also due to the hydrophilic nature of polyester. The fiber-reinforced composites absorb water very rapidly at the initial stage and later a saturation level is attained, and there is no further increase in water absorption. As the fiber content increased the water absorption also increased due to the hydrophilic nature of the fiber [101].

Sisal Fiber-Reinforced Urea-Formaldehyde Composite

Urea-formaldehyde resins (UFR) are the most prominent examples of the class of thermosetting resins usually referred to as amino resins. There are various advantages to the use of UFR, including low cost, ease of use under a wide variety of curing conditions, low cure temperatures, water solubility, resistance to micro organisms and to abrasion, hardness, excellent thermal properties, etc.

Impact Strength

The impact properties of composite materials are directly related to its overall toughness. The impact strength of sisal-reinforced urea-formaldehyde composite with 30 wt% sisal fiber is 5.78 KJ/m². While increasing the sisal fiber loading from 30 to 50 wt%, the impact strength increased by 62.98% but on further increasing sisal fiber volume up to 60 wt%, the impact strength decreased [103]. Composites with 50 wt% fiber volume showed higher strength which may be due to the proper interfacial adhesion between the fiber and matrix; the fibers with desired quantity act as better stress transferring media. In addition, the interspaces and stress concentrations shoot up with the increase of the sisal fiber. These fibers could have acted as crack initiation points during impact. Therefore, inferior impact strength was obtained in the composite containing 60 wt% sisal fiber [103].

Flexural Property

It is observed from the work done by earlier researchers (Table 22.7) that sisal-reinforced urea-formaldehyde composite with fiber volume 30 wt%, showed higher flexural strength (58.58 MPa) and on further increasing the fiber volume from 30 to 70 wt%, the flexural strength decreased from 58.58 to 15.28 MPa. Meanwhile, the flexural modulus decreased from 7.63 to 1.59 GPa [103].

Table 22.7 Flexural properties of sisal fiber-urea formaldehyde composite

S. No.	Fiber volume (%)	Density (g/cm ³)	Flexural strength (MPa)	Flexural modulus (GPa)	Specific strength (MPa.cm ³ /g)	Specific modulus (GPa.cm ³ /g)	Reference
1.	30	1.53	58.58	7.63	38.29	4.99	Zhong et al. [103]
2.	40	1.52	55.80	5.27	36.71	3.47	
3.	50	1.48	53.07	4.93	35.86	3.33	
4.	60	1.44	37.73	4.09	26.20	2.84	
5.	70	1.22	15.28	1.59	12.52	1.31	

Water Absorption Property

Rong et al. [38] reported that the water absorption of composite with 30 wt% sisal fiber was only 0.98%. This may be because of the greater adhesion between the fiber and matrix and the low water absorption nature of the matrix. It was observed that with an increase in sisal fiber content from 30 to 70 wt%, water absorption increased. This might be because of the poor distribution of fibers in the composite, which converts into lumps of fiber. These lumps require more force to deform during hot pressing, and as a result more stresses might have got incorporated in the composites. When the composites were tested for water absorption, a greater proportion of these stresses was released, causing high water absorption. It is evident that because of its hydrophilic nature, sisal fiber absorbs moisture readily [103].

Thus, it is concluded that fiber as a filler in a matrix enhances the mechanical properties because sisal has high tensile properties and its composite have high strength to weight ratio.

Fiber Matrix Interphase Adhesion

The mechanical properties of fiber-reinforced polymer composites are controlled by factors such as nature of matrix, fiber–matrix interface, fiber volume or weight fraction, fiber aspect ratio, etc. Due to the hydrophilic nature, the fibers pulled out from polyester and polyethylene matrices, they were compared with the fibers pulled out from the epoxy matrix, which carry polymer particles on their surfaces. On the other hand, fracture of the fibers occurs at the crack plane in phenolic composites. From SEM microstructures of different composites, it was observed that the bonding of sisal fiber with the four matrices are found to be in the order of phenolic > epoxy > polyester > polyethylene [58, 59].

From SEM studies, it can be observed that the untreated sisal fiber has a network structure and includes waxes and other low molar mass impurities whereas sisal fiber gets thinner after treatment. It is possible that treatment leads to microfibrillation. The surfaces of the treated sisal fiber become smoother as compared to those of untreated sisal fiber. The effective surface area of fiber available for contact with the matrix also increases in composites while also reducing the diameter of sisal fibers and thereby increasing their aspect ratio. This may offer better fiber–matrix interface adhesion and improve stress transfer. These will give rise to improvement in mechanical properties [78].

Chemical Modification and its Effect on Fiber Matrix Adhesion

To modify the fiber surface and its internal structure, various treatments were done, and when the treated fibers were incorporated into the matrix, treatments showed two types of importance related to interface: one between fiber bundles and the matrix and the other between the ultimate cells. In general, fiber treatments can

increase interphase adhesion and also lead to penetration of the matrix resin into the fibers, thereby influencing the mechanical properties of fiber and composites, which are illustrated here.

Treatment of sisal fiber with alkali for making composites to increase interfacial adhesion is very common, but extent of effect is determined on the basis of quantity and duration of treatment. Alkali treatment makes the sisal fiber surface rougher by removing the waxy materials. The rough surface produced on the sisal fiber leads to better mechanical anchoring with the matrix [34].

The surface modification process usually affects the morphology, mechanical properties, and thermal degradation of natural fiber. Alkali treatment improves the surface structure of sisal fiber and decreases the diameter of fiber. Due to the removal of cementing substances on the inner surface of lumen, polymer can easily penetrate into the cavities of sisal fiber. Moreover, alkali treatment increases the numbers of possible reactive sites and allows better fiber wetting. Sisal fiber surface was wrapped with some cementing substances before alkali treatment, which made the epidermal cells of sisal fiber combine with neighboring cells closely. The alkali reagent has an effect on the chemical composition of the fiber, the degree of polymerization, and the molecular orientation of the cellulose crystallite due to cementing substances such as lignin and hemicelluloses that were removed during the treatment process. TGA studies showed that in the untreated fibers, degradation temperature is 355°C while after mercerization of fibers it is 377°C means thermal stability increased after treatment [78].

In permanganate treatment for increasing the adhesion between sisal fiber and polymer, acetone solution of KMnO_4 is used to induce grafting of polymer on to sisal fibers. Here MnO_4^- ion is responsible for initiating permanganate induced grafting. These chemical modifications increased the viscosity of the hybrid composites because of the increased fiber–matrix interaction [35].

In stearic acid treatment, solution of stearic acid is used to induce interfacial adhesion of the sisal fiber. It was found that due to the presence of hydroxyl groups on the sisal fiber, stearic acid enhanced the viscosity of the hybrid composite [35].

In silane treatment, the level of fiber matrix adhesion is further enhanced by the presence of a silane coupling agent. The interfacial shear strength between natural fiber and matrix improved by morphological modification of the fiber surface. Fiber surface silanization results in improving the wetting of fiber. The reduction of the hydrophilic tendency of sisal fiber due to the treatments and the reduction of moisture absorption obtained with silane treatment can be associated with the interpenetration of the coupling agent into the cell wall of the fibers through its pores and its deposition in the interfibrillar region, generating a barrier that binds the moisture access to fibers [39].

In peroxide treatment, peroxides were added to a molten mass of the polymer at the time of mixing with fibers. After treatment, the peroxide-treated composites showed higher viscosity than untreated composites because of the grafting of polymer on the sisal fiber surface in the presence of peroxides [104].

In acrylation treatments, fiber densities decreased due to the extraction of soluble products in acrylamide which also affect fiber texture and its dispersion in the resin

when manufacturing composites. The SEM of treated and untreated sisal fiber were compared and results showed that *N*-iso propyl-acrylamide 1, 2, and 3% gradually attacks the fiber, exposing its inner layers, and in the case of 3% treatment, significantly altering its surface. The increase of the crystallinity index of acrylamide-treated sisal samples suggests that the acrylamide extracts an amorphous portion (lignin and hemicellulose) of the fibers [35].

In bleaching, untreated fibers were treated in sodium chlorite solution with a liquor ratio of 25:1 and anticolored with 2% solution of sodium sulfite [36, 37].

In cyanoethylation grafting, polyester composites made up of cyano ethylated sisal showed improved mechanical properties as compared to the control. This may be due to bonding of P-cyanoethyl groups of the fiber with the polyester, thereby improving the fiber matrix orientation [36, 37].

The graft copolymerization of acrylonitrile and methylmethacrylate (MMA) onto 5% alkali-treated sisal fiber were carried out at a temperature of 40°C in an aqueous medium to get acrylonitrile-grafted and MMA-grafted sisal fiber with a different percentage of grafting [36, 37].

Physical and Mechanical Properties of Chemically Modified Sisal Fiber-Reinforced Thermoset Polymer Composite

Treatment of natural fiber has been done to improve interfacial adhesion for making sisal-reinforced thermoset polymer composites. Studies were carried out on the properties of fiber with various treatments and the effect of treatment on the polyester composite's mechanical properties (30% fiber volume) [36, 37]. Results from Table 22.8 showed that 5% alkali-treated sisal composite showed enhancement in the impact strength of almost 35 J/m as compared to untreated polyester composite, but an increase in alkali concentration from 5 to 10% resulted in a decrease in the impact strength as compared to 5% alkali-treated composite. Bleached, defatted, and cyanoethylated sisal composite showed almost similar impact strength of 171 J/m, indicating that treatment increases the impact strength of fiber. Cyanoethylation of sisal was done at various temperatures (50°C, 60°C, 70°C); treatment at 60°C cyanoethylated sisal showed a higher impact strength of 192.46 J/m as compared to cyanoethylated sisal at 50°C or 70°C (171 J/m). An increase from 5 to 10% concentration in acrylonitrile grafting increased tensile strength, but on increasing concentration up to 20% the impact strength fell suddenly [36, 37].

Mishra et al. [36, 37] tested the tensile and impact strength of maleic anhydride-treated sisal composite at different fiber volumes and found that tensile and impact strength decreased gradually from 40% fiber volume composite to 55% fiber volume polyester composite. It was concluded that maleic anhydride-treated composite at fiber volume 40% showed higher and better mechanical properties [36, 37]. Related to tensile properties evaluation, Mishra et al. [36, 37] concluded that a composite of alkali treated (5%) sisal fiber was found to achieve better mechanical properties as compared to untreated, dewaxed, 10% alkali treated and bleached sisal fiber-reinforced composites. A 5% alkali-treated sisal fiber-reinforced composite

Table 22.8 Effect of sisal fiber treatment on different properties of Sisal fiber reinforced polyester thermoset composite

S. No	Treatment	Fiber volume (%)	Tensile strength (MPa)	Flexural strength (MPa)	Impact strength (J/m)	Reference
1.	Untreated	30	39.057	52.11	261	Present study by authors
2.	Alkali (5–10% concentration)	30	–	–	167.2–197.8	Mishra et al. [46]
3.	Bleached	30	47.5	112.19	171.17	
4.	Cyanoethylation (60°C)	30	84.29	149.09	171.27–192.46	
5.	Acrylonitrile grafting (5–10% concentration)	30	–	–	160.27–171.15	
6.	MMA grafted (5–10% concentration)	30	–	–	158.29–169.71	
7.	MMA (methyl-methacrylate) grafted (5% concentration)	–	72.3 ± 4.3	81.2 ± 7.2	–	Bismarck et al. [93]

showed enhancement in tensile strength (22%), flexural strength (43%), and impact strength (21%) as compared to the untreated composite. This increase can be attributed to fibrillation, which means a breaking down of fiber bundles into smaller fibers and thereby increasing the effective surface area for matrix adhesion. At higher alkali concentration treatment, brittleness of fiber increases, which may have resulted in lowering of mechanical properties. The defatted sisal polyester composite showed better mechanical properties because dewaxing of fiber helps in improving fiber–matrix interaction. Delignification occurs in the bleaching process, which results in lowering of tensile strength because lignin acts as a cementing material. After delignification, there is less stiffness and more flexibility in bleached composites, which results in better flexural strength. After delignification, the polyester resin replaces the role of lignin in fiber and interfacial fiber–matrix adhesion increases, which results in high impact strength of the composite [36, 37].

With cyanoethylation, treatment of sisal fiber at 60°C showed higher tensile strength (84.29 MPa) and flexural strength (149.09 MPa) compared with its treatment at 50°C, as shown in Table 22.8. As the temperature increases from 50 to 60°C, the composite showed enhanced mechanical properties, but above 60°C, the values of all properties decreased. With acrylonitrile grafting on sisal, tensile strength increased 1.1% and flexural and impact strength decreased 5.1% and 2%, respectively. But an increase in grafting percentage up to 10%, increased the tensile strength, flexural strength, and impact strength by about 10.3%, 25.8%, and 4.6%, respectively [36, 37].

The impact strength of methyl-methacrylate (MMA)-grafted (5%) sisal fiber composites was found to be 158.29 J/m. However, composites produced from 10% MMA grafted sisal fiber showed high tensile strength, flexural strength, and impact strength of 7%, 13.3%, and 2.7%, respectively [36, 37]. In fact, an increase in MMA

concentration up to 20% reduced the impact strength [36, 37]. A comparison of the result of tests done on fiber grafted with acrylonitrile and MMA shows that acrylonitrile grafting is better than MMA-grafting. At a higher percentage of grafting, fiber becomes porous, which results in lower values. The variation in the impact strength explains why there is no significant variation in results between different concentrations of treatment of MMA. However, the work done at AMPRI shows the impact properties of neat polyester composite, sisal-reinforced polyester composite, jute-reinforced fly ash polyester composite, and jute-reinforced red mud polyester composite showed an impact strength of 2,250 J/m², 3,600 J/m², 2,660 J/m², 4,560 J/m², respectively. Results showed that the impact strength increased predominantly by reinforcing the polymer with sisal fiber.

22.5.3.1 Sisal Fiber-Reinforced Thermoplastic Polymer Composite

Thermoplastic resin softens when heated, hardens when cooled, and allows for reprocessing and remelting without any chemical structure or properties. Thermosets are plastics that cannot be melted once cured and include resins such as epoxies; considerable interest has been generated in the manufacture of thermoplastic composites due to their unique properties, such as high strength to weight ratio, good dimensional stability, good fracture toughness, scratch resistance, thermal stability, and good resistance against chemicals [105, 106]. With more stringent demands for recycling, standard thermoplastic polymers are being used as substitutes for thermosetting polymers as matrix materials for high-volume consumer-driven composites. Natural fiber thermoplastic composites have been used for applications such as transportation, manufacturing of sporting goods, packaging, and similar industries because they are reusable, reshapable, and repairable; the composites are ecofriendly as they are developed with renewable material. Thermoplastic resins have some disadvantages in that they are prone to creep and have poor melt flow characteristics; they degrade at medium and high temperature and for mixing with fiber need to be heated well above the melting point for the polymer to wet the fibers sufficiently [74, 107, 108].

The most commonly used thermoplastic resins are polyethylene (PE), polypropylene (PP), polyether ether ketone (PEEK), polyvinyl chloride (PVC), polystyrene (PS), polyolefin etc., which have been reported as the matrices [76]. Polyethylene is the cheapest and has excellent toughness and impact strength, but the lowest in service temperature. The resin can be used both in virgin and recycled form. All polyethylene grades [i.e., Low Density Polyethylene (LDPE) and High Density Polyethylene (HDPE)] are used for the manufacture of thermoplastic composites. PVC is the strongest resin with the highest service temperature, high stiffness capability, mechanical strength, and weather resistance properties. Polyvinyl chloride resins are being used in thermoplastic composites for manufacture of window panels in construction because it is cheap, durable, and easy to assemble [96].

To make natural fiber thermoplastic composites, fiber and thermoplastics resin can be mixed in any one of the two following methods:

- (a) Melt mixing
- (b) Solution mixing

In melt mixing, the fiber is added to a melt of thermoplastics, and mixing is performed using a mixer at a specified temperature and speed and for a specified time. Then the mix is taken out from the mixer while hot and extruded in the form of long and thick rods using an injection molding machine.

In solution mixing, the fibers are added to a viscous solution of thermoplastics in a solvent in a stainless-steel beaker with a stainless-steel stirrer. The temperature is maintained for some time and the mix is transferred to a flat tray and kept in a vacuum oven to remove the solvent. The solution mixing process avoids fiber damage that normally occurs during blending of fiber and thermoplastics by melt mixing.

Randomly oriented sisal fiber reinforced composites are prepared by standard injection molding of the blends. Oriented sisal composites are processed by aligning the long extruded rods with compression molding [88, 89].

Physical and Mechanical Properties of Sisal Fiber-Reinforced Thermoplastic Polymer Composite

Testing of mechanical properties such as tensile strength (ASTM-D-638), flexural strength (ASTM-D-790), and impact strength (ASTM-D-256) was done following standard methods. The water absorption of both untreated and treated composites was determined as per ASTM-D-570. The variation in tensile, impact, and flexural properties of thermoplastic composites, viz. sisal–polypropylene and sisal polystyrene, is explained here, and the change in fiber volume also given here.

The Effect of Fiber Loading on the Mechanical Properties of Sisal Fiber Thermoplastic Composites

The work done by Mishra and Naik [109] shows that an increase in the fiber volume in the matrix leads to a reduction in the mechanical properties of the composite due to lack of adhesion between fiber and polymer. The grafting of sisal fiber with maleic anhydride resulted in better adhesion with polymer [109]. Antich et al. [110] reported that there was an increase in the Young's modulus with fiber loading, but tensile strength and deformation at break were found to be decreased (Table 22.9). The deformations at break decreased to 3.88% without sisal fiber and 0.97% with 25% sisal fiber as a consequence of the weak fiber–matrix interface derived from the divergent behavior in polarity between the hydrophilic sisal fiber and the hydrophobic polymer matrix [110]. These studies conducted by Sreekumar et al. [111] using wheat flour-based thermoplastic polymer-based sisal fiber composites showed not much increase in the tensile strength; Young's modulus, however, increased. The mechanical properties of composites with varying sisal fiber content were measured and these measurements are shown in Table 22.9 [111].

Table 22.9 Mechanical properties of sisal fiber (Different fiber loading) reinforced thermoplastic composites

S. No.	Composite matrix	Fiber/matrix content (wt%)	Tensile strength (MPa)	Young's modulus (GPa)	Elongation at break (%)	Flexural strength (MPa)	Flexural modulus (GPa)	Reference
1.	Sisal-PS	0	20.64	1.22	3.35	45.55	3.42	Mishra and Naik [109]
	Sisal-PS	40/60	8.63	1.30	3.30	16.55	3.04	
	Sisal-PS	45/55	6.97	0.90	2.75	19.33	2.90	
	Sisal-PS	50/50	3.30	0.66	2.50	17.21	2.79	
	Sisal-PS	55/45	2.79	0.46	2.00	15.7	2.47	
2.	Sisal-HIPS	0	21.88-22.14	1.84-1.96	3.88-4.04	-	-	Antich et al. [110]
	Sisal-HIPS	5	15.97-17.01	1.94-2.08	1.46-1.68	-	-	
	Sisal-HIPS	10	14.18-14.62	2.22-2.34	1.01-1.11	-	-	
	Sisal-HIPS	15	12.82-13.98	2.43-2.67	0.42-1.3	-	-	
	Sisal-HIPS	20	11.52-11.30	2.22-2.48	0.65-1.27	-	-	
3.	Sisal-HIPS	25	12.29-10.75	1.87-3.15	0.55-0.97	-	-	Sreekumar et al. [111]
	SFR-WFT	0	1.8-2.0	41.2-48.8	31.4-38.6	-	-	
	SFR-WFT	1	1.6-1.8	39.7-46.6	42.7-59.6	-	-	
	SFR-WFT	3	1.5-1.9	44.4-49.6	42.6-43.4	-	-	
	SFR-WFT	5	2.0-2.2	61.0-65.0	36.0-40.0	-	-	
	SFR-WFT	10	1.8-2.2	83.2-102.8	17.2-24.8	-	-	

PS Polystyrene

HIPS High impact polystyrene

SFR-WFT Sisal fiber reinforced wheat flour thermoplastic composites

Studies carried by Leao et al. [28] showed that 70% sisal fiber content in sisal polypropylene composites gave maximum tensile strength and Young's modulus, but flexural strength and flexural modulus property were found to be optimum in 60% sisal fiber, as given in Table 22.10 [28].

The work done by Jarukumjorn and Suppakarn [112] reported that when sisal fiber percentage increased in polypropylene composites the tensile strength increased. Young's modulus, flexural strength, and flexural modulus in polypropylene sisal composites increased by 55%, 9%, and 58%, respectively. But impact strength decreased from 85.80 KJ/m² (no sisal fiber) to 12.78 KJ/m² (30% sisal fiber) (Table 22.10). The mechanical properties of sisal fiber-reinforced thermoplastic composites under different fiber loading, chemical treatments (alkali, acetylated, stearic acid, permanganate, silane, peroxide, isocyanate, cyanoethylation, benzoylation) and maleic anhydride treatment are shown in Tables 22.11, 22.12, and 22.13, respectively. For better adhesion and improved mechanical strength, Jarukumjorn and Suppakarn [112] used polypropylene grafting with maleic anhydride (PP-g-MA) which resulted in increased tensile strength (23.83–28.66 MPa), Young's modulus (2.11–2.29 GPa), flexural strength (60.88–65.88 MPa), and impact strength (12.78–14.42 KJ/m²). The increase in the value of these properties was due to covalent linkage formation between maleic anhydride groups and the OH group of the sisal fiber [112]. Further details about the mechanical properties of maleic anhydride-treated sisal fiber composites studied by different researchers are shown in Table 22.13.

Mohanty et al. [105] reported gradual increases in the tensile, flexural, and impact strength of composites. When fiber loading was varied from 10 to 30%, the composites showed increased tensile strength. Tensile strength and flexural strength increased to about 60–70% and 140–150%, respectively. Moreover, impact

Table 22.10 Mechanical properties of sisal fiber (different fiber loading) reinforced polypropylene composites

S. No.	Fiber/matrix content (wt%)	Tensile strength (MPa)	Young's modulus (GPa)	Flexural strength (MPa)	Flexural modulus (GPa)	Impact strength (J/m)	Reference
1.	80/20	11.12	1.25	16.36	1.36	–	Leao et al. [28]
2.	70/30	25.41	2.35	23.76	1.83	–	
3.	60/40	23.25	1.97	32.3	2.78	–	
4.	30/70	23.88	2.11	60.88	3.91	12.78	Jarukumjorn and Suppakarn [112]
5.	0	17.80	–	19.60	–	23.25	
6.	10	24.17	–	34.83	–	40.50	Mohanty et al. [105]
7.	15	26.11	–	46.35	–	46.10	
8.	30	29.25	–	48.96	–	51.79	
9.	45	23.21	–	43.41	–	39.83	
10.	80/20	–	–	49	2.4	19	Oksman et al. [113]
11.	75/25	–	–	45	8	23	
12.	66/34	–	–	46	3.0	27	
13.	63/43	–	–	48	3.6	29	

Table 22.11 Mechanical properties of Sisal fiber (Different fiber loading and orientation) reinforced thermoplastic composites

S. No	Composite matrix	Fiber content (wt%)	Tensile strength (MPa)	Young's modulus (MPa)	Elongation at break (%)	Reference
1.	Sisal – PP (L and R)	0	35.00	498	15.00	Joseph et al. [3]
	Sisal – PP	10	36.00 (29.00)	730 (605)	7.82 (8.00)	
	Sisal – PP	20	39.10 (31.14)	798 (971)	7.11 (8.33)	
	Sisal – PP	30	44.40 (33.84)	1,040 (940)	8.33 (8.50)	
2.	Sisal – PS (L and R)	0	34.90	390	9.00	
	Sisal – PS	10	21.30 (18.16)	629 (516)	9.00 (7.00)	
	Sisal – PS	20	43.20 (25.98)	999 (553)	8.00 (6.00)	
	Sisal – PS	30	45.06 (20.42)	999 (624)	7.00(4.00)	
3.	Sisal – LDPE (L and R)	0	9.20	140	200.00	
	Sisal – LDPE	10	15.61 (10.80)	1,429 (324)	4.00 (27.00)	
	Sisal – LDPE	20	21.66 (12.50)	2,008 (453)	3.00 (10.0)	
	Sisal – LDPE	30	31.12 (14.70)	3,086 (781)	2.00 (7.00)	
4.	Sisal – PS (L)	0	34.9	390	9	Nair et al. [79]
	Sisal – PS	20	43.20	999.9	8	
	Sisal – PS	30	45.06	998	7	

(Properties of randomly orientation of sisal fiber composites are shown in parentheses)

PP Polypropylene

PS Polystyrene

L Longitudinally and *R* randomly oriented solution mixed sisal fiber

LDPE Low density polyethylene

strength increased 23.25 J/m to 51.79 J/m with 10% sisal fiber and 120–125% with 30% sisal fiber [105].

Oksman et al. [113] reported the flexural properties and impact strength of sisal polypropylene (pp) composites with different fiber content. Test results showed that flexural modulus and impact strength increased with increased fiber content but flexural strength was not affected (Table 22.10). Oskman et al. used maleated polypropylene (epolene 43 WAX) as a coupling agent, whereby flexural strength was increased: the flexural modulus of maleated-treated fiber was 4.6 GPa [113].

Joseph et al. [3] worked on sisal thermoplastic composites using three different types of thermoplastic polymer PP (polypropylene), PS (polystyrene), and PE (polyethylene [LDPE]). Joseph et al. [3] reported mechanical properties of sisal thermoplastic composites on the basis of varying fiber loads (0–30%) and orientation (longitudinally and randomly). Joseph et al. [3] found an increase in sisal–PP and sisal–PE composites tensile strength and Young's modulus with an increase in fiber loading, but a decrease in elongation. Sisal–PS composites showed an initial decrease in tensile strength when fiber loading was of 10%, but it increased gradually as the fiber loading went up to 20 and 30% (Table 22.11); flexural

Table 22.12 Tensile properties of treated Sisal fiber thermoplastic composite

S. No	Treatments	Composite	Tensile strength (MPa)	Young's modulus (MPa)	Elongation at break (%)	Reference
1.	Alkali	LDPE Sisal (30/70)	34.27 (31.12)	3,328 (3,086)	1 (2)	Joseph et al. [58, 59]
		SGRP (Sisal/Glass 70/30)	31.26 (27.86)	831.27 (831)	5 (5)	Kalaprasad et al. [114]
		Sisal PP	31.23 (29.55)	–	–	Mohanty et al. [105]
2.	Acetylated	SGRP (Sisal/Glass 70/30)	32.23 (27.86)	919.535 (831)	5 (5)	Kalaprasad et al. [114]
3.	Stearic (4 wt%)	SGRP (Sisal/Glass 70/30)	32.79 (27.86)	1,000.785 (831)	5 (5)	
4.	Permanganate (0.06 wt%)	SGRP (Sisal/Glass 70/30)	32.97 (27.86)	1,081.825 (831)	5 (5)	
		LDPE Sisal (30/70)	38.80 (31.12)	3,816 (3,086)	3 (2)	Joseph et al. [58, 59]
		Sisal – PP (30/70)	45.7 (37)	1,271 (735)	8 (8)	Joseph [115]
5.	Silane	SGRP (Sisal/Glass 70/30)	34.34 (27.86)	1,185 (831)	4 (5)	Kalaprasad et al. [114]
6.	DCP (Peroxide)	SGRP (Sisal/Glass 70/30)	35.03 (27.86)	1,303.7 (831)	4.7 (5)	
		LDPE Sisal (30/70)	41.80 (31.12)	4,156 (3,086)	4 (2)	
7.	BPO (Peroxide)	SGRP (Sisal/Glass 70/30)	35.77 (27.86)	1,401.75 (831)	5 (5)	Joseph et al. [58, 59]
		LDPE Sisal (30/70)	40.90 (31.12)	4,018 (3,086)	3 (2)	Kalaprasad et al. [114]
		LDPE Sisal (30/70)	41.50 (31.12)	4,068 (3,086)	4 (5)	Joseph et al. [58, 59]
8.	Isocyanate	Sisal-pp (30%)	35.64 (29.55)	–	–	Mohanty et al. [105]
9.	Cyanoethylation	Sisal-PP (30/70)	45.8 (37)	1,342 (735)	7 (8)	Joseph [115]
10.	Benzoylation	Sisal-PS (30/70)	48.3 (45.06)	1,125 (998)	8 (7)	Nair et al. [79]

(Properties of untreated composites are shown in parentheses)

SGRP Sisal glass reinforced polypropylene

Table 22.13 Tensile properties of maleic anhydride treated sisal fiber composite

S. No	Composite	Fiber/matrix content (wt%)	Tensile strength (MPa)	Young's modulus (MPa)	Elongation at break (%)	Flexural strength (MPa)	Flexural modulus (MPa)	Reference
1.	Sisal-PS	40/60	9.89 (8.63)	1,705.66 (1,308)	2.75 (3.00)	37.74 (16.55)	4,565 (3,047)	Mishra and Naik [109]
2.	Sisal-PS	45/55	7.65 (6.97)	1,274.91 (900)	3.25 (2.75)	12.73 (19.13)	4,246 (2,896)	
3.	Sisal-PS	50/50	5.51 (3.30)	852.78 (660)	2.75 (2.50)	10.99 (17.21)	3,747 (2,793)	
4.	Sisal-PS	55/45	4.16 (2.79)	555.1 (466)	2.75 (2.00)	18.514 (15.70)	3,217 (2,470)	
5.	SGRP	70/30 (Sisal/Glass)	34.97 (27.86)	1,139.32 (831)	5 (5)	–	–	Kalaprasad and Thomas [34]
6.	Sisal – PP	30/70	45.8 (37)	1,342 (735)	7 (8)	–	–	Joseph [115]

(Properties of untreated composites are shown in parentheses)

strength showed a rapid increase. Joseph et al. [3] observed the mechanical properties in both types of orientation. It was found that the composites containing longitudinally oriented fibers exhibit better mechanical properties than those with randomly oriented fibers. Of all the three types of sisal thermoplastic composites, sisal polypropylene showed the optimum increase in mechanical properties; it was therefore concluded that PP would be a good matrix for sisal polyolefin composites (Table 22.11) [79].

In a natural fiber polymer composite, natural fiber of a definite volume is incorporated in the polymer matrix. Mechanical properties can be enhanced by increasing the fiber volume in composites but once the volume reaches an optimum level, the properties thereafter start to decrease. Nair et al. [79] studied the sisal fiber-reinforced polystyrene composite behavior and they found that tensile strength and Young's modulus increases as a result of the increase in the fiber volume from 0 to 40%, whereas elongation at break decreases on increasing fiber volume. Nair et al. [79] used three different types of orientation: L (longitudinal), T (transverse), and R (randomly); longitudinal orientations gave good mechanical result compared to other orientations (Table 22.11) [79].

An increasing trend in the tensile strength with fiber volume fraction was reported by Joseph et al. [3]. They reported that sisal fiber addition increased the tensile strength from 9 MPa (0% sisal) to 14–15 MPa (30% sisal) and the reinforcement effect largely on matrix ductility, that is, the resistance to crack propagation [3].

Fiber Matrix Interphase

Thermoplastic composite materials frequently showed a lack of fiber matrix adhesion when exposed to adverse/aggressive environmental conditions. Moreover,

their composites were prone to swell/warp and shrink when exposed to moist and hot weather conditions. In order to develop composites with better mechanical properties and environmental performance, it is necessary to impart hydrophobicity to the fibers by chemical reaction with suitable coupling agents. This is typically remedied using fiber surface modification. Chemical modification or the addition of a third phase bridging the fiber and matrix phases were successfully applied to improving the interfacial characteristics of many polymer composite systems. Such surface modification of natural fiber would not only decrease moisture absorption, but also increase wet-ability of fibers with resin and improve the interfacial bond strength, which are critical factors for obtaining better mechanical properties of composites. Natural fiber-reinforced thermoplastic composites have poor interfacial bonding between sisal fiber and thermoplastic matrix. To overcome this poor interfacial bonding, a number of fiber pretreatment techniques, such as alkaline treatment, heat treatment, and coupling agent treatment were found to be appropriate [116].

The fiber–matrix interfacial bond strength is expected to be very poor in composites of cellulosic fiber, which is hydrophilic, and thermoplastic polymer, which are hydrophobic in nature. Several treatments have been developed for the above system to improve interface bonding, which improves the mechanical properties and dimensional stability of cellulosic fiber of sisal–LDPE composites [58, 59, 117].

Chemical Modification and its Effect on Fiber Matrix Adhesion

For pretreatment of sisal fiber chemicals such as alkali (NaOH), permanganate (KMnO_4), acetylation, peroxide (BPO and DCP), isocyanate treatment, stearic acid, silane, benzoylation [79], maleic anhydride modification, PPG–TDI [34, 60, 61], and cold-plasma treatment are used [76, 118].

It is known that alkali treatment improves the fiber–matrix adhesion due to the removal of natural and artificial impurities from the fiber surface as well as the change in the crystal structure of the cellulose [119]. Moreover, alkali treatment reduces fiber diameter and thereby increases the aspect ratio. Therefore, the development of a rough surface topography and enhancement in aspect ratio offer better fiber–matrix interface adhesion and an increase in mechanical properties was reported by Mohanty et al. [68]. Alkali treatment increases surface roughness resulting in better mechanical interlocking due to the amount of cellulose exposed on the fiber surface [53]. Several other studies were conducted on alkali treatment and the results are discussed elsewhere [36, 37, 41, 86].

To reduce the surface hydrophilicity, the fiber surface is treated with MAPP. The anhydride rings of MAPP covalently link with the hydroxyl groups of the fibers to form an ester linkage. The surface tension of the fiber increases its wettability within the matrix [68].

Fiber modification reduces hydrophilicity of the fiber and improves the physical/chemical interactions between the fiber and polystyrene matrix. The improvement in tensile properties of benzoylated fiber composite is attributed to the presence of a

phenyl structure in fiber treated similarly to that of polystyrene, which improves the thermodynamic compatibility between the fiber and polystyrene benzoylated fiber composites. The leach out of alkali-soluble fractions like the waxy layer, lignin, etc., during treatment makes the surface of the fiber very rough and provides better mechanical interlocking with the polymer matrix.

Physico-Mechanical Properties of Chemically Modified Sisal Fiber-Reinforced Thermoplastic Polymer Composite

When a composite is subjected to mechanical forces, the load is transferred between the matrix and the fiber and is governed by the shear deformation of the matrix around the fibers. This shear deformation is produced because of the high Young's modulus of the fiber and the large differences between the mechanical properties of the composite constituents. The mechanical properties of the composites are influenced by component properties, fiber orientation, and fiber–matrix interfacial adhesion.

The interface is a region at least several molecular layers thick with properties intermediate between those of the fiber and matrix phases and arises due to the peculiar restrictions on molecular motions in this zone. Matrix molecules may be anchored to the fiber surface by chemical reaction or adsorption and determine the extent of interfacial adhesion. Fiber modification reduces hydrophilicity of the fiber and improves the physical/chemical interactions between the fiber and matrix. Treatment makes the surface of the fiber very rough and provides better mechanical interlocking with the polymer matrix.

Extensive work was carried out by Joseph et al. on many treatments of natural fiber (alkali, permanganate, peroxide (DCP and BPO), isocyanate) for improving the mechanical properties of sisal fiber LDPE composites. The results showed that in every case the mechanical properties were increased with chemical treatment but peroxide treatment showed the best results (Table 22.12) [58, 59].

Mohanty et al. [105] used 30% sisal fiber with a 6-mm average length of fiber for different types of chemical treatment such as NaOH, cyanoethylation and 2-type maleic anhydride-grafting polypropylene (G-3015) and hostaprim (HC₅). Results showed that the NaOH and cyanoethylation treatments improved the mechanical properties; details are shown in Table 22.12. With the treatment of G-3015 and HC₅, the tensile strength attained was 43.66 MPa and 43.84 MPa, respectively (HC₅), which was higher than that of untreated sisal fiber composites (29.25 MPa). Moreover, with the G-3015 and HC₅ treatments results, the flexural strength was 62.42 MPa and 63.66 MPa, respectively, which were found to be higher than the flexural strength of untreated sisal fiber composites (48.96 MPa). The impact strength of sisal fiber composites under different treatments NaOH, cyanoethylation, G-3015, and HC₅ were 53.69 J/m, 60.43 J/m, 60.43 J/m, and 81.57 J/m, respectively (The impact strength of untreated sisal fiber composite was 51.79 J/m) [105].

Increase in the surface area of fibre, enhances the fibre matrix adhesion and contributing to the improvement of mechanical properties. Grafting of fiber increases the adhesion property of fiber with matrix and its composites showed improved mechanical properties (Table 22.12) [105].

The work carried out by Kalaprasad and Thomas [34] shows different chemical surface modifications such as alkali, acetic anhydride, stearic acid, permanganate, maleic anhydride, silane, and peroxides improving the interfacial adhesion and compatibility between the fiber and matrix. A polyethylene thermoplastic matrix with sisal and glass hybrid composites was developed. The results showed that in all treatments, tensile strength increased about 10–30% and peroxide treatment showed maximum tensile strength and Young's modulus [34].

Ichazo et al. [120] reported the mechanical properties of treated and untreated sisal fiber. Polyolefin composites were developed using 20% fiber loading. Acetic anhydride was used and acetylated treatment showed an improved tensile modulus by 30–40%. But the impact strength and elongation at break decreased because of the rigid interface between fiber and matrix [120].

22.6 Application of Sisal Fiber-based Composites

Using sisal fiber in composites provides several advantages in terms of product design flexibility, noise absorption, insulation; impact resistance in a crash followed by weight reduction contributes to saving fuel [154].

Sisal fiber has not been optimally utilized and commercially exploited given its abundant availability and good characteristics. Sisal fiber has potential in manufacturing composites that can be used in building materials, automobiles, locomotives, and aerospace applications and it can also replace synthetic fibers such as asbestos and glass fiber in roofing sheets [121]. There is growing interest in the use of sisal fiber due to its high specific strength, significant processing advantages, and low density in composites [122, 123]. In the face of growing industrialization the automotive, packaging, and construction industries, have been forced by the new environmental policies to search for new materials that can substitute for the traditional composite materials consisting of a plastic matrix and inorganic filler as reinforcement matrices. Inorganic fibers have several disadvantages: nonbiodegradability, the abrasion in the processing equipment, and the human health problems associated with operation, processing, and handling of the manmade fibers such as glass, aramid, carbon, and asbestos fibers used in thermoplastic/thermoset composites [104, 124]. However, a major technological gap in sisal technology is the manufacture of the sisal yarn for which the continuous sisal fiber needs to be made and spindling it on bobbins for looming. To achieve this, various techniques such as mechanical extraction of sisal fiber using Raspador machine, softening, sisal yarn-making process, and fabric making using a handloom machine are under progress at AMPRI (CSIR) Bhopal [121].

Sisal is used by industry in three grades (World of Sisal home page 2006). Lower grade fiber is processed by the paper industry because of its high content of cellulose and hemicelluloses. Medium grade fiber is used in the cordage industry for making ropes and baler and binder twine. Whereas ropes and twines are widely employed for marine, agricultural, and general industrial use, high grade fiber is converted after treatment into yarns and used by the carpet industry.

In the ancient period, clay reinforced with straw was used to build walls of dwellings [125, 126]. However, with the development of more durable materials such as metals, the interest in natural materials was lost [125]. In 1941, composites, particularly those based on natural fiber reinforcement received increased attention [41]. Natural fibers were used for making seats, bearings, and fuselages in aircrafts during World War II, which was due to the shortage at that time of aluminum for bearings in ships [127]. However, now attention is given to use natural fiber due to various global environmental threats.

For effective utilization of sisal as reinforcement material, an entire chain-based process is to be followed. This includes the farming, extraction, and processing of fiber, yarn and fabric making, manufacturing of the component, and release of the required product to the user agency/industry. The use of sisal fiber in composites for different applications may follow two different routes, as explained in the flow chart in Fig. 22.7. In the first, the green fiber of the sisal plant is extracted using a mechanical extraction process (Raspador) followed by processing of the fiber. Thereafter two methodologies may be adopted for making the composites. In the first process, fiber will be used for reinforcement in different types of polymer matrices, whereas in the second case, the processed fiber is crimped, by chemical and physical means and the yarn produced mechanically. This yarn, using looms, is converted into fabric to get textile composites for applications such as building, automotive, defense, railways, and geotextiles.

22.6.1 Applications of Sisal Fiber Composites in Building Materials

The traditional building material aggregate such as sand, stone, gravel, cement, steel, brick, block, tiles, paint, and timber have been produced from existing natural resources. Over exploitation of all such building materials leads to environmental damage. Also, due to the high transportation costs of these raw materials and environmental restrictions, there is a mismatch in the demand and supply positions both in rural and urban centers. It is essential, therefore, to find an alternative, a substitute for conventional building materials for the construction industry. Keeping in view the depletion of available natural resources, for instance, deforestation, reduction in availability of fine and coarse aggregates and environmental restrictions, it is necessary to use the available natural resources suitably and develop alternative building materials.

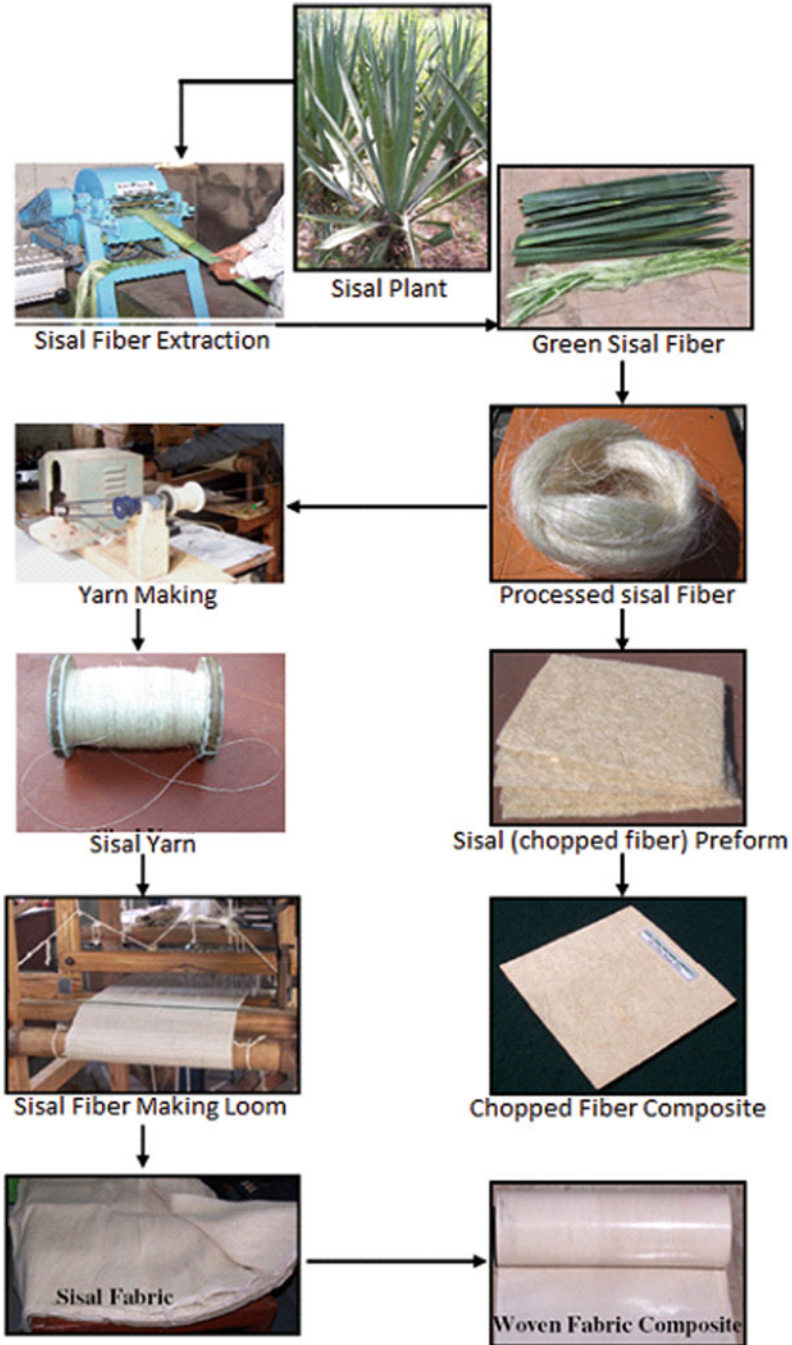


Fig. 22.7 Flow chart for development of Sisal fiber composites

The building industry is under enormous pressure and is unable to meet the demands from different construction sectors. Wood is in short supply, and it is difficult to procure seasoned timber in required quantities. There is a serious need to combat wood scarcity. Existing wood substitutes such as reconstituted panel products: particle/fiber boards, ply wood, and other materials cannot meet the increasing demand for wood without the development of wood substitutes. One important option is to promote development and utilization of natural fibers for the development of composites.

Various attempts have been made recently to rationally utilize abundantly available natural fibers such as jute, sisal, coir, palm, bagasse, and wood fibers in polymer matrices such as polyester, epoxy, and phenolics, to be used as building materials. Developmental work on low-cost building materials based on henequen/palm/sisal fibers and unsaturated polyester resins have been undertaken as a cooperative research project between the government of Mexico and UNIDO [128]. Sisal and coir are one of the most studied fibers, but bamboo, jute, hemp, and grasses have also been studied for making fiber concrete and sheeting materials [129]. The Swedish Cement and Concrete Institute has also been involved with sisal products for many years, especially with respect to research in their durability. Field experience has also been gained by installing sisal fiber-based roofing tiles in South Africa [130]. A new potential application of sisal is for manufacturing corrugated roofing panels that are strong and cheap with good fire resistance [5]. Asbestos fibers are carcinogenic; therefore, sisal fiber cement corrugated roofing sheets are manufactured, which are eco-friendly and an effective alternative to asbestos fiber. Figure 22.8 shows sisal fiber cement corrugated roofing sheet.

Under a mission mode program of AMPRI (CSIR) Bhopal, India, the major tasks involved are exploitation of sisal fiber for engineering applications.

This program is expected to create major employment potential in the rural sector for sisal cultivation; fiber extraction and processing; ropes and cordages; handicrafts; fiber looming; yarn making; carpets and mats; and other value added products.

However, in order to effectively utilize some of the natural fiber as a raw material in developing alternative building materials, the physical–chemical, engineering, mineralogical, and morphological properties of the fiber and other additives have been evaluated at AMPRI Bhopal. Various lab and bench scale experiments were conducted and the process details for commercial scale trials were optimized. In this context, this section of the work addresses the processes and technologies developed at AMPRI Bhopal for large-scale utilization of jute fiber – industrial waste in building materials, wood substitute products, and sisal fiber-reinforced roofing sheets, etc. [121].

Asbestos fiber presently used in cement matrix for the production of asbestos sheets leads to serious health hazards. AMPRI, Bhopal has developed a technology to effectively utilize fly ash along with organic fibers for the production of corrugated roofing sheets.

Sisal Fiber-Reinforced-Fly Ash Cement Roofing Sheets

This product is an alternative to the carcinogenic asbestos cement sheets. The strength of sisal/cement sheet is comparable with asbestos cement sheets. The microstructure of sisal fiber within a cement matrix is shown in Fig. 22.9, showing good improved interfacial bonding. Sheets can be made manually or mechanically. It thus has great potential for use in rural areas. These products can be used in roofing, partitions, etc.

The salient features of this material are:

- It is a good substitute for asbestos cement roofing sheets
- Only renewable natural resources are used
- It is eco-friendly
- It can be repaired
- It has no health hazards
- It can generate employment in the rural areas
- It is cost-effective



Fig. 22.8 Sisal fiber cement roofing sheet

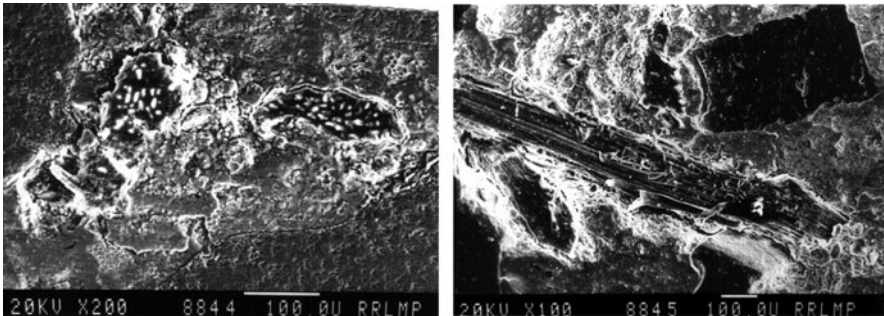


Fig. 22.9 Cross section of Sisal fiber with cement matrix

Wood Substitute Products

Natural fiber (jute fabric) and industrial wastes are used along with polymer to make composite wood substitute products. In this process, processed fabric of jute fiber and industrial wastes such as fly ash/red mud/marble slurry dust with polymer were synthesized in molds of required length and width. The composite laminates were fabricated with requisite pressure and cured at room temperature. Various products such as full size door shutters and panels can be fabricated and designed according to requirement. The industrial waste-based polymer composite products are comparable to natural wood and thus could be used as a wood substitute for doors, windows, ceilings, flooring, partitions, and furniture, etc. The products are cost-effective and no further maintenance is required. This is an environment friendly product with fruitful utilization of fly ash/red mud/marble slurry dust (Table 22.14).

The salient features of the products are:

- Stronger than wood
- Weather resistant and durable
- Corrosion resistant
- Termite fungus, rot and rodent resistant
- Fire retardant, self-extinguishing
- Cost effective and maintenance free

Table 22.14 Properties of the developed composites

S. No.	Properties	Red mud jute fiber polymer composite	Red mud sisal fiber polymer composite	Fly ash jute fiber polymer composite	Fly ash sisal fiber polymer composite
1.	Density (gm/cm ³)	1.72–1.76	1.60–1.64	1.64–1.68	1.60–1.68
2.	Moisture content (%)	0.20–0.38	0.48–0.56	0.42–0.48	0.40–0.50
3.	Modulus of rupture (N/mm ²)	85.00–95.00	78.00–88.00	80.00–92.00	83.00–90.00
4.	Tensile strength (N/mm ²)	22.00–24.00	18.00–23.00	20.00–22.00	20.00–23.00
5.	Compressive strength perpendicular to surface (N/mm ²)	78.48–101.00	70.00–95.00	75.00–95.00	78.00–98.00
6.	Compressive strength parallel to surface, (N/mm ²)	44.00–51.00	42.00–50.00	42.50–51.50	41.00–48.00
7.	Water absorption				
	2 h (%)	0.15–0.40	0.20–0.35	0.18–0.38	0.17–0.32
	24 h (%)	1.10–1.50	1.15–1.40	1.15–1.30	1.25–1.35
8.	Swelling in water				
	Length (%)	0.00–0.36	0.00–0.48	0.00–0.52	0.00–0.80
	Width (%)	0.00–0.47	0.00–0.62	0.00–0.70	0.00–0.95
	Thickness (%)	0.00–1.38	0.00–1.30	0.00–1.78	0.00–1.78
9.	Fire residency's (duration of self extinguishing)	15	20	18	22

Source: Saxena et al. [121]

Table 22.15 Building materials/components

S. No	Building materials	Composites	Plant fiber used	Institute(s)
1.	Furniture, doors, panels	R-Wood	Jute	AMPRI, Bhopal
2.	Doors and panels	Bamboo mat board (BMB) Bamboo mat veneer composites (BMVC)	Bamboo	AMPRI, Bhopal IPIRTI, Bangalore BMTPC, New Delhi
3.	Panels	Sandwich composites	Sisal and jute	AMPRI, Bhopal CBRI, Roorkee
4.	Roofs	Corrugated roofing sheets	Sisal Coir/wood wool	AMPRI, Bhopal CBRI, Roorkee
5.	Doors	Jute pultruded door frames, medium density composites	Bamboo Jute coir	IPIRTI, Bangalore CBRI, Roorkee
6.	Wood substitute	Poly coir	Coir fiber	NIIST, Tiruvananthapuram
7.	Partitioning, false ceiling, surface paneling, roofing, furniture, cupboards, wardrobes	Natural fiber reinforced boards	Jute and coir	Natural Fibertech, Bangalore NIRJAFT, Kolkata

Source: <http://www.expresstextile.com>, 2005

- Incorporation of jute fabric with other raw materials such as in red mud/fly ash/marble slurry to polyester increased the tensile strength, modulus of rupture, and resistance to abrasion (Table 22.14).
- Suitable combination of jute fabric, polyester, and industrial wastes can be used to get the desired properties of the laminates.
- The developed composites have the potential to be used in a variety of engineering applications, for instance, as wood substitutes, which will help in reduction of deforestation and environmental pollution.

Addition of jute fabric improved reinforcement in the composites leading to improvement in the latter's mechanical properties. Incorporation of red mud in these composites increased the density, modulus of rupture, and resistance to abrasion. However, the impact strength is reduced. This property can be improved to some extent by the addition of sisal fibers. Reinforcement of red mud imparts high abrasion resistance, which makes it suitable for flooring tiles. Various building components manufactured by using some plant fibers are shown in Table 22.15.

Sisal Fiber Composites

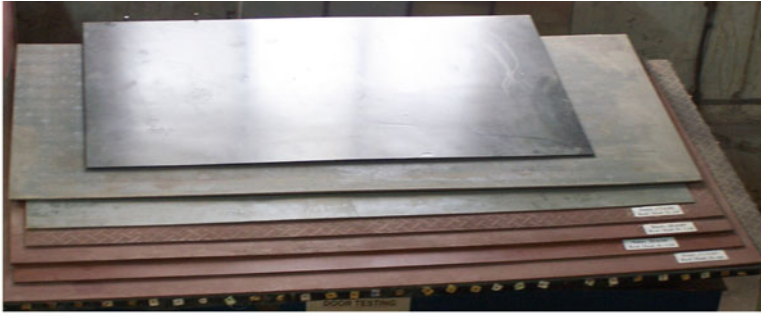
In order to effectively exploit the potential of sisal fiber, jute fibre for various engineering applications, the building materials development group at Advanced Materials and Processes Research Institute (AMPRI) Bhopal has set up facilities for the advanced and user-friendly inputs on sisal fiber-based technologies for sustainable rural employment, income generation, followed by training for entrepreneurs and rural Indians. In addition, deliverables drive the development of sustainable processes, with a comprehensive package of green technologies for sisal fiber-reinforced composites for use in a wide spectrum of applications, as shown in Fig. 22.10.

22.6.2 *Automotive Applications of Sisal Fiber*

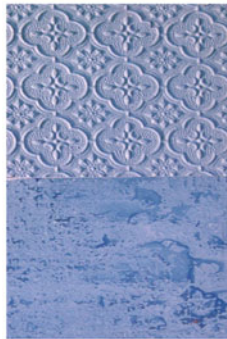
Plant fibers show significant contribution in automobile applications due to characteristics such as high stiffness with light weight per unit area, easy to recycle, 30–40% lighter than glass fiber; reduced fuel consumption, low cost, no wear of tooling, no health hazard, good thermal and acoustic insulating properties etc. Actual industrial demand for natural fibers has increased only over the past few years. In 2005, the first time natural fibers (without wood and cotton) were used in automotive composites [131]. Natural fiber composite materials are being used for making many components in the automotive sector [132].

Sisal and jute fibers have been used in the German automotive industry for years [121]. Mercedes first used jute-based door panels in its E-Class vehicles in 1996. Then in September 2000, Daimler Chrysler began using natural fibers for their vehicle production based in East London, South Africa. The company was able to implement technology transfer from their German plants to South Africa for the entire process chain. This included farming of sisal, processing of fibers, manufacturing of components and the release to the Mercedes Benz Plant of Daimler Chrysler South Africa [26]. In recent years, there has been increasing interest in the replacement of glass fibers in reinforced plastic composites by natural plant fibers such as flax, hemp, and sisal parts [53]. Like glass, the natural fibers combine readily with a thermoplastic or thermosetting matrix to produce commodity goods [133]. The automotive industry requires composite materials to meet performance criteria as determined in a wide range of tests. Typical market specification includes ultimate breaking force and elongation, flexural properties, impact strength, fogging characteristics, flammability, acoustic absorption, suitability for processing: temperature and dwell time, odor, water absorption, dimensional stability, and crash behavior [26].

Plant fibers are currently only used in the interior of passenger cars and truck cabins. Besides their use in trim parts such as door panels or cabin linings, plant fibers are used extensively for thermo-acoustic insulation. Such insulating materials, mainly based on cotton fibers recycled from textiles, have relatively high fiber content of more than 80% by weight. Trim parts in Brazilian trucks, made of a mixture of jute, coffee bag wastes, and polypropylene bags show that recycling



Panels for partitions



Tiles



Doors

Fig. 22.10 Natural fiber based wood substitute products

sometimes can lead to advanced applications. Another well-established field of application is the use of coconut fibers bonded with natural latex for seat cushions. For this application the ability of plant fibers to absorb large amounts of humidity leads to an increased comfort that cannot be reached with synthetic materials. Aside from this kind of developments, fundamentally new applications have not been realized in recent years.

Table 22.16 Various automotive parts made with plant fiber composites

S. No.	Automobile	Parts	Plant fiber used
1.	Brazilian Trucks	Trim parts seat cushions	Jute coir
2.	Mercedes Benz (E-Class)	Door panels	Sisal/flax
3.	Mercedes Benz (C-Class)	Rear panel shelf	Sisal, cotton
4.	Mercedes Benz (S-Class)	Inner door panels	Hemp
5.	Chevrolet Impala	Trim panels	Flax
6.	Daimler Chrysler (M-B Travego Coach)	Engine and transmission cover 95% recyclable vehicles	Sisal, flax, coir, hemp, cotton
7.	General Motors (Opel Astra/Vectra)	Inner door panels, Seatbacks	Hemp, Kenaf, Flax
8.	Toyota	Package shelves	Kenaf

Sources: Rai and Jha [134], <http://www.osec.ch>, <http://www.acmainfo.com>, <http://www.siamindia.com>, Sharma [135]

Natural fiber composites with thermoplastic and thermoset matrices have been embraced by European car manufacturers and suppliers for door panels, seat backs, headliners, package trays, dashboards, and many interior parts (Table 22.16). Natural fibers such as kenaf, hemp, flax, jute, and sisal offer such benefits as reduction in weight, cost and CO₂, less dependence on foreign oil sources and recyclability. Glass fiber reinforced plastics have proven to meet the structural and durability demands of automobile interior and exterior parts. However, it exhibits shortcomings such as its relatively high fiber density (40% higher than natural fibers), difficulty to machine, poor recycling property, and potential health hazard. An ecological evolution of natural fiber mat as compared to glass fiber mat offers another prospective use of natural fiber reinforcement. Flax, sisal, and hemp are processed into door cladding, seatback linings, floor panels, and various other automotive parts [53].

Various automotive parts made of natural fiber composites are shown in Table 22.16. The use of plant fiber (sisal/flax/hemp etc.) based automobile parts such as trim parts, various panels, shelves, and brake shoes are attracting automobile industries worldwide because of its weight reduction, energy and cost saving. Conservative estimates indicate that about 6,000 TPA plant fiber-based composite parts can find their way into passenger cars and multi-utility vehicles [17].

Sisal is used in door cladding, seatback linings, and for packaged shelves (the space behind the rear seats of sedans). The BMW group incorporates a considerable amount of renewable raw materials in to its vehicles. Each BMW 7 series car boats 24 kg of renewable raw materials, with flax and sisal in the interior door lining panels [136].

Prospects for the Use of Sisal Fiber in Automotive Industry

Door panels; cabin linings; brake liners; thermo-acoustic insulation; trim parts: seat cushions and backs; headliners; package trays; dash boards; trunk liners. The possible stakeholders for the utility of sisal fiber in automotive components industry

are: Mercedes Benz, Freightliner, Daimler Chrysler, Chevrolet, and General Motors, Mahindra & Mahindra, Tata Motors and Hero Honda etc.

The cost benefit analysis, techno-commercial feasibility, and the challenges for sisal fiber exploitation for various engineering applications are as follows:

- Sisal is a xerophyte, grows in wastelands. Conserves soil and earns carbon credits
- Assured sustainable fiber production: 2.5 ton/ha for 6–8 years
- Surface treatments enable sisal fibers to be used as reinforcement in a polymer matrix
- Advantageous over mineral and other conventional natural fibers

22.6.3 *Electrical Application of Sisal Fiber*

In order to utilize sisal fiber for electrical applications, several researchers have studied different electrical properties of sisal fiber at different temperatures and frequencies. The work carried out by Xin et al. [138] showed that an increase in frequency decreases the dielectric constant ' ϵ' ' whereas an increase in temperature increases at all frequencies. Increasing the plant age shifts the dissipation factor ($\tan \delta$) peak to higher temperature.

Further, these phenomena were explained on the basis of structural charges. Water absorbed by sisal fibers has OH^- anions which act as dipoles. Other than OH^- anions, there are several impurities and ions on the fibers. These dipoles and ions contribute to the ϵ' and $\tan \delta$ behaviors of sisal fiber. At low frequencies, high ϵ' and $\tan \delta$ values in sisal fiber are caused by the dipolar contribution of absorbed water molecules. ϵ' Values at intermediate frequencies are the result of contributions from space charge polarization. At high frequencies, the contribution of polarization of absorbed water molecules and space charge decreases and electronic and atomic polarization becomes operative. Increase in temperature affects the mobility of ions and consequently changes the ionic contributions [139, 140].

The electrical properties of sisal fiber reinforced LDPE have been studied with respect to the effects of frequency, fiber content, and fiber length. The dielectric constant increases steadily with increasing fiber content for all frequencies in the range $1-10^7$ Hz. It is also noted that dielectric constant decreases with an increase in fiber length and frequency. Maximum dielectric constant values are obtained at low frequencies. Sisal/LDPE composites of 1 mm fiber length and 30% fiber content have the highest values of dielectric constants at all frequencies. The values of volume receptivity decrease with increase of frequency and fiber content i.e., the electric conductivity of composites are greater than neat LDPE. When compared to glass/LDPE composites, the same trend in electrical properties is observed, but the charges of dielectric constants of the latter composites with frequency and fiber content are smaller as a result of their lower interfacial polarization. The dielectric constant, dielectric loss factor, and electrical conductivity of 25% sisal LDPE can be increased considerably by adding 5% carbon black. The composites can be used in antistatic applications to dissipate static charges [56, 57].

22.6.4 Application of Sisal Fiber in Railways

Composite materials offer some significant advantages to metals in many structural applications in railways to the effect that they are lightweight, cost-effective, corrosion resistant, energy saving, wear resistance and fire retardant. In railways, the gear case, main doors, luggage racks, floor/roof panels, berths, chair backings, interior panels and partitions, interior furnishing and seating, modular toilets, and lightweight coaches are made from different natural fiber composites and their combinations. Weight savings of up to 50% for structural and 75% for nonstructural applications bring associated benefits of high speed, reduced power consumption, lower inertia, less track wear, and the ability to carry greater pay-loads. Natural hard fibers such as coir, jute, etc. impregnated with phenolic resins are used for manufacturing of composite boards. Eighty percent of the materials used in the composite are natural fibers [121]. In the railways, sisal fiber has major role for potential application in many areas. Indian Railways have initiated action for introducing composites in the coaches. In facts, for a mass transit system, lightweight coaches are important for achieving higher speed. The present use of GRP products due to its corrosion resistance and workability would also be substituted with natural fiber composites. Already, the natural 1.6-mm thick fiber thermoset composites are being used by the railways for roof ceiling, flooring, and is targeted to substitute timber and plywood usage in the coach [155]. Natural fiber-based composite materials in India have great scope in the railways where the resulting performance improvements would be significant in terms of weight savings, high-speed, reduced power consumption, lower inertia, less track wear, etc. It is estimated that about 350 TPA fiber composites is required in the Indian railways for manufacturing of doors, luggage racks, panels, partitions, seating, etc. [17, 141].

22.6.5 Application of Sisal Fiber in Geotextiles

Geotextiles have been used for many years in roadway construction and soil stabilization to avoid soil erosion. Geotextiles were made of natural fibers, fabrics or vegetation mixed with soil even in the past. In recent days, geotextiles have been in use for modern road construction. Geotextiles are the subfamily in the large family of “Geosynthetics”; other subfamilies include geogrids, geonets, geomembranes, geosynthetic clay liners (GCL), geopipes, and geocomposites. Geotextiles are woven and nonwoven fabrics. A geotextile can be made either using synthetic or natural fibers. It is designed in such a way as to be permeable to filtrate fluids and control migration of soil. Geotextiles can be woven, knitted, or nonwoven and can be fabricated suitable for different applications. The nonwoven geotextile is an arrangement of fibers either oriented or randomly patterned. These geotextiles support water flow in addition to stabilization of

soil. There are many other uses of geotextiles such as roads, aggregate drains, pavement overlays, and erosion control. Recent development in this area is the use of natural geotextiles, which include fabric formed using coir, sisal, and the natural fiber from the husk of coconuts. These geotextiles have exceptional strength due to the high content of cellulose lignin polymer in them. Besides, they are naturally degradable, which may be attractive in certain applications such as natural stream bank restoration. Other natural fiber geotextiles include jute, mixed coir jute, and mixed sisal jute. The market potential of geotextiles for roads, paved road networks, and railways applications in India is estimated to be 272,500 tons, for which sisal textile can also be used [130, 142, 143, 150].

22.6.6 Defense Applications of Sisal Fiber

There are six main fields of applications for military use that might be of immediate interest in the use of biofiber materials. These are uniforms and other textile applications, personal safety equipment, transportation vehicles, field housing and other construction, packaging, weapon components, and utility tools. Defense applications include protective clothing and systems integration in the textile itself. In addition to the different composite materials, a steel composite hybrid system is also made. With the current generation of biocomposites for military transport vehicles, most applications would be interior, such as various panels, dashboards, and also textiles. The basic advantages would be the same as for the civilian industry. Cellulose fiber-based composites would make excellent packaging materials due to their light weight and biodegradability.

22.6.7 Application of Sisal Fiber in Packaging Industry

Sisal fiber has very important contribution to meet the future challenges of environmental sustainability in the packaging market. This has further mass scope when it combined with bio-based polymers in developing composite materials to use as packaging materials in the future. The packaging materials for bags, boxes, crates, containers, which are now made of wood can be replaced by cost-effective sisal fiber reinforced composites [17]. The estimated demand for the package materials works out to 93 lakh tons.

22.6.8 Other Applications of Sisal Fiber

AMPRI, Bhopal is involved in R&D activities on sisal fiber extraction, processing, and product design. It has developed a versatile machine (Raspador) for the

mechanical extraction of sisal fiber. The laboratory has been imparting training to people in rural areas, especially women, to make handicrafts of sisal fiber. AMPRI has also developed vermicomposting technology using sisal leaf residue to produce eco-friendly manure. Based on its expertise, the laboratory has developed sisal fiber-reinforced corrugated roofing sheets and sisal fiber-polymer composites, which are alternate building materials superior in quality, eco-friendly, noncarcinogenic, and cost-effective. Basic research and design need to be carried out for the development of crimp to make yarn and various surface treatments and processes to overcome its hydrophilic nature, improving the interfacial bonding and mechanical properties of the fiber. The “Building Materials Characterization and Testing Center” and “Technology Enabling Center” for natural fiber composites are the additional expertise and facilities available. Sisal fiber research and its allied activities such as cultivation, fiber extraction, processing and making value added products are proven sources of employment opportunity and income generation. The present experience indicates that trained artisans and women are able to generate a sustained income through the sisal-related activities. The engineering applications of sisal fiber such as buildings, automobiles, railways etc. are prospective areas that can generate employment. The ease with which fiber can be produced on wastelands in a wide range of agro-climates, the sustained fiber yield for a considerably long duration, and the versatility of the fiber as a potential input material for various applications make it a viable option for employment generation and rural development.

1. *Use in Vermicomposting:* After extraction of the fiber from the leaves about 95% green pulp is obtained in the form of residue. The sisal green pulp is a source of organic matter and this residue will be utilized for manufacturing eco-friendly and valuable vermicompost. This aspect covers the comprehensive utilization of sisal. In vermicomposting, degradation of bio-residues is done with the help of earthworms (*Eisenia Foesia*). This ecofriendly organic manure is rich in nitrogen, phosphorous, potassium, and organic matter [16].
2. *Use in Biodegradable Polymers:* Development of biodegradable materials as an alternative to synthetic materials such as glass fiber-reinforced plastics and other synthetic plastics is the challenge for the present and future generations in the context of global climate change. Moreover, there are various problems associated with synthetic polymer composites due to the inherent problem of life cycle assessment and waste management at the end of its service life. At this juncture, biodegradable materials offer significant advantages provided they are techno-economically viable. Worldwide, considerable work is being done by several researchers for the development of biodegradable polymers leading to manufacturing of biodegradable polymer composites for various engineering applications. The problem related to finding available landfill areas for the final disposal of nonrecyclable polymers has also given rise to the development of biodegradable polymers and blends able to fulfill the new environmental requirements regarding the effective management of waste. Biodegradable polymers have been combined with natural fibers to produce environmentally sound

biocomposites. The addition of short sisal fibers is found to be cost beneficial by decreasing the polymer volume fraction with additional improvement in properties, such as thermal stability, creep behavior, and mechanical properties [18, 144].

3. *Biogas from Sisal Fiber Waste*: In most developing countries, agro-industrial residues are available in abundance. Sisal fiber extraction by-products have been evaluated for animal food production and sisal waste is a good material for biogas production [145]. These wastes have great potential in catering to the energy demand, especially in the small-scale local energy sector. Bio-methane from sisal fiber wastes, a waste product of the sisal industry, is of great importance as a renewable energy carrier that could be used for cooking and power generation [8]. Sisal waste has proved a good feed for anaerobic reactors to produce biogas and this biogas could be used for the generation of electricity [146]. Pilot scale demonstrations show that it is a valuable feedstock for biogas plants to cater to local and rural energy requirements. One ton of sisal pulp can generate 54.3 m³ of biogas by the methanogenesis [146]. Sisal leaves are known to contain wax (0.38%) and hecogenin (0.10%). These expected spin offs are in the form of secondary/allied activities which are labor intensive and have applications in rural and small-scale industrial sectors. The stored biogas made by sisal waste can be used to run two 150 Kw electricity generators for a rated total electricity output of 300 Kw; biogas can also be used in cooking [147]. One of the latest study reports for the first time a two-stage fungi pretreatment for enhanced biogas production from sisal leaf decortication residues. The increase in methane yield is attributed to improved biodegradability of sisal residues after pretreatment. However, there is a great potential of methane generation from biological pretreatment using fungi; further research is required to establish the mechanism of such improvements [7].

22.7 Conclusions and Future Prospects

The results of recent research revealed that plant-based fibers can be effectively used as a reinforcement in polymer matrix composites, replacing synthetic fibers to some extent.

Sisal fiber has relatively high stiffness and low cost, but the disadvantages are high moisture sensitivity and variation in fiber properties. Interest in using sisal fiber in composites has increased in recent years because such composites are lightweight, nonabrasive, nontoxic, and biodegradable. The physical and chemical methods of treating sisal fiber composites improved their mechanical properties because of increased fiber matrix adhesion. Sisal fiber is a potential reinforcement material in polymers, rubber, and in gypsum and cement matrices. This has resulted in innovative technological applications beyond its traditional uses in ropes, carpets, mats, handicrafts, etc. The use of sisal fiber as a renewable raw material in the

plastics industry shows potential uses in the manufacture of different composites. Use of sisal waste has also shown to conserve resources, produce manure and other valuable byproducts (wax and hecogenin) and generate energy (biogas and electricity).

Recently sisal fiber has been autoclaved to get pulp for spinning into the yarn. Further research may focus on the utilization of better or mechanized yarn making/spinning technology to achieve better yarn consistency and higher productivity leading to production of high quality sisal fabric. Also, serious efforts may be initiated for sisal yarn and fabric making as it has not yet been commercially exploited as a reinforcement in composites. Because of the low density and high specific properties of sisal fibers, composites based on these fibers have good applications in the electrical, automotive, railways, buildings materials, boats, geotextiles, defense, and packaging industries. Moreover, reduced equipment abrasion and subsequent reduction of cost will make these composites more attractive.

The present scenario indicates that the use of plant fiber (sisal/flax/hemp etc)-based automobile parts such as trim parts, various panels, seat backs, shelves, brake shoes, etc., are picking up momentum worldwide. Conservative estimates indicate that about 6,000 TPA plant fiber-based composite parts can find their way into passenger cars and multiutility vehicles. Railways are also a potential application industry where it is estimated that about 350 TPA fiber composites will be required in India for manufacture of doors, luggage racks, panels, partitions, seating, etc.

There is a scarcity of sisal fiber supply and a sustainable supply chain needs to be established. For the sustained supply of sisal fiber to make sisal chopped strand mats, sisal fabrics, and composites for user industries, fiber production has to be increased. To achieve this, a larger area has to be brought under sisal cultivation. Mechanical extraction using raspador/decorticator consumes energy; besides, the fiber gets damaged resulting in poor mechanical properties. Therefore, to make the fiber cost-effective and technically sound for engineering applications, further modification in the existing decorticator needs to be made. Sisal textile composites are showing better performance as compared to chopped strand mat composites. The problem faced in making the fabric from sisal fiber is crimping. This is hindering the process of yarn and fabric making. The existing processes for generation of crimp in sisal fiber/fabric looms are only of academic interest, lab scale, and not commercially viable. Hence, some alternative path needs to be evolved following suitable methodologies such as separation of cellulose microfibrils following a microbiological approach for spinning into the yarn. Future research may focus on utilization of better or mechanized spinning technology to get better yarn evenness and higher productivity.

A study on hybrid composites of sisal fiber with other natural fibers or synthetic fiber is needed to achieve optimum benefit for broader applications. Sisal fiber/matrix interface and relationship between interface and bulk composites need to be studied in detail for a better understanding leading to the development of a unique process for better bonding between fiber and matrix and compatibility with a wider range of other materials/components. Further R&D, new initiatives, and innovation are needed to develop a unique mechanism for the manufacture of environmental

friendly and cost-effective processing methods for the composites, and to understand the relationship between processing methods and mechanical properties of the composites and recycling characteristics/options of the sisal fiber reinforced composites, gaining energy and ecological advantage. It is essential to develop/use matrix materials based on renewable/biodegradable resources such as biodegradable polymers. The engineering applications of sisal fibers are the prospective areas and the utility of the sisal fiber makes it a viable option for employment generation and rural development. Further systematic and persistent research on sisal fiber-based technologies will lead to greater scope in the use of this plant resource

Acknowledgment The authors are thankful to Dr. Anil K. Gupta, Director, Advanced Materials and Processes Research Institute (AMPRI) Bhopal, Council of Scientific and Industrial Research (CSIR) India, for the guidance support and permission to publish this article. Authors are also thankful to members of SAPNA (Sisal Action Program for Novel Applications) group of AMPRI, Bhopal, India for necessary support. The contribution of Mr. Pavan K. Srivastava in the preparation of manuscript is thankfully acknowledged. Thanks to Mr. Dharam Raj and other staff of the Building Materials Development Group AMPRI, Bhopal for their valued contribution. The authors are grateful to BMTPC, MoEF and CSIR, New Delhi, India for financial support.

References

1. Berglund L (2006) New concepts in natural fiber composites. Proceeding of the 27th Riso International Symposium on Materials Science. Polymer Composite Materials for Wind Power Turbines: 1-9.
2. John MJ et al (2003) Lignocellulosic fiber reinforced rubber composites, Chap 10. Old City, Philadelphia, pp 252–269
3. Joseph K, Filho RDT, James B, Thomas S et al (1999a) A reviews on sisal fiber reinforced polymer composite. R. Bras. Eng. Agríc. Ambiental, Campina Grande V.3 n.3: 367–379
4. George J, Sreekala MS, Thomas S (2001) A Review on Interface Modification and Characterization of Natural fibre Reinforced Plastic Composites. Polym Eng Sci 41(9): 1475–1485
5. Bisanda ETN (1993) The manufacture of roofing panels from sisal fiber reinforced composites. J Mater Process Technol 38:369–380
6. Sinha MK et al (2009) Crop diversification for profitability in jute and allied fiber crops. Indian J Agron 54(2):221–225
7. Muthangya M et al (2009) Two-stage fungal pre-treatment for improved biogas production from sisal leaf decortication residues. Int J Mol Sci 10:4805–4815
8. Chynoweth DP et al (2001) Renewable methane from anaerobic digestion of biomass. Renew Energy 22:1–8
9. Oksman K, Wallstro L, Berglund LA et al (2002) Morphology and mechanical properties of unidirectional sisal–epoxy composites. J Appl Polym Sci 84:2358–2365
10. Kar CS (2008a) Improved package and practices of sisal cultivation in India. In: Sisal fiber technologies for sustainable rural employments generation. Allied Publication, Delhi, pp 1–7
11. Kar CS (2008b) Nursery management of sisal production of quality planting material. sisal fiber technologies for sustainable rural employments generation. Allied Publication, Delhi, pp 15–23
12. Leadon DA (2006) Brazil sisal producers aim to recapture market share lost to synthetic fibers. Int Fiber J 21. <http://www.braziliansources.com>
13. Wilson PI (1971) Sisal, vol 2. In: Hard fibers research series No. 6. FAO, Rome

14. Li Y, Mai YW, Ye L (2000) Sisal fiber and its composites: a review of recent developments. *Compos Sci Technol* 60:2037–2055
15. Lewin M (2007) *Handbook of fiber chemistry*, Chap 8, 3rd edn. Taylor and Francis, London, pp 460–462
16. Saxena M et al (1998) Fly ash vermicompost from non- ecofriendly organicwastes. *Pollut Res* 17(1):5–11
17. Saxena M, Murali S, Nandan MJ et al (2005) Sisal Potential for employment generation and rural development. In: 3rd International Conference Rural India, pp 208–212
18. Alvarez VA, Vazquez A (2004) Thermal degradation of cellulose derivatives/starch blends and sisal short fiber biocomposites. *Polym Degrad Stab* 84:13–21
19. Das PK, Nag D, Debnath S et al (2010) Machinery for extraction and traditional spinning of plant fibers. *Indian J Tradit Knowl* 9(2):386–393
20. Mukherjee PS, Satyanarayana KG (1984) Structure and properties of some vegetable fibers part 1 Sisal fiber. *J Mater Sci* 19:3925–3934
21. Li Y, Mai YW, Ye L (2000) Sisal fiber and its composites a review of recent developments. *Compos Sci Technol* 60:2037–2055
22. Bai SL, Li RKY, Mai W et al (2002) Morphological study of sisal fibers. *Adv Compos Lett Abst* 11(3)
23. Chand N, Tiwary RK, Rohatgi PK (1988) Bibliography resource structure properties of natural cellulosic fibers –an annotated bibliography. *J Mater Sci* 23:381–387
24. Young R et al (1992) Activation and characterization of fibre surface for composites in emerging technologies for materials and chemicals for biomass. *ACS Symp Ser* 476:12
25. Chand N, Hashmi S (1993) Effect of plant age on structure and strength of sisal fiber. *Met Mater Process* 5:51–57
26. Mohanty AK, Misra M, Drzal LT (2005) *Natural fibers biopolymers and biocomposites*. CRC, Boca Raton
27. Babu MS, Bakshi S, Srikant G et al (2004) Thermoplastic Composites – Technology and business opportunities. In: Proceedings of the international conference & exhibition on reinforced plastics (ICERP 2004), Chennai, India, 12–14 Feb 2004, pp 226–237
28. Leao AL, Rowell R, Tavares N (1997) Application of natural fiber in automotive industry in Brazil- thermofforming process. In: 4th International conference on frontiers of polymers and advanced materials conference proceedings, Caoro, Egypt, Plenum, New York, pp 755–760
29. Young RA (1992) Activation and characterization of fiber surfaces for composites. In: Rowell RM, Schultz T, Narayanan R (eds) *Emerging technologies for materials and chemicals from biomass*, Chap 9. American Chemical Society, Washington DC, pp 115–135
30. Wakida T, Tokino S (1999) *Indian J Fiber Text Res* 21:69.
31. Dong S et al (1992) Rheological properties of corona modified cellulose polyethylene composites. *Polym Eng Sci* 32:1734
32. Albano C, Poleo R, Reyes J et al (2003) Considerations on the mechanical properties of gamma irradiated polyethylene reinforced with sisal fibers. *Revista de la Facultad de Ingeniería de la U.C.V*, vol 18, pp 83–87
33. Kalia S, Kaith BS, Kaur I (2009) Pretreatment of natural fiber and their application as reinforcing material in polymer composites – a review. *Polym Eng Sci* 49:1253–1272
34. Kalaprasad G, Thomas S (2003) Melt rheological behavior of intimately mixed short sisal-glass hybrid fiber-reinforced low-density polyethylene composites. II chemical modification. *J Appl Polym Sci* 89:443–450
35. Sydenstricker THD, Mochnaz S, Amico SC (2003) Pullout and other evaluations in sisal-reinforced polyester biocomposites. *Polym Test* 22:375–380
36. Mishra S, Misra M, Tripathy SS et al (2001) Graft copolymerization of acrylonitrile on chemically modified sisal fibers. *Macromol Mater Eng* 286:107–113
37. Mishra S et al (2001) Potentiality of pineapple leaf fiber as reinforcement in PALF polyester composite surface modification and mechanical performance. *J Reinf Plast Comp* 20 (4):321–334

38. Rong MZ, Zhang MQ, Liu Y et al (2001) The effect of fiber treatment on the mechanical properties of unidirectional sisal-reinforced epoxy composites. *Compos Sci Technol* 61:1437–1447
39. González L, Cervantes-Uc JM, Olayo R et al (1999) Chemical modification of henequen fibers with an organosilane coupling agent. *Compos B* 30:321–331
40. Jacob M, Varughese KT, Thomas S et al (2006) Dielectric characteristics of sisal-oil palm hybrid bio-fiber reinforced natural rubber bio-composites. *Society of Plastics Engineers*, pp 671–680
41. Joseph K et al (2000) Natural fiber reinforced thermoplastic composites, in *Proceeding, Natural Polymers and Agro-fibers Composites*. In: Frollini E, Leão AL, Mattoso LHC (eds) *Natural polymers and agrofibers composites*. São Carlos (Brazil): Embrapa, USP-IQSC, UNESP, pp 159–201
42. Gassan J, Bledzki AK (1999) Alkali treatment of jute fibers: relationship between structure and mechanical properties. *J Appl Polym Sci* 71:623
43. Garcia-Jaldon C, Dupeyre D, Vignon MR (1998) Fibers from semi-retted hemp bundles by steam explosion treatment. *Biomass Bioenergy* 14:251
44. Sreekala MS, Kumaran MG, Joseph S et al (2000) Oil palm fiber reinforced phenol formaldehyde composites influence of fiber surface modifications on the mechanical performance. *Appl Comp Mater* 7:295–329
45. Morrison WH, Archibald DD, Sharma HSS et al (2000) Chemical and physical characterization of water- and dew-retted flax fibers. *Ind Crops Prod* 12:39–46
46. Mishra S, Misra M, Tripathy SS et al (2002) The influence of chemical surface modification on the performance of sisal- polyester bio composite. *Polym Compos* 23(2):164–170
47. Bisanda ETN (2000) The effect of alkali treatment on the adhesion characteristics of sisal fibers. *Appl Compos Mater* 7:331–339
48. Andersson M, Andersson M, Tillman AJ (1989) Acetylation of jute: effects on strength rot resistance, and hydrophobicity. *J Appl Polym Sci* 37:3437. doi:10.1002/app.1989.070371214
49. Rowell RM (1983) *For Prod Abstr* 1:363
50. Hill CAS, Khalil HPS, Hale MD (1998) A study of the potential of acetylation to improve the properties of plant fibers. *Ind Crops Prod* 8:53. <http://www.thefreelibrary.com/Natural+Fibers>
51. Ebrahimzadeh PR (1997) Dynamic mechanical studies of wood, paper and some polymers subjected to humidity changes. Ph.D. thesis, Chalmers University of Technology, Göteborg, <http://www.Fiber2fashion.com>
52. Flemming M, Ziegmann G, Roth S (1995) *Faserverbundbauweisen: fasern und matrices*. Springer, Berlin
53. Bledzki AK, Gassan J (1999) Composites reinforced with cellulose based fibers. *Prog Polym Sci* 24:221–274
54. Mishra S et al (2003) Studies on mechanical performance of biofibre/glass reinforced polyester hybrid composites. *Compos Sci Technol* 63:1377–1385
55. Sreekala MS, Kumaran MG, Thomas S (2002) The mechanical performance of hybrid phenol-formaldehyde-based composites reinforced with glass and oil palm fibers. *Compos Sci & Technol* 62:339–353
56. Paul A, Joseph K, Thomas S (1997) Effect of surface treatments on the electrical properties of low-density polyethylene composites reinforced with short sisal fibers. *Compos Sci Technol* 57:67–79
57. Paul A et al (1997) Electrical properties of natural fiber reinforced low-density polyethylene composites a comparison with carbon black and glass fiber filled low-density polyethylene composites. *J Appl Polym Sci* 63:247–266
58. Joseph K, Thomas S, Pavithran C (1996) Effect of chemical treatment on the tensile properties of short sisal fiber-reinforced polyethylene composites. *Polymer* 37(23): 5139–5149

59. Joseph K, Varghese S, Kalaprasad G et al (1996) Influence of interfacial adhesion on the mechanical properties and fracture behaviour of short sisal fiber reinforced polymer composites. *Eur Polym J* 32(10):1243–1250
60. Joseph PV, Mathew G, Joseph K et al (2003) Dynamic mechanical properties of short sisal fiber reinforced polypropylene composites. *Composites Part A: Applied Science and Manufacturing* 34:275–290
61. Joseph PV, Joseph K, Thomas S et al (2003) The thermal and crystallisation studies of short sisal fiber reinforced polypropylene composites. *Compos A* 34:253–266
62. Williams GI, Wool RP (2000) *Appl Compos Mater* 7:421
63. Coutinho FMB, Costa THS, Carvalho DS (1997) Polypropylene–wood fiber composites: effect of treatment and mixing conditions on mechanical properties. *J Appl Polym Sci* 65:1227
64. González L (1997) Applications of an azide sulfonyl silane as elastomer crosslinking and coupling agent. *J Appl Polym Sci* 63:1353
65. Culler SR, Ishida H, Koenig JL (1986) The silane interphase of composites: Effects of process conditions on γ -aminopropyltriethoxysilane. *Polym Compos* 7:231
66. Ghatge ND, Khisti RS (1989) Performance of new silane coupling agents alongwith phenolic no- bake binder for sand core. *J Polym Mater* 6:145
67. Sefain MZ et al (1993) Kinetics of heterogenous cyanoethylation of cellulose. *Polym Int* 32:251
68. Mohanty AK, Misra M, Drzal LT et al (2001) Surface modifications of natural fibers and performance of the resulting biocomposites an overview. *Compos Interf* 8(5):313–343
69. Monte SJ, Sugeran G (1984) *Polym Eng Sci* 24:1369
70. Zahran MK, Rehan MF, ElRafie MH (2005) single bath full bleaching of flax fibers using an activated sodium chlorite/hexamethylene tetramine system. *J Nat Fibers* 2:49–67
71. Raj RG et al (1988) *Polym Compos* 9:404
72. George J, Janardhan R, Anand J et al (1996) Melt rheological behaviour of short pineapple fibre reinforced low density polyethylene composites. *Polymer* 37:5421–5431
73. Nair KCM, Thomas S, Groeninckx G (2001) *Compos Sci Technol* 61:2519
74. Wang B (2004) Pre-treatment of flax fibers for use in rotationally molded biocomposites. M. Sc. Thesis, University of Saskatchewan, Canada
75. Saxena M, Kathal A (2004) Development of innovative building materials using polyester, red mud and sisal fiber fabric. In: *RTBM Proceedings*, pp 238–248
76. Li Y et al (2007) Chemical treatments of natural fiber use in natural fiber–reinforced composites: a review. *J Polym Environ* 15:25–33
77. Joseph PV, Rabello MS, Mattoso LHC et al (2002) Environmental effects on the degradation behaviour of sisal fiber reinforced polypropylene composites. *Compos Sci Technol* 62:1357–1372
78. Ganan P, Garbizu S, Llano-Ponte R et al (2005) Surface modification of sisal fibers effects on the mechanical and thermal properties of their epoxy. *Polym Compos* 26:121–127
79. Nair KCM, Diwan SM, Thomas S (1996) Tensile properties of short sisal fiber reinforced polystyrene composites. *J Appl Polym Sci* 60:1483–1497
80. Idicula M, Boudenne A (2006) Thermo physical properties of natural fiber reinforced polyester composites. *Compos Sci Technol* 66:2719–2725
81. Dostal CA (1987) *Engineered materials handbook: composites, vol 1*. ASM International, Metals Park, OH, USA
82. Strong AB (1989) *Fundamentals of composites manufacturing: materials, methods, and applications*. Society of Manufacturing Engineers (SME), Dearborn, Michigan, 252 p
83. Washington DC: US environmental Protection Agency U.S. Office of enforcement and Compliance Assurance (1995) *Introduction to composites, 3rd edn*. Society of the Plastics Industry, Washington DC
84. Silva FA, Chawla N, Filho RDT (2008) Tensile behavior of high performance natural (sisal) fibers. *Compos Sci Technol* 68:3438–3444
85. Barkakaty BC (1976) Some structural aspects of sisal fibers. *J Appl Polym Sci* 20:2921–2940

86. Bisanda ETN, Ansell MP (1991) The effect of silane treatment on the mechanical and physical properties of sisal-epoxy composites. *Compos Sci Technol* 41:165–178
87. Joseph K, Thomas K, Pavithran C (1992) Viscoelastic properties of short sisal fiber filled low-density polyethylene composites. Effect of fiber length and orientation. *Mater Lett* 15:224
88. Joseph K, Thomas K, Pavithran C (1993) Dynamic mechanical properties of short sisal fiber reinforced low-density polyethylene composites. *J Reinf Plastics Compos* 12:139
89. Joseph K, Thomas K, Pavithran C et al (1993) Tensile properties of short sisal fiber reinforced polyethylene composites. *J Appl Polym Sci* 47:1731
90. Khazanchi AC et al (1990) Material science of natural organic fiber reinforced composites in polymer/cement/mud matrix for construction engineering. In: Hamelin P, Verchery G (eds) *A book on textile composites in building construction*. Pluralis, France, pp 69–76
91. Mattoso LHC, Ferreira FC, Curvelo AAS (1997) Sisal fiber Morphology and applications in polymer composites. In: Leao AL, Carvalho FX, Frollin E (eds) *Lignocellulosic-plastics composites*. USP/UNESP, Sao Paello, pp 21–51
92. Yi C, Tian L, Tang F et al (2009) Crystalline transition behavior of sisal in cycle process. *Society of Plastics Engineers*. <http://dx.doi.org/10.1002/pc.20885>
93. Bismarck A, Mohanty AK, Aranberri-Askargorta I et al (2001) Surface characterization of natural fiber surface properties and water up take behaviour of modified sisal and coir fiber. *Green Chem* 3:100–107
94. Bogoeva G, Avella M, Malinconico M et al (2007) Natural fiber eco composites. *Polym Compos* 28:98–107
95. Shibata M, Ozawa K, Teramoto N et al (2003) Biocomposites made from short abaca fiber and biodegradable polyesters. *Macromol Mater Eng* 288:35–43
96. Geethamma VG et al (1999) Composite of short coir fibers and natural rubber: effect of chemical modification, loading and orientation of fiber. *Polymer* 39:1483–1491
97. Lubin G (1982) *Handbook of composites*. Van Nostrand Reinhold, New York
98. Li Y (2006) Processing of sisal fiber reinforced composites by resin transfer molding. *Mater Manuf Process* 21(2):181–190
99. Arzondo LM, Vazquez A, Carella JM et al (2004) A low-cost, low-fiber breakage, injection-molding process for long sisal fiber reinforced polypropylene. *Polym Eng Sci* 44(9):1766–1772
100. Pal S, Mukhopadhyay D, Sanyal S et al (1988) Studies on process variables for natural fiber composites—effect of PEAP as interfacial agent. *J Appl Polym Sci* 35:973–985
101. Sree Kumar PA, Joseph K, Unnikrishnan K et al (2007) A comparative study on mechanical properties of sisal-leaf fiber-reinforced polyester composites prepared by resin transfer and compression moulding techniques. *Compos Sci Technol* 67:453–461
102. Singh B, Gupta M, Verma A (1995) Mechanical behaviour of particulate hybrid composite laminates as potential building materials. *Construct Build Mater* 9:39–44
103. Zhong JB, Lv J, Wei C (2007) Mechanical properties of sisal fiber reinforced urea formaldehyde resin composites. *Express Polym Lett* 1(10):681–687
104. Kim HJ, Seo DW (2006) Effect of water absorption fatigue on mechanical properties of sisal textile-reinforced composites. *Int J Fatigue* 28:1307–1314
105. Mohanty AK, Verma SK, Nayak SK et al (2004) Influence of fiber treatment on the performance of sisal polypropylene composite. *J Appl Polym Sci* 94:1336–1345
106. Khoathane MC (2005) The processing properties of natural fiber reinforced higher α -olefin based thermoplastics. *Magister Technology Polymer Technology*, pp 1–85
107. Beckermann G (2007) Performance of hemp fiber reinforced polypropylene composites materials. Thesis, Materials and process engineering, Waikato University
108. Bourmaud A, Baley C (2007) Investigations on the recycling of hemp and sisal fiber reinforced polypropylene composites. *Polym Degrad Stab* 92:1034–1045
109. Mishra S, Naik JB (2005) Effect of treatment of maleic anhydride on mechanical properties of natural fiber polystyrene composites. *Polym Plastics Technol Eng* 44:663–675

110. Antich P, Vazquez A, Mondragonb I et al (2006) Mechanical behavior of high impact polystyrene reinforced with short sisal fibers. *Compos A* 37:139–150
111. Sreekumar PA, Leblanc N, Saiter JM (2009) Characterization of bulk agro-green composites sisal fiber reinforced wheat flour thermoplastics. *Polym Compos* 31:939–945
112. Jarukumjorn K, Suppakam N (2009) Effect of glass fiber hybridization on properties of sisal fiber polypropylene composites. *Compos B* 40:1–5
113. Oksman K, Mathew AP, Langstrom R (2009) The influence of fiber microstructure on fiber breakage and mechanical properties of natural fiber reinforced polypropylene. *Compos Sci Technol* 69:1847–1853
114. Kalaprasad G, Francis B, Thomas S et al (2004) Effect of fiber length and chemical modifications on the tensile properties of intimately mixed short sisal/glass hybrid fiber reinforced low-density polyethylene composites. *Polym Int* 53:1624–1638
115. Joseph PV (2001) Studies on short sisal fiber reinforced isotactic polypropylene composites. Thesis, Mahatma Gandhi University, Kerala
116. Fung KL, Xing XS, Li RKY (2003) An investigation on the processing of sisal fiber reinforced polypropylene composites. *Compos Sci Technol* 63:1255–1258
117. Albano C, Gonzalez J, Ichazo M et al (1999) Thermal stability of blends of polyolefins and sisal fiber. *Polym Degrad Stab* 66:179–190
118. Martin AR, Manolache S, Mattoso LHC et al (2000) Plasma modification of sisal and high-density polyethylene composite, effect on mechanical properties. In: *Natural polymers and composites*, pp 431–436
119. Rahman MM, Khan MA (2007) Surface treatment of coir (*Cocos nucifera*) fibers and its influence on the fibers physico-mechanical properties. *Compos Sci Technol* 67:2369–2376
120. Ichazo MN, Albano C, Gonzalez J (2000) Behavior of polyolefin blends with acetylated sisal fibers. *Polym Int* 49:1409–1416
121. Saxena M, Asokan P, Bakshi P (2008) Sisal potential for engineering application – an overview. In: *Sisal fiber technologies for sustainable rural employment generation*. Allied Publications, New Delhi, pp 112–154
122. Satyanarayana KG et al (1990a) Handbook of ceramic and composites. In: Cherimisin off NP (ed) *Lignocellulosic fiber reinforced polymer composites*, vol 1. Marcel Decker, New York, pp 339
123. Satyanarayana KG, Sukumaran K, Mukherjee PS et al (1990b) Natural fiber-polymer composites. *Cement Concrete Compos* 12:117–136
124. Sanadi AR, Prasad SV (1986) Sun hemp fiber reinforced polyester part-I. Analysis of tensile and impact properties. *J Mater Sci* 21:4299–4304
125. Suddell BC (2002) A survey into the application of natural fiber composites in the automotive industry. In: Mattoso LHC, Leao A, Follini E (eds) *Proceedings ISNaPol natural polymers and composites IV*, Sao Paulo, Brazil, pp 1–7
126. Suddell BC (2003) The current situation and future outlook for natural fibers within the automotive industry, food and agriculture organization (FAO) of the United Nations Joint Meeting of the 32nd session of the Intergovernmental group on Hard Fibers and the 34th session of the Intergovernmental Group on Jute, kenaf and allied fibers. Salvador, Brazil.
127. Hughes M (2002) Sustainable composites-fact or fiction, oral presentation, composites processing composites processing association, Holiday Inn, Birmingham airport, 24 Jan 2002
128. Belmares H et al (1981) New composite materials from natural hard fibers. *Ind Eng Chem Prod Res Dev* 20:555
129. Swamy RN (ed) (1988) *Natural fiber reinforced cement and concrete*, vol 1. Concrete technology and design. Blackie, London
130. Gram H-E (1983) *Durability of natural fibers in concrete*. Swedish Research and Concrete Research Institute, Stockholm
131. Karus M, Gahle GC (2006) Use of natural fibers in composites for the German automotive production from 1999 till 2005. Slowed growth in the past two years new production techniques arising. Nova-Institut, Hürth

132. Taj S, Munawar MA, Khan SU (2007) Review: Natural fiber-reinforced polymer composites. *Proc Pakistan Acad Sci* 44(2):129–144
133. Brouwer WD (2002) Natural fiber composites where can flex compete with glass. *SAMPE J* 36:18–23
134. Rai A, Jha CN (2004) Natural fiber composites and its potential as building material. *Express Textile*, 25 Nov 2004
135. Sharma D (2004) India automotive components industry, Swiss Business Hub India, pp 1–20
136. Sink SE (2005) Specials reported cars made of plants. <http://www.edmunds.com>
137. Bolton J (1997) Plant fibers in composite materials: a review of technical challenges and opportunities. The Burgess-Lane Memorial Lectureship in Forestry, March 5
138. Xin X, Xu CG, Qing LF (2007) Friction properties of sisal fiber reinforced resin brake composites. *Wear* 262:736–741
139. Chand N, Joshi SK (1994) Temperature dependence of dielectric behaviour of sisal fiber. *J Mater Sci Lett* 13:156–158
140. Patra A, Bisoyi DK (2010) Dielectric and impedance spectroscopy studies on sisal fiber-reinforced polyester composite. *J Mater Sci* 45(21):5742–5748
141. Tudu P (2009) Processing and characterization of natural fiber reinforced polymer composites a thesis submitted in partial fulfillment of the requirements for the degree of bachelor of technology in mechanical Engineering. Department of mechanical engineering National institute of technology, Rourkela, India, pp 1–52
142. Shukla JP, Ram R, Peters E (2008) Scope of sisal based geotextile application. In: *Sisal fiber technologies for sustainable rural employments generation*. Allied Publication, New Delhi, pp 45–59
143. Oosthuizen D, Kruger D (1994) The use of Sisal Fiber as natural geotextile to control erosion. In: Rao GV, Balan K (eds) *proceeding of the fifth international conference on geotextiles, geomembranes and related products*, Singapore, coir geotextiles – emerging trends. The Kerala State Coir Corporation, Kerala, India
144. Lu X, Zhang MQ, Rong MZ et al (2004) Environmental degradability of self-reinforced composites made from sisal. *Compos Sci Technol* 64:1301–1310
145. Osuna MS (2007) *Projects and programmes*, Unido, Vienna, Austria
146. Oudshoorn (1995) Biogas from sisal waste – a new opportunity for the sisal industry in Tanzania. *Energy Sustain Dev* 2(4):46–49
147. Rica C (2002) The sisal “zero” waste cleaner production programme in Tanzania study case. *Common Fund for Commodities*, pp 23–27
148. Albano C, Ichazo M, Reyes J et al (2002) Analysis of the mechanical, thermal and morphological behaviour of polypropylene compounds with sisal fiber and wood flour, irradiated with gamma rays. *Polym Degrad Stab* 76:191–203
149. Belgacem MN, Bataille P, Sapiuha S (1993) Effect of corona modification on the mechanical effect of corona modification on the mechanical properties of polypropylene/cellulose composites. *J Appl Polym Sci* 53:397
150. Gonzalez et al (1999) Effect of fibre surface treatment on the fibre matrix bond strength of natural fibre reinforced composites. *Composites: Part B* 30:309–320
151. Vibrant Gujarat (2004) *Project proposals: global investors summit-2004*. Government of Gujarat, India
152. Yi C, Tian L, Tong Y et al (2008) Thermal stability and mechanical properties of sisal in cycle process. *J Thermal Anal Calorim* 94(1):129–135
153. AMPRI, home page, Accessed on 22/2/2010. <http://en.wikipedia.org>
154. AMPRI, home page, Accessed on 22/2/2010. <http://www.sisal.ws/specialapplication.html>
155. AMPRI, home page, Accessed on 22/2/2010. <http://www.tifac.org.in>

Chapter 23

Natural Fibre-Reinforced Polymer Composites and Nanocomposites for Automotive Applications

James Njuguna, Paul Wambua, Krzysztof Pielichowski,
and Kambiz Kayvantash

Abstract Natural fibre-reinforced composites have recently received much attention because of their attractive properties such as lightweight, non-abrasive, combustible, non-toxic, low cost and biodegradable. This chapter examines the applications of natural fibre-reinforced composites and nanocomposites in automotive structural applications. Various applied and promising natural fibre-reinforced composites and nanocomposites including flax, hemp, kenaf, wood, pineapple, banana and sisal are presented. Key determinants to performance-specific properties of natural fibre-reinforced composites are discussed in detail. These include fibre–matrix adhesion, fibre mechanical properties, moisture, impact and fatigue, thermal stability and preparation of fibre-reinforced composites. The chapter further looks into lightweight component manufacturing techniques including their potentials and limitations. Examples of current applications are given, and future trends are outlined while addressing the main drawbacks faced by these composites to lightweight components or vehicle manufacturing.

Keywords Automotive applications · Autoparts manufacturing · Mechanical properties · Nanocomposites · Natural fibres

Contents

23.1	Introduction	662
23.2	Selection of Natural Fibres	663
23.3	Selected Examples of Fibre-Reinforced Composites	664
23.3.1	Flax Composites	664
23.3.2	Hemp Composites	665
23.3.3	Kenaf Composites	667
23.3.4	Wood Composites	668
23.3.5	Pineapple Composites	671
23.3.6	Banana Composites	671

J. Njuguna (✉)

Department of Sustainable Systems, Cranfield University, Cranfield, Bedfordshire MK43 0AL, UK

e-mail: j.njuguna@cranfield.ac.uk

23.3.7	Sisal Composites	674
23.4	Key Determinants to Performance Specific Properties of Natural Fibre-Reinforced Composites	676
23.4.1	Fibre–Matrix Adhesion	676
23.4.2	Fibre Mechanical Properties	677
23.4.3	Moisture	679
23.4.4	Fatigue Behaviour	679
23.4.5	Thermal Stability	680
23.4.6	Preparation of Fibre–Matrix Composites	682
23.5	Natural Fibre-Reinforced Nanocomposites	684
23.6	Lightweight Component Manufacturing Techniques	691
23.6.1	Compression and Injection Moulding	691
23.6.2	Resin Transfer Moulding	691
23.6.3	Vacuum Assisted Resin Transfer Moulding	692
23.7	Applications and Future Trends	692
23.8	Conclusions	696
	References	697

23.1 Introduction

As industry attempts to lessen the dependence on petroleum-based fuels and products, there is an increasing need to investigate more environmentally friendly, sustainable materials to replace the existing glass fibre and carbon fibre-reinforced materials. Therefore, attention has recently shifted to the fabrication and properties of natural fibre-reinforced materials. The automotive industries have demonstrated an interest in using more natural fibre-reinforced composites. For example, in order to reduce vehicle weight, automotive companies have already shifted from steel to aluminium and now are shifting from aluminium to fibre-reinforced composites for some applications [1]. This has led to predictions that in the near future plastics and polymer composites will form a significant fraction of total automobile weight.

Natural fibres exhibit many advantageous properties as reinforcement for composites. They are a low-density material, yielding relatively lightweight composites with high specific properties. Reinforcing biodegradable plastics with natural fibres leads to green composite that is easy to degrade by bacteria or enzyme. Natural fibres also offer significant cost advantages and benefits associated with processing, when compared with synthetic fibres. Finally, they are a highly renewable resource, which reduces the dependency on foreign and domestic petroleum oil. As a result of the increasing demand for environmentally friendly materials and the desire to reduce the cost of traditional fibre (i.e., carbon, glass and aramid) reinforced petroleum-based composites, new bio-based composites have been developed.

The natural fibre-reinforced composites have a very light weight potential due to the low density of the fibres as shown in both Table 23.1 and Fig. 23.1, for example [2].

The processing characteristics and acoustic properties are further advantages of the natural fibres. Additional advantages like good life-cycle assessment and industrial medicine relating advantages compared with glass fibres are also to be

Table 23.1 Properties of natural fibres in relation to those of E-glass [2]

Properties	Fibres							
	E-glass	Hemp	Jute	Ramie	Coir	Sisal	Flax	Cotton
Density (g/cm ³)	2.55	1.48	1.46	1.5	1.25	1.33	1.4	1.51
Tensile strength (MPa)	2,400	550–900	400–800	500	220	600–700	800–1,500	400
E-Modulus (GPa)	73	70	10–30	44	6	38	60–80	12
Specific (E/d)	29	47	7–21	29	5	29	26–46	12
Elongation at failure (%)	3	1.6	1.8	2	15–25	2–3	1.2–1.6	3–10
Moisture absorption (%)	–	8	12	12–17	10	11	7	8–25

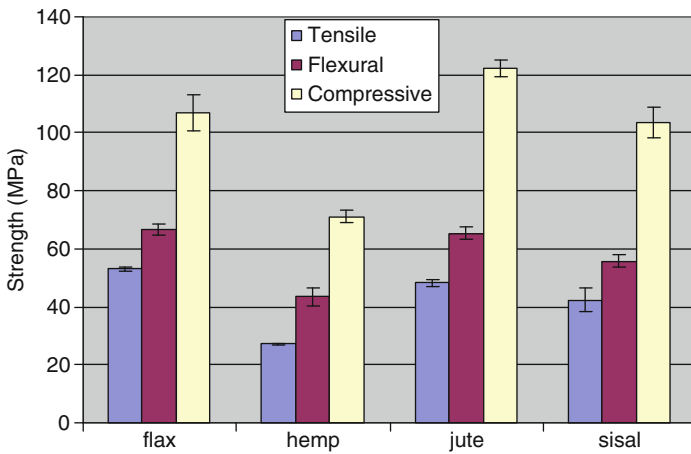


Fig. 23.1 Tensile, flexural (in warp/weft direction) and out-of-plane compressive strengths of hemp, flax and sisal fabric reinforced polypropylene composites at $V_f = 37\%$

taken into account. One disadvantage of natural fibres is the unevenness of the fibre quality and characteristics through, e.g., soil, climate and the kind of fibre separation. Often the natural fibre is not sufficiently heat resistant compared with the glass fibre for the usual processing techniques.

23.2 Selection of Natural Fibres

Natural fibres are classified into three main groups, namely, bast (or stem), leaf and seed (or fruit). Bast fibres such as jute, hemp, kenaf and flax are fibrous bundles found in the inner bark of the plant stem. The fibre bundles consist of filaments of fibre cells made up of mainly cellulose and hemicelluloses. The cementing material between the fibre bundles is lignin while the filaments are held together by pectins. These fibres are separated from the woody matter through a process of natural

decomposition (retting) to soften, dissolve and wash away the gummy tissues followed by breaking and scotching [3]. Leaf fibres, also known as hard fibres, run in the length of the leaves. Sisal is the most common; others include banana (abaca) and pineapple fibres. The most commonly used fruit fibre in composites applications is coir. Of the three groups, bast fibres have the highest mechanical properties and this has contributed to their utilization as reinforcement to polymers in the manufacture of natural fibre composites. For each application, the choice of bast, stem or fruit fibres depends on the required properties and expected performance.

Cellulose is the basic structural unit of all natural fibres. The alignment of cellulose molecules to form molecular bundles confers crystalline properties in this group of fibres. These molecules, referred to as micelles, further align themselves to form micro-fibrils in the plant fibre. Natural cellulose fibres are multicellular [4] and consist of fibre cells with high aspect ratio. The cell walls have a homogeneous lattice structure of lignin and hemicelluloses in which the cellulose micro-fibrils are embedded [5–7]. Lignin has a high molecular weight and three-dimensional polymer structure, and is responsible for the rigidity of the fibres. The orientation of the micro-fibrils in relation to the fibre's lengthwise direction influences the properties of the fibre. If the orientation is low, the fibre will be more extensible and less stiff. The higher the orientation or micro-fibril angle, the higher the tensile strength. The cellulose content also contributes to the tensile strength of the fibres. Other factors that influence the mechanical properties of plant fibres are degree of crystallization, lumen size, density, diameter, degree of polymerization and porosity [8].

23.3 Selected Examples of Fibre-Reinforced Composites

Natural fibres are presently being considered as possible replacements for glass and other non-recyclable fibres in certain applications. In the following sections, a few examples are provided on some of the most promising bast and leaf fibre-reinforced composites for automotive applications. While the bast fibres exhibit a superior flexural strength and modulus of elasticity, the leaf fibres show superior impact properties. These types of composites present many advantages compared with synthetic fibre-reinforced plastics such as low tool wear, low density, cheap cost, availability and biodegradability. These materials have already been embraced by a number of leading carmakers.

23.3.1 Flax Composites

Among all the natural fibres, flax is considered to be one of the strongest and easily available. The tensile strength of elementary flax fibres is found to be in the region of 1,500 MPa [9]. There are many studies where specific properties of natural fibres such as hemp, kenaf, jute, flax and sisal have been compared with traditional

composite reinforcements. Research shows that the density of these natural fibres is much lower than the traditional materials thereby leading to strength/weight ratios comparable with those of such widely used materials as E-glass and aramid. The advantages of using polypropylene as matrix in flax composites are their relatively low processing temperature which is essential because of low thermal stability of natural fibres, their good properties and lower cost. Non-wovens are one of the products popularly used as reinforcements in composites for many applications since they possess a good combination of strength, lightweight and flexibility compared with conventional materials [10]. Although there have been many studies on lignocellulosic short-fibre composites, only a few mention the use of non-wovens as reinforcement in flax composites. The biggest advantage of this type of composite is their low processing cost, combined with their ecological and technological benefits.

John and Anandjiwala [11] investigated the effect of reinforcement of polypropylene matrix with flax non-wovens. As would be expected, the tensile strength and modulus were found to increase with increasing fibre loading. Flexural strength and modulus also registered an increase. Zein modification of the flax non-wovens was found to enhance the mechanical properties of the composites. This was attributed to better interfacial bonding between matrix and non-wovens. Impact strength was found to decrease due to zein modification. Scanning electron microscopic studies revealed the presence of fibre breakage in chemically modified composites. Viscoelastic properties like storage modulus increased while damping properties were found to decrease with the incorporation of flax non-wovens. The increase of storage modulus indicated better interfacial adhesion. The variation of excitation frequency was found to affect the secondary relaxations of the composites significantly. Further studies are required to investigate the polarity changes by zeta potential measurements on flax non-wovens.

23.3.2 *Hemp Composites*

Traditionally, hemp has been grown for its valuable and versatile high-quality bast fibres. Bast fibres account for 20–30% of the stalk (depending on the seed variety and planting density). Bast (long) fibres make up approximately 70% of the fibres and are long, high in cellulose and low in lignin. Long bast fibres are the most valuable part of the stalk, and are generally considered to be among the strongest plant fibres known. Secondary bast (hurds) fibres make up the remaining 30% of the bast fibres and are medium in length and higher in lignin. They are less valuable and become more prevalent when the hemp plants are grown less densely, making shorter fatter stalks since they do not have to compete for light.

The production or extraction of the primary bast fibres has traditionally been a very labour-intensive process, but recently an alternative fibre separation process has been developed using technologies such as ultrasound and steam explosion, which are much less labour intensive. Once separated, the bast fibres are ready for spinning and weaving into textiles, or for pulping into high-quality pulp.

In an interesting study, Beckermann and Pickering [12] investigated the properties of hemp fibre-reinforced polypropylene composites after alkali treatment. It was found that injection moulded hemp fibre-reinforced polypropylene composite consisting of 40 wt% NaOH/Na₂SO₃ treated fibre, 4% maleic anhydride modified polypropylene (MAPP) and polypropylene had the highest tensile strength (50.5 MPa) and Young's modulus (5.31 GPa) of all the composites studied. As seen in Fig. 23.2,

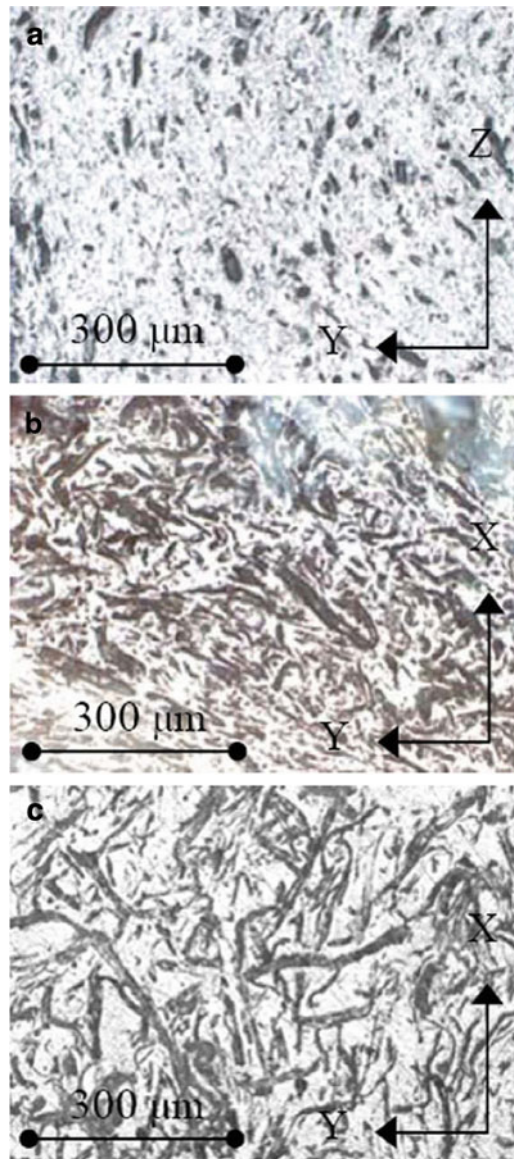


Fig. 23.2 Optical micrograph of: (a) specimen cross-section; (b) specimen centre and (c) specimen surface. In reference to these micrographs, the X-direction corresponds to the mould-filling direction, the Y-direction corresponds to the sample width and the Z-direction corresponds to the sample thickness [12]

it is shown that a large number of fibre cross-sections seen in the $Y-Z$ plane (a) indicate some level of orientation in the mould flow direction, and the fibres in the $X-Y$ plane appear to be randomly oriented (b and c). The orientation correction factor (K_1) value also indicates that only a small fraction of the fibres effectively contribute to the strength of the composite.

Mohanty et al. [13] evaluated biocomposites formed using chopped hemp fibre and cellulose ester biodegradable plastic. The effect of two different processing approaches was studied. For the first process, the chopped fibre (30% by weight) was mechanically mixed in a kitchen mixer for 30 min followed by compression moulding using a picture-frame mould. The second process involved two steps: first an extrusion process yielded pellets of cellulose acetate plastic (CAP); second, the pellets were fed into a twin-screw extruder while chopped hemp fibres were fed into the last zone of the extruder.

This process yielded thin strands of the composite, which were pelletized for injection moulding into tensile test coupons. One of the main advantages of melt mixing is the superior mixing of fibre and matrix, but at the cost of high shear forces, which may lead to fibre damage. The mechanical mixing and compression moulding process allows for these forces to be avoided. In addition, preforms are produced in one step. However, the lack of adequate mixing may adversely affect the overall performance. The composites formed using the second process, extrusion and injection moulding, showed superior overall strength due to the adhesion and distribution of the fibres.

Investigations have shown that it is possible to manufacture all-natural composites using hemp and flax fibres using soy oil resins [14]. The tensile and flexural properties of the resins were shown to be improved by the addition of the fibres as observed for regular thermoset resins. However, this type of composite gave lower values than polymer-natural fibre-reinforced composites. Wollerdorfer and Bader [15] made similar observations for different all-natural composites using soya resins. Researchers [16] have reported studies on the properties of composites from hemp non-woven mats and polyester resin. The authors observed that mechanical properties were found to reach maximum at a fibre loading of 30%.

23.3.3 *Kenaf Composites*

Kenaf is an herbaceous annual plant that is grown commercially in the USA in a variety of weather conditions, and it has been previously used for rope and canvas. Kenaf has been deemed extremely environmentally friendly for two main reasons: (a) kenaf accumulates carbon dioxide at a significantly high rate and (b) kenaf absorbs nitrogen and phosphorous from the soil [17]. In addition, kenaf, like most other natural fibres, demonstrates low density, high specific mechanical properties, is easily recycled and maintains a competitive price.

Nishino et al. [18] used kenaf fibre sheets in an attempt to fabricate composites with better dispersion and adhesion. The kenaf fibre was dried, and then soaked in a dioxane solution under vacuum. These samples were easily fabricated and exhibited

good performance with a fibre content of approximately 70% by volume. This study concluded that the fibre orientation plays an important role in the final properties of the composite. Zampaloni et al. [19] has successfully fabricated kenaf–polypropylene natural fibre composites. The optimal fabrication method for the compression moulding process was proven to be the layered sifting of a microfine polypropylene powder and chopped kenaf fibres. A fibre content of both 30 and 40% by weight was proven to provide adequate reinforcement to increase the strength of the polypropylene matrix. The use of the coupling agent, 3% Epolene G3015, has enabled successful fibre–matrix adhesion. The kenaf–PP composites compression moulded during the study provide both tensile and flexural strength that is very similar to the 40% by weight flax and hemp polypropylene systems. In contrast, the tensile strength was higher and the flexural strength was almost doubled when compared with the coir and sisal systems. It was also shown that kenaf–PP composites have a higher modulus/cost and a higher specific modulus than sisal, coir, hemp, flax and E-glass. This implies that the 30% by weight kenaf polypropylene composite that was compression moulded compares favourably with the more commonly used hemp and flax fibre polypropylene composites that are 40% fibre by weight.

23.3.4 Wood Composites

Wood is a natural and complex polymeric composite, which essentially contains cellulose, hemicellulose, lignin and extractives. A wide range of different substances is included under the extractives heading: flavonoids, lignans, stilbenes, tannins, inorganic salts, fats, waxes, alkaloids, proteins, simple and complex phenolics, simple sugars, pectins, mucilages, gums, terpenes, starch, glycosides, saponins and essential oils. Extractives content in most temperate and tropical wood species are 4–10 and 20% of the dry weight, respectively. Although extractives contribute merely a small percent to the entire wood composition, they have significant influence on its properties, such as mechanical strength, and the quality of wood can be affected by the amount and type of these extractives.

Shebani et al. [20] noted that removing extractives improved the thermal stability of different wood species. Therefore, using extracted wood for the production of wood–plastic composite (WPCs) would improve the thermal stability of WPCs. Because wood and other bio-fibres easily undergo thermal degradation beyond 200°C, thermoplastic matrix used in the composites is mainly limited to low-melting-temperature commodity thermoplastics like polyethylene (PE) and polypropylene (PP). However, the inherently unfavourable thermomechanical and creep properties of the polyolefin matrix limit some structural applications of the materials.

Although there have been quite a number of studies on the WPCs as new generation of reinforcing materials in recent years, so far, not much attention has been paid to the effect of chemical composition of wood on the mechanical and physical properties. The effective use of wood-based particles and fibres as fillers or reinforcements in thermoplastic composites requires a fundamental understanding of

the structural and chemical characteristics of wood. Several attempts have been made to correlate the properties of wood-based particles and fibres to WPC properties. Maldas et al. [21] investigated the effect of wood species on the mechanical properties of wood/thermoplastic composites. They observed differences in morphology, density and aspect ratios across wood species, which accounted for varying reinforcement properties in thermoplastic composites. A high aspect ratio (length/width) is very important in fibre-reinforced composites, as it indicates potential strength properties. Lu et al. [22] reported that the mechanical properties of the resultant WPC increase only at low weight percentages of wood filler. They found that tensile and flexural strengths reach a maximum at 15 and 35 wt% wood particle contents, respectively, and gradually decrease with a further increase in wood particle content. Michell [23] studied different types of composites containing wood pulp fibres. Michell has shown that wood pulp fibres are cheaper than other organic polymers and also lead to improvements of both the strength and tensile modulus of composites. The study concluded that although the wood pulp fibres were already being used in thermoset applications, there exists an opportunity for use as reinforcements in thermoplastic composites.

Research studies on Kraft fibre-reinforced polypropylene (PP) composites found the properties to decrease while failure strain increased with decreasing fibre length [24]. Modest levels of fibre beating increased the tensile strength of composites, which related to improved interfacial bonding. During hygrothermal ageing, the diffusion coefficient increased with increased ageing temperature (Fig. 23.3). Composites without coupling agent showed higher water uptake and diffusion coefficient than those with coupling agent.

Tensile strength and Young's modulus were found to decrease for hygrothermal ageing due to fibre damage (Fig. 23.4) and reduced fibre–matrix interfacial bonding, whereas failure strain and impact strength were found to increase due to the plasticizing effect of water [24].

McKenzie and Yuritta [25] compared different types of wood fibre-reinforced polymers to determine if wood fibre has advantages as a reinforcing material over other fibrous materials. Comparisons were made with nylon, rayon, glass and Kevlar. The short length of the wood fibre led to the conclusion that the bonding of the matrix with the fibre was crucial since the full strength of the fibre would only be utilized if a strong bond were formed. It was also found that a wood fibre composite would have to be 67% thicker than a glass fibre composite in order to have the same strength. This increased polymer matrix requirement reduces the cost benefit of wood fibre over glass, but wood fibre provides advantages by consuming less energy during fibre manufacture and the potential for lower mass structures.

Bhattacharyya et al. [26] showed that wood fibre–polypropylene composites are indeed formable. The sheets they manufactured used pinus radiate fibres along with polypropylene powder, for a total through thickness of 1.3 mm. Two types of composites were made, layered and homogeneous with polypropylene and wood fibres mixed during formation. Results showed a tensile modulus increase of up to 250% with a 25–30% fibre mass fraction. Several formability tests were studied, dome forming with matched die and cup drawing being most relevant. For both

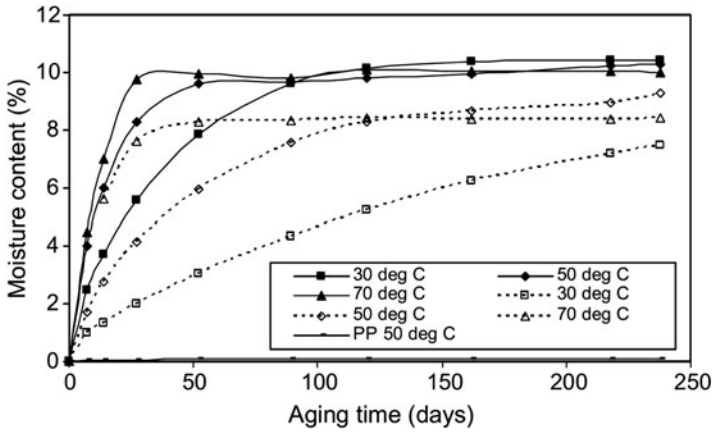


Fig. 23.3 Hydrothermal ageing time versus moisture content of 40 wt% fibre composites with 4 wt% maleated polypropylene (MAPP) (dotted line) and without MAPP (solid line) at 30, 50 and 70°C hydrothermal ageing temperature [24]

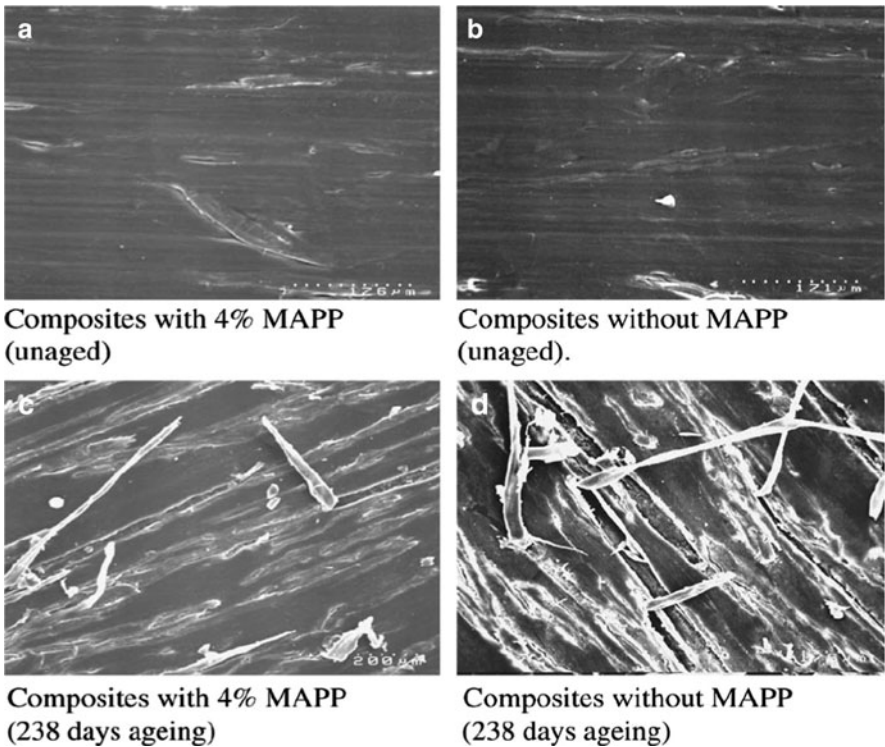


Fig. 23.4 Comparison of the effects of hydrothermal ageing showing SEMs of composite (40 wt% fibre) surfaces after hydrothermal ageing at 70°C compared with unaged surface [24]

forming techniques, the material was heated to approximately 190°C (374 °F) before beginning formation. This study demonstrated the ability to form these composites into not only two-dimensional shapes, but also simple three-dimensional shapes.

23.3.5 *Pineapple Composites*

Pineapple leaf fibre (PALF), which is rich in cellulose, relatively inexpensive and abundantly available has the potential for polymer-reinforced composite. PALF at present is a waste product of pineapple cultivation. Hence, without any additional cost input, pineapple fibres can be obtained for industrial purposes. Among various natural fibres, PALFs exhibit excellent mechanical properties. These fibres are multicellular and lignocellulosic. They are extracted from the leaves of the plant *Ananus cosomus* belonging to the Bromeliaceae family by retting. The main chemical constituents of pineapple fibres are cellulose (70–82%), lignin (5–12%) and ash (1.1%). The superior mechanical properties of PALFs are associated with their high cellulose content.

George et al. [27] studied stress relaxation behaviour of pineapple fibre-reinforced polyethylene composites. They found stress relaxation to be decreased with an increase of fibre content due to better reinforcing effect. It is also reported by George et al. [28] that properties of fibre-reinforced composites depend on many factors like fibre–matrix adhesion, volume fraction of fibre, fibre aspect ratio, fibre orientation as well as stress transfer efficiency of the interface. Luo and Netravali [29] found an increase in the mechanical properties of “green” composites prepared from PALFs and poly(hydroxybutyrate-co-valerate) resin (a biodegradable polymer) with the fibres in the longitudinal direction. However, the researchers reported a negative effect of the fibres on the properties in the transverse direction.

The use of PALF as reinforcement to improve mechanical properties of polycarbonate (PC) has been investigated [30]. The study focused on the tensile and flexural behaviours of PALF–polypropylene composites as a function of volume fraction. It follows that relatively soft polymeric surface of PC can easily scratch, and notch sensitivity at lower temperatures limits PC in some applications. The tensile modulus and tensile strength of the composites were found to be increasing with fibre content in accordance with the rule of mixtures, Fig. 23.5.

The flexural modulus gives higher value at 2.7% volume fraction. The flexural strength of the composites containing 5.4% volume fraction was found to be higher than that of pure polypropylene resin by 5.1%.

23.3.6 *Banana Composites*

Banana fibre (BaF) is extracted from the waste product of banana cultivation. Due to high cellulose content and comparatively low micro-fibrillar angle, it has superior mechanical properties, especially tensile strength and modulus. It is thus

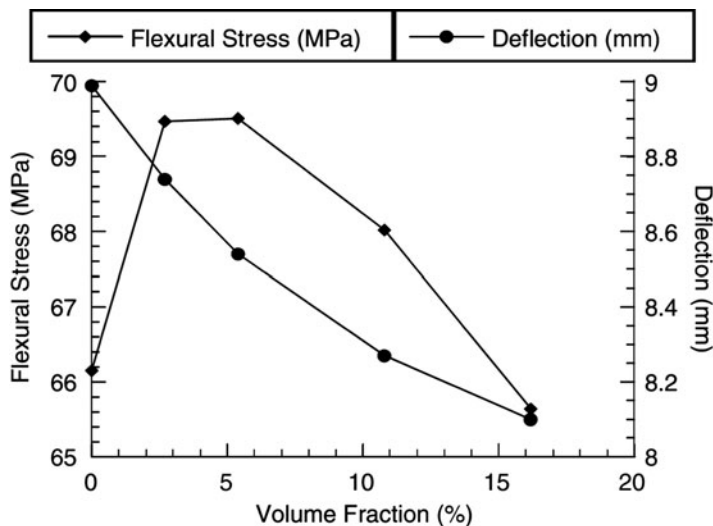


Fig. 23.5 Flexural stress and deflection versus volume fraction [30]

considered as a promising candidate for replacing conventional glass fibres in the fibre-reinforced composites. Earlier studies showed that BaF provided good reinforcement for various thermosetting resins such as unsaturated polyester (UPE), phenol formaldehyde (PF) and epoxy. Chemical treatments of the fibre and hybridization with other fibres are able to further enhance the properties of composites [31]. Studies have shown that compositional changes occur in the fibre structure during hydrolysis for the untreated banana fibre, the alkaline solution-treated banana fibre, the bleached banana fibre and the hydrolysed banana fibre samples as shown in Fig. 23.6 [32]. Nevertheless, cellulose micro-fibres prepared by using the different reaction conditions show very similar spectral patterns to that of cellulose.

To promote interfacial adhesion between BaF and hydrophobic matrix, various modification strategies, including addition of compatibilizers, chemical treatment of the fibre and use of maleic anhydride grafted polyolefin as a matrix may be adopted. For various BaF-filled thermosetting or thermoplastic composites, it was found that a decrease in fibre loading and/or chemical modification of the fibre reduced water absorption (WA) of the composites at ambient temperature [33]. This was attributed to better adhesion between the matrix and the fibre. However, most of current studies focus on individual polymer as matrix, while the utilization of high-melting point and high-performance engineering plastics (e.g., Nylon-6, $T_m = 220^\circ\text{C}$) as a blending component has rarely been attempted.

Recently, Liu et al. [34] prepared banana fibre (BaF)-filled composites based on high-density polyethylene (HDPE)/polyamide-6 (PA 6) blends via a two-step extrusion method. Maleic anhydride grafted styrene/ethylene-butylene/styrene triblock polymer (SEBS-g-MA) and maleic anhydride grafted polyethylene (PE-g-MA) were used to enhance impact performance and interfacial bonding between BaF and the resins. Mechanical, crystallization/melting, thermal stability, water absorption and

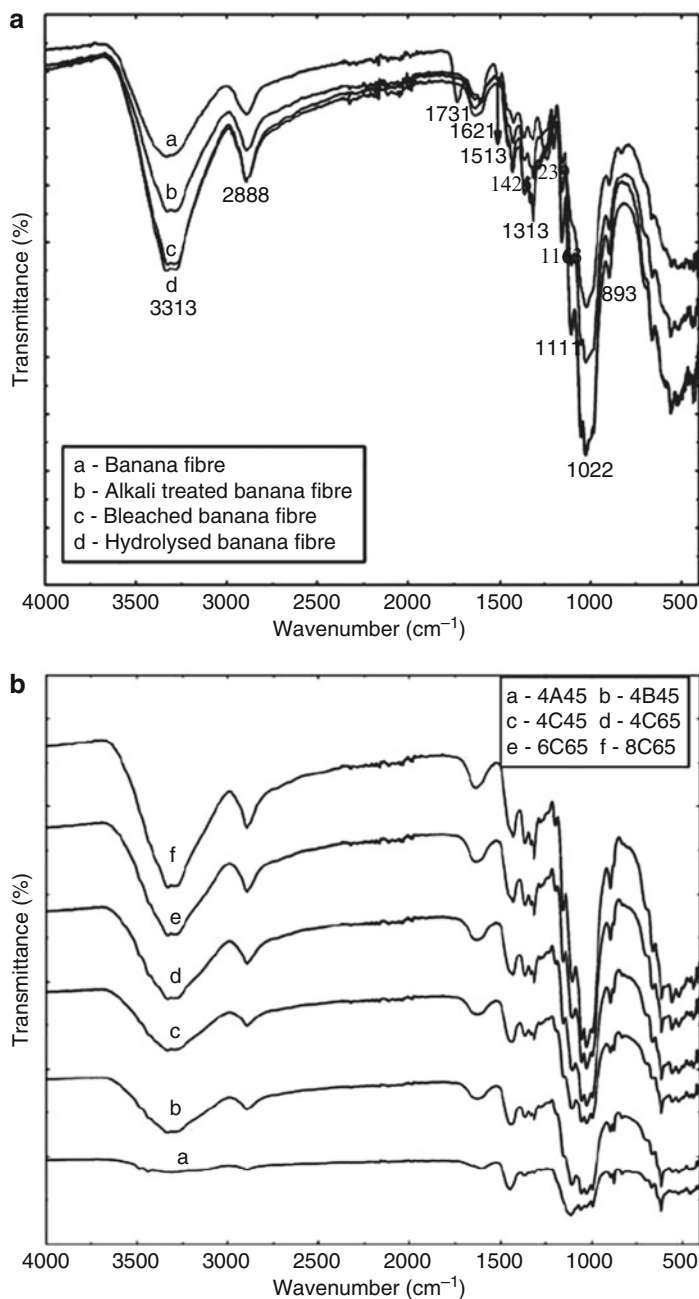


Fig. 23.6 (a) FT-IR spectra of banana fibres after different treatments. (b) FT-IR spectra of cellulose micro-fibres produced under different reaction conditions [32]

morphological properties of the composites were investigated. In the presence of SEBS-g-MA, better strengths and moduli were found for HDPE/PA 6-based composites compared with corresponding HDPE-based composites. At a fixed weight ratio of PE-g-MA to BaF, an increase of BaF loading up to 48.2 wt% led to a continuous improvement in moduli and flexural strength of final composites, while impact toughness was lowered gradually. Predicted tensile modulus by the Hones–Paul model for three-dimensional random fibre orientation agreed well with experimental data at the BaF loading of 29.3 wt%. However, the randomly oriented fibre models underestimated experimental data at higher fibre levels. It was found that the presence of SEBS-g-MA had a positive influence on reinforcing effect of the PA 6 component in the composites. Thermal analysis results showed that fractionated crystallization of the PA 6 component in the composites was induced by the addition of both SEBS-g-MA and PE-g-MA. Thermal stability of both composite systems differed slightly, except an additional decomposition peak related to the minor PA 6 for the composites from the HDPE/PA 6 blends. In the presence of SEBS-g-MA, the addition of PA 6 and increased BaF loading level led to an increase in the water absorption value of the composites.

Agarwal et al. [35] analysed the variation of thermal conductivity and thermal diffusivity of banana fibre-reinforced polyester composites caused by the addition of glass fibre. They observed that the thermal conductivity of composites increased when compared with the matrix. However, the thermal conductivity of the composites with increased percentage of glass fibre decreases in comparison to composite of pure banana fibre.

Annie Paul et al. [36] studied short randomly oriented PP/banana fibre composites. The thermophysical properties of the above composites were studied on the basis of different banana fibre loading and different chemical treatments given to the banana fibres. The incorporation of banana fibres into PP matrix induced a decrease of the effective thermal conductivity of the composite. The use of the theoretical series conduction model allowed to estimate the transverse thermal conductivity of untreated banana fibre composites. As was expected, the series model appears sufficient for the effective thermal conductivity estimation of this kind of composites. All the chemical treatments enhanced both thermal conductivity and diffusivity of the composite considerably in varying degrees. This indicates that the chemical treatment allows a better contact between the fibre and the matrix and reduces considerably the thermal contact resistance. Nevertheless, a significant increase of the thermal conductivity was observed only for benzoylated and 10% NaOH-treated fibre composites. Besides, the variations of density and specific heat upon fibre chemical treatment are small compared to their associated uncertainties.

23.3.7 Sisal Composites

Sisal fibre is an effective reinforcement of polymer, rubber, gypsum and cement matrices. This has created a range of technological applications beyond its

traditional usage as ropes, carpets and mats. The mechanical and physical properties of sisal fibre not only depend on its source, position and age which will affect the structure and properties, but also depend on the experimental conditions, such as fibre diameter, gauge length, strain rate and test temperature. Fibre-surface treatment can improve the adhesion properties between sisal fibre and matrix and simultaneously reduce water absorption. Such methods include [37]:

- Silane and other coupling agents to introduce long chain structures onto the sisal fibre to change its hydrophilic characteristics
- Peroxide to promote grafting reactions
- Permanganate and alkali to increase the roughness of fibre surface hence increasing the surface area available for contact with the matrix
- Thermal treatment

Different matrix systems have different properties. The mechanical and physical properties of sisal fibre-reinforced composites are very sensitive to processing methods, fibre length, fibre orientation and fibre-volume fraction. Sisal and glass fibres can be combined to produce hybrid composites which take full advantage of the best properties of the constituents. Almost all the mechanical properties show “positive” hybrid effects. Research has shown that the tensile strength and elastic modulus of the thermoset sisal fibre-reinforced composites containing up to 40% fibre-volume fraction (V_f) increase linearly with V_f in good agreement with the rule of mixtures. The work of fracture, as determined by Izod impact test, also increases linearly with V_f . Analysis of the energy-absorption mechanisms during impact fracture shows that fibre pull-out and interface fracture are the major contributors to the high toughness of these composites. This result indicates that sisal fibres have potential to produce inexpensive materials with high toughness.

Comparison of the impact properties of different natural fibre-reinforced composites, including sisal, pineapple, banana and coir, shows that sisal-fibre composites possess the highest impact toughness owing to the optimal micro-fibrillar angle of the fibre (21° for sisal, 12° for banana, 14° for pineapple and 45° for coir). It has been proven that the toughness of composites increases with the micro-fibrillar angle of the fibres and reaches a maximum at $15\text{--}20^\circ$ [38]. It will then decrease with increasing angle. The optimal micro-fibrillar angle of sisal fibre (21°) leads to better impact resistance with a work of fracture of 98.7 kJ/m^2 when the fibre-volume fraction is 50%. For the same volume fraction of pineapple fibres, this is 79.5 kJ/m^2 ; for banana and coir fibres, they are 51.6 and 43.5 kJ/m^2 , respectively. When compared with synthetic fibre composites, the specific impact work of fracture for the natural fibre composites is not much worse. The specific work of fracture (i.e., toughness per unit density) of 60% volume fraction sisal fibre/polyester composites is $115 \text{ kJ/m}^2/\text{g}$, while for ultra-high-modulus polyethylene (UHMPE) and E-glass fibres these values are 125 and $165 \text{ kJ/m}^2/\text{g}$, respectively.

Li et al. [37] showed that the tensile properties of sisal fibres are not uniform along their length. Parameters such as fibre length, test speed, gauge length, fibre age or temperature were all found to have effects on the mechanical properties of sisal and sun-hemp fibres. Most of these effects are explained by the internal structure of

the fibres (cell structure, micro-fibrillar angle, imperfections and water content). However, Van Voorn et al. [14] found that the temperature and the moisture content have a limited influence on the tensile strength of sisal and flax fibres.

The environmental properties of sisal-fibre composites are very important because, as a natural fibre, sisal ages and causes degradation. The effects of ageing on the physical and mechanical properties of sisal fibre-reinforced polyethylene composites have been studied [39]. The tensile properties and dimensional stability were evaluated under two different ageing conditions: (a) by immersing samples in boiling water for 7 h under atmospheric pressure; and (b) by heating the samples at 70°C in an air circulating oven for 7 days. Both cardanol derivative of toluene diisocyanate (CTDIC) treated and untreated sisal fibre-reinforced composites have been studied. The ageing properties of the sisal composites are also compared with those of glass-fibre composites aged under identical conditions. It was concluded that CTDIC-treated composites showed better mechanical properties and dimensional stability when compared with untreated composites as a result of the existence of an effective interfacial bond between fibre and matrix. Better dimensional stability is offered by glass/LDPE composite because of the hydrophobic nature of the glass fibre. With suitable fibre-surface treatment, mechanical properties such as strength and elastic modulus of sisal/LDPE composites can be improved to comparable levels as those of glass/LDPE.

23.4 Key Determinants to Performance Specific Properties of Natural Fibre-Reinforced Composites

23.4.1 Fibre–Matrix Adhesion

Natural fibres are hydrophilic in nature as they are lignocellulosic, which contain strongly polarized hydroxyl groups. These fibres, therefore, are inherently incompatible with hydrophobic thermoplastics, such as polyolefins. The major limitations of using these fibres as reinforcements in such matrices include poor interfacial adhesion between polar-hydrophilic fibres and non-polar-hydrophobic matrix, and difficulties in mixing due to poor wetting of the fibres with the matrix. Hence, it is imperative that natural fibres should be subjected to chemical modification to increase the compatibility and adhesion between fibres and matrix.

Therefore, the first and the most important problem is the fibre–matrix adhesion. The role of the matrix in a fibre-reinforced composite is to transfer the load to the stiff fibres through shear stresses at the interface. This process requires a good bond between the polymeric matrix and the fibres. Poor adhesion at the interface means that the full capabilities of the composite cannot be exploited and leaves it vulnerable to environmental attacks that may weaken it, thus reducing its life span. Insufficient adhesion between hydrophobic polymers and hydrophilic fibres result in poor mechanical properties of the natural fibre-reinforced polymer composites. Pre-treatments of the natural fibre can clean the fibre surface,

chemically modify the surface, stop the moisture absorption process and increase the surface roughness. These properties may be improved by: physical treatments (cold plasma treatment and corona treatment) and chemical treatment (maleic anhydride, organosilanes, isocyanates, sodium hydroxide, permanganate and peroxide). Among the various pre-treatment techniques, graft copolymerization and plasma treatment are the best methods for surface modification of natural fibres. Graft copolymers of natural fibres with vinyl monomers provide better adhesion between matrix and fibre.

Gauthier et al. [40] reported that adhesion may be improved by using coupling agents like maleic anhydride to incorporate hydroxyl groups on the matrix through hydrophilization and consequently enhancing the wetting effect of the resin on the fibres. The hydroxyl groups then interact with $-OH$ molecules on the lignocellulosic fibres via hydrogen bonding thus producing a stronger bond. George et al. [41] attempted to solve the problem of fibre–matrix adhesion when manufacturing biocomposites by applying an alkaline solution to the fibres. Natural fibres are mainly composed of cellulose, whose elementary unit, anhydro d-glucose, contains three hydroxyl ($-OH$) groups. These hydroxyl groups form intramolecular and intermolecular bonds, causing all vegetable fibres to be hydrophilic. The alkaline solution regenerated the lost cellulose and dissolved unwanted microscopic pits or cracks on the fibres resulting in better fibre–matrix adhesion. Another method of improving fibre–matrix adhesion discussed in this work was through the use of coupling agents. The coupling agents had two functions: to react with $-OH$ groups of the cellulose and to react with the functional groups of the matrix with the goal of facilitating stress transfer between the fibres and the matrix. There have been numerous studies conducted on the use of coupling agents for improving the adhesion between natural fibres and polypropylene, with the most common approach being the use of a coupling agent containing maleic anhydride, creating MAPP, which has been shown to immensely improve the properties of these materials.

23.4.2 Fibre Mechanical Properties

Natural fibres consist mainly of cellulose. These fibres are made of micro-fibrils in a matrix of lignin (or pectin) and hemicellulose. The strength and stiffness of the fibres are provided by hydrogen bonds and other linkages. The overall properties of the fibres depend on the individual properties of each of its components. Hemicellulose is responsible for the biodegradation, moisture absorption and thermal degradation of the fibre. On the other hand, lignin (or pectin) is thermally stable but is responsible for UV degradation of the fibre. On average, natural fibres contain 60–80% cellulose, 5–20% lignin (or pectin) and up to 20% moisture.

Treatment of natural fibres is beneficial in order to improve the water resistance of fibres, enhance the wettability of the natural fibre surface by polymers (mainly non-polar polymers) and promote interfacial adhesion. The performance of fibres is critical to obtain the improved physical and mechanical properties of the resulting

composites. Physical treatments (e.g., electronic discharge in the different media such as plasma and corona technologies) may create a hydrophilic or hydrophobic fibre surface by changing the surface energy to consequently increase the compatibility of the treated fibre with the polymer matrices. These surface treatments only modify a very shallow surface of cell walls and thus do not change the hygroscopic characteristics of fibres.

Bledzki and Gassan [42] observed that the characteristic values of natural fibres are comparable to those of glass fibres. The strength of natural fibres greatly depends on the process used to produce them. In theory, the elastic moduli of cellulose chains can reach values of 250 GPa. However, there is no existing procedure to separate these chains from the micro-fibrils and therefore obtain such values. At present, the pulp and paper industry is able to produce cellulose fibres with moduli around 70 GPa. Moreover, some experimental data obtained from flax and pineapple fibres show that the tensile strength of these fibres is significantly more dependent on the length of the fibre than for the case of glass fibres. Natural fibres seem to be less homogeneous than synthetic fibres. It can be concluded that even if natural fibres are well suited to replace glass fibres in composite materials, many improvements can still be done concerning their mechanical properties. Experimental data giving the tensile strength, flexural strength, modulus, impact force and compressive force are available in the literature for different types of natural-fibre composites.

Natural fibres seem to be less homogeneous than synthetic fibres. Natural fibre properties are highly variable and depend on conditions of growth. It is therefore very difficult to get the same mechanical properties after repeat testing. The fibre properties, such as dimensional instability, have been found to improve after treatment with chemicals such as maleic anhydride, acetic anhydride and silanes. It can be concluded that even if natural fibres are well suited to replace glass fibres in composite materials, many improvements can still be done concerning their mechanical properties. Experimental data giving the tensile strength, flexural strength, modulus, impact force and compressive force are available in the literature for different types of natural-fibre composites. Though natural fibres' mechanical properties are much lower than those of glass fibres (Table 23.1), their specific properties, especially stiffness, are comparable to the stated values of glass fibres. Moreover, natural fibres are about 50% lighter than glass, and in general cheaper.

It is widely acknowledged that natural fibre composites combine good mechanical properties with a low specific mass and offer an alternative material to glass fibre-reinforced plastics in some technical applications. However, their high level of moisture absorption, poor wettability by non-polar plastics and insufficient adhesion between untreated fibres and the polymer matrix can lead to debonding with age. It is also reported by Abdelmouleh et al. [43] that because fibre has low interaction with matrix, load transfer from matrix into fibre is not good. Therefore, fibre surface needs to be modified to reduce the polarity of fibre, and thus the compatibility at interface region is improved. The modification methods are alkaline treatment, grafting with maleic anhydride copolymer and using silane coupling agent.

23.4.3 *Moisture*

Another important aspect is the moisture content of natural fibres. These fibres are hydrophilic and absorb water. The moisture content can be as high as 20%, but in most cases it will be in the range of 5–10%. Lack of good interfacial adhesion with the polymer phase, due to the inherently poor compatibility and the ability of the hydrophilic cellulose fibres to disperse with the hydrophobic resins, makes the use of cellulose-based fibre-reinforced composites less attractive. During processing, the presence of water can create voids in the matrix and also lead to a poor adhesion of the fibres with the hydrophobic resin. The hydrophilic nature of natural fibres can be a problem in the finished composites as well.

The presence of free water and hydroxyl groups, especially in the amorphous regions, worsens the ability of plant fibres to develop adhesive characteristics with most binder materials. High water and moisture absorption of the cellulose fibre causes swelling and a plasticizing effect resulting in dimensional instability and poor mechanical properties. Plant fibres are also prone to micro-biological attack leading to weak fibres and reduction in their life span. However, these drawbacks can be overcome by treating the cellulose fibres with appropriate chemicals. For instance, varying concentrations of caustic soda have been applied to cellulose materials for surface and fine structure modifications. The absorption of steam by sisal, hemp and banana fibre/novolac resin composites was found to reduce after esterification of the –OH groups with maleic anhydride [44]. The tensile strength of the maleic anhydride-treated fibre composites was found to be higher than that of untreated fibre composites.

Cellulose-based fibres absorb moisture causing reversible and non-reversible swelling. In composite products, this can result in undesirable dimensional changes. To arrest this problem, the reinforcing cellulose fibres are subjected to certain modifications. These processes involve either the stabilization of the cell wall matrix to restrain swelling, reduction of the hygroscopic tendency of the cell wall and bulking the cell wall polymers to maintain the wet volume so that moisture does not cause any additional swelling [45]. Formaldehyde has been extensively applied to create dimensional stability in cellulose materials, whereby it reacts with the cell wall hydroxyl groups bonding together micro-fibril units. The reaction takes place under strong acid catalyst.

23.4.4 *Fatigue Behaviour*

In general, the fatigue of composites is a rather complex phenomenon, which is characterized by initiation of cracks, which is dependent on the ductility of the matrix and fibre modulus. The damage is diffused and grows by fibre–matrix debonding or crack bridging and is governed by the fibre–matrix interaction. The properties of the composites show a progressive reduction in strength and stiffness coupled with a

significant increase in the material's damping. The latter two characteristics can be monitored as a function of increasing load cycles or increasing peak loads.

The most important damping mechanisms result from Hwang and Gibson [46]:

- The viscoelastic nature of the matrix and fibre
- The thermoelastic damping
- The Coulomb friction damping due to slip among the unbonded, debonded and bonded regions of fibre–matrix interface
- The energy dissipation occurring at cracks or delaminations

Although, in general, the use of fibre-reinforced plastic composites is continually increasing, certain aspects of their behaviour are still poorly understood. An example is their viscoelastic, viscoplastic or time-dependent behaviour due to creep and fatigue loadings (Fig. 23.7).

The creep and fatigue behaviour for natural fibre-reinforced plastics is less well understood than for glass fibre-reinforced plastics because of the lack of systematic and detailed information. Limited information is currently available on the effects on the fatigue behaviour of natural fibre-reinforced plastics of different composite parameters such as fibre type, the quality of fibre–matrix adhesion and fibre properties and their content.

Wambua et al. [2] evaluated several different natural fibre–polypropylene composites to determine if they had the ability to replace glass fibre-reinforced materials. Polypropylene with a very high melt flow index was used to aid in fibre–matrix adhesion and to ensure proper wetting of the fibres. Samples were made with 40% fibre content of kenaf, coir, sisal, hemp and jute. After the samples were fabricated, tensile and impact tests were run to compare the properties of these composites with those made with glass fibre. The tensile strengths all compared well with glass, except for the coir, but the only sample with the same flexural strength was hemp. It was shown with kenaf fibres that increasing fibre weight fraction increased ultimate strength, tensile modulus and impact strength. However, the composites tested showed low impact strengths compared with glass mat composites. This study demonstrated that natural fibre composites have a potential to replace glass in many applications that do not require very high load bearing capabilities.

23.4.5 Thermal Stability

The interaction of thermal energy (i.e., heat) with the atoms which constitute a material determines some of the most important physical properties of the material. The properties describing this interaction at the most fundamental level are often called thermophysical properties which include heat capacity, thermal diffusivity and thermal conductivity [48]. A complete characterization of the thermal properties of materials requires the determination of the thermal conductivity and thermal diffusivity [49]. Thermal conductivity is a property of materials that expresses the heat flux that will flow through the material if a certain temperature gradient exists

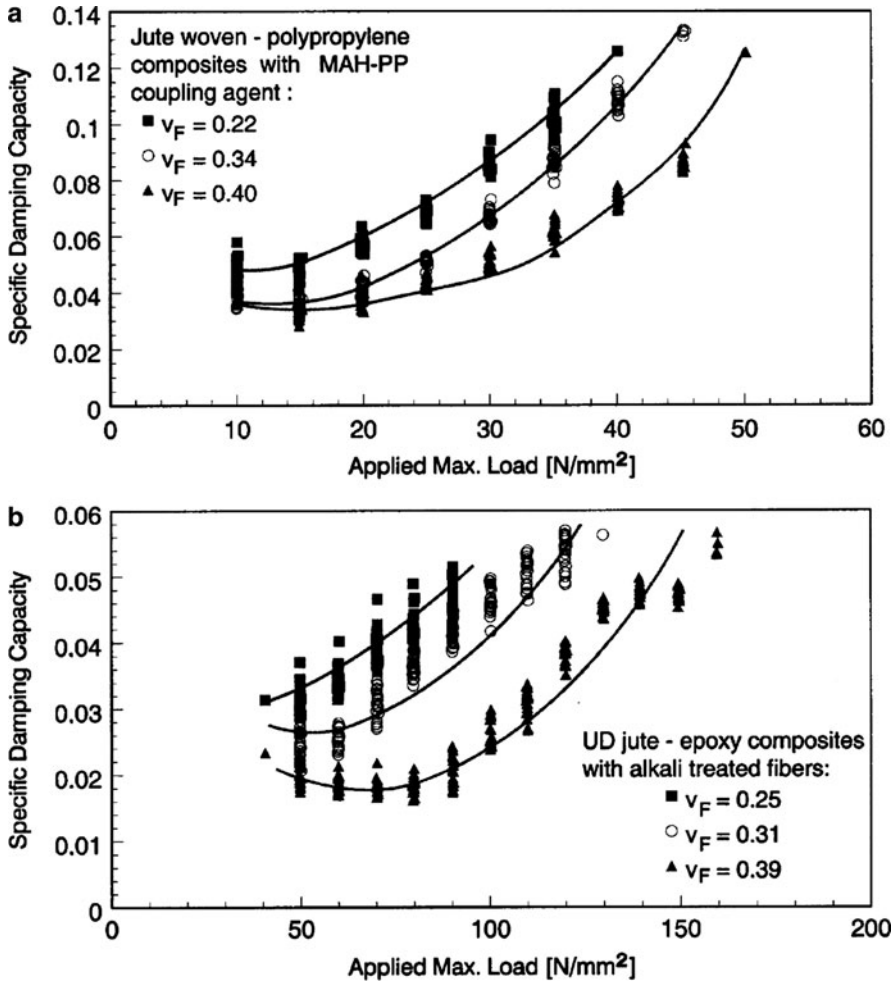


Fig. 23.7 Specific damping capacity versus applied maximum load (10^4 load cycles/load level) for: (a) polypropylene-based composites with MAH-PP-treated jute wovens; (b) epoxy-based composites with alkali-treated (shrinkage = 0%) unidirectional jute fibre [47]

over the material. Thermal diffusivity describes the time-dependent non-steady-state aspects of heat flow. Thermal conductivity is a bulk property analogous to mechanical modulus. Moreover, it is well accepted that a mathematical analogy exists between thermal conduction and elasticity of fibre composites.

Natural fibre-reinforced polymer composites are considered as replacement for metals or carbons in situations where they have better mechanical properties. But the thermal properties of these composites are in general much lower than that of metals. Consequently, it is more difficult to dissipate the heat, and in some situations this can be an important consideration, particularly if electronic components

are situated very close to the material. The combination of reinforcement with high thermal conductivity embedded in a resin matrix with low thermal conductivity is desirable to dissipating the heat flux for electronic packaging components. Studies on the mechanical properties of short fibre-reinforced polymer composites have shown that both fibre length distribution and fibre orientation distribution play a very important role in determining the mechanical properties. A number of analytical models have been proposed to predict the thermal conductivity of short-fibre composites. Thermal conductivity is a bulk property analogous to mechanical modulus. Moreover, it is well accepted that a mathematical analogy exists between thermal conduction and elasticity of fibre composites.

The thermal stability of the reinforcing fibres is a key parameter in composite processing, especially in the case of thermosetting resins and their exothermic curing behaviour as discussed by Pielichowski and Njuguna [48]. Wielage et al. [50] studied the thermal stability of flax and hemp fibres using differential scanning calorimetric (DSC) and thermo-gravimetric (TGA) methods. They noticed a slight decrease of the mass of natural fibres between 200 and 220°C. Above this last temperature, irreversible degradation was observed. Below 160°C, no degradation was taking place. These results suggest that hemp and flax fibres have the thermal stability to endure thermoset cure reactions encountered during composite manufacturing.

Thermal conductivity, diffusivity and specific heat of polyester/natural fibre (banana/sisal) composites were investigated by Idicula et al. [51] as a function of filler concentration and for several fibre-surface treatments. Short randomly oriented intimately mixed banana/sisal hybrid fibre-reinforced polyester composites were processed by varying the fibre-volume fraction. The thermophysical properties of the above composites were studied. The incorporation of the banana/sisal fibre induces a decrease of the effective thermal conductivity of the composite. This shows that thermal conductivity of polymeric matrix seems to be more important than the banana/sisal fibre. The opposite effect was noted for PALF/glass fibre composites. Using NaOH and polystyrene maleic anhydride (PSMA) chemical treatment of fibre allow a significant increase of both thermal conductivity and density values of banana/sisal fibre composites. This shows that the chemical treatment allows a better contact between the components (fibre-matrix) and reduces considerably the thermal contact resistance. Besides, it was shown that a good agreement was obtained between thermal conductivity measurement values and series model predictions in the case of PALF/glass fibre hybrid composites (Fig. 23.8). This last appears sufficient for the effective thermal conductivity estimation of his kind of composites.

23.4.6 Preparation of Fibre-Matrix Composites

A lot of research work has been performed all over the world on the use of natural fibres as a reinforcing material for the preparation of various types of composites.

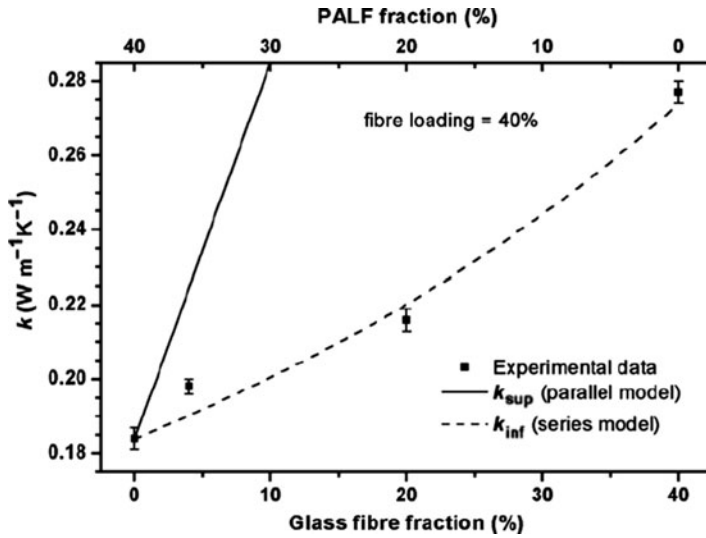


Fig. 23.8 Effect of PALF and glass fibre-volume fraction on experimental and theoretical thermal conductivity of PALF/glass hybrid fibre composites [51]

However, lack of good interfacial adhesion, low melting point, and poor resistance towards moisture make the use of natural fibre-reinforced composites less attractive. Pre-treatments of the natural fibre can clean the fibre surface, chemically modify the surface, stop the moisture absorption process and increase the surface roughness. Among the various pre-treatment techniques, graft copolymerization and plasma treatment are the best methods for surface modification of natural fibres. Graft copolymers of natural fibres with vinyl monomers provide better adhesion between matrix and fibre.

Natural fibre composites are prepared using various composites manufacturing methods such as compression moulding, injection moulding, Resin transfer moulding (RTM) and vacuum bagging. The preforms are mostly fibres, fabrics or non-wovens (Fig. 23.9).

Prepregs are also used. It is often necessary to preheat the natural fibres to reduce the moisture before processing the composites. Equation (23.1) is commonly used in the preparation of composites.

$$V_f = \frac{W_f/\rho_f}{(W_f/\rho_f) + (W_m/\rho_m)}, \tag{23.1}$$

where V_f is the fibre-volume fraction, W_f is the weight of fibre and W_m is the weight of matrix. ρ_f and ρ_m are the densities of the fibre and matrix, respectively.



Fig. 23.9 Non-woven natural fibres for press moulding

The production of the composites is optimized in relation to temperature, pressure and moulding time. High temperatures degrade the cellulose; thus, negatively affecting the mechanical properties of the composites. Inefficient fibre dispersion in the matrix causes fibre agglomeration which decreases the tensile strength.

Most of the previous research on natural fibre composites has focused on reinforcements such as flax, hemp, sisal and jute, and thermoplastic and thermoset matrices. Some of these composites have been produced using matrices made of derivatives from cellulose, starch and lactic acid to develop fully biodegradable composites or biocomposites [52]. The emerging diversity of applications of natural fibre composites has seen the production of sandwich structures based on natural fibre composite skins (see Fig. 23.10).

In some cases, these sandwich composites have been produced from paper honeycomb and natural fibre-reinforced thermoplastic or thermoset skins, depending on the applications.

23.5 Natural Fibre-Reinforced Nanocomposites

Nanoparticles, when engineered appropriately, exhibit a variety of unique and tuneable physicochemical properties [53, 54]. These characteristics have made engineered nanoparticles as central components in an array of emerging technologies with widespread potential applications in material sciences and engineering. Large quantities of nanomaterials are already commercially available for commercial scale applications due to the establishment of well-developed nanomaterial production methods such as chemical vapour deposition and electrospinning. As a



Fig. 23.10 Natural fibre skins for sandwich structures

result, more practical applications are being uncovered due to the ease of bulk manufacture.

Carbon nanotubes, carbon nanofibres, and polyhedral oligomeric silsesquioxanes (POSS) are being used commercially in nanocomposites [55, 56]. Nanoclays, however, are the most dominant commercial nanomaterials, accounting for nearly 70% of the total volume of nanomaterials commercially used [57–59]. The first clay nanocomposite, PA 6/montmorillonite clay nanocomposite, is known to be developed by Toyota back in 1993 [60, 61]. Since then, the concept of nanostructured material design has gained widespread importance in automotive industry mainly due to low cost and availability, when compared with other nanomaterials such as POSS and carbon nanotubes. Automotive and packaging market segments are presently expected to account for nearly 80% of total nanocomposite consumption. The use of nanomaterials in current and future automobiles will allow environmentally friendly automotive materials with higher performance and low manufacture costs, as discussed in the following sections. However, nanotechnology might also have detrimental effects to the environment and it is paramount to understand both the hazards associated with nanomaterials and the levels of exposure that are likely to occur, while still taking advantage of the technology.

The incorporation of nanoclays and natural fibres in resin systems thus provides reinforcements to resin systems at two scales. The nanoclay enhances the bio-based polymer system in stiffness and hygrothermal properties, while the natural fibres provide the main stiffness and strength. In addition, the enhanced barrier properties of the nano-reinforced resin retard moisture from reaching the natural fibres and thereby providing a synergetic effect between scales for an efficient bio-based composite. Hybrid bio-based composites that exploit the synergy between natural fibres (industrial hemp) in a nano-reinforced bio-based polymer can lead to

improved properties while maintaining environmental appeal. Bio-based resins obtained by partial substitution of UPE with epoxidized soybean oil (ESO) increase toughness but compromise stiffness and hygrothermal properties. Reinforcement of the bio-based resin with nanoclays permits to retain stiffness without sacrificing toughness, while also improving barrier and thermal properties.

Longkullabutra et al. [62] recently reported improvement in the tensile strength of epoxy resin and hemp/epoxy resin composites using carbon nanotubes (CNTs). The CNTs adding nanopowder were vibrated via the vibration milling technique for 6–48 h. Different volume percentages of CNTs were dispersed for hemp/epoxy resin composites. The results indicate that adding the milled CNTs can improve tensile properties of composites. Elsewhere, Liu and Erhan [63] fabricated an epoxidized soybean oil (ESO)-based composites reinforced with flax fibres and nanocomposites reinforced with organoclay. The flexural modulus and tensile modulus of the developed composites increased proportionally with the amount of epoxy resin, 1,1,1-tris(*p*-hydroxyphenyl)ethane triglycidyl ether (THPE-GE). The flexural modulus also increased with fibre contents lower than 10 wt%, but showed a decrease beyond 10 wt%. The tensile modulus increases with fibre content until a maximum, at 13.5 wt%, and then it decreases. X-ray diffraction (XRD) and transmission electron microscopy (TEM) data indicated that the organophilic clay was well dispersed in the matrix. An intercalated structure of the composite is developed. Dynamic mechanical study shows that the ESO/clay nanocomposites with 5–10 wt% clay content possess storage modulus ranging from 2.0 to 2.70 MPa at 30°C. As T_g , about 20°C was measured from a dynamic mechanical study. The mechanical study predicates these materials are promising as alternative to petrochemical polymers.

In another example, Faruk and Matuana [64] investigations aimed at identifying the best approach of incorporating nanoclay into WPCs to enhance their mechanical properties. Two different methods of introducing nanoclays into HDPE-based WPCs were examined. The first method involved the reinforcement of HDPE matrix with nanoclay, which was then used as a matrix in the manufacture of the WPCs (melt blending process). The second method consisted of a direct addition of nanoclay into HDPE/wood–flour composites during conventional dry compounding (direct dry blending process). The melt blending process, in which nanoclay/HDPE nanocomposite was used as matrix, appeared to be the best approach of incorporating nanoclay in WPCs. The experimental results indicated that the mechanical properties of HDPE/wood–flour composites could be significantly improved with an appropriate combination of the coupling agent content and nanoclay type in the composites.

CaCO₃/wood cellulose nanocomposite materials have been prepared by controlled generation of carbonate in aqueous solution from an organic precursor (DMC) in the presence of wood cellulose fibres and CaCl₂ [65]. The work demonstrated that the quantity and morphology of CaCO₃ particles deposited at the surface of cellulose fibres were strongly influenced by the hydrolysis conditions. The amount and size of CaCO₃ deposited on the cellulose fibres increased with increasing reaction time. Besides, the reactions performed at room temperature originated

nano-sized CaCO_3 particles with spheroid morphology, while at 70°C micrometric aggregates of $\text{Ca}(\text{OH})_2$ were obtained. In addition, lower mass fractions of fibres in the reacting suspensions favoured the formation of spheroid particles of CaCO_3 . Finally, the presence of carboxyl groups at the substrate surface increased the selectivity of precipitation of CaCO_3 particles on the surface of the fibres. It is acknowledged that the mechanism by which CaCO_3 particles are retained at the surface of cellulosic fibres is not understood yet. Nevertheless, CaCO_3 /cellulose nanocomposites might be considered as potential reinforcing fillers in PE matrix-based composites since preliminary dynamic mechanical analysis (DMA) studies demonstrated that PE composites with CaCO_3 /cellulose fibres showed a much higher mechanical performance as shown in Fig. 23.11.

It follows that silane coupling chemicals have three main advantages: (a) they are commercially available in a large scale; (b) at one end, they bear alkoxy silane groups capable of reacting with OH-rich surface, and (c) at the second end, they have a large number of functional groups which can be tailored as a function of the matrix to be used [66]. The last feature ensures, at least, a good compatibility between the reinforcing element and the polymer matrix or even covalent bonds between them. The reaction of silane coupling agents with lignocellulose fibres (mainly: cellulose and lignin) was found to be quite different to compare with that observed between them and glass surface, in the sense that with cellulose macromolecules, only prehydrolyzed silanes underwent the reaction with cellulose surface. Research work by Abdelmouleh et al. [67] clearly shows that cellulose fibres can be effectively used as reinforcing elements in thermoplastic low-density polyethylene and natural rubber matrices. Cellulose fibres were incorporated into the matrices, as such or after chemical surface modification involving three silane coupling agents, namely, γ -methacryloxypropyltrimethoxy

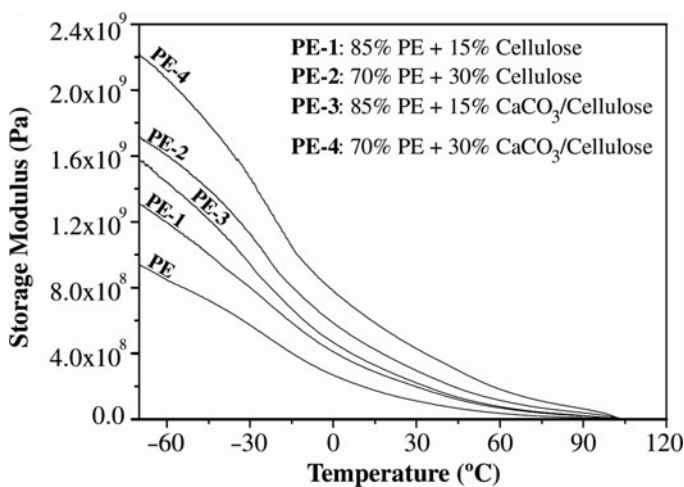


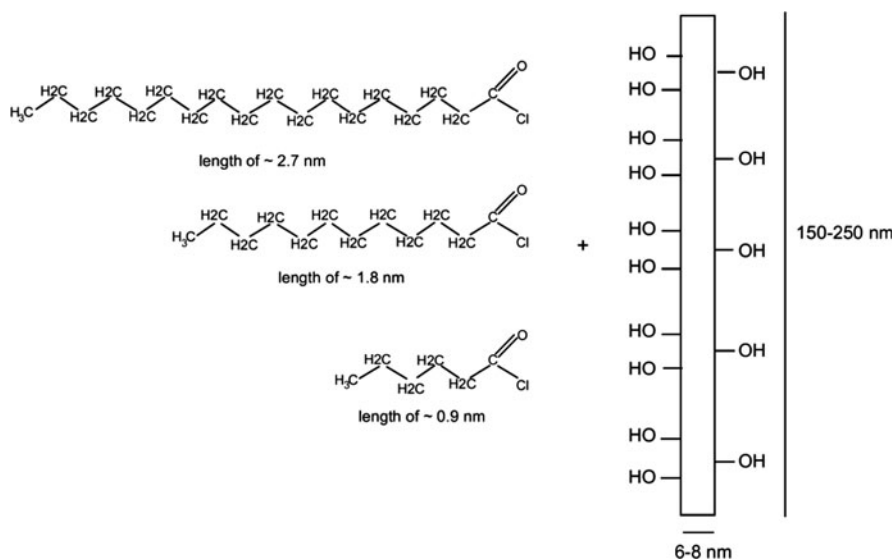
Fig. 23.11 The dynamic storage modulus curves of PE and PE-based composites [65]

(MPS), γ -mercaptopropyltrimethoxy silane (MRPS) and hexadecyltrimethoxy silanes (HDS). As expected, the mechanical properties of the composites increased with increasing average fibre length, and the composite materials prepared using both matrices and cellulose fibres treated with MPS and MRPS displayed good mechanical performances. On the other hand, with HDS bearing merely aliphatic chain only, a modest enhancement on composite properties was observed which was imputed to the incapacity of HDS to bring about covalent bonding with matrix.

A study on extrusion of functionalized ramie cellulose whiskers chemically modified the cellulose whiskers by grafting organic acid chlorides (Scheme 23.1) presenting different lengths of the aliphatic chain by an esterification reaction [68].

The crystallinity of the particles was not altered by the chain grafting, but it was reported that covalently grafted chains were able to crystallize at the cellulose surface when using C18. Both unmodified and functionalized nanoparticles were extruded with low-density polyethylene (LDPE) to prepare nanocomposite materials. The homogeneity of the ensuing nanocomposites was found to increase with the length of the grafted chains. A significant improvement in terms of elongation at break was observed when sufficiently long chains were grafted on the surface of the nanoparticles. It was ascribed to improve dispersion of the nanoparticles within the LDPE matrix.

The reinforcement by cellulose nanofibres instead of micro-sized fibres is recognized as being more effective due to interactions between the nano-sized elements that make up a percolated network connected by hydrogen bonds or entanglements,



Scheme 23.1 Chemical structures of the various chemical grafting agents and their typical dimensions compared with cellulose whiskers [68]

once a good dispersion in the matrix is achieved. Micro-fibrillated cellulose (MFC), therefore, has a great potential as reinforcing medium in composites. More specifically, MFC delivers enhanced toughness to the composites compared with pulp fibres. Nevertheless, the adequate dispersion of hydrophilic cellulosic fibres in a matrix of mostly hydrophobic polymers is a critical aspect to be addressed, which is especially difficult in the case of nanofibres. Very recently, a new process to produce MFC/PLA composites by compression moulding of sheets made of uniformly dispersed MFC and PLA fibres by a procedure similar to papermaking has been developed [69]. The method is similar to papermaking, with reduced dewatering time, and it is claimed to be simple enough to be readily applicable at an industrial scale. The method delivered high yields and reduced dewatering times and could be easily adopted by the industry. Good dispersions were obtained even at high MFC contents up to 90 wt% and as a result the tensile modulus, strength and strain at fracture of the composites increased linearly as a function of MFC content. The modulus was doubled and the strength was tripled as the MFC content increased from 10 to 70 wt%. The reinforcement attained by the incorporation of MFC resulted in better mechanical properties (Fig. 23.12) over neat PLA, especially regarding the enhancement in toughness.

In a different study, characterization of different hybrid composites have verified this synergistic behaviour in which systems with 10% ESO and 1.5 wt% nanoclay retained the original stiffness, strain to failure (Fig. 23.13), and hygrothermal properties of the original resin while improving toughness [70]. Optimum designs that maximize the synergy of the constituents are thus possible and the presented results provide an initial benchmark to identify such balance, and thus increase the potential applications of bio-based composites.

As lamented on earlier, fatigue and impact resistance remains a major drawback in many potential applications of natural fibre-reinforced composites, just like their synthetic counterparts. And although numerous new nanocomposites have been developed in various research fields, the research on energy absorption capability of

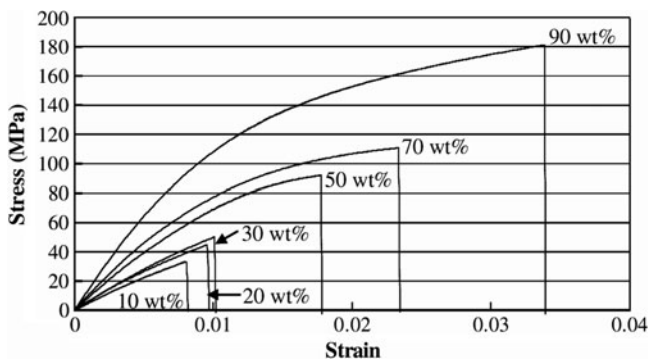


Fig. 23.12 Typical stress–strain curves of MFC/PLA composites at different MFC fibre contents. Percentages indicate MFC fibre contents [69]

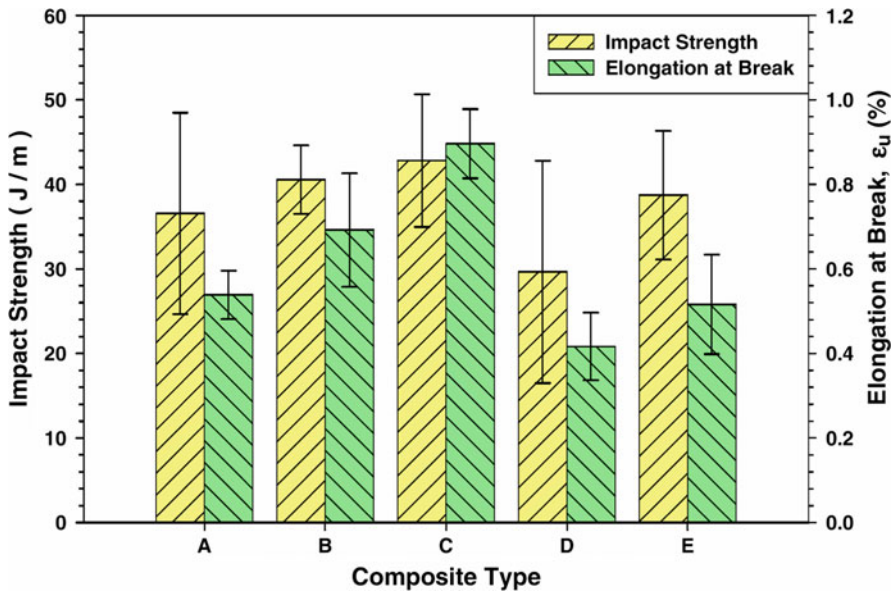


Fig. 23.13 Impact strengths from notched Izod tests and tensile strains at failure [70]

nanocomposites is still in the early stages [71]. The technical issues to be addressed include [72]:

- Lack of acceptable evaluation parameters and methods for energy absorption capability of nanocomposites, such as evaluating indicators, test methods and test conditions
- Lack of theoretical models that can predict the energy absorption capability
- Lack of a systematic comparison of limitations and advantages among the existing research methods
- Lack of a fundamental understanding of energy absorption mechanisms in nanocomposites
- Need for finding potential applications of energy-absorbing nanocomposites

The environmental concerns linked to the use of halogen-based fire retardants open new routes to develop fire-resistant composites. The elaboration of polymer–silicate clay nanocomposites has already addressed to these fireproof issues. Indeed, the nano-scale dispersion of clay layers forms a passive barrier, a sort of inorganic labyrinth, which hinders the out-diffusion of volatile decomposition products from thermal cracking. For instance, Guigo et al. [73] studies on nanocomposites composed of isolated lignin, natural fibres and natural additives which are elaborated through conventional thermoplastic processes such as injection moulding. The obtained composites have wood-like mechanical behaviour and some properties lies in the range of those of polyamides. For certain practical applications such as automotive, the thermal stability and fire resistance of the nanocomposites need further improvement.

23.6 Lightweight Component Manufacturing Techniques

23.6.1 *Compression and Injection Moulding*

Injection moulding process is suitable to form complex shapes and fine details with excellent surface finish and good dimensional accuracy for high production rate and low labour cost [1]. On the other hand, the compression technique is also widely used and involves sheet moulding compound (SMC), which is a semi-finished product that is moulded into parts by compression moulding technology. The material consists of roughly 45% mineral filler, 30% glass fibres and 25% polymeric matrix and different additives. The reinforcing glass fibres are manufactured under high use of energy and bear a fairly high density of roughly 2.5 g/cm^3 . The matrix polymers mainly used are UPE or vinylester resins that are both derived from crude oil. As SMC material offers high potential for lightweight design and application, the use of raw materials coming from renewable resources is sustainable.

The advantages of these procedure are the short cycle time, the low scrap arising and the low orientation in the mouldings. Processing times of < 2 min are reached during the compression moulding of three-dimensional components with a high forming degree. It has also been shown that the adhesion of natural fibres and matrix resin is important in order to obtain good mechanical properties of natural fibre composites, and the mechanical properties were improved by the moulding condition, the moulding pressure and temperature. A question that needs to be addressed in compression moulding is: what is the maximum pressure which can be applied for improving the mechanical properties before damaging the structure of the fibres, so that meaningful reinforcement takes place?

23.6.2 *Resin Transfer Moulding*

Resin transfer moulding (RTM) process is commonly used in the aerospace and automotive industry. The process consists of mixing resin with a hardener and injecting the combination at low pressure into a mould, which contains fibres. The resulting part is cured at room temperature or above until the end of the curing reaction. Several types of resins (epoxy, polyester, phenolic and acrylic) can be used for this process as long as their viscosity is low enough to ensure a proper wetting of the fibres. Parameters such as injection pressure, fibre content or mould temperature have a great influence on the development of the temperature profiles and the thermal boundary layers, especially for thin cavities. Good knowledge of all the operating steps is very important to obtain high-quality parts.

Richardson and Zhang [74] presented an experimental study of the mould-filling process for a non-woven hemp-phenolic resin system. Fibre washing (unexpected displacement of the reinforcement in the mould during the RTM process) was shown to be a problem at low fibre concentration due to poor clamping. This

could lead to the failure of the process. This effect was reduced by increasing the fibre concentration and improving the clamping system. Edge flow was observed during the mould filling as well. It was found to be very sensitive to fibre concentration. Using preforms larger than the mould solved this problem. Finally, in the rectangular mould used for this study, the “quasi-one dimensional steady state” flow (equal resin advancement distance or velocity at any moment during the injection in the resin advancement direction) was required to obtain a complete preform impregnation. All these parameters were found to depend greatly on the injection pressure and on the fibre concentration.

A few other studies investigated the possibility of using the RTM process to prepare natural fibres composites. Sèbe et al. [75] obtained very good results for hemp fibre-reinforced polyester composites. No major problem was noticed during the RTM process. Williams and Wool [76] did not report any problems as well with natural fibres–soy oil resins systems. More recently, Oksman [77] manufactured high-quality flax fibre composites using a RTM process. Good flow properties were observed in the mould and high fibre content was attained. The composites were found to have very promising mechanical properties.

23.6.3 Vacuum Assisted Resin Transfer Moulding

The vacuum assisted resin transfer moulding (VARTM) process is a variant of vacuum-infusion RTM in which one of the solid tool faces is replaced by a flexible polymeric film (Fig. 23.14).

This process or a modified version is also known as vacuum infusion or SCRIMP. The VARTM process is a very clean and economical manufacturing method: the process draws resin into a dry reinforcement on a vacuum bagged tool, using only the partial vacuum to drive the resin. The process increases the component mechanical properties and fibre content by reducing void percentage, when compared with other large-part manufacturing processes, such as hand lay-up [78]. For higher performance composites, VARTM offers the potential for reduced tooling costs where matched tooling is being used, such as that used in RTM or compression moulding. As one of the tool faces is flexible, the moulded laminate thickness depends in part on the compressibility of the fibre–resin composite before curing and the vacuum negative pressure.

23.7 Applications and Future Trends

Despite significant improvement in properties, disposal and recycling problems, combined environmental and societal concerns make continued use of petroleum-based nanocomposites unattractive. As a consequence, natural fibre-reinforced thermoset and thermoplastic composites have been intensively studied in the last

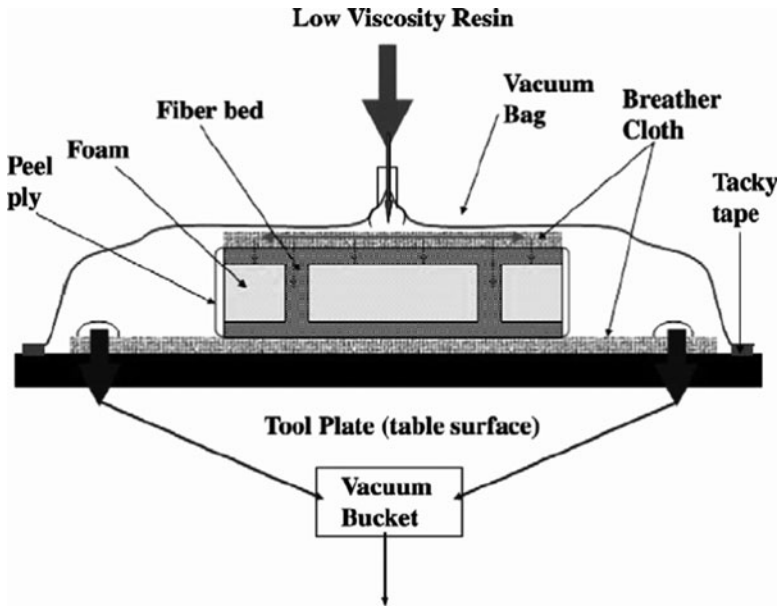


Fig. 23.14 A schematic showing VARTM process when a structural part is infused [78]

years since they present a positive environmental impact and interesting characteristics. Moreover, all plant fibre composites are characterized as being easy to process, economic to produce and friendly to process, presenting good mechanical properties, light weight, no skin irritation and in some cases they can promote thermal and acoustic insulation. Even so, some disadvantages such as moisture or odours must be over passed. Regarding the mechanical performance, as the fibre length increases, the material stiffness and strength tends to increase, but it also becomes more difficult to produce complex parts.

Of late many of the major car manufacturers now use biocomposites in various applications, e.g., door trim panels made of polyurethane (PU)-flax/sisal mat in Audi A2 midrange car; jute-based door panels in Mercedes E-class; polyester-cotton fibres in “Trabant” car; under floor protection trim of Mercedes A class made from banana fibre-reinforced composites and the Mercedes S class automotive components made from different bio-fibre-reinforced composites. All these so-called “biocomposites” use natural fibres but the resin matrix is always an oil-derived synthetic material.

To date, many of the major car manufacturers such as Daimler Chrysler, Mercedes, Volkswagen, Audi Group, BMW, Ford and Opel now use biocomposites in various applications as demonstrated in Fig. 23.15 [79].

Interior trim components such as dashboards and door panels using polypropylene and natural fibres have been produced for Daimler Chrysler for a while. The use of flax fibres in car disc brakes to replace asbestos fibres is also another

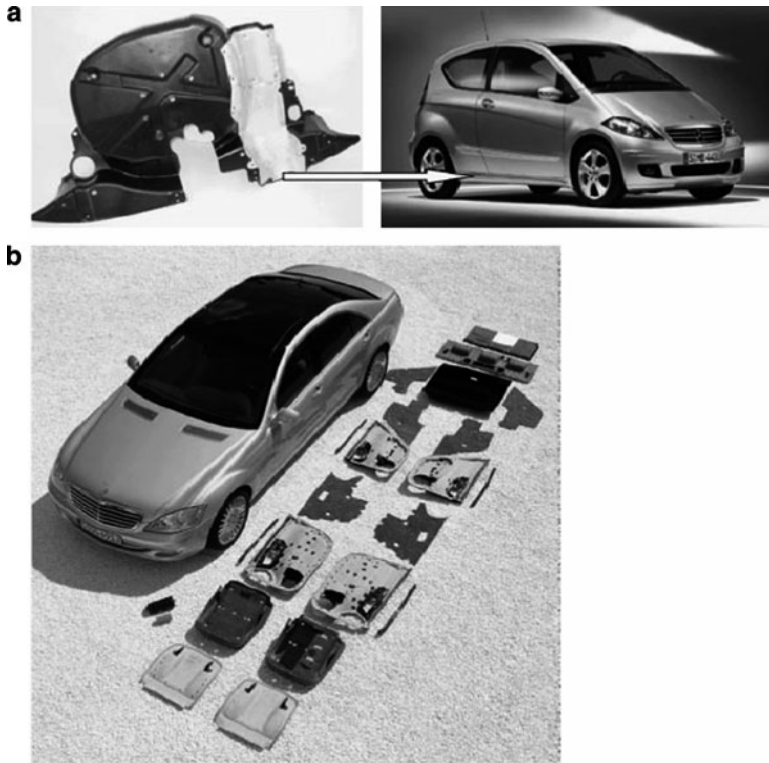


Fig. 23.15 (a) Under floor protection trim of Mercedes A class made from banana fibre-reinforced composites. (b) Newest Mercedes S class automotive components made from different bio-fibre-reinforced composites [79]

example. In 2000, Audi launched the A2 midrange car in which door trim panels were made of polyurethane reinforced with mixed flax/sisal mat.

Daimler Chrysler has been increasing its research and development in flax-reinforced polyester composites for exterior applications for a number of years now [80]. Mercedes also used jute-based door panels in its E-class vehicles in 1996 [81]. Cotton fibres embedded in polyester matrix were used in the body of the East German “Trabant” car [82]. Some other applications are on Mercedes A and S class made from different bio-fibre-reinforced composites [83]. Lotus manufactured “Eco Elise” bodyworks which contains hemp fibres, while sisal fibres are used for interior trimmings while the inner door panels for the BMW 7 Series contain 70% of sisal fibres. Plant fibre-reinforced polylactic acid composites with improved rigidity and reduced processing times have been applied in the Toyota Lexus HS250h hybrid vehicle recently.

It is therefore acknowledged that natural fibre production requires much less non-renewable energy than glass fibres production. The non-renewable energy

consumed by the production of glass fibre mat (54.7 MJ/kg) is more than five times higher than the value estimated for the flax fibre mat (9.55 MJ/kg) [84]. While natural fibres growth mainly demands solar energy, glass fibres production process including melting stages at extreme temperatures depends on intensive fossil fuels consumption. The only trouble spot of natural fibre crops is related to the use of fertilizers that could potentially lead to increased nitrate emissions and result in eutrophication effects. Nevertheless, if the contributions of atmospheric NO_x emissions to eutrophication phenomenon are taken into account, GFR composites production environmental impact is more severe [85]. Moreover, to facilitate wide-scale applications, a better understanding is required to properly quantify the added benefit of green composites. For mass production in applications like automotive, special considerations need to be given on damage tolerances, impact behaviour (failure and resistance), fatigue life and vehicle safety margins.

Upgrading these greener composites through biodegradable bioplastic-nanocomposites remains the most feasible route to environmentally friendly green nanocomposites using extrusion followed by compression moulding or injection moulding. By employing nanomaterial, much of this objective can be achieved as shown by Njuguna et al. [86]. In particular, incorporating a small amount of appropriate compatibilizer is expected to enhance miscibility of composite matrix and clay nanofillers and thus further improve mechanical and thermal properties of the nanocomposites. These nanocomposites may ultimately replace existing petroleum-based polypropylene/thermoplastic polyolefins (PP/TPO) in automotive applications.

Further, Daimler-Benz has been exploring the idea of replacing glass fibres with natural fibres in automotive components since 1991 [79]. Mercedes Benz pioneered this concept with the “Beleem project” based in Sao Paulo, Brazil, through which, coconut fibres were used in the commercial vehicles over a 9-year period. Evidently nanoclays are being used to replace other fillers and provide an improved balance of stiffness and toughness while reducing weight. For example, 5% of nanoclay can replace 15–50% of standard fillers like calcium carbonate thereby reducing the cost and improving the mechanical properties. Nanoclays typically replace talc or glass fillers at a 3:1 ratio, with 5–8% of a nanoclay replacing 15% of glass filler, for example [87]. The balance of flexural modulus and impact strength in nanocomposites allows polyolefins to compete with engineering materials like PC/ABS. Notably, polyolefin nanocomposites are less expensive and do not need drying, resulting in a 15–25% system cost savings over some engineering resins.

If current research efforts for the development of fully biodegradable green composites are of utmost importance, use of biocomposites represents a necessary intermediate step. Mechanical properties and strengths of widespread thermoset or thermoplastic resins (PP, PE, PEEK, etc.) can be significantly increased by employing natural fibres as reinforcement. Natural fibres present the advantage to have a higher specific strength when compared with common glass fibres and to be carbon dioxide neutral. Most of them are vegetal, extracted from leaves (abaca, banana, sisal and pineapple), stem (jute, flax, hemp, kenaf and ramie), fruits (coir and oil palm), seeds (cotton) grasses (bamboo) or roots (broom), but some fibres of animal (wool and silk) and mineral (basalt) origin are produced. Another alternative consists

in mixing synthetic and natural fibres or different types of natural fibres to obtain hybrid composites (basalt/glass/PP, basalt/hemp/PP, etc.) and make the most of the specific properties of each constituent. Up to now, natural fibre-reinforced polymeric composites are used for applications like particleboards, printed circuit boards, window frames, and asbestos replacement in car disc brakes, car door panels, interior trim boards or dashboards.

Automotive manufacturers are constantly searching for material solutions for both interior and exterior parts that improve part aesthetics and acoustic, reducing weight, increase the performance or reduce time and cost. It is expected that increased use of green (nano)composites made using renewable and environmentally benign materials such as biofibres and bio-based resins derived from soybeans, pure cellulose acetate, citrate-based plasticizer, and organically modified montmorillonite nanofillers, for example, will prevail [86]. Notably, attempts have been made to use natural fibre composites in place of glass mostly in non-structural applications. So far, a good number of automotive components previously made with glass fibre composites are now being manufactured using environmentally friendly composites [88, 89].

23.8 Conclusions

The application of natural fibres is being targeted in various fields due to both environmental and economical benefits. Natural fibres are renewable, biodegradable, safe to use and the most important reason being their high specific strength to weight ratio. This is of special significance in transportation applications as it leads to weight reductions and thus savings in fuel consumption. In this chapter, natural fibre-reinforced polymer composites and nanocomposites for applications in automotive as a class of structural materials have been presented. Their ease of fabrication, relatively low cost and superior mechanical properties compared with polymer resins is beneficial.

The chapter demonstrates that in spite of the incompatibility between hydrophilic natural fibres and hydrophobic polymeric matrices, the properties of natural fibre composites can be enhanced through chemical modifications. The chemical treatments have therefore played a key role in the increased applications of natural fibre composites in the automotive sector. Recent work has also shown that if some of the drawbacks of natural fibres can be adequately addressed, these materials can easily replace glass fibres in many applications. The chapter has also shown that there have been attempts to use natural fibre composites in structural applications, an area which has been hitherto the reserve of synthetic fibres like glass and aramid. The use of polymer nanocomposites in applications of natural fibre-reinforced composites, though at infancy, may provide means to address these efficiencies. Evidence-based life-cycle assessment of natural fibre-reinforced composites is required to build confidence in the green composites applications in automotive sector.

References

1. Mouti Z, Westwood K, Kayvantash K et al (2010) Low velocity impact behavior of glass filled fiber-reinforced thermoplastic engine components. *Materials* 3:2463–2473
2. Wambua P, Ivens J, Verpoest I (2003) Natural fibres: can they replace glass in fibre reinforced plastics? *Compos Sci Technol* 63:1259–1264
3. Wambua PM (2004) Protective low price composite materials based on natural fibres. PhD thesis, Katholieke Universiteit Leuven, Belgium
4. Lee SC, Mariatti M (2008) The effect of bagasse fibers obtained (from rind and pith component) on the properties of unsaturated polyester composites. *Mater Lett* 62:2253–2256
5. Jústiz-Smith NG, Virgo GJ, Buchanan VE (2008) Potential of jamaican banana, coconut coir and bagasse fibres as composite materials. *Mater Charact* 59:1273–1278
6. Reed AR, Williams PT (2003) Thermal processing of biomass natural fibre wastes by pyrolysis. *Int J Energy Res* 28:131–145
7. Cahn RW (1990) *Encyclopedia of materials science and engineering supplementary*. Pergamon Press, Oxford
8. Hamad W (2002) *Cellulosic materials: fibers, networks, and composites*. Kluwer Academic Publishers, The Netherlands
9. Bos HL, Van Den Oever MJA, Peters OCJJ (2002) Tensile and compressive properties of flax fibres for natural fibre reinforced composites. *J Mater Sci* 37:1683–1692
10. Bhat GS (1995) Nonwovens as three-dimensional textiles for composites. *Mater Manuf Process* 10:667–688
11. John MJ, Anandjiwala RD (2009) Chemical modification of flax reinforced polypropylene composites. *Compos A* 40:442–448
12. Beckermann GW, Pickering KL (2009) Engineering and evaluation of hemp fibre reinforced polypropylene composites: micro-mechanics and strength prediction modelling. *Compos A* 40:210–217
13. Mohanty AK, Wibowo A, Misra M et al (2004) Effect of process engineering on the performance of natural fiber reinforced cellulose acetate biocomposites. *Compos A* 35:363–370
14. Van Voorn B, Smit HHG, Sinke RJ et al (2001) Natural fibre reinforced sheet moulding compound. *Compos A* 32:1271–1279
15. Wollerdorfer M, Bader H (1998) Influence of natural fibres on the mechanical properties of biodegradable polymers. *Ind Crop Prod* 8:105–112
16. Mehta G, Drzal LT, Mohanty AK et al (2006) Effect of fiber surface treatment on the properties of biocomposites from nonwoven industrial hemp fiber mats and unsaturated polyester resin. *J Appl Polym Sci* 99:1055–1068
17. Mitchell AJ (1986) Composites of commercial wood pulp fibres and cement. *Appita J* 30:229
18. Nishino T, Hirao K, Kotera M et al (2003) Kenaf reinforced biodegradable composite. *Compos Sci Technol* 63:1281–1286
19. Zampaloni M, Pourboghraat F, Yankovich SA et al (2007) Kenaf natural fiber reinforced polypropylene composites: a discussion on manufacturing problems and solutions. *Compos A* 38:1569–1580
20. Shebani AN, van Reenen AJ, Meincken M (2008) The effect of wood extractives on the thermal stability of different wood species. *Thermochim Acta* 471:43–50
21. Maldas D, Kokta BV, Daneault C (1989) Thermoplastic composites of polystyrene: effect of different wood species on mechanical properties. *J Appl Polym Sci* 38:413–439
22. Lu JZ, Wu Q, Negulescu II (2005) Wood-fiber/high-density-polyethylene composites: coupling agent performance. *J Appl Polym Sci* 96:93–102
23. Michell AJ (1986) Composites containing wood pulp fibres. *Appita* 39:223–229
24. Beg MDH, Pickering KL (2008) Mechanical performance of kraft fibre reinforced polypropylene composites: influence of fibre length, fibre beating and hygrothermal ageing. *Compos A* 39:1748–1755
25. McKenzie AW, Yuritta JP (1979) Wood fiber reinforced polymers. *Appita* 32:460–465

26. Bhattacharyya D, Bowis M, Jayaraman K (2003) Thermoforming woodfibre-polypropylene composite sheets. *Compos Sci Technol* 63:353–365
27. George J, Sreekala MS, Thomas S et al (1998) Stress relaxation behavior of short pineapple fiber reinforced polyethylene composites. *J Reinforc Plast Compos* 17:651–672
28. George J, Bhagawan SS, Prabhakaran N et al (1995) Short pineapple-leaf-fiber-reinforced low-density polyethylene composites. *J Appl Polym Sci* 57:843–854
29. Luo S, Netravali AN (1999) Mechanical and thermal properties of environment-friendly ‘green’ composites made from pineapple leaf fibers and poly(hydroxybutyrate-co-valerate) resin. *Polym Compos* 20:367–378
30. Arib RMN, Sapuan SM, Ahmad MMHM et al (2006) Mechanical properties of pineapple leaf fibre reinforced polypropylene composites. *Mater Des* 27:391–396
31. Pothan LA, Thomas S (2003) Polarity parameters and dynamic mechanical behaviour of chemically modified banana fiber reinforced polyester composites. *Compos Sci Technol* 63: 1231–1240
32. Elanthikkal S, Gopalakrishnanapanicker U, Varghese S et al (2010) Cellulose microfibrils produced from banana plant wastes: isolation and characterization. *Carbohydr Polym* 80:852–859
33. Sreekumar PA, Albert F, Unnikrishnan G et al (2008) Mechanical and water sorption studies of ecofriendly banana fiber-reinforced polyester composites fabricated by RTM. *J Appl Polym Sci* 109:1547–1555
34. Liu H, Wu Q, Zhang Q (2009) Preparation and properties of banana fiber-reinforced composites based on high density polyethylene (HDPE)/Nylon-6 blends. *Bioresour Technol* 100: 6088–6097
35. Agarwal R, Saxena NS, Sharma KB et al (2003) Thermal conduction and diffusion through glass-banana fiber polyester composites. *Indian J Pure Appl Phys* 41:448–452
36. Annie Paul S, Boudenne A, Ibos L et al (2008) Effect of fiber loading and chemical treatments on thermophysical properties of banana fiber/polypropylene commingled composite materials. *Compos A* 39:1582–1588
37. Li Y, Mai Y, Ye L (2000) Sisal fibre and its composites: a review of recent developments. *Compos Sci Technol* 60:2037–2055
38. Gordon JE, Jeronimidis G (1980) Composites with high work of fracture. *Philos Trans R Soc Lond A Math Phys Sci* 294:545–550
39. Joseph K, Thomas S, Pavithran C (1995) Effect of ageing on the physical and mechanical properties of sisal-fiber-reinforced polyethylene composites. *Compos Sci Technol* 53:99–110
40. Gauthier R, Joly C, Coupas AC et al (1998) Interfaces in polyolefin/cellulosic fiber composites: chemical coupling, morphology, correlation with adhesion and aging in moisture. *Polym Compos* 19:287–300
41. George J, Sreekala MS, Thomas S (2001) A review on interface modification and characterization of natural fiber reinforced plastic composites. *Polym Eng Sci* 41:1471–1485
42. Bledzki AK, Gassan J (1999) Composites reinforced with cellulose based fibres. *Prog Polym Sci* 24:221–274
43. Abdelmouleh M, Boufi S, Belgacem MN et al (2004) Modification of cellulosic fibres with functionalised silanes: development of surface properties. *Int J Adhes Adhes* 24:43–54
44. Mishra S, Naik JB, Patil YP (2000) The compatibilising effect of maleic anhydride on swelling and mechanical properties of plant-fiber-reinforced novolac composites. *Compos Sci Technol* 60:1729–1735
45. Dash BN, Rana AK, Mishra HK et al (1999) Novel, low-cost jute-polyester composites. part 1: processing, mechanical properties, and SEM analysis. *Polym Compos* 20:62–71
46. Hwang SJ, Gibson RF (1992) Use of strain energy-based finite element techniques in the analysis of various aspects of damping of composite materials and structures. *J Compos Mater* 26:2585–2605
47. Gassan J (2002) A study of fibre and interface parameters affecting the fatigue behaviour of natural fibre composites. *Compos A* 33:369–374

48. Pielichowski K, Njuguna J (2005) Thermal degradation of polymeric materials. RAPRA Technologies Limited, Shawbury, Surrey
49. Pandey JK, Raghunatha Reddy K, Pratheep Kumar A et al (2005) An overview on the degradability of polymer nanocomposites. *Polym Degrad Stab* 88:234–250
50. Wielage B, Lampke T, Marx G et al (1999) Thermogravimetric and differential scanning calorimetric analysis of natural fibres and polypropylene. *Thermochim Acta* 337:169–177
51. Idicula M, Boudenne A, Umadevi L et al (2006) Thermophysical properties of natural fibre reinforced polyester composites. *Compos Sci Technol* 66:2719–2725
52. Mishra S, Mohanty AK, Drzal LT et al (2004) A review on pineapple leaf fibers, sisal fibers and their biocomposites. *Macromol Mater Eng* 289:955–974
53. Leszczyńska A, Njuguna J, Pielichowski K et al (2007) Polymer/montmorillonite nanocomposites with improved thermal properties: part I. Factors influencing thermal stability and mechanisms of thermal stability improvement. *Thermochim Acta* 453:75–96
54. Leszczyńska A, Njuguna J, Pielichowski K et al (2007) Polymer/montmorillonite nanocomposites with improved thermal properties: part II. Thermal stability of montmorillonite nanocomposites based on different polymeric matrixes. *Thermochim Acta* 454:1–22
55. Markarian J (2005) Automotive and packaging offer growth opportunities for nanocomposites. *Plastics Addit Compound* 7:18–21
56. Auto Applications Drive Commercialization of Nanocomposites (2002) *Plastics. Addit Compound* 4:30–33
57. BCC Research (2006) Nanocomposites, nanoparticles, nanoclays, and nanotubes. 1 Jun 2006
58. Lux Research (2004) The Nanotech Report 2004 retrieved on February 10, 2011 from <http://www.luxresearchinc.com/products/subscription-intelligence/state-of-the-market-reports.html>
59. Principia Partners (2005) Polymer Nanocomposites Create Exciting Opportunities in the Plastics Industry: Updated Study from Principia. Retrieved on February 10, 2011 from Special Chem at <http://specialchem4polymers.com/resources/latest/displaynews.aspx?id=1965>
60. Kojima Y, Usuki A, Kawasumi M et al (1993) Mechanical properties of nylon 6-clay hybrid. *J Mater Res* 8:1185–1189
61. Kojima Y, Usuki A, Kawasumi M et al (1993) Sorption of water in nylon 6-clay hybrid. *J Appl Polym Sci* 49:1259–1264
62. Longkullabutra H, Thamjaree W, Nhuapeng W (2010) Improvement in the tensile strength of epoxy resin and hemp/epoxy resin composites using carbon nanotubes. *Adv Mater Res* 93–94: 497–500
63. Liu Z, Erhan SZ (2008) “Green” composites and nanocomposites from soybean oil. *Mater Sci Eng A* 483–484:708–711
64. Faruk O, Matuana LM (2008) Nanoclay reinforced HDPE as a matrix for wood-plastic composites. *Compos Sci Technol* 68:2073–2077
65. Vilela C, Freire CSR, Marques PAAP et al (2010) Synthesis and characterization of new CaCO₃/cellulose nanocomposites prepared by controlled hydrolysis of dimethylcarbonate. *Carbohydr Polym* 79:1150–1156
66. Xie Y, Hill CAS, Xiao Z et al (2010) Silane coupling agents used for natural fiber/polymer composites: a review. *Compos A* 41:806–819
67. Abdelmouleh M, Boufi S, Belgacem MN et al (2007) Short natural-fibre reinforced polyethylene and natural rubber composites: effect of silane coupling agents and fibres loading. *Compos Sci Technol* 67:1627–1639
68. Junior de Menezes A, Siqueira G, Curvelo AAS et al (2009) Extrusion and characterization of functionalized cellulose whiskers reinforced polyethylene nanocomposites. *Polymer* 50: 4552–4563
69. Nakagaito AN, Fujimura A, Sakai T et al (2009) Production of microfibrillated cellulose (MFC)-reinforced polylactic acid (PLA) nanocomposites from sheets obtained by a paper-making-like process. *Compos Sci Technol* 69:1293–1297
70. Haq M, Burgueño R, Mohanty AK et al (2008) Hybrid bio-based composites from blends of unsaturated polyester and soybean oil reinforced with nanoclay and natural fibers. *Compos Sci Technol* 68:3344–3351

71. Njuguna J, Michalowski S, Pielichowski K, Kayvantash K, Walton AC (2011) Fabrication, characterisation and low-velocity impact on hybrid sandwich composites with polyurethane/layered silicate foam cores. *Polym Compos* 32:6–13
72. Sun L, Gibson RF, Gordaninejad F et al (2009) Energy absorption capability of nanocomposites: a review. *Compos Sci Technol* 69:2392–2409
73. Guigo N, Vincent L, Mija A et al (2009) Innovative green nanocomposites based on silicate clays/lignin/natural fibres. *Compos Sci Technol* 69:1979–1984
74. Richardson MOW, Zhang ZY (2000) Experimental investigation and flow visualisation of the resin transfer mould filling process for non-woven hemp reinforced phenolic composites. *Compos A* 31:1303–1310
75. Sèbe G, Cetin NS, Hill CAS et al (2000) RTM hemp fibre-reinforced polyester composites. *Appl Compos Mater* 7:341–349
76. Williams GI, Wool RP (2000) Composites from natural fibers and soy oil resins. *Appl Compos Mater* 7:421–432
77. Oksman K (2001) High quality flax fibre composites manufactured by the resin transfer moulding process. *J Reinf Plast Compos* 20:621–627
78. Dweib MA, Hu B, O'Donnell A et al (2004) All natural composite sandwich beams for structural applications. *Compos Struct* 63:147–157
79. John MJ, Thomas S (2008) Biofibres and biocomposites. *Carbohyd Polym* 71:343–364
80. Automotive Industries (2000) "Goes Natural" for large body panel. DaimlerChrysler 9
81. Pervaiz M, Sain MM (2003) Sheet-molded polyolefin natural fiber composites for automotive applications. *Macromol Mater Eng* 288:553–557
82. Suddell BC, Evans WJ, Mohanty AK, Misra M, Drzal LT (eds) (2005) Natural fiber composites in automotive applications: Natural fibers. Biopolymers and Biocomposites. CRC Press, p 231
83. Bledzki AK, Faruko O, Sperher VE (2006) Cars from bio-fibres. *Macromol Mater Eng* 291:449–457
84. Diener J, Siehler U (1999) Ökologischer vergleich von NMT-und GMT-bauteilen. *Angew Makromol Chem* 272:1–1
85. Corbiere-Nicollier T, Gfeller Laban B, Lundquist L et al (2001) Life cycle assessment of biofibres replacing glass fibres as reinforcement in plastics. *Resour Conservat Recycl* 33:267–287
86. Njuguna J, Pena I, Zhu H et al (2009) Opportunities and environmental health challenges facing integration of polymer nanocomposites: technologies for automotive applications. *Int J Polym Technol* 1:113–122
87. PolyOne Corporation (2010) <http://www.polyone.com/en-us/products/Pages/default.aspx>. Accessed 30 Apr 2010
88. Leao A, Rowell R, Tavares N (1997) Applications of natural fibres in automotive industry in brazil-thermoforming process. In: 4th International Conference on Frontiers of Polymers and Advanced Materials Conference Proceedings, pp 755–760
89. Dahlke B, Larbig H, Scherzer HD et al (1998) Natural fiber reinforced foams based on renewable resources for automotive interior applications. *J Cell Plast* 34:361–378

Chapter 24

Natural Fiber-Based Composite Building Materials

B. Singh, M. Gupta, Hina Tarannum, and Anamika Randhawa

Abstract Jute and allied fibers have gained interest as reinforcing materials in the composite industry for low-cost housing applications. Their advantages have been increasingly recognized with the major motivation being the environmental friendliness, low cost, renewability, and high specific strength and stiffness. In this chapter, an overview of efforts made during the previous decades on natural fiber composites is presented. Research and development carried out at CBRI on natural fiber composites with reference to jute is outlined. A three cornered approach: surface treatment of fibers, matrix resin modification, and selection of an appropriate processing technique for designing innovative building products have been adopted to develop dimensionally stable products. Based on these findings, various products such as composite panels, roofing sheets, door shutters, frames, and shuttering plates alternative to plywood have been prepared. Industrial trials for the manufacturing of standard size panel products are also carried out to know their commercial viability. The suitability of these products was assessed as per existing standard specifications for use as alternate building materials.

Keywords Building materials · Composites · Door shutters · Jute · Natural fibers

Contents

24.1	Introduction	702
24.2	An Overview on Natural Fiber Based Building Materials	702
24.3	Jute Fibers and Their Modification	704
24.4	Composite Matrix Resins	706
24.5	Properties of Jute Composites	708
	24.5.1 Jute/Phenolic Composites	708
	24.5.2 Jute/Polyester Composites	710
	24.5.3 Jute/Thermoplastic Composites	711
24.6	Applications Development	712

B. Singh (✉)

CSIR-Central Building Research Institute, Roorkee 247 667, India

e-mail: singhb122000@yahoo.com

24.6.1	Jute Composite Door Shutters	712
24.6.2	Jute Profile Door Frames	714
24.6.3	Roofing Sheets	715
24.6.4	Wall Panels	717
24.7	Standardization of Jute Building Products	718
24.8	Conclusions	718
	References	719

24.1 Introduction

Natural fibers are a major renewable resource material throughout the world specifically in the tropics. According to the Food and Agricultural Organization Survey, Tanzania and Brazil produce the largest amount of sisal. Henequen is produced by Mexico. Abaca and hemp are produced by Philippines. The largest producers of jute are India, China, and Bangladesh [1, 2]. Presently, the annual production of natural fibers in India is about six million tons compared with worldwide production of about 25 million tons. Natural fibers can be considered as naturally occurring composites consisting mainly of cellulose fibrils embedded in a lignin matrix. They are inexpensive, lignocellulosics in nature, and locally available in abundance.

In low pressure laminating, the use of glass fibers is almost a monopoly. In recent times, the lack of competitiveness of glass fiber reinforced plastic components in applications where strength characteristics are not paramount, has led molders to seek a reinforcement that will give necessary properties while reducing the cost. This has given rise to a growing interest in natural fibers' reinforcement. Thus, the diversification of natural fibers from its traditional markets not only strengthen the activity in the area of wood substitutes and molded products, but also conserve forest resource that help in maintaining our ecological balance. It is well known [1–4] that the drawback of jute composites is its weakness of absorbing moisture. It causes loss of adhesion or debonding at the fiber/matrix interface, which may be followed by diffusion of water into this area. In turn, this may cause a reduction in dimensional stability and strength of the composites. Another disadvantage of jute fibers is their limited resistance toward biological attacks [5] and weathering agents. To overcome some of these drawbacks, surface modification of jute fibers is an important step to develop specification grade products.

24.2 An Overview on Natural Fiber Based Building Materials

Jute and allied fibers have gained interest as a reinforcing material in the composite industry to produce new and alternate building materials for low cost housing applications [6–14]. The typical applications include: building panels, roofing sheets, boards partitions, doors and windows, tiles, etc. Currently, the

import of industrial round wood in India is two million cubic meter annually and is expected to grow triple by 2012 as they are during the last decades [15]. The increased wood demand cannot be met by either falling trees from the existing forests, secondary plantation timber, or other man-made materials used for this purpose. One strong option in this direction is to develop natural fibers-based composites and wood substitute products. The construction of primary school buildings in Bangladesh [7], prototype of low-cost housing units and food grain silos using jute/polyester composites in India [7], and low-cost building materials based on composites of henequen/palm/sisal fibers and polyester resin in Mexico [8] have been widely acknowledged for the appropriate utilization of natural fibers. Semsarzadeh et al. [10] worked on the reinforcement of polyester resin with jute in Iran for low cost housing applications. The British Jute Research Association has also carried out natural weathering trials on jute/polyester laminates for 2 years. The use of glass fabric as an outer skin on jute composite is suggested to minimize loss in strength.

In cement matrix, sisal and coir are two of the most studied fibers, but bamboo, jute, hemp, reeds, and grasses have also been studied for making fiber concrete and sheeting materials [11]. The Swedish Cement and Concrete Institute has been involved with sisal products for many years especially with respect to their durability. Field experience has also been gained by installing sisal fiber-based roof tiles in South Africa [12]. Appropriate Technology International (ATI) and Save for Child Federation (SCF) have actively promoted fiber-cement roofing tiles since the 1970s. Thousands of tiles have been made in countries such as Kenya, Sri Lanka, and Latin America using indigenous plant fibers as reinforcement. Based on their findings, both ATI and SCF have concluded that as currently manufactured such fiber reinforced tiles are unsuitable for rural housing. In 1987, International Labor Organization (ILO) supported some craft industries for the production of fiber-cement roofing tiles in Ivory Coast-West African Country. Studies indicate that the quality of tiles produced by these manufacturers is generally poor because of inadequate quality control in the production [13]. CSIRO, Australia adopted an autoclave process using wood fibers as reinforcement for making asbestos-free cement products in the 1980s [14].

It is known that these composites failed in wet conditions either by surface roughening caused by fiber swelling or delamination possibly owing to crack propagation between the plies [5, 16]. With the advent of surface modification techniques [17], moisture-resistant natural fibers are utilized in a low-pressure molding for making composites to overcome their well-defined problem of high water absorption. The properties of these composites depend on a combination of system heterogeneity consequent to processing limitations, wettability and chemical compatibility between the natural fibers and polymer matrices. In spite of continuous thrust given on the research and development, natural fibers-based building products have not been exploited commercially and their practical applications are still limited to only low value products. Acceptability of these products requires fresh efforts to meet the requisite minimum performance that conform to the existing specifications.

24.3 Jute Fibers and Their Modification

Jute fibers are obtained from the stem of plants. Among the naturally occurring lignocellulosic fibers, jute contains the highest proportion of the stiff natural cellulose that forms its main structural component [18]. India has the highest cultivation area, largely concentrated in the east and the north-eastern states. The current production of jute fibers in India is 1.4 million tons. It is reported that out of 1.6 million tons jute goods produced, 1.03 million tons are sacks while only 0.28 million tons are jute-diversified products. Thus, the product mix of jute industry comprises of low value added products. High sensitivity to moisture is an important hindrance to the performance of jute. Therefore, it is necessary to impart hydrophobicity to the fiber surface. The improvement in mechanical properties and reduction in water uptake of these composites are achieved by pretreatment of jute with alkali [19–21], coupling agents [3, 5, 17, 19], coatings [22, 23], etc. via increased fiber–matrix adhesion.

At CBRI, jute fibers of different plant species such as *Chorcorous olitorius* and *Corchorus capsularis* and *Hibiscus sabdariffa* and *Hibiscus cannabinus* are used for experiments. SEM studies of these jute fibers are made to know their surface characteristics, lumen size, and cell structure (Fig. 24.1). The high aspect ratio and minimum cell number of fibers are selected as reinforcement in composites [24]. Moisture resistant jute is prepared by applying a coupler on to jute under an optimized condition. The efficacy of treatments is assessed in terms of their adsorptive nature. Figure 24.2a shows IR image of the untreated and organotitanate treated mercerized jute fibers. The cell lumen in the treated jute was clearly visible compared with the untreated ones probably because of the loss of waxy surface layer along with lignin. The difference spectra recorded between the untreated and the treated jute showed a splitting of broaden hydroxyl region

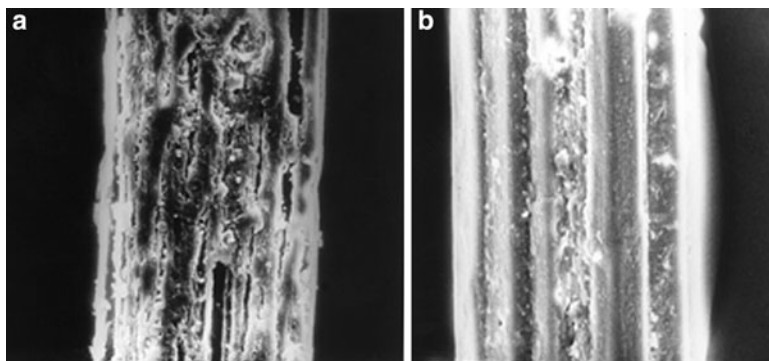


Fig. 24.1 Scanning electron micrograph of jute fiber obtained from two different plant species showing internal structure (a) *C. capsularis*, (b) *H. cannabinus*

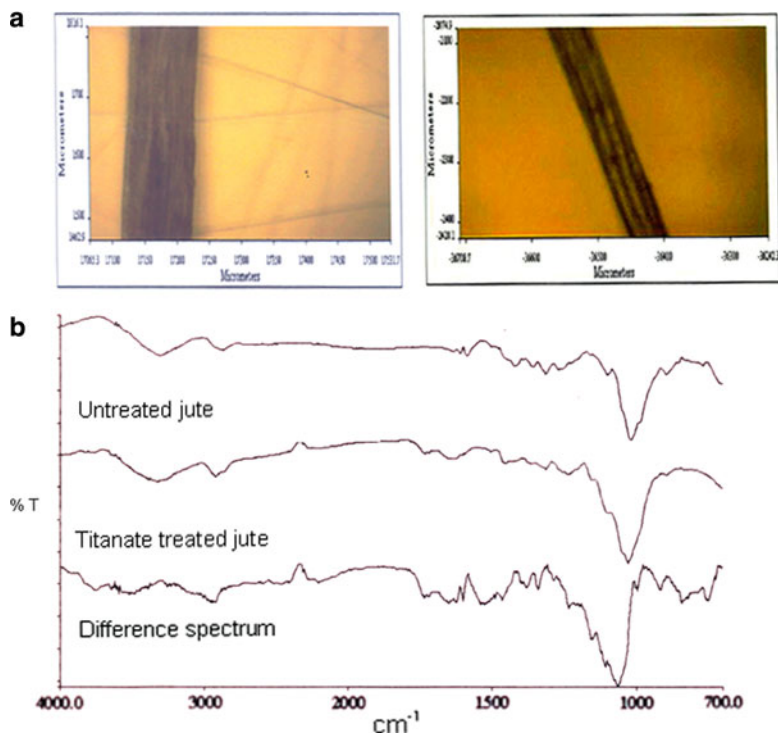


Fig. 24.2 (a) IR image of untreated and titanate-treated jute fiber, (b) difference spectra of untreated and treated jute fiber

between $3,500$ and $3,350\text{ cm}^{-1}$, presence of split carbonyl group and adsorbed species between $1,750$ and $1,000\text{ cm}^{-1}$ (Fig. 24.2b). The appearance of additional —OH stretching band after splitting confirmed the participation of the surface-free hydroxyl groups in the chemical modification reactions. The surface-treated jute gives a split carbonyl absorption band near $1,732\text{ cm}^{-1}$. The shoulder near $1,730\text{ cm}^{-1}$ appears specific for titanate coupling agent due to hydrogen-bonded carbonyl group. The emergence of new absorption bands between $1,700$ and $1,000\text{ cm}^{-1}$ is attributed to the pyrophosphate organofunctionality of titanate coupling agent. The adsorption of these chemical species supported the change in nature of fiber surfaces from hydrophilic to hydrophobic. The modified jute was subsequently assessed for wettability characteristics using water as a probe liquid under dynamic contact angle analyzer. Contact angle of the treated jute is reduced to a level of $22\text{--}40\%$ compared with the untreated ones suggesting its usefulness as reinforcement (better wetting with resin matrix). The low value of water absorption of treated jute is an indicative of its hydrophobic nature (moisture resistant). These treated jute fibers were used with unsaturated polyester resin for making laminates.

24.4 Composite Matrix Resins

Various kinds of matrix resins such as phenolics [25, 26], unsaturated polyester [3, 5, 6, 27, 28], vinyl ester [29], and epoxy [30, 31] have been used in the manufacturing of jute composites. It is known that unsaturated polyester resins are widely used as composite matrices because of their low cost, low viscosity, and optimum strength. However, they are prone to microcracking and secondary bond failures because of poor toughness, less adhesion with fibers, and high volume shrinkage during curing process [32]. Therefore, improvements in the properties of polyester are highly desirable to enhance their toughness by interpenetrating polymer techniques [33]. In this method, hybrid polymer network can be formed through the cross-link reactions, i.e., copolymerization of unsaturated polyester resin with styrene and polyaddition between terminal hydroxyl groups of polyester and isocyanate groups. Adequate control of phase separation and interlocking of both resins enhances the impact strength of the hybrid polymer networks.

At CBRI, an optimum stoichiometric NCO/OH ratio of unsaturated polyester–urethane hybrid polymer network matrix resin has been developed for jute composites [34] and also for sandwich core foamable compositions (Table 24.1). An advantage of using this matrix resin is that during cold press molding, the process shortens several times. The isocyanate-terminated hybrid network reacts with the surface hydroxyl groups of jute fibers to form a strong chemical bond avoiding the known necessity of jute pretreatment with coupling agent, coating, etc. The gel time of these resins ranged between 25 and 30 min. An improvement of 103–136% in the energy to break and 37–43% in the tensile strength of network resin were observed over the polyester resin at a NCO/OH ratio of 0.76 and 1.15, respectively. On the contrary, the elastic modulus of hybrid network resin is reduced by 17–32%. On the basis of these results and economics, an optimized NCO/OH ratio of 0.76 of hybrid network is finalized for composite preparation. The hybrid polymer network exhibited superior curing characteristics than the polyester resin in terms of larger size of network and reduced damping ratio. Lack of multiple glass transition temperatures in the differential scanning calorimetry, sharp Tan delta peak in the dynamic

Table 24.1 Physicomechanical properties of unsaturated polyester–isocyanate resins

NCO/OH ratio	Gel time (min)	Flexural strength (MPa)	Tensile strength (MPa)	Elongation (%)	Tensile modulus (MPa)	Energy to break (J)
0	70	53.67	51.60	4.72	1,376	3.85
0.23	50	41.93	42.19	4.10	1,321	3.12
0.38	40	69.98	56.70	5.78	1,209	5.06
0.76	36	94.90	70.70	7.10	1,130	7.81
1.15	30	103.94	73.70	8.26	932	9.07
1.53	25	70.24	49.19	4.80	1,463	4.37

Standard deviation \pm 5%

mechanical analysis, and particulate composite type morphology viewed in an atomic force microscope in which urethane domain dispersed in the matrix are clearly demonstrated the formation of phase-mixed domains in the hybrid networks. The storage modulus and loss modulus master curves obtained by dynamic mechanical analysis indicate that hybrid polymer networks retained higher modulus at low and intermediate frequencies over the polyester resin showing their superior time dependent response.

Efficacy of hybrid polymer network as a composite matrix for jute reinforcement is compared with the polyester resin and also with polyester–polyurethane interpenetrating network (Table 24.2). Various composites have been prepared using these matrix resins and nonwoven jute fabrics (45–47 wt%). It is observed that tensile strength and energy to break of hybrid network matrix composites are improved by 23% and 20%, respectively, whereas tensile modulus of system is reduced by 26% only. Elongation at break increased marginally. The improvement in the properties of these composites may consider due to increased fiber–matrix adhesion. The jute composite samples are aged for 2 h in boiling water. A decrease of 13–25% in the tensile strength and ~54% in the tensile modulus are observed in both polyester and hybrid network matrix composites. It is noted that network resin composites retained ~12% more tensile strength than the polyester resin composites. This indicates that hybrid polymer network has superior hydrothermally stable bond at the interface in the composites than the polyester resin. The elongation at break of the aged samples increased (16–34%) because of slipping deformation of matrix resin and debonding between the fiber and the resin. Fractographic evidences such as matrix adherence on to jute and fiber breakage also support hybrid network matrix for its advantages over other matrices (Fig. 24.3).

Table 24.2 Comparative properties of polyester matrix and hybrid polymer network matrix jute composites

Property	Unsaturated polyester resin	Hybrid polymer network (HPN)	HPN with chain extender	Polyester–polyurethane network
Density (g cm^{-3})	1.20	1.25	1.19	1.24
Water absorption (%)				
2 h	1.85	1.29	1.41	1.71
24 h	6.277	3.966	3.597	5.509
Thickness swelling (%)				
2 h	1.98	0.87	0.45	1.75
24 h	4.608	1.577	1.319	3.584
Tensile strength (MPa)	57.5	71	71.2	66.6
Elongation at break (%)	5.86	5.40	6.12	6.30
Tensile modulus (MPa)	1,568	1,862	1,153	1,737
Energy to break (J)	4.156	4.270	5.01	4.570
Toughness (MPa)	25	29	34	30

Standard deviation $\pm 5\%$

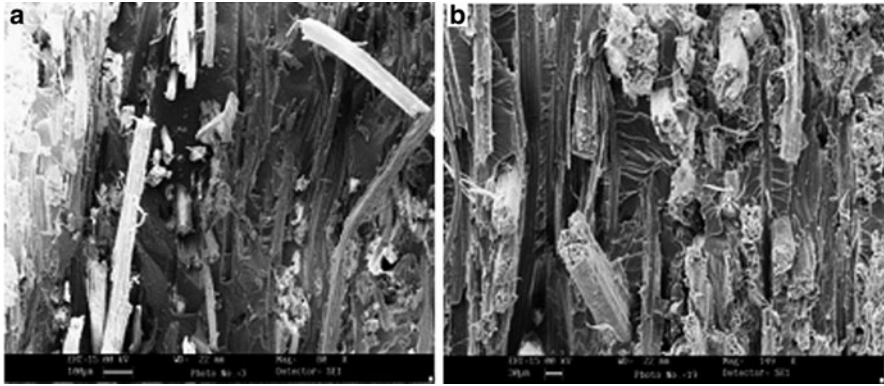


Fig. 24.3 SEM micrographs showing fractured surface under tensile mode (a) unsaturated polyester/jute composite, (b) hybrid polymer network/jute composite

24.5 Properties of Jute Composites

24.5.1 Jute/Phenolic Composites

The composites are made from jute hessian cloth (80 wt%) and water soluble phenolic resin by a compression molding technique under 8–10 MPa for making building panels/boards. The density of composite is 0.953 g cm^{-3} . Immersing in water at 27°C , the composite has gained weight to the extent of $\sim 10\%$ after 2 h. Subsequent exposure has resulted in the increase of $\sim 12\%$ after 24 h. The thickness swelling of composite is $\sim 6\%$ of which 14% is due to the surface absorption and the remaining is due to absorption at the cut edge. The tensile, flexural, and internal bond strengths of jute composites are 26, 44, and 1.20 MPa, respectively (Table 24.3). The plucking of fibers in the form of chips at cut edge is often noticed. During humidity exposure program, moisture content of the composites at saturation is $\sim 7\%$ while thickness swelling is in the order of 10–12%. Under alternate wetting and drying cycle, there is no sign of bulging or delamination at the edge of the samples. However, $\sim 50\%$ reduction in the strength under both tension and flexure modes is observed when compared with the fresh samples. During weathering, it is found that the loss of tensile and flexural strengths is severe ($< 50\%$) as compared with the glass fiber-reinforced plastics after 3.5 years exposure. The mycological studies of jute composite panels are carried out at a level of different humidity for 8–10 weeks to ascertain fungal disfigurement. An increase in the intensity and spreading of fungal growth over the surface is observed with increasing humidity due to the reduced vapor transmission from the surface. A notable decrease in fungal infestation is noticed when suitable toxicant is incorporated during processing stage [35].

Table 24.3 Physicomechanical properties of jute fiber-reinforced polymer composites

Property	Jute/polyester composites		Jute/phenolic composites	Pultruded jute/phenolic profiles
	Untreated	Treated		
Density (g cm^{-3})	1.05	1.12	0.953	0.873
Moisture content (%)	3.5	2.0	3.04	4.41
Water absorption (%), 24 h	6.45	3.03	12	12.31
Thickness swelling (%), 24 h	3.32	1.50	6	0.37
Flexural strength (MPa)	44.10	65	44	62.60
Flexural modulus (GPa)	1.15	1.28	3.02	5.31
Tensile strength (MPa)	47.08	56.92	26	33
Tensile modulus (GPa)	2.29	3.42	3.82	7.98
Elongation (%)	2.06	2.31	0.96	0.86
Internal bond strength (MPa)	0.90	1.2	1.20	0.66
Screw withdrawal load (N)				
(a) Face	1,550	1,680	–	1,800
(b) Edge	1,310	1,350	–	–
Thermal conductivity ($\text{kcal h}^{-1} \text{ }^\circ\text{C}^{-1} \text{ m}^{-1}$)	0.21	0.20	0.15	–

Standard deviation $\pm 5\%$

The jute profiles are prepared by woven jute mats and phenolic resin by a pultrusion technique for making flat- and complex-shaped items. The mats are impregnated with the resin and passed through a hot die at a speed of $0.4\text{--}1 \text{ m min}^{-1}$ to produce a profile. The product is then pulled by two sets of pullers followed by an automatic cutting to the desired length. The cured profiles contain 50–60 wt% jute fibers. The profiles are evaluated for their various physicomechanical properties (Table 24.3). The stress–strain response of the jute profiles in tension and flexure is given in Fig. 24.4. The onset of nonlinearity in the tensile curve is mainly due to the failure of resin matrix and critically stressed first ply as a result of the lower fracture strain of fibers to the resin matrix. In flexure mode, load carried out by the fiber plies alone in the samples. Kinks in the curve are an indicative of failure of the plies. The internal bond strength is satisfactory enough (0.66 MPa) to hold screws and performed well against nailing action. During water absorption, the weight gain in the profiles is 3.6% after 2 h and 12% after 24 h immersion, respectively. The surface absorption of water in the samples is only 1.5% of the total water gained. This indicates that most of the water is absorbed by the samples through their cut edges. The change in dimensional stability in terms of thickness swelling is negligible after 24 h water immersion. The pultruded sections are aged under humidity, hydrothermal, and weathering conditions. It is observed that dimensional change of the sections is only upto 4% even in an accelerated water aging for 2 h. The effect of absorbed moisture/water on the jute section is more pronounced in an accelerated water aging than the samples are being exposed to high humidity and alternate wetting and drying cycles. The changes in the values of internal bond strength of the sections could be used as an indicator because of its sensitivity toward aging. Accentuation of fibers on the weathered samples along with severe resin erosion has been suggested to layer the surface of the sections with rich resin prior to use in the outdoors [36].

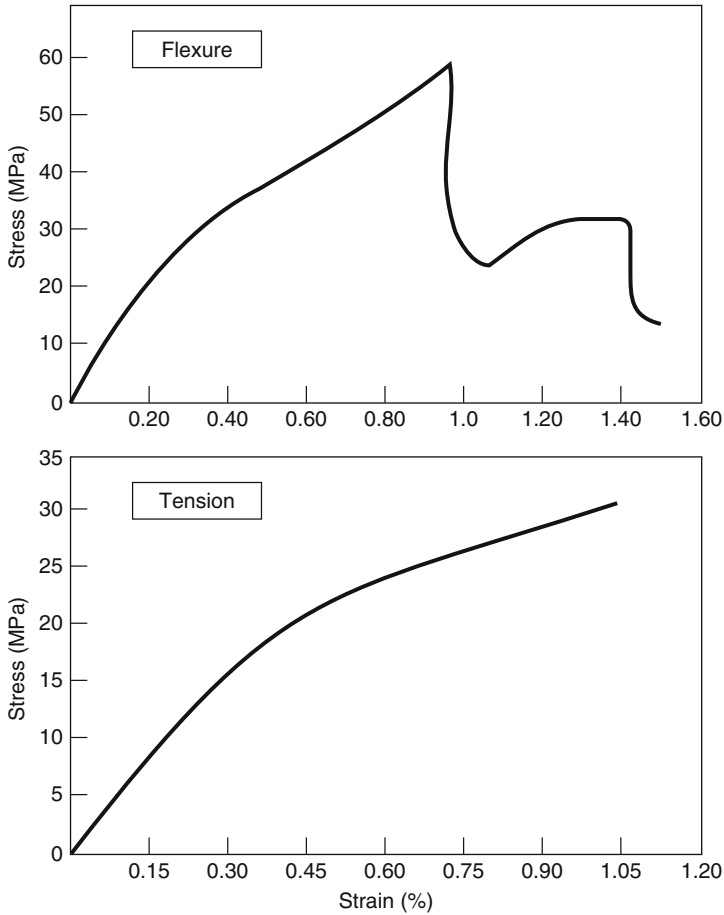


Fig. 24.4 Stress–strain response of the jute profiles under flexural and tension

24.5.2 Jute/Polyester Composites

Attempts have been made for producing composites by a compression molding at a pressure of 2–6 MPa using untreated and a combination of alkali-titanate coupling agent treated nonwoven jute mats and unsaturated polyester resins. The properties of these composites are given in Table 24.3. It is observed that composites made from the treated jute exhibited superior properties than the composites made from untreated jute probably due to the good bonding between the fiber and the resin matrix. The treated jute samples absorb less water (3%) than the untreated samples (6%) after 24 h immersion. The improvement of 21% in tensile strength and 49% in

tensile modulus for the treated composites is observed over the untreated jute composites. The elongation at the break of the treated composites is also increased by 12%. The flexural strength and modulus of the treated jute composites are increased by 47% and 11%, respectively, as compared to the untreated samples. The screw holding power of composites is 1,680 N in the face direction while 1,350 N in the edge direction. In the case of untreated composites, poly (vinyl acetate) emulsion provides hydrophobicity and a good resin wet-out to the fibers by an interaction between lignocellulosic groups of jute and proton-accepting groups of polymer. During resin impregnation of mats, poly (vinyl acetate) is dissolved in the unsaturated polyester resin leaving fiber with a clean surface, indicating poor bonding between the fiber and resin. The thick deposition of emulsion on the fiber surface during mat formation resulted in deterioration of the mechanical properties of the composites. This is attributed mainly to the formation of distinct matrix interphase consisting of poly (vinyl acetate) and polyester resin near the fiber surface [37].

It has been suggested that due to low density and relatively high modulus of the jute, serious considerations are given to its use with glass fibers in hybrid composites to obtain superior performance characteristics [38]. The hybrid laminates are found to be tougher in impact having higher value of work of fracture. They are more environmental resistant than the simple jute composites [39].

24.5.3 Jute/Thermoplastic Composites

In recent years, considerable attempts have been made on use of thermoplastic matrices for jute composites in making low-cost items such as automotive components, door profiles and window frames, pellets, furniture, etc. Compared to the inorganic filled systems, thermoplastic-cellulose composites offer several advantages such as low cost per unit volume, lightweight, stiffness, easily recyclable, and ease of processing. The major issue in the composites is the compatibility between the hydrophilic jute and the hydrophobic thermoplastics. During mixing of jute and thermoplastics (polypropylene, polyethylene, etc.), the fiber tends to agglomerate, unless fibers are sufficiently wetted to reduce fiber to fiber bonding. There are many types of dispersing agents such as stearic acid, solid paraffin wax, etc. used in the melt-blending process to obtain a homogeneous mix. A coupling agent can react with both the fiber and the polymer. As a result, an interface would have intermediate to transfer stress between two physically mismatched phases. Rana et al. [40] studied the effect of compatibilizer on short jute-reinforced polypropylene composites. They reported a marked improvement in flexural, tensile, and impact strengths even with 1 wt% compatibilizer. Water uptake in the jute composites suggests that swelling of wetted jute fibers has resulted in higher shear strength between the fiber and the matrix during fracture.

24.6 Applications Development

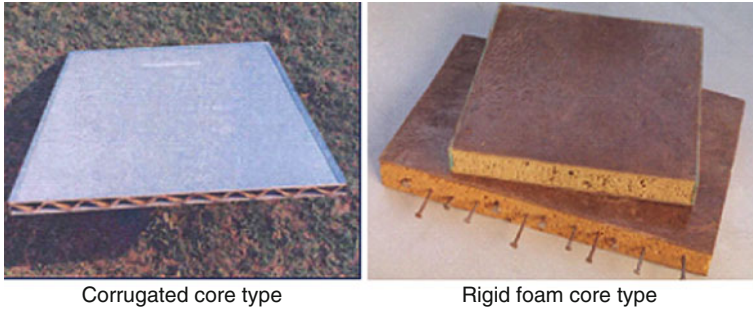
24.6.1 Jute Composite Door Shutters

The sandwich composites are made from jute laminate (3 mm) as a face and plastic wood of unsaturated polyester–urethane foam (28 mm) as a core. The physico-mechanical properties of this composite are given in Table 24.4. The density of panels is 0.60 g cm^{-3} . During tapping test, it is noted that there is no debonded area between the face and core in the panels. Impact indentation values of the samples are negligible ($<0.2 \text{ mm}$) when 500 g of steel ball of 50 mm diameter is dropped on the sample from a height of 750 mm. The samples exhibited satisfactory bending strength of 9 MPa to resist against operational loads for use as panel insert/door shutter materials. The screw withdrawal load of the sandwich panels (1,500 N) is higher than the specified value (1,000 N) for commercial wooden doors. The sandwich composites are also exposed to *Microcerotermus bessoni* termite colony. It was noted that termites are survived in all cases after 60 days. The maximum weight loss in the samples is in the order of 1.5% only probably due to termiticidal activity of styrene/isocyanate present in the hybrid core and also the existence of pyrophosphate in jute. The samples exhibited only cling of termite on their surfaces. When the samples are treated with copper chrome arsenic compound, the weight loss in the samples is 0.52% only. According to ASTM classification, these samples fall under rating 10 – sound. During natural decay in *Aspergillus niger* strain, weight loss in the samples is $<2\%$ only. The samples exhibited no residual locus of fungus even after cleaning. This indicates that the jute composites are resistant to natural decay [37].

The composite door shutters of standard size ($2,005 \times 900 \times 35 \text{ mm}$) have been prepared using jute sandwich composites (Fig. 24.5). The properties of these door shutters are given in Table 24.5. Local planeness of the door shutter is in the

Table 24.4 Properties of sandwich composite panels using jute laminate face and hybrid resin foam core

Property	Value
Density (g cm^{-3})	0.60
Water absorption (%), 24 h	5.50
Impact energy (J)	17.10
Impact indentation test (mm)	<0.2
Bending strength (MPa)	9.0
Tapping test	No unbonded area between face and core
Flat wise tensile strength (N)	Adhesive failure
Screw withdrawal load (N)	1,500
Thermal conductivity ($\text{kCal h}^{-1} \text{ }^\circ\text{C}^{-1}\text{m}^{-1}$)	0.18
Natural decay – weight loss (%) (ASTM D 2017)	<2
Termite resistance test – weight loss (%) (ASTM D 3345)	<1.5
Standard deviation $\pm 5\%$	



Jute sandwich panels



Fig. 24.5 Jute sandwich panels and door shutter

range of 0.02–0.1 mm. When the door is immersed to a depth of 300 mm in water, the bonding between the face and the core is intact even applying knife for delamination purpose after alternate wetting and drying cycle exposure. During impact, depth of steel ball indented on the surface of door panel is <math><0.2\text{ mm}</math>. Under soft body impact, the hung door shutter is free from visual damage either in the face/core parts or in the integrity of doors when 5 kg sand filled leather ball is allowed to blow 25 times from the striking place. The rigidity of door is assessed under edge loading and buckling conditions. In edge loading, deflection in the door noted at the loaded edge is 3 mm only against the specified value of 5 mm while in buckling test, the residual deflection is 3 mm after 15 min on removal of loads. In order to know normal working conditions, Sal wood slip is inserted in the bottom of hinged stile of door. After an application of 20 kg load in the direction of closing, the door is defect-free at the point of fixing. Under slamming, the door is also intact

Table 24.5 Comparative properties on jute composite door shutters vis-à-vis wooden door shutters

Property	Wooden door shutters (IS: 2202-99)	Jute composite door shutters
Local planeness test	Depth of depression at any point <0.50 mm	0.02–0.1 mm
General flatness	Twist <1.5 mm, cupping <1.5 mm, warping <1.5 mm	Twist 1.0 mm, cupping 1.2 mm, warping 0.8 mm
Dimensions and defects of squareness	Squareness – deviation not more than 1 mm in a length of 500 mm	0.75 mm
Edge loading test	Deflection of edge at max. load <5 mm	3 mm
Impact indentation test	No abnormal defect after a drop of 500 g steel ball from a height of 750 mm. Depth of indentation : <0.2 mm	No abnormal defects 0.15 mm
Shock resistance test	No visible damage in any part of the door after 25 blows of 5 kg sand ball on each end	No visible damage
Slamming test	No visible damage caused in any part of the door by 50 drops at an angle of 30° at the hinged edge	No visible damage
End immersion test	No delamination	No delamination
Glue adhesion test	No delamination	No delamination in the glue line
Knife test	No delamination	Bonding between face and core intact
Screw withdrawal resistance test	>1,000 N	1,500 N
Buckling	Max. residual deflection at bottom level not to be more than 5 mm	3 mm
Misuse test	No permanent deformation	Defect-free

when it was dropped 50 times from an angle of 30° at the hinged edge under its own weight. A photo view of some tests conducted on jute composite door shutter is given in Fig. 24.6. The properties of these door shutters are comparable to the commercial wooden door shutters. Fixtures such as handle locks and hinges are easily fixed in the door without inserting wood inside it because of good screw holding power of face/core of composites [41, 42].

24.6.2 Jute Profile Door Frames

The pultruded jute profile sections are assembled before fixing them in the wall by meter joints fortified with a reinforced adhesive pack to form a door frame (Fig. 24.7). The frame section comprises of a 3 mm thick section with 127 mm in width and 63.5 mm in height. One side has a 12.7 mm chamfer for the aesthetic purpose. Three holdfasts are fixed on each side of the doorframe, one at the center and the remaining two at 30 cm from the top and the bottom of the frame.

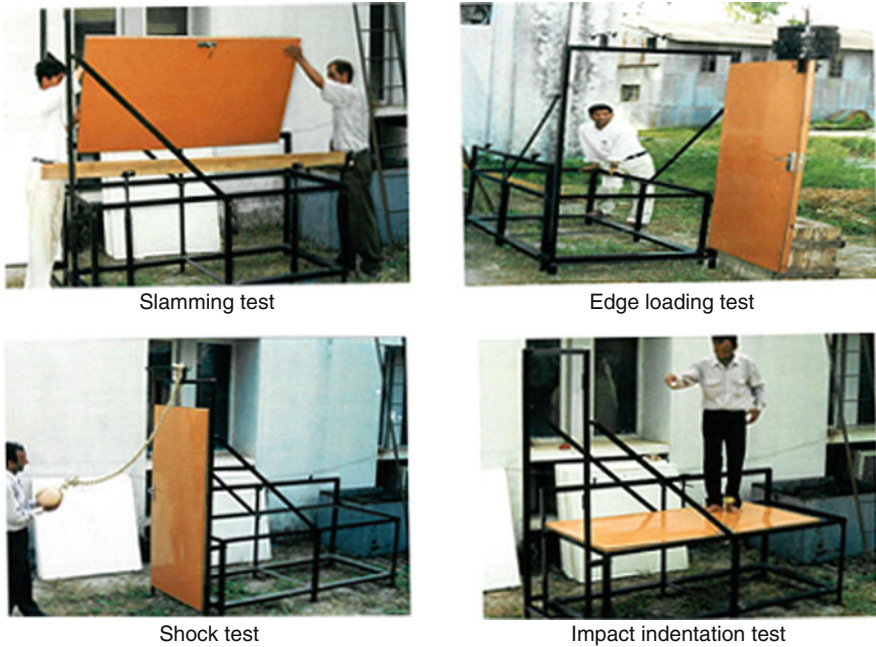


Fig. 24.6 Photo view of some tests conducted on jute composite door shutters

The properties of jute door frame are evaluated according to IS: 4021-83 – Indian standard specification for timber door, window, and ventilator frames. The moisture content of the jute profiles is roughly half or nearly three times less than the moisture content of the wooden frame materials (Table 24.6). The weathering performance of the door frame is improved either by applying a UV-stabilized resin rich layer on its outer surface during molding or through application of a polyurethane coating similar to the wooden frames. The door frame has been installed in the Institute’s premises to evaluate its actual behavior under the condition of use. The procedure for the installation of jute door frame is similar to that of wooden frame. The door frame is placed in position at a correct height from the finished floor level. During placing, the frame is checked for its uprightness, and kept free from twisting. Building of walls on each side of frame is made and cement/concrete mortar is grouted inside the frame so as to make a solid contact with the jute pultruded door frame leaving no voids. The installed frame has indicated no sign of dimensional instability (warping and bulging) after 3.5 years [36, 43].

24.6.3 Roofing Sheets

An appropriate technology for the production of coir–cement roofing sheets has been developed at the Institute. In the manufacturing process, coir fibers are first

Fig. 24.7 Jute profile door frame

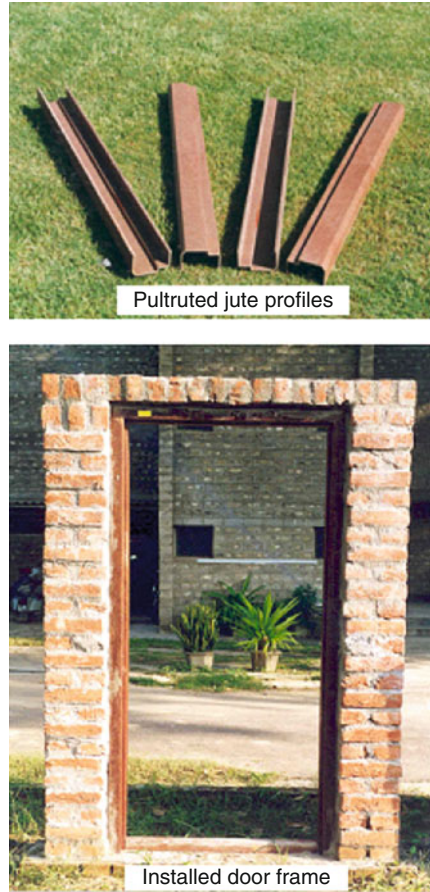


Table 24.6 Comparative properties of pultruded jute profile door frame vis-à-vis wooden door frame

Property	Wooden door frame (IS: 4021-83)	Pultruded jute door frame
Moisture content (%)	8–14	4.4
Seasoning/treatment	Prevented from warping and mold growth	Not required
Dimensions/size (cm)	H-199-209, W 79-99	H-214, W-92
Thickness (mm)	60	60
Hold fasts	3	3
Gluing of joints	BWR adhesive	Reinforced adhesive
Installation	Solid door frame, no grouting is required to fill inside of frame	Frame cavity is filled by concrete/foams
Finish	Priming followed by varnish/paint	PU paint/varnish/melamine
Weathering	Aluminum priming required	Resin rich layer
Dimensional stability	No warping/twisting	Dimensionally stable

soaked in mineralized water for at least 2 h. The free water is drained from the fiber, which is then mixed with dry cement in a 1:5 ratio by weight. The sheet can be made with a wet mix of cement-coated fibers either by a manual process or a semi-mechanized process. It is held under pressure for 4–8 h, then demolded and cured in the shade. A cement wash can be applied on both sides of the dried sheets. It can be produced in the size of $2 \times 1 \text{ m}^2$ of 6–8 mm thickness. Experimental structures constructed in 1990 with coir–cement roofing sheets have shown satisfactory performance with little maintenance needed [44].

Roofing sheets of thickness 3–4 mm have been prepared from chopped fiber strand mats, fibrous reinforcing filler, antiaging agent, and unsaturated polyester resin. Wooden blocks with corrugated face are used as molding male and female dies. It has been observed in the load–deflection curve that sheet cannot break under flexure when peak load of sheet is reached. The sheets have an adequate strength and rigidity to merit application as roofing materials. To improve outdoor durability, neopentylglycol-based gelcoat is used on exterior sides of the sheets [24, 41]. Photo view of roofing sheet is given in Fig. 24.8.

24.6.4 Wall Panels

Jute sandwich composite wall panels have been developed using jute laminate as a face and plastic wood/honeycomb as a core material for prefabricated structure. The thickness of panels is ranged between 25 and 65 mm. The panels are lightweight, rigid, and easy to install with simple tools to an open frame work. During impact test, the panels withstand against 5 and 25 kg sand-filled leather balls after several blows. The face material coated with gelcoat on the outer surface is water resistant.



Fig. 24.8 Photo view of roofing sheets

24.7 Standardization of Jute Building Products

It is known that in natural, there is a wide variation in the properties of fibers from its origin age, growing conditions, extraction methods, and extent of vulnerability toward various environments. As a consequence, natural fiber composites exhibit an unusual performance. Standardization is a difficult problem when it comes to local materials as they differ widely from place to place. Production of natural fibers-based composite products such as panels, roofing sheets, door shutters, door and window frames, and sandwich wall panels requires market support. To promote this, various user agencies have to be advised to include such items in the schedules of specification. Validation and certification on the basis of actual performance testing would go a long way in the adaptation of natural fiber composites. A design guide/code of practice on the product specification is necessary for wider acceptance on a large scale.

With a view to encourage the use of natural fiber composite, Bureau of Indian Standard has formulated some standards on coir veneer boards for general purposes – specification, IS: 14842-2000 and bamboo–jute composites corrugated and semicorrugated sheets, CED 20 (7627). A series of standards published on particle boards, fiber boards, and plywood are also being followed as a guideline for user agencies.

24.8 Conclusions

Jute composites – an environmentally benign material are already making their way into the building industry with the active support of UNDP, UNIDO, and State Governments. Their use with moderate strength will perform for many noncritical structural applications in housing. Since the significant attraction of jute is its low cost, inexpensive yet effective surface treatments that avoid organic solvents are logical ways of making a reactive jute fiber surface. Through utilization of an “engineered jute fibers” concept, jute composites with superior strength can be obtained. These materials have the potential to replace commodity plastics if the products are lightweight with high performance at comparable cost.

In essence, there is a real need for a quality assurance protocol for natural fibers to be established. Initiatives from R&D institutions are required to develop new diversified jute products (composites and molded items) through the involvement of jute mills and a new class of entrepreneurs. Further research is necessary to gain a better understanding to develop sustainable economically viable materials and processes for jute-based composites and to design innovative products of common interest.

Acknowledgments This chapter forms the part of a Supra Institutional Project of CSIR R&D program (Govt. of India) and is published with the permission of Director, CSIR- Central Building Research Institute, Roorkee. The authors are thankful to M/s TIPCO Polymers for providing the pultruded jute profiles for experimental work.

References

1. Mohanty AK, Misra M, Drazel LT (2005) Natural fiber, biopolymers and biocomposites. Taylor & Francis, New York, NY
2. Semsarzadeh MA (1985) Low cost, high strength, hard cellulosic fiber reinforced polyester structures and units. *Polym Plast Technol Eng* 24:323
3. Varma IK, Ananthkrishnan SR, Krishnamoorthy S (1989) Composites of glass/modified jute fabric and unsaturated polyester resin. *Composites* 20:383–388
4. Bisanda ETN, Ansell MP (1991) The effect of silane treatment on the mechanical and physical properties of sisal-epoxy composites. *Compos Sci Technol* 41:165–178
5. Singh B, Gupta M, Verma A (1996) Influence of fiber surface treatment on the properties of sisal fiber reinforced polyester composites. *Polym Compos* 17:910–918
6. Schirp A, Wolcott M (2005) Influence of fungal decay and moisture absorption on mechanical properties of extruded wood-plastic composites. *Wood Fiber Sci* 37:643–652
7. Winfield AG (1979) Jute reinforced polyester project for UNIDO/ Govt. of India. *Plast Rubber Int* 4:23–28
8. Belmares H, Barrera A, Castillo E, Verhuegen VE, Monjarsa M, Paltfort GA, Buequoye EN (1981) New composites materials from natural hard fibers. *Ind Eng Chem Prod Res Dev* 20:555–561
9. Pal PK, Ranganathan SR (1986) Jute plastics composites for the building industry. *Pop Plast* 31:22–24
10. Semsarzadeh MA (1986) Fiber matrix interactions in jute reinforced polyester resin. *Polym Compos* 7:23–25
11. Swamy RN (1988) Natural fiber reinforced cement and concrete, vol 1, Concrete technology and design. Blackie, London
12. Gram HE (1983) Durability of natural fibers in concrete. Swedish Research and Concrete Research Institute, Stockholm
13. Lola CR (1986) Fiber reinforced concrete roofing technology appraisal report in RILEM FRC. In: Swamy RN, Wagstaffe RL, Oakley DR (eds) RILEM Technical Committee 49-TFR, paper 2:12
14. Clouts RSP (1992) From forest to factory fabrication fiber reinforced cement and concrete. In: Swamy RN (ed) Proceedings of the 4th RILEM International Symposium E & FN, SPON, Tokyo, 20–23 July, p. 31
15. Muthoo M (2006) India in the global timber market place. *Wood News* 15:18–23
16. Zadorecki P, Flodin P (1985) Surface modification of cellulose fibers. II. The effect of cellulose fiber treatment on the performance of cellulose-polyester composites. *J Appl Polym Sci* 30:3971–3983
17. Yanjun X, Hill CAS, Xiao Z, Militz H, Mai C (2010) Silane coupling agents used for natural fiber/polymer composites. *Compos A* 41:806–819
18. Roe PJ, Ansell MP (1985) Jute-reinforced polyester composites. *J Mater Sci* 20:4015–4020
19. Ray D, Sarkar BK (2001) Characterization of alkali-treated jute fibers for physical and mechanical properties. *J Appl Polym Sci* 80:1013–1020
20. Gassan J, Bledzki AK (1999) Possibilities of improving the mechanical properties of jute/epoxy composites by alkali treatment of fibers. *Compos Sci Technol* 59:1303–1309
21. Singh B, Gupta M, Verma A (1998) Studies on adsorptive interaction between natural fiber and coupling agents. *J Appl Polym Sci* 70:1847–1858
22. Mukherjee RN, Sanyal SN, Pal SK (1983) Studies on jute fibers composites with polyester-amide polyols as interfacial agent. *J Appl Polym Sci* 28:3029–3040
23. Mitra BC, Basak RK, Sarkar M (1998) Studies on jute-reinforced composites, its limitations and some solutions through chemical modifications of fibers. *J Appl Polym Sci* 67:1093–1100
24. Bhal NS, Singh B (1998) Potential of natural fiber reinforced polymer composites for civil engineering applications in India. In: Saadatmanesh H, Ehsani M R (eds) Proceedings of

- second international conference on composites in infrastructure, Arizona, USA, 5–7 Jan 1998, pp 661–673
25. Datta C, Basu D (2002) Mechanical and dynamic mechanical properties of jute fibers novolac-epoxy composite laminates. *J Appl Polym Sci* 85:2800–2807
 26. Sarkar S, Adhikari B (2001) Jute felt composites from lignin modified phenolic resin. *Polym Compos* 22:518–527
 27. Ahmad KS, Vijayanjan S (2007) Experimental characterization of woven jute fabrics reinforced isophthalic polyester composites. *J Appl Polym Sci* 104:2650–2662
 28. Dash BN, Rana AK, Nayak SK (1999) Novel low cost jute polyester composites part I: processing, mechanical properties and SEM analysis. *Polym Compos* 20:62–71
 29. Ray D, Sarkar BK, Das S, Rana AK (2002) Dynamic mechanical and thermal analysis of vinyl ester resin matrix composites reinforced with untreated and alkali-treated jute fibers. *Compos Sci Technol* 62:911–917
 30. Gassan J, Bledzki AK (1999) Effect of cyclic moisture absorption on the mechanical properties of silanized jute epoxy composites. *Polym Compos* 20:604–611
 31. Tripathy SS, Landro LD (2000) Mechanical properties of jute fiber and interface strength with an epoxy resin. *J Appl Polym Sci* 75:1585–1596
 32. Gunduz G, Erol D, Akkas N (2005) Mechanical properties of unsaturated polyester-isocyanate hybrid polymer network and its E-glass fiber reinforced composites. *J Compos Mater* 39:1577–1589
 33. Yu JL, Liu YM, Jang BZ (1994) Mechanical properties of carbon fiber reinforced polyester/urethane hybrid network composites. *Polym Compos* 15:488–495
 34. Gupta M, Rhandhawa A, Singh B (2009) Jute composites: properties and end use in buildings. In: Agarwal SK, Rai A (eds) *Proceedings of the international seminar on green building materials and construction technologies using agricultural and industrial wastes*, New Delhi, 12–13 Nov 2009, pp 184–189
 35. Singh B, Gupta M, Verma A (2000) The durability of jute fiber-reinforced phenolic composites. *Compos Sci Technol* 60:581–589
 36. Singh B, Gupta M (2005) Performance of pultruded jute fiber reinforced phenolic composites as building materials for door frame. *J Polym Environ* 13:127–137
 37. Singh B, Gupta M, Tarannum H (2010) Jute sandwich composite panels for building applications. *J Biobased Bioenergy* 4:397–407
 38. Aquino EMF, Sarmiento LPS (2007) Moisture effect on degradation of jute/glass hybrid composites. *J Reinforc Plast Compos* 26:219–233
 39. Mishra S, Mohanty AK, Drzal LT, Misra M, Parija S, Nayak SK, Tripathy SS (2003) Studies on mechanical performance of biofiber/glass reinforced polyester hybrid composites. *Compos Sci Technol* 63:1377–1385
 40. Rana AK, Mandel A, Mitra BC, Jacobson R, Rowell R, Banerjee AN (1998) Short jute fiber-reinforced polypropylene composites: effect of compatibilizer. *J Appl Polym Sci* 69:329–338
 41. Singh B, Gupta M (2005b) In: Mohanty AK, Misra M, Drzal LT (eds) *Natural fibers, biopolymers and biocomposites*, Chap 8. Taylor & Francis, New York, pp 261–290
 42. Singh B, Gupta M (2005c) Report No. O (G)/0002, Development of composites and moulded products from jute and allied fibers. CBRI, Roorkee
 43. Singh B, Gupta M (1998) Report No. F(C) 0176, Suitability assessment of JRP pultruded profile as door frame materials in buildings. CBRI, Roorkee
 44. Singh SM (1975) Corrugated roofing sheets and building panels from coir waste. Coir 3-6 (CBRI Project Proposal No. 53, 1985, Corrugated roofing sheets from coir waste or wood wool and portland cement)

About the Editors

Dr. Susheel Kalia is Assistant Professor in Department of Chemistry, Bahra University, Wagnaghat (Shimla Hills), Solan (H.P.) India. He did his Ph.D. research work at National Institute of Technology (Deemed University) Hamirpur and submitted his Ph.D. thesis at PTU Jalandhar, India. He worked as an Assistant Professor (Reader) and Head of Chemistry Department in Singhania University (Rajasthan), India, for 3 years. He has 30 research papers to his credit in international journals of repute along with 45 publications in proceedings of national and international conferences and five book chapters. He has guided seven M.Phil. students and presently guiding a number of Ph.D. students. He is a reviewer for many international journals and member of editorial board for various international journals. He is a life member of Asian Polymer Association and Indian Cryogenics Council. He is also editing a book “Biopolymers: Biomedical and Environmental Applications” – Wiley-Scrivener Publishing along with Professor Luc Averous of France. Presently he is working in the field of polymer composites, cellulose nanofibers, hydrogels, and cryogenics.



Dr. B.S. Kaith did his Ph.D. in Panjab University Chandigarh in 1990. He joined National Institute of Technology Hamirpur as Lecturer in 1991. He joined Department of Chemistry, National Institute of Technology, Jalandhar (Pb.), as Professor in 2007. In September 2009 he took over as the Head, Department of Chemistry, Dr. B.R. Ambedkar National Institute of Technology – Jalandhar. Seven students have completed their Ph.D. degree under his supervision. He has a wide experience in the field of natural products, polymers composites, hydrogels, removal of toxic heavy metal ions from waste water, removal of colloidal particles, sustained drug delivery, controlled release of insecticides/pesticides, etc. He has more than 80 research papers in various reputed international journals. He has more than 60 research papers in the proceedings of the international conferences and



more than 100 research papers in the proceedings of the national conferences. He has handled many sponsored research projects successfully.

Dr. (Mrs.) Inderjeet Kaur did her doctoral study on “Graft Copolymerization of Vinyl Monomers on to Wool” and joined Chemistry Department, H.P. University, Shimla, India, as Lecturer in 1981 and presently she is working as Professor of Chemistry in the department. She is actively engaged in research involving modification of polymers both natural and synthetic through graft copolymerization and utilizing them in various processes. Modification of polymeric films for use as membranes in separation processes, modification of cotton fabric to induce antibacterial and flame retarding properties, modification of polyolefin such as PE and PP to impart biodegradable behavior, use of natural biofibers for use in composite materials, hydrogels, and polymer supported reagents are few to mention. She has been credited with major projects from BARC, DST, DRDO, and CSIR. She has published more the 120 papers in national and international journals of repute. She has successfully guided 19 Ph.D. and more than 20 M.Phil. students and a number of them are pursuing Ph.D. Apart from teaching and research, she has a keen interest in planning and designing of research documents. She has published a number of chapters in books published by prestigious publishers.



Index

A

- Abaca, 226, 230, 231
- Abdominal wall, 574–576
- Abrasion resistance, 643
- Acetic anhydride, 604, 637
- Acetobacter xylinum*, 545, 551, 568
- Acetylation, 85, 109, 603, 604, 635
- Acid
 - coupled steam treatment, 555
 - hydrolysis, 540, 549, 555, 556, 558, 559
- Acidification, 437
- Acknowledgment, 653
- Acne, 429
- Acrylamide, 435
- Acrylate latex, 550, 562, 563
- Acrylation, 110–111, 603, 605, 607, 625
- Acrylic monomers, 561
- Acrylic resin, 609
- Acrylonitrile, 434, 435
- Activation function neuron (FAN), 226
- Activation neurons function, 226
- Adhesion, 107, 109, 112, 241, 243, 246, 254, 255, 258, 259, 294, 296, 308, 309, 311, 312, 314, 317–319, 321, 323
- Adhesives, 438, 440, 444
- Adsorption, 349, 360, 363, 366
- Advanced Materials and Processes Research Institute (AMPRI), 609, 613, 615, 628, 637, 640, 643, 644, 649, 650
- Aerosil, 359–362, 364, 370
- Agave fibre, 17, 18
- Agave sisalana*, 592–594
- Agricultural crops, 544, 548
- Agricultural fibers, 549
- Agro-polymers
 - poly(lactic acid), 456–459
 - polyhydroxyalkanoates, 459–461
- Aircrafts, 114–116
- Algae, 545, 550, 555, 573
- Algal nanocellulose, 550–551
- Algorithm, 218, 226, 231
- Aliphatic copolyesters, 462, 464
- Alkaline treatment, 382, 386, 388
- Alkali treatment, 85, 603–604, 607, 609, 625, 635
- Alkyldimethylchlorosilanes, 559
- All-cellulosic, 399–419
- Alpha cellulose
 - carboxymethylation, 53–54
 - characteristics, 53
 - cyanoethylation, 54–55
 - hydroxypropylation, 55–56
 - isolation, 52–53
- Aminopropyl, 334
- Ammonium peroxydisulfate, 561
- Amorphous, 331, 541, 544, 549, 555
- Amylase, 433
- Amylolytic enzymes, 433
- Amylopectin, 433
- Anaerobic, 426, 445
- Anhydro-D-glucosecapyranose, 331
- 1,4- β anhydroglucose units, 601
- Animal fibre, 5–6
- Animal wound dressing, 545
- Anisotropic, 402–405, 409, 410, 418, 419
- Anisotropy
 - axial, 159
 - transverse, 159
- Annual plant, 72
- Antimicrobial agent, 559
- Antimicrobially active, 559
- Antimicrobials, 81
- Antioxidants, 81
- Applications, 216–218, 222, 224, 225, 227, 229, 230, 234, 236
 - automotive, 393, 394

- Applications (*cont.*)
 building, 393
 packaging, 393
 sisal fiber polymer composite, 589–653
- Arithmetic average, 232, 236
- Aromatic compounds, 81
- Aromatic copolyesters, 462, 464
- Articular capsule, 574
- Articulation, 576
- Artificial blood vessels, 545
- Artificial cardiovascular tissues, 567
- Artificial neural network, 224, 226, 230, 236
- Ash
 black, 349, 363, 364
 white, 349, 360, 362, 364
- Aspect ratio, 411–413
- Aspen, 391–392
- ASTM International, 79
- Atomic force microscopy (AFM), 15–17,
 23, 28, 31, 32, 34–36, 402, 405–407,
 414, 445
- Autograft skin, 571
- Autologous cells, 567
- Automotive applications, 644–647
- Automotive industry, 644, 646–647
- Automotive parts, 217
- Availability, 593, 637, 638
- B**
- Bacteria, 71, 72, 85, 86, 426, 432, 435, 437,
 440, 445
- Bacterial cellulose (BC), 169–173, 545,
 551–554, 556, 558, 560, 562, 565,
 566, 569, 570, 573
- Bacterial cellulose/poly(ethylene oxide)-
 nanocomposites, 563
- Bacterial nanocellulose, 545, 551–554, 568
 grafts, 567
- Bacteriostatic, 71
- Bagasse, 217, 219, 221
- Ballistic, 393
- Bamboo, 232, 233, 235
- Banana, 217, 219–221, 224, 544, 549, 558
- Banana fibre (BaF), 30, 33, 219, 224,
 671–676, 679, 682, 683, 694
- Band structure, 404
- Barley, 549
- Bast fibers, 65, 73, 75, 97–117
- Benzoylation, 333, 609, 631, 633, 635
- Benzoylation-acetylation, 333, 334
- Bioactivity, 568
- Biobased monomers, 521–522
- Biocellulose, 573, 574
- Biocompatibility, 545, 567, 568
- Biocomposite, 61–87, 544, 649, 651
 mechanical properties, 471–474
 thermal properties, 467–471
- Biodegradability, 425–446
- Biodegradable, 5, 6, 24, 26, 326, 338
- Biodegradable aliphatic copolyesters, 462
- Biodegradable aromatic copolyesters, 462
- Biodegradable plastics, 435, 440–442, 445
- Biodegradable polymers, 521–522, 650
 classification, 455–456
- Biodegradation, 426, 431–433, 440–441, 445,
 509–516, 521
- Bioenergy, 80
- Biofibers, 544
- Biogas, 598, 612, 651, 652
- Biological mechanism, 553
- Biological protection, 577
- Biomass, 113, 116
- Biomaterial, 564, 568, 574
- Biomax[®], 462
- Biomedical application, 549, 556, 559, 562
- Bioplastic films, 444
- Biopolyesters, 457
- Biopolymerization, 552
- Biopolymers, 114, 116, 429, 430, 439,
 441–446, 563
 consumption, 116
 nanocomposites, 527–530
- Bioproducts, 80
- Biosynthesis, 545, 546, 552, 558
- Biotechnology, 545, 577
- Bladder, 577
- Bleaching, 549, 550, 608, 626, 627
- Blood remnants, 567
- Blood vessels, 545, 564–567, 576, 577
- Bone colonization, 568
- Bone graft, 567–569
- Brazilian fibers, 216, 222, 223, 232
- Brittle materials, 226
- Building materials, 637, 638, 640, 643,
 644, 650
 delamination, 703, 708, 713
- Buriti fibers, 219, 232, 235, 243
- Burns, 564, 571–572, 577
- C**
- Calcium-deficient hydroxyapatite (CDHAP),
 567, 568
- Calender, 76, 77
- Canada, 64, 74, 75
- Capsular tissue, 569
- Car, 99, 100, 114–116

- Carbodiimide derivatives, 561
Carbohydrate, 436, 540, 545, 559
Carbon dioxide, 99, 117
Carbon fiber, 242–244, 259
Carboxylated MFC, 563
Carboxylated nanocellulose, 560
Carboxymethyl cellulose (CMC), 437, 563
Cardiovascular surgery, 567
Carotid artery, 566, 567, 569
Cartilage, 574, 576
Castor oil, 439
Cellobiose, 540
Cells, 215, 219, 223, 229
 entrapment, 562
 growth, 229
Cellulose, 7–9, 11–15, 17–22, 24, 26–37,
 97–117, 329–331, 348, 360, 361, 364,
 365, 367, 368, 434–438, 441, 539–577,
 592, 600–604, 606–609, 611, 613, 614,
 616, 625, 635, 638, 649, 652
 applications, 48–50
 chain, 541–543, 555
 chemical functionalization, 43–57
 esters and ethers, 47–49
 fiber, 379, 380, 389, 390, 392, 481–484
 implant, 569
 membrane, 552, 574, 575
 microfibrils, 181, 183, 194, 203–205
 nanocomposites, 525, 539–577
 nanofibers, 540, 544–547, 549, 553, 554,
 556–558, 562
 nanoparticles, 549, 558
 non conventional sources, 43–57
 reactivity, 46, 47, 50
 sources, 45, 46, 50
 structure, 46, 181–182, 198
 type, 181
 wall, 565
 γ -cellulose, 437
Cellulose I, 541, 542
Cellulose II, 541, 542
Cellulose III, 541, 542
Cellulose IV, 542
Cellulose acetate butyrate, 560, 563
Cellulosic fibrils
 cryocrushing, 124
 fibre saturation point (FSP), 125
 fibrillated cellulose, 123
 fibril-water interactions, 125
 grinding, 123–125
 hierarchical structure, 123
 homogenisation, 123
 mechanical disintegration, 123
 rheology, 124, 125
 ultrasound sonication, 123
Characteristic life, 229, 230
Characterization, 650
Chelator, 165
Chemical composition, 69, 70, 83, 85, 219
Chemical constituents, 215
Chemical methods, 603–611
Chemical modification, 558–561, 624–626,
 635–636
Chemical processing, 542
Chemical reactivity, 299
Chemical-retting, 73
Chemical treatments, 108, 159, 172, 246, 254,
 545, 553
Chemistry, 545
Chiral nematic, 402, 403
Chitosan, 429
Chitosan/chitin nanocomposites, 525
Chlorophyceae, 550
Chondrocytes, 574
Chronic ulcers, 571, 577
Chronic venous ulcers, 572
Chronic wounds, 571–572
Clemson Fiber Flax (CFF), 72, 73
CLP curves, 248–252
Coconut, 549
 fiber, 379, 380, 392–394
Cocrystallizations, 561
Coefficient variation, 225, 229, 235
Cohesion, 67
Coir fiber, 219–225, 222, 223, 225, 227–229,
 232–235, 245, 250–252, 544
Collagen, 568, 570
Compatibility, 159, 172
Compatibilization, 379, 381–383
Compatibilizers, 378, 383, 384, 386, 389, 390
Composite properties
 crystallinity, 199, 200, 204
 glass-rubber transition, 198, 199
 melting temperature, 199
 microstructure, 196–198
 percolation theory, 202, 204
 storage modulus, 201
 swelling, 203–205
 thermal decomposition, 200
 water vapor transmission/permeability, 205
Composites, 63–65, 75, 80, 82–87, 97–117,
 217, 218, 221, 222, 226, 231, 235, 236,
 241–259, 345–370, 427, 428, 702–704,
 706–712, 714, 718
 fiber moving, 268
 interphase, 272–280

- Composites (*cont.*)
 laminates, 389
 mechanical properties, 264–285
 paper, 123, 135–146, 150
 rupture, 248
 transcrystallinity, 264, 285
- Composition, 600, 602, 603, 611–613, 625
- Compost, 511, 512, 514
- Compounding, 484–488
- Compression molding, 82, 86, 235, 618–619, 621, 629, 668, 683, 689, 691, 692, 695
- Compressive stress, 160
- Computer analysis, 234
- Conclusions, 651–653
- Consistency, 87
- Constant strain rate, 232
- Consumption scenario, 597–598
- Contact angle, 705
- Conventional usage, 217
- Copolymer, 550, 559
- Copolymerization, 334
- Corn, 549, 569
- Cornea, 574, 577
- Corona treatment, 382, 390
- Correlation, 216, 218, 223, 224, 235
- Cosmetics, 545, 547, 573–574, 577
- Cosmetic tissues, 545, 573–574
- Cotton, 219, 221, 223, 540, 544, 545, 555–558
 fibers, 223
 standards, 78
- Council of Scientific and Industrial Research (CSIR), 615, 637, 640
- Coupling agent (CA), 490–492, 494, 495, 497, 498, 500–502
 IR spectrum, 705
- Cox, 411
- Critical length, 243, 246–254, 258
- Critical length pullout (CLP), 243, 246–252, 258
- Critical surface energy, 162, 163, 173
- Crop mulcher, 442
- Cross-linking, 400–402, 406–409, 413–415, 417, 418
- Cross section, 220, 223, 229, 232, 243, 244, 249
- Crushing rollers, 75, 76
- Crystalline, 331, 333
 forms, 541–544
 nanocrystals, 549
- Crystallinity, 8, 9, 15, 16, 22
 X-ray diffraction, 167
- Crystallinity index, 219
- Crystallization, 552, 561, 563
- Crystal modulus, 544
- Crystal structure
 cellulose I α , 541, 542
 cellulose I β , 542, 562
- Cultivation, 594–598, 615, 640, 650, 652
- Culture, 169, 170, 172, 173
- Cumulative distribution functions, 229
- Curaua fiber, 217, 219, 221, 222, 232, 233, 235, 236, 243, 245, 250, 252, 380, 387–388, 393
- Cutin, 432
- Cyanoethylation, 334, 337, 608, 626, 627, 631, 633, 636
- D**
- Debonding, 247, 249, 252, 256
- Decomposition, 332
- Decortication equipment, 75
- Defects, 218, 219, 222–224, 228–231, 233, 236
 population, 239
- Defects/flaws, 228
- Defense, 638, 649, 652
- Defibrillation, 329
- Degradation, 159, 161, 162, 164, 166, 167, 326, 329, 336, 339, 601, 603, 606, 613, 615, 625, 650
 thermal, 345–370
- Degree of crystallinity, 549
- Degree of polymerisation, 157, 158
- Degree of polymerization, 552, 555
- Dehydration, 613, 615
- Density, 65–67, 72, 74, 80, 82, 83, 85, 86, 100, 105, 112, 117
- Dental, 564
- Deproteinized, 550
- Dermis, 571
- Dermolysis, 577
- Dewaxing, 337, 607–608, 627
- Dew-retting, 73, 74, 84, 85
- Dextrin, 433
- D13.17 (Flax and Linen), 79
- Dialysis, 555
- Diameter, 102, 104, 105, 107, 243–245, 247–249, 251, 254–256
 range, 221
 variation, 226, 249
- Diclofenac, 429
- Dielectric, 540
- Differential scanning calorimetry (DSC), 612, 614
- Digestive tract, 576
- Diisocyanates, 400–402, 417
- Dimensional change, 709

- Dimensional variation, 223
 - Dimensionless shape parameter, 231
 - Dimensions, 218, 221–224, 232, 236, 243, 258
 - Dinitrophenylation, 333, 334
 - Disaccharides, 434
 - Discontinuous reinforcement composites, 86
 - Dislocations, 67
 - Dispersant, 563
 - Dispersion
 - of strength, 231
 - in stress, 248, 251
 - in stress values, 248, 251
 - Disposal diapers, 563
 - DNA oligomers, 561
 - Door frame, Holdfasts, 714
 - Door panels, 693, 694, 696
 - Door shutter, Termite, 712
 - Drawbacks, 218
 - Drug delivery, 562, 563
 - Duodenal lesions, 577
 - Duramater, 576
 - Dynamic mechanical analysis, 612
 - Dynamic mechanical thermal analysis, 317–318
- E**
- Ecoflex[®], 462
 - Elastic modulus, 552
 - Electrical application, 647
 - Electric discharge, 602
 - Electroluminescent, 553
 - Electrolyte solvent, 563
 - Electron microscopy, 567
 - Electrospinning, 558
 - Elementary fibers, 65, 67
 - Elongation, 612, 613, 616, 621, 630, 632–634, 637, 644
 - Embedded area, 257
 - Embedded length, 245, 247, 248, 250, 251, 256, 258
 - E-modulus, 563
 - Endogenous cells, 565
 - Endoprosthesis, 564–567
 - Endothelial cell, 567
 - Energy, 80–82, 100, 110, 114–116
 - Engineered paper grades, 122
 - Engineering materials, 218
 - Environment, 98, 113, 114
 - Environmental aspects, 520–521, 530–531
 - Environmental benign, 521
 - Environmental friendly, 394
 - Environment-friendly, 326, 426–430, 438, 444, 445
 - Enzyme-retting, 71, 73, 74
 - Epicutaneous test, 573
 - Epidermis layer, 571
 - Epithelial lesions, 577
 - Epoxy, 563
 - Epoxy, 243, 250–252, 256, 257, 259
 - composites, 620, 621
 - resins, 562
 - Epoxypropyltrimethylammonium chloride (EPTMAC), 559
 - Equivalent diameter, 232, 243, 247
 - Esophagus, 576
 - Esterification, 109, 117, 558, 559
 - Etherification, 558
 - Ethyl 2-bromoisobutyrate, 561
 - Ethyl cellulose, 429, 437
 - European Union, 63, 82
 - E.U.'s End-of-Life Vehicle (ELV), 82
 - Exothermic process, 300
 - Extract fibers, 74
 - Extraction, 163–169, 326, 328–329, 338
 - method, 219
 - process, 222
- F**
- Fabric, 612, 618, 637, 638, 642, 643, 648, 649, 652
 - Facial peeling, 577
 - Failure mode, 254, 257
 - Fatigue, 679–680, 689, 1 695
 - Fatty acids, 167
 - Feminine hygiene, 435
 - Femoral trochlea, 574
 - Fermentation, 567, 569
 - Ferromagnetic, 540
 - Fertilizer, 72
 - Fiber, 215–236
 - cross section, 220
 - diameter, 235
 - dimensions, 221
 - distribution, 486, 498
 - extractions, 598–599
 - fragmentation, 252–255
 - fragmentation test, 252–255
 - length, 621–622
 - length distribution, 486–487
 - loading, 622, 629–634
 - pellets, 487–488
 - pollution, 244–246
 - pullout test, 244–246
 - quality, 69, 73, 77, 79, 82–84, 87
 - reinforced polymer, 617–637
 - rupture, 247

- Fiber (*cont.*)
 selection, 218, 222, 236
 strength, 223, 225, 229
 strength variation, 223, 224, 229
 surface modification, 601–617
- Fiber/matrix interface, 258
- Fibre-matrix, 668, 669, 671, 676–680, 682–684
 adhesion, 617–618, 624–626, 635–636
 coupling, 489–490, 500–502
 decoupling, 500–502, 504
 interphase, 634–635
 interphase adhesion, 624
- Fibril-calcium carbonate composites, 123
- Fibril distribution, 233
- Fibrillated pulp, 546
- Fibrillation, 333
- Fibroblasts, 553, 554, 576
- Fibrocartilage, 574
- Fibrous plants, 99–102, 105, 112, 116, 117
- Fickian diffusion, 428
- Filament winding, 619
- Fillers, 113, 117, 345–370
- Filters, 117
- Fineness, 66, 69, 72, 73, 77, 79, 80, 84
- Flaw
 distribution, 225
 size distributions, 223
- Flax (*Linum usitatissimum* L.), 62, 98–108,
 114, 217, 221, 379, 380, 383–384, 443,
 544, 548, 556, 562
 composites, 664–665
 fibers, 61–87
- Flax seed, 64, 65, 71, 72, 81, 82
- Flax seed industry, 82
- Flexible polymer, 563
- Flexural performance, 86
- Flexural properties, 622, 623
- Flexural strength, 665
- Flocculation, 563
- Fly ash, 628, 640, 642
- Food packaging, 415, 418, 419
- Fractographic studies, 236
- Fractographs, 219, 222, 235
- Fracture
 mechanism, 222
 mode, 219
 strength, 227–229, 232
- Frictional, 66, 71
- FT-IR, 445
- Functional composites, 553
- Functionalized nanocellulose, 559
- Fungi, 164, 166–169, 173, 426, 440, 445
- Furfuryl alcohol, 561
- Fusarium lini*, 432
- Future prospects, 651–653
- G**
- Gamma treatment, 603
- Gas, 402, 408, 415–419
- Gauge lengths, 225, 226, 229, 231
- Gels, 124, 125, 127, 150
- Geometric properties, 558
- Geotextiles, 117, 638, 648–649, 652
- Glacial acetic acid, 604
- Glass fiber, 484, 615, 618, 637, 644, 646, 650
- Gluconacetobacter xylinus*, 545, 551
- Glycosidic linkage, 540
- α -1,4 glycosidic linkage, 433
- Good wetting, 83
- Grading systems, 77
- Graft copolymerization, 626
- Grafting, 334, 337, 383, 391
- Grafting copolymerization, 110, 117
- Grafting-from, 560
- Grafting-onto, 560
- Granulation tissue, 571
- Green methods, 531–532
- Griffith's theory, 218
- Growing market, 217
- H**
- Halpin-Tsai equation, 228, 231, 411, 412
- Hammer milling, 64, 75, 80
- Hammers, 75
- Hand lay-up/spray up, 618
- Hardwood, 556
- Harvesting, 72, 74, 84, 87, 594–598
- Health benefits, 64–65, 81
- Heat stability, 493–495
- Hemicellulose, 102, 104, 105, 107, 329–331,
 333, 348, 361, 364, 365, 367, 368, 438,
 545, 553, 600, 601, 604, 611, 613, 614,
 625, 626, 638
- Hemp, 98–100, 102–106, 113, 114, 116, 379,
 380, 384, 386, 393, 427, 443, 544, 548,
 556, 558, 562, 563
- Hemp composites, 665–667
- Henequen fiber, 254, 379, 380, 388
- Herbicide, 72, 73
- Hernias, 577
- Hexamethylenetetramine, 337
- Hierarchical composites, 172, 173
- High-density polyethylene (HDPE), 382, 387,
 388, 390–392
- High-strength materials, 419
- Histograms, 225, 229, 230, 232

Histology, 564, 566, 567
 Hollocellulose, 330
 Homogenization process, 546, 558
 Human patch test, 573
 Human skin, 553, 564
 Humidity, 106, 114
 fungal disfigurement, 708
 Hybrid composites, 86
 Hybrid polymer network, 706–708
 Hybrid textiles, 86
 Hydrogel, 547, 563
 Hydrogen bonding, 541–542
 Hydrophilic, 83, 84, 158, 159, 172, 333
 Hydrophilic fibres, 676, 678, 679, 689
 Hydrophilic flax fibers, 83
 Hydrophobic, 158–160, 162, 163, 167
 Hydrophobic polymers, 83
 Hydroxyl groups, 157, 159, 167, 556, 558, 560, 561
 Hydroxyls, 331, 333
 Hydroxypropyl cellulose (HPC), 401–410, 414, 416–418, 429, 437
 Hygroscopicity, 549
 Hyperbolic equation, 233
 Hypertrophic scars, 572
 Hypromellose, 437

I

Impact, 706, 711–715, 717
 properties, 482, 492–493, 497–499
 strength, 319–322, 608, 621–623, 626–629, 631, 632, 636, 637, 643, 644
 Improved performance, 218
 IMZ implant, 564
 Incontinence pads, 547
 Indigenous fungi, 72
 Industrial oil, 80, 81
 Industrial sectors, 222
 Inguinal hernias, 577
 Injection molding, 618, 619, 629
 Inoculating, 567
 Insecticide, 72
 Insects, 426, 445
 In situ chemical polymerization, 547
 In situ polymerization, 561
 Insulating/Insulation, 100, 114, 428, 432
 Intercropping, 596
 Interface, 326, 327, 332, 337
 Interface resistance, 246
 Interfacial, 326, 334, 338
 Interfacial adhesion, 85, 381, 386, 388, 390, 394, 561
 Interfacial debonding, 252

Interfacial shear strength (IFSS), 241–259
 Interfacial shear stress, 160
 Interfacial strength, 83, 85
 Intermolecular, 331
 Intermolecular hydrogen bond, 541–542
 Intestinal tube, 576
 Intramolecular, 331
 In vivo tissue, 567
 Ionic liquids (ILs), 531–532
 Irregularities, 243–245
 Irrigation, 595, 596
 Isocyanate-mediated coupling, 561
 Isocyanates, 85, 111–112, 117
 Isocyanate treatment, 608, 635
 Isolation, 541, 546, 549, 555–558, 577
 Isora fibre, 101–103, 105, 106
 chemical composition, 295–296
 chemical reactivity, 299
 materials and experimental techniques, 295
 physical and mechanical properties, 296
 surface morphology, 297–298
 theoretical strength, 296–297
 thermal analysis, 300–302
 wide angle X-ray diffraction studies, 302
 Isotropic, 402–418

J

Jute, 98–107, 114, 217, 219, 221, 225, 226, 230–232, 235, 379, 380, 384–386, 393, 427, 428, 443, 544

K

Kenaf fibers, 98, 100, 102–106, 114, 256, 257, 544
 Keratinocytes, 553
 Keratosis pilaris, 429
 Keratoconjunctivitis sicca, 437
 Knee joint, 570, 574
 Kopak, 219
 Kraft pulp, 546, 562, 572
 Kulkarni, 227–229

L

Lactic acid, 456–457
 Lacuna, 219, 229
 Laminates, 618, 642, 643
 Laminectomy, 574
 Landfiller, 444
 Land preparation, 595
Lantana camara and Bamboo, proximate analysis, 43, 51
 Lanthanide alkoxides, 430
 Larger diameter, 234

- Large scatter, 222, 223, 227
 Leaf fiber, 100, 112, 219, 230, 231
 Leaf fibre, 6, 17, 30, 34
 Leaf sheaths, 219
 Length, 65–67, 76, 77, 79, 80, 86, 105
 Light, 82
 Lignin, 65, 69–71, 81, 84, 102, 104, 105, 107, 110, 111, 219, 222, 330, 331, 333, 348, 361, 364, 365, 367, 368, 545, 549, 553, 559, 600, 601, 604, 608, 611, 613, 615, 616, 625–627, 636, 649
 Lignin–carbohydrate, 559
 Lignocellulose-based fibers, chemical composition, 455
 Lignocellulose fillers (LF), 466–467
 Lignocellulosic fibers, 215–236, 241–259, 326, 333, 428
 adhesion, 268, 281, 282, 284, 285
 flax, 274, 278
 hemp, 267, 282
 mercerization, 267, 269, 276
 modification, 269, 275–277, 282–284
 nucleation, 264, 271, 277–280, 285
 pulling, 265–272
 surface, 274–276, 282, 285
 topography, 271, 275, 276, 285
 Lignocellulosics, 4, 6, 8
 Linear relationship, 228
 Linear thermal coefficient of expansion, 160
 Linen, 62–65, 71, 75, 78, 79, 84
 Lipids, 69, 80
 Liquid ammonia treatment, 108, 117
 Liquid-crystalline, 402, 403, 410, 411, 418, 419
 Long-line fibers, 64, 74, 75
 Low-density polyethylene (LDPE), 382, 387–389, 392, 514
 Lower heat value, 80
 Lumen, 4, 6, 15, 19–21, 219
 Lyotropic, 403, 404
- M**
- Macromolecules, 426, 440, 441
 Magnetic, 540
 Mammary teats, 574
 Man-made cellulose fiber, 481–484
 Marble slurry dust, 642
 Material performance, 224
 Matrix, 65, 69, 73, 82–86, 104, 107, 109, 110, 112, 117, 216, 218, 219, 226, 231, 236, 427, 428, 436, 437, 440, 441
 adhesion, 83
 materials, 216, 218
 shear strength, 247
 Matrix–fiber interface, 231, 236
 Maximum likelihood technique, 229, 230
 Maximum packing fraction, 412, 414
 Mean roughness, 407
 Mean strength, 225
 Mechanical disintegration, 545
 Mechanical interlock, 167, 169, 173
 Mechanical properties, 79, 82, 83, 87, 244, 255, 256, 258, 601–603, 607, 609, 611–617, 619–622, 624–627, 629–637, 643, 651–653, 664, 665, 667–669, 671, 675–679, 681
 Mechanical strength, 430, 434, 440
 Mechanical treatments, 125, 150
 Medical applications, 150, 564
 Medical devices, 545, 564
 Medicine, 545, 547, 564–577
 Meniscal lesions, 568
 Meniscal tissue, 569
 Meniscus, 568–570, 577
 Meniscus implant, 568–570
 Mercerization, 108, 112, 117, 333
 Methacrylate propyl trimethoxy silane, 334
 Methodology, 218, 219, 224
 Microbial cellulose, 551, 567, 568, 576
 Microbial degradation, 441, 445
 Microbond tests, 243, 244, 255–258
 Microcrystalline cellulose (MCC), 418, 557, 558
 Microdebond, 243, 257
 Microdroplet, 255–256
 Microdroplet test, 255, 256
 Microfibrillar, 331, 336
 Microfibrillar cellulose, 123, 150
 Microfibrillated cellulose (MFC), 121–150, 545–547, 549, 562, 563
 Microfibrils, 7, 8, 12–14, 16, 21, 26–28, 36, 67, 69, 219–221, 231, 436, 544, 546, 549, 550, 552, 555, 562, 664, 671–673, 675–679, 689
 Microindentation test, 243, 257, 258
 Micromechanical method, 244, 252, 255
 Micromechanical properties, 244
 Micronerves, 577
 Microorganisms, 426, 430, 431, 436, 440, 441, 445
 Microsurgery, 565, 566, 577
 Microsurgical, 565–567
 Microsurgical suture, 565
 Microvessel endoprosthesis, 564–567
 Microvessel replacement, 565
 Mineral cellulosic fibril composites
 abalone shell, 127

- biopolymers, 126–132
- colloidal PCC, 127, 129, 131
- composite PCC, 127–131
- co-precipitation, 127–132
- Hollander, 132–134
- particle size, 129–133
- PCC morphology, 129–132
- pigments, 126–132
- refining, 127, 130, 132–134
- rhombohedral PCC, 127, 129, 130, 132
- scalenoahedral PCC, 127, 129–131
- scanning electron microscopy (SEM), 129, 130, 132, 133
- Supermass colloid, 127, 132–134
- surface area, 129, 131–133
- Mineral pigments
 - filler content, 135
 - in situ precipitation, 135
 - Lumen loading, 135
 - magnetic compounds, 135
 - microfines-filler composite, 135
 - papermaking, 134–135
 - preflocculation, 135
- Modeling, 243, 252
- Moisture, 663, 670, 676–679, 683, 685, 693
 - content, 159
- Monomer, 334
- Monosaccharides, 434, 540
- Morphological factors, 223
- Morphology, 215–236
- Mucoadhesive, 563
- Multicellular flax fibers, 65
- N**
- Nanocellulose, 150, 544–577
 - esterification, 559
 - film, 559
- Nanocellulosic fibrils, 123, 124, 134–150
- Nanocellulosic gel composites, 123–134
- Nanocellulosic material, 545, 559
- Nanocomposites, 523–524, 661–696
- Nanocrystal production
 - acid hydrolysis, 185–187, 189
 - effect of experimental parameters, 186
 - stability, 186
 - surface charge, 186
- Nanocrystals, 544, 549
- Nanodimension, 546
- Nanofibres, 26–37
- Nanofibrillar cellulose, 144, 150
- Nanofibrillated cellulose (NFC), 121–150
- Nanofibrillated cellulose production
 - carboxymethylation, 185
 - enzymatic hydrolysis, 185
 - mechanical processing, 183, 185
 - TEMPO-mediated oxidation, 185
- Nanofibrils, 27, 28, 33
- Nanomaterials, 546, 550
- Nanoparticle morphology
 - aspect ratio, 190
 - geometry, 189
 - nature, 184
- Nanowhiskers, 540, 544, 563
- NaOH, 230, 246, 256
- Native composite, 545
- Natural fibers, 216–219, 223–227, 231, 236, 243–245, 254, 255, 544, 552, 611–617
 - bast, 379, 380, 383–386
 - leaf, 379, 380, 386–389
 - seed, 379, 389
- Natural fibres, 3–37
 - cellulose, 157, 158, 166, 167, 169–173
 - hemicellulose, 157, 158, 167, 173
 - jute, 701–718
 - lignin, 157, 158, 167, 168, 173
 - pectin, 157, 164–166, 173
 - waxes, 157
- Natural oil polyols (NOPs), 438–439
- Natural rubber composites
 - bonding agent effects, 312, 314–315
 - cure characteristics, 305
 - effect of fibre length, 307
 - fibre breakage, 304–305
 - fibre loading, 313–314
 - fibre orientation effects, 307–308
 - green strength measurements, 306
 - preparation and characterisation, 303–304
- Nature's composite, 65, 82
- Near-infrared spectroscopy, 71, 79, 80
- Needle-punched, 328
- Nerves microsurgery, 565
- Nervus ischiadicus, 565, 566
- Nettle, 100–103, 105, 106
- Neural network, 226, 231
- Never-dried cellulose membranes, 571
- New uses, 222
- Nielsen, L.E., 412
- NIR spectroscopy, 80
- N-isopropylacrylamide, 561
- Nitration, 333, 334
- N-octadecyl isocyanate, 560, 563
- Nodes, 67
- Noncellulosic, 331, 332
- Noncellulosic compounds, 556
- Noncellulosic polysaccharides, 69
- Nonfibrous, 329

- Nonionic surfactants, 559
 Nonpolar polymers, 559
 Nonpolar solvents, 559
 Nontoxic, 651
 Nonuniform distribution, 229
 Nonuniformity, 218
 Nonwood cellulose, 548
 Nonwood plants, 549
 Nonwovens, 117, 328, 337, 665
 North American textile mills, 64
 Norway spruce, 557
 Novel composite paper
 - bending stiffness, 138–140
 - bulk, 136, 138, 139
 - cellulosic nanofines, 136
 - composite paper, 136, 141–144
 - consistency, 137, 144, 146
 - FIB-SEM microscopy, 144
 - filled paper, 135
 - fracture toughness, 138, 141–143
 - glue, 136
 - handsheets, 137–146
 - honeycomb structure, 145
 - light scattering, 138, 144, 145
 - optical properties, 135, 136
 - PCC content, 137–142, 144
 - permeability, 140
 - precipitated calcium carbonate (PCC), 135–146
 - reinforcing fibres, 137, 142, 143
 - strength, 135–138, 140–144
 - strengthening agents, 136
 - Supermass colloid, 137, 146
- Nucleating agent, 394
 Nursery, 594–595
 Nutraceutical, 81
 Nutritional oil, 81
 Nutritional uses, 80
- O**
- Oil based nanocomposites, 527
 Oilseed, 63, 64, 71, 84
 Oligosaccharides, 434, 559
 Omega-3, 81
 Omega-3 fatty acids, 64, 65, 81
 Opening and cleaning equipment, 76
 Optical properties, 135, 136, 150
 Optimized derivatives
 - characterization, 56–57
 - rheology, 56–57
- Order parameter, *S*, 404, 405, 410, 411, 413
 Oregon, 63
 Organic fatty acid chlorides, 559
- Osseous defects/Osseus defects, 564, 568
 Osteoarthritis, 568
 Osteochondral, 574
 Oxidase, 432
 Oxidation, 558, 560
 Oxidative polymerization, 561
 Oxygen-permeable polymer, 567
- P**
- Packaging material, 427–429, 442–443, 628, 637, 649, 652
 PALF nanocellulose, 549
 Palm, 111, 112, 556
 Palmyrah, 224
 Paper, 121–150
 Paracrystalline, 555
 Parapatellar skin incision, 574
 Parenchyma cells, 69
 Patella, 574, 575
 PCC-cellulosic fibril composites
 - air permeability, 148
 - bending stiffness, 148, 149
 - composite fillers, 147–149
 - composite handsheets, 147
 - density, 147, 148
 - finer, 146–148
 - internal bond strength, 148
 - light scattering, 148, 149
 - network structure, 147, 149
 - optical pores, 149
 - PCC morphology, 131, 147–150
 - reference handsheets, 147
 - Supermass colloid, 146
- Peanut oil, 439
 Pectin, 102, 104, 105, 330, 332
 Pelvic floor, 576
 Peptide coupling, 561
 PE-rayon: 20
 Percolation effect, 473
 Peripheral nerves, 574
 Permanganate treatment, 604–606, 625
 Permeability, 84, 416–418
 Permeation, 415, 416
 Peroxide treatment, 85, 607, 625, 636, 637
 Pesticide, 72
 Petroleum-based polyesters
 - biodegradable aliphatic copolyesters, 462
 - biodegradable aromatic copolyesters, 462
 - polycaprolactone, 461–462
- Pharmaceuticals, 545
 PHB-rayon, 502–504
 Phenol formaldehyde, 562
 Photodegradation, 426, 440, 441, 509, 512–515

- Photo-oxidation resistance, 444
Physical methods, 107, 602–611
Physical treatments, 107
Physico-chemical, 611–617
Piassava, 219, 220, 232, 233, 235, 243, 246, 250–252
Pineapple, 219, 221, 222, 224, 544, 549
Pineapple leaf, 325–339, 379, 380, 388–389, 544, 549
PLA/MFC, 563
Plantation, 593, 595–597
Plant fibers, 544, 592, 601–603, 611, 617, 643–646, 652
PLA-rayon, 498–502
Plasma
 abrasion, 160
 atmospheric pressure, 162–163
 cleaning, 160
 crosslinking, 160
 etching, 161, 162
 free radicals, 160
 functionalisation, 160
 low pressure, 160–162
 treatment, 381, 383, 602, 635
Plastic deformation, 409
Plasticizers, 432, 435
Plastics, 116, 150
Polarized optical microscopy (POM), 402, 403
Polyaniline, 561
Polyanionic, 560
Poly-anionic cellulose (PAC), 437
Polybutylene succinate (PBS), 435
Polybutylene succinate adipate (PBSA), 435
Polycaprolactone (PCL), 431, 461–462, 560, 561, 563
Poly- ϵ -caprolactone (PCL), 429, 431
Polyelectrolyte multilayers (PEMs), 563
Polyester, 223, 225, 236, 243, 246, 250–252, 258
Polyester-based composites, 235
Polyester composites, 621, 622, 626, 628
 characterisation, 317
 dynamic mechanical thermal analysis, 317–318
 flexural properties, 318–319
 impact strength, 319–322
 preparation, 315–317
 tensile properties, 318
Polyester matrix, 258
Polyesters, 427, 429, 430, 432, 434–435
Polyglycolic acid (PGA), 429–430
Polyhydroxyalkanoates (PHAs), 430–431, 459–461
Polyhydroxybutyrate (PHB), 430, 564
Poly (3-hydroxybutyrate-*co*-3-hydroxyvalerate) (PHBV), 515
Polyhydroxyoctanoate (PHO), 430, 431, 563, 564
Poly(lactic acid) (PLA), 338, 428–429, 434, 443, 456–459, 515, 559, 563
Poly(oxyethylene), 563
Poly(styrene-*co*-butyl acrylate) latex, 562, 563
Polymer, 107, 109–114, 116, 117, 243, 345–370
 composites, 241–259, 547, 589–653
 grafting, 558, 560
 matrix, 600, 615, 620, 629, 634, 636, 651
Polymer-based composites, 231
Polymeric coating, 609–611
Polymeric fibers, 223, 226
Polymeric matrices, 244, 245, 247, 250, 252, 258, 259
Polymeric resins, 257
Polymorphic, 558
Polymorphs, 541
Polypropylene, 511, 514
 β -phase, 265
 composite, 264, 265, 268, 270–285
 crystallization, 271, 272, 274, 277–280
 functions, 226
 MAH grafted PP, 384, 387, 389
 nucleation, 274, 277–280, 285
 polymorphism, 265
 processing, 264, 265, 282
 structure, 265, 266
Polypyrrole, 547
Polysaccharide, 433–440
Polysiloxanes, 335, 563
Polystyrene, 258, 515
Polysulfonates, 563
Polytetrafluoroethylene (ePTFE), 575
Polyurethane, 561, 563
Poly(vinyl acetate), 563
Poly(vinyl alcohol) (PVA), 515–516, 562, 563
Polyvinyl chloride, 563, 567
Postsurgery, 564
Poultry feed, 82
PP-rayon, 490–496
Prehistoric, 62
Premature rupture, 233
Pre-treatment, 676, 677, 683
Probability, 224, 226, 229, 230, 233, 234
Probability density, 226, 229
Probability density function (PDF), 226, 231
Probability plot, 229, 234
 techniques, 230
Processing, 598–599, 601, 612, 617, 618, 637, 638, 640, 644, 649, 650, 653

- Processing condition, 242, 250, 252, 256
 Processing extrusion, 271
 Processing fiber pulling, 272
 Processing injection molding, 271–272, 284
 Processing of cellulose nanocomposites
 electrospinning, 194–195
 extrusion, 193
 hydrodispersable polymers, 191
 hydrosoluble polymers, 191
 impregnation, 194
 layer-by-layer films, 196
 long chain grafting, 192–193, 195
 nonaqueous, 191–192
 polymer latexes, 190–191
 Processing press molding, 272, 283, 284
 Producers, 593, 594
 Profiles, 716
 Properties, 217–224, 226, 231, 232, 235, 236,
 601–604, 606, 607, 609, 611–637, 640,
 642–644, 647, 650–653
 Protein, 5–6, 24, 550, 563
 Protein nanocomposites, 526
 Pseudo-plastic, 150
 PU-cellulose, 562
 Pullers, 73, 74
 Pullout, 244–259
 mechanism, 250
 test, 244–247, 249, 250
 Pultrusion, 618
 Pyrolysis, 349, 351, 358–360, 362, 363,
 365, 366
- Q**
- Quality fibers, 219
 Quasi-stationary, 226
- R**
- Radiation, 110
 Railways, 638, 648–650, 652
 Ramie fibers, 98–106, 219, 222, 232–236, 250,
 252, 255–257, 443, 555
 Random distribution, 226
 Raspador, 597–599, 609, 637, 638, 649, 652
 Reactor, fluidized bed, 351, 353, 354, 357, 358
 Reconstruction of nerves, 577
 Recyclable, 394
 Red mud, 628, 642, 643
 Reepithelialization process, 553, 571
 Regenerated cellulose, 563
 Reinforcement, 98, 99, 101, 112–117,
 215–236, 242, 243, 246, 612, 617, 621,
 622, 634, 637, 638, 643, 646, 647,
 651, 652
- Renewable biosources, 540
 Renewable material, 216, 544
 Renewable resources, 98, 116
 Resins, 81, 85
 Resin transfer moulding (RTM), 84, 618, 621,
 683, 691–692
 Resorcinol, 337
 Retinaculum, 574, 575
 Retroperitoneum, 577
 Retting, 9–11, 219, 329, 333
 dew, 164, 165, 167, 173
 enzyme, 164–166, 173
 natural, 168
 water, 163–164, 173
 Rheological behavior, 335, 390, 556
 Rheology, 563
 Rice, 549
 Rice husks, 345–370
 Rigorous cleaning techniques, 75
 Ring-opening polymerization (ROP), 430,
 431, 561
 Rod-like nanocellulose, 556
 Rollertop card, 76, 78
 Roofing/Roofing sheet, 637, 640, 641, 643,
 650, 703
 Rubber, 347, 349, 357, 367–370
 composites, 323
 Ruminants, 436
- S**
- Sanitary napkins, 547
 Scaffold, 549, 564, 567
 Scanning electron microscope (SEM), 232,
 251, 445, 609, 610, 624, 626
 Scatter properties, 218, 222
 Scatter strength properties, 231
 Scutching wheel, 76, 77
 Seed fibers, 100
 cotton, 379, 389, 394
 Self-reinforcing, 418
 Serrations, 248, 250
 Shape determining factor, 230
 Shear deformation, 636
 Shear rate, 403, 404
 Shear strength, 241–259, 625
 Shive, 65, 69, 71, 73, 75–77, 80, 81, 84, 86
 Shive-containing fiberboards, 80
 Short fibre composites (SFCs), 404, 411, 412
 Silane treatment, 381, 382, 606–607, 625
 Silanization, 109, 117
 Silica, 347–360, 362, 364, 368–370
 Silk, 5, 6, 24
 Silylation, 558–560

- Simulations, 226
- Single fiber fragmentation (SFF), 243, 252–255, 258
- Single fiber pullout (SFP) test, 244–246
- Sisal fiber-reinforced–fly ash cement roofing sheets, 641
- Sisal fibers, 98–100, 217, 219–224, 226, 229–233, 235, 236, 246, 250–252, 258, 379, 380, 382, 386–388, 394, 544, 548, 556, 558, 589–653
- composites, 638–644
 - waste, 651
- Sisal growth, 595
- Sisal-production, 597–598
- Skin-cleansing cloths, 547
- Skin grafting, 553, 564, 571, 577
- Skin wounds, 553
- Small angle light scattering (SALS), 402, 404, 411, 413
- Smaller diameter, 234
- Soft contact lens, 562
- Soft tissue, 554, 576
- Soft tissue augmentation material, 554
- Softwood, 556, 558
- Solid dosage forms, 547
- Songe gourde, 219, 243
- Sonication/cavitation techniques, 73
- Sorghum, 549
- Sorption, 106, 107
- Soy bean oil, 439
- Soy beans, 439, 440
- Soybean stock-based nanofiber, 562
- Soy plastics, 439–440
- Spherical nanocelluloses, 557
- Stability, 604, 625, 628, 635, 644, 651
- Standard deviations, 236
- Standardization, 718
- Stand-retting, 73
- Starch, 433–436, 440, 441, 443
- Starch-aliphatic polyester blends, 434–435
- Starch-based biodegradable polymers, 433–434
- Starch-based polymers, 563
- Starch nanocomposites, 525
- Static friction coefficient, 160
- Statistical analysis, 223, 226, 229, 232, 236, 249
- Statistical approach, 218, 226, 231
- Statistical distribution, 231–233
- Statistical distribution function, 231
- Statistical evaluation, 222
- Statistical model, 226, 231, 236
- Statistical techniques, 254
- Statistic methods, 244
- Steam explosion techniques, 73
- Stearic acid treatment, 606, 625
- Stem, 101, 102
- Stick–slip, 248, 250
- Stiffness, 608, 617, 627, 628, 644, 651, 677–679, 685, 686, 689, 693, 695
- Storage modulus, 563
- Strength, 65, 67, 71, 73, 74, 77, 79, 80, 82–87
- Strengthening mechanism, 219, 236
- Strength–length dependency, 231
- Strength properties, 135, 141, 149
- Strength variation, 223, 224, 229
- Stress transfer, 171
- Strong, 65, 71, 82, 83, 86, 87
- Structural defects, 233, 243
- Structural hierarchy, 541
- Structural parameters, 215
- Structure, 593, 594, 600, 601, 603, 606, 611, 623–625, 628, 635, 636
- Structure of natural fibers, 104
- Styrenebutyl acrylate latex, 563
- Subcutaneous tissue, 571, 574, 576
- Subjectively judged, 79
- Submicron, 546
- Sugar beet pulp, 556, 562
- Sugarcane, 217, 219, 221, 549
- Superabsorbents, 435
- Superficial, 571
- Superior performance, 219, 236
- Surface acetylation, 559
- Surface cationization, 559
- Surface chemical treatment, 246, 254, 259
- Surface energy, 160, 558
- Surface modification, 107, 111, 601–617, 625, 635, 637
- chemical, 381, 392
 - physical, 381
 - silane coupling agent, 392, 393
- Surface-modified nanocellulose, 559
- Surface roughness, 160, 168
- Surface treatment, 71, 83–85, 87, 155–173
- Surfactant, 558, 559, 563
- Sustainability, 217
- Sustainable development, 217
- Sutures, 565–567, 569, 570, 574–576
- Swelling, 107, 117
- Synthetic fibers, 216–218, 222–225, 227, 232, 242–244, 249, 255, 257–259
- Synthetic fibre
- carbon, 156, 160
 - glass, 156, 173
- Synthetic polymers, 217

T

Takayanagi's model, 474
 Talipot fibers, 224
 Technical textiles, 117
 TEMPO-oxidized, 560
 Tensile properties, 219, 221, 226, 231, 482,
 490–492, 494–499, 501–502, 504, 609,
 621, 624, 626, 633–635
 Tensile rupture, 250, 251
 Tensile strength, 65, 67, 83, 87, 106, 112, 218,
 219, 221, 223, 229–231, 233, 235, 236,
 247, 249, 663–666, 668, 669, 671, 675,
 676, 678–680, 684, 686
 Tensile stress, 408, 414
 Tensile test, 244, 247, 253
 Termites, 436
 Test lengths, 223, 228
 Textiles, 379, 389
 Theoretical strength, 296–297
 Therapeutic application, 553
 Thermal analysis, 300–302, 445
 Thermal-degradation, 426
 Thermal expansion coefficient, 548, 553, 562
 Thermal gravimetric analysis (TGA), 612,
 614, 625
 Thermal properties, 613–615, 623
 Thermal stability, 553, 557, 577, 665, 668, 672,
 674, 680–682
 Thermogravimetric, 331, 335
 Thermoplastic composites, 378, 628–630, 632,
 634, 635
 Thermoplastic matrices, 254
 Thermoplastic polymer composite, 628–637
 Thermoplastics, 427–429, 432, 434
 Thermoset, 427, 432, 440
 Thermoset polymer composite, 619–620,
 626–628
 Thermotropic, 403
 Thinner fibers, 218, 232–234
 Thixotropic behavior, 556
 Tissue-engineered application, 549
 Tissue-engineered constructs, 549
 Tissue regeneration, 577
 T50-median, 230
 Topography, 402, 404, 405
 Top shaker, 76, 77
 Total rupture, 233
 Trachea, 576
 Transparent, 547, 548, 553, 554, 562, 564
 Transparent cellulose, 562, 564
 Triglycerides, 167
 Trimethoxy silane, 334
 Trochlear groove, 574, 575

Trochleoplasty, 574, 576
 Tunicates, 540, 541, 544, 549, 550, 555, 556,
 559–561
 Tunicin, 550, 551, 558
 Turners, 73, 74
 Two nonlinear equations, 229
 Two-parameter analysis, 224
 Two parameters, 227, 229, 230

U

Ulcers, 564, 571, 572, 577
 Ultimate fibers, 79
 Ultrasonic treatment, 556, 558
 Uniform distribution, 229
 Unimodal, 224, 225, 229, 233
 Unimodal distribution, 224, 225
 United States Department of Agriculture
 1995, 78
 Universal Standards, 79
 Unsaturated polyester resin, 294, 705–707,
 710, 711
 Unsaturation, 432
 Urea-formaldehyde composite, 623
 Ureter, 576
 US Cotton Standards Act, 78
 USDA Flax Pilot Plant (Flax-PP), 73, 75, 76

V

Vacuum-assisted resin transfer molding
 (VARTM), 84
Valonia cellulose, 555
 Variety, 593, 595, 615, 617, 623, 643
 Vascular wall, 565
 Vegetable fibers, 455
 Vegetable oils, 438, 439
 Velocity, fluidizing, 353–357
 Vermicomposting, 650
 Vessel implants, 565
 Veterinary medicine, 564, 574–577
 Vinyl monomers, 561
 Vitro scaffold, 567
 Voids, 230, 231
 Volume fraction, 617, 619, 620, 622, 634, 651

W

Wall panels, Gelcoat, 717
 Warts, 429
 Waste, 99, 113, 116, 346, 348, 359, 369, 370
 management, 650
 Water absorption, 606, 618, 622–624, 629,
 642, 644
 Water resistant, 440, 442
 Water-retting, 73, 85

- Water uptake, 704, 711
 - Wax, 65, 69–71, 80, 81, 85
 - Wax content, 80
 - Weak links, 233
 - Weak points, 244, 245
 - Weeds
 - industrial feedstock, 57
 - management, 51, 57
 - Weibull analysis, 218, 222–227, 229, 230, 232, 236, 244
 - Weibull distribution, 224, 225, 229, 230, 232, 236, 253
 - Weibull method, 249
 - Weibull model, 225, 230, 236
 - Weibull modulus, 224, 229
 - Weibull parameters, 224, 253
 - Weibull plots, 225
 - Weibull-weak link, 224
 - Wettability, 71, 159–162, 173
 - Wheat/Wheat straw, 549, 556, 558
 - Wood, 100, 109, 112, 114, 116
 - composites, 668–671
 - fibers, 544, 546, 547
 - nanocellulose, 547
 - pulp, 545, 546
 - substitute, 640, 642–643, 645
 - Wood fiber, bamboo, 379, 390, 394
 - Wool fibers, 223–226
 - Wound covering bandage, 562
 - Wound dressings, 564, 571
 - Wound healing, 553, 571, 572, 577
 - Wrinkle resistance, 432
- X**
- Xerophyte, 647
 - Xyloglucan, 559
- Y**
- Yarns, 637, 638, 640, 650, 652
 - Yeasts, 426, 445
 - Yield, 593, 594, 597, 600, 650, 651
 - Yield stress, 408, 409, 414, 415
 - Young's modulus, 218, 221, 230, 231, 411, 412, 547, 548, 553, 562, 563, 569, 570
- Z**
- Zeta potential, 167